

1 $x=2, y=1, z=2, R=H$ (cyclam)

2 $x=2, y=2, z=2, R=H$ (isocyclam)

3 $x=2, y=1, z=2, R=CH_2N(CH_2)_2$ (scorpionate)

4 $x=1, y=1, z=1, R=H$ (cyclen)

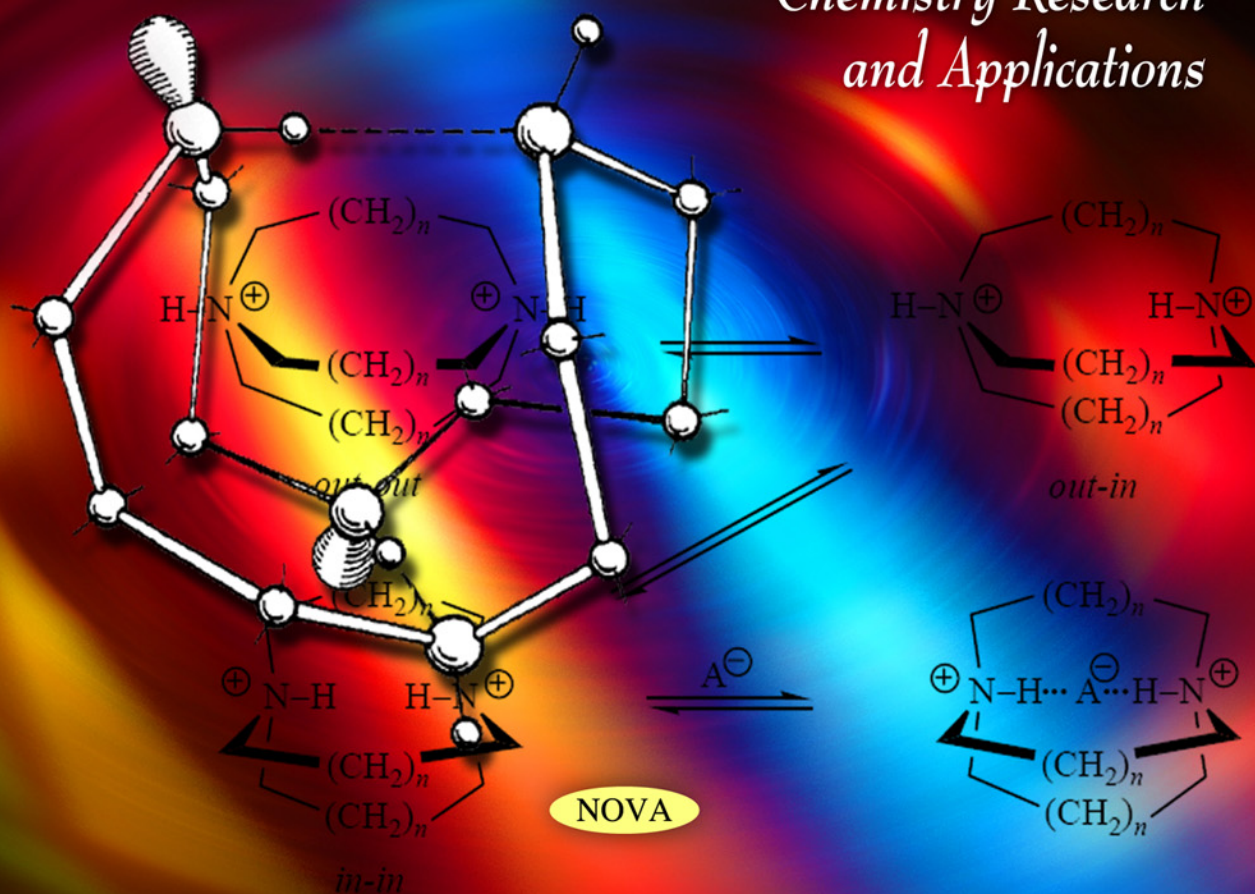
Daniel W. Fitzpatrick
Henry J. Ulrich

Editors

MACROCYCLIC CHEMISTRY

NEW RESEARCH DEVELOPMENTS

*Chemistry Research
and Applications*



CHEMISTRY RESEARCH AND APPLICATIONS

MACROCYCLIC CHEMISTRY: NEW RESEARCH DEVELOPMENTS

No part of this digital document may be reproduced, stored in a retrieval system or transmitted in any form or by any means. The publisher has taken reasonable care in the preparation of this digital document, but makes no expressed or implied warranty of any kind and assumes no responsibility for any errors or omissions. No liability is assumed for incidental or consequential damages in connection with or arising out of information contained herein. This digital document is sold with the clear understanding that the publisher is not engaged in rendering legal, medical or any other professional services.

CHEMISTRY RESEARCH AND APPLICATIONS

Applied Electrochemistry

Vijay G. Singh (Editor)

2009. ISBN: 978-1-60876-208-8

Handbook on Mass Spectrometry: Instrumentation, Data and Analysis, and Applications

J. K. Lang (Editor)

2009. ISBN: 978-1-60741-580-0

Handbook of Inorganic Chemistry Research

Desiree A. Morrison (Editor)

2010. ISBN: 978-1-61668-010-7

2010. ISBN: 978-1-61668-712-0 (E-book)

Solid State Electrochemistry

Thomas G. Willard (Editor)

2010. ISBN: 978-1-60876-429-7

Mathematical Chemistry

W. I. Hong (Editor)

2010. ISBN: 978-1-60876-894-3

2010. ISBN: 978-1-61668-440-2 (E-book)

Physical Organic Chemistry: New Developments

Karl T. Burley (Editor)

2010. ISBN: 978-1-61668-435-8

2010. ISBN: 978-1-61668-469-3 (E-book)

Chemical Sensors: Properties, Performance and Applications

Ronald V. Harrison (Editor)

2010. ISBN: 978-1-60741-897-9

Macrocyclic Chemistry: New Research Developments

Dániel W. Fitzpatrick and Henry J. Ulrich (Editors)

2010. ISBN: 978-1-60876-896-7

Electrolysis: Theory, Types and Applications

Shing Kuai and Ji Meng (Editors)

2010. ISBN: 978-1-60876-619-2

**Energetic Materials:
Chemistry, Hazards and Environmental Aspects**

Jake R. Howell and Timothy E. Fletcher (Editors)

2010. ISBN: 978-1-60876-267-5

Chemical Crystallography

Bryan L. Connelly (Editor)

2010. ISBN: 978-1-60876-281-1

2010. ISBN: 978-1-61668-513-3 (E-book)

**Heterocyclic Compounds: Synthesis, Properties
and Applications**

Kristian Nylund and Peder Johansson (Editors)

2010. ISBN: 978-1-60876-368-9

Influence of the Solvents on Some Radical Reactions

*Gennady E. Zaikov, Roman G. Makitra, Galina G. Midyana
and Liliya I. Bazylyak*

2010. ISBN: 978-1-60876-635-2

Dzhemilev Reaction in Organic and Organometallic Synthesis

Vladimir A. D'yakonov

2010. ISBN: 978-1-60876-683-3

**Analytical Chemistry of Cadmium: Sample Pre-Treatment
and Determination Methods**

Antonio Moreda-Piñeiro and Jorge Moreda-Piñeiro

2010. ISBN: 978-1-60876-808-0

**Binary Aqueous and CO₂ Containing Mixtures
and the Krichevskii Parameter**

*Aziz I. Abdulagatov, Ilmutdin M. Abdulagatov
and Gennadii V. Stepanov*

2010. ISBN: 978-1-60876-990-2

Advances in Adsorption Technology

Bidyut Baran Saha and Kim Choon Ng (Editors)

2010. ISBN: 978-1-60876-833-2

Electrochemical Oxidation and Corrosion of Metals

Elena P. Grishina and Andrew V. Noskov

2010. ISBN: 978-1-61668-329-0

2010. ISBN: 978-1-61668-329-0 (E-book)

**Modification and Preparation of Membrane
in Supercritical Carbon Dioxide**
Guang-Ming Qiu, Rui Tian, Yang Qiu and You-Yi Xu
2010. ISBN: 978-1-60876-905-6

**Thermostable Polycyanurates: Synthesis, Modification,
Structure and Properties**
Alexander Fainleib (Editor)
2010. ISBN: 978-1-60876-907-0

Combustion Synthesis of Advanced Materials
B. B. Khina
2010. ISBN: 978-1-60876-977-3

**Structure and Properties of Particulate-Filled Polymer Composites:
The Fractal Analysis**
G. V. Kozlov, Y. G. Yanovskii and G. E. Zaikov
2010. ISBN: 978-1-60876-999-5

Information Origins of the Chemical Bond
Roman F. Nalewajski
2010. ISBN: 978-1-61668-305-4

Cyclic β -Keto Esters: Synthesis and Reactions
M.A. Metwally and E. G. Sadek
2010. ISBN: 978-1-61668-282-8

Wet Electrochemical Detection of Organic Impurities
F. Manea, C. Radovan, S. Picken and J. Schoonman
2010. ISBN: 978-1-61668-661-1
2010. ISBN: 978-1-61668-491-4 (E-book)

Quantum Frontiers of Atoms and Molecules
Mihai V. Putz (Editor)
2010. ISBN: 978-1-61668-158-6

Molecular Symmetry and Fuzzy Symmetry
Xuezhuan Zhao
2010. ISBN: 978-1-61668-528-7
2010. ISBN: 978-1-61668-375-7 (E-book)

Molybdenum and Tungsten Cofactor Model Chemistry
Carola Schulzke, Prinson P. Samuel
2010. ISBN: 978-1-61668-750-2
2010. ISBN: 978-1-61668-828-8 (E-book)

Rock Chemistry

Basilio Macías and Fidel Guajardo (Editors)

2010. ISBN: 978-1-60876-563-8

Boron Hydrides, High Potential Hydrogen Storage Materials

Umit B. Demirci and Philippe Miele (Editors)

2010. ISBN: 978-1-61668-362-7

Tetraazacyclotetradecane Species as Models of the Polyazacrown Macrocycles

Ryszard B. Nazarski

2010. ISBN: 978-1-61668-487-7

2010. ISBN: 978-1-61668-9001 (E-book)

Chemical Reactions in Gas, Liquid and Solid Phases: Synthesis, Properties and Application

G.E. Zaikov and R.M. Kozłowski (Editors)

2010. ISBN: 978-1-61668-671-0

2010. ISBN: 978-1-61668-906-3 (E-book)

Ion Transfer at Liquid/Liquid Interfaces

Rodrigo Alejandro Iglesias and Sergio Alberto Dassie

2010. ISBN: 978-1-61668-684-0

2010. ISBN: 978-1-61728-255-3 (E-book)

Calixarene Complexes with Solvent Molecules

O.V. Surov, M.I. Voronova, A.G. Zakharov

2010. ISBN: 978-1-61668-755-7

2010. ISBN: 978-1-61728-250-8 (E-book)

Nobel Laureates and Nanotechnologies of Applied Quantum Chemistry

Vladimir A. Babkin and Gennady E. Zaikov

2010. ISBN: 978-1-61668-849-3

2010. ISBN: 978-1-61728-057-3 (E-book)

Lanthanum: Compounds, Production and Applications

Ryan J. Moore (Editor)

2010. ISBN: 978-1-61728-111-2

Spin-Orbit Interactions in PtF₆ and in Related Octahedral Molecules and Fluorocomplexes

Svetlana G. Kozlova and Svyatoslav P. Gabuda

2010. ISBN: 978-1-61668-838-7

2010. ISBN: 978-1-61728-471-7 (E-book)

Interactions of Aqueous-Organic Mixtures with Cellulose

M.I. Voronova, O.V. Surov, A.G. Zakharov

2010. ISBN: 978-1-61668-766-3

2010. ISBN: 978-1-61728-457-1 (E-book)

CHEMISTRY RESEARCH AND APPLICATIONS

**MACROCYCLIC CHEMISTRY:
NEW RESEARCH DEVELOPMENTS**

DÁNIEL W. FITZPATRICK

AND

HENRY J. ULRICH

EDITORS

Nova Science Publishers, Inc.

New York

Copyright © 2010 by Nova Science Publishers, Inc.

All rights reserved. No part of this book may be reproduced, stored in a retrieval system or transmitted in any form or by any means: electronic, electrostatic, magnetic, tape, mechanical photocopying, recording or otherwise without the written permission of the Publisher.

For permission to use material from this book please contact us:

Telephone 631-231-7269; Fax 631-231-8175

Web Site: <http://www.novapublishers.com>

NOTICE TO THE READER

The Publisher has taken reasonable care in the preparation of this book, but makes no expressed or implied warranty of any kind and assumes no responsibility for any errors or omissions. No liability is assumed for incidental or consequential damages in connection with or arising out of information contained in this book. The Publisher shall not be liable for any special, consequential, or exemplary damages resulting, in whole or in part, from the readers' use of, or reliance upon, this material.

Independent verification should be sought for any data, advice or recommendations contained in this book. In addition, no responsibility is assumed by the publisher for any injury and/or damage to persons or property arising from any methods, products, instructions, ideas or otherwise contained in this publication.

This publication is designed to provide accurate and authoritative information with regard to the subject matter covered herein. It is sold with the clear understanding that the Publisher is not engaged in rendering legal or any other professional services. If legal or any other expert assistance is required, the services of a competent person should be sought. FROM A DECLARATION OF PARTICIPANTS JOINTLY ADOPTED BY A COMMITTEE OF THE AMERICAN BAR ASSOCIATION AND A COMMITTEE OF PUBLISHERS.

LIBRARY OF CONGRESS CATALOGING-IN-PUBLICATION DATA

Macrocyclic chemistry : new research developments / editors, Daniel W.

Fitzpatrick and Henry J. Ulrich.

p. cm.

Includes index.

ISBN 978-1-61209-255-3 (eBook)

Published by Nova Science Publishers, Inc. † New York

CONTENTS

Preface		xi
Chapter 1	Tetraazacyclotetradecane Species as Models of the Polyazacrown Macrocycles: Molecular Structure and Reorganizations in Aqueous Media (pH 0-14) as Probed by NMR Spectroscopy and Computational Methods - Problems and Solutions	1
	<i>Ryszard B. Nazarski</i>	
Chapter 2	Calixarene Complexes with Solvent Molecules	51
	<i>O. V. Surov, M. I. Voronova and A. G. Zakharov</i>	
Chapter 3	Molecular Discrimination Behavior, Discrimination Level and Discrimination Factor of Cyclodextrins and Their Derivatives to Guest Molecules	87
	<i>Le Xin Song, Xue Qing Guo, Zheng Dang and Mang Wang</i>	
Chapter 4	Macrocyclic Glycopeptide-Based Chiral Stationary Phases in High Performance Liquid Chromatographic Analysis of Amino Acid Enantiomers and Related Analogs	129
	<i>I. Ilisz, Z. Pataj and A. Péter</i>	
Chapter 5	From Macrocyclic Ligands to Fluorescent Molecular Sensors for Metal Ions: Recent Results and Perspectives	159
	<i>Carlos Lodeiro, Vito Lippolis and Marta Mameli</i>	
Chapter 6	Study of Polysaccharides Thermal Stability in the Aspect of their Future Applications	213
	<i>Wojciech Ciesielski</i>	
Chapter 7	Interactions of Cyclodextrins with Amino Acids, Peptides and Proteins	233
	<i>Katarzyna Guzow and Wiesław Wiczak</i>	
Chapter 8	Inclusion Complex Formation of Cyclodextrins with Aminobenzoic Acids in Aqueous Solution	263
	<i>Irina V. Terekhova</i>	

Chapter 9	Thermodynamics of Cesium Complexes Formation with 18-Crown-6 in Hydrophobic Ionic Liquids. A Correlation with Extraction Capability	287
	<i>A. G. Vendilo, D. I. Djigailo, H. Rönkkömäki, M. Lajunen, E. A. Chernikova, L. H. J. Lajunen, I. V. Pletnev and K.I. Popov</i>	
Chapter 10	Macrocycles Role in Competitive Transport and Extraction of Metal Cations	307
	<i>Azizollah Nezhadali</i>	
Chapter 11	Chiral Calixarenes	325
	<i>Abdulkadir Sirit, Mustafa Yilmaz and Richard A. Bartsch</i>	
Chapter 12	New Trends in Modifications and Applications of Resorcinarenes	363
	<i>Cezary A. Kozłowski, Wiesława Kudelska and Joanna Konczyk</i>	
Chapter 13	Imine Macrocyclics: Building Blocks in Polymer Synthesis	393
	<i>Mircea Grigoras and Loredana Vacareanu</i>	
Chapter 14	The Recognition and Activation of Molecules and Anions by Polyaza Macrocyclic Ligands and their Complexes	417
	<i>Tong-Bu Lu</i>	
Chapter 15	New Therapeutically Agent with Increased Antifungal Activity	435
	<i>Mariana Spulber, Mariana Pinteala, Adrian Fifere, Valeria Harabagiu and Bogdan C Simionescu</i>	
Chapter 16	Food Antioxidants Cyclodextrin Inclusion Compounds: Molecular Spectroscopic Studies and Molecular Modelling	447
	<i>Aida Moreira da Silva</i>	
Chapter 17	A New Sprouting Inhibitor: <i>n@NO-Sprout</i>[®], B-Cyclodextrin/ S-Carvone Inclusion Compound	459
	<i>Marta Costa e Silva, Cristina Galhano and Aida Moreira da Silva</i>	
Chapter 18	Urea as an Adductor for the Branched Drug Molecules	469
	<i>A.K. Madan and Seema Thakral</i>	
Index		499

PREFACE

A macrocycle is, as defined by IUPAC, "a cyclic macromolecule or a macromolecular cyclic portion of a molecule. In the chemical literature, organic chemists may consider any molecule containing a ring of seven or more atoms to be a macrocycle. Coordination chemists generally define a macrocycle more narrowly as a cyclic molecule with three or more potential donor atoms that can coordinate to a metal center. This new book brings together the latest research results from around the world.

Chapter 1 - Three aliphatic molecules {*cyclam* (1, 1,4,8,11-tetraazacyclotetradecane), its 1,4,7,11-isomer *isocyclam* (2), and a single pendant arm derivative of 1 [*scorpiand*, 3, 1-(2-aminoethyl)-*cyclam*]} and their subsequently formed protonated congeners are considered as representatives of the macrocyclic polyamines (azacrowns) and related polyammonium salts. Important methodological aspects of structural investigations on these highly mobile aza-substituted macrorings are taken into account, especially concerning aqueous solutions over a whole pH range. Various issues about ascertaining donating sites and sequences of the protonation, dynamics and conformational preferences of such multidentate polyamino ligands as potential chelators (complexones) are considered. The scopes and limitations of different title tools and approaches applied in the field of azacrown macrocycles are discussed in detail. However, the extensively studied design and structures of their chelate complexes with metal cations are out of the scope of this overview, in principle.

Some important problems usually occurring in multinuclear resonance spectroscopy experiments performed for azacrowns as polyprotic bases in water solutions are considered. In particular, various issues involved with proper use of the NMR pH-titration technique supported by potentiometric results (instrumentation, software, acidic and alkaline errors in the pH measurements, an influence of the ionic strength, deuterium isotope effects, chemical-shift references for aqueous media) and resonance signal assignments [by using the amino protonation-induced shifts in δ_{XS} (where X = ^1H and, especially, ^{13}C), empirical 'shielding constants' or 'amine shift parameters', resemblance of pH titration profiles, and line broadening effects] are discussed in detail.

Different theoretical (computational) treatments suitable for reliable molecular modeling of the most probable, usually time-averaged and multicomponent, overall conformations of the polyaza macrocycles (as free amines or related polyammonium cations) and for subsequent empirically corrected (linearly scaled) GIAO-based predictions of NMR chemical shifts of these macrocyclic species assessed at different HF or DFT (B3LYP) quantum-chemical levels, are also considered. Selected results on the intramolecularly H-bonded and

non-H-bonded conformers of the macrocycles **1-3** are presented. The strengths and weaknesses of empirical force-fields methods (MMX vs. OPLS-AA and DREIDING) and simulations of the surrounding medium (mainly of solvent water molecules) with use of PCM and/or ONIOM techniques are enclosed, as well.

Beside the selected the author's own known results on the guiding polyamines **1-3**, some related (not published, corrected or accessible with some difficulty) experimental findings as well as theoretical predictions from this laboratory are also presented. In addition, the work is supplemented with several relevant literature data and reports on another structurally similar hetero-macrocycles. Moreover, some other selected recent results, new ideas and research directions in this topic are briefly discussed.

Chapter 2 - Solid calixarenes as receptors are characterized by phase transitions, which occur in binding of neutral molecules of guest compounds with the formation of clathrates or guest-host intercalation compounds. The binding of a guest by a solid host compound is largely a cooperative process. It begins after the attainment of a certain threshold thermodynamic activity (relative pressure p/p_0) of the guest and is completed in a narrow range of p/p_0 values. The process of clathrate formation in the binding of a guest by a host is accompanied by a significant rearrangement of the packing of host molecules, and the result of this rearrangement can depend considerably on the molecular structure of the guest. Moreover, the "induced correspondence" of the clathrate structure to the molecular structure of the guest is observed; in some cases, this effect endows solid hosts with improved selectivity.

Scattered information is available as to guest-removal, -addition, and -exchange properties of many host systems, including calix[n]arene derivatives. Upon recrystallization, host can form stoichiometric guest-host adducts, where guest molecules are included in each cavity maintained by the hydrogen-bonded network of the host. Volatile guests can be removed upon heating, to give polycrystalline guest-free apohost. The apohost subsequently binds various guests not only as liquids or gases but also, in some cases, as solids in the same guest-host stoichiometry as in recrystallization. The resulting adducts exhibit the same X-ray powder diffractions as the corresponding single-crystalline samples. Guest exchange also occurs. Despite such phenomenologically rich information, the authors are still far away from a thorough understanding of how solid-state complexation takes place. There are number of fundamental questions which are related to each other: Do the solid host and its solid adduct share the same phase or constitute different phases? Do guest-binding cavities maintained by an organic network survive or collapse upon guest-removal? How do guest molecules diffuse in the solid host?

Chapter 3 - This review briefly describes the molecule-molecule and molecule-ion interactions in cyclodextrin (CD) chemistry. And then the interactions were carefully compared on the basis of data from published papers. According to this, the authors concluded that the binding behaviors and discrimination abilities of CDs to a group of similar guests could be divided into four levels (A, B, C and D) in the light of the combination between the formation constants (K) of inclusion complexes and the ratio values (ξ , discrimination factor) of K of different complexes of the same host or guest. The author's objective is to present a useful method of categorizing host-guest complexes of CDs, and to elucidate the difference and relationship in concepts among inclusion phenomenon, molecular discrimination and molecular recognition. In addition, the physical significance of ξ , as well

as the contributions of ξ and K to the molecular discrimination between CDs and guests, is described in the present work.

Chapter 4 - The past 20 years has seen an explosive growth in the field of chirality, as illustrated by the rapid progress in the various facets of this intriguing field. The impetus for advances in chiral separation has been highest in the past decade and this still continues to be an area of high focus. This paper reviews direct separations of amino acid enantiomers and related analogs using macrocyclic glycopeptide-based high performance liquid chromatographic methods, focusing on the literature published in the last decade.

Chapter 5 - The design and synthesis of fluorescent molecular sensors that selectively and specifically respond to the presence of a given analyte (in particular metal ions) in a complex matrix is a vigorous research area of supramolecular chemistry. Applications can span from process control to environmental monitoring, food analysis, and medical diagnosis, to give some examples.

The most common synthetic approach to fluorescent chemosensors is to link covalently, through an appropriate spacer, a fluorogenic fragment (signalling unit) to a guest-binding site (receptor unit). The recognition of the target species by the receptor unit as a result of a selective host-guest interaction between the two is converted into an optical signal expressed as an enhancement or quenching of the fluorophore emission. The choice of both the signalling- and the receptor-units can be critical to both the performance and the selectivity/specificity of the sensor, especially if a direct interaction between the fluorophore and the target species is possible.

Different fluorophores (anthracene, 8-hydroxyquinoline, dansylamide, coumarin, phenanthroline, *etc*) are used as signalling sites, whereas macrocyclic receptors continue to represent the first choice as guest-binding sites for metal cations due to the extensive possibilities which they can offer for modulation of the topology and nature of the binding domain, thus providing an easy route to achieving strong and possibly selective interactions with the substrate of interest.

In this chapter will be reviewed the use of macrocyclic ligands essentially as receptor units in fluorescent molecular sensors for metal ions. The reported systems are mainly based on the work developed by the authors in the last ten years and compared with other related similar systems published. Some interesting properties beyond sensing ionic and/or neutral substrates by fluorescence can arise from these compounds; in particular pH, metals and light can be used as external stimuli to modulate the sensing properties through energy and electron transfer mechanisms.

Chapter 6 - The interaction of polysaccharides and cereal grains with transition metal ions is of a biochemical importance, mostly due to the presence of those complexes in biological systems. Metal polysaccharide chemistry plays a crucial role in crosslinking of various biomolecules, and formed polysaccharide/metal complexes are promising for various application, *e.g.* as drilling muds, heavy metal collectors and material for production of carbonizate and gaseous substances allowing preparation of second generation biofuels. In the study of cereal/metal complexes, the thermogravimetric measurements were also made in order to explain the influence of CoCl_2 , $\text{Cr}_2(\text{SO}_4)_2$, $\text{K}_2\text{Cr}_2\text{O}_7$, CuCl_2 , FeCl_3 , MnCl_2 , NiCl_2 , and ZnCl_2 on thermal decomposition of barley, oat, rye, triticale, and wheat grains in aspect of their applications for biofuels production. In investigation of polysaccharide/metal complexes, mainly concerning their conductivity as well as thermal stability and rheological properties, a special attention was paid to interactions of transition metal salts ($\text{Co}(\text{NO}_3)_2$,

Cu(NO₃)₂, Ni(NO₃)₂, Co(CH₃COO)₂, Cu(CH₃COO)₂, Mn(CH₃COO)₂, Ni(CH₃COO)₂, CoCl₂, CuCl₂, FeCl₃, MnCl₂, NiCl₂, CoSO₄, Cr₂(SO₄)₃, CuSO₄, Fe₂(SO₄)₃, MnSO₄) with potato, amarantus and cassava starch, potato amylose and potato as well as corn amylopectin.

Chapter 7 - For many years cyclodextrins and their inclusion complexes with different compounds have been widely studied by means of different experimental as well as theoretical methods. Among most popular compounds used as host molecules in the inclusion complexes are biologically active compounds, especially peptides and proteins as well as amino acids as model molecules. Such interest is a result of searching for new drug carriers. To study interactions of cyclodextrins with above mentioned host molecules, experimental methods such as ¹H NMR, fluorescence spectroscopy and microcalorimetry are used. In this review, basing on literature as well as own research, the application of those methods will be widely and critically discussed. Also, the influence of different factors such as distance between chromophore and functional groups, presence of protective groups, peptide chain conformation and amino acid chirality on the binding constants with cyclodextrins and thermodynamic parameters of the inclusion or other types of complexes formed will be described.

Chapter 8 - This chapter is a summary review devoted to inclusion complex formation of native and substituted α - and β -cyclodextrins with isomeric aminobenzoic acids. Complex formation of cyclodextrins with aniline and benzoic acid is also considered. The thermodynamic characteristics of complex formation are calculated and discussed in terms of the influence of the reagent's structure and pH on the binding process. Binding modes and driving forces of complexation are proposed.

The obtained results show that α - and β -cyclodextrins display selectivity in interactions with aminobenzoic acids. Complexation of α -cyclodextrin with *para*- and *meta*-aminobenzoic acids is highly exothermic and, consequently, it is enthalpy driven. Insertion of aminobenzoic acids into the α -cyclodextrin cavity is shallow and it is governed predominantly by the van der Waals interactions. On the contrary, the deeper inclusion of aminobenzoic acids into the β -cyclodextrin cavity takes place, and this process is accompanied by intensive dehydration. Complex formation of β -cyclodextrin with aminobenzoic acids is characterized by higher enthalpy and entropy changes. Thus, complexes formed by β -cyclodextrin are enthalpy-entropy stabilized. The size of the cyclodextrin cavity does not affect the complex stability, while the structure of aminobenzoic acids has a noticeable influence on the values of binding constants. *Para*- and *ortho*-aminobenzoic acids form more stable complexes with cyclodextrins. Ionization of the carboxylic group which is located inside the cyclodextrin cavity results in weakness of binding. The introduction of methyl- and hydroxypropyl-groups into the β -cyclodextrin molecule does not change the binding mode revealed for native β -cyclodextrin. Complex formation of aminobenzoic acids with these modified β -cyclodextrins is less enthalpy- and more entropy-favorable due to an increased contribution from dehydration of bulky substituents surrounding the macrocyclic cavity.

Chapter 9 - Thermodynamic data for cesium complexes formation with 18-crown-6 (18C6, L) [Cs(18C6)]⁺ and [Cs(18C6)₂]⁺ in hydrophobic room temperature ionic liquids (RTIL): trioctylmethylammonium salicylate ([TOMA][Sal]), tetrahexylammonium dihexylsulfosuccinate ([THA][DHSS]), 1-butyl-3-methylimidazolium hexafluorophosphate ([BMIM][PF₆]), 1-butyl-3-methylimidazolium bis(trifluoromethyl)sulphonylimide ([BMIM][N(Tf)₂]), 1-hexyl-3-methylimidazolium bis(trifluoromethyl)sulphonylimide ([HMIM]

$[N(Tf)_2]$ and 1-(2-ethylhexyl)-3-methylimidazolium bis[trifluoromethylsulphonyl]imide ($[EtHMIM][N(Tf)_2]$) were measured with NMR ^{133}Cs technique at 27 to 50 °C. Only $[Cs(18C6)]^+$ complexes are found for $[TOMA][Sal]$, $[THA][DHSS]$, $[BMIM][PF_6]$, while in $([BMIM][N(Tf)_2])$ and $([HMIM][N(Tf)_2])$ both $[Cs(18C6)]^+$ and $[Cs(18C6)_2]^+$ are formed. The stability of cesium complex in RTILs is estimated to be in the range between water and acetonitrile. Stability constants for $[Cs(18C6)]^+$ revealed much weaker dependence on temperature than those, measured in hydrophilic RTIL. The following values for $\log K(Cs+L)$ and $\Delta H(Cs+L)$ at 25 °C are determined: 1.43 (0.05), 3.85 (0.25) kJ/mol ($[TOMA][Sal]$); 0.76 (0.06), 2.1 (0.3) kJ/mol ($[THA][DHSS]$); 2.4 (0.2), -21.0 (1.4) kJ/mol ($[BMIM][PF_6]$); 3.4 (0.5), -6.8 (1.9) kJ/mol ($[BMIM][N(Tf)_2]$); 4.4 (0.1), -9.5 (0.4) kJ/mol ($[HMIM][N(Tf)_2]$), and 3.4 (0.4), 9 (18) kJ/mol ($[EtHMIM][N(Tf)_2]$). Besides, for $([HMIM][N(Tf)_2])$ and $([EtHMIM][N(Tf)_2])$ $\log K(CsL+L)$ and $\Delta H(CsL+L)$ at 25 °C are also found: 1.13 (0.07), -17.8 (0.3) kJ/mol ($[HMIM][NTf_2]$) and 1.16 (0.08); -17.5 (0.3) kJ/mol ($[EtHMIM][NTf_2]$).

It is demonstrated that unlike hydrophilic RTIL the entropy change with an exception of $[BMIM][PF_6]$, promotes complex formation while the corresponding enthalpy change is either positive or gives rather small contribution to the complex stability. The stability constants correlate well with crown ether assisted extraction degree of cesium from water into RTIL indicating an importance of complex stability for the extraction process.

Chapter 10 - A considerable number of investigation of the transport and extraction of transition and post- transition metal cations through bulk liquid and polymer inclusion membranes using a wide range of synthetic macrocyclic ionophores have now be reported by researchers. A motivation for these studies has been the potential for obtaining new metal ion separation processes for use in the range of industrial and analytical applications. A variety of membrane types have been used in metal ion transport experiments. A lot of competitive transport experiments involving metal ion transport from an aqueous source phase across an organic membrane phase into an aqueous receiving phase have been studied using open-chain mixed-donor ligands or macrocycles as the ionophore in the organic phase. For similar source and receiving phases the presence of the ionophore in the organic phase acts as a carrier for the metal ion until the concentrations in both aqueous source and receiving phases equalize and the system reaches equilibrium. It is well known that transport efficiency and selectivity can be influenced by a range of parameters with the transport limiting step differing from one system to another one. This chapter reports some of the factors that affect on the selectivity and efficiency of a macrocyclic ligand for transport and extraction of metal cations. A macrocycle has an important role to selecting a cation from a mixture of cations during the transport or extraction process. In the arrangement of transport process for carriers with protonation capability, the metal ion in the source phase comes into contact with the protonated or free ionophore at the source phase/ organic phase interface. A neutral complex is formed at this interface and the donor groups on the ligand are deprotonated upon complexation. The metal-ligand complex then diffuses through the organic phase until it comes into contact with the more acidic receiving phase where the metal ion is displaced by protons. The protonated form of the ligand then moves back through the organic phase to repeat the cycle. Typically, both aqueous phases are buffered appropriately in order to maintain the required pH gradient. The direction of the proton transport is in the opposite direction to that of the metal ions and this enables the concentration of the transported ion to exceed the equilibrium concentration. Among the multidentate ligands, the macrocyclic ones

which have many properties in common with the naturally occurring ionophores and distinguished by special arrangement of binding sites that controls their coordination environment and stereochemistry display remarkable and often unique stabilities and selectivities for complexation of various cations.

Chapter 11 - The development of calixarene-based host molecules containing chiral residues at either the lower or the upper rims of the calixarene macrocyclic ring is reviewed in this chapter. These supramolecular models are of particular significance for understanding the interactions between biological molecules, design of asymmetric catalysis systems, development of new pharmaceutical agents, and analysis and separation of enantiomers.

Chapter 12 - Easily accessible, resorcinarenes are valuable three dimensional building blocks for the coordination chemistry. They can be functionalized by introducing many different ligand moieties containing atoms O, S, N, P both at upper and lower rim. The possibility of the modifications of resorcinarenes resulted in the formation of coordination preorganized structures of molecular dimensions and complexes which can selectively encapsulate a variety of molecules. All the fascinating properties of resorcinarenes make this class of compounds very prospective from the point of view of supramolecular chemistry and creation valuable receptor molecules as well as new systems mimicking nature. In this connection, chiral derivatives of resorcinarenes are particular interest due to new possibilities of activities and applications. Recent developments of the resorcinarenes application as ion carriers for alkali metal, alkaline earth metal cations as well as transition metal ions removal and separation will be presented. The effect of structural studies of ring size variation, lower and upper rim functionalization on the selectivity and efficiency of solvent extraction and liquid membrane metal ions transport will be also described.

The authors present the recent applications of resorcinarenes and their derivatives as new ion carrier immobilized in polymers and as analytical devices achieved *via* their attachment to solid supports.

Chapter 13 - Two imine macrocycles with rhomboidal shape have been synthesized in excellent yields through [2+2] cyclocondensation reaction between (R,R)-1,2-diaminocyclohexane with 4,4'-bisformyl triphenylamine and 4,4'-bisformyl 4''-bromo triphenylamine. The macrocycles structure was assigned by electrospray ionization mass spectrometry (EIS-MS), ¹H-NMR, and elemental analysis. UV and FTIR spectroscopy and TG measurements were also used to characterize these compounds. These macrocycles have used as bricks in building of polymers containing macrocycles in the main chain (polyrhombimines). Chemical and electrochemical oxidative polymerization of rhombimine (R=H) and Suzuki polycondensation (R=Br) were applied in order to obtaining polymers containing imine macrocycles in the main polymer chain.

Chapter 14 - Molecular recognition and activation occur frequently in biological systems to achieve the physiological actions, and it is important to understand the process of recognition between receptors and substrates. In this chapter, the authors present the recent progress in the recognition of molecules and anions by cryptands, protonated cryptands and cryptates, the chiral recognition of amino acids by chiral polyaza macrocyclic ligands, the asymmetrical catalysis by chiral macrocyclic complexes, and the activations of bicarbonate and nitriles by dinuclear cryptates.

Chapter 15 - The effect of various native cyclodextrins and hydroxy propyl- β -cyclodextrin onto flucytosine water solubility has been investigated in phosphate buffer aqueous solution of the same pH value (7.0-7.2) and 37° C, corresponding to human body

normal conditions, using Higuchi and Connors phase solubility method. The cyclodextrins increase the drug solubility, making drug molecules more available for cell metabolism; the complexation stoichiometry is obtained by using two different methods (the phase solubility and Rose-Drago method). The enhancement of the solubility and the characteristics of the obtained phase diagram recommend the analyzed cyclodextrins as useful therapeutic agents promoters for sulconazole nitrate in conditions mimic to those characteristic for human bodies. The best results were obtained for hydroxypropyl β -cyclodextrin and β -cyclodextrin, that is why the flucytosine- β -cyclodextrin and hydroxypropyl β -cyclodextrin water soluble inclusion complex were used for further studies. The formation of inclusion complex between β -cyclodextrins and flucytosine has been studied and fully described in the author's previous work [1]. In this paper the authors are describing also, the results obtained concerning the antifungal activity of this new compounds. As expected the new inclusion complexes presents an important increase of the antifungal activity, illustrated by the reduction of the minimal inhibitory concentrations for 50 % and 90 % of the tested strains decreased. Also, the acute toxicity of the flucytosine - β cyclodextrin and hydroxypropyl β cyclodextrin complex is smaller comparing with the pure drug, analyzed alone. These results recommend the described conjugates as future promising therapeutic agents.

Chapter 16 - Certain plant-derived foods are rich in chlorogenic, caffeic and gallic acids, potent antioxidants. Its interaction with β -cyclodextrin leads to formation of inclusion compounds which affect the physicochemical properties of the guest molecule. Raman and $^1\text{H-NMR}$ spectroscopic studies of the interactions between β -cyclodextrin (β -CD) and included *PPO* (polyphenol oxidase) substrate molecules, chlorogenic acid, (CGA) and caffeic acid (CA) in aqueous and solid medium are reported.

Data analysis by Job's method shows that all the complexes have 1:1 stoichiometry in the studied range of temperatures. Values for the apparent association constant of the inclusion compound are estimated at different temperatures. The obtained thermodynamic parameters are compared with previously reported values for other inclusion systems. These molecules also provide characteristic vibrations with group frequencies for probing the guest on complex formation. The results confirm that inclusion occurs.

This work was complemented by evaluating the energy differences involved in the inclusion reactions for the considered guests and the energies involved in the conformational changes occurring both in the included guests and in the CD macrocycles. Molecular modelling was carried out for the inclusion complexes using the Gaussian 98 system of programs (Gaussian 98, 1998). Inclusion modes for the 1:1 inclusion complexes of gallic, caffeic and chlorogenic acids in β -cyclodextrin (β -CD) and the structures of the included and free host (β -CD) and guest molecules were determined at the HF/6-31G//HF/PM3 level. In addition, the total energy for the 1:1 inclusion as well as the interaction energies between CD and the guest molecules in their non-relaxed inclusion complex geometries were evaluated.

Chapter 17 - The main goal of this work was to develop a new potato sprouting inhibitor. Why? Because there is an unquestionable increasing research interest on finding alternatives to traditional chemical control methods. In fact, it is well recognized the high importance of obtaining a human health innocuous and environmentally-friendly potato anti-sprouting compound to take Chlorpropham's (CIPC) place. In many countries, this carbamate is not currently being used due to both legislative and marketing reasons. However, potato sprouting is a common significant problem during winter storage of potato tubers, which needs to

prevented. Potato is the fourth most important food crop in the world, mainly due to its starch content, high quality protein, substantial amount of essential vitamins, minerals, and very low fat content.

In this work, the potential potato sprouting inhibition effect on two systems, S-carvone and the inclusion compound *n@NO-sprout*[®] was studied and, simultaneously, compared with the traditionally used CIPC. S-(+)-carvone, a monoterpene compound, which is the main compound if the essential oil of caraway (*Carum carvi* L.) is extracted using hydrodistillation and the supercritical method. The inclusion compound, *n@NO-sprout*[®], based on β -cyclodextrin and S-carvone (yield *ca.* 95% (w/v)) was synthesised through the precipitation method. Firstly, small-scale bioassays were carried out using 70 potato tubers/treatment. Secondly, bioassays were carried out on a large scale in semi-practical conditions at a chips industry. The obtained results showed the significant sprout inhibition effect of *n@NO-sprout*[®] on potato tubers. Finally, to access possible detectable flavour differences between industrial chips obtained from potato tubers which were previously submitted to the different treatments and industrial chips obtained from potato tubers which were not submitted to any treatment, sensory discriminative analysis, triangular tests, were performed. Through statistical analysis, significant differences ($p < 0.05$) were only found for the CIPC treatment.

To sum up the findings a new promising sprout inhibitor agent for potato tuber storage, the β -cyclodextrin/S-carvone inclusion compound registered as *n@NO-sprout*[®] was found as an alternative to CIPC.

Chapter 18 - Urea has the interesting property of forming solid inclusion compounds. An inclusion compound is a unique form of chemical complex formed by the inclusion of one kind of molecules into cavities of a crystalline framework composed of molecules of another kind. Unlike the case of traditional chemical compounds, chemical reactivity does not determine whether inclusion occurs.

Urea – widely used as an adductor for diverse range of linear organic compounds- can also be utilized for adduction of cyclic/ branched drug molecules having sufficient anchor length in the presence of suitable RAE, through a modified technique. Resulting co-inclusion compounds of drug in urea offer wide range of applications of diverse nature, which are exemplified, but not limited by, steep improvement in dissolution profile of poorly soluble drugs; improved content uniformity especially important for potent drugs; protection from moisture, light, atmospheric oxygen leading to improved stability and shelf life; conversion of liquid medicaments into solids and improvement in safe handling characteristics. Thus, urea inclusion compounds are gradually emerging as simple and viable substitute for solid dispersions for the improvement in dissolution profile of poorly soluble drugs and as substitute for microcapsules for stabilization of air/moisture/photo sensitive drugs. However, further studies are needed to exploit the full potential of urea as an adductor, which can be a promising alternative also to cyclodextrins for improvement of pharmaceutical characteristics. There are exciting prospects for the continued studies on urea co-inclusion compounds to unravel their potential applications.

Chapter 1

**TETRAAZACYCLOTETRADECANE SPECIES AS
MODELS OF THE POLYAZACROWN MACROCYCLES:
MOLECULAR STRUCTURE AND REORGANIZATIONS
IN AQUEOUS MEDIA (pH 0-14) AS PROBED BY NMR
SPECTROSCOPY AND COMPUTATIONAL METHODS -
PROBLEMS AND SOLUTIONS**

*Ryszard B. Nazarski**

Laboratory of Molecular Spectroscopy, Faculty of Chemistry, University of Łódź,
Tamka 12, 91-403 Łódź, Poland.

ABSTRACT

Three aliphatic molecules {*cyclam* (**1**, 1,4,8,11-tetraazacyclotetradecane), its 1,4,7,11-isomer *isocyclam* (**2**), and a single pendant arm derivative of **1** [*scorpiand*, **3**, 1-(2-aminoethyl)-*cyclam*]} and their subsequently formed protonated congeners are considered as representatives of the macrocyclic polyamines (azacrowns) and related polyammonium salts. Important methodological aspects of structural investigations on these highly mobile aza-substituted macrorings are taken into account, especially concerning aqueous solutions over a whole pH range. Various issues about ascertaining donating sites and sequences of the protonation, dynamics and conformational preferences of such multidentate polyamino ligands as potential chelators (complexones) are considered. The scopes and limitations of different title tools and approaches applied in the field of azacrown macrocycles are discussed in detail. However, the extensively studied design and structures of their chelate complexes with metal cations are out of the scope of this overview, in principle.

Some important problems usually occurring in multinuclear resonance spectroscopy experiments performed for azacrowns as polyprotic bases in water solutions are considered. In particular, various issues involved with proper use of the NMR pH-

* Corresponding author: E-mail: nazarski@uni.lodz.pl.

titration technique supported by potentiometric results (instrumentation, software, acidic and alkaline errors in the pH measurements, an influence of the ionic strength, deuterium isotope effects, chemical-shift references for aqueous media) and resonance signal assignments [by using the amino protonation-induced shifts in δ_{Xs} (where X = ^1H and, especially, ^{13}C), empirical 'shielding constants' or 'amine shift parameters', resemblance of pH titration profiles, and line broadening effects] are discussed in detail.

Different theoretical (computational) treatments suitable for reliable molecular modeling of the most probable, usually time-averaged and multicomponent, overall conformations of the polyaza macrocycles (as free amines or related polyammonium cations) and for subsequent empirically corrected (linearly scaled) GIAO-based predictions of NMR chemical shifts of these macrocyclic species assessed at different HF or DFT (B3LYP) quantum-chemical levels, are also considered. Selected results on the intramolecularly H-bonded and non-H-bonded conformers of the macrocycles **1-3** are presented. The strengths and weaknesses of empirical force-fields methods (MMX vs. OPLS-AA and DREIDING) and simulations of the surrounding medium (mainly of solvent water molecules) with use of PCM and/or ONIOM techniques are enclosed, as well.

Beside the selected our own known results on the guiding polyamines **1-3**, some related (not published, corrected or accessible with some difficulty) experimental findings as well as theoretical predictions from this laboratory are also presented. In addition, the work is supplemented with several relevant literature data and reports on another structurally similar hetero-macrocycles. Moreover, some other selected recent results, new ideas and research directions in this topic are briefly discussed.

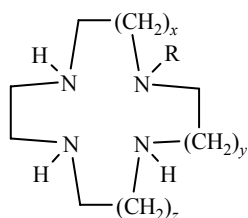
Keywords: Macrocycles, polydentate ligands, macrocyclic receptors, polyamines, azacrown ethers, polyazacycloalkanes, cyclam, isocyclam, scorpiand, aqueous solutions, glass-electrode potentiometry, pH-titration, protonation, NMR titrations, NMR reference standards, MMX / OPLS-AA force fields, DFT calculations, intramolecular hydrogen bond, conformations.

1. INTRODUCTION - AZACROWNS AS MULTIPURPOSE LIGANDS OR RECEPTORS (STRUCTURAL ASPECTS)

Crown ether chemistry was begun in 1967 with an accidental discovery by Pedersen [1] for one member of the macrocyclic polyethers and clear recognizing their potential as complexing agents. During these and later works, Pedersen gave these macrocycles, containing oxygen atoms (O-atoms) suitably positioned in the internal cavity to permit selective complexing with many metal cations or even some organic molecules, their trivial 'crown' nomenclature. The stability of such complexes depends primarily upon how well the cation fits as a guest into the polyether macrocycle (host). Other factors are the charge density of the cation and (in solution) the solvating power of the medium [2]. This kind of species can *inter alia* assist the transport of inorganic cations into organic media from the solid phase or aqueous solution, by the formation of chelate complexes soluble in organic solvents (phase-transfer catalysis). In the organic medium, which may be a relatively non-polar or polar aprotic solvent, the ionic compound is dissociated into a cation tightly chelated with the crown ether and a 'naked' anion. The cation is shielded from close interactions with an anion because of the surrounding crown system (intramolecular encapsulation). But, the anion is

also transported into the solvent to maintain electroneutrality. As a result, it is unsolvated ('naked') and at a relatively high energy and, so, highly reactive [3].

The availability of crown ethers possessing various sizes of an intramolecular cavity permits highly selective chelation of cations of matching size, including all the alkali metal ions. Numerous applications of such type chelating agents were repeatedly reviewed [4]. However, macrocycles containing ring heteroatoms apart from oxygen are also of large value or even irreplaceable in some particular applications. Indeed, a large variety of such homologous and mixed, *e.g.*, oxaza, oxathia, thiaaza, thiaphospha, azaphospha [5], *etc.*, hetera-macrocycles showing various crown-ether like chelating properties is well known. However, the aza-substituted crown ethers (*i.e.*, azacrown ethers or, shorter, azacrowns) are most important among all of such homogeneous crown-type multidentate ligands with non-oxygen heteroatoms in the macroring [6].



- 1 $x = 2, y = 1, z = 2, R = H$ (cyclam)
- 2 $x = 2, y = 2, z = 1, R = H$ (isocyclam)
- 3 $x = 2, y = 1, z = 2, R = CH_2CH_2NH_2$ (scorpiand)
- 4 $x = 1, y = 1, z = 1, R = H$ (cyclen)

In the reality, this was recognized quickly enough that the substitution of some O-atoms as donating sites in the polyoxa macrocycles by nitrogens results in tremendous changes in their molecular properties in relation to those concerning ordinary crown ethers. Strictly, the azacrowns were known earlier. For example, the first tentative structure of the 1,4,8,11-tetraazacyclotetradecane (**1**, named *cyclam* [7]) as an internally hydrogen-bonded (H-bonded) free-base cyclic ligand (Figure 1a) and five idealized intramolecular cavities in its octahedral complexes with metal cations was proposed by Bosnich *et al.* [7] already in 1965, *i.e.*, before spectacular Pedersen's works, while the compound **1** itself was known since 1937 [8].

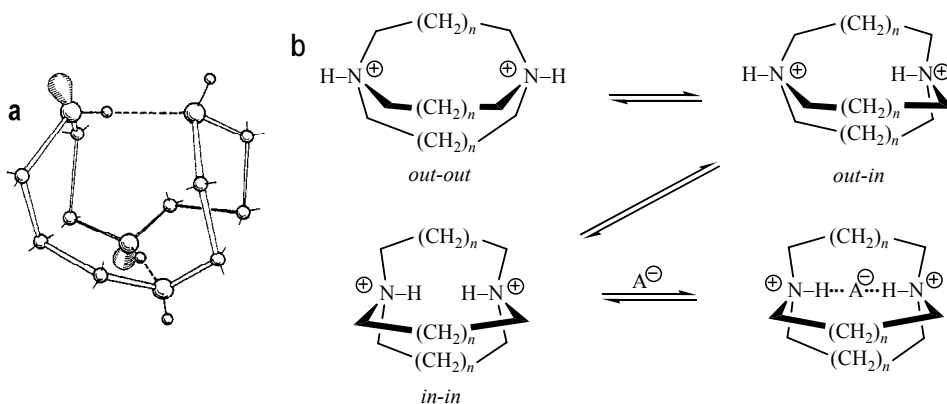


Figure 1. (a) The first proposed 3D picture of a possible compact structure of the dication $H_2\mathbf{1}^{2+}$ with two internal H-bonds. Reproduced with kind permission, from Bosnich *et al.* [7]. Copyright © 1965, American Chemical Society. (b) Schematic representation [9] of the encapsulation of a single spherical halide (Cl, Br, I) anion A^- within a diprotonated *katapinand* ($6 \leq n \leq 8$).

However the inherent possibilities of water-soluble macrocyclic polybasic ligands of this type, especially their chelating properties, were not diagnosed through a long time and, so, not appreciated. This fundamentally changed with the discovery of crown ethers. Indeed, the first macrobicyclic diammonium cages for anions, coordinating to the spherical halide ions *via* electrostatic interactions and H-bonds together (Figure 1b), were ^1H NMR investigated at 220 MHz and reported in 1968 by Park and Simmons [9] – only one year after crown ethers appeared in the literature. Their results in solution were fully confirmed throughout the solid-state study [10]. After years, the hexaprotonated *in-in* form of a triply bridged anion receptor of a similar oxaaza type (*cryptand*) was found by Lehn and his group as being responsible for the encapsulation of a single nitrate anion inside its intramolecular tridimensional (3D) cavity, *i.e.*, crypt, of the formed inclusion complex termed, for this reason, *cryptate* [11]. On the whole, ammonium groups along macrocyclic or polymacrocyclic systems preferentially adopt the *out* configurations. This effect that has already been realized by Park and Simmons who showed that diprotonated bicyclic diaza hosts favor the *out-out* conformation, while the less favorable *in-in* conformation is optimal for anion recognition [9].

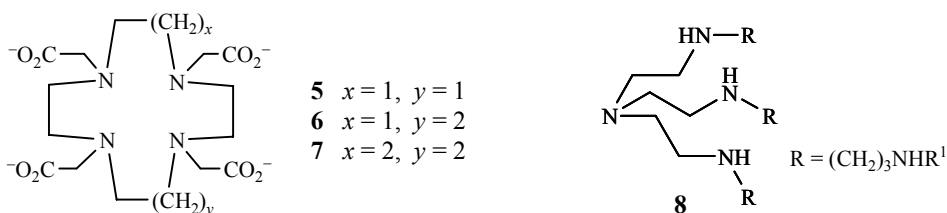
As a matter of fact, the simple preparation of macromonocyclic polyamines and related amino-ethers has long been sought. The introduction of non-template Richman-Atkins cyclization [12] opened, however, a general route for easy synthesis of such macrocycles and their mono-*N*-substituted derivatives [13]. An original procedure of this method has been modified during the last years and new conditions for this cyclization reaction were reported recently [14]. Azacrowns show most interesting features among different multidentate macrocyclic systems used for the electron donor-acceptor (EDA) complexation in solutions. In addition, these systems create considerably stronger interactions with metallic and organic cations in comparison to structurally similar crown ethers. Therefore, selective chelation and extraction of numerous ions is possible. The variety of types such selectively recognized chemical entities is also considerably greater [6]. For some interesting remarks concerning many earlier related investigations, which predate Pedersen's first papers on crown ether chemistry and supramolecular chemistry, in general, see, *e.g.*, Ref. [15].

Indeed, cyclam (**1**) and its aliphatic and aromatic derivatives or analogues, such like polyamino systems **2** and **3** discussed here in details, form one of the most prominent groups of 14-membered-ring tetrahetera macrocyclic ligands, because of the high thermodynamic stability and kinetic inertness of their important transition-metal (lanthanides, in particular) ion chelates that has provided several fields of applications in new processes of organic synthesis, *e.g.*, asymmetric homogenous catalysis, or as simple chemical models for the study of certain biological reactions or systems (the mimicking of enzymes). One of the most interesting features of the cyclam-type ligands when compared to those based on the 1,4,7,10-tetraazacyclododecane (cyclen, **4**) backbone is their high selectivity towards certain metal ions [16]. According to results of Hancock and co-workers [17], the strength of cation binding is determined by the ion size, internal macrocyclic cavity (hole) size, and ligand conformation. In every case, the stability of such complexes results from the combination of various factors (conformational, thermodynamic and kinetic).

Very important is also an incorporation of the amide group(s) into macrocyclic polyamino rings, for the first time done by Tabushi *et al.* [18]. Indeed, a planarity of the $-\text{NHCO}-$ moiety in the macrocycle reduces the flexibility of its skeleton and defines the ring conformation, which can lead to novel coordination geometry around a central metal ion in

certain metal complexes. This inflexibility of the macrocyclic oxopolyamines is expected to be related to their unique selectivity. Indeed, their structure bears the dual features of macrocyclic polyamines and oligopeptides [19]. Moreover, such a structural change $\text{CH}_2 \rightarrow \text{CO}$ in the macrocycle also decreased the basicity of adjacent ring nitrogen donors and thereby changes their coordination properties [20].

Functionalization of the azamacrocycles can be achieved using either a carbon or a nitrogen atom of the ring as an attaching point. Generally, the modifications have been focused on *N*-substituted pendant-arm groups, while *C*-substituted researches are relatively rare [18b,19]. Various *N*-functionalized azamacrocycles containing one or several linear (open-chain) chelators can considerably enhance their selectivity towards certain ionic species [21]. Fabbrizzi and co-workers [22] coined the term ‘scorpiands’ for this class of macrocyclic molecules with the one *N*-pendant arm possessing donor atoms. Indeed, such a dangling aminoalkyl side arm somewhat represent the tail of the scorpion that folds to bind the metal ion encircled by the macrocycle.



According to Martell and co-workers [23], as the ring size of the homologous tetraazamacrocyclic ligands changes from 14 (cyclam, **1**) to 13 and 12-members (cyclen, **4**) the value of the first protonation constants ($\log K_1$) decreased. This would suggest that 1,3-propylenediamino moiety (bridge) has higher affinity for the proton than 1,2-ethylenediamino unit. However, the reverse relation was found [16a,c,24] for derivatives **5-7** [24] of the above polyamines, with four easily ionizable *N,N',N'',N'''*-pendant carboxymethyl ($-\text{CH}_2\text{CO}_2\text{H}$) groups capable of further coordination to the centrally placed metal ion.

A great importance of the pendant-armed cyclic ligands able to form neutral metal-ion chelates for biomedical applications and in the broad field of radiotherapy (as radioimmuno diagnostic agents or radiopharmaceuticals) and of medical use [as magnetic-resonance-imaging (MRI) contrast agents] is especially worth of mention [25]. Tetraazacyclododecane polycarboxylic acid complexones proved to be especially suitable multidentate chelating agents (chelators) in regard of the thermodynamic and kinetic stability of their Gd^{3+} chelates. In particular, the ligand **5** [DOTA or H_4dota (where $\text{dota}^{4-} = 1,4,7,10$ -tetracyclododecane-*N,N',N'',N'''*-tetraacetate)] became a popular metal-chelating agent due to its strong capability to encapsulate the highly toxic Gd^{3+} ion, while allowing the cation to keep one H_2O molecule in the inner coordination sphere. This H_2O molecule conveys the paramagnetic effects of the metal ion to the bulk water [26]. Such selectivity towards different ions has been pointed before [16], and even explored by using **5** for determination of Ca^{2+} in the presence of other alkaline-earth metal ions [16b]. However $\text{Gd}(\text{dota})^-$ is a charged chelate complex and, in this respect, seemed that neutral chelates formed with the 10-membered triaza triacetate macrocyclic ligands would be more favorable for clinical use.

Generally, the polyamines are water-soluble ambivalent multidentate receptors capable of interacting with cationic and anionic entities. Coordinative interactions with metal ions will occur when pH is high enough to allow for a sufficiently large number of available electron pairs. Binding interaction with anionic or polar species will be mainly driven by electrostatic interactions when the pH is low enough for having a sufficiently high number of protonated amino groups within the receptor. Additionally, if the polyamine has a high number of nitrogen donor atoms appropriately distributed in the molecule, intermediate situations in which such a receptor is able to interact with the metal ions and anions in separated compartments can also be envisaged, especially in the case of non-cyclic (open chain) tripodal polyamines **8**. All of these binding modes can be modulated by the length of hydrocarbon chains between the amino groups as well as by the attachment of aromatic functionalities. The large structural variability of the polyamines and an easy pH-regulation of their complexing properties allow for many applications such as a selective cation and anion chelation and detection [27].

In past 40 years, although the host-guest chemistry of a metal cation encapsulation has become well developed, the field of coordination chemistry of anions is still in its infancy. Indeed, the design and synthesis of artificial macromolecular receptors for anions are particularly challenging. The main reason is that anions have a lower charge-to-radius ratio so as to have less effective electrostatic binding interactions than do isoelectronic cations [28]. Several artificial oxaza macropolycyclic host molecules has been synthesized, which are able to bind different kind of guest substrates such as ammonium salts, neutral molecules or anionic guests inside their 3D cavities. Their properties to specifically recognize the other chemical entities are especially precious (ion-selective electrodes, specific sensors). As it was already mentioned above, the coordination of anions can be achieved using as receptors the polyprotonated forms of the aza or oxaza macrobicyclic hosts, which can interact with the negatively charged guests *via* the distance-dependent Coulomb attracting forces and spatially more specific H-bonds. In a consequence, the basicity properties of such anion receptors are strictly correlated with their binding features [29].

The azacrowns and their metal chelates have been extensively investigated for about four decades [6d,15a,30]. Among the important properties of these multidentate chelating agents, the large majority of microscopic ionization sequences, *i.e.*, protonation schemes, have not been thoroughly explained until now. However, the detailed knowledge of such processes at the molecular level is often essential for understanding the chemistry of these polyamino macrocycles.

An elucidation of the structure of subsequently formed variously protonated intermediate species of any azacrowns is very important for understanding different aspects of their pH-driven molecular reorganizations and associated chelating processes. Obviously, the greater rings make more serious exploratory problems, owing to usually larger conformational mobility of such macrocycles and, so, much greater number of their geometries accessible in space. Therefore, the title fully saturated tetraazacrowns became chosen for recognizing the chemical structures of related polyammonium ions, their conformational preferences and equilibria. Every one of these three azacrowns creates the somewhat other issues. Thus, 1,4,7,11-tetraazacyclotetradecane (**2**, named *isocyclam* [31]) is isomeric with the foregoing system of cyclam (**1**). Instead, the last system discussed in detail, *i.e.*, 1-(2-aminoethyl)-1,4,7,10-tetraazacyclododecane, {or shorter 1-(2-aminoethyl)-cyclam, also called *scorpiand* [22], **3**}, is considered as a good representative of various *N*-mono-functionalized pendant-

armed azamacrocycles containing additional donor atom(s) on the periphery of a central core of the molecule. This macrocycle is especially challenging, owing to a fully unsymmetrical nature of its backbone. Undoubtedly, a deeper knowledge about molecular properties of all these tetraaza macrorings **1-3** will permit to better understand the various molecular behaviors of another considerably more complicated azacrown-based ligands or receptors.

2. NMR SPECTROSCOPY OF TETRAAZACYCLOTETRADECANES AND STRUCTURALLY SIMILAR POLYAZA MACRORINGS

While it is possible to determine, through classic pH-potentiometric titrations, a large majority of the pK_a values for any n -protic macrocyclic ligands, L_s , it is not possible, on the simple basis of the glass-electrode potentiometric experiment, to assign unambiguously the correct pK_a value to each one of the n basic sites in these molecular systems. Indeed, the protonation constants (expressed usually just by pK_a values) being a measure of the ‘macroscopic’ basicity of such polybasic ligands, by themselves do not indicate the protonation sequence, which is necessary for the correct interpretation of the complexation reactions of L_s at the microscopic level.

However, this can be achieved, in principle, by NMR techniques, following the chemical shifts of the NMR-active nuclei in the system of as a function of pH or pD. In fact, for L_s , whose NMR spectra were fully resolved and assigned, the determination of the dependence(s) of their chemical shifts on pH has been extensively used in the literature to elucidate the protonation schemes. Such an analysis of various types of chemical-shift plots, as a function of pH, will be described below in details. The majority of NMR studies dealing with acid-base properties of n -protic polyaza macrocyclic systems makes use with the results previously determined by classical potentiometry. Moreover, the instrumentarium of the latter technique is always applied. Therefore, a brief discussion of his essential elements and of the applied methodology seemed necessary to consider here.

The potentiometric titrations [strictly speaking, adequate EMF (electromotive force) measurements] are typically performed with the assembly consisting of a digital pH meter, combined (glass / reference) electrode and automatic burette. Before titrations the electrode must be calibrated against, at least two, standard aqueous pH buffers. Freshly-titrated solutions of HCl or HNO₃ and NaOH, KOH or Me₄NOH [16a,c,21f,26,32] in bidistilled carbonate-free H₂O are usually applied as titrants. The water-thermostated titration vessel is maintained at 20°C or (usually) 25°C. Atmospheric CO₂ is excluded from the cell by passing highly purified N₂ or Ar across the top of an experimental solution. Alternatively, an organic layer, *e.g.*, of cyclohexane, covers this solution to exclude CO₂ [33]. Very frequently the titration procedure is automatically controlled by the software, allowing for long unattended experimental runs.

Minimum three measurements are commonly used for each pH-titrated polyamine. Sometimes these operations are made both in the salt formation and in dissociation direction (from alkaline to acidic pH and *vice versa*) to check the reversibility of reactions and repeatability of measurements. Obviously, any change of the solute (and titrant) concentration affects its ionization through a change of the ionic strength I of solution. Therefore, the constant value of I must be adjusted by an addition of adequate amounts of the supporting

electrolyte, for example KCl, KNO₃, NaX and Me₄NX (where X = NO₃, ClO₄, Cl) or Bu₄NNO₃. Occasionally, different ammonium nitrates as non-complexing background media were preferably chosen to maintain the ionic strength of solution, *e.g.*, for macrocycle **5** that forms the complexes with K⁺ ions [16a].

Finally, subsequent macroscopic protonation (dissociation) constants K_a of any ligand, H_{*n*}L, for the simple one-proton reactions (H_{*i-1*}L + H⁺ ⇌ H_{*i*}L⁺) can be obtained as follows:

$$K_a = [\text{H}_i\text{L}^+] / [\text{H}_{i-1}\text{L}][\text{H}^+] \quad (1)$$

where K_a [expressed normally as p K_a (or $-\log K_a$)] is calculated from potentiometric pH-titration EMF data. Such experimental data are usually handled with the aid of suitable non-linear least-squares curve-fitting programs, because the use of simple graphical methods leads, as a rule, to incorrect p K_a values [34]. Really, many powerful computer programs for the determination of these equilibrium constants from the EMF data and, so, for the study of a speciation in solution have been developed and reviewed [35], such like *e.g.*, MINIQUAD, TITFIT, SUPERQUAND or HYPERQUAND. With use of rigorous procedures for the first critical titration step of the analysis, experimental and simulated pH-titration curves were found as completely superimposable [16a]. Species distribution diagrams are finally plotted from the calculated acidity constants p K_a using the HYSS [36] or another similar program.

Generally, values of p K_a s for many polyaza macrocyclic ligands L have already been described in the literature. Some of the deviations (up to ~0.5 log units) between these data may be easily correlated with differences in used experimental parameters such as temperature T and ionic strength I . On the other hand, according to some authors [37], for several polyamine ligands L some (de)protonation processes can not be reliably followed potentiometrically since the corresponding reactions take place in strongly acidic {pH < 2 [37c] (or even < 3) [37b]} or basic {pH > 12 [21e,38] (or even > 11) [37b]} solutions. It is felt that such an opinion (maybe a little exaggerated; see Ref. 37b, in particular) can result in part from the pure instrumental problems (*vide infra*) as well as difficulties with a confident interpretation of the EMF data at both extremes of the pH scale, *i.e.*, the need of use of special computer programs. Therefore, NMR pH-titrations based on the protonation-induced changes in chemical shifts of nuclei present in the molecules of interest, are usually applied in all these cases; for low p K_a values (between 0 and 2) accurately determined by the ¹H NMR titration, see Ref. 39.

Almost all pH glass electrodes have sufficient properties for working in the most popular pH range, from ~1 till ~12 pH units. But, certain problems appear with EMF measurements in the strongly acidic and strongly alkaline solutions. There are different types pH glass electrodes, some of them have improved characteristics for working in such acidic or *vice versa* alkaline aggressive medium. Indeed, because of the ion-exchange nature of a glass membrane, it is possible for some other ions to concurrently interact with ion-exchange centers of the glass and to distort a linear dependence of the measured electrode potential on the pH function.

Accordingly, *at low values of pH*, the influence of anions of corresponding acid solution can be detected and the systematic *acidic error* occurs as a consequence. This error typically starts below pH 1 and increases as the pH of the solution decreases, especially at pH < 0 and in solutions of high electrolyte content. It may be as high as 0.5 pH unit. Most glass pH

electrodes exhibit a lower than actual pH value in concentrated acids [40]. Instead, *at high values of pH*, the contributions of interfering alkaline ions (like Li^+ , Na^+ and K^+) are comparable with that of hydrogen ions [H^+ ; strictly say, hydronium ions H_3O^+ (or, rather, a lot more hydrated)]. In this situation, dependence of the potential on pH becomes non-linear (*alkaline error*). The electrode responds to such ions as though they were H^+ ions, giving a pH reading that is consistently too low. Depending on the pH-glass formulation, this can occur as low as pH 10 (normally above pH 12). The error may be as little as 0.05 pH and up to 0.5 pH unit within specified pH electrode measuring range. Thus, this error is of decisive meaning for all pH-titrations of strongly basic polyamine macrocycles (*vide infra*). Therefore, where accurate high pH readings are required, the upper pH limit of the electrode should be always checked and specially scaled. From the nomographs frequently furnished by the manufacturers [37a], being only a rough guide to the behavior of any individual electrode, it appeared initially that this error is slightly greater in heavy water (D_2O) than in light water (H_2O), however its current theoretical prediction is rather reverse [41]. Generally, the special high-pH electrode should be used if necessary. Compared to sodium, lithium ions will produce a larger error, while the effect of K^+ ions is negligible. Because ions Na^+ are much more common, the effect is often called the *sodium (ion) error* [40a,41].

Some important issues involved with all of the aforementioned fields will be discussed below more in detail, especially in context of NMR measurements.

2.1. NMR Measurements for Polyamines in Aqueous Solutions (General Remarks)

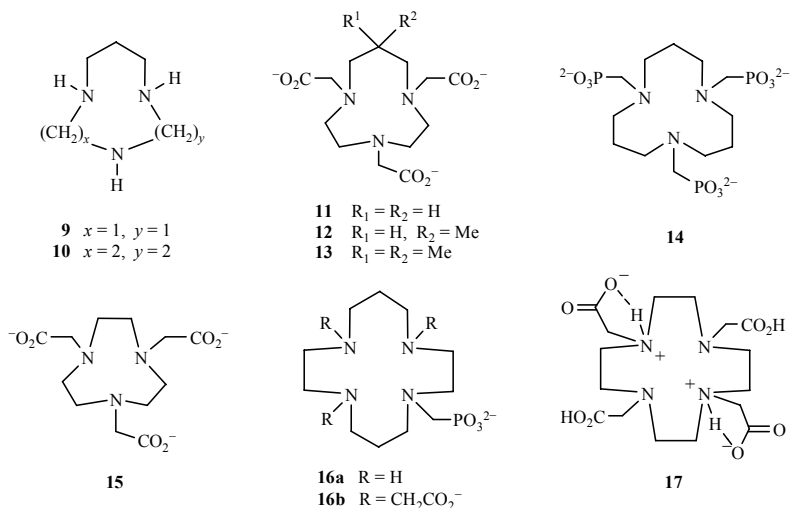
The classical (glass-electrode) potentiometric pH determination of the first protonation constants $\log K_1$ higher than ~ 12 is difficult, and in many cases, only approximate values can be obtained. The problem of the inadequacy of standard potentiometric methods in these cases was recognized probably for the first time by Riedo and Kaden [37a] in their study on two cyclic triamines **9** and **10**. Fortunately, very high values of $\log K_1$ s for this type of polyamino ligands **L** can be determined by NMR spectroscopy if some chemical shifts δ_{Xs} of their nuclei exhibit marked chemical shift changes upon deprotonation ($\Delta\delta_{\text{Xs}}$). Such a situation was *inter alia* reported for the three 10-membered triaza triacetate ligands **11-13** possessing one ring-N atom of an unusually high basicity [33]. Similar problems involved with an accurate determination of $\log K_1$ were also reported for systems **14** [32a], **15** [42], and two cyclam derivatives **16** [21e,f] with the ionized carboxylatemethyl (acetate) and/or phosphonatemethyl *N*-pendant arm(s), respectively. We recognized the case of ligands **11-13** [33] as very interesting and instructive. Therefore, it will be presented in more detail below.

The deprotonation of *N*-monoprotonated forms HL^{-2} of the ligands **11-13** did not occur below pH 12.8 and signals of their non-exchangeable protons shift upfield (lower frequency) with increasing concentration of KOH. Thus, ^1H NMR pH-titration curves, $\delta_i = f(\text{pH})$, for different protons *i* in these complexones were determined at different KOH concentrations between 0.01 and 1.0 mol L^{-1} , with the ionic strength held constant at 1 mol L^{-1} by addition of KCl [33]. The chemical shifts characteristic ($\delta_{i,\text{HL}}$) of their *N*-monoprotonated species HL^{-2} were obtained from the ^1H NMR data measured between pH 8 and 12, where the δ_{HS} were found constant. Analogous characteristic of the non-protonated species L^{-3} ($\delta_{i,\text{L}}$) could not be

obtained experimentally because their deprotonation is not full at 1.0 mol L^{-1} KOH concentration. Since the analyzed proton exchange was fast, the time-averaged chemical shifts (δ_i^{exp}) observed for these simple two-component systems may be expressed as the weighted sum of chemical shifts of HL^{-2} and L^{-3}

$$\delta_i^{\text{exp}} = x_{\text{HL}} \delta_{i,\text{HL}} + x_{\text{L}} \delta_{i,\text{L}} \quad (2)$$

where $x_{\text{HL}} = [\text{HL}^{-2}] / [\text{L}]_{\text{tot}}$ and $x_{\text{L}} = [\text{L}^{-3}] / [\text{L}]_{\text{tot}}$, *i.e.*, the pH dependent mole fractions of equilibrium species HL^{-2} and L^{-3} . Given that $x_{\text{HL}} + x_{\text{L}}$ must equal 1 over this pH interval, $\log K_1$ was estimated by assuming various values for δ_{L} and computer fitting the curves to Eq. (2). For each curve, the sum of the squares of residuals reached a minimum value, as δ_{L} was incremented through its true value. The value of δ_{L} at that minimum was accepted as a true value, and in each instance this value of δ_{L} agreed reasonably well with that predicted on the basis of ‘shielding constants’ C_{NS} (*vide infra*) proposed for other similar-type ligands [33]. It should be noted, that the value of $\log K_1$ of 14.8 ± 0.2 determined in this way for **11** was substantially higher than its value of 13.5 obtained from NMR data taken in the presence of NaCl [43].

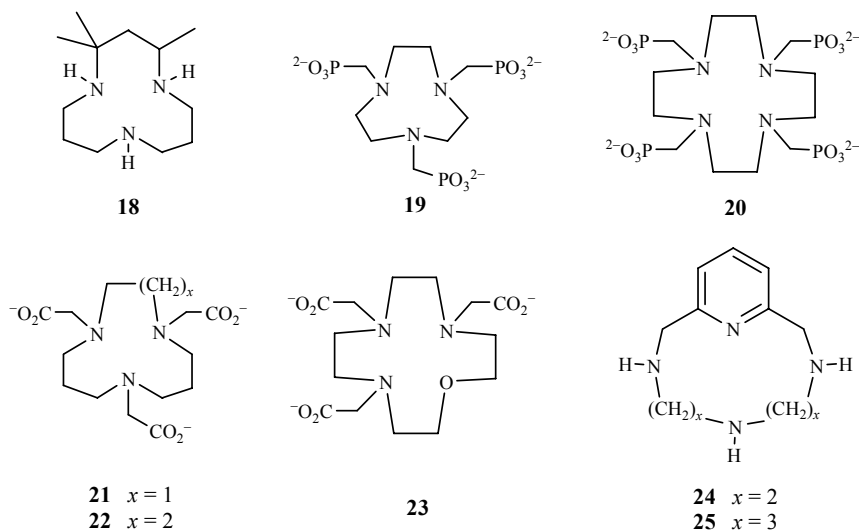


Comparable problems occur with a correct analysis of NMR data for strongly acidic solutions, but resulting, in turn, from not fully protonated species H_nL^{n+} [42,44]. Such a situation was reported *e.g.*, for ligands **5** and **7**, for which even two N-atoms belonging to their internal cavities are essentially unprotonated in very strongly acidic media (pH 0.1–0.4). According to these data, the neutral form H_4L of **5** having the structure **17** with two carboxy ($-\text{CO}_2\text{H}$) and two coordinated carboxylate ($-\text{CO}_2^-$) groups was proposed [44].

The experimental data necessary for unambiguous assigning NMR signals of differently protonated forms H_nL^{n+} ($n = 1, 2, 3, \dots$) of any macrocyclic polyamino ligand **L** in aqueous solution and, so, to establish their protonation mechanism are usually attained in X NMR pH-titrations, *i.e.*, through carrying out rather long series of standard 1D X NMR spectra [where $X = {}^1\text{H}, {}^{13}\text{C}$ (or other NMR active nuclei present in the molecule, *e.g.*, ${}^{31}\text{P}$)] recorded at different pH values. A fully automated NMR pH-titration set-up was also reported [35b]. In a

usual procedure, solutions of **L** in D₂O are applied and their pD values adjusted to the desired pD by dotting with relatively concentrated DCl or DNO₃ (and CO₂-free KOD, NaOD, Me₄NOH or CsOD [32b,45]) to minimize dilution. Potassium hydroxide is strongly preferred as a titrant over sodium hydroxide. Except the sodium ion error in the pH determination, other issues were also signalized.

Indeed, Bhula and Weatherburn [46] reported that in the ¹³C NMR pH-titrations some additional lines appeared above pH 13 in the spectra of aqueous solutions of tri-*C*-methylated triazamacrocycle **18** where NaOH was used to control the pH. Because these extra lines were absent when Me₄NOH was applied, the authors suggested that, under such conditions, the triamine **18** forms a sodium complex which gives rise to the additional signals. Also Gerald *et al.* [32a] found different ¹H and ³¹P NMR titration curves above pH ~10 for polyazacyclic phosphonate ligands **14**, **19** and **20**, in the presence and absence of Na⁺ ions, by using NaOD or Me₄NOH. Simultaneously, markedly different values of the log *K*₁ (of 10.9 and 12.6) were determined potentiometrically for **20**, by applying NaCl and Me₄NCl as an ionic background, respectively.



Similar situation was found for the analogous triacetate ligands **15**, **21** and **22** with use of NaOD and KOD [43]. In the case of **15**, larger concentrations of Na⁺ were also recognized as directly responsible for the decrease of its potentiometric log *K*₁. For all these three ligands, the presence of Na⁺ ions also markedly affects their ¹H NMR spectra and titration curves for solutions of high pH values. According to the authors [43], this indicates that, at pH > 11, Na⁺ ions bind within the cavity of these chelators, and, by interacting with both the N and carboxylate O donor atoms, induce low frequency proton shifts similar to those observed for **14**, **19** and **20** [32a]. However, the use of KOD instead of NaOD in NMR pH-titrations was found as not sufficient, in some cases. Indeed, *N*-acetate oxaaza macrocyclic ligand **23** was titrated with CsOD since it forms complexes with K⁺ that are stable enough to cause broadening of its ¹H signals at high concentrations of added base [45]. As mentioned above, the formation of a complex with K⁺ by its tetraaza analogue **5** is a well-known fact [16a].

The pH of solutions is measured with an accuracy of ± 0.01 pH unit (frequently, both before and after recording the NMR spectrum) applying the equipment described above for

H₂O solutions. Then, the acid content of samples is determined with the pH meter fitted with previously calibrated combination electrode (*vide supra*). By using adequate microelectrode, the pH (= $-\log [H^+]$, strictly $-\log a_{H^+}$) can be measured directly in the standard 5-mm NMR tube. The direct pH-meter readings made in D₂O give the pD* (or pH^D) values, *i.e.*, so-called apparent (or ‘operational’) pD uncorrected for any deuterium isotope effect on the glass electrode (since the used pH meter was calibrated against respective pH buffers in H₂O) [32b], which usually are recalculated to actual pD values ($-\log [D^+]$ in D₂O) applying the equation [Eq. (3)]

$$pD = pD^* + \delta_{\text{glass}} \quad (3)$$

where the temperature dependent [41] empirical correction term δ_{glass} was found to be 0.40 [47] or 0.41 ± 0.03 at 25°C [41,48] or even 0.44 [49]. Therefore, this is customary to add the correction factor of 0.4 [32b,50].

Sometimes (for ¹³C NMR pH-titrations, in particular) the samples of polyamino ligands **L** are dissolved in water (H₂O) containing enough D₂O (5-10 vol.%) for internal deuterium locking the magnetic field **B**₀ onto the HDO resonance signal. In this case, the adequate pH adjustments are made with small amounts of HCl, HNO₃, NaOH, KOH or NMe₄OH solutions in H₂O, respectively. These pH-meter readings (strictly pD*s, *vide supra*) are most commonly not corrected for small (< 10, 15 or even 20%) [51] contributions of D₂O present, though the correction relation have been published for such mixtures [48]; for D₂O 20% content, $\delta_{\text{glass}} = 0.07$ pH unit.

All chemical shifts (δ_H and δ_C) in aqueous media are normally measured and reported relative to the signal of a used NMR reference substance ($\delta_X = 0$ ppm). However, there is no generally accepted reference compound for ¹³C NMR chemical shifts [52]. Typically, small amounts of water-soluble ‘zero-point’ sodium salts as, *e.g.*, DSS [sodium 3-(trimethylsilyl)-propanesulfonate, Me₃Si(CH₂)₃SO₃⁻Na⁺] (pH independent) [53] or TSP [sodium 3-(trimethylsilyl)-propionate, Me₃Si(CH₂)₂CO₂⁻Na⁺] (sensitive to pH) [53a,54], are applied in their non-deuterated or deuterated forms, which are either external or directly added to the samples. But, the disadvantageous interactions with the titrated polyamine are possible in the later case (internal referencing), which can deform the shape of obtained pH-titration profiles. Moreover the corrections, Eqs (4 and 5) [53,55], for the pH dependence should be always used for TSP applied as the δ_H or δ_C reference.

$$\delta_H^{\text{corr}} [\text{ppm}] = \delta_H^{\text{exp}} - 0.019 / [1 + 10^{(5.0 - \text{pH})}] \quad (4)$$

$$\delta_C^{\text{corr}} [\text{ppm}] = \delta_C^{\text{exp}} - 0.10 / [1 + 10^{(5.0 - \text{pH})}] \quad (5)$$

Also *tert*-butyl alcohol [21f,32a,34,42,56] and 1,4-dioxane are frequently served as internal references in water, the latter especially for acquiring ¹³C NMR spectra [52,53b,54b]. Unfortunately, there has been much confusion in the literature concerning the ¹³C chemical shift of dioxane relative to tetramethylsilane (TMS) used as an external reference in the contemporary spectrometers equipped with superconducting magnets, in which the NMR-tube axis is parallel to the magnetic field **B**₀. According to the reports from two different laboratory, this difference, $\Delta\delta_C$, was of 67.85 ± 0.01 ppm for typical aqueous media (10-20%

D₂O v/v, at 15-30°C) [57]. A little lower value was used for studies in 5% D₂O v/v (67.62 ppm) [58]. Still lower value of δ_C (67.4 ppm) is in common use for D₂O solutions [59], including numerous works in the field of polyamino macrocycles [21a,27,29,33,46,60]. Instead, Geraldès *et al.* [43] used its reference line at 67.0 ppm (pH ~1.0). In the reality, this $\Delta\delta_C$ amounts to 66.61 ppm for 10 % (w/w) solution in 99.8% D₂O at 25°C, according to our 50.29 MHz ¹³C NMR measurements with an external neat liquid TMS placed in a sealed cylindrical capillary [61]. Our result is in good agreement with the analogously found $\Delta\delta_C = 66.58$ ppm [54b] or values of 66.5 ppm [53b] or 66.53 ppm [59c], which were recommended for ¹³C chemical shift referencing in biomolecular NMR studies.

On the other hand, $\Delta\delta_C$ of 67.72 ± 0.01 ppm [62] or 67.8 ppm [63] (*vs.* external TMS) has been usually applied for internal dioxane in earlier NMR investigations performed in D₂O solutions with use of conventional electromagnets (axis $\perp \mathbf{B}_0$). At this point, it is perhaps worth emphasizing that a direct comparison of δ_C s obtained from spectra externally referred to the same substance but recorded on NMR instruments equipped with magnets of both generations (*i.e.*, with the NMR-tube axis \parallel and $\perp \mathbf{B}_0$) leads to erroneous results, unless an adequate correction for the effect of variable diamagnetic susceptibility (χ) of the samples is applied [64]. Moreover, an application of two dissimilar reference substances, *e.g.*, an internal TSP and external dioxane [65], additionally complicates comparing the experimental NMR data from different research groups.

Alternatively, the separate coaxially inserted capillary glass tube filled with neat TMS [51,62e,66] {or any suitable liquid secondary NMR reference substance, *e.g.*, dioxane (as a neat liquid or in D₂O [59a]) or *t*-butyl alcohol [67]} can be used in the standard 5-mm NMR sample tube to provide an external reference signal (inner capillary method). Obviously, all of the disadvantageous ‘polyamine–NMR reference’ interactions are excluded in this case. But, the chemical shifts so evaluated should be, in turn, corrected for bulk magnetic susceptibility effects if these NMR data are to be meaningfully compared with those of other workers applying the diverse reference substances. Unfortunately, such a correction for the difference in χ values of two used dissimilar liquids, *e.g.*, heavy water–TMS, is commonly done only sporadically (*vide infra*).

In the simplest case of an one-proton region ($\text{H}_{i-1}\mathbf{L} + \text{H}^+ \rightleftharpoons \text{H}_i\mathbf{L}^+$) in the ¹H NMR pH-titration curve of any species $\text{H}_n\mathbf{L}^{n+}$ formed from the polybasic ligand \mathbf{L} , the acidity constant pK_a of a titratable site can be very easily evaluated using Eq. (8) derived [39,63b,68] from the Henderson-Hasselbach chemical-exchange equation [Eq. (6)]

$$pK_a = \text{pH} + \log ([\text{H}_i\mathbf{L}^+] / [\text{H}_{i-1}\mathbf{L}]) \quad (6)$$

$$pK_a = \text{pH} + \log ([\delta_{\text{H}_{i-1}\mathbf{L}} - \delta^{\text{exp}}] / [\delta^{\text{exp}} - \delta_{\text{H}_i\mathbf{L}^+}]) \quad (7)$$

$$\delta^{\text{exp}} = [\delta_{\text{H}_i\mathbf{L}^+} + \delta_{\text{H}_{i-1}\mathbf{L}} \cdot 10^{(\text{pH} - pK_a)}] / [1 + 10^{(\text{pH} - pK_a)}] \quad (8)$$

where δ^{exp} is the chemical shift experimentally observed at any measured pH value, $\delta_{\text{H}_i\mathbf{L}^+}$ and $\delta_{\text{H}_{i-1}\mathbf{L}}$ is, respectively, the chemical shift of the protonated form $\text{H}_i\mathbf{L}^+$ and the deprotonated form $\text{H}_{i-1}\mathbf{L}$. As easily to notice, a point of the curve inflection corresponding to the situation that both these forms are in an equal concentration occurs at $\delta = (\delta_{\text{H}_i\mathbf{L}^+} + \delta_{\text{H}_{i-1}\mathbf{L}}) / 2$; at the same time, $\text{pH} = pK_a$. Thus, each signal of the NMR spectrum can be associated with the pK_a

taken as a midpoint of the typical one-proton *S*-shape titration curve. However, this will be the case only if stepwise (de)protonations do not overlap. Indeed, $pK_{a,s}$ calculated by curve fitting to Eq. (8) could be in error when successive $pK_{a,s}$ differ by less than 3 pK_a units [69]. So, the use of NMR spectroscopy to determine $pK_{a,s}$ of the individual amino groups is rather scarce for the polyamines. Nevertheless, such ^1H NMR pH-titrations allowed successful determination of all three protonation constants for **24** and **25** in D_2O solutions [70]. The log $K_i(\text{D}_2\text{O})_s$, $i = 1-3$, obtained in this way were in good agreement with the equation, Eq. (9), correlating the acidity constants $pK_{a,s}$ evaluated for cyclic polyamines in H_2O and with those found in D_2O . Three other similar relationships concerning various chemical systems, Eqs. (10), are also frequently applied in the literature.

$$pK_a(\text{D}_2\text{O}) = 1.10 pK_a(\text{H}_2\text{O}) + 0.11 \quad (9) [32b]$$

$$pK_a(\text{D}_2\text{O}) \cong 1.015 pK_a(\text{H}_2\text{O}) + 0.45 \quad (10a) [71]$$

$$pK_a(\text{D}_2\text{O}) = pK_a(\text{H}_2\text{O}) + 0.63 (\pm 0.07) \quad (10b) [62f]$$

$$pK_a(\text{D}_2\text{O}) = 1.044 pK_a(\text{H}_2\text{O}) + 0.32 \quad (10c) [32b]$$

It is obvious that for any analyzed polybasic systems a single global value for each pK_a must exist which is common to all various individual pH-titration curves. Because a given NMR-active nucleus may not exhibit marked changes in chemical shift at all pK_a values, computing pK_a values using each titration curve individually can give inaccurate or biased $pK_{a,s}$ [62c]. The value of computer curve fitting is particularly obvious when there are strongly overlapping dissociations (ionisations) whose separate pK_a values cannot be obtained by simple inspection. Therefore, as above with classical potentiometric pH titrations, special programs (also commercial ones, *e.g.*, HYPNMR [72]) based on a non-linear least-squares fit of the chemical-shifts have been developed for determining these macroscopic equilibrium constants from NMR pH-titration data. On the other hand, it is obvious that an earlier knowledge of $pK_{a,s}$ strongly facilitates the assignment of NMR signals of any pH-titrated polybasic system.

Relatively high concentrated solutions of **Ls** are usually employed to obtain good ^{13}C NMR lines. Therefore, some displacements of inflection points on such obtained pH-curves are normally observed then in relation to pK_a values established by classical potentiometric measurements carried out, as a rule, for the more diluted solutions [56a,b,66]. All these displacements can be rationalized mainly in the light of a difference in the ionic strengths I of analyzed samples.

In general, the higher reliability of equilibrium data ($pK_{a,s}$) based on NMR measurements in the ranges $2 \geq \text{pH}$ and $\text{pH} \geq 12$ is widely recognized. Some of the issue outlined by us above in context of studies on the polybasic macrocycles, were also critically discussed by Popov *et al.* in the IUPAC guidelines for NMR measurements for determination of high and low pK_a values [50b]. These include *inter alia*: (i) the avoidance of measurement with glass electrode in highly acidic (basic) solutions, (ii) exclusion of D_2O as a solvent or even co-solvent, (iii) use of external reference and lock compounds, (iv) use of a medium of constant ionic strength, and (v) use of $\text{Me}_4\text{NCl}/\text{Me}_4\text{NOH}$ or KCl/KOH as a supporting electrolyte in basic solution.

2.2. Determining Protonation Mechanisms Through NMR pH-Titration Spectroscopy

The use of ^1H NMR spectra for the determination of protonation schemes is based upon measurement of the chemical shift values of non-labile protons as a function of pH. Indeed, such protons attached to carbon atoms adjacent to any functional group are sensitive to changes in the electronic environment caused by protonation, as it was shown by Grunwald *et al.* for the first time [73]. As a matter of fact, less or more successful attempts of determining the sites and sequences of the protonation for various macrocyclic polyamino ligands **L** in aqueous media, by using the NMR spectroscopy, are carried out for a long time. Also, different efforts of the parallel utilization to this end several of theoretical approaches are performed for some time past. For example, the formation and/or disruption of internal H-bonds in the macromonocyclic tetraaza ligands **1-3** and related polyammonium cations H_nL^{n+} (where **L** = **1-3**) has been also preliminary considered at the University of Łódź (Poland) on the basis of approximate gas-phase quantum-chemical calculational results [66]. However, the simulation for such discrete solute-solvent supermolecular assemblies in the aqueous phase is not a trivial task. Indeed, the species (solute) size and number of explicit solvent molecules (H_2O) were recognized to be of crucial importance [74]. Fortunately, a valuable information relevant to the structures of physically real associates of this kind is usually attainable experimentally, at least in part, by means of X NMR pH-titration spectroscopy, where X = ^1H , ^{13}C or the other NMR active nucleus, *e.g.*, ^{31}P [21f,32a,35b] or ^{15}N [75].

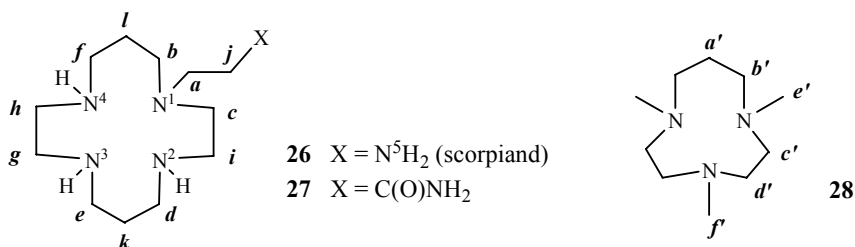
^1H NMR signals of free macrocyclic polyamino ligands **L** are commonly assigned on the basis of observed $^nJ_{\text{HH}}$ couplings, relative intensities and multiplicity (or signal patterns) of the resonances, homonuclear spin decouplings or empirically known relations between δ_{XS} and molecular structures. Also observations of the nuclear Overhauser effect (NOE) were carried out in some instances [76]. Obviously, various standard two-dimensional (2D) homo- and heteronuclear-correlated NMR experiments (including ^{13}C nuclei) are usually helpful, especially for asymmetric molecules. In general, the ^{13}C NMR data are more suitable for all structural considerations on such entities. However, only analysis of changes in pH-dependent chemical shifts $\Delta\delta_{\text{X}}$, where X = ^1H and especially ^{13}C , observed in the progress of gradual acidification of the solution of **L** (the first protonation step, at least), supplies a relevant structural information on the free polyamine in all cases of more complicated systems, such like *e.g.*, the macrocyclic pentaamine **3** [77].

As mentioned above, the data necessary for assigning the NMR signals of differently protonated forms of any macrocyclic polyamines **L** are usually attained in adequate NMR pH-titrations. Strictly say, the whole analysis is realized by elucidating the chemical structures of successively formed polyammonium cations H_nL^{n+} ($n = 1,2,3,\dots$). Under such conditions, all ^1H signals coming from the protons on ring nitrogens are not observable because of exchange broadening [55].

Some problems arise from the extensive crossing-over or coincidence of NMR signals, which occurs as the pH is altered. This leads to serious ambiguities in connecting the data points into the plots of chemical shifts against pH. Such an incorrectly recognized [54] crossover between the two ^1H NMR pH-titration curves for unsymmetrical linear triamine $\text{H}_2\text{N}(\text{CH}_2)_3\text{NH}(\text{CH}_2)_2\text{NH}_2$ was found *inter alia* by Hague and his co-workers [65a]. The ambiguities of this kind can be minimized by collecting data at closely spaced pH values, and,

especially, by fitting the data to the Henderson-Hasselbach equation (*vide supra*). In all such situations, the ^1H - ^1H and ^1H - ^{13}C correlation 2D (or others) NMR spectra are additionally recorded at selected pHs, easily available with modern NMR. In the second more conceptual step of the analysis of NMR pH-titration data, the amino protonation shift-based or other empirical approaches are customarily used.

Occasionally, some additional unconventional techniques had also to be employed, namely, the analysis of ‘signal-width effects’ (line broadening) and/or an application of the criterion based on the ‘similarity of NMR pH-titration profiles’ (*vide infra*). Indeed, these two supplementary methods were used with success in the case of a relatively complicated scorpianid system $\text{H}_n\mathbf{3}^{n+}$ ($n = 0, 1, 2, \dots$) [77] in which the N^2 atom is protonated first, then N^4 , N^5 , N^3 , and N^1 [66,78]; for the adopted atom labeling, see Formula **26**. Similar conclusion about an initial protonation was drawn for the close structurally amide tetraamine **27** studied in CDCl_3 solution [79]. In this case, observed upfield ^{13}C NMR shifts of C-atoms *c* and *k* are in agreement with a monoprotonation taking place preferentially on nitrogen N^2 or in dynamic exchange between N^2 and N^3 . A complexity of the problem is good represented by selected NMR pH-titration curves determined for the former pendant-arm macrocycle in aqueous medium as a function of added nitric acid (Figure 2). The publication *inter alia* about the attempt to rationalize an origin of some ‘wrong-way’ (*i.e.*, negative or reverse) amino-protonation shifts found for the pentaamine **26** (= **3**) appeared very recently [80,81].



On the whole, there are four main approaches, which were till now applied in the analysis of NMR pH-titration profiles of the polyamino macrocycles, *i.e.*, three classical: (i) amino protonation-induced changes in δ_{Xs} , where X = ^1H and, especially, ^{13}C (of general purpose), (ii) approach based on empirical ‘shielding constants’, (iii) method based on empirical ‘amine shift parameters’, and two unconventional: (iv) use of the resemblance of ^1H and ^{13}C NMR pH-titration profiles, and (v) consideration of the ^{13}C NMR line-broadening effects. All these approaches will be less or more in detail discussed below.

2.2.1. Amino protonation-induced changes in δ_{Xs}

The assignment of the pH-dependent chemical shifts (δ_{HS}) for the polyamino ligand **L** are normally aided by the observed magnitude of so-called ‘intrinsic pH titration shifts’, that is chemical-shifts changes ($\Delta\delta_{\text{HS}}$) protonation-induced during the titration of proximate basic groups by an addition of acid. Indeed, the carbon-bonded protons closest to the *N*-protonation site, *i.e.*, being in the α -position(s), generally have the largest decrease in shielding (the downfield NMR pH-titration shift) [55] and, concomitantly, the largest chemical-shift changes to the higher ppm values (frequencies) [25,56a]. These $\Delta\delta_{\text{H}}$ changes observed in the (de)protonation reactions are mainly due to through-bond electrostatic effects [25a]. The term

‘intrinsic titration shift’ was originally used for the pH-dependent variations of δ_{HS} that arise from interactions with an ionizable group mediated exclusively *via* covalent bonds [55]. However, translation of the measured $\Delta\delta_{\text{HS}}$ into molecular structures of various protonation states H_nL^{n+} is usually difficult because the observed changes in the δ_{HS} are concentration weighted averages of different isomers of the species H_nL^{n+} present at a particular pH.

On the contrary, for the analogous assignments of pH-dependent ^{13}C chemical shifts, δ_{CS} , an upfield (increase in shielding) ‘protonation shift’ for the carbon nuclei that are in α and β positions with respect to an *N*-protonation site in various amines and polyamines is generally accepted, the largest shift being observed for the β carbon (therefore usually called ‘ β shift’ or ‘ β effect’) [29,51,54,59b,60b,62a].

Really, some deviations from two aforementioned empirical guidelines were occasionally found in ^1H and (more seldom [25b,45,60a-c,62h,66,80]) ^{13}C NMR spectra of open-chain as well as macrocyclic polyamines. Such ‘abnormal’ titration $\Delta\delta_{\text{HS}}$ for the aminocarboxylate compounds, observed already in 1964 [56a], were explained [25a,55] as arising from the conformational-dependent through-space interactions, especially internal H-bonding between the $^+\text{N-H}$ (or N-H) protons and anionic carboxylate O-atoms. Analogous changes in $\Delta\delta_{\text{HS}}$, attributed to formation of the H-bonds shown in the Formula 17 [44] and/or associated conformational alterations were also reported for carboxylatealkyl-polysubstituted azacrowns [20,25a,32a,43,76]. In the absence of such or similarly ionized phosphonatealkyl *N*-groups, various intramolecular hydrogen bonds involving only ring N-atoms can exist, additionally complicated the macromolecular arrangement, owing to the disruption and subsequent formation of new H-bonds [21f,66]. Indeed, the protonation in any polyamino system is governed by electrostatic effects and its overall conformation is altered to accommodate the introduced positive charges and minimize the necessarily higher electrostatic repulsions at a short distance between such charges on the formed ammonium groups [46,70]. As a result, these *N*-sites are preferentially protonated in opposite positions of the macroring, to minimize such repulsions [21f]. Moreover, in certain azacrowns the discussed $\Delta\delta_{\text{H}}$ effects occur due to a simultaneous accommodation of the proton on a few nitrogens [43,45,60a,c,70,79] and/or the competition between some N-atoms, involving progressive deprotonation of the others [45].

2.2.2. Use of empirical ‘shielding constants’

Under conditions of any fast equilibrium, *e.g.*, proton exchange, among various protonated species H_nL^{n+} (where $n = 0, 1, 2, \dots$) the observed weighted average of the X NMR chemical shift, δ_{X} , of the *i*th nucleus X in these entities is given by

$$\delta_i^{\text{exp}} = \sum_n \delta_{i,n} x_{\text{H}_n\text{L}} \quad (11)$$

where $\delta_{i,n}$ are the intrinsic chemical shifts of involved H_nL^{n+} species and $x_{\text{H}_n\text{L}}$ ($= [\text{H}_n\text{L}] / [\text{L}]_{\text{tot}}$) is the mole fraction of each species. By using the protonation constants K_i obtained by potentiometry (*vide supra*), the $\delta_{i,n}$ values for all non-labile protons can be, in principle, calculated *via* a suitable multiple-linear-regression based program, which minimizes the sum of squares of the deviations between the observed and calculated δ_i^{exp} values [26,32]. However, the ^1H NMR pH-titration of **L** made in the medium being very similar to that applied in the potentiometric pH titration is the *sine qua non* condition of full success of such

an approach [56a,b]. This concerns especially the magnitude of the maintained ionic strength I of the solution and preferential use of the counter-ion (*e.g.*, K^+), which not bind significantly to the ligand L under analysis (*vide supra*). Then, the observed shifts δ_i^{exp} can be used to calculate the percentage protonations at the basic sites of L at each pH, by using an empirical procedure proposed by Sudmeier and Reilley [56a].

It is well known that changes in ^1H NMR chemical shifts, $\Delta\delta_{\text{H}}$, can indicate successive protonation sites of various basic sites existing in any polyamino ligand L , because the protonation of its nitrogen donor atoms generally results in a deshielding of nearby non-exchangeable protons (*vide supra*). On this basis, Sudmeier and Reilley [56a] have suggested that a chemical shift due to protonation can be given by relation:

$$\Delta\delta_i = \sum C_{ij}f_j \quad (12)$$

where $\Delta\delta_i$ is the change in chemical shifts of the i th nucleus caused by protonation ($i = \alpha, \beta$, or γ -position in regard to a titratable donor group), C_{ij} - the mean empirical protonation shift (or so-called substituent 'shielding constant') of the i th proton due to the protonation of the j th site [*i.e.*, either an amino nitrogen or oxygen of the anionic carboxylate group ($-\text{CO}_2^-$)], and f_j - the protonation population of the j th site (or an average fraction of time during which the j th site is protonated). Various methylenic constants C_j , *e.g.*, $C_{\text{N}} = 0.75$ ppm for the italicized methylene protons in $-\text{CH}_2\text{NR}_2$, $C_{\text{N}'} = 0.35$ ppm for $-\text{CH}_2\text{CH}_2\text{NR}_2$, and $C_{\text{O}} = 0.20$ ppm for $-\text{CH}_2\text{CO}_2^-$, were originally determined for a number of the open-chain polyamino polycarboxylic acids. Generally, Eq. (12) is based on the three assumptions that: (*i*) the contributions of protonating different sites to the δ_i of a relevant proton are perfectly additive, and (*ii*) linearly related to the fractions of time for which the sites are protonated, and (*iii*) contributing factors other than the deshielding effect of the protonation are unchanged by protonation. On the basis of Eq. (12), therefore, the distribution of proton(s) on protonated basic sites in the molecule of interest can be, in principle, calculated from δ_i^{exp} s determined at different stages of the ^1H NMR pH-titration.

This empirically established procedure has been successfully applied to many open-chain polyamines [56b,c] and macrocyclic N -pendant-armed polyamino ligands possessing the carboxylate or phosphonate groups ($-\text{CO}_2^- / -\text{PO}_3^{-2}$) [26,44]. However, certain modifications of this protocol were necessary in some cases. For example, somewhat different value of C_{N} was applied by Desreux *et al.* [44] for the macrocycles **5** and **7**. The other authors [32a,42,43,45,76] confirmed such results and concluded that the determination of the protonation sequences of different tetraaza, thiaaza or oxaaza polyfunctional macrocycles by the Sudmeier and Reilley's method is complicated by an abnormal conformational behavior of these cyclic systems, when compared with their acyclic analogues [76]. Such a difference results from changes in conformational equilibria of various groups caused by restricted flexibility, electrostatic repulsions and H-bond formation that are difficult to predict *a priori*. These restrictions seem to be even more severe in the cyclic triaza macrocycles than in the tetraaza analogues [42]. It was also found that the foregoing assumption (*iii*) does not fully hold for the structurally different macrocyclic oxopolyamines possessing pendant N -acetate functionalities [20].

2.2.3. Use of empirical ‘amine shift parameters’

Certain attempts of obtaining still better results for non-functionalized polyamines were undertaken by Hague and co-workers [62e]. They found that ^{13}C NMR chemical shifts of linear aliphatic polyamines, where the N-atoms are separated by two or three CH_2 groups, can be analyzed by using a two-term empirical relationship based on ‘amine shift parameters’ π and π^+ . Indeed, the observed $\delta_{\text{C}}\text{s}$ has been found as being sums of contributions associated with two nearest amino groups, $[(\pi_1 \text{ or } \pi_1^+) + (\pi_2 \text{ or } \pi_2^+)]$, whose magnitudes depend on the type (primary or secondary) and distance (α , β , or γ) along the chain from the C-atom in question; Eq. (13).

$$\delta_{\text{C}} = f_1 \pi_1^+ + (1 - f_1) \pi_1 + f_2 \pi_2^+ + (1 - f_2) \pi_2 \quad (13)$$

One series of parameters (π) has been determined for the unprotonated polyamines (with $f_i = 0$) and another (π^+) for their fully protonated forms (with $f_i = 1$). This relation was applied to determine the protonation sites in the charged forms of several linear aliphatic polyamines. Also the nature of their partially protonated intermediates formed during the pH-titration was successfully investigated [62h,65a]. However such an approach, especially designed for the polyamines, could not be used to predict ^{13}C NMR protonation shifts experimentally observed for the macrocyclic triamine **18** [46].

2.2.4. Similarity of pH-titration profiles (^1H and ^{13}C NMR spectra)

During the course of our NMR investigations [77] on the macrocyclic system $\text{H}_n\mathbf{3}^{n+}$ ($n = 0, 1, 2, \dots$) a full set of routine homo- and heteronuclear 2D NMR experiments (COSY, HMQC, and TOCSY) were made. However, some of their ^1H and ^{13}C signals were distinguished only based on the similarity between the profiles of relevant pH vs. chemical shift plots. For the convenience of discussion, a useful working labeling **a-l** of all nuclei in the CH_2 groups was originally applied, in which lines **a** and **l** were found as the most high- and low-frequency signals, respectively, in an initial ^{13}C NMR spectrum of **3** at pH 12.3 (native solution in H_2O) [81].

Thus, a large similarity between profiles (shapes) of titration curves, $\delta_{\text{H}} = f(\text{pH})$, observed at pH 10-11.5 for the proton pairs **e/g** and **f/h** of **3** (Figure 2a) allowed us for a tentative assumption that the remaining two not assigned CH_2 groups **g** and **h** are attached to atoms N^3 and N^4 , respectively. Previously, such a resemblance between pH-titration shapes had been applied for assigning of ^1H NMR signals of some polyaza macrocycles only sporadically, and without reasonable discussion [45,70,76]. We found also a close similarity of the ^1H NMR-pH titration profiles for pairs **b’e’** and (to some extent) **d’f’** reported for the tri-*N*-methylated triaza macrocycle **28** [43]. Its corresponding curve **c’** lies between curves **b’** and **d’**, as one could expect.

Such an empirically established method is based on the foundation that NMR pH-titration curves of nuclei in comparable chemical environments have comparable shapes. In order to confirm the validity both the foregoing **g/h** assignment and the concept mentioned above, the ROESY experiment was performed additionally at pH 10.75, which fully supported this **g/h** identification and the legality of the used method.

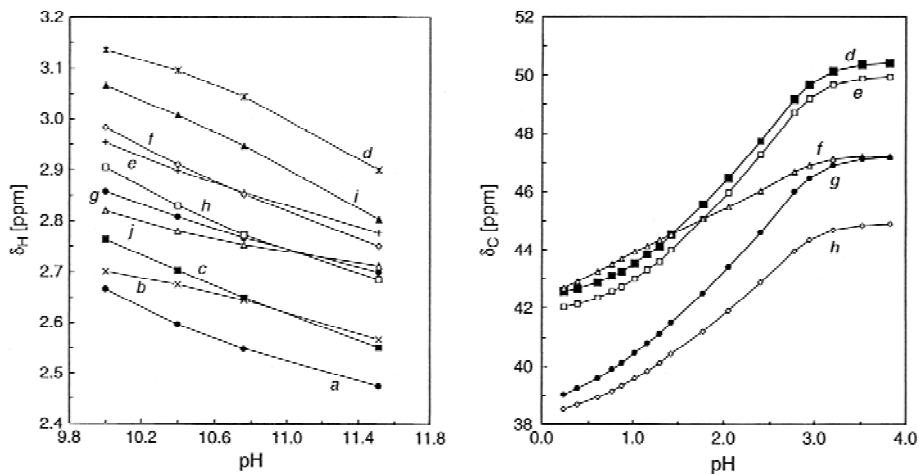


Figure 2. Plots of selected chemical shifts of **3** as a function of pH: a (left side) ^1H NMR profiles (alkaline region), b (right side) ^{13}C NMR profiles (acidic region). Reproduced with kind permission, from Nazarski [77]. Copyright © 2002 John Wiley & Sons, Ltd.

Likewise, Figure 2b shows that pH-titration curves coming from carbons **d** and **e** of the $\text{N}^2\text{CH}_2\text{CH}_2\text{CH}_2\text{N}^3$ unit of **3** are very similar in shape as the pH is lowered below 3.8. Thus, it was reasonable to expect, basing on the above-presented idea, that an analogous regularity would be also true for the adjacent $\text{N}^3\text{CH}_2\text{CH}_2\text{N}^4$ fragment. So, the profiles of pH-titration curves belonging to the carbon nuclei **f** and **g** should be similar, respectively, to shapes of such curves belonging to the relevant nuclei close in space. An assumption that the carbons **f** and **g** are responsible for the titration plot with the least and greatest slope, respectively, gives series of pairs with the slope increasing as follows $f < h < d \approx e < g$ for carbon pairs **f/h** (proximity of N^4), **h/g** ($\text{N}^3\text{CH}_2\text{CH}_2\text{N}^4$) and **g/e** (proximity of N^3) at pH 0.25-3.3, in full agreement with the profile similarity concept [77]. To the best of our knowledge, this was the first use of the resemblance of pH-titration profiles as a tool in recognizing the ^{13}C NMR lines of polyaza macrocycles.

2.2.5. ^{13}C NMR line-broadening effects

During our study on the macrocycle **3** some effects associated with the broadening of its ^{13}C lines were also applied. For example, lines **b** and **c** in the region of their close vicinity on a titration plot, pH range 3.5-6.6, and the crossed lines **h** and **i** (see Figure 3 in Ref. 66) were easily distinguished from each other by an essentially unchanging the full linewidth measured at half-height, $W_{1/2}$, of related resonance signals; always $b > c$ and $i > h$.

On the other hand, the foregoing identification of the **g/h** ^{13}C nuclei (based on the similarity of pH-titration profiles) was also fully consistent with a maximal broadening of their resonances (and also the signals **d**, **e** and **k**) at pH 2.05. Indeed, the $W_{1/2}$ of these lines increases in the order f (3.6 Hz) $< k < h < e \approx g \approx d$ (8.6 Hz) under such measurement conditions, in good agreement with an increase of their slope. The line broadening of these five latter ^{13}C NMR signals was very recently [80] explained as coming from a dynamic equilibrium mostly between the conformers of two co-existing polyammonium cations $\text{H}_n\mathbf{3}^{n+}$, $n = 3-4$ (*vide infra*) [82].

To the best of our knowledge, this was the first application of line-widths effects as an additional aid to recognizing the ^{13}C NMR lines of polyaza macrocycles. The pH-dependent line broadening of some ^1H -resonance signals, indicative of dynamic behavior, was only noticed for a few such polyamino systems [42,44]. Similar ^1H NMR observations made for the series of pendant-armed oxopolyamines were explained by the protonation accompanied by a slow proton exchange process [20].

2.3. pH-Driven Internal Dynamics in Azacrowns as Probed by the ^{13}C T_1 Rates [83]

An attempt was made in our studies to resolve some aspects of the molecular behavior of two intermediate ions $\text{H}_n\mathbf{3}^{n+}$ ($n = 1$ and 5) of scoriand (**3**) associated with the hypothetical participation of a single nitrate ion (NO_3^-) in the complex formed by the ammonium cation $\text{H}_5\mathbf{3}^{5+}$ in very acidic solution (*vide infra*). More precisely, it was paid attention on the need of recognition of internal dynamics in both these 12-carbon-ring macrocyclic species, especially in their pendant-arm fragments. Accordingly, two suitable 50.29 MHz ^{13}C NMR experiments were performed to obtain an insight into the dynamics of these macrocyclic ions [83].

Thus, ^{13}C spin-lattice (longitudinal) relaxation times (rates), T_{1s} , were measured under proton decoupling for two aqueous solutions of **3** at pH of 0.24 and 11.50, by using the fast inversion-recovery pulse sequence with 8-12 different relaxation delays. The T_1 values of all well-resolved ^{13}C -resonance lines are summarized in Table 1. They were calculated applying the fitting program implemented within standard software provided with a Varian Gemini BB 200 MHz (^1H) NMR spectrometer used in these experiments. Such relaxation data afforded the dynamic information about a segmental mobility of penta- and monoprotonated forms $\text{H}_5\mathbf{3}^{5+}$ and $\text{H}\mathbf{3}^+$, respectively, in acidic and basic solution in H_2O . All these numerical results can be directly compared, because only ^{13}C nuclei of the methylene groups occur in both analyzed ionic species.

As one can easily see, dynamics of the 14-membered-ring tetraaza-macrocyclic core in **3** is considerably smaller (T_{1s} are shorter) in strongly acidic medium. According to these relaxation data, the mobility of the pendant-arm CH_2 groups in two considered molecular fragments $^\alpha\text{CH}_2^\beta\text{CH}_2\text{NH}_3^+$ and $^\alpha\text{CH}_2^\beta\text{CH}_2\text{NH}_2$ increases with increasing distance from the ring center (T_{1s} becomes longer). In both cases, the ^{13}C relaxation times determined for α -carbons are equal to the greatest value found for related macrocyclic cores. On the contrary, T_{1s} determined for both β -carbons are identical (within error limits) and, simultaneously, they are the longest in both series of the relaxation data (~ 0.66 s).

Such a relative inflexibility of the macrocycle in acidic medium most likely results from efficient mutual Coulombic repulsions between the five positively charged ammonium sites ‘fixing’ the preferred ring conformers of the perprotonated species $\text{H}_5\mathbf{3}^{5+}$ in their maximally extended *out* forms (*vide infra*) and from intermolecular H-bond interactions between the cationic sites and surrounding solvate water molecules. On the other hand, a larger flexibility of the core of the monoprotonated amine (cation $\text{H}\mathbf{3}^+$) is in agreement with the time-averaged value of vicinal interproton couplings of ~ 5.3 Hz, which was crudely estimated for all its ring-proton multiplets found in the 500 MHz ^1H NMR spectrum measured at pH 11.50 [77]. In this case, H-bonding to the adjacent N-atom (or even being in dynamic H^+ -exchange

between the two N-atoms, $\text{NH}\cdots\text{H}^+\cdots\text{HN}$), as it was suggested in [79], is highly probable. As a result, internal fluctuations of CH_2 protons in the macrocyclic ring framework of $\text{H}_n\mathbf{3}^{n+}$ are always slower than that of CH_2 protons in the pendant 2-ammonio(amino)ethyl group. Similar situation was also observed for other pendant-armed macrocycles (the broadening of some ^1H NMR signals) [20].

Indeed, the main contribution to the spin-lattice relaxation of ^{13}C nuclei connected to protons is provided by the dipolar relaxation originating from protons in the same or in neighboring molecules, which move with the molecular motion. From this, it follows that the ^{13}C spin-lattice relaxation is linked to the mobility of the whole molecule or its molecular unit [84]. Undoubtedly, the measurements of ^{13}C T_1 s can carry an essential information on the mobility of different molecular fragments (segmental mobility) of much more complicated macrocycles. The results of such measurement performed at pH of 11.5 were practically used in an initial stage of our analysis of the scorpiand system (**3**) [66].

Table 1. Experimental ^{13}C longitudinal relaxation time, T_1 (s), for CH_2 group carbons in $\text{H}_5\mathbf{3}^{5+}$ and $\text{H}\mathbf{3}^+$ (for *ca.* 0.01 mol L $^{-1}$ solutions in $\text{H}_2\text{O}/\text{D}_2\text{O}$, ~90:10 vol. %) evaluated by exponential data analysis

Carbon No. ^a	$\text{H}_5\mathbf{3}^{5+}$ (pH 0.24)	$\text{H}\mathbf{3}^+$ (pH 11.50)
1	0.29	0.46
2	0.27	0.42
3	– ^b	0.45
4	0.38	0.42
5	0.29 ₅	0.49
6	0.32	0.40
7	0.30	0.41
8	– ^b	0.41
9	0.36	0.39
10	0.32	0.47
11	0.38 ₅	0.49
12	0.67	0.65

^a For the used atom-numbering scheme, see below (Figure 3).

^b Not determined owing to a practical overlap of the ^{13}C NMR lines due to C3 and C8.

2.4. Polyamine **3** in the Strongly Acidic Medium: a Rejection of the Working Proposal of an Active Participation of the Nitrate Anion [85]

In the foregoing study [80] concerning an origin of ‘wrong-way’ amino-protonation shifts very well observed at pH below 3 for the pH-profiles of atoms C11 and C12 of **3** (see Figure 3) [81] the close proximity of C11/C12 to the both adjacent ammonium centers in $\text{H}_5\mathbf{3}^{5+}$ was considered as one of the possibilities leading to these specific short-range NMR effects. It was noticed that, at least in principle, such an atom arrangement would make possible the electrostatic and/or H-bonding attractive interactions of two cationic sites at N^1 and N^5 with the surrounding NO_3^- anion persisting in the outer spheres of both C-atoms mentioned above. Indeed, some literature reports indicate for ion pairing of a simple ammonium dication $^+\text{H}_3\text{NCH}_2\text{CH}_2\text{NH}_3^+$ with NO_3^- or Cl^- in aqueous solution [86]. Therefore, supermolecular

interactions of the type $N^+-H\cdots O^--N$ with an active participation of the single nitrate ion seemed to be rational, at least as a coexistent occurrence.

The T_1 values evaluated for the ^{13}C sites in two cations H_3^+ and H_5^+ (Table 1) indicate a comparable mobility of their pendant-arm CH_2 groups and, so, suggest similar solute-solvent interactions of these ‘outer’ molecular units with a surrounding aqueous medium. On the other hand, the aminoalkyl dangling arm of the former species was previously found as its mobile fragment [77]. Indeed, an average coupling constant $^3J_{HH}$ of ~ 7.1 Hz was estimated for the side-chain protons of H_3^+ at pH 11.50, showing that they are typical of the so-called ‘free rotating’ ethane fragments. The equality of ^{13}C T_1 s found for β -carbons of both pendant-arms strongly suggest that analogous fast rotation also occurs around the $CH_2-CH_2NH_3^+$ bond in H_5^+ . Unfortunately, related vicinal J_{HH} couplings were not experimentally evaluated for the side-chain rotamers of this pentacation.

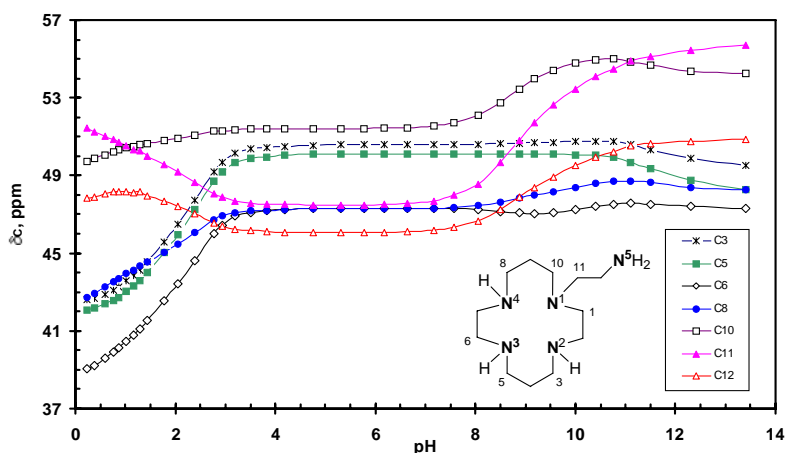


Figure 3. Selected 50.29 MHz $^{13}C\{^1H\}$ NMR pH-titration profiles of ca. 0.01 mol L^{-1} solution of the ligand **3** in H_2O/D_2O $\sim 90:10$ v/v solution at $\sim 21^\circ C$ (isotope effect for pH neglected, δ_C s originally [66] measured relative to an external liquid TMS corrected [77] by $+0.72$ ppm to account for the difference in diamagnetic susceptibilities of both liquids involved). The C12 atom curve vertically shifted by $+12$ ppm, for brevity of plot. Reproduced with kind permission, from Nazarski [80]. Copyright © 2009 John Wiley & Sons, Ltd.

As a matter of fact, the discussed unusual trends found in the ^{13}C NMR pH-profiles of **3** were reproduced quite well in the δ_C values computed for the multicomponent shapes of related ions $H_n\mathbf{3}^{n+}$ coexisting in acidic medium [80]. Related overall conformations were, in turn, elucidated by the best fitting of experimental δ_C data to those predicted by the GIAO DFT B3LYP/6-31G**/B3LYP/6-31G* method. In view of all these results, *i.e.*, reported here and already published, one can suppose that the hypothetically considered supermolecular interactions of the type $N^+-H\cdots O^--N$ not operate in reality. Without any doubt, such interactions would enforce some rigidity of the pendant-arm fragment of $H_5\mathbf{3}^{5+}$. However, the awaited slowdown of dynamics of its constituent C-atoms was not found experimentally.

3. COMPUTATIONAL METHODS FOR AZACROWN MACROCYCLES AND RELATED POLYPROTONATED SPECIES

It is well known, that correct assessing the overall (mean, time-averaged) conformations of various protonation states of the title and other structurally similar macrocyclic polyamines is extremely important in developing a comprehensive understanding the molecular properties (including also spectroscopic features) of such macrospecies throughout the whole pH range. Indeed, advanced molecular-modeling studies are necessary to determine the mean shapes of numerous species H_nL^{n+} ($n = 0, 1, \dots$) dynamically coexisting in solution, especially taking into account a great mobility of their macrocyclic cores. Really, the large structure averaging owing to very fast, on the NMR time scale, flexing between different forms of H_nL^{n+} was found for the typical 14-membered macrocycles **1-3** [66,75,80,87].

Adequately, the Monte Carlo (MC)-type GMMX subroutine of the PCMODEL program [88] was *inter alia* applied to initial search for minima on pertinent potential-energy surfaces (PESs) of various species of the scoriand system **3** [80]. Thus, a full randomization [89] over their main macrocyclic units and all rotatable bonds in the pendant side-chain fragments was performed. In this case, the default MMX [88] method was applied in the beginning, but with the passage of time an another force field (OPLS-AA) [90] was recognized as a much better molecular mechanics (MM) method for modeling the distinct conformers of the penta- and tetraprotonated forms $H_n\mathbf{3}^{n+}$, but not for related triprotonated species (*vide infra*). Each simulation was executed for up to approximately 150 000 MC steps. A relatively large molecular size of these polyammonium cations forced to make all these calculational efforts without explicit considering the solvent influences (a ‘free-molecule’ approach), but dielectric permittivity of 78.4 was always applied for a rough modeling the aqueous solution.

Such generated low-energy forms [typically 20-40 unique MM structures for every one ionic species $H_n\mathbf{3}^{n+}$ ($n = 3-5$), embracing the energy window of *ca.* 5.5 kJ mol⁻¹] were subjected next to the full *in vacuo* relaxation at the HF/3-21G level of theory. The resulting models were verified, initially with total electronic energies and then [after the additional geometry refinement in the HF/6-31G* and (finally) DFT B3LYP/6-31G* calculations] with magnetic shieldings, σ_{CS} , predicted for all lowest-energy structures pre-selected in this manner, by using a GIAO method [91] at the DFT B3LYP/6-31G* level. Adequate statistical evaluation of the agreement between theoretical σ_{CS} and experimental chemical shifts, δ_{CS} , was ultimately applied to draw relevant conclusions (*vide infra*).

A close examination of such *in vacuo* designed models of the three successive ions $H_n\mathbf{3}^{n+}$ with respect to their structural goodness for the NMR parameters (δ_{CS}) measured in aqueous solution was of crucial importance. Indeed, many initially good geometrical candidates were found in this way as reflecting the local gas-phase energy minima only. Moreover, it was gradually recognized that only the overall conformations, *i.e.*, families of several dynamically interconverting forms, are satisfactory representatives of the cationic species of interest (*vide infra*). According to our earlier results on the other flexible molecular systems [87,92], the ‘*solution* (more precisely, spectroscopic) *match criterion*’ revealed to be much strongest determinant for the goodness of all such ‘theory – experiment’ comparisons, besides the principal ‘*minimum-energy criterion*’. In consequence, the usually recommended [93] calculations weighted with respect to Boltzmann population statistics of various lowest-energy structures of the studied species were practically not applicable. Therefore, various

NMR spectroscopic data showed to be indispensable for adequate molecular modeling the macrocyclic systems $H_n\mathbf{3}^{n+}$ in solution and *vice versa*.

In general, there are three (or four) main issues involved with the treatment of fully complementary NMR data for solution and related theoretical predictions on the macrocyclic entities under consideration: (i) adequate choice of initial geometric models of the species $H_n\mathbf{L}^{n+}$ ($n = 0, 1, 2, \dots$), (ii) overall multicomponent conformations forced by a large dynamics of the macrocyclic cores of $H_n\mathbf{L}^{n+}$, (iii) empirical correction of the DFT GIAO predictions of δ_{XS} applying the linear regression analysis, and (iv) use of the PCM model or ONIOM technique in the ‘behind a free-molecule’ approach. All of these issues will be less or more in detail discussed below.

3.1. MMX vs. OPLS-AA Force Field (Creation of Initial Molecular Models)

During the course of detailed DFT studies [80] on the differently protonated states of a pentaprotic macrocyclic base **3**, an important observation was accomplished about practical utility of the MMX [88] *versus* OPLS-AA [90] force field for modeling related ammonium cations of the polyamino macrocycles. Thus, the former of two molecular mechanics (MM) methods was found as more appropriate for the pentabasic macrocycle **3** in initial generating of the intramolecularly H-bonded *in* conformers of the ions $H_3\mathbf{3}^{3+}$ with the multiple binding interactions comprising different $N^+ - H \cdots N$ hydrogen bonds, whereas the latter – for the *out* forms of the more hydrophilic ions $H_4\mathbf{3}^{4+}$ and $H_5\mathbf{3}^{5+}$ (*vide supra*). In this way, two or three internal H-bridges of type $N^+ - H \cdots N$, including also some bifurcated H-bond systems, were found in the preferred *in* conformers of $H_3\mathbf{3}^{3+}$ being in agreement with experimental ^{13}C NMR data.

Because the B3LYP/6-31G*-optimized geometries of analogous dication of the parent cyclam (**1**) did not be published to date, their selected examples elucidated at initial use of the both aforementioned MM methods are presented below. These forms of $H_2\mathbf{1}^{2+}$ were DFT computed in standard *in vacuo* approach or at simulated presence of the surrounding bulk solvate water molecules. The latter simulations were performed applying the polarizable continuum model with the integral equation formalism (IEF-PCM) [94] (*vide infra*). The key energy and structural data for such predicted conformers of $H_2\mathbf{1}^{2+}$ are summarized in Table 2.

The three low-energy endodontate (*in*-type, *vide supra*) conformers **A-C** of the dication $H_2\mathbf{1}^{2+}$ with a planar or bend arrangement of intramolecular bifurcated H-bonds are pictured in Figure 4. All these forms were initially generated with the MMX force field. Undoubtedly, several of such or similar H-bonded conformers of $H_2\mathbf{1}^{2+}$ are in equilibrium [66,75,87]. Moreover, a single exodontate (*out*) non-H-bonded form **D** of much higher energy, which was optimized starting from the OPLS-AA geometry, is also given for the purpose of comparison. In all of these four cases, the more compact molecules were obtained in PCM simulations of the surrounding aqueous environment, as was simply estimated from the $N^+ \cdots N^+$ distances within their diprotonated macrocyclic cores (Table 2). Inspection of the content clearly reveals that the form **D** is really more susceptible on the interactions with polar solvent. However its energy increases the lack of internal H-bonds strongly stabilizing the endodontate structures **A-C**. Finally, it should be noted that these latter preferred conformers of the

dication $\text{H}_2\mathbf{1}^{2+}$ strongly differ from its tentative models proposed previously basing only on the HF/STO-3G level calculational results [66].

Table 2. Important energetic and geometric data B3LYP/6-31G*-predicted for the forms A-D of $\text{H}_2\mathbf{1}^{2+}$ ^a

Calculational result \ species	A		B		C		D	
	gas	water	gas	water	gas	water	gas	water
$\Delta\Delta G$, kJ mol ⁻¹	0 ^b	0 ^{c,d}	10.99	9.40 ^c	14.30	8.16 ^c	114.72	92.77 ^c
N ⁺ ...N ⁺ distance, Å	4.342	4.325	4.377	4.298	4.154	4.037	6.702	6.476
Short N ⁺ -H...N distance, Å	1.927	1.954	1.949	1.952	1.866	1.848	–	–
Long N ⁺ -H...N distance, Å	2.713	2.704	2.704	2.638	2.628	2.609	–	–
H-bond system	planar		bent		bent		–	
Hydration energy, kJ mol ⁻¹ ^e	–	-724.04	–	-724.36	–	-729.02	–	-742.20
Molecular symmetry	C _i		C ₂		C ₂		C ₂	

^a Data for the gas phase (in vacuum, 0 K) or solution in water (by an IEF-PCM model, 298 K).

^b Absolute energy of -614.861331 hartrees; 1 Ha = 1 au = 2625.50 kJ mol⁻¹.

^c Total free energy in solution with all non-electrostatic terms.

^d Absolute energy of -615.446031 Ha.

^e PCM result for the term [(polarized solute) – solvent].

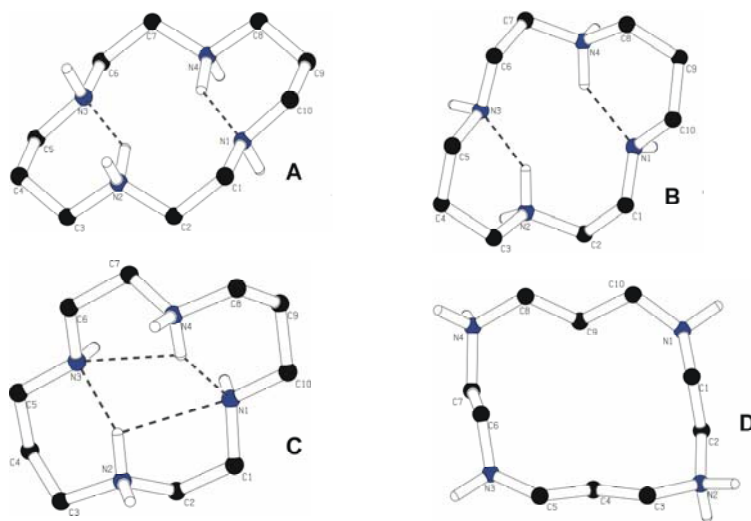


Figure 4. PLUTON drawings of the four selected forms A-D of $\text{H}_2\mathbf{1}^{2+}$ found at the B3LYP/6-31G* level [83]. Dashed thick lines indicate multiple intramolecular H-bonds; only NH hydrogen atoms are shown. Two unsymmetrical bifurcated H-bond systems are explicitly shown only in the conformer C because of stiff settings of the used software [95].

On the contrary, only *out* orientations of the macroring ⁺N-H bonds were found in the favored conformers of the perprotonated species $\text{H}_4\mathbf{1}^{4+}$ as well as analogous scorpiand cations $\text{H}_4\mathbf{3}^{4+}$ and $\text{H}_5\mathbf{3}^{5+}$ (*vide infra*). The initial geometries of all these ions were generated in the OPLS-AA force field. The dominant DFT GIAO-supported exodentate conformers of the later ionic species, $\text{H}_5\mathbf{3}^{5+}$, will be discussed in the next section in detail. It was obvious, that such a maximally extended configuration of the 1,4,8,11-tetraaza-macrocyclic core, arising

from repulsive forces of the Coulomb type between four positively charged cationic sites, is much more favorable for hydration and other electrostatic interactions in aqueous medium. Indeed, the OPLS-AA approach was originally designed for liquid simulations and, so, it is more suitable for doing of all predictions concerning the polar media. One of the important differences among these MM methods is that in the OPLS-AA force field there are no 'lone pairs' at the heteroatoms, whereas they appear as pseudoatoms in its MMX counterpart [88].

3.2. Overall Conformations of the Macrocycles Forced by Their Dynamics

As mentioned earlier, in our NMR study on the scorpionid system **3** we quickly realized that only overall (weighted averages) shapes of various rapidly interconverting conformers of the species H_n3^{n+} were satisfying representatives of these macrocyclic entities in the aqueous medium [80]. Indeed, all 1H NMR spectra showed single resonances for each magnetically equivalent group of nuclei over the entire pH range, indicating rapid exchange between all of the coexisting species. Moreover identical HF/3-21G structures of H_33^{3+} and H_43^{4+} were often found departing from their different initial MM models, especially for H_33^{3+} . This latter finding can be easily explained with considerable macrocycle flexibility involving nitrogen inversions, which was previously observed for all polyamines **1-3** and related polyammonium cations in aqueous solution [66,75,87,96,97]. Therefore, weaker correlations δ_C^{calc} vs. δ_C^{exp} found for two ions of **3** mentioned above can partially result from their mobility and, so, from the need to consider a lot of different conformers of similar energy.

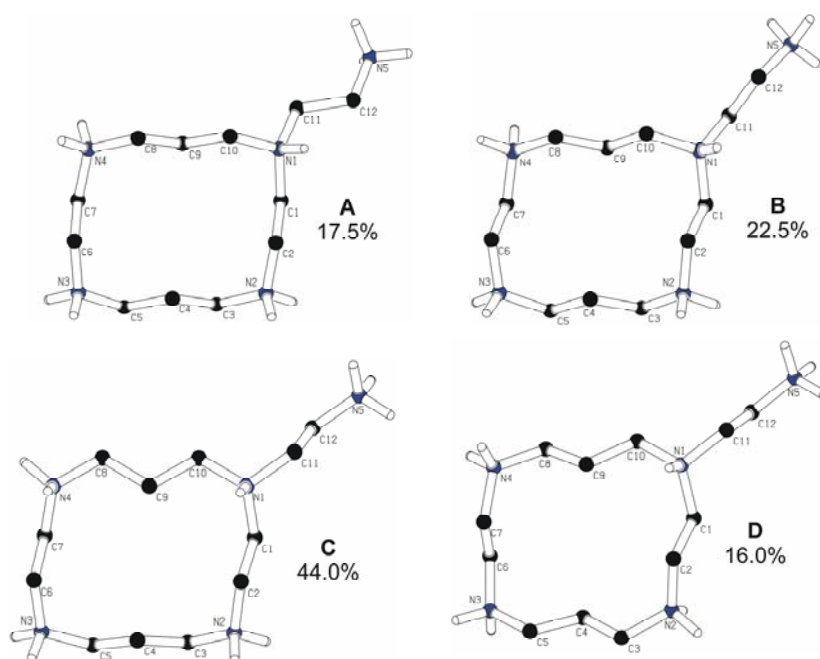


Figure 5. The four main B3LYP/6-31G*-optimized *out* components **A-D** (with their percentages) of the DFT GIAO-supported overall four-composite conformation of the cation H_33^{5+} [80,83].

In general, the population of specific structures in the mean shape (*i.e.*, an ensemble of species that constitutes the ‘overall’ conformation) of any flexible polyazamacrocycles can be determined from the extent of NMR pH-titration shifts [55]. In the particular case of the scorpionand (**3**), the best result was obtained for H_53^{5+} ($r = 0.9882$ for δ_C^{exp} vs. δ_C^{calc} relation, *vide infra*). Thus, 0.175:0.225:0.44:0.16 ‘superposition’ of four B3LYP/6-31G*-optimized forms **A–D** (as depicted in Figure 5) was elucidated as a reasonable time-averaged shape of this ionic specimen in solution, because related δ_C s both measured at pH 0.24 and *in vacuo* DFT GIAO computed were in the best way accommodated in such four-composite overall conformation (named H_53^{5+} **ABCD**) [80]. Indeed, when observing the average NMR signals originated from any equilibrium, a normal procedure to estimate the composition of the mixture under analysis is to use interpolation.

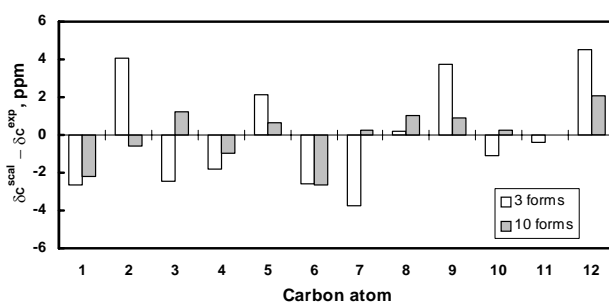


Figure 6. Bar graph of the δ_C differences between linearly scaled *in vacuo* results and values measured for **3** at pH 2.05, for two different approaches applied. Related data from the DFT GIAO predictions for 3 forms contributing to a single mean shape of H_53^{4+} **ABC** ($r = 0.953$) and for 10 forms coming from the three consecutive cations H_n3^{n+} , $n = 3-5$, coexisting in solution ($r = 0.990$) [80]; see also text.

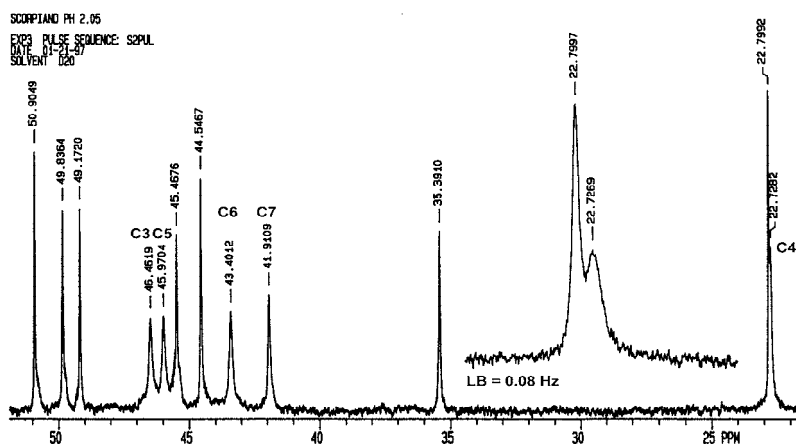


Figure 7. 50.29 MHz $^{13}C\{^1H\}$ NMR spectrum of the pentamine **3** in H_2O/D_2O at pH 2.05 [10 900 transients, the 0.65 Hz line broadening (LB) was applied in processing the spectrum; for the other experimental details and atom-numbering scheme, see Figure 3]. The broadened signals are due to the macroring atoms C3–C7 [80,82].

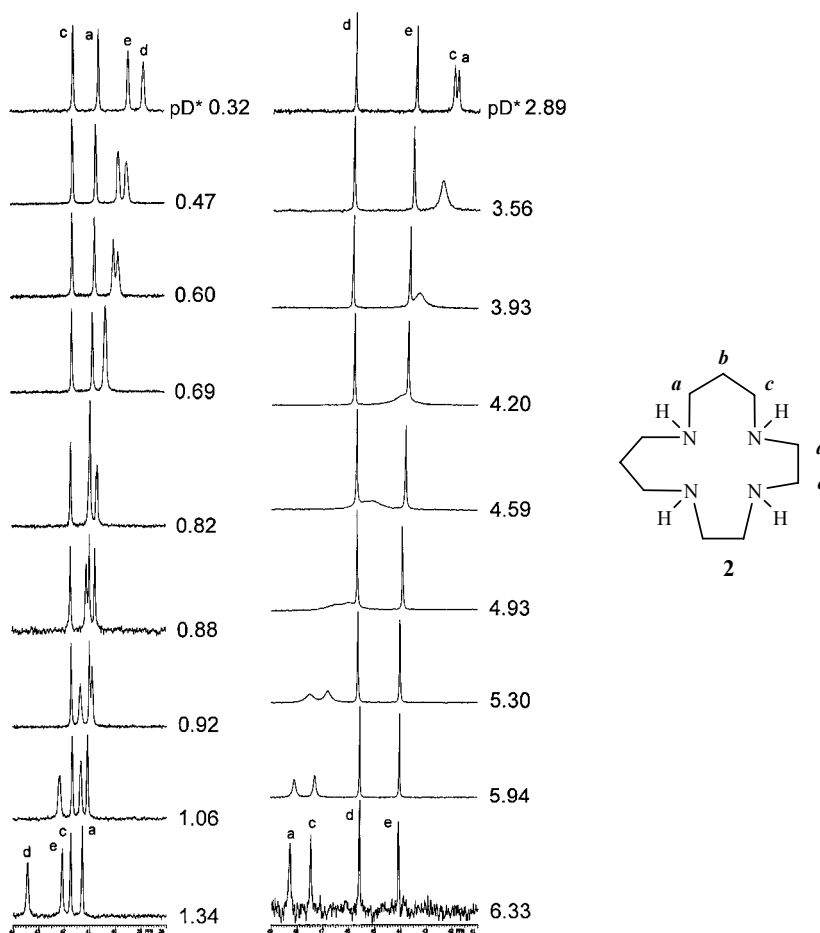


Figure 8. The dynamic processes observed for the isocyclam system **2** in D_2O in the pD* range 0.3-1.3 (44-38 ppm, on the left) and 2.9-6.3 (49-41 ppm, on the right side). The low-field region of 50.29 MHz ^{13}C NMR spectra (Varian Gemini 200 BB, $\sim 21^\circ\text{C}$; the δ_{C} values relative to an external pure TMS, no susceptibility correction of +0.67 ppm [83] was used) For the labeling of resonance signals, see Formula above. Reproduced with kind permission, from Nazarski [87,99]. Copyright © 2000 Institute of Molecular Physics, Polish Academy of Science.

Unfortunately, such a treatment is considerably more difficult for the species occurring in small amounts. For example, an intermediate ion $\text{H}_4\mathbf{3}^{4+}$ reaches the maximum concentration of only $\sim 55\%$. In consequence, its direct NMR spectroscopic observation was practically impossible [80]. Indeed, any two processes of the protonation overlap measurably unless associated $\text{p}K_{\text{a}}$ values differ by more than about 4 logarithm units [98]. As a result, the multicomponent mixture of three ionic entities $\text{H}_3\mathbf{3}^{3+}\text{ABCD}$ ($\sim 37.5\%$), $\text{H}_4\mathbf{3}^{4+}\text{BC}$ ($\sim 34.5\%$) and $\text{H}_5\mathbf{3}^{5+}\text{ABCD}$ ($\sim 28\%$) embracing ten single forms being in fast equilibrium was proposed in order to explain the ^{13}C NMR spectrum of the pentaamine **3** at pH 2.05. The differences $\delta_{\text{C}}^{\text{scal}} - \delta_{\text{C}}^{\text{exp}}$ found in this case by using linear scaling of the data are shown in Figure 6. Two different approaches were applied, *i.e.*, considering only the one single overall conformation $\text{H}_4\mathbf{3}^{4+}\text{ABC}$ (three forms A-C) or all ten forms coexisting in the mentioned multicomponent

mixture. Obviously, an adequate statistical analysis of NMR results, *i.e.*, experimental δ_C^{exp} s and pertinent DFT GIAO predicted δ_C^{calc} s, is absolutely necessary in all considerations of this kind (*vide infra*). The Pearson correlation coefficient r of 0.988 and 0.990 was obtained for two sets of δ_{CS} concerning the system **3** analyzed at pH 0.24 and 2.05, respectively.

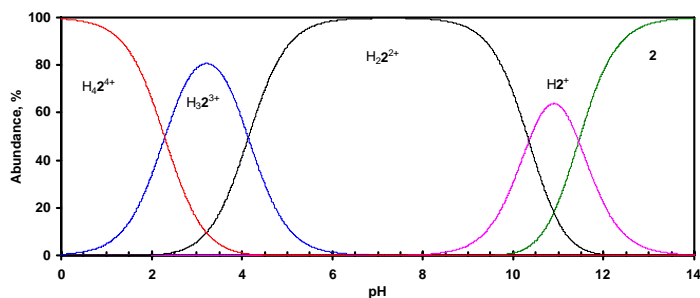


Figure 9. Distribution diagram of the protonated species formed from macrocyclic tetraamine **2** in H_2O , as a function of pH. The plot was calculated from protonation constants found potentiometrically ($I = 0.1 \text{ mol L}^{-1} \text{ KNO}_3$, 25°C) [66,74], by using the PlotPhi program [100].

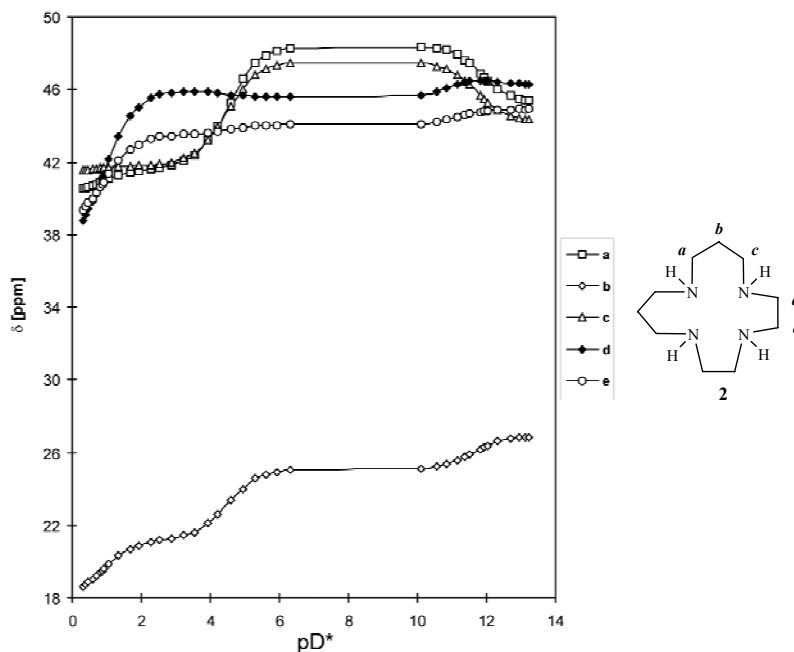


Figure 10. The plot of ^{13}C NMR chemical shifts against pD^* for isocyclam (**2**) in D_2O . Reproduced with kind permission of Springer Science and Business Media, from Sroczynski *et al.* [66,99]. Copyright © 1999 Kluwer Academic Publishers.

The aforementioned ^{13}C NMR spectrum measured at pH 2.05, formally belonging to a single ion $\text{H}_4\mathbf{3}^{4+}$, is also interesting from the other reason. Thus, some broadening of ^{13}C lines of the five consecutive ring atoms C3–C7 in the macrocyclic core **3** were best observed under such conditions (Figure 7). In full agreement with the calculational structural results, this

signal broadening was attributed to relatively slow, on the NMR time scale, equilibrium mostly between the six different components of the two multi-composite entities $H_3\mathbf{3}^{3+}\mathbf{ABCD}$ (internally H-bonded) and $H_4\mathbf{3}^{4+}\mathbf{BC}$ (non H-bonded) [80]. Indeed, there are numerous disruptions and formations of intramolecular H-bridges of the type $N^+-H\cdots N$ in such dynamic equilibria. As a consequence, the ^{13}C NMR lines of the five macroring C-atoms adjacent to three amino N^2-N^4 sites involved in these processes are substantially broadened [82]. For similar H-bonded forms **A-C** and non-bonded form **D** of a dication of the parent cyclam ($H_2\mathbf{1}^{2+}$), see Figure 4.

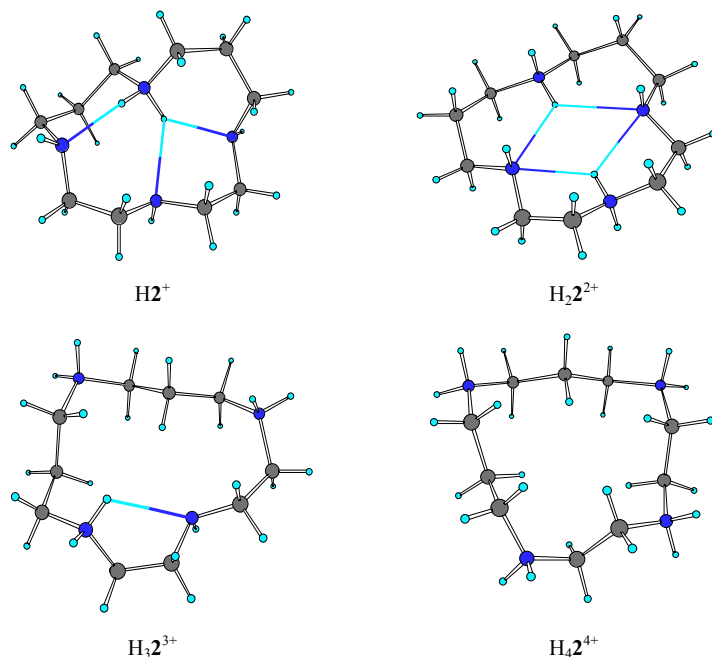


Figure 11. Tentatively proposed [96] HF/6-31G*-level *in vacuo* global energy minima of the ions $H_n\mathbf{2}^{n+}$. The N-atoms are in blue while the multiple binding interactions comprising different $N^+-H\cdots N$ intramolecular H-bonds are shown with aquamarine-blue lines.

One can safely accept that an analogous dynamic process very well observable at $\text{pD}^* 3-6$ for the isomeric isocyclam system **2** (Figure 8) has also the same origin [87,99]. In this case the equilibrium $H_2\mathbf{2}^{2+} \rightleftharpoons H_3\mathbf{2}^{3+}$ takes place. The distribution diagram of different molecular species coexisting for the tetraamine **2** in aqueous solution is given in Figure 9. This plot, calculated from potentiometrically evaluated protonation constants [66,74] using PlotPhi [100], explicitly shows five macrospecies $H_n\mathbf{2}^{n+}$ ($n = 0-4$) characterized by their mean shapes. Obviously, a real situation regarding individual components of these superimposed states, *i.e.*, particular species and their conformers considered as physically distinct microspecies, is much more complicated [101]. According to these data, there is a significant pH range [about 4.14 (= $\text{p}K_{23}$ of **2** [66,74]), *vide supra*] in which both aforementioned ammonium dications coexist in comparable amounts. This pH range was not the same in ^{13}C NMR pH-titrations in D_2O , but was rather similar. The inflection point on pH-curves for nuclei **a-c** of **2** is very well observed at $\text{pD}^* \sim 4.3$ (Figure 10). By using Eqs. (9)–(10) we obtained $\text{p}K_a(\text{D}_2\text{O})$ of 4.64–4.77.

Such a small (~ 0.4 unity) difference in pK_{a} s is easily attributable to different ionic strengths I , which were applied in both measurement conditions (*vide supra*).

Some *ab initio* HF/3-21G and 6-31G* results on isocyclam species $\text{H}_n\mathbf{2}^{n+}$, $n = 0-4$, were presented previously [96] (Figure 11). Thus, the unsymmetrical bifurcated intramolecular H-bond systems were found in pertinent cations, including the species $\text{H}\mathbf{2}^+$. The three internal H-bonds found in $\text{H}\mathbf{2}^+$ are probably responsible for the high basicity of its N1 nitrogen; for an adopted atom-numbering scheme, see Figure 12. Very high pK_1 values, most likely being a consequence of the formation of strong intramolecular H-bonds between the ring-nitrogens in some macrocycles, were discussed in the literature [33,46]. Current large-scale ($\sim 75\,000$ MC steps of initial MMX searches with a wide energy window of ~ 14.5 kJ mol $^{-1}$) and more advanced *in vacuo* DFT B3LYP/6-31G* level computations [83] supported a large majority of these preliminary findings. The located lowest-energy C_s symmetrical forms **A** and **B** of the chemically different (tautomerism due to an intramolecular prototropy) structures **a** and **b** of the cation $\text{H}_2\mathbf{2}^{2+}$ are shown in Figure 12.

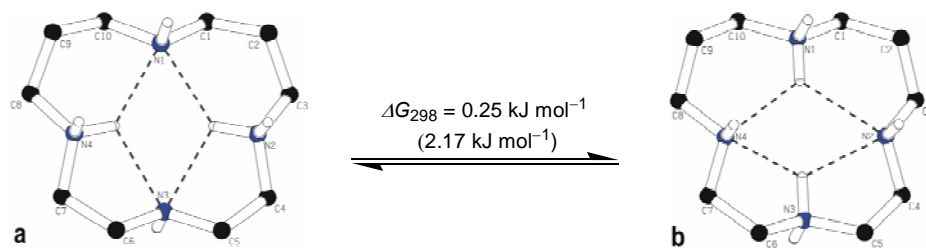


Figure 12. The lowest-energy *in vacuo* conformers **A** and **B** of tautomers **a** and **b**, respectively, of the isocyclam ion $\text{H}_2\mathbf{2}^{2+}$ as predicted on the 0.96-scaled [102] B3LYP/6-31G* level; the 0.9135-scaled [103] HF/6-31G* value of ΔG_{298} in parenthesis [96]. Dashed thick lines indicate internal H-bridges; only NH hydrogens are depicted [83].

A comparison of geometric data of the H-bond systems in both these positional isomers, predicted at two levels of theory, is given in Table 3. The 4,11-distribution of the positive charges in the form **B** is negligible thermodynamically favored by 0.25 kJ mol $^{-1}$ over the 1,7-one in **A** (gas-phase 0.96-scaled [102] DFT result). As a consequence, dication $\text{H}_2\mathbf{2}^{2+}$ of the types **a** and **b** are undoubtedly in fast equilibrium, also in solution. In other words, two protons are shared between the four secondary N-atoms to a practically equal extent. Such a conclusion is in full agreement with our old suggestion on the positive-charge spread over all nitrogenous basic centers in $\text{H}_2\mathbf{2}^{2+}$, which was based on a tentative analysis of the ^{13}C NMR pH-titration data [66].

It should be noted that serious problem was met with initial finding of chemically different conformers **A** and **B** of $\text{H}_2\mathbf{2}^{2+}$ from among the lots of MM generated forms of types **a** and **b**. Due to some limitations of the applied software, *i.e.*, the lack of a possibility of the symmetry imposition using PCMODEL, their unsymmetrical models **A'** and **B'** were really located as relatively high-energetic species, with $\Delta E(\text{MMX})$ of 13.82 and 5.00 kJ mol $^{-1}$ in relation to originally found unsymmetrical lowest-energy forms of the structures **a** and **b**, respectively. In fact, both forms **A** and **B** were initially designed ‘by hand’, in the trial-and-error method, starting from various forms of $\text{H}_2\mathbf{2}^{2+}$. They were also obtained from the models **A'** and **B'** after their earlier symmetrization, *e.g.*, by applying the AM1 procedure.

Table 3. Distances and valence angles concerning bifurcated H-bonds (\AA , $^\circ$) in the best conformers A and B of the structures a and b of H_22^{2+} as *in vacuo* predicted at two levels of theory^{a,b}

1,7-Protonated form A		4,11-Protonated form B	
N1...H2	2.319 (2.356)	N2...H1	2.447 (2.471)
N1...N2	3.118 (3.132)	N1...N2	3.159 (3.168)
N1-H2-N2	132.8 (132.7)	N1-H1-N2	125.3 (125.6)
N3...H2	2.329 (2.343)	N2...H3	2.231 (2.266)
N2...N3	2.838 (2.833)	N2...N3	2.822 (2.829)
N2-H2-N3	108.8 (108.6)	N2-H3-N3	114.2 (113.7)

^a The B3LYP/6-31G* level data [83]; the HF/6-31G* geometries in parentheses [96].

^b H_n = H-bonded proton linked to the N_n atom.

3.3. Empirically Corrected (Linearly Scaled) DFT GIAO-based Predictions of δ_X s for Aqueous Solutions

The adequate statistical evaluation of an agreement between the theoretically evaluated magnetic shieldings (σ_X^{calc} s) and experimentally measured chemical shifts (δ_X^{exp} s) is essential for the whole analysis, *i.e.*, an initial selection of the promising models of coexisting macrocyclic species H_nL^{n+} ($n = 0, 1, 2, \dots$) and final elucidation of the overall multi-composite conformations $\text{H}_n\text{L}^{n+}\text{AB}\dots$ of these macromolecular entities.

There are basically two ways of comparing isotropic σ_X^{calc} s predicted by the GIAO [91] technique (applied as a method of choice) and δ_X^{exp} s found for solution. In the approach proposed at the beginning [91a-d,f,g], one additionally calculates the shielding constant for a used reference compound, σ_X^{ref} , and then transforms all of the theoretical data in question according to the simple formula:

$$\delta_X^{\text{calc}} [\text{ppm}] = \sigma_X^{\text{ref}} - \sigma_X^{\text{calc}} \quad (14)$$

However, such a procedure suffers from two significant drawbacks [104]. The foundation of the second, so-called ‘scaled,’ approach recommended by Chesnut [105] as well as Forsyth and Sebag [91e] and numerous later authors, is the belief that deficiencies of the theory can be partially compensated by a linear scaling of the GIAO-based predictions, assuming one of two equivalent relationships, Eq. (15):

$$\delta_X^{\text{scal}} [\text{ppm}] = a \cdot \sigma_X^{\text{calc}} + b \quad (15a)$$

$$\delta_X^{\text{scal}} [\text{ppm}] = a' \cdot (s - \sigma_X^{\text{calc}}) \quad (15b)$$

For any reliable theoretical model, the value of a' or $(-a)$ found by linear regression is expected to be close to unity. Instead, the value of s should not differ very much from σ_X^{ref} calculated for the NMR signal lying at 0 ppm, which can be used as another indication of the

correctness of data analysis [104b]. An example of such an approach, applicable for the four-component conformation $H_5 3^{5+} ABCD$ in solution is shown in Figure 13a.

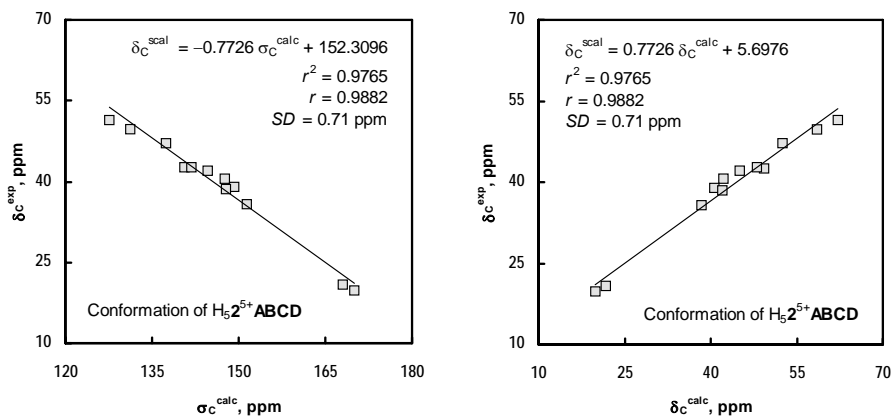


Figure 13. Scatter plots of isotropic δ_C^{exp} vs. σ_C^{calc} (or δ_C^{calc}) for the DFT B3LYP/6-31G* level overall GIAO-supported four-component conformation of $H_5 3^{5+} ABCD$ found in two differently performed scaled approaches. The best-fit straight lines are also shown, respectively. Part a (left): classical one-stage treatment; Eq. (15) [83]. Part b (right): two-stage approach used in the work [80]; Eq. (16). Reproduced with kind permission, from Nazarski [80]. Copyright © 2009 John Wiley & Sons, Ltd.

For any reliable theoretical model, the value of a' or $(-a)$ found by linear regression is expected to be close to unity. Instead, the value of s should not differ very much from σ_X^{ref} calculated for the NMR signal lying at 0 ppm, which can be used as another indication of the correctness of data analysis [104b]. An example of such an approach, applicable for the four-component conformation $H_5 3^{5+} ABCD$ in solution is shown in Figure 13a.

Still another two-step ‘chemical shift–chemical shift’ correlation (see, Refs 92 and 106) was applied in our studies on the systems **3** in aqueous solution [80] that uses the advantages of both above approaches. Thus, all desired δ_C^{calc} s were initially calculated with Eq. (14), by using σ_C^{calc} s *in vacuo* evaluated by a GIAO method at the DFT B3LYP/6-31G*//B3LYP/6-31G* level and the analogously found σ_C^{ref} of 189.7709 ppm, for neat liquid TMS externally applied in the coaxial capillary [66]. This simple procedure gives a comfort of the fast, direct and transparent visualization of divergences between experiment and theory, which was especially important in initial selections of the promising macrocyclic models. In the second step of this approach, an empirical best fit scaling equation of type

$$\delta_X^{\text{scal}} [\text{ppm}] = a'' \cdot \delta_X^{\text{calc}} + b'' \quad (16)$$

(where $X = C$) was determined for every low-energy conformer, by using the least-square procedure. As usual, the Pearson correlation coefficient value (r) was used to measure a strength of such obtained relations $\delta_C^{\text{exp}} = f(\delta_C^{\text{calc}})$, and the linear regression equation of type $y_i = a'' \cdot x_i + b''$ to mathematically define these relationships [92]. In this way, two regression parameters, the slope $a'' (= -a)$ and intercept (intersect) b'' , were finally employed to correct for systematic errors in an applied treatment regarding the direct ‘theory (vacuum, 0 K) vs.

experiment (solution, RT)' comparison. The practical use of such a two-step protocol for an overall solution conformation $H_5\mathbf{3}^{5+}\mathbf{ABCD}$ is also shown in Figure 13b [80]. How easy to see, both approaches concerning the linearly scaled values of δ_{CS} are fully equivalent.

3.4. Behind a 'Free-Molecule' Approach

In general, when solvation plays a major role in short-range solute-solvent interactions further theoretical treatment should be basically applied, such like *e.g.*, the polarizable continuum model with an integral equation formalism (IEF-PCM) [94] or, much more computationally requiring, two-layer version of the ONIOM procedure (ONIOM2) [107]. Especially, the latter technique is a conceptually simple approach whereby both long-range and local environmental effects on the properties of molecules (studied in an explicit solvent) can be captured. The foregoing satisfactory *in vacuo* results on the per-protonated and, so, strongly hydrophilic ion $H_5\mathbf{3}^{5+}$ (*vide supra*) were intended to compare with related structural data and GIAO predictions of δ_{CS} performed in the presence of bulk water simulated by applying the IEF-PCM approach at the DFT level. Unexpectedly, a bad convergence was generally found for these calculation efforts, because only three of the six pre-selected low-energy B3LYP/6-31G* geometries of $H_5\mathbf{3}^{5+}$ were successfully examined in this way [80].

These failures decided us to perform some supermolecular GIAO DFT calculations of δ_{CS} at the ONIOM2 B3LYP/6-31G*:STO-3G level using the Gaussian 03 program [108], in order to study the expected solvent H-bonding effects. At the beginning, six boxes with ~445 water models (as described by three-site TIP3P potentials [109]) surrounding the six forms of $H_5\mathbf{3}^{5+}$ were constructed applying the solvent-box option of HyperChem [110]. Such models were subjected next to normal energy minimizations with this software, by using the OPLS-AA force field [90]. Final geometry optimizations of these supermolecules were performed at the ONIOM2 B3LYP/6-31G*:DREIDING level applying the Gaussian 03 package.

There was some analogy to molecular dynamics (MD) simulations, because the 'ducked' cations were initially compressed from equilibrium (in the OPLS-AA force field) and then fully relaxed using an ONIOM2 approach. The $H_5\mathbf{3}^{5+}\cdot(H_2O)_n$ aggregates generated in this way fulfilled all requested criterions of the convergence. These 'hydrated states' of $H_5\mathbf{3}^{5+}$ were found as structures only slightly stabilized by a complex 3D network of intermolecular H-bonds. The most abundant such computed supramolecular cluster $H_5\mathbf{2}^{5+}\cdot(H_2O)_{462}$ of the type **B** is depicted in Figure 14. However, the macrocyclic cores of a large majority of these $H_5\mathbf{3}^{5+}\cdot(H_2O)_n$ supramolecules were found as being structurally similar to the initial gas-phase models. Also related NMR data were comparable, in general [80].

Above results suggest that the use of standard *in vacuo* approach is normally sufficient for elucidating the structure and behavior of the discussed macrocyclic polyamino species $H_n\mathbf{L}^{n+}$, particularly taking into account their large mobility in strongly polar aqueous solution. So, the overall multicomponent conformations should be rather taken into account, as a rule. In such a case, there is most likely some cancellation of small errors arising from the change in their molecular properties on going from the gas to solution phase. Moreover, all 'behind a free-molecule' approaches are extremely computationally time-consuming treatments.

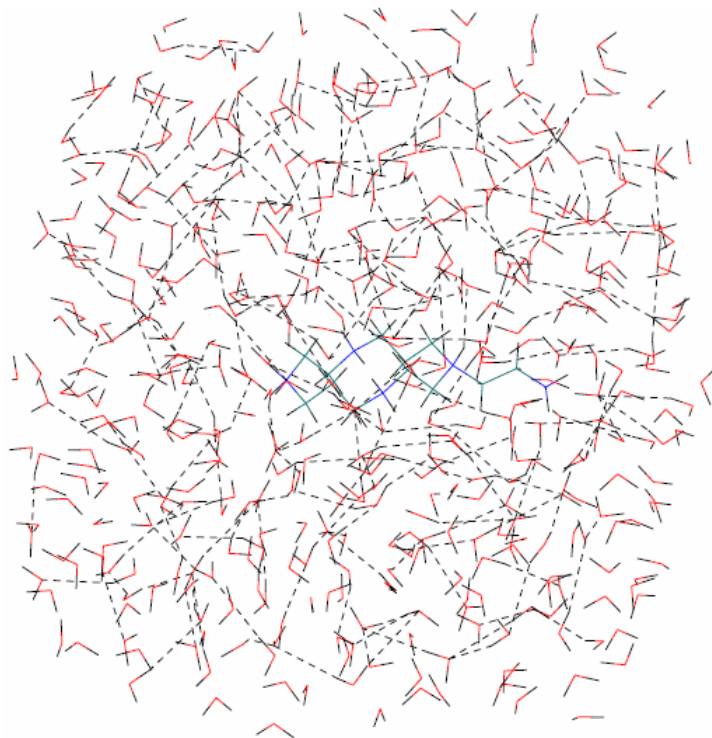


Figure 14. A stick drawing of the most abundant (~45.5%) supramolecular cluster $\text{H}_5\text{2}^{5+} \cdot (\text{H}_2\text{O})_{462}$ of type **B** computed at the ONIOM2 B3LYP/6-31G*:DREIDING level, by starting from an output geometry of the OPLS-AA force field optimization (solvent box of 23.988 \AA^3 , 462 TIP3P water models [109] added and cutoff from 7.994 to 11.994 \AA were initially employed). The dashed thick lines indicate a complex 3D network of intermolecular H-bonds; the HyperChem [110] depiction. Only axially oriented $^1\text{N}^1\text{H}$ hydrogen atom of the cation $\text{H}_5\text{2}^{5+}$ is engaged in the $\text{N}^+-\text{H}\cdots\text{OH}_2$ hydrogen bond. Reproduced with kind permission, from Nazarski [80]. Copyright © 2009 John Wiley & Sons, Ltd.

Table 4. Torsion angles ($^\circ$) in the macroring of $\text{H}_4\text{1}^{4+}$ determined experimentally in the crystal [112] or MM predicted in vacuum ^{a,b}

Torsion	Crystal ^c	Crystal _{av} ^d	MM+	DREIDING	MMX
N4–C1–C2–C3	174.95(15)	172.88	173.64	173.03	174.66
C1–C2–C3–N1	–170.80(15)	–172.88	–173.64	–173.03	–174.66
C2–C3–N1–C4	54.5(2)	56.92	58.52	55.94	51.44
C3–N1–C4–C5	58.6(2)	63.45	63.02	63.45	65.97
N1–C4–C5–N2	–173.47(13)	–173.47	–169.18	–164.82	–165.32
C4–C5–N2–C6	68.3(2)	63.45	63.02	63.45	65.97
C5–N2–C6–C7	59.33 ^e	56.92	58.52	55.94	51.44

^a Only one half of the macroring was taken into account due to C_i symmetry of the analyzed form.

^b For an arbitrary atom numbering see Figure 15.

^c Angles determined [112] in the crystal of $\text{D}_8\text{1}^{4+} \cdot 4\text{NO}_3^{3-} \cdot 2\text{D}_2\text{O}$.

^d Adequately averaged values found in the crystalline state (neighboring column).

^e Calculated from atomic coordinates, by using the Mercury program [113].

The use of the DREIDING [111] force field, in a second step of the ONIOM2 modeling of $\text{H}_3\mathbf{3}^{5+} \cdot (\text{H}_2\text{O})_n$ clusters, deserves some comment. Actually, it is the only one empirical force field accessible in Gaussian 03. Moreover, this MM tool was previously successfully tested *versus* its MM+ and MMX field congeners implemented within HyperChem and PCMODEL [112]. Some comparison of their predictions about the geometry of the particular form of the ion $\text{H}_4\mathbf{1}^{4+}$ is given in Table 4. Torsion angles were mainly used because these geometrical parameters are, in general, especially sensitive to any changes in the molecular shape.

Thus, our *in vacuo* calculational results were confronted with adequately averaged values of related torsion angles in the macrocyclic core of a free (hypothetical) tetracation $\text{H}_4\mathbf{1}^{4+}$. In turn, experimental values of these angles were determined in a single-crystal X-ray diffraction analysis of the normal [114] or partially deuterated form [112] of the dihydrate form of cyclam tetranitrate; for a view of the latter form ($\text{D}_8\mathbf{1}^{4+} \cdot 4\text{NO}_3^{3-} \cdot 2\text{D}_2\text{O}$), see Figure 15. The 14-membered-ring macrocyclic unit of this salt adopts a puckered conformation of the type (3.4.3.4)-A [115], with the ring *N*-atoms occupying four corners of the molecular polygon and all $\text{N}^+ - \text{H}$ bonds situated outward an internal macrocyclic cavity. In such an *out* disposal of H-atoms all positive sites in the macrocycle are as far apart as possible in order to achieve minimum electrostatic repulsion. Similar arrangement of the central *N*-atoms was found in the perprotonated cation $\text{H}_3\mathbf{3}^{5+}$ studied in aqueous solution (*vide supra*).

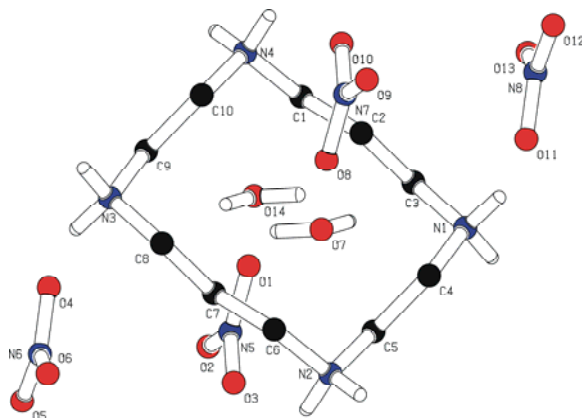


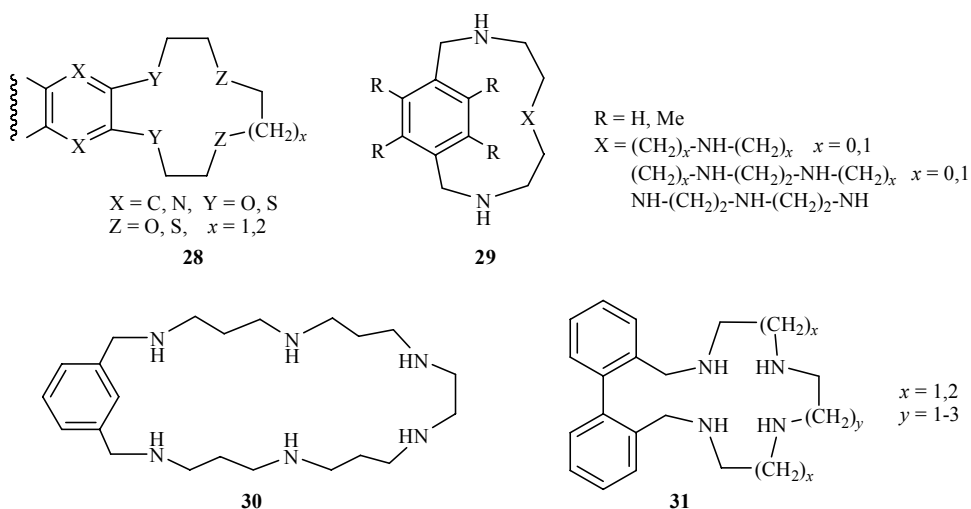
Figure 15. PLUTON [95] view of the molecular structure of $\text{D}_8\mathbf{1}^{4+} \cdot 4\text{NO}_3^{3-} \cdot 2\text{D}_2\text{O}$; the atoms C, N and O are shown in black, blue and red, respectively. Only ND and OD deuterium atoms are given [112].

4. POLYAZA AND OTHER MACROCYCLES - SOME CURRENT ACHIEVEMENTS

In the last section of this chapter a few additional arbitrarily chosen research subtopics are briefly discussed, which are currently undertaken in the field of azacrowns and other structurally close macromolecular ligands acting as chelators. In our opinion, they are interesting from the protonation sequences, NMR-based results and/or widely understood

conformational analysis points of view. The reader should clearly understand that this material does not pretend to the titer of an overview of the rich literature in this subject.

Typical crown ethers are generally conformationally mobile macrocycles. To, reduce their intramolecular flexibility, it is possible to insert a rigid and/or voluminous structural fragment into the saturated macrocyclic moiety. Such oxathia crown ethers **28** containing different *ortho*-substituted aromatic subunits were studied with application of various NMR techniques, including variable-temperature (VT) measurement [116]. Simultaneously, their global-minima structures determined theoretically from the MM studies were analyzed with respect to barriers to the ring interconversion and mobility in solution.



On the other hand, by introduction of single *para*- or *meta*-substituted benzene as well as 2,2'-biphenylene aromatic spacers into saturated polyaza macrocyclic systems, related aza cyclophane receptors **29-31** with 3-6 nitrogen donor atoms in an intramolecular cavity were synthesized [60a,c,117]. Two former groups of the ligands (**29** and **30**) were fully analyzed by 1H and ^{13}C NMR pH-titrations in the pH range from ~ 2 to ~ 12 . According to their protonation behavior, these polyamines can be classified into three different sets, namely (i) with only ethylenic (CH_2CH_2) chains, (ii) containing only propylenic ($CH_2CH_2CH_2$) chains, and (iii) having both these chains in the polyaza bridge [60a].

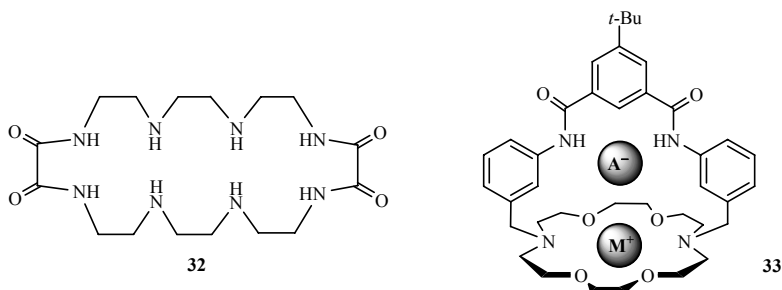
The ligands **29** of the first group display lower basicities in the protonation steps. In their diprotonated forms H_229^{2+} both protons seem to bind to benzylic N-atoms, mainly due to an effect of entropy. The NMR analysis of the second groups of ligands does not show preferred coordination sites. Thus, the protons should be randomly shared over all protonation sites in these systems. As already observed for other polyamines, the presence of propylenic chains between protonation sites strongly reduces the electrostatic repulsions (*vide supra*). The third group of ligands displays, in their all three first protonation steps, analogous basicities to that of the second group [60a].

The protonation behavior of hexaaza *meta*-cyclophane **30** is a little different. Firstly, in sharp contrast to what was found for tetraaza *para*-cyclophanes **29** [60a], the first protonation of the system **30** does not affect its benzylic nitrogen atoms. However, also in this ligand the entropy stabilization was attenuated by the presence of propylenic subunits. Secondly, the

next protonation steps seem to proceed randomly on the different N-atoms as long as both nitrogens separated by the ethylenic chain are simultaneously protonated. Thirdly, last proton binds **30** in the second N-atom of the ethylenic chain, which is the position mainly affected by unfavorable electrostatic repulsions between the same sign charges [60c].

On the other hand, an important role of intramolecular H-bonds playing in the flexibility of the tetraaza-2,2,-biphenylophanes **31** was investigated by ^1H NMR spectroscopy and MD simulations [117]. It was found that the ^1H NMR spectrum (in CDCl_3) of the largest studied system **31** ($x = 2, y = 3$), containing one butylenic and two propylenic spacers, did not change upon heating to 60°C . A similar situation was observed for the smallest macrocycle **31** ($x = y = 1$). Such a conformational rigidity of both these compounds was in sharp contrast to that found for two other systems **31** ($x = 2, y = 1, 2$) existing, under identical conditions, in fast equilibrium between two equivalent biphenyl rotamers. This behavior of the macrocycle **31** ($x = 2, y = 3$) was explained by a strong tendency to form an intramolecular H-bond bridging its central amino group. This H-bonding is especially stable due to the formation of an internal seven-membered ring that permits an almost linear disposition of the three atoms involved ($\text{N}-\text{H}\cdots\text{N}$) [117]. So, the larger macrocycles are not always more flexible.

A little other behavior was established for the large, 28-mer conformationally flexible tetraazamacrocyclic host **32** containing two oxamido units capable of complexing guest ions through O- and/or N-donor atoms [118]. Thus, single-crystal structure determinations of two its host-guest complexes demonstrated that this macrocycle is capable of complexing two NO_3^- anions at pH 3-4 (protonated form) or two copper(II) ions in the presence of aqueous solution of KOH (deprotonated form), involving a large structural reorganization in the whole macrocycle conformation on coordination of the Cu^{2+} cations when compared to the nitrate.

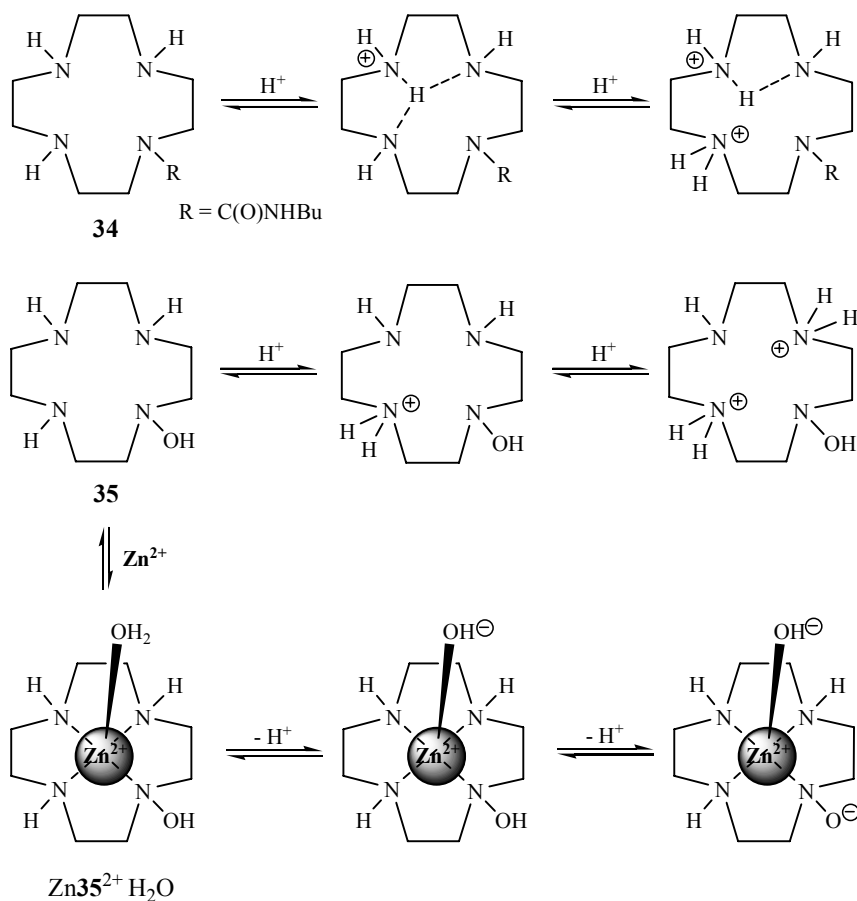


The quite other situation concerns the amide macrobicycles extensively studied by Smith and co-workers [119]. This ditopic salt receptor, shown as its complex **33** with bound salt M^+A^- , is able to extract a range of monovalent salts, *e.g.*, alkali halides, into CHCl_3 solution as associated ion-pairs, in sharp contrast to the action of typical polyoxa crown ethers (*vide supra*). The structures of this receptor complexed with KAcO , MNO_3 ($\text{M} = \text{Li}, \text{Na}, \text{K}$), and NaNO_2 were characterized in the solid state by an X-ray crystallography and in solution using an NMR spectroscopy. In this case, unusual NMR shielding effects were observed, such as upfield movements of the receptor NH proton signals upon salt complexation, apparently induced by the diamagnetic anisotropy of the aforementioned trigonal oxyanions encapsulated within the intramolecular 3D cavity.

Let us come back to tetraazacrowns. Two interesting *N*-substituted derivatives of cyclen (**4**), *i.e.*, amide compound **34** and *N*-hydroxy ligand **35**, were studied by König and co-

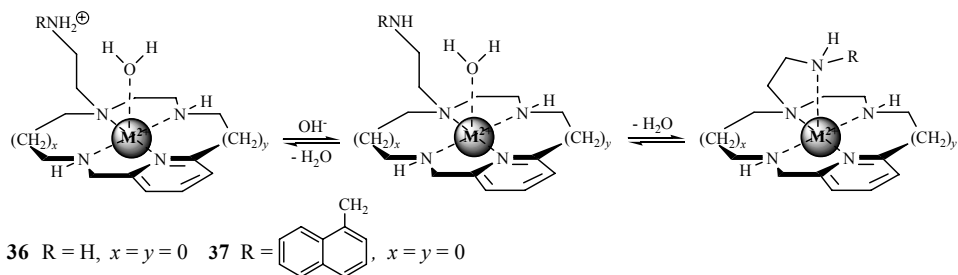
workers using only potentiometric titrations [120]. In comparison to the parent system **4** [having two N-atoms with high basicity (pK_a 11.0 and 9.9) and two remaining with low basicity ($pK_a < 2$)], compound **34** has one amino group with pK_a of 11.3, one with reduced basicity (pK_a 6.3), and one with low basicity ($pK_a < 2$) [120a]. Instead, hydroxylamine **35** shows markedly greater basicity; pK_a s of 11.6, 10.2, and 8.5 [121b]. So, an incorporation of the N–OH moiety into the azamacrocyclic ring system changes its N-basicity significantly.

Unfortunately, the authors did not perform related NMR pH-titration measurements and, so, no final assignment of pK_a s to the protonation of specific N-atoms was possible. The different (!) proposed protonation equilibria are presented in Scheme 1; final trivalent species H_3L^{3+} with the last protonated secondary amino group not shown. A neutral form of ligand **35** forms the zinc(II) chelate, *i.e.*, $Zn35^{2+} \cdot 2ClO_4^- \cdot H_2O$. Two pH dependent protonation equilibria were found; suggested protonation sequence is also given in Scheme 1. Generally, such hydrated structures involving participation of the divalent metal cation are typical for chelates formed by tetraazacrowns and similar to those previously found for the scorpionand-like ligands (Scheme 2) [21c,d,22,60d].

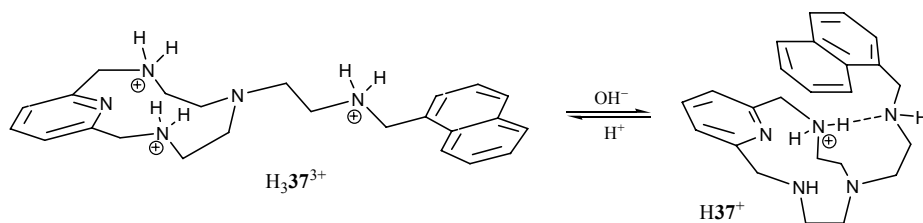


Scheme 1. Originally proposed protonation equilibria of the species **34**, **35** and $Zn35^{2+} \cdot H_2O$ [120].

Two interesting ligands of the above-mentioned type, *i.e.*, *N*-pendant arm derivatives **36** and **37** of the pyridine-containing compound **24** [70], were recently prepared and investigated in detail by Verdejo *et al.* [60d]. Thus, X-ray data on the monohydrates of the complexes $H_3\mathbf{37}^+ClO_4^-$ and $H_3\mathbf{37}^+(H_2PO_4^-)_3$, obtained at pH of 9 and 4, respectively, show the movement of the 2-aminoethyl pendant arm as a result of the change in the protonation degree of these macrocycles and the formation of an intramolecular H-bond. Similar results on two their copper(II) complexes show a great importance of the N-atom of the arm in the binding to the metal cation, as was earlier observed by others [21c,d,22]. Moreover, it was found that the pH-driven movement that performs the pendant arm in **36** and **37** function to bind or unbind the metal ion can also be achieved in the absence of any metal ion [60d].



Scheme 2. pH-Dependent coordination of the side-chain amino group in the scorpiand-like ligands [21c,d,22,60d].

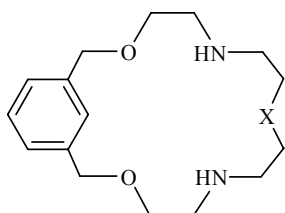


Scheme 3. pH-Driven molecular rearrangement found for **37** from X-ray diffraction data [60d].

The latter behavior, which has not been reported previously for other scorpiand-like ligands, is powered by the formation of intramolecular H-bonds between the amino group of the *N*-pendant arm and the protonated ammonium group in a macrocyclic core, with additional contributions from π - π stacking interactions between the naphthalene and pyridine rings. Both molecular movements associated to the changes of pH are presented in Schemes 2 and 3. In general, **36** and **37** can be regarded as functional models for molecular machines, because they contain a moving part, whose motion can be reversibly and repeatedly carried out. Indeed, these macrocycles convert the chemical energy into mechanical work and can be therefore considered as machines operating at the molecular level [121].

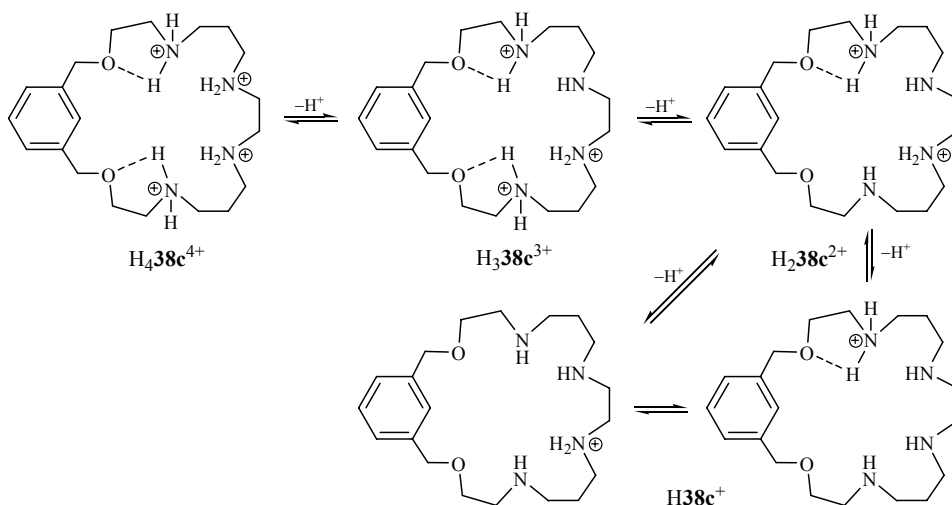
In final discussion we will say some words about results on dioxapolyaza cyclophanes **38a-d** as receptors for the anionic molecular subunits, which were reported by Burguete *et al.* [122]. It was found that the substitution of two methylene groups by two ethyleneoxy groups is reflected in higher basicity and significant increase in the $\log K$ values for the interaction

with nucleotides (AMP^{-2} , HADP^{-2} and HATP^{-3} , in particular) relative to that of related aza cyclophanes **29** and **30**. This can be generated either by a participation of O-atoms *via* H-bonding in the protonation process, or by providing additional conformational flexibility so that disadvantageous electrostatic repulsions are better accommodated in the macrocycle.



- 38a** X = $\text{CH}_2\text{-NH-CH}_2$
38b X = $\text{NH-(CH}_2)_2\text{-NH}$
38c X = $\text{CH}_2\text{-NH-(CH}_2)_2\text{-NH-CH}_2$
38d X = $\text{CH}_2\text{-NH-(CH}_2)_4\text{-NH-CH}_2$

All oxaza cyclophanes **38** were subjected to potentiometric and ^1H NMR pH-titrations. According to these mutually supplementing experimental data, related protonation sequences could be determined. Such a sequence proposed for **38c** is shown in Scheme 4. Two alternative forms of H_2L^{2+} and, especially, of H_1L^+ were generally found as coexisting for the macrocycles **38a-c**. Instead, protons located at the two central N-atoms were mostly found for the species $\text{H}_2\text{38b}^{2+}$ and $\text{H}_1\text{38b}^+$ with the large aliphatic (butylenic) spacer.



Scheme 4. Protonation sequence for macrocyclic pentaamine **38c** according to the ^1H NMR data and MM results [122].

5. CONCLUSION

Several selected problems of decisive meaning which are frequently met during the course of usually non-trivial studies on the acid-base behavior and pH-dependent molecular structures of typical and *N*-pendant-armed azacrown ligands **L** or the other structurally similar

hetera-azamacrocycles, were outlined in this short review. Simultaneously, a lot of practical solutions or ways of overcoming of such and similar issues were given. Especially, NMR measurements for the macrocyclic polyamines in aqueous solutions (including strongly acidic and strongly basic media), the determination of protonation mechanisms through ^1H and ^{13}C NMR pH-titrations, as well as various theoretic methods adequate for the polyazamacrocycles (molecular modeling), DFT-level computational results on neutral or charges forms of the azacrowns, and rational final statistical analysis of all of the data obtained in this way, were discussed in great detail.

An elucidation of overall conformations of the free polyamine macrocyclic ligands L , on the one hand, and subsequently formed protonated intermediates H_nL^{n+} , on the other, is very important for understanding the different aspects of their pH-driven gradually changing reorganizations in 3D space. Among the numerous polyazamacrocyclic ligands of this sort, polycarboxylate and polyphosphonate or such mixed chelators are especially important. The knowledge of conformational preferences of these and other N -pendant arm chelating systems in aqueous solution is thus of the utmost importance in predicting their complexational behavior, *i.e.*, the remarkable host-guest type interactions resulted from a complementary stereoelectronic arrangement of binding sites in the host and the guest, and understanding their mechanism of action.

Undoubtedly, all advanced experimental studies in this topic are of an interdisciplinary nature because of the necessity of intensive use of NMR spectroscopy in aqueous solutions, *i.e.*, pH-titrations and various 2D correlation experiments additionally performed depending on needs, which should be obligatorily supported by potentiometric measurements and specialized software. Also other structural techniques are often very useful, especially the single-crystal X-ray diffraction analysis. On the other hand, advanced MM modeling of the polyaza macrocycles of this sort followed by a theoretical quantum-chemical computational treatment involving the GIAO DFT calculations of NMR chemical shifts, performed at least for the gaseous phase (a 'free-molecule' approach), seems to be the additional indispensable supplement of all experimental results of this kind, at the current time. As it was shown here, an elucidation of overall conformations of the complicated pendant-arm molecular system of scorpianid (**3**) in the acidic media was possible only with a broad and parallel use of both these complementary approaches.

REFERENCES

- [1] (a) Pedersen, C. J. *J. Am. Chem. Soc.* **1967**, *89*, 2495-2496 (b) Pedersen, C. J. *J. Am. Chem. Soc.* **1967**, *89*, 7017-7036.
- [2] (a) Pedersen, C. J. *Angew. Chem.* **1988**, *100*, 1053-1059; *Angew. Chem., Int. Ed. Engl.* **1988**, *27*, 1021-1027. (b) Pedersen, C. J.; Frensdorff, H. K. *Angew. Chem.* **1972**, *84*, 16-26; *Angew. Chem., Int. Ed. Engl.* **1972**, *11*, 16-25.
- [3] Carey, F. A.; Sundberg, R. J. *Advanced Organic Chemistry. Part A: Structure and mechanisms*, 5th edition, Springer Science + Business Media, New York, 2007, pp. 363-364.
- [4] See, *e.g.*, (a) Cram, D. J. *Angew. Chem.* **1988**, *100*, 1041-1052; *Angew. Chem., Int. Ed. Engl.* **1988**, *27*, 1009-1020. (b) Gokel, G. W. *Crown Ether and Cryptands in:*

- Monographs in Supramolecular Chemistry*, Editor, Stoddard, J. F., The Royal Society of Chemistry, Cambridge, 1991 (c) *Crown Compounds: Towards Future Applications*, Editor, Cooper, S. R., VCH Publishers, Inc., New York, 1992.
- [5] Ranocchiarì, M.; Mezzetti, A. *Organometallics*, **2009**, *28*, 1286-1288 and refs therein.
- [6] See, e.g., (a) Christensen, J. J.; Eatough, D. J.; Izatt, R. M. *Chem. Rev.* **1974**, *74*, 351-384. (b) Izatt, R. M.; Bradshaw, J. S.; Nielsen, S. A.; Lamb, J. D.; Christensen, J. J.; Sen, D. *Chem. Rev.* **1985**, *85*, 271-339. (c) Izatt, R. M.; Pawlak, K.; Bradshaw, J. S.; Bruening, R. L. *Chem. Rev.* **1991**, *91*, 1721-2085. (d) Bradshaw, J. S.; Krakowiak, K. E.; Izatt, R. M. *Aza-Crown Macrocycles*, John Wiley & Sons, Inc., New York, 1993. (e) Izatt, R. M.; Pawlak, K.; Bradshaw, J. S.; Bruening, R. L. *Chem. Rev.* **1995**, *95*, 2529-2586.
- [7] Bosnich, B.; Poon, C. K.; Tobe, M. L. *Inorg. Chem.* **1965**, *4*, 1102-1108 and refs therein.
- [8] Van Alphen, J. *Recl. Trav. Chim. Pays-Bas.* **1937**, *56*, 343-350.
- [9] Park, C. H.; Simmons, H. E. *J. Am. Chem. Soc.* **1968**, *90*, 2431-2432.
- [10] (a) Lehn, J.-M. *Acc. Chem. Res.* **1978**, *11*, 49-57 and refs therein. (b) Motekaitis, R. J.; Martell, A. E.; Lehn, J.-M.; Watanabe, E.-I. *Inorg. Chem.* **1982**, *21*, 4253-4257.
- [11] Kubik, S.; Reyheller, C.; Stüwe, S. *J. Incl. Phenom. Macrocycl. Chem.* **2005**, *52*, 137-187.
- [12] (a) Richman, J. E.; Atkins, T. J., *J. Am. Chem. Soc.* **1974**, *96*, 2268-2270. (b) Atkins, T. J.; Richman, J. E.; Oettle, W. F. *Org. Synth.* **1978**, *58*, 86-98; *Org. Synth., Coll. Vol.* **1988**, *6*, 652-661.
- [13] (a) Hediger, M.; Kaden, T. A. *J. Chem. Soc., Chem. Commun.* **1978**, 14-15. (b) Leugger, A. P.; Herli, L.; Kaden, T. A. *Helv. Chim. Acta* **1978**, *61*, 2296-2306.
- [14] Burguete, M. I.; López-Diago, L.; García-España, E.; Galindo, F.; Luis, S. V.; Miravet, J. F.; Sroczynski, D. *J. Org. Chem.* **2003**, *68*, 10169-10171.
- [15] (a) Gokel, G. W.; Korzeniowski, S. H. *Macrocyclic Polyether Syntheses*, Springer-Verlag, Berlin, 1982, pp. 1-11. (b) Schalley, C. A. in: *Analytical Methods in Supramolecular Chemistry*, Editor, Schalley, C. A., Wiley-VCH Verlag GmbH & Co. KGaA, Weinheim, 2007, pp. 1-16.
- [16] (a) Delgado, R.; Fraústo da Silva, J. J. R. *Talanta* **1982**, *29*, 815-822. (b) Maitra, N.; Herlinger, A. W.; Jaselskis, B. *Talanta* **1988**, *35*, 231-234. (c) Chaves, S.; Delgado, R.; Fraústo da Silva, J. J. R. *Talanta* **1992**, *39*, 249-254.
- [17] (a) Thöm, V. J.; Fox, C. C.; Boeyens, J. C. A.; Hancock, R. D. *J. Am. Chem. Soc.* **1984**, *106*, 5947-5955. (b) Hancock, R. D.; Dobson, S. M.; Evers, A.; Wade, P. W.; Ngwenya, M. P.; Boeyens, J. C. A.; Wainwright, K. P. *J. Am. Chem. Soc.* **1988**, *110*, 2788-2794. (c) Hancock, R. D.; Wade, P. W.; Ngwenya, M. P.; de Sousa, A. S.; Damu, K. V. *Inorg. Chem.* **1990**, *29*, 1968-1974. (d) Chantson, T. E.; Hancock, R. D. *Inorg. Chim. Acta* **1995**, *230*, 165-167.
- [18] (a) Tabushi, I.; Okino, H.; Kuroda, Y. *Tetrahedron Lett.* **1976**, 4339-4342. (b) Tabushi, I.; Taniguchi, Y.; Kato, H. *Tetrahedron Lett.* **1977**, 1049-1052.
- [19] Su, X.-C.; Zhou, Z.-F.; Lin, H.-K.; Zhu, S.-R.; Sun, H.-W.; Zhao, G.-H.; Chen, Y.-T. *Can. J. Chem.* **2001**, *79*, 221-225 and refs therein.
- [20] Inoue, M. B.; Oram, P.; Inoue, M.; Fernando, Q. *Inorg. Chim. Acta* **1995**, *232*, 91-98 and refs therein.

- [21] (a) Alcock, N. W.; Kingston, R. G.; Moore, P.; Pierpoint, C. *J. Chem. Soc., Dalton Trans.* **1984**, 1937-1943. (b) Zhang, Z.; Mikkola, S.; Lönnberg, H. *Org. Biomol. Chem.* **2003**, *1*, 854-858. (c) Siegfried, L.; Honecker, M.; Schlageter, A.; Kaden, T. A. *Dalton Trans.* **2003**, 3939-3948. (d) Siegfried, L.; McMahon, C. N.; Kaden, T. A.; Palivan, C.; Gescheidt, G. *Dalton Trans.* **2004**, 2115-2124. (e) Füzervová, S.; Kotek, J.; Čísařová, I.; Hermann, P.; Binnemans, K.; Lukeš, I. *Dalton Trans.* **2005**, 2908-2915. (f) Lima, L. M. P.; Delgado, R.; Drew, M. G. B.; Brandão, P.; Félix, V. *Dalton Trans.* **2008**, 6393-6608 and refs therein.
- [22] Pallavicini, P. S.; Perotti, A.; Poggi, A. Seghi, B.; Fabbrizzi, L. *J. Am. Chem. Soc.* **1987**, *109*, 5139-5144.
- [23] Sun, Y.; Chen, D.; Martell, A. E.; Welch, M. J. *Inorg. Chim. Acta* **2001**, *324*, 180-187 and refs therein.
- [24] Stetter, H.; Frank, W. *Angew. Chem., Int. Ed. Engl.* **1976**, *15*, 686-686.
- [25] Keire, D. A.; Jang, Y. H.; Li, L.; Dasgupta, S.; Goddard III, W. A.; Shively, J. E. *Inorg. Chem.* **2001**, *40*, 4310-4318 and refs therein.
- [26] André, J. P.; Brücher, E.; Kiraly, R.; Carvalho, R. A.; Mäcke, H.; Geraldès, C. F. G. C. *Helv. Chim. Acta* **2005**, *88*, 633-646.
- [27] Albelda, M. T.; García-España, E.; Jiménez, H. R.; Llinares, J. M.; Soriano, C.; Sornosa-Ten, A.; Verdejo, B. *Dalton Trans.* **2006**, 4474-4481 and refs therein.
- [28] Beer, P. D.; Gale, P. A., *Angew. Chem., Int. Ed.* **2001**, *40*, 486-516.
- [29] Bazzicalupi, C.; Bencini, A.; Bianchi, A.; Fusi, V.; Paoletti, P.; Valtancoli, B. *J. Chem. Soc., Perkin Trans. 2*, **1994**, 815-820 and refs therein.
- [30] (a) Bernhardt, P. V.; Lawrance, G. A. *Coord. Chem. Rev.* **1990**, *104*, 297-343. (b) Martell, A. E.; Hancock, R. D. *Metal Complexes in Aqueous Solutions*, Plenum Press, New York, 1996.
- [31] Sabatini, L.; Fabbrizzi, L. *Inorg. Chem.* **1979**, *18*, 438-444.
- [32] (a) Geraldès, C. F. G. C.; Sherry, A. D.; Cacheris, W. P. *Inorg. Chem.* **1989**, *28*, 3336-3341. (b) Delgado, R.; Fraústo Da Silva, J. J. R.; Amorim, M. T. S.; Cabral, M. F.; Chaves, S.; Costa, J. *Anal. Chim. Acta* **1991**, *245*, 271-282.
- [33] Brucher, E.; Cortes, S.; Chavez, F.; Sherry, A. D. *Inorg. Chem.* **1991**, *30*, 2092-2097.
- [34] Letkeman, P.; Martell, A. E. *Inorg. Chem.* **1979**, *18*, 1284-1289.
- [35] (a) Gans, P.; Sabatini, A.; Vacca, A. *Talanta* **1996**, *43*, 1739-1753. (b) Peters, M.; Siegfried, L.; Kaden, T. A. *J. Chem. Soc., Dalton Trans.* **1999**, 1603-1607.
- [36] Alderighi, L.; Gans, P.; Ienco, A.; Peters, D.; Sabatini, A.; Vacca, A. *Coord. Chem. Rev.* **1999**, *184*, 311-318.
- [37] (a) Riedo, T. J.; Kaden, A. T. *Chimia* **1977**, *31*, 220-222. (b) Briellmann, M.; Kaderli, S.; Meyer, C. J.; Zuberbühler, A. D. *Helv. Chim. Acta* **1987**, *70*, 680-689. (c) Hancock, R. D.; Motekaitis, R. J.; Mashishi, J.; Cukrowski, I.; Reibenspies, J. H.; Martell, A. E. *J. Chem. Soc., Perkin Trans. 2*, **1996**, 1925-1929.
- [38] Sánchez-Moreno, M. J.; Gómez-Coca, R. B.; Fernández-Botello, A.; Ochocki, J.; Kotynski, A.; Griesser, R.; Sigel, H. *Org. Biomol. Chem.* **2003**, *1*, 1819-1826.
- [39] Szakács, Z.; Hägele, G. *Talanta*, **2004**, *62*, 819-825.
- [40] (a) Instrument Engineers' Handbook, Vol. 1: Process Measurement and Analysis, 4th edition, Editor-in Chief, Lipták, B. G., CRS Press, Boca Raton, 2003, pp.1578-1579. (b) Minimizing User Errors in pH Measurements: Features, Limitations & Potential Errors

- of the Tools of pH Measurements, Advanced Sensor Technologies, Inc., 603 North Poplar Street Orange, CA 92868-1011, USA; <http://www.astisensor.com>
- [41] Covington, A. K.; Paabo, M.; Robinson, R. A.; Bates, R. G. *Anal. Chem.* **1968**, *40*, 700-706 and refs therein.
- [42] Geraldès, C. F. G. C.; Alpoim, M. C.; Marques, M. P. M.; Sherry, A. D.; Singh, M. *Inorg. Chem.* **1985**, *24*, 3876-3881.
- [43] Geraldès, C. F. G. C.; Sherry, A. D.; Marques, M. P. M.; Alpoim, M. C.; Cortes, S. J. *Chem. Soc., Perkin Trans. 2*, **1991**, 137-146.
- [44] Desreux, J. F.; Merciny, E.; Loncin, M. F. *Inorg. Chem.* **1981**, *20*, 987-991.
- [45] Bhula, R.; Weatherburn, D. C. *J. Chem. Soc., Perkin Trans. 2*, **1988**, 1161-1164 and refs therein.
- [46] Amorim, M. T. S.; Ascenso, J. R.; Delgado, R.; Fraústo da Silva, J. J. R. *J. Chem. Soc., Dalton Trans.* **1990**, 3449-3455.
- [47] Li, N. C.; Tang, P.; Mathur, R. *J. Phys. Chem.* **1961**, *65*, 1074-1076 and refs therein.
- [48] Salomaa, P.; Schaleger, L. L.; Long, F. A. *J. Am. Chem. Soc.* **1964**, *86*, 1-7.
- [49] Mikkelsen, K.; Nielsen, S. O. *J. Phys. Chem.* **1960**, *64*, 632-637.
- [50] (a) Bates, R. G. *Determination of pH: Theory and Practice*, 2nd edition, John Wiley & Sons, Inc., New York, 1973, pp. 251-253, 375-376. (b) Popov, K.; Rönkkömäki, H.; Lajunen, L. H. *J. Pure Appl. Chem.* **2006**, *78*, 663-675.
- [51] (a) Ciampolini, M.; Micheloni, M.; Nardi, N.; Paoletti, P.; Dapporto, P.; Zanobini, F. *J. Chem. Soc., Dalton Trans.* **1984**, 1357-1362 and refs therein. (b) Clay, R. M.; Corr, S.; Micheloni, M.; Paoletti, P. *Inorg. Chem.* **1985**, *24*, 3330-3336.
- [52] Gottlieb, H. E.; Kotlyar, V.; Nudelman, A. *J. Org. Chem.* **1997**, *62*, 7512-7515.
- [53] (a) De Marco, A. *J. Magn. Reson.* **1977**, *26*, 527-528. (b) Wishart, D. S.; Bigam, C. G.; Yao, J.; Abildgaard, F.; Dyson, H. J.; Oldfield, E.; Markley, J. L.; Sykes, B. D. *J. Biomol. NMR.* **1995**, *6*, 135-140.
- [54] Delfini, M.; Segre, A. L.; Conti, F.; Barbucci, R.; Barone, V.; Ferruti, P. *J. Chem. Soc., Perkin Trans. 2*, **1980**, 900-903 and refs therein.
- [55] Bundi, A.; Wüthrich, K. *Biopolymers* **1979**, *18*, 299-311.
- [56] (a) Sudmeier, J. L.; Reilley, C. N. *Anal. Chem.* **1964**, *36*, 1698-1706. (b) Sudmeier, J. L.; Reilley, C. N. *Anal. Chem.* **1964**, *36*, 1707-1712. (c) Letkeman, P.; Westmore, J. B. *Can. J. Chem.* **1971**, *49*, 2086-2095.
- [57] (a) Beinert, W.-D.; Rüterjans, H.; Müller, F.; Bacher, A. *Eur. J. Biochem.* **1985**, *152*, 581-587. (b) Berman, E.; Lis, H.; James, T. L. *Eur. J. Biochem.* **1986**, *161*, 589-594. (c) Richter, G.; Weber, S.; Römisch, W.; Bacher, A.; Fischer, M.; Eisenreich, W. *J. Am. Chem. Soc.* **2005**, *127*, 17245-17252.
- [58] Gelb, R. I.; Schwartz, L. M.; Radeos, M.; Edmonds, R. B.; Laufer, D. A. *J. Am. Chem. Soc.* **1982**, *104*, 6283-6288.
- [59] (a) Kimberly, M. M.; Goldstein, J. H. *Anal. Chem.* **1981**, *538*, 789-793. (b) Kalinowski, H.-O.; Berger, S.; Braun, S. *Carbon-13 NMR Spectroscopy*, John Wiley & Sons, Chichester, 1988, pp. 85, 222-232. (c) The SUGABASE database, <http://boc.chem.uu.nl/sugabase/sugabase.html>. (d) Loß, A.; Stenutz, R.; Schwarzer, E.; von der Lieth, C. W. *Nucleic Acids Res.* **2006**, *34*, W733-W737.
- [60] (a) Bianchi, A.; Escuder, B.; García-España, E.; Luis, S. V.; Marcelino, V.; Miravet, J. F.; Ramírez, J. A. *J. Chem. Soc., Perkin Trans. 2*, **1994**, 1253-1259. (b) Bazzicalupi, C.; Bencini, A.; Bianchi, A.; Fusi, V.; Giorgi, C.; Paoletti, P.; Stefani, A.; Valtancoli, B. J.

- Chem. Soc., Perkin Trans. 2*, **1995**, 275-280 and refs therein. (c) Aguilar, J. A.; García-España, E.; Guerrero, J. A.; Luis, S. V.; Llinares, J. M.; Ramírez, J. A.; Soriano, C. *Inorg. Chim. Acta* **1996**, *246*, 287-294. (d) Verdejo, B.; Ferrer, A.; Blasco, S.; Castillo, C. E.; González, J.; Latorre, J.; Mániz, M. A.; Basallote, M. G.; Soriano, C.; García-España, E. *Inorg. Chem.* **2007**, *46*, 5707-5719.
- [61] Nazarski, R. B.; Pasternak, B. unpublished results.
- [62] (a) Sarneski, J. E.; Surprenant, H. L.; Molen, F. K.; Reilley, C. N. *Anal. Chem.* **1975**, *47*, 2116-2124 and refs therein. (b) Rabenstein, D. L.; Sayer, T. L. *J. Magn. Reson.* **1976**, *24*, 27-39. (c) Surprenant, H. L.; Sarneski, J. E.; Key, R. R.; Byrd, J. T.; Reilley, C. N. *J. Magn. Reson.* **1980**, *40*, 231-243. (d) Appleton, T. G.; Hall, J. R.; Harris, A. D.; Kimlin, H. A.; McMahan, I. J. *Aust. J. Chem.* **1984**, *37*, 1833-1840. (e) Dagnall, S. P.; Hague, D. N.; McAdam, M. E. *J. Chem. Soc., Perkin Trans. 2*, **1984**, 435-440. (f) Dagnall, S. P.; Hague, D. N.; McAdam, M. E.; Moreton, A. D. *J. Chem. Soc., Faraday Trans. 1*, **1985**, *81*, 1483-1494. (g) Głowacki, Z.; Hoffmann, M. *Magn. Reson. Chem.* **1990**, *28*, 184-186. (h) Hague, D. N.; Moreton, A. D. *J. Chem. Soc., Perkin Trans. 2*, **1994**, 265-270.
- [63] (a) Wüthrich, K. *NMR in Biological Research: Peptides and Proteins*, North Holland, Amsterdam, 1976. (b) Richarz, R.; Wüthrich, K. *Biopolymers*, **1978**, *17*, 2133-2141.
- [64] Live, D. H.; Chan, S. I. *Anal. Chem.* **1970**, *42*, 791-792 and refs therein.
- [65] (a) Dagnall, S. P.; Hague, D. N.; McAdam, M. E. *J. Chem. Soc., Perkin Trans. 2*, **1984**, 1111-1114. (b) Frassinetti, C.; Alderighi, L.; Gans, P.; Sabatini, A.; Vacca, A.; Ghelli, S. *Anal. Bioanal. Chem.* **2003**, *376*, 1041-1052.
- [66] Sroczyński, D.; Grzejdzia, A.; Nazarski, R. B. *J. Incl. Phenom. Macrocycl. Chem.* **1999**, *35*, 251-260.
- [67] Creaser, S. P.; Lincoln, S. F.; Pyke, S. M. *J. Chem. Soc., Perkin Trans. 1*, **1999**, 1211-1213.
- [68] Cohen, J. S.; Shrager, R. I.; McNeel, M.; Schechter, A. N. *Nature* **1970**, *228*, 642-644 and refs therein.
- [69] Rabenstein, D. L.; Sayer, T. L. *Anal. Chem.* **1976**, *48*, 1141-1146.
- [70] Costa, J.; Delgado, R. *Inorg. Chem.* **1993**, *32*, 5257-5265.
- [71] Martin, B. R. *Science*, **1963**, *139*, 1198-1203.
- [72] Frassinetti, C.; Ghelli, S.; Gans, P.; Sabatini, A.; Moruzzi, M. S.; Vacca, A. *Anal. Biochem.* **1995**, *231*, 374-382.
- [73] Grunwald, E.; Loewenstein, A.; Meiboom, S. *J. Chem. Phys.* **1957**, *27*, 641-642.
- [74] Sroczyński, D. Protolytic properties and complexes of some polyazamacrocyclic amines with the silver ions (in Polish), Ph.D. Thesis, University of Łódź, Łódź, Poland, 1999.
- [75] Nazarski, R. B.; Sroczyński, D. poster P-32 at the *IIIrd Symposium on Application of Magnetic Resonance in Chemistry and Related Areas*, Warsaw, Poland, June 24-26, 1998, Book of Abstracts, P-32.
- [76] Ascenso, J. R.; Delgado, R.; Fraústo da Silva, J. J. R. *J. Chem. Soc., Perkin Trans. 2*, **1985**, 781-788.
- [77] Nazarski, R. B. *Magn. Reson. Chem.* **2003**, *41*, 70-74.
- [78] Nazarski, R. B.; Sroczyński, D.; Urbaniak, P.; Dziegieć, J.; Grzejdzia, A., poster SB-I16 at the *36th IUPAC Congress*, Geneva, Switzerland, August 17-22, 1997 (*Chimia* **1997**, *51*, 432).

- [79] Fensterbank, H.; Berthault, P.; Larpent, C. *Eur. J. Org. Chem.* **2003**, 3985-3990.
- [80] Nazarski, R. B. *J. Phys. Org. Chem.* **2009**, *22*, xxx-xxx. (Published Online: Mar 9 2009. DOI: 10.1002/poc.1529)
- [81] The useful working labeling *a-l* of methylenic nuclei in the pentaamine **3** is shown in Formula **26**. Instead, the arbitrary notation 1-12, which was also used throughout this work, is given in Fig. 3.
- [82] In the original paper, Ref. 80, the atoms C4-C8 and sites N³/N⁴ were erroneously given as associated with these equilibria.
- [83] Nazarski, R. B., unpublished results.
- [84] Breitmaier, E. *Structure Elucidation by NMR in Organic Chemistry: A Practical Guide*, John Wiley & Sons, Chichester, 1993, Chapter 2.6.2.
- [85] (a) Nazarski, R. B., will be presented at the *Vth Symposium on NMR in Chemistry, Physics and Biological Sciences*, Warsaw, Poland, September 23-25, 2009, Book of Abstracts, poster P-xx. (b) Nazarski, R. B., to be submitted for publication.
- [86] Cascio, S.; De Robertis, A.; Foti, C. *Fluid Phase Equilib.* **2000**, *170*, 167-181 and refs therein.
- [87] Nazarski, R. B. *Mol. Phys. Rep.* **2000**, *29*, 176-179.
- [88] PCMODEL V 8.5, Molecular Modeling Software for Windows Operating System, Apple Macintosh OS, Linux and Unix, Serena Software, Box 3076, Bloomington, IN 47402-3076, USA, August 2003.
- [89] (a) Saunders, M. *J. Am. Chem. Soc.* **1987**, *109*, 3150-3152. (b) Saunders, M.; Houk, K. N.; Wu, Y.-D.; Still, W. C.; Lipton, M.; Chang, G.; Guida, W. C. *J. Am. Chem. Soc.* **1990**, *112*, 1419-1427 and refs therein.
- [90] (a) Jorgensen, W. L.; Maxwell, D. S.; Tirado-Rives, J. *J. Am. Chem. Soc.* **1996**, *118*, 11225-11236. (b) Rizzo, R. C.; Jorgensen, W. L. *Am. Chem. Soc.* **1999**, *121*, 4827-4836. (c) Tirado-Rives, J. *OPLS and OPLS-AA Parameters for Organic Molecules, Ions, and Nucleic Acids*, Yale University, New Haven, CT 065520-8107, USA, November 2000.
- [91] (a) Wolinski, K.; Hilton, J. F.; Pulay, P. *J. Am. Chem. Soc.* **1990**, *112*, 8251-8260 and refs therein. (b) Rauhut, G.; Puyear, S.; Wolinski, K.; Pulay, P. *J. Phys. Chem.* **1996**, *100*, 6310-6316. (c) Cheeseman, J. R.; Trucks, G. W.; Keith, T. A.; Frisch, M. J. *J. Chem. Phys.* **1996**, *104*, 5497-5509. (d) Foresman, J. B.; Frisch, M. *Exploring Chemistry with Electronic Structure Methods*, 2nd edition, Gaussian, Inc. Pittsburgh, PA 15106, USA, 1996. Chapter 4 + Errata. (e) Forsyth, D. A.; Sebag, A. B. *J. Am. Chem. Soc.* **1997**, *119*, 9483-9494. (f) Wiberg, K. B. *J. Comput. Chem.* **1999**, *20*, 1299-1303. (g) Aminova, R. M.; Schamov, G. A.; Aganov, A. V. *J. Mol. Struct. Theochem* **2000**, *498*, 233-246 and refs therein. (h) Wiitala, K. W.; Hoye, T. R.; Cramer, C. J. *J. Chem. Theory Comput.* **2006**, *2*, 1085-1092.
- [92] Michalik, E.; Nazarski, R. B. *Tetrahedron* **2004**, *60*, 9213-9222.
- [93] (a) Barone, G.; Duca, D.; Silvestri, A.; Gomez-Paloma, L.; Riccio, R.; Bifulco, G. *Chem. Eur. J.* **2002**, *8*, 3240-3245. (b) Tähtinen, P.; Bagno, A.; Klika, K. D.; Pihlaja, K. *J. Am. Chem. Soc.* **2003**, *125*, 4609-4618 and refs therein.
- [94] (a) Mennucci, B.; Tomasi, J. *J. Chem. Phys.* **1997**, *106*, 5151-5158. (b) Cancès, E.; Mennucci, B.; Tomasi, J. *J. Chem. Phys.* **1997**, *107*, 3032-3041. (c) Cossi, M.; Barone, V.; Mennucci, B.; Tomasi, J. *Chem. Phys. Lett.* **1998**, *286*, 253-260.

- [95] (a) A. L. Spek, *J. Appl. Cryst.* **2003**, *36*, 7-13. (b) A. L. Spek, *PLATON, A Multipurpose Crystallographic Tool*, Version 230203, Utrecht University, Utrecht, The Netherlands, **2003**; <http://www.cryst.chem.uu.nl/platon>.
- [96] Nazarski, R. B., poster P-95 at the *6th International Conference on Heteroatom Chemistry*, Łódź, Poland, June 22-27, 2001; Book of Abstracts, p. 223.
- [97] A full conformational investigations on macrocycles **1-3** (including equilibria between their multiple ring forms and a deeper analysis of the formed intramolecular H-bonds) is still in progress. Its final results will be published elsewhere.
- [98] Hunter, K. A. *Acid-base Chemistry of Aquatic Systems*, University of Otago, Dunedin, New Zealand, 1998.
- [99] The pH symbol was erroneously used instead of pD* in the description of x-axes for pH-titration curves presented in Figs 1 and 2 in Ref. 66. Unfortunately, the same also concerns traces of ^{13}C NMR spectra of ligand **2** originally shown in the Fig. 1 in our latter work (Ref. 87). Both these facts were noticed during the preparation of this chapter.
- [100] Sroczyński, D., unpublished work (Ref. 74). *PlotPhi*, The C computer program generating distribution plots of the species H_nB^{n+} (where **B** = any *n*-protic base) according to the stepwise macroscopic protonation constants $K_{i,i+1}^{\text{H}} = [\text{H}_i\text{B}^{i+}]/[\text{H}_{i-1}\text{B}^{(i-1)+}][\text{H}^+]$, $i = 1\sim n$, by using general formulas given in: J. Inczédy, *Analytical Applications of Complex Equilibria*; E. Horwood, Ltd., Chichester, 1976, Chapter 1.
- [101] See, e.g., Szakács, Z.; Kraszni, M.; Noszál, B. *Anal. Bioanal. Chem.* **2004**, *378*, 1428-1448 and refs therein.
- [102] Curtiss, L. A.; Raghavachari, K.; Redfern, P. C.; Pople, J. A. *Chem. Phys. Lett.* **1997**, *270*, 419-426.
- [103] Scott, A. P.; Radom, L. *J. Phys. Chem.* **1996**, *100*, 16502-16513.
- [104] (a) van Eikema Hommes, N. J. R.; Clark, T. *J. Mol. Model.* **2005**, *11*, 175-185. (b) Dybiec, K.; Gryff-Keller, A. *Magn. Reson. Chem.* **2009**, *47*, 63-66 and refs therein.
- [105] Chesnut, D. B. *The Ab Initio Computation of Nuclear Magnetic Resonance Chemical Shielding* in: *Reviews in Computational Chemistry*, Editors, Lipkowitz, K. B.; Boyd, D. B., VCH Publishers, Inc., New York, 1996, Vol. 8, pp.245-297.
- [106] Aliev, A. E.; Courtier-Murias, D.; Zhou, S. *J. Mol. Struct. Theochem* **2009**, *893*, 1-5 and refs therein.
- [107] (a) Svensson, M.; Humbel, S.; Froese, R. G. J.; Matsubara, T.; Sieber, S.; Morokuma, K. *J. Phys. Chem.* **1996**, *100*, 19357-19363. (b) Dapprich, S.; Komáromi, I.; Byun, K. S.; Morokuma, K.; Frisch, M. J. *J. Mol. Struct. Theochem* **1999**, *461/462*, 1-12. (c) Tschumper, G. S.; Morokuma, K. *J. Mol. Struct. Theochem*, **2002**, *592*, 137-147. (d) Jiang, N.; Yuan, S.; Wang, J.; Jiao, H.; Qin, Z.; Li, Y.-W. *J. Mol. Catal. A* **2004**, *220*, 221-228.
- [108] *Gaussian[®] 03, Revision E.01*, Frisch, M. J.; Trucks, G. W.; Schlegel, H. B.; Scuseria, G. E.; Robb, M. A.; Cheeseman, J. R.; Montgomery, J. A., Jr.; Vreven, T.; Kudin, K. N.; Burant, J. C.; Millam, J. M.; Iyengar, S. S.; Tomasi, J.; Barone, V.; Mennucci, B.; Cossi, M.; Scalmani, G.; Rega, N.; Petersson, G. A.; Nakatsuji, H.; Hada, M.; Ehara, M.; Toyota, K.; Fukuda, R.; Hasegawa, J.; Ishida, M.; Nakajima, T.; Honda, Y.; Kitao, O.; Nakai, H.; Klene, M.; Li, X.; Knox, J. E.; Hratchian, H. P.; Cross, J. B.; Bakken, V.; Adamo, C.; Jaramillo, J.; Gomperts, R.; Stratmann, R. E.; Yazyev, O.; Austin, A. J.;

- Cammi, R.; Pomelli, C.; Ochterski, J. W.; Ayala, P. Y.; Morokuma, K.; Voth, G. A.; Salvador, P.; Dannenberg, J. J.; Zakrzewski, V. G.; Dapprich, S.; Daniels, A. D.; Strain, M. C.; Farkas, O.; Malick, D. K.; Rabuck, A. D.; Raghavachari, K.; Foresman, J. B.; Ortiz, J. V.; Cui, Q.; Baboul, A. G.; Clifford, S.; Cioslowski, J.; Stefanov, B. B.; Liu, G.; Liashenko, A.; Piskorz, P.; Komaromi, I.; Martin, R. L.; Fox, D. J.; Keith, T.; Al-Laham, M. A.; Peng, C. Y.; Nanayakkara, A.; Challacombe, M.; Gill, P. M. W.; Johnson, B.; Chen, W.; Wong, M. W.; Gonzalez, C.; Pople, J. A.; Gaussian, Inc.: 340 Quinnipiac St., Bldg. 40, Wallingford, CT 06492, USA, September 11, 2007.
- [109] Jorgensen, W. L.; Chandrasekhar, J.; Madura, J. D.; Impey, R. W.; Klein, M. L. *J. Chem. Phys.* **1983**, *79*, 925-935.
- [110] HyperChem. Molecular Modeling System. Release 7.0 for Windows. Hypercube Inc., Gainesville, FL 32601, USA, January **2002**.
- [111] Mayo, S. L.; Olafson, B. D.; Goddard III, W. A. *J. Phys. Chem.* **1990**, *94*, 8897-8909.
- [112] Domagała, M.; Nazarski, R. B., poster A-17 at the *46th Polish Crystallographic Meeting*, Wrocław, Poland, June 24-25, 2004, Book of Abstracts, p. 55.
- [113] Mercury 2.2 (Build RC5), Copyright Cambridge Crystallographic Data Centre, 2001-2008; <http://www.ccdc.cam.ac.uk/mercury>.
- [114] Harrowfield, J. M.; Miyamae, H.; Shand, T. M.; Skelton, B. W.; Soudi, A. A.; White, A. H. *Aust. J. Chem.* **1996**, *49*, 1051-1066.
- [115] Meyer, M.; Dahaoui-Gindrey, V.; Lecomte, C.; Guillard, R. *Coord. Chem. Rev.* **1998**, *178-180*, 1313-1405 and refs therein.
- [116] Holzberger, A.; Holdt, H.-J.; Kleinpeter, E. *Org. Biomol. Chem.* **2004**, *2*, 1691-1697.
- [117] Burguete, M. I.; Escuder, B.; García-España, E.; López, L.; Luis, S.; Miravet, J. F.; Querol, M. *Tetrahedron Lett.* **2002**, *43*, 1817-1819.
- [118] Cronin, L.; McGregor, P. A.; Parsons, S.; Teat, S.; Gould, R. O.; White, V. A.; Long, N. J.; Robertson, N. *Inorg. Chem.* **2004**, *43*, 8023-8029.
- [119] Mahoney, J. M.; Stucker, K. A.; Jiang, H.; Carmichael, I.; Brinkmann, N. R.; Beatty, A. M.; Noll, B. C.; Smith, B. D. *J. Am. Chem. Soc.* **2005**, *127*, 2922-2928 and refs therein.
- [120] (a) König, B.; Pelk, M.; Subat, M.; Dix, I.; Jones, P. G. *Eur. J. Org. Chem.* **2001**, 1943-1949. (b) Reichenbach-Klinke, R.; Zabel, M.; König, B. *Dalton. Trans.* **2003**, 141-145.
- [121] Castillo González, C. E.; Verdejo, B.; Ferrer, A.; Blasco, S.; González, J.; Latorre, J.; Máñez, M. A.; Basallote, M. G.; Soriano, C.; García-España, E., an oral presentation at the *9th European Biological Inorganic Chemistry Conference (EUROBIC9)*, Wrocław, Poland, September 2-6, 2008, Book of Abstracts, p.108.
- [122] Burguete, M. I.; García-España, E.; López-Diago, L.; Luis, S. V.; Miravet, J.; Sroczynski, D. *Org. Biomol. Chem.* **2007**, *5*, 1935-1944.

*Chapter 2***CALIXARENE COMPLEXES WITH SOLVENT
MOLECULES***O. V. Surov, M. I. Voronova and A. G. Zakharov*Institute of Solution Chemistry, Russian Academy of Sciences, 153045,
Ivanovo, Academicheskaya Str, 1, Russia.**ABSTRACT**

Solid calixarenes as receptors are characterized by phase transitions, which occur in binding of neutral molecules of guest compounds with the formation of clathrates or guest–host intercalation compounds. The binding of a guest by a solid host compound is largely a cooperative process. It begins after the attainment of a certain threshold thermodynamic activity (relative pressure p/p_0) of the guest and is completed in a narrow range of p/p_0 values. The process of clathrate formation in the binding of a guest by a host is accompanied by a significant rearrangement of the packing of host molecules, and the result of this rearrangement can depend considerably on the molecular structure of the guest. Moreover, the “induced correspondence” of the clathrate structure to the molecular structure of the guest is observed; in some cases, this effect endows solid hosts with improved selectivity.

Scattered information is available as to guest-removal, -addition, and -exchange properties of many host systems, including calix[n]arene derivatives. Upon recrystallization, host can form stoichiometric guest-host adducts, where guest molecules are included in each cavity maintained by the hydrogen-bonded network of the host. Volatile guests can be removed upon heating, to give polycrystalline guest-free apohost. The apohost subsequently binds various guests not only as liquids or gases but also, in some cases, as solids in the same guest-host stoichiometry as in recrystallization. The resulting adducts exhibit the same X-ray powder diffractions as the corresponding single-crystalline samples. Guest exchange also occurs. Despite such phenomenologically rich information, we are still far away from a thorough understanding of how solid-state complexation takes place. There are number of fundamental questions which are related to each other: Do the solid host and its solid adduct share the same phase or constitute different phases? Do guest-binding cavities maintained by an organic network survive or collapse upon guest- removal? How do guest molecules diffuse in the solid host?

INTRODUCTION

Calix[n]arenes represent an interesting class of preorganized aromatic hosts exhibiting an enhanced ability for cation- π interaction and inclusion of small neutral organic guests. In many biological systems, metal cation- π interactions play an important role in molecular recognition, and atmospheric detection of odorant vapours of organic compounds is one of the most important problems of environment monitoring. Moreover the recognition of neutral organic molecules and cations by synthetic receptors is a topic of current interest in supramolecular and analytical chemistry. It was shown that some compounds such crown ethers and calixarenes forming inclusion complexes with some organic guest molecules and cations can be used for the development of sensors and components of microelectronic systems [1]. The growing interest in these materials is due to the simplicity of their synthesis, thermal stability and the extreme ease of deposition under thin film form [2-5]. From the study of crystal structures of calixarene hosts including organic molecules and research of host-guest calixarene chemistry in the gas phase by mass spectroscopy as well as results obtained by solution chemistry, several conclusions of general validity were drawn [6]. Probably, the strength of the host-guest interaction depends on the potential guest molecule nature, the cavity size and the conformation of the macrocycles, substituents on the upper and lower rim of the calixarenes which influence the cavity size, the conformation and the flexibility of the host molecule, the number of the ligating sites of the host (e.g., the number of the oxygen atoms in the polyether ring). In spite of available facts, conclusions regarding the relationship between the structure and the binding properties of a particular host are rather difficult because of the complex relations between the complex formation constants and the structure of both the host and the guest molecules.

There is evidence that the small neutral guest selectivity in the cavity of solid calixarene host is closely related to the free energy of complexation in solution [7]. In the last ten years, host-guest chemistry in the gas phase has been studied by mass spectroscopy [8], and it turns out that the ionization mode determines whether the results obtained by mass spectroscopy reflect those of solution chemistry. Shinkai *et al.* [9] have studied organic cation complexes with several calix[n]arenes of differing conformation and ring size by the use of positive secondary ion mass spectrometry. Relative peak intensities have been shown to reflect the complex stability in the gas phase but selectivity of the complexation with respect to the size of both the host and the guest differs greatly from that observed in solution. Whereas the conformation selectivity found in the gas phase paralleled that of the solution, the hole-size selectivity of guests was found to be different for the gas and the condensed phases. Despite the enormous work developed to characterize calixarene receptors and investigate their chemistry in solution, very few studies have been undertaken to date to investigate the interaction between them and organic guest molecules in the gas phase [10]. However gas-phase studies provide interesting perspective for host-guest interactions. As the solvent is absent, no solvation effects can modify the electronic and thermodynamic properties nor the geometrical constraints of supramolecular binding, so that pure intrinsic interaction between the two counterparts is uncovered, free from any third-body influence.

There has been much recent interest in organic and metal-organic network materials whose guest-binding properties are reminiscent of traditional zeolites. Lattice inclusion compounds have so far been studied mostly from the static viewpoint (stoichiometry, crystal

structure, selectivity, etc.) on recrystallized host-guest adducts. In the context of zeolite analogues, it is also essential to know how preformed solid hosts interact with guests.

As was shown in a study of polymorphism by Atwood *et al.* [11, 12], under certain conditions, the wellknown compound-host, *p*-tert-butylcalix[4]arene, underwent a phase transitions in single crystals. The authors showed that *p*-tert-butylcalix[4]arene could form a bilayer-type structure, where calixarenes are slightly shifted relative to each other. This results in the formation of isolated cavities with approximate volume 235 Å³ per dimeric unit. In spite of the inaccessibility of these cavities, the crystal is capable of adsorption of guest molecules into its lattice with a side shift of adjacent bilayers relative to each other. The surface of bilayers is formed by bulky *tert*-butyl groups alternating with calixarene cavities and gaps between neighboring *tert*-butyl fragments. It is therefore easy to image how neighboring layers can slip one above other favoring the absorption or removal of guests in the intercalation reaction of the solid–liquid or solid–vapor type.

The temperature dependences of vapor pressure of some calix[4]arenes and their complexes with solvent molecules were determined by the Knudsen effusion method [13, 14]. It was found that calix[4]arenes could form intramolecular compounds with solvents retaining their stoichiometric composition during sublimation. Molecules of organic solvents intercalated into calix[4]arene cavities then stabilize the crystal lattice by increasing the enthalpy of sublimation.

On the other hand, some attempts were made to study the adsorption of organic vapors on calixarene thin films prepared by various methods including Langmuir–Blodgett deposition, centrifugation, and self-assembly. It should be noted that the adsorption on films is very often a nonselective process, because the compounds under investigation behave similarly, which is indicative of weak nonspecific interactions between guest molecules and calixarene films [1]. As distinct from crystalline samples, the binding of neutral guests by calixarene films is not a cooperative process accompanied by the formation of a new host–guest phase.

Calixarenes are often used in modeling membrane transport in biological systems because of their unique conformational properties. The size, shape, and electrostatic profile of biological pores are considered basic determining factors of their functioning. The intuitively simple idea of molecular transport through some matrix suggests the presence of channels of the appropriate size limited by van der Waals surfaces. The molecular hydrodynamics, for example, can be considered only when the narrowest part of the channel is at least sufficiently wide for the passage of a separate water molecule. The problems of transport of small mobile molecular particles through a hydrophobic matrix, in particular, water through a thiacalixarene crystal, are discussed in [15, 16]. The conclusion was made that the traditional concept of a porous crystal structure could be incorrect. The formation of clathrates of thiacalixarenes differs essentially from water sorption on activated carbon, where a “step” in the sorption isotherm is supposedly caused by the formation of water clusters [17], and step sorption on zeolites, which are characterized by structure deformation after a significant primary sorption in micropores.

Crystal Structures of Calixarene Complexes

Many of the calixarenes form crystalline complexes in the solid state with a variety of small molecules, this property having been observed even before the basic structures of the calixarenes were established. For example, *p*-tert-butylcalix[4]arene forms complexes with chloroform, toluene, pyridine [18], benzene, xylene and anisole [19]; *p*-tert-butylcalix[5]arene forms complexes with isopropyl alcohol [20] and acetone [21]; *p*-tert-butylcalix[6]arene forms a complex containing chloroform and methanol [18]; *p*-tert-butylcalix[7]arene forms a complex containing methanol [22]; *p*-tert-butylcalix[8]arene forms a complex with chloroform [18]; *p*-tert-butylidihomooxalix[4]arene forms a complex with methylene chloride [18]. That the guest molecule is located within the calix of the host molecule is indicated by the X-ray crystallographic pictures of the cyclic tetramer [23] and cyclic pentamer complexes [21]. Derivatives of the calixarenes also frequently show a marked tendency to form complexes. For example, the tetraacetate of *p*-tert-butylcalix[8]arene retains methanol, chloroform, and ethyl acetate far more tightly than does the parent compound [24].

It is well known that calix[4]arenes, particularly when in their *cone* conformation, possess an intramolecular cavity which can host neutral guest molecules of complementary size [25]. Larger calix[*n*]arenes are also known to form inclusion complexes but because of the usually greater conformational flexibility of these macrocycles and the relatively limited range of studies so far made of them, the factors controlling their inclusion selectivity are not well understood. Calix[4]arenes showed good inclusion properties, in particular with aromatic guests, in the solid state but not in solution [25, 26]. Only recently was it verified that in these media the calixarene cavity can host neutral organic molecules of complementary size. It was also established that the efficiency of the recognition process is strongly determined by the rigidity of the hosts and by the nature of the guest, which should bear acid CH-groups. On this basis it has been hypothesised that specific CH- π interactions stabilise the complexes formed [27-29].

Numerous crystallographic studies have been made of complexes of neutral organic molecules having acidic CH-groups with calix[4]arenes, calix[4]resorcinols and thiacalix[4]arenes in the *cone* conformation. Data retrieved from the Cambridge Structural Database (CSD) concern inclusion resulting fortuitously from the choice of recrystallisation solvent as well as studies deliberately focussed on inclusion complex formation [30]. The influences of molecular symmetry and guest acidity were important issues in the latter group. Solid state structural determinations are frequently complicated by "disorder" problems which have often not been fully resolved [31].

There is the plethora of X-ray crystal structures reported for calixarene complexes, for example with acetonitrile [32, 33-49] and dichloromethane [33, 50-62]. The crystal structures of *p*-tert-butylcalix[4]arene complexes with long-chain guests such as *n*-hexane, 1-pentanol, 1-octanol, dodecan are also well-known [31]. The crystal structures of calix[4]arene *bis*(crown ether)s and their solvent complexes reported up to now are summarized in review article [63].

Concurrent Insertion of Solvent Molecules in Solutions

p-Tert-butylcalix[4]arene appears to show little or no selectivity in complexing chloroform and toluene, as indicated by the data on aromatic solvent induced shift (ASIS) and by the fact that strong endo-calix complexes are formed with both of these solvent molecules in the solid state [64]. With any exceptions, for example, complexes with amines, attempts to find guest molecules that can form endo-calix complexes with a calix[4]arene in chloroform solution have been unsuccessful. The problem apparently arises from the fact that the putative guest compounds do not form complexes that are strong enough to “out-compete” the chloroform to an extent sufficient to make the guest detectable by spectral means. The compounds tested included anisole, nitrobenzene, *p*-xylene, bromobenzene, (trichloromethyl)benzene, (trifluoromethyl)benzene, acetone, tert-butylcyclohexanol, *p*-tert-butylphenol, benzonitrile, acetonitrile, (trimethylaceto)nitrile, and phenylacetylene. The host molecules used were *p*-allyl-calix[4]arene and its tetra-*p*-toluenesulfonate, the latter being chosen because it is known to be fixed in the cone conformation and, therefore, to possess an “enforced cavity” [65]. Concentrations up to 10% of the “guest” molecules were used, and changes in ¹H NMR spectral shifts and coalescence temperatures for conformational inversion in the case of the parent calixarene were sought. In no case, however, were significant changes observed. *p*-2-Hydroxyethylcalix[4]arene and its *p*-toluenesulfonate are soluble in a 3:1 mixture of acetonitrile and water. It was hoped that complex formation might be demonstrated in these cases as the result of the lipophobic forces that presumably account for the formation of complexes of cyclodextrins in Me₂SO solution. However, the ¹H NMR spectra of CH₃CN/H₂O solutions of *p*-2-hydroxyethylcalix[4]arene (or its tosylate) in (trichloromethyl)benzene, toluene, chloroform, benzonitrile, or *p*-nitrophenol showed no significant changes. Similar results were obtained when 3:1 Me₂SO/H₂O was used as the solvent. The failure to observe complex formation may again arise from competition between the solvent components (H₂O, CH₃CN, Me₂SO) and the putative guest molecules for complexation with the calixarenes.

Representative examples demonstrate that in liquid phase, the solvent alters the stability of the complex in a selective way [66, 67]. Many findings indicate that the solvent effect plays an important role in complexation processes involving ionic or neutral species and macrocyclic ligands in general and calixarenes in particular [68-72].

Danil de Namor's group is very active in the field of the thermodynamic studies of calixarenes which deal with the equilibrium of complex formation with alkali ions and the effects of the solvent [73]. They also studied the thermodynamics of the interactions of calixarenes with ions and neutral molecules. During the investigations they change the applied calixarene host, the guest molecule or ion and the solvent. More than 10 years ago [74] Danil de Namor summarized the problems in the thermodynamics of macrocycles. The role of the reaction media was pointed out in the binding properties of the calixarene esters toward the alkali metal ions. In this field, the properties of the lithium complexes have special importance for constructing high capacity accumulators. The thermodynamics of the dissolution of calixarene derivatives substituted by polar groups at the lower rim was in the focus of Ref. [75]. The solutes are esters with *N*-di(isopropyl)carbamic acid and ethers with 2-hydroxypyridine moieties substituting all the four lower rim hydroxy groups. The applied polar solvents were nitriles, alcohols and *N,N*-dimethylformamide among others. The free energy, enthalpy and entropy of solution were calculated from solubility and calorimetric

data. In some cases, formation of the solvate layer was observed. The presence of water seriously perturbs the nonaqueous system. This work group summarized the advances on thermodynamics of calixarenes until 1998 in a review article [76]. Properties of about hundred compounds were discussed. Of course, this publication also contains their own results. In this work one can find several very useful data, i.e. tables of thermodynamic data of dissolution of *p*-tert-butylcalix[*n*]arenes (*n* = 4, 6, 8) in solvents of different polarity were published. Another table showed a detailed list of equilibrium constants of lower rim calixarene derivatives with alkali ions in solution. The detailed list of stability constants with neutral species in various solvents was also included. Moreover, one can find a list of the thermodynamic parameters of complexation of calixcrown ligands with metal cations in nonaqueous solvents: equilibrium constants, free energies, enthalpies and entropies of the processes. The last table of this survey contains the properties of the protonation–deprotonation equilibria of upper rim calixarene derivatives in aqueous solutions. During the first years of the present decade several articles were published by this group, dealing with the synthesis of calixarene derivatives, their complex building process and the structure of the complexes. Lower rim calix[4]arene keto derivatives were studied in *N,N*-dimethylformamide and acetonitrile [77]. Stability constants and standard thermodynamic functions of the complexation with Na⁺ were measured. The new 5,11,17,23-tetra-tert-butyl-25,26,27,28-tetra(benzoyl)methoxycalix[4]arene compound was synthesized and its complex with Na⁺ and acetonitrile was studied [78]. This molecular complex was isolated and its molecular structure was determined by X-ray diffraction. Thermodynamics of the aforementioned system was reported. Similarly, the compound 5,11,17,23-tetra-tert-butyl[25,27-bis(ethylethanoate)oxy-26,28-bis(ethylthioethoxy)]-calix[4]arene was synthesized [79]. Its hosting capacity was determined toward the metal cations Li⁺, Na⁺, Ag⁺, Ca²⁺, Cu²⁺, Hg²⁺, and Pb²⁺. The capacity was greater in acetonitrile than in *N,N*-dimethylformamide and ethanol. The effect of the pendant arms of the host molecule was discussed. Thermodynamics of the complexation process was discussed. Recently, similar measurements were carried out for the investigation of complexation of 4-hydroxypyridine ethers of calix[4]arenes with several metal ions in solutions [80]. The article lists the equilibrium constants and the changes of the thermodynamic functions (free energy, enthalpy, entropy) during the solvation. Liu *et al.* [81] published some articles about the thermodynamics of calixarene complexation during the last years. As model host molecules they used water soluble sulfonate derivatives. They studied the complexation process of 5,11,17,23-tetrasulfonato-25,26,27,28-tetrakis(hydroxyl-carbonylmethoxy)calix[4]arene and 5,11,17,23-tetrasulfonato-thiacalix[4]arene with La³⁺, Gd³⁺ and Tb³⁺ cations [81]. The host:guest ratio was stoichiometric 1:1 in aqueous solution. The complexations were entropy driven. The large positive entropy change and the smaller positive enthalpy change contribute to the stability of the complexes. In another work [82] they continued the elucidation of the complexation capability of calixarene sulfonates with calix[4]arene tetrasulfonate and thiocalix[4]arene tetrasulfonate. The guest molecules were diazacycloalkanes, i.e. piperazine, homopiperazine and 1,5-diazacyclooctane. The complexes were found enthalpy stabilized. The stability constants and the changes in the thermodynamic functions were presented. This work was continued using the same host molecules but their guests were in this case pyridinium ions [83]. The highest complex building ability showed the 2,6-dimethylpyridine/2,6-pyridinedicarboxylic acid pair. Similarly, the stability constants and the changes of the thermodynamic function for the complexation processes were determined.

Gas-Phase Interactions of Calixarenes with Molecular Guests

The extensive development of this important class of molecular receptors in the last two decades has expanded considerably the number and variety of substituents carried by the original calixarene structure, especially for the tetrameric calix[4]arene [25, 26, 84-88]. Both the phenolic hydroxyl and the *para*-substituent were derivatized in many ways, in order to increase the selectivity of the receptor or to modify its flexibility and solubility properties [25, 89]. Despite the enormous work developed throughout the world to synthesize and characterize all these molecular receptors and to investigate their chemistry in solution, very few studies have been undertaken to date to investigate the interaction between them and organic guest molecules and ions in the gas-phase by means of mass spectrometric methods. This lack of interest for the gas-phase chemistry of calixarene- and resorcinarene-cavitands is difficult to understand: even if the practical applications of host-guest chemistry are likely to be developed for the condensed phase, gas-phase studies nevertheless provide a different and interesting perspective for host-guest interactions. As the solvent is absent, no solvation effects can modify the electronic and thermodynamic properties nor the geometrical constraints of supramolecular binding, so that the pure intrinsic interaction between the two counterparts is uncovered, free from any third-body influence.

Much more extensive literature deals with the gas-phase interaction of alkali metal ions with crown ethers, cryptands and other macrocyclic hosts [8, 90]. Another application of mass spectrometry to supramolecular chemistry, quite developed in the past, is the recognition of optically active guests by chiral crown ethers and cyclodextrins [91]. Other recent and rapidly growing fields where mass spectrometry is utilized to characterize complex non-covalent aggregates are, respectively those of organometallic supramolecular architectures [92] and biological protein-substrate and DNA pairing aggregates [93]. Several factors account for the scarcity of work on the gas-phase reactions of calixarenes and resorcinarenes. One reason is that just the basic structures, not the most interesting derivatives, are readily available by commercial sources. Another reason is that complex host structures can not be maintained with ease in an unexcited state in the vapor phase before they react with a charged or neutral guest. The third and more crucial factor is that the interactions between these hosts and neutral molecular guests, which represent the obvious target, are generally very weak and difficult to occur in the gas-phase. It is generally much simpler to pre-form the complexes in solution and then to ionize and isolate them in the gas-phase, as is performed in electrospray ionization (ESI).

The most simple calixarenes are among the molecular receptors that provide too weak interactions to be observed with ease in the gas-phase. The large flexibility of the calixarene structure is emphasized in the gas-phase, where no solvent molecule limits the free conformational changes of the molecule. Consequently, the constraints associated with the formation of host-guest complexes correspond to a strongly negative entropic contribution, resulting in the weakening of the supramolecular interaction. Then very little internal energy is sufficient to dissociate the host-guest complex inside the mass spectrometer, preventing its detection. Even in a specific case studied by Wong and coworkers, where the host had considerable steric hindrance to the free conformational change and the guest carried a positive charge, *tert*-butylcalix[4]arene proved to be a less effective ligand than crown ethers toward benzylammonium ions [94]. The formation of host-guest complexes in the gas-phase is favored by any form of derivatization, that reduces the flexibility of the calixarene

backbone. This decreases the entropic loss associated to the formation of the host-guest complex, making it energetically feasible. A secondary effect of the reduced flexibility of the ligand is its increased selectivity, as the rigid three-dimensional arrangement of its binding sites should complement those of the guest to produce strong interaction. The stiffening of the calixarene structure has been achieved in several ways. One way is to introduce bulky substituents, especially in the lower rim of the molecule, in order to block its structure in the cone conformation. In such a case, it may happen that the calixarene oxygen become quite inaccessible to the candidate guests, restricting the binding properties of the ligand to the π -electrons of its aromatic rings. Thus, other substituents with target binding properties are frequently introduced at the upper rim of the calixarene structure. This solution, was successfully demonstrated by Schalley and coworkers, who studied a series of calix[4]arenes functionalized with urea substituents at their upper rim (i.e., the calixarene opening not containing the hydroxyl oxygen) [92, 95]. Urea substituents are particularly interesting, since they can act both as donor and acceptor in hydrogen bonding. The consequence is that, under ESI conditions, these calixarenes tend to dimerize, forming a two-valve shell held together by hydrogen bonding, in which guest species of molecular dimension can be trapped. Even if the trapped species described in the original work were typically charged (i.e., tetraalkylammonium ions) [92, 95], yielding extremely stable 2:1 complexes, it is not unlikely that also neutral organic molecules capable of hydrogen bonding could be captured inside these supramolecular architectures. More complex ligands, where two calixarene units are covalently linked by means of an hexyl chain produced 1:1 complexes with tetraalkylammonium ions by self-closure of the ligand halves around the guest ion under ESI conditions [95, 96]. When these and other multiple-calixarene ligands were mixed with monomeric urea-substituted calixarenes and alkylammonium salts, the ESI mass spectra showed evidence of stable supramolecular aggregates, containing the three species in specific stoichiometries. These depended on the structure of the coordinating ligand, forming aggregates with up to seven non-covalently bound subunits in a 1:3:3 stoichiometry [95]. Also melamine substituents were introduced into the calixarene structure to form hydrogen-bonded supramolecular assemblies with diethylbarbituric acid and similar monomers exhibiting concurrent donor and acceptor properties [97]. By covalently bridging three calixarene moieties by means of their melamine substituents, large molecular boxes were obtained [98], capable of forming complex molecular aggregates, that were characterized by MALDI-TOF.

Unless time-resolved experiments are performed after ionization, plain ESI mass spectra represent a chemical system where charged host-guest complexes are either pre-formed in solution or are generated at the high-voltage conditions used in ESI. In both cases, the observation of molecular aggregates in the mass spectrum demonstrates the stability of such complexes in the gas-phase, at least for the time-frame of mass analysis. Due to the rather energetic conditions needed inside the mass spectrometer to isolate the analyte ions, the positive finding of a mass peak corresponding to the host-guest complex in the ESI spectrum is generally accepted as a good demonstration of its existence also in solution. In other words, ESI-MS is supposed to provide a reasonable guess of what chemical reactions may take place in *solution*. Analogous description of mainly the condensed phase chemistry is provided by LSIMS as well as any other technique in which the two counterparts are dissolved together in a liquid matrix and introduced simultaneously inside the ion source of the mass spectrometer. The investigation of *gas-phase* chemistry requires that the reagents are introduced separately

into the mass spectrometer, frequently at different steps of the experiment and using different methods to vaporize them. The most appropriate instruments to perform these studies are time-resolved mass analyzer, capable of trapping ions for long time period, such as Fourier transform ion cyclotron resonance (FTICR) or quadrupole ion-trap mass spectrometers. In these instruments, a substrate ion (for example, the charged host) is first isolated and then allowed to interact with vapors of a neutral reagent species, which is generally pulsed into the reaction chamber. The subsequent mass analysis at various time intervals allows one to determine both the products and the kinetics for their formation.

From the study of the specific gas-phase reactivity of calixarenes with various esters and alcohols, several conclusions of general validity were drawn by authors of [99]. (a) The presence of one or more bridges at the upper rim of the cavity dramatically increases the calixarene ability to form inclusion complexes, provided that these bridges are rather rigid, i.e., all the atoms forming the bridge are linked to at least one unsaturated carbon. (b) The size of the bridge and the nature of its substituents drives the selectivity of the calixarenes toward different guests [100]. (c) Some extreme forms of selectivity that have been experimentally observed may be peculiar to the mass spectrometric context, where the charge location plays the major role.

The possibility of utilizing conventional chemical-ionization (CI) and electron-impact (EI) mass spectrometry as a method for probing gas-phase guest-host chemistry between *p*-tert-butylcalix[*n*]arenes (*n*=4,6) and fluoroaromatics, benzene or 2,2,2-trifluoroethanol as guest molecules is explored in reference [101]. Only with benzene a tiny cluster ion at *m/z* 727 (*p*-tert-butylcalix[4]arene+H+PhH)⁺ and *m/z* 726 (*p*-tert-butylcalix[4]arene+PhH)⁺ observed, which did not increase in intensity when the source temperature was lowered to 120 °C.

Previous desorption chemical ionization (DCI) complexation studies [102] pointed to a mechanism in which gaseous neutral cavitand molecules encapsulate neutral guests prior to ionization. Mechanisms in which either the charged guest or the host form the guest-host complex could be excluded. Therefore, the lack of complexation in the CI and EI modes may be due to a faster ionization rate of the thermally vaporized neutral species (having more internal energy) relative to their complexation rate. Once the host is ionized it does not complex. The absence of a guest-host cluster in the gas phase from a pre-formed guest-host cluster in the condensed phase shows that the complex undergoes thermal decomplexation prior to (or upon) volatilization/ionization, in line with DCI studies [102]. The mechanistic picture that emerges for gas-phase guest-host complexation between oligomeric macrocycles and neutral guests is that surface-desorbed intact neutral species of low internal energy must be first generated, these subsequently complexing in the DCI plasma [103]. The generated complex is then immediately ionized and detected. EI or CI conditions generate neutral species of higher energy which do not complex.

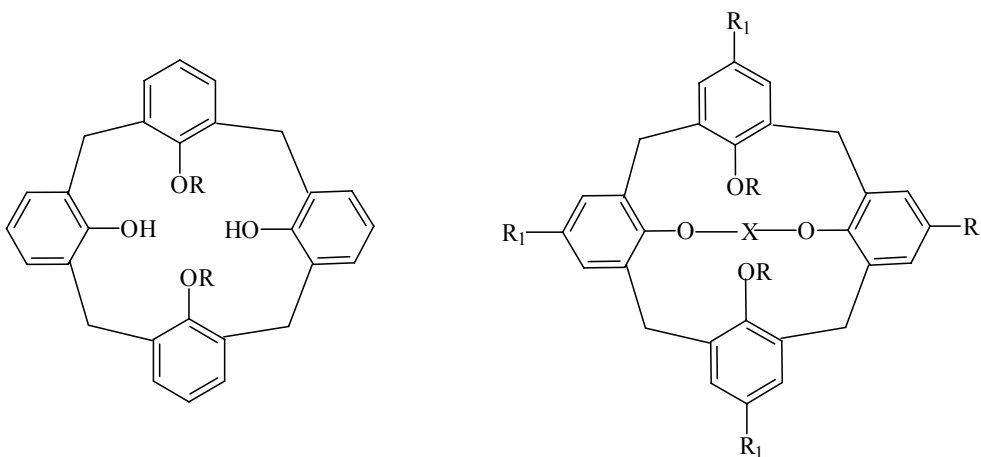
The inclusion of small neutral organic guests (C₆H₁₄, CH₂Cl₂, CH₃OH) by calix[4]arene receptors was found by ¹H NMR spectroscopy and microanalysis in [104]. The studied calix[4]arenes can form stable intramolecular complexes with solvent molecules which keep the stoichiometric composition without changing under conditions of the sublimation experiment. The saturated vapor pressures of calix[4]arenes and complexes of calix[4]arenes with solvent molecules were determined for the first time by the Knudsen's effusion method in the wide temperature range. The changing of standard thermodynamic parameters of complexation by transfer process from condensed state to vapor phase was estimated. It was

shown that the large flexibility of the calixarene ligand structure corresponds to a strongly negative entropic contribution as well as negative enthalpy term to the Gibbs energy of formation of host-guest complexes in the gas phase.

In this study, the temperature dependences of the saturated vapor pressures of calix[4]arenes and complexes of calix[4]arenes with solvent molecules were determined with the aim to estimate the changing of relative standard thermodynamic parameters of complexation by transfer process from condensed state to vapor phase. 25,27-Dimethoxy-26,28-dihydroxycalix[4]arene (II), 25,27-dimethoxy-calix[4]arene crown-6 (III), 25,27-dimethoxy-5,11,17,23-tetra-*p*-tert-butylcalix[4]arene crown-5 (IV), 25,27-diethoxy-5,11,17,23-tetra-*p*-tert-butylcalix[4]arene crown-5 (V), 25,27-bis(benzyloxy)-5,11,17,23-tetra-*p*-tert-butylcalix[4]arene crown-5 (VI), 25,27-dimethoxy-5,11,17,23-tetra-*p*-tert-butylcalix[4]arene crown-6 (VII) were synthesized used available from Aldrich 25,26,27,28-tetrahydroxycalix[4]arene (I) (Figure 1) according to methods described in ref. [105-108].

Calix[4]arenes (I-IV, VII) are present as a *cone* structure, compounds (V, VI) are in the *partial cone* conformation. The complexes (I)·C₆H₁₄·CH₂Cl₂, (II)·C₆H₁₄, (III)·C₆H₁₄ and (VII)·CH₃OH were obtained by crystallization from mixture CH₃OH/C₆H₁₄/CH₂Cl₂. The complex (I)·CH₂Cl₂ was obtained by solution of (I) in CH₂Cl₂ and then by evaporation of the solvent. ¹H NMR spectra were recorded with Bruker VC-300 (300 MHz) spectrometer in CDCl₃.

Compound (I)·CH₂Cl₂. Found: C, 68.32; H, 5.07; Cl, 13.94. Anal. Calcd for C₂₈H₂₄O₄·CH₂Cl₂: C, 68.38; H, 5.14; Cl, 13.97. ¹H NMR δ 7.97 (s, 4H, OH), 7.39 (d, *J* = 7.4 Hz, 8H, ArH *meta*), 6.73 (t, *J* = 7.6 Hz, 4H, ArH *para*), 5.65 (s, 2H, CH₂Cl₂), 4.33 (s, 4H, ArCH₂Ar), 3.42 (s, 4H, ArCH₂Ar).



I. R=H

II. R=CH

III. R=CH₃, R₁=H, X=CH₂CH₂(OCH₂CH₂)₄

IV. R=CH₃, R₁=*t*-Bu, X=CH₂CH₂(OCH₂CH₂)₃

V. R=C₂H₅, R₁=*t*-Bu, X=CH₂CH₂(OCH₂CH₂)₃

VI. R=CH₂C₆H₅, R₁=*t*-Bu, X=CH₂CH₂(OCH₂CH₂)₃

VII. R=CH₃, R₁=*t*-Bu, X=CH₂CH₂(OCH₂CH₂)₄

Figure 1. The structural formulas of the calix[4]arenes under investigation [104].

Compound (I)·C₆H₁₄·CH₂Cl₂. Found: C, 70.59; H, 6.72; Cl, 11.93. Anal. Calcd for C₂₈H₂₄O₄ · C₆H₁₄ · CH₂Cl₂: C, 70.56; H, 6.70; Cl, 11.91. ¹H NMR δ 7.95 (s, 4H, OH), 7.41 (d, *J* = 7.6 Hz, 8H, ArH *meta*), 6.71 (t, *J* = 7.1 Hz, 4H, ArH *para*), 5.68 (s, 2H, CH₂Cl₂), 4.31 (s, 4H, ArCH₂Ar), 3.40 (s, 4H, ArCH₂Ar), 0.98 (m, 8H, C₆H₁₄), 0.58 (t, 6H, C₆H₁₄).

Compound (II)·C₆H₁₄. Found: C, 80.30; H, 7.80. Anal. Calcd for C₃₀H₂₈O₄ · C₆H₁₄: C, 80.27; H, 7.78. ¹H NMR δ: 7.71 (s, 2H, OH), 7.82 (d, *J* = 7.5 Hz, 4H, ArH *meta*), 6.87 (d, *J* = 7.6 Hz, 4H, ArH *meta*), 6.74 - 6.66 (m, *J* = 7.2 Hz, 4H, ArH *para*), 4.31 (d, *J* = 13.1 Hz, 4H, ArCH₂Ar), 3.82 (s, 6H, OCH₃), 3.41 (d, *J* = 13.2 Hz, 4H, ArCH₂Ar), 0.97 (m, 8H, C₆H₁₄), 0.55 (t, 6H, C₆H₁₄).

Compound (III)·C₆H₁₄. Found: C, 74.59; H, 8.11. Anal. Calcd for C₄₀H₄₆O₈ · C₆H₁₄: C, 74.56; H, 8.08. ¹H NMR δ: 7.80 (d, *J* = 7.6 Hz, 4H, ArH *meta*), 7.41 (d, *J* = 7.6 Hz, 4H, ArH *meta*), 6.71 - 6.63 (m, *J* = 7.1 Hz, 4H, ArH *para*), 4.41 (d, *J* = 13.2 Hz, 4H, ArCH₂Ar), [4.10, 4.02, 3.92, 3.85 (m, 16H, -OCH₂CH₂O-)], 3.71 (s, 4H, -OCH₂CH₂O-), 3.12 (s, 6H, OCH₃), 3.38 (d, *J* = 13.2 Hz, 4H, ArCH₂Ar), 0.95 (m, 8H, C₆H₁₄), 0.52 (t, 6H, C₆H₁₄).

Compound (VII)·CH₃OH. Found: C, 75.16; H, 9.01. Anal. Calcd for C₅₆H₇₈O₈ · CH₃OH: C, 75.13; H, 8.97. ¹H NMR δ: 7.78 (s, 4H, ArH *meta*), 7.39 (s, 4H, ArH *meta*), 4.44 (d, *J* = 13.1 Hz, 4H, ArCH₂Ar), [4.15, 4.06, 3.93, 3.81 (m, 16H, -OCH₂CH₂O-)], 3.64 (s, 4H, -OCH₂CH₂O-), 3.25 (s, 3H, CH₃OH), 3.10 (s, 6H, OCH₃), 3.40 (d, *J* = 13.2 Hz, 4H, ArCH₂Ar), 1.30 (s, 18H, -C(CH₃)₃), 1.26 (s, 18H, -C(CH₃)₃), 1.10 (s, 1H, CH₃OH).

Sublimation enthalpy is an important property of the condensed phase as far as this quantity is a macroscopic measure of the magnitude of intermolecular interactions. A variety of experimental techniques have been developed to measure the sublimation enthalpies of solids. In the paper [104] the sublimation experiments were carried out by the Knudsen's effusion method. A weighed in a glass container (± 0.05 mg) sample is placed into the effusion cell. The experimental cell was made of stainless steel with internal volume of about 4 cm³. The internal diameter of the glass container is about 10 mm, the ratio of sample surface area to effusion orifice area is about from 80 to 300. The design of the experimental cell provides a device for vapor-proof effusion orifice closing during establishing the steady regime of measurements. The temperature of the effusion cell is maintained by means of thermocouples battery with accuracy ± 0.1 °C. The vapour pressure in the effusion cell is determined by Knudsen's equation (1):

$$P = (\Delta m / \alpha \cdot \beta \cdot S_{\text{eff}} \cdot \tau) \cdot (2\pi \cdot R \cdot T / M)^{1/2} \quad (1)$$

where Δm is a weight loss through an orifice of area S_{eff} , β is the Klauising's factor which takes into account the finite length of the orifice, α is a condensation coefficient, τ is the effusion time, M is the molecular weight, T is a temperature and R is the ideal gas constant.

The effusion equipment was calibrated using naphthalene (m.p.353.43 K) and benzoic acid (m.p.395.5 K). The obtained values of sublimation enthalpies of naphthalene 72.4 ± 0.6 kJ mol⁻¹ and benzoic acid 89.8 ± 0.7 kJ mol⁻¹ are in good agreement with recommended values [109]. In addition calix[4]arenes (I-VII) and their complexes with solvent molecules were purified by sublimation in a high vacuum of 10⁻⁵ Torr using a temperature gradient furnace. The absence of decomposition and impurities was controlled by ¹H NMR spectra. To estimate a condensation coefficient α the sublimation measurements were carried out using two orifices of different effective areas $\beta \cdot S_{\text{eff}}$ ($2.21 \cdot 10^{-7}$ m² and $8.48 \cdot 10^{-7}$ m²) as well as Langmuir method (sublimation from surface of the effusion material). It was found that the

measured vapour pressure was independent of both the orifice area and the measurement method (Knudsen or Langmuir). Thus for all compounds under investigation α was equal 1.

The experimentally determined vapor pressure data were described in coordinates $\ln P$ versus $1/T$ by equation (2):

$$\ln P = A + B/T \quad (2)$$

The value of the sublimation enthalpy is calculated by the Clausius-Clapeyron equation (3):

$$\Delta H_{\text{sub}}^T = -R \cdot \partial(\ln P) / \partial(1/T) \quad (3)$$

The value of sublimation entropy is calculated as

$$\Delta S_{\text{sub}}^T = -\partial(\Delta G_{\text{sub}}^T) / \partial T \quad (4)$$

where $\Delta G_{\text{sub}}^T = -RT \cdot \ln(P/P_0)$ and $P_0 = 1.013 \cdot 10^5$ Pa. (5)

The results of vapor pressure measurements are plotted in Figure 2. The least squares constants A and B corresponding to (2) as well as enthalpies and entropies of sublimation are presented in Table 1.

It has been shown by us earlier [13] that the studied compounds can be classified into roughly two groups. The compounds (I), (II), (III) and (VII) can form stable intramolecular aggregates (I)·CH₂Cl₂, (I)·C₆H₁₄·CH₂Cl₂, (II)·C₆H₁₄, (III)·C₆H₁₄ and (VII)·CH₃OH which keep the stoichiometric composition without changing under conditions of the sublimation experiment. The calix[4]arenes (IV), (V) and (VI) do not form stable host-guest complexes with the solvent molecules. The calix[4]arenes (V) and (VI) are in the *partial cone* conformation and their potential cavities are full with their own groups (“endo-positioned” ethoxy and benzyloxy groups, respectively) [105]. The structure difference of the calix[4]arenes (IV) and (VII) is the additional group OCH₂CH₂ in the crown polyether ring of (VII). Calix[4]arene (VII) forms the stable intramolecular aggregate with the solvent molecule as a result of the increase of the length of the polyether ring of (VII). The inclusions of organic molecules to the cavities of calixarenes (II), (III) and (VII) stabilize the crystal lattice energies increasing the values of the sublimation enthalpies. The sublimation enthalpy of ligand (I) is higher than enthalpies of (I)·CH₂Cl₂ and (I)·C₆H₁₄·CH₂Cl₂. The complex (I)·C₆H₁₄ is unstable and decomposed under sublimation. The large flexibility of the calixarene structure is emphasized in the gas phase, where no solvent molecule limits the free conformational changes of the molecule. Consequently, the constraints associated with the formation of host-guest complexes correspond to a strongly negative entropic contribution, resulting in the weakening of the supramolecular interaction. The formation of host-guest complexes in the gas phase is favored by any form of derivatization that reduces the flexibility of the calixarene backbone. This decreases the entropic loss associated to the formation of the host-guest complex, making it energetically feasible. A secondary effect of the reduced flexibility of the ligand is its increased selectivity, as the rigid three-dimensional arrangement of its binding sites should complement those of the guest to produce strong interaction. The stiffening of the calixarene structure has been achieved in several ways. One way is to introduce bulky substituents, especially in the lower rim of the molecule, in order to

block its structure in the cone conformation. In such a case, it may happen that the calixarene oxygen become quite inaccessible to the candidate guests, restricting the binding properties of the ligand to the π -electrons of its aromatic rings.

Table 1. The least squares constants A and B corresponding to equation (2), sublimation enthalpies and entropies of studied compounds.

Compound	A	B/1000	$\Delta H_{\text{sub}}^{\text{T}}$, kJ mol ⁻¹	$\Delta S_{\text{sub}}^{\text{T}}$, J mol ⁻¹ K ⁻¹
(I)	36.5±0.6	-20.1±0.3	167±2	207±5
(I)·CH ₂ Cl ₂	15±1	-11.7±0.4	98±3	35±5
(I)·C ₆ H ₁₄ ·CH ₂ Cl ₂	36.6±0.9	-15.7±0.3	131±3	208±8
(II)	17.7±0.6	-9.0±0.2	75±2	71±5
(II)·C ₆ H ₁₄	28±1	-14.7±0.5	122±4	134±10
(III)	24.6±0.7	-9.9±0.2	82±2	109±6
(III)·C ₆ H ₁₄	25±1	-11.7±0.4	97±3	118±12
(IV)	28.0±0.6	-10.8±0.2	90±2	137±5
(V)	19.2±0.5	-9.5±0.2	79±2	65±4
(VI)	20.5±0.8	-9.3±0.3	78±3	74±7
(VII)	20.8±0.5	-9.3±0.2	78±1	76±3
(VII)·CH ₃ OH	24±1.4	-12.1±0.5	100±4	100±12

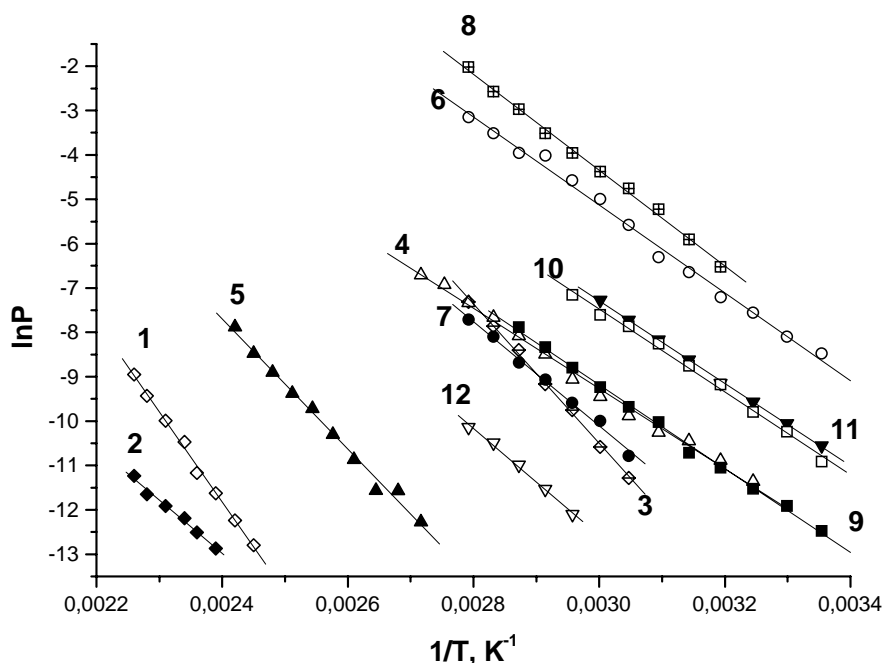
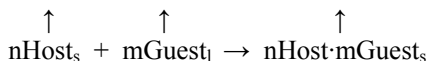
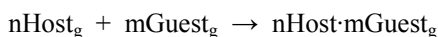


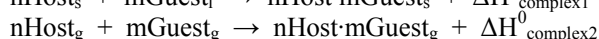
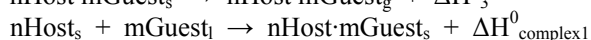
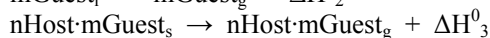
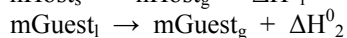
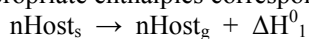
Figure 2. The temperature dependence of the vapor pressures of the studied compounds: 1 - (I); 2 - (I)·CH₂Cl₂; 3 - (I)·CH₂Cl₂·C₆H₁₄; 4 - (II); 5 - (II)·C₆H₁₄; 6 - (III); 7 - (III)·C₆H₁₄; 8 - (IV); 9 - (V); 10 - (VI); 11 - (VII); 12 - (VII)·CH₃OH.

The unique property of complexes of calixarenes with solvent molecules to keep the stoichiometric composition without changing under conditions of the sublimation experiment

efforts an opportunity to estimate the thermodynamic functions of complexation using data on temperature dependence of saturated vapour pressures. The thermodynamic cycle for the transfer process of calixarene, solvent and the complex of calixarene with solvent from the condensed state to the gas phase is considered to be:



The appropriate enthalpies correspond to the stages:



The relative binding enthalpy is computed by the difference:

$$\Delta(\Delta H^0_{\text{complex}}) = \Delta H^0_{\text{complex2}} - \Delta H^0_{\text{complex1}} = \Delta H^0_3 - (\Delta H^0_1 + \Delta H^0_2)$$

Similarly, assuming that the system is reversible:

$$\Delta(\Delta G^0_{\text{complex}}) = \Delta G^0_{\text{complex2}} - \Delta G^0_{\text{complex1}} = \Delta G^0_3 - (\Delta G^0_1 + \Delta G^0_2)$$

where, *Host* is a calixarene; *Guest* is a solvent; *nHost·mGuest* is a complex of the calixarene with the solvent; *n* and *m* characterize the stoichiometry of the complex; the subscript signs *s*, *l* correspond to the condensed state, *g* corresponds to the gas phase, respectively; $\Delta H^0_{1,2,3}$ and $\Delta G^0_{1,2,3}$ are the standard enthalpies and Gibbs energies of vapour formation of calixarene, solvent and the complex of the calixarene with the solvent, respectively; $\Delta H^0_{\text{complex1}}$, $\Delta H^0_{\text{complex2}}$ and $\Delta G^0_{\text{complex1}}$, $\Delta G^0_{\text{complex2}}$ are the standard enthalpies and Gibbs energies of complexation in the condensed state and in the gas phase, respectively.

Table 2. The relative standard thermodynamic functions of complexation by transfer process from the condensed state to the gas phase

Compound	$\Delta(\Delta G^0_{\text{complex}})$, kJ mol ⁻¹	$\Delta(\Delta H^0_{\text{complex}})$, kJ mol ⁻¹	$T\Delta(\Delta S^0_{\text{complex}})$, kJ mol ⁻¹
(I)·CH ₂ Cl ₂	-19	-98	-80
(I)·CH ₂ Cl ₂ ·C ₆ H ₁₄ ^a	-43	-96	-54
(II)·C ₆ H ₁₄	19	16	-3
(III)·C ₆ H ₁₄	10	-16	-26
(VII)·CH ₃ OH	11	-15	-26
(I)·CH ₂ Cl ₂ ·C ₆ H ₁₄ ^b	-24	2	26

^acomplexation process: (I) + CH₂Cl₂ + C₆H₁₄ → (I)·CH₂Cl₂·C₆H₁₄

^bcomplexation process: (I)·CH₂Cl₂ + C₆H₁₄ → (I)·CH₂Cl₂·C₆H₁₄

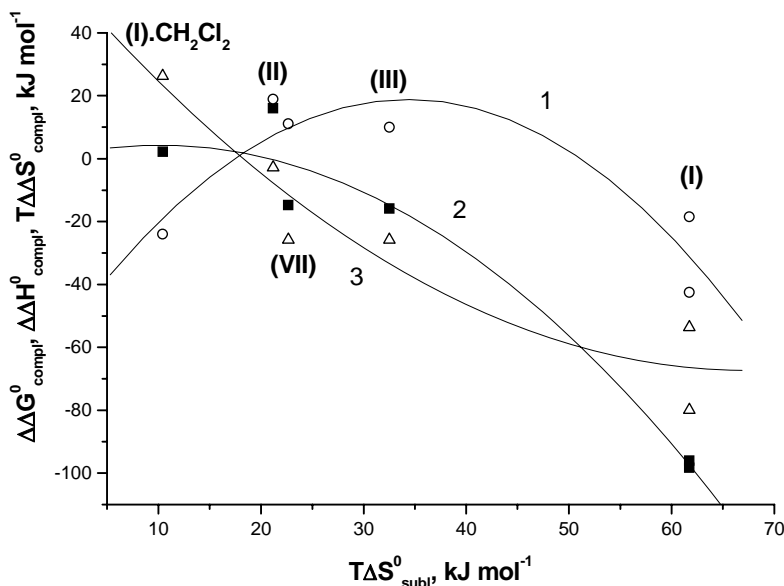


Figure 3. The relative standard thermodynamic functions of complexation by transfer process from the condensed state to the gas phase. $T\Delta S_{\text{subl}}^0$ is sublimation entropy of calixarene ligands (I), (II), (III), (VII) and (I)·CH₂Cl₂; 1 – $\Delta(\Delta G_{\text{compl}}^0)$; 2 – $\Delta(\Delta H_{\text{compl}}^0)$; 3 – $T\Delta(\Delta S_{\text{compl}}^0)$.

Thus the certain values of $\Delta H_{1,2,3}^0$ and $\Delta G_{1,2,3}^0$ allow us to calculate the relative binding enthalpies $\Delta(\Delta H_{\text{complex}}^0)$ and Gibbs energies $\Delta(\Delta G_{\text{complex}}^0)$ of complexation by transfer process from the condensed state to the gas phase and the corresponding changing of entropy $T\Delta(\Delta S_{\text{complex}}^0) = \Delta(\Delta H_{\text{complex}}^0) - \Delta(\Delta G_{\text{complex}}^0)$. The relative standard thermodynamic functions of complexation $\Delta(\Delta H_{\text{complex}}^0)$, $\Delta(\Delta G_{\text{complex}}^0)$, $T\Delta(\Delta S_{\text{complex}}^0)$ for the complexes (I)·CH₂Cl₂, (I)·CH₂Cl₂·C₆H₁₄, (II)·C₆H₁₄, (III)·C₆H₁₄ and (VII)·CH₃OH are presented in Table 2.

The sublimation enthalpies at the mean temperatures of measurements were assumed as the standard sublimation enthalpies of calixarenes and complexes of calixarenes with solvents (Table 1). The evaporation enthalpies of C₆H₁₄, CH₂Cl₂ and CH₃OH at 298.15 K are 7.4; 6.8 and 8.94 kcal mol⁻¹, respectively. The standard sublimation Gibbs energies ΔG^0 of calixarenes and their complexes were calculated by equation (5) using vapour pressures values obtained by extrapolation of the temperature dependence of vapour pressures to 298.15 K (Table 1). The standard evaporation Gibbs energies ΔG^0 of solvents were calculated using vapour pressures values at 298.15 K.

As the sublimation entropy characterizes the free conformational changes of the molecule by the transfer process to the gas phase, it is possible to estimate the correlation between flexibility of the calixarene structure and the complexation properties.

Grootenhuis *et al.* [110] assessed some of the structural and energetical properties of calix[4]arenes by various computational methods. They found that the preferred conformation of calix[4]arene depends on the number and the positions of the substituents on the oxygen atoms and is mainly determined by electrostatic interactions. In a number of cases the conformation with the lowest calculated energy is different from the conformation found in solution and in the solid state. In order to study conformational interconversions the authors [110] carried out molecular dynamics simulations on one isolated molecule of 25,26,27,28-tetrahydroxy-5,11,17,23-tetra-*p*-methylcalix[4]arene at temperatures of 300, 600, and 800 K

for 50 ps. Inspection of MD movies suggested that at 300 K the motions of the two phenol moieties opposite to each other were initially strongly coupled when the calixarene was in its *cone* conformation. After 35 ps one of the phenol moieties did break its hydrogen bonds with the other phenols and flipped through the cavity, resulting in the *partial cone* conformation. After adopting the *partial cone* conformation for a few picoseconds the molecule started interconverting between the *1,2-* and *1,3-* *alternate* conformations and the *partial cone*. At 600 K only one conformational interconversion was observed in the 50-ps trajectory. However, the amplitude of the coupled movements of the phenolic moieties was much larger at this temperature. At 800 K an almost continuous interconversion of the calixarene was observed. It is quite clear from the MD movies that the strongly coupled movement of the two pairs of opposite phenol moieties favors the conformational transitions. So compound (I) is conformationally mobile in the gas phase and can interconvert between the *cone*, *partial cone*, *1,2-alternate*, *1,3-alternate* conformations, although in the solid state it is present exclusively as a *cone* structure due to strong intramolecular hydrogen bonding [105]. Consequently, the transfer of calixarene (I) from the solid state to the gas phase must be accompanied by high value of sublimation entropy.

The conformational analysis of calixarene (II) is described in [110]. For the dimethyl ether (II) none of the conformations is clearly preferred in the calculations. The *cone* conformation is not anymore the only conformation in which all possible (in this case two) *H* bonds can be accommodated, and therefore, other conformations that have a more favorable VDW or bonded energy or have a lower electrostatic repulsion between the oxygen atoms become important. On the other hand, the dimethyl ether (II) can in principle assume every possible conformation due to its flexibility in the gas phase. Thus the sublimation process should be characterized in this case by low value of sublimation entropy.

The flexibility of (I)·CH₂Cl₂ (which is considered as the ligand in the complexation process (I)·CH₂Cl₂ + C₆H₁₄ → (I)·CH₂Cl₂·C₆H₁₄) is constrained greatly as a result of the formation of host-guest complex. The presence of the crown polyether ring at the lower rim of the cavity reduces the flexibility of the calixarene structures (III) and (VII) in comparison with (I) and (II). *tert*-Butyl groups introduced at the upper rim of the calixarene structure (VII) reduce the flexibility of the calixarene backbone as compared to (III).

The relative standard thermodynamic functions of complexation by transfer process from the condensed state to the gas phase versus sublimation entropy of calixarene ligands, $T\Delta S_{\text{subl}}^0$, are shown in Figure 3.

It is obvious that the smaller value of sublimation entropy ($T\Delta S_{\text{subl}}^0$ values decrease in order (I) > (III) > (VII) > (II) > (I)·CH₂Cl₂) corresponds to the more positive entropic term $T\Delta(\Delta S_{\text{complex}}^0)$ to the relative standard Gibbs energy of complexation $\Delta(\Delta G_{\text{complex}}^0)$. On the other hand, the negative enthalpy contribution $\Delta(\Delta H_{\text{complex}}^0)$ to the Gibbs energy of complex formation $\Delta(\Delta G_{\text{complex}}^0)$ increases with increasing of $T\Delta S_{\text{subl}}^0$. As a result the flexibility dependence of the relative standard Gibbs energy of complexation ($\Delta(\Delta G_{\text{complex}}^0)$ versus $T\Delta S_{\text{subl}}^0$) is an extremal function. The negative values of $\Delta(\Delta G_{\text{complex}}^0)$ correspond to the maximal and minimal conformational changes of the calixarene ligand structures by transfer process from the solid state to the gas phase. The entropic contribution to the relative free energy of complexation dominates when the flexibility of calixarene is reduced whereas the enthalpy term prevails when the flexibility is large. The complex formation (I)·CH₂Cl₂ + C₆H₁₄ → (I)·CH₂Cl₂·C₆H₁₄ is accompanied by negligible enthalpy effect and is governed by the entropic contribution to the relative Gibbs energy of the complexation process. The values

of the relative Gibbs energy of complexation of (II), (III) and (VII) are positive since negative values of $T\Delta(\Delta S_{complex}^0)$ are not balanced by negative values of $\Delta(\Delta H_{compl}^0)$. Hence the preferred complexation occurs in the condensed state coming out of insufficient rigid structures of calixarene ligands (II), (III) and (VII). Thus it must be taken into consideration that the large flexibility of the calixarene ligand structure corresponds to a strongly negative entropic contribution as well as negative enthalpy term to the Gibbs energy of formation of host-guest complexes in the gas phase.

More than two decades after their introduction, calixarene and resorcinarene cavitands are nowadays investigated for their possible practical applications. To this respect, gas-phase interaction studies have limited direct impact on applications, and should still be regarded chiefly as fundamental studies. However, they provide a unique perspective and information, since the dynamic character of the gas-phase interaction makes the attractive forces established between host and guest depend uniquely on their relative structures and the intrinsic energy of the system.

Moreover, the major source of interference, that is the solvent, is absent in gas-phase studies. The simplicity of the reacting system has the potential of revealing the specific nature and strength of each supramolecular binding. Thus, the thermodynamic parameters associated to subtle structural attributes such as, for example, synergic multiple binding, conformational dynamics and steric constraints can be measured. In order to undertake these studies, it is convenient to establish strong cooperation between synthetic chemists and mass spectroscopists, and to have access to instruments capable of time-resolved experiments, particularly FTICR mass spectrometers. But, above all, it is essential that the scientist investigating supramolecular architectures become aware of the significance of gas-phase studies in elucidating the intrinsic nature of supramolecular interactions.

Adsorption of Organic Vapors within Calixarene Thin Films

Atmospheric detection of odorant vapors of organic compounds is one of the most important problems of environment monitoring. A number of vapor sensors and sensor arrays have been developed during the last few years. The majority of these sensors are based on the use of different polymer coatings and employ several transduction techniques, such as, using a mass sensitive quartz crystal microbalance (QCM) [111-115] and surface acoustic wave (SAW) [116, 117] devices, chemical field effect transistors (ChemFETs) [118], conductivity [111, 119-121] and interdigitated capacitance [122] measurements.

Several attempts to study the adsorption of organic vapors within thin calixarene films formed with different techniques, including Langmuir-Blodgett (LB) film deposition, spin coating and self-assembly, have been made [123-129]. In publications [128, 129] it has been shown that the vapors of benzene and toluene, as well as some hydrocarbons (hexane), can be adsorbed at calixarene LB films. This adsorption process is very fast, and full recovery of the film has been observed after flushing with clean air. It has to be pointed out, however, that the detected vapors were of a high concentration (a few percent in volume) and the adsorption was not selective since all vapors studied yielded a similar response. These effects are attributed to weak and non-specific interactions between guest molecules and the calixarene LB film. It was also shown that the adsorption of organic vapors occurs in the whole bulk of

the LB films, and that the number of adsorbed molecules is much higher than the number of calixarene molecules [128]. The proposed mechanism of adsorption included swelling of the film and even condensation of adsorbate within the film. The swelling of the film has been confirmed directly by ellipsometry and surface plasmon resonance (SPR) measurements [128, 129], but the mechanism of adsorption is still unclear.

Adsorption of vapors of benzene, toluene, *p*-xylene, aniline, hexane and chloroform in LB films of two calix[4]resorcinarene derivatives was studied *in situ* using QCM, ellipsometry and SPR techniques [130]. Isotherms of adsorption obtained by both QCM and SPR show that the adsorption ability depends on the condensed vapor pressures of the adsorbates rather than on a structural coincidence between host cavities and guest molecules. The results were interpreted in terms of capillary condensation of organic vapors in the nanoporous matrix of calixarene LB films accompanied by film swelling. Ellipsometric measurements show changes of both the thickness and refractive index of the LB films caused by adsorption, and thus confirm condensation and further accumulation of liquid adsorbate within the film matrix.

In the paper [131] a systematic study is reported of modified calixarenes with various side groups and various sizes to optimize their recognition properties towards specific molecules. Thin films of calix[4]arenes, calix[6]arenes, and calix[8]arenes have been prepared by thermal evaporation onto Au electrodes of quartz oscillators. Since polar O-containing groups are present in para-positions of the aromatic rings, double-layer structures can be formed in thin calix arene films, similar to the geometric structure of toluene/ *p*-tert-butylcalix[4]arene crystals [84]. The first set of experiments in this study deals with the determination of thermodynamic and kinetic parameters which describe the interaction of thin calixarene layers with organic solvent molecules. Perchloroethylene (C_2Cl_4) was chosen as a solvent with particular relevance in environmental control. The parameters include the equilibrium surface and bulk concentrations, molar heats of absorption, diffusion coefficients, and activation energies of diffusion. They are obtained from thickness, partial pressure, temperature, and time dependent measurements of mass changes which occur during the solvent/calixarene interaction. These parameters are also important from a practical viewpoint in characterizing and comparing the different properties of calixarenes for specific applications as chemical sensors. In a second set of experiments, activation energies were determined for desorption and diffusion of C_2Cl_4 molecules by means of thermodesorption spectroscopy (TDS). The latter is performed under ultra-high-vacuum conditions with well defined calixarene layers prepared *in-situ* by Knudsen evaporation onto gold substrates. Finally experimental results obtained for different solvents were compared (i.e. perchloroethylene (C_2Cl_4), chloroform ($CHCl_3$), benzene (C_6H_6), and toluene ($C_6H_5CH_3$)) with theoretical force field calculations of geometric structures and binding energies of molecule/calixarene complexes. From thickness dependent measurements of mass changes during subsequent exposure of different solvents to these films surface effects were separated from bulk effects in the solvent/calixarene interactions. Thermodesorption spectra give additional evidence for diffusion processes occurring from surface to subsurface sites even at low temperatures $T \sim 240$ K. Force field calculations indicate strong key-lock interactions between individual solvent molecules with molecular cavities of calix[4]arenes. The larger cavities of calix[6]arenes and calix[8]arenes form supramolecular units which capture two or more small organic solvent molecules.

Molecular Recognition of Organic Guest Vapors by Solid Calixarenes

Molecular recognition in solid-phase host-guest binding is generally a more complex phenomenon than solvation selectivity in liquids. For liquid solutions the linear structure-energy relationship is usually observed in the absence of specific solute-solvent coordination or for simple solvent-solute interaction with the single donor-acceptor or H-bond [132]. Molecular recognition in the supramolecular systems is based on host-guest structural complementarity [133], which is essentially a nonlinear property. This nonlinearity can be found in the discrete changes of the stoichiometry of host-guest inclusion compounds with variation of the guest molecular structure [134-138]. More guest and host structural features are relevant for the guest inclusion than for solvation of organic compounds. For liquid solutions the knowledge of the solute and solvent molecular group composition is often enough for the prediction of solvation parameters [139]. The guest inclusion parameters depend, besides, on the host shape and symmetry, conformational flexibility/rigidity, and configuration of the H-bonding network [134, 140]. The knowledge of parameters of guest molecular recognition by solid hosts can help to improve the host molecular design, especially when the full structural picture of the guest inclusion is not available. An effective strategy for the study of the host structural influence on guest inclusion can be the examination of the structure-affinity relationships for hosts with a few different structural features. This approach was realized consistently only for the stoichiometry of the inclusion compounds [134, 135, 141-143]. The ability of the inclusion compound to crystallize from the host solution in liquid guest is often used as a qualitative host-guest affinity parameter [134, 135, 141-143]. Another related parameter is the difference between the guest boiling temperature and the decomposition temperature of the inclusion compounds [144]. Estimation of the guest binding energy is not a simple problem for the inclusion process due to its high cooperativity [145-148], sensitivity to temperature [149-151], and the presence of other components [146, 152-156]. These effects, if not controlled, can considerably distort the relationship between the obtained inclusion parameters and the host and guest molecular structure.

The structure-affinity relationships were studied for the guest inclusion parameters of solid tert-butylthiacalix-[4]arene and tert-butylcalix[4]arene in [157, 158]. The inclusion stoichiometry and inclusion free energy were calculated by the sorption isotherms obtained for guest vapor-solid host systems by the static method of headspace gas chromatographic analysis at 298 K. The obtained sorption isotherms have an inclusion threshold for guest thermodynamic activity corresponding to the phase transition between the initial host phase and the phase of inclusion compound.

The influence of the calixarene macrocycle size on the thermodynamic parameters of inclusion formation in organic guest vapor-solid host systems was studied in the series of tert-butylcalix[4]arene, tert-butylcalix[6]arene, and tert-butylcalix[8]arene [159]. For this purpose, sorption isotherms of a guest vapor by a solid host were determined using the static method of headspace gas chromatographic analysis. Besides, the stoichiometry and decomposition temperatures of saturated clathrates formed in these systems were determined using thermogravimetry. The compositions of some of these clathrates differ substantially from those of clathrates crystallized from a host solution in a liquid guest.

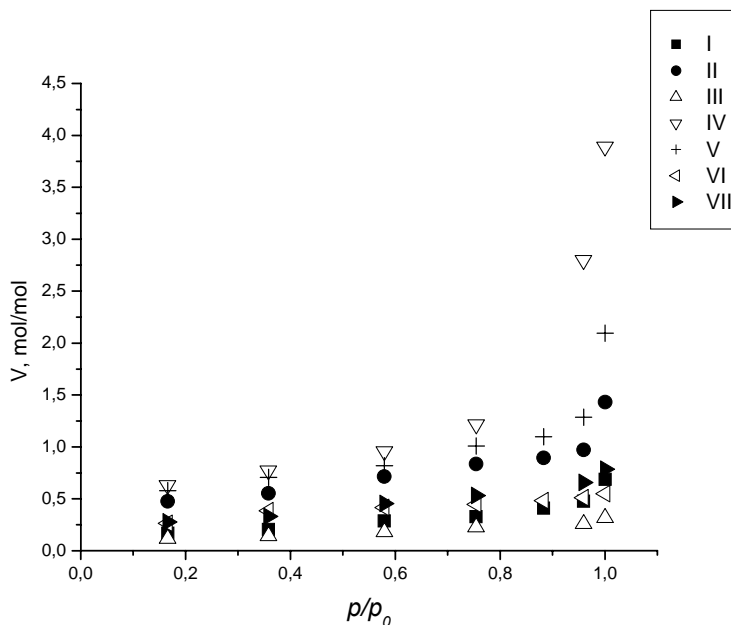


Figure 4. Isotherms of water sorption on calixarenes I–VII at 298 K.

The special features of water interaction with classic calixarenes were studied [160] by measuring water sorption isotherms on seven powdered calix[4]arenes (I–VII) (Figure 1) at 298 K by the isopiestic method (storage in a desiccator at controlled humidity). Isopiestic experiments were performed at relative pressures p/p_0 from 0.15 to 1. Calixarene powders (fractions with particle size 0.16–0.28 mm separated by screening through calibrated sieves) with weight about 500 mg were dried in a vacuum at 338–343 K to a constant weight and brought to isopiestic equilibrium with aqueous solutions of sulfuric acid with a given concentration at the known vapor pressure over solution. The experiments were performed in an air thermostat; the temperature was controlled to an accuracy of ± 0.1 K. The time of the establishment of equilibrium was from 7 to 21 days. The content of sorbed water was determined gravimetrically. Figure 4 shows water sorption isotherms on calixarenes at 298 K.

As can be seen from the figure, all isotherms are similar and show a pronounced trend to a sharp increase in water sorption as p/p_0 approaches 1. The complete coincidence between the sorption and desorption branches of isotherms and the absence of hysteresis are indicative of an insignificant porosity of crystalline calixarenes. A comparative analysis of sorption isotherms and the structural formulas of calixarenes shows that the water sorption value is independent of the number of potential sorption sites (oxygen atoms in calixarene molecules). The maximum number of oxygen atoms is characteristic of calixarenes III and VII, and maximum water sorption is observed for calixarenes IV and V. Maximum water sorption on various calixarene samples is 0.5–1 mol/mol on average, except samples V and IV characterized by water sorption of 2 and 4 mol/mol calixarene, respectively. An analysis of the isotherms showed that the experimental data were linearized in the coordinates of the Harkins–Jura equation. Figure 5 demonstrates isotherms of water sorption on the calixarenes in the coordinates of the Harkins–Jura equation.

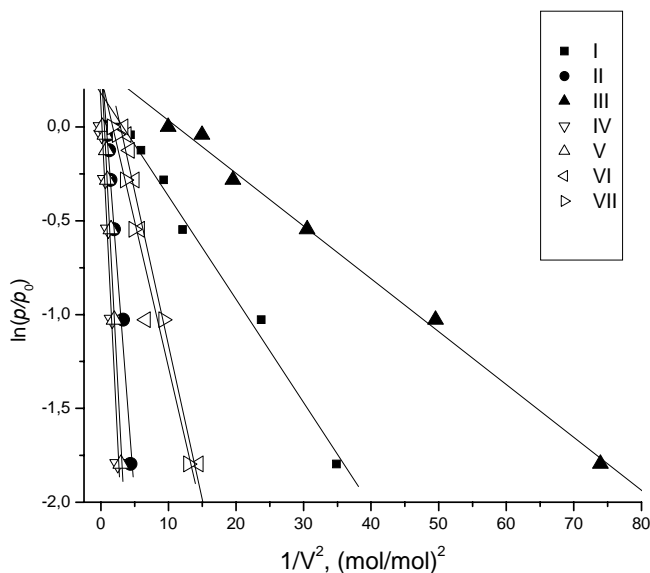


Figure 5. Isotherms of water sorption on calixarenes I–VII in the coordinates of the Harkins–Jura equation.

By analyzing the phase diagrams of surface layers constructed from the experimental isotherms of gas and vapor adsorption on solid adsorbents, Harkins and Jura proved that the state of two-dimensional surface films was similar to that of adsorption layers on solid surface [161]. The works by Harkins and Jura confirmed that there were well-defined regions of the curves of compression of the surface layers of solid adsorbents similar in properties to various film phases, for example, oil on water. Each of five phases of oil-on-water films demonstrates a relation between film pressure π and molecular surface area σ characteristic of the given phase only. Harkins and Jura showed that the isothermal equation of state for a condensed film is described by the equation

$$\pi = b - a\sigma, \quad (6)$$

where π is the surface pressure of the film, σ is the molecular surface area, and a and b are constants. This equation can be transformed as

$$\ln(p/p_0) = B - A/V^2, \quad (7)$$

where p/p_0 is the relative pressure of adsorbate vapors, A and B are constants, and V is the amount of the adsorbed substance.

According to the data by Harkins and Jura, the surface area of a solid can easily be calculated from a vapor adsorption isotherm provided that the adsorbed film forms a condensed phase along part of the isotherm; the surface area of a solid can be calculated by the equation

$$\Sigma = kA^{1/2}, \quad (8)$$

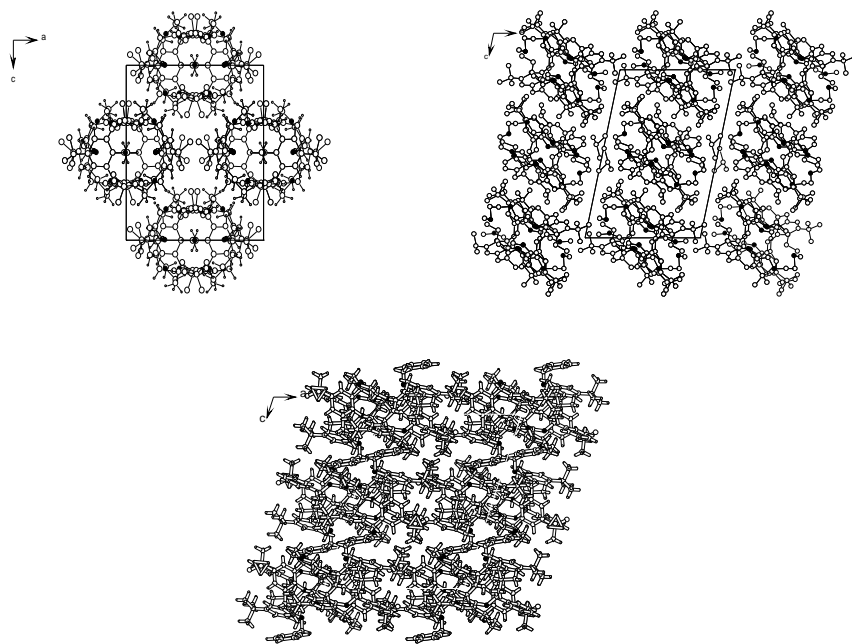


Figure 6. Porous structure of calixarenes IV, V, and VI.

where Σ is the surface area, k is the constant depending on the adsorbate used, and A is the constant of Eq. (7). For water at 25°C, $k = 3.83$ [161]. The surface areas (m^2/g) of calixarenes I–VII calculated using the Harkins–Jura approach are given below: 2.1 (I), 5.8 (II), 9.8 (III), 3.6 (IV), 3.5 (V), 1.4 (VI), and 1.6 (VII).

An analysis of the X-ray diffraction data on single crystals of IV, V, and VI [105] shows that the enhanced sorption on samples IV and V can be related to the presence in the crystal lattices of a developed network of through channels favoring the penetration of water molecules into hydrophobic crystals (Figure 6).

Water is not adsorbed on specific sorption sites but forms a condensed film, which, in the presence of a sufficient number of branched channels, can form a polymolecular film. As distinct from classic calixarenes, water absorption by thiacalixarene follows a complex mechanism including rotations of *tert*-butyl groups accompanied by deformation of the host molecule with the removal of peripheral aromatic rings that form the cavity [16]. Such a deformation most likely involves rotation around C–S thioether bonds. It is well known that, compared with classic calixarenes, thiacalixarenes are characterized by improved mobility in solutions and conformational peculiarities in the solid state [162]. The improved conformational mobility of solid thiacalixarenes is probably responsible for the intercalation of water molecules into a calixarene crystal without the obvious presence of suitable channels [16]. According to [16], the three-dimensional lattice and molecular cavities in the structure of thiacalixarene are the determining factors for water diffusion. Although the cavities do not merge to form channels, water molecules can probably use these cavities as steps in their motion through the lattice. Therefore, the mechanism of water transport should involve jumps of water molecules between cavities until a thermodynamically favorable arrangement is found. In the case of classic calixarenes I–VII without enhanced conformational mobility in the solid state, water cannot supposedly be intercalated into hydrophobic cavities, and is

adsorbed on the surface of crystals or through pores with fairly large diameters to produce a condensed film.

Binding of small neutral guest with solid monodeoxycalix[4]arene host was carried out in references [163, 164]. It was found that the solid apo-host can bind gaseous small organic guest; the guest selectivity in the cavity of solid apo-host is closely related to the free energy of complexation in solution. Structure elucidation of the inclusion complexes of monodeoxycalix[4]arene with small organic guests was carried out by X-ray crystallographic analysis and molecular dynamic simulation. Although the guest moves rapidly in the host cavity, the time averaged structure resembles the one obtained by the X-ray crystallography. Chemical shift simulation succeeded to reproduce the observed complexation induced shift.

It was shown that a potassium salt of *p*-tert-butylthiacalix[6]arene shows highly-extensive coordination nature to give rise to zeolitic crystal which has huge cavity with the widest span of ca. 19 Å and is capable of crystalline phase guest-addition and –removal [165]. This work suggests a potential utility of the bridging sulfur moieties of thiacalixarene for construction of extensively-coordinated structures in the crystalline state. The sulfur-bridged cyclic hexamer drastically differs from a methylene-bridged counterpart *p*-tert-butylcalix[6]arene in that a former can bind as much as four potassium cations at once, while a latter usually forms the complexes with not more than two alkali metal ions [166, 167]. The obtained highly-coordinated crystal may be regarded as intermediate between pure organic crystals involving porosity based on phase transition [148] upon guest binding and metal-coordinated ones possessing permanent or genuine porosity.

The solid state inclusion of various organic solvent molecules in *p*-tert-butylcalix[4]arene and *p*-tert-butylcalix[6]arene has been studied by thermal gravimetry and electron impact mass spectrometry (EI-MS) in [168]. The host–guest ratio varies from 1:2 to 4 :1 and the nature of included guest has been determined by EI-MS. Thermal gravimetric analysis of solvent–*p*-tert-butylcalix[*n*]arene complexes gives a qualitative order of intramolecular forces involved. Structural information obtained by cross-polarization magic angle spinning (CP-MAS) ¹³C NMR spectroscopy is in good agreement with known data from single crystal X-ray diffraction analysis.

In [169] the authors report evidence for an inclusion complex between carbon dioxide and *p*-tert-butylcalix[4]arene. The complex was studied with infrared spectroscopy, single-crystal X-ray diffraction, solid-state NMR, and thermogravimetric analysis. Results indicate that 70% of the *p*-tert-butylcalix[4]arene cavities could be occupied by a CO₂ molecule following exposure at 30 MPa and 40 °C.

With recent developments in materials chemistry and nanotechnology, extensive studies have been undertaken in the search for stable nano- or microporous networks. Most of these networks utilize coordination polymers, the porosity of which can be programmed depending on the applications. A variety of metal organic frameworks (MOFs) has been designed for gas storage and transport [170-179]. MOFs were found to effectively absorb N₂, O₂, Ar, CO₂, N₂O, H₂ and CH₄. The remarkable ability of certain MOFs in sorption of H₂ and CH₄ makes them very attractive candidates for vehicular gas storage. Much less effort has been devoted to assessment of pure organic solids as gas sorbents since organic molecules typically adhere to close-packing principles and do not afford porous structures. Calixarenes offer a remarkable exception. Atwood and co-workers showed that CH₄, CF₄, C₂F₆, CF₃Br and other low-boiling halogenated alkanes could be reversibly entrapped and retained within the lattice voids of a crystalline calix[4]arene framework [180]. Such gas-storing crystals appeared to be

extremely stable and release their guests only at elevated temperatures, several hundreds of °C above their boiling points. Ripmeester discovered that the calix[4]arene cavities in such crystals are directly involved in the gas complexation [181]. The Atwood team further demonstrated that *p*-tert-butylcalix[4]arene dimerizes in a crystalline phase into a hourglass-shaped cavity, capable of gas entrapment [182]. These crystals soak up gases when stored in air. Absorption of CO₂ was particularly rapid, but CO, N₂, and O₂ were also trapped. Of special importance, the calixarene crystals selectively absorbed CO₂ from a CO₂ - H₂ mixture, leaving the H₂ behind. This phenomenon can be used for purification of H₂. More recently, Atwood showed that calix[4]arene crystals can also absorb H₂ at higher pressures [183]. Cavity-containing solid materials for gas entrapment and storage have thus emerged. While polymers with intrinsic calixarene cavities have not yet been constructed [184], He, H₂, N₂, N₂O, and CO₂ were encapsulated in the solid state by hemicarcerand [185]. These gases were shown to replace each other in the solid hemicarcerand. The scope of gas encapsulation was thus expanded from solution to the gas-solid interface. In summary, calixarenes can be employed in the design of cavity containing solid materials for gas entrapment, storage and release. Polymers with intrinsic calixarene cavities are still not known, but this is just a matter of time. The major drawback of reversible encapsulation complexes with gases is in their low thermodynamic stability. Even well preorganized cavities of calixarenes and hemicarcerands derived from them cannot complex strongly, due to the lack of binding interactions. An alternative approach is based on reversible chemical transformation of gases upon complexation. In this case, they produce reactive intermediates with higher affinities for the receptor molecules.

Transport of Small Mobile Particles Through a Calixarene Crystal

More than two decades ago, Andreotti and coworkers reported the X-ray structural analysis of a 1:1 complex of *p*-tert-butylcalix[4]arene with toluene, *Ia* [23]. This pioneering study unambiguously confirmed the cone conformation of the host molecule, and showed that its cavity is capable of accommodating small aromatic species. Subsequent studies have revealed that inclusion compounds involving *p*-tert-butylcalix[4]arene most often crystallize with the host molecules packed as bilayers. Furthermore, the bilayer packing mode can be subdivided into two major categories (Figure 7): *A*, space group *P4/n*, host:guest ratio 1:1 and the guest is partially inserted into the calixarene cavity; *B*, space group *P4/nnc*, host:guest ratio 2:1 and two calixarene molecules face one another to form a dimeric capsule which can completely enclose the guest.

Thermogravimetric analysis of the 1:1 host:guest complex of *p*-tert-butylcalix[4]arene and toluene yields two distinct weight-loss events, each accounting for half of the total amount of toluene originally present in the material. The first weightloss occurs with an onset temperature of 108 °C. It was shown [15] that this corresponds to a transition from a structure of type *A* to one of type *B* as adjacent bilayers shift laterally by *ca.* 9 Å relative to one another. This process occurs as a single-crystal-to-single-crystal phase transformation and is triggered by relatively weak van der Waals interactions between host and guest molecules. Loss of the remaining toluene occurs with an onset temperature of 120 °C, yielding the host material in its pure, unsolvated form.

Ripmeester reported the crystal structure of pure *p*-tert-butylcalix[4]arene grown over a period of three days at 70 °C from a tetradecane solution of the compound [138]. In this phase, *Ib*, the host molecules associate with one another as mutually self-included dimers in which each molecule inserts one its *butyl*-groups into the other's cavity. This arrangement is relatively well packed with an efficiency of 0.67. In the absence of any known polymorphic structures of pure *p*-tert-butylcalix[4]arene, it was reasonable to speculate that *Ib* might be the phase that obtains upon guest removal. Indeed, this assumption was endorsed in a subsequent report [157] dealing with solid–vapor guest inclusion/decomposition processes involving *p*-tert-butylcalix[4]arene and a related compound. Therefore, in light of the recent interest in solid–solid phase transitions of *p*-tert-butylcalix[4]arene, it is relevant to finally address this issue conclusively.

Atwood obtained diffraction-quality single crystals of *p*-tert-butylcalix[4]arene by sublimation of the compound at 280 °C under reduced pressure [11]. The structure of this sublimed phase, *Ic*, has already been described in detail [15]. Phase *Ic* proves to be a polymorphic form of pure *p*-tert-butylcalix[4]arene and, in contrast to *Ib*, has a relatively low packing efficiency of 0.59. The molecules pack in the familiar bilayer motif with facing calixarenes slightly offset relative to one another (Figure 7). This arrangement results in the formation of skewed capsules, each with an estimated free volume of 235 Å³. Furthermore, these capsules are unoccupied, thus accounting for the rather low efficiency of packing. Following previously reported procedures [23, 138] Atwood also prepared crystals of *Ia* and *Ib*. The former were heated at 220 °C under reduced pressure for three hours in order to remove all of the toluene guest molecules. X-Ray powder diffraction patterns of the various materials were recorded and it was revealed that, upon removal of toluene by heating, *Ia* undergoes a phase transition to eventually yield *Ic*.

Atwood and coworkers have similarly investigated 1:1 host:guest adducts of *p*-tert-butylcalix[4]arene with *p*-chlorotoluene, *p*-fluorotoluene, chlorobenzene and fluorobenzene. In each case, they found that guest removal results in phase *Ic*. Although the authors concede that it may still be possible to form phase *Ib* by means of guest removal, they have not yet observed this to be the case for the limited series of inclusion compounds considered here. It is important to note that, with regard to the arrangement of the calixarene molecules, the fundamental difference between *Ic* and the structures of types *A* and *B* is that adjacent bilayers are shifted laterally relative to one another (Figure 7).

In all three structural types, the molecular spacing, both within and between the bilayers, is practically identical. The surfaces of the bilayers are composed of bulky *But*-groups, interspersed with calixarene cavities and the crevices between adjacent *But*- moieties. Thus it is not difficult to envision how adjacent bilayers are able to slide over one another in order to facilitate guest uptake or release as a solid/liquid or solid/vapor inclusion reaction. As yet, the influence of weak van der Waals interactions on both the stability as well as the dynamics of molecules in the solid state has been largely overlooked. However, Atwood and coworkers have shown that studies of simple, yet elegant model systems provide valuable insight into the organic solid state, and that a high degree of cooperativity exists between molecules during phase transitions.

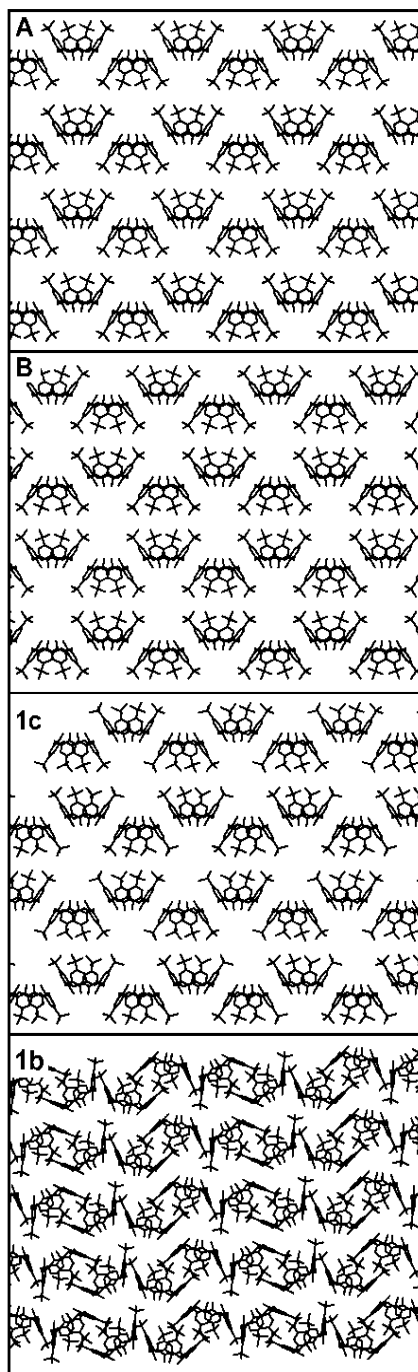


Figure 7. X-Seed projections contrasting 1c with the two most commonly observed bilayer packing arrangements (A and B) of *p*-tert-butylcalix[4]arene. In A, facing calixarenes are offset with respect to one another and the guest molecules (not shown) are partially inserted into their cavities. Adjacent bilayers of B are translated laterally relative to those of A such that facing calixarenes form dimeric capsules. In 1c, facing calixarenes are slightly offset and form skewed, unoccupied capsules. The self-included dimer structure, 1b, obtained from a tetradecane solution of *p*-tert-butylcalix[4]arene is also shown.

Single-crystal to single-crystal phase transformations have received considerable attention in recent years [186]. However, very few examples are known to date because crystals normally do not retain the single crystallinity after the transformation. Most of the reported cases involve guest exchange in porous materials in which structural transformation of the host framework is triggered by guest exchange or removal [187]. Exchange of guest molecules in porous metal-organic frameworks is a well-known but poorly understood phenomenon [188-190]. In contrast, single-crystal to single-crystal transformations caused by guest inclusion in crystals that are held together by weak van der Waal forces are very rare [186]. Host framework retention is a useful strategy for the storage and separation, storage, and transportation of gases [191-195]. Calixarenes are versatile inclusion compounds that have been studied for gas sorption and sensor applications [16, 196-200]. The adsorption of gases, particularly carbon dioxide, is very important for carbon capture and sequestration technology and is one of the most challenging aspects of transportation of carbon dioxide. In this regard, Atwood and coworkers have reported several papers on the CO₂ absorption properties of calix[4]arene derivatives, which demonstrate advantages compared to other porous materials [201]. During the process of gas uptake and release, the host framework should not undergo phase transformation because such transformations are associated with an energy penalty. For instance, Atwood and coworkers have recently reported the “gas-induced transformation and expansion” of an organic solid upon CO₂ or N₂O uptake [202]. The authors discovered that the guest-free thermodynamic form of *p*-tert-butylcalix[4]arene may be converted to the 1:1 host:guest tetragonal form. Such a process should involve a considerable energy barrier, and surprisingly, this transformation process occurs much faster at low temperatures (-10 °C). However, low pressures (100 psi) may require up to 10 days to effect the transformation. In communication [203], Atwood *et al.* have found that a range of gases as well as solvent molecules can effect the transformation of guest-free high-density *p*-tert-butylcalix[4]arene to the 1:1 host:guest tetragonal form.

Similarly, they extended this phenomenon to a range of gases and solvents molecules using the guest free thermodynamic form under ambient conditions. At room temperature and 0.70 MPa (100 psig) of propane, *Ib* was found to transform to *A* in just 10 min. The presence of indicative peaks corresponding to phase of 1:1 host:guest form in the powder diffraction pattern suggests that the transformation from *Ib* to *A* occurs through phase of *p*-tert-butylcalix[4]arene complex. As a result of the transformation, the crystal volume increases by 13% going from *Ib* to *A*. The powder plot of *A* with propane inclusion is near-identical to that of *A* with CO₂ and N₂O. However, the transformation from *Ib* to *A* with CO₂ is rather slow and it is possible to isolate the kinetic form *p*-tert-butylcalix[4]arene with CO₂ (i.e., as a 2:1 host:guest phase *B* prior to conversion to the 1:1 form *A* over a given period of time). As a result, *Ib* expands 33% along the [100] direction and shrinks by 17 and 7% along the [010] and [001] directions, respectively, upon changing to *p*-tert-butylcalix[4]arene complex. The experimental powder plots with these gases are near-identical to that of simulated powder patterns of the 1:1 host:guest complex suggest these gases can form 1:1 host:guest inclusion complexes with *p*-tert-butylcalix[4]arene. Because of the near-identical powder patterns, it is possible to speculate that each calixarene void is filled with one gas molecule. Several experiments were conducted to determine the exact location of the gas molecules in the 1:1 complex using single-crystal X-ray diffraction experiments, but all failed. Though the powder looked identical to the 1:1 host:guest complex, it's possible that the location of gas molecules may look different. To further confirm the molar ratios of the various gases in *p*-tert-

butylcalix[4]arene, gas sorption measurements were conducted on *Ib* at various pressures of CO₂, N₂O, and propane using volumetric analyzer. Previous studies on *p*-tert-butylcalix[4]arene complex at low pressures of CO₂ and N₂O (moles of gas:calixarene ratio = 0.5:1) showed that only a single molecule of the gas can be accommodated within each void formed by two calixarene molecules [204-206], i.e., host:guest = 2:1. Similar experiments on *Ib* at 1 atm pressure indicate phase *Ib* is dead for sorption, which further supports the observation in which at lower pressures (0.70 MPa, 100 psig) of CO₂ and N₂O the conversion from *Ib* to *A* is very slow and takes as long as 10 days to a month. However, the same measurements on *p*-tert-butylcalix[4]arene complex and *Ib* at high pressure indicate instantaneous pressure drop and reaches equilibrium in just 2 h. At this pressure, 1.07 moles of gas occupied per calixarene void, i.e., host:guest = 1:1. Similar experiments on *Ib* at various pressures of propane indicate the molar ratio of the propane approaches close to one. At 1, 3, and 7 bar of propane, the molar ratio is found to be 0.3, 0.5, and 0.7. Therefore, it is possible to selectively transform *Ib* to the desired host:guest = 1:1, 2:1, or 1:2 forms simply through gas selection or by employing higher pressures of the same gas.

The authors also examined the effects of solvents and their vapors on form *Ib*. Freshly grown crystals of *Ib* were placed in two separate vials. One set of crystals was soaked in acetone, whereas for the others, CS₂ vapors were allowed to diffuse through the crystals for 10 min. Both crystal batches were crushed into fine powders and the corresponding powder plots indicate the transformation from *Ib* to the 1:1 host:guest (acetone and CS₂) forms. Shatz *et al.* [207] reported the formation of an acetone complex with a 2:1 host:guest ratio, which unfortunately has not been fully characterized. The powder patterns suggest that the molar ratio of host and guest is 1:1. The observations are in good agreement with the simulated powder diffraction plots of 1:1 acetone and CS₂ complexes obtained simply by recrystallizing *p*-tert-butylcalix[4]arene from CS₂ and acetone, as reported by Klinoski and Schatz *et al.* [207, 208]. X-ray analysis on *Ib* at various temperatures suggests that at low temperature, three out of four *tert*-butyl groups are disordered over two positions, whereas all are disordered at room temperature. Therefore, one can further speculate that limited rotation of *tert*-butyl groups in *Ib* would allow the gas molecules to diffuse through the solid, and simultaneously the energy released after the gas is trapped in crystal is sufficient to transform *Ib* to the more stable form *A* or *B* with included gas or solvent molecules. The existence of 2:1, 1:1, and higher gas inclusion complexes and failure of similar transformation to occur with other gases (H₂, He, and CH₄) suggest the possibility of exploiting these materials for carbon capture and separation applications.

REFERENCES

- [1] Nabok, AV; Hassan, AK; Ray, AK. *J. Mater. Chem.*, 2002, 10, 189-194.
- [2] Chaabane, RB; Gamoudi, M; Guillaud, G; Jouve, C; Lamartine, R; Bouazizi, A; Maaref, H. *Sens. Actuators B*, 1996, 31, 41-44.
- [3] Mlika, R; Dumazet, I; Gamoudi, M; Lamartine, R; Ben Ouada, H; Jaffrezic-Renault, N; Guillaud, G. *Anal. Chem. Acta*, 1997, 354, 283-289.
- [4] Mlika, R; Ben Ouada, H; Hamza, MA; Gamoudi, M; Guillaud, G; Jaffrezic-Renault, N. *Synth. Met.*, 1997, 90, 173-179.

- [5] Mlika, R; Ben Ouada, H; Jaffrezic-Renault, N; Dumazet, I; Lamartine, R; Gamoudi, M; Guillaud, G. *Sens. Actuators B*, 1998, 47, 43-47.
- [6] Abraham, W. J. *Incl. Phenom. Macrocycl. Chem.*, 2002, 43, 159-174.
- [7] Hirakata, M; Yoshimura, K; Usui, S; Nishimoto K; Fukazawa, Y. *Tetrahedron Lett.*, 2002, 43, 1859-1861.
- [8] Vincenti, M. *J. Mass Spectrosc.*, 1995, 30, 925-939.
- [9] Inokuchi, F; Araki, K; Shinkai, S. *Chem. Lett.*, 1994, 23(8), 1383-1386.
- [10] Vincenti, M; Irico, A. *Int. J. Mass Spectrom.*, 2002, 214, 23-36.
- [11] Atwood, JL; Barbour, LJ; Jerga, A. *Chem. Commun.*, 2002, 2952-2953.
- [12] Atwood, JL; Barbour, LJ; Lloyd, GO; Thallapally, PK. *Chem. Commun.*, 2004, 922-923.
- [13] Surov, OV; Mamardashvili, NZh; Shaposhnikov, GP; Koifman, OI. *Russ. J. Gen. Chem.*, 2006, 76 (6), 974-979.
- [14] Surov, OV; Mamardashvili, NZh; Shaposhnikov, GP; Koifman, OI. *Russ. J. Phys. Chem., A* 2007, 81(12), 1936-1941.
- [15] Atwood, JL; Barbour, LJ; Jerga, A; *Schottel, BL. Science*, 2002, 298, 1000-1002.
- [16] Thallapally, PK; Lloyd, GO; Atwood, JL; Barbour, LJ. *Angew. Chem. Int. Ed.*, 2005, 44 (25), 3848-3851.
- [17] Alcaciz-Monge, A; Linares-Solano, A; Rand, B. *J. Phys. Chem., B* 2001, 105, 7998-8001.
- [18] Gutache, CD; Dhawan, B; No, KH; Muthukrishnan, R. *J. Am. Chem. Soc.*, 1981, 103, 3782-3791.
- [19] Coruzzi, M; Andreotti, GD; Bocchi, V; Pochini, A; Ungaro, R. *J. Chem. Soc. Perkin Trans.*, 1982, 2, 11, 33-44.
- [20] Ninagawa, A; Matauda, H. *Makromol. Chem. Rapid Commun.*, 1982, 3, 65-67.
- [21] Coruzzi, M; Andreotti, GD; Bocchi, V; Pochini, A; Ungaro, R. *J. Chem. Soc. Perkin Trans.*, 1982, 2, 1133-1141.
- [22] Nakamoto, Y; Ishida, S. *Makromol. Chem. Rapid Commun.*, 1982, 3, 705-706.
- [23] Andreotti, GD; Ungaro, R; Pochini, A. *J. Chem. Soc. Chem. Commun.*, 1979, 1005-1007.
- [24] Gutsche, C.D. *Acc. Chem. Res.* 1983, 16, 161-170.
- [25] Gutsche, CD. In *Calixarenes Revisited*; JF; Stoddart, (Eds.), Monographs in Supramolecular Chemistry; The Royal Society of Chemistry: Cambridge, U.K., 1998, Vol. 6.
- [26] Pochini, A; Ungaro R. In *Comprehensive Supramolecular Chemistry*; In: F; Vögtle, (Eds.), Elsevier: 1996, Vol. 2, Chapt. 4, 103-142.
- [27] Nishio, M; Hirota, M; Umezawa Y. In *The CH/π Interaction*; AP; Marchand, (Eds.), Methods in Stereochemical Analysis; Wiley-VCH: 1998, No. 11.
- [28] Umezawa, Y; Tsuboyama, S; Honda, K; Uzawa, J; Nishio, M. *Bull. Chem. Soc. Jpn.*, 1998, 71, 1207-1213.
- [29] Braga, D; Grepioni, F; Tedesco, E. *Organometallics*, 1998, 17, 2669-2672.
- [30] Arduini, A; Pochini, A; Secchi, A; Ugozzoli, F. In Z; *Calixarenes* Asfari, et al; (Eds.), *Kluwer Academic Publishers: Dordrecht*, NL, 2001, Chapt. 25, 457-475.
- [31] Brouwer, EB; Enright, GD; Ratcliffe, CI; Ripmeester, JA; Udachin, KA. In *Calixarenes* Z; Asfari, (Eds.), Eds; *Kluwer Academic Publishers: Dordrecht*, NL, 2001, Chapt. 16, 296-311.

- [32] Arduini, A; McGregor, WM; Paganuzzi, D; Pochini, A; Secchi, A; Ugozzoli, F; Ungaro, R. *J. Chem.Soc. Perkin Trans.*, 1996, 2, 839-846.
- [33] Abidi, R; Baker, MV; Harrowfield, JM; Ho, DSC; Richmond, WR; Skelton, BW; White, AH; Varnek, A; Wipff, G. *Inorg. Chim. Acta*, 1996, 246, 275-286.
- [34] McKervey, MA; Seward, EM; Ferguson, G; Ruhl, BL. *J. Org. Chem.*, 1986, 51, 3581-3584.
- [35] Gibson, VC; Redshaw, C; Clegg, W; Elsegood, MRJ. *J. Chem. Soc. Chem. Commun.*, 1997, 1605-1606.
- [36] Harrowfield, JM; Ogden, MI; Richmond, WR; Skelton, BW; White, AH. *J. Chem. Soc. Perkin Trans.*, 1993, 2, 2183-2190.
- [37] Beer, PD; Drew, MGB; Leeson, PB; Lyssenko, K; Ogden, MI. *J. Chem. Soc. Chem. Commun.*, 1995, 929-930.
- [38] Beer, PD; Drew, MGB; Leeson, PB; Ogden, MI. *J. Chem. Soc. Dalton Trans.*, 1995, 1273-1283.
- [39] Xu, W; Puddephatt, RJ; Manojlovic-Muir, L; Muir, KW; Frampton, CS. *J. Incl. Phenom. Macrocycl. Chem.*, 1994, 19, 277-290.
- [40] MacGillivray, LR; Atwood, JL. *J. Am. Chem. Soc.*, 1997, 119, 6931-6932.
- [41] Zhen-Lin, Z; Yuan-Yin, C; Xue-Ran, L; Bao-Sheng, L; Liao-Rong, C. *Jiegou Huaxue (J. Struct. Chem.)*. 1996, 15, 358-360.
- [42] Reichwein, AM; Verboom, W; Harkema, S; Spek, AL; Reinhoudt, DN. *J. Chem. Soc. Perkin Trans.*, 1994, 2, 1167-1172.
- [43] Aleksyuk, O; Grynszpan, F; Biali, SE. *J. Incl. Phenom. Macrocycl. Chem.* 1994, 19, 237-256.
- [44] Biali, SE; Böhmer, V; Cohen, S; Ferguson, G; Güttner, C; Grynszpan, F; Paulus, EF; Thondorf, I; Vögt, W. *J. Am. Chem. Soc.*, 1996, 118, 12938-12949.
- [45] Szemes, F; Heseck, D; Chen, Z; Dent, SW; Drew, MGB; Goulden, AJ; Graydon, AR; Grieve, A; Mortimer, RJ; Wear, T; Weightman, JS; Beer, PD. *Inorg.Chem.*, 1996, 35, 5868-5879.
- [46] Danil de Namor, AF; Piro, OE; Pulcha Salazar, LE; Aguilar-Cornejo, AF; Al-Rawi, N; Castellano, EE; Sueros Velarde, FJ. *J. Chem. Soc. Faraday Trans.*, 1998, 94, 3097-3104.
- [47] Verboom, W; Struck, O; Reinhoudt, DN; van Duynhoven, JPM; van Hummel, GJ; Harkema, S; Udachin, KA; Ripmeester, JA. *Gazz. Chim. Ital.*, 1997, 127, 727-739.
- [48] Pitarch, M; Walker, A; Malone, JF; McGarvey, JJ; McKervey, MA; Creaven, B; Tobin, D. *Gazz.Chim. Ital.*, 1997, 127, 717-721.
- [49] Akdas, H; Bringel, L; Graf, E; Hosseini, MH; Mislin, G; Pansanel, J; De Cian, A; Fischer, J. *Tetrahedron Lett.*, 1998, 39, 2311.
- [50] Airola, K; Böhmer, V; Paulus, EF; Rissanen, K; Schmidt, C; Thondorf, I; Vogt, W. *Tetrahedron*, 1997, 53, 10709-10724.
- [51] Giannini, L; Caselli, A; Solari, E; Floriani, C; Chiesi-Villa, A; Rizzoli, C; Re, N; Sgamellotti, A. *J. Am.Chem. Soc.*, 1997, 119, 9709-9719.
- [52] Beer, PD; Drew, MGB; Grieve, A; Kan, M; Leeson, PB; Nicholson, G; Ogden, MI; Williams, G. *Chem. Commun.*, 1996, 1117-1118.
- [53] Gardiner, MG; Koutsantonis, GA; Lawrence, SM; Nichols, PJ; Raston, CL. *Chem. Commun.*, 1996, 2035-2036.
- [54] Shevchenko, I; Zhang, H; Lattman, M. *Inorg. Chem.*, 1995, 34, 5405-5409.

- [55] Beer, PD; Drew, MGB; Grieve, A; Ogden, MI. *J. Chem. Soc. Dalton Trans.*, 1995, 3455-3466.
- [56] Beer, PD; Drew, MGB; Kan, M; Leeson, PB; Ogden, MI; Williams, G. *Inorg. Chem.*, 1996, 35,2202-2211.
- [57] Beer, PD; Drew, MGB; Leeson, PB; Ogden, MI. *Inorg. Chim. Acta.*, 1996, 246, 133-141.
- [58] Mislin, G; Graf, E; Hosseini, MH; Bilyk, A; Hall, AK; Harrowfield, JM; Skelton, BW; White, H. *Chem. Commun.*, 1999, 373-374.
- [59] Böhmer, V; Ferguson, G; Gallagher, JF; Lough, AJ; McKervey, MA; Madigan, E; Moran, MB; Phillips, J; Williams, G. *J. Chem. Soc. Perkin Trans*, 1993, 1, 1521-1527.
- [60] Leigh, DA; Linnane, P; Pritchard, RG; Jackson, G. *Chem. Commun.*, 1994, 389-390.
- [61] Helgeson, RC; Knobler, CB; Cram, DJ. *Chem. Commun.*, 1995, 307-308.
- [62] Sartori, G; Porta, C; Bigi, F; Maggi, R; Peri, F; Marzi E. *Tetrahedron*, 1997, 53, 3287-3300.
- [63] Thuéry, P; Nierlich, M; Lamare, V; Dozol, JF; Asfari, Z; Vicens, J. *J. Incl. Phenom. Macrocycl. Chem.*, 2000, 36, 375-408.
- [64] Bauer, LJ; Gutsche, CD. *J. Am. Chem. Soc.*, 1985, 107, 6063-6069.
- [65] Gutsche, CD; Levine, JA. *J. Am. Chem. Soc.*, 1982, 104, 2652-2659.
- [66] Danil de Namor, AF; Zapata-Ormachea, ML; Hutcherson, RG. *J. Phys. Chem., B* 1998, 102, 7839-7851.
- [67] Danil de Namor, AF; Hutcherson, RG; Sueros Velarde, JF; Alvarez-Larena, A; Briansó-Penalva, JL. *J. Chem. Soc. Perkin Trans.*, 1998, 1, 2933-2940.
- [68] Danil de Namor, AF; Zapata-Ormachea, ML; Hutcherson, RG. *J. Phys. Chem., B* 1999, 103, 366-377.
- [69] Arena, G; Contino, A; Gulino, FG; Magr'ı, A; Sciotto, D; Ungaro, R. *Tetrahedron Lett.*, 2000, 41, 9327-9336.
- [70] Kunsági-Máté, S; Nagy, G; Kollár, L. *Anal. Chim. Acta*, 2001, 428, 301-308.
- [71] Kunsági-Máté, S; Nagy, G; Kollár, L. *Sens. Actuators B*, 2001, 76, 545-549.
- [72] Kunsági-Máté, S; Bitter, I; Grün, A; Nagy, G; Kollár, L. *Anal. Chem. Acta*, 2002, 461, 273-279.
- [73] Danil de Namor, AF; Cleverley, RM; Zapata-Ormachea, ML. *Chem. Rev.*, 1998, 98, 2495-2525.
- [74] Danil de Namor, AF. *Pure Appl. Chem.*, 1993, 65, 193-197.
- [75] Danil de Namor, AF; Hutcherson, RG; Sueros Velarde, FJ; Zapata-Ormachea, ML; Pulcha Salazar, LE; al Jammaz, I; al Rawi, N. *Pure Appl. Chem.*, 1998, 70, 769-774.
- [76] Danil de Namor, AF; Cleverley, RR; Zapata-Ormachea, ML. *Chem. Rev.*, 1998, 98, 2495-2497.
- [77] Danil de Namor, AF; Kowalska, D; Marcus, Y; Villanueva-Salas, J. *J. Phys. Chem. B*, 2001, 105, 7542-7548.
- [78] Danil de Namor, AF; Kowalska, D; Castellano, EE; Piro, OE; Sueros Velarde, FJ; Villanueva-Salas, J. *Phys. Chem. Chem. Phys.*, 2001, 3, 4010-4016.
- [79] Danil de Namor, AF; Chahine, S; Castellano, EE; Piro, OE. *J. Phys. Chem B*, 2004, 108, 11384-11394.
- [80] Danil de Namor, AF; Aguilar-Cornejo, A; Soualhi M. Shehab, R; Nolan, KB; Ouazzani, N; Mand, L. *J. Phys. Chem. B*, 2005, 109, 14735-14741.
- [81] Liu, Y; Wang, H; Wang, LH; Zhang, HY. *Thermochim. Acta*, 2004, 414, 65-71.

- [82] Liu, Y; Yang, EC; Chen, Y. *Thermochim. Acta*, 2005, 429, 163-171.
- [83] Liu, Y; Yang, EC; Chen, Y; Guo, DS; Ding, F. *Eur. J. Org. Chem.*, 2005, 21, 4581-4585.
- [84] Vicens, J; Böhmer, V. *Calixarenes: A Versatile Class of Macrocyclic Compounds*; Kluwer Academic Publishers: Dordrecht, NL, 1991.
- [85] Vicens, J; Asfari, Z; Harrowfield, JM. *Calixarenes 50th Anniversary*; Commemorative Volume; Kluwer Academic Publishers: Dordrecht, NL, 1994.
- [86] Böhmer, V. *Angew. Chem. Int. Ed.*, 1995, 34, 713-718.
- [87] Ikeda, A; Shinkai, S. *Chem. Rev.*, 1997, 97, 1713-1717.
- [88] van Wageningen, AMA; Verboom, W; Reinhoudt, DN. *Pure Appl. Chem.*, 1996, 68, 1273-1276.
- [89] Mandorlini, L. In *Calixarenes in Action*; R; Ungaro, (Eds.), Imperial College Press: London, U.K., 2000.
- [90] Brodbelt, JS; Dearden, DV. In *Mass Spectrometry, Comprehensive Supramolecular Chemistry*; In: JED; Davies, JA; Ripmeester, Eds; Pergamon Press: Oxford, U.K., 1996, Vol. 8.
- [91] Sawada, M. *Mass Spectrom. Rev.*, 1997, 16, 73-84.
- [92] Schalley, CA. *Int. J. Mass Spectrom.*, 2000, 194, 11-23.
- [93] Loo, JA. *Mass Spectrom. Rev.*, 1997, 16, 1-20.
- [94] Wong, PSH; Yu, XJ; Dearden, DV. *Inorg. Chim. Acta*, 1996, 246, 259-268.
- [95] Schalley, CA; Castellano, RK; Brody, MS; Rudkevich, DM; Siuzdak, G; Rebek Jr., J. *J. Am. Chem. Soc.*, 1999, 121, 4568-4579.
- [96] Brody, MS; Schalley, CA; Rudkevich, DM; Rebek Jr., J. *Angew. Chem. Int. Ed.*, 1999, 38, 1640-1642.
- [97] Jolliffe, KA; Crego Calama, M; Fokkens, R; Nibbering, NMM; Timmerman, P; Reinhoudt, DN. *Angew. Chem. Int. Ed.*, 1998, 37, 1247-2249.
- [98] Cardullo, F; Crego Calama, M; Snellink-Ruël, BHM; Weidmann, JL; Bielejewska, A; Fokkens, R; Nibbering, NMM; Timmerman, P; Reinhoudt, DN. *J. Chem. Soc. Chem. Comm.*, 2000, 367-369.
- [99] Vincenti, M; Irico, A. *Int. J. Mass Spectrom.*, 2002, 214, 23-36.
- [100] Vincenti, M; Minero, C; Pelizzetti, E; Secchi, A; Dalcanale, E. *Pure Appl. Chem.*, 1995, 67, 1075-1079.
- [101] Liang, TM; Laali, KK; Cordero, M; Wesdemiotis, C. *J. Chem. Research (S)*, 1991, 354-355.
- [102] Vincenti, M; Dalcanale, E; Soncini, P; Guglielmetti, G. *J. Am. Chem. Soc.*, 1990, 112, 445-451.
- [103] Cotter, RJ. *Anal. Chem.*, 1980, 52, 1589A.
- [104] Surov, OV; Mamardashvili, NZh; Shaposhnikov, GP; Koifman, OI. *J. Incl. Phenom. Macrocycl. Chem.*, 2007, 58, 329-335.
- [105] Ghidini, E; Ugozzoli, F; Ungaro, R; Harkema, S; Abu El-Fadl, A; Reinhoudt, DN. *J. Am. Chem. Soc.*, 1990, 112(19), 6979-6985.
- [106] Klenke, B; Friederichsen, W. *J. Chem. Soc. Perkin Trans.*, 1998, 1, 998(20), 3377-3380.
- [107] Yam, VWW; Cheung, KL; Yuan, LH; Wong, KMC; Cheung, KK. *Chem. Commun.*, 2000, 16, 1513-1514.

- [108] van Loon, JD; Arduini, A; Coppi, L; Verboom, W; Pochini, A; Ungaro, R; Harkema, S; Reinhoudt, D. *J. Org. Chem.*, 1990, 55, 5639-5646.
- [109] Chickos, JS; Acree, Jr, WE. *J. Phys. Chem. Ref. Data*, 2002, 31(2), 537-698.
- [110] Grootenhuis, PDJ; Kollman, PA; Groenen, LC; Reinhoudt, DN; van Hummel, GJ; Ugozzoli, F; Andreetti, GD. *J. Am. Chem. Soc.*, 1990, 112(11), 4165-4176.
- [111] Kunugi, Y; Nigorikawa, K; Harima, Y; Yamashita, K. *J. Chem. Soc. Chem. Commun.*, 1994, 873-874.
- [112] Lu, CJ; Shin, JS. *Anal. Chem. Acta*, 1995, 306, 129-133.
- [113] Chen, ZK; Ng, SC; Li, SFY; Zhong, L; Xu, LG; Chan, HSO. *Synth. Met.*, 1997, 87, 201-211.
- [114] Zhou, XC; Zhong, L; Li, SFY; Ng, SC; Chan, HSO. *Sens. Actuators B*, 1997, 42, 59-68.
- [115] Barko, G; Hlavay, J. *Anal. Chim. Acta*, 1998, 367, 135-142.
- [116] Deng, ZP; Stone, DC; Thompson, M. *Analyst*, 1996, 121, 1341-1349.
- [117] Cao, Z; Cao, D; Lei, ZG; Lin, HG; Yu, RQ. *Talanta*, 1997, 44, 1413-1419.
- [118] Papes, V; Brodska, S. *Sens. Actuators B*, 1997, 40, 143-150.
- [119] Costello, BPJD; Evans, P; Ewen, RJ; Honeybourne, CL; Ratcliffe, NM. *J. Mater. Chem.*, 1996, 6, 289-297.
- [120] Milella, E; Musio, F; Alba, M.B. *Thin Solid Films*, 1996, 285, 908-911.
- [121] De Wit, M; Vanneste, E; Geise, HJ; Nagels, LJ. *Sens. Actuators B*, 1998, 50, 164-166.
- [122] Buhlmann, K; Schladtt, B; Cammann, K; Shulga, A. *Sens. Actuators B*, 1998, 49, 156-159.
- [123] Dickert, FL; Baumler, UPA; Zwissler, GK. *Synth. Met.*, 1993, 61, 47-53.
- [124] Nelli, P; Delcanale, E; Faglia, G; Sberveglieri, G; Soncini, P. *Sens. Actuators B*, 1993, 13-14, 302-312.
- [125] Schierbaum, KD; Weiss, T; Thoden van Velzen, EU; Engbersen, JFJ; Reinhoudt, DN; Gopel, W. *Science*, 1994, 265, 1413-1415.
- [126] Dalcanale, E; Hartman, J. *Sens. Actuators B*, 1995, 24, 39-41.
- [127] Rickert, J; Weiss, T; Gopel, W. *Sens. Actuators B*, 1996, 31, 45-50.
- [128] Nabok, AV; Lavrik, NV; Kazantseva, ZI; Nesterenko, BA; Markovskiy, LN; Kalchenko, VI; Shivaniuk, AN. *Thin Solid Films*, 1995, 259, 244-248.
- [129] Nabok, AV; Hassan, AK; Ray, AK; Omar, O; Kalchenko, VT. *Sens. Actuators B*, 1997, 45, 115-118.
- [130] Nabok, AV; Hassan, AK; Ray, AK. *J. Mater. Chem.*, 2000, 10, 189-194.
- [131] Schierbaum, KD; Gerlach, A; Göpel, W; Müller, WM; Vögtle, F; Dominik, A; Roth, HJ. *Fresenius J. Anal. Chem.* 1994, 349, 372-379.
- [132] Abraham, M. H; Platts, J. A. *J. Org. Chem.*, 2001, 66, 3484-3496.
- [133] Lehn, JM. *Supramolecular Chemistry: Concepts and Perspectives*; VCH: Weinheim, BD, 1995.
- [134] Weber, E. In *Comprehensive Supramolecular Chemistry*; J. L., Atwood, J. E., Davies, D. D., MacNicol, F., Vogtle, (Eds.), Elsevier Science: Oxford, U.K., 1996, Vol. 6, Chapt. 17, 535-592.
- [135] Weber, E; Hens, T; Brehmer, T; Csöreg, I. *J. Chem. Soc. Perkin Trans.*, 2000, 2, 235-238.
- [136] Gorbachuk, VV; Tsifarkin, AG; Antipin, IS; Solomonov, BN; Kononov, AI. *Mendeleev Commun.*, 1999, 11-13.

- [137] Gorbachuk, VV; Tsifarkin, AG; Antipin, IS; Solomonov, BN; Konovalov, AI; Seidel, J; Baitalov, F. *J. Chem. Soc. Perkin Trans.*, 2000, 2, 2287-2289.
- [138] Brouwer, EB; Udachin, KA; Enright, GD; Ripmeester, JA; Ooms, KJ; Halchuk, PA. *Chem. Commun.*, 2001, 565-567.
- [139] Fredeslund, A; Jones, RL; Prausnitz, JM. *AIChE J.*, 1975, 21, 1086-1089.
- [140] Bishop, R. *Chem. Soc. Rev.*, 1996, 25, 311-313.
- [141] Weber, E; Wierig, A; Scobridis, K. *J. Prakt. Chem.*, 1996, 338, 553-558.
- [142] Weber, E; Hens, T; Gallardo, O; Csöreg, I. *J. Chem. Soc. Perkin Trans.*, 1996, 2, 737-742.
- [143] Weber, E; Hens, T; Li, Q; Mak, TC. *W. Eur. J. Org. Chem.*, 1999, 1115-1121.
- [144] Schatz, J; Schildbach, F; Lentz, A; Rastätter, S. *J. Chem. Soc. Perkin Trans.*, 1998, 2, 75-82.
- [145] Dickert, FL; Keppler, M; Zwissler, GK; Obermeier, E. *Ber. Bunsen-Ges. Phys. Chem.*, 1996, 100, 1312-1319.
- [146] Furusho, Y; Aida, T. *Chem. Commun.*, 1997, 2205-2207.
- [147] Coetzee, A; Nassimbeni, LR; Achleitner, K. *Thermochim., Acta* 1997, 298, 81-88.
- [148] Dewa, T; Endo, K; Aoyama, Y. *J. Am. Chem. Soc.*, 1998, 120, 8933-8940.
- [149] Beketov, K; Weber, E; Seidel, J; Köhnke, K; Makhkamov, K; Ibragimov, B. *Chem. Commun.*, 1999, 91-93.
- [150] Nassimbeni, LR. In *Molecular Recognition and Inclusion*; A. W., Coleman, (Eds.), Kluwer: Dordrecht, NL, 1998, 135-152.
- [151] Brouwer, EB; Udachin, KA; Enright, GD; Ripmeester, JA. *Chem. Commun.*, 2000, 1905-1907.
- [152] Ungaro, R; Pochini, A; Andretti, GD; Sangermano, V. *J. Chem. Soc. Perkin Trans.*, 2 1984, 1979-1985.
- [153] Toda, F; Tanaka, K; Miyahara, I; Akutsu, S; Hirotsu, K. *Chem. Commun.*, 1994, 1795-1797.
- [154] Lee, SO; Harris, KDM. *Chem. Phys. Lett.*, 1999, 307, 327-333.
- [155] Kuruma, K; Nakagawa, H; Imakubo, T; Kobayashi, K. *Bull. Chem. Soc. Jpn.*, 1999, 72, 1395-1401.
- [156] Brehmer, TH; Weber, E; Cano, FH. *J. Phys. Org. Chem.*, 2000, 13, 63-72.
- [157] Gorbachuk, VV; Tsifarkin, AG; Antipin, IS; Solomonov, BN; Konovalov, AI; Lhotak, P; Stibor I. *J. Phys. Chem., B* 2002, 106, 5845-5851.
- [158] Gorbachuk, VV; Tsifarkin, AG; Antipin, IS; Solomonov, BN; Konovalov, AI. *J. Incl. Phenom. Macrocycl. Chem.*, 1999, 35, 389-396.
- [159] Ziganshin, MA; Yakimov, AV; Konovalov, AI; Antipin, IS; Gorbachuk, VV. *Russ. Chem. Bull. Int. Ed.*, 2004, 53(7), 1536-1543.
- [160] Surov, OV; Voronova, MI. *Russ. J. Phys. Chem., A* 2009, 83(5), 822-825.
- [161] Jura, G; Harkins, WD. *J. Am. Chem. Soc.*, 1944, 66(8), 1356-1373.
- [162] Lhotak, P; Himl, M; Stibor, I. et al. *Tetrahedron*, 2003, 59, 7581-7586.
- [163] Hirakata, M; Yoshimura, K; Usui, S; Nishimoto, K; Fukazawa, Y. *Tetrahedron Lett.*, 2002, 43, 1859-1861.
- [164] Iwamoto, H; Hirakata, M; Usui, S; Haino, T; Fukazawa, Y. *Tetrahedron Lett.*, 2002, 43, 85-87.
- [165] Endo, K; Kondo, Y; Aoyama, Y; Hamada, F. *Tetrahedron Lett.*, 2003, 44, 1355-1358.
- [166] Murayama, K; Aoki, K. *Inorg. Chim. Acta*, 1998, 281, 36-42.

- [167] Leverd, PC; Berthault, P; Lance, M; Nierlich, M. *Eur. J. Inorg. Chem.*, 1998, 1859-862.
- [168] Schatz, J; Schildbach, F; Lentz, A; Rastätter, S. *J. Chem. Soc. Perkin Trans.*, 1998, 2, 133-144.
- [169] Graham, BF; Harrowfield, JM; Tengrove, RD; Lagalante, AF; Bruno, TJ. *J. Incl. Phenom. Macrocycl. Chem.*, 2002, 43, 179-182.
- [170] James, SL. *Chem. Soc. Rev.*, 2003, 32, 276-288.
- [171] Janiak, C. *J. Chem. Soc. Dalton Trans.*, 2003, 2781-2804.
- [172] Rosi, NL; Eckert, J; Eddaoudi, M; Vodak, DT; Kim, J; O'Keeffe, M; Yaghi, OM. *Science*, 2003, 300, 1127-1130.
- [173] Pan, L; Sander, MB; Huang, X; Li, J; Smith, M; Bittner, E; Bockrath, B; Johnson, JK. *J. Am. Chem. Soc.*, 2004, 126, 1308-1309.
- [174] Düren, T; Sarkisov, L; Yaghi, O. M; Snurr, R. Q. *Langmuir* 2004, 20, 2683-2689.
- [175] Eddaoudi, M; Kim, J; Rosi, N; Vodak, D; Wachter, J; O'Keeffe, M; Yaghi, OM. *Science*, 2002, 295, 469-472.
- [176] Kitagawa, S; Kitaura, R; Noro, S. *Angew. Chem. Int. Ed.* 2004, 43, 2334-2375.
- [177] Sharma, AC; Borovik, AS. *J. Am. Chem. Soc.*, 2000, 122, 8946-8955.
- [178] Padden, KM; Krebs, JF; MacBeth, CE; Scarrow, RC; Borovik, AS. *J. Am. Chem. Soc.*, 2001, 123, 1072-1079.
- [179] Rowsell, JLC; Yaghi, OM. *Angew. Chem. Int. Ed.*, 2005, 44, 4670-4679.
- [180] Atwood, JL; Barbour, LJ; Jerga, A. *Science*, 2002, 296, 2367-2369.
- [181] Enright, GD; Udachin, KA; Moudrakovski, IL; Ripmeester, JA. *J. Am. Chem. Soc.*, 2003, 125, 9896-9897.
- [182] Atwood, JL; Barbour, LJ; Jerga, A. *Angew. Chem. Int. Ed.*, 2004, 43, 2948-2950.
- [183] Thallapally, PK; Lloyd, GO; Wirsig, TB; Bredenkamp, MW; Atwood, JL; Barbour, LJ. *Chem. Commun.*, 2005, 5272-5274.
- [184] McKeown, NB; Budd, PM; Msayib, KJ; Ghanem, BS; Kingston, HJ; Tattershall, CE; Makhseed, S; Reynolds, KJ; Fritsch, D. *Chem. Eur. J.*, 2005, 11, 2610-2620.
- [185] Leontiev, AV; Rudkevich, DM. *Chem. Commun.*, 2004, 1468-1469.
- [186] Atwood, JL; Barbour, LJ; Jerga, A. *Science*, 2006, 296, 2367-2369.
- [187] Kitagawa, S; Kitaura, R; Noro, SI. *Angew. Chem. Int. Ed.*, 2004, 39, 2334-2337.
- [188] Zhang, JP; Lin, YY; Zhang, WX; Chen, ZM. *J. Am. Chem. Soc.*, 2005, 127, 14162-14165.
- [189] Toh, NL; Nagarathinam, M; Vittal, J. *Angew. Chem. Int. Ed.*, 2005, 44, 2237-2239.
- [190] Chen, CL; Goforth, AM; Smith, MD; Su, CY; Zur Loye, HC. *Angew. Chem. Int. Ed.*, 2005, 44, 6637-6639.
- [191] Dalgarno, SJ; Thallapally, PK; Barbour, LJ; Atwood, JL. *Chem. Soc. Rev.*, 2007, 36, 236-238.
- [192] Eddaoudi, M; Kim, J; Rosi, N; Vodak, D; Wachter, J; O'Keeffe, M; Yaghi, OM. *Science*, 2002, 295, 469-472.
- [193] Kitagawa, S; Kondo, M; Seki, K. *Angew. Chem. Int. Ed.*, 2000, 39, 2082-2085.
- [194] Zhao, X; Xiao, B; Fletcher, J; Thomas, KM; Bradshaw, D; Rosseinsky, MJ. *Science*, 2004, 306, 1012-1014.
- [195] Barbour, LJ. *Chem. Commun.*, 2006, 1163-1164.
- [196] Atwood, JL; Barbour, LJ; Jerga, AJ. *Angew. Chem. Int. Ed.*, 2004, 43, 2948-2950.
- [197] Thallapally, PK; Dalgarno, SJ; Atwood, JL. *J. Am. Chem. Soc.*, 2006, 128, 15060-15063.

-
- [198] Atwood, JL; Barbour, LJ; Thallapally, PK; Wirsig, TB. *Chem. Commun.*, 2005, 51-53.
- [199] Thallapally, PK; Wirsig, TB; Barbour, LJ; Atwood, JL. *Chem. Commun.*, 2005, 4420-4422.
- [200] Thallapally, PK; Lloyd, GO; Barbour, LJ; Atwood, JL. *Angew. Chem. Int. Ed.*, 2005, 44, 3848-3851.
- [201] Thallapally, PK; Kirby, KA; Atwood, JL. *New J. Chem.*, 2007, 31, 628-632.
- [202] Thallapally, PK; McGrail, BP; Dalgarno, SJ; Schaef, HT; Tian, J; Atwood, JL. *Nat. Mater.*, 2008, 7, 146-151.
- [203] Thallapally, PK; McGrail, PB; Dalgarno, SJ; Atwood, JL. *Cryst. Growth Des.*, 2008, 8(7), 2090-2092.
- [204] Thallapally, PK; Dobrzanska, L; Gingrich, TR; Wirsig, TB; Barbour, LJ; Atwood, JL. *Angew. Chem. Int. Ed.*, 2006, 45, 6506-6509.
- [205] Thallapally, PK; McGrail, BP; Atwood, JL. *Chem. Commun.*, 2007, 1521-1522.
- [206] Thallapally, PK; McGrail, BP; Atwood, JL; Gaeta, C; Tedesco, C; Neri, P. *Chem. Mater.*, 2007, 19, 3356-3360.
- [207] Shatz, J; Schildbach, F; Lentz, A; Rastatter, S. *J. Chem. Soc. Perkin Trans.*, 2 1998, 75-81.
- [208] Benevelli, F; Kolodziejski, W; Wozniak, K; Klinoski, J. *Phys. Chem. Chem. Phys.*, 2001, 3, 1762-1766.

Chapter 3

**MOLECULAR DISCRIMINATION BEHAVIOR,
DISCRIMINATION LEVEL AND DISCRIMINATION
FACTOR OF CYCLODEXTRINS AND THEIR
DERIVATIVES TO GUEST MOLECULES**

*Le Xin Song^{1,2}, * Xue Qing Guo¹,
Zheng Dang² and Mang Wang²*

¹ CAS Key Laboratory of Soft Matter Chemistry,
Department of Polymer Science and Engineering,
University of Science and Technology of China,
Hefei, Anhui 230026, China.

² Department of Chemistry, University of Science and
Technology of China, Hefei, 230026, Anhui, China.

ABSTRACT

This review briefly describes the molecule-molecule and molecule-ion interactions in cyclodextrin (CD) chemistry. And then the interactions were carefully compared on the basis of data from published papers. According to this, we concluded that the binding behaviors and discrimination abilities of CDs to a group of similar guests could be divided into four levels (A, B, C and D) in the light of the combination between the formation constants (K) of inclusion complexes and the ratio values (ζ , discrimination factor) of K of different complexes of the same host or guest. Our objective is to present a useful method of categorizing host-guest complexes of CDs, and to elucidate the difference and relationship in concepts among inclusion phenomenon, molecular discrimination and molecular recognition. In addition, the physical significance of ζ , as well as the contributions of ζ and K to the molecular discrimination between CDs and guests, is described in the present work.

Keywords: Cyclodextrin; Inclusion complex; Molecular discrimination; Discrimination level; Discrimination factor; Molecular recognition.

1. INTRODUCTION

There are molecular or ionic inclusion phenomena in a system possessing natural or semi-natural macrocyclic hosts that usually have predisposing conditions, such as one or more inner cavities with particular structures, sizes, shapes, and polarities.[1–3] Cyclodextrins (CDs) and their derivatives are one of the most representative macrocyclic host groups. They are cyclic oligosaccharides composed of several glucopyranose units with a molecule like a truncated cone. The macrocyclic geometry is formed by linking six, seven and eight glucose units to get the most common α -, β - and γ -CD, respectively.[4,5] Their molecular structures are illustrated in Figure 1.

CDs, having both hydrophobic intracavity with a chiral microenvironment and hydrophilic surface with exposed OH-groups, can interact with many kinds of guests like inorganic ions, coordination compounds, polymers and even biomacromolecules to form supramolecules and solid-state architectures.[1,3,6–17] The interactions between native CDs and most of the guest molecules are weak, so many researchers have concentrated on chemical modification of CDs to improve the binding affinity and structural selectivity of a CD to one specific guest in recent 30 years.[18–24] So far, many CD derivatives have been extensively used as molecular receptors, artificial enzyme models and drug carriers in many scientific fields for their inclusion properties.[25–34]

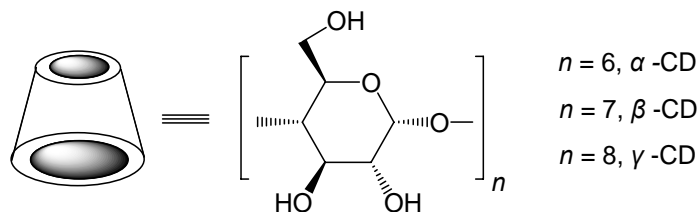


Figure 1. Molecular structural features of CDs.

With the development of cyclodextrin chemistry, some important concepts, like inclusion complexation and encapsulation interaction; molecular recognition and molecular discrimination; free CD, complexed CD (guest–CD inclusion complex) and recovered CD (after removal of guest in a complex); complexation energy and interaction energy, and so on need to be clearly defined and identified. Recently, we have reported the structural transformation among free CD, complexed CD and recovered CD.[35] Also, the distinction between inclusion complexation and encapsulation interaction was discussed in another paper.[36] The current work emphasizes the molecular discrimination behaviors in cyclodextrin chemistry.

It is well known that molecular recognition behavior plays an important role in supramolecular chemistry.[37] As a part of supramolecular chemistry, one of the emphases of cyclodextrin chemistry is to comprehend completely and correctly the mechanism of the molecular recognition between CDs and a group of guests. As we know, molecular recognition phenomenon came from the affinity, selectivity and specificity of an enzyme for substrate in biology and biochemistry.[38] It means a selective binding process between host and guest, as well as between acceptor and donor, in which several intermolecular interactions exert a key influence on supramolecular formation.[37] The strong affinity ability

and highly selective complexation between CDs and some guest molecules are somewhat like the recognition interaction between enzyme and substrate.

In the recent years, the recognition behaviors concerning CDs and their derivatives to those guests with a similar structure have been widely researched.[39–56] Indeed, these efforts are of great significance not only in supramolecular chemistry but also in biology in revealing the ultimate secret of life itself. However, due to the limitation of the structure of CDs themselves as well as current technical limitation, it is very difficult to prepare a CD derivative like enzyme in nowadays. In guest–CD supramolecular systems, affinity, selectivity and specificity, are often not enough comparable to the molecular recognition phenomenon in nature. If there are no significant differences in the formation constants (K) of the complexes of a CD with several similar guests, it means the lack of high selectivity of the CD to minor structure of the guests. Therefore, in this study we propose to use the concept of molecular discrimination to describe those between a low-level molecule-ion adduct phenomenon in supramolecular chemistry and a high-level molecular recognition behavior in living nature in order to create an integrated logical concept chain. After comparing the K values of many CD inclusion complexes,[18,19,21,41] we recommend the use of the discrimination factor (ζ , the ratio of two K values) to reflect the differences between the intermolecular interactions of a group guests with the same host (ζ_G), as well as a group hosts with the same guest (ζ_H), so as to represent the molecular discrimination ability.

The binding behaviors and discrimination abilities of CDs to a group of similar guests are roughly divided into four levels (A, B, C and D) based on a combination between the values of K and ζ_G . This method could be applied to the large amount of literature as well as to other established and new host systems. The present work not only can provide a clear understanding of some of the important issues related to molecular recognition, but also will play an important role in the development of organic chemistry and supramolecular chemistry, especially cyclodextrin chemistry. We believe that, with the development of supramolecular chemistry, the records of affinity and selectivity between CD derivatives and guests will be continuously broken, and some of them will mimic, or even transcend naturally species in the future.

2. AN APPROXIMATE EVALUATION OF POSSIBLE INFLUENCE FACTORS ON THE INTERMOLECULAR INTERACTIONS BETWEEN CDS AND GUESTS

The cavity environment of a CD molecule exhibits rather low polarity, but a few water molecules are always found in the cavity of CD to form a hydrate both in solution and in crystal.[5] Supposing that a CD hydrate and a low-polar organic guest react in a stoichiometric ratio of 1:1, as shown in Figure 2, when the guest is added into a CD aqueous solution, the hydrophobic property of the guest offers an opportunity to displace some of the water molecules into the hydrophobic cavity of CD forming an inclusion complex.

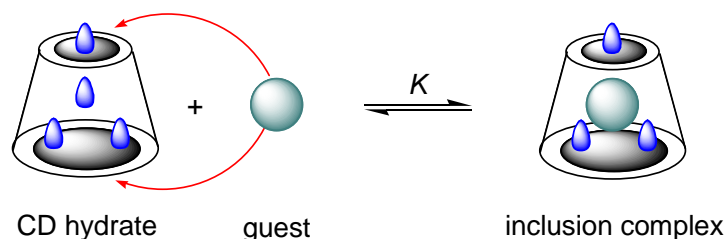


Figure 2. Inclusion complexation between CD and guest.

The phenomenon seems to be an extension of the “like dissolves like” rule in the field of supramolecular chemistry. The formation of the so called “inclusion complex” is due to the intermolecular interaction between the CD and the guest, by which the guest may be embedded in the CD cavity whole or partly either from larger opening at one end or from smaller opening at the other end (see Figure 2). Although the same CD can form inclusion complexes with various similar guests by molecule-molecule or molecule-ion interactions, the stability of the complexes may be very different because of the minor differences of the guests in structure.[19,21] We can even extract those components more suitable for the microenvironment of CD cavity from natural or synthetic samples, by means of large differences in K values of the formed complexes.[18,19]

The inclusion process between CD and guest is driven by intermolecular interactions mainly including electrostatic force, hydrogen bonding, van der Waals force, hydrophobic interaction and so on.[57–60] Interestingly, in most case, an inclusion complex exhibits a strict stoichiometry between host and guest.[61–63] The configuration matching degree between the cavity of a CD and the structure of a guest has great effects on the formation and stability of the guest–CD complex by reason of the rigidity of the cavities and the intermolecular hydrogen bonding networks formed by hydroxyl groups on the rims of the cavities.[64,65]

There are two popular theories used to explain molecular recognition phenomena. One is the famous “lock and key” model proposed by Fischer in 1894,[66] giving an emphasis to the matching degree in volume or size between host and guest. The other is the “induced-fit” theory proposed by Koshland in 1958,[67] stressing that it is the interaction between host and guest that makes the shape of a flexible guest match the dimensions of the rigid cavity of host to the greatest extent. Obviously, they both set out from the high selectivity between enzyme and substrate, and both emphasize the importance of size matching in intermolecular interactions.

The cavity volumes of α -, β - and γ -CD are 0.174, 0.262 and 0.427 nm³, respectively.⁵ If the volume of a guest molecule is too small relative to the cavity size of a CD, it cannot usually form a stable supramolecular complex,[68–70] due to a very weak van der Waals interaction between them. This is the reason why many small organic molecules, like acetonitrile, ethanol and isopropanol, cannot form stable complexes, since they are far away from the size requirement of the cavity of α -CD.[68]

Inorganic ions in size are usually small. In particular, most of them have a much higher polarity than water. Hence, they are not compatible with the size and environment of CD cavities, and cannot form stable complexes with CDs. The K values of the molecule-ion complexes, are often less than 100 dm³·mol⁻¹,[69,70] so many of the complexes can be regarded as adducts by an encapsulation interaction between CDs and inorganic salts.³⁶ It is

worth noting that the structures and formation mechanisms of some of the special complexes are still not clear.

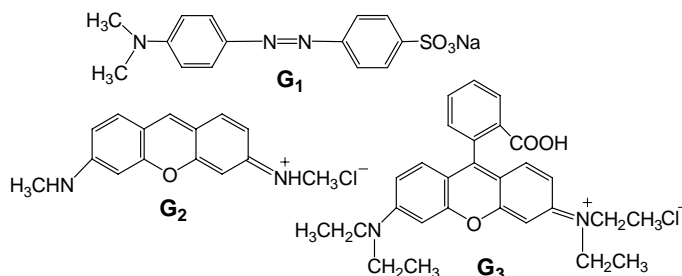
According to the limited data available, it is found that for the same anion, the influence of different cations on the stability of CD complexes is very small. Furthermore, for the same inorganic alkali salts, the stability of their complexes with different CDs seems to have the same order: α - > β - > γ -CD, and is rather poor ($K < 35 \text{ dm}^3 \cdot \text{mol}^{-1}$, see Table 1).

Table 1. K values of the complexes of CDs with inorganic alkali salts in D_2O ⁶⁹

Guest	α -CD	β -CD	γ -CD
NO_3^-	1.4 ± 0.1	–	–
Br^-	1.6 ± 0.1	–	–
I^-	18.6 ± 0.7	8.5 ± 0.4	4.9 ± 0.3
SCN^-	28.4 ± 0.9	9.2 ± 0.5	4.1 ± 0.2
ClO_4^-	33.0 ± 1.1	13.6 ± 0.7	–

Apparently, this phenomenon reflects the significance of volume matching degree and polarity matching degree in CD supramolecular chemistry. The order of the K values, for the five α -CD complexes listed in Table 1, is approximately identical to the order in the hydrophobic strength of the five anions.[69] Besides, SO_4^{2-} and PO_4^{3-} can hardly form complexes with CDs,[64] possibly because they carry more negative charges and possess a higher polarity. For all these reasons, we think that, for the small size inorganic ions with charges, even if they can go into CD cavity casually, a large mismatching stress often makes them difficult to locate in the cavity. Possibly, they prefer to stay at the two openings of the cavity.

Unlike small organic molecules and inorganic ions described above, some of large or even very large organic molecules or ions may form rather stable complexes with CDs by partial inclusion into the hydrophobic cavities of the CDs.[71] For instance, the value of K for the inclusion complex of α -CD with a large guest, \mathbf{G}_1 , reaches $9000 \text{ dm}^3 \cdot \text{mol}^{-1}$. [72] And β -CD can not only form stable inclusion complexes with substituted benzenes with bulky substituent groups,[73] such as 4-*tert*-butylphenol- β -CD (K , $36000 \text{ dm}^3 \cdot \text{mol}^{-1}$),[74] but also include benzene derivatives with a larger planar structure, such as \mathbf{G}_2 and \mathbf{G}_3 (K , $> 1000 \text{ dm}^3 \cdot \text{mol}^{-1}$). [75] Also, γ -CD with a larger cavity size can interact well with the guests having a very large size, such as anthracene[76] and fullerene in aqueous solution.[77,78] There are many reported examples referring to the inclusion phenomenon that a partial inclusion is often more efficient than a complete inclusion in cyclodextrin chemistry.[79,80]



The guests with a long alkyl chain can well match the cavity of α -CD for their flexibility, such as the value of K for the inclusion complex, 1,10-decanediol- α -CD, is up to $7115 \text{ dm}^3 \cdot \text{mol}^{-1}$. [81] However, the values of K for α -CD complexes descend rapidly with the shortening of carbon chain length and the strengthening of the rigidity of guest skeleton. For example, the value of K for 1,9-nonanediol- α -CD is $3575 \text{ dm}^3 \cdot \text{mol}^{-1}$, while the K values for the complexes of α -CD with 1,8-octanediol, 1,7-heptanediol, 1,6-hexanediol, 1,5-pentanediol, 1,4-butanediol and 1,3-propanediol are 1195, 318, 101.4, 28.3, 7.8 and $2.2 \text{ dm}^3 \cdot \text{mol}^{-1}$, respectively. [81] For these results, it can be explained that the carbon chain of an alkyl guest become more flexible with the increase of the carbon atoms number of alkanes, and the increase of the flexibility is advantageous to improve binding ability because more flexibility may induce more conformation changes which allow a guest to adjust its shape for filling a cavity. Again, the addition of carbon atoms on alkyl chain also can effectively expand the interaction area between α -CD and guest molecules.

The spatial structure of guest molecules also has a great effect on the intermolecular interaction between host and guest. That is to say, there is a structural requirement for the interaction between the hollow truncated cone shape of CD cavity and the skeleton structure of guest. For a certain CD, a suitable size, polarity, shape and structure for a guest may lead to a very strong interaction between them. For instance, it is the well-fitting relationship between the cavity of β -CD and the globular adamantane frame that results in the large K values of the complexes of β -CD with adamantane derivatives. [82] This gives an impression that a strong complexation seems to be necessary for the harmonization between the accommodation of CD cavity and the penetration of guest, possibly somewhat like the match between lock and key.

It should be noted that unlike inorganic ions and simple organic molecules, some of coordination compounds formed by inorganic atoms or ions with simple organic molecules, such as dicyclopentadienyl iron, its derivatives and so on, may produce strong intermolecular interactions with CDs, even form crystal inclusion complexes of CDs. [83–95] Hapiot and his co-workers have summarized the formation of four types of CD inclusion complexes of organometallic compounds in a recent review in detail. [85]

Until now, many efforts have been paid to the study of inclusion phenomena between CDs and polymers to build particular supramolecular systems. [96–107] For instance, when α -CD interacts with a poly(propylene oxide)-poly(ethylene oxide)-poly(propylene oxide) triblock copolymer, it is found that the long alkyl chain is coated with cavities of α -CD molecules and the cavities are located at the outside surface of polyethylene oxide through intermolecular interactions. [108] What's more, α -CD as well as β - and γ -CD may form inclusion complexes with some specific polymers selectively. For example, α -CD formed a complex of polyethylene glycol with high yield but β -CD did not. [109] Conversely, β -CD formed a complex with polypropylene glycol but α -CD did not. [110] Again, poly[(*R*)-3-hydroxybutyrate] can only be included by α -CD while poly[(*R,S*)-3-hydroxybutyrate] can only form a stable inclusion complex with γ -CD. [111] Strikingly, γ -CD molecules allow the same two polymer chains, such as poly(ethylene adipate) [112] or poly(ϵ -caprolactone), [113] to pass through their cavities in the form of two parallel lines simultaneously, forming a polyrotaxane structure surrounded by the cavities.

All these inclusion phenomena described above reveal the importance of adaptive selection, including both host selection for guest and guest selection for host in size, shape, structure, polarity and flexibility, in the formation of a supramolecule between host and guest.

Except for the factors, the charges in guests especially in hosts also exhibit a pronounced effect on the interaction between them. For example, it is found that the coordination compound formed by β -CD with Cu^{2+} possessed a rather strong binding ability to *L*-tryptophan, *L*-phenylalanine, *L*-tyrosine or *L*-histidine (K , from 24000 to 110000 $\text{dm}^3 \cdot \text{mol}^{-1}$) in an alkaline environment.[64] Under the same conditions, parent β -CD has a weak or even no inclusion interaction to the above amino acids.[64] These findings powerfully demonstrate that the presence of coordination centers in a modified CD has an obvious enhancement in the adaptive selection between host and guest, owing to the occurrence of additional interaction sites.

With the exception of the intrinsic factors from hosts or guests themselves, there are also other extrinsic factors, such as temperature, pH, ion strength and so on, making an effect on the intermolecular interaction between host and guest. For example, the K values of butanoate- α -CD at the conditions of weak acid (pH 6.9) and alkalescence (pH 11.3) are 12.6 and 85.1 $\text{dm}^3 \cdot \text{mol}^{-1}$, respectively.[114,115] And the K values of 4-nitrophenolate- α -CD at pH of 10 are 3548 $\text{dm}^3 \cdot \text{mol}^{-1}$ and 1821 $\text{dm}^3 \cdot \text{mol}^{-1}$ in aqueous solution and in the solution of 1 $\text{mol} \cdot \text{dm}^{-3}$ sodium chloride, respectively.[116,117] In addition, the influence of reaction medium, is also important, such as the K values of 1-naphthol- β -CD in aqueous solution and in the solution of $\text{H}_2\text{O}-\text{CH}_3\text{OH}$ (1:1, v/v) are 1230 and 4.3 $\text{dm}^3 \cdot \text{mol}^{-1}$, respectively.[118,119]

3. A CAREFUL COMPARISON OF THE INCLUSION INTERACTIONS BETWEEN CDS AND A SERIES OF ANALOGUES

When a series of analogous organic compounds form inclusion complexes with the same CD, the complexes usually display different stabilities in solution, which are dependent on how change in volume, number and position of substituent groups of the analogs is experienced. Additionally, the changes in molecular polarity and charge distribution of the analogs also strongly influence the interactions between CDs and them.[120,121] Just like the different inclusion phenomena of the same CD with a series guests, the behaviors of the same guest bound by a series of CDs, such as α -, β - and γ -CD, as well as their derivatives, are likely to be very different from one another, owing to the difference of the cavity diameter and modification character of CDs.[122,123] In a word, CDs can respond to changes in shape, size, polarity, and charge distribution of those guest molecules reacting with them, and vice versa.

For example, when α -CD interacts with 1-propanol, 1-butanol, 1-pentanol, 1-hexanol and 1-heptanol, the K values of the formed complexes are 28.8, 79.4, 275.4, 870.9 and 1174.9 $\text{dm}^3 \cdot \text{mol}^{-1}$, respectively, gradually increasing with the increase of carbon atoms in these guest molecules (see Figure 3).[64] It also can be seen from Table 2 that there is a similar inclusion phenomenon between β -CD and several primary unbranched aliphatic alcohols, such as 1-butanol, 1-pentanol and 1-hexanol.[124]

Interestingly, as shown in Figure 3, the binding ability of α -CD is obviously weaker to a cyclitol than to a short-chain alcohol with the same carbon atom number, since the values of K for the α -CD complexes of cyclobutanol, cyclopentanol, cyclohexanol, cycloheptanol and cyclooctanol are 30.2, 36.3, 57.5, 67.6 and 234.4 $\text{dm}^3 \cdot \text{mol}^{-1}$, respectively.[64] Although the K values increase with the increase of carbon atom number as well, the stabilities of the α -CD

complexes of the short-chain alcohols have a faster increase than those of the complexes of the corresponding cyclitols. The different flexibilities of the two kinds of alcohols are probably one of the important reasons responsible for the different inclusion phenomena.

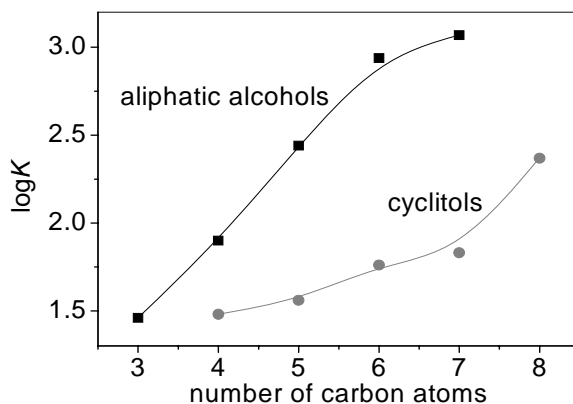


Figure 3. The change trend of $\log K$ with increasing carbon atoms of aliphatic alcohols and cyclitols in the inclusion systems between α -CD and them.[64]

Table 2. K values of β -CD inclusion complexes of several sets of homologous organic guests

Guest	$K/\text{dm}^3\cdot\text{mol}^{-1}$	Method ^a	pH	Refs ^b
G_2	2630	fl	7.2	75
G_3	4240	fl	7.2	75
1-butanol	16.6	CD	7.2	124
1-pentanol	63	CD	7.2	124
1-hexanol	219	CD	7.2	124
cyclopentanol	168 ± 3	cal	7.2	125
cyclohexanol	707 ± 4	cal	7.2	125
cycloheptanol	2344 ± 92	cal	7.2	125
(+)-borneol	18640 ± 110	cal	7.2	125
2-methoxyphenol	8900 ± 230	fl	–	126
syringic acid	16600 ± 500	fl	–	126
eugenol	396000	uv	–	127

^a Method employed: CD, circular dichroism; uv, uv–vis spectrophotometry; cal, calorimetry; fl, fluorimetry.

^b Refs is an abbreviation of references.

What's more, α -CD can form inclusion complexes with many aromatic guests such as derivatives of phenol, but the stabilities of the complexes are different. For example, the K values of α -CD complexes of 2-methoxyphenol (disubstituted benzene),[126] eugenol (trisubstituted benzene)[127] and syringic acid (tetrasubstituted benzene)[126] are 174000 ± 36000 , 49500 ± 2300 and $1880 \pm 280 \text{ dm}^3\cdot\text{mol}^{-1}$, respectively. Clearly, the inclusion ability of α -CD to 2-methoxyphenol with less substituents is over 92 times stronger than to syringic acid, and 3 times stronger than to eugenol. Further, the order of the K values is quite different

from that of the complexes of β -CD with the three guests (see Table 2). The complex of β -CD with eugenol has the largest K value, indicating that β -CD, as well as α -CD, have different responses to the structure of the guests with two, three or four substituent groups. It is reasonable that the structural selectivity between host and guest is dependent on how suitable the structures between two reactants are when a stable complex is formed. It is worth mentioning that the structural diversity of parent CDs involves the change in cavity diameter and macrocyclic conformation, which greatly affects the penetration behaviors of guests with various sizes.

In general chemistry, molecular identification means to point out a special atom, ion or molecule through the difference in basic chemical reactions or instrument analyses. It is easy and feasible to distinguish between alcoholic hydroxyl groups and aldehyde groups using their respective characteristic reactions. Nonetheless, it is difficult for a general chemist to discern a series of homologous organic compounds, in particular a set of geometric isomers or a pair of chiral isomers.

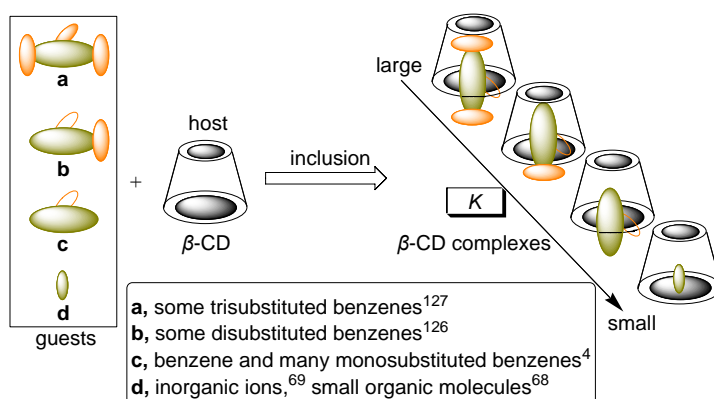


Figure 4. A schematic drawing depicting the formation of 1:1 guest- β -CD complexes with different stabilities.

As well, the idea of molecular identification in CD supramolecule chemistry may be regarded as molecular discrimination behaviors by CDs. The so-called molecular discrimination means to distinguish a certain guest, such as an atom, ion or molecule, from a group of guests through the difference in intermolecular interactions (see Figure 4). Such a discrimination process can be performed due to different affinity abilities, induced or dominated by CD cavity, to different guests. When CDs or their derivatives actually take part in the inclusion processes, even if the guests are a set of geometric isomers or a pair of optical isomers with little distinction in structure and character, an observable difference in spectral properties can be found due to different inclusion modes and interaction intensities.

So far, there have been many reports relating to molecular discrimination behaviors in cyclodextrin chemistry.[19, 39, 128–131] Most of them claim that the constructed inclusion systems can be regarded as examples of molecular recognition. However, to date there have no reports on the difference between a low-level molecular discrimination and a high-level molecular recognition in supramolecular chemistry, as well as in nature. Preferably, we suggest using the concept of “molecular discrimination” to express the structural selectivity between CDs and guests in this case. The large value of K is a token of the matching degree

between the cavity of CD and the structure of a guest. By comparing the K values of the complexes with a certain chemical stoichiometry, formed by many series of analogous guests with the same CD, we can evaluate the molecular discrimination ability of the CD to a series of guests according to Equation 1.

$$\zeta_G = K_{Gn} / K_{G1} \quad (1)$$

In Equation 1, K_{Gn} represents the K value of the complex of the same CD with any one of the series of similar guests, and K_{G1} is the lowest value of K of the complexes. The ratio value of K_{Gn} to K_{G1} is defined as the discrimination factor (ζ_G) of the CD to several similar guests.

Interestingly, we can also detect the difference of CDs, as well as their derivatives, in structure by means of the interaction between them and the same guest with a special structure. Similarly with Equation 1, the discrimination factor (ζ_H) of a guest to several CDs is expressed in Equation 2.

$$\zeta_H = K_{Hn} / K_{H1} \quad (2)$$

In Equation 2, K_{Hn} represents the K value of the inclusion complex of the same guest with any one of CDs, and K_{H1} is the lowest value of K of the complexes. Equation 2 is suitable for describing those inclusion systems with a certain stoichiometry.

At first appearance, there seems to be not much physical significance for ζ as a ratio of K values. However, as a matter of fact, it is very important in supramolecular systems, as will be explained below.

First, the intermolecular interactions between CDs (H) and guests (G), such as 1:1, 2:1, 1:2 and $x:y$ stoichiometries, can be represented by Equations 3, 4, 5 and 6, respectively.



where HG , H_2G , HG_2 and H_xG_y denote inclusion complexes of H and G. Supposing that when an inclusion complexation system reaches equilibrium, the equilibrium concentration ($[G]$) of a guest is just equal to half of the initial concentration of the guest, when the initial concentrations of H and G are $[H_0]$ and $[G_0]$ respectively, then the relationships among K , $[H_0]$ and $[G_0]$ are shown in Equations 7, 8, 9 and 10 for 1:1, 2:1, 1:2 and $x:y$ stoichiometries, respectively.

$$K_{11} = 1/([H_0] - 0.5 [G_0]) \quad (7)$$

$$K_{21} = 1/([H_0] - [G_0])^2 \quad (8)$$

$$K_{12} = 1/[G_0] \cdot ([H_0] - 0.25 [G_0]) \quad (9)$$

$$K_{xy} = 2^{y-1} (G_0)^{1-y} / [y \cdot (H_0 - G_0 \cdot x/2y)^x] \quad (10)$$

The initial concentrations of H' and G' in the other inclusion system are $[H_0]'$ and $[G_0]'$ respectively. If in two compared systems with the same pH, temperature and ionic strength, and $[G_0]'$ is equal to $[G_0]$, then for 1:1, 2:1, 1:2 and $x:y$ stoichiometries, the relationship between $[H_0]'$ and $[H_0]$ can be expressed in Equations 11, 12, 13 and 14 respectively.

$$[H_0]' = \zeta_G \cdot [H_0] - 0.5(\zeta_G - 1) [G_0] \quad (11)$$

$$[H_0]' = (\zeta_G)^{0.5} \cdot [H_0] - [(\zeta_G)^{0.5} - 1] [G_0] \quad (12)$$

$$[H_0]' = \zeta_G \cdot [H_0] - 0.25(\zeta_G - 1) [G_0] \quad (13)$$

$$[H_0]' = (\zeta_G)^{1/x} \cdot [H_0] - x/2y[(\zeta_G)^{1/x} - 1] [G_0] \quad (14)$$

It is found that the correlations among the values of ζ_G , chemical stoichiometries and the ratios of $[H_0]/[G_0]$ (RHG) are closely associated with the initial concentration ratios of the host ($[H_0]'/[H_0]$, RHH) for the molecular discrimination behavior of any two similar guests by the same host. The calculation results are listed in Table 3. Figure 5 illustrates the relationship among stoichiometries, RHH and RHG in the case of ζ_G 1.5.

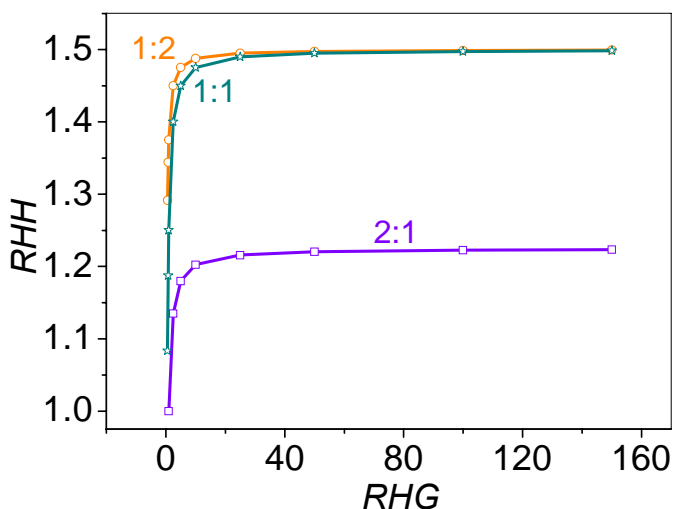


Figure 5. A schematical figure depicting the relationship among stoichiometries, RHH and RHG in the case of ζ_G 1.5.

According to Figure 5, the profile difference in the three curves provides some significant information concerning the values of RHH and ζ_G : (1) In the case of the same RHG , the higher the values of $x:y$, the lower the values of RHH as summarized in Table 3; (2) With the increase of RHG , the curves approach to a horizontal asymptote with an intercept on the ordinate equal to ζ_G , *i.e.*, 1.5 for 1:2 and 1:1 stoichiometries, but equal to $(\zeta_G)^{0.5}$, *i.e.*, $(1.5)^{0.5}$ for a 2:1 stoichiometry.

Similarly, for those systems using the same guest to discriminate a group of hosts, supposing that when an inclusion system reaches equilibrium, $[H]$ is just equal to half of $[H_0]$, then the correlations among ζ_H , $[H_0]$ and $[G_0]$ are shown in Equations 15, 16 and 17 and 18 for 1:1, 2:1, 1:2 and $x:y$ stoichiometries, respectively.

$$[G_0]' = \zeta_H \cdot [G_0] - 0.5(\zeta_H - 1) [H_0] \quad (15)$$

$$[G_0]' = \zeta_H \cdot [G_0] - 0.25(\zeta_H - 1) [H_0] \quad (16)$$

$$[G_0]' = (\zeta_H)^{0.5} \cdot [G_0] - [(\zeta_H)^{0.5} - 1] [H_0] \quad (17)$$

$$[G_0]' = (\zeta_H)^{1/y} \cdot [G_0] - y/2x[(\zeta_H)^{1/y} - 1] [H_0] \quad (18)$$

The relationships among the values of ζ_H , chemical stoichiometries and the ratios of $[G_0]/[H_0]$ (RGH) are closely related with the initial concentration ratios of the guest ($[G_0]'/[G_0]$ RGG) for the molecular discrimination ability of any two similar hosts by the same guest. Also, the calculated results are listed in Table 3. Figure 6 displays the curves expressing the relationship among stoichiometries, RGH and RGG in the case of ζ_H 3.0.

Unlike those systems with the same host to discriminate a group of guests, for the systems using the same guest to discriminate a group hosts in the case of the same RGH , the lower the values of $x:y$, the lower the values of RGG . With the increase of RGH , the curves also approach to a horizontal asymptote with an intercept on the ordinate equal to ζ_H , *i.e.*, 3.0 for 2:1 and 1:1 stoichiometries, but equal to $(\zeta_H)^{0.5}$, *i.e.*, $3^{0.5}$ for a 1:2 stoichiometry, as shown in Figure 6.

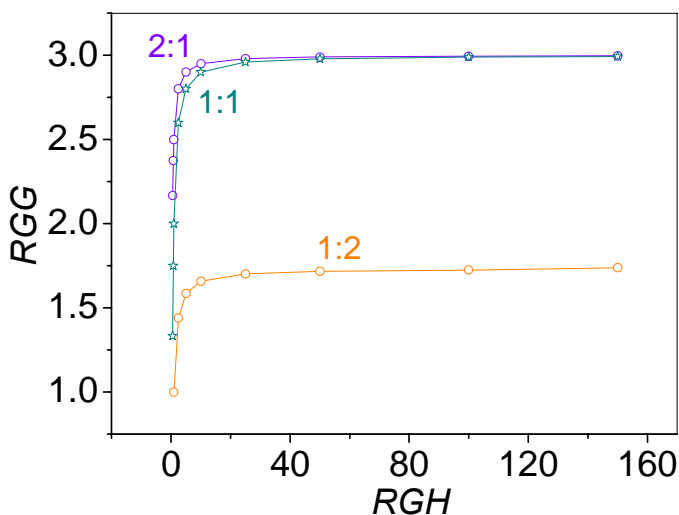


Figure 6. A schematic figure depicting the relationship among stoichiometries, RGH and RGG in the case of ζ_G 3.0.

Table 3. The relationship between ξ and chemical stoichiometries of complexes

ξ_G	RHG	RHH in various stoichiometries of H to G			
		1:1	1:2	2:1	x:y
1.5	1:1	1.2500	1.3750	1.0000	$(1.5)^{1/x} - x/2y[(1.5)^{1/x}-1]$
	10:1	1.4750	1.4875	1.2020	$(1.5)^{1/x} - x/20y[(1.5)^{1/x}-1]$
	50:1	1.4950	1.4975	1.2202	$(1.5)^{1/x} - x/100y[(1.5)^{1/x}-1]$
	100:1	1.4975	1.4987	1.2224	$(1.5)^{1/x} - x/200y[(1.5)^{1/x}-1]$
3.0	1:1	2.0000	2.5000	1.0000	$(3)^{1/x} - x/2y[(3)^{1/x}-1]$
	10:1	2.9000	2.9500	1.6588	$(3)^{1/x} - x/20y[(3)^{1/x}-1]$
	50:1	2.9800	2.9900	1.7174	$(3)^{1/x} - x/100y[(3)^{1/x}-1]$
	100:1	2.9900	2.9950	1.7247	$(3)^{1/x} - x/200y[(3)^{1/x}-1]$
10	1:1	5.5000	7.7500	1.0000	$(10)^{1/x} - x/2y[(10)^{1/x}-1]$
	10:1	9.5500	9.7750	2.9485	$(10)^{1/x} - x/20y[(10)^{1/x}-1]$
	50:1	9.9100	9.9550	3.1188	$(10)^{1/x} - x/100y[(10)^{1/x}-1]$
	100:1	9.9950	9.9775	3.1404	$(10)^{1/x} - x/200y[(10)^{1/x}-1]$
ξ_H	RGH	RGG in various stoichiometries of G to H			
		1:1	1:2	2:1	x:y
1.5	1:1	1.2500	1.0000	1.3750	$(1.5)^{1/y} - y/2x[(1.5)^{1/y}-1]$
	10:1	1.4750	1.2020	1.4875	$(1.5)^{1/y} - y/20x[(1.5)^{1/y}-1]$
	50:1	1.4950	1.2202	1.4975	$(1.5)^{1/y} - y/100x[(1.5)^{1/y}-1]$
	100:1	1.4975	1.2224	1.4987	$(1.5)^{1/y} - y/200x[(1.5)^{1/y}-1]$
3.0	1:1	2.0000	1.0000	2.5000	$(3)^{1/y} - y/2x[(3)^{1/y}-1]$
	10:1	2.9000	1.6588	2.9500	$(3)^{1/y} - y/20x[(3)^{1/y}-1]$
	50:1	2.9800	1.7174	2.9900	$(3)^{1/y} - y/100x[(3)^{1/y}-1]$
	100:1	2.9900	1.7247	2.9950	$(3)^{1/y} - y/200x[(3)^{1/y}-1]$
10	1:1	5.5000	1.0000	7.7500	$(10)^{1/y} - y/2x[(10)^{1/y}-1]$
	10:1	9.5500	2.9485	9.7750	$(10)^{1/y} - y/20x[(10)^{1/y}-1]$
	50:1	9.9100	3.1188	9.9550	$(10)^{1/y} - y/100x[(10)^{1/y}-1]$
	100:1	9.9950	3.1404	9.9775	$(10)^{1/y} - y/200x[(10)^{1/y}-1]$

These observations imply that if a host and a group of guests can form inclusion complexes with a high stoichiometric ratio of host to guest, such as 2:1, then the host will have a relatively lower cost (the need of initial concentration ratio) to perform the discrimination for the guests in the same level (ζ_G) in comparison with those with a lower stoichiometries such as 1:1 and 1:2. On the contrary, if a guest and several similar hosts can form complexes that possess a low stoichiometric ratio of host to guest, such as 1:2, then the guest will have a relatively lower need of initial concentration ratio to perform the molecular discrimination for these hosts in the same level (ζ_H) in comparison with those with a higher stoichiometries such as 1:1 and 2:1. Therefore, the physical significance of ζ can be considered as the initial concentration need of a host to discriminate a group of guests or a guest to discriminate a group of hosts. In the case of the same stoichiometry, the larger the values of ζ , the higher the values of RHH and RGG . Moreover, in the case of the same ζ and the same stoichiometry, the higher the values of RHG or RGH , the higher the values of RHH and RGG , the more difficult the molecular discrimination.

Further, when the equilibrium concentration ratio ($[H]'/[H]$) of host is defined as a new physical quantity η for two inclusion systems with the same measurement conditions, including temperature, initial concentration of guests, pH, ionic strength and so on, then, according to Equations 3 and 5, η for 1:1 and 1:2 stoichiometries can be represented by Equation 19 as follows.

$$\eta = [H]'/[H] = K_{Hn}/K_{H1} = \zeta \quad (19)$$

Based on Equations 4 and 6, η for 2:1 and $x:y$ stoichiometries can be represented by Equations 20 and 21.

$$\eta = [H]'/[H] = (K_{Hn}/K_{H1})^{0.5} = \zeta^{0.5} \quad (20)$$

$$\eta = [H]'/[H] = (K_{Hn}/K_{H1})^{1/x} = \zeta^{1/x} \quad (21)$$

So, Equation 15 can be simplified as Equation 22.

$$[H_0]' \geq \eta[H_0] - x/2y(\eta-1) G_0 \quad (22)$$

As discrimination factors, the values of ζ are to hold the balance, to set the boundary conditions within which the similar inclusion systems are to compare. However, the expression of discrimination ability is not only dependent on the values of ζ (the relative values of K), but also on the absolute values of K . For instance, in some compared systems with very large K values, although ζ may be rather low, the huge differences in absolute values of K will allow reasonable discrimination between hosts and guests. Contrarily, those compared systems with very low values of K often indicate a low discrimination ability though sometimes ζ is very large. Equation 23 and 24 are presented to evaluate the contribution of ζ and K to the molecular discrimination between hosts and guests.

$$\Phi = 0.1996 \log (K_2 - K_1) + 0.8004 \log (K_2/K_1) \quad (23)$$

$$\Phi = 0.2 \log (K_2 - K_1) + 0.8 \log \zeta \quad (24)$$

where Φ represents total discrimination ability, K_1 and K_2 is the formation constants of any two of compared inclusion system. Generally, the discrimination behavior of one component to two similar components is enhanced with the increased value of Φ . The normalization factors 0.2 and 0.8 are approximations resulting from more than 800 sets of data points based on reported values in the literature.⁴

Generally speaking, ζ_G is more usual than ζ_H , though they are a reflection of the difference in inclusion behavior. Here, we attempt to allot four levels reflecting the discrimination ability of a host to a set of guests in constructed inclusion systems, according to the correlation between values of K and ζ_G from the reported data.

- i Level A, there are both very large values of K , such as larger than 10^4 ($\text{dm}^3 \cdot \text{mol}^{-1}$)^{x+y-1}, and very high values of ζ_G , such as 10.0 or higher. In this level, hosts not only have very strong affinity ability to one or more of a group guests, but also have a very high discrimination behavior for at least two or more among these guests. The host-guest systems in Level A can be expected to approach successfully molecular recognitions of enzyme-substrate interactions.
- ii Level B, there are both large values of K , such as larger than 10^3 ($\text{dm}^3 \cdot \text{mol}^{-1}$)^{x+y-1}, and high values of ζ_G , such as higher than 3.0, but not including those in Level A. In this level, there are a strong interaction between host and guest, and a high discrimination ability of hosts to at least two of compared guests.
- iii Level C, there are both medium values of K , such as larger than 10^2 ($\text{dm}^3 \cdot \text{mol}^{-1}$)^{x+y-1} and moderate values of ζ_G , such as higher than 1.5, but other than belonging to Levels A and B. In this level, hosts have a common affinity ability to selected guests, and a common discrimination ability to at least two of compared guests.
- iv Level D, there are either small values of K , such as smaller than 10^2 ($\text{dm}^3 \cdot \text{mol}^{-1}$)^{x+y-1} or low values of ζ_G , such as lower than 1.5. In this level, hosts have a weak affinity ability to the selected guests, or a low discrimination ability between the guests.

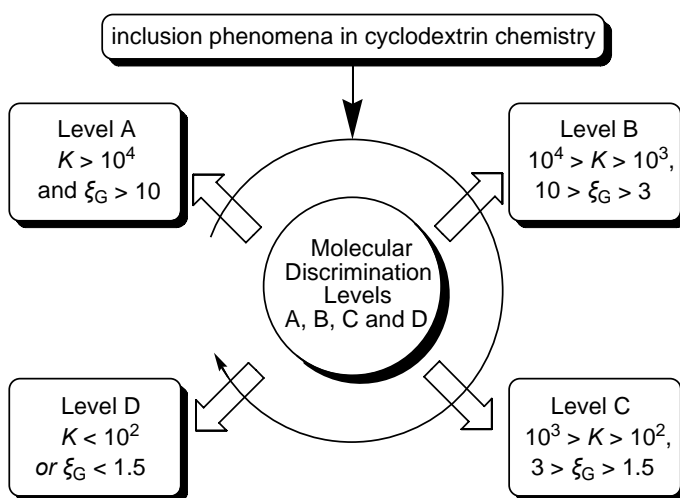


Figure 7. Four levels depicting the affinity ability and molecular discrimination ability of inclusion phenomena in cyclodextrin chemistry.

The molecular discrimination levels A, B, C and D are illustrated in Figure 7. It is important to note that the values of K and ζ_G in levels C and D are too small to use or have no value in practice, but there are lots of examples of host–guest inclusion systems belonging to the two categories (see Table 4). Further, when the values of K are lower than 10^3 ($\text{dm}^3 \cdot \text{mol}^{-1}$) ^{$x+y-1$} , in our opinion to discuss molecular discrimination ability for such systems are insignificant whether ζ_G is big enough or not. Even so, in view of the fact that the systems involving the two levels widely exist in CD inclusion complexes, they will be discussed below.

The values of K and ζ_G in Level B, especially in Level A, are large enough to have a great value both in theory helping to develop such a scheme applied in enzyme and substrate engineering, and in practice helping to separate the analogous guests. Also, there are many examples involving the two categories (see Table 4). However, some inclusion systems, either having a large K value but a low ζ_G value, or having a small K value but a high ζ_G value, are classified to a relative lower level.

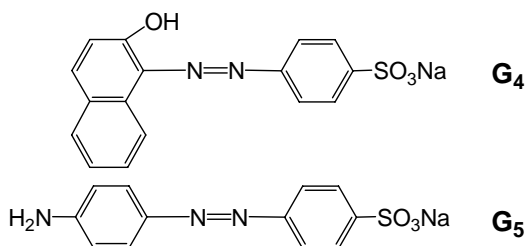
4. REPRESENTATIVE INCLUSION SYSTEMS IN LEVEL D

A weak discrimination level means that the value of K or ζ_G for several similar inclusion systems of the same CD is quite small. That is to say, the binding effect or structural selectivity of a CD to the selected guests is inappreciable. There are many such examples in cyclodextrin chemistry. For instance, the values of K_R and K_S of the two inclusion complexes of protonated monoaminated(6-amino-6-deoxy)- β -CD (mono-NH₃⁺- β -CD) with *R-N*-acetylated phenylalanine (*R-N*-AcPhe) and *S-N*-AcPhe are only 55 ± 7 and 67 ± 8 $\text{dm}^3 \cdot \text{mol}^{-1}$, respectively, and ζ_G is merely 1.2.[132] This inclusion phenomenon reflects a rather negative effect characteristic arising from modification behavior for either β -CD or Phe, since higher binding affinity and better structural selectivity of β -CD to a pair of optical isomers of Phe were observed.[133]

It is shown that β -CD has a weak binding ability to some simple di- and trisubstituted benzenes with polar substituent groups. For example, the K values of the complexes formed by β -CD with 1-chloro-2-nitrobenzene, 4-nitrobenzoic acid and 1-chloro-2,4-dinitrobenzene, are 79, 60 and 63 $\text{dm}^3 \cdot \text{mol}^{-1}$, [134] respectively, and less than 100 $\text{dm}^3 \cdot \text{mol}^{-1}$. The discrepancy in stability between them seems to be insignificant, since the ζ_G values of the latter two and the former two are 1.1 and 1.3, respectively. Many of β -CD complexes of substituted benzenes modified by simple polar groups have lower stabilities than the complex formed by parent benzene and β -CD. On one hand, the complexation between the rigid cavity of β -CD and the rigid benzene ring has difficulty in building a strong association. On the other hand, the simple polar groups introduced to the benzene ring do not play a promoting role in the formation of complexes. In this case, it seems that the intermolecular hydrogen bondings between the hydroxyl groups of β -CD and the polar groups of the guests are not responsible for the stabilities of the complexes.

Guest **G**₁ formed stable inclusion complexes with α -⁷² and β -CD[135] in aqueous solution with the K values of 9000 and 3560 $\text{dm}^3 \cdot \text{mol}^{-1}$, respectively. However, in aqueous 40% formic acid, the K value of the complex of **G**₁ and β -CD was sharply decreased to 69.2 $\text{dm}^3 \cdot \text{mol}^{-1}$. In the same acid solution, guests **G**₄ and **G**₅ with similar structure to **G**₁ also have

similar inclusion behaviors, and the K values of the complexes formed by G_4 and G_5 with β -CD are 38.9 and 97.7 $\text{dm}^3\cdot\text{mol}^{-1}$, respectively.[136]

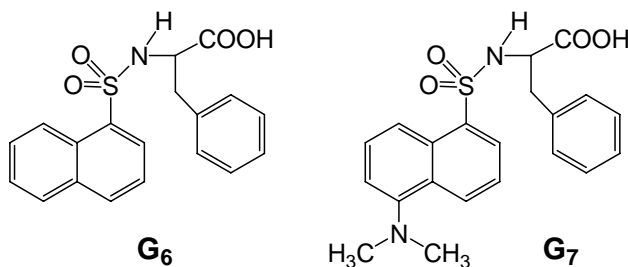


The guests G_1 and G_5 are all the diazo derivatives of benzenesulfonic acid sodium salt. In G_1 and G_5 molecules, two *para*-substituted benzenes are on the two sides of a diazo group. From the above data, β -CD has difficulty in distinguishing between NH_2 group and $\text{N}(\text{CH}_3)_2$ group ($\zeta_G = 1.4$, the ratio between the K values of G_1 - β -CD and G_5 - β -CD) in aqueous 40% formic acid.

Clearly, the inclusion ability and discrimination level of CD to inorganic ions (see Table 1) belong to Level D. Such inclusion systems can only be regarded as weak molecular-ion interactions. It has no practical meaning for the systems to discuss molecular discrimination or molecular recognition because of too low K values.

5. REPRESENTATIVE INCLUSION SYSTEMS IN LEVEL C

With respect to many simple organic guests, CDs as well as their derivatives can form inclusion complexes with them, and this is reflected by the values of K . A moderate ζ_G value means that a CD shows some ability in distinguishing the selected guests. For instance, the system consisted of the two inclusion complexes formed by β -CD with G_6 and G_7 [137] is a typical example of this discrimination level, *i.e.*, Level C.



Guest G_7 has one extra dimethylamino group in position C-5 of the substituted naphthalene in comparison with G_6 , and the subsequent influence on the formation and stability of β -CD inclusion complexes is considerable. On one hand, the inclusion complex formed by β -CD and L - G_6 is more stable than that formed by β -CD and D - G_6 . The K values of L - G_6 - β -CD and D - G_6 - β -CD are 565 and 328 $\text{dm}^3\cdot\text{mol}^{-1}$, respectively, and the corresponding ζ_G value is about 1.7. Hence, β -CD can, to some extent, discriminate between

*L-G*₆ and *D-G*₆. On the other hand, with respect to the inclusion complexes formed by β -CD with *D-G*₇ and *L-G*₇, on the contrary, *D-G*₇- β -CD (K , 412 dm³·mol⁻¹) is more stable than *L-G*₇- β -CD (368 dm³·mol⁻¹). The corresponding value of ζ_G is only about 1.1. Therefore, β -CD becomes markedly less effective in distinguishing them. Structurally, guests *G*₆ and *G*₇ are intramolecularly stacked molecules, and when they penetrate into the cavity of β -CD, there are two modes, one is parallel with the cavity and the other is perpendicular. Possibly, different penetration modes will give different circumstances around chiral carbon atom, thus causing the different discrimination level of isomers by the same CD. This phenomenon should be a significant reflection on the diversity of inclusion behaviors.

Due to the lack of interaction sites, the chiral cavity of a parent CD can only provide the limited discrimination ability to a pair of optical isomers. Relatively speaking, the discrimination level of a parent CD to geometric isomers, especially organic homologues, is often higher than to chiral isomers even though sometimes the values of K for the complexes are low.⁴

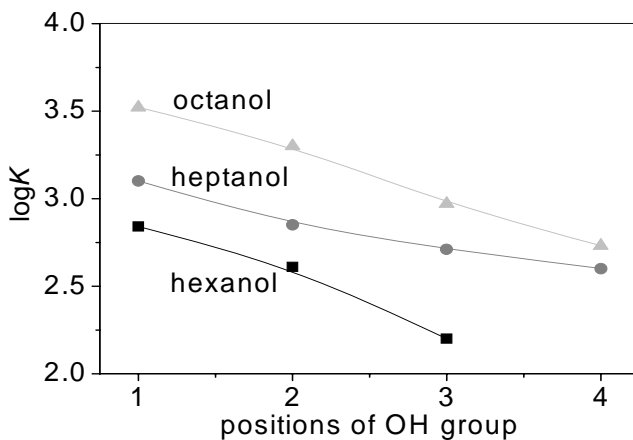
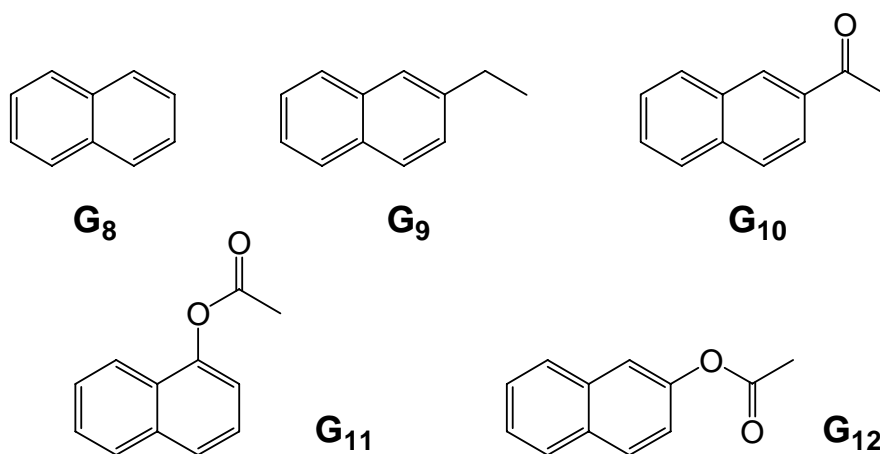


Figure 8. The relationship between the positions of OH group in monoaliphatic alcohols and the values of $\log K$ of the complexes of the alcohols with α -CD.[138]

α -CD possesses a weak binding ability to many normal-chain and branched-chain alkyl derivatives, but has a certain discrimination power to them. For instance, the K values of the complexes formed by α -CD with 1-pentanol, 2-pentanol and 3-pentanol are 378, 108 and 45 kg·mol⁻¹, respectively,[138] which are decreasing markedly as the OH group moved toward the center of the chain. Similarly, such an inclusion phenomenon occurs in the systems between α -CD and hexanol homologues (K , 1-hexanol, 689; 2-hexanol, 412 and 3-hexanol, 159 kg·mol⁻¹), and the systems between α -CD and heptanol homologues (K , 1-heptanol, 1270; 2-heptanol, 713; 3-heptanol, 508 and 4-heptanol, 379 kg·mol⁻¹).[138] The calculated ζ_G values in the above systems are all higher than 1.5, suggesting that parent α -CD possesses a moderate ability to distinguish the difference in the location of the OH group. Undoubtedly, when the OH group having a strong hydrophilicity is transferred towards the chain center, it seems to be disadvantageous for the hydrophobic-hydrophobic interaction between the cavity of α -CD and the alkyl chain (see Figure 8). That is the reason why the position change of the OH group led to a decreased stability of the inclusion complexes.

There are sufficient data available to discuss the discrimination behavior in Level C. For another example, the K value of the complex formed by β -CD and G_8 is $608 \text{ dm}^3 \cdot \text{mol}^{-1}$ at 298 K, while the K values of the complexes formed by β -CD and the four derivatives of G_8 , G_9 – G_{12} , are 752, 491, 252 and $950 \text{ dm}^3 \cdot \text{mol}^{-1}$, respectively.[139] G_{11} - β -CD and G_{12} - β -CD are the least stable and the most stable of the five complexes. Interestingly, the two guests are just a pair of geometrical isomers. The stability difference between the two complexes is big enough (ζ_G , 3.8), indicating a considerable ability of β -CD to discriminate between G_{11} and G_{12} .

By appearances, they have more similarity to each other than to any other guests at least in constitution and properties. The largest difference in inclusion intensities between the two guests and β -CD is only related to the substitution positions of one ester group, implying that the position change of the same substituted group at the naphthalene ring seems to have a larger influence than the structural change of the different substituted groups.



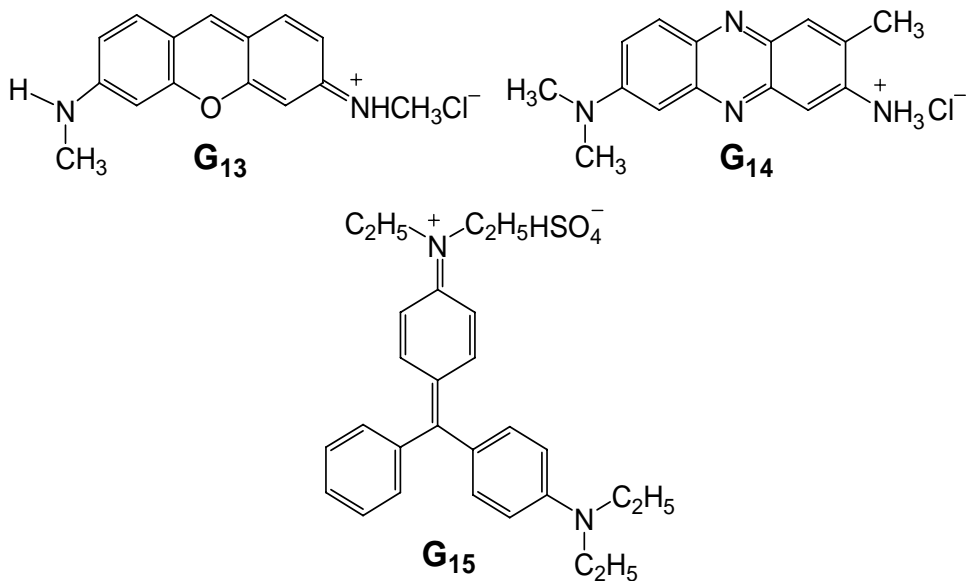
From the structural comparison among G_8 , G_9 and G_{12} , the existence of ethyl group or ester group in position C-2 on the naphthalene ring is advantageous to improve the interaction between β -CD and naphthalene ring. And the positive effect of the ester group is larger than that of the ethyl group. Contrarily, the ester group in position C-1, as well as acetyl group in position C-2, seems to play a role in weakening the interaction between β -CD and naphthalene ring based on the structural comparison among G_8 , G_{10} and G_{11} . The binding abilities of β -CD to G_8 and G_9 are very close to each other (ζ_G , 1.2), according to the ratio of their K values. Nonetheless, the stability of G_9 - β -CD is larger than that of G_{10} - β -CD (ζ_G , 1.5). In light of the observations described above, it suggests that the structural change of substituted groups on the rigid naphthalene ring plays an important role in discriminating between naphthalene and monosubstituted naphthalenes.

Overall, the systems in Level C are mainly composed of the same parent CD and homologous organic guests. And α - or β -CD has certain discrimination ability to the guests with similar structure, but relative low stabilities are serious problems in face of the inclusion systems. That is to say, the low values of K set a limit to the actual application of the systems.

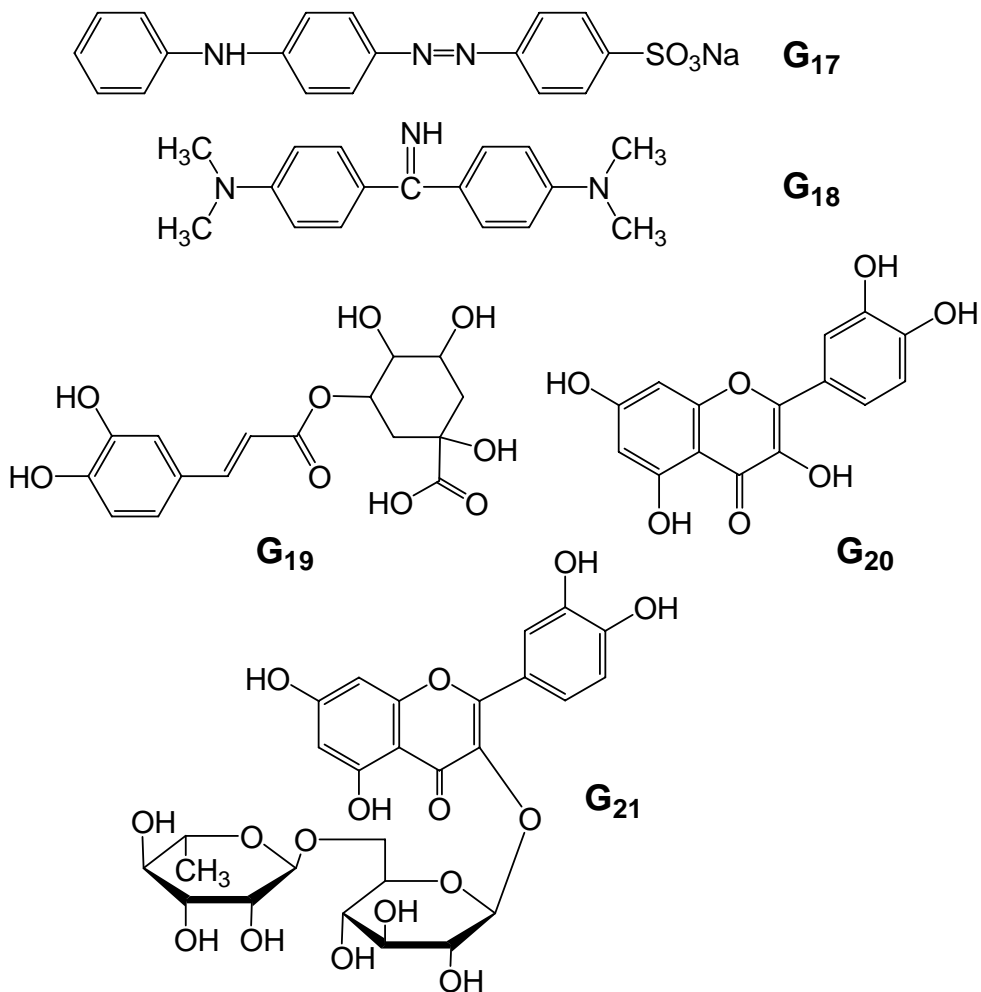
6. REPRESENTATIVE INCLUSION SYSTEMS IN LEVEL B

If the inclusion systems between the same CD and a series of guests are expected to have a practical application in solving the problem of homologue separation, particularly in geometrical isomer separation and optical isomer separation, the CD must provide both a strong enough binding ability to one or some of the guests and a high enough discrimination level between the guests.

Many studies indicate that such inclusion systems are available. For instance, the K values of the complexes formed by β -CD with dye molecules G_{13} , G_{14} , G_{15} and G_3 are 2089, 480, 2187 and 4240 $\text{dm}^3 \cdot \text{mol}^{-1}$, respectively.[135,140] Taking the least K value of G_{14} - β -CD as a reference, the ξ_G values between G_{14} and the other three guests are 4.4 (for G_{13}), 4.6 (for G_{15}) and 8.8 (for G_3), in terms of our calculations. From the data, it is reasonable that β -CD possesses a good discrimination ability to distinguish between G_{14} and the others. Since the inclusion ability of β -CD to any one of the three guests G_{13} - G_{15} is much lower than the guest G_3 , this reflects the significance of the structural difference of the guests, including the arrangement and number of rigid aromatic rings, the heteroatoms in the rings and the nature of substituted groups.



In this case of the same CD, whether inclusion effect is strong or weak depends on guest structure and its response to the CD structure, and whether the discrimination level between analogous guests is high or low depends on both the differences of the guests in structure and the discrepancies of their responses to the CD structure. The structural factors from a CD include the diameter of cavity and the position and number of modified OH groups. And the structural factors from a guest mainly include the length of carbon chain; the position, polarity and volume of substituted groups; the kind, number and arrangement of ring.



In Level B, due to the large values of K and high values of ξ_G , it allows us to consider the actual application of constructed supramolecular systems. For example, the K values of the complexes of β -CD with three guest molecules **G₁**, **G₁₇** and **G₁₈** are 3560, 5530 and 819 $\text{dm}^3\cdot\text{mol}^{-1}$, respectively.[135] The structural relationship between **G₁** and **G₁₇**, as well as between **G₁** and **G₁₈**, is clear at a glance. That is to say, one side (benzene sulfonate) of the asymmetric guest **G₁** is the same as one side of the asymmetric guest **G₁₇**, and the other side (*N,N*-dimethylaniline) of **G₁** is the same as one side of symmetric guest **G₁₈**. However, such an inclusion result shows that the complexations between β -CD and two diazo derivatives **G₁** and **G₁₇** are much stronger than that between β -CD and **G₁₈**. Taking the least K value of **G₁₈**- β -CD as a reference, the ξ_G values between **G₁₈** and the other two guests are 4.3 (for **G₁**) and 6.7 (for **G₁₇**). This observation indicates that the introduction of benzene sulfonate with a negative charge, possibly as well as the presence of a diazo group in the middle, has a positive effect on the discrimination between the complex benzene derivatives using the formation of supramolecules with β -CD.

Table 4. The structural selectivities of the same CDs to a series of homologous guests

Level	Group	Host	Guest	$K/ \text{dm}^3 \cdot \text{mol}^{-1}$	ζ_G	pH	Method ^a	Refs
D	1	α -CD	NaCl	no reaction	–	–	cal	6
D	1	α -CD	NaBr	1.7 ± 0.3	1.0	–	cal	6
D	1	α -CD	NaI	19.5 ± 0.9	11.5	–	cal	6
D	2	α -CD	KCl	no reaction	–	–	cal	6
D	2	α -CD	KBr	2.3 ± 0.8	1.0	–	cal	6
D	2	α -CD	KI	17 ± 3	7.4	–	cal	6
D	3	α -CD	methyl propionate	48 ± 9	1.0	–	cal	6
D	3	α -CD	ethyl propionate	64 ± 20	1.3	–	cal	6
D	4	α -CD	cyclobutanol	23 ± 2	1.0	–	st	138 ^b
D	4	α -CD	cyclopentanol	40 ± 5	1.7	–	st	138 ^b
D	4	α -CD	cyclohexanol	50 ± 8	2.2	–	st	138 ^b
D	5	β -CD	4-nitrobenzoic acid	60	1.0	–	uv	134
D	5	β -CD	1-chloro-2,4-dinitrobenzene	63	1.1	–	uv	134
D	5	β -CD	1-chloro-2-nitrobenzene	79	1.2	–	uv	134
D	6	β -CD	G₄	38.9	1.0	^c	uv	136
D	6	β -CD	G₁	69.2	1.8	^c	uv	136
D	6	β -CD	G₅	97.7	2.5	^c	uv	136
D	7	γ -CD	benzoic acid	3	1.0	–	cze	123
D	7	γ -CD	2-methylbenzoic acid	7	2.3	–	cze	123
D	7	γ -CD	3-methylbenzoic acid	6	2.0	–	cze	123
D	7	γ -CD	4-methylbenzoic acid	8	2.7	–	cze	123
D	8	mono-NH ₃ ⁺ - β -CD	<i>R-N</i> -AcPhe	55 ± 7	1.0	6.0	nmr	132
D	8	mono-NH ₃ ⁺ - β -CD	<i>S-N</i> -AcPhe	67 ± 8	1.2	6.0	nmr	132
C	1	α -CD	methyl formate	8 ± 5	1.0	–	cal	6
C	1	α -CD	ethyl formate	38 ± 1	4.8	–	cal	6
C	1	α -CD	propyl formate	116 ± 9	14.5	–	cal	6
C	2	α -CD	methyl acetate	21 ± 1	1.0	–	cal	6
C	2	α -CD	ethyl acetate	53 ± 3	2.5	–	cal	6
C	2	α -CD	propyl acetate	120 ± 7	5.7	–	cal	6
C	3	α -CD	3-pentanol	45 ± 2^c	1.0	–	st	138
C	3	α -CD	2-pentanol	108 ± 8^c	2.4	–	st	138
C	3	α -CD	1-pentanol	378 ± 25^c	8.4	–	st	138
C	4	α -CD	2-methyl-2-pentanol	244 ± 5	1.0	–	st	138

Level	Group	Host	Guest	$K/\text{dm}^3\cdot\text{mol}^{-1}$	ζ_G	pH	Method ^a	Refs
C	4	α -CD	2-hexanol	412 ± 9	1.7	–	st	138
C	4	α -CD	2-heptanol	713 ± 9	2.9	–	st	138
C	5	β -CD	<i>D</i> - G ₆	328 ± 20	1.0	6.9	nmr	137
C	5	β -CD	<i>L</i> - G ₆	565 ± 20	1.7	6.9	nmr	137
C	6	β -CD	<i>L</i> - G ₇	368 ± 10	1.0	6.9	nmr	137
C	6	β -CD	<i>D</i> - G ₇	412 ± 14	1.1	6.9	nmr	137
C	7	β -CD	G ₁₀	491	1.0	–	fl	139
C	7	β -CD	G ₉	752	1.5	–	fl	139
C	7	β -CD	G ₁₂	950	1.9	–	fl	139
C	8	β -CD	G ₁₁	252	1.0	–	fl	139
C	8	β -CD	G ₁₂	926	3.8	–	fl	139
C	9	β -CD	ethylenediamine	83.4	1.0	7.2	uv	41
C	9	β -CD	ethylene diaminetetraacetic	265.0	3.2	7.2	uv	41
C	9	β -CD	diethylenetriamine	368.0	4.4	7.2	uv	41
C	9	β -CD	triethylamine	748.0	9.0	7.2	uv	41
C	10	heptakis(2,6-di- <i>O</i> -methyl) β -CD	<i>D</i> -Phenylalanine	155.7	1.0	6.84	uv	133
C	10	heptakis(2,6-di- <i>O</i> -methyl) β -CD	<i>L</i> -Phenylalanine	264.1	1.7	6.84	uv	133
C	11	<i>L</i> -Trp- β -CD ^d	(+)-menthol	429	1.0	7.2	fl	18
C	11	<i>L</i> -Trp- β -CD	(–)-menthol	810	1.9	7.2	fl	18
C	12	<i>L</i> -Trp- β -CD	nerol	197	1.0	7.2	fl	18
C	12	<i>L</i> -Trp- β -CD	geraniol	384	1.9	7.2	fl	18
Table 4 (Continued)								
Level	Group	Host	Guest	$K/\text{dm}^3\cdot\text{mol}^{-1}$	ζ_G	pH	Method ^a	Refs
B	1	α -CD	1-octanol	3316 ± 75	6.1	–	st	138
B	1	α -CD	2-octanol	1973 ± 23	3.6	–	st	138
B	1	α -CD	3-octanol	942 ± 11	1.7	–	st	138
B	1	α -CD	4-octanol	543 ± 5	1.0	–	st	138
B	2	β -CD	G ₁₄	480	1.0	7.2	fl	140
B	2	β -CD	G ₁₃	2089	4.4	7.2	fl	140
B	2	β -CD	G ₁₅	2187	4.6	7.2	uv	140
B	2	β -CD	G ₃	4240	8.8	7.2	fl	140
B	3	β -CD	G ₁₈	819	1.0	7.2	fl	135
B	3	β -CD	G ₁	3560	4.3	7.2	fl	135
B	3	β -CD	G ₁₇	5530	6.8	7.2	fl	135

Table 4. (Continued).

Level	Group	Host	Guest	$K/ \text{dm}^3 \cdot \text{mol}^{-1}$	ζ_G	pH	Method ^a	Refs
B	4	β -CD	G₂₁	250 ± 48	1.0	7.0	fl	141
B	4	β -CD	G₁₉	420 ± 50	1.7	7.0	fl	141
B	4	β -CD	G₂₀	1284 ± 106	5.1	7.0	fl	141
B	5	per-CO ₂ ⁻ - β -CD ^d	Λ -Ru(phen) ^d ₃ ²⁺	590 ± 40	1.0	7.0	cze	130
B	5	per-CO ₂ ⁻ - β -CD	Δ -Ru(phen) ₃ ²⁺	1250 ± 50	2.1	7.0	cze	130
B	6	per-CO ₂ ⁻ - γ -CD ^d	Λ -Ru(phen) ₃ ²⁺	890 ± 40	1.0	7.0	cze	130
B	6	per-CO ₂ ⁻ - γ -CD	Δ -Ru(phen) ₃ ²⁺	1140 ± 50	1.3	7.0	cze	130
B	7	per-NH ₃ ⁺ - β -CD ^d	<i>R-N</i> -AcPhe	2000 ± 130	1.0	6.0	nmr	132
B	7	per-NH ₃ ⁺ - β -CD	<i>S-N</i> -AcPhe	2180 ± 130	1.1	6.0	nmr	132
B	8	H₁	G₂₅	4170	1.0	7.2	fl	142
B	8	H₁	G₂₄	8040	1.9	7.2	fl	142
B	9	ND- β -CD ^e	cyclohexanol	368	1.0	-	CD	143
B	9	ND- β -CD	cyclohexane	2016	5.5	-	CD	143
A	1	H₁	G₂₅	4170	1.0	7.2	fl	142
A	1	H₁	G₂₄	8040	1.9	7.2	fl	142
A	1	H₁	G₂₂	16700	4.0	7.2	fl	142
A	1	H₁	G₂₃	41900	10.0	7.2	fl	142
A	1	H₁	G₂₆	103900	24.9	7.2	fl	142
A	2	H₂	G₂₂	6380	1.0	7.2	fl	142
A	2	H₂	G₂₅	7600	1.2	7.2	fl	142
A	2	H₂	G₂₄	10230	1.6	7.2	fl	142
A	2	H₂	G₂₆	59800	9.4	7.2	fl	142
A	2	H₂	G₂₃	117000	18.3	7.2	fl	142
A	3	H₃	cyclohexanol	1430	1.0	7.2	fl	143
A	3	H₃	cyclohexane	20650	14.4	7.2	fl	143
A	4	H₄	G₃₀	12405 ± 545	1.0	7.2	fl	125
A	4	H₄	G₂₉	49760 ± 490	4.0	7.2	fl	125
A	4	H₄	G₂₈	89570 ± 750	7.2	7.2	fl	125
A	4	H₄	G₂₇	133450 ± 2450	10.8	7.2	fl	125
A	5	heptakis(2,6-di- <i>O</i> -methyl) β -CD	syringic acid	1730 ± 110	1.0	7.2	fl	126
A	5	heptakis(2,6-di- <i>O</i> -methyl) β -CD	2-methoxyphenol	51900 ± 800	30	7.2	fl	126

Level	Group	Host	Guest	$K/\text{dm}^3\cdot\text{mol}^{-1}$	ζ_G	pH	Method ^a	Refs
A	5	heptakis(2,6-di- <i>O</i> -methyl) β -CD	eugenol	93300 ± 7400	53.9	7.2	uv	127
A	6	β -CD	G₂₄	2510	1.0	7.2	cal	19
A	6	β -CD	2-NS ^e	234000	93.4	7.2	cal	19
A	7	β -CD	C ₁ C ₇ V ²⁺ ^f	440	1.0	7.0	uv	21
A	7	β -CD	C ₁ C ₈ V ²⁺	890	2.0	7.0	uv	21
A	7	β -CD	C ₁ C ₉ V ²⁺	2400	5.5	7.0	uv	21
A	7	β -CD	C ₁ C ₁₀ V ²⁺	7800	17.7	7.0	uv	21
A	7	β -CD	C ₁ C ₁₂ V ²⁺	12000	27.3	7.0	uv	21

^a method employed: st, surface tension; cze, capillary zone electrophoresis; nmr, nuclear magnetic resonance. ^b the unit of these K values is $\text{kg}\cdot\text{mol}^{-1}$. ^c in aqueous 40% formic acid. ^d *L*-Trp- β -CD is *L*-tryptophan-modified β -CD. Per-CO₂⁻ β - and per-CO₂⁻ γ -CD are anionic heptakis[6-carboxymethylthio-6-deoxy]- β - and heptakis[6-carboxymethylthio-6-deoxy]- γ -CD, respectively. Phen is 1,10-phenanthroline. Per-NH₃⁺- β -CD is protonated heptakis(6-amino-6-deoxy)- β -CD. ^e ND- β -CD is 6-[(*N*-2-naphthoyl-2-aminoethyl)amino]-6-deoxy- β -CD; 2-NS: 2-naphthalenesulfonate. ^f C₁C_{*n*}V²⁺: methylalkyl viologens (C₁C_{*n*}V²⁺, *n* = 7–10, 12).

Further, it is shown that, during the inclusion interaction, the steric factors associated with the structures of host and guest molecules strongly influence the stability magnitude of host–guest complexes. In many instances, such as in the inclusion systems formed by β -CD with three guests **G**₁₉, **G**₂₀ and **G**₂₁, which are the derivatives of catechol, the *K* values (**G**₁₉, 420 ± 50 ; **G**₂₀, 1284 ± 106 and **G**₂₁, $250 \pm 48 \text{ dm}^3 \cdot \text{mol}^{-1}$) of their complexes of β -CD are quite different.[141]

Taking the least *K* value of **G**₂₁– β -CD as a reference, the ζ_G values between **G**₂₁ and the other two guests are 3.1 (for **G**₁₉) and 5.1 (for **G**₂₀). The only difference in structure between **G**₂₀ and **G**₂₁ is that a hydroxyl group in the former is substituted by a monomethylated disaccharide group in the latter, but the difference in inclusion effect is the decrease of five times in the *K* value. Certainly, the existence of the bulky disaccharide group causes a steric hindrance effect on the supramolecular formation. For this reason, we can be expected to realize at least partially the separation of an excessive reactant such as **G**₂₀ and a target product such as **G**₂₁ by means of the difference in their affinity abilities to β -CD.

7. REPRESENTATIVE INCLUSION SYSTEMS IN LEVEL A

The *K* values and ζ_G values in the systems of Levels B, C and D discussed above are not comparable with the strong binding ability and high selectivity of enzyme to substrate in biological system. By modification of CDs to increase the probability of higher values of *K* and ζ_G , it is possible to obtain some of the functions of enzymes.

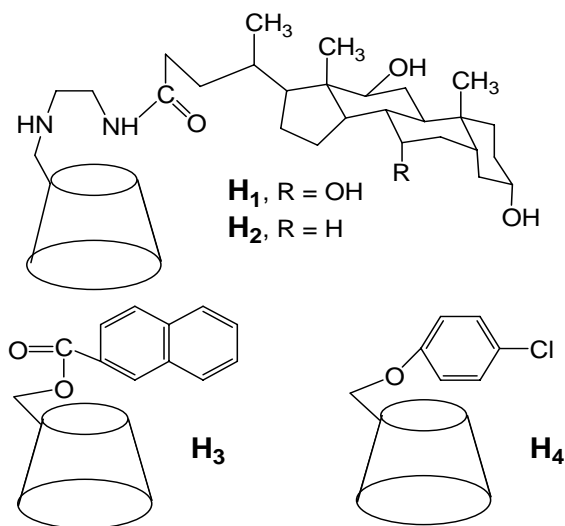
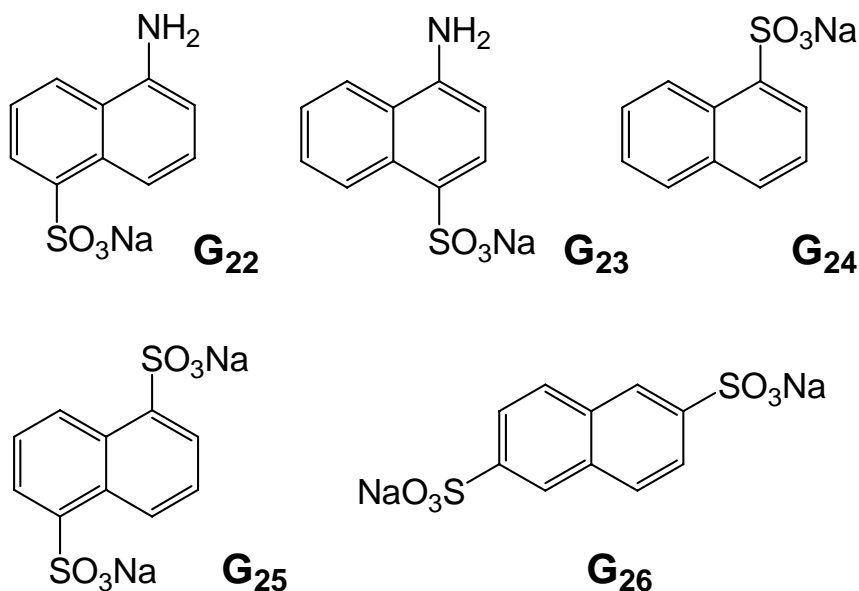


Figure 9. Structures of mono(6-*O*-substituted)- β -CD molecules.

For example, in the constructed systems of β -CD derivatives **H**₁ and **H**₂ (modified by bulky nonaromatic groups, see Figure 9) with a group of naphthalenesulfonates sodium derivatives (**G**₂₂–**G**₂₆), the *K* values of the complexes are obviously higher than those of the complexes of parent β -CD with the guests.[142] To be specific, the *K* values of the complexes of **H**₁ with **G**₂₂, **G**₂₃, **G**₂₄, **G**₂₅ and **G**₂₆ are 16700, 41900, 8040, 4170 and 103900 $\text{dm}^3 \cdot \text{mol}^{-1}$

respectively, and the K values of the complexes of \mathbf{H}_2 with the corresponding binding partners are 6380, 117000, 10230, 7600 and 59800 $\text{dm}^3\cdot\text{mol}^{-1}$, respectively.[142] According to the data, the nature of the substituent groups of the hosts as well as the guests, such as properties (\mathbf{H}_1 and \mathbf{H}_2 ; \mathbf{G}_{22} and \mathbf{G}_{25}), position (\mathbf{G}_{22} and \mathbf{G}_{23} ; \mathbf{G}_{25} and \mathbf{G}_{26}) and quantity (\mathbf{G}_{24} and \mathbf{G}_{25}), has a significant effect on the K values of the host–guest complexes.

The ratios (ζ_G) of the K values of the complexes of \mathbf{H}_1 with \mathbf{G}_{22} , \mathbf{G}_{23} , \mathbf{G}_{24} and \mathbf{G}_{26} to that of the complex $\mathbf{G}_{25}\text{--}\mathbf{H}_1$ are 4.0, 10.0, 1.9 and 24.9 respectively, indicating that \mathbf{H}_1 is able to distinguish between \mathbf{G}_{23} and \mathbf{G}_{25} or between \mathbf{G}_{26} and \mathbf{G}_{25} , as well as between \mathbf{G}_{26} and \mathbf{G}_{22} or between \mathbf{G}_{26} and \mathbf{G}_{24} , because for the four systems, the values of ζ_G are 10 and above. By the inducement of the bulk substituent in position C-6 of β -CD, \mathbf{G}_{26} is inserted into the cavity of \mathbf{H}_1 . [142] The huge K values ($> 10^5 \text{ dm}^3\cdot\text{mol}^{-1}$) of the two complexes, $\mathbf{G}_{26}\text{--}\mathbf{H}_1$ and $\mathbf{G}_{23}\text{--}\mathbf{H}_2$, not only reflects the existence value of the large modification group on the narrower rim of β -CD, but also suggests that the disubstitution of sulfonic ions in positions C-2 and C-6 on a naphthalene ring, as well as the substitutions of an amino group and a sulfonic ion in positions C-1 and C-4 respectively, is much more advantageous than the substitutions of two sulfonic ions, as well as an amino group and a sulfonic ion, in positions C-1 and C-5 to promote the stability of the inclusion complexes of \mathbf{H}_1 with naphthalene derivatives. We can explain the phenomenon by considering the effects of the steric hindrance resulted from the substitutions of H atoms in positions C-1 and C-5 by substituent groups such as NH_2 and SO_3^- . As shown in Figure 9, the substituent R in \mathbf{H}_1 or \mathbf{H}_2 , seems to be far away from the openings of the cavity, but the K values of the complexes of the same guest with the two hosts were markedly changed following the replacement of R in OH group by R in H atom, implying the presence of structural self-organization of the two hosts during inclusion complexation process.

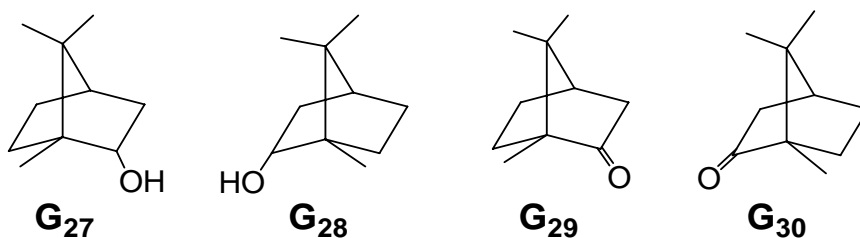


The K values of the complexes of \mathbf{H}_3 (modified by an aromatic group, see Figure 9) with cyclohexanol and cyclohexane are 1430 and 20650 $\text{dm}^3\cdot\text{mol}^{-1}$, respectively,[143] and ζ_G is up to 14.4. The inclusion ability of \mathbf{H}_3 to cyclohexane is large enough, and much larger than to

cyclohexanol. Therefore, such a system can be expected to open up a wide range of applications in separation of simple organic compounds with similar structure. It is worth stressing that the structure of modification groups in **H₃** plays an important role because it influences both affinity ability and discrimination behavior. For example, the complexes of the two guests with ND- β -CD¹⁴³ ($\zeta_G = 5.5$, see Table 4) show a much lower stability than those of them with **H₃**.

It is well known that the polarity of cyclohexanol is different from that of cyclohexane, and the former is much more hydrophilic than the latter. Their complexes of the same host show rather different stability level owing to the slight difference between H atom and OH group. It is the structural difference that makes a significantly different intermolecular interaction between host and guest. The observation provides a new way for effective identification, discrimination and recognition of the similar organic molecules in quantitative analysis, chemical separation and modern synthetic chemistry with the aid of forming their CD supramolecules.

The *K* values of the inclusion complexes of **H₄** with four guests **G₂₇**, **G₂₈**, **G₂₉** and **G₃₀** are 133450 ± 2450 , 89570 ± 750 , 49760 ± 470 and $12405 \pm 545 \text{ dm}^3 \cdot \text{mol}^{-1}$, respectively.[125] They are all large enough ($K > 12000 \text{ dm}^3 \cdot \text{mol}^{-1}$), showing the complexes are quite stable. It is worth mentioning that the four guests with the same skeleton structure (borneol and camphor derivatives) and a similar heteroatom O (in OH group or in C=O bond). The very strong interactions between **H₄** and the guests mean that such a guest frame with tricyclic structure can well match to the cavity of **H₄**. This inclusion phenomenon is very similar to that of β -CD and adamantane, implying that there is a prominent structural correlation between the three-dimensional cavity and the tricyclic structural unit.



It is certain that, in Level A as discussed above, the interactions between CD derivatives and guests seem to be comparable with the interaction between enzyme and substrate in biological system in a way. The supramolecular systems with huge binding ability and high discrimination behavior offer us a platform for the expansion of the application in separation, purification, immunoassay, enzyme mimic, chemical sensor, and other fields.

Additionally, the binding interactions of **H₄** to **G₂₇** and **G₂₈** are stronger than to **G₂₉** and **G₃₀**. The two guests **G₂₇** and **G₂₈**, as well as the two guests **G₂₉** and **G₃₀**, are both a pair of enantiomers. Significantly, there is an obviously different discrimination level of **H₄** to the two groups of enantiomers. By contrast with the ζ_G value of 4.0 between **G₂₉** and **G₃₀**, the value of ζ_G less than 1.5 between **G₂₇** and **G₂₈** is rather low. The result shows that, under the same frame, the fine adjustment of the guests in structure of substituent groups can lead to a rather different discrimination effect of the same host to the chiral molecules.

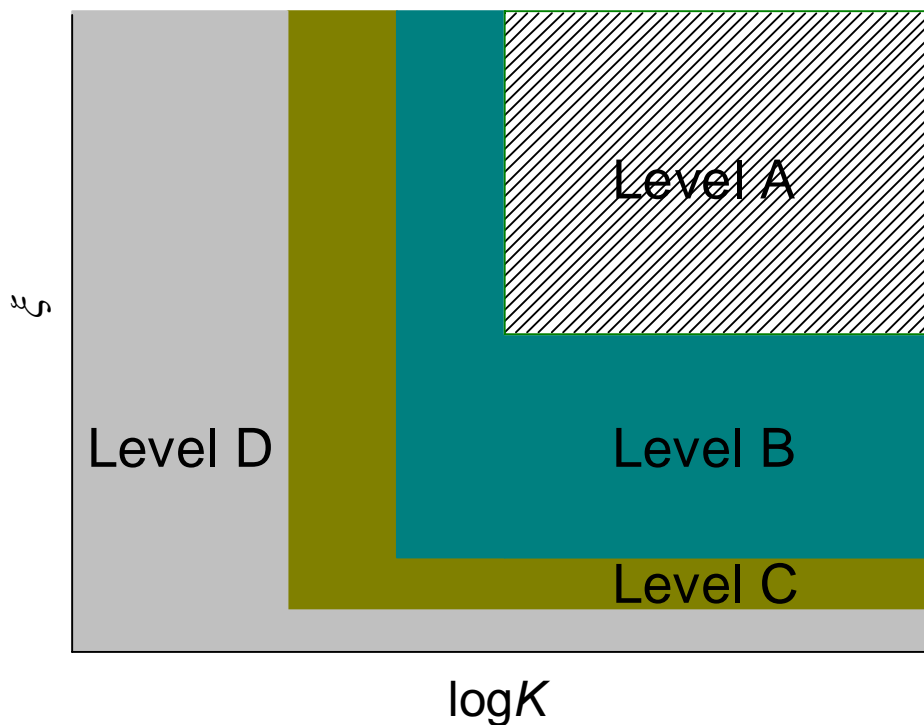


Figure 10. A schematic feature depicting the molecular discrimination levels A, B, C and D of the same CDs to different guests.

As can be seen in Figure 10, the schematic feature describing the four levels A, B, C and D of molecular discrimination abilities of the same CDs to different guests clearly summarizes the relationship among the levels.

8. THE DISCRIMINATION BEHAVIOR OF THE SAME GUEST TO A GROUP CDs

Like the discrimination behavior of the same host to a group of analogous guests, the same guest also can discriminate the difference of a group CDs in structure. For instance, the K values of complexes of G_2 with α -, β - and γ -CD, are 49.7, 1380 and 117 $\text{dm}^3 \cdot \text{mol}^{-1}$, respectively.[144] In comparison with the K value of complex G_2 - β -CD, the values of ζ_H to G_2 - α -CD and G_2 - γ -CD are 27.8 and 11.8, respectively. Thus it can be seen that the cavity of β -CD is fitter to accommodate G_2 than that of α - or γ -CD, possibly because the cavity of α -CD is too small but that of γ -CD is too big. This example exhibits that such a guest as AR is likely to be used to extract β -CD from the mixture containing the three parent CDs by forming their complexes of G_2 .

Table 5. The structural selectivity of the same guest to different CDs

Level	Group	Guest	Host	$K/\text{dm}^3\cdot\text{mol}^{-1}$	ζ_{H}	pH	Method	Refs
D	1	benzoate	γ -CD	3	1.0	–	cze	123
D	1	benzoate	α -CD	16	5.3	–	cze	123
D	1	benzoate	β -CD	23	7.7	–	cze	123
D	2	4-methyl benzoate	γ -CD	8	1.0	–	cze	123
D	2	4-methyl benzoate	α -CD	36	4.5	–	cze	123
D	2	4-methyl benzoate	β -CD	66	8.3	–	cze	123
D	3	salicylic acid	α -CD	8 ± 0.3	1.0	–	cze	22
D	3	salicylic acid	heptakis(2,6-di- <i>O</i> -methyl) β -CD	79 ± 6	9.9	–	cze	22
D	3	salicylic acid	β -CD	82 ± 3	10.3	–	cze	22
D	4	1-butanol	H₅	7.4	1.0	7.2	CD	124
D	4	1-butanol	H₆	12.8	1.7	7.2	CD	124
C	1	cyclopentanol	β -CD	168 ± 3	1.0	7.2	cal	125
C	1	cyclopentanol	H₄	629 ± 3	3.7	7.2	cal	125
C	2	Λ -Ru(phen) ₃ ²⁺	per-CO ₂ ⁻ β -CD	590 ± 40	1.0	7.0	cze	130
C	2	Λ -Ru(phen) ₃ ²⁺	per-CO ₂ ⁻ γ -CD	890 ± 40	1.5	7.0	cze	130
C	3	nimodipine	α -CD	62 ± 14	1.0	–	uv	128
C	3	nimodipine	β -CD	550 ± 32	8.9	–	uv	128
C	4	1-pentanol	β -CD	180 ± 10	1.0	–	nmr	80
C	4	1-pentanol	α -CD	434 ± 68	2.4	–	nmr	80
C	5	cyclohexanol	H₅	183	1.0	7.2	CD	124
C	5	cyclohexanol	H₆	590	3.2	7.2	CD	124
C	5	cyclohexanol	β -CD	707 ± 4	3.9	7.2	cal	125
B	1	cycloheptanol	β -CD	2344 ± 92	1.0	7.2	cal	125
B	1	cycloheptanol	H₄	7925 ± 32	3.4	7.2	cal	125
B	2	G₂	α -CD	49.7	1.0	6.0	fl	144
B	2	G₂	γ -CD	117	11.8	6.0	fl	144
B	2	G₂	β -CD	1380	27.8	6.0	fl	144
B	3	<i>L</i> - G₇	β -CD	368 ± 14	1.0	6.9	nmr	137
B	3	<i>L</i> - G₇	γ -CD	2600 ± 150	7.0	6.9	nmr	137
B	4	<i>D</i> - G₇	β -CD	412 ± 10	1.0	6.9	nmr	137
B	4	<i>D</i> - G₇	γ -CD	3800 ± 150	9.2	6.9	nmr	137
B	5	cyclohexanol	ND- β -CD	368	1.0	–	CD	143
B	5	cyclohexanol	H₃	1430	3.9	–	CD	143

Level	Group	Guest	Host	K/ dm ³ ·mol ⁻¹	ξH	pH	Method	Refs
B	6	<i>S-N</i> -AcPhe	mono-NH ₃ ⁺ -β-CD	67 ± 8	1.0	6.0	nmr	132
B	6	<i>S-N</i> -AcPhe	per-NH ₃ ⁺ -β-CD	2180 ± 130	32.5	6.0	nmr	132
A	1	1-adamantanol	H ₅	7300	1.0	7.2	CD	124
A	1	1-adamantanol	H ₆	278000	38.1	7.2	CD	124
A	2	2-adamantanol	H ₅	14600	1.0	7.2	CD	124
A	2	2-adamantanol	H ₆	435000	29.8	7.2	CD	124
A	3	G ₂₃	β-CD	50	1.0	7.2	fl	142
A	3	G ₂₃	H ₁	41900	838	7.2	fl	142
A	3	G ₂₃	H ₂	117000	2340	7.2	fl	142
A	4	G ₃₁	H ₈	3600 ± 150	1.0	7.2	nmr	75
A	4	G ₃₁	H ₉	5000 ± 200	1.4	7.2	nmr	145
A	4	G ₃₁	H ₇	11800 ± 600	3.3	7.2	nmr	145
A	5	C ₁ C ₁₀ V ²⁺	β-CD	7800	1.0	7.0	uv	21
A	5	C ₁ C ₁₀ V ²⁺	N-β-CD ^a	19700	2.5	7.0	uv	21
A	5	C ₁ C ₁₀ V ²⁺	Ns-β-CD ^b	33000	4.2	7.0	uv	21
A	6	cyclohexane	ND-β-CD	2016	1.0	–	CD	143
A	6	cyclohexane	H ₃	20650	10.2	–	CD	143
A	7	G ₂₆	β-CD	1950	1.0	7.2	cal	142
A	7	G ₂₆	H ₂	59800	30.7	7.2	fl	142
A	7	G ₂₆	H ₁	103900	53.3	7.2	fl	142
A	8	G ₂	H ₇	5300 ± 200	1.0	7.2	fl	145
A	8	G ₂	H ₈	9420 ± 400	1.8	7.2	fl	75
A	8	G ₂	H ₉	27500 ± 400	5.2	7.2	fl	145

^a N-β-CD: mono-6-*O*-(2-naphthyl)-β-CD.

^b Ns-β-CD: mono-6-*O*-(2-sulfonato-6-naphthyl)-β-CD.

It is shown that the values of K and ζ_{H} are seriously influenced by the minor difference of the selected guest in structure. For instance, the K values of the complexes of 1-adamantanol with \mathbf{H}_5 and \mathbf{H}_6 (see Figure 11) are 7300 and 278000 $\text{dm}^3 \cdot \text{mol}^{-1}$, large enough to form stable complexes.[124] What is more, the value of ζ_{H} between them is up to 38.0, which results from, so to speak, so small structural change between \mathbf{H}_5 and \mathbf{H}_6 , where the difference is only between one methoxyl group and one methyl group. It seems to be a good example of an applicable and rather high-level molecular discrimination, perhaps somewhat like the molecular recognition of a certain substrate to some specific enzymes.

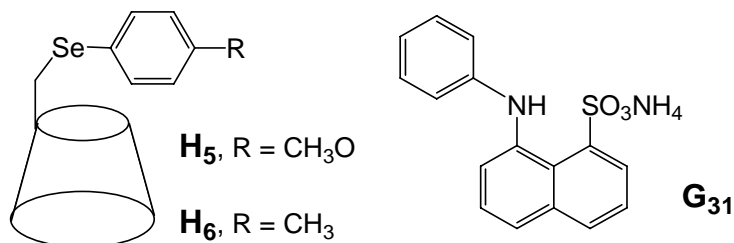


Figure 11. Structural features of guest \mathbf{G}_{31} and two mono(6-*O*-substituted)- β -CD molecules \mathbf{H}_5 and \mathbf{H}_6 .

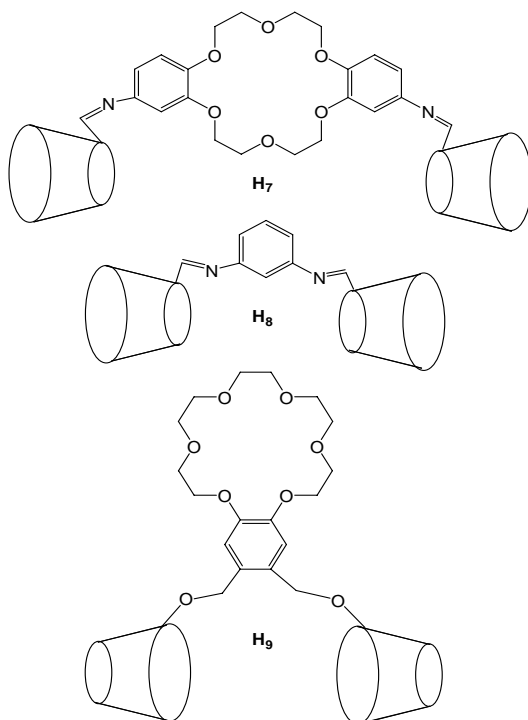


Figure 12. Structural features of β -CD dimers \mathbf{H}_7 – \mathbf{H}_9 .

In order to increase the intermolecular interaction sites between host and guest, many types of bridged CD dimers or multimers were synthesized to improve the inclusion ability and the discrimination level of CDs effectively. For instance, the K values of complexes of \mathbf{G}_{31} (Figure 11) with three β -CD dimers \mathbf{H}_7 , \mathbf{H}_8 and \mathbf{H}_9 (see Figure 12) are 11800 ± 600 , 3600

± 150 and $5000 \pm 200 \text{ dm}^3 \cdot \text{mol}^{-1}$, respectively.[145] The values are all rather big, and the observed ratios between them, especially between $\mathbf{G}_{31}\text{-H}_7$ and $\mathbf{G}_{31}\text{-H}_8$ (ζ_{H} , 3.2), are considerable. This result indicates that \mathbf{G}_{31} is able to detect the difference in structure between the bridged groups of \mathbf{H}_7 and \mathbf{H}_8 .

Besides the inclusion systems discussed above, some examples about the structural selectivity of a specific guest to a group of CDs are listed in Table 5. Generally speaking, as can be seen from Table 5, modified CDs usually have much stronger affinity ability than parent CDs to the same guest, even though there are some exceptions. We believe that this inclusion phenomenon may be applied in separating between parent CDs and their derivatives in future.

It is well known that it is difficult to make the chemical separation between CDs and their derivatives, as well as between the derivatives. We believe that the further investigation on the different discrimination behaviors of CDs or their derivatives to the same guest will result in the realization of the chemical separation between them by the aid of supramolecular formation. In addition, for a CD dimer, though the synergistic effects among bridged groups and double cavities have been considerably reported,[135,146] the synergistic mechanisms in many host-guest systems are still not clear.[145,146] For this reason we consider that further studies are needed to deeply understand the phenomena.

9. SEVERAL EXAMPLES OF CD INCLUSION COMPLEXES WITH STOICHIOMETRIES OTHER THAN 1:1

There are a few examples about the molecular discrimination systems with stoichiometries other than 1:1. As mentioned above, the definition of ζ_{G} and ζ_{H} can also be used to discuss the systems with 1:2 and 2:1 stoichiometries, and so on.

For instance, it is reported that benzene can form 1:2 inclusion complexes with α - and β -CD, with K_{12} values of 97 ± 4 and $2270 \pm 30 \text{ dm}^6 \cdot \text{mol}^{-2}$, respectively.[56] The value of ζ_{H} 23.4 is much higher than the discrimination ability (K_{11} , benzene- α -CD, $31.6 \pm 0.1 \text{ dm}^3 \cdot \text{mol}^{-1}$, benzene- β -CD, $169 \pm 0.1 \text{ dm}^3 \cdot \text{mol}^{-1}$; ζ_{H} , 5.4) of benzene to the two CDs in forming 1:1 complexes,[56] implying that benzene seems to have a stronger ability to perform the molecular discrimination between α - and β -CD by means of forming complexes with a 1:2 stoichiometry.

Owing to small molecular volumes, 1-propanol and 1-butanol can form 1:1 and 1:2 inclusion complexes with β -CD. The values K_{11} and K_{12} of the two complexes are 5.0 ± 0.5 and $27.6 \pm 1.2 \text{ dm}^3 \cdot \text{mol}^{-1}$, 7.3 and $62 \text{ dm}^6 \cdot \text{mol}^{-2}$, respectively.[54] Although the value of ζ_{G} is up to 5.5 for 1:1 stoichiometry and 8.5 for 1:2 stoichiometry, these values of K in either of two stoichiometries are inappreciable.

Similarly with those molecules with small volumes, some bulky guests like sodium deoxycholate also can form 1:2 inclusion complexes with β -CD (K_{12} , $39 \pm 0.4 \times 10^3 \text{ dm}^6 \cdot \text{mol}^{-2}$) or its derivative 6-deoxy-6-amino- β -CD (K_{12} , $49.1 \pm 0.1 \times 10^3 \text{ dm}^6 \cdot \text{mol}^{-2}$).[55] A quite low value of ζ_{H} 1.3 mean that sodium deoxycholate cannot fully reflect the difference between an amino group and a hydroxyl group. But then sodium cholate only can form 1:1 complexes with CDs.[55]

β -CD can form both 1:1 and 2:1 inclusion complexes with some guests, such as a group of hydrocarbon derivatives ($C_xH_{2x+1}CO_2Na$, $x = 11$ and 13) and a family of perfluorocarbon derivatives ($C_xF_{2x+1}CO_2Na$, $x = 7-9$). The K values increase with the increase of carbon chain length, regardless of stoichiometries. For example, the K values of $C_xH_{2x+1}CO_2Na-\beta$ -CD are $2.15 \pm 1.08 \times 10^2 \text{ mol}^{-2}\cdot\text{kg}^2$ for $x = 11$, and $3.00 \pm 1.50 \times 10^2 \text{ mol}^{-2}\cdot\text{kg}^2$ for $x = 13$, respectively. There is only a very low value of ζ_G 1.4. The K values of $C_xF_{2x+1}CO_2Na-\beta$ -CD, $x = 7-9$ are $1.20 \pm 0.6 \times 10^3$, $2.00 \pm 1.00 \times 10^3$ and $3.50 \pm 1.50 \times 10^3 \text{ mol}^{-2}\cdot\text{kg}^2$ respectively.[53] There is the highest value of ζ_G 2.92. Although the number of carbon atoms in each of the perfluorocarbon surfactants is fewer than that of hydrocarbon surfactants, the stabilities of the complexes of the perfluorocarbon surfactants, as well as the difference in stabilities, are considerably higher than those of the complexes of the hydrocarbon surfactants, indicating that the introduction of fluorine into the organic guests substantially improved the affinity and selectivity between host and guest simultaneously.

10. SEVERAL EXAMPLES ON THE APPLICATION OF MOLECULAR DISCRIMINATION PHENOMENA OF CDS TO A GROUP OF GUESTS IN MODERN CHEMISTRY

β -CD is most widely used in decades past because it is easily available. For instance, the derivatives of β -CD modified by silane analogs can be used to resolute a pair of enantiomers by means of chromatography.[146–149] The cyclam-capped β -CD-bonded silica particles were prepared and used as chiral stationary phases in capillary electrochromatography, exhibiting excellent enantioselectivity.[150]

There are many studies on selective catalysis in the presence of CDs and its derivatives in organic synthesis. [151,152] For instance, the addition of β -CD into the system of carboxylation reaction not only increases the yield of the reaction, but also improves the percent of *para* selectivity in forming *para*-carboxylated phenol from 55% to 99%.[153] This example indicates that β -CD appears to function as enzyme in a reaction of asymmetric synthesis. Additionally, CDs also have been applied in coordination catalysis and molecular assembly. For instance, the Monflier group has made a great progress in the synthesis of catalyst.[154–159] The acceleration in rate of isomerization of some organic compounds has been observed when β -CD is introduced into the reaction system of the compounds.[160]

To the best of our knowledge, considerable progress in enzyme-mimetic model compounds has been made by using exogenously applied compounds, it has been pointed out that artificial chemical treatments rarely mimic natural responses in quantitative terms,[161] It is well known that unique catalytic properties of enzyme owe to the ability of enzyme to form a stable complex with substrate. Compared with crown ether analogs, CDs and their derivatives have a more powerful ability to be solubilized in aqueous media due to many terminal polar hydroxyl groups, which is more close to *in vivo* conditions. In the present, the discrimination behaviors on the basis of CDs and their derivatives have been widely researched. Especially, the Inoue and Liu groups have done a lot of great work on many fields about it, such as the chiral discrimination for amino acids. Further, there are a few valuable reports on how, based on the frame of CDs, enzyme-mimetic models are constructed efficiently so far.[162–170] We believe that more and more reactions that cannot be

performed under common conditions will be performed in the presence of CDs or their derivatives.

11. CONCLUSION

The selective inclusion phenomena between CDs and guests are the foundation of the molecular discrimination behavior of a CD to a group of guests with similar structure. At present, the boundary between molecular discrimination for a host–guest system in supramolecular chemistry and molecular recognition for an enzyme–substrate system in nature, to a certain extent, is not clear. This, of course, poses some serious problems on the application of molecular recognition concept. As described in this paper, only a very high level (Level A) of molecular discrimination behaviors can be approximately regarded as an approach for molecular recognition phenomena in nature (see Figure 13). Nowadays, it is still difficult to achieve the level of biological recognition in current research of cyclodextrin chemistry. However, molecular discrimination behaviors of CDs to guests are one of the main concerns of is cyclodextrin chemistry, and many of them have been regarded as successful and exemplary examples of molecular recognition in supramolecular chemistry. Indeed, with a large number of tests, some of them will achieve or exceed the level of biological recognition in the future as the development of cyclodextrin chemistry.

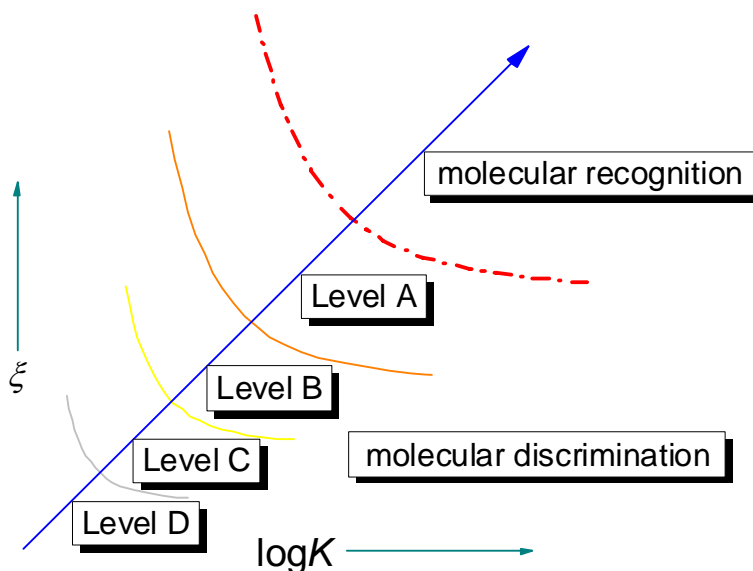


Figure 13. A schematic feature depicting the relationship between the molecular recognitions and the molecular discrimination levels A, B, C and D of the same CDs to different guests.

The molecular discrimination abilities between the same CD and analogous guests are divided into four levels according to the values of both K and ζ . ζ is not only a simple ratio of K values, but also an important physical quantity that has a decisive influence on the expression of discrimination level. The inclusion systems in Level B, only inferior to those of

Level A, indicate high discrimination abilities of CDs to selected guests. However, the systems in Levels C and D only indicate a weak inclusion phenomenon. It should be mentioned that, though direct observations from many modern physical methods, such as ^1H and ^{13}C nuclear magnetic resonance, circular dichroism, and spectrophotometric, chromatographic and fluorimetric methods, are important and significant to reveal the molecular discrimination behaviors between host and guest, the combination between values of K and ζ , determined based on the observations, is an important quantitative indicator to show the level of molecular discrimination. We believe that the method of categorizing host-guest complexes of CDs is useful in promoting the development of supramolecular chemistry, especially cyclodextrin chemistry.

REFERENCES

- [1] Zhang, X. X.; Bradshaw, J. S.; Izatt, R. M. *Chem. Rev.* 1997, 97, 3313–3361.
- [2] Wenz, G. *Angew. Chem. Int. Ed. Engl.* 1994, 33, 803–822.
- [3] Saenger, W. *Angew. Chem. Int. Ed. Engl.* 1980, 19, 344–362.
- [4] Rekharsky, M. V.; Inoue, Y. *Chem. Rev.* 1998, 98, 1875–1917.
- [5] Szejtli, J. *Chem. Rev.* 1998, 98, 1743–1753.
- [6] Spencer, J. N.; He, Q.; Ke, X. M.; Wu, Z. Q.; Fetter, E. *J. Sol. Chem.* 1998, 27, 1009–1019.
- [7] Song, L. X.; Wang, H. M.; Yang, Y.; Xu, P. *Bull. Chem. Soc. Jpn.* 2007, 80, 2185–2195.
- [8] Dong, H. Q.; Li, Y. Y.; Cai, S. J.; Zhuo, R. X.; Zhang, X. Z.; Liu, L. *J. Angew. Chem. Int. Ed.* 2008, 47, 5573–5576.
- [9] Tsutsumi, T.; Hirayama, F.; Uekama, K.; Arima, H. *J. Pharm. Sci.* 2008, 97, 3022–3034.
- [10] Choi, S. H.; Kim, S. Y.; Ryoo, J. J.; Lee, K. P. *J. Incl. Phenom. Macrocycl. Chem.* 2001, 40, 139–146.
- [11] Zhang, S. X.; Fan, M. G.; Liu, Y. Y.; Ma, Y.; Zhang, G. J.; Yao, J. N. *Langmuir* 2007, 23, 9443–9446.
- [12] Vaz de Melo Mattos, S.; Fernando Cappa de Oliveira, L.; Nascimento, A. A. M.; Peres Demicheli, C.; Dario Sinisterra, R. *Appl. Organometal. Chem.* 2000, 14, 507–513.
- [13] Liu, L. X.; Zhu, S. Y.; *Carbohydr. Polym.* 2007, 68, 472–476.
- [14] Galia, A.; Navarre, E. C.; Scialdone, O.; Ferreira, M.; Filardo, G.; Tilloy, S.; Monflier, E. *J. Phys. Chem. B* 2007, 111, 2573–2578.
- [15] He, L. H.; Huang, J.; Chen, Y. M.; Xu, X. J.; Liu, L. P. *Macromolecules* 2005, 38, 3845–3851.
- [16] Ren, L. X.; Ke, F. Y.; Chen, Y. M.; Liang, D. H.; Huang, J. *Macromolecules* 2008, 41, 5295–5300.
- [17] Jiao, H.; Goh, S. H.; Valiyaveetil, S. *Macromolecules* 2002, 35, 3997–4002.
- [18] Liu, Y.; Han, B. H.; Sun, S. X.; Wada, T.; Inoue, Y. *J. Org. Chem.* 1999, 64, 1487–1493.

- [19] Inoue, Y.; Hakushi, T.; Liu, Y.; Tong, L. H.; Shen, B. J.; Jin, D. S. *J. Am. Chem. Soc.* 1993, *115*, 475–481.
- [20] Liu, Y.; Chen, G. S.; Li, L.; Zhang, H. Y.; Cao, D. X.; Yuan, Y. J. *J. Med. Chem.* 2003, *46*, 4634–4637.
- [21] Park, J. W.; Lee, S. Y. *J. Incl. Phenom. Macrocycl. Chem.* 2003, *47*, 143–148.
- [22] Lee, Y. H.; Lin, T. *Electrophoresis* 1996, *17*, 333–340.
- [23] Kodama, S.; Yamamoto, A.; Sato, A.; Suzuki, K.; Yamashita, T.; Kemmei, T.; Taga, A.; Hayakawa, K. *J. Agric. Food Chem.* 2007, *55*, 6547–6552.
- [24] Yamamura, H.; Rekharsky, M. V.; Ishihara, Y.; Kawai, M.; Inoue, Y. *J. Am. Chem. Soc.* 2004, *126*, 14224–14233.
- [25] Villalonga, R.; Cao, R.; Fragoso, A. *Chem. Rev.* 2007, *107*, 3088–3116.
- [26] Yamasaki, H.; Makihata, Y.; Fukunaga, K. *J. Chem. Technol. Biot.* 2008, *83*, 991–997.
- [27] Scriba, G. K. E. *J. Sep. Sci.* 2008, *31*, 1991–2011.
- [28] Davis, M. E.; Brewster, M. E. *Nat. Rev. Drug. Discov.* 2004, *3*, 1023–1035.
- [29] Burgos, A. E.; Belchior, J. C.; Sinisterra, R. D. *Biomaterials* 2002, *23*, 2519–2526.
- [30] Wang, B.; He, J.; Sun, D. H.; Zhang, R.; Han, B. X. *J. Incl. Phenom. Macrocycl. Chem.* 2006, *55*, 37–40.
- [31] Anselmi, C.; Centini, M.; Maggiore, M.; Gaggelli, N.; Andreassi, M.; Buonocore, A.; Beretta, G.; Maffei Facino, R. *J. Pharm. Biomed. Anal.* 2008, *46*, 645–652.
- [32] Binkowski-Machut, C.; Canipelle, M.; Bricout, H.; Tilloy, S.; Hapiot, F.; Monflier, E. *Eur. J. Inorg. Chem.* 2006, 1611–1619.
- [33] Sueur, B.; Leclercq, L.; Sauthier, M.; Castanet, Y.; Mortreux, A.; Bricout, H.; Tilloy, S.; Monflier, E. *Chem. Eur. J.* 2005, *11*, 6228–6236.
- [34] Cassez, A.; Ponchel, A.; Hapiot, F.; Monflier, E. *Org. Lett.* 2006, *8*, 4823–4826.
- [35] Xu, P.; Song, L. X. *Acta Phys. Chim. Sin.* 2008, *24*, 727–734.
- [36] Song, L. X.; Bai, L.; Xu, X. M.; He, J.; Pan, S. Z. *Coord. Chem. Rev.* 2009, *253*, 1276–1284.
- [37] Lehn, J. M. *Angew. Chem. Int. Ed. Engl.* 1988, *27*, 89–112.
- [38] Wei, Y.; Huan, H.; Dale, G. D. *Angew. Chem. Int. Ed.* 2001, *113*, 1764–1768.
- [39] Yang, Y.; Shuang, S. H.; Chao, J. B.; Zhang, G. M.; Ding, H. Y.; Dong, C. *Acta. Chim. Sin.* 2004, *62*, 176–181.
- [40] Zhao, Y.; Yang, Z. M.; Zhu, H. Y.; Gu, J.; Wang, Y. F. *Acta Phys. Chim. Sin.* 2007, *23*, 394–398.
- [41] Wang, H. M.; Song, L. X.; Teng, C. F.; Bai, L. *Chin. J. Inorg. Chem.* 2008, *24*, 1–9.
- [42] Wang, Z. H.; Wang, Y. M.; Luo, G. *Analyst* 2002, *127*, 1353–1358.
- [43] Callari, F.; Petralia, S.; Sortino, S.; *Chem. Commun.* 2006, 1009–1011.
- [44] Bardelang, D.; Rockenbauer, A.; Karoui, H.; Finet, J. P.; Biskupska, I.; Banaszak, K.; Tordo, P. *Org. Biomol. Chem.* 2006, *4*, 2874–2882.
- [45] Lu, R. Yang, H.; C.; Cao, Y. J.; Wang, Z. Z.; Wada, T.; Jiao, W.; Mori, T.; Inoue, Y. *Chem. Commun.* 2008, 374–376.
- [46] Pham, D. T.; Clements, P.; Easton, C. J.; Papageorgiou, J.; May, B. L.; Lincoln, S. F. *New J. Chem.* 2008, *32*, 712–718.
- [47] B. Y.; Xia, W. S.; Cai, X. G.; Shao, Q. X.; Guo, B.; Maigret, Z. X. Pan, *J. Mol. Struct. (Theochem.)* 2001, *546*, 33–38.
- [48] Liu, L.; Li, X. S.; Mu, T. W.; Guo, Q. X.; Liu, Y. C. *J. Incl. Phenom. Macrocycl. Chem.* 2000, *38*, 199–206.

- [49] Chan, W. K.; Yu, W. Y.; Che, C. M.; Wong, M. K. *J. Org. Chem.* 2003, *68*, 6576–6582.
- [50] Buschmann, H. J.; Cleve, E.; Schollmeyer, E. *J. Incl. Phenom. Macrocycl. Chem.* 1999, *33*, 233–241.
- [51] Liu, Y.; Yang, Y. W.; Yang, E. C.; Guan, X. D. *J. Org. Chem.* 2004, *69*, 6590–6602.
- [52] Song, L. X.; Wang, H. M.; Guo, X. Q.; Bai, L. *J. Org. Chem.* 2008, *73*, 8305–8316.
- [53] Wilson, L. D.; Verrall, R. E. *J. Phys. Chem. B* 1997, *101*, 9270–9279.
- [54] Buvári, A.; Szejtli, J.; Barcza, L. *J. Incl. Phenom.* 1983, *1*, 151–157.
- [55] Ramos Cabrer, P.; Alvarez-Parrilla, E.; Meijide, F.; Seijas, J. A.; Rodriguez Nunez, E.; Vazquez Tato, J. *Langmuir* 1999, *15*, 5489–5495.
- [56] Tucker, E. E.; Christian, S. D. *J. Am. Chem. Soc.* 1984, *106*, 1942–1945.
- [57] Liu, L.; Guo, Q. X. *Chem. Rev.* 2001, *101*, 673–695.
- [58] Liu, L.; Guo, Q. X. *J. Chem. Inf. Comput. Sci.* 1999, *39*, 133–138.
- [59] Guo, Q. X.; Liu, L.; Cai, W. S.; Jiang, Y.; Liu, Y. C. *Chem. Phys. Lett.* 1998, *290*, 514–518.
- [60] Liu, L.; Song, K. S.; Li, X. S.; Guo, Q. X. *J. Incl. Phenom. Macrocycl. Chem.* 2001, *40*, 35–39.
- [61] Miyake, K.; Irie, T.; Arima, H.; Hirayama, F.; Uekama, K.; Hirano, M.; Okamoto, Y. *Int. J. Pharm.* 1999, *179*, 237–245.
- [62] Schneiderman, E.; Stalcup, A. M. *J. Incl. Phenom. Macrocycl. Chem.* 2002, *43*, 37–42.
- [63] Lu, Z. D.; Lu, C. G.; Meng, Q. J. *J. Incl. Phenom. Macrocycl. Chem.* 2008, *61*, 101–106.
- [64] Liu, Y.; You, C. C.; Zhang, Y. H. *Supramolecular Chemistry, Molecular Recognition and Assembly of Synthetic Receptor*; Nankai University Publishers: Tianjin, 2000.
- [65] Harata, K. *Chem. Rev.* 1998, *98*, 1803–1827.
- [66] Fischer, E. *Ber. Dtsch. Chem. Ges.* 1894, *27*, 2985–2993.
- [67] Koshland, D. E. Jr. *Proc. Natl. Acad. Sci. USA.* 1958, *44*, 98–104.
- [68] Gelb, R. I.; Schwartz, L. M.; Radeos, M.; Edomonds, R. B.; Laufer, D. A. *J. Am. Chem. Soc.* 1982, *104*, 6283–6288.
- [69] Matsui, Y.; Ono, M.; Tokunaga, S. *Bull. Chem. Soc. Jpn.* 1997, *70*, 535–541.
- [70] Yamashoji, Y.; Fujiwara, M.; Tanaka, M. *Chem. Lett.* 1993, 1029–1032.
- [71] Wenz, G.; Han, B. H.; Muller, A. *Chem. Rev.* 2006, *106*, 782–817.
- [72] Miyajima, K.; Komatsu, H.; Inoue, K.; Handa, T.; Nakagaki, M. *Bull. Chem. Soc. Jpn.* 1990, *63*, 6–10.
- [73] Yamashoji, Y.; Tanaka, M.; Shono, T. *Chem. Lett.* 1990, 945–948.
- [74] Matsui, Y.; Nishioka, T.; Fujita, T. *Top. Curr. Chem.* 1985, *128*, 61–89.
- [75] Liu, Y.; Yang, Y. W.; Zhao, Y.; Li, L.; Zhang, H. Y.; Kang, S. Z. *J. Incl. Phenom. Macrocycl. Chem.* 2003, *47*, 155–160.
- [76] Munoz de la Pena, A.; Zung, T.; Ndou, J. B.; Warner, I. M. *J. Phys. Chem.* 1991, *95*, 3330–3334.
- [77] Anderson, T.; Nilsson, K.; Sundahl, M.; Westman, G.; Wennerstrom, O. *J. Chem. Soc. Chem. Commun.* 1992, 604–606.
- [78] Yoshida, Z.; Takakuma, H.; Takakuma, S.; Matsubara, Y. *Angew. Chem. Int. Ed. Engl.* 1994, *33*, 1597–1599.
- [79] Sasaki, K.; Nagasaka, M.; Kuroda, Y. *Chem. Commun.* 2001, 2630–2631.

- [80] Ahmed, J.; Yamamoto, T.; Matsui, Y. *J. Incl. Phenom. Macrocycl. Chem.* 2000, 38, 267–276.
- [81] Bastos, M.; Briggner, L. E.; Shehatta, I.; Wadso, I. *J. Chem. Thermodyn.* 1990, 22, 1181–1190.
- [82] Gelb, R. I.; Schwartz, L. M. *J. Incl. Phenom. Mol. Recognit. Chem.* 1989, 7, 537–543.
- [83] Harada, A.; Takahashi, S. *J. Chem. Soc. Chem. Commun.* 1986, 1229–1230.
- [84] Isnin, R.; Salam, C.; Kaifer, A. E. *J. Org. Chem.* 1991, 56, 35–41.
- [85] Hapiot, F.; Tilloy, S.; Monflier, E. *Chem. Rev.* 2006, 106, 767–781.
- [86] Lu, C. S.; Zhang, W. W.; Ren, X. M.; Hu, C. J.; Zhu, H. Z.; Meng, Q. *J. Chem. Soc., Dalton Trans.* 2001, 3052–3055.
- [87] Braga, S. S.; Marques, M. P. M.; Sousa, J. B.; Pillinger, M.; Teixeira-Dias, J. J. C.; Goncalves, I. S. *J. Organomet. Chem.* 2005, 690, 2905–2912.
- [88] Fernandes, J. A.; Lima, S.; Braga, S. S.; Ribeiro-Claro, P.; Rodriguez-Borges, J. E.; Teixeira, C.; Pillinger, M.; Teixeira-Dias, J. J. C.; Goncalves, I. S. *J. Organomet. Chem.* 2005, 690, 4801–4808.
- [89] Marques, J.; Anjo, L.; Marques, M. P. M.; Santos, T. M.; Almeida Paz, F. A.; Braga, S. S. *J. Organomet. Chem.* 2008, 693, 3021–3028.
- [90] Ferreira, P.; Goncalves, I. S.; Pillinger, M.; Rocha, J.; Santos, P.; Teixeira-Dias, J. J. C. *Organometallics* 2000, 19, 1455–1457.
- [91] Braga, S. S.; Goncalves, I. S.; Pillinger, M.; Ribeiro-Claro, P.; Teixeira-Dias, J. J. C. *J. Organomet. Chem.* 2001, 632, 11–16.
- [92] Braga, S. S.; Gago, S.; Seixas, J. D.; Valente, A. A.; Pillinger, M.; Santos, T. M.; Goncalves, I. S.; Romao, C. C. *Inorg. Chim. Acta* 2006, 359, 4757–4764.
- [93] Petrovski, Ž.; Norton de Matos, M. R. P.; Braga, S. S.; Pereira, C. C. L.; Matos, M. L.; Goncalves, I. S.; Pillinger, M.; Alves, P. M.; Romao, C. C. *J. Organomet. Chem.* 2008, 693, 675–684.
- [94] Braga, S. S.; Goncalves, I. S.; Lopes, A. D.; Pillinger, M.; Rocha, J.; Romao, C. C.; Teixeira-Dias, J. J. C. *J. Chem. Soc. Dalton Trans.* 2000, 2964–2968.
- [95] Klingert, B.; Rihs, G. *Organometallics* 1990, 9, 1135–1141.
- [96] Okumura, Y.; Ito, K. *Adv. Mater.* 2001, 13, 485–487.
- [97] Sakai, T.; Murayama, H.; Nagano, S.; Takeoka, Y.; Kidowaki, M.; Ito, K.; Seki, T. *Adv. Mater.* 2007, 19, 2023–2025.
- [98] Li, J.; Yang, C.; Li, H. Z.; Wang, X.; Goh, S. H.; Ding, J. L.; Wang, D. Y.; Leong, K. W. *Adv. Mater.* 2006, 18, 2969–2974.
- [99] Yui, N.; Ooya, T. *Chem. Eur. J.* 2006, 12, 6730–6737.
- [100] Rusa, C. C.; Wei, M.; Bullions, T. A.; Shuai, X.; Uvar, T.; Tonelli, A. E.; *Polym. Adv. Technol.* 2005, 16, 269–275.
- [101] Li, J.; Li, X.; Ni, X. P.; Wang, X.; Li, H. Z.; Leong, K. W. *Biomaterials* 2006, 27, 4132–4140.
- [102] Lu, J.; Mirau, P. A.; Tonelli, A. E. *Prog. Polym. Sci.* 2002, 27, 357–401.
- [103] Kidowaki, M.; Zhao, C. M.; Kataoka, T.; Ito, K. *Chem. Commun.* 2006, 4102–4103.
- [104] Mahammad, S.; G. Robert, W.; Khan, S. A. *Soft Matter* 2007, 3, 1185–1193.
- [105] Ionita, G.; Meltzer, V.; Pincu, E.; Chechik, V. *Org. Biomol. Chem.* 2007, 5, 1910–1914.
- [106] Araki, J.; Ito, K. *Soft Matter* 2007, 3, 1456–1473.
- [107] Karaky, K.; Brochon, C.; Schlatter, G.; Hadziioannou, G. *Soft Matter* 2008, 4, 1165–1168.

- [108] Li, J.; Ni, X. P.; Zhou, Z. H.; Leong, K. W. *J. Am. Chem. Soc.* 2003, *125*, 1788–1795.
- [109] Harada, A.; Kamachi, M. *Macromolecules* 1990, *23*, 2821–2823.
- [110] Harada, A.; Kamachi, M. *J. Chem. Soc. Chem. Commun.* 1990, 1322–1323.
- [111] Shuai, X. T.; Porbeni, F. E.; Wei, M.; Bullions, T.; Tonelli, A. E. *Macromolecules* 2002, *35*, 3778–3780.
- [112] Harada, A.; Nishiyama, T.; Kawaguchi, Y.; Okada, M.; Kamachi, M. *Macromolecules* 1997, *30*, 7115–7118.
- [113] Kawaguchi, Y.; Nishiyama, T.; Okada, M.; Kamachi, M.; Harada, A. *Macromolecules* 2000, *33*, 4472–4477.
- [114] Rekharsky, M. V.; Mayhew, M. P.; Goldberg, R. N.; Ross, P. D.; Yamashoji, Y.; Inoue, Y. *J. Phys. Chem. B* 1997, *101*, 87–100.
- [115] Castronuovo, G.; Elia, V.; Fessas, D.; Velleca, F.; Viscardi, G. *Carbohydr. Res.* 1996, *287*, 127–138.
- [116] Korpela, T. K.; Himanen, J. P. *J. Chromatogr.* 1984, *290*, 351–361.
- [117] Eftink, M. R.; Harrison, J. C. *Bioorg. Chem.* 1981, *10*, 388–398.
- [118] Guo, Q. X.; Zheng, X. Q.; Luo, S. H.; Liu, Y. C. *Chin. Chem. Lett.* 1996, *7*, 357–360.
- [119] Mohseni, R. M.; Hurtubise, R. J. *J. Chromatogr.* 1991, *537*, 61–71.
- [120] Wang, Y. H.; Zhang, H. M.; Liu, L.; Liang, Z. X.; Guo, Q. X.; Tung, C. H.; Inoue, Y.; Liu, Y. C. *J. Org. Chem.* 2002, *67*, 2429–2434.
- [121] Wagner, B.; Fitzpatrick, S. J. *J. Incl. Phenom. Macrocycl. Chem.* 2000, *38*, 467–478.
- [122] Fukuhara, G.; Mori, T.; Wada, T.; Inoue, Y. *J. Org. Chem.* 2006, *71*, 8233–8243.
- [123] Larsen, K. L.; Endo, T.; Ueda, H.; Zimmermann, W. *Carbohydr. Res.* 1998, *309*, 153–159.
- [124] Liu, Y.; You, C. C.; Wada, T.; Inoue, Y. *J. Org. Chem.* 1999, *64*, 3630–3634.
- [125] Liu, Y.; Yang, E. C.; Yang, Y. W.; Zhang, H. Y.; Fan, Z.; Ding, F.; Cao, R. *J. Org. Chem.* 2004, *69*, 173–180.
- [126] Song, L. X.; Wang, H. M.; Xu, P.; Yang, Y.; Zhang, Z. Q. *Chem. Pharm. Bull.* 2008, *56*, 468–474.
- [127] Yang, Y.; Song, L. X. *J. Incl. Phenom. Macrocycl. Chem.* 2005, *53*, 27–33.
- [128] Kopecky, F.; Kopecka, B.; Kaclik, P. *J. Incl. Phenom. Macrocycl. Chem.* 2001, *39*, 215–217.
- [129] Meier, M. M.; Luiz, M. T. B.; Farmer, P. J.; Szpoganicz, B. *J. Incl. Phenom. Macrocycl. Chem.* 2001, *40*, 291–295.
- [130] Kano, K.; Hasegawa, H. *J. Am. Chem. Soc.* 2001, *123*, 10616–10627.
- [131] Franchi, P.; Lucarini, M.; Mezzina, E.; Pedulli, G. F. *J. Am. Chem. Soc.* 2004, *126*, 4343–4354.
- [132] Kitae, T.; Nakayama, T.; Kano, K. *J. Chem. Soc., Perkin Trans. 2.* 1998, *2*, 207–212.
- [133] Song, L. X.; Zhang, L.; Guo, Z. J. *Chin. J. Inorg. Chem.* 2002, *18*, 897–901.
- [134] Ramaraj, R.; Kumar, V. M.; Raj, C. R.; Ganesan, V. *J. Incl. Phenom. Macrocycl. Chem.* 2001, *40*, 99–104.
- [135] Liu, Y.; Li, B.; You, C. C.; Wada, T.; Inoue, Y. *J. Org. Chem.* 2001, *66*, 225–232.
- [136] Buschmann, H. J.; Schollmeyer, E. *J. Incl. Phenom. Macrocycl. Chem.* 1997, *29*, 167–174.
- [137] Hembury, G.; Rekharsky, M.; Nakamura, A.; Inoue, Y. *Org. Lett.* 2000, *2*, 3257–3260.
- [138] Saito, Y.; Watanabe, K.; Hashizaki, K.; Taguchi, H.; Ogawa, N.; Sato, T.; Ueda, H. *J. Incl. Phenom. Macrocycl. Chem.* 2000, *38*, 445–452.

- [139] Garcia-Zubiri, I. X.; Gonzalez-Gaitano, G.; Isasi, J. R. *J. Incl. Phenom. Macrocycl. Chem.* 2007, *57*, 265–270.
- [140] Liu, Y.; Li, L.; Zhang, H. Y.; Song, Y. *J. Org. Chem.* 2003, *68*, 527–536.
- [141] Alvarez-Parrilla, E.; Rosa, L. A. D. L.; Torresrivras, F.; Rodrigo-Garcia, J.; Gonzalez-Aguilar, G. A. *J. Incl. Phenom. Macrocycl. Chem.* 2005, *53*, 121–129.
- [142] Zhao, Y. L.; Zhang, H. Y.; Wang, M.; Yu, H. M.; Yang, H.; Liu, Y. *J. Org. Chem.* 2006, *71*, 6010–6019.
- [143] Gao, X. M.; Zhang, Y. L.; Tong, L. H.; Ye, Y. H.; Ma, X. Y.; Liu, W. S.; Inoue, Y. *J. Incl. Phenom. Macrocycl. Chem.* 2001, *39*, 77–80.
- [144] Liu, Y.; Han, B. H.; Chen, Y. T. *J. Phys. Chem. B* 2002, *106*, 4678–4687.
- [145] Liu, Y.; Yang, Y. W.; Li, L.; Chen, Y. *Org. Biomol. Chem.* 2004, *2*, 1542–1548.
- [146] Song, L. X.; Meng, Q. J.; You, X. Z. *Acta. Chim. Sinica.* 1996, *54*, 777–782.
- [147] Levkin, P. A.; Levkina, A.; Schurig, V. *Anal. Chem.* 2006, *78*, 5143–5148.
- [148] Sun, P.; Krishnan, A.; Yadav, A.; Singh, S.; MacDonnell, F. M.; Armstrong, D. W. *Inorg. Chem.* 2007, *46*, 10312–10320.
- [149] Gong, Y. H.; Lee, H. K. *Anal. Chem.* 2003, *75*, 1348–1354.
- [150] Campos, I. B.; Brochsztain, S. *J. Incl. Phenom. Macrocycl. Chem.* 2002, *44*, 207–211.
- [151] Bhosale, S. V.; Bhosale, S. V. *Mini-Rev. Org. Chem.* 2007, *4*, 231–242.
- [152] Narender, M.; Reddy, M. S.; Kumer, V. P.; Reddy, V. P.; Nageswar, Y. V. D.; Rao, K. R. *J. Org. Chem.* 2007, *72*, 1849–1851.
- [153] Komiyama, M.; Hirai, H. *J. Am. Chem. Soc.* 1984, *106*, 174–178.
- [154] Cabou, J.; Bricout, H.; Hapiot, F.; Monflier, E. *Catal. Commun.* 2004, *5*, 265–270.
- [155] Torque, C.; Bricout, H.; Hapiot, F.; Monflier, E. *Tetrahedron* 2004, *60*, 6487–6493.
- [156] Torque, C.; Sueur, B.; Cabou, J.; Bricout, H.; Hapiot, F.; Monflier, E. *Tetrahedron* 2005, *61*, 4811–4817.
- [157] Travers, C.; Essayem, N.; Delage, M.; Quelen, S. *Catal. Today* 2001, *65*, 355–361.
- [158] Lacroix, T.; Bricout, H.; Tilloy, S.; Monflier, E. *Eur. J. Org. Chem.* 1999, 3127–3129.
- [159] Kirschner, D.; Green, T.; Hapiot, F.; Tilloy, S.; Leclercq, L.; Bricout, H.; Monflier, E. *Adv. Synth. Catal.* 2006, *348*, 379–386.
- [160] Yamauchi, K.; Takashima, Y.; Hashidzume, A.; Yamaguchi, H.; Harada, A. *J. Am. Chem. Soc.* 2008, *130*, 5024–5025.
- [161] Heil M.; Baldwin, I. T. *Trends. Plant. Sci.* 2002, *7*, 61–67.
- [162] Breslow, R.; Doherty, J.; Guillot, G.; Lipsey, C. *J. Am. Chem. Soc.* 1978, *100*, 3227–3229.
- [163] Katakya, R.; Morgan, E. *Biosens. Bioelectron.* 2003, *18*, 1407–1417.
- [164] Fan, Z.; Diao, C. H.; Song, H. B. *J. Org. Chem.* 2006, *71*, 1244–1246.
- [165] Shen, J. R.; Lei, Z. L.; Ding, Z. G. *Anal. Lett.* 2007, *40*, 1622–1631.
- [166] Zhang, B. L.; Breslow, R. *J. Am. Chem. Soc.* 1997, *119*, 1676–1681.
- [167] Iglesias, E. *J. Am. Chem. Soc.* 1998, *120*, 13057–13069.
- [168] Milovic, N. M.; Badjic, J. D.; Kostic, N. M. *J. Am. Chem. Soc.* 2004, *126*, 696–697.
- [169] Ortega-Caballero, F.; Rousseau, C.; Christensen, B.; Petersen, T. E.; Bols, M. *J. Am. Chem. Soc.* 2005, *127*, 3238–3239.
- [170] Fang, Z.; Breslow, R. *Bioorg. Med. Chem. Lett.* 2005, *15* 5463–5466.

Chapter 4

MACROCYCLIC GLYCOPEPTIDE-BASED CHIRAL STATIONARY PHASES IN HIGH PERFORMANCE LIQUID CHROMATOGRAPHIC ANALYSIS OF AMINO ACID ENANTIOMERS AND RELATED ANALOGS

I. Ilisz, Z. Pataj and A. Péter

Department of Inorganic and Analytical Chemistry, University of Szeged,
H-6720 Szeged, Dóm tér 7, Hungary.

ABSTRACT

The past 20 years has seen an explosive growth in the field of chirality, as illustrated by the rapid progress in the various facets of this intriguing field. The impetus for advances in chiral separation has been highest in the past decade and this still continues to be an area of high focus. This paper reviews direct separations of amino acid enantiomers and related analogs using macrocyclic glycopeptide-based high performance liquid chromatographic methods, focusing on the literature published in the last decade.

Keywords: Chirality, enantiomers, amino acids, high-performance liquid chromatography, chiral stationary phases, macrocyclic antibiotics, glycopeptides.

1. INTRODUCTION

The phenomenon of optical isomerism has been known for many years and the importance of chirality with respect to biological activity is nowadays clearly recognized. Chirality exists throughout the universe and plays a vital role in our lives. It is well known that the L and D forms of amino acids in peptides can differ significantly with respect to stability and biological activity. Evaluation of the degree to which racemization occurs in the peptides produced is regularly required. Aspects of chirality are also very important in the

environment, and particularly in the pharmaceutical, food and beverages, agrochemical and petrochemical industries.

Initially chiral analyses were relatively difficult and most separations were carried out with derivatization prior to analysis. The main methodologies utilized for enantioseparation nowadays are enzymatic degradation, crystallization, membrane-based, spectroscopic, capillary electrophoretic (CE) and chromatographic methods. In chromatographic methods, two main strategies have evolved for chiral separation: *indirect methods*, based on the formation of diastereomers by the reactions of chiral compounds with a chiral derivatizing agent (CDA) and separation of the diastereomeric derivatives on an achiral stationary phase; and *direct methods*, based on the formation of diastereomers on a chiral stationary phase (CSP), or with a chiral selector in the mobile phase on an achiral stationary phase. Both approaches have their advantages and disadvantages.

The first CSP for gas chromatography was described in 1966 [1]. Davankov and Rogozhin [2] introduced chiral ligand-exchange chromatography (LEC) in 1971, and LEC became the first direct high-performance liquid chromatographic (HPLC) method for the resolution of amino acids. With increasing experience and knowledge and continuous development in the field, the chiral separation techniques have subsequently become a very sophisticated field of analytical chemistry. The number of CSPs now exceeds 200, and studies focusing on the development of new types of chiral selectors are published virtually daily. The most important classes currently applied are ligand exchangers, polysaccharides, cyclodextrins, crown ethers, proteins, antibiotics, and Pirkle-type CSPs.

In 1994 Armstrong *et al.* proposed the use of vancomycin in the separation of amino acid enantiomers [3] since the target of these antibiotics is the D-Ala-D-Ala group. The macrocyclic antibiotics have unique structural features and functionalities that allow various interactions (i.e. electrostatic, hydrophobic, H-bonding, steric repulsion, dipole stacking, π - π -interactions, etc.) between the analyte and the stationary phase. In the past decade, macrocyclic antibiotics have proved to be an exceptionally useful class of chiral selectors for the separation of enantiomers of biological and pharmacological importance by means of high-performance liquid chromatography, thin-layer chromatography and electrophoresis. The glycopeptides avoparcin, teicoplanin, ristocetin A and vancomycin have been extensively used as chiral selectors in the form of chiral bonded phases in HPLC, and HPLC stationary phases based on these glycopeptides have been commercialized. In the early stages of the application of macrocyclic antibiotics, Beesley and Scott [4] and Bojarski [5], and more recently Aboul-Enein *et al.* [6], Ward *et al.* [7], Dolezalova *et al.* [8], Dungalova *et al.* [9,10], Gasparrini *et al.* [11], Xiao and Armstrong [12], Beesley and Lee [13] and Ilisz *et al.* [14,15] have surveyed the application of macrocyclic antibiotics in different fields of chromatography.

This review sets out to characterize the physicochemical properties of these antibiotics and their application in the enantioseparations of amino acids and related analogs. The mechanism of separation, the sequence of elution of the stereoisomers and the relation to the absolute configuration are also discussed.

2. THE PHYSICOCHEMICAL PROPERTIES OF MACROCYCLIC ANTIBIOTICS

Macrocyclic antibiotics possess several characteristics that allow them to interact with analytes and serve as chiral selectors. There are hundreds of these compounds and, unlike other classes of chiral selectors, they comprise a large variety of structural types, including polyene-polyols, ansa compounds, glycopeptides, peptides, peptide-heterocycle conjugates, etc. In general, these compounds have molecular masses greater than 600, but less than 2200. There are acidic, basic and neutral types, and depending on chemical structure they may or may not display significant UV-Vis absorbance. The macrocyclic antibiotics used for chiral separations in HPLC include the ansamycins (rifamycins), the glycopeptides (avoparcin, teicoplanin, ristocetin A, vancomycin and their analogs), and the polypeptide antibiotic thiostrepton. Although not strictly considered to be macrocyclic antibiotics, the aminoglycosides (fradiomycin, kanamycin and streptomycin) have been used as chiral selectors in CE [16,17]. A number of the physicochemical properties of the most important macrocyclic antibiotics applied in HPLC enantioseparations are listed in Table 1.

2.1. The Ansamycins

The ansamycins are of historical significance in that they were the first chiral selectors used exclusively in CE prior to their use in HPLC [18]. Their physicochemical data are listed in Table 1. They have a characteristic ansa structure, consisting of a ring structure of a chromophore spanned by an aliphatic bridge. The ansamycins differ in the nature and position of substituents on their naphthohydroquinone ring (Figure 1). The ansamycins most commonly used in chiral HPLC separations are rifamycin B and rifamycin SV [19], but their importance as CSPs has declined.

2.2. The Glycopeptide Antibiotics

The macrocyclic glycopeptide antibiotics and its analogs, appear to be the most successful chiral selectors used to date. They include avoparcin, teicoplanin and its analogs, ristocetin A and vancomycin analogs.

Avoparcin is a macrocyclic glycopeptide antibiotic complex produced as a fermentation product by a strain of *Streptomyces candidus* (Table 1) [20]. Avoparcin exists in two major forms, α and β , differing only in the molecular mass of one chlorine versus one hydrogen atom of the aglycone rhamnoside (Figure 2). The molecular masses of α - and β -avoparcin are 1908 and 1943, respectively. The ratio of α - to β -avoparcin is 1:3 or 1:4 [20]. The aglycone portion of the avoparcin molecule contains three connected semi-rigid macrocyclic rings (one 12-membered and two 16-membered, which form a “pocket” suitable for analyte interactions in the reversed-phase mode (RPM). This glycopeptide antibiotic also contains seven aromatic rings with four phenolic moieties, five carbohydrate side-chains, 16 hydroxy groups, one carboxylic acid, two primary amines, one secondary amine, six amide linkages, two chlorine

atoms in β -avoparcin (only one in α -avoparcin), and 32 stereogenic centers. The primary amines are located on the carbohydrate side-chains, which are free to rotate. All these diverse functional groups provide a variety of possible interactions as mentioned above. Avoparcin was the fourth macrocyclic antibiotic evaluated as a CSP in HPLC.

Teicoplanin is produced by *Actinoplanes teichomyceticus* and is active against aerobic and anaerobic Gram-positive bacteria both *in vitro* and *in vivo* [21,22]. The aglycone consists of four fused macrocyclic rings which form a “semi-rigid basket” (Figure 3). It contains seven aromatic rings, two of which have chlorine-substituents and four of which are ionizable phenolic moieties. The aglycone contains a single primary amine which (together with the phenolic moieties) maintains its charge at the pHs normally used in HPLC (i.e. 3.5-8.0). Teicoplanin A₂₋₂ has three carbohydrate moieties consisting of D-glucosamine and D-mannose. The most unique feature of teicoplanin is that one glucosamine contains an *N*-acyl hydrocarbon chain. Consequently, teicoplanin is considerably more surface-active than other related glycopeptides. Teicoplanin is a mixture of five closely related analogs, designated T-A₂₋₁ through T-A₂₋₅ [21,23]. They differ by approximately 20 molecular mass units because of the variation in length (i.e. C₁₀-C₁₁) and substituent groups of the acyl side-chain attached to the amino sugar. Teicoplanin A₂₋₂ is the most common or abundant product produced.

The antibiotic A-40,926 is a complex of glycopeptides produced by the *Actinomadura* strain ATCC 39726, from which factors A and B are the major recoverable species [24-27]. The chemical structure of the prevalent component of the A-40,926 glycopeptide complex (factor B, >70%) is structurally related to teicoplanin A₂₋₂ (Figure 3). The five differences between the molecules are: (i) the β -D-*N*-acetylglucosamine unit of teicoplanin A₂₋₂ is not present in A-40,926 factor B; instead, there is a simple hydroxy group; (ii) the primary alcohol of the *N*-acylglucosamine unit of teicoplanin is oxidized to the carboxylic acid in A-40,926; (iii) the primary amine group on the aglycone portion of teicoplanin is a methyl-substituted secondary amine in A-40,926; (iv) the chlorine substituent on phenyl ring 2 in teicoplanin is not present in A-40,926, which in turn possesses a chlorine atom on its phenyl ring 3; (v) the nine-carbon chain of teicoplanin A₂₋₂ is replaced by an eleven-carbon chain in A-40,926 B₀ or a ten carbon chain in A-40,926 B₁. The first three structural differences listed above are the most important in terms of chiral recognition and enantioselectivity.

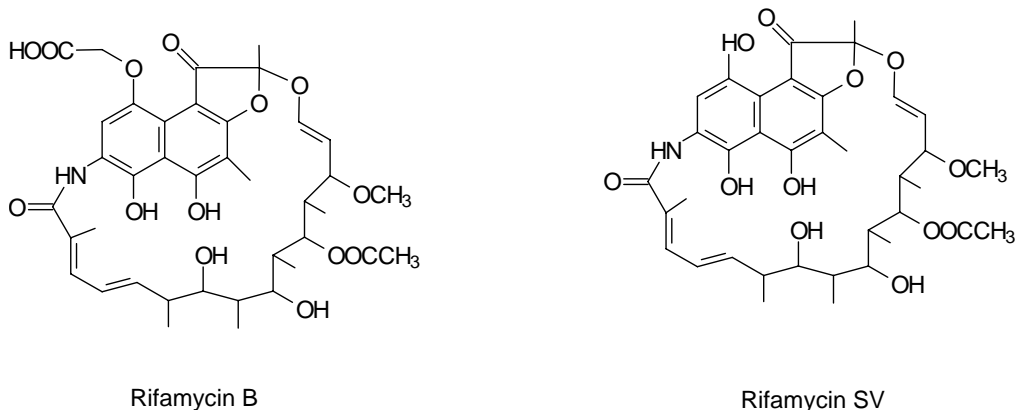


Figure 1.

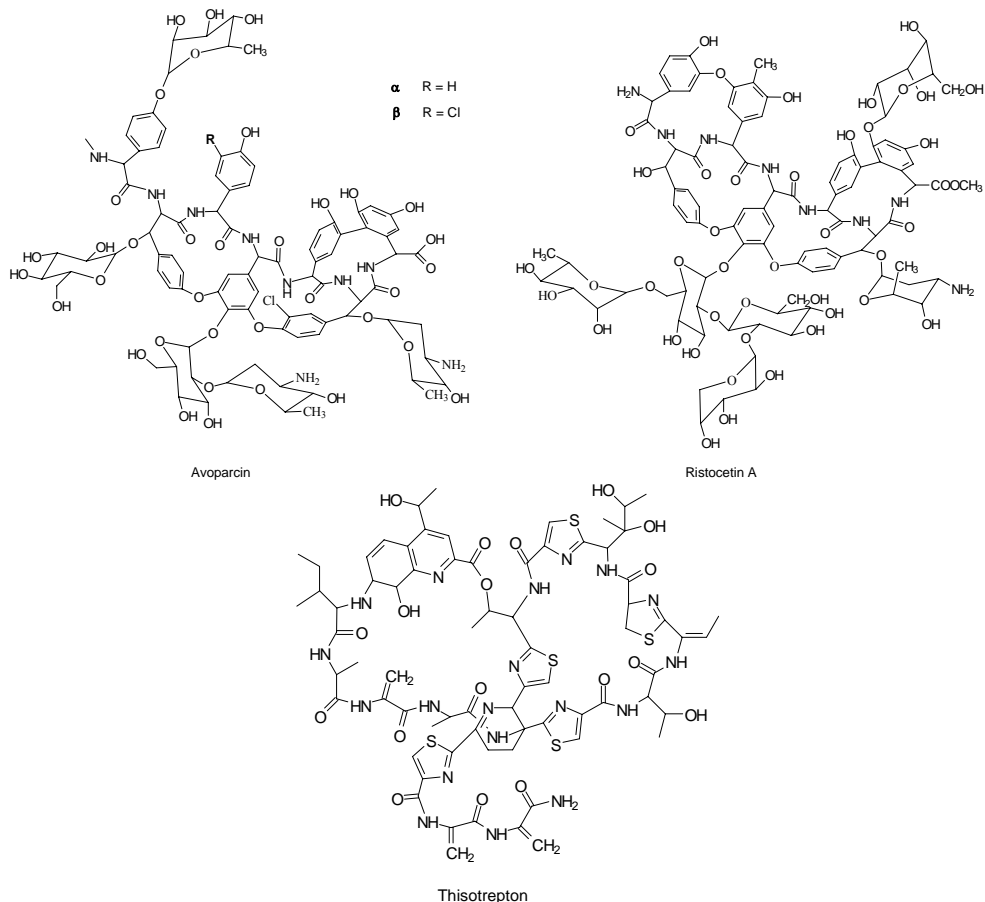


Figure 2.

A new CSP was recently prepared by reacting MDL 63,246, a glycopeptide antibiotic belonging in the teicoplanin family, with diol-silica particles [28,29]. The differences between the T-A₂₋₂ and MDL 63,246 molecules are (Figure 3): (i) the β -D-N-acetylglucosamine unit of teicoplanin A₂₋₂ is not present in MDL 63,246; instead, there is a simple hydroxy group; (ii) the primary amine group on the aglycone portion of teicoplanin is replaced by a methyl-substituted secondary amine in MDL 63,246; (iii) the anionic site ($-\text{COO}^-$) of the teicoplanin A₂₋₂ is replaced by a substituted amide, $-\text{NH}-(\text{CH}_2)_3-\text{N}(\text{CH}_3)_2$, (iv) substituents R₁ and R₃ (Cl and H) in T-A₂₋₂ are inverted in MDL 63,246; and (v) the hydrophobic chain in A₂₋₂ is one carbon atom shorter than that in MDL 63,246.

Antibiotic studies revealed that certain vancomycin derivatives with altered carbohydrate moieties killed bacteria by a mechanism differing from that for native vancomycin. In some cases, the carbohydrate units alone had antibiotic activity [30]. When these findings are transposed to the chiral recognition process, the question arises of the exact role of the sugar moieties in the highly efficient teicoplanin CSP. To answer this question and to investigate the role of the teicoplanin sugar units, the three carbohydrate units of the teicoplanin molecule were removed and the teicoplanin aglycone “basket” was isolated and used for the preparation of teicoplanin aglycone CSP [31]. The differences between the molecules are: (i) the β -D-N-acylglucosamine unit (with a nonyl chain) is not present in teicoplanin aglycone;

instead, there is a phenolic hydroxy group; (ii) the α -D-mannose unit is replaced by a phenolic hydroxy group; and (iii) the β -D-*N*-acetylglucosamine unit of teicoplanin A_{2.2} is replaced by a secondary alcoholic hydroxy group (Figure 3).

Ristocetin A is produced as a fermentation product of *Nocardia lurida*, and (like vancomycin and teicoplanin) is very active against Gram-positive bacteria [32]. *Nocardia lurida* produces a structurally similar compound, known as ristocetin B, differing in the number of carbons in one of the sugar moieties. Ristocetin A has a molecular mass of 2066, and consists of an aglycone portion with four joined macrocyclic rings (one twelve-membered, one fourteen-membered, and two sixteen-membered rings), to which several sugars (including arabinose, glucose, mannose and rhamnose) are covalently bonded (Figure 2) [33,34]. The molecule contains 38 stereogenic centers, seven aromatic rings, six amide linkages, twenty-one hydroxy groups, two primary amino groups, and one methyl ester. All these various functional groups are useful for chiral recognition through the interactions listed above.

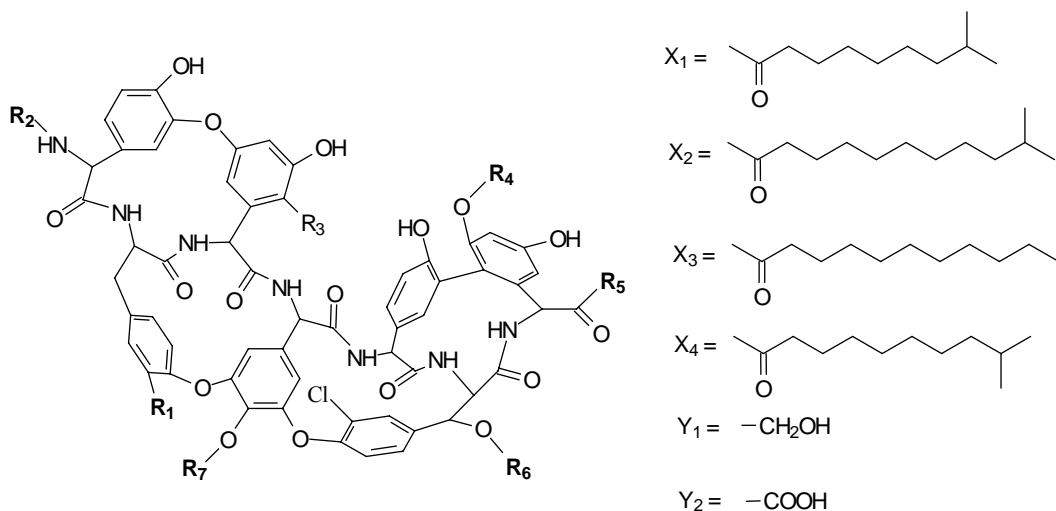
Vancomycin, rifamycin B and thiostrepton were the first macrocyclic antibiotics evaluated as CSPs in HPLC [19]. Vancomycin is an amphoteric glycopeptide produced by *Streptomyces orientalis* or *Amycolatopsis orientalis* and it exists as a mixture of similarly structured compounds (Figure 4) [35,36]. The potential impurities are therapeutically less active than the parent molecule vancomycin B. It has a molecular mass of 1449. There are three macrocyclic portions in the molecule, which also contains five aromatic rings. There are two side-chains, one of which is a carbohydrate dimer and the other an *N*-methylamino acid. Native vancomycin contains 18 stereogenic centers, nine hydroxy groups, two amine groups (one primary and one secondary), seven amido groups, and two chlorine moieties (substituents on two aromatic rings).

Norvancomycin, a new glycopeptide antibiotic, is produced by *Streptomyces orientalis* when the methyl group connected to the secondary amine nitrogen is lost (Figure 4), i.e. there is a leucine rather than *N*-methylleucine in the molecule of norvancomycin [37]. It has a molecular mass of 1435, the loss of the methyl group meaning that two primary amino groups are present [38].

Crystalline degradation products formed by the hydrolytic loss of ammonia from vancomycin (CDPM and CDPm [36]) have been covalently linked to silica gel and have been used for the enantioseparation of Trp and 4-hydroxyphenylglycine [39]. Berthod et al. [40] linked (*R*)- and (*S*)-naphthylethyl carbamate to six of the hydroxy groups of native vancomycin (not the phenolic hydroxy group), but this new phase proved to be less effective in enantioseparation of *N*-protected protein amino acids. Vancomycin has also been derivatized with 3,5-dimethylphenyl isocyanate and evaluated as a CSP [19]. Other vancomycin analogs (A35512B, A82846B, LY333328 and LY307599) were developed by Strege et al. [41] and Sharp et al. [42-44] and applied as chiral mobile phase additives (CMPAs) in narrow-bore HPLC, mainly in the enantioseparation of *N*-dansyl-blocked amino acids.

Table 1. Comparison of the physicochemical properties of macrocyclic antibiotics.

Characteristics	Ansamycins		Glycopeptides							Polypeptide
	Rifamycin B	Rifamycin SV	Avoparcin	Teicoplanin A _{2,2}	Teicoplanin A-40,926	Teicoplanin aglycone	Ristocetin A	Vancomycin	Nor- vancomycin	Thiostrepton
Molecular weight	755	698	α = 1908 β =1943	1877	B ₀ =1732 B ₁ =1718	1197	2066	1449	1435	1665
Number of stereogenic centers	9	9	32	23	B ₀ =19 B ₁ =18	8	38	18	18	17
Number of macrocycles	1	1	3	4	4	4	4	3	3	2
Number of aromatic rings	2	2	7	7	7	7	7	5	5	1
Number of sugar moieties	0	0	5	3	2	0	6	2	2	0
Hydrophobic tail	0	0	0	1	1	0	0	0	0	0
Number of hydroxy groups	4	5	16	14	11	7	21	9	9	5
Number of primary amines	0	0	2	1	0	1	2	1	2	0
Number of secondary amines	0	0	1	0	1	0	0	1	0	1
Number of amido groups	1	1	6	8	7	6	6	7	7	11
Number of carboxylic groups	1	0	1	1	2	1	0	1	1	0
Number of methoxy groups	1	1	0	0	0	0	0	0	0	0
Number of methyl esters	1	1	0	0	0	0	1	0	0	0
Produced by	<i>Nocardia mediterranei</i>	<i>Nocardia mediterranei</i>	<i>Streptomyces candidus</i>	<i>Actinoplanes teichomyceticus</i>	<i>Nonomuraea ATCC 39727</i>	<i>Chemically synthesized from Teicoplanin</i>	<i>Nocardia lurida</i>	<i>Streptomyces orientalis</i>	<i>Streptomyces orientalis</i>	<i>Streptomyces azureus</i>
References	[7]	[7]	[7]	[7, 23]	[14]	[14, 150]	[7, 23]	[7, 23]	[14]	[7]



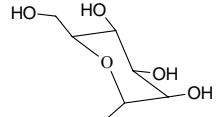
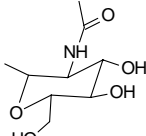
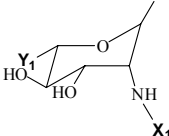
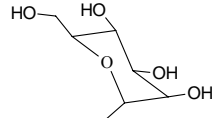
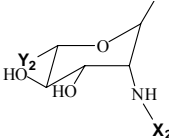
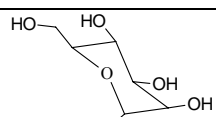
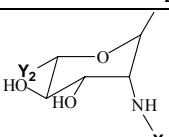
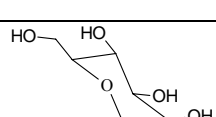
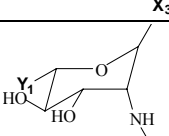
Compound	R ₁	R ₂	R ₃	R ₄	R ₅	R ₆	R ₇
Teicoplanin A ₂₋₂	Cl	H	H		-OH		
Teicoplanin A-40,926 B ₀	H	-CH ₃	Cl		-OH	H	
Teicoplanin A-40,926 B ₁	H	-CH ₃	Cl		-OH	H	
Teicoplanin MDL 63,246	H	-CH ₃	Cl		(CH ₃) ₂ N-(CH ₂) ₃ -NH-	H	
Teicoplanin aglycone	Cl	H	H	H	-OH	H	H

Figure 3.

The macrocyclic antibiotic chiral selectors actaplanin A [45] and D-(+)-tubocurarine chloride [46] have been applied in CE, and erythromycin [47] in TLC.

2.3. Polypeptide Antibiotics and Aminoglycosides

The macrocyclic polypeptide thiostrepton, with five thiazole rings and one quinoline ring, is produced by *Streptomyces azureus* [48] (Figure 2). It contains 17 stereogenic centers, five

hydroxy groups, ten amide linkages and one secondary amine [19]. Today, the application of thioestrepton as a CSP has significantly declined.

The aminoglycosidic antibiotics are not macrocycles, and are not of such great importance. Kanamycin sulfate is produced from the bacterium *Streptomyces kanamyceticus*, streptomycin is produced from *Streptomyces griseus* [49] and fradiomycin is produced from *Streptomyces fradiae* [50].

All macrocyclic antibiotic stationary phases are multimodal CSPs, i.e. they can be used in different modes: normal-phase mode (NPM), RPM, polar-organic mode (POM) or polar-ionic mode (PIM). The polar-organic or polar-ionic mobile phases are composed of a polar organic solvent such as acetonitrile (MeCN) with small amounts of acetic acid (AcOH) and triethylamine (TEA). A certain quantity of an organic solvent such as methanol (MeOH) is usually added to adjust the retention time. The ionization of the analyte can be controlled through protonation and deprotonation by varying the ratio of AcOH to TEA.

3. CHIRAL SEPARATION ON MACROCYCLIC GLYCOPEPTIDE CSPS WITH SOME MECHANISTIC CONCEPTS

3.1. Separation on Avoparcin CSP

The application of avoparcin as CSP [20] or CE additive [51] was evaluated for the enantiomeric separations of a variety of compounds of biological and pharmaceutical importance. Four important compounds, verapamil, thyroxine, mephentyoin and 2-imidazolidone-4-carboxylic acid, were baseline-resolved in the RPM only on the avoparcin CSP [20]. The major types of molecular interactions taking place in the RPM are probably (1) electrostatic (charge-charge) interactions between the analyte and one of the free amine groups of the avoparcin molecule, and (2) hydrophobic-driven inclusion between the analyte and the hydrophobic "pocket" formed by the macrocyclic rings in the aglycone portion of the avoparcin molecular complex. Other secondary interactions may involve steric effects and H-bonding associations [20]. In the RPM, the pH can also greatly affect retention, enantioselectivity and resolution. A pH decrease from 7.0 to 4.0 led to increased retention and enantioselectivity. The fact that different mobile phase modes give rise to the separations of different classes of enantiomeric compounds implies that different retention mechanisms are involved. In the POM, the major interactions believed to take place between the analyte and the avoparcin CSP are of H-bonding type. Secondary interactions are thought to involve electrostatic and steric forces. In the NPM, one expects to see the same/similar types of interactions as in the POM, with the addition of π - π interactions [20].

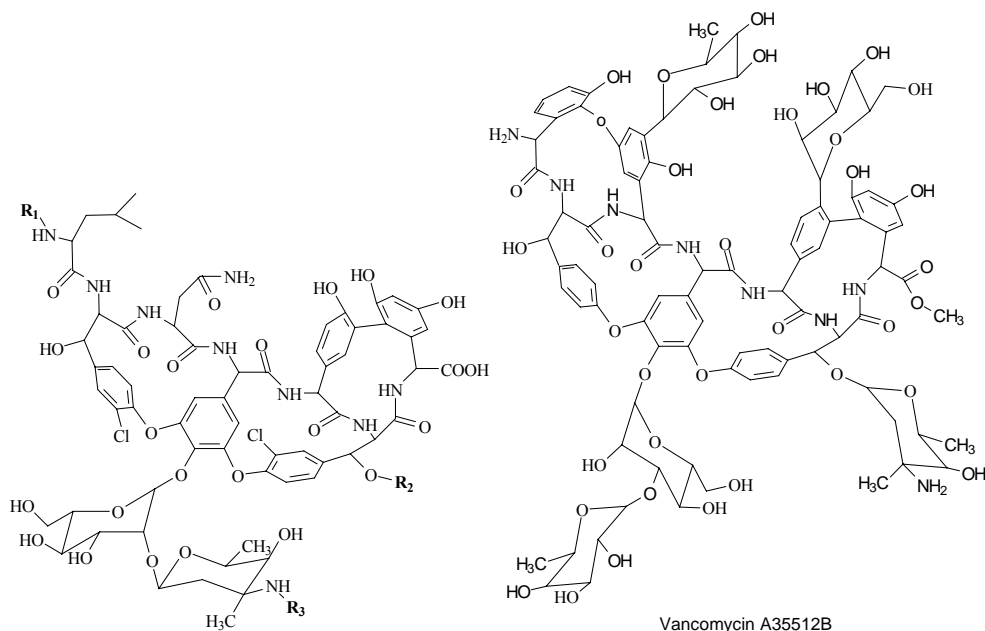
3.2. Separation on Teicoplanin and Teicoplanin-Related CSPS

Most of the investigations relating to separation mechanisms were carried out on T-A₂₋₂ and teicoplanin aglycone as CSPs. The first considerations were published by Armstrong *et al.* [22, 52]. It was presumed that the primary interaction is electrostatic in nature. There are two possibilities: the teicoplanin ammonium group can interact with the carboxylate group of

the amino acid, or the ammonium group of the amino acid with the teicoplanin carboxylate. It was established that dual electrostatic interactions can not occur. The distance between the amine and carboxylate group on the aglycone is ~ 12 Å. This distance and their relative positions on the aglycone would prevent their simultaneous ionic interactions with the corresponding groups of an amino acid. For chiral compounds with acid groups, the ammonium group of teicoplanin is the most available and logical site for the initial docking. A hydrophobic cleft on the aglycone is also available at or near that site, together with additional H-bonding and dipolar groups associated with the aglycone peptide bonds and the pendant sugar moieties. The secondary and tertiary structures of the teicoplanin molecule supply appropriate H-bonding, hydrophobic and steric interaction sites. Any factor hampering this interaction weakens the chiral recognition. The results of Armstrong *et al.* [22] indicate that the surface loading of the chiral selector also affects separation. A denser surface coverage of the selector could prevent deep penetration by steric means.

A similar separation mechanism was presumed by Péter *et al.* [53-58] from analyses of a number of unusual primary and secondary α - and β -amino acid enantiomers on T-A_{2,2} as CSP under different conditions. Most of the α -amino acid enantiomers exhibited excellent resolution, whereas no or only partial separation could be achieved for alicyclic β -amino acids. The retention factor versus organic modifier content curves in most cases exhibited a U-shaped character. The increase in retention factor with increasing water content was due to the increased hydrophobic interactions in the water-rich mobile phase, while the increase in retention factor with increasing MeOH content was due to the decreased solubility of the polar amino acids in the MeOH-rich mobile phase. From the temperature dependence and thermodynamic data obtained for the separation of different β -methyl-substituted amino acids, it was concluded that, besides charge-charge interactions, hydrophobic and in most cases steric interactions play important roles in enantio-recognition [54]. From enthalpy-entropy compensation data (compensation temperature), it was concluded that the two enantiomers are retained via similar mechanisms. Four years later, Carr *et al.* [59] showed that the only thing that can be concluded from the identical compensation temperature is that the relative contributions of enthalpy and entropy to the overall free energy in the processes are the same. Since it is possible that two processes occur via different mechanisms that, by chance, result in the same relative blends of enthalpy and entropy, the observation of identical compensation temperatures can not be used as evidence for mechanistic identity. If two processes exhibit different compensation temperatures, however, it can logically be concluded that the two processes are mechanistically distinct.

Chen [60,61] and Chen and Ward [62] applied a variety of electrophilic tagging agents (alkyl isothiocyanates, and nitro-, dinitro- and halobenzyl chlorides) to elucidate the chiral recognition sites on T-A_{2,2}. It was noted that: (i) chiral recognition on T-A_{2,2} was appreciably sensitive to size, indicating that the hydrophobic pocket of teicoplanin plays a significant role in chiral recognition in the POM; (ii) the resolution was sensitive to the size of the alkyl group present in the isothiocyanate reagent; the interaction between the isothiocyanate group and the chiral selector was important; (iii) resolution was enhanced due to relocation of the H-receptor site from sulfur to nitrogen on the isothiocyanate fragment of the derivatizing reagent, which in turn alters the selectivity; (iv) chiral recognition was more pronounced when the stereogenic center of the analyte was near the tagging moiety and surrounded by functional groups (*e.g.* carboxylic acid, *etc.*) which are favorable for H-bonding.



Compound	R ₁	R ₂	R ₃
Vancomycin	-CH ₃	H	H
Vancomycin A82846B	-CH ₃		H
Vancomycin LY307599	-CH ₃		
Vancomycin LY333328	-CH ₃		
Norvancomycin	H	H	H

Figure 4.

The study by Wu and Furlanut [63] demonstrated that H-binding plays an important role in the mechanism of the chiral separation of D,L-dopa and D,L-3-O-methyl-dopa on a T-A₂₋₂ column. Gasparri *et al.* [64] separated chiral mono- and dinuclear Ru(II) complexes on T-A₂₋₂ CSP. They concluded that the conformational homogeneity and the presence of a cleft-like cavity with an aromatic moiety available for π -stacking in the peptide backbone make the CSP capable of chiral recognition in a hydro-organic mobile phase.

Tesarova *et al.* [65,66] found that the chiral separation of β -adrenergic antagonists, profen non-steroidal anti-inflammatory drugs, chlorphenoxypropionic acid herbicides, *N-tert.*-butoxycarbonyl amino acids and their non-blocked analogs on T-A₂₋₂ is pH-dependent. It was postulated that the ionization of the functional groups of teicoplanin and the amino group of analytes play an important role in the stereoselective CSP-analyte interaction.

Schlauch *et al.* [67,68] investigated the influence of the mobile phase composition and pH on the enantioseparation of several cyclic β -substituted α -amino acids on T-A₂₋₂. It was demonstrated that the discrimination mechanism for the enantiomers and diastereomers (amino acids with two chiral centers) differed, probably in consequence of the different effects caused by the changes in the conformation of teicoplanin. The reproducibility depended strongly on the preconditioning of the column. Jandera *et al.* [69] reported that, on T-A₂₋₂, the concentration of MeOH or EtOH in the hydro-organic mobile phase and the pH of the mobile phase affected not only the retention, selectivity, saturation capacity and isotherm profile, but also the solubility of acids, which should be taken into account in preparative separations.

In recent years, a new teicoplanin-based CSP was introduced by the Armstrong group [31]: teicoplanin without sugar units, teicoplanin aglycone. From the aspect of chiral separation, the sugar moieties of the native teicoplanin may intervene in the chiral recognition process in at least three ways [31]: (i) steric hindrance, where the sugar units occupy space inside the “basket”, which limits the access of other molecules to the binding sites; (ii) the blocking of possible interaction sites on the aglycone, where two sugars are linked through phenolic hydroxy groups and the third sugar is linked through an alcohol moiety; and (iii) the offer of competing interaction sites, where the three sugars are themselves chiral and have hydroxy, ether and amido functional groups. Berthod *et al.* [31] separated amino acids and structurally related compounds on both T-A₂₋₂ and teicoplanin aglycone CSPs. On teicoplanin aglycone as selector, the retention factor in most cases decreased with increasing organic modifier content in the mobile phase, while on T-A₂₋₂ a U-shaped curve was generally obtained. It was concluded that sugar moieties hindered the chiral recognition, and that better resolutions were obtained for α -amino acids on teicoplanin aglycone than on T-A₂₋₂. They also concluded that sugar moieties can contribute significantly to the resolution of a number of enantiomeric pairs, such as bromacil, coumachlor, warfarin, carnitine, atenolol and pindolol.

Péter *et al.* [70,71] compared the separation efficiencies of T-A₂₋₂ and teicoplanin aglycone as CSPs for a series of unusual α - and β -amino acids. All the investigated α -amino acid enantiomers were separated on both selectors, but in most cases, similarly as observed by Berthod *et al.* [31], teicoplanin aglycone proved to be more efficient.

Enantioselective ion-exclusion separations were developed on teicoplanin aglycone CSP for *Dns*-protected protein amino acids by Steffeck and Zelechonok [72], who considered that the separation mechanism was due to the carboxylic acid group of teicoplanin aglycone, which can be partially ionized to exclude anionic analytes by ionic repulsion.

Xiao *et al.* [73] separated a wide variety of racemic analytes on T-A₂₋₂, teicoplanin aglycone and methylated teicoplanin aglycone in the RPM and POM. In both separation modes, improved separation efficiencies for acidic analytes were obtained on methylation of the H-bonding groups of teicoplanin aglycone. Ionic/dipolar interactions between the carboxylate groups of the analytes and the amine groups on T-A₂₋₂, teicoplanin aglycone and methylated teicoplanin aglycone are important for chiral discrimination. Hydrophobic interactions are important for enantiomeric separations in the RPM, where the H-bonding interactions between the analytes and the chiral selectors are relatively weak. Methylated teicoplanin aglycone offers higher hydrophobicity, which can accentuate the interactions of analytes with hydrophobic moieties, but these interactions are not necessarily stereoselective.

In the POM, electrostatic/dipolar interactions between polar functional groups are the predominant interactions in chiral recognition. Another important factor is the steric fit, which can be changed with every modification of the T-A_{2,2} structure.

D'Acquarica *et al.* [26] and Berthod *et al.* [27] evaluated a new teicoplanin-related macrocyclic glycopeptide selector, A-40,926, and applied it for separation of the enantiomers of amino acids, amino acid-related compounds, bromacil, terfenadine, verapamil, warfarin, carnitine, pindolol, norephedrine, *etc.* [27]. On both CSPs, *k'* changed in parallel with variation of the mobile phase composition and the elution sequence was the same. Comparison of the separation efficiencies of two CSPs, T-A_{2,2} and A-40,926, revealed that A-40,926 was complementary to T-A_{2,2} CSP, thereby enlarging the number of enantiomers that can be separated.

Shen *et al.* [74] compared the separation efficiencies of T-A_{2,2} and the phenyl isocyanate derivative of T-A_{2,2} in the separation of amino alcohols in the POM. The derivatized T-A_{2,2} CSP was not as efficient as the original T-A_{2,2} CSP. π - π and dipole-dipole interactions were believed to contribute to the retention on both CSPs, while H-bonding and steric interactions play important roles in chiral recognition.

Fanali *et al.* [28,29] introduced a teicoplanin analog, MDL 63,246 (Hepta-Tyr), for the enantioseparation of hydroxy acids in capillary LC. Good enantioresolution was achieved for most of the analytes, though long analysis times were required.

3.3. Separation on Ristocetin a CSP

The covalently bonded macrocyclic glycopeptide ristocetin A was first applied as a CSP for enantioseparation by Ekborg-Ott *et al.* [33]. All of the compounds resolved in the RPM were either anionic or neutral. The authors therefore concluded that the main molecular interactions taking place in the RPM are charge-charge (electrostatic between the analyte and the free amine group of ristocetin A) and hydrophobic associations of the analyte with the hydrophobic “cleft” or “pocket” of ristocetin A CSP. Secondary interactions undoubtedly involve H-bonding and steric effects. Although π - π interactions are possible, they are not likely to be as significant in the polar solvents used in the RPM. Clearly, π - π and H-bonding interactions are most important in the NPM, where nonpolar organic solvents are used as mobile phase. Conversely, the hydrophobic interactions that are essential in RPM must by definition be absent in NPM. In the POM, the main interactions are H-bonding, π - π , dipole stacking and steric interactions. Charge-charge interactions may be seen to some extent. The nature of the mobile phase solvents controls the interactions between the analyte and the CSP, thereby giving rise to different enantioselective mechanisms. It was demonstrated that the most important factor in the selectivity in the peptide separation was the stereochemistry of the carboxy terminal amino acids.

Various primary and secondary α -amino acid enantiomers were resolved on ristocetin A as selector by Péter *et al.* [57,58,75-77]. This selector proved as efficient as T-A_{2,2} in the separation of unusual primary and secondary α -amino acid enantiomers. From the temperature dependence of the retention of Trp analogs, 1,2,3,4-tetrahydroisoquinoline analog and γ -butyrolactone analog, and from the thermodynamic data, Péter *et al.* [77] concluded that in the RPM the main interactions are charge-charge, hydrophobic, H-bonding,

dipole stacking and steric interactions. In the NPM and POM, the lack of charge-charge and hydrophobic interactions resulted in shorter retention, but enantioselective retention was still possible due to H-bonding, dipolar and perhaps π - π interactions.

3.4. Separation on Vancomycin and Vancomycin Analog CSPs

In 1994, Armstrong *et al.* [19] separated 70 compounds, including amino acid enantiomers, as *Dns*, *Z* and *Bz* derivatives, β -blockers, lactones, *etc.*, on vancomycin or 3,5-dimethylphenyl-derivatized vancomycin as selector. Briefly, the retention behavior of organic analytes in RPM indicates the importance of hydrophobic interactions (hydrophobic inclusion complexes or merely an association with a hydrophobic cleft or pocket). H-bonding, dipole stacking, steric interactions and (in the NPM and POM) π - π complexation are also thought to be essential for chiral recognition. The selectivity of vancomycin for anionic compounds may be related to its amino groups.

The cornerstone work of Nair *et al.* [78] investigated the enantioselectivity of native vancomycin and the copper-vancomycin complex by using capillary electrophoresis. Since copper coordinates with the secondary amine (present on the aglycone basket), while the primary amine (present on the disaccharide side-chain) remains free, by comparing the enantioselectivities of native vancomycin and the copper-vancomycin complex, the authors concluded that the secondary amine of the *N*-methylleucine of vancomycin is a necessary interaction site for chiral recognition. The primary amine present on the disaccharide chain did not appear to be of primary importance.

Berthod *et al.* [40] demonstrated that *R*- or *S*-(naphthylethyl)carbamate (NEC) derivatization of vancomycin may block some useful sites on the vancomycin molecule. Moreover, *R*- and *S*-NEC are themselves chiral and can contribute additional interaction sites not available on native vancomycin. Tesarova *et al.* investigated the enantioseparation of different ergot alkaloids [79], promethazines [80] and β -blockers and profens [81] on vancomycin CSP. The main factors influencing the chromatographic behavior were the charge-charge (electrostatic) interactions, the size and polarity of the molecules, the π - π interactions and the vancomycin coverage on the silica. Vancomycin CSP was used in supercritical fluid chromatography by Donneck *et al.* [82]. The large differences in enantioselectivity on vancomycin in homologous series of local anesthetic compounds indicated that the fit of a host-guest interaction could be very precise. Nonlinear van't Hoff plots implied that the enantiomers of metoprolol and the modifiers evaporated from their absorption sites at different temperatures. Improved chiral selectivity was observed for numerous compounds when vancomycin was added to the mobile phase on a Chirobiotic V column [83]. A substantial increase in the difference in enthalpy of transfer, $\Delta\Delta H$, and in the difference in entropy of transfer, $\Delta\Delta S$, for two enantiomers was observed when vancomycin was used as both mobile phase additive and the chiral selector of the stationary phase. Ward *et al.* [84] used vancomycin dimers attached via covalent bonding, and native vancomycin whose dimers self-assemble in solution, to separate chiral amino acids. Significant differences in separation effectiveness were observed between the covalent dimers and the dimers of native vancomycin formed in the mobile phase.

The separation of barbiturates, piperidine-2,6-diones, and mephencytoin on vancomycin as chiral selector [85] showed that the substituents on the chiral carbon of the racemic drugs affect the chiral resolution. The ring size may also play a role as regards the formation of analyte-CSP inclusion complexes. In contrast with the piperidine-2,6-diones, the chromatographic parameters for the barbiturates are much the same under NPM and POM conditions. The separation of flurbiprofen and ketoprofen on vancomycin-based CSP revealed that these negatively charged acidic compounds interact electrostatically with the positively charged chiral selector [86]. In the separation of zolmitriptan on the vancomycin selector in POM, Zhang *et al.* [87] observed that the ionic interactions, H-bonding and steric interactions may play key roles together.

A novel norvancomycin-bonded CSP was applied by Ding *et al.* [38,88], who separated several *N-Dns*-amino acid enantiomers in the RPM. Both ionic and hydrophobic interactions were involved between the analyte and macrocycle in this chromatographic system. The process of enantioseparation for *Dns*-threonine was enthalpy-controlled at pH 3.5, while at pH 7.0 it was entropy-controlled according to the thermodynamic parameters $\Delta\Delta H^\circ$ and $\Delta\Delta S^\circ$ afforded by the van't Hoff plots. In the combination of vancomycin as mobile phase additive with the norvancomycin-CSP, noteworthy increases in enantioselectivity were observed for all the compounds, as a result of the synergistic effect, due to the presence of the vancomycin dimer.

The vancomycin analog A82846B provides excellent selectivity as a chiral recognition agent for some acidic test analytes in HPLC [89]. A82846B outperforms vancomycin as a chiral selector, probably due to the increased dimerization constant of over 100 in comparison with vancomycin. Dimerization of A82846B in solution is proposed as an explanation as to why A82846B gave enhanced separations for acidic racemates.

The crystalline degradation product (CDP) of vancomycin was applied as CSP by the Aboul-Enein group [39, 90-92] in the separation of different chiral compounds (*e.g.* amino acids, β -blockers and agrochemical toxins, haloxyfop-methyl, fenoxaprop-*p*-ethyl and indoxacarb). Chiral discrimination in the NPM and POM was due to the combination of attractive forces such as H-bonding, dipole-dipole interactions and π - π interactions between the enantiomers and the polar groups of the CDP-CSP.

The newly developed macrocyclic glycopeptide balhimycin was applied as CE additive by Schurig *et al.* [93-95]. Briefly, a glycopeptide dimerization-based mechanism was proposed to explain the enantioselectivity of balhimycin in CE.

Staroverov *et al.* [96-99] used eremomycin as chiral selector for the separation of α -amino-, α -hydroxy- and α -methylphenylcarboxylic acids (profens). The chromatographic retention of the enantiomers of amino acids is determined by the interplay of hydrophobic and ion-exchange interactions, H-bonds, and π - π and dipole-dipole interactions, and can be regulated by changing the composition of the mobile phase. From the pH dependence of the separation, it was established that the ion-exchange interactions between the analyte and eremomycin greatly affect the retention of the amino acid enantiomers, but they have little effect on the enantioselectivity of their separation, which reaches its maximum at the eluent pH close to the corresponding values of the isoelectric points of the amino acids. From the dependence of the MeOH concentration of the mobile phase, it was concluded that the ion-exchange interactions and the formation of H-bonds make the main contribution to the retention. Removal of the disaccharide residue from the eremomycin molecule increased the

enantioselectivity of separation of the racemates of the amino acids with aliphatic side-chains, decreased it for the cyclic amino acids, and led to the complete disappearance of enantioselectivity for aromatic amino acids. In aromatic amino acids, the absence of the disaccharide residue does not pose noticeable difficulties for the first-eluting enantiomer, and the retention increases 2- to 4-fold up to the retention of the second-eluting enantiomer.

3.5. Parallel Application of Macrocyclic Glycopeptide CSPs and Comparison of their Separation Efficiencies

Enantiomer separations by HPLC using the macrocyclic glycopeptides teicoplanin, teicoplanin aglycone, and ristocetin A CSPs were achieved on a racemic analog of dihydrofurocoumarin [100]. The teicoplanin CSP exhibited the broadest enantioselectivity. All three mobile phase modes, *i.e.* the NPM, RPM, and POM, were evaluated. The NPM proved most effective for the separation of chiral dihydrofurocoumarins on all CSPs tested. The structural characteristics of the analytes and steric effects are very important factors leading to chiral recognition. H-bonding was found to play a secondary role in chiral discrimination in the NPM and POM. Hydrophobic interactions are important for chiral separation in the RPM.

Separation of chiral sulfoxides by HPLC was carried out on T-A_{2,2}, teicoplanin aglycone, ristocetin A, vancomycin and vancomycin aglycone selectors [101]. The T-A_{2,2} and teicoplanin aglycone in the NPM and RPM were most effective. An important feature involved in the chiral recognition mechanism of sulfoxide compounds seems to be steric repulsion. It also appears that the intramolecular stacking of some of the larger chiral sulfoxides can greatly affect the enantioselectivity.

Macrocyclic glycopeptide CSPs containing T-A_{2,2}, ristocetin A or vancomycin have been evaluated in packed-column subcritical fluid chromatography for the separation of nonsteroidal anti-inflammatory compounds, β -blockers, sulfoxides and amino acids [102,103]. The Chirobiotic TAG CSP proved most effective, followed by the chirobiotic T column.

The separation of β -amino acid enantiomers seems to be more crucial than that of α -amino acids. Attempts to resolve β -amino acid enantiomers with different alkyl or aryl substituents on C2 were made by Péter *et al.* [53, 70,104-108] on T-A_{2,2}, teicoplanin aglycone and ristocetin A as selectors. In the RPM, better enantioselectivity was achieved on T-A_{2,2} than on ristocetin A. Change to the POM did not improve the separation efficiency. For alicyclic β -amino acid enantiomers, with a few exceptions, only partial separation was achieved on T-A_{2,2} and ristocetin A, but the separation efficiency of teicoplanin aglycone was demonstrated to be higher.

For the separation of aryloxypropanols T-A_{2,2} and teicoplanin aglycone selectors were applied by Lehotay *et al.* [109]. The highest resolution of aryloxypropanols was achieved on T-A_{2,2}. The interactions needed for chiral resolution involve charge-charge, H-bonding and steric interactions. Electrostatic interaction can substitute for H-bonding interaction in the POM. Aryloxyaminopropanol-based β -blockers were separated by Lehotay *et al.* [110-112] on T-A_{2,2}, teicoplanin aglycone, methylated teicoplanin aglycone and vancomycin selectors. For potential β -blockers of secondary amine type, the saccharide moieties on the selector play an

important role in the chiral recognition due to charge-charge and steric interactions [110,111], while the teicoplanin aglycone is responsible for the enantioseparation of morpholine-type potential β -blockers [112].

The enantioseparation of alkoxy-substituted analogs of phenylcarbamic acid was carried out by Lehotay *et al.* [113,114]. The mechanism of enantioseparation on T-A₂₋₂ and teicoplanin aglycone selectors involves charge-charge, H-bonding and steric interactions; the environment of the asymmetric carbon atom has a substantial influence on the efficiency of enantioseparation. From the temperature dependence and thermodynamic values of enantioseparation of alkoxy-substituted analogs of phenylcarbamic acid, it was concluded that both the change in enthalpy (ΔH_i) and entropy (ΔS_i) decreased with increasing length of the alkoxy chain on the benzene ring [115,116]. Both the enthalpy and entropy of this system and the number of carbon atoms in the alkoxy chain play important roles in chiral recognition. Enthalpy-entropy compensation plots revealed that all the compounds were separated via the same enthalpy-driven chiral recognition mechanism [116]. The work of Carr [59] indicated that the validity of enthalpy-entropy compensation does not automatically mean identity of the separation mechanisms for the two enantiomers.

The efficiencies of T-A₂₋₂, teicoplanin aglycone, methylated teicoplanin aglycone and vancomycin selectors in the separation of phenylcarbamic acid analogs at different temperatures have been investigated [117,118]. It was concluded that the change in enthalpy was most important when a teicoplanin-type selector was used, and the change in entropy was significant on the vancomycin selector. It appears that the number of carbon atoms in the alkoxy chain plays an important role. The enantioseparation of *Dns*-amino acids on T-A₂₋₂ and vancomycin CSPs confirms the presumed mechanism mentioned above [119].

From the results of thermodynamic studies of the enantioseparation of chiral sulfoxides on teicoplanin-based (T-A₂₋₂, teicoplanin aglycone, methylated teicoplanin aglycone) CSPs, it was concluded that energetic and steric interactions are most important in chiral recognition [120,121]. In the case of halogen sulfoxides, besides steric interactions, the energetic interactions probably have a predominant influence. This is related with the electronegativity of halogen atoms, increasing electronegativity inducing a positive dipole-dipole effect. The enantioseparations were enthalpically driven, but the extents of the enthalpy and entropy contributions differed for each CSP.

4. MECHANISTIC CONSIDERATIONS

Berthod *et al.* traced the possible interactions related to the retention and enantioselectivity of T-A₂₋₂-based CSP through two experiments with HPLC [122]. In one experiment, Cu²⁺ was added to the mobile phase to block the *N*-terminal amino group via complex formation. It was found that the enantioselectivity of the T-A₂₋₂-based CSP was decreased for the separations of most underivatized amino acids forming complexes with Cu²⁺. However, the complex formation had no significant effect on the separation of enantiomers other than those of amino acids. In a second experiment, an MeCN/D₂O mobile phase was used to evaluate the H-bonding interactions through isotopic exchange. It was found that the retention times of amino acids decreased; however, those of enantiomers without amino groups were increased. In all cases, deuterium exchange did not influence the

enantioselectivity of the CSP. It was proposed that the electrostatic interactions are decreased in the deuterated mobile phases and the solute-accessible stationary-phase volume is somewhat swollen by deuterium oxide. The balance of these effects is a decrease in the amino acid retention times and an increase in the polar solute retention times.

Cavazzini *et al.* [123] studied the mechanisms of chiral discrimination of amino acids and their *N*-acylated derivatives on T-A_{2,2}, and formulated some general conclusions: (i) the importance of the formation of the complex between the carboxylic moiety of the enantiomer and the aglycone basket; (ii) formation of a H-bond between the amidic hydrogen of the acylated analyte and an amidic group on the stationary phase is pivotal for the stability of the complex aglycone D-enantiomer; (iii) esterification leads to complete loss of the apparent enantioselectivity; (iv) one or both enantiomers can be excluded from the selector owing to ionic interactions between the CSP, the analytes and the surrounding medium and/or a steric hindrance effect; (v) selection appears better for MeOH as modifier than for MeCN as modifier.

Much work has been done in this field by Peyrin *et al.* [124-131] and Guillaume *et al.* [132-136]. Peyrin *et al.* [124-131] recently investigated the retention behavior of *Dns*-amino acid enantiomers and the enantioselective mechanism of T-A_{2,2} and vancomycin-based CSPs. On T-A_{2,2} CSP [124,125], it was concluded from the effects of the pH and the concentration of added citrate anion in the mobile phase and from the thermodynamic parameters that: (i) the solute retention is governed by the salting-out effect of the citrate anion; (ii) there is a competitive displacement of the *Dns*-amino acids from their teicoplanin binding site by the citrate anion; (iii) hydrophobic interactions and H-bond formation are important for chiral discrimination; and (iv) the chiral discrimination is essentially controlled by the interactions between the anionic form of the solute and the stationary phase. The main conclusions relating to the mechanisms of the separations on vancomycin CSP [126-128] are: (i) *Dns*-amino acids bind to the active aglycone pocket of the selector and this interaction is enantioselective; steric hindrance at the CSP aglycone pocket is responsible for the loss of chiral recognition for the largest molecules; (ii) thermodynamic analysis demonstrates that only the compounds which exhibit specific short-range interactions (H-bonding and van der Waals interactions) with the vancomycin selector are resolved on this CSP; (iii) the enantioselectivity is enthalpically or entropically driven; and (iv) with vancomycin as mobile phase additive, vancomycin dimerization enhances the enantioselectivity by a factor of 3.7 for D,L-*Dns*-Val enantiomers. The mechanism was also studied by use of displacement and perturbation techniques, thermodynamic investigations and the addition of NaClO₄ in the course of Trp binding to T-A_{2,2} and to teicoplanin aglycone [129-131]. The experimental data revealed that (i) the bi-Langmuir model is able to describe D- and L-enantiomer retention, similarly as observed by Jandera *et al.* [137]; (ii) the apparent selectivity increases on the addition of ClO₄⁻ to the mobile phase; (iii) this chiral recognition enhancement is governed by an increase in the difference in adsorption constant for the high-affinity aglycone pocket between the two enantiomers; (iv) there is an enhancement of the number of aglycone chiral regions interacting with D-Trp, suggesting that an ion-pair formation mechanism between ClO₄⁻ and the solute/or selector is responsible for this behavior; (v) sugar moieties on the CSP inhibit the contacts with the low-affinity binding regions on the aglycone; (vi) in the presence of sugar units on the CSP, the stereoselective properties for the high-affinity bonding pockets decrease; and (vii) the Grünwald model for enthalpy-entropy compensation demonstrates that

the enantioselective binding mode is dependent on an interface dehydration process. The changes observed in the enantioselective process between the aglycone and T-A₂₋₂ are characterized by the difference of *ca.* 2-3 ordered water molecules released from the species interface.

Guillame *et al.* [132,133] studied the chiral recognition mechanisms of *Dns*-amino acids on T-A₂₋₂ in the presence of the tension modifier sucrose, the chaotropic agent ClO₄⁻ and Na⁺ added to the mobile phase in the RPM. Thermodynamic studies and the enthalpy-entropy compensation data indicated that (i) the sucrose molecule acts only on the hydrophobic part of the teicoplanin/*Dns*-amino acid interaction and not on the specific chiral part; (ii) enhancement of the separation factor as the ClO₄⁻ concentration is increased is enthalpically controlled owing to stereoselective binding interactions; and (iii) from the number of Na⁺ excluded from the solute-teicoplanin interface when analyte transfer occurs, it is clear that the teicoplanin is balanced between two conformational states characterized by distinct enantioselective properties. From the dependences on the pH, the temperature and the MeOH concentration in the mobile phase in the enantioseparations of phenoxypropionic acid, Guillaume *et al.* [134-136] confirmed the earlier results: (i) chiral recognition was controlled by the interactions between the anionic form of the analyte and T-A₂₋₂, while those with the neutral form played only a minor role; (ii) the mechanism was described well by the bi-Langmuir model; (iii) enhancement of the separation factor with increasing MeOH content in the mobile phase was enthalpically controlled owing to stereoselective binding interactions; (iv) secondary sites with low affinity on the teicoplanin surface were involved in the process determining both the retention and the selectivity, were not affected by the temperature change and were not involved in the chiral recognition mechanism.

Seventy-one chiral compounds were separated on four macrocyclic glycopeptide chiral selectors: T-A₂₋₂, its aglycone, ristocetin A and vancomycin, using three possible separation modes: the RPM, NPM and PIM in the temperature range 5-45 °C [138]. All the van't Hoff plots were linear, indicating that the selector did not change in the temperature range studied. The calculated enthalpy and entropy variations showed that the interaction of the solute with the stationary phase was always enthalpy-driven with the NPM and RPM. It could be both enthalpy and entropy-driven with PIM mobile phases strongly dependent on the solute. The plots of $\Delta(\Delta H)$ vs. $\Delta(\Delta S)$ were in most cases linear (enthalpy-entropy compensation). This observation cannot be used to ascertain clear information on chiral recognition mechanisms, but it allows the identification of specific stationary phase-solute interactions because the points corresponding to the respective thermodynamic parameters were clearly delineated from the general compensation lines.

The linear solvation (free) energy relationship (LSER; LFER) is a general relationship linking analyte retention factors or partition coefficients to numerical measures of properties of the analyte, the mobile phase and the stationary phase [139]. One of the more widely accepted symbolic representations of the LSER model was proposed by Abraham [140] in the form:

$$\log k' = c + eE + sS + aA + bB + vV$$

in which k' is the solute retention factor. E , S , A , B and V are the solute descriptors independent of the mobile and/or the stationary phase used. E is the solute excess molar

refraction modeling the solute polarizability due to n - and/or π -electrons in excess of that of a comparable sized n -alkane, while S is the solute descriptor for the dipolar character and also polarizability of the molecule, A and B are the H-bond solute acidity (H-donor) and basicity (H-acceptor) descriptors, respectively, and V is the McGowan characteristic molecular volume calculated by using the solute structure.

c , e , s , a , b , and v are the system parameters or constants reflecting the difference in solute interactions between the mobile and stationary phases. The constant c is the intercept obtained in the regression calculation; it depends on the experimental system used (the nature of the organic modifier and the phase ratio) and not on the solute. The system parameter e indicates the tendency of the mobile and stationary phases to interact with the solute through π - or n -electron pairs; the parameter s is related to dipole- or induced dipole-type interactions; the system parameter a denotes the difference in H-bond basicity between the phases and the solute since an acidic solute (corresponding descriptor A) will interact with a basic stationary phase; the parameter b is a measure of the difference in H-bond acidity between phases and solute; and the system parameter v corresponds to the difference in cavity formation energy between the mobile and stationary phases [140,141].

Tesarova *et al.* [142,143] used three teicoplanin-based CSPs: T-A_{2,2}, teicoplanin aglycone and methylated teicoplanin aglycone. To examine the importance of various interaction types in the chiral recognition mechanism, the three related CSPs were evaluated and compared via an LSER. The retention factors of 19 widely different solutes, with known solvation parameters, were determined on each of the columns under the same mobile phase conditions. Statistically derived standardized regression coefficients were used to evaluate the contributions of the individual molecular interactions within one stationary phase. Although the LSER model does not address chiral aspects, the authors attempted to explore the importance of the individual interactions in the chiral discrimination of amino acids and their *N*-*tert*-butyloxycarbonyl derivatives. Intermolecular interactions of the hydrophobic type contribute significantly to retention on all the CSPs studied here. Hydrophobic interactions play a major role in the mobile phases at high buffer contents. The more hydrophobic the CSP, the more important these interactions are in the retention mechanism. With increase of the MeOH content in the mobile phase, the major role in the interaction mechanism is shifted to more polar forces in which basicity and dipolarity/polarizability predominate. Other retention-increasing factors are n - and π -electron interactions and dipole-dipole or dipole-induced dipole interactions, while H-donating or accepting interactions are more predominant with the mobile phase than with the stationary phase. However, these types of interactions are not equally significant for all the CSPs studied.

Five-parameter LSERs are known to have little or no shape-recognition ability. However, Armstrong *et al.* [144,145] recently proposed the use of LSER studies to acquire insight into chiral recognition mechanisms. Since two enantiomers with exactly the same five A - V solute descriptors are still separated by CSPs, it can be considered that they form two different transient diastereoisomers with the CSP. It is then possible to perform LSER studies on the enantiomer retention factor ratios. In the first step, the five a - v system parameters of four CSPs of macrocyclic glycopeptide type (T-A_{2,2}, teicoplanin aglycone, ristocetin A and vancomycin) were determined by using a set of test solutes with known A - V descriptors, in both the RPM and the NPM. In the second step, the A - V descriptors of 18 enantiomeric pairs were tentatively established through the use of five achiral columns with known a - v

parameters. This was successful only for the five molecular enantiomers. The predicted retention factor for the molecular enantiomers separated on a given CSP corresponded either to the retention factor of the first experimentally eluted enantiomer, or to that of the second one, or to neither. When the enantioselectivity factors were applied, it was possible to obtain the $\Delta\alpha - \Delta\nu$ parameters corresponding to the difference in CSP properties seen for the two enantiomers. For the five molecular enantiomeric pairs in the RPM with a T-A₂₋₂ CSP, there was an elevated contribution by the coefficient e , which the authors interpret as a possible interaction between surface charges on the T-A₂₋₂ CSP and solute-induced dipoles. Steric effect, seen on the parameter ν , are second in magnitude, followed by H-bond and polar interactions (coefficients b and s). Only one solute could be studied in the NPM, showing a different mechanism with polar and steric major interactions. It was concluded that the enantiorecognition mechanisms in the two modes were completely different for the same enantiomer separated on the same CSP. The results also showed that a particular interaction that may have a minor effect on the solute retention may be essential for solute enantiorecognition and *vica versa*.

It is important that the data measured under linear conditions give only a qualitative picture. Determination of the equilibrium adsorption isotherms furnishes more information [146]. The analysis of band profiles based on stochastic theory by Jandera *et al.* [137] revealed that the band broadening can be attributed to at least two additional chiral centers of adsorption in the CSP, contributing to the retention of the more strongly retained enantiomer in addition to the adsorption of the less retained one. Another conclusion relating to the adsorption sites was that the description of the distribution of the enantiomers on the basis of the bi-Langmuir model is probably oversimplified, in spite of the formally good fit of the experimental distribution data.

The chiral discrimination of phenoxypropionic acid herbicides by RP chromatography on a T-A₂₋₂ phase was reexamined by Andre and Guillaume [136], who used the perturbation method to calculate the solute distribution isotherms. The effects of both temperature and the MeOH content of the mobile phase on the chiral discrimination mechanism were well described by the bi-Langmuir model. The method confirmed a change in the mechanism of enantiomer retention at a critical temperature, T^* , and demonstrated that the mechanism was independent of the herbicide molecular structure, *i.e.* the position of the chloro group on the phenol ring, and the absolute configuration of the carbon atom. The enantioselectivity was enhanced by increasing the mobile phase MeOH content. Use of this approach revealed that secondary sites on the teicoplanin surface were involved in the processes determining both retention and selectivity. These secondary sites of low affinity were not affected by temperature change and were not involved in the chiral recognition mechanism.

Petrusevska *et al.* [147] separated racemic α -amino acids on a new CSP based on eremomycin. In order to evaluate the potential with respect to preparative separations, the adsorption isotherms of D- and L-methionine were determined for one mobile phase composition, the elution applied involving the characteristic point method. The isotherms were validated by comparing experimentally determined elution profiles with predictions based on the equilibrium dispersive model. Finally, the performance of the eremomycin CSP was compared with that of a commercially available CSP based on the T-A₂₋₂. After determination of the isotherms of D- and L-methionine for the T-A₂₋₂ phase, the equilibrium dispersive model was used for both CSPs to identify the optimal operating conditions. For the

separation and conditions considered, the new eremomycin CSP revealed a better performance relative to that of the teicoplanin CSP.

Modern CSPs are often combined with eluents comprising a mixture of organic solvents and polar additives. The latter may cause extreme deformations of the eluted enantiomer bands in both analytical and preparative separations. Arnell *et al.* [148] gave a theoretical background for these deformations. They separated the enantiomers of different β -blockers on T-A_{2,2} CSP in the presence of TEA/AcOH. It was found that TEA is strongly adsorbed on the T-A_{2,2} CSP for typical MeOH/MeCN/AcOH/TEA eluents. For different compositions, the β -blocker peaks had either Langmuirian or anti-Langmuirian shapes. It was possible to tune the peak shapes of the two enantiomers by varying the organic solvent composition (MeOH/MeCN ratio), probably because the initial slopes of the additive and solute adsorption isotherms display different polarity dependences. By changing this ratio, it was possible to tune the initial slope of the additive in relation to those of the β -blockers. A very interesting situation arose when the additive isotherm had a higher initial slope than that of the first-eluting enantiomer, but lower than that of the second enantiomer, and if the perturbation peak eluted before both enantiomer peaks. An advantageous situation occurs when the first-eluted peak is transformed to an anti-Langmuirian shape, while that of the second enantiomer maintains a normal Langmuirian shape. In this situation, the two peaks tail in opposite directions, with their sharp sides pointing closely toward each other. It is then possible to obtain baseline resolution at a higher load than when both enantiomer peaks tail in the same direction. Adsorption isotherm parameters were determined by using the inverse method; no other method could be used, due to the system complexity. Computer simulations based on these parameters agreed very well with the observed deformations.

The adsorption behavior of two amino acids, L,D-threonine and L,D-methionine, was studied by Poplewska [149] on a CSP column packed with T-A_{2,2}, under nonlinear adsorption isotherm conditions for various types of organic modifiers (MeOH, EtOH, propan-2-ol and MeCN) in the RPM. A heterogeneous adsorption mechanism of amino acids was identified that was strongly affected by the nature of the organic modifier. The isotherm nonlinearity and retention generally decreased with decrease of the modifier content in the mobile phase, exhibiting a minimum for water-rich mobile phases. These trends probably result from a combined effect of both the mobile and the adsorbed phase composition. To determine the composition of the adsorbed phase, the excess adsorption of the modifiers in aqueous solutions was measured and their binary adsorption equilibria were quantified and compared. Strongly nonideal behavior of solvents in the mobile phase and the adsorbed phase was accounted for by the activity coefficients. The fraction of the modifiers in the adsorbed phase decreased in the sequence MeOH > EtOH > propan-2-ol > MeCN.

According to the generally accepted three-point model, chiral recognition requires a minimum of three simultaneous interactions between the CSP and the model compound, where at least one of the interactions is stereochemically dependent. Transitory diastereomeric complexes formed on CSPs with different physical and chemical properties can be resolved during the separation procedure. Chiral recognition mechanisms differ from one CSP to another. Macrocyclic antibiotic-based CSPs have demonstrated broad selectivity in the RPM, NPM, POM and PIM [150]. Since CSPs may contain several ionizable groups, the enantioselectivity may be significantly different in each of these modes. The POM enhances solubilization and may be favored in the case of neutral analytes. Obviously,

changes in pH may affect the ionization state of both the analyte and the CSP. Compounds containing ionizable groups require the addition of small amounts of acid and/or base (PIM), *i.e.* the ionization state of the CSP should finally be tuned. The PIM enhances several interactions, especially ionic ones, and therefore several chiral separations can be achieved [150].

From the results relating to the possible chiral recognition mechanism, it can be concluded that there is no generally valid conception for the chiral recognition of racemic compounds on macrocyclic glycopeptide-based CSPs. There are probably several mechanisms and, besides electrostatic interactions, hydrophobic, H-bond, steric, dipole-dipole, *etc.* interactions can all contribute to the retention and chiral recognition, depending on the nature of the analyte and the mode of chromatography. Further efforts should be made to elucidate the real mechanism, which can help in the optimization of the separation of these types of analytes on macrocyclic antibiotic CSPs.

5. ELUTION SEQUENCE AND ABSOLUTE CONFIGURATION

Macrocyclic glycopeptides are very active against Gram-positive bacteria. They bind selectively to terminal D-Ala-D-Ala sequences in mucopeptides and thereby inhibit bacterial cell wall synthesis. Accordingly, the sequence L<D is to be expected in the course of separations. Berthod *et al.* [52], Ekborg-Ott *et al.* [33] and Schmid *et al.* [151] reported that, in agreement with this, D-terminated peptides were more retained than L-terminated ones. Moreover dipeptides and peptides with D-amino acids at the C-terminal exhibited higher retention. This means that peptides with a D-configuration at the carbon atom adjacent to the carboxyl group display the greater affinity for the CSP. In contrast, Zhang [152] found that all peptides exhibiting D-amino acid polymorphism eluted before the corresponding L-amino acid-containing peptides.

Following the introduction of macrocyclic glycopeptide CSPs, an appreciable length of time elapsed before any deviation from the expected sequence L<D was observed for amino acids. In 1998, Péter *et al.* [53] reported the reverse elution sequence, D<L, for the enantioseparation of *trans*-(1*S*,2*S* and 1*R*,2*R*)-2-amino-4-cyclohexene-1-carboxylic acid, and for *diexo*-cycloalkane- and alkeneaminocarboxylic acids on T-A_{2,2}. Other examples of the reverse elution sequence have since been published for α -amino acids on ristocetin A in the RPM [76], for β -amino acids in the POM [104] and also for β -amino acids on T-A_{2,2} and teicoplanin aglycone in both the RPM and the POM [105]. Schlauch *et al.* [67] similarly observed the reverse elution sequence for *cis*- and *trans*-1-amino-2-hydroxycyclohexanecarboxylic acids on T-A_{2,2}, as did Xiao *et al.* [153] for *Dns*- α -amino acids on ristocetin A, Chen [61] for *N*-benzoylisothiocyanated- α -amino acids on T-A_{2,2} and Haroun *et al.* [154] for Tyr, Trp and their analogs on C18 and C8 stationary phases dynamically coated with teicoplanin. Since some amino acids show the opposite elution sequence from that expected, it is not yet possible to predict the absolute configuration of an amino acid via its retention behavior on a macrocyclic glycopeptide CSP.

ACKNOWLEDGMENTS

This work was supported by OTKA grant K 67563. I. Ilisz wishes to express his thanks for a Bolyai János Postdoctoral Fellowship supporting his research work.

ABBREVIATIONS

CE, capillary electrophoresis; CDA, chiral derivatizing agent; CSP, chiral stationary phase; LEC, ligand-exchange chromatography; HPLC, high-performance liquid chromatography; AcOH, acetic acid; *Bz*, benzyl; *Dns*, dansyl; EtOH, ethanol; MeCN, acetonitrile; MeOH, methanol; NPM, normal phase mode; PIM, polar ionic mode; POM, polar organic mode; RPM, reversed-phase mode; TEA, triethyl amine;

REFERENCES

- [1] Gil-Av, E., Feibush, B. & Charles-Sigler, R. (1966). *Tetrahedron Lett.*, 7, 1009.
- [2] Davankov, V. A., Rogozhin, S. V. & Chromatogr. J. (1971). 60, 280.
- [3] Armstrong, D. W. (1994). Pittsburg Conference Abstracts, Pittcon, 572.
- [4] Beesley, T. E. & Scott, R. P. W. (1998). Chiral Chromatography, *John Wiley & Sons*, Chichester.
- [5] Bojarski, J. (1999). *Wiadomosci Chemiczne*, 53, 235.
- [6] Ali, I., Kumerer, K. & Aboul-Enein, H. Y. (2006). *Chromatographia*, 63, 295.
- [7] Ward, T. J., Farris, A. B. & Chromatogr. J. A. (2001). 906, 73.
- [8] Dolezalova, M. & Tkaczykova, M. (2000). *Chemicke Listy*, 94, 994.
- [9] Dungelova, J., Lehotay, J. & Rajkovicova, T. (2004). *Chem. Anal.*, 49, 1.
- [10] Dungelova, J., Lehotay, J., Rojkovicova, T. & Cizmarik, J. (2003). *Ceska a Slovenska Farmacie*, 52, 119.
- [11] Gasparrini, F., D'Acquarica, I., Misiti, D., Pierini, M. & Villani, C. (2003). *Pure and Applied Chem.*, 75, 407.
- [12] Xiao, T. L. & Armstrong, D. W. (2004). *Methods in Molecular Biology*, (Totowa, NJ, United States) Vol., 243, Chiral Separations, 113-171, Publisher: Humana Press Inc.,.
- [13] Beesley, T. E. & Lee, J. T. (2007). *Advanced Separation Technologies*, Editor(s): G. Subramanian, Chiral Separation Techniques (3rd Edition), Wiley-VCH Verlag GmbH & Co. KGaA, Weinheim, Germany, 1-28.
- [14] Ilisz, I., Berkecz, R., Péter, A. (2006). *J. Sep. Sci.*, 29, 1305.
- [15] Ilisz, I., Berkecz, R. & Péter, A. (2009). *J. Chromatogr. A*, 1216, 1845.
- [16] Ward, T. J. & Ward, K. D. In H., Aboul Enein, I., Wainer, (Eds), The Impact of Stereochemistry on Drug Development and Use, *Chemical Analysis Series*, Vol. 142, John Wiley & Sons, New York,
- [17] Armstrong, D. W., Nair, U. B. (1997). *Electrophoresis*, 18, 2331.
- [18] Armstrong, D. W., Rundlett, K. L. & Reid III, G. L. (1994). *Anal. Chem.*, 66, 1690.

- [19] Armstrong, D. W., Tang, Y., Chen, S., Zhou, Y., Bagwill, C. & Chen, J. R. (1994). *Anal. Chem.*, *66*, 1473.
- [20] Ekborg-Ott, K. H., Kullman, J. P., Wang, X., Gahm, K., He, L. & Armstrong, D. W. (1998). *Chirality*, *10*, 627.
- [21] Barna, J. C. J., Williams, D. H., Stone, D. J. M., Leung, T. W. C., Dodrell, D. M. & Amer, J. (1984). *Chem. Soc.*, *106*, 4895.
- [22] Armstrong, D. W., Liu, Y. & Ekborg-Ott, K. H. (1995). *Chirality*, *7*, 474.
- [23] Gasper, M. P., Berthod, A., Nair, U. B. & Armstrong, D. W. (1996). *Anal. Chem.*, *68*, 2501.
- [24] Goldstein, B. P., Selva, E., Gastaldo, C., Berti, M., Pallanza, R., Ripamonti, F., Ferrari, P., Denaro, M., Arioli, V. & Cassani, G. (1987). *Antimicrob. Agents Chemother.*, *31*, 1961.
- [25] Beltrametti, F., Jovetic, S., Feroggio, M., Gastaldo, L., Selva, E., Marinelli, F. & Antibiot, J. (2004). *57*, 37.
- [26] D'Acquarica, I., Gasparri, F., Misiti, D., Zappia, G., Cimarelli, C., Palmieri, G., Carotti, A., Cellamare, S. & Villani, C. (2000). *Tetrahedron: Asymmetry*, *11*, 2375.
- [27] Berthod, A., Yu, T., Kullman, J. P., Armstrong, D. W., Gasparri, F., D'Acquarica, I., Misiti, D., Carotti, A. & Chromatogr. J. (2000). *897*, 113.
- [28] Fanali, S., Catarcini, P., Presutti, C., Stancanelli, R., Quaglia, M. G. (2003). *J. Chromatogr.*, *A 990*, 143.
- [29] Fanali, S. P., Catarcini, C., Presutti, J. & Chromatogr. A. (2003). *994*, 227.
- [30] Ge, M., Chen, Z., Onoshi, H. R., Kohler, J., Silver, L. L., Kerns, R., Fukusawa, S., Thompson, C., Kahne, D. (1999). *Science*, *284*, 507.
- [31] Berthod, A., Chen, X., Kullman, J. P., Armstrong, D. W., Gasparri, F., D'Acquarica, I., Villani, C. (2000). *Anal. Chem.*, *72*, 1767.
- [32] Jordan, D. C. (1967). Ristocetin, In: D., Antibiotics, P., Gottlieb, Shaw, (Eds.), New York: Springer, Vol. *1*, 84.
- [33] Ekborg-Ott, K. H., Liu, Y. & Armstrong, D. W. (1998). *Chirality*, *10*, 434.
- [34] Ekborg-Ott, K. H., Wang, X. & Armstrong, D. W. (1999). *Microchem. J.*, *62*, 26.
- [35] Best, G. K., Best, N. H. & Durham, N. N. (1968). *Antimicrob. Agents Chemother.*, *4*, 115.
- [36] Diana, J., Visky, D., Roets, E., Hoogmartens, J. & Chromatogr. J. (2003). *A 996*, 115.
- [37] Gao, W., Zhang, S., Liu, H., Zhang, Y., Diao, M., Han, H. & Du, L. (2004). *J. Antibiotics*, *57*, 45.
- [38] Ding, G. S., Liu, Y., Cong, R. Z. & Wang, J. D. (2004). *Talanta*, *62*, 997.
- [39] Ghassempour, A., Abdollahpour, A., Tabar-Heydar, K., Nabid, M. R., Mansouri, S. & Aboul-Enein, H. Y. (2005). *Chromatographia*, *61*, 151.
- [40] Berthod, A., Nair, U. B., Bagwill, C. & Armstrong, D. W. (1966). *Talanta*, *3*, 1767.
- [41] Strege, M. A., Huff, B. E. & Risley, D. S. (1996). *LC-GC*, *14*, 144.
- [42] Sharp, V., Risley, D. S., McCarthy, S., Huff, B. E. & Strege, M. A. (1997). *J. Liq. Chromatogr.*, *20*, 887.
- [43] Sharp, V. S. & Risley, D. S. (1999). *Chirality*, *11*, 75.
- [44] Sharp, V. S., Letts, M. N., Risley, D. S. & Rose, J. P. (2004). *Chirality*, *16*, 153.
- [45] Trelli-Seifert, L. A., Risley, D. S. (1998). *J. Liq. Chromatogr.*, *21*, 299.
- [46] Nair, U. B. & Armstrong, D. L. W. W. (1998). *Hinze, Anal. Chem.*, *70*, 1059.

- [47] Bhushan, R., Parshad, V. (1996). *J. Chromatogr. A*, 736, 235.
- [48] Pagano, J. F., Weinstein, M. J., Stout, M. A. & Donovick, R. (1956). *Antibiot. Ann.*, 554.
- [49] Budavari, S. (Eds.), (1996). The Merck Index, 12th ed., Merck, Whitehouse Station, NJ,.
- [50] Pollock, J. R. A. & Stevens, R. (Eds.), (1965). Dictionary of Organic Compounds, 4th ed., Oxford University Press, New York,.
- [51] Ekborg-Ott, K. H., Zientara, G. A., Schneiderheinze, J. M., Gahm, K. & Armstrong, D. W. (1999). *Electrophoresis*, 20, 2438.
- [52] Berthod, A., Liu, Y., Bagwill, C. & Armstrong, D. W. (1996). *J. Chromatogr. A*, 731, 123.
- [53] Péter, A., Török, G. & Armstrong, D. W. (1998). *J. Chromatogr.*, A, 793, 283.
- [54] Péter, A., Török, G., Armstrong, D. W., Tóth, G. & Tourwé, D. (1998). *J. Chromatogr. A*, 828, 177.
- [55] Péter, A., Olajos, E., Casimir, R., Tourwé, D., Broxterman, Q. B., Kaptein, B., Armstrong, D.W. (2000). *J. Chromatogr. A*, 871, 105.
- [56] Török, G., Péter, A., Vékes, E., Sági, J., Laronze, M. & Armstrong, D. W. (2000). *Chromatographia*, 51, S 165.
- [57] Péter, A., Vékes, E., Gera, L., Stewart, J. M. & Armstrong, D. W. (2002). *Chromatographia*, 56, S 79.
- [58] Péter, A., Vékes, E., Armstrong, D. W. & Tourwé, D. (2002). *Chromatographia*, 56, S 41.
- [59] Ravatunga, R., Vitha, M. F. & Carr, P. W. J. (2002). *Chromatogr. A*, 946, 47.
- [60] Chen, S. & Liq, J. (2003). *Chromatogr. Rel. Technol.*, 26, 3475.
- [61] Chen, S. (2006). *Biomed. Chromatogr.*, 20, 718.
- [62] Chen, S. & Ward, T. (2004). *Chirality*, 16, 318.
- [63] Wu, G. & Furlanut, M. (1999). *Il Farmaco*, 54, 188.
- [64] Gasparrini, F., D'Aquarica, I., Vos, J. G., O'Connor, C. M. & Villani, C. (2000). *Tetrahedron: Asymmetry*, 11, 3535.
- [65] Kafkova, B., Bosakova, Z., Tesarova, E., Coufal, P. (2005). *J. Chromatogr. A*, 1088, 82.
- [66] Tesarova, E., Bosakova, Z. & Pacakova, V. (1999). *J. Chromatogr. A*, 838, 121.
- [67] Schlauch, M. & Frahm, A. W. (2000). *J. Chromatogr. A*, 868, 197.
- [68] Schlauch, M., Kos, O. & Frahm, A. W. (2002). *J. Pharm. Biomed. Anal.*, 27, 409.
- [69] Jandera, P., Skavrada, M., Klemmova, K., Backovska, V. & Guiochon, G. (2001). *J. Chromatogr. A*, 917, 123.
- [70] Péter, A., Árki, A., Vékes, E., Tourwé, D., Forró, E., Fülöp, F. & Armstrong, D. W. (2004). *J. Chromatogr. A*, 1031, 159.
- [71] Péter, A., Török, A. R., Armstrong, D. W. (2004). *J. Chromatogr. A*, 1057, 229.
- [72] Steffek, R. J. & Zelechonok, Y. (2003). *J. Chromatogr. A*, 983, 91.
- [73] Xiao, T. L., Tesarova, E., Anderson, J. L., Egger, M. & Armstrong, D. W. (2006). *J. Sep. Sci.* 29, 429.
- [74] Shen, B. C., Zhang, D. T. Xu, B. J. & Xu, X. Z. (2007). *Anal. Letters*, 40, 2821.
- [75] Péter, A., Török, G., Armstrong, D. W., Tóth, G. & Tourwé, D. (2000). *J. Chromatogr. A*, 904, 1.

- [76] Török, G., Péter, A., Armstrong, D. W., Tourwé, D. & Tóth, G. (2001). *J. Sári, Chirality*, 13, 648.
- [77] Péter, A., Vékes, E. & Armstrong, D. W. (2002). *J. Chromatogr. A*, 958, 89.
- [78] Nair, U. B., Chang, S. S. C., Armstrong, D. W., Rawjee, Y. Y., Eggleston, D. S. & McArdle, J. V. (1996). *Chirality*, 8, 590.
- [79] Tesarova, E., Záruba, K. & Flieger, M. (1999). *J. Chromatogr. A*, 844, 137.
- [80] Bosakova, Z., Klouckova, I. & Tesarova, E. (2002). *J. Chromatogr. B*, 770, 63.
- [81] Bosakova, Z., Curinova, E. & Tesarova, E. (2005). *J. Chromatogr. A*, 1088, 94.
- [82] Donnecke, J., Svensson, L. A., Gyllenhaal, O., Karlsson, K. E., Karlsson, A. & Vessman, J. (1999). *J. Microcolumn Sep.*, 11, 521.
- [83] Sun, Q. & Olesik, S. V. (2000). *J. Chromatogr. B: Biomed. Sci. Appl.*, 745, 159.
- [84] Ward, T. J., Baker, B. A., Gilmore, A. C., Vowell, C. L. & Oglesbee, M. D. (2007). Abstracts of Papers, 233rd ACS National Meeting, Chicago, IL, USA, March, 25-29.
- [85] Aboul-Enein, H. Y. & Serignese, V. (1998). *Chirality*, 10, 358.
- [86] Pehourcq, F., Jarry, C. & Bannwarth, B. (2001). *Biomed. Chromatogr.*, 15, 217.
- [87] Zhang, D., Xu, X. & Ma, S. (2005). *J. Sep. Sci.*, 28, 2501.
- [88] Ding, G. S., Huang, X. J., Liu, Y. & Wang, J. D. (2004). *Chromatographia*, 59, 443.
- [89] Reilly, J., Sanchez-Felix, M. & Smith, N. V. (2003). *Chirality*, 15, 731.
- [90] Mojtahedi, M. M., Chalavi, S., Ghassempour, A., Tabar-Heydar, K., Sharif, S. J. G., Malekzadeh, M. & Aboul-Enein, H. Y. (2007). *Biomed. Chromatogr.*, 21, 234.
- [91] Ghassempour, A., Alizadeh, R., Najafi, N. M., Karami, A., Rompp, A., Spengler, B. & Aboul-Enein, H. Y. (2008). *J. Sep. Sci.*, 31, 2339.
- [92] Gholami, M., Ghassempour, A., Alizadeh, R. & Aboul-Enein, H. Y. (2009). *J. Sep. Sci.*, 32, 918.
- [93] Kang, J., Bischoff, D., Jiang, Z., Bister, B., Suessmuth, R. D. & Schurig, V. (2004). *Anal. Chem.*, 76, 2387.
- [94] Jiang, Z., Kang, J., Bischoff, D., Bister, B., Suessmuth, R. D. & Schurig, V. (2004). *Electrophoresis*, 27, 2687.
- [95] Jiang, Z., Bertazzo, M., Suessmuth, R. D., Yang, Z., Smith, N. W. & Schurig, V. (2006). *Electrophoresis*, 27, 1154.
- [96] Staroverov, S. M., Kuznetsov, M. A., Nesterenko, P. N., Vasiyarov, G. G., Katrukha, G. S. & Fedorova, G. B. (2006). *J. Chromatogr. A*, 1108, 263.
- [97] Zhang, L., Geddicke, K., Kuznetsov, M. A., Staroverov, S. M. & Seidel-Morgenstern, A. (2007). *J. Chromatogr. A*, 1162, 90.
- [98] Kuznetsov, M. A., Nesterenko, G. G. & Vasiyarov, S. M. (2006). Staroverov, Applied Biochem. Microbiol., 42, 536.
- [99] Kuznetsov, M. A., Nesterenko, P. N., Vasiyarov, G. G. & Staroverov, S. M. (2008). *J. Anal. Chem.*, 63, 57.
- [100] Xiao, T. L., Rozhkov, R. V., Larock, R. C. & Armstrong, D. W. (2003). *Anal. Bioanal. Chem.*, 377, 639.
- [101] Berthod, A., Xiao, T. L., Liu, Y., Jenks, W. S. & Armstrong, D. W. (2002). *J. Chromatogr. A*, 955, 53.
- [102] Medvedovici, A., Sandra, P., Toribio, L. & David, F. (1997). *J. Chromatogr. A*, 785, 159.

- [103] Liu, Y., Berthod, A., Mitchell, C. R., Xiao, T. L., Zhang, B. & Armstrong, D. W. (2002). *J. Chromatogr. A*, 978, 185.
- [104] Péter, A., Lázár, L., Fülöp, F. & Armstrong, D. W. (2001). *J. Chromatogr. A*, 926, 229.
- [105] Árki, A., Tourwé, D., Solymár, M., Fülöp, F., Armstrong, D. W. & Péter, A. (2004). *Chromatographia*, 60, S 43.
- [106] Péter, A., Árki, A., Vékes, E., Tourwé, D., Lázár, L., Fülöp, F. & Armstrong, D. W. (2004). *J. Chromatogr. A*, 1031, 171.
- [107] Berkecz, R., Ilisz, I., Benedek, G., Fülöp, F., Armstrong, D. W. & Péter, A. (2009). *J. Chromatogr. A*, 1216, 927.
- [108] Pataj, Z., Berkecz, R., Ilisz, I., Misicka, A., Tymecka, D., Fülöp, F. & Armstrong, D. W. A. Péter, *Chirality* (in press).
- [109] Hrobonova, K., Lehotay, J., Cizmarikova, R. & Armstrong, D. W. (2001). *J. Liquid Chromatogr. & Related Technol.*, 24, 2225.
- [110] Hrobonova, K., Lehotay, J. & Cizmarikova, R. (2004). *Pharmazie*, 59, 828.
- [111] Cizmarikova, R., Racanska, E., Hrobonova, K., Lehotay, J., Aghova, Z. & Halesova, D. (2003). *Pharmazie*, 58, 237.
- [112] Hrobonova, K., Lehotay, J. & Cizmarikova, R. (2005). *Pharmazie*, 60, 888.
- [113] Lehotay, J., Hrobonova, K., Cizmarik, J., Reneova, M. & Armstrong, D. W. (2001). *J. Liquid Chromatogr. & Related Technol.*, 24, 609.
- [114] Rojkovicova, T., Lehotay, J., Dungelova, J., Cizmarik, J. & Armstrong, D. W. (2002). *J. Liquid Chromatogr. & Related Technol.*, 25, 2723.
- [115] Rojkovicova, T., Lehotay, J., Krupcik, J., Fedurcova, A., Cizmarik, J. & Armstrong, D. W. (2004). *J. Liquid Chromatogr. & Related Technol.*, 27, 1653.
- [116] Rojkovicova, T., Lehotay, J., Mericko, D., Cizmarik, J. & Armstrong, D. W. (2004). *J. Liquid Chromatogr. & Related Technol.*, 27, 2477.
- [117] Rojkovicova, T., Lehotay, J., Armstrong, D. W. & Cizmarik, J. (2004). *J. Liquid Chromatogr. & Related Technol.*, 27, 3213.
- [118] Rojkovicova, T., Lehotay, J., Armstrong, D. W. & Cizmarik, J. (2006). *J. Liquid Chromatogr. & Related Technol.*, 29, 2615.
- [119] Lehotay, J., Hrobonova, K. & Krupcik, J. (1998). *J. Cizmarik, Pharmazie*, 53, 863.
- [120] Mericko, D., Lehotay, J., Skacani, I. & Armstrong, D. W. (2006). *J. Liquid Chromatogr. Related Technol.*, 29, 623.
- [121] Mericko, D., Lehotay, J., Skacani, I. & Armstrong, D. W. (2007). *J. Liquid Chromatogr. Related Technol.*, 30, 1401.
- [122] Berthod, A., Valleix, A., Tizon, V., Leonce, E., Caussignac, C. & Armstrong, D. W. (2001). *Anal. Chem.*, 73, 5499.
- [123] Cavazzini, A., Nadalini, G., Dondi, F., Gasparini, F., Ciogli, A. & Villani, C. (2004). *J. Chromatogr. A*, 1031, 143.
- [124] Peyrin, E., Ravel, A., Grosset, C., Villet, A., Ravalet, C. & Nicolle, E. (2001). *J. Alary, Chromatographia*, 53, 645.
- [125] Peyrin, E., Ravalet, C., Nicolle, E., Villet, A., Grosset, C., Ravel, A. & Alary, J. (2001). *J. Chromatogr. A*, 923, 37.
- [126] Slama, I., Villet, A., Ravel, A., Grosset, C. & Peyrin, E. (2002). *J. Chrom. Sci.*, 40, 83.

- [127] Slama, I., Jourdan, E., Villet, A., Grosset, C., Ravel, A. & Peyrin, E. (2003). *Chromatographia*, 58, 399.
- [128] Slama, I., Dufresne, C., Jourdan, E., Fahratt, F., Villet, A., Ravel, A., Grosset, C. & Peyrin, E. (2002). *Anal. Chem.*, 74, 5205.
- [129] Slama, I., Jourdan, E., Grosset, C., Ravel, A., Villet, A. & Peyrin, E. (2003). *Chromatogr. J. B*, 795, 115.
- [130] Loukili, B., Dufresne, C., Jourdan, E., Grosset, C., Ravel, A., Villrt, A. & Peyrin, E. (2003). *J. Chromatogr. A*, 986, 45.
- [131] Haroun, M., Ravalet, C., Ravel, A., Grosset, C., Villet, A. & Peyrin, E. (2005). *J. Sep. Sci.*, 28, 409.
- [132] Courderot, C. M., Perrin, F. X., Guillaume, Y. C., Truong, T. T., Millet, J., Thomassin, M., Chaumont, J. P. & Nicod, L. (2002). *Anal. Chim. Acta*, 457, 149.
- [133] Ismaili, L., Truong, T. T., Andre, C., Thomassin, M., Mozer, J. L., Robert, J. F., Xicluna, A., Refouvelet, B., Millet, J., Nicod, L. & Guillaume, Y. C. (2003). *J. AOAC Int.*, 86, 222.
- [134] Guillaume, Y. C., Truong, T. T., Millet, J., Nicod, L., Guinchard, C., Robert, J. F. & Thomassin, M. (2002). *Chromatographia*, 55, 143.
- [135] Guillaume, Y. C., Ismaili, L., Truong, T. T., Nicod, L., Millet, J. & Thomassin, M. (2002). *Talanta*, 58, 951.
- [136] Andre, C. & Guillaume, Y. C. (2003). *Chromatographia*, 58, 201.
- [137] Jandera, P., Backovska, V. & Felinger, A. (2001). *J. Chromatogr. A*, 919, 67.
- [138] Berthod, A., He, B. L. & Beesley, T. E. (2004). *J. Chromatogr.*, A 1060, 205.
- [139] Kalisz, R. (1997). *Structure and Retention in Chromatography: A Chemometric Approach*, Harwood Academic Publishers, Amsterdam.
- [140] Abraham, M. H., Ibrahim, A. & Zissimos, A. M. (2004). *J. Chromatogr. A*, 1037, 29.
- [141] Vitha, M. & Carr, P. W. (2006). *J. Chromatogr. A*, 1126, 143.
- [142] Lokajova, J., Tesarova, E. & Armstrong, D. W. (2005). *J. Chromatogr. A*, 1088, 57.
- [143] Kalikova, K., Lokajova, J. & Tesarova, E. (2006). *J. Sep. Sci.*, 29, 1476.
- [144] Berthod, A., Mitchell, C. R. & Armstrong, D. W. (2007). *J. Chromatogr. A*, 1166, 61.
- [145] Mitchell, C. R., Armstrong, D. W. & Berthod, A. (2007). *J. Chromatogr. A* 1166, 70.
- [146] Guiochon, G., Shirazi, S. G. & Katti, A. (1994). *Fundamentals of Preparative and Nonlinear Chromatography*, Boston MA: Academic Press.
- [147] Petrusevska, K., Kuznetsov, M. A., Gedicke, K., Meshko, V., Staroverov, S. M. & Sidel-Morgenstern, A. (2006). *J. Sep. Sci.*, 29, 1447.
- [148] Arnell, R., Forssen, P. & Fornstedt, T. (2007). *Anal. Chem.*, 79, 5838.
- [149] Poplewska, I., Kramarz, R., Piatkowski, W., Seidel-Morgenstern, A. & Antos, D. (2007). *Dorota, J. Chromatogr. A*, 1173, 58.
- [150] Astec, (2004). Advanced Separation Technologies Inc., Whippany, NJ, USA,
- [151] Schmid, M. G., Grobuschek, N., Pessenhofer, V., Klostius, A. & Gübitz, G. (2003). *J. Chromatogr. A*, 990, 83.
- [152] B. Zhang, R. Soukup, D.W. Armstrong, *J. Chromatogr. A* 1053 (2004) 89.
- [153] Xiao, T. L., Zhang, B., Lee, J. T., Hui, F., Armstrong, D. W. & Liq, J. (2001). *Chromatogr. Rel. Technol.*, 24 2673.
- [154] Haroun, M., Ravalet, C., Grosset, C., Ravel, A., Villet, A. & Peyrin, E. (2006). *Talanta*, 68, 1032.

Chapter 5

FROM MACROCYCLIC LIGANDS TO FLUORESCENT MOLECULAR SENSORS FOR METAL IONS: RECENT RESULTS AND PERSPECTIVES

Carlos Lodeiro^{1*}, *Vito Lippolis*^{2*} and *Marta Mameli*²

¹University of Vigo, Physical-Chemistry Department, Faculty of Science, BIOSCOPE Research Team, Ourense Campus, E-32004 (OU) Spain.

²Università degli Studi di Cagliari, Dipartimento Chimica Inorganica e Analitica, S.S. 554, Bivio Sestu, I-09042 Monserrato (CA) Italy.

ABSTRACT

The design and synthesis of fluorescent molecular sensors that selectively and specifically respond to the presence of a given analyte (in particular metal ions) in a complex matrix is a vigorous research area of supramolecular chemistry. Applications can span from process control to environmental monitoring, food analysis, and medical diagnosis, to give some examples.

The most common synthetic approach to fluorescent chemosensors is to link covalently, through an appropriate spacer, a fluorogenic fragment (signalling unit) to a guest-binding site (receptor unit). The recognition of the target species by the receptor unit as a result of a selective host-guest interaction between the two is converted into an optical signal expressed as an enhancement or quenching of the fluorophore emission. The choice of both the signalling- and the receptor-units can be critical to both the performance and the selectivity/specificity of the sensor, especially if a direct interaction between the fluorophore and the target species is possible.

Different fluorophores (anthracene, 8-hydroxyquinoline, dansylamide, coumarin, phenanthroline, *etc*) are used as signalling sites, whereas macrocyclic receptors continue to represent the first choice as guest-binding sites for metal cations due to the extensive possibilities which they can offer for modulation of the topology and nature of the binding domain, thus providing an easy route to achieving strong and possibly selective interactions with the substrate of interest.

* Principal authors equally contributing to this work

In this chapter will be reviewed the use of macrocyclic ligands essentially as receptor units in fluorescent molecular sensors for metal ions. The reported systems are mainly based on the work developed by the authors in the last ten years and compared with other related similar systems published. Some interesting properties beyond sensing ionic and/or neutral substrates by fluorescence can arise from these compounds; in particular pH, metals and light can be used as external stimuli to modulate the sensing properties through energy and electron transfer mechanisms.

Keywords: Poly-aza-macrocycles; Oxa-aza macrocycles; Thia-aza macrocycles; Other macrocycles; Chemosensors; Fluorescence.

1. INTRODUCTION

In the last decades, coordination chemistry has entered a phase of creative rather than investigative chemistry. The study of the simple molecular systems which was Werner's focus has lost its central role in this major area of chemical science and a new area termed supramolecular chemistry has emerged.[1,2] According to J.M. Lehn (Nobel prize 1987), [3] "the coordination chemistry of the ligands of supramolecular chemistry is the chemistry of artificial receptor molecules which strive to achieve control over the strength, selectivity and dynamics of the binding process" with appropriate substrates to give new supramolecular structures/assemblies which exhibit highly specific molecular functions and show new physical and chemical properties; certainly, in this puzzle game, macrocyclic and macropolycyclic structures have played, and continue to play, a crucial role. Macrocyclic ligands offer a great potential structural diversity which is essential for the design of artificial receptor molecules having the appropriate structural features that will confer strength and selectivity to the binding process to the desired substrate (ionic or neutral). The great effectiveness of macrocyclic compounds as receptors to bind specific guest species, especially towards metal ions, is strongly related to structural factors, such as nature of the donor atoms, size and shape of the ring cavity, as well as to the topology, rigidity and spatial organization of the macrocyclic architecture. A general trend in macrocyclic chemistry over the last 50 or so years has been the design of ever more pre-organised and structurally complex ligands showing increased selectivity for the substrate of interest.[4-9] Host-guest chemistry has become a new discipline within supramolecular chemistry and many practical applications based on selective binding, recognition and sensing of a substrate by specifically designed receptors containing a macrocyclic moiety are now possible.

According to IUPAC, [10] a chemical sensor is a macroscopic device that transforms chemical information, ranging from the concentration of the analyte of interest to total composition analysis, into an analytical useful signal (change in pH, light emission, electronic distribution). Chemical sensor devices are conceived to bypass classical analytical methodologies which normally require laborious sample pre-treating, expensive instrumentation and trained staff, and to allow *in situ* and in real time detections and quantification of analytes at the lowest cost possible. It is hardly necessary any longer to stress the importance of the development of new chemical sensors; applications span from process control, environmental monitoring, food analysis and medical diagnosis, and many disciplines need sensing systems for their development, including chemistry, biology, clinical

biology and environmental science. The list of interesting analytes to be detected is lengthy, however, among all possible analytes, metal ions occupy a central role in all aspects of human life and for this reason there has always been a need for rapid and low-cost testing methods for a wide range of them in areas of chemical, biological and environmental importance.

A very useful approach recently adopted by chemists for the design of new and efficient chemical sensors takes right advantage of the principles of supramolecular chemistry. This “bottom-up” approach starts the design of a device from a molecular level, ensuring a resolution unachievable with a classic “top-down” approach. The resulting molecular indicators or supramolecular species are normally referred to as molecular sensors or chemosensors, mostly to distinguish them from chemical sensors, which usually are intended as macroscopic devices. [11] The integration of chemosensors into a truly sensory device without loss of sensitivity and selectivity, but actually with an increase of these parameters, is also increasingly captivating the attention of scientists. New implementation strategies based on polymers, sol-gel materials, surfactant aggregates, glass and gold surfaces, silica nanoparticles and quantum dots (to mention some of them) have been developed for new chemosensing materials. [12,13] However, especially when targeting metal ions, the availability of selective and specific molecular sensors is crucial in many cases in order to build in a subsequent work-step the integrated sensor devices.

In general, because of the two main processes occurring during analyte detection (molecular recognition and signal transduction) a chemosensor consists of a receptor unit or binding sub-unit (which is the part of the supramolecular species that interacts with the substrate) and of a signaling or active unit (which is the part that changes its physical-chemical properties when the receptor binds the substrate) generally separated by a spacer. According to this supramolecular modular scheme, if the signaling unit is a fluorogenic fragment the systems are referred as a fluorescent chemosensor. [14,30] Many factors make fluorescence one of the most powerful transduction mechanisms to report the chemical recognition event. Fluorescence does not consume analytes and no reference is required. A number of fluorescence microscopy and spectroscopy techniques have been developed, as well as laser fiber optics and detection technologies are well established. These techniques are extremely sensitive and allow even the detection of single molecules. Therefore, fluorescence techniques are considered for their sensitivity, response time and cost as the most important detection method for the development of chemical sensors for screening metal ions in biological, industrial and environmental samples. [14-30]

Important aspects of fluorescence chemosensors design for metal ions include analyte affinity, choice of chromophore or fluorophore, binding selectivity and specificity and transduction signaling mechanism. All these aspects can be in principle targeted by changing the receptor, the signaling and the spacer units. [14-30]

About the choice of the fluorophore, one important aspect is that the absorption wavelength must be comparable with the light-absorbing properties of the medium in which measurements are to be made and with the light source (for example, for analytes in biological fluids or in cells, λ_{max} values for absorption larger than 400 nm are required). With regard to molecular recognition and selective binding of metal ion species, macrocyclic ligands are extensively studied, and the development of abiotic chemosensors has been deeply intertwined to that of macrocyclic chemistry since the pioneering work of Pedersen, Cram and Lehn; from then onwards, hundreds of possible sensor molecules featuring macrocyclic moieties were listed. In fact, by changing some structural features of the macrocyclic

framework such as number and disposition of donor atoms, cavity size, and conformational flexibility, it is possible in principle to design highly pre-organised ligands or receptor units capable of recognizing and binding selectively to certain metal ion guests. From a structural point of view, fluorescent chemosensors for metal ions can be classified into two main classes: intrinsic chemosensors in which both functions of recognizing and signaling a given analyte are performed by a fluorophore; conjugated chemosensors which consist of a fluorogenic fragment (signaling unit) covalently linked, through an appropriate spacer, to a guest-binding site (receptor unit). The latter class of fluorescent chemosensors is the most common and studied; the selective host-guest interaction of the target species with the receptor unit (recognition event) is converted into an optical signal expressed in general as an enhancement or quenching of the fluorophore emission.

According to this simple “receptor-spacer-fluorophore” supramolecular modular scheme, the selectivity/specificity of conjugated chemosensors would be determined solely or mainly by the nature of the receptor unit, while the transduction mechanism that is triggered upon the host-guest interaction, and the sensitivity or sensor-performance would be determined mainly by the fluorogenic fragment. This subdivision of the roles played by the receptor and fluorescent signaling units, which can be translated into the operative synthetic strategy “find the appropriate receptor and attach to it a fluorogenic fragment”, although very simplistic, certainly represents a useful guide to the design of a conjugated fluorescent chemosensor, and it has worked very well for metal cation sensors featuring anthracenyl derivatives of crown ethers. However, the choice of the “read-out” or signaling unit can be critical to both the performance and the selectivity/specificity of the sensor, especially if a direct interaction of the fluorophore with the target species is implied. In this respect, the complementary approach of changing the signaling unit attached to a pre-defined receptor unit (not necessarily the best in the binding process) could therefore represent a promising alternative to the common practice in the design of specific and selective conjugated fluorescent chemosensors, of using different receptors linked to the same fluorophore.

The selectivity/specificity as well as the sensitivity of a fluorescent chemosensor are also determined by the medium (in particular the solvent) in which the “host-guest” interaction takes place. It has been observed that non-selective chemosensors became so when dispersed into supported PVC liquid membranes, liposomes or micelles. In fact, under these conditions other parameters such as lipophilicity of the chemosensor and its metal ion complex, their mobility within the membrane and other parameters governing the transport processes can strongly influence the performances of the fluorescent chemosensor improving the selectivity as well as the sensitivity observed in solution.[14-30]

In this chapter, we will review the chemical systems from our groups containing macrocyclic frameworks and able to act as fluorescent chemosensors for metal ions. As a method, we will gather the various chemosensors in different classes, according to the nature of the macrocyclic framework as receptor unit and we will discuss them in comparison to other related similar systems from the literature.

2. POLY-AZA-MACROCYCLIC SYSTEMS

The concept of fluorescence chemosensor was reported for the first time in 1977 by L. R. Sousa; he used several naphthalene-functionalised crown ether ligands as molecular probes for alkaline metal ions. [31]

In 1990, A.W. Czarnik reported the first water-soluble fluorescent chemosensors possessing a polyamine macrocyclic receptor linked to an anthracene chromophore: compounds **1-4** (Figure 1). [32]

The presence of a polyamine receptor unit usually provides to the sensor water-solubility, in great part due to the protonation equilibria that the polyamine unit can undergo in water. Furthermore, the protonation of the polyamine unit at acidic pH values offers an anionic sensor while at basic pH the unprotonated forms are ideal to complex metal ions.

The first fluorescent chromophores explored as signalling units in fluorescent chemosensors were anthracene and naphthalene, [33] but other emitters were considered later, as for example dansyl, [34] 8-hydroxyquinoline, [35] coumarine, [36] pyrene, [37] indole, [38] or ruthenium tris-bipyridyl derivatives. [39] In all cases the fluorescence emission of the sensing unit should be increased or decreased upon binding of the analyte to the receptor.

Regarding the mechanisms through which the chemosensor operates, photo-induced electron transfer (PET) involving the excited sensing unit and the polyamine receptor is the most common. In the case of anthracene and naphthalene the PET occurs from the lone pair of the nitrogens to the excited fluorophore.

In all receptor units in which an aromatic nitrogen heterocycle such as pyridine, phenanthroline, terpyridine or bipyridyl has been integrated into the receptor, the new binding properties modulate the PET mechanism. Protonation of the aromatic nitrogen at acidic pH values also gives rise to PET from the excited fluorophore to the protonated heterocycle, resulting in fluorescence quenching. Systems containing both aliphatic amines and nitrogen heterocycles are only effective in a pH window whose width is dependent on the structure of the molecule. [40]

In 1995, the groups of E. García-España and F. Pina introduced for the first time, the systematic superposition of two different families of data obtained in solution by potentiometric and fluorescence emission spectroscopy, to study the interaction of polyazacyclophane macrocyclic receptors **5** (Figure 2), with the anion, hexacyanocobaltate (III). [41, 29] This approach was later on complemented by the use of NMR titrations. [42] The combining of these three techniques, fluorescence emission, potentiometry, and NMR spectroscopy, used as a function of pH, proved to be a powerful analytical strategy to investigate the behaviour in water of fluorescent polyamine chemosensors. [29] In particular, it is possible to assign the protonation sequence of the nitrogen atoms of the chemosensor, and thus identify the contribution of each species to the fluorescent emission, at each pH value.

It is very important to underline that the sensing unit can play a central role in the performance of the chemosensor. Aromatic hydrocarbons such as anthracene, naphthalene, pyrene, pyridine, phenanthroline, bipyridile, terpyridine, etc have been extensively used, due to their good fluorescence emission quantum yields and because they can easily communicate with the polyamine receptor through PET. In some macrocycles where the sensing unit possesses two or more chromophores (see compound **6** in Figure 2), formation or disappearance of intramolecular excimers can also be used together with the monomer emission to sensing target compounds. [43]

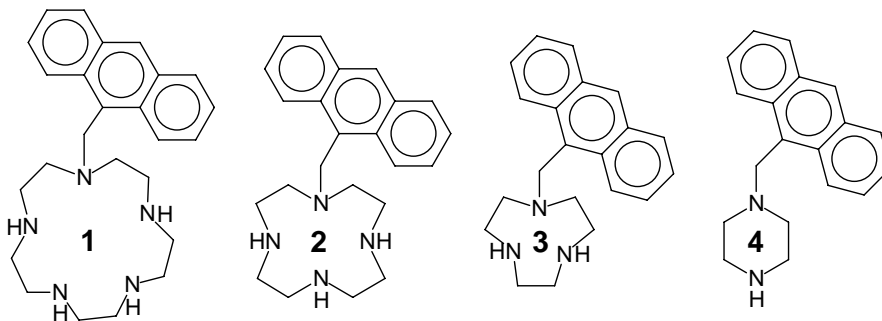


Figure 1. For compound **1**, protons, as well as Zn^{2+} and Cd^{2+} , switch ON the fluorescence of the sensor.

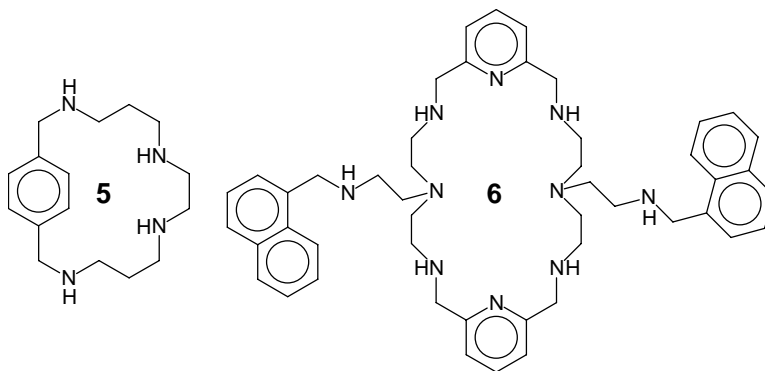


Figure 2.

In these cases the absorption spectra are practically independent on the protonation sequence, but in contrast the fluorescence emission is dramatically affected, see Figure 3A. The excimer emission is clearly identified by the observation of its red shifted and unstructured emission band. Full protonation of the polyamine receptor prevents PET and confers rigidity to the ligand; by consequence $(\text{H}_6\mathbf{6})^{6+}$ exhibits the highest fluorescence emission intensity.

An example of this approach is reported for macrocycle **6** in Figure 3. The relative contribution to the fluorescence emission of each species can be measured. The maximum of the fluorescence emission is observed for the more protonated forms, $(\text{H}_6\mathbf{6})^{6+}$, because protonation prevents the quenching process by electron transfer and in contrast at high pH values the emission is not observed or highly quenched, due to the PET quenching process.

Formation of excimer was also described for macrocycles **7** and **8** (Figure 4). [44] The different central spacer unit with different connections to the central benzene groups with the polyamine chain, leads to small but significant differences in the photophysical behaviour of the two compounds, namely in the rate of excimer formation at acidic pH values. Excimer formation at acidic pH values when the protonation of the polyamine bridges is extensive (all six secondary amines) is observed. Identically excimer emission was detected for compound **6**. In this case time-resolved fluorescence data, obtained by single photon counting showed that a significant percentage of excimer is preformed as ground state dimers. [43]

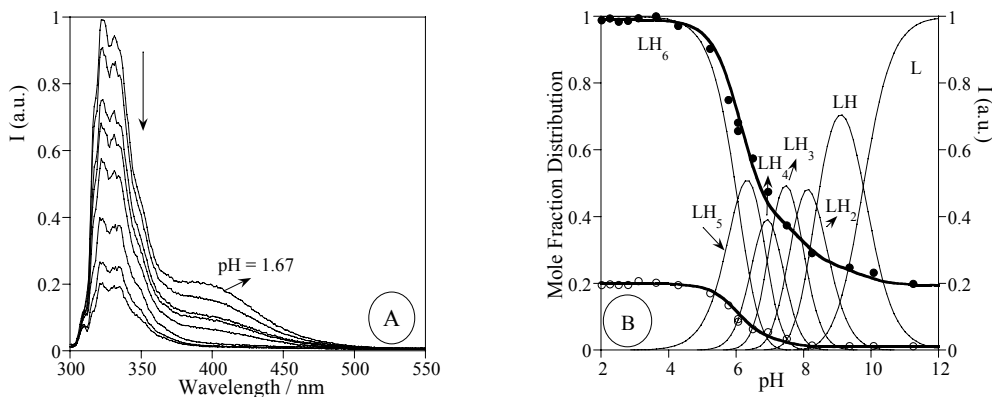


Figure 3. (A) Fluorescence emission spectra of **6** recorded at 298.1 K as function of pH. (B) Steady-state fluorescence emission titration curves of **6** ($\lambda_{\text{exc}} = 280$ nm) in water. (●) emission followed at 323 nm (monomer) and (○) emission followed at 400 nm (exciplex). Molar fractions distribution (solid lines).

Complexation of **6** with Cu^{2+} and Zn^{2+} gave mono- and dinuclear complexes in which the nitrogen atoms located in the pendant arms did not provide a strong contribution to the overall stability. In both cases the excimer emission was not observed. As usual, copper(II) complexation gives rise to a CHEQ (Chelation Enhancement of Quenching) effect while zinc(II) complexation originates a slight CHEF (Chelation Enhancement of Fluorescence) effect. The lack of significant CHEF effect expected upon coordination of Zn^{2+} was attributed to a compensating effect due to the coordination of the pyridine units in the Zn^{2+} complexes that is expected to give a CHEQ effect.

Sensing metal ions can be performed by the fluorescence emission not only from excimers but also from exciplexes, upon complexation with macrocycle-based chemosensors. The coordination environment re-organizes the structure of the ground and excited states of the chemosensor, in some cases inducing and in other cases preventing the formation of these excited state species.

An example of this behaviour was observed with the Zn^{2+} complex of compound **9**. [29,30] Coordination/detachment of a pendant functionality in the Zn^{2+} complex with the macrocyclic ligand **9** gives rise to ON/OFF switching of exciplex emission, defining elementary movements that can be driven by both pH and light (see Figure 5).

Steady-state and time-resolved fluorescence studies with the Zn^{2+} complex of **9** were reported in an ethanolic solution and in the solid state. In solution, from the temperature dependence of the photostationary ratio ($I_{\text{Exc}}/I_{\text{M}}$), the activation energy ($E_{\text{a}} = \text{kJ mol}^{-1}$) for exciplex formation and the binding energy of the exciplex ($\Delta H = -7.9 \text{ KJ mol}^{-1}$) were determined.

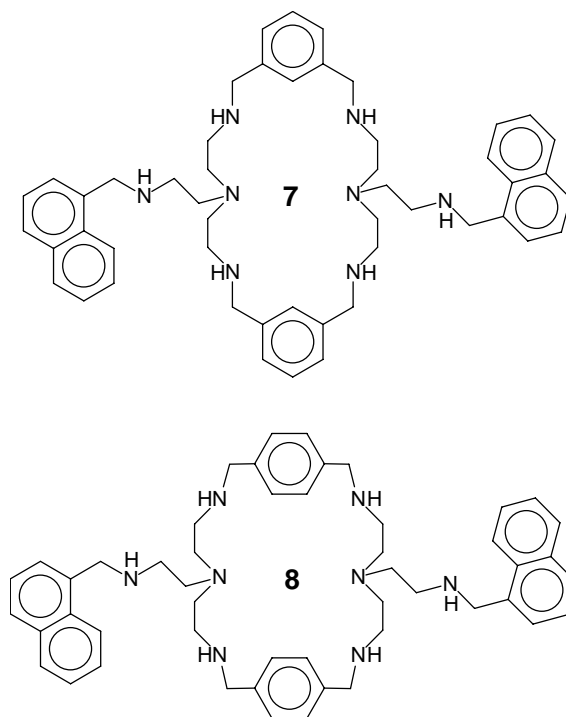
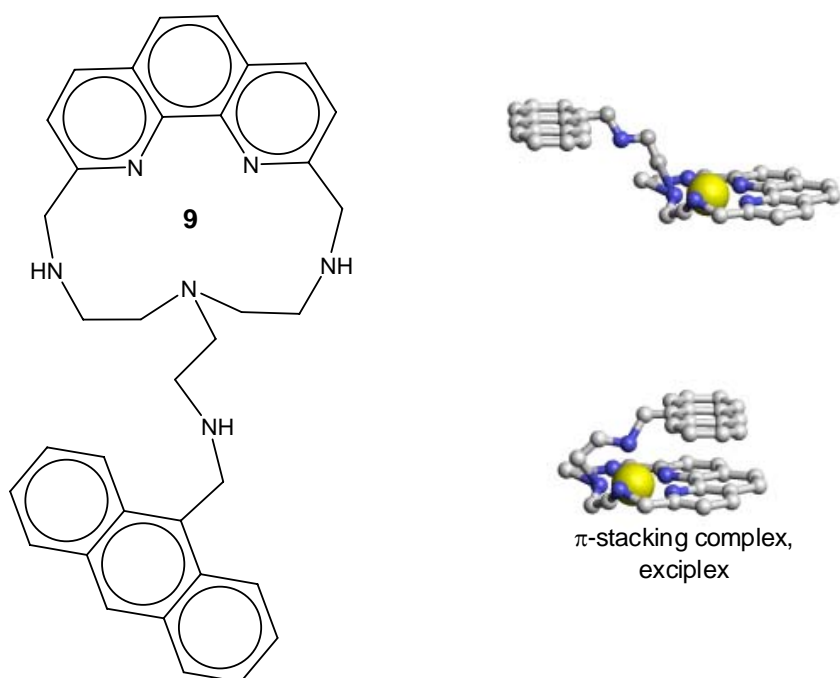
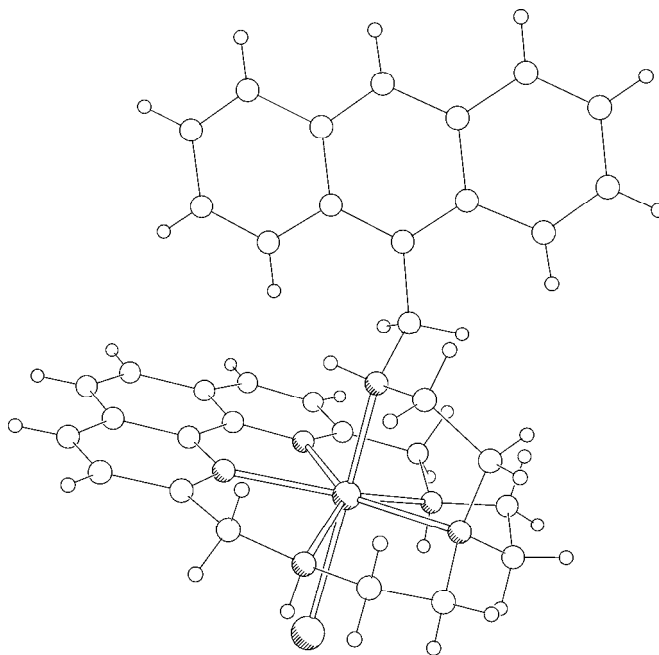
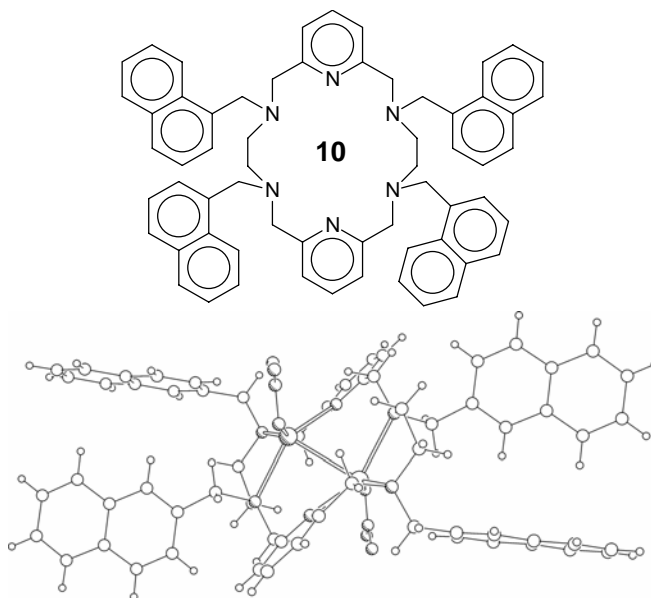


Figure 4.

Figure 5. Compound 9 and its [Zn9]²⁺ complex in the π -stacked and detached forms.

Figure 6. $[\text{Zn}9(\text{Br})]^+$.Figure 7. **10**; $[\text{Ag}_2\mathbf{10}(\text{NO}_3)_2]$.

An interesting result comes from the solid state. The absorption spectrum of a thin film containing the 1:1 complex between Zn^{2+} and **9** is red-shifted relatively to the solution spectra whereas its emission spectrum reveals the unique featureless exciplex band but blue shifted relatively to the one obtained in solution. In conjunction with X-ray data (See Figure 6) the solid-state data were interpreted as being due to a new exciplex where differently from the

results in water no π -stacking (full overlap of the π -electron cloud of the anthracene and phenanthroline units) was observed.

Another clear evidence for an exciplex emission was obtained in compound **10** (Figure 7). [47] In this case the exciplex emission (excited CT state) is centred *ca.* 440 nm, and was interpreted as an exciplex-like structure involving the naphthalene pendant-arms and the pyridine units.

Complexation of **10** with Zn^{2+} and Cd^{2+} leads to a total disappearance of the exciplex emission, and the interaction with the transition metal complexes, Cu^{2+} , Ni^{2+} and Co^{2+} leads to a formation of mononuclear non-emissive complexes.

In figure 7 the crystal structure of the dinuclear silver complex of **10** is shown. Complexation with two equivalents of Ag^+ produces a non-emissive complex due to the participation of both pyridine units present in the macrocyclic ligand upon the coordination. The fluorescence quantum yield for the binuclear silver(I) complex was 0.016, smaller than the value obtained for the free ligand (0.021), confirming the quenching effect upon chelation to the pyridine rings.

Incorporating of heterocycles such as phenanthroline, bipyridine and terpyridine into the macrocyclic skeletons of the fluorescent chemosensor has been a subject of recent research by several research groups. [48]

In collaboration with the group of A. Bianchi and A. Bencini several examples of chemosensors based on macrocyclic polyamine designed following this strategy have been reported since 1999. [49] In these systems the aromatic nitrogen atoms can be used for two functions: binding and sensing.

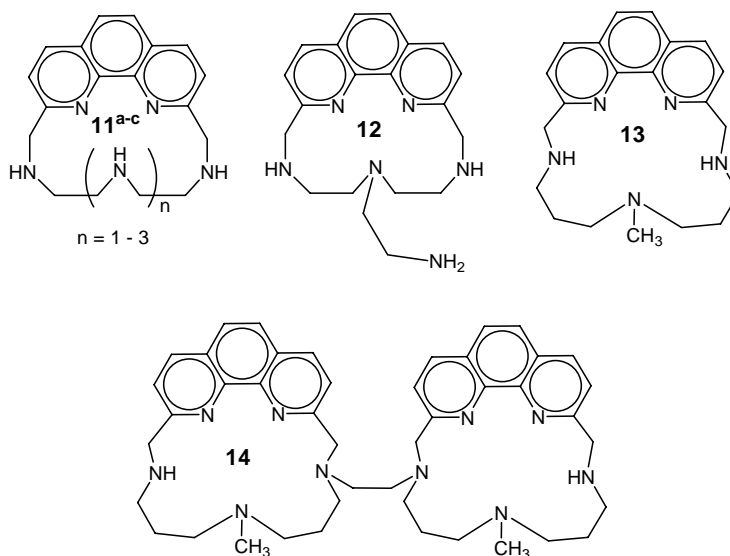


Figure 8.

In Figure 8 the family of compounds having the phenanthroline chromophore incorporated into the polyamine macrocycle is represented. The fluorescence emission of the free ligands on changing the pH presents the common trend of the compounds possessing at the same time both aromatic and aliphatic amines, a bell shaped fluorescence emission

titration curve. The quenching effect at lower pH values for compounds **11^{a-c}** depends on the chain length and is stronger for $n = 3$ as expected by the easier protonation of the phenanthroline unit for the larger macrocycle.

In the case of Zn^{2+} complexes of compound **11^a** ($n=1$) (Figure 8) it was shown that the benzylic nitrogens are weakly bound to the metal ion, and for this reason no fluorescence emission was observed because the benzylic amines are available to the PET process of quenching. On the other hand a decreasing of the stability trend for the complexes with Zn^{2+} from **11^a** ($n=1$) to **11^c** ($n=3$) was observed. This fact suggests that the number of donor atoms participating in the coordination does not parallel the increasing number of donors in the ligands. Moreover an increasing number of uncoordinated amine groups favours the formation of protonated complexes, as was observed for **11^b** ($n=2$) and **11^c** ($n=3$), and allows the larger ligand to have enough free donor atoms to bind a second metal. **[Error! Bookmark not defined.b]** In order to observe the fluorescence emission, the nitrogens should be involved in the binding with the metal or protected by protons. This is in agreement with the observation that the largest fluorescence emission occurs for the diprotonated metal complex with **11^c** ($n=3$).

Ligand **12** was studied in the presence of the divalent metals, Zn^{2+} , Cd^{2+} , and Hg^{2+} . In all cases mononuclear complexes were formed and the fluorescence emission quenched. [49bb]

Similar behaviour was found recently for the phenanthroline-containing systems **13** and **14** (Figure 8). [49d] While ligand **13** permits coordination of divalent metal ions such as Cu^{2+} , Zn^{2+} , Cd^{2+} , Pb^{2+} and Hg^{2+} to give mononuclear complexes, with **14** both mono- and dinuclear complexes were obtained. Unfortunately, all these metal complexes with **13** and **14** do not display fluorescence emission, due to the presence of amine groups not involved in metal coordination.

The dinuclear Zn^{2+} complex with macrocycle **14** shows remarkable hydrolytic ability for bis-(*p*-nitrophenyl) phosphate (BNPP), due to the simultaneous presence within this complex of two metal centers and two hydrophobic units. In fact, the two Zn^{2+} ions act cooperatively in substrate binding, probably through a bridging interaction of the phosphate ester; the interaction is further reinforced by π -stacking pairing and hydrophobic interactions between the phenanthroline unit(s) and the *p*-nitrophenyl groups of BNPP. [49d]

Ligand **15** bearing two naphthalene and two phenanthroline units was investigated in the presence of transition metals such as Cu^{2+} and Zn^{2+} (Figure 9). [50] The fluorescence emission spectra of **15** show the simultaneous presence of three bands: a short wavelength emission band (naphthalene monomer), a middle emission band (phenanthroline emission) in addition to a long-wavelength band. All three bands were found to be dependent on the protonation state of the macrocyclic unit (including the aliphatic polyamine and phenanthroline moieties). The long wavelength emission was analysed in great detail and it was attributed to an intramolecular interaction between a ground state phenanthroline and an excited state phenanthroline, suggesting that phenanthroline can give rise to excimer emissions. [50] The excimer formation is dramatically increased in the presence of Zn^{2+} and decreased with Cu^{2+} . It is shown that depending on the metal the long-emission band presents a different wavelength maximum, which can be considered as a characteristic to validate the ligand **15** as a fluorescent chemosensor for a given and specific metal.

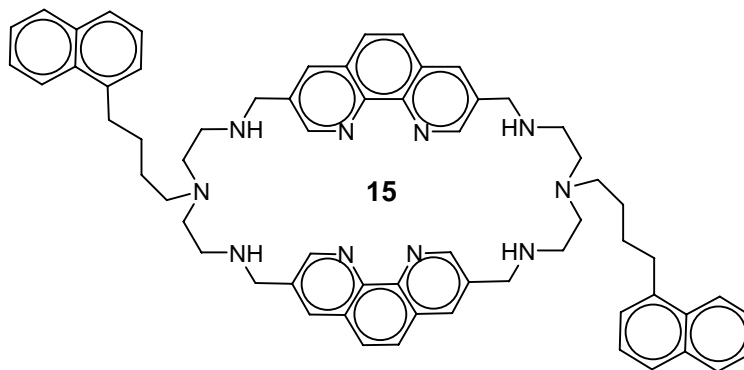
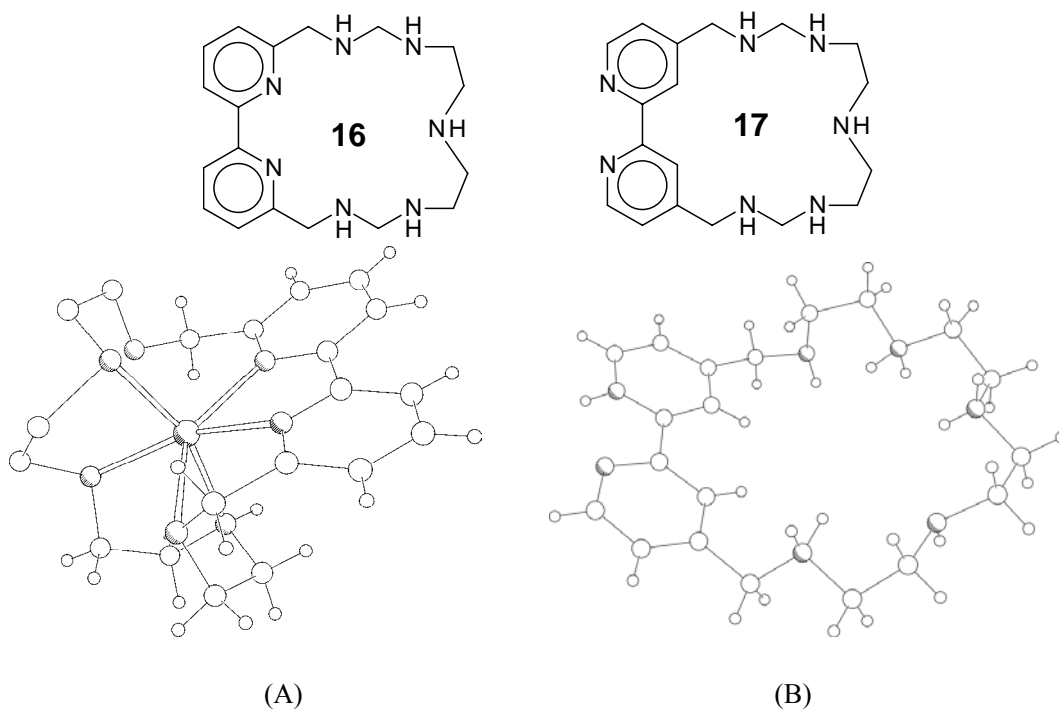


Figure 9.

Figure 10. **16**; **17**; (A) $[\text{Zn16}]^{2+}$; (B) $(\text{H}_4\text{17})^{4+}$.

A more flexible emissive chromophore such as bipyridine was used to synthesize compounds **16** and **17** (Figure 10) [51]. In the former the disposition of the heteroaromatic and aliphatic nitrogen donors is convergent towards the macrocyclic cavity, while in the latter two aromatic nitrogens point outside the cavity.

A crystal structure of the tetraprotonated species $(\text{H}_4\text{17})^{4+}$ (Figure 10B) shows two well-separated binding zones, the macrocycle cavity and the external dipyrindine units. The crystal structure of the complex cation $[\text{Zn16}]^{2+}$ (Figure 10A) indicates that the metal is coordinated inside the cavity bound to the heteroaromatic nitrogen donors and to the three amines of the aliphatic chain. The benzylic nitrogens are not involved in the bonding; facile protonation of

these two nitrogens takes place at acidic pH values and by consequence this species is the one exhibiting the largest fluorescence emission. In the case of the mononuclear Zn^{2+} complex of compound **17**, the metal is encapsulated inside the cavity, not coordinated by the dipyridine unit. Protonation of the complex occurs on the aliphatic polyamine chain and gives rise to a translocation of the metal outside the cavity, bound to the heteroaromatic nitrogens (Figure 11).

Similar effects have also been reported for Cu^{2+} and Ni^{2+} with macrocycle **17** but in both cases a non emissive species was observed. In Figure 12 are represented the X-ray structure of the Cu^{2+} and Ni^{2+} complexes of ligand **16** [52]. In both cases the metal ion is encapsulated into the macrocyclic cavity, similarly to what was observed in $[\text{Zn}\mathbf{16}]^{2+}$ (Figure 10A).

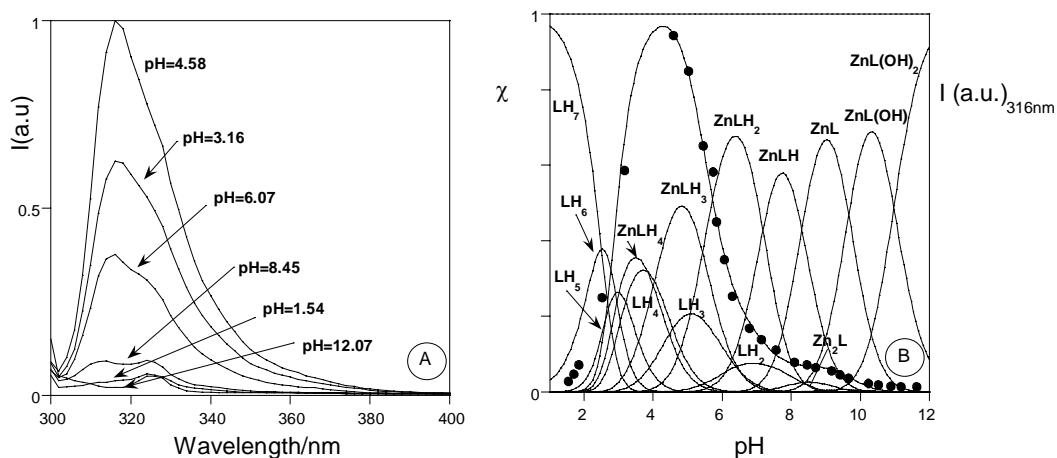


Figure 11. (A) Fluorescence emission spectra of the $\text{Zn}(\text{II})$ complexes with **16** at different pH values ($\lambda_{\text{exc}} = 293 \text{ nm}$). (B) Fluorescence emission (\bullet) and molar fractions of the protonated and complexed species of **16** (dashed lines) in the presence of $\text{Zn}(\text{II})$ (1:1 molar ratio) as a function of pH.

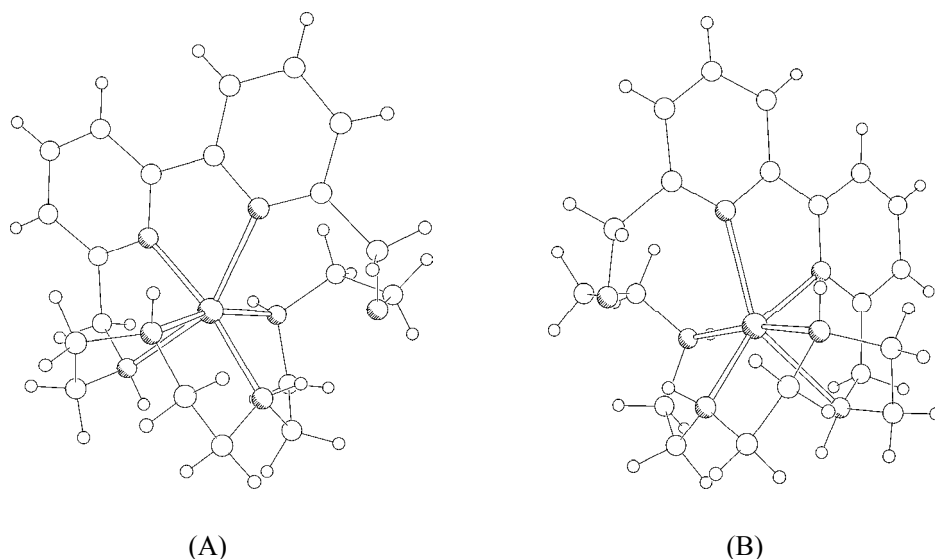


Figure 12. (A) $[\text{Ni}\mathbf{16}]^{2+}$; (B) $[\text{Cu}\mathbf{16}]^{2+}$.

Macrocyclic ligand **18** containing a terpyridine unit was reported (see Figure 13). [53] Several studies in water solution (potentiometric, ¹H NMR, UV-vis spectrophotometric and fluorescence emission) showed that the first four protonation steps in ligand **18** occur on the polyamine chain, while the terpyridine nitrogens are involved in proton binding only in the last protonation step at strongly acidic pH values. Mono and dinuclear complexes with Cu²⁺, Zn²⁺, Cd²⁺ and Pb²⁺ are formed in solution. Cu²⁺ and Zn²⁺ can form both mono and dinuclear complexes in solution, while the larger Cd²⁺ and Pb²⁺ give only mononuclear complexes. In the [M**18**]²⁺ complexes (M = Zn²⁺ or Cd²⁺) the metal is unequivocally bound to the terpyridine unit. Crystal structures were obtained and show two [M(H**18**)]³⁺ units coupled by a bridging OH⁻ or Br⁻ anion (Figure 14). In both complexes, a π -stacking interaction between the terpyridine moieties helps stabilizing the systems. A potentiometric and spectrophotometric study showed that, in the case of Cu²⁺ and Zn²⁺, the dimeric assemblies are also formed in aqueous solution containing the ligand and the metals in 1:1 molar ratio. Protonation of the complexes or addition of a second metal ion leads to disruption of the dimers, due to the increased electrostatic repulsions between the two monomeric units. [53]

The fluorescence emission of compound **18** is also strongly affected by metal coordination. Figure 13A and 13B reports the pH dependence of the fluorescence emission spectra recorded on solutions containing the ligand and Zn²⁺ in 1:1 molar ratio. The comparison of the fluorescence emission intensity of the ligand **18** in absence and in presence of Zn²⁺ (Figure 13B) clearly shows an increase of the fluorescence emission in the presence of the metal in the acidic pH region, where the [Zn(H₃**18**)]⁵⁺ complex is formed. A similar behavior is also found in the case of Cd²⁺, where only the [Cd(H₂**18**)]⁴⁺ complex is emissive.

2.1. Sensing Effects

Macrocyclic ligands like compound **17** containing endotopic cavities and exotopic coordination sites can be used as ligands in the construction of water soluble fluorescent metal complexes. These coordination compounds can operate as luminescence chemosensors based on the emission intensity as well as in long lifetime measurements-based sensing (life time of species in solution) for cations and anions.

As could be expected, coordination ability of **19** (Figure 15) towards Zn²⁺ and Cu²⁺ is reduced in comparison with the parent ligand **17** due to the electrostatic repulsion brought by the ruthenium core. The absorption and emission of the mononuclear Zn²⁺ complexes with **19** is only slightly red-shifted relative to the non-complexed compound **17**. While Cu²⁺ is also able to form dinuclear species, ligand **19** does not display a great tendency to bind the second metal. In this case the emission shows a dramatic quenching upon coordination to the metal. The quenching of the emission of [Ru(bpy)₃]²⁺ by polyamine complexes of Cu²⁺ ion was previously described by Moore and Alcock and attributed to energy transfer from the excited state of {[Ru(bpy)₃]²⁺}^{*} to the copper complex, promoting a d-d transition of Cu²⁺. [54]

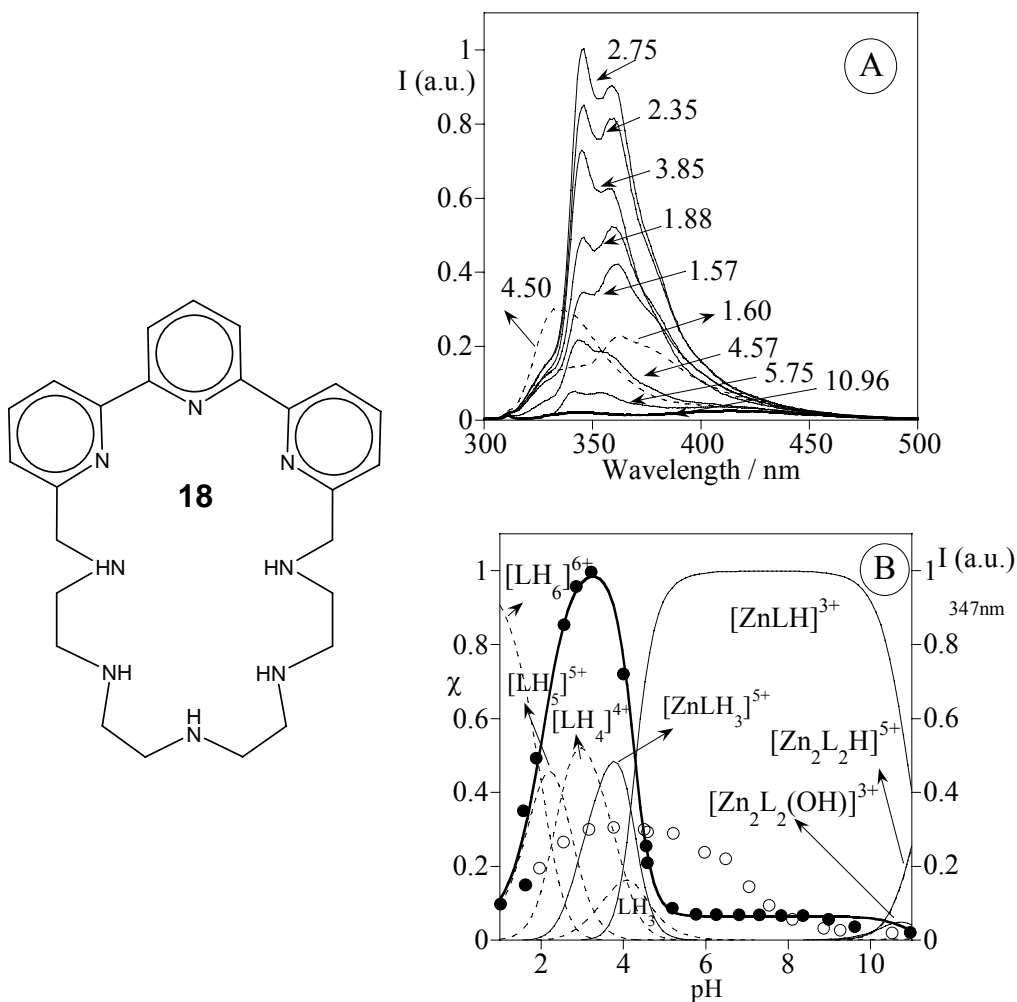


Figure 13. (A): Fluorescence emission spectra of the Zn^{2+} complexes with **18** at different pH values ($\lambda_{\text{exc}} = 282$ nm). (B): fluorescence emission at 347 nm of **18** in the absence (o) and in the presence of Zn^{2+} (1:1 molar ratio) (•) and molar fractions of the protonated (dashed lines) and complexed species of **18** as a function of pH.

An interesting effect was the possibility of exploring the cavity of the macrocycle in **19** as a photocatalytic center capable to host substrates amenable to react upon electron or energy transfer involving the metal center. [55]

An example of this photocatalytic effect is the adduct formed between compound **19** and iodide (See Figure 16). [55]. Excitation of compound **19** in the MLCT band allows the transfer of one electron from I^- to the Ru^{2+} complex, leading to the formation of an iodine radical and reduced Ru^{2+} complex (the electron goes to one of the bpy moieties). The iodine radical gives I_3^- as a final product by a sequence of well known reactions. [56] The cycle is completed by re-oxidation of the reduced bpy moiety of the complex by dioxygen.

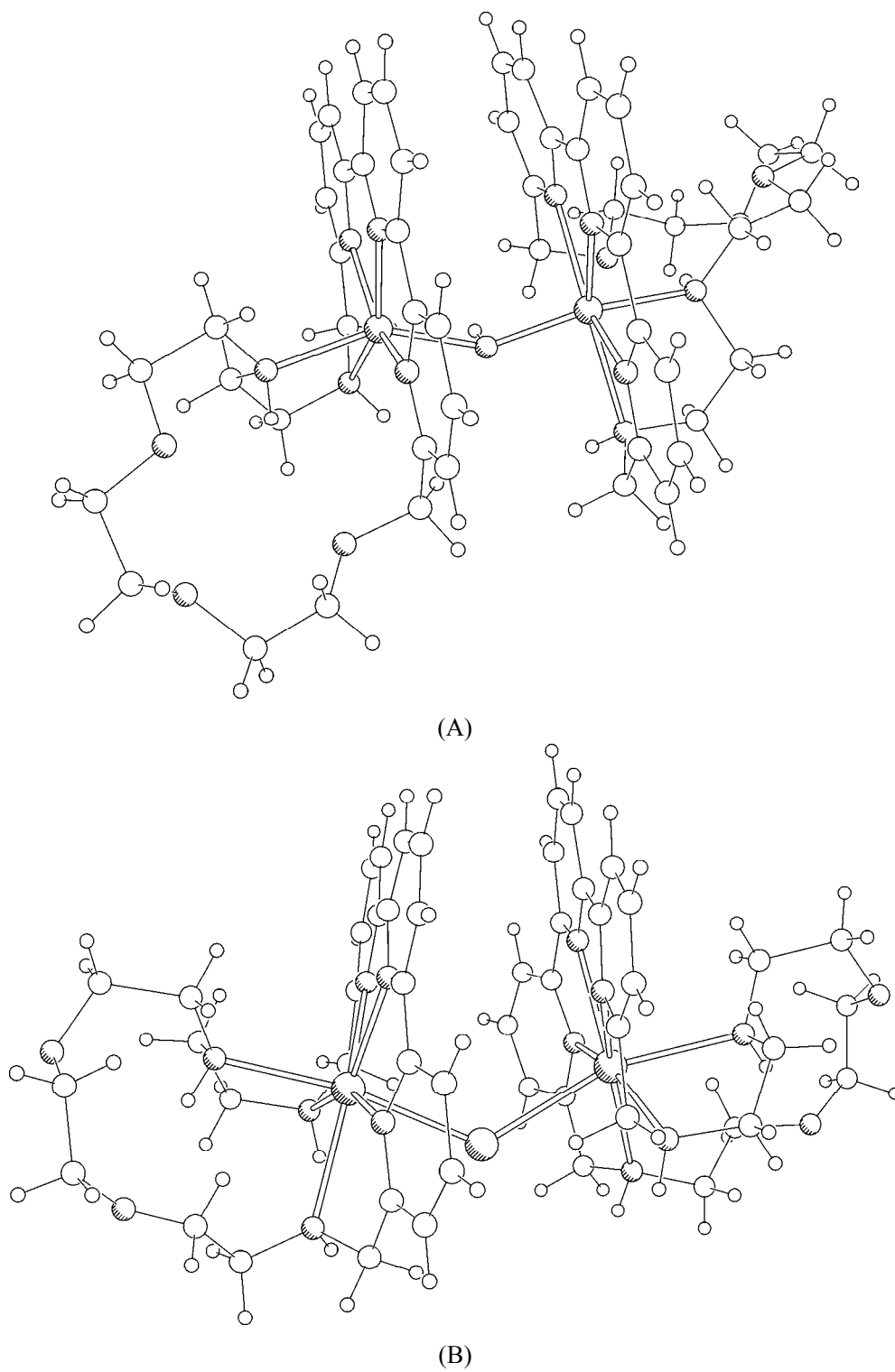


Figure 14. (A) $\{[\text{Zn}(\text{H18})]_2(\mu\text{-OH})\}^{5+}$; (B) $\{[\text{Cd}(\text{H18})]_2(\mu\text{-Br})\}^{5+}$.

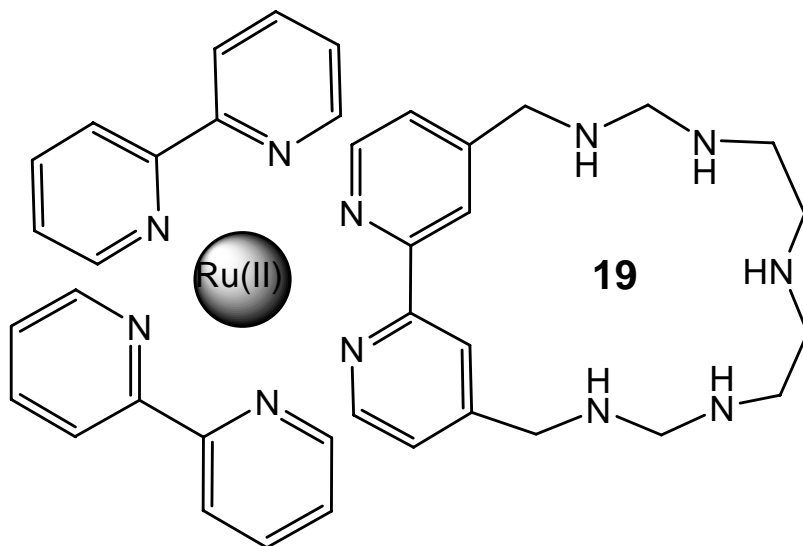
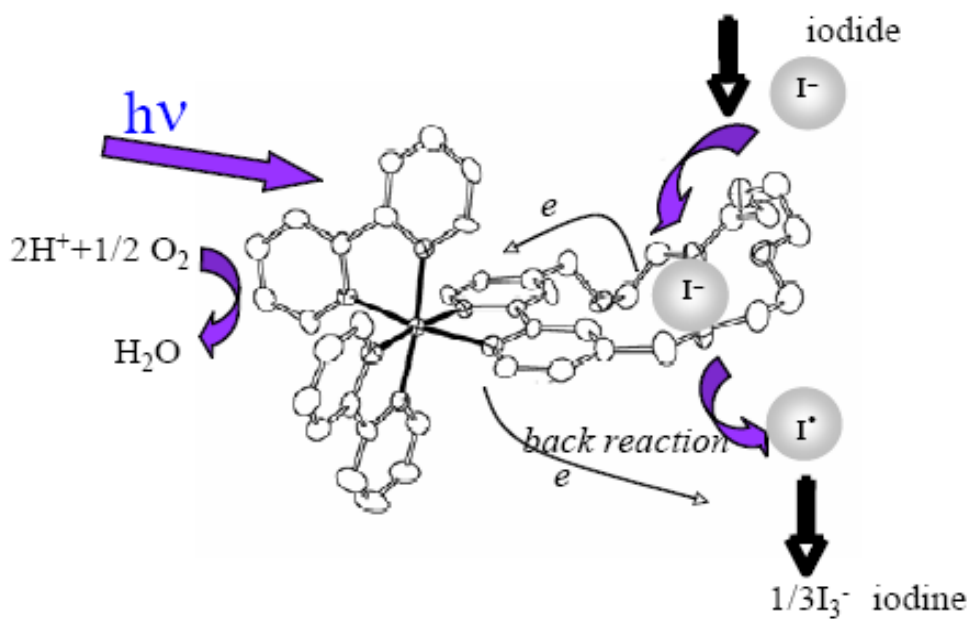


Figure 15.

Figure 16.- Photocatalytic cycle for the oxidation of iodide to iodine by dioxygen by **19**.

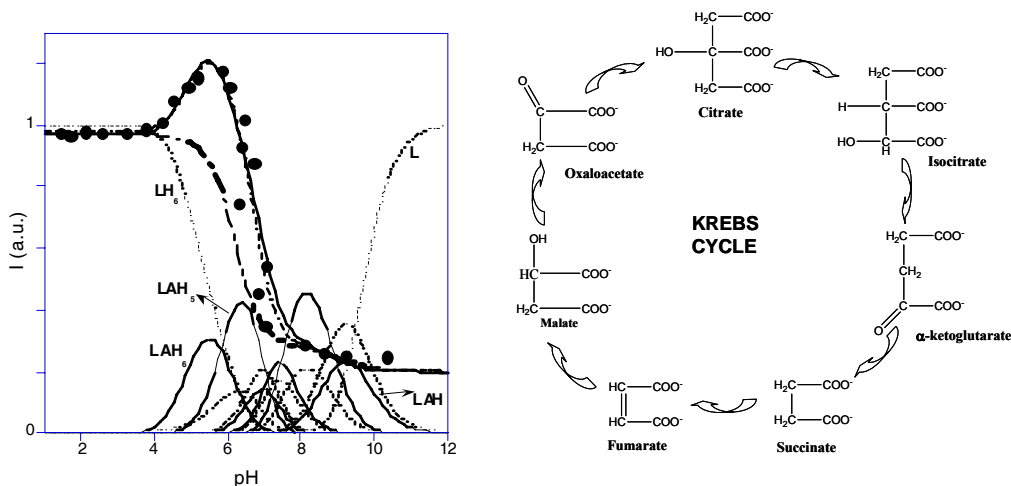


Figure 17. Fluorescence emission titration curves of **6** in water, in the presence of citrate. The other components of the Krebs cycle do not affect the fluorescence of the free compound **6**, trace-point line.

The relatively low efficiency of this system (0.35 in solution saturated with dioxygen) can be attributed to the fact that only 5% of the excited state can be quenched by iodide. In addition there is evidence, from preliminary flash photolysis experiments, that the back reaction from the reduced Ru^+ complex to I_3^- is a competitive process that decreases the net formation of photo-products.

It is well known that macrocyclic polyamines in their protonated forms are efficient receptors of anionic species in solution. [57] In particular very stable adducts are formed with cyanide complexes such as $[\text{Fe}(\text{CN})_6]^{4-}$ and $[\text{Fe}(\text{CN})_6]^{3-}$, principally due to the high negative charge of such anions. [58-62] Compound **19** contains the basic ruthenium sensing unit, and in addition possesses an extra binding polyamine receptor, that can be protonated and, therefore, it is expected to influence the overall process, improving the efficiency in anion sensing. The interaction between compound **19** with $[\text{Fe}(\text{CN})_6]^{4-}$ and $[\text{Fe}(\text{CN})_6]^{3-}$, was studied by the Stern-Volmer plots of the fluorescence intensity (I_0/I) and lifetimes (τ_0/τ) and compared with the behaviour of $[\text{Ru}(\text{bpy})_3]^{2+}$, in identical conditions. The studies were carried out at $\text{pH}=4$ and at this pH value the polyamine of compound **19** is tetra-protonated $(\text{H}_4\mathbf{19})^{4+}$. The quenching process observed was essentially dynamic in both cases studied.

Another interesting example of anions sensing was reported with compound **6** (Figure 2). Among the Krebs cycle components, just citrate enhances the fluorescence of this compound, see Figure 17. [63]

The main species responsible for the enhancement of the emission of compound **6** in the presence of citrate are $\{(\text{H}_6\mathbf{6})\text{A}\}^{2+}$ and $\{(\text{H}_5\mathbf{6})\text{A}\}^{2+}$ ($\text{A} = \text{citrate}$) and it was proved that citrate

García-España, E; Micheloni, M; Paoletti, P; Bianchi, A. *Inorg. Chim. Acta*, 1985 102, L9-L11.

Bencini, A; Bianchi, A; García-España, E; Giusti, M; Mangani, S; Micheloni, M; Orioli, P; Paoletti, P; *Inorg. Chem.*, 1987, 26, 3902-3907.

Aragó, J; Bencini, A; Bianchi, A; Domenech, A; García-España, E. *J. Chem. Soc., Dalton Trans.*, 1992, 319-324.

is the anion better suited for forming hydrogen bonds with the arms of compound **6** thus enhancing the fluorescence.

2.2. Antenna Effect

The photophysical properties of the rare-earth complexes of Eu^{3+} and Tb^{3+} , and the Ru^{3+} complexes with dipyrindine containing cryptands, such as compound **20** (Figure 18), have been extensively studied in the past few years. [64, 66]

Encapsulation of Eu^{3+} inside this type of ligands allows overcoming the drawback of the extremely low absorption coefficient of the un-complexed rare-earth metal, the so-called antenna effect. Cryptands are capable not only to efficiently bind to the metal, but also to protect it from the solvent, especially in aqueous solution where coordinated water is an efficient quencher of the emission.

Cryptand **21** was synthesized in order to contain a coordinative cleft as potential binding site for metals. [67] However, the most significant difference from previously reported cryptands, such as compound **20**, is the presence of an aliphatic polyamine chain which can easily bind protons in aqueous solutions. These structural features make compound **21** an appropriate ligand for simultaneous Eu^{3+} and H^+ binding.

As expected, the luminescence spectrum of the Eu^{3+} cryptate in aqueous solution at $\text{pH}=6.8$, in the absence of chloride, shows the characteristic visible emission of the metal with a maximum at 617 nm, upon excitation at 306 nm. The emission from the metal upon excitation of the ligand was previously observed for many other Eu^{3+} cryptate complexes. The observed emission from Eu^{3+} can thus be explained by an intramolecular energy transfer to the metal ion mainly from the higher energy triplet state of the cryptand.

2.3. Nucleotide Recognition

Nucleotide recognition and sensing in water is an important challenge in supramolecular chemistry due to its many biological implications. One of the most important anions is the ATP because it plays a basic role in the bioenergetics of all living organisms, the center for chemical energy storage and transfer being its triphosphate chain. As a consequence, many papers have been published regarding the interaction of ATP with abiotic systems, in particular those with polyamine based sensors which were described above. [68]

In Nature, ATPases hydrolyze ATP only in the presence of softer metal cations such as Ca^{2+} , Mg^{2+} , Zn^{2+} . The metal is involved in the catalytic mechanism, acting as binding site for ATP or as cofactor, favouring the phosphoryl transfer process.[69]

(a) Rodriguez-Ubis, JC; Alpha, B; Plancherel, D; Lehn, JM. *Helv. Chim. Acta*, 1984, 67, 2264-2269.

(b) Alpha, B; Lehn, JM; Mathis, G. *Angew. Chem. Int. Ed. Engl.*, 1987, 26, 266-267.

(c) PaulRoth, CO; Lehn, JM; Guilheim, J; Pascard, C. *Helv. Chim. Acta*, 1995, 78, 1895-1903.

In the mononuclear Zn^{2+} complex with ligand **18**, the metal is bound to the terpyridine nitrogens, the polyamine chain is not involved or weakly involved in metal binding and can easily be protonated in aqueous solutions to give $[\text{Zn}(\text{H}_x\mathbf{18})]^{2+x}$ complexes [53]; furthermore, a second Zn^{2+} ion can be coordinated affording dinuclear complexes (Figure 19). [70]

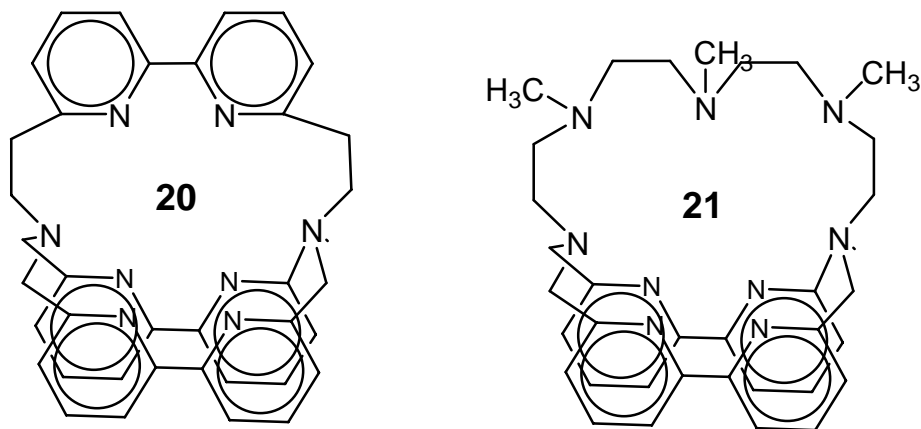


Figure 18.

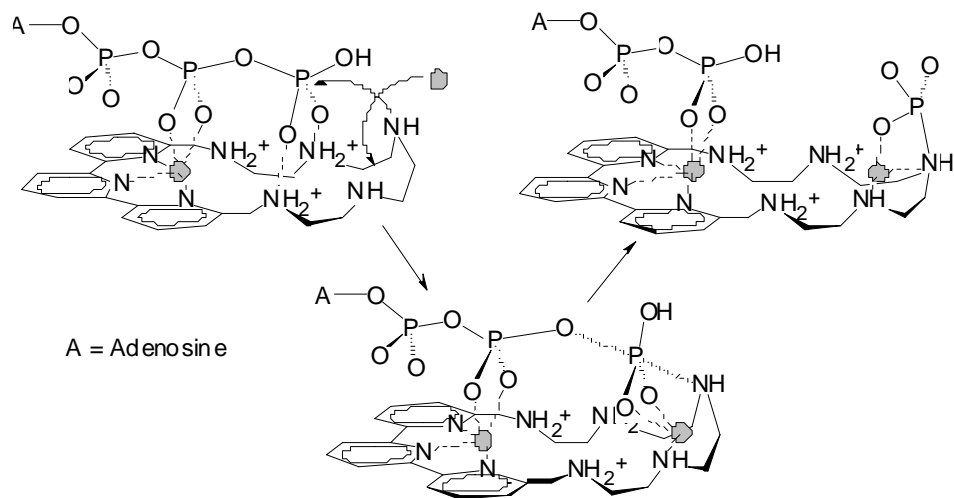


Figure 19. A Zinc(II)-based receptor featuring **18** for ATP binding and hydrolysis.

The protonated $[\text{Zn}(\text{H}_x\mathbf{18})]^{2+x}$ complexes, therefore, behave as multifunctional receptors for ATP, due to the simultaneous presence of metal-donor bonds, electrostatic and hydrogen bonding interactions and π -stacking pairing. The potentiometric study of this system shows that the Zn^{2+} complexes with **18** display a markedly higher affinity for ATP than the simple protonated species of the ligand **18** alone, confirming the crucial role of Zn^{2+} in ATP binding. The mononuclear Zn^{2+} complexes, however, do not show any significant ability in ATP hydrolysis. Addition of an equivalent of Zn^{2+} ion to solutions containing the mononuclear ternary complexes with ATP leads to the formation of dinuclear Zn^{2+} complexes with the nucleotide (See Figure 19). The second metal ion is coordinated to the polyamine chain

competing with protonation of the aliphatic amine groups. At this point, a fast cleavage process is observed by ^{31}P NMR at pH = 4, where the $[\text{Zn}(\text{H}_4\mathbf{18})\text{ATP}]^{2+}$ complex and the free Zn^{2+} are coexisting in solution.

The rate constants observed for the process $\text{ATP} \rightarrow \text{PN} + \text{ADP}$ fit the distribution curve of the tetra-protonated species $[\text{Zn}(\text{H}_4\mathbf{18})\text{ATP}]^{2+}$ species, with a maximum at pH 4 ($k_{\text{OBS}} = 3.2 \cdot 10^{-2} \text{ min}^{-1}$), thus indicating that this complex is the active species.

At pH 4, the phosphoramidate intermediate is formed, together with ADP, in the first few minutes up to a relatively high percentage (30%), compared with other polyammonium receptors able to hydrolyze ATP.

This system represents an unique case of ATP dephosphorylation promoted by the simultaneous action of a Zn^{2+} complex, which is used essentially for substrate anchoring, and of a second metal ion, which acts as cofactor, assisting the phosphoryl transfer from ATP to an amine group of the receptor.

3. OXA-AZA MACROCYCLES

In order to confer additional “hard” properties to the ligand and increase the range of metal ions to be complexed and detected, profit was taken from the introduction of oxygen atoms in the polyamine chain. [71] This strategy has however sometimes a drawback of rendering the chemosensor less soluble in water and by consequence some of the systems reported in this section were studied in organic solvents or mixtures of water/organic solvents.

With the collaboration of the group of R. Bastida the synthesis of a comprehensive family of macrocyclic ligands (See Figure 20) designed for metal complexation has been reported [72] and their interaction with lanthanide(III), transition metal ions, such as Cu^{2+} , Ni^{2+} , Co^{2+} , Mn^{2+} , post-transition metals Zn^{2+} , Cd^{2+} and the alkaline-earth Ca^{2+} were explored. In particular mono- and dinuclear complexes with ligands **22-30** were reported. No fluorescence emission was detected from all these ligands.

Reduction of the double C=N imine bonds to a C-NH amine bond, leads to more flexible structures, see Figure 21, and in some cases to the appearance of emissive properties, specially when a high emissive chromophore is linked as flexible pendant-arm. Similarly to what was observed for the polyamine receptors, protonation of the nitrogen atoms is a necessary requirement to observe the fluorescence but in these cases is not enough.

For example, the fully protonated form is not the most emissive species like happens in the polyamine systems due to the non-radiative decay involved in the hydrogen-bond formation between the oxygens and the protonated benzylic nitrogens. In this way in compound **31** (solid state) only one amine nitrogen atom is protonated, and the PET (photoinduced electron transfer) from the non protonated nitrogen prevents any emission. [72aa] Similar results were observed for macrocycles **32** and **34**.

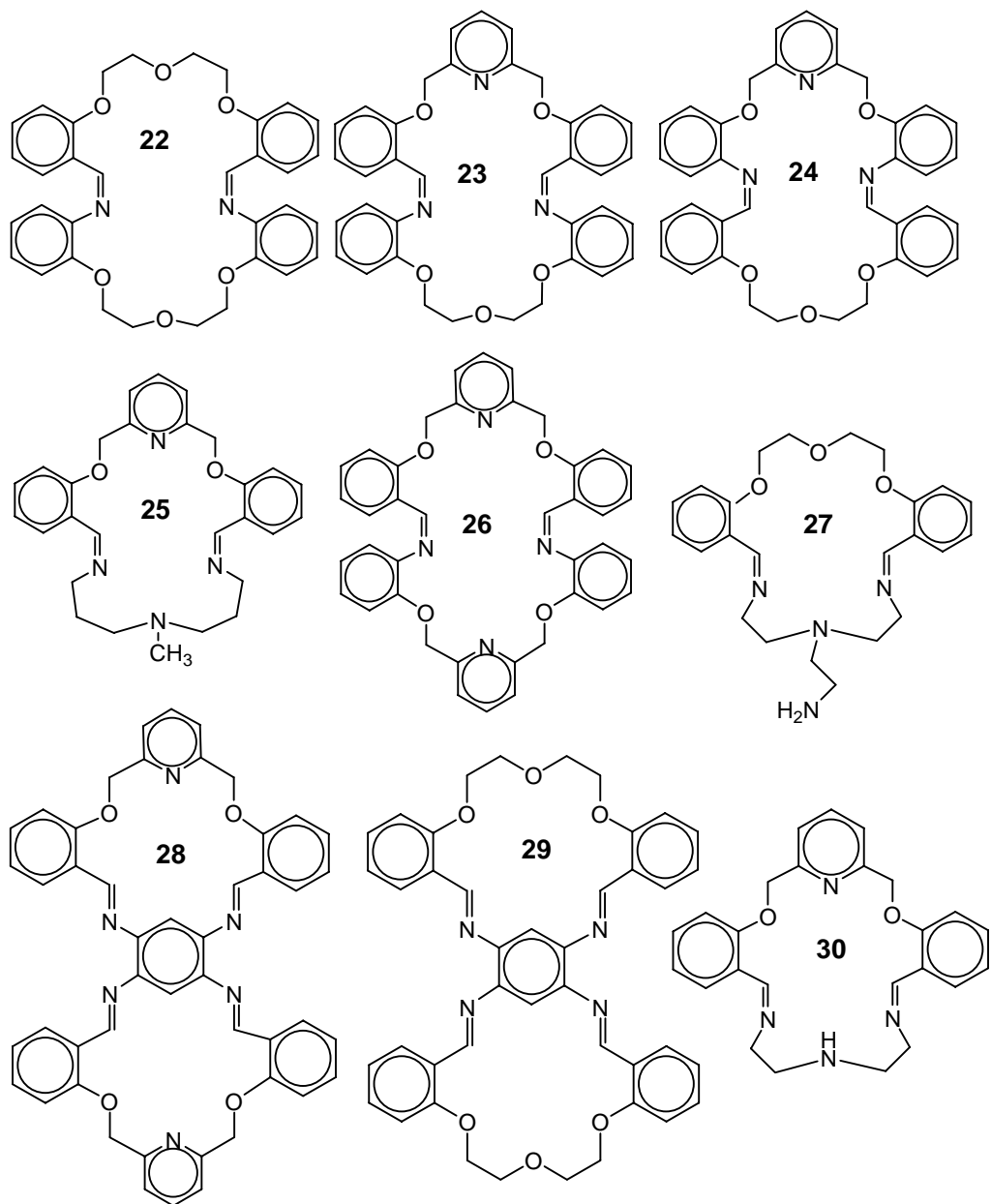


Figure 20.

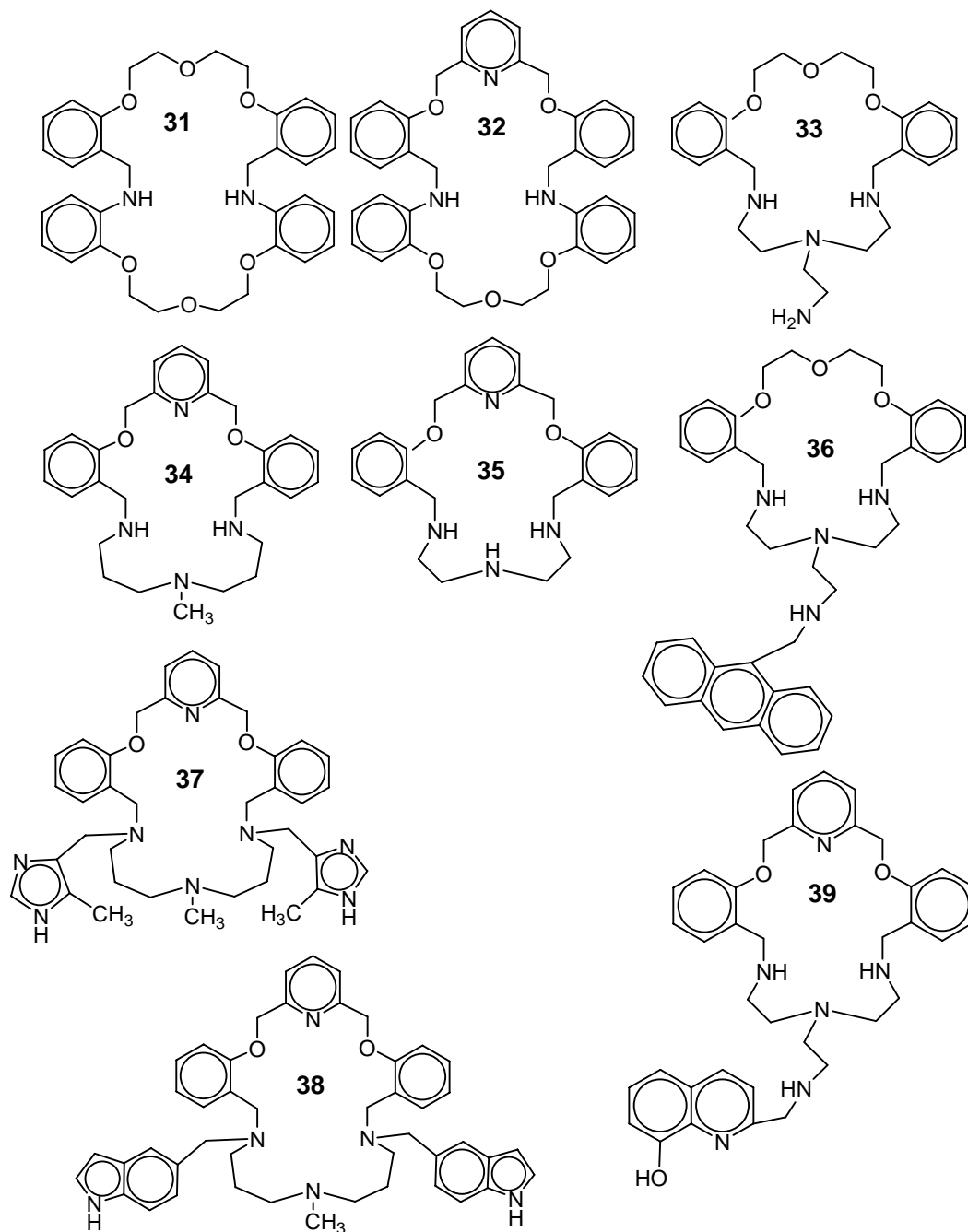


Figure 21.

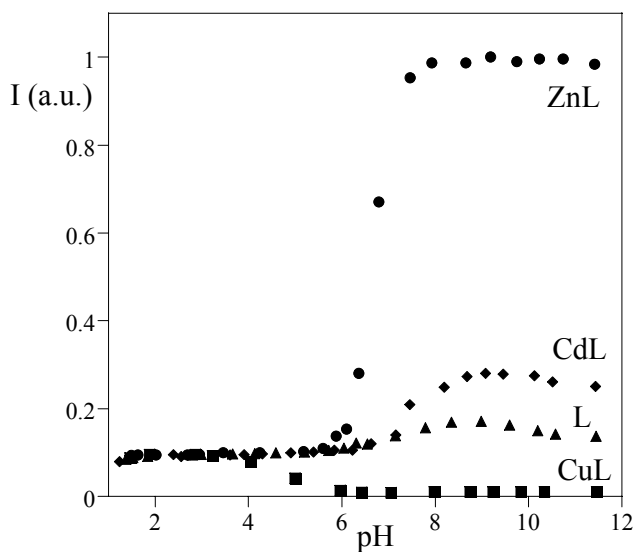
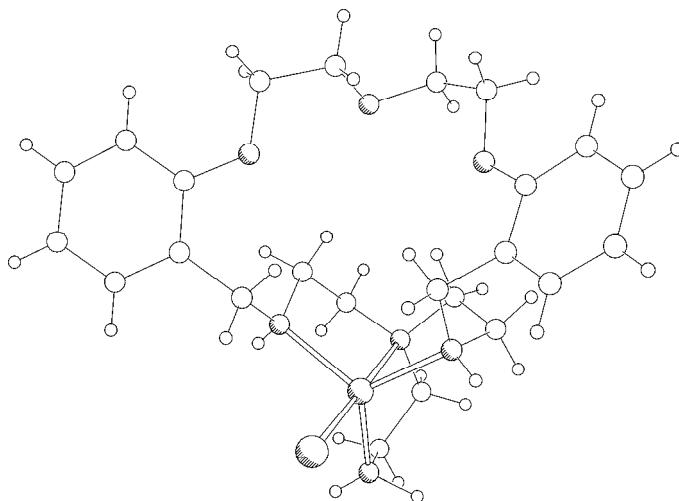


Figure 22. Fluorescence emission titration curves of **33** (▲) in the presence of equimolar amounts of Cu^{2+} (■), Cd^{2+} (◆) and Zn^{2+} (●). ($\lambda_{\text{exc}} = 275 \text{ nm}$, $\lambda_{\text{em}} = 303 \text{ nm}$).

Another example of the appearance of fluorescence upon reduction of the imine C=N bond to a C-NH amine bond was observed for compounds **27** and **33**. While compound **27** is not emissive in solution, compound **33** reveals fluorescence properties in water, see Figure 22.



(A)

Figure 23. (Continued).

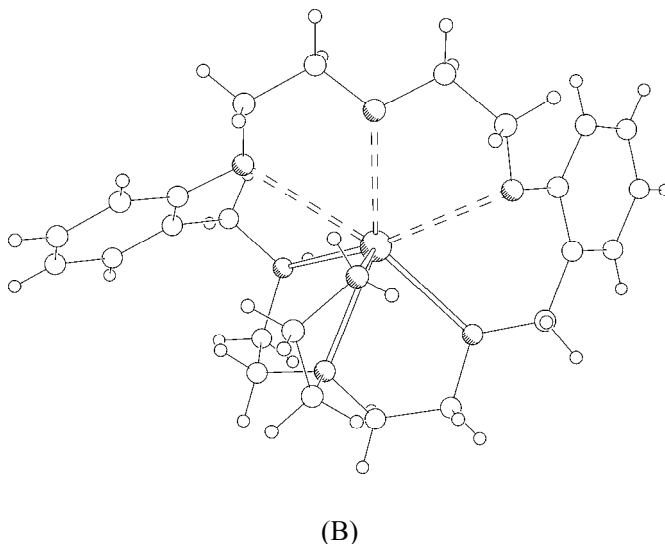


Figure 23. (A) $[\text{Zn}\mathbf{33}(\text{Cl})]^+$; (B) $[\text{Pb}\mathbf{33}]^{2+}$.

The binding properties of macrocyclic **33** towards Cu^{2+} , Zn^{2+} , Cd^{2+} and Pb^{2+} were studied by potentiometry, absorption and fluorescence spectroscopies. The behavior of this system is quite similar to the one reported for the polyamine based receptors. All the Cu^{2+} complexes species exhibit a strong CHEQ effect attributed to an energy transfer quenching of the π^* emissive state through low-lying metal-centered states. [73]

On the other hand, Zn^{2+} and Cd^{2+} complexes are emissive species leading to a CHEF effect. Figure 22 compares the titration curves of **33** in the absence and in the presence of three different cations in order to evaluate the chemosensor ability of the ligand towards Cu^{2+} , Zn^{2+} and Cd^{2+} .

The titration curves of these metals exhibit different fluorescence responses for $\text{pH} \geq 4$, and below this value only protonated forms of ligand **33** are present in solution. The fluorescence of ligand **33** in the presence of alkaline and alkaline-earth metals and some transition metal ions such as Co^{2+} , Ni^{2+} and Hg^{2+} were also studied. Only small changes on the fluorescence intensity took place, except for Co^{2+} and Hg^{2+} for which a CHEQ effect similar to Cu^{2+} was achieved.

It is worth of note that the enhancement of fluorescence in the presence of Zn^{2+} is almost independent of a huge excess of Li^+ , K^+ , Mg^{2+} and Ca^{2+} (up to 1:100). The increase observed in the fluorescence emission upon Zn^{2+} complexation can be enlightened from the type of coordination of this metal. Figure 23A shows the X-ray structure of the complexes $[\text{Zn}\mathbf{33}(\text{Cl})]^+$. The crystal structure shows that the metal ion is coordinated by all nitrogen atoms presents in the ligand preventing the PET quenching effect. On the other hand coordination with Pb^{2+} to all the donor-atoms present shows a strong quenching effect (Figure 23B).

In order to separate the binding function from the signaling function an anthracene pendant-arm was introduced in ligand **33**, see ligand **36**. [74]

This strategy allows obtaining a chemosensor exhibiting a more intense and red-shifted fluorescence emission. In this case the interaction with Al^{3+} and Cr^{3+} in methanol or

water/methanol solutions was studied and a CHEF effect, leading to an increase of 1.80-folds for Al^{3+} and 2.0-fold for Cr^{3+} was observed. See Figure 24.

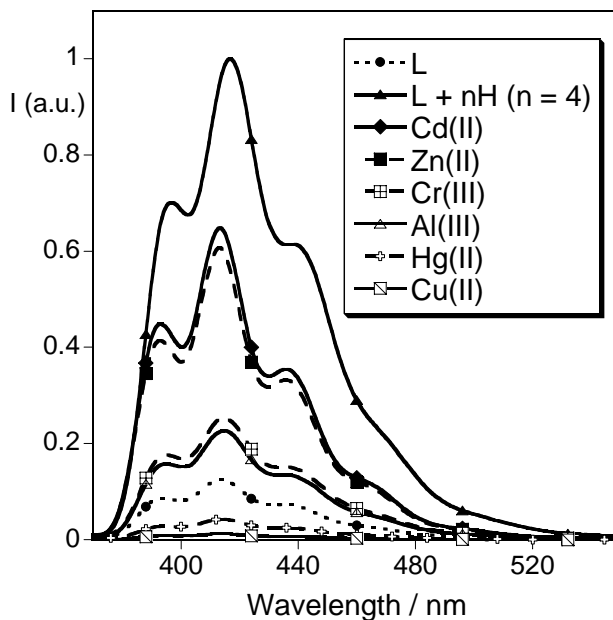


Figure 24. Fluorescence emission spectra of methanol solutions of **36** in the presence of 1 equiv. of $\text{Zn}(\text{NO}_3)_2$, $\text{Cd}(\text{NO}_3)_2$, $\text{Cr}(\text{NO}_3)_3$, AlCl_3 , $\text{Hg}(\text{CF}_3\text{SO}_3)_2$ and $\text{Cu}(\text{CF}_3\text{SO}_3)_2$. ($\lambda_{\text{exc}} = 367 \text{ nm}$).

The interaction with the same metal ions studied with ligand **36** was explored using ligand **39** and its family. [75] An 8-hydroxyquinoline was introduced as emissive pendant-arm in the ligand in order to have the emission band in the visible region (555 nm). Addition of Zn^{2+} and Cd^{2+} to ligand **39** gave the mononuclear emissive complexes followed by an increase in the fluorescence intensity, CHEF effect. (see figure 25). With the complexation of Al^{3+} , Cr^{3+} and Cu^{2+} metal ions, the emission of the ligand was always quenched (CHEQ effect). [75]

Ligand **39** and its derivatives [75] also react with these metal ions in the gas phase. As an example, using dithranol as MALDI-TOF-MS matrix, addition of Zn^{2+} or Al^{3+} to **39** confirms the formation of the mononuclear complexes.

Macrocyclic ligand H_2 **40** possessing two carboxylic-acid as pendant-arms was studied in acetonitrile, water and mixtures of water/acetonitrile solutions. [76] The ligand is non-emissive in solution as well in the presence of several metal ions such as alkaline, alkaline-earth and transition metals. [76] However, similarly to what was observed for polyamine **21**, the characteristic visible emission bands from complexes of Eu^{3+} and Tb^{3+} in water at 618 and 586 nm respectively were observed, upon excitation at *ca.* 270 nm. Coordination with Zn^{2+} reveals the presence of a polymeric non-emissive material in which the metal ion is coordinated by the both pendant-arms and the nitrogen donor atoms present in the ligand. (See figure 26)

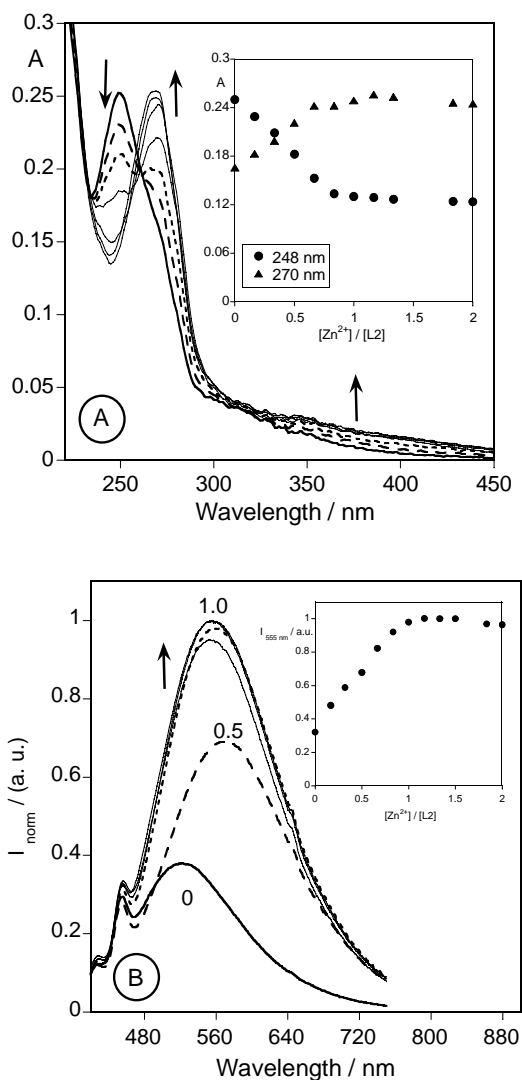


Figure 25. Absorption (A) and fluorescence emission (B) titration of absolute ethanol solutions of **39** as a function of increasing amounts of Zn^{2+} ions. The inset shows the absorption at 248 and 270 nm, and the normalized fluorescence intensity at 555 nm.

Ligands **41** to **45** were designed using as building block a 15-crown-5 unit as macrocyclic ligand. [77] (Figure 27).

In the case of ligand **41**, and similarly to other Schiff-base macrocycles, no fluorescence emission was detected for the free ligand or after complexation with metal ions. In contrast, compound **42** in acetonitrile/water solution shows a fluorescence emission band centered at 365 nm, attributed to the 15-benzocrown-5 moiety. [77aa] This emission is quenched by Cu^{2+} , Pb^{2+} and Al^{3+} complexation as it was previously observed in the parent ligand, 15-benzo crown-5, with alkaline ions.[78]

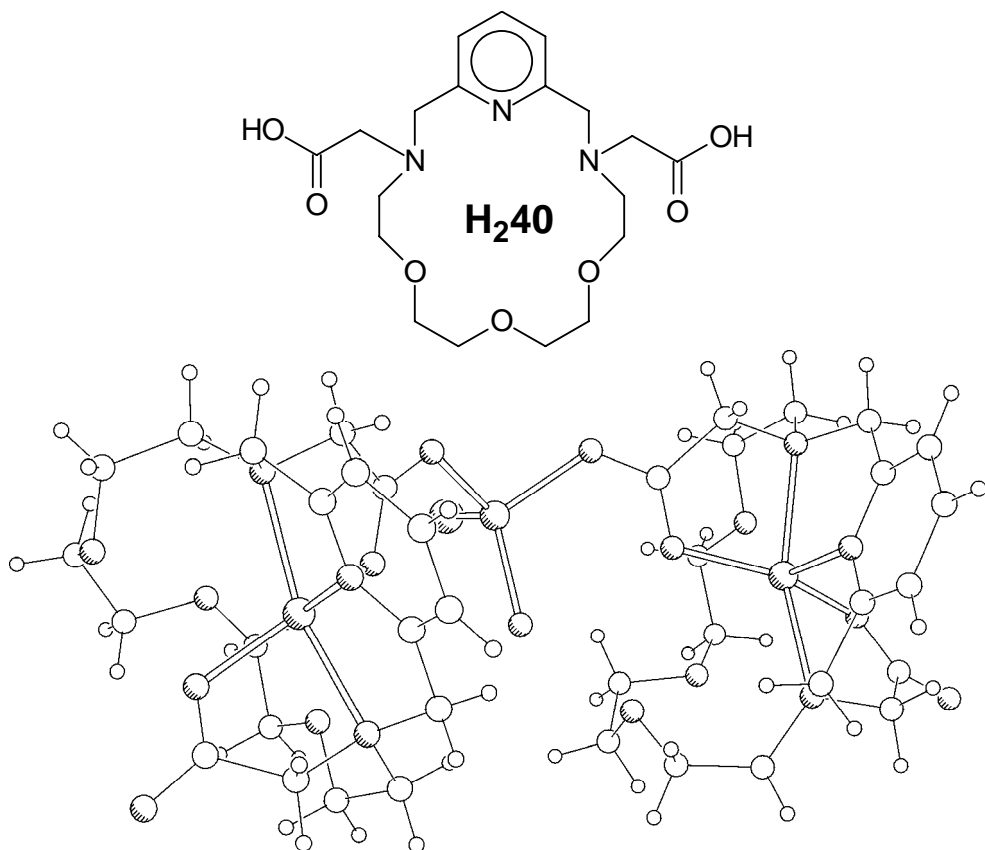
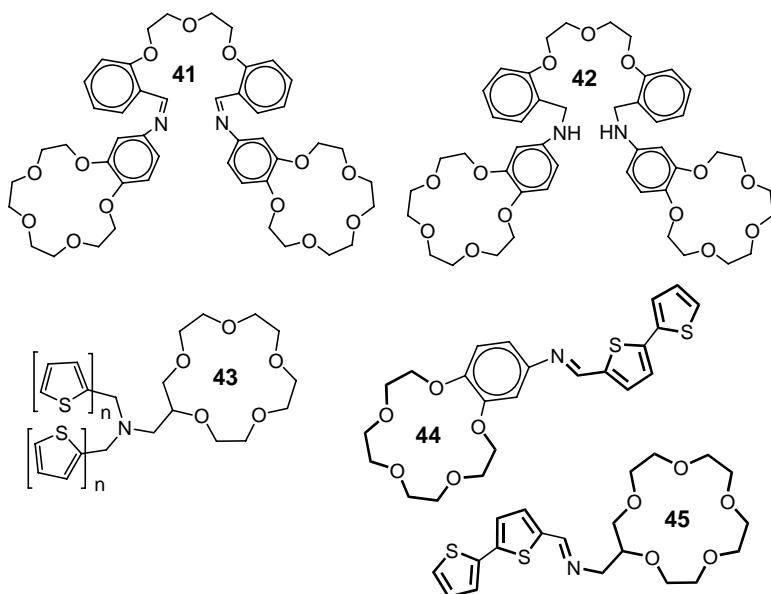
Figure 26. **40**; partial view of $\{[Zn_2(\mathbf{40})(Cl)(H_2O)]^+\}_\infty$.

Figure 27.

Interesting colour changes in the absorption spectra from yellow to blue-violet (absorbance at 590 nm), were observed upon Cu^{2+} complexation with **41** or **42**. In the same conditions other transition metal ions studied (Zn^{2+} , Ni^{2+} , Co^{2+} , Cd^{2+} , Pb^{2+} and Al^{3+}) gave non significant effects, and thus **41** or **42**, could be used as a colorimetric chemosensor to determine the presence of Cu^{2+} in acetonitrile solution. For the complex $[\text{Cu41}]^{2+}$, the absorbance increase was linear up to 1.05×10^{-4} M, for $[\text{Cu42}]^{2+}$, the linearity in the absorption was up to 5.30×10^{-5} M.

Ligand **43** featuring an (oligo)thiophene bipendant-arm unit gave an emissive system when the number of thiophene units, n , was 2 or 3. The emission band observed was centered at 378 and 437 nm respectively. Addition of protons, sodium(I) or palladium(II) produced an increase in the fluorescence intensity emission being higher when Na^+ and Pd^{2+} were added simultaneously.

The effect of Ni^{2+} , Pd^{2+} and Hg^{2+} complexation on absorption, fluorescence and MALDI-TOF-MS spectra of ligands **44** and **45** were studied dissolving both ligands in acetonitrile and titrating with the metal ions. Ligand **45** proves to be useful as absorption and fluorescence molecular probe for Ni^{2+} , Pd^{2+} and Hg^{2+} . Addition of Ni^{2+} and Hg^{2+} induced a red shift of *ca.* 15 nm in the absorption spectra while Pd^{2+} showed a *ca.* 45 nm red-shift. At the same time a very strong emission was observed upon Pd^{2+} complexation. The intensity of emission observed upon Ni^{2+} and Hg^{2+} addition was very small when compared with the Pd^{2+} complex. This emission is not affected after the addition of an excess of Na^+ (up to 100 equivalents). Fluorescence titration of **45** is represented in Figure 28 upon excitation in the isosbestic point at 360 nm. Significant enhancement of the fluorescence intensity and a strong red-shift was observed upon addition of one equivalent of Pd^{2+} . Addition of the second equivalent of Pd^{2+} showed a partial quenching of the emission. The inset of Figure 28B depicts the emission at 410 nm (ligand band) and at 480 nm (complex band); this effect could be attributed to a conformational change in the position and involvement of the bithiophene chromophore in coordination to the metal center.

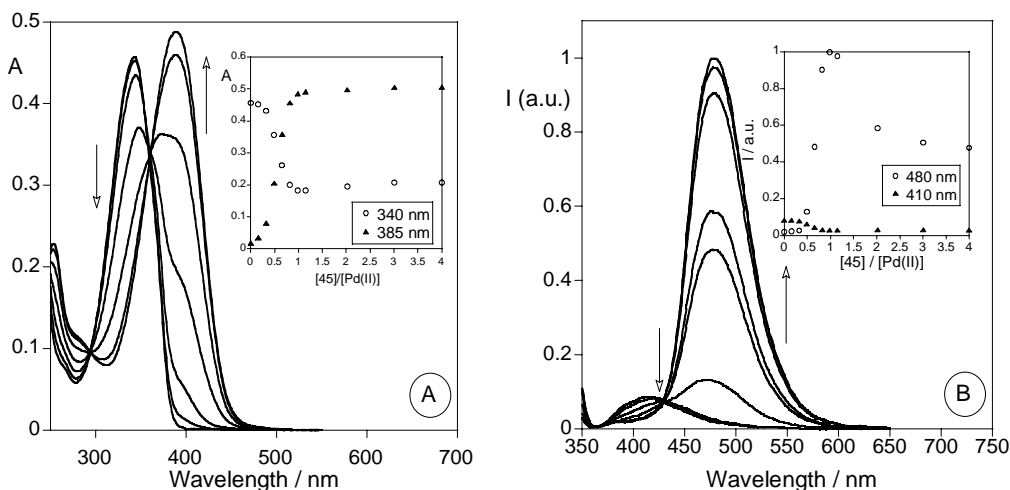


Figure 28. Absorption (A) and Emission (B) titration of **45** in the presence of Pd^{2+} after addition of an initial one equivalent of Na^+ in acetonitrile.

4. THIA-AZA MACROCYCLES

As already pointed out in the previous paragraphs, most of the reported fluoroionophores based on macrocyclic receptor units feature polyoxa-, polyaza, and aza/oxa-macrocycles as the guest binding site, whereas the potential of S- or mixed N/S-, and N/S/O-donating macrocyclic sites as selective receptors in fluorescent molecular sensors remains much less untapped, reflecting a general increased synthetic difficulty encountered in the preparation of this type of ligands. [79-82] On the other hand according to Pearson rule, the use of receptor units containing soft donors such as sulfur atoms in the design of fluorescent chemosensors, should allow, in principle, a better selective recognition and sensing of soft metal ions with marked thiophilycity. In this context, following our interest in both coordination chemistry of mixed thia-aza and thia-oxa macrocycles, and their analytical applications as selective ionophores towards heavy transition and post-transition metal ions, [83-89] we have synthesized and studied quite a good number of fluorescent chemosensors featuring sulfur atoms in the donor set of their macrocyclic receptor units. Our main aim was also to demonstrate the potential of the complementary strategy of linking different fluorophores to the same receptor unit (not necessarily the most selective in the binding process) trusting to a cooperation between the two in determining a substrate-selective response.

A systematic functionalization of the pyridine-based N₂S₂-donating 12-membered macrocycle **46** with pendant arms bearing different fluorogenic fragments was carried out, and the conjugated chemosensors **47-51** were synthesized (Figure 29). [90, 91]

Potentiometric studies in aqueous solution demonstrated that metal complexation of **46** occurs at acidic pH values to give [M**46**]²⁺ species and it is followed by the formation of mono hydroxo-complexes [M**46**(OH)]⁺ at alkaline pHs, at least in the case of Cu²⁺ and Hg²⁺. The formation constants of the 1:1 complexes [M**46**]²⁺ decrease in the order Hg²⁺ (10.68) > Cu²⁺ (10.05) > Cd²⁺ (9.12) > Pb²⁺ (8.45) > Zn²⁺ (7.13) (log K in parenthesis) with the Cu²⁺ and Hg²⁺ displaying the higher stability as generally observed in the complexes with polyamine ligands. Interestingly, and as contrary to expectation, the presence of S-donors in the macrocyclic framework, did not confer on **46** a marked thermodynamic selectivity towards any of the “borderline” and “soft” metal ions considered. [90]

Bronson, RT; Bradshaw, JS; Savage, PB; Fuangswasdi, S; Lee, SC; Krakowiak, KE; Izatt, RM. *J. Org. Chem.*, 2001, 66, 4752-4760.

Xue, G; Bradshaw, JS; Song, H; Bronson, RT; Savage, PB; Krakowiak, KE; Izatt, RM; Prodi, L; Montalti, M; Zaccheroni, N. *Tetrahedron*, 2001, 57, 87-91.

Shamsipur, M; Poursaberi, T; Rezapour, M; Ganjali, MR; Mousavi, MF; Lippolis, V; Montesu, DR. *Electroanal.*, 2004, 16, 1336-1342.

Shamsipur, M; Hosseini, M; Alizadeh, K; Mousavi, MF; Garau, A; Lippolis, V; Yari, A. *Anal. Chem.*, 2005, 77, 276-283.

Lippolis, V; Blake, AJ; Cooke, PA; Isaia, F; Li, WS., Schröder, M. *Chem. Eur. J.*, 1999, 5, 1987-1991.

Arca, M; Blake, AJ., Lippolis, V; Montesu, DR; McMaster, J; Tei, L; Schröder, M. *Eur. J. Inorg. Chem.*, 2003, 1232-1241.

Shamsipur, M; Hashemi, OR; Lippolis, VJ. *Memb. Science*, 2006, 282, 322-327.

The optical response of **47-49** to the presence of Hg^{2+} , Cu^{2+} , Cd^{2+} , Pb^{2+} or Zn^{2+} was studied in MeCN/ H_2O (4:1 v/v) solutions buffered at pH = 7, due to the scarce solubility of these ligands in other mixtures containing a higher content of water. [90] With **47**, where the anthracenyl moiety does not participate in the complexation process, no substrate-selective changes in the fluorescence emission were observed upon interaction with the metal ions considered.

In particular, with Cd^{2+} , Pb^{2+} , Zn^{2+} , the complexation processes led to a relevant enhancement of the fluorescence intensity (CHEF effect) of **47** ($\lambda_{\text{ex}} = 364$, $\lambda_{\text{em}} = 417$ nm) up to a $\text{M}^{2+}/\mathbf{47}$ molar ratio of 1. With Hg^{2+} and Cu^{2+} , a CHEF effect up to a $\text{M}^{2+}/\mathbf{47}$ molar ratio of 1, followed by a quenching of the luminescence intensity (CHEQ effect) for higher molar ratios was observed. [90] The presence of coordinatively active fluorogenic fragments in **48** and **49** resulted in different sensing performances. In fact, the former responded with the same efficiency only to the presence of Hg^{2+} or Cu^{2+} via a CHEQ effect ($\lambda_{\text{ex}} = 336$, $\lambda_{\text{em}} = 522$ nm), while the latter only to the presence of Cd^{2+} or Zn^{2+} via a CHEF effect ($\lambda_{\text{ex}} = 244$, $\lambda_{\text{em}} = 548$ nm), with a preference twice as much for Zn^{2+} . In all cases, inflection points in the spectrofluorimetric titrations curves indicated the formation of 1:1 complex species. [90]

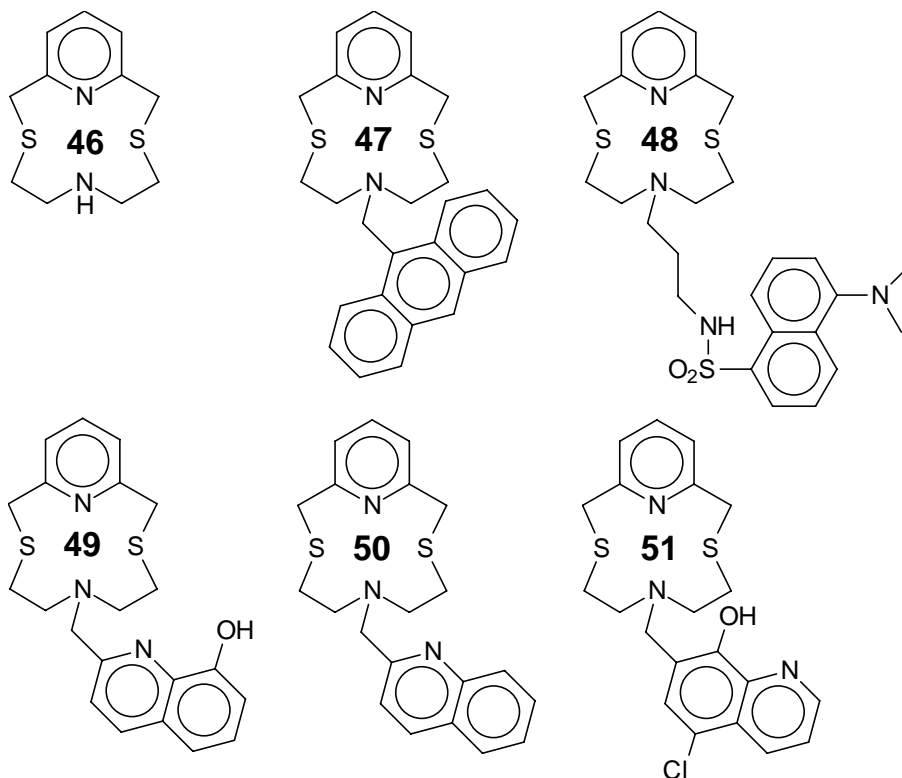


Figure 29.

From the complexation reaction of **49** with $\text{Zn}(\text{NO}_3)_2 \cdot 6\text{H}_2\text{O}$ in MeCN followed by diffusion of Et_2O vapor into the reaction mixture, single crystals of $[\text{Zn}\mathbf{49}](\text{NO}_3)_2 \cdot \text{MeNO}_2$ were grown suitable for X-ray diffraction analysis. The coordination environment around the metal center (Figure 30A) resembles that observed in $[\text{Zn}\mathbf{46}(\text{NO}_3)_2]$ (Figure 30B): four

positions of a distorted octahedral coordination sphere are occupied by the N_2S_2 -donor set of the macrocyclic framework, and the remaining two sites taken up by the donor atoms of the bidentate 8-hydroxyquinoline moiety; these sites in $[Zn46(NO_3)_2]$ are occupied by two monodentate nitrate ligands. In both complexes the macrocyclic framework adopts a similar folded conformation resembling an open book with the spine along the S-Zn-S direction and an N-Zn-N hinge angle very close to 90° . [90]

With **50** and **51**, which are very similar to **49** from a structural point of view (Figure 29), a much higher substrate-selective response was observed in terms of fluorescence intensity changes upon adding Hg^{2+} , Cu^{2+} , Cd^{2+} , Pb^{2+} or Zn^{2+} . [91]

50 and **51** resulted soluble in MeCN/ H_2O (1:1 v/v) and therefore, the binding properties of the two ligands were first studied potentiometrically in this solvent mixture. These studies were generally limited to the acidic pH region because of complex precipitation beyond neutral pH values. Only for the systems $Hg^{2+}/50$ and $Zn^{2+}/51$ the potentiometric measurements were carried out over a wider pH range. All metals form 1:1 complexes at acidic pH with both **50** and **51**. In the case of Zn with **51** the formation of species with a 1:2 metal-to-ligand stoichiometry is also observed. Presumably 1:2 species with the other metal ions are also formed but at higher pH values and are too insoluble to be detected potentiometrically. [91]

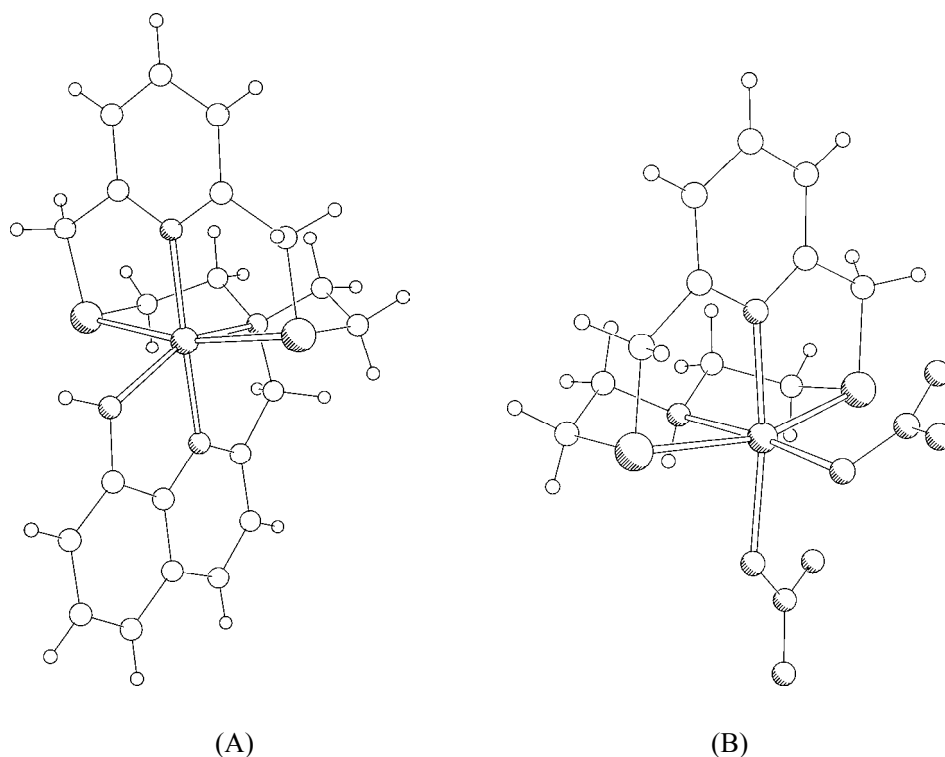


Figure 30. (A) $[Zn49]^{2+}$; (B) $[Zn46(NO_3)_2]$.

However, for both **50** and **51** the stability of the 1:1 complex species follow the same order of stability observed for the un-functionalised macrocycle **46**, but **51** forms slightly more stable 1:1 complexes than **50** with all metal ions considered. It is reasonable to suppose

that in all 1:1 complexes with both ligands the coordinating groups belonging to the fluorogenic fragment are involved in metal coordination. However, neither **50** nor **51** show a particular thermodynamic selectivity, they bind all metal ions considered with quite high formation constants of the corresponding 1:1 complexes. [91]

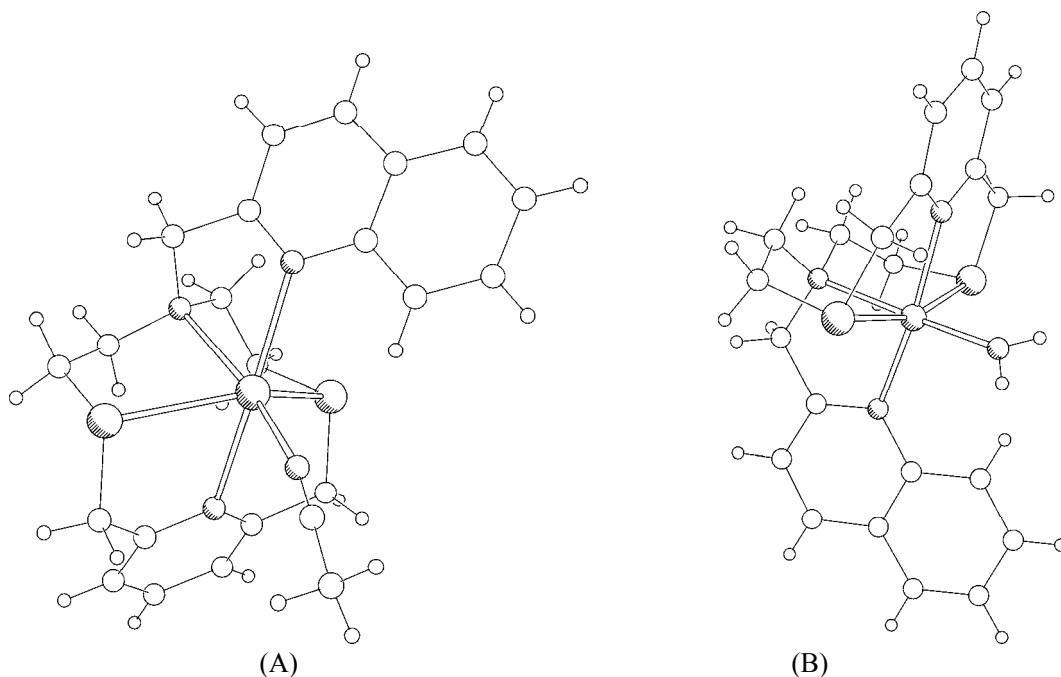


Figure 31. (A) $[\text{Hg}\mathbf{50}(\text{MeCN})]^{2+}$; (B) $[\text{Zn}\mathbf{50}(\text{H}_2\text{O})]^{2+}$.

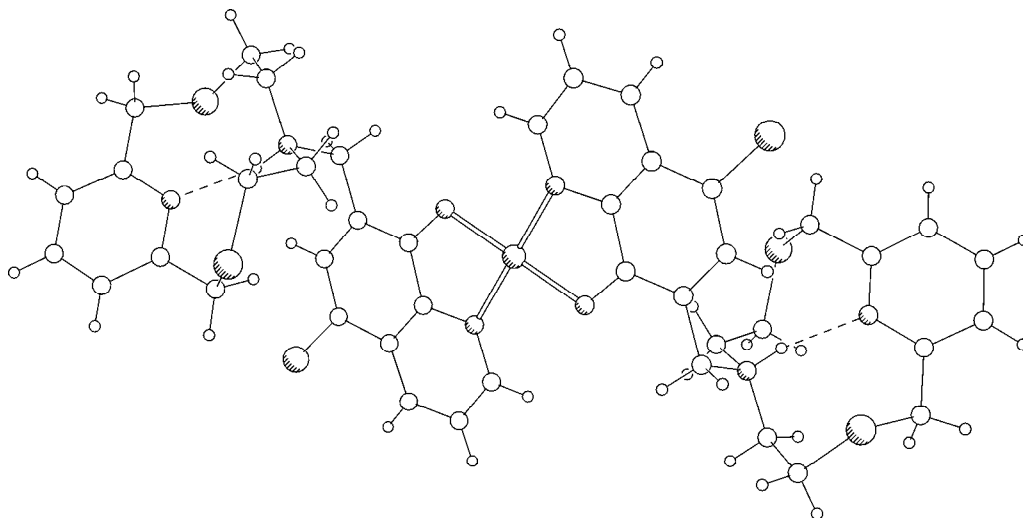


Figure 32. $[\text{Cu}(\mathbf{51})_2]^{2+}$.

The coordination behaviour of **50** and **51** in solution was also confirmed at the solid state; the complexes $[\text{Hg}\mathbf{50}(\text{MeCN})](\text{ClO}_4)_2$, $[\text{Cu}\mathbf{50}](\text{ClO}_4)_2 \cdot \frac{1}{2}\text{MeCN}$, $[\text{Zn}\mathbf{50}(\text{H}_2\text{O})](\text{ClO}_4)_2$,

[Pb**50**(ClO₄)₂] and [Cu(**51**)₂](BF₄)₂·2MeNO₂ were isolated and structurally characterised. In all four 1:1 complex with **50**, the ligand interacts with each metal centre through all its donor atoms, the coordination site(s) left free by the N₃S₂-donor set of **50** are either left unoccupied in [Cu**50**]²⁺ or occupied by a solvent molecule in [Hg**50**(MeCN)]²⁺ and [Zn**50**(H₂O)]²⁺ (Figure 31) or counter-anion molecules in [Pb**50**(ClO₄)₂]. [91]

In the complex cation [Cu(**51**)₂]²⁺, the metal center is coordinated in a square planar geometry by the two deprotonated and *trans* bidentate hydroxyquinoline moieties from two **51** molecules. The two macrocyclic units are not involved in metal coordination, but in each, the aliphatic N-donor is protonated to give a NH··N hydrogen bond that presumably determines the observed folded conformation of the macrocyclic framework (Figure 32). [91]

Taking advantage of the solubility of **50** and **51** in a solvent mixture having a high water content, and because the fluorescence of molecular sensors like **47-51** is often pH sensitive, the effect of pH on the fluorescence of both **50** and **51** and their 1:1 metal complexes with Hg²⁺, Cu²⁺, Cd²⁺, Pb²⁺ or Zn²⁺ in MeCN/H₂O (1:1 v/v) was initially studied. In fact, in **47** and **50** a photoinduced electron transfer (PET) mechanism between the tertiary nitrogen atom of the macrocyclic moiety and the quinoline or anthracene fragments, mainly operates in determining the fluorescence changes upon the interaction with the metal cations; in **49** and **51**, besides a PET mechanism, also an intramolecular photoinduced proton transfer (PPT) operates between the hydroxyl group and the quinoline nitrogen, which also depends on the nature of the solvent.

Both **50** ($\lambda_{\text{ex}} = 316$, $\lambda_{\text{em}} = 382$ nm) and **51** ($\lambda_{\text{ex}} = 332$, $\lambda_{\text{em}} = 520$ nm) did not change their fluorescence OFF state over the range of pH values considered. A significant enhancement of the fluorescence intensity was observed in the presence of Zn²⁺ for **50** in the pH range 3.0-9.0 with a maximum at around pH = 7.0, and in the presence of Cd²⁺ for **51** in the pH range 4.0-9.0 with a maximum at around pH = 6.0. [91]

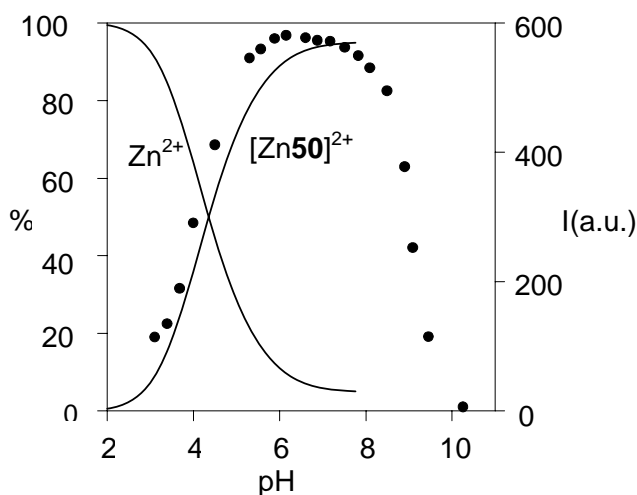


Figure 33. Distribution diagram and pH dependence of the fluorescence emission for the systems Zn²⁺/**50** in MeCN/H₂O (1:1 v/v) ($\lambda_{\text{exc}} = 316$ nm, $\lambda_{\text{em}} = 382$ nm).

The comparison between the distribution curves derived from potentiometric measurements and the pH dependence of the fluorescence emission for the systems Zn²⁺/**50**

and $\text{Cd}^{2+}/\mathbf{51}$ (see Figure 33 for the case of $\text{Zn}^{2+}/\mathbf{50}$) clearly indicates that in both cases the corresponding 1:1 metal complex species are responsible for the selective CHEF effects observed. The subsequent return of the ligands to an OFF state at higher pH values (>7) could be the result of the formation of hydroxylated or 1:2 metal-to-ligand complex species in which either PPT, PET, or both are possibly restored. [91]

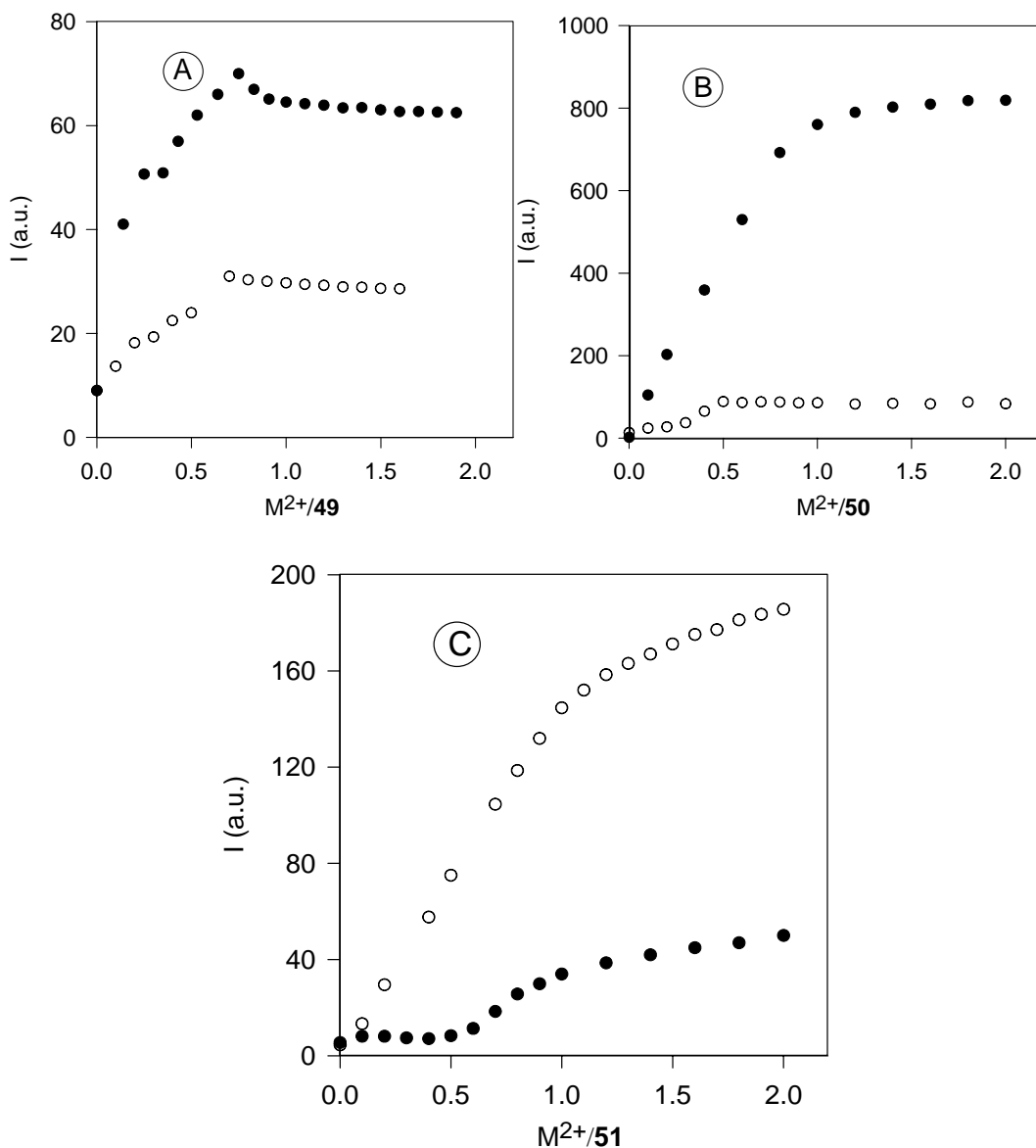


Figure 34. Fluorescence intensity/ molar ratio plots in solution buffered at $\text{pH} = 7.0$ for **49** (MeCN/ H_2O , 4:1 v/v) (A); **50** (MeCN/ H_2O , 1:1, v/v) (B); **51** (MeCN/ H_2O , 1:1, v/v) (C) in the presence of increasing amounts of Zn^{2+} (●) and Cd^{2+} (○) ($\lambda_{\text{exc}} = 244 \text{ nm}$, $\lambda_{\text{em}} = 548 \text{ nm}$ for **49**; $\lambda_{\text{exc}} = 316 \text{ nm}$, $\lambda_{\text{em}} = 382 \text{ nm}$ for **50**; $\lambda_{\text{exc}} = 332 \text{ nm}$, $\lambda_{\text{em}} = 520 \text{ nm}$ for **51**).

It is interesting to compare the fluorescence intensity/ molar ratio plots for **49**, **50** and **51** in solution buffered at $\text{pH} = 7.0$ in the presence of increasing amounts of each metal ion

considered (Figure 34). [90, 91] It is clear that small changes in the coordination environment around the metal ion by substitution of the signalling unit brings to a dramatic change in the substrate-selectivity of the resulting chemosensor as a whole in term of optical response. As compared to **49**, **50** is much more selective towards Zn^{2+} with a much better sensitivity, while **51** is definitively selective for Cd^{2+} although, a much less pronounced enhancement effect is observed in the presence of Zn^{2+} with inflection points at metal-to-ligand ratio vales of 0.5 and 1 (in agreement with potentiometric studies). Therefore, a synergic cooperation between the signalling and the receptor units in determination of the substrate-selective response by a fluorescent chemosensor is possible when the signalling unit can coordinate the metal centre. Even though the receptor unit is not thermodynamically selective in the host-guest interaction, the chemosensor having a coordinating signalling unit can give a selective response to one of the metal ions considered. Furthermore, changing the signalling unit it is possible to change the metal ion towards which the chemosensor shows a selective optical answer.

The importance of having a coordinating signalling unit that cooperates with the receptor units within a conjugated fluorescent chemosensor in reaching a substrate-selective optical response is also proved by the optical properties of **53-55** (Figure 35) studied in dichloromethane solutions in the presence of different transition metal ions such as Ag^+ , Cd^{2+} , Cu^{2+} , Zn^{2+} , Co^{2+} , Ni^{2+} , Pd^{2+} , Hg^{2+} . [92-95] **53-55** can be considered structural analogous of **47** with the main difference that the receptor unit is the pyridine-based N_2S_2 -donating 14-membered macrocycle **52** (Figure 35) characterized by a ring cavity bigger than that in **46** (Figure 29).

Several emissive mononuclear complexes have been obtained with **53** and **54** in the solid state, [93, 94, 95] while the formation of dinuclear species was observed in solution for **55**. [93] Interestingly, as contrary to what was observed in the X-ray crystal structure of $[\text{Cu53}(\text{ClO}_4)]\text{ClO}_4$ (Figure 36A), [12] in which all donor atoms from the macrocyclic framework are involved in metal coordination, in the neutral species $[\text{Cd53}(\text{NO}_3)_2]$ and $[\text{Hg53}(\text{Cl})_2]$ (Figures 36B and 36C) the tertiary nitrogen atom from the receptor unit is not involved in metal binding. [94, 95]

In any case, a CHEF effect was observed in dichloromethane solution with all metal ions considered, in some cases followed by a quenching of the fluorescence intensity for increased metal-to-ligand molar ratios. Changes in the fluorescence intensity emission were observed to be, in some cases, the result of a strong competition between complexation and protonation of the ligands. [95]

Tamayo, A; Lodeiro, C; Escriche, L; Casabó, J; Covalo, B; González, P. *Inorg. Chem.*, 2005, 44, 8105-8115.

Tamayo, A; Oliveira, E; Covalo, B; Casabó, J; Escriche, L; Lodeiro, CZ. *Anorg. Allg. Chem.*, 2007, 633, 1809-1814.

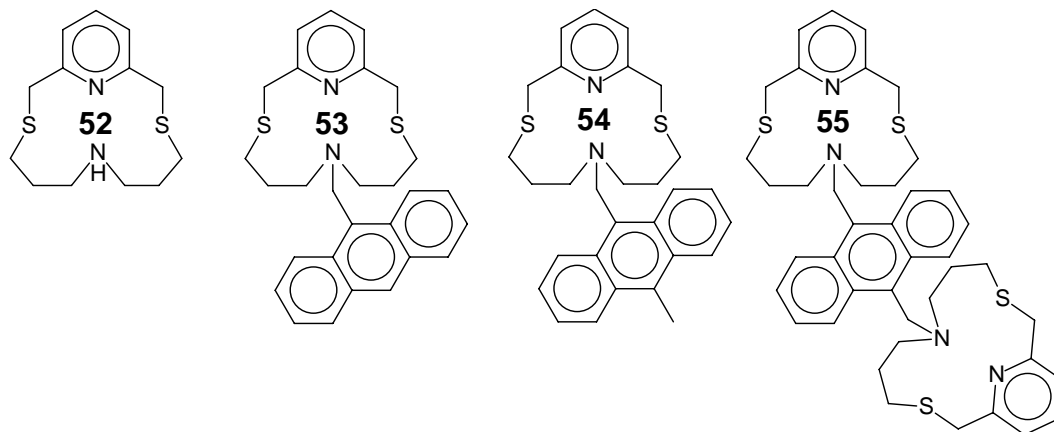


Figure 35.

This notwithstanding, analytical studies demonstrated the ability of **53** as dissolved in dichloromethane to extract Hg^{2+} from aqueous solution at pH = 8.0. [95]

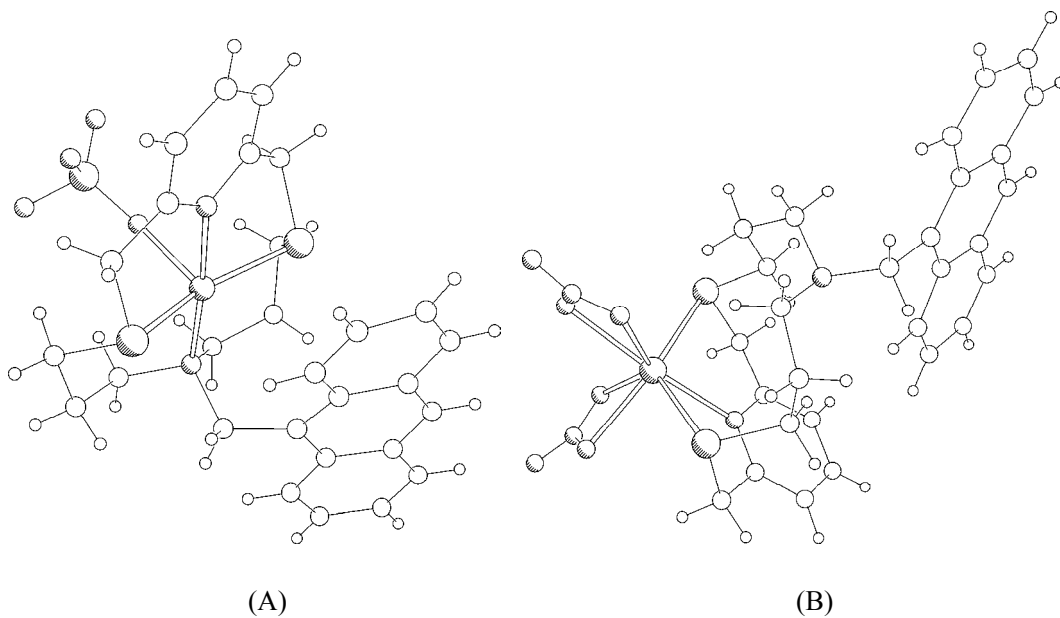
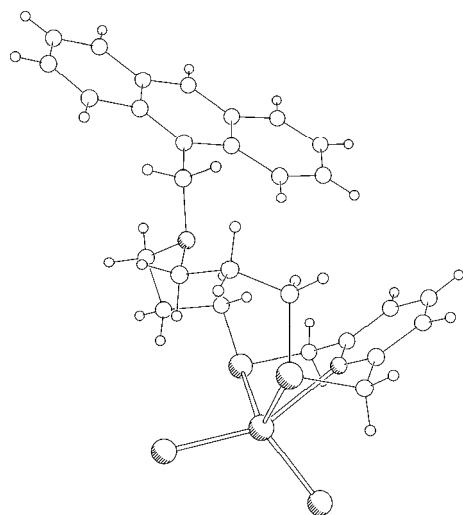


Figure 36. (Continued).



(C)

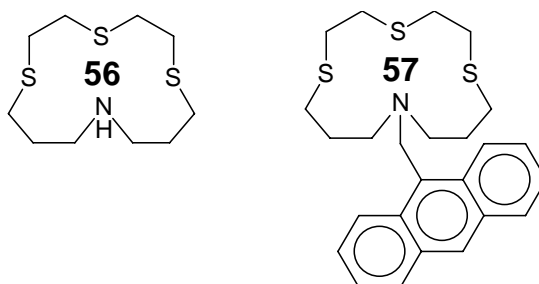
Figure 36. (A) $[\text{Cu}53(\text{ClO}_4)]^+$; (B) $[\text{Cd}53(\text{NO}_3)_2]$ and $[\text{Hg}53(\text{Cl})_2]$ (C).

Figure 37.

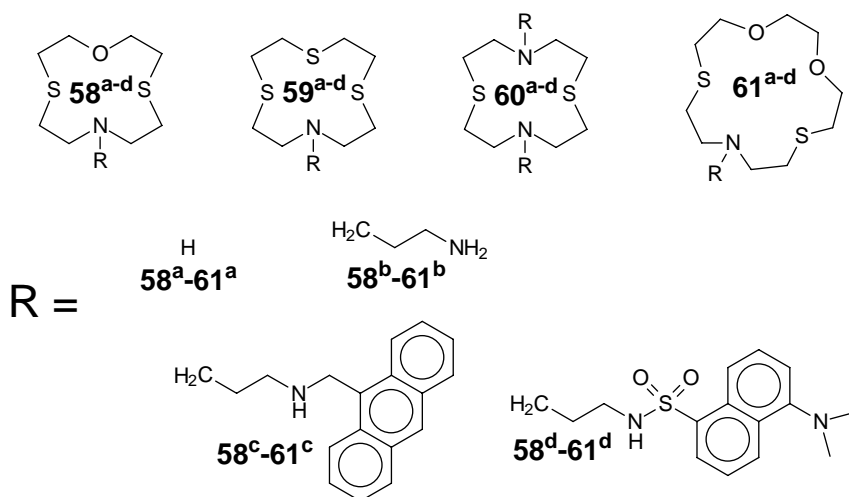


Figure 38.

An optical behaviour similar to that observed for **53-55** was also shown by **57** which features the NS₃-donating 14-membered aliphatic macrocycle **56** bearing a non coordinating anthracenylmethyl pendant arm (Figure 37). [94, 96]

Conjugated fluorescent chemosensors have also been synthesized having different mixed N/S- and N/S/O-donating aliphatic macrocyclic receptors and coordinating signaling units. In particular, the macrocycles **58^a-61^a** were functionalised with N-(9-anthracenylmethyl)aminopropyl (**58^c-61^c**) and N-dansylamidopropyl (**58^d-61^d**) pendant arm(s) (Figure 38) and the optical response of the resulting fluorescent chemosensors was investigated towards Hg²⁺, Cu²⁺, Cd²⁺, Pb²⁺ or Zn²⁺ in MeCN/H₂O (4:1 v/v) solutions buffered at pH = 7.0. [97]

Although in these systems the fluorescent moiety is remote from the cavity of the macrocyclic receptor, the linker heteroatom of the fluorophore (i.e. the amine or amide nitrogen atom of the pendant arm(s)) can participate in complexation to the metal ion, thereby possibly improving the signal transduction mechanism and allowing a cooperation between the receptor and the signaling units leading to a reliable substrate-selective optical response by the sensor(s).

Initially, potentiometric studies in water for all four macrocycles and for their amino propyl pendant arm derivatives (**58^b-61^b**) were performed to understand the coordinating properties of the binding domain of **58^{c/d}-61^{c/d}**. [97, 66] All ligands in both series form 1:1 metal complexes, in some cases starting from acidic pH values. For both series of ligands the stability constants decrease in the order Hg²⁺ > Cu²⁺ > Cd²⁺ > Pb²⁺ > Zn²⁺ analogously to what was found with the previous family of sensors based on **46**. The presence of aminopropyl arms increases the stability constant in agreement with the higher number of N-donors potentially present for metal coordination. Interestingly only for the ligands having aminopropyl side arms it is observed the formation at acidic pH of monoprotonated and diprotonated complex species. This suggests that protonation of complexes takes place on the amino group of the pendant arm with possible consequent detachment of this N-donor from the metal centre. [97] The coordination behaviour in solution was also confirmed in the solid state by isolation and structural characterisation of 1:1 metal complexes with both un-functionalised macrocycles and aminopropyl pendant arm derivatives. In them (see Figure 39 for some representative examples) the macrocyclic moieties coordinate through all their donor atoms adopting folded conformations, and the metal ions are displaced out of the ring cavity completing their coordination sphere by coordinating solvent molecules or counter anions. In the complexes with aminopropyl pendant arm derivatives, the primary amino group of the pendant arm(s) is involved in metal coordination as supported by potentiometric studies. [97, 98]

In terms of optical response to the presence of metal ions, **58^{c/d}-61^{c/d}** maintained their fluorescence ON state in the presence of Cd²⁺, Pb²⁺ or Zn²⁺ in MeCN/H₂O (4:1 v/v) solutions buffered at pH = 7.0. While for **58^c-61^c** and **59^d** and **60^d** a CHEQ effect was observed only in the presence of Cu²⁺ and Hg²⁺ up to a 1:1 metal-to-ligand molar ratio, with **58^d** and **61^d** a highly selective and efficient quenching of the fluorescence intensity was observed only in the presence of Hg²⁺ (Figure 40) suggesting a synergic cooperation between the receptor and signalling units in these fluorescent chemosensors in reaching a substrate-selective optical response. [97]

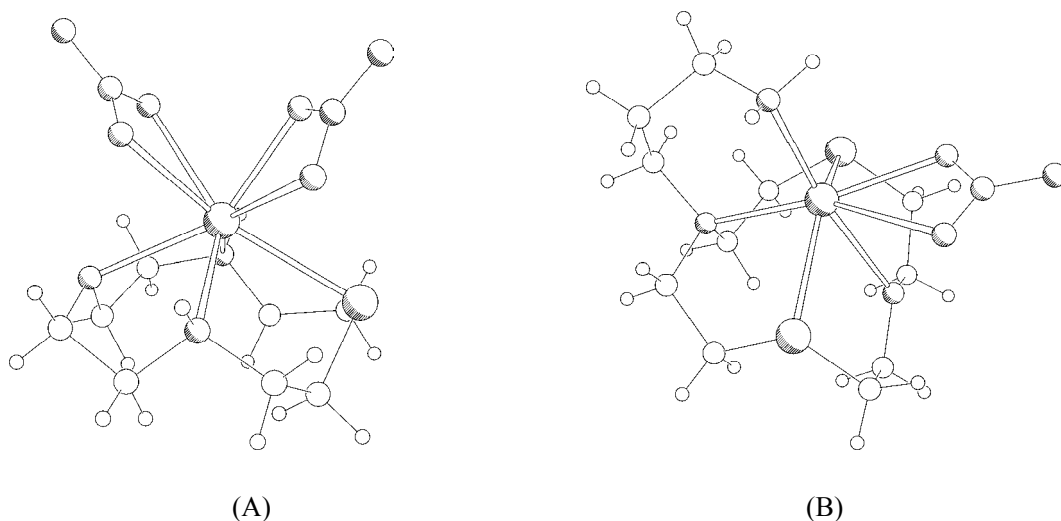


Figure 39. $[\text{Cd}58^{\text{a}}(\text{NO}_3)_2]$ (A); $[\text{Cd}58^{\text{b}}(\text{NO}_3)]^+$ (B).

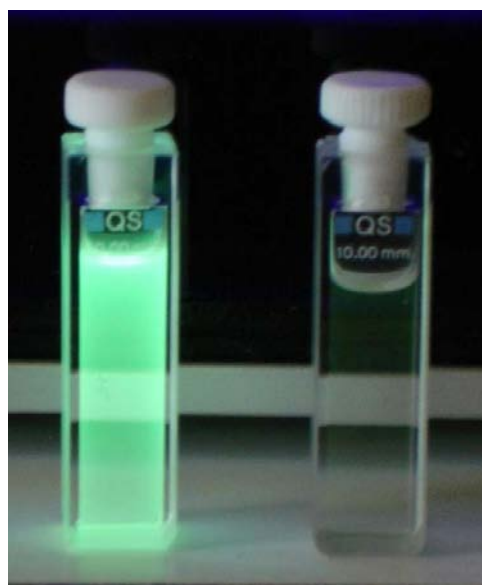


Figure 40. Changes in the fluorescent emission of 58^{d} (left) upon addition of 1 equiv. of Hg^{2+} (right) in MeCN/ H_2O (4:1 v/v) solutions buffered at pH = 7.0.

58^{d} was then used as neutral carrier in the construction of a highly sensitive and selective fluorimetric bulk optode membrane for subnanomolar detection of Hg^{2+} ions in water solutions, displaying a calibration curve over a wide concentration range ($1.0 \times 10^{-4} - 5.0 \times 10^{-12}$ M) and a relatively fast response time (less than 1 min.). [99] On the contrary 59^{d} resulted suitable for the construction of a highly sensitive and selective fluorimetric optode membrane for the determination of trace amounts of Ag^+ ions. [100]

Mixed-donor atom (N,S,O) macrocycles such as **58^a** and **61^a** (Figure 38) have been integrated as simple receptor modules to a variety of supramolecular signaling architectures such as those shown in Figure 41.

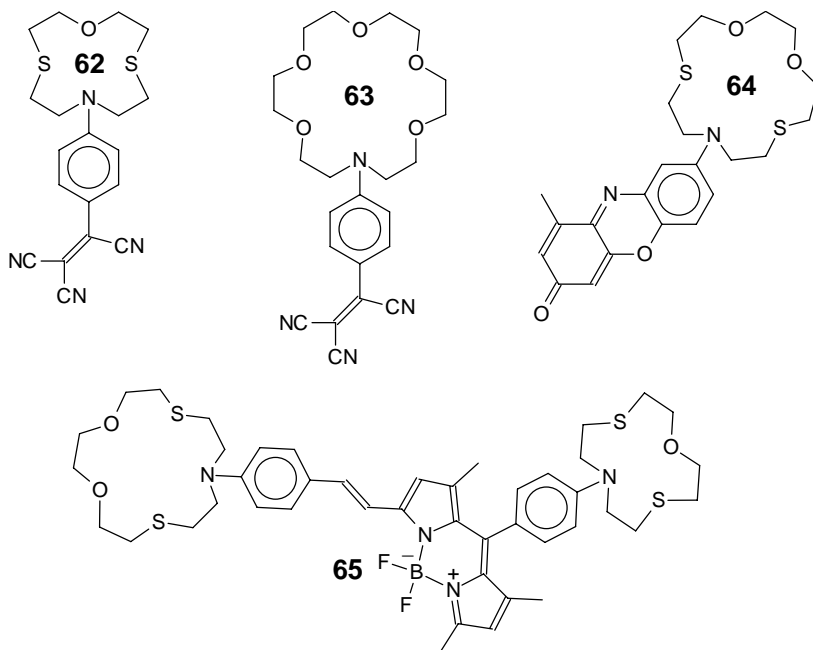


Figure 41.

The systems reported in Figure 41 represent a step forward towards the development of “clever” fluorescent sensor molecules such as multi-channel sensors or molecular logic gates that still take advantage from the chemistry of macrocyclic ligands. As already extensively pointed out, fluorescent chemosensors have mainly been designed by coupling a binding site for the selective coordination of a guest and a fluorescent signaling subunit for the transduction of the binding event into quenching or enhancement of the emission intensity of the fluorophore. According to this “traditional” or “classical” single-signaling approximation only two emissive states of the probe are observed directly related to the presence or absence of a certain guest. Natural developments of this receptor-spacer-fluorophore supramolecular modular scheme are represented by multi-channel signaling chemosensors and molecular logic gates. In the former, the host-guest binding event is transduced in more than one observable signal; in the latter, various signaling and/or receptor groups are attached to suitable skeletons so to give multi-responsive and/or multi-functional chemosensors able to cooperatively recognize two or more different analytes as well as to bind a single analyte with cooperative forces.

For example, **62** (Figure 41) shows a Hg^{2+} -selective color change from pink to yellow in MeCN solution, and a CHEF effect in the presence of the same ion; furthermore, a remarkable anodic shift of the reversible one-electron reduction process of **62** in MeCN is observed in the presence of Hg^{2+} and Pb^{2+} . [101] On the contrary, the structural analogue of **62**, **63**, featuring a crown ether macrocycle as binding site, shows selective color change in the presence of Pb^{2+} , a significant CHEF effect in the presence of the same ion but a

remarkable CHEQ effect in the presence of Cu^{2+} and Fe^{3+} , while large anodic shifts were found for Hg^{2+} , Pb^{2+} and Fe^{3+} . Systems like **62** and **63** can therefore be described as electro-optical signaling sensors which offer the possibility of sensing different metal ions via multiple signaling patterns. [101]

64 (Figure 41) was designed to give highly selective dual chromo- and fluorogenic response towards Hg^{2+} in water. While, the phenoxazinone moiety guarantees enough solubility in water and intense fluorescence in the visible region, the mixed donor macrocyclic unit **61**^a, binds selectively the target species. Furthermore, the donor-acceptor ensemble in **64** can also be considered a ditopic probe: the macrocyclic binding site for Hg^{2+} and the carbonyl group for all potentially interfering species communicating via the amino-keto conjugated backbone. In MeCN solutions a selective CHEQ effect is observed in the presence of Hg^{2+} accompanied by a selective drastic hypochromic shift of the absorption band from pink to yellow. A bathochromic shift is instead observed in the presence of other metal ions and protons. Most remarkable is the fact that the selective and reversible response of **64** towards Hg^{2+} at nanomolar level is preserved in water thus rendering this chemosensor suitable for Hg^{2+} sensing by using either absorption or emission measurements in this medium. [102]

65 represents a very interesting ditopic fluorescent probe designed to operate as molecular IMPLICATION logic gate. An asymmetrically core-extended boron-dipyrrromethane dye is equipped with two electron-donating macrocyclic units having different metal ion preferences. While the tetraoxa-aza crown ether is π -conjugated with the chromophore, the dithia-oxa-aza crown is electronically decoupled from the boron-dipyrrromethane unit. Accordingly, a CHEQ effect is observed on the fluorescence emission of **65** only in the case in which Na^+ is bound to the tetraoxa-aza crown ether and the other macrocyclic unit is free; vice-versa, a high fluorescence output is observed when either only Ag^+ is bound to the N,S,O mixed-donor macrocyclic moiety or both Na^+ and Ag^+ interact with **65** at the appropriate binding sites. [103]

5. OTHER MACROCYCLE LIGANDS

Most of the fluorescent chemosensors so far discussed are conjugated molecular sensors and feature a macrocyclic receptor unit covalently linked to a fluorophore via a spacer. Macrocyclic intrinsic chemosensors in which the signaling unit is part of the macrocyclic structure are much rarer especially if containing S-donor atoms. Figure 42 shows two classes of mixed donor macrocycles featuring a phenanthroline (**66-68**) and an anthraquinone (**69-71**) sub-units, respectively, as integral part of the macrocyclic architecture. [104-106]

66-68 in MeCN show an absorption band at about 280 nm and a fluorescent band around 360 nm. The effect on the fluorescence intensity upon addition of increasing amounts of Pb^{2+} , Cd^{2+} , or Hg^{2+} to an MeCN solution of **66**, **67** or **68** was investigated. The shape and position of the fluorescence emission bands do not change in the presence of the metal ions compared to those of free ligands, whereas the emission intensities change as function of the M^{2+}/L

($M^{2+} = Pb^{2+}, Cd^{2+}, Hg^{2+}$; L = **66-68**) molar ratio according to the curves reported in Figure 43. [104]

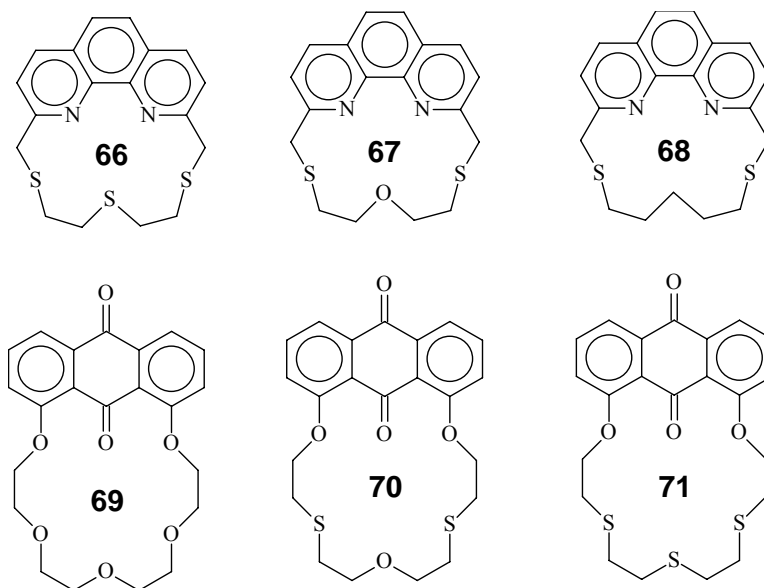


Figure 42.

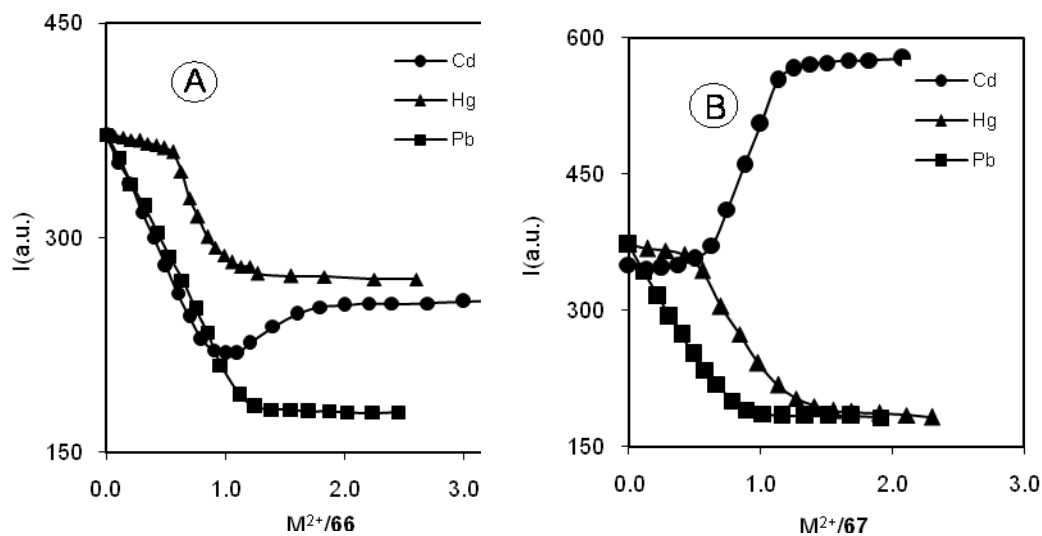


Figure 43. (Continued).

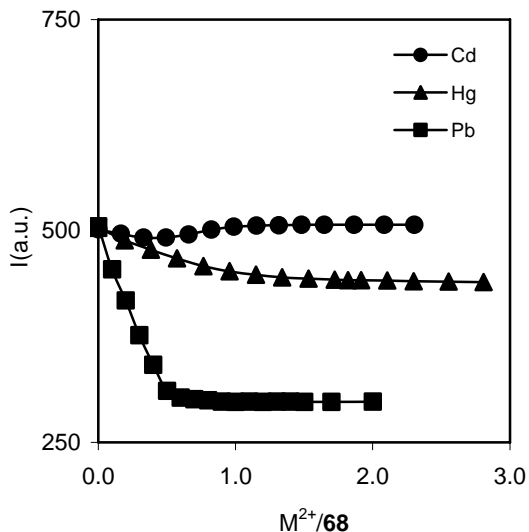


Figure 43. Fluorescent intensity/molar ratio plots for **66** ((A), **67** (B), and **68** (C) in the presence of increasing amounts of Pb^{2+} , Cd^{2+} , and Hg^{2+} ($\lambda_{\text{exc}} = 275$ nm for **66** and **67**, 285 nm for **68**; $\lambda_{\text{em}} = 365$ nm for **66** and **67**, 355 nm for **68**).

A CHEQ effect is observed for all three ligands on addition of increasing amounts of Pb^{2+} and Hg^{2+} . From the inflection points in the fluorescence intensity/molar ratio plots it can be inferred that 1:1 $[\text{M}(\text{L})]^{2+}$ complexes ($\text{M} = \text{Pb}^{2+}$, Hg^{2+} ; $\text{L} = \mathbf{66}$, **67**) are formed. The formation of $[\text{M}(\text{L})_2]^{2+}$ species appears to take place only with **68** for Pb^{2+} and with both **66** and **67** for Hg^{2+} . [104] A different trend of the fluorescence intensity variation is observed upon addition of Cd^{2+} to MeCN solution of the three ligands. A CHEQ effect followed by a chelation enhancement of fluorescence (CHEF) is observed with **66** and **68** (Figures 43A, 43C); the inflection points in the spectrofluorometric titration curves indicate the formation of the species $[\text{Cd}(\mathbf{66})]^{2+}$, $[\text{Cd}_2(\mathbf{66})]^{4+}$, $[\text{Cd}(\mathbf{68})]^{2+}$, and $[\text{Cd}(\mathbf{68})_2]^{2+}$. In the case of **67** (Figure 43B) a selective CHEF effect is observed throughout the whole range of $\text{Cd}^{2+}/\mathbf{67}$ molar ratios explored with formation of the 1:1 and 1:2 metal-to-ligand complexes. **67** is therefore the only ligand among the three under consideration that allow to distinguish Cd^{2+} from Hg^{2+} and Pb^{2+} in terms of substrate-selective optical response. [104] The stoichiometry of the species formed during the spectrofluorometric titrations was confirmed by conductometric measurements and by the best fitting of the experimental data to the appropriate complexation models. [104] Interestingly, a complex cation corresponding to the formulation $[\text{Pb}(\mathbf{68})_2]^{2+}$ was demonstrated by cyclic voltammetry to be responsible of the assisted transfer of Pb^{2+} at the polarised water/1,2-dichloroethane junction by interfacial coordination with **68**. [107]

The complexation properties of **66-68** towards Pb^{2+} , Cd^{2+} , and Hg^{2+} were also investigated in the solid state. The reaction between the ligands and the metal ions always afforded 1:1 metal complexes, except the reaction of **68** with Pb^{2+} which always gave in the solid state a compound having a formulation corresponding to a 1:2 $\text{Pb}^{2+}/\mathbf{68}$ stoichiometry. Crystals suitable for X-ray diffraction analysis were obtained for the complexes $[\text{Pb}(\mathbf{66})][\text{ClO}_4]_2 \cdot \frac{1}{2}\text{H}_2\text{O}$, $[\text{Pb}(\mathbf{67})][\text{ClO}_4]_2 \cdot \text{MeNO}_2$, $[\text{Pb}(\mathbf{68})_2][\text{ClO}_4]_2 \cdot 2\text{MeCN}$, and $[\text{Cd}(\mathbf{68})][\text{NO}_3]_2$ (Figure 44). [104] In all cases the three ligands adopt a folded conformation similarly to that observed in related complexes with Group VIII transition metal ions with the

aliphatic portion of the ring folded over the plane of the phenanthroline moiety. [83] However, the ring cavity is not large enough to fully encapsulate larger d^{10} metal ions such as Cd^{2+} and Pb^{2+} , which therefore are “perching” above the macrocyclic cavity of **66-68** rather than “nesting” within it. In $[\text{Pb}(\mathbf{66})][\text{ClO}_4]_2 \cdot \frac{1}{2}\text{H}_2\text{O}$, two perchlorate ions and a water molecule bridge two symmetry related $[\text{Pb}(\mathbf{66})]^{2+}$ units to form a binuclear species.

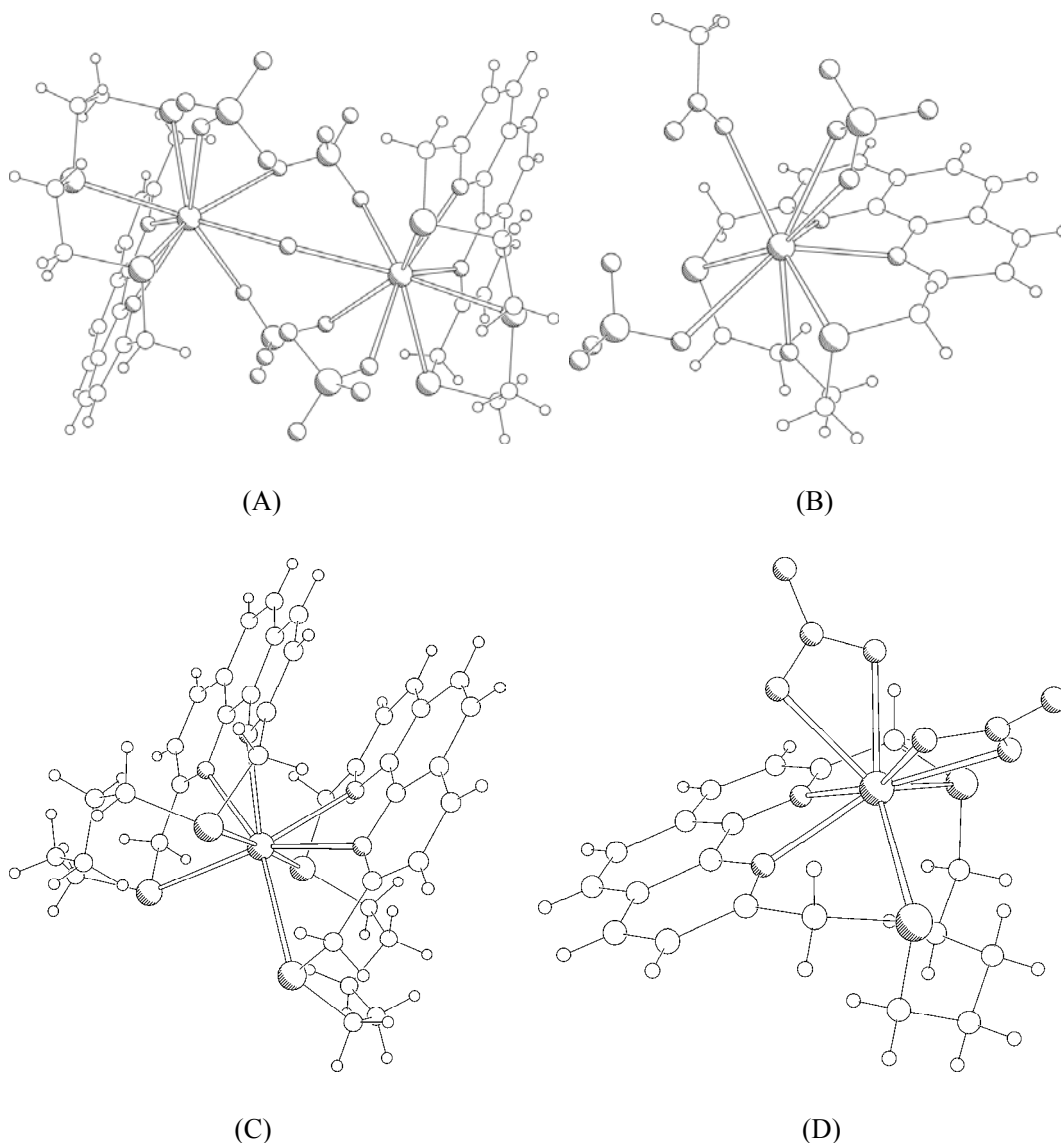


Figure 44. $[\text{Pb}(\mathbf{66})][\text{ClO}_4]_2 \cdot \frac{1}{2}\text{H}_2\text{O}$ in its dimeric form (A), $[\text{Pb}(\mathbf{67})][\text{ClO}_4]_2 \cdot \text{MeNO}_2$ (B), $[\text{Pb}(\mathbf{68})]^{2+}$ (C), and $[\text{Cd}(\mathbf{68})][\text{NO}_3]_2$ (D).

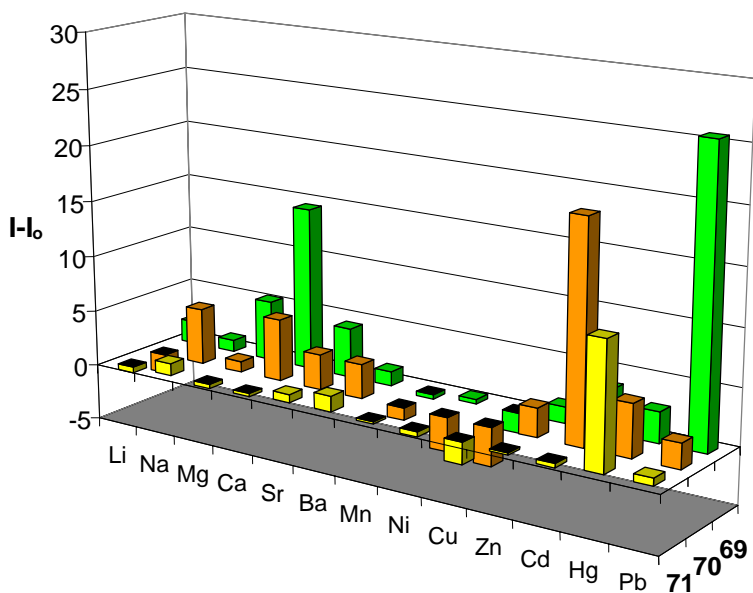


Figure 45. Fluorescence changes of **69-71** after addition of two equivalents of metal perchlorate salts.

The structure of the complex cation $[\text{Pb}(\mathbf{68})_2]^{2+}$ represents a rare example of a sandwich complex for Pb^{2+} with macrocyclic ligands and nicely supports the formation in solution of 1:2 M/L species ($\text{M} = \text{Pb}^{2+}, \text{Cd}^{2+}, \text{Hg}^{2+}$; $\text{L} = \mathbf{66-68}$). [104]

In **69-71**, the macrocyclic scaffold integrates an anthraquinone lumophore with an oxa-, thia- or mixed thia-oxa receptor that incorporates an intra-annular carbonyl oxygen. Complexation by a metal cation of sufficiently high charge density would involve the carbonyl oxygen thus resulting in luminescence turn-ON of the chemosensor because of the consequent inversion of the non-radiative $n\text{-}\pi^*$ and radiative $\pi\text{-}\pi^*$ transitions. A CHEF effect is selectively observed on adding Pb^{2+} , Cd^{2+} and Hg^{2+} to **69**, **70** and **71**, respectively. Interestingly, interference from alkaline earth metals decrease with increasing number of sulfur atoms in the aliphatic portion of the macrocyclic structure (Figure 45); this is in agreement with Mg^{2+} , Ca^{2+} and Sr^{2+} interfering in the CHEF effect induced by Pb^{2+} on **69**, and with the soft mercuric ion preferring the macrocycle with the greatest number of sulfur atoms, **71**. [105, 106]

X-ray crystallography on the 1:1 complexes of **69** and **70** with Pb^{2+} , Mg^{2+} , Cd^{2+} , Mn^{2+} and Zn^{2+} showed the metal center within the cavity of the macrocyclic system coordinated to four ligand donors including the intra-annular carbonyl one. (see Figure 46 for the case of Cd^{2+} with **70**). Two solvent molecules, two counter-anion molecules or one solvent and one counter-anion molecules cap the metal center above and below the plane of the same encapsulating macrocycle. [105, 106] The metal ion is not centered within the cavity, as the intra-annular carbonyl oxygen that extends into the aliphatic portion of the ring constrains the M^{2+} ion to be offset. As a consequence the anthraquinone moiety is not perfectly planar but assumes a slightly bent conformation.

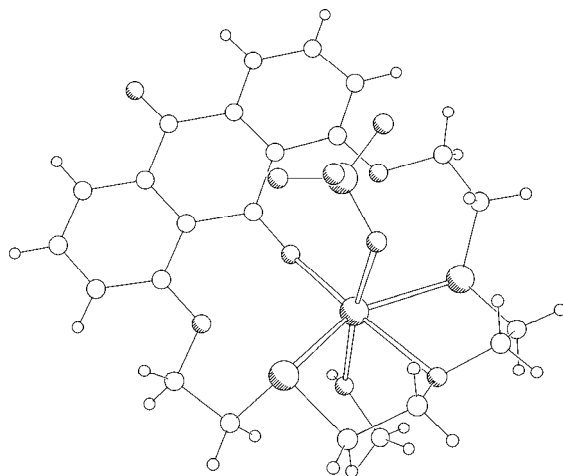


Figure 46. $[\text{Cd}70(\text{MeOH})(\text{ClO}_4)]^+$.

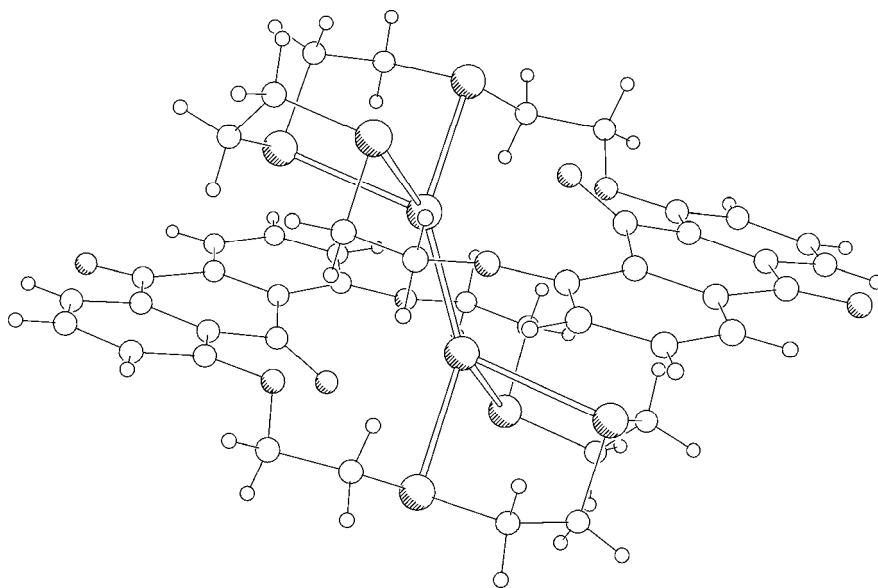


Figure 47. $[\text{Hg}_2(71)_2]^{2+}$.

Interestingly, reduction of Hg^{2+} by the solvent DMF in the presence of **71** gave the complex $[\text{Hg}_2(71)_2](\text{ClO}_4)_2$ in which Hg_2^{2+} bridges two molecules of **71** via sulfur ligation (Figure 47).

6. CONCLUSIONS

Macrocyclic chemistry has grown considerably since the pioneering work of Pedersen, Cram and Lehn. The possibility of a precise molecular recognition between macrocyclic ligands and their guests has many applications in supramolecular science and applicative disciplines. The results summarized in this chapter cover several publications which have

been published during the recent years in the field of fluorescence chemosensors featuring macrocyclic sub-units. These results give a clear idea of the role that macrocyclic systems can have in developing selective and sensitive fluorescent probes for metal ions. It is expectable that the scientific community will continue to pay attention to this area of research both in its fundamental and applicative aspects.

ACKNOWLEDGMENTS

We would like to thank our co-workers and all collaborators for their contribution to this research program.

C.L. thanks Xunta de Galicia for the Isidro Parga Pondal Research Program, the Xunta de Galiza (Spain) by projects PGIDT04PXIB2091PR and 09CSA043383PR, INOU UVIGO/VICOU/K914-122P64702/2009 Project and the FCT-MCTES/FEDER (Portugal) through projects POCTI/32442/2000, POCTI/QUI/47357/2002, POCI/QUI/55519/2004, PDTC/QUI/66250/ 2006, as well as the European Commission project HPTN-CT-2000-00029 for financial support. VL and MM thank MIUR (Ministero dell'Istruzione, dell'Università e della Ricerca Scientifica) for financial support (Project PRIN 2007C8RW53).

REFERENCES

- [1] Lehn, JM. *Supramolecular Chemistry Concepts and Perspectives*; Wiley-VCH: Weinheim, DE, 1995.
- [2] Steed, JW; Atwood, JL. *Supramolecular Chemistry*, 2nd Edition; *John Wiley & Sons: Chichester*, UK, 2009.
- [3] Lehn, JM. In *Perspectives in Coordination Chemistry*; AF; Williams, C; Floriani, AE; Merbach, (Eds.); VHC: Basel, SZ & VCH: Weinheim, DE, 1992.
- [4] Lindoy, LF. *The Chemistry of Macrocyclic Ligand Complexes*; Cambridge University Press: *Cambridge*, UK, 1989.
- [5] *Coord. Chem Rev.* special issue on Macrocyclic Chemistry. 1996; 148,
- [6] *Macrocyclic Synthesis*: In: A; practical Approach, D; Parker, (Eds.), Oxford University Press: Oxford, UK, 1996.
- [7] *Macrocyclic Compounds In Analytical Chemistry*; In: YA; Zolotov, (Eds.), *Chemical Analysis*, Vol. 143; John Wiley & Sons: New York, USA, 1997.
- [8] *Macrocyclic Chemistry Current Trends and Future Perspectives*, In: K; Gloe, (Eds.), Springer: Dordrecht, NL, 2005.
- [9] *Modern Supramolecular Chemistry: Strategy for Macrocyclic Synthesis*; In: F; Diederich, P; Stang, RR; Tykwinski, (Eds.), Wiley-VCH: Weinheim, DE, 2008.
- [10] Hulanicki, A; Glab, S; Ingman, F. *Pure Appl. Chem.*, 1991, 63, 1247-1250.
- [11] Balzani, V; Credi, A; Venturi, M. *Molecular Devices and Machines: Concepts and Perspectives for the Nanoworld*, 2nd Edition; Wiley-VCH: Weinheim, DE, 2008.
- [12] *Chem Rev.* 2000, 100 (7), special issue on Chemical Sensors.

- [13] Comprehensive Supramolecular Chemistry; In: JM; Lehn, JL; Atwood, JED; Davies, DD; MacNicol, F; Vögtle, DN; Reinhoudt, (Eds.), Pergamon: Oxford, UK, 1996, Vol. 10.
- [14] Czarnik, AW. *Acc. Chem. Res.*, 1994, 27, 302-308.
- [15] Chemosensors of Ions and Molecular Recognition; In: AW; Czarnik, JP; Desvergne, (Eds.), NATO ASI Series C; Kluwer Academic Publishers: Dordrecht, NL, 1997, Vol. 492.
- [16] de Silva, AP; Gunaratne, HQG; Gunnlaugsson, T; Huxley, AJM; McCoy, CP; Rademacher, JT; Rice, TE. *Chem. Rev.*, 1997, 97, 1515-1565.
- [17] Kimura, E; Koike, T. *Chem. Soc. Rev.*, 1998, 27, 179-183.
- [18] Bergonzi, R; Fabbrizzi, L; Licchelli, M; Mangano, C. *Coord. Chem. Rev.*, 1998, 170, 31-46.
- [19] *Coord. Chem. Rev.*, 2000, 205, special issue on Luminescent Sensors.
- [20] Rurack, K. *Spectrochim. Acta, Part, A* 2001, 57, 2161-2195.
- [21] Wiskur, SL; Haddou, A; Lavigne, JJ; Anslyn, EV. *Acc. Chem. Res.*, 2001, 34, 963-972.
- [22] Parack, K; Resch-Genger, U. *Chem. Soc. Rev.*, 2002, 31, 116-127.
- [23] Fabbrizzi, L; Licchelli, M; Taglietti, A. *Dalton Trans.*, 2003, 3471-3479.
- [24] Martínez-Mañez, R; Sancenón, F. *Chem. Rev.*, 2003, 103, 4419-4476.
- [25] Prodi, L. *New. J. Chem.*, 2005, 29, 20-31.
- [26] Mater, J. *Chem.* 2005, 15, special issue on Fluorescent Sensors.
- [27] Amendola, A; Fabbrizzi, L; Foti, F; Licchelli, M; Mangano, C; Pallavicini, P; Poggi, A; Sacchi, D; Taglietti, A. *Coord. Chem. Rev.*, 2006, 250, 273-299.
- [28] Basabe-Desmonts, L; Reinhoudt, DN; Crego-Calama, M. *Chem. Soc. Rev.*, 2007, 36, 993-1017.
- [29] Lodeiro, C; Pina, F. *Coord. Chem. Rev.*, 2009, 253, 1353-1383.
- [30] Pallavicini, PS; Diaz-Fernandez, YA; Pasotti, L. *Coord. Chem. Rev.*, 2009, 2226-2240.
- [31] Sousa, LR; Larson, JM. *J. Am. Chem. Soc.*, 1977, 99, 307-310.
- [32] Askaya, EU; Huston, ME; Czarnik, AW. *J. Am. Chem. Soc.*, 1990, 112, 7054-7056.
- [33] Yoon, J; Ohler, NE; Vance, DH; Aumiller, WD; Czarnik, AW. *Tetrahedron Lett.*, 1997, 38, 3845-3848.
- [34] Prodi, L; Montalti, M; Zaccheroni, N; Dallavalle, F; Folesani, G; Lanfranchi, M; Corradini, R; Paglari, S; Marchelli, R. *Helve. Chim. Acta*, 2001, 84, 690-706.
- [35] a) Bordunov, AV; Bradshaw, JS; Dalley, NK; Kou, XL; Izatt, RM. *Inorg. Chem.*, 1996, 35, 7229-7240. b) Prodi, L; Bargossi, C; Montalti, N; Su, N; Bradshaw, JS; Izatt, RM; Savage, PB. *J. Am. Chem. Soc.*, 2000, 122, 6769-6770. c) Farruggia, G; Lotti, S; Prodi, L; Montalti, M; Zaccheroni, N; Savage, PB; Trapani, V; Wold, F. I. *J. Am. Chem. Soc.*, 2006, 128, 344-350.
- [36] a) Alonso, MT; Brunet, E; Hernandez, C; Rodriguez-Ubis, JC. *Tetrahedron Lett.*, 1993, 46, 7465-7468. b) Alonso, MT; Brunet, E; Juanes, O; Rodríguez-Ubis, JC. *J. Photochem. Photobiol. A Chem.*, 2002, 147, 113-125.
- [37] a) Bilyk, A; Harding, MM; Turner, P; Hambley, TW. *J. Chem. Soc. Dalton Trans.*, 1994, 19, 2783-2790. b) Bodenant, B; Weil, T; Businelli-Pourcel, M; Fages, F; Barbe, B; Pianet, I; Laguerre, M. *J. Org. Chem.*, 1999, 64, 7034-7039.
- [38] a) Black, DSC; Rothnie, NE; Wong, LCH. *Tetrahedron Lett.*, 1980, 21, 1883-1886. b) Rurack, K; Bricks, YL; Slominski, YL; Resch, U. *Dyes and Pigments*, 1998, 36, 121-138.

- [39] a) Beer, P; Dent, SW; Fletcher, NC. *Polyhedron*, 1996, 15, 2983-2996.
b) Lodeiro, C; Pina, F; Parola, AJ; Bencini, A; Bianchi, A; Bazzicalupi, C; Ciattini S; Giorgi, C; Masotti, A; Valtancoli, B; Melo, J. S. *Inorg. Chem.*, 2001, 40, 6813-6819.
- [40] a) Aucejo, R; Alarcón, J; García-España, E; Llinares, JM; Marchin, KL; Soriano, C; Lodeiro, C; Bernardo, MA; Pina, F; Pina, J; de Melo, JS. *Eur. J. Inorg. Chem.*, 2005, 4301-4308.
b) de Silva, AP; Gunaratne, HQN; Lynch, PLM. *J. Chem. Soc. Perkin Trans.*, 1995, 2, 685-690.
c) de Silva, SA; Zavaleta, A; Baron, DE; Allam, O; Isidor, EV; Kashimura, N; Percapio, JM. *Tetrahedron Lett.*, 1997, 38, 2237-2240.
d) de Silva, SA; Amorelli, B; Isidor, DC; Loo, KC; Crooker, KE; Pena, YE. *Chem. Commun.*, 2002, 1360-1361.
e) Fabbriizzi, L; Gatti, F; Pallavicini, P; Parodi, L. *New. J. Chem.*, 1998, 1403-1407.
- [41] Bernardo, MA; Parola, AJ; Pina, F; García-España, E; Marcelino, V; Luis, SV; Miravet, JF. *J. Chem. Soc. Dalton Trans.*, 1995, 993-997.
- [42] Bernardo, MA; Guerrero, JA; García-España, E; Luis, SV; Llinares, JM; Pina, F; Ramirez, JA; Soriano, C. *J. Chem. Soc. Perkin Trans.*, 1996, 2, 2335-2342.
- [43] Clares, MP; Aguilar, J; Aucejo, R; Lodeiro, C; Albelda, MT; Pina, F; Lima, JC; Parola, AJ; Pina, J; Melo, JS; Soriano, C; García-España, E. *Inorg. Chem.*, 2004, 43 6144-6122.
- [44] Melo, JS; Pina, J; Pina, F; Lodeiro, C; Parola, AJ; Lima, JC; Albelda, MT; Clares, M. P; García-España, E. *J. Phys. Chem. A.*, 2003, 107, 11307-11318.
- [45] Bencini, A; Bianchi, A; Lodeiro, C; Masotti, A; Parola, AJ; Pina, F; Melo, JS; Valtancoli, B. *Chem. Commun.*, 2000, 1639-1640.
- [46] Bencini, A; Berni, E; Bianchi, A; Fornasari, P; Giorgi, C; Lima, JC; Lodeiro, C; Melo, MJ; Melo, JS; Parola, AJ; Pina, F; Pina, J; Valtancoli, B. *Dalton Trans.*, 2004, 2180-2187.
- [47] Nuñez, C; Oliveira, C; Giestas, L; Valencia, L; Macías, A; Lima, JC; Bastida, R; Lodeiro, C. *Inorg. Chim. Acta.*, 2008, 361, 2183-2194.
- [48] a) Baxter, PNW. *J. Org. Chem.*, 2001, 66, 4170-4179.
b) Chen, Y; Fan, QL; Wang, P; Zhang, B; Huang, YQ; Zhang, GW; Lu, XM; Chan, HSO; Huang, W. *Polymer*, 2006, 47, 5228-5232.
c) Costero, AM; Gil, S; Parra, M; Huguet, N; Allouni, Z; Lakhmir, R; Atlamsani, A. *Eur. J. Org. Chem.*, 2008, 1079-1084.
d) Loren, JC; Siegel, JS. *Ang. Chem. Int. Ed.*, 2001, 40, 754-757.
e) Goze, C; Ulrich, G; Charbonniere, L; Cesario, M; Prange, T; Ziesel, R. *Chem. Eur. J.*, 2003, 9, 3748-3755.
f) Leslie, W; Batsanov, AS; Howard, JAK; Williams, JAG. *Dalton Trans.*, 2004, 623-631.
g) Schmittel, M; Kalsani, V; Kishore, RSK; Colfen, H; Bats, JW. *J. Am. Chem. Soc.*, 2005, 127, 11544-11545.
h) Song, B; Wang, GL; Tan, MQ; Yuan, JL. *J. Am. Chem. Soc.*, 2006, 128, 13442-13450.
- [49] a) Bazzicalupi, C; Bencini, A; Bianchi, A; Giorgi, C; Fusi, V; Valtancoli, B; Bernardo, MA; Pina, F. *Inorg. Chem.*, 1999, 38, 3806-3813.
b) Bencini, A; Bernardo, MA; Bianchi A; Fusi, V; Giorgi, C; Pina, F; Valtancoli, B. *Eur. J. Inorg. Chem.*, 1999, 11, 1911-1948.
c) Bazzicalupi, C; Bencini, A; Berni, E; Bianchi, A; Giorgi, C; Borsari, L; Giorgi, C; Valtancoli, B; Lodeiro, C; Lima, JC; Parola, AJ; Pina, F. *Dalton Trans.* 2004, 591-597.
d) Bazzicalupi, C; Bencini, A; Bianchi, A; Borsari, L; Danesi, A; Giorgi, C; Lodeiro, C; Mariani, P; Pina, F; Santarelli, S; Tamayo, A; Valtancoli, B. *Dalton Trans.*, 2006, 4000-4010.

- [50] Pina, J; de Melo, JS; Pina, F; Lodeiro, C; Lima, JC; Parola, AJ; Soriano, C; Clares, MP; Albelda, MT; Aucejo, R; García-España, E. *Inorg. Chem.*, 2005, 44, 7449-7458.
- [51] Lodeiro, C; Parola, AJ; Pina, F; Bazzicalupi, C; Bencini, A; Bianchi, A; Giorgi, C; Masotti, A; Valtancoli, B. *Inorg. Chem.*, 2001, 40, 2968-2975.
- [52] Anda, C; Bazzicalupi, C; Bencini, A; Bianchi, A; Fornasari, P; Giorgi, C; Valtancoli, B; Lodeiro, C; Parola, AJ; Pina, F. *Dalton Trans.*, 2003, 1299-1307.
- [53] Bazzicalupi, C; Bencini, A; Berni, E; Bianchi, A; Danesi, A; Giorgi, C; Valtancoli, B; Lodeiro, C; Lima, JC; Pina, F; Bernardo, MA. *Inorg. Chem.*, 2004, 43, 5134-5146.
- [54] (a) Rawle, SC; Moore, P; Alcock, NW. *J. Chem. Soc., Chem. Commun.*, 1992, 684-687. (b) Alcock, NW; Clarke, AJ; Errington, W; Josceanu, AM; Moore, P; Rawle, SC; Sheldon, P; Smith, SM; Turonek, ML. *Supramol. Chem.*, 1996, 6, 281-291.
- [55] Lodeiro, C; Pina, F; Parola, AJ; Bencini, A; Bianchi, A; Bazzicalupi, C; Ciattini, S; Giorgi, C; Masotti, A; Valtancoli, B; de Melo, JS; *Inorg. Chem.*, 2001, 40, 6813-6819.
- [56] Pina, F; Ciano, M; Moggi, L; Balzani, V. *Inorg. Chem.*, 1985, 24, 844-847.
- [57] Bianchi, A; Bowman-James, K; García-España, E. (Eds.), 1997, *Supramolecular Chemistry of Anions*, Wiley-VCH, New York.
- [58] (a) Peter, F; Gross, M; Hosseini, MW; Lehn, JM; Sessions, RBJ. *Chem. Soc. Chem. Commun.*, 1981, 1067-1069. (b) Peter, F; Gross, M; Hosseini, MW; Lehn, JM. *Electroanal. Chem.*, 1983, 144, 279-292
- [59] García-España, E; Micheloni, M; Paoletti, P; Bianchi, A. *Inorg. Chim. Acta*, 1985 102, L9-L11.
- [60] Bencini, A; Bianchi, A; García-España, E; Giusti, M; Mangani, S; Micheloni, M; Orioli, P; Paoletti, P; *Inorg. Chem.*, 1987, 26, 3902-3907.
- [61] Aragón, J; Bencini, A; Bianchi, A; Domenech, A; García-España, E. *J. Chem. Soc., Dalton Trans.*, 1992, 319-324.
- [62] Bianchi, A; Domenech, A; García-España, E; Luis, S. *Anal. Chem.*, 1993, 65, 3137-3142.
- [63] Clares, MP; Lodeiro, C; Fernández, D; Parola, AJ; Pina, F; García-España, E; Soriano, C; Tejero, R. *Chem. Commun.*, 2006, 3824-3826.
- [64] (a) Azéma, J; Galaup, C; Picard, C; Tisnès, P; Ramos, O; Juanes, O; Rodríguez-Ubis, JC; Brunet, E. *Tetrahedron*, 2000, 56, 2673-2681. (b) Galaup, C; Carrié, MC.; Tisnès, P; Picard, C. *Eur. J. Org. Chem.*, 2001, 2165-2175.
- [65] (a) Rodríguez-Ubis, JC; Alpha, B; Plancherel, D; Lehn, JM. *Helv. Chim. Acta*, 1984, 67, 2264-2269. (b) Alpha, B; Lehn, JM; Mathis, G. *Angew. Chem. Int. Ed. Engl.*, 1987, 26, 266-267. (c) PaulRoth, CO; Lehn, JM; Guilheim, J; Pascard, C. *Helv. Chim. Acta*, 1995, 78, 1895-1903.
- [66] (a) Barigelletti, F; De Cola, L; Balzani, V; Belser, P; von Zelewsky, A; Vögtle, F; Ebmeyer, F; Grammenudi, S. *J. Am. Chem. Soc.*, 1989, 111, 4662-4668. (b) Balzani, V; Ballardini, R; Bolletta, F; Gandolfi, MT; Juris, A; Maestri, M; Manfrin, MF; Moggi, L., Sabbatini, N; *Coord. Chem. Rev.*, 1993, 125, 75-88 and references therein. (c) Sabbatini, N; Guardigli, M; Lehn, JM. *Coord. Chem. Rev.*, 1993, 123, 201-228. (d) Balzani, V; Credi, A; Venturi, M. *Coord. Chem. Rev.*, 1998, 171, 3-16 and references therein.
- [67] (a) Bazzicalupi, C; Bencini, A; Bianchi, A; Giorgi, C; Fusi, V; Masotti, A; Valtancoli, B; Roque, A; Pina, F. *Chem. Commun*, 2000, 561-562. (b) Bazzicalupi, C; Bencini, A;

- Berni, E; Bianchi, A; Giorgi, C; Fusi, V; Valtancoli, B; Lodeiro, C; Roque, A; Pina, F. *Inorg. Chem.*, 2001, 40 6172-6179.
- [68] (a) Bazzicalupi, C; Bencini, A; Bianchi, A; Faggi, E; Giorgi, C; Lodeiro, E; Oliveira, Pina, F; Valtancoli, B. *Inorg. Chim. Acta.*, 2008, 361, 3410-3419. (b) Swamy, KMK; Kwon, SK; Lee, HN; Kumar, SMS; Kim, JS; Yoon, J. *Tetrahedron Let.*, 2007, 48, 8683-8686. (c) Hershinkel, M; Silverman, WF; Sekler, I., *Mol. Med.*, 2007, 7-8, 331-336. (d) Ojida, A; Miyahara, Y; Wongkongkatap, A; Tamaru, S; Sada, K; Hamachi, I. *Chem. Asian J.*, 2006, 1, 555-563.
- [69] (a) Dugas, H; "Bioorganic Chemistry: a Chemical Approach to Enzyme Action", Springer, New York, USA. 1996. (b) Kühlbrandt, W. *Nat. Rev. Mol. Cell. Biol.*, 2004, 5, 282-295. (c) Sharma, R; Rensing, C; Rosen, BP; Mitra, B. *J. Biol. Chem.*, 2000, 275, 3873-3878. (d) Hou, Z; Mitra, B. *J. Biol. Chem.*, 2003, 278, 28455-28461.
- [70] Bazzicalupi, C; Bencini, A; Bianchi, A; Danesi, A; Giorgi, C; Lodeiro, C; Pina, F; Santarelli, S; Valtancoli, B. *Chem. Commun.*, 2005, 2630-2632.
- [71] Pearson, RG. *J. Am. Chem. Soc.*, 1963, 85, 3533-&.
- [72] (a) Vicente, M; Lodeiro, C; Adams, H; Bastida, R; De Blás, A; Fenton, DE; Macías, A; Rodríguez, A; Rodríguez-blás, T. *Eur. J. Inorg. Chem.*, 2000, 1015-1024. (b) Bértolo, E; Bastida, R; Fenton, DE; Lodeiro, C; Macías, A; Rodríguez, A. *J. Alloys Comp.*, 2001, 323, 155-158. (c) Lodeiro, C; Bastida, R; Bértolo, E; Macías, A; Rodríguez, A. *Polyhedron*, 2003, 22, 1701-1710. (d) Bértolo, E; Bastida, R; Fenton, DE; Lodeiro, C; Macías, A; Rodríguez, A. *J. Inclus. Phen. Macro. Chem.*, 2003, 45, 155-160. (e) Lodeiro, C; Bastida, R; Bértolo, E; Macías, A; Rodríguez, A. *Trans. Metal. Chem.*, 2003, 28, 388-394. (f) Lodeiro, C; Bastida, R; Bértolo, E; Macías, A; Rodríguez, A. *Inorg. Chim. Acta.*, 2003, 343, 133-140. (g) Lodeiro, C; Capelo, JL; Bértolo, E; Bastida, R; Anorg, Z. *Allg. Chem.*, 2004, 630, 1110-1115. (h) Lodeiro, C; Bastida, R; Bértolo, E; Rodríguez, A. *Can. J. Chem.*, 2004, 82, 443-447. (i) Lodeiro, C; Bértolo, E; Capelo, JL; Bastida, R. *Z. Anorg. Allg. Chem.*, 2004, 630 914-920.
- [73] Czarnik, AW., *Fluorescent Chemosensors for Ion and Molecule Recognition*; 538, 1-9, American Chemical Society: Washington, DC, 1993.
- [74] Oliveira, E; Vicente, M; Valencia, L; Macías, A; Bértolo, E; Bastida, R; Lodeiro, C. *Inorg. Chim. Acta*, 2007, 360, 2734-2743.
- [75] Nuñez, C; Bastida, R; Macías, A; Bértolo, E; Fernandes, L; Capelo, JL; Lodeiro, C. *Tetrahedron*, 2009, 65, 6179-6188.
- [76] Freiria, A; Bastida, R; Valencia, L; Macías, A; Lodeiro, C; Adams, H. *Inorg. Chim. Acta*, 2006, 359, 2383-2394.
- [77] (a) Lodeiro, C; Capelo, JL; *J. Inclu. Pheno. Macro. Chem.*, 2004, 49, 249-258. (b) Batista, RMF; Oliveira, E; Costa, SPG; Lodeiro, C; Raposo, MMM. *Tetrahedron Let.*, 2008, 49, 6575-6578. (c) Pedras, B; Fernandes, L; Oliveira, E; Rodríguez, L; Raposo, MMM; Capelo, JL. *Lodeiro, C.*, 2009, 79-85.
- [78] (a) Gocmen, A; Erk, C. *J. Inclu. Phen. Mol. Rec. Chem.*, 1996, 26, 67-72. (b) Erk, C; Gocmen, A., *Talanta*, 2000, 53, 137-140.
- [79] Lee, SC; Izatt, RM; Zhang, XX; Nelson, EG; Lamb, JD; Savage, PB; Bradshaw, JS. *Inorg. Chim. Acta*, 2001, 317, 174-180.
- [80] Bronson, RT; Bradshaw, JS; Savage, PB; Fuangswasdi, S; Lee, SC; Krakowiak, KE; Izatt, RM. *J. Org. Chem.*, 2001, 66, 4752-4760.

- [81] Xue, G; Bradshaw, JS; Song, H; Bronson, RT; Savage, PB; Krakowiak, KE; Izatt, RM; Prodi, L; Montalti, M; Zaccheroni, N. *Tetrahedron*, 2001, 57, 87-91.
- [82] De Santis, G; Fabbrizzi, L; Licchelli, M; Mangano, C; Sacchi, D. *Inorg. Chem.*, 1995, 34, 3581-3582.
- [83] Lippolis, V; Shamsipur, M. *J. Iran. Chem. Soc.*, 2006, 2, 105-127.
- [84] Shamsipur, M; Poursaberi, T; Rezapour, M; Ganjali, MR; Mousavi, MF; Lippolis, V; Montesu, DR. *Electroanal.*, 2004, 16, 1336-1342.
- [85] Shamsipur, M; Hosseini, M; Alizadeh, K; Mousavi, MF; Garau, A; Lippolis, V; Yari, A. *Anal. Chem.*, 2005, 77, 276-283.
- [86] Lippolis, V; Blake, AJ; Cooke, PA; Isaia, F; Li, WS., Schröder, M. *Chem. Eur. J.*, 1999, 5, 1987-1991.
- [87] Arca, M; Blake, AJ., Lippolis, V; Montesu, DR; McMaster, J; Tei, L; Schröder, M. *Eur. J. Inorg. Chem.*, 2003, 1232-1241.
- [88] Shamsipur, M; Hashemi, OR; Lippolis, VJ. *Memb. Science*, 2006, 282, 322-327.
- [89] Shamsipur, M; Mizami, F; Alizadeh, K; Mousavi, MF; Lippolis, V; Garau, A; Caltagirone, C. *Sens. And Actuators B*, 2008, 130, 300-309.
- [90] Blake, AJ; Bencini, A; Caltagirone, C; De Filippo, G; Dolci, LS; Garau, A; Isaia, F; Lippolis, V; Mariani, P; Prodi, L; Montalti, M; Zaccheroni, N; Wilson, C. *Dalton Trans.*, 2004, 2771-2779.
- [91] Aragoni, MC; Arca, M; Bencini, A; Blake, AJ; Caltagirone, C; De Filippo, G; Devillanova, FA; Garau, A; Gelbrich, T; Hursthouse, MB; Isaia, F; Lippolis, V; Mameli, M; Mariani, P; Valtancoli, B; Wilson, C. *Inorg. Chem.*, 2007, 46, 4548-4559.
- [92] Tamayo, A; Casabó, J; Escriche, L; González, P; Lodeiro, C; Rizzi, AC; Brondino, CD; Passeggi, MCG; Kivekäs, R; Sillanpää, R. *Inorg. Chem.*, 2007, 46, 5665-5672.
- [93] Tamayo, A; Lodeiro, C; Escriche, L; Casabó, J; Covalo, B; González, P. *Inorg. Chem.*, 2005, 44, 8105-8115.
- [94] Tamayo, A; Oliveira, E; Covalo, B; Casabó, J; Escriche, L; Lodeiro, CZ. *Anorg. Allg. Chem.*, 2007, 633, 1809-1814.
- [95] Tamayo, A; Pedras, B; Lodeiro, C; Escriche, L; Casabó, J; Capello, JL; Covalo, B; Kivekäs, R; Sillanpää, R. *Inorg. Chem.*, 2007, 46, 7818-7826.
- [96] Tamayo, A; Escriche, L; Casabó, J; Covalo, B; Lodeiro, C. *Eur. J. Inorg. Chem.*, 2006, 2997-3004.
- [97] Aragoni, MC., Arca, M; Bencini, A; Blake, AJ; Caltagirone, C; Decortes, A; Demartin, F; Devillanova, FA; Faggi, E; Dolci, LS; Garau, A; Isaia, F; Lippolis, V; Prodi, L; Wilson, C; Valtancoli, B; Zaccheroni, N. *Dalton Trans.*, 2005, 2994-3004.
- [98] Caltagirone, C; Bencini, A; Demartin, F; Devillanova, FA; Garau, A; Isaia, F; Lippolis, V; Mariani, P; Papke, U; Tei, L; Verani, G. *Dalton Trans.*, 2003, 901-909.
- [99] Shamsipur, M; Hosseini, M; Alizadeh, K; Alizadeh, N; Yari, A; Caltagirone, C; Lippolis, V. *Anal. Chim. Acta*, 2005, 533, 17-24.
- [100] Shamsipur, M; Alizadeh, K; Hosseini, M; Caltagirone, C; Lippolis, V. *Sens. and Actuators B*, 2006, 113, 892-899.
- [101] Jimenéz D; Martínez-Máñez, R; Sancenón, F; Soto, J. *Tet. Lett.*, 2004, 45, 1257-1259.
- [102] Descalzo, AB; Martínez-Máñez, R; Radaglia, R; Rurack, K; Soto, J. *J. Am. Chem. Soc.*, 2003, 125, 3418-3419.
- [103] Rurack, K; Trieflinger, C; Koval'chuck, A; Daub, J. *Chem. Eur. J.*, 2007, 13, 8998-9003.

- [104] Aragoni, MC; Arca, M; Demartin, F; Devillanova, FA; Isaia, F; Garau, A; Lippolis, V; Jalali, F; Papke, U; Shamsipur, M; Tei, L; Yari, A; Verani, G. *Inorg. Chem.*, 2002, 41, 6623-6632.
- [105] Kadarkaraisamy, M; Sykes, AG. *Polyhedron*, 2007, 26, 1323-1330.
- [106] Kadarkaraisamy, M; Sykes, AG. *Inorg. Chem.*, 2006, 45, 779-786.
- [107] Ferreira, ES; Garau, A; Lippolis, V; Pereira, CM; Silva, FJ. *Electroanal. Chem.*, 2006, 587, 155-160.

Chapter 6

STUDY OF POLYSACCHARIDES THERMAL STABILITY IN THE ASPECT OF THEIR FUTURE APPLICATIONS

*Wojciech Ciesielski**

Institute of Chemistry and Environmental Protection, Jan Długosz University,
Armii Krajowej Ave. 13/15, 42 201 Częstochowa, Poland.

ABSTRACT

The interaction of polysaccharides and cereal grains with transition metal ions is of a biochemical importance, mostly due to the presence of those complexes in biological systems. Metal polysaccharide chemistry plays a crucial role in crosslinking of various biomolecules, and formed polysaccharide/metal complexes are promising for various application, *e.g.* as drilling muds, heavy metal collectors and material for production of carbonizate and gaseous substances allowing preparation of second generation biofuels. In the study of cereal/metal complexes, the thermogravimetric measurements were also made in order to explain the influence of CoCl_2 , $\text{Cr}_2(\text{SO}_4)_2$, $\text{K}_2\text{Cr}_2\text{O}_7$, CuCl_2 , FeCl_3 , MnCl_2 , NiCl_2 , and ZnCl_2 on thermal decomposition of barley, oat, rye, triticale, and wheat grains in aspect of their applications for biofuels production. In investigation of polysaccharide/metal complexes, mainly concerning their conductivity as well as thermal stability and rheological properties, a special attention was paid to interactions of transition metal salts ($\text{Co}(\text{NO}_3)_2$, $\text{Cu}(\text{NO}_3)_2$, $\text{Ni}(\text{NO}_3)_2$, $\text{Co}(\text{CH}_3\text{COO})_2$, $\text{Cu}(\text{CH}_3\text{COO})_2$, $\text{Mn}(\text{CH}_3\text{COO})_2$, $\text{Ni}(\text{CH}_3\text{COO})_2$, CoCl_2 , CuCl_2 , FeCl_3 , MnCl_2 , NiCl_2 , CoSO_4 , $\text{Cr}_2(\text{SO}_4)_3$, CuSO_4 , $\text{Fe}_2(\text{SO}_4)_3$, MnSO_4) with potato, amarantus and cassava starch, potato amylose and potato as well as corn amylopectin.

Keywords: Cereals, complex, metal, polysaccharides, soil.

* Corresponding author: E-mail: w.ciesielski@interia.pl

INTRODUCTION

There exist a fairly abundant number of reports describing Werner-type complexes of mono- and di-saccharides as O-ligands [1-11]. Consequently, also polysaccharides are able to O-ligate metal ions [12-25]. Particular attention has been paid to starch as the ligand of metal ions. Relevant studies involved coordination of granular as well as pregelatinized starches of various botanical origin with numerous metal salts [26-27]. Structure of the inner coordination spheres of these complexes depends on cations and anions of used salts, however the coordination capacity of starches only in random cases is influenced by their botanical origin.

Coordination of metal ions with starch can result in the metal ion uptake by living organisms and their excretion from organisms within a food chain, therefore the life processes may be affected [28]. Coordination of starch to the central metal ions could be a positive phenomenon if starches are considered as, for instance, aids for soil cementation [29-40], depressants in the flotation of complex metal ores [41,42], as well as binders and plasticizers in metal oxide based ceramics [43-45]. Such coordination can also be advantageous if starches are used as collectors of heavy metals, for example from a wastewater, and as components of drilling muds [59-62].

Problem of the coordination of starch to metal ions is complex since counterions of salts used also interact strongly with starch [28, 46]. In the case of granular starch an additional factor has also to be taken into account, since on swelling, depending on the nature of the metal ion, either cations or anions penetrate the granule interior. It is known that anions penetrate granular starch suspended in aqueous solutions of metal salts of the first main group [25]. In contrast, cations of metals from higher main groups [26] and from transition groups [20] are bound in granules by coordination, as it was confirmed by EPR and thermal studies [13-20]. Starch gels coordinate to metal ions more efficiently than native starch; it is noteworthy that amylopectin binds metal ions stronger than amylose [17]. Potato starch and amylopectin from this starch, exhibiting anionic character, additionally coordinate metal ions to the phosphate groups [19,48].

In aqueous solutions, carbohydrate complexes with metal ions are fairly unstable because of low donor properties of hydroxyl groups. Computations of gas phase basicity performed for the hydroxyl groups of α -D-glucose [49] point to the hydroxyl group at C6 as the most basic center of this saccharide. Ability to form complexes increases by several orders in acidic media [50]. Only low selectivity between potential coordination sites in saccharides was observed [11]. In polysaccharides the hydroxyl groups at C2 and C3 are also involved in coordination, and this process does not influence the saccharide units conformation [27]. Disordered conformations of polysaccharide chains predominate at low salt concentration, whereas with the concentration increase the ordering of the macrostructures of complexes occurs [51-53].

Our former EPR studies [16-20] showed that complexes of starches with metal salts, namely Fe(III) chloride as well as Ni(II) acetate, chloride and nitrate had tetrahedral inner coordination spheres. However, Cu(II) nitrate and chloride formed complexes of the square planar inner coordination spheres, whereas Co(II) salts, except for acetate, had octahedral inner coordination spheres.

Although formation of the Werner-type complexes of metal salts with starches [16-20] has been proven, and structures of their inner coordination spheres, formation enthalpies, and thermal stabilities have been reported, neither macrostructure of such complexes nor capacity of starches in coordination of metal ions was explained. The problem was approached quantitatively involving conductivity and rheological measurements of starch pastes formed upon addition of metal salts [68,69]. The results are promising for future use of starches for example in drilling muds, or in soil conditioning, as well as for other applications.

Cations and anions of studied salts also affect significantly the thermal stability of complexes, the course and rate of their decomposition and amounts of carbonizate and gaseous products. In some cases temperature of decomposition can be considerably lowered, pointing out to a possibility of energy saving if starch would be used for production of carbonizate and/or synthetic gas (syngas) for Fischer-Tropsch production of fuels. The carbonizate could potentially replace coal, and serve as a supplement of biomass and wood as the source of syngas [63-67]. Because of versatile, renewable sources used for their production, such fuels might be classified as a biofuels. Additional benefit from the use of crops for this purpose would come from the fact that the crop quality and its potential contaminations bioaccumulated during the plant growth will not be essential for such type of application. A design of crops for production of biofuels not only from biomass and wood would keep agricultural production going, in spite of some limits put by European Union and Government [70] of the United States for production of crops for nutritional purposes only [71].

The catalytic effect of metal salts on the thermal decomposition and rheology of polysaccharides has been described, having in view selection of metal salts offering the most suitable pathway of polysaccharides decomposition for their non-food applications [68,69].

1. POLYSACCHARIDES AS METAL IONS COLLECTORS

Non-substituted carbohydrates are very weak acids ($pK_a > 12$) [72]. Computations of gas phase basicity for α -D-glucose [49] have assigned the hydroxyl group at C6 as the most basic center of this saccharide. In aqueous solutions, complexes are formed by replacement of water molecules coordinating central metal atom by hydroxyl groups of carbohydrates ligands [6]. Carbohydrate complexes with metal ions are unstable because of low donor properties of hydroxyl groups. Ability of starches to form complexes increases by several orders in acidic media [50]. In polysaccharides the hydroxyl groups at C2 and C3 are also involved in coordination and this process does not influence the saccharide units conformation [27]. It was found that the selectivity between potential coordinating sites in saccharides is very weak [73]. Disordered conformations of polysaccharide chains have a priority at low salt concentration but the increase in the salt concentration results in the ordering of macrostructures [52,53,74]. Depending on reaction conditions, the reagent conformations cause exclusion of potential coordination sites for steric reasons [75]. Around pH 7, the binding capacity of starches is low, ca 10 mg of metal ion per 1 g of starch [68]. On titration of starch gels with aqueous solutions of metal salts, before achievement of the saturation point, the conductivity of titrated solutions only slightly increases. Because in aqueous solutions the anions interact with starch even stronger than cations do [76,77], one cannot

state whether the observed effect might be associated with entering of cations into the inner coordination sphere of the central metal atoms.

Investigation of metal derivatives deals, first of all, with starches as metal ion carrying bioelements of a potential heterogeneous catalytic activity. Moreover the effect of metal ions on the thermal dextrinization of starches into British gums and production of starch carbonizate was studied. It should be mentioned also that dextrinization is a promising source of carbon monoxide and other gaseous products for hydrogenation affording hydrocarbons [78]. The known starch metal derivatives can be classified into three categories: (i) ion pairs, (ii) Werner complexes, and (iii) derivatives with the metal-oxygen valence bonds.

Salts of metals from the first main group form ion pairs with starch [25]. Anions of these salts interact with starch stronger than cations do. Therefore, anions sorb on starch, which acts as a hydrogen donor for starch/anion hydrogen bonds, whereas cations are held by Coulombic interactions. Such interactions influence considerably the starch decomposition [79]. Metals of higher main groups form Werner complexes [76] in which starch with its hydroxyl groups being sites of coordination, constitutes a polycentered macroligand.

The pregelatinized starch forms complexes more readily than granular starch. The observation of essential differences in the coordination of metal ions by potato and corn starches [19] induced a study on transition metals complexes with potato [19], amaranthus [16], and cassava [18] starches as well as on metal complexes of potato amylose and amylopectin [17]. These investigations involved determination of the structure of the coordination sphere around central atoms (Co(II), Cu(II), Fe(III), Mn(II), and Ni(II)), the role of counterion (chloride, nitrate and acetate), and thermal characteristics up to 500°C. Generally, except for potato starch and potato amylopectin, typical Werner complexes were formed. Because of the presence of phosphoric acid moieties in potato starch and its amylopectin, the metal cations are covalently bound to these sites and they are additionally coordinated by vicinal hydroxyl groups. In this way clathrates are formed, and in their cavities considerable amounts of water are closed. It was shown that transition metal ions also control the path of ligands thermolysis.

Recently, it was reported that potato starch was reacted with lanthanum [80], vanadium(III), chromium(III), molybdenum(V), tungsten(V) [81], as well as with bismuth(III) [82], and sodium bismuthate(V) [82]. These solid state reactions performed by a microwave heating yielded metal "starchates". Starch was crosslinked in them in various manners with the O-Metal-O linkages. They were stable towards hydrolysis suggesting that the metals forming -O-metal bonds can be additionally chelated. Thallation(I) was applied [83] for recognizing reaction sites in starch.

1.1. Numeric Calculations

Ability to coordinate metal ions and stability of complexes depend, among others, on dimension of the coordination centre and steric distribution of the coordination sites in ligands [73]. In the case of polysaccharides an analogy to smaller saccharide molecules, *e.g.* mono- and disaccharides often is found [84,85].

The DFT computations performed for studied complexes revealed an extent to which dissociation and subsequent intramolecular coordination influence the energy of HOMO and

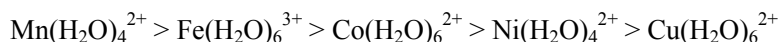
LUMO orbitals, and change the delocalization of electrons. The changes of planar and dihedral angles of the metal-oxygen bonds were reported basing on the optimized geometry of complexes with six glucose ligands [86].

The density of HOMO orbitals is localized mainly in the D-glucose rings with a dominating control of the electronegative oxygen atoms, while the density of LUMO orbitals is localized mainly on the central metal ion. As a result, the D-glucose units undergo a deformation, and also the changes of dihedral angles between the central metal ion and the oxygen atoms of the hydroxyl groups occur. These changes were accompanied by an increase in the ionization energy and the electron affinity, a decrease in the energy difference between HOMO and LUMO, and delocalization of the total electron density in the direction of coordinated D-glucose units [87].

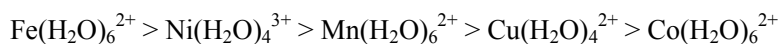
The comparison of energy values and HOMO and LUMO orbitals densities of the individual α -D-glucose unit to those of their metal complexes has shown a strong localization of electrons around a central metal atom of complexes [88]. The stability of such complexes expressed as their dissociation energy, increases with the number of D-glucose units in the inner coordination sphere.

Calculations were performed for α -D-glucose as a ligand coordinated to Co(II), Cu(II), Fe(III), Mn(II) and Ni(II) central ions; the presence of counterions was also taken into account. Based on the lowest energy criterion, the oxygen atoms of the hydroxyl groups at C2 and C3 appeared to be the most probable coordination sites in α -D-glucose.

Computations revealed that the stability of hydrated cations in the presence of either chloride or nitrate counterions decreases in the order:



whereas in the presence of the acetate counterion the corresponding order was as follows [86]:



The central metal ion in complexes with α -D-glucose was either anhydrous (in the case of MnCl_2 , CoCl_2 , $\text{Fe}(\text{NO}_3)_3$, $\text{Mn}(\text{NO}_3)_2$, $\text{Co}(\text{CH}_3\text{COO})_2$, $\text{Mn}(\text{CH}_3\text{COO})_2$, CuCl_2 , NiCl_2 , $\text{Ni}(\text{NO}_3)_2$, $\text{Cu}(\text{CH}_3\text{COO})_2$, $\text{Ni}(\text{CH}_3\text{COO})_2$) or it was coordinated with α -D-glucose units and water molecules (in the case of FeCl_3 , $\text{Co}(\text{NO}_3)_2$, $\text{Cu}(\text{NO}_3)_2$, $\text{Fe}(\text{CH}_3\text{COO})_3$) [68,69].

It was found that α -D-glucose can act as a bidentate ligand. Some formation heat values of complexes are positive, indicating that coordination of these centers with metal ions is impossible. Such results could be expected because of steric reasons. The chelation by tetraordinating metal ion with O1 and O2 oxygen atoms of hydroxyl groups is the most likely, and is followed by chelation with O3 and O4 atoms and then with O6 and O1 atoms. In the case of hexacoordinating metal ion, the chelation with O2 and O3 atoms, is the most probable, decreasing in the chelation of O1 and O2 atoms and then with O3 and O4 atoms [86]. The studies indicate also that complexes with single α -D-glucose ligands are energetically more stable than those containing α -D-glucose molecules bound linearly.

1.2. Conductivity of Solutions of Starch Complexes with Metal Salts

The influence of the cations on conductivity of starch complexes with metal salts was studied. It was observed that the starch gels upon addition of metal salts strongly increase their conductivity. One should mention that the opposite situation, *i.e.* when the metal salt solution is titrated with starch gels, no conductivity increase was observed. In most cases the titration of starch gels with FeCl_3 and NiCl_2 solutions proceeds differently than with other metal ions. The investigated starch gels had $\text{pH} > 7$, therefore chlorides could be transformed into hydroxides, which prior to dehydration, could in micellar form adhere to starch micelles [68,69].

Certainly, anionic character of potato starch has no essential effect on binding of metal ions. The viscosity of starch gels also does not affect the course of titration. It is known [55] that cassava gels contain residual lipids, but they also do not influence the metal binding. Thus, it may be suggested that the macrostructure of starch gels and their specific tendency to retrogradation [89,56], is dependent on kind of metal ions.

In investigation of Cu(II) salts, the experiments with $\text{Cu}(\text{CH}_3\text{COO})_2$, $\text{Cu}(\text{NO}_3)_2$ and CuCl_2 were performed. The acetate anion is a typical bidentate ligand, therefore its binding to the central metal atom is more efficient than that of nitrate or chloride and its interaction with hydroxyl groups is the strongest. The binding efficiency of anions decreases in the order: acetate > nitrate > chloride [68].

The influence of anions as counterions on the conductivity of complexes solutions plays also an essential role. For titration of corn, cassava and amaranthus starches a monotonous increase in the conductivity up to the saturation point was practically identical for used salts. Only CuCl_2 provided higher conductivity than other metals, it nearly monotonously increased up to the saturation point, then each subsequent dose of titrating solution caused a sharp conductivity increase. As mentioned above, it should be noted that the viscosity of solutions was not decisive for the conductivity of complexes solutions [69].

The properties of starch complexes with metal ions enable the use of dextrans as selective depressants in flotation of metal ores and as collectors of heavy metals in wastewater. If the temperature of decomposition of starch/metal complexes is appropriate, the obtained products have a different character, therefore they may be applied for selective separation of metals ores. This behavior is of a great practical importance in metallurgy industry. In the copper production, the removal of toxic lead complexes from copper concentrates may be performed by replacement of a highly toxic thioglycolic acid by modified dextrans.

2. POLYSACCHARIDES AS COMPONENTS OF DRILLING MUDS

2.1. Rheological Studies of Starch Complexes with Metal Salts

It was established that the addition of any metal salt solution (0.1M) dramatically reduces pseudoplasticity of starch gels and their thixotropy properties; the nature of the salt only weakly influences the observed phenomenon. A similar effect was found for more concentrated, 0.1 – 0.5M solutions. However the metal salt solution of above 0.5M concentration has only negligible effect upon pseudoplasticity and thixotropy of these systems;

such results indicate that the coordination to metal ions destroys the network of starch gels, this process occurring more efficiently for solutions of metal salts at higher concentrations. Relation of shear rate to shear stress for potato starch and its complexes with metal salts (0.1-0.5M and 0.01 – 0.0001M) shows that the surface area of the hysteresis loop depends on the concentration of salts, namely for solutions of low concentration this area is larger [68].

The strong decrease in the shear stress upon addition of salts suggests that the coordination sphere around the central metal atom is occupied by D-glucose units of the same molecule of starch, leading to the formation of globular structures. This behavior makes impossible the existence of stable, rigid network of the gel [69].

These studies point out that the starch/metal complexes may evolve water, this property being of an importance in mining processes, in which they are applied as components of drilling muds. An important objective of a drilling mud is to remove heat from the borehole. In the absence of starch/metal complexes in drilling muds, during mining process the decrease of water occurs, therefore the viscosity and plasticity of material become lower. This may result in the loss in the stability of walls and in the disturbance of work. Such difficulties may be avoided by use of starch/metal complexes which by water evolvment may improve conditions of the mining procedure [90].

3. POLYSACCHARIDES AS COMPONENTS OF BIOFUELS

It was established that the thermolysis of cereal grain complexes with metal ions may be controlled in aspect of carbonizate (*i.e.* residue) and gaseous products yields, on the contrary to thermolysis of non-coordinated cereal grains, where such control is not possible.

3.1. Biofuels from Cereal Grains/Metal Complexes

Study of thermolysis of cereal grain/metal complexes was made in the aspect of carbonizate and gaseous substances production.

The catalytic effect of CoCl_2 , $\text{Cr}_2(\text{SO}_4)_2$, $\text{K}_2\text{Cr}_2\text{O}_7$, CuCl_2 , FeCl_3 , MnCl_2 , NiCl_2 , and ZnCl_2 on the thermal decomposition of barley, oat, rye, triticale, and wheat grains was studied in order to select metal salts offering the most suitable pathway for decomposition of cereal grains, leading to gasification. It was found that the thermal stability and pathway for decomposition of cereal grains is different since it depends on their particular botanical varieties. The investigations were made by using TG, DTG and DSC measurements [???].

At first the thermolysis of non-coordinated cereal grains was studied; the results are summarized below.

Barley grains decompose in several steps. The fastest step is accompanied by a subsequent, nearly 50% weight loss, however up to 500°C the almost monotonous weight decrease was observed.

Oat grains are more thermally stable than barley grains. The degradation slows down around 250°C and turns into a monotonous process leaving at 500°C carbonizate in the yield of ca 80% of original grains weight.

Triticale grains are less thermally stable than barley and oat. The initially slow process accelerates from 250°C, and at 300°C the original weight of the sample is reduced to 32.5%. At 500°C the sample undergoes a complete volatilization.

Rye grains are more thermally stable than triticale grains, their decomposition starts around 300°C and leaves carbonizate in the 47.5% yield. The completely gasification occurs up to 500°C.

Wheat grains decompose similarly as rye grains. A fast single step decomposition at ca 300°C leaves carbonizate in 55% yield; this amount does not decrease up to 500°C [91].

3.1.1. Carbonizate production from cereal grains/metal complexes

Having in view the carbonizate production the following results were obtained.

Barley grains complexes, so with Co(II) as with Cu(II) ions decompose in a similar way. Both ions prolonged the first decomposition step and shortened the second step after which a fast reduction of the carbonizate amount occurred. The Fe(III) and Mn(II) ions closely resembled Co(II) and Cu(II) ions in their catalytic activity. Ni(II) ion is a catalyst changing the decomposition pattern of barley grain to a least extent. The decomposition pathway in the presence of either Cr(III), Cr(VI) or Zn(II) proceeded in a completely different way for each of these ions. In the case Cr(III) ion the degradation proceeds slowly and almost steadily up to 500°C; at this temperature the grains leave 30% of carbonizate. The Zn(II) ions very well stabilize the material of grains; a considerable degradation starts at ca 300°C and proceeds rapidly leaving no carbonizate. For Cr(VI) ion the degradation of fats occurs; no carbonizate was left up to 500°C.

Oat grains complexes with some salts cause a complete gasification up to 500°C, although non-coordinated oat grains are thermally stable and cannot be fully gasified up to this temperature. It was found that in the presence of Co(II) ions the gasification is practically completed already at 450°C. Such result was also obtained for Cr(III) and Mn(II) ions, however, in the case Cr(III) ions the thermolysis is more favorable due to its lower temperature; the fast weight loss begins already at 100°C. In contrast, the decomposition in the presence of Mn(II) ions requires heating to ca 260°C; in this process no weight loss was observed. The Fe(III) ions caused a complete volatilization around 450°C, but a weight loss of the sample started just above 375°C. The oat grains in the presence of Cr(VI) ions up to 500°C lose only 40% of their original weight. Similarly, Cu(II) and Ni(II) complexes do not undergo a complete decomposition; up to 500°C they lose 30 and 50% weight, respectively.

Triticale grains complexes with Fe(III) ions offered the most beneficial conditions for their full thermolysis. Up to 280°C the weight of sample decreased by 80%; at 500°C the complete volatilization of sample occurred. The promising results were achieved also by

heating triticale grains with Zn(II), Ni(II), and Cu(II) ions. The degradation in the presence of Co(II) and Mn(II) ions left about 20% of carbonizate up to 500°C.

Rye grains complexes with Cr(VI) ions are more thermally stable than the non-coordinating rye. For Cr(VI) complexes at 500°C the carbonizate (40%) was obtained. The degradation in the presence of the Zn(II) and Fe(III) ions at 500°C leaves 35 and 30% weight of sample, respectively. When grains were thermolysed in the presence of either Cu(II) or Mn(II) ions, the 10% of carbonizate was found at 500°C. It should be pointed out that only the Ni(II) ion offered complete decomposition, and its course was very promising; at 450°C the whole sample practically volatilized.

Wheat grains complexes with Mn(II) and Zn(II) ions undergo complete decomposition, in this process Mn(II) ions are more efficient catalysts than Zn(II) ions. However the non-coordinated wheat grains leave 55% carbonizate up to 500°C. In the case of Cu(II), Cr(III) and Cr(VI) the complete decomposition was not observed. The Fe(III), Co(II) and Ni(II) ions are only weak catalysts; at 500°C the carbonizate amounts of 30, 40 and 60%, respectively, were found [91].

In the conclusion concerning thermolysis of cereal grain complexes in the aspect of carbonizate production it may be established that Mn(II) ion is a better catalyst than Zn(II) ion. The Cu(II), Cr(III) and Cr(VI) ions do not cause a complete decomposition; in every case 10% of carbonizate was left at 500°C. Except for two cases, *i.e.* oat and triticale grains with Fe(III), the production of carbonizate was increased when concentration of the salt was lower.

3.1.2. Syngas production from cereal grains

In these investigations, as a first experiment the thermolysis of non-coordinated cereal grains was studied.

The decomposition of cereal grains and cereal grains/metal complexes affords gaseous products containing CO, methane, alkenes and CO₂.

The carbon monoxide evolving began from ca 250°C, it reached maximum yield (35-40% of the total volatile fraction) around 350°C, and its amount declined to 20-25% at 500°C. Potato starch is the best source of CO while the corn starch is for CO the worse source. The appearance of CO₂ as a sole gaseous product of starch degradation was observed already at 200°C [54] and was on the same level up to 500°C. The yield of CO₂ was only slightly dependent on the botanical origin of starch.

Methane appears in the volatile fraction already at 250°C but in 1% yield only. This amount increases to 40-50% at 450°C and then declines to 25-40% at 500°C. Similarly as in the case of CO production, potato strach is also the best source for methane whereas corn starch is the worst source for this gas. At 250°C alkenes form in the 1-1.5% amount, and their yield reaches maximum around 375°C. Acetic acid, aldehydes, ketones and tars constitute a minor fraction of organics. At elevated temperature tars undergo degradation to products of a lower molecular weight.

Comparing the thermal stability and pathway of degradation of considered grains one may conclude that for generation of CO from cereals, the triticale and rye grains are the best, the barley grains are worse, whereas the full gasification of the oat and wheat grains up to 500°C is impossible.

The thermolysis of cereal grains complexes with metal ions was investigated; the following results were obtained. It was observed that the cereal grains upon soaking in aqueous metal salts solutions strongly change their thermal properties. Salts can simply adsorb on the surface of grains as well as in their interior, or they may coordinate to the grain components, *e.g.* polysaccharides and proteins.

The complete gasification of grains treated with metal salts which would occur at possibly lowest temperature is essential from the practical point of view. Decrease in onset temperature of treated grain and rate of particular stages of degradation are also important, since faster degradation requires a lower amount of material to be heated.

In the case of barley grain complexes with Zn(II) ions a very efficient production of methane (94% of mass of the whole system) was established. Methane is also obtained for barley with Cr(VI) ions, however in this case its production is much lower (only 24%). Upon addition of Cu(II), Fe(III) and Mn(II) ions to barley grains, the obtained CO yields were in the range of 40- 60%.

In the case of oat grain complexes with Fe(III) ions large amounts (86%) of methane may be obtained. For Zn(II), Co(II) and Mn(II) ions large yields of CO (ca 65%) are formed. The thermolysis of the oat with Cu(II) ions affords small amounts of methane (and additionally CO). Thermolysis of oat with Ni(II) ions gives very small quantities of gaseous products, along with high yields (38%) of carbonizate. The lowest yields of gaseous products were found for Cr(VI) ions.

In the case of wheat grain complexes with Mn(II), Cr(III) and Cu(II), the large amounts of CO (ca 80%) are formed. Upon Fe(III) addition to wheat grains the large yields of carbonizate (33%) and large yields of gaseous products, mainly CO (above 50%) are obtained. The lowest amounts of gaseous products are found upon addition of Ni(II) and Co(II) ions to wheat; for Co(II) it is methane.

In the case of rye grain complexes with Cu(II) and Mn(II) ions the large amounts of CO (ca 70%) are formed. In the presence of Zn(II) ions, similarly as in the case of wheat with Fe(III) ions, the large amounts of carbonizate (35%) and of gaseous products in the form of CO (45%) are obtained. For Cr(VI) ions the lowest production of gaseous substances occurs, however large amounts of carbonizate are formed. Using Co(II) ions causes formation of gaseous substances (ca 25%), consisting mainly of methane and alkene.

In the case of triticale grain metal complexes only very small amounts of carbonizate are obtained, however high production of gaseous substances (mainly CO) is achieved. Solely for Ni(II) and Zn(II) ions the alkene fractions and CO₂ may form. Except for Cr(III) and Cr(VI) ions, the production of gases during the thermolysis is in the range of 55 - 85%.

In the summary one can state that barley grain complexes with Co(II), Cu(II), Fe(III), Mn(II) and Ni(II) ions decompose under most convenient conditions. The Fe(III) and Mn(II) ions enabled the lowest onset temperature of decomposition while the Cu(II) and Ni(II) ions caused the most efficient decomposition up to 300°C, accompanied by 61 and 60% weight loss, respectively; for Cu(II) ions the earlier weight loss than in the case Ni(II) ions was observed, *i.e.* Cu(II) ion is more efficient catalyst than Ni(II). Low amount of carbonizate in the case of Cu(II) ion confirmed the advantageous properties of the Cu(II) catalyst in gasification. Only Co(II) and Cr(III) ions caused a complete gasification of oat starch; among both of them, the Co(II) ion showed to be a better catalyst. Although the onset temperature of degradation (160°C) in the case Co(II) ion is higher than that for Cr(III) ion (100°C), in the case of Co(II) the 52% weight loss was achieved just up to 300°C. Triticale grain complexes

with Ni(II) and Cu(II) ions can be completely gasified up to 500°C. Both ions have comparable catalytic properties but advantage in using the Ni(II) ions results from a lower onset temperature of degradation. The Ni(II) ion is a catalyst providing complete decomposition of the rye grains up to 500°C. The wheat grains were efficiently thermolyzed in the presence of Zn(II) and Mn(II) ions.

In conclusion, having in view the economic problems, concerning production of carbonizate and gaseous substances it may be established that many systems of cereal grains with transition metal ions can serve for preparation of large amounts of carbonizate and of gaseous products. Among considered cereal grains/Co(II) systems, the highest production of carbonizate at relatively low temperature (230°C) is achieved in the case of barley/Co(II). The rye grains with metal ions afford carbonizate, however in lower yield than in the case of barley.

It was found that the treatment of the studied cereal grains with Zn(II) salts is very promising. Zinc is serving as catalyst for hydrogenation in coal pyrolysis, the use of the cereal/Zn(II) system for this purpose allows a better utilization of its catalytic properties by coordination of Zn(II) ions with hydroxyl groups of starch. Besides Zn(II) ions, also Ni(II) ions are very promising, in this case the carbonization begins at ca 250°C and affords large amounts of carbonizate. Complexes of oat with Ni(II) ion afford also high yields of carbonizate.

In the case of the triticale systems, the temperature of carbonization is relatively high, and the yields of carbonizate and gaseous products are very small; therefore from an economic point of view the application of triticale is unprofitable. Only the use of triticale in triticale/Cr(III) complex is promising (80% of carbonizate), but the loss of mass is linear and it is difficult to find the degradation onset temperature.

Having in view the yields of gaseous substances (CO and methane), the systems of cereal grains with metal ions are very suitable; they mainly afford high amounts of these products. Among the systems used, the barley/Zn(II) is the most promising. In the thermolysis of the oat/metal ions systems, the oxidation of polysaccharides, fats and proteins can occur, resulting in different composition of evolved gases, mainly consisting of methane. For the most efficient production of methane the Fe(III) ions are used, and for the CO production Cu(II) and Mn(II) ions are the best [91].

3.2. Biofuels from Polysaccharide Starches

Similarly as in the case of study of biofuels production from cereal grain/metal complexes, also investigation of production of biofuels obtained on the basis of three starch kinds of different botanical origin (potato, amaranthus and cassava starches), potato amylose and potato as well as corn amylopectin with metal salts (Co(NO₃)₂, Cu(NO₃)₂, Ni(NO₃)₂, Co(CH₃COO)₂, Cu(CH₃COO)₂, Mn(CH₃COO)₂, Ni(CH₃COO)₂, CoCl₂, CuCl₂, FeCl₃, MnCl₂, NiCl₂, CoSO₄, Cr₂(SO₄)₃, CuSO₄, Fe₂(SO₄)₃, MnSO₄) was performed.

It should be pointed out that the possible use of starch complexes with transition metal ions is of great importance in view of economy and of environment protection problems.

A unique character of potato starch among all known starches results from the large size of its granules and, first of all, from the chemical structure of its amylopectin. The phosphoric

acid moieties residing in every 12th to 200th D-glucose unit make this starch anionic, thus this starch has the natural cation-exchanging properties. The non-coordinated potato starch holds a certain amount and variety of cations collected from the soil on which potato plant was grown. Usually, they are sodium, potassium, magnesium, and calcium ions.

There exist procedures transforming potato starch into the cation-free, hydrogen starch [92-99]. Hydrogen starch is unstable for storage and undergoes the proton-catalysed autohydrolysis. Similarly, the cations originally residing in potato starch can be exchanged into a number of other cations [48]. The phosphoric acid moieties of potato starch are a primary place to which the metal ions can be bound. Up to now it is not known to what extent the addition of metal ions, involving solely the phosphoric acid moieties, would affect the ability of such starch to coordinate to a further number of cations, leading to Werner complexes.

The formation of complexes of various starches with metal ions was studied by many authors [26,77] and it was proven [20] that the Werner-type complexes are formed. The transition metal ions introduced into the phosphoric acid moiety of potato starch might fill their empty orbitals by coordination to the oxygen atoms of the hydroxyl groups of the D-glucose units. Under such circumstances a number of the intra and/or inter-molecular -(H)O-Metal-O(H)- bridges would be formed which might sterically inhibit formation of Werner complexes with further metal ions.

In the study of the TG/DTG/DSC diagrams of starch complexes with metal ions it was found that the patterns of their thermal decomposition were not superpositions of the diagrams for pure starch and a given pure salt, but they presented diagrams of complexes.

In the case when the increase in the temperature of the transition point exists, this fact is attributed to the coordination of metal ions with hydroxyl groups of starch or dextrin resulting from it. However, in the case when the decrease in the temperature of the transition point occurs, this fact can be tentatively assigned to the formation of eutectics, *i.e.* to the known effect of decrease of melting point of contaminated species. However, this behaviour is not so common as the former one.

Previous investigation [13-20,41,68,69,79,86,87,90] focus on the formation of starch complexes with metal ions, and on types of resulting complexes (sorption or helical complexes), as well as types of bonds existing in them. This study showed also that the coordination of starches of a different botanical origin influences thermal degradation of their metal complexes.

The thermolysis of starch/metal complexes at different temperatures is depending on the metal salt used; the stages of decomposition proceed at a different speed, also the yields of carbonizate and gaseous products are different. All these factors are crucial for the potential application of starch complexes for preparation of second generation fuels.

For these purposes the most suitable systems are those in which the onset temperature of decomposition is precisely determined, and possibly is the lowest. Moreover the carbonizate yield at that temperature should be high and not decreasing upon further heating. The weight loss (TG curve) should occur in a single, precisely shaped step, and not during many small steps. Similarly, the thermal effect (DSC curve) should be only one, ascribed to a given weight loss. Such process affords the largest amount of carbonizate, and the low decomposition temperature is very advantageous from economic point of view.

The studies show that some polysaccharide complexes with transition metal ions may serve for production of large quantities of carbonizate. In the case of potato starch, the use of

$\text{Cu}(\text{CH}_3\text{COO})_2$ is the most convenient, however for all studied complexes of amaranthus starch only “negative yields” of carbonizate are found, *i.e.* the carbonizate yield from starch complexes was lower than that for non-coordinated starch. In the case of cassava starch complexes with $\text{Cu}(\text{NO}_3)_2$, the carbonizate yield is highest among considered systems. The highest yields of gaseous products are obtained for cassava starch complexes. It should be noted that these products contain large amounts of CO (ca 65%). High amount of CO (ca 40%) in gaseous products are also observed for potato and amaranthus starch complexes. However, in the use of corn amylopectin complexes, the CO amount in gaseous products is much lower (ca 20%). All complexes affording high yields of CO also contain water, this fact suggesting that they are suitable substrates for production of syngas.

4. SOIL STABILIZATION BY POLYSACCHARIDES

Effect of polysaccharides on soil structure at the level of aggregation is varied in nature. Polysaccharides can create complex systems with other components of soil by adsorption of natural minerals. This is the case with montmorillonites [35]. Humic components in soil structure include numerous polysaccharides. In the presence of metal (e.g. of Fe and Al) oxides, and/or of multivalent metal ions their interaction with soil results in its microaggregation. When the soil conditions allow gelation of polysaccharides, the resulting gels afford with metal ions from soil not only micro- but also macroaggregation structures [100].

Polysaccharides are metal ion ligands, especially for transition metal ions. Depending on conditions, metal ions present in the soil coordinate, if it is possible, with polysaccharides. This behavior can substantially change the structure of polysaccharides, and thus the nature of interactions with the environment. In this case ionic or polar interactions are very important, since they strongly influence physicochemical and mechanical properties of soil. It should be pointed that the recent research results concerning the supplementation of soil by complexes of polysaccharides with metal ions, prepared in laboratory, is here very promising. Many transition metal ions are micronutrients, therefore such supplementation can have an additional importance in practice. The coordination by polysaccharides may cause a temporary immobilization of metal ions in soil. It should be pointed out that this behavior influences the bioaccumulation of metals in plants. Coordination of metal ions by polysaccharides may also affect gelation of these ligands and therefore control the soil micro- and macroaggregation.

Since fifties of last century, various measures of soil conditioning were used in agriculture. In this way prevention of soil erosion was achieved, along with the higher fertility and decrease of soil dehydration. Polysaccharides may also increase the soil plasticity [101] and improve its mechanical properties [102]. The soil conditioning by polysaccharides, such as starch and its copolymers have been used in the end years of last century [38,103]. Their cost is lower compared to the applied today synthetic copolymers, such as poly(vinyl alcohol), poly(acrylamide), hydrolyzed poly(acrylonitrile) and other [104]. Such treatments are also effective in the case of sandy soils [40,105]. The study shows that starch coordination with metal ions, regardless of their kind, lowers pseudoplasticity of gels and changes their

tixotropy properties. Therefore, it appears that this effect would be beneficial for soil cementation.

Upon addition of polysaccharides to soil, which contains metal ions, the earth structures will undergo the volume contraction. Such processes enable the formation of soil aggregates, strongly cementing the soil. This phenomenon can be used to obtain short-term protective layer, resistant against rain water erosion. The above behavior is particularly important in the case of a large area of slope angle, *i.e.* for embankments and slopes at bridges [106].

CONCLUSION

Along with a rapid development of science and technology the growing interest in non-food use of polysaccharides and cereals is observed. Today many reports concerning a wide variety of potential applications of these materials appear. The above paper shows unconventional examples of polysaccharides applications, *e.g.* as components of drilling muds, as well as soil stabilizers and collectors of heavy metal ions.

As a result of a fast development of civilization, the resources of various kinds of natural fuels are being more and more exhausted, and the search for new energy sources is necessary. However, this process requires major investments. In order to solve the above difficult and important problems, a growing attention is paid now to renewable energy sources. Having this in mind, the investigations of thermolysis of cereal grains and starches with metal ions are performed. The obtained results have shown that such procedures are promising for production of carbonizate and of volatile substances, and it should be pointed out that their yields may be controlled.

Resources of plant products (grains, straw, and their constituents - polysaccharides) are practically inexhaustible. They are a major source of renewable energy. These renewable energy sources can and should play an important role in enhancing the profitability of agriculture and in the activation of the rural population. It is therefore necessary to create the global energy system for future generations and provide the participation of many countries in these processes.

REFERENCES

- [1] Bandwar, R; Giralt, M; Hidalgo, J; Rao, C. Metal-saccharide chemistry and biology: saccharide complexes of zinc and their effect on metallothionein synthesis in mice, *Carbohydr. Res.*, 1996, 284, 73.
- [2] Bandwar, RC. Rao, Transition-metal-saccharide chemistry: synthesis and characterisation of D-galactose, D-fructose, D-glucose, D-xylose, D-ribose and maltose complexes of Mn(II), *Carbohydr. Res.*, 1996, 287, 157.
- [3] Bandwar, R; Rao, Ch. Transition-metal saccharide chemistry: synthesis and characterization of d-glucose, D-fructose, D-galactose, D-xylose, D-ribose, and maltose complexes of Ni(II), *Carbohydr. Res.*, 1996, 297, 341.

- [4] Bandwar, R; Sastry, M; Kadam, R; Rao, Ch. Transition-metal saccharide chemistry: synthesis and characterization of d-glucose, d-fructose, d-galactose, d-xylose, d-ribose, and maltose complexes of Co(II), *Carbohydr. Res.*, 1997, 297, 333.
- [5] Gyurcsik, B; Gajda, T; Nagay, L; Burger, K; Rockenbauer, A; Korecz, L. Proton, copper (II) and nickel (II) complexes of some Amadori rearrangement products of D-glucose and amino acids, *Inorg. Chim. Acta*, 1993, 57, 214.
- [6] Gyurcsik, B; Nagy, L. Carbohydrates as ligands: coordination equilibria and structure of metal complexes, *Coord. Chem. Rev.*, 2000, 203, 81.
- [7] Lu, Y; Deng, G; Miao, F; Li, Z. Metal ion interactions with sugars. The crystal structure and FT-IR study of the NdCl₃-ribose complex, *Carbohydr. Res.*, 2003, 338, 2913
- [8] Nagy, L; Burger, K; Kürti, J; Mostafa, MA; Korecz, L; Kiricsi, I. Iron(III) complexes of sugar-type ligands, *Inorg. Chim. Acta*, 1986, 124, 55
- [9] Nagy, L; Gajda, T; Burger, K; Pali, T. Saccharose complexes of manganese in different oxidation states, *Inorg. Chim. Acta*, 1986, 123, 35.
- [10] Norkus, E; Vaskelis, A; Vaitkus, R. On Cu (II) complex formation with saccharose and glycerol in alkaline solution, *J. Inorg. Biochem.*, 1995, 60, 299.
- [11] Saladini, M; Menabue, L; Ferrari, E. Sugar complexes with metal²⁺ ions: thermodynamic parameters of associations of Ca²⁺, Mg²⁺ and Zn²⁺ with galactaric acid, *Carbohydr. Res.*, 2001, 336, 55.
- [12] Burger, K; Illes, J; Gyurcsik, B; Gazdag, M; Forrai, E; Dekany, I; Mihalyfi, K. Metal ion coordination of macromolecular bioligands: formation of zinc(II) complex of hyaluronic acid, *Carbohydr. Res.*, 2001, 332, 197.
- [13] Ciesielski, W. Complexes of anionic polysaccharides with metal salts. Part II: Kappa carrageenan, *J. Food, Agr. Env.*, 2004, 2(1), 17.
- [14] Ciesielski, W. Complexes of anionic polysaccharides with metal salts. Part III: Iota carrageenan, *J. Food, Agr. Env.*, 2004, 2(1), 26.
- [15] Ciesielski, W; Tomasik, P. Metal complexes of xanthan gum, *EJPAU*, 2008, 11, 25.
- [16] Ciesielski, W; Kozioł, JJ; Tomasik, P. Complexes of amaranthus starch with selected metal salts and their thermolysis, *Thermochim. Acta*, 2003, 403, 161.
- [17] Ciesielski, W; Tomasik, P. Complexes of amylose and amylopectins with transition metal salts and their thermal properties, *J. Inorg. Biochem.*, 2004, 98, 2039.
- [18] Ciesielski, W; Tomasik, P. Coordination of cassava starch to metal ions and thermolysis of resulting complexes, *Bull. Chem. Soc. Ethiopia*, 2003, 17, 155.
- [19] Ciesielski, W; Tomasik, P; Werner-type metal complexes of potato starch, *Int. J. Food Sci. Technol.*, 2004, 39, 691.
- [20] Ciesielski, W; Tomasik, P; Lii, CY; Yen, MT. Interactions of starch with salts of metals from the transition groups, *Carbohydr. Polym.*, 2003, 51, 47.
- [21] Cross, H; Pepper, T; Keasley, W; Birch, GG. Mineral complexing properties of food carbohydrates, *Starch/Stärke*, 1985, 37, 132.
- [22] Debon, SJJ; Taster, RT. In vitro binding of calcium, iron and zinc by non-starch polysaccharides, *Food Chem.*, 2001, 73, 401.
- [23] Gough, B; Pybus, J. Effect of metal cations on the swelling and gelatinization behaviour of large wheat starch granules, *Starch/Stärke*, 1973, 25, 129.
- [24] Jane, J. ¹³C-NMR study of interactions between amylopectin and neutral salts, *Starch/Stärke*, 1993, 45, 172.
- [25] Lii, CY; Tomasik, P; Wei-Ling Hung, Vivian, MF. Lai, Revised look at starch interactions with electrolyte. Interactions with salts of metals from the first nontransition group, *Food Hydrocoll.*, 2002, 16, 35.

- [26] Lii, CY; Tomasik, P; Yen, MT; Lai, VMF. Re-examination of the interactions between starch and salts of metals from the non-transition groups, *Int. J. Food. Sci. Technol.*, 2001, 36, 321.
- [27] Lugovaya, Z; Tolmachev, V; Illenko, I. Study of the optical rotation of dextran solutions containing metal ions, *Vysokomol. Soedin.*, 1981, 23, 434.
- [28] Burger, K; Nagy, L. Biocoordination chemistry: coordination equilibria in biologically active systems, Ellis Harwood, London, 1990, 236.
- [29] Carter, MR; Andrews, SS; Drinkwater, LE. Managing soil quality: Challenges In modern agriculture; P; Schjønning, S; Elmholt, BT; Christensen, (Eds.), CAB International, Oxford, UK, 2004, 261.
- [30] Hu, S; Coleman, DC; Beare, MH; Hendrix, PF. Soil carbohydrates inaggrading and degrading agroecosystems: influences of fungi and aggregates, *Agricult. Ecosyst. Environm*; 1995, 54, 77.
- [31] Mehta, NC; Streuli, H; Muller, M; Deuel, H. Role of polysaccharides in soil aggregation, *J. Sci. Food Agric*; 1960, 11, 40.
- [32] Lado, M; Ben-Hur, M. Soil mineralogy effects on seal formation, runoff and soil loss, *Appl. Clay Sci*; 2004, 24, 209.
- [33] Bronick, C; Lal, R. Soil structure and management: a review, *Geoderma*, 2005, 124, 3.
- [34] Martin, JP. Microorganisms and soil aggregation. II. Influence of bacterial polysaccharides on soil structure, *Soil. Sci.*, 1946, 61, 157.
- [35] Greenland, DJ. The adsorption of sugars by montmorillonite. II. Chemical studies, *J. Soil Sci.*, 1956, 7, 329.
- [36] Carter, MR; Stewart, BA. Structure and organic matter storage in agricultural soils, Lewis/CRC Press, Boca Raton, FL, 1996, 55.
- [37] Ball Ball, BC; Cheshire, MV; Robertson, EAG; Hunter, EA. Carbohydrate composition inrelation to structural stability, compactibility and plasticity of two soils in a long-term experiment, *Soil & Till. Res*; 1996, 39, 143.
- [38] De Boodt, MF. Soil conditioning a modern procedure for restoring physical soil degradation, *Pedologie*, 1993, 43, 157.
- [39] Darling, FE; Crofting agriculture, Its practice in the Western Highland, Olivier and Boyd, Edinburg, 1945, 163.
- [40] Chapman, VJ. Seaweeds and their uses, 2nd Edn, Methuen, London, 1970, 304.
- [41] Kapuśniak, J; Ciesielski, W; Kozioł, JJ; Tomasik, P. Starch based depressors for selective flotation of metal sulfide ores, *Starch/Staerke*, 1999, 51, 416.
- [42] Drzymała, J; Tomasik, P; Sychowska, B; Sikora, M. Dextrins as selective flotation depressants for sulfide minerals, *Phys. Probl. Min. Proc.*, 2002, 36, 273.
- [43] Schilling, CH; Biner, SB; Goel, H; Jane, J. Plastic shaping of aqueous alumina suspensions with sucrose and maltodextrin additives, *J. Environ. Polym. Degr.*, 1995, 3, 153.
- [44] Schilling, CH; Tomasik, P; Sikora, M; Kim, CJ; Garcia, VJ; Li, CP. Molding technical ceramics with polysaccharides, *Żywn. Technol. Jakość*, 1998, 4(17), Suppl; 217.
- [45] Sikora, M; Schilling, C; Tomasik, P; Li, CY. Dextrin plasticizers for aqueous colloidal processing of alumina, *J. Eur. Ceramic Soc.*, 2002, 22, 625.
- [46] Tomasik, P; Schilling, C. Chemical Modification of Starch, *Adv. Carbohydr. Chem. Biochem.*, 2004, 59, 176.
- [47] Mazurkiewicz, J; Nowotny-Rozanska, M; Tomasik, P. Viscosimetric studies on hydration of ions, *Chem. Scripta*, 1988, 28, 375.

- [48] Leszczyński, W. Properties of potato starch saturated with ferric salts, *Acta Aliment. Pol.*, 1985, 11, 21.
- [49] Jebber, KA; Zhang, K; Casady, CJ; Chung-Phillips, A. Ab Initio and Experimental Studies on the Protonation of Glucose in the Gas Phase, *J. Am. Chem. Soc.*; 1996, 118, 10515.
- [50] Hay, B; Hancock, R. The role of donor group orientation as a factor in metal ion recognition by ligands, *Coord. Chem. Rev.*, 2001, 212, 61.
- [51] Lakatos, B; Meisel, J; Rockenbauer, A; Simon, P; Korecz, L. EPR and Mössbauer spectroscopic studies on metal complexes of pectic acid and their derivatives, *Inorg. Chim. Acta*, 1983, 79, 269.
- [52] Cheetham, N; Mashimba, E. Proton and ¹³C-NMR studies on xanthan derivatives, *Carbohydr. Polym.*, 1992, 17, 127.
- [53] Cheetham, N; Tao, L. Solid state NMR studies on the structural and conformational properties of natural maize starches, *Carbohydr. Polym.*, 1998, 36, 285.
- [54] Muzimbaranda, C; Tomasik, P. Microwaves in physical and chemical modification of starch, *Starch/Staerke*, 1994, 46, 469.
- [55] Gibinski, M; Palasinski, M; Tomasik, P. Physicochemical properties of defatted oat starch, *Starch/Staerke*, 1993, 45, 354.
- [56] Jane, J. Chemical and functional properties of food saccharides, Tomasik, P; (Ed), CRC Press, Boca Raton, 2004, Ch. 7.
- [57] Steffe, JF. Rheological methods in food process engineering, Freeman Press, East Lansing, MI, 1996, 21.
- [58] Polish Standards, Potato starch, PN-68/C-89034, 2000.
- [59] Wojnar, K. Wiertnictwo-Technika i Technologia, Wyd. Naukowe PWN, Warszawa-Kraków, 1997.
- [60] Herczak, M; Sawicka-Żukowska, R; Jędrychowska, B. Płuczki do wiercenia otworów hydrogeologicznych, *Tech. Poszuk. Geol.*; 3, 33 (1989).
- [61] Bielewicz, D; Bahrynowski, S. Analysis of drilling muds in view of their resistivity to microflora, using Merck metod, *Zesz. Nauk. AGH Wiertnictwo, Nafta, Gaz*, 21/1, 2004, 61.
- [62] Berkhuisen, JE. Płuczka polimerowo-potasowa firmy BDC, *Nafta-Gaz*, (7-8), 1992, 178.
- [63] Boerrigter, H. Greek diesel production with Fischer-Tropsch synthesis, http://www.senternovem.nl/mmfiles/26674_tcm23-279868.pdf
- [64] Pimentel, D; Patzek, TW. Ethanol production using corn, switchgrass, and wood. Biodiesel production using soybean and sunflower. *Nat. Resour. Res.*; 2005, 14(1), 65-76.
- [65] Schanke, D; Hansen, R; Sogge, J; Hoftad, KH; Wesenberg, MH; Rytter, E. Optimum integration of Fischer-Tropsch synthesis and syngas production, US Patent 6696501.
- [66] Srinivas, S; Malik, RK; Mahajani, SH. Fischer-Tropsch synthesis using biosyngas and CO₂, *Adv. Energy Res.*; 2006, 317-322.
- [67] Zwart, R. Large scale Fischer-Tropsch diesel production, <http://www.tu-freiberg.de/~wwwiec/conference/conf07/pdf/7.1.pdf>.
- [68] Ciesielski, W; Sikora, M; Krystyjan, M; Tomasik, P. Quantitative studies on coordination of starches and their polysaccharides to the transition metal atoms and its consequences, *Starch. Recent Progress in Biopolymer and Enzyme Technology*, Ed. Tomasik, P; Yuryev, V. P; Bertoft, E. 2008, 183.

- [69] Ciesielski, W; Krystyan, M; Starch-metal complexes and their rheology, *E-Polymers*, 2009, 092.
- [70] Website of European Commission: <http://ec.europa.eu/>.
- [71] Sahn, David, E. The Impact of Export Crop Production on Nutritional Status in Cote D'Ivoire. *World Development*, Vol. 18, No. 12, pp. 1635-1653, December 1990. Available at SSRN: <http://ssrn.com/abstract=455560>.
- [72] Hegetschweiler, K; Schmalle, H; Streit, H; Schneider, W. Synthesis and structure of a novel hexanuclear iron(III) complex containing six terminal and twelve bridging alkoxo groups and one μ_6 -oxo bridge, *Inorg. Chem.*, 1990, 29, 3625.
- [73] Dewar, MJS; Zebisch, EG; Healy, EF; Stewart, JJP. AM1: A New General Purpose Quantum Mechanical Molecular Model, *J. Am. Chem. Soc.*; 1985, 107, 3902.
- [74] Lakatos, B; Meisel, J; Rockenbauer, A; Simon, P; Korecz, L. EPR and Mössbauer spectroscopic studies on metal complexes of pectic acid and their derivatives, *Inorg. Chim. Acta*, 1983, 79, 269.
- [75] Parker, A; Boulenger, P; Kravchenko, T. *Food Hydrocolloids*, Plenum Press, New York, 1992, 307.
- [76] Braudo, E; Plashchina, I; Semenova, M; Yuryev, V. Structure formation in liquid solutions and gels of polysaccharides. A review of the authors work, *Food Hydrocoll.*, 1998, 12, 253.
- [77] Tomasik, P; Schilling, C. Starch complexes. Part I. Complexes with inorganic guests, *Adv. Carbohydr. Chem. Biochem.*; 1998, 53, 263.
- [78] Okkerse, C. van Bekkum, H. Starch 96, *The Book* (eds. H. Van Doren and N. Van Swaaij), Zestec Carbohydrate Research Foundation, Nordwijkhout, 1997, Ch. 1.
- [79] Ciesielski, W; Koziol, JJ; Tomasik, P. Effect of mineral salts on thermal homolytic decomposition of starch, *Pol J. Food Nutr. Sci.*, 2001, 10, 37.
- [80] Tomasik, P; Schilling, C; Refvik, M; Anderegg, J. Starch-lanthanum complexes, *Carbohydr. Polym.*; 2000, 41, 61.
- [81] Tomasik, P; Anderegg, JW; Jane, J; Baczkowicz, M. Potato starch derivatives with some chemically bound bioelements, *Acta Pol. Pharm., Drug. Res.*, 2001, 58, 447.
- [82] Baczkowicz, M; Wojtowicz, A; Anderegg, JW; Schilling, CH; Tomasik, P. Starch complexes with Bismuth (III) and (V), *Carbohydr. Polym.*; 52, 263 (2003).
- [83] Baran, W; Tomasik, P; Sikora, M; Anderegg, J. Thallium (I) starchate, *Carbohydr. Polym.*, 1997, 32, 209.
- [84] Yang, L; Tian, W; Zhao, Y; Jin, X; Weng, S; Wu, J; Xu, G. Sugar interaction with metal ions. The crystal structure and Raman spectra study of SmCl_3 -galactitol complex, *J. Inorg. Biochem.*, 2001, 83, 161.
- [85] Yang, L; Su, Y; Liu, W; Jin, X; Wu, J. Sugar interaction with metal ions. The coordination behavior of neutral galactitol to Ca(II) and lanthanide ions, *Carbohydr. Res.*, 2002, 337, 1485.
- [86] Ciesielski, W. Quantum-mechanical simulation of the structure and stability of starch – metal cation complexes, *E-Polymers*, 2009, 092.
- [87] Ciesielski, W; Generation and structure of oligosaccharide free radicals, *J. of Phys.*, 2007, 79, 012041.
- [88] Ciesielski, W; Koziol, JJ; Tomasik, P. Structure and properties of D-glucosyl radicals, *Food Sci. Agric. Chem.*; 2001, 3, 109.
- [89] Shao, YY; Tseng, YH; Chang, YH; Lin, JH; Li, Ch, Y. Rheological properties rice amylose gels and their relationships to the structures amylose and its subfractions, *Food Chem.*, 2007, 103, 1324.

-
- [90] Ciesielski, W. Studium nad nowymi sposobami wykorzystania skrobi do celów niespożywczych (kolektory jonów ciężkich metali, stabilizatory gleby, płuczki wiertnicze), Wydawnictwo Akademii Jana Długosza, Częstochowa, 2008.
- [91] Ciesielski, W. Cereal grains as source for syngas, EJPAU, 2009, 12(2), #14.
- [92] Pałasiński, M; Studies on physicochemical properties of potato starch. V. Saturation of phosphoric acid in starch with sodium and potassium (in Polish). , Zesz. Nauk. WSR Kraków, Rolnictwo, 1964, 211, 65.
- [93] Pałasiński, M. Autohydrolysis of hydrogen starch (in Polish), Zesz. Nauk. AR Kraków, Rozpr; 7, 1968, 1-93.
- [94] Pałasiński, M. Ueber die Phosphorsaeure in der Kartoffelstaerke, Starch/Staerke, 1980, 32, 405-408.
- [95] Pałasiński, M; Bussek, J. Studies on physicochemical properties of potato starch. VI. Saturation of phosphoric acid in starch with calcium (in Polish). Roczn. Technol. Chem. Żywn; 1964, 10, 47-53.
- [96] Pałasiński, M; Schierbaum, F. Die Selbsthydrolyse der Kartoffelsaerke. II. Starch/Staerke, 1971, 23, 383-390.
- [97] Pałasiński, M; Fortuna, T; Nowotna, A. Autohydrolysis of hydrogen starch with limited water content, *Acta Aliment. Pol*; 1981, 7, 127-136.
- [98] Gibiński, M. Preparation of ammonium starch (in Polish), Zesz. Nauk AR Kraków, 1987, 213(2), 35.
- [99] Winkler, Eigenschaften und Bedeutung der H-Staerke, Starch/Staerke, 1961, 10, 319.
- [100] Carter, MR; Stewart, BA. (Eds.), Structure and Organic Matter Storage in Agricultural Soils. Lewis/CRC Press, Boca Raton, FL, 1996, 477-55.
- [101] Ball, BC; Cheshire, MV; Robertson, EAG; Hunter, EA. Carbohydrate composition in relation to structural stability, compactibility and plasticity of two soils in a long-term experiment, *Soil & Till. Res*; 1996, 39, 143.
- [102] Rahimi, H; Pazira, E; Tajik, F. Effect of soil organic matter, electrical conductivity and sodium adsorption ratio on tensile strength of aggregates, *Soil & Tillage Res*; 2000, 54, 145.
- [103] Azam, RAI. Agricultural polymers, polyacrylamide preparation, application and prospects in soil conditioning, *Comm. Soil Sci. Plant Anal.*, 1980, 11, 767.
- [104] Öztürk, HS; Türkmen, C; Erdogan, E; Baskan, O; Dengiz, O; Parlak, M. Effects of a soil conditioner on some physical and biological features of soils: results from a greenhouse study, *Biores. Techn.*, 2005, 96, 1950.
- [105] Darling, FE; Crofting agriculture, Its practice in the Western Highland, Olivier and Boyd, Edinburg, 1945, 163.
- [106] Ciesielski, W. Soil stabilization by polysaccharides, *J. of Phys.*, 2010, accepted, in press.

Chapter 7

INTERACTIONS OF CYCLODEXTRINS WITH AMINO ACIDS, PEPTIDES AND PROTEINS

*Katarzyna Guzow and Wiesław Wiczek**

Faculty of Chemistry, University of Gdańsk, Sobieskiego 18, 80-952 Gdańsk, Poland.

ABSTRACT

For many years cyclodextrins and their inclusion complexes with different compounds have been widely studied by means of different experimental as well as theoretical methods. Among most popular compounds used as host molecules in the inclusion complexes are biologically active compounds, especially peptides and proteins as well as amino acids as model molecules. Such interest is a result of searching for new drug carriers. To study interactions of cyclodextrins with above mentioned host molecules, experimental methods such as ^1H NMR, fluorescence spectroscopy and microcalorimetry are used. In this review, basing on literature as well as own research, the application of those methods will be widely and critically discussed. Also, the influence of different factors such as distance between chromophore and functional groups, presence of protective groups, peptide chain conformation and amino acid chirality on the binding constants with cyclodextrins and thermodynamic parameters of the inclusion or other types of complexes formed will be described.

INTRODUCTION

The intriguing structure of cyclodextrins has attracted chemists, physicist, biologists, and many others in attempts to take advantage of the unique properties. Cyclodextrins are among the most important molecular receptors studied in supramolecular chemistry. They have raised many questions and provided answers to academic and industrial problems. One of the most interesting subject of cyclodextrin science is the mode of interaction with the hydrophobic guest molecule as well as investigation of driving forces responsible for

* Corresponding author: Phone: (+48)-(58)-5235353, Fax: (+48)-(58)-5235472, E-mail: ww@chem.univ.gda.pl.

inclusion complex formation, its stability and structure. When guest molecules are peptides or proteins, especially biologically active compounds, the importance of such studies considerably increases. In this review, the nature of interaction of naturally occurring and chemically modified cyclodextrins with amino acids and their derivatives, peptides and proteins are discussed.

STRUCTURE OF CYCLODEXTRINS

Cyclodextrins (CDs) are a family of macrocyclic compounds which comprises of three well-known industrially produced major cyclic oligosaccharides as well as several rare minor ones. The three major cyclodextrins are crystalline, homogenous and nonhygroscopic substances which are torus-like macro-rings of glucopyranose units. As the nomenclature of cyclodextrins is not exact, the practically important, industrially produced CDs are named α -, β -, and γ -CDs and referred to as first generation or parent cyclodextrins [1]. Table 1 lists some basic properties of the native CDs.

The α -, β -, and γ -CDs are composed of six, seven and eight glucopyranose units, respectively, connected through α -(1,4)-glycosidic bond as presented in Fig. 1 [1]. The glucopyranose rings are in the rigid 4C_1 conformation (Fig. 1), however, C^1 -O- C^4 bridges between these units are responsible for the flexibility of CD, observed also in the solid state [2,3]. As the consequence the glucose residues are in such arrangement that the secondary hydroxyl groups (C^2 and C^3) are located on one edge of the ring whereas the primary hydroxyl groups (C^6) on the other one, resulting in torus-shaped, or better said wreath-shaped, truncated cone molecule (Fig. 1).

Table 1. Physicochemical properties of α -, β - and γ -cyclodextrins.

	α -CD	β -CD	γ -CD
Number of glucopyranose unit	6	7	8
Empirical formula (anhydrous form)	$C_{36}H_{60}O_{30}$	$C_{42}H_{70}O_{35}$	$C_{48}H_{80}O_{40}$
Molecular weight [g/mol] (anhydrous form)	972.85	1134.99	1297.14
Solubility in H_2O (room temp.) [mol/dm ³]	0.1211	0.0163	0.168
Optical rotation [α] _D 25°C	+150.5	+162.0	+177.4
Height of cavity h [Å]	7.8	7.8	7.8
Inner diameter a [Å]	4.7-5.3	6.0-6.5	7.5-8.3
Outer diameter b [Å]	14.6 ± 0.4	15.4 ± 0.4	17.5 ± 0.4
Approx. cavity volume V [Å ³]	174	262	427
Crystalline water [% molecular weight]	10.2	13.2-14.5	8.13-17.7
pK_a (potenciometric) 25 °C	12.332	12.202	12.081
ΔH° (solution) [kJ/mol]	32.1	34.8	32.4
ΔS° (solution) [J/mol*K]	57.8	49.0	61.6

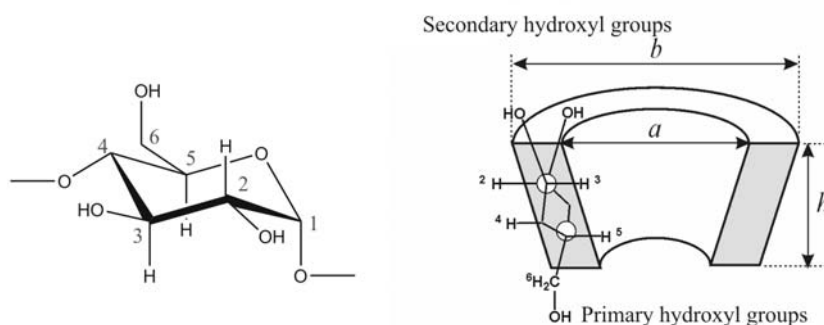


Figure 1. Structure of cyclodextrin (on the right) and conformation of glucose residue with atom numbering (on the left).

The C²-OH group of one glucopyranose unit can form a hydrogen bond with C³-OH group of the adjacent glucopyranose unit. These hydrogen bonds form a complete secondary belt in the CD molecule. Because of that β -CD is a rather rigid structure which explains its lowest water solubility among all CDs (Table 1). The hydrogen bonds belt is incomplete in the α -CD molecule, because of distorted position of one of its glucopyranose unit resulting in only four fully established hydrogen bonds instead of six possible ones. The γ -CD is nonplanar, more flexible structure and the most soluble in water among these three CDs (Table 1). Also, it is worth mentioning that the strength of the hydrogen bonds depends on the environment in which CD molecule is dissolved [1-3].

For a long time only the three major CDs (α , β and γ) were known and well-characterized. However, series of larger CDs have been isolated and studied. For example the nine-membered δ -CD had greater aqueous solubility than the β -CD but less than that of α - and γ -CDs. The larger CDs are not regular cylinder-shaped structures. They are collapsed and their real cavity is even smaller than that of γ -CD.

The apolar C³ and C⁵ hydrogens and ether-like oxygens of CD are inside whereas the hydroxyl groups are outside this molecule. This results in a molecule with a hydrophilic outside, which can dissolve in water, and an apolar cavity, which provides a hydrophobic matrix, enabling cyclodextrins to form inclusion complexes with a wide variety of nonpolar, amphiphilic and bola-amphiphilic compounds [2]. The three dimensional structure and size provide an important parameter for complex formation. The formation of axial inclusion complexes is mainly governed by the thickness of the guest compared to the internal diameter of the CD. The guest experiences a bottleneck at the level of H⁵ hydrogens invading the CD cavity [4]. The diameter of the hydrophobic part of the guest has to be less than the minimal diameter of the CD to permit the formation of a stable axial inclusion complex. X-ray, NMR and theoretical calculations show that the CD with the included guest molecule has axial symmetry C_n (n=6, 7, 8) with the glucosidic oxygen atoms lying in the plane and all glucopyranose units with chair conformations.

Apart from naturally occurring cyclodextrins, many cyclodextrin derivatives have been synthesized. These derivatives are usually produced by aminations, esterifications or etherifications of primary and secondary hydroxyl groups of cyclodextrins [5]. Depending on the substituent, the solubility of the cyclodextrin derivatives is usually different from that of their parent cyclodextrins. Virtually, all derivatives have hydrophobic cavity volume changed

and also these modifications can improve solubility and stability against the light or oxygen as well as help control the chemical activity of guest molecule and toxicity for parental drug administrations [6]. For the better control of the binding strength towards organic guests having various shapes and chemical functions or for the use of modified cyclodextrins as the chemosensor molecules [7], different capped cyclodextrins derivatives have been also synthesized [8].

POSSIBLE DRIVING FORCES OF COMPLEXATION PROCESS

A primary criterion for the inclusion of guest within the host's cavity is obviously its size (size selectivity). The complexation is based, depending on the solvent and type of host and guest, on a combination of several intramolecular interaction (and possibly hydrophobic effects): electrostatic interactions (ion-ion interactions, ion-dipole interaction and dipole-dipole interactions), charge-transfer interactions, release of conformational strain, van der Waals interactions, removing of the high energy water molecules from cavity, hydrogen bonding, entropy changes.

Electrostatic Interactions

The electrostatic interaction is usually the energy of interaction between ion-ion, ion-dipole and dipole-dipole. As CDs are neutral molecules, the ion-ion interactions do not occur unless the CD is appropriately substituted. CDs molecule are polar with permanent dipole moment (about 2-4 D) caused by the presence of polar hydroxyl groups on the both rims of the molecule as well as the nonbonding electron pairs of the glucosidic oxygen bridges directed toward the inside of the cavity producing a high electron density there and lending it some Lewis base characteristics. Thus the ion-dipole and dipole-dipole interactions must play a role in their complexation. Moreover, dipole-dipole interactions play an essential role in stabilization of the complex as well as determining its orientation [9].

Charge-Transfer Interactions

The charge-transfer interactions, comprehended as the transfer of charge/electron from the higher-lying occupied molecular orbitals of one molecule into the lower-lying unoccupied molecular orbitals of another molecule, are observed between the substituted group of CD and the guest compounds [10]. Moreover, the direct charge-transfer interaction between CD skeleton and the substrate has also been observed [11].

Relief of Conformational Strain

The crystalline packing and the presence of water molecules in the solid state causes that the geometry of a CD molecule does not correspond to the global energy minimum and

usually is less symmetrical than in solution. However, the relief of conformational strain upon complexation is not a driving force of CD complexation in the solution [12]. The CD molecules usually undergo a significant conformational change upon complex formation to optimize opportunity of other mode of interactions. Thus, the “induced fit” mechanism is an experimental behaviour, not a driving force in CD complexation.

Van Der Waals Interactions

Van der Waals force mostly seems to mean either the induction and dispersion forces combined or dispersion force alone. As CDs have modestly large dipole moments, the induction force could be strong in CD complexation. However, the importance of dispersion force is hard to show, because dipole-induced dipole interactions are always present. It should be mentioned that van der Waals interactions also exist between the solvent molecules and the substrates of CD. Thus, in the CD complexation the substrate is exchanging one set of van der Waals interactions (with the solvent molecules) to another set (in CD cavity). This type of exchange is the reason why ion-dipole interactions are not significant in CD complexation. The polarizability of water molecule is lower than that of organic component lying in the CD cavity and it is expected that van der Waals interaction should be stronger between CD and substrate than between water and substrate [9].

Exclusion of Cavity-Bounded High-Energy Water

Two kinds of water molecules can be found within the CD or at the gate and in the proximity of cyclodextrins: water molecules bounded at the hall of the cage and structurally different networks of water molecules in the vicinity of the host [13]. The number of water molecules trapped inside the cavity or bounded to the gate is limited (about seven molecules for crystalline β -CD) and energy to cooperate is higher compared to the bulk water. Neutron scattering experiment showed that the disorder of water molecules inside the cavity is dynamic in nature, however, exhibits a larger degree of spatial and orientational order than in the bulk phase [14]. The exclusion upon the CD complexation of the “high energy” cavity-bounded water molecules was postulated as a driving force leading to the complex formation. However, the solvent reorganization energy is a process of enthalpy-entropy compensation without any free-energy contribution. The incorporation of a guest molecule leads through the decrease in the number of degrees of freedom of the guest (translational and rotational) to a decrease in entropy and is accompanied by the negative enthalpy change. However, the free energy of the process is not necessarily negative. Thus, the exclusion of cavity-bounded water is not a driving force of the complexation [12].

Hydrogen Bonding

The important role of hydrogen bonding in the CDs complexation has been well established in the solid state [12,15,16]. However, the role of hydrogen bonding in CD

complexation in aqueous solution is controversial as water can compete with CDs in forming hydrogen bonds with the substrate molecule. Nevertheless, many examples of hydrogen bonding in CD complexation in aqueous solution have been shown. Ross and Rekharsky shown that the binding of the phenolic hydroxyl substituted derivatives of phenylethylamine and hydrocinnamate, which are capable to form an additional hydrogen bond, to β -CD is characterized by 1.4 to 2.0 kcal/mol more exothermic values of ΔH^0 and more negative values of ΔS^0 than the reference compounds [17]. The formation of an additional hydrogen bond between the glucosidic oxygen atoms and tyrosine phenolic hydroxyl group explains a higher binding constant compared to that of phenylalanine [18].

Hydrophobic Interactions

Hydrophobicity was considered to be the result of the enhanced structure of the water molecule in the vicinity of the non-polar solute, which would bring about a usually large entropy loss during hydration. According to this model, the destructive overlap of the hydrophobic hydration shell, which is entropically favourable due to the release of the structured hydration water, constituted the driving force for the aggregation of nonpolar solute in aqueous solution. These driving forces are usually named the hydrophobic interaction. The hydrophobic effect refers to the fact that nonpolar substances are less soluble in water than in organic solvent. The CDs cavity is relatively nonpolar (especially compared with the surrounding aqueous solution) and hydrophobic guest will prefer the environment inside cavity. Molecular dynamics simulation has shown nearly 50% decrease of the dielectric constant of water molecules confined in the cavity [14]. There are many studies on the estimation of the polarity of the CD's cavity, where various kinds of fluorescence probes have been used [19]. However, there are many discrepancies regarding the polarity values (ϵ) of the CD's cavity which are in the wide range from 2.2 to 74, but more values are around the polarity of different kind of alcohols (1-octanol $\epsilon=10.3$, 1-pentanol $\epsilon=13.9$, methanol $\epsilon=32.7$ or ethylene glycol $\epsilon= 37.7$) [19]. The estimated ϵ values most likely depend not only on the kind of fluorescent probe but also on the environment around it, that is the type of the inclusion complex, as the probe used does not necessarily totally enter the cavity, because the interior of the CD cavity is not wide and deep enough for each probe. Hydrophobic effects are sometimes analyzed in terms of two factors: a/ the cavitation energy, which corresponds to the unfavourable energy required to make a cavity in water, and b/ the energy of interactions between the solute and solvent, which corresponds to the energy required to put a solute into an appropriately sized and solvent-surrounded cavity. Both factors are directly related to the surface area of the guest. It was found that the hydrophobic effect on binding correlates with the change of the exposed surface area that occurs upon binding [20].

In CD chemistry, evidence of the presence of hydrophobic interactions is the observation that in the CD complex the most non-polar portions of the guest molecules are usually enclosed in the CD cavities as well as the fact that the increasing hydrophobicity of substituent of the guest molecule enhances the complexation [17]. Another evidence of the hydrophobic interactions is that the strength of CD complexation is usually weakened upon addition of organic co-solvent [21].

The driving forces leading to the inclusion complexation of cyclodextrins should include all mentioned above interactions. Usually, it is found that van der Waals and hydrophobic interactions constitute the major driving forces for cyclodextrins complexation, whereas electrostatic interactions and hydrogen bonding can significantly affect the conformation of a particular inclusion complex.

Enthalpy-entropy compensation is the phenomenon in which the change in enthalpy is offset by corresponding change in entropy resulting in a smaller net free energy change. The compensatory enthalpy-entropy relationship has been often observed empirically [1,9,17,22-24], while no explicit relationship between the enthalpy change and the entropy change can logically be derived from fundamental thermodynamics [13,26]. In these papers, it was shown that the diverse chemical and biochemical supramolecular systems, including cyclodextrins, can be analysed consistently using the following equations:

$$T\Delta\Delta S^0 = \alpha\Delta\Delta H^0 \quad (1)$$

$$\Delta\Delta G^0 = (1-\alpha)\Delta\Delta H^0 \quad (2)$$

Thus, the slope (α) of the $T\Delta S^0$ versus ΔH^0 plot (eq. 1) indicates to what extent the enthalpic gain ($\Delta\Delta H^0$), which is induced by the alternations in host, guest, or solvent, is cancelled by the accompanying entropic loss ($\Delta\Delta S^0$). In the other words, only a fraction ($1-\alpha$) of the enthalpic gain can contribute to the enhancement of complex stability. Moreover, the intercept ($T\Delta S_0^0$) represents the inherent complex stability (ΔG^0) obtained at $\Delta H^0=0$, which means that the complex is stabilized even in the absence of enthalpic gain, as far as the $T\Delta S_0^0$ term is positive. The slope (α) and the intercept ($T\Delta S_0^0$) of the regression line are related to the degree of conformational changes and the extent of desolvation of both host and guest upon complexation, respectively [17,22]. However, more recently it has been suggested that the actual source of the compensation effect should be related to contributions due to solvent reorganization [9,23,24]. Some authors state that because temperature dependence of binding constant is not measured with high precision over a large temperature range, the experimental error rather than any fundamental principle may be responsible for the apparent correlation between ΔH and ΔS [20,25]. The linear relationship between ΔH and ΔS is really just a statement that ΔG is a constant in such cases.

STOICHIOMETRY AND BINDING CONSTANT DETERMINATION

Research in host/guest chemistry should follow several well-defined steps: proof of the inclusion, determination of the complex stoichiometry, determination of the association constant and eventually determination of the inclusion complex geometry and thermodynamic parameters of the complex formation. Many experimental techniques allow to confirm the formation of an inclusion complex. Also, some descriptions of determination of complex stoichiometry exist in the literature. Among these, the Job diagram is probably the most reliable [26,27].

The 1:1 (guest:host) stoichiometry is the common type of CD's complexes. Another complex stoichiometries such as 1:2, 2:1, 2:2, 1:1:1 and 1:1:2 are also frequently observed.

For a given guest, the stoichiometry, stability, and structure of the complex can depend on the type of CD, mainly because of its cavity size.

Many different experimental techniques which can give information about concentration of the “free” and complexed components in solution are used for the binding constant determination. Among them, the UV-Vis spectroscopy, fluorescence spectroscopy (steady-state and time-resolved), NMR spectroscopy and microcalorimetry are the most popular ones. Each method has some limitations and is characterized by different accuracy. Thus, the selection of appropriate method needs to consider many parameters. The concentrations of the “free” and complexed guest and host molecules have to be suitable for the sensitivity of the selected method. The component used in low concentration (usually guest) is responsible for the choice of the method, however, the higher concentration component (usually host) causes the change of the observable. Moreover, the smallest deviation of the binding constant is obtained when the low-concentration component is bounded in 20% to 80%. Thus, ^{13}C NMR is applied when the binding constant is lower than $K < 10^2 \text{ M}^{-1}$, whereas ^1H NMR for $K < 10^4 \text{ M}^{-1}$ [28]. The spectrophotometric method allows to determine binding constant $K < 10^5 \text{ M}^{-1}$ when molar absorption coefficient is equal to $10^4 \text{ M}^{-1}\text{cm}$, whereas steady-state fluorimetric titration method is useful when $K < 10^8 \text{ M}^{-1}$ [29].

UV-Vis Spectroscopy

For the 1:1 guest:host complex the binding constant can be determined by Benesi-Hildebrand method [30] using the equation:

$$\frac{1}{\Delta A} = \frac{1}{[G]_T \Delta \varepsilon} + \frac{1}{\Delta \varepsilon \times K [G]_T [CD]_T} \quad (3)$$

where: $\Delta \varepsilon$ is the difference of molar absorption coefficients of „free” and bounded host molecules, $[G]_T$ and $[CD]_T$ – is the total concentration of host and cyclodextrin, respectively, K is the binding constant, ΔA – is the difference of absorbances at measured wavelength.

A good fit of the eq. 3 to the experimental points indicates on the 1:1 stoichiometry. However, for the low cyclodextrin concentration the calculated binding constant is overestimated. The more precise binding constant is obtained from the non-linear fitting to the equation:

$$\Delta A = \frac{\Delta \varepsilon \times K [G]_T [CD]_T}{1 + K [CD]_T} \quad (4)$$

whereas eq. 3 is used for the stoichiometry determination [31].

For the nonchromogenic substrate a competitive spectrophotometric method may be used [32,33].

Fluorescence Spectroscopy

Among all methods applied, fluorescence spectroscopy is one of the widest used because of its high sensitivity, very low background and small amount of studied compound requirement. In this method, properties of fluorescent guest such as fluorescence band position, fluorescence quantum yield, fluorescence lifetime or anisotropy are measured as the host molecule is nonfluorescent. The observed changes are a result of differences in microenvironment of the bulk solution and CD cavity. In the fluorimetric titration method, the equilibrium constant of complex with 1:1 stoichiometry is usually calculated using the non-linear least-squares method applying following equation [34,35]:

$$I_f = \frac{I_G^0 + I_{G:CD}^0 K [CD]_0}{1 + K [CD]_0} \quad (5)$$

or in linear form:

$$\frac{1}{I_f - I_G^0} = \frac{1}{K(I_{G:CD}^0 - I_G^0)[CD]_0} + \frac{1}{I_{G:CD}^0 - I_G^0} \quad (6)$$

For successive 1:2 complex formation one obtains:

$$I_f = \frac{I_G^0 + I_{G:CD}^0 K_1 [CD]_0 + I_{G:CD^2}^0 K_1 K_2 [CD]_0^2}{1 + K_1 [CD]_0 + K_1 K_2 [CD]_0^2} \quad (7)$$

where: I_f - the fluorescence intensity of the guest in the presence of various [CD] concentration; I_G^0 - the fluorescence intensity of the guest in water; $I_{G:CD}^0$ and $I_{G:CD^2}^0$ - the fluorescence intensity of 'pure' 1:1 (G:CD) and 1:2 (G:CD²) complex, respectively, whereas K_1 and K_2 - denote the stepwise association constants for 1:1 and 1:2 complexes, respectively.

According to Pistolis and Malliaris, the use of non-linear least-squares fitting method (eqs 5 and 7) as well as so-called double reciprocal plots (eq. 6) for the determination of the stoichiometry and equilibrium constant of reaction involving weak complex formation does not always suggest the correct parameters of such reactions [36].

Equations (5), (6) and (7) are valid for a large excess of CD over dyes and with the assumption that during the excited state lifetime the conversion of the uncomplexed dye to the complexed one and *vice versa* can be excluded since the corresponding guest exchange rate constants are small [37,38]. In most cases, the condition $[CD]_0 \gg [G]_0$ is easy to meet and $[CD]_0$ can be used for [CD] in the data analysis. However, for the system with high K value, typically $K > 10^4 \text{ M}^{-1}$, it is sometimes difficult to maintain the condition throughout the experiment. In this case for the 1:1 complex stoichiometry the binding constant can be obtained from non-linear fitting of eq. 8 to the experimental data [39]:

$$I_f = I_G^0 + \frac{(I_{G:CD}^0 - I_G^0) \{ ([G]_0 + [CD]_0 + 1/K_1) - \sqrt{([G]_0 + [CD]_0 + 1/K_1)^2 - 4[G]_0[CD]_0} \}}{2[G]_0} \quad (8)$$

For a more complicated systems appropriate equations can be found in [21,40].

Time-Resolved Fluorescence Spectroscopy Method

If fluorescence intensity decay of the guest molecule is mono-exponential one can expect that the guest molecule incorporated into the CD cavity will change its fluorescence lifetime because of different microenvironment. If lifetime of “free” (τ_G) and bounded guests (τ_{GCD}) distinctly differ, fluorescence intensity decay of the mixture can be described by bi-exponential function with one of the fluorescence lifetime corresponding to the lifetime of “free” guest, whereas the second to the lifetime of the complex:

$$F(t) = \alpha_G \exp(-t / \tau_G) + \alpha_{GCD} \exp(-t / \tau_{GCD}) \quad (9).$$

Moreover, pre-exponential factors (α_G and α_{GCD}) are proportional to the concentrations of both forms. Thus, the binding constant can be calculated using formula:

$$K = \frac{\alpha_{GCD}}{\alpha_G [CD]} \quad (10)$$

where: α_G is the pre-exponential factor connected with the fluorescence lifetime of “free” guest, α_{GCD} is the pre-exponential factor connected with the fluorescence lifetime of inclusion complex, $[CD]$ is the concentration of cyclodextrin.

However, the ratio of the pre-exponential factors is equal to the ratio of concentrations of bounded and “free” guest molecules according to the following equation:

$$\frac{\alpha_{GCD}}{\alpha_G} = \frac{\varepsilon_{GCD} \Phi_{GCD} \tau_G [G \cdot CD]}{\varepsilon_G \Phi_G \tau_{GCD} [G]} \quad (11),$$

if the following assumptions are fulfilled:

a/ there is no change in the absorption spectra or excitation is at the isosbestic wavelength ($\varepsilon_G = \varepsilon_{GCD}$);

b/ only nonradiative processes are affected ($\Phi_G / \Phi_{GCD} = \tau_G / \tau_{GCD}$),

or c/ $\varepsilon_{GCD} \Phi_{GCD} \tau_G = \varepsilon_G \Phi_G \tau_{GCD}$;

d/ there is no shift in the emission spectra or observation is at the isoemissive wavelength [41].

The examples of application of this method to the calculation of binding constant of tyrosine and phenylalanine and their analogues with CDs are given in [42,43].

NMR Spectroscopy

NMR spectroscopy is widely used in the CDs chemistry, especially in the studies of structure and molecular arrangement of inclusion complexes using 2D technique [35,44,45].

Moreover, NMR spectroscopy is also used in the binding constant determination if the chemical shift of the “free” and bounded guest signals are not too small or binding constant is small. The appearance of the NMR spectrum of the guest-host mixture would depend on the binding constant and the rate of the exchange rate. In the case of similar exchange rate of the host-guest complexation equilibrium compared to the NMR time scale, the NMR peaks broaden and/or disappear, so it is impossible to measure them. There are two following cases suitable for the measurement by NMR spectroscopy.

1. The host-guest complexation equilibrium which has very slow exchange rate compared to the NMR time scale. In this case, the peaks which are assigned to the host parts in the complex and those of the “free” host are observed individually at the same NMR spectrum.
2. The host-guest complexation equilibrium which has a very fast exchange rate compared to the NMR time scale. In this case, peaks which are assigned to the host parts in the complex and those to the “free” host are fused and appear at the weight average chemical shift of the “free” and complexed host [28,29].

Studies of the dynamics of CD inclusion complex formation and dissociation reveal that the inclusion rate constant is in the order of $10^8 \text{ M}^{-1}\text{s}^{-1}$, which is much lower than the diffusion controlled rate constant. This is a result of association complex formation, being in equilibrium with the substrate, before the inclusion complex forms. Thus, the measured association rate constant is an apparent value. The dissociation rate constant is in the order of 10^5 s^{-1} [37,46-48]. Thus, the second case is the most frequent in the CDs chemistry and appropriate computer program for binding constant calculation using chemical shifts is available in literature [49]. However, there has been growing interest in the use of pulsed field gradient methods that give information on binding constant via the molecular self-diffusion coefficient [50,51].

Microcalorimetric Titration

In the isothermal calorimetric titration (ITC) method the heat of reaction is used to follow a titration experiment. The pattern of these heat effects as a function of the molar ratio [ligand]/[macromolecule] can then be analyzed to give the thermodynamic parameters of the interaction under study from a single experiment. This permits determination of the mid point (stoichiometry) of a reaction as well as its enthalpy (ΔH), entropy (ΔS) and of primary concern the binding constant (K). Application of ITC method is determined by the solubility of the reactant. In order to obtain a binding constant with a high accuracy the product of value of binding constant molar concentration of macromolecule (the Wiseman parameter “ c ”) should be higher than about 10. However, under certain circumstances the determination of the binding constant is possible for a lower value of “ c ” [52]. One of the advantage of this method is the possibility of determination of thermodynamic parameters of reaction at constant temperature. For all aforementioned methods, to determine the enthalpy and entropy changes Van't Hoff equation should be used after repeating experiments at different temperatures. Moreover, these methods give the thermodynamic parameters values with a lower accuracy because of assumption of constant heat capacity in the measured temperature range.

Application of different experimental methods (microcalorimetry, fluorescence and NMR spectroscopy) allows to determine stoichiometry, binding constant and thermodynamic parameters of guest-host interaction in solution. However, binding constants determined by fluorescence spectroscopy and microcalorimetry for complex guest molecules do not necessarily have to coincide, because the observables for these two techniques are quite different and the guest/host concentration ratio for all applied methods are different. For example, in the fluorescence spectroscopy methods the microenvironment influences the photophysical properties and the information obtained refer to the nearest surrounding of fluorophore, whereas for the microcalorimetric method the total heat of all interactions between guest and host molecules is measured.

BINDING OF AMINO ACIDS BY CYCLODEXTRINS

The binding constants of amino acids and their derivatives and analogues with naturally occurring as well as modified cyclodextrins are collected in Table 2.

The data were obtained applying different experimental methods, but in most cases microcalorimetry, UV, fluorescence and NMR spectroscopies. Some of the data were obtained using ultrasonic relaxation or affinity capillary electrophoresis. The solvent used was water or D₂O at different pH or different buffer solution. Thus, direct comparison of the values of binding constants and the discussion of the influence of size of side chain of amino acid residue, protonation of amino acid moiety and size of CDs cavity on the binding constants is not possible. However, some general conclusions can be drawn. Using all data presented in Table 2 the distribution plot of CDs complexes within each 0.2 range of pK unit (a frequency distribution), like those presented by Connors [1] and Houk at al. [20] was prepared (Fig. 2).

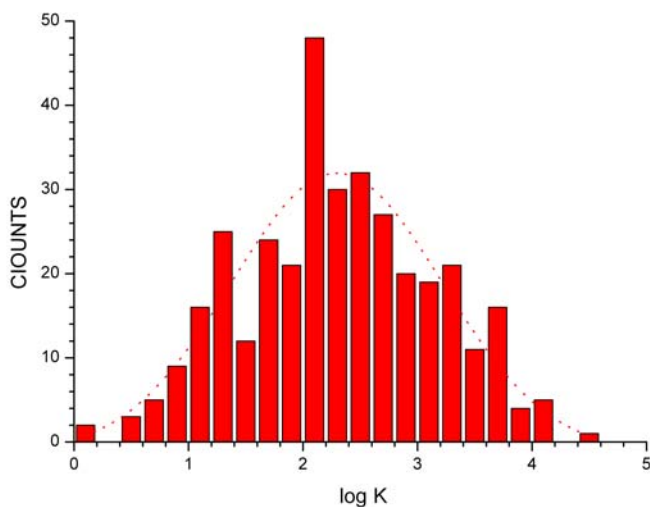


Figure 2. Frequency distribution (bars) and Gaussian distribution (dashed line) calculated for binding constants of 350 complexes of amino acids and their derivatives and analogues with various cyclodextrins.

Table 2. Binding constants of amino acids and their derivatives and analogues with various cyclodextrins.

Compound (charge)	Solvent	pH	T [K]	<i>K</i> [dm ³ /mol]	Method ^c	Ref.
<i>α</i>-CD						
L-Ala	H ₂ O	-	298	1122.0 ± 1.0	Cal	A
Gly	H ₂ O	-	298	562.3 ± 1.1	Cal	A
L-His	H ₂ O	-	298	9 ± 4	Cal	B
	H ₂ O	11.3 ^a	298	12 ± 1	Cal	B
L-Leu	D ₂ O	-	290	6.3 ± 0.3	NMR	C
L-Phe	D ₂ O	-	290	14.3 ± 0.4	NMR	C
	H ₂ O	-	298	15 ± 1	Cal	B
	H ₂ O	-	298	257.0 ± 1.1	Cal	A
	H ₂ O	-	298	13.6 ± 1.0	Cal	D
	H ₂ O	5.01 ^b	298	8 ± 5	Cal	E
	H ₂ O	6.84	298	125.0	UV	F
	H ₂ O	7.4 ^a	298	42.3	UV	G
	H ₂ O	7.4 ^a	296	13 ± 0.4	UV	H
	H ₂ O	7.6	298	25.5	NMR	I
	H ₂ O	11.0 ^a	298	15.5 ± 0.5	Cal	J
	H ₂ O	11.3 ^a	298	25 ± 1	Cal	B
	H ₂ O	13.6	298	7.9 ± 1.4	Fl	K
	H ₂ O	13.6 ^a	298	8 ± 3	Cal	B
D-Phe	H ₂ O	5.01	298	8 ± 6	Cal	E
	H ₂ O	6.84	298	70.4	UV	F
	H ₂ O	11.0 ^a	298	18.1 ± 2.8	Cal	J
D,L-Phe	H ₂ O	6.84	298	99.8	UV	F
L-Phe-NH ₂ (+1)	H ₂ O	5.01 ^b	298	12.0 ± 1.1	Cal	E
L-Phe-NH ₂	H ₂ O	10.02 ^c	298	18.6 ± 2.3	Cal	E
L-Trp	H ₂ O	7.2 ^a	298	61.7 ± 1.07	Cal	L
	H ₂ O	-	298	31.62 ± 8.19	Cal	M
	H ₂ O	-	298	19.05 ± 3.85	Cal	N
	H ₂ O	-	298	19 ± 4	Cal	B
	H ₂ O	7.4	298	21.4	Cal	G
	H ₂ O	7.4 ^a	298	17.0 ± 0.2	Cal	O
	H ₂ O	11.3 ^a	298	28 ± 1	Cal	B
	H ₂ O	11.3	298	28.18 ± 1.33	Cal	N
	H ₂ O	11.3	298	28.2 ± 1.0	Cal	J
L-Tyr	H ₂ O	-	298	794.3	Cal	N
	H ₂ O	-	293	8 ± 5	Fl	P
	H ₂ O	7.4	298	27.5	Cal	G
	H ₂ O	10.0	298	-	Cal	B
L-Val	H ₂ O	-	298	1621.8 ± 1.1	Cal	A
Mono[6-(1-Pyridinio)-6-deoxy]-<i>α</i>-CD						
L-Ala	H ₂ O	-	298	2344.2	UV	R

Table 2. (Continued)

Compound (charge)	Solvent	pH	T [K]	K [dm ³ /mol]	Method ^e	Ref.
D-Ala	H ₂ O	-	298	1548.8	UV	R
L-Asp	H ₂ O	-	298	4466.8	UV	R
L-Cys	H ₂ O	-	298	977.2	UV	R
L-Ile	H ₂ O	-	298	5248.1	UV	R
L-Leu	H ₂ O	-	298	3981.1	UV	R
D-Leu	H ₂ O	-	298	2238.7	UV	R
L-Pro	H ₂ O	-	298	2187.8	UV	R
L-Ser	H ₂ O	-	298	1412.5	UV	R
D-Ser	H ₂ O	-	298	831.8	UV	R
L-Trp	H ₂ O	7.2 ^a	298	245.5 ± 1.1	Cal	L
L-Val	H ₂ O	-	298	3630.8	UV	R
D-Val	H ₂ O	-	298	2138.0	UV	R
Sulfated-α-CD						
Arg	H ₂ O	4.5	295	87.3 ± 18.3	ACE	S
	H ₂ O	9.4	295	121.6 ± 18.9	ACE	S
Cys	H ₂ O	9.4	295	40.3 ± 17.8	ACE	S
Citrulline	H ₂ O	4.5	295	222.1 ± 97.8	ACE	S
	H ₂ O	9.4	295	231.8 ± 24.7	ACE	S
Lys	H ₂ O	4.5	295	103.3 ± 11.9	ACE	S
	H ₂ O	9.4	295	167.2 ± 12.4	ACE	S
Orn	H ₂ O	4.5	295	181.8 ± 14.8	ACE	S
	H ₂ O	9.4	295	139.1 ± 4.8	ACE	S
β-CD						
<i>N</i> -t-Boc-L-Ala (-1)	H ₂ O	6.9 ^a	298	367 ± 4	Cal	T
<i>N</i> -t-Boc-D-Ala (-1)	H ₂ O	6.9 ^a	298	392 ± 4	Cal	T
<i>N</i> -t-Boc-L-Ala-OMe	H ₂ O	6.9 ^a	298	578 ± 4	Cal	T
<i>N</i> -t-Boc-D-Ala-OMe	H ₂ O	6.9 ^a	298	659 ± 6	Cal	T
<i>N</i> -Cbz-L-Ala (-1)	H ₂ O	6.9 ^a	298	147 ± 4	Cal	T
<i>N</i> -Cbz-D-Ala (-1)	H ₂ O	6.9 ^a	298	149 ± 4	Cal	T
L-Cys	H ₂ O	9.88	298	1	Fl	U
<i>N</i> -Cbz-Gly (-1)	H ₂ O	6.9 ^a	298	157 ± 4	Cal	T
L-Ile	H ₂ O	-	298	4.9 ± 0.4	UR	V, W
L-Leu	H ₂ O	-	298	3.3	UR	V
	H ₂ O	9.88	298	9.35	Fl	U
DL-Norleucine	H ₂ O	9.88	298	6.3	Fl	U
DL-Norvaline	H ₂ O	9.88	298	0.4	Fl	U
L-Phe	H ₂ O	-	298	18.2 ± 3.18	Cal	N
	H ₂ O	-	293	15.3	Fl	X
				10.5 ± 6.2		
	H ₂ O	5.01 ^b	298	3 ± 7	Cal	E
H ₂ O	-	298	18 ± 3	Cal	B	

Table 2. (Continued)

Compound (charge)	Solvent	pH	T [K]	K [dm ³ /mol]	Method ^c	Ref.
	H ₂ O	6.84	298	26.5	UV	F
	H ₂ O	7.2 ^d	-	2000 ± 200	Fl	Y
	H ₂ O	7.4 ^a	296	17 ± 0.6	UV	H
	H ₂ O	9.88	298	50	Fl	U
	D ₂ O	11.0	304	454.5	NMR	Z
	H ₂ O	11.3	298	107.2 ± 13.03	Cal	N
	H ₂ O	11.3	298	107.2 ± 1.1	Cal	J
	H ₂ O	11.3 ^a	298	106 ± 12	Cal	B
D-Phe	H ₂ O	6.84	298	8.80	UV	F
	H ₂ O	7.2 ^d	-	2000 ± 200	Fl	Y
D,L-Phe	H ₂ O	6.84	298	17.0	UV	F
<i>o</i> -MePhe	H ₂ O	-	293	51.8	Fl	X
3,4-(OH) ₂ -L-Phe	H ₂ O	7.2 ^d	-	3500 ± 200	Fl	Y
3,4-(OH) ₂ -D-Phe	H ₂ O	7.2 ^d	-	3500 ± 300	Fl	Y
βPhe	H ₂ O	-	293	25.1	Fl	X
βHph	H ₂ O	-	293	23	Fl	X
				32.6 ± 7.6		
Hph	H ₂ O	2	293	98.7 ± 8.7	Fl	X
				78.2 ± 4.9		
				81.4 ± 8.9		
Tic	H ₂ O	-	293	11.5	Fl	X
<i>N</i> -Ac-L-Phe (-1)	H ₂ O	6.9 ^a	298	60.7 ± 1.3	Cal	B
	H ₂ O	6.9 ^a	298	67.5 ± 1.4	Cal	T, A1
	D ₂ O	6.9 ^a	298	80 ± 2	Cal	A1
<i>N</i> -Ac-L-Phe- <i>d</i> ₅ (-1)	H ₂ O	6.9 ^a	298	63.3 ± 1.5	Cal	A1
	D ₂ O	6.9 ^a	298	75 ± 2	Cal	A1
<i>N</i> -Ac-L-Phe- <i>d</i> ₈ (-1)	H ₂ O	6.9 ^a	298	62.7 ± 1.5	Cal	A1
	D ₂ O	6.9 ^a	298	73.6 ± 1.5	Cal	A1
<i>N</i> -Ac-D-Phe (-1)	H ₂ O	6.9 ^a	298	67.5 ± 1.4	Cal	B
	H ₂ O	6.9 ^a	298	60.7 ± 1.3	Cal	T
Dans-L-Phe	H ₂ O	6.9 ^a	298	368 ± 14	Cal	B1
Dans-D-Phe	H ₂ O	6.9 ^a	298	412 ± 10	Cal	B1
Naph-L-Phe	H ₂ O	6.9 ^a	298	565 ± 20	Cal	B1
Naph-D-Phe	H ₂ O	6.9 ^a	298	328 ± 20	Cal	B1
Nal	H ₂ O	-	288	460 ± 74	Fl	C1
			293	428 ± 57		
			303	305 ± 60		
			313	278 ± 40		
			323	206 ± 38		
	H ₂ O	-	298	190 ± 11	Cal	C1

Table 2. (Continued)

Compound (charge)	Solvent	pH	T [K]	K [dm ³ /mol]	Method ^c	Ref.
Ac-Nal-NH ₂	H ₂ O	-	288	600 ± 64 (K ₁) 42 ± 63 (K ₂)	Fl	C1
			293	445 ± 80 (K ₁) 48 ± 97 (K ₂)		
			303	373 ± 60 (K ₁) 8 ± 83 (K ₂)		
			313	350 ± 150 (K ₁) 221 ± 384 (K ₂)		
			323	329 ± 68 (K ₁) 46 ± 176 (K ₂)		
	H ₂ O	-	298	486 ± 9	Cal	C1
L-Phe-NH ₂ (+1)	H ₂ O	5.01 ^b	298	22 ± 2	Cal	E
L-Phe-NH ₂	H ₂ O	10.02 ^c	298	107 ± 3	Cal	E
	H ₂ O	10.0 ^c	298	109 ± 1	Cal	T
D-Phe-NH ₂	H ₂ O	10.0 ^c	298	101 ± 1	Cal	T
L-Phe-OMe (+1)	H ₂ O	4.8 ^b	298	12 ± 1	Cal	T
D-Phe-OMe (+1)	H ₂ O	4.8 ^b	298	11 ± 2	Cal	T
L-Phg	H ₂ O	7.2 ^d	-	1200 ± 100	Fl	Y
D-Phg	H ₂ O	7.2 ^d	-	1200 ± 100	Fl	Y
3-(4-hydroxyphenyl)propionic acid (3-(4-OH)PPA)	H ₂ O	2	293	588.4 ± 19.8	Fl	X
				589.4 ± 50.3		
				687 ± 22		
3-(4-hydroxyphenyl)propionate (-1) (3-(4-OH)PPA)	H ₂ O	6.9 ^a	298	297 ± 4	Cal	A1, D1
	D ₂ O	6.9 ^a	298	363 ± 4	Cal	A1
	H ₂ O	8.0	293	285 ± 28	Fl	X
L-Ser(Bzl)	H ₂ O	6.9 ^a	298	69 ± 3	Cal	T
D-Ser(Bzl)	H ₂ O	6.9 ^a	298	71 ± 4	Cal	T
<i>N</i> -t-Boc-L-Ser (-1)	H ₂ O	6.9 ^a	298	285 ± 2	Cal	T
<i>N</i> -t-Boc-D-Ser (-1)	H ₂ O	6.9 ^a	298	306 ± 2	Cal	T
<i>N</i> -CBZ-L-Ser (-1)	H ₂ O	6.9 ^a	298	109 ± 2	Cal	T
Tyramine (4-hydroxyphenethylamine) (+1)	H ₂ O	6.9 ^a	298	70 ± 2	Cal	A1, D1
	D ₂ O	6.9 ^a	298	82.1 ± 1.0	Cal	A1
	H ₂ O	-	293	26.2 ± 5.6	Fl	X
43.1 ± 6.0						
45 ± 11						
<i>p</i> -ethylphenol	H ₂ O	-	293	582.8 ± 11.1	Fl	X
				581.9 ± 15.3		
				653 ± 58		
	H ₂ O	-	298	457 ± 9	Cal	X
D-Trp	H ₂ O	8.9	298	12.9 ± 1.6	Fl	K
	H ₂ O	7.2 ^d	-	100 ± 10	Fl	Y

Table 2. (Continued)

Compound (charge)	Solvent	pH	T [K]	K [dm ³ /mol]	Method ^e	Ref.
L-Trp	H ₂ O	7.4	298	213.8	Cal	G
	H ₂ O	7.2	298	1819.7 ± 1.1	Cal	L
	H ₂ O	7.2 ^d	-	100 ± 10	Fl	Y
	H ₂ O	9.88	298	22.2	Fl	U
N-Ac-L-Trp (-1)	H ₂ O	6.9 ^a	298	17.1 ± 0.5	Cal	B, T
	H ₂ O	6.9 ^a	298	71.3 ± 0.7	Cal	E1
	H ₂ O	5.0 ^b	298	63.0 ± 0.7	Cal	E1
N-Ac-D-Trp (-1)	H ₂ O	6.9 ^a	298	12.7 ± 0.5	Cal	T, A1
L-Tyr	H ₂ O	-	293	50 ± 4	Fl	P
				40 ± 5		
				50.2 ± 5.4		
	H ₂ O	7.0	293	48 ± 5	Fl	F1
	H ₂ O	7.4	298	33.1	Cal	G
	H ₂ O	9.88	298	17.8	Fl	U
	D ₂ O	11	304	107.5	NMR	Z
	H ₂ O	11.3	298	148 ± 7.0	Cal	N
H ₂ O	11.3 ^a	298	147 ± 6	Cal	B	
Phg(OH)	H ₂ O	-	293	18 ± 10	Fl	X
				21.7 ± 9.1		
L-Phg(OH)	H ₂ O	7.2 ^d	-	1000 ± 100	Fl	X
D-Phg(OH)	H ₂ O	7.2 ^d	-	1000 ± 300	Fl	Y
Phg(Me)	H ₂ O	-	293	43 ± 15	Fl	X
				54 ± 13		
Tyr(Me)	H ₂ O	-	293	26.1 ± 4.8	Fl	X
				22.0 ± 5.8		
				20 ± 14		
βTyr(Me)	H ₂ O	-	293	15.9 ± 5.2	Fl	X
				21.0 ± 5.7		
				198 ± 6		
βHty	H ₂ O	-	293	118 ± 4	Fl	X
				121.0 ± 4.4		
				137 ± 58		
	H ₂ O	-	298	82.5 ± 5.7	Cal	X
βHty(Me)	H ₂ O	-	293	115.2 ± 4.8	Fl	X
				117.8 ± 3.3		
				116 ± 40		
	H ₂ O	-	298	138 ± 12	Cal	X
N-Ac-L-Tyr	H ₂ O	-	293	164.4 ± 16.3	Fl	X
				157.48 ± 17.9		
	H ₂ O	-	298	157.4 ± 17.9	Fl	G1
	H ₂ O	-	298	142 ± 4.7	Cal	G1

Table 2. (Continued)

Compound (charge)	Solvent	pH	T [K]	K [dm ³ /mol]	Method ^e	Ref.
<i>N</i> -Ac-L-Tyr (-1)	H ₂ O	6.9 ^a	298	130 ± 2	Cal	T, A1
	D ₂ O	6.9 ^a	298	156 ± 2	Cal	A1
<i>N</i> -Ac-D-Tyr (-1)	H ₂ O	6.9 ^a	298	125 ± 2	Cal	T
	D ₂ O	6.9 ^a	298	80 ± 2	Cal	A1
<i>N</i> -Ac-Tyr-NH ₂	H ₂ O	-	298	270.7 ± 50.9	Fl	G1
	H ₂ O	-	298	130 ± 7.8	Cal	G1
<i>N</i> -Ac-Tyr-NHMe	H ₂ O	-	298	118.6 ± 26.4	Fl	G1
	H ₂ O	-	298	122 ± 5.5	Cal	G1
<i>N</i> -Ac-Tyr-NHEt	H ₂ O	-	298	145.8 ± 32.9	Fl	G1
	H ₂ O	-	298	159 ± 15	Cal	G1
<i>N</i> -Ac-Tyr-NHPr ^g	H ₂ O	-	298	181.9 ± 35.1	Fl	G1
	H ₂ O	-	298	142 ± 11	Cal	G1
<i>N</i> -Ac-Tyr-NHPr ^l	H ₂ O	-	298	125.3 ± 13.0	Fl	G1
	H ₂ O	-	298	135 ± 12	Cal	G1
<i>N</i> -Ac-Tyr-NHBu ^h	H ₂ O	-	298	186.5 ± 27.6	Fl	G1
	H ₂ O	-	298	153 ± 28	Cal	G1
<i>N</i> -Ac-Tyr-NHBu ^s	H ₂ O	-	298	162.2 ± 14.4	Fl	G1
	H ₂ O	-	298	188 ± 23	Cal	G1
<i>N</i> -Ac-Tyr-NHBu ^t	H ₂ O	-	298	726.0 ± 123.6	Fl	G1
	H ₂ O	-	298	513 ± 17	Cal	G1
<i>N</i> -Ac-Tyr-NH(Me) ₂	H ₂ O	-	298	436.4 ± 38.1	Fl	G1
	H ₂ O	-	298	269 ± 4	Cal	G1
<i>N</i> -Ac-Tyr-NH(Et) ₂	H ₂ O	-	298	705.1 ± 33.2	Fl	G1
	H ₂ O	-	298	414 ± 10	Cal	G1
<i>N</i> -Ac-Tyr-NH(Pr ^g) ₂	H ₂ O	-	298	338.7 ± 15.2	Fl	G1
	H ₂ O	-	298	368 ± 19	Cal	G1
<i>N</i> -Ac-Tyr-NH(Bu ^h) ₂	H ₂ O	-	298	370.3 ± 55.7	Fl	G1
<i>N</i> -Ac-Tyr-NH(Bu ^t) ₂	H ₂ O	-	298	539.6 ± 76.4	Fl	G1
	H ₂ O	-	298	405 ± 15	Cal	G1
L-Val	H ₂ O	9.88	298	3.92	Fl	U
Partially methylated β-CD						
L-Phe	H ₂ O	7.4 ^a	296	4 ± 0.5	UV	H
Hydroxypropyl-β-CD						
L-Phe	H ₂ O	7.4 ^a	296	5 ± 0.5	UV	H
Sulfated-β-CD						
Arg	H ₂ O	4.5	295	151.8 ± 10.6	ACE	S
	H ₂ O	9.4	295	324.9 ± 93.8	ACE	S
Cys	H ₂ O	4.5	295	250.5 ± 49.1	ACE	S
	H ₂ O	9.4	295	719.5 ± 37.8	ACE	S
Citrulline	H ₂ O	4.5	295	231.8 ± 24.7	ACE	S
	H ₂ O	9.4	295	1068.6 ± 57.8	ACE	S

Table 2. (Continued)

Compound (charge)	Solvent	pH	T [K]	<i>K</i> [dm ³ /mol]	Method ^e	Ref.
Lys	H ₂ O	4.5	295	173.6 ± 3.1	ACE	S
	H ₂ O	9.4	295	142.0 ± 13.7	ACE	S
Orn	H ₂ O	4.5	295	368.8 ± 24.6	ACE	S
	H ₂ O	9.4	295	192.2 ± 22.0	ACE	S
Trp	H ₂ O	4.5	295	49.5 ± 4.9	ACE	S
Mono[6-(1-Pyridinio)-6-deoxy]-β-CD						
L-Ala	H ₂ O	7.2 ^a	298	1380.4	UV	H1
D-Ala	H ₂ O	7.2 ^a	298	1148.2	UV	H1
L-Asp	H ₂ O	7.2 ^a	298	4073.8	UV	H1
L-Cys	H ₂ O	7.2 ^a	298	269.2	UV	H1
L-Glu	H ₂ O	7.2 ^a	298	758.6	UV	H1
L-Ile	H ₂ O	7.2 ^a	298	7943.3	UV	H1
L-Leu	H ₂ O	7.2 ^a	298	4897.8	UV	H1
D-Leu	H ₂ O	7.2 ^a	298	2884.0	UV	H1
L-Lys	H ₂ O	7.2 ^a	298	204.2	UV	H1
L-Met	H ₂ O	7.2 ^a	298	331.1	UV	H1
L-Pro	H ₂ O	7.2 ^a	298	1202.3	UV	H1
L-Ser	H ₂ O	7.2 ^a	298	1174.9	UV	H1
D-Ser	H ₂ O	7.2 ^a	298	660.7	UV	H1
L-Trp	H ₂ O	7.2 ^a	298	5128.6 ± 1.1	Cal	L
L-Val	H ₂ O	7.2 ^a	298	4466.8	UV	H1
D-Val	H ₂ O	7.2 ^a	298	2187.8	UV	H1
Mono[6-[[[(1-methylpyrrolidin-2-ylidene)amino]sulfonyl]amino]-6-deoxy]-β-CD						
L-Phg	H ₂ O	7.2 ^d	-	4000 ± 200	Fl	Y
D-Phg	H ₂ O	7.2 ^d	-	3300 ± 200	Fl	Y
L-Phe	H ₂ O	7.2 ^d	-	2500 ± 100	Fl	Y
D-Phe	H ₂ O	7.2 ^d	-	6600 ± 400	Fl	Y
3,4-(OH) ₂ -L-Phe	H ₂ O	7.2 ^d	-	1000 ± 100	Fl	Y
3,4-(OH) ₂ -D-Phe	H ₂ O	7.2 ^d	-	10000 ± 400	Fl	Y
L-Phg(OH)	H ₂ O	7.2 ^d	-	2200 ± 100	Fl	Y
D-Phg(OH)	H ₂ O	7.2 ^d	-	33000 ± 500	Fl	Y
L-Trp	H ₂ O	7.2 ^d	-	150 ± 10	Fl	Y
D-Trp	H ₂ O	7.2 ^d	-	1000 ± 40	Fl	Y
Mono[6-[2-[[[(1-methylpyrrolidin-2-ylidene)amino]sulfonyl]amino]ethyl]amino]-6-deoxy]-β-CD						
L-Phg	H ₂ O	7.2 ^d	-	2000 ± 200	Fl	Y
D-Phg	H ₂ O	7.2 ^d	-	1800 ± 100	Fl	Y
L-Phe	H ₂ O	7.2 ^d	-	5000 ± 200	Fl	Y
D-Phe	H ₂ O	7.2 ^d	-	10000 ± 400	Fl	Y
3,4-(OH) ₂ -L-Phe	H ₂ O	7.2 ^d	-	6000 ± 300	Fl	Y
3,4-(OH) ₂ -D-Phe	H ₂ O	7.2 ^d	-	7500 ± 400	Fl	Y
L-Phg(OH)	H ₂ O	7.2 ^d	-	450 ± 20	Fl	Y
D-Phg(OH)	H ₂ O	7.2 ^d	-	4200 ± 200	Fl	Y
L-Trp	H ₂ O	7.2 ^d	-	120 ± 20	Fl	Y

Table 2. (Continued)

Compound (charge)	Solvent	pH	T [K]	<i>K</i> [dm ³ /mol]	Method ^e	Ref.
D-Trp	H ₂ O	7.2 ^d	-	2500 ± 100	Fl	Y
Mono[6-(<i>O</i>-diphenylphosphoryl)]-β-CD						
L-Ala	H ₂ O	7.2 ^a	298	218.8	UV	I1
D-Ala	H ₂ O	7.2 ^a	298	131.8	UV	I1
L-Asp	H ₂ O	7.2 ^a	298	363.1	UV	I1
L-Cys	H ₂ O	7.2 ^a	298	331.1	UV	I1
D-Cys	H ₂ O	7.2 ^a	298	512.9	UV	I1
L-Glu	H ₂ O	7.2 ^a	298	251.2	UV	I1
L-His	H ₂ O	7.2 ^a	298	1819.7	UV	I1
L-Ile	H ₂ O	7.2 ^a	298	660.7	UV	I1
L-Leu	H ₂ O	7.2 ^a	298	1412.5	UV	I1
D-Leu	H ₂ O	7.2 ^a	298	1689.2	UV	I1
L-Met	H ₂ O	7.2 ^a	298	631.0	UV	I1
L-Pro	H ₂ O	7.2 ^a	298	660.7	UV	I1
L-Ser	H ₂ O	7.2 ^a	298	407.4	UV	I1
D-Ser	H ₂ O	7.2 ^a	298	1479.1	UV	I1
L-Trp	H ₂ O	7.2 ^a	298	95.5 ± 1.2	Cal	L
L-Val	H ₂ O	7.2 ^a	298	741.3	UV	I1
D-Val	H ₂ O	7.2 ^a	298	1412.5	UV	I1
Mono[6-(<i>O</i>-ethoxyhydroxyphosphoryl)]-β-CD						
L-Ala	H ₂ O	7.2 ^a	298	234.4	UV	I1
D-Ala	H ₂ O	7.2 ^a	298	56.2	UV	I1
L-Cys	H ₂ O	7.2 ^a	298	269.2	UV	I1
D-Cys	H ₂ O	7.2 ^a	298	588.8	UV	I1
L-Leu	H ₂ O	7.2 ^a	298	380.2	UV	I1
D-Leu	H ₂ O	7.2 ^a	298	489.8	UV	I1
L-Ser	H ₂ O	7.2 ^a	298	123.0	UV	I1
D-Ser	H ₂ O	7.2 ^a	298	30.2	UV	I1
L-Trp	H ₂ O	7.2 ^a	298	2290.9 ± 1.1	Cal	L
Mono(6-phenylseleno-6-deoxy)-β-CD						
L-Trp	H ₂ O	7.2 ^a	298	117.5 ± 1.1	Cal	L
Mono[6-[(<i>p</i>-tolyl)seleno]-6-deoxy]-β-CD						
L-Trp	H ₂ O	7.2 ^a	298	173.8 ± 1.1	Cal	L
Mono(6-benzylseleno-6-deoxy)-β-CD						
L-Trp	H ₂ O	7.2 ^a	298	104.7 ± 1.0	Cal	L
Mono(6-anilino-6-deoxy)-β-CD						
L-Ala	H ₂ O	7.2 ^a	298	4168.7	UV	H1
D-Ala	H ₂ O	7.2 ^a	298	3311.3	UV	H1
L-Asp	H ₂ O	7.2 ^a	298	10964.8	UV	H1
L-Cys	H ₂ O	7.2 ^a	298	446.7	UV	H1
L-Glu	H ₂ O	7.2 ^a	298	14791.1	UV	H1
L-Ile	H ₂ O	7.2 ^a	298	6166.0	UV	H1
L-Leu	H ₂ O	7.2 ^a	298	5011.9	UV	H1
D-Leu	H ₂ O	7.2 ^a	298	4677.4	UV	H1

Table 2. (Continued)

Compound (charge)	Solvent	pH	T [K]	<i>K</i> [dm ³ /mol]	Method ^e	Ref
L-Lys	H ₂ O	7.2 ^a	298	371.5	UV	H1
L-Pro	H ₂ O	7.2 ^a	298	4365.2	UV	H1
L-Ser	H ₂ O	7.2 ^a	298	3090.3	UV	H1
D-Ser	H ₂ O	7.2 ^a	298	2691.5	UV	H1
L-Val	H ₂ O	7.2 ^a	298	6606.9	UV	H1
Mono[6-(m-toluidinyl)-6-deoxy]-β-CD						
L-Ala	H ₂ O	7.2 ^a	293-296	1197	Fl	J1
D-Ala	H ₂ O	7.2 ^a	293-296	1430	Fl	J1
L-Leu	H ₂ O	7.2 ^a	293-296	1439	Fl	J1
D-Leu	H ₂ O	7.2 ^a	293-296	1002	Fl	J1
L-Ser	H ₂ O	7.2 ^a	293-296	843	Fl	J1
D-Ser	H ₂ O	7.2 ^a	293-296	1406	Fl	J1
L-Val	H ₂ O	7.2 ^a	293-296	416	Fl	J1
D-Val	H ₂ O	7.2 ^a	293-296	609	Fl	J1
Mono[6-[[9-fluorenylamino)ethyl]amino]-6-deoxy]-β-CD						
L-Ala	H ₂ O	7.2 ^a	293-296	707.9	Fl	K1
D-Ala	H ₂ O	7.2 ^a	293-296	1047.1	Fl	K1
L-Ser	H ₂ O	7.2 ^a	293-296	323.6	Fl	K1
D-Ser	H ₂ O	7.2 ^a	293-296	2041.7	Fl	K1
L-Val	H ₂ O	7.2 ^a	293-296	660.7	Fl	K1
D-Val	H ₂ O	7.2 ^a	293-296	631.0	Fl	K1
γ-CD						
Cbz-Gly (-1)	H ₂ O	6.9 ^a	298	19 ± 3 (K ₁) 8.5 ± 1.5 (K ₂)	Cal	L1
<i>N</i> -Cbz-L-His (-1)	H ₂ O	6.9 ^a	298	16 ± 2	Cal	L1
<i>N</i> -Cbz-D-His (-1)	H ₂ O	6.9 ^a	298	13 ± 2	Cal	L1
<i>N</i> -Cbz-L-Phe (-1)	H ₂ O	6.9 ^a	298	185 ± 4	Cal	L1
<i>N</i> -Cbz-D-Phe (-1)	H ₂ O	6.9 ^a	298	175 ± 3	Cal	L1
Dans-L-Phe	H ₂ O	6.9 ^a	298	2600 ± 150	Cal	B1
Dans-D-Phe	H ₂ O	6.9 ^a	298	3800 ± 150	Cal	B1
Naph-L-Phe	H ₂ O	6.9 ^a	298	1200 ± 80	Cal	B1
Naph-D-Phe	H ₂ O	6.9 ^a	298	1940 ± 50	Cal	B1
L-Trp	H ₂ O	7.2	298	89.1 ± 1.2	Cal	L
<i>N</i> -Cbz-L-Trp (-1)	H ₂ O	6.9 ^a	298	57 ± 5	Cal	L1
<i>N</i> -Cbz-D-Trp (-1)	H ₂ O	6.9 ^a	298	53 ± 5	Cal	L1
L-Tyr	H ₂ O	-	293	1.4 ± 2	Fl	P
<i>N</i> -Cbz-L-Tyr (-1)	H ₂ O	6.9 ^a	298	192 ± 3	Cal	L1
<i>N</i> -Cbz-D-Tyr (-1)	H ₂ O	6.9 ^a	298	175 ± 4	Cal	L1

^a phosphate buffer, ^b acetate buffer, ^c glycine buffer, ^d tetraborate buffer

^e ACE – affinity capillary electrophoresis, Cal – calorimetric titration, Fl – fluorometric titration, NMR – magnetic resonance spectroscopy, UR – ultrasonic relaxation method, UV – UV-VIS spectrometry

Cbz – carbobenzyloxy group, Dans – dansyl group, Naph – naphthyl group

[A] Buschmann, HJ; Schollmeyer, E; Mutihac, L. *Thermochim. Acta*, 2003, 399, 203-208.

[B] Castronuovo, G; Elia, V; Fessas, D; Giordano, A; Velleca, F. *Carbohydr. Res.*, 1995, 272, 31-39.

[C] Gonzales-Gaitano, G; Sainz-Rozas, PR; Isasi, JR; Guerrero-Martinez, A; Tardajos, G. *J. Phys. Chem. B*, 2004, 108, 14154-14162.

- [D] Paduano, L; Sartorio, R; Vitagliano, V; Castronuovo, G. *Thermochim. Acta*, 1990, 162, 155-161.
- [E] Rekharsky, MV; Schwarz, FP; Tewari, YB; Goldberg, RN. *J. Phys. Chem.*, 1994, 98, 10282-10288.
- [F] Song, LX; Zhao, L; Guo, ZJ. *Chin. J. Inorg. Chem.*, 2002, 18, 897.
- [G] Matsuyama, K; El-Gizawy, S; Perrin, JH. *Drug Dev. Ind. Pharm.*, 1987, 13, 2687-2691.
- [H] Horský, J; Pitha, J. *J. Incl. Phenom. Mol. Rec. Chem.*, 1994, 18, 291-300.
- [I] Sompornpisut, P; Deechalao, N; Vongsvivut, J. *Science Asia*, 2002, 28, 263-270.
- [J] Cooper, A; MacNicol, DD. *J. Chem. Soc., Perkin Trans. 2*, 1978, 760-763.
- [K] Tabushi, I; Kuroda, Y; Mizutani, T. *J. Am. Chem. Soc.*, 1986, 108, 4514-4518.
- [L] Liu, Y; Han, BH; Li, B; Zhang, YM; Zhao, P; Chen, YT; Wada, T; Inoue, Y. *J. Org. Chem.*, 1998, 63, 1444-1454.
- [M] Lewis, EA; Hansen, LD. *J. Chem. Soc., Perkin Trans. 2*, 1973, 2081-2085.
- [N] Hallén, D; Schön, A; Shehatta, I; Wadsö, I. *J. Chem. Soc., Faraday Trans.*, 1992, 88, 2859-2863.
- [O] Nishijo, J; Tsuchitani, M. *J. Pharm. Sci.*, 2001, 90, 134-140.
- [P] Wiczek, W; Mrozek, J; Szabelski, M; Karolczak, J; Guzow, K; Malicka, J. *Chem. Phys. Lett.*, 2001, 341, 161-167.
- [R] Liu, Y; Zhang, YM; Sun, SX; Zhang, ZH; Chen, YT. *Acta Chim. Sin. (Huaxue Xuebao)*, 1997, 55, 779-785.
- [S] Lantz, AW; Rodriguez, MA; Wetterer, SM; Armstrong, DW. *Anal. Chim. Acta*, 2006, 557, 184-190.
- [T] Rekharsky, M; Inoue, Y. *J. Am. Chem. Soc.*, 2000, 122, 4418-4435.
- [U] Tee, OS; Gadosy, TA; Gorgi, JB. *Can. J. Chem.*, 1996, 74, 736-744.
- [V] Ugawa, T; Nishikawa, S. *J. Phys. Chem. A*, 2001, 105, 4248-4251.
- [W] Fukahori, T; Ugawa, T; Nishikawa, S. *J. Phys. Chem. A*, 2002, 106, 9442-9445.
- [X] Rekharsky, J; Banecki, B; Karolczak, J; Wiczek, W. *Biophys. J.*, 2005, 116, 237-250.
- [Y] Kumar, VP; Suryanarayana, I; Nageswar, YVD; Rao, KR. *Helv. Chim. Acta*, 2008, 91, 753-758.
- [Z] Kuan, F; Inoue, Y; Miyata, Y; Chûjô, R. *Carbohydr. Res.*, 1985, 142, 329-332.
- [A1] Rekharsky, MV; Inoue, Y. *J. Am. Chem. Soc.*, 2002, 124, 12361-12371.
- [B1] Hembury, G; Rekharsky, M; Nakamura, A; Inoue, Y. *Org. Lett.* 2000, 2, 3257-3260.
- [C1] Mrozek, J; Lewandowska, A; Guzow, K; Malicka, J; Banecki, B; Wiczek, W. *J. Incl. Phenom. Macrocycl. Chem.*, 2009, 65, 361-375.
- [D1] Ross, PD; Rekharsky, MV. *Biophys. J.*, 1996, 71, 2144-2154.
- [E1] Rekharsky, MV; Goldberg, RN; Schwarz, FP; Tewari, YB; Ross, PD; Yamashoji, Y; Inoue, Y. *J. Am. Chem. Soc.*, 1995, 117, 8830-8840.
- [F1] Bekos, IJ; Gardella, Jr., JA; Bright, FV. *J. Incl. Phenom. Mol. Recogn. Chem.*, 1996, 26, 185-195.
- [G1] Mrozek, J; Banecki, B; Sikorska, E; Skwierawska, A; Karolczak, J; Wiczek, W. *Chem. Phys.*, 2008, 354, 58-70.
- [H1] Liu, Y; Zhang, YM; Sun, SX; Li, YM; Chen, YT. *J. Chem. Soc., Perkin Trans. 2*, 1997, 1609-1614.
- [I1] Liu, Y; Li, B; Han, BH; Li, YM; Chen, RT. *J. Chem. Soc., Perkin Trans. 2*, 1997, 1275-1278.
- [J1] Liu, Y; Zhang, YM; Qi, AD; Chen, RT; Yamamoto, K; Wada, T; Inoue, Y. *J. Org. Chem.*, 1998, 63, 10085.
- [K1] Liu, Y; Zhang, YM; Qi, AD; Chen, RT; Yamamoto, K; Wada, T; Inoue, Y. *J. Org. Chem.*, 1997, 62, 1826-1830.
- [L1] Rekharsky, M; Inoue, Y. *J. Am. Chem. Soc.*, 2000, 122, 10949-10955.

The average value of the logarithm of the binding constant is equal to 2.29 ± 0.92 , for 350 complexes. The distribution can be approximated by the Gaussian distribution (dashed line in Fig. 2). The obtained value is only a little lower than that presented by Houk et al. [20] ($\log K = 2.5 \pm 1.1$) for 1257 complexes formed by α -, β - and γ -cyclodextrins with different kinds of organic molecules. The calculated average free energy of amino acids binding with CDs is -3.2 kcal/mol and it is comparable to this obtained by Houk et al. (-3.5 kcal/mol) [20]. Thus, the interactions of amino acids and their derivatives and analogues with naturally occurred and modified cyclodextrins statistically do not differentiate from the interactions of the CDs with other organic molecules. A similar analysis of the binding constants of presented compounds with only naturally occurring cyclodextrins is presented in Fig. 3.

For α -CD, after removing the data higher than 100 which seem to be overestimated, the arithmetic average of gives is $\log K = 1.25 \pm 0.26$, for $n = 31$. Moreover, the distribution plot can be well approximated by Gaussian distribution with the $\log K = 1.24 \pm 0.33$. For β -CD, the arithmetic average of gives is $\log K = 1.91 \pm 0.81$ for $n = 81$ and Gaussian distribution gives $\log K = 1.97 \pm 1.01$. For γ -CD, because of small number of data, only arithmetic average was calculated and $\log K$ value for $n = 16$ is equal to 2.03 ± 0.97 . The difference between binding constants of amino acids by α -CD and β -CD is substantial and arises from the size fit of amino acid side chain into the CD cavity. Most of proteinogenic amino acids possess as a side chain a small aliphatic hydrocarbon chain which is too small to interact strongly with CDs. Moreover, an aromatic amino acid or derivatives containing an aromatic substituent are too

large to perfectly fit into α -CD cavity, however, they accurately fit into β -CD cavity. On the other hand, the cavity of γ -CD is too large to provide strong interactions with amino acid side chain, except a bulky substituent like dansyl or naphthyl group. However, because of its flexibility it can adopt to some extent its structure to increase the binding force. Its average value of $\log K$ is similar to that of β -CD, however, much less data available and their dispersion cause that the value is less reliable than those for other CDs.

Data presented in Table 2 indicate that among the studied substances higher binding constants possess neutral compounds in comparison to the corresponding charged species derived from the same guest molecule, for instance: 3-(4-OH)PPA at pH=2 and pH=8, Tyr and AcTyr. Another examples are Phe at different pH ($K=107$ at pH=11 and $K=3$ at pH=5), AcPhe ($K=61$) and Phe as well as phenylalanine amide at different pH ($K=22$ and $K=107$ at pH=5 and 10, respectively). For the interactions of amino acid with cyclodextrins, the hydration of amino acid moiety is also essential beside the presence of charged amino and carboxyl groups being outside the binding site. The hydration shell around the charged group (amino or carboxyl) includes about two C–C bond lengths [53]. Also, the cyclodextrin possesses its own strong and diversified sphere [13,18,53]. Thus, the displacement of the amino group from α - to β -carbon atom in the phenylalanine or tyrosine analogues (β -analogues) while the carboxyl group stands at α -carbon atom stretches the hydration sphere to the phenyl (phenol ring) causing shallow penetration of the cyclodextrin cavity resulting in lower constant binding. Moreover, the standoff the carboxyl group from the phenyl group for more than one methylene group increases substantially the binding constant of benzoic acid analogues with β -CD [17]. This conclusion is also supported by the data presented in Table 2 ((Phg(OH), Tyr and Hty; Tyr(Me) and β Hty(Me)). Such conclusion cannot be drawn from the binding constant data for phenylalanine analogues because of their low diversification. The binding constants of phenylalanine derivatives depend on the substitution in the phenyl ring of phenylalanine. Small methyl group in position 2 of phenylalanine (o-MePhe) causes an increase of hydrophobic interaction rising the binding constant with β -CD, whereas bigger substituent as in the case of Tic decreases its value because of steric hindrance and unfavourable location of charged amino group. It has been shown that the phenolic group in a guest as tyramine or 3-(4-OH)PPA forms hydrogen bonds inside cyclodextrin cavity [17,53]. The same interactions were observed for tyrosine analogues causing that tyrosine and its analogues with free hydroxyl of the phenol group interact with β -cyclodextrin stronger than phenylalanine and its appropriate analogues. As stated by Rekharsky et al. [54], for β -cyclodextrin values of the equilibrium constants of the formation of inclusion complexes increase in the order $\text{OCH}_3 > \text{CH}_3 > \text{OH} > \text{H}$. Methylation of the hydroxyl group of p-hydroxyphenylglycine increases the equilibrium constant of the inclusion complex with β -CD twice times, whereas for tyrosine it decreases twice times while for β -homo-tyrosine it remains the same. It indicates that van der Waals forces and hydrophobic interactions play the major role in β -CD complexation of guest molecules devoid of polar groups, however, for tyrosine derivatives and analogues the hydrogen bond formation is also important [43]. The substituent on amide nitrogen atom influences also on the interactions of N-acetyl-tyrosine amides with β -cyclodextrin. In comparison with AcTyrOH a primary amide group only in a small degree modifies the binding constant with β -CD, regardless of the structure (linear or branched) and the length of n-alkyl substituent, except for t-butyl substituent for which the additional complex with t-butyl group incorporated into CD cavity is formed. Moreover, for a

branched substituent the binding constant is a little higher in comparison with n-alkyl one. Also, for secondary amides the binding constants are higher [55].

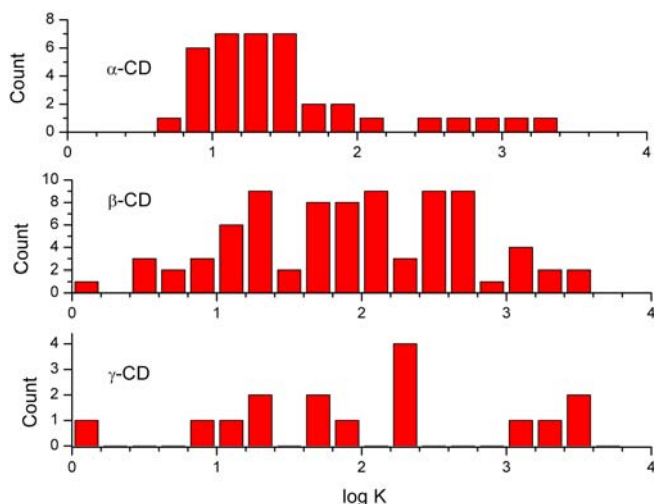


Figure 3. Frequency distributions calculated for binding constants of complexes of amino acids and their derivatives and analogues with α -, β - and γ -cyclodextrins.

Since the CD's cavity, apart from being hydrophobic, is also chiral in nature, CDs can be further explored for chiral recognition of amino acids and their derivatives. The analysis of the data collected in Table 2 reveals that the chirality of amino acid has a low influence on the binding constant with naturally occurred cyclodextrins. Moreover, modification of the amino or carboxyl group of amino acids do not alter the enantioselectivity of the CD or the mode of penetration as far as the degree of hydrophobicity of the substituents around the asymmetric center is conserved. Rekharsky and Inoue [53] conclude that a/ it is a direct correlation between the mode of penetration and chiral recognition by β -CD for aromatic amino acid derivatives, b/ chiral guests with a less symmetrical, nonpolar penetrating group and chiral guests with a larger distance between chiral center and most hydrophobic group are more likely to exhibit chiral recognition, c/ alternation made to the guest molecule that result in the stronger binding with CD lead to a loose of chiral recognition. Thus, a high level of chiral recognition can only be achieved when the host molecule has a shape and location of specific functional groups that are complementary to the structure of the guest. Such requirements are fulfilled by derivatized CDs. The CDs are chemically modifying at the primary side by appending a flexible moiety which leads to significant changes in complex stability. A wide variety of cyclodextrin derivatives have been synthesized in order to increase molecular recognition ability of amino acids [56]. Some of them are listed in Table 2. As can be seen, the binding constants of amino acid with modified α - and β -CD are substantially higher than that of naturally occurring CDs. Also, the enantiomeric selectivity has been substantially increased for example for mono-(6-*O*-diphenoxyphosphoryl)- β -cyclodextrin enantioselectivity is up to 3.6 for D/L-serine [57] and more than 20 for D/L-Trp [58]. The enhancement of the binding constants and enantioselectivity of modified cyclodextrins is mostly caused by the induced-fit interaction and the complementary geometrical relationship between the host and guest molecules. Apart from these driving forces, the electrostatic

interaction between host and guest as well as the microstructural changes of the modified cyclodextrin apparently governs the chiral recognition of amino acid molecules to some extent.

Also, in the gas phase protonated amino acids formed inclusion complexes with cyclodextrins showing a rather good enantioselectivity which was analyzed basing on the "three point attachment" model which included hydrogen bonding, inclusion, and steric hindrance [60].

AMINO ACID AND PEPTIDE MODIFIED CYCLODEXTRINS

It has been amply demonstrated that modified cyclodextrins possessing nucleophilic or electrophilic substituents significantly alter the original complexation behaviour and enantioselectivity of native CDs. Spectroscopically inert CDs molecules can be converted into fluorescent CDs by covalent attachment of a fluorophore. Fluorescent CDs change their fluorescence intensity upon addition of guest molecule, as it causes a change of the location of the fluorophore mostly from inside to outside of the CD cavity [61]. Tryptophan modified β -CD [62,63] or β -CD containing DNS-Leu [64] or DNS-Phe [65] or DNS-Lys [66] were used as chemosensor molecules. To improve sensitivity and selectivity of the CD-based chemosensor molecules, novel CD-peptide hybrids possessing two different photoreactive moieties were synthesized. Alanine was chosen as a main component of the peptides to obtain semi-rigid α -helix peptide conformation. The alanine peptides contain also lysine or glutamic acid that can form α -helix-stabilization intramolecular salt-bridges [67-69].

INTERACTIONS OF SMALL PEPTIDES WITH CYCLODEXTRINS

As have been shown by Horsky and Pitha [32], the binding constants of the complexes between CDs and dipeptides are higher than those of particular amino acid alone and depend on the sequence and amino acid residues configuration. For β -CD, the stability constant of Gly-L-Phe is equal to 76 M^{-1} while for L-Phe-Gly $K=57 \text{ M}^{-1}$, and for Gly-D-Phe $K=67 \text{ M}^{-1}$. The similar dependence is also valid for α -CD as well as for partially methylated or hydroxypropyl modified cyclodextrins. The responsibility for such behaviour probably bears the influence of peptide geometry on the thermodynamics of its interactions with host molecules as well as presence of an aromatic amino acid residue in the sequence (N- or C-terminal, i.e. the position of charged amino group of the peptide in the relation to aromatic amino acid residue), the cavity size of CDs and the kind of CD peripheral pendant substituent [71].

The sequence selective binding of small peptides in aqueous solution can be substantially improved by using bis(CD)s linked with a short tether possessing binding abilities and selectivities much higher than the native CDs [72-74]. This is a result of the size-fit and cooperative multi-point recognition. In some bridged-bis(CD)s, the bridge can also interact with the guest molecule [73] as well as change the mode of interaction depending on the acidity of the solution [74].

INTERACTIONS OF CDS WITH POLYPEPTIDES AND PROTEINS

The formation of α -CD and β -CD complexes with free tyrosine and two pentapeptides containing tyrosine residue (YIGSR and YGGFL) reveals that the peptides stronger bind to the CDs and binding process depends on the size (tyrosine vs. peptide), structure (sequence selectivity) and peptide conformation [75]. This is a result of favourable interactions of the unincorporated residues within the individual pentapeptides with the exterior of the CD cavity which provide secondary stabilization effect (hydrogen bonding). This general trend might increase with the number of amino acid residues until reaching the point at which the accessibility of aromatic amino acid ring itself becomes occluded by another amino acid residues. The presence of two side chains which are able to penetrate CD cavity as well as possibility of hydrogen bonds formation between CD and a peptide chain and hydrophobic interactions of the peptide side chains result in competition for binding, affecting the binding constant and complex structure leading to the formation of mixed complexes. In such cases not only inclusion complexes are formed in which the aromatic amino acid residue can penetrate the cavity from both wider and narrower sides but also association complexes can exist [35,54].

However, molecules of many peptides and proteins are too hydrophilic and bulky to penetrate entirely into the CD cavity. Also, the topological constraints of the peptide backbone may influence on the formation of inclusion complexes. Thus, their interactions with CDs could only be local meaning that accessible hydrophobic side chains may form inclusion complexes with CDs [32,71,76-80]. Camillieri et al. [81] discovered that the amyloid A β (1-40) peptide interacts with β -CD and diminishes its aggregation. Moreover, Qin et al. [82] and Danielson et al. [83] showed that only aromatic amino acid (Phe¹⁹ or/and Phe²⁰) and hydrophobic Val¹⁸ of the peptide A β (12-28) interact with β -CD. Additional studies shown that A β (12-28)G¹⁹G²⁰ as well as A β (1-9) do not show measurable affinity to β -CD, whereas in the full-length peptide A β (1-40) the binding occurs at two sides, at Phe¹⁹ or/and Phe²⁰ and Tyr¹⁰. These results as well as the results presented in [79] on the interaction of model protein: insulin mutant, ubiquitin, S6 and chymotrypsin inhibitor 2, as well as salmon calcitonin [84], melittin [78], to name a few, suggested that every solvent-exposed aromatic or bulky aliphatic amino acid residue is an interaction site. However, in some cases even solvent-exposed residues do not always take part in the interaction. A sequence and close proximity of charged residue(s) can prevent the inclusion complex formation with CDs. The examples of such behaviour are fragments of NOTCH membrane receptor (H₂N–YKIEAVQSETVEPPPPAQ–CONH₂ (I), H₂N–TLYPLVSVVSESLTPER–CONH₂ (II), H₂N–PYPLRDVRGEPLPEPS–CONH₂ (III)). Among these three peptides, only peptide (III) forms with β -CD stable inclusion complex ($K=136\text{ M}^{-1}$). Peptide (II) interacts very weakly ($K=5\text{ M}^{-1}$), whereas peptide (I) does not interact at all [85]. Thus, the exact effect of cyclodextrins on a given polypeptide or protein will always be limited by the particular structure of this polypeptide or protein.

CONCLUSION

The interactions of CDs with amino acids, polypeptides and proteins may help to explain the wide range of different effects. If residues responsible for aggregation are highly solvent accessible CDs can suppress this process. The weak interactions of CDs with unfolded proteins may enhance the solubility of denaturated proteins by masking the exposed hydrophobic residues, thereby possibly assisting the refolding of the proteins. In this way CDs might act as a small chaperone-mimic in the protein folding process when refolding is inhibited by poorly reversible aggregation entanglement mechanisms. If point of attack of protease is sterically "masked" by CD it can protect against degradation. Such effects of the interactions of CDs with amino acids, polypeptides and proteins are important in the enzyme technology [86], artificial enzymes [87], and pharmaceutical science, especially in drug delivery systems [88-91]. Another applications of CDs in the technologies and analytical methods can be found in [6]. However, the mentioned above CDs applications will not be discussed in details as it is beyond the scope of this review. The interested readers can find some information in the above-mentioned excellent reviews [6,86-91].

ACKNOWLEDGMENT

This work was financially supported by the Polish Ministry of Science and Higher Education under grant DS-8441-4-0132-9.

REFERENCES

- [1] Connors, KA. *Chem. Rev.*, 1997, 97, 1325-1357.
- [2] Saenger, W; Jacob, J; Gessler, K; Steiner, T; Hoffmann, D; Sanbe, H; Koizumi, K; Smith, SM; Takaha, T. *Chem. Rev.*, 1998, 98, 1787-1802.
- [3] Raffaini, G; Ganazzoli, F. *Chem. Phys.*, 2007, 333, 128-134.
- [4] Wenz, G; Han, BH; Müller, A. *Chem. Rev.*, 2006, 106, 782-817.
- [5] Khan, AR; Forgo, P; Stine, KJ; D'Souza, VT. *Chem. Rev.*, 1998, 98, 1977-1996.
- [6] Del Valle, EMM. *Process Biochem.*, 2004, 39, 1033-1046.
- [7] Ikeda, H; Ueno, A. In *Cyclodextrins Materials Photochemistry, Photophysics and Photobiology*, Douhal, A; Ed; Chemical, Physical and Biological Aspects of Confined Systems; Elsevier: *Amsterdam*, 2006, 267-283.
- [8] Engeldinger, E; Armspach, D; Matt., D. *Chem. Rev.*, 2003, 103, 4147-4185.
- [9] Liu, L; Guo, QX. *J. Incl. Phenom. Macrocycl. Chem.*, 2002, 42, 1-14.
- [10] Rademacher, JT; Czarnik, AW. *J. Am. Chem. Soc.*, 1993, 115, 3018-3019.
- [11] Harata, K. *Bull. Chem. Soc. Jpn.*, 1990, 63, 2481-2486.
- [12] Harata, K. *Chem. Rev.*, 1998, 98, 1803-1828.
- [13] Douhal, A. *Chem. Rev.*, 2004, 104, 1955-1976.
- [14] Senapati, S; Chandra, A. *J. Phys. Chem. B*, 2001, 105, 5106-5109.
- [15] Clark, JL; Stezowski, JJ. *J. Am. Chem. Soc.*, 2001, 123, 9880-9888.
- [16] Clark, JL; Booth, BR; Stezowski, JJ. *J. Am. Chem. Soc.*, 2001, 123, 9888-9895.

- [17] Ross, PD; Rekharsky, MV. *Biophys. J.*, 1996, 71, 2144-2154.
- [18] Rekharsky, MV; Inoue, Y. *J. Am. Chem. Soc.*, 2002, 124, 12361-12371.
- [19] Hamai, S; Nakamura, A. In Handbook of Photochemistry and Photobiology; Nalwa, HS; Ed; American Scientific Publisher: CA, 2003, Vol. 3, 59-119.
- [20] Houk, KN; Leach, AG; Kim, SP; Zhang, X. *Angew. Chem. Int. Ed.*, 2003, 42, 4872-4897.
- [21] Mrozek, J; Guzow, K; Szabelski, M; Karolczak, J; Wiczek, W. *J. Photochem. Photobiol. A: Chem.*, 2002, 153, 121-128.
- [22] Rekharsky, MV; Inoue, Y. *Chem. Rev.*, 1998, 98, 1875-1917.
- [23] Liu, L; Guo, QX. *Chem Rev.*, 2001, 101, 673-696.
- [24] Meo, PL; D'Anna, F; Gruttauria, M; RIELA, S; Noto, R. *Tetrahedron*, 2004, 60, 9099-9111.
- [25] Sharp, K. *Protein Sci.*, 2001, 10, 661-667.
- [26] Job, P. *Ann. Chim.*, 1928, 9, 113.
- [27] Landy, D; Tetart, F; Truant, E; Blach, P; Fourmentin, S; Surpateanu, G. *J. Incl. Phenom. Macrocycl. Chem.*, 2007, 57, 409-413.
- [28] Fielding, L. *Tetrahedron*, 2000, 56, 6151-6170.
- [29] Hirose, K. *J. Incl. Phenom. Macrocycl. Chem.*, 2001, 39, 193-209.
- [30] Benesi, HA; Hildebrand, JH. *J. Am. Chem. Soc.*, 1949, 71, 2703-2707.
- [31] Milewski, M; Maciejewski, A; Augustyniak, W. *Chem. Phys. Lett.*, 2007, 272, 225-231.
- [32] Horsty, J; Pitha, J. *J. Incl. Phenom. Mol. Recogn.*, 1994, 18, 291-300.
- [33] Yuexian, F; Yu, Y; Shaomin, S; Chuan, D. *Spectrochim. Acta A*, 2005, 61, 953-959.
- [34] Shen, X; Belletete, M; Durocher, G. *J. Phys. Chem. B*, 1998, 102, 1877-1883.
- [35] Mrozek, J; Lewandowska, A; Guzow, K; Malicka, J; Banecki, B; Wiczek, W. *J. Incl. Phenom. Macrocycl. Chem.*, 2009, 65, 361-375.
- [36] Pistolis, G; Malliaris, A. *Chem. Phys. Lett.*, 1999, 303, 334-340.
- [37] Nau, WM; Zhang X. *J. Am. Chem. Soc.*, 1999, 121, 8022-8032.
- [38] Mohanty, J; Bhasikuttan, AC; Nau, WM; Pal, H. *J. Phys. Chem. B*, 2006, 110, 5132-5138.
- [39] Park, JW. In Cyclodextrin Materials Photochemistry, Photophysics and Photobiology, Douhal, A; Ed; Chemical, Physical and Biological Aspects of Confined Systems; Elsevier: Amsterdam, 2006, 1-26.
- [40] Lee, C; Sung, YW; Park, JW. *J. Phys. Chem. B*, 1999, 103, 893-898.
- [41] Szmacki, H; Lakowicz, JR. In Probe Design and Chemical Sensing; Lakowicz, JR; Ed; Topics In Fluorescence Spectroscopy; Plenum Press: New York, London, 1994, Vol. 4, 295-329.
- [42] Wiczek, W; Mrozek, J; Szabelski, M; Karolczak, J; Guzow, K; Malicka, J. *Chem. Phys. Lett.*, 2001, 341, 161-167.
- [43] Mrozek, J; Banecki, B; Karolczak, J; Wiczek, W. *Biophys. Chem.*, 2005, 116, 237-250.
- [44] Kieda, H. *Chem. Rev.*, 1998, 98, 1755-1785.
- [45] Mrozek, J; Sikorska, E; Skwierawska, A; Malicka, J; Karolczak, J; Banecki, B; Wiczek, W. *J. Incl. Phenom. Macrocycl. Chem.*, 2009, 62, 269-278.
- [46] Barros, TC; Stefaniak, K; Holzward, JF; Bohne, C. *J. Phys. Chem.*, 1998, 102, 5639-5651.
- [47] Ugawa, T; Nishikawa, S. *J. Phys. Chem. A*, 2001, 105, 4248-4251.

- [48] Al-Soufi, W; Reija, B; Novo, M; Felekyan, S; Kuhnemuth, R; Seidel, CAM. *J. Am. Chem. Soc.*, 2005, 127, 8775-8784.
- [49] Salvatierra, D; Diez, C; Jaime, C. *J. Incl. Phenom. Mol. Recogn.*, 1997, 27, 215-231.
- [50] Cameron, KS; Fielding, L. *J. Org. Chem.*, 2001, 66, 6891-6895.
- [51] Wimmer, R; Achmann, FL; Larsen, KL; Petersen, SB. *Carbohydr. Res.*, 2002, 337, 841-849.
- [52] Turnbull, B; Daranas, AH. *J. Am. Chem. Soc.*, 2003, 125, 14859-14866.
- [53] Rekharsky, MV; Inoue, Y. *J. Am. Chem. Soc.* 2000, 122, 4418-4435.
- [54] Rekharsky, MV; Goldberg, RN; Schwarz, FP; Tewari, YB; Ross, PD; Yamashoji, Y; Inoue, Y. *J. Am. Chem. Soc.*, 1995, 117, 8830-8840.
- [55] Mrozek, J; Banecki, B; Sikorska, E; Skwierawska, A; Karolczak, J; Wiczak, W. *Chem. Phys.*, 2008, 345, 58-70.
- [56] Liu, Y; Han, BH; Li, B; Zhang, YM; Zhao, P; Chen, YT; Wada, T; Inoue, Y. *J. Org. Chem.*, 1998, 63, 1444-1454.
- [57] Liu, Y; Li, B; Han, BH; Li, YM; Chen, RT. *J. Chem. Soc. Perkin Trans. 2*, 1997, 1275-1278.
- [58] Kumar, YP; Suryanarayana, I; Nageswar, YVD; Rao, KR. *Helv. Chim. Acta*, 2008, 91, 735-758.
- [59] Eaton, CJ; Lincoln, SF. *Chem. Soc. Rev.*, 1996, 163-170.
- [60] Lebrilla, CB. *Acc. Chem. Res.*, 2001, 31, 653-661.
- [61] Ueno, A. *Supramolecular Sci.*, 1996, 3, 31-36.
- [62] Liu, Y; Han, BH; Sun, SX; Wada, T; Inoue, Y. *J. Org. Chem.*, 1999, 64, 1487-1493.
- [63] Wang, H; Cao, R; Ke, CF; Liu, Y; Wada, T; Inoue, Y. *J. Org. Chem.*, 2005, 70, 8703-8711.
- [64] Ikeda, H; Nakamura, M; Ise, N; Oguma, N; Nakamura, A; Ikeda, T; Toda, F; Ueno, A. *J. Am. Chem. Soc.*, 1996, 118, 10980-10988
- [65] Pagliari, S; Corradini, R; Galaverna, G; Sforza, S; Dossena, A; Marchelli, R. *Tetrahedron Lett.* 2000, 41, 3691-3695.
- [66] Ueno, A; Ikeda, A; Ikeda, T; Toda, F. *J. Org. Chem.*, 1999, 64, 382-387.
- [67] Matsumura, S; Sakamoto, S; Ueno, A; Mihara, H. *Chem. Eur. J.*, 2000, 6, 1781-1788.
- [68] Yana, D; Shimizu, T; Hamasaki, K; Mihara, H; Ueno, A. *Macromol. Rapid Commun.*, 2002, 23, 11-15.
- [69] Hossain, MA; Takahashi, K; Mihara, H; Ueno, A. *J. Incl. Phenom. Macrocycl. Chem.*, 2002, 43, 271-277.
- [70] Yamamura, H; Rekharsky, MV; Ishihara, Y; Kawai, M; Inoue, Y. *J. Am. Chem. Soc.*, 2004, 126, 14224-14233.
- [71] Breslow, R; Yang, Z; Ching, R; Trojandt, G; Odobel, F. *J. Am. Chem. Soc.*, 1998, 120, 3536-3537.
- [72] Maletic, M; Wennemers, H; McDonald, DQ; Breslow, R; Still, WC. *Angew. Chem. Int. Ed. Eng.*, 1996, 35, 1490-1492.
- [73] Liu, Y; Yang, YW; Song, Y; Zhang, HY; Ding, F; Wada, T; Inoue, Y. *Chem. Bio. Chem.*, 2004, 5, 868-871.
- [74] Liu, Y; Chen, GS; Chen, Y; Ding, F; Liu, T; Zhao, YL. *Bioconjugate Chem.*, 2004, 15, 300-306.
- [75] Bekos, EJ; Gardella, Jr., JA; Bright, FV. *J. Incl. Phenomen. Mol. Recogn. Chem.*, 1996, 26, 185-195.

- [76] Cooper A. *J. Am. Chem. Soc.*, 1992, 114, 9208-9209.
- [77] Matsubara, K; Irie, T; Uekama, K. *Chem. Pharm. Bull.*, 1997, 5, 378-383.
- [78] Khajehpour, M; Troxler, T; Nanda, V; Vanderkooi, JM. *Proteins*, 2004, 55, 275-287.
- [79] Aachmann, FL; Otzen, DE; Larsen, KL; Wimmer, R. *Protein Eng.*, 2003, 16, 905-912.
- [80] Giragossian, C; Schschke, N; Moroder, L; Mierke, DF. *Biochemistry*, 2004, 43, 2724-2731.
- [81] Camilliere, P; Haskins, NJ; Howlett, DR. *FEBS Lett.*, 1994, 341, 256-258.
- [82] Qin, XR; Abe, H; Nakanishi, H. *BBRC*, 2002, 297, 1011-1015.
- [83] Danielson, J; Jarvet, J; Damberg, P; Gräslund, A. *Biochemistry*, 2004, 43, 6261-6269.
- [84] Sigurjonsdottir, JF; Loftsson, T; Masson, M. *Int. J. Pharm.*, 1999, 186, 205-213.
- [85] Mrozek, J; Czaplewska, P; Czaplewski, C; Wiczek, W. unpublished results.
- [86] Villanoga, R; Cao, R; Fragoso, A. *Chem. Rev.*, 2007, 107, 3088-3116
- [87] Bierre, J; Rousseau, C; Marinescu, L. *Appl. Microbiol. Biotechnol.*, 2008, 81, 1-11.
- [88] Uekama, K; Hirayama, F; Irie, T. *Chem. Rev.*, 1998, 98, 2045-2076.
- [89] Irie, T; Uekama, K. *Adv. Drug. Deliv. Rev.* 1999, 36, 101-123.
- [90] Vyas, A; Saraf, S; Saraf, S. *J. Incl. Phenom. Macrocycl. Chem.*, 2008, 62, 23-42.
- [91] Stella, VJ; Rao, VM; Zannou, EA; Zia, V. *Adv. Drug Deliv. Rev.*, 1999, 36, 3-16.

Chapter 8**INCLUSION COMPLEX FORMATION OF
CYCLODEXTRINS WITH AMINOBENZOIC ACIDS IN
AQUEOUS SOLUTION*****Irina V. Terekhova****

Akademicheskaya Str. 1, 153045 Ivanovo, Russian Federation.

ABSTRACT

This chapter is a summary review devoted to inclusion complex formation of native and substituted α - and β -cyclodextrins with isomeric aminobenzoic acids. Complex formation of cyclodextrins with aniline and benzoic acid is also considered. The thermodynamic characteristics of complex formation are calculated and discussed in terms of the influence of the reagent's structure and pH on the binding process. Binding modes and driving forces of complexation are proposed.

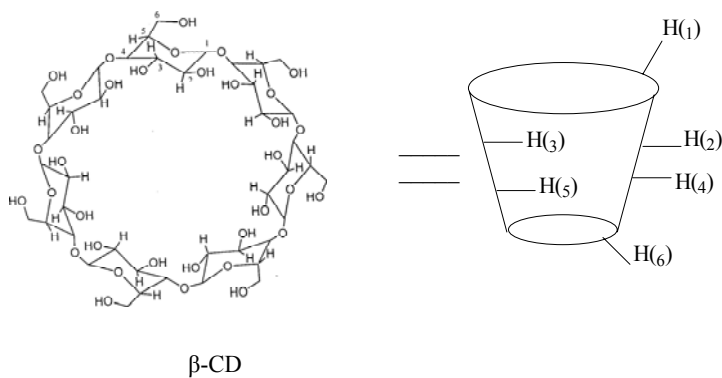
The obtained results show that α - and β -cyclodextrins display selectivity in interactions with aminobenzoic acids. Complexation of α -cyclodextrin with *para*- and *meta*-aminobenzoic acids is highly exothermic and, consequently, it is enthalpy driven. Insertion of aminobenzoic acids into the α -cyclodextrin cavity is shallow and it is governed predominantly by the van der Waals interactions. On the contrary, the deeper inclusion of aminobenzoic acids into the β -cyclodextrin cavity takes place, and this process is accompanied by intensive dehydration. Complex formation of β -cyclodextrin with aminobenzoic acids is characterized by higher enthalpy and entropy changes. Thus, complexes formed by β -cyclodextrin are enthalpy-entropy stabilized. The size of the cyclodextrin cavity does not affect the complex stability, while the structure of aminobenzoic acids has a noticeable influence on the values of binding constants. *Para*- and *ortho*-aminobenzoic acids form more stable complexes with cyclodextrins. Ionization of the carboxylic group which is located inside the cyclodextrin cavity results in weakness of binding. The introduction of methyl- and hydroxypropyl-groups into the β -cyclodextrin molecule does not change the binding mode revealed for native β -cyclodextrin. Complex formation of aminobenzoic acids with these modified β -

* Corresponding author: E-mail ivt@isc-ras.ru

cyclodextrins is less enthalpy- and more entropy-favorable due to an increased contribution from dehydration of bulky substituents surrounding the macrocyclic cavity.

INTRODUCTION

Cyclodextrins (CDs) represent a class of macrocyclic receptors which are also known as cycloamyloses and Schardinger dextrins. They are cyclic oligosaccharides obtained by the enzymatic degradation of starch and consisting of six (α -CD), seven (β -CD), eight (γ -CD), nine (δ -CD) and up to 13 D-glucose units linked by $\alpha(1\rightarrow4)$ glycosidic bonds. The first three of the CDs mentioned above were easily isolated and characterized and their structure, and properties have been well established and described in many books and articles [1-5]. CDs have a toroidal truncated cone structure with hollow cavity, the wider side of which is surrounded by the secondary 2- and 3-hydroxyl groups and the narrower side by the primary 6-hydroxyls, thus the interior of CD molecule is relatively hydrophobic and the exterior is hydrophilic. The internal cavity of CDs is capable of including a wide range of organic molecules as well as small inorganic anions. Inclusion complexes (or host-guest) of CDs are formed due to noncovalent interactions which include van der Waals, hydrophobic, electrostatic and charge-transfer interactions and hydrogen bonding [5, 6]. Complex formation is released in accordance with the principles of geometric and energetic complementarity. Recently, various modified CDs have been synthesized with the purpose of extending the physicochemical properties and complexation capacity of parent CDs [7, 8]. Chemical modification of outer hydroxyls yields methylated, ethylated, hydroxypropylated, carboxymethylated and sulfated CD derivatives that are more usable in recent years.

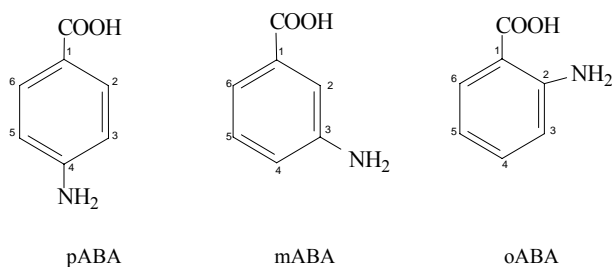


Scheme 1. Schematic representation of β -CD structure.

Inclusion complexes of CDs find numerous practical applications. It has been determined that the physicochemical properties (e.g., stability, taste and solubility) of a guest molecule placed inside the CD cavity can be considerably changed. Therefore, CDs are used as encapsulating materials in food, cosmetic and textile industries in order to improve the quality of the products [9, 10]. Owing to their capacity for selective complex formation, CDs are widely employed in separation technology, especially as chiral receptors in chromatography and capillary electrophoresis [11, 12]. In biochemistry, CDs can serve as models of enzymes

[13]. In pharmaceutical chemistry, CDs are applied as solubilizing agents and drug delivery systems [14-17]. The external surface of a CD molecule is polar and induces the solubilization of poorly soluble drugs inserted into the hydrophobic cavity. It was detected that CDs enhance drug delivery through biomembranes by increasing the drug availability at the membrane surface [16]. Moreover, CD complexation prolongs the therapeutic action of drugs and eliminates drug irritation. Thus, the importance of CD inclusion complexes is evident, and the necessity for their investigation is obvious.

This chapter is devoted to a review of complex formation of native as well as some modified α - and β -CDs with isomeric aminobenzoic acids. Interest in aminobenzoic acids is excited by the biological importance and properties of these compounds. *p*-Aminobenzoic acid (pABA) is considered a member of the B-vitamin complex [18]. It plays an important physiological role as a metabolic inhibitor and it is also involved in the biosynthesis of folic acid [19]. Moreover, pABA is used in the synthesis of some medicines (analgesics and vasodilators) [20], and as a UV-absorber in commercial sunscreen products [21]. *o*-Aminobenzoic acid (oABA) is known as vitamin L and is used as an intermediate for production of dyes, pigments and pharmaceuticals [22]. *m*-Aminobenzoic acid (mABA) displays no biological activity and it is employed in the synthesis of dyes. Aminobenzoic acids are also of interest because the existence of structural isomers allows comparison of their complexation with CDs.



Scheme 2. Isomeric aminobenzoic acids.

This chapter focuses on complex formation of CDs with isomeric aminobenzoic acids in aqueous solution and describes this process on our data and that of the literature. It is aimed at analyzing the influence of the structure of both CDs and aminobenzoic acids on complex formation and revealing the binding mode and driving forces of interaction.

RESULTS AND DISCUSSION

In our recent publications, complex formation of α -CD, β -CD and some β -CD derivatives with pABA and mABA was studied by calorimetry, ^1H NMR, UV-vis spectroscopy and densimetry [23-26]. There are also some available works in the literature devoted to the complexation of CDs with isomeric aminobenzoic acids in solution and in the solid state [27-35]. Crystal structures of β -CD complexes with pABA and oABA have been considered by Zhang et al. [27]. In particular, complexes of β -CD with pABA of 1:1 stoichiometry and

those with oABA of 2:3 stoichiometry have been revealed by single-crystal X-ray diffraction. It was found that these two complexes have different molecular packing structures. Intermolecular hydrogen-bond interactions stabilize both structures. Harata [28] investigated complexes of α -CD and β -CD with isomeric aminobenzoic acids in aqueous solution by circular dichroism spectroscopy and obtained thermodynamic parameters for 1:1 binding. The vibrational circular dichroism spectroscopy was also used by Setnička et al. [29] to study complex formation of pABA with α -CD and β -CD in water and DMSO solutions. Selectivity in interactions of pABA with α -CD, β -CD and hydroxypropyl- β -CD was revealed by Shuang et al. [30] using steady-state fluorescence measurements at 293 K. The influence of pH on complexation was also analyzed in this work. Calorimetric investigation of interactions of pABA and oABA with α -CD and β -CD has been carried out by Lewis and Hansen [31], and thermodynamic parameters of complex formation (K , ΔG_c , ΔH_c and ΔS_c) have been obtained and discussed. Stalin et al. showed that β -CD forms inclusion complexes with mABA [32], pABA [33] and oABA [34]. Complexes were investigated by UV-vis spectroscopy, fluorimetry, ^1H NMR and semiempirical quantum calculations (AM1).

All thermodynamic parameters of inclusion complex formation of CDs with aminobenzoic acids, which will be considered in the present work, refer to the process that is described by the following equation:



The 1:1 complex formation of CDs with ABA was observed in our previous works [23-26] and in the literature [28-35].

Complex Formation with α -CD

Thermodynamic parameters (stability constants, free energy, enthalpy and entropy changes) of complex formation of α -CD with aminobenzoic acids are listed in Table 1. Data relating to complexation of CDs with aniline [31] and benzoic acid [28, 31, 36] are also presented herein. It should be mentioned, that values of stability constants obtained for each complex by different experimental methods are close. The enthalpy and entropy values of complex formation with pABA obtained by us [25] are in accordance with data reported by Harata [28]. Nevertheless, ΔH_c and ΔS_c corresponding to interaction with mABA and evaluating from calorimetric measurements [23, 25] differ from those obtained by circular dichroism method [28].

It follows from Table 1 that α -CD forms complexes with mABA, pABA and oABA as well as with benzoic acid. However, no complex formation between α -CD and aniline was observed [31]. This means that availability of carboxylic group is the main factor determining the inclusion complex formation. It has been well established that the carboxylic group binds within α -CD, especially in its non-ionized form [37, 38]. Complex formation is accompanied by high negative enthalpy and entropy changes.

Table 1. Thermodynamic parameters of 1:1 complex formation of α -CD with some benzene derivatives

Complex	lgK	ΔG_c	ΔH_c	$T\Delta S_c$	Experimental conditions	Method	Ref.
		kJ·mol ⁻¹					
α -CD/aniline	a				H ₂ O, 298 K	calorimetry	[31]
α -CD/benzoic acid	2.88±0.01	-16.4±0.1	-42.5±0.6	-26.0±0.6	H ₂ O, 298 K	potentiometry	[36]
α -CD/benzoic acid	3.0±0.1	-17.1±0.4	-40.2±0.4	-22.5	H ₂ O, 298 K	calorimetry	[31]
α -CD/benzoic acid	2.5	-14.4	-41.8±1.0	-27.4±2.9	H ₂ O, 298 K	circular dichroism	[28]
α -CD/oABA	5.0±1.3	-28.5±7.5	-1.3±0.4	26.2	H ₂ O, 298 K	calorimetry	[31]
α -CD/mABA	1.73	-9.9	-32.5±0.3	-22.6±0.8	H ₂ O, 298 K	circular dichroism	[28]
α -CD/mABA ^b	1.8±0.4	-10.3	–	–	H ₂ O, 298 K	¹ H NMR	[24]
α -CD/mABA ^b	1.7±0.2	-9.7	–	–	H ₂ O, 298 K	densimetry	[25]
α -CD/mABA ^b	1.8±0.2	-10.3	-21.9±0.6	-11.6±1.5	H ₂ O, 298 K	calorimetry	[25]
α -CD/pABA	2.80	-16.0	-43.6±0.8	-27.6±2.5	H ₂ O, 298 K	circular dichroism	[28]
α -CD/pABA	2.8±0.1	-15.9±0.4	-49±2	-33	H ₂ O, 298 K	calorimetry	[31]
α -CD/pABA	3.0±0.4	-16.8	–	–	pH 2.0, 293 K	fluorescence	[30]
α -CD/pABA	3.1±0.1	-17.6	–	–	pH 3.5, 293 K	fluorescence	[30]
α -CD/pABA	a				pH 10.5, 293 K	fluorescence	[30]
α -CD/pABA ^b	3.1±0.6	-17.7	–	–	H ₂ O, 298 K	¹ H NMR	[24]
α -CD/pABA ^b	2.8±0.2	-16.0	–	–	H ₂ O, 298 K	densimetry	[25]
α -CD/pABA ^b	3.2±0.2	-18.3±1.1	-41.0±0.4	-22.7	H ₂ O, 298 K	calorimetry	[25]
α -CD/p-aminobenzoate	0.58	-3.30	–	–	298 K	molecular modeling	[35]

a – indication that either no complex formation takes place or a negligible enthalpy change occurs during reaction;
b – data obtained by author

For complexation of mABA and pABA with α -CD, the negative free energy is due to negative enthalpy values and complexes are enthalpy-stabilized in this case. On the contrary, complexation of α -CD with oABA is characterized by small negative enthalpy and high positive entropy. The entropy contribution is dominant and determines the binding in this system.

The enthalpy and entropy of CD complex formation contain the contributions from the following processes: (1) dehydration of reagents; (2) release of cavity-bound water from the CD cavity [6]; (3) binding due to non-covalent interactions such as van der Waals, electrostatic and hydrophobic interactions as well as the hydrogen bonding [6]; (4) hydration of the complex. The first three processes are particularly important and mainly determine the magnitudes of $\Delta_c H$ and $\Delta_c S$.

For complex formation of aminobenzoic acids with α -CD, the following tendency of change of the stability constants, enthalpy and entropy was revealed:

$$K: \text{oABA} > \text{pABA} > \text{mABA}$$

$$\Delta H_c: \text{oABA} > \text{mABA} > \text{pABA}$$

$$T\Delta S_c: \text{oABA} > \text{mABA} > \text{pABA}$$

These results testify that position of amino group in the aromatic ring considerably influences the binding mode and thermodynamic parameters of complexation.

It is clear from Table 1 that thermodynamic parameters of α -CD complex formation with pABA and benzoic acid are similar. This fact denotes that amino group located in *para*-position of benzene ring has no influence on the binding. In common with benzoic acid, carboxylic group of pABA is included into α -CD cavity, while the amino group is outside the cavity and placed in the bulk solvent. Large negative ΔH_c value is due to predominantly van der Waals interactions. The negative ΔS_c is explained by the loss in conformation mobility of the solutes.

The gradual increase of ΔH_c and ΔS_c was observed for complex formation of α -CD with mABA and next with oABA (Table 1). In comparison with pABA, mABA exists in aqueous solution as zwitterion having the negatively and positively charged carboxylic and amino groups, respectively [39, 40]. Zwitterionic forms are more strongly hydrated than molecular forms. This can restrict complex formation due to increased endothermic contribution caused by the dehydration.

In the case of oABA, the amino group is very close to carboxylic group and able to penetrate into α -CD cavity. This induces the intensive dehydration of NH_2 and $COOH$ polar groups. In comparison with pABA and mABA, the positive contribution from dehydration in ΔH_c and ΔS_c is larger. Thus, low exothermicity of α -CD binding with oABA is due to considerable changes in solvation of both reagents. The large positive entropy contribution favors the formation of very stable α -CD/oABA complexes.

As it was demonstrated for mABA complexation, ionization of the carboxylic group results in weaker binding with macrocyclic cavity. This fact can be additionally confirmed by comparison of α -CD binding with molecular and anionic forms of pABA. The molecular form of pABA is dominate in aqueous solution [39, 40]. Stability of complexes formed by α -CD and molecular pABA is significantly higher comparing to complexes with *p*-aminobenzoate (Table 1). Decrease of binding affinity of α -CD to substituted benzoic acids being in the ionization state has been noted by Simova and Schneider [37].

The 1H NMR measurements were carried out to reveal the binding modes of CD with mABA and pABA. 1H NMR spectra were recorded on Bruker AC-200 spectrometer operating at 200 MHz and temperature of 298.15 K. This technique also allows to determine the stoichiometry and stability constants of the complexes.

The continuous variation method (Job method) [41] was used for determination of stoichiometric ratio. For all systems under study, the 1:1 stoichiometry of the complexes was revealed in continuous variation plots (Figure 1). Minima of curves shown in Figure 1 correspond to $R=0.5$, confirming the existence of complexes of single 1:1 composition within the range of concentrations studied.

Stability constants were obtained by measuring the chemical shift changes of aminobenzoic acid protons at fixed aminobenzoic acid concentration ($0.005 \text{ mol}\cdot\text{kg}^{-1}$) and variable concentration of α -CD. Some concentration dependences of $\Delta\delta$ are shown in Figure 2. Calculation of K was done by non-linear regression analysis of the following equation [24]:

$$K = C_{ABA} \cdot \Delta\delta / (\Delta\delta_c \cdot (C_{CD} - C_{ABA} \cdot \Delta\delta / \Delta\delta_c) \cdot (C_{ABA} - C_{ABA} \cdot \Delta\delta / \Delta\delta_c)) \quad (2)$$

where K is stability constant; $\Delta\delta$ is the experimental chemical shift change; $\Delta\delta_c$ is chemical shift change induced by 100-% complex formation; C_{CD} and C_{ABA} are concentrations of CD

and aminobenzoic acid, respectively. Values of K and $\Delta\delta_c$ are listed in Tables 1 and 2, respectively.

The results presented in Table 2 show that complex formation of α -CD with mABA and pABA induces the downfield shift for H(2) and H(6) protons which are close to the carboxylic group. It suggests that penetration of pABA and mABA into α -CD cavity is shallow. The carboxylic group is located inside the cavity, whereas the amino group resides within the polar exterior of α -CD molecule. To confirm this fact the consideration of α -CD ^1H NMR spectrum is necessary.

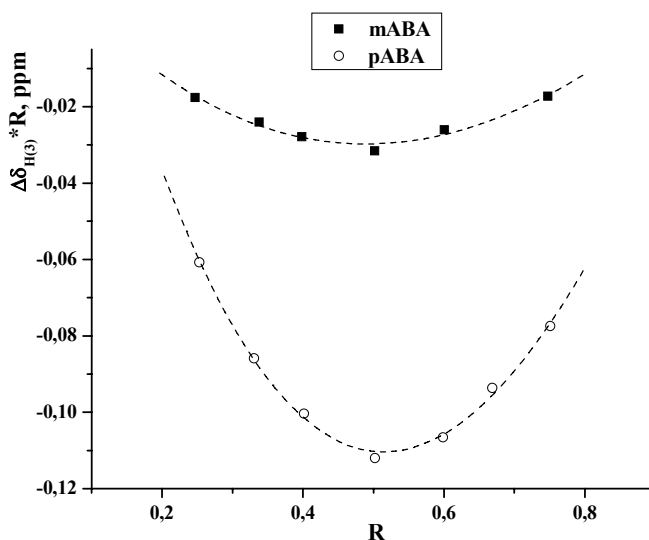


Figure 1. Job plots for complexation of α -CD with mABA and pABA at 298.15 K.

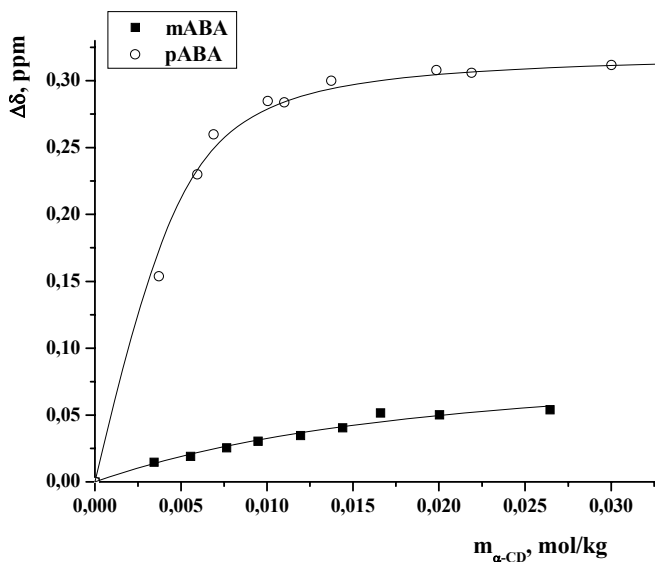


Figure 2. Chemical shift changes for H(2) protons of aminobenzoic acids vs. α -CD concentration.

Table 2. Complexation induced chemical shifts of protons of aminobenzoic acids in complexes with α -CD (298.15 K)

Complex	$\Delta\delta_c$, ppm				
	H(2)	H(3)	H(4)	H(5)	H(6)
mABA/ α -CD	0.09±0.02	—	~0	~0	0.09±0.02
pABA/ α -CD	0.32±0.01	~0	—	~0	0.32±0.01

Figure 3 shows the partial ^1H NMR spectra of α -CD alone and in the presence of mABA and pABA. The ^1H NMR spectrum of CD consists of the signals of H(1), H(2), H(3), H(4), H(5) and H(6) protons. It is necessary to note, that H(1), H(2), H(4) and H(6) protons are located on the CD exterior (see Scheme 1). To the contrary, H(3) and H(5) protons are placed inside the macrocyclic cavity at the wider and narrow rims, respectively, and they are most sensitive to the inclusion process [42].

As can be seen from Figure 3, addition of pABA induces the pronounced upfield shift for H(3) proton of α -CD ($\Delta\delta_c = -0.32\pm 0.01$ ppm) and downfield shift for H(5) proton ($\Delta\delta_c = 0.19\pm 0.01$ ppm). The negligible upfield shift for H(1), H(2), H(4) and H(6) protons was also observed. These $\Delta\delta_c$ values were obtained by measuring $\Delta\delta$ of α -CD protons at constant concentration of α -CD and variable concentration of aminobenzoic acids.

The influence of the mABA on the α -CD ^1H NMR spectrum is analogous (Figure 3). The “external” protons of α -CD are practically unaffected in the presence of mABA, whereas the signals of the “internal” H(3) and H(5) protons exhibit an upfield ($\Delta\delta_c = -0.35\pm 0.01$ ppm) and downfield ($\Delta\delta_c = 0.16\pm 0.01$ ppm) shift, respectively. The magnitude and sign of $\Delta\delta_c$ for the H(3) and H(5) protons indicate that pABA and mABA are inserted into macrocyclic cavity predominantly from the wider rim of α -CD molecule. The depth of penetration is approximately the same for both acids under study. The location of the aromatic ring of aminobenzoic acids inside the macrocyclic cavity induces the observed shielding of the H(3) proton. The carboxylic group positioned near the H(5) protons causes their deshielding. The similar results were found for complex formation of α -CD with some substituted benzoic acids [37] and phenyl derivatives [43].

To get information on the nature of CD-ABA interactions and structural rearrangements in solution occurring upon inclusion complex formation the densimetry can be employed. The densities of solutions were measured at 298.15 ± 0.01 K using a vibrating-tube digital densimeter (model DMA 4500, Anton Paar, Austria) with a precision of 1×10^{-5} g cm $^{-3}$. Detailed description of the density measurements has been done previously [25]. The apparent molar volumes (V_ϕ) were calculated on the basis of the following relation:

$$V_\phi = M/d + 10^3(d-d_0)/mdd_0 \quad (3)$$

where M is the solute molar mass; m is the molality; d_0 and d are the densities of solvent and solution, respectively. For binary systems (CD+H $_2$ O) or (ABA+H $_2$ O), water was the reference solvent with $d_0 = 0.99704$ g·cm $^{-3}$. For ternary systems (CD+ABA+H $_2$ O), the reference solvents were aqueous solutions of CD or aminobenzoic acid.

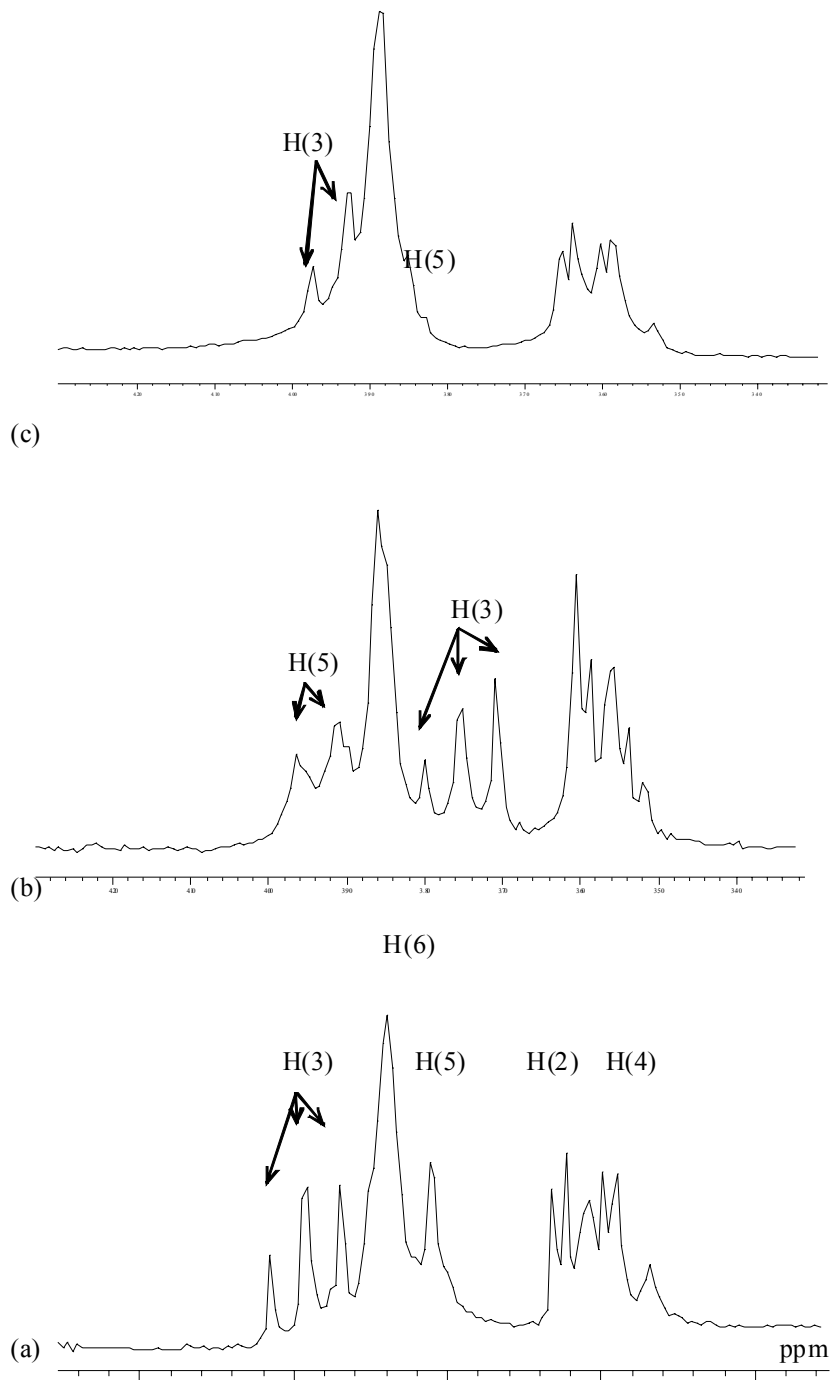


Figure 3. Partial ^1H NMR spectra (200 MHz, 298.15 K) of 5 mM α -CD alone (a) and in the presence of 5 mM pABA (b) and 5 mM mABA (c).

The two sets of experiments were carried out. The apparent molar volumes of CDs ($V_{\phi}(\text{CD})$) were determined at constant CD concentration ($0.005 \text{ mol}\cdot\text{kg}^{-1}$) and variable concentration of aminobenzoic acid ($0\div 0.04 \text{ mol}\cdot\text{kg}^{-1}$) and vice versa the apparent molar

volumes of aminobenzoic acids ($V_{\Phi}(\text{ABA})$) were determined at constant concentration of aminobenzoic acid ($0.005 \text{ mol}\cdot\text{kg}^{-1}$) and changeable α -CD concentration ($0\div 0.08 \text{ mol}\cdot\text{kg}^{-1}$). As an example, some concentration dependences of V_{Φ} are plotted in Figure 4.

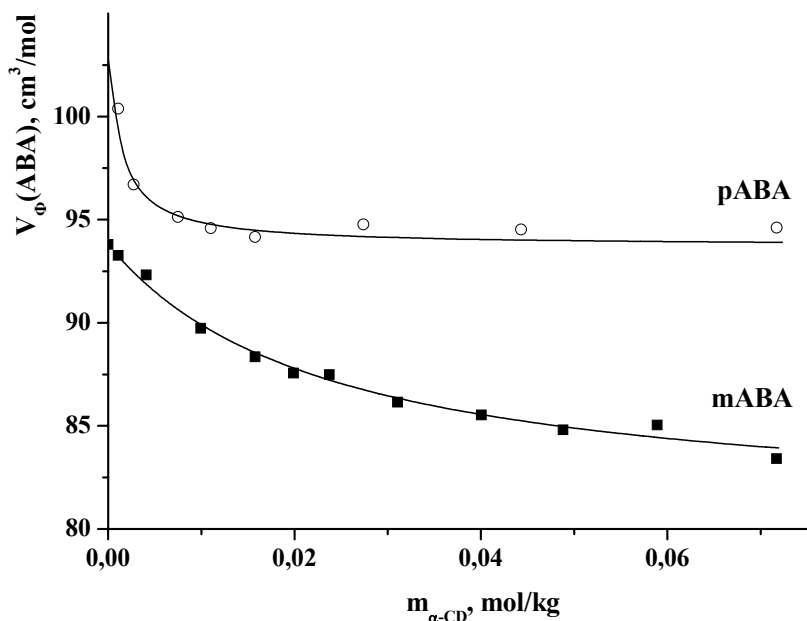


Figure 4. Dependences of the apparent molar volumes of aminobenzoic acids from α -CD concentration (298.15 K).

According to the Young's rule [44] for 1:1 complexation mode, V_{Φ} contains the contributions from volumes of free and complexed species presented in the system:

$$V_{\Phi} = (1 - \alpha_c)V_{\Phi,f} + \alpha_c V_{\Phi,c} \quad (4)$$

where α_c is the fraction of the complexes; $V_{\Phi,f}$ and $V_{\Phi,c}$ are the volumes of free and fully complexed species, respectively. Contributions due to ionization/protonation of aminobenzoic acids were considered as negligible in the concentration ranges under study since the measured pH of the solutions (pH=3.6 for pABA and pH=3.9 for mABA) corresponded to the predominant existence of neutral (or zwitterionic) structures [45]. CDs do not dissociate under experimental conditions [46].

Some mathematical rearrangements of equation (4) result in:

$$V_{\Phi} = (V_{\Phi,f} + K \cdot V_{\Phi,c} m) / (1 + K m) \quad (5)$$

where K is stability constant of 1:1 complexes and m is the solute concentration. Analytical solution of equation (5) by nonlinear least-squares fitting gives K and $V_{\Phi,c}$. The values of $V_{\Phi,f}$ were found to be 603.3 , 102.8 and $93.8 \text{ cm}^3\cdot\text{mol}^{-1}$ for α -CD, pABA and mABA, respectively.

They are in a good agreement with values reported for α -CD ($604 \pm 2 \text{ cm}^3 \cdot \text{mol}^{-1}$) [47], pABA ($103.61 \text{ cm}^3 \cdot \text{mol}^{-1}$) [48] and mABA ($90.3 \text{ cm}^3 \cdot \text{mol}^{-1}$) [49].

The change in the molar volumes ($\Delta V_{\phi,c}$) induced by complex formation can be calculated as

$$\Delta V_{\phi,c} = V_{\phi,c} - V_{\phi,f} \quad (6)$$

Values of K and $\Delta V_{\phi,c}$ are listed in Tables 1 and 3, respectively.

Table 3. Volume data for complex formation of aminobenzoic acids with α -CD at 298.15 K

Complex	$V_{\phi,c}(\text{ABA})$	$\Delta V_{\phi,c}(\text{ABA})$	$V_{\phi,c}(\alpha\text{-CD})$	$\Delta V_{\phi,c}(\alpha\text{-CD})$
	$\text{cm}^3 \cdot \text{mol}^{-1}$			
α -CD/mABA	82.3 ± 1.9	-11.5 ± 0.9	595.0 ± 0.5	-8.3 ± 0.7
α -CD/pABA	93.7 ± 0.8	-9.1 ± 0.9	596.5 ± 0.5	-6.8 ± 0.6

It can be seen from Table 3 that transfer of mABA and pABA from water to aqueous solutions of α -CD is accompanied by negative volume changes ($\Delta V_{\phi,c}(\text{ABA}) < 0$). The same character of volume changes was obtained for transfer of α -CD to aqueous solutions of both mABA and pABA ($\Delta V_{\phi,c}(\alpha\text{-CD}) < 0$).

The $\Delta V_{\phi,c}$ values can be interpreted on the basis of the reorganization of solvent (water) molecules during complex formation [47, 50-52]. It is known, that cavity of α -CD contains 2 water molecules, which are partially or completely replaced by the guest molecules upon binding [53]. This process gives the positive contribution to the $\Delta V_{\phi,c}$ values [47, 51, 52]. In addition, complex formation is accompanied by the partial destruction of hydration shells of aminobenzoic acid and α -CD. Restructurization of the hydration shells of the solutes can be explained using cosphere overlap model proposed by Friedman and Krishnan [54]. According to this model, hydrophilic-hydrophilic interactions result in positive contribution to $\Delta V_{\phi,c}$, whereas hydrophilic-hydrophobic and hydrophobic-hydrophobic interactions contribute negatively in $\Delta V_{\phi,c}$.

Taking into account all these processes one can suppose that negative $\Delta V_{\phi,c}$ values are the result of dominant contribution from interactions of hydrophobic cavity of α -CD with polar groups as well as with aromatic ring of aminobenzoic acids. The realization of these interactions is in agreement with the established by ^1H NMR shallow penetration of aminobenzoic acids into α -CD cavity.

Complex Formation with β -CD

The molecule of β -CD consists of seven glucose units and, consequently, possesses the larger cavity diameter. It is interesting to investigate the interactions of β -CD with aminobenzoic acids with the purpose to analyze the influence of cavity dimensions on

complex formation. Thermodynamic parameters of complex formation of β -CD with aminobenzoic acids, benzoic acid and aniline are listed in Table 4.

It can be seen from Table 4 that, contrary to α -CD which binds only benzoic acid (see Table 1), β -CD participates in complex formation with both aniline and benzoic acid. According to Hoshino et al. [55], hydrophobic interactions are important in the inclusion complex formation of β -CD with aniline and its derivatives. Results of molecular dynamics study show that aniline is included with molecular axis strongly inclined. Hydrogen bonding between the hydroxyl groups of the top torus in the β -CD molecule and nitrogen atom of the aniline molecule was observed [56]. The inclination of molecular axis of aniline is in agreement with circular dichroism data [57], which also indicate deviation from axial inclusion during binding of β -CD with aniline.

Compared to aniline, benzoic acid is included with larger deviation from the axial orientation and with higher stability constant [57]. The data of circular dichroism are compatible with the inclusion mode proposed by Bergeron et al. [58]. According to it, benzoic acid is inserted in CD cavity by carboxyl group. Stability of the complex is determined by van der Waals forces and hydrogen-bonding between the deeply inserted COOH group and OH groups surrounding the bottom rim of the cavity [57, 58]. Location of carboxylic group in the β -CD cavity was confirmed by ^1H NMR in Ref. [59]. As follows from Table 4, stability constant for complex of benzoic acid with β -CD is slightly lower than that for α -CD. Binding with β -CD is characterized by higher enthalpy and entropy changes, as compared with α -CD. These differences can be caused by the deeper penetration of benzoic acid molecule into β -CD cavity.

Thermodynamic parameters of complex formation between β -CD and aminobenzoic acids obtained by different experimental methods differ. Values of ΔH_c and ΔS_c reported by Harata [28] and Stalin et al. [32-34] were estimated from temperature dependence of stability constants. It is well known, that uncertainty of van't Hoff analysis is higher [60]. Unusually considerable discrepancy with values obtained by Stalin et al. [32, 33] can be explained by the presence of DMSO as cosolvent.

According to our data derived from calorimetry and presented in Table 4, complex formation of β -CD with mABA and pABA is accompanied by negative enthalpy and positive entropy changes. Complexes are stabilized by both the enthalpy and entropy terms. Positive entropy changes testify the considerable contribution from dehydration that is accompanied by the release of water molecules from the solvation shells of reagents and macrocyclic cavity in the bulk aqueous solution. Furthermore, hydrophobic interactions of the aromatic ring of aminobenzoic acid with apolar cavity of cyclodextrins can play significant role in the complexation resulting in positive ΔS_c and small negative ΔH_c .

Analysis of the data summarized in Tables 1 and 4 shows that revealed for α -CD complexation influence of the position of amino group in the benzene ring is displayed for β -CD complexation. In particular, binding of β -CD with pABA and oABA results in formation of more stable complexes (Table 4). On the contrary to pABA and mABA, which form only 1:1 complexes with β -CD, oABA is able to 1:1 and 1:2 binding at pH 7 when it exists as anion [34]. The 1:2 complexes are found to be very stable (Table 4). As compared to mABA, interaction with pABA is more exothermic. As it was discussed above, this difference is due to predominant existence of molecular forms of pABA, which are less hydrated in comparison with zwitterionic forms of mABA.

Table 4. Thermodynamic parameters of 1:1 complex formation of β -CD with some benzene derivatives

Complex	lgK	ΔG_c	ΔH_c	$T\Delta S_c$	Experimental conditions	Method	Ref.
β -CD/ aniline	1.7±0.1	-9.7	–	–	H ₂ O, 301 K	fluorescence	[55]
β -CD/ aniline	2.1±0.3	-12.0	–	–	pH 7.5, 298 K	circular dichroism	[57]
β -CD/ benzoic acid	2.1±0.4	-12±2	-32±11	-20	H ₂ O, 298 K	calorimetry	[31]
β -CD/ benzoic acid	2.5	-14.4	-22.3±0.3	-7.8±0.8	H ₂ O, 298 K	circular dichroism	[28]
β -CD/ benzoic acid	2.6±0.3	-14.7	–	–	pH 6.2, 298 K	circular dichroism	[57]
β -CD/ oABA	2.18	-12.67	–	–	pH~1.0, 303 K	Uv-vis	[34]
β -CD/ oABA	2.58	-14.95	–	–	pH~1.0, 303 K	fluorescence	[34]
β -CD/ oABA	2.31	-10.77	–	–	pH~7.0, 303 K	Uv-vis	[34]
β -CD/ oABA ^a	5.62	-32.62	–	–	pH~7.0, 303 K	Uv-vis	[34]
β -CD/ oABA	2.50	-13.76	–	–	pH~7.0, 303 K	fluorescence	[34]
β -CD/ oABA ^a	5.85	-34.76	–	–	pH~7.0, 303 K	fluorescence	[34]
β -CD/ mABA	1.8	-10.3	-8.7±0.3	1.6±1.3	H ₂ O, 298 K	circular dichroism	[28]
β -CD/ mABA	2.20	-12.74	-68.00	-55.26	pH~1.0, 303 K	Uv-vis	[32]
β -CD/ mABA	2.11	-12.23	–	–	pH~1.0, 303 K	fluorescence	[32]
β -CD/ mABA	1.83	-10.63	-68.00	-57.97	pH~7.0, 303 K	Uv-vis	[32]
β -CD/ mABA	1.98	-11.47	–	–	pH~7.0, 303 K	fluorescence	[32]
β -CD/ mABA ^b	1.8±0.3	-10.3	–	–	H ₂ O, 298 K	¹ H NMR	[24]
β -CD/ mABA ^b	1.85±0.03	-10.56	–	–	H ₂ O, 293 K	UV-vis	[23]
β -CD/ mABA ^b	1.8±0.2	-10.3	–	–	H ₂ O, 298 K	densimetry	[25]
β -CD/ mABA ^b	1.8±0.1	-10.2	-2.2±0.1	8.0	H ₂ O, 298 K	calorimetry	[25]
β -CD/ pABA	2.7	-15.4	-23.4±0.4	-8.0±1.3	H ₂ O, 298 K	circular dichroism	[28]
β -CD/ pABA	1.95	-11.31	-70.75	-59.44	pH~1.0, 303 K	Uv-vis	[33]
β -CD/ pABA	2.33	-13.51	–	–	pH~1.0, 303 K	fluorescence	[33]
β -CD/ pABA	1.52	-8.81	-70.75	-61.94	pH~7.0, 303 K	Uv-vis	[33]
β -CD/ pABA	2.36	-13.72	–	–	pH~7.0, 303 K	fluorescence	[33]
β -CD/ pABA	2.4±0.3	-13.5	–	–	pH 2.0, 293 K	fluorescence	[30]
β -CD/ pABA	2.8±0.2	-15.6	–	–	pH 3.5, 293 K	fluorescence	[30]
β -CD/ pABA ^c					pH 10.5, 293 K	fluorescence	[30]
β -CD/ pABA ^b	2.8±0.6	-16.0	–	–	H ₂ O, 298 K	¹ H NMR	[24]
β -CD/ pABA ^b	2.8±0.2	-16.0	–	–	H ₂ O, 298 K	densimetry	[25]
β -CD/ pABA ^b	2.9±0.1	-16.6	-14.2±0.2	2.4	H ₂ O, 298 K	calorimetry	[25]

a – complexes of 1:2 stoichiometry; b – data obtained by author; c – indication that either no complex formation takes place or a negligible enthalpy change occurs during reaction.

The influence of cavity dimensions is not reflected on the stoichiometry of the complexes and their stability. The 1:1 stoichiometric ratio of β -CD complexes is evident from Job plots illustrated in Figure 5. Stability of the complexes formed by one acid and different CDs is approximately the same (Tables 1 and 4). On the contrary, cavity dimensions have a significant influence on the enthalpy and entropy of complex formation. Values of ΔH_c and ΔS_c corresponding to β -CD complexation are higher than those for α -CD complex formation. This can be attributed to deeper inclusion of aminobenzoic acids into β -CD cavity and, as a consequence, to more intensive dehydration of the reagents.

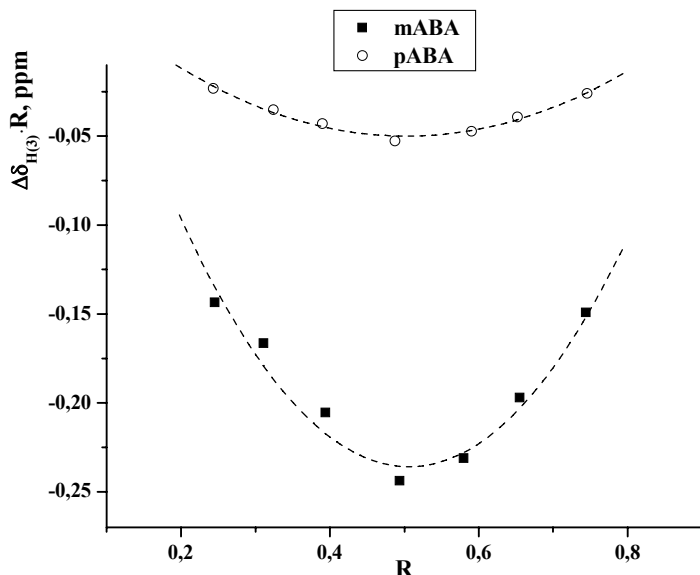


Figure 5. Job plots for complexation of β -CD with mABA and pABA at 298.15 K.

Binding mode of β -CD can be predicted on the basis of ^1H NMR data presented in Table 5 and Figure 6. The signals of all protons of the aromatic ring of aminobenzoic acids are upfield shifted upon complex formation with β -CD (Table 5). It indicates the location of whole benzene ring inside β -CD cavity and, consequently, the deep insertion of pABA and mABA.

Table 5. Complexation induced chemical shifts of protons of aminobenzoic acids in complexes with β -CD (298.15 K)

Complex	$\Delta\delta_c$, ppm				
	H(2)	H(3)	H(4)	H(5)	H(6)
mABA/ β -CD	-0.33 ± 0.04	—	-0.17 ± 0.07	-0.14 ± 0.05	-0.36 ± 0.06
pABA/ β -CD	-0.09 ± 0.01	-0.13 ± 0.01	—	-0.13 ± 0.01	-0.09 ± 0.01

Figure 6 shows the partial ^1H NMR spectra of β -CD alone and in the presence of pABA and mABA. It is not difficult to see that addition of both acids induces the upfield shift for H(3) and H(5) protons of β -CD, the shifting of the H(5) being more sizeable. For pABA complexes, the values of $\Delta\delta_c = -0.18\pm 0.01$ ppm and $\Delta\delta_c = -0.24\pm 0.01$ ppm were obtained for H(3) and H(5) protons, respectively. For mABA complexes, the following $\Delta\delta_c$ were estimated: $\Delta\delta_c = -0.19\pm 0.01$ ppm and $\Delta\delta_c = -0.23\pm 0.01$ ppm for H(3) and H(5), respectively. The measurable upfield shifts obtained for both H(3) and H(5) protons demonstrate that the aromatic ring of pABA and mABA is deeply included into the β -CD cavity and located between H(3) and H(5) planes. The signal of H(6) proton placed near the narrow rim of the torus is affected by complex formation of β -CD with both acids. Probably, the shifting of signal of H(6) proton is caused by the location of carboxylic group in the area of primary

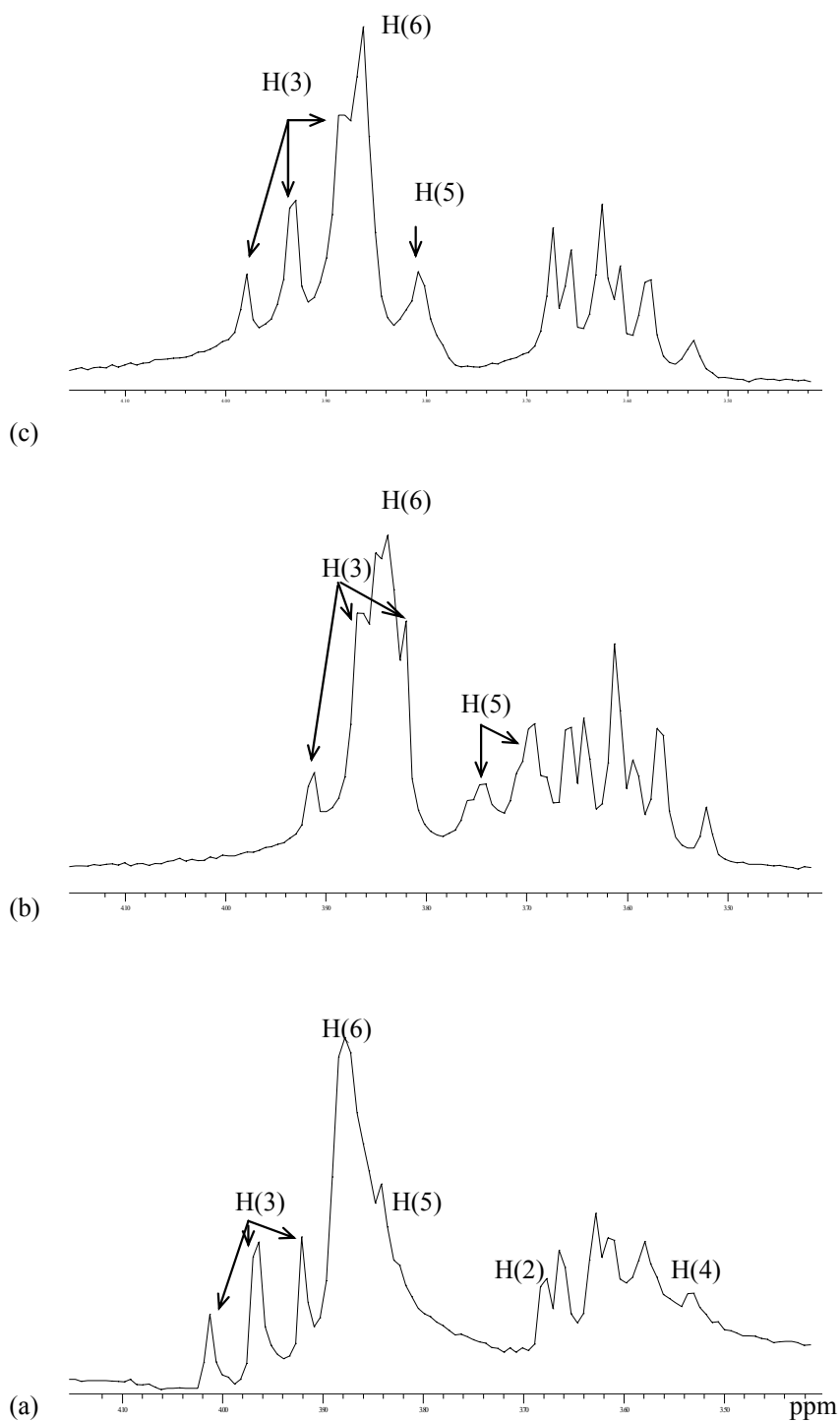


Figure 6. Partial ^1H NMR spectra (200 MHz, 298.15 K) of 5 mM β -CD alone (a) and in the presence of 5 mM pABA (b) and 5 mM mABA (c).

hydroxyl groups. Hydrogen bonding between COOH and OH groups is not excluded in this case. It has been shown by Stalin et al. [32, 33] that the COOH group of mABA as well as pABA is located in the non-polar part of the β -CD cavity during the complex formation in water-DMSO mixture. It should be mentioned that the presence of DMSO as organic cosolvent does not change the binding mode of β -CD with aminobenzoic acids. The proposed binding mode of β -CD with aminobenzoic acids is also in accordance with complexation of β -CD with benzoic acid [57, 58]. It should be noted, that the structure of β -CD complexes in solution and in the solid state is the same. According to Zhang et al. [27], in the crystalline β -CD/pABA complex, the guest molecule is deeply included into the cavity of β -CD while the amino group is located on the wide site of cavity and the carboxyl at the narrow site.

As it was found, the deeper penetration of aminobenzoic acids into β -CD cavity takes place and this process is accompanied by considerable dehydration of the solutes. Volumetric properties given in Table 6 are sensitive to these structural changes in solution occurring during complex formation. The $\Delta V_{\phi,c}$ values (Table 6) obtained for β -CD complex formation are large and positive in comparison with negative $\Delta V_{\phi,c}$ observed for α -CD complexation (Table 3). Positive $\Delta V_{\phi,c}$ are related to release of more water molecules from β -CD cavity than from α -CD cavity. This fact is also confirmed by less negative ΔH_c and positive ΔS_c obtained for β -CD complexation (Table 4). It was assumed above, that small negative ΔH_c and positive ΔS_c are also typical for hydrophobic interactions. According to cosphere overlap model [54], which is used for the assignment of volume changes, hydrophobic interactions contribute negatively to $\Delta V_{\phi,c}$. However, the positive $\Delta V_{\phi,c}$ values detected for β -CD complex formation (Table 6) testify that hydrophobic interactions are not the driving force of β -CD binding with aminobenzoic acids. Comparison of $\Delta V_{\phi,c}$ allows to note that inclusion of mABA is accompanied by more intensive dehydration and, as consequence, binding in this system is generally entropy driven.

Table 6. Volume data for complex formation of aminobenzoic acids with β -CD at 298.15 K

Complex	$V_{\phi,c}(\text{ABA})$	$\Delta V_{\phi,c}(\text{ABA})$	$V_{\phi,c}(\beta\text{-CD})$	$\Delta V_{\phi,c}(\beta\text{-CD})$
	$\text{cm}^3 \cdot \text{mol}^{-1}$			
β -CD/mABA	111.8 \pm 0.9	18.0 \pm 0.8	732.4 \pm 0.9	27.2 \pm 0.6
β -CD/pABA	117.4 \pm 0.8	14.6 \pm 0.9	728.1 \pm 1.0	22.9 \pm 0.5

It is well known that the empty cavity of β -CD cavity is filled by approximately five to seven water molecules [61, 62]. Fukahori et al. [63] proposed a simplified expression that describes the volume change upon substitution of cavity-bound water by guest molecule:

$$\Delta_{tr}V = nV(\text{H}_2\text{O}) - V(\text{g}) \quad (7)$$

where n is the number of ejected molecules of cavity-bound water; $V(\text{H}_2\text{O})$ and $V(\text{g})$ are the molar volumes of water and included guest molecule. It is known that $V(\text{H}_2\text{O}) = 18.07 \text{ cm}^3 \text{ mol}^{-1}$ [51, 64]. The partial molar volumes of mABA ($93.8 \text{ cm}^3 \text{ mol}^{-1}$) and pABA ($102.8 \text{ cm}^3 \text{ mol}^{-1}$) obtained earlier [25] were taken for $V(\text{g})$ since, as it was concluded above, these acids deeply penetrate into β -CD cavity and the whole molecule of aminobenzoic acid is placed

inside. It is easy to calculate that 7.0 and 6.7 water molecules are expelled when mABA and pABA, respectively, enter the β -CD cavity. This result is in agreement with literature data [63, 65, 66]. In particular, González-Gaitano et al. [65] obtained $n = 6.5$ for complex formation of β -CD with decyltrimethylammonium bromide. The number of water molecules released from β -CD cavity upon binding with adenosine 5'-monophosphate and acetylsalicylic acid was found as $n = 6$ [66] and $n = 5.5$ [63], respectively.

Complex Formation with Modified β -CDs

Modified CDs become more popular during the last years due to their higher solubility in aqueous medium and improved complexing properties [7, 8]. Complex formation of aminobenzoic acids with hydroxypropyl- β -CD (HP- β -CD) and methyl- β -CD (M- β -CD) was studied in this work. These CDs were randomly substituted with the average substitution degree of 0.6 and 1.8 per glucose unit for HP- β -CD and M- β -CD, respectively. Table 7 reports the stability constants, free energy, enthalpy and entropy of complex formation of modified β -CDs with mABA and pABA. Data obtained by Shuang et al. [30] for complexation of HP- β -CD with pABA at different pH are also presented herein.

Results of calorimetric study showed that complexation of HP- β -CD and M- β -CD with mABA is accompanied by thermal effects that were too small to calculate K and ΔH_c . Therefore, the UV-vis spectroscopy was used for this purpose. Absorption spectra of mABA were recorded in the range of 200-400 nm on a UV-2401 PC UV-VIS Recording Spectrometer (Shimadzu, Japan) equipped with TCC-240 A temperature controlled cell holder.

Figure 7 shows the absorbance spectra of mABA in the presence of HP- β -CD. The addition of HP- β -CD increases the intensity and induces the red shift of absorption maxima, which is displayed for pure mABA at 306 nm.

The absorbance spectra reflect the isosbestic points, the availability of which suggests the occurrence of 1:1 complex formation. Figure 8 illustrates the concentration dependences of the absorbance obtained for several temperatures.

Stability constants of the complexes were estimated using the nonlinear curve fitting procedure based on of the following equation:

$$A = A_0 + (\Delta\varepsilon \cdot K \cdot C_{\text{mABA}} \cdot C_{\text{HP-}\beta\text{-CD}}) / (1 + K \cdot C_{\text{HP-}\beta\text{-CD}}) \quad (8)$$

where A and A_0 are the absorbance of mABA in the presence and absence of HP- β -CD, respectively; $\Delta\varepsilon$ is the difference in molar absorptivities between free and complexed mABA; C_{mABA} and $C_{\text{HP-}\beta\text{-CD}}$ are the initial concentrations of mABA and HP- β -CD, respectively; K is stability constant. The values of K corresponding to different temperatures are given in Table 8. As it is seen from Table 8, stability constants do not depend on temperature. The invariance of K with temperature increase for binding of mABA with HP- β -CD denotes the approximately zero enthalpy change, which is consistent with the calorimetry results. The same situation was typical for complex formation of M- β -CD with mABA (Table 7).

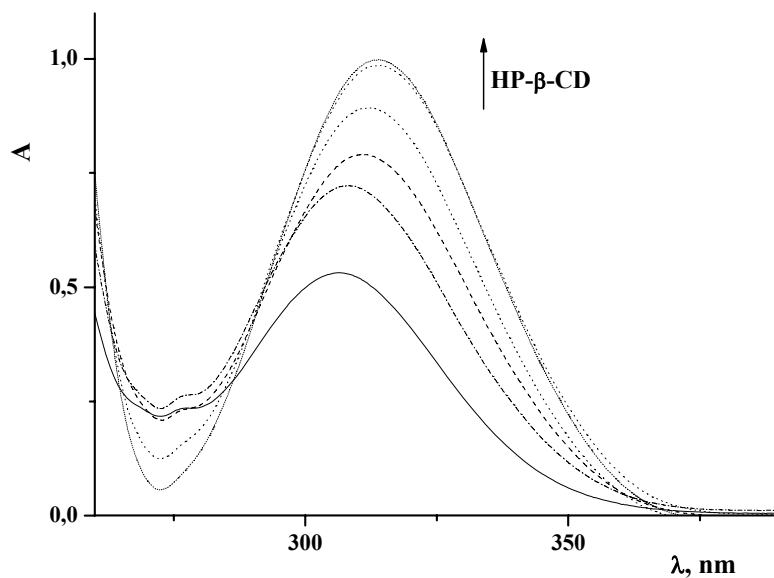


Figure 7. The effect of HP- β -CD on UV-vis spectrum of mABA (298.15 K).

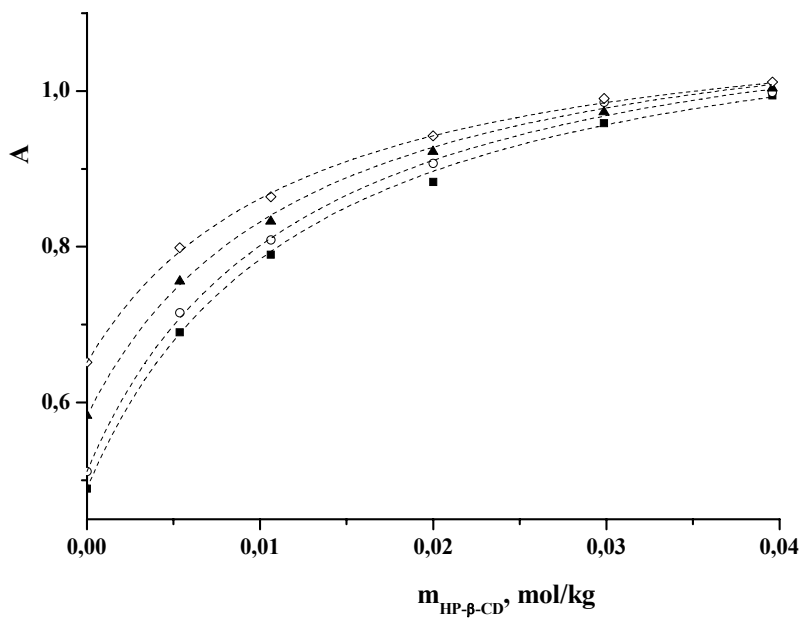


Figure 8. Dependences of the mABA absorbance from HP- β -CD concentration (! - 293.15 K; -- 298.15 K, 7 - 308.15 K; M - 318.15 K).

Table 7. Thermodynamic parameters of 1:1 complex formation of modified β -CDs with aminobenzoic acids

Complex	lgK	ΔG_c	ΔH_c		T ΔS_c	Experimental conditions	Method	Ref
			kJ·mol ⁻¹					
HP- β -CD/mABA ^b	1.9±0.3	-10.8	–	–	–	H ₂ O, 298 K	¹ H NMR	[23]
HP- β -CD/mABA ^b	2.0±0.1	-11.4	≈0	≈ 11.4	–	H ₂ O, 298 K	UV-vis	[26]
M- β -CD/mABA	1.9±0.2	-10.8	–	–	–	H ₂ O, 298 K	¹ H NMR	[23]
M- β -CD/mABA	1.91±0.07	-10.7	–	–	–	H ₂ O, 293 K	UV-vis	[23]
M- β -CD/mABA	–	–	≈0	–	–	H ₂ O, 298 K	calorimetry	[23]
HP- β -CD/ pABA	2.3±0.5	-13.1	–	–	–	pH 2.0, 293 K	fluorescence	[30]
HP- β -CD/ pABA	2.8±0.1	-16.0	–	–	–	pH 3.5, 293 K	fluorescence	[30]
HP- β -CD/ pABA ^a	–	–	–	–	–	pH 10.5, 293 K	fluorescence	[30]
HP- β -CD/ pABA ^b	2.8±0.4	-15.9	–	–	–	H ₂ O, 298 K	¹ H NMR	[26]
HP- β -CD/ pABA ^b	2.9±0.2	-16.6	-11.7±0.3	4.9	–	H ₂ O, 298 K	calorimetry	[26]

a – indication that either no complex formation takes place or a negligible enthalpy change occurs during reaction; b – data obtained by author

Table 8. Stability constants of mABA/HP- β -CD complexes at different temperatures

T, K	K, kg·mol ⁻¹
293.15	94±3
298.15	96±3
308.15	96±3
318.15	98±3

Substitution of OH-groups surrounding the β -CD cavity by the functional groups can cause the increase of depth and diameter of the cavity as well as the change of hydrophobicity, promoting sometimes more effective binding. As it was found, introduction of hydroxypropyl- and methyl-groups in the β -CD molecule results in increase of ΔH_c and ΔS_c and practically does not affect the stability constants (Tables 4 and 7). Invariance of stability constants of complexes formed by β -CD and HP- β -CD was also detected by Shuang et al. [30].

Complexes of modified β -CDs with pABA are enthalpy-entropy stabilized, while the complexes with mABA are only entropy stabilized. The increased entropy contribution, in comparison with the native β -CD, is due to stronger dehydration of bulky substituents surrounding the macrocyclic cavity. Hydration shells of modified CDs are partially broken up upon the binding, and the release of more water molecules to the disordered bulk solvent takes place, producing the positive contribution to ΔH_c and ΔS_c .

The same influence of the position of the amino group in the benzene ring that was found for complexation of native β -CD was observed for modified β -CDs. In particular, binding of pABA with HP- β -CD is more exothermic and results in formation of more stable complexes as compared to binding with mABA.

Analyzing the influence of pH on complex formation of HP- β -CD with pABA, Shuang et al. [30] demonstrated that the binding ability of HP- β -CD is decreased in the following order:

neutral > cationic > anionic species. The authors explained this phenomenon by the higher hydrophobicity of the uncharged species.

^1H NMR spectra of aminobenzoic acids were examined in the absence and presence of various amounts of HP- β -CD and M- β -CD. ^1H NMR spectra of HP- β -CD and M- β -CD were not examined because of the overlapping of some peaks. Chemical shift changes corresponding to 100% complex formation of aminobenzoic acids with HP- β -CD and M- β -CD are reported in Table 9. Evidently, the considerable $\Delta\delta_c$ were detected for all protons of the aromatic ring, the $\Delta\delta_c$ being maximal for H(2) and H(6) protons which are close to the carboxylic group. This means that deep insertion of mABA and pABA into the cavity of the CDs under study and the location of the carboxylic group inside the cavity take place. Thus, the obtained results are in agreement with the binding mode of native β -CD.

Table 9. Complexation induced chemical shifts of protons of aminobenzoic acids in complexes with HP- β -CD and M- β -CD (298.15 K)

Complex	$\Delta\delta_c$, ppm				
	H(2)	H(3)	H(4)	H(5)	H(6)
M- β -CD/mABA	-0.40±0.01	—	-0.22±0.01	-0.13±0.01	0.41±0.01
HP- β -CD/mABA	-0.31±0.01	—	-0.19±0.01	-0.11±0.01	-0.33±0.01
HP- β -CD/pABA	-0.08±0.01	-0.13±0.01	—	-0.13±0.01	-0.08±0.01

CONCLUSION

The results showed that α -CD and β -CD form with mABA and pABA inclusion complexes of 1:1 stoichiometry. The shallow insertion of the carboxylic group of pABA and mABA into α -CD takes place. In this case, inclusion complexes are mainly enthalpy stabilized due to the prevalence of van der Waals interactions. The deeper penetration of pABA and mABA into β -CD was observed. The molecules of cavity-bound water are fully replaced by the molecule of aminobenzoic acid during complexation of β -CD. Thus, solvent reorganization plays an important role in β -CD complex formation. The position of the amino group in the aromatic ring was found to influence considerably the thermodynamic parameters of complex formation. Introduction of hydroxypropyl- and methyl-substituents in the β -CD molecule does not dramatically change the binding mode with aminobenzoic acids and thermodynamic parameters of complex formation.

REFERENCES

- [1] Bender, MI; Komiyama, M. *Cyclodextrin chemistry*. Berlin: Springer Verlag; 1978.
- [2] Szejtli, J. *Cyclodextrins and their inclusion complexes*. Budapest: Akadémiai Kiadó; 1982.
- [3] Bergeron, RJ. Cycloamylose-substrate binding. In: JL; Atwood, JED; Davies, DD; MacNicol, editors. *Inclusion compounds*. London: Academic Press; 1984; 391-443.
- [4] Duchene, D. *Cyclodextrins and their industrial uses*. Paris: Editions de Santé; 1987.

- [5] Connors, KA. The stability of cyclodextrin complexes in solution. *Chem. Rev.*, 1997, 97, 1325-1357.
- [6] Liu, L; Guo, QX. The driving forces in the inclusion complexation of cyclodextrins. *J. Inclusion Phenom. Macrocycl. Chem.*, 2002, 42, 1-14.
- [7] Szente, L; Szejtli, J. Highly soluble cyclodextrin derivatives: chemistry, properties, and trends in development. *Adv. Drug Deliv. Rev.*, 1999, 36, 17-38.
- [8] Duchene, D. *New trends in cyclodextrins and derivatives*. Paris: Editions de Santé; 1991.
- [9] Hedges, AR. Industrial applications of cyclodextrins. *Chem. Rev.*, 1998, 98, 2035-2044.
- [10] Szejtli, J. Industrial applications of cyclodextrins. In: JL; Atwood, JED; Davies, DD; MacNicol, (Eds.), *Inclusion compounds*. London: Academic Press, 1984, 331-390.
- [11] Scriba, GKE. Selected fundamental aspects of chiral electromigration of chiral electromigration techniques and their application to pharmaceutical and biomedical analysis. *J. Pharm. Biomed. Anal.*, 2002, 27, 373-399.
- [12] Chankvetadze, B. *Capillary Electrophoresis in Chiral Analysis*. Chichester: Wiley; 1997.
- [13] Breslow, R; Dong, SD. Biomimetic reactions catalyzed by cyclodextrins and their derivatives. *Chem. Rev.*, 1998, 98, 1997-2012.
- [14] Uekama, K; Hirayama, F; Irie, T. Cyclodextrin drug carrier systems. *Chem. Rev.*, 1998, 98, 2045-2076.
- [15] Loftsson, T; Brewster, M. Pharmaceutical applications of cyclodextrins. 1. Drug solubilization and stabilization. *J. Pharm. Sci.*, 1996, 85, 1017-1025.
- [16] Loftsson, T. Cyclodextrins and the biopharmaceutics classification system of drugs. *J. Inclusion Phenom. Macrocycl. Chem.*, 2002, 44, 63-67.
- [17] Challa, R; Ahuja, A; Ali, J; Khar, RK. Cyclodextrins in drug delivery: an updated review. *AAPS PharmSciTech.*, 2005, 6, E329-E357.
- [18] Elvehjem, CA. *Am. Scientist*, 1944, 32, 25-30.
- [19] Staunton, E; Todd, WR; Mason, HS; Bruggen, JTV. *Textbook of Biochemistry*. New York: MacMillan Company; 1967.
- [20] Palafox, MA; Gil, M; Nunez, JL. Meta-aminobenzoic acid: structures and spectral characteristics. *Spectrosc. Lett.*, 1996, 29, 609-629.
- [21] Tomasella, FP; Zuting, P; Love, LJC. Determination of sun-screen agents in cosmetic products by micellar liquid chromatography. *J. Chromatogr.*, 1991, 587, 325-328.
- [22] Samsonowicz, M; Hrynaskiewicz, T; Świsłocka, R; Regulaska, E; Lewandowski, W. Experimental and theoretical IR, Raman, NMR spectra of 2-, 3- and 4-aminobenzoic acids. *J. Molec. Struct.*, 2005, 744-747, 345-352.
- [23] Terekhova, IV; Obukhova, NA. Study on inclusion complex formation of m-aminobenzoic acid with native and substituted β -cyclodextrins. *J. Solut. Chem.*, 2007, 36, 1167-1176.
- [24] Terekhova, IV; Kumeev, RS; Alper, GA. Inclusion complex formation of α - and β -cyclodextrins with aminobenzoic acids in aqueous solution studied by ^1H NMR. *J. Inclusion Phenom. Macrocycl. Chem.*, 2007, 59, 301-306.
- [25] Terekhova, IV. Volumetric and calorimetric study on complex formation of cyclodextrins with aminobenzoic acids. *Mend. Commun.*, 2009, 19, 110-112.

- [26] Zielenkiewicz, W; Terekhova, IV; Wszelaka-Rylik, M; Kumeev, RS. Thermodynamics of inclusion complex formation of hydroxypropylated α - and β -cyclodextrins with aminobenzoic acids in water. *J. Therm. Anal. Calorim.* submitted.
- [27] Zhang, Y; Yu, Sh; Bao, F. Crystal structure of cyclomaltoheptaose (β -cyclodextrin) complexes with p-aminobenzoic acid and o-aminobenzoic acid. *Carbohydr. Res.*, 2008, 343, 2504-2508.
- [28] Harata, K. Induced circular dichroism of cycloamylose complexes with meta- and para-disubstituted benzenes. *Bioorg. Chem.*, 1981, 10, 255-265.
- [29] Setniča, V; Urbanová, M; Král, V; Volka, K. Interactions of cyclodextrins with aromatic compounds studied by vibrational circular dichroism spectroscopy. *Spectrochim. Acta A*, 2002, 58, 2983-2989.
- [30] Shuang, S.-m; Yang, Y; Pan, J.-h. Study on molecular recognition of para-aminobenzoic acid species by α -, β - and hydroxypropyl- β -cyclodextrin. *Anal. Chim. Acta*, 2002, 458, 305-310.
- [31] Lewis, EA; Hansen, LD. Thermodynamics of binding of guest molecules to α - and β -cyclodextrins. *J. Chem. Soc. Perkin Trans. 2*, 1973, 2081-2085.
- [32] Stalin, T; Rajendiran, N. Intramolecular charge transfer effects on 3-aminobenzoic acid. *Chem. Phys.*, 2006, 322, 311-322.
- [33] Stalin, T; Shanthi, B; Vasantha Rani, P; Rajendiran, N. Solvatochromism, prototropism and complexation of para-aminobenzoic acid. *J. Incl. Phenom. Macrocycl. Chem.*, 2006, 55, 21-29.
- [34] Stalin, T; Rajendiran, N. Intramolecular charge transfer associated with hydrogen bonding effects on 2-aminobenzoic acid. *J. Photochem. Photobiol. A*, 2006, 182 137-150.
- [35] Klein, CT; Polheim, D; Viernstein, H; Wolschann, P. Predicting the free energies of complexation between cyclodextrins and guest molecules: linear versus nonlinear models. *Pharm. Res.*, 2000, 17, 358-365.
- [36] Gelb, RI; Schwartz, LM; Johnson, RF; Laufer, DA. The complexation chemistry of cyclohexaamyloses. 4. Reactions of cyclohexaamylose with formic, acetic, and benzoic acids and their conjugate bases. *J. Am. Chem. Soc.*, 1979, 101, 1869-1874.
- [37] Simova, S; Schneider, H-J. NMR analyses of cyclodextrin complexes with substituted benzoic acids and benzoate anions. *J. Chem. Soc. Perkin Trans. 2*, 2000, 1717-1722.
- [38] Inoue, Y; Hoshi, H; Sakurai, M; Chûjô, R. Geometry of cyclohexaamylose inclusion complexes with some substituted benzenes in aqueous solution based on carbon-13 NMR chemical shifts. *J. Am. Chem. Soc.* 1985, 107, 2319-2323.
- [39] He, Y; Wu, C; Kong, WJ. A theoretical and experimental study of water complexes of m-aminobenzoic acid MABA·(H₂O)_n (n=1 and 2). *J. Phys. Chem. A*, 2005, 109, 748-753.
- [40] Gopal, L; Jose, CI; Biswas, AB. *Spectrochim. Acta*, 1967, 23A, 513-518.
- [41] Job, P. *Ann. Chim.*, 1928, 9, 113-203.
- [42] Schneider, H-J; Hacket, F; Rüdiger V. NMR studies of cyclodextrins and cyclodextrin complexes. *Chem. Rev.*, 1998, 98, 1755-1785.
- [43] Rüdiger, V; Eliseev, A; Simova, S; Schneider, H-J; Blandamer, MJ; Cullis, PM; Meyer, AJ. Conformational, calorimetric and NMR spectroscopic studies on inclusion complexes of cyclodextrins with substituted phenyl and adamantane derivatives. *J. Chem. Soc. Perkin Trans., 2*, 1996, 2119-2123.

- [44] Young, TF; Smith, MB. Thermodynamic properties of mixtures of electrolytes in aqueous solutions. *J. Phys. Chem.*, 1954, 58, 716-724.
- [45] Christensen, JJ; Wrathall, DP; Izatt, RM; Tolman, DO. Thermodynamics of proton dissociation in dilute aqueous solutions. IX. pK , ΔH^0 , and ΔS^0 values for proton ionization from *o*-, *m*-, and *p*-aminobenzoic acids and their methyl esters at 25. *J. Phys. Chem.*, 1967, 71, 3001-3006.
- [46] Gelb, RI, Schwartz, LM, Bradshaw, JJ, Laufer, DA. Acid dissociation of cyclohexaamylose and cycloheptaamylose. *Bioorg. Chem.*, 1980, 9, 299-304.
- [47] Spildo, K; Høiland, H. Complex formation between alkane- α,ω -diols and cyclodextrins studied by partial molar volume and compressibility measurements. *J. Solut. Chem.*, 2002, 31, 149-164.
- [48] Hynčica, P; Hnědkovský, L; Cibulka, I. Partial molar volumes of organic solutes in water. VII. *o*- and *p*-Aminobenzoic acids at $T = 298$ K to 498 K and *o*-diaminobenzene at $T = 298$ K to 573 K and pressures up to 30 MPa. *J. Chem. Thermodyn.*, 2002, 34, 861-873.
- [49] Cohn, EJ; McMeekin, TL; Edsall, JT; Blanchard, MH. Studies in the physical chemistry of amino acids, peptides and related substances. I. The apparent molar volume and the electrostriction of the solvent. *J. Am. Chem. Soc.*, 1934, 56, 784-794.
- [50] Milioto, S; Bakshi, MS; Crisantino, R; De Lisi, R. Thermodynamic properties of water- β -cyclodextrin-dodecylsurfactant ternary systems. *J. Solut. Chem.*, 1995, 24, 103-120.
- [51] Wilson, LD; Verrall, RE. A volumetric study of β -cyclodextrin/hydrocarbon and β -cyclodextrin/fluorocarbon surfactant inclusion complexes in aqueous solution. *J. Phys. Chem. B*, 1997, 101, 9270-9277.
- [52] Wilson, LD; Verrall, RE. A volumetric study of cyclodextrin- α,ω -alkyl dicarboxylate anion complexes in aqueous solutions. *J. Phys. Chem. B*, 2000, 104, 1880-1886.
- [53] Manor, PC; Saenger, W. Topography of cyclodextrin inclusion complexes. III Crystal and molecular structure of cyclohexaamylose hexahydrate, the water dimmer inclusion complex. *J. Am. Chem. Soc.*, 1974, 96, 3630-3639.
- [54] Friedman, HL; Krishnan, CV. Water, *A Comprehensive Treatise*. New York: Plenum; 1973.
- [55] Hoshino, M; Imamura, M; Ikehara, K; Hama, Y. Fluorescence enhancement of benzene derivatives by forming inclusion complexes with β -cyclodextrin in aqueous solutions. *J. Phys. Chem.*, 1981, 85, 1820-1823.
- [56] Manunza, B; Deiana, S; Pintore, M; Gessa, C. A molecular dynamics study of the inclusion of mono- and disubstituted benzenes with β -cyclodextrin. *J. Mol. Graphics Mod.*, 1997, 15, 79-81.
- [57] Kamiya, M; Mitsuhashi, S; Makino, M; Yoshioka, H. Analysis of the induced rotational strength of mono- and disubstituted benzenes included in β -cyclodextrin. *J. Phys. Chem.*, 1992, 96, 95-99.
- [58] Bergeron, R; Channing, MA; McGovern, KA. Dependence of cycloamylose-substrate binding on charge. *J. Am. Chem. Soc.*, 1978, 100, 2878-2883.
- [59] Salvatierra, D; Jaime, C; Virgili, A; Sánchez-Ferrando, F. Determination of the inclusion geometry of the β -cyclodextrin/benzoic acid complex by NMR and molecular modeling. *J. Org. Chem.*, 1996, 61, 9578-9581.

-
- [60] Hirose, K. A practical guide for the determination of binding constants. *J. Inclusion Phenom. Macrocycl. Chem.*, 2001, 39, 193-209.
- [61] Lindner, K; Saenger, W. β -Cyclodextrin-dodecahydrat: haufung von wassermolekullen in einer hydrophoben hohlraum. *Angew. Chem.*, 1978, 90, 738-740.
- [62] Marini, A; Berbenni, V; Bruni, G; Massarotti, V; Mustarelli, P. Dehydration of the cyclodextrins: a model system for the interaction of biomolecules with water. *J. Chem. Phys.*, 1995, 103, 7532-7540.
- [63] Fukahori, T; Kondo, M; Nishikawa, S. Dynamic study of interaction between β -cyclodextrin and aspirin by the ultrasonic relaxation method. *J. Phys. Chem. B*, 2006, 110, 4487-4491.
- [64] Manabe, M; Ochi, T; Kawamura, H; Katsu-ura, H; Shiomi, M; Bakshi, MS. Volumetric study on the inclusion complex formation of α - and β -cyclodextrin with 1-alkanols at different temperatures. *Colloid. Polym. Sci.*, 2005, 283, (738-746).
- [65] González-Gaitano, G; Crespo, A; Compostizo, A; Tardajos, G. Study at a molecular level of the transfer process of a cationic surfactant from water to β -cyclodextrin. *J. Phys. Chem. B*, 1997, 101, 4413-4421.
- [66] Kondo, M; Nishikawa, S. Inclusion kinetics of a nucleotide into a cyclodextrin cavity by means of ultrasonic relaxation. *J. Phys. Chem. B*, 2007, 111, 13451-13454.

Chapter 9

**THERMODYNAMICS OF CESIUM
COMPLEXES FORMATION WITH 18-CROWN-6 IN
HYDROPHOBIC IONIC LIQUIDS. A CORRELATION
WITH EXTRACTION CAPABILITY**

*A. G. Vendilo^a, D. I. Djigailo^b, H. Rönkkömäki^c,
M. Lajunen^d, E. A. Chernikova^e, L. H. J. Lajunen^d,
I. V. Pletnev^b and K.I. Popov^{d,f,*}*

^aState Research Institute of Reagents and High Purity Substances (IREA),
Bogorodskii val 3, 107258 Moscow, Russia.

^bDepartment of Chemistry, M.V. Lomonosov State University, 1/3 Leninskiye gory,
119992, Moscow, Russia.

^cFinnish Institute of Occupational Health, Aapistie 1, FI-90220 Oulu, Finland.

^dUniversity of Oulu, Department of Chemistry, P.O. Box 3000, FI-90014,
University of Oulu, Finland.

^eZelinsky Institute of Organic Chemistry RAS, Moscow, 119991, Leninsky pr. 47,
Russia.

^fDepartment of Physical and Colloid Chemistry, Moscow State University of Food
Technologies, Volokolamskoye Sh.11, 125080, Moscow, Russia.

ABSTRACT

Thermodynamic data for cesium complexes formation with 18-crown-6 (18C6, L) $[\text{Cs}(18\text{C}6)]^+$ and $[\text{Cs}(18\text{C}6)_2]^+$ in hydrophobic room temperature ionic liquids (RTIL): trioctylmethylammonium salicylate ([TOMA][Sal]), tetrahexylammonium dihexylsulfosuccinate ([THA][DHSS]), 1-butyl-3-methylimidazolium hexafluorophosphate ([BMIM][PF₆]), 1-butyl-3-methylimidazolium bis(trifluoromethyl)sulphonylimide ([BMIM][N(Tf)₂]), 1-hexyl-3-methylimidazolium bis(trifluoromethyl)sulphonylimide ([HMIM]

* Corresponding author: E-mail: ki-popov@mtu-net.ru

[N(Tf)₂] and 1-(2-ethylhexyl)-3-methylimidazolium bis[trifluoromethylsulphonyl]imide ([EtHMIM][N(Tf)₂]) were measured with NMR ¹³³Cs technique at 27 to 50 °C. Only [Cs(18C6)]⁺ complexes are found for [TOMA][Sal], [THA][DHSS], [BMIM][PF₆], while in ([BMIM][N(Tf)₂] and ([HMIM][N(Tf)₂]) both [Cs(18C6)]⁺ and [Cs(18C6)₂]⁺ are formed. The stability of cesium complex in RTILs is estimated to be in the range between water and acetonitrile. Stability constants for [Cs(18C6)]⁺ revealed much weaker dependence on temperature than those, measured in hydrophilic RTIL. The following values for log*K*(Cs+L) and Δ*H*(Cs+L) at 25 °C are determined: 1.43 (0.05), 3.85 (0.25) kJ/mol ([TOMA][Sal]); 0.76 (0.06), 2.1 (0.3) kJ/mol ([THA][DHSS]); 2.4 (0.2), -21.0 (1.4) kJ/mol ([BMIM][PF₆]); 3.4 (0.5), -6.8 (1.9) kJ/mol ([BMIM][N(Tf)₂]); 4.4 (0.1), -9.5 (0.4) kJ/mol ([HMIM][N(Tf)₂]), and 3.4 (0.4), 9 (18) kJ/mol ([EtHMIM][N(Tf)₂]). Besides, for ([HMIM][N(Tf)₂]) and ([EtHMIM][N(Tf)₂]) log*K*(CsL+L) and Δ*H*(CsL+L) at 25 °C are also found: 1.13 (0.07), -17.8 (0.3) kJ/mol ([HMIM][NTf₂]) and 1.16 (0.08); -17.5 (0.3) kJ/mol ([EtHMIM][NTf₂]).

It is demonstrated that unlike hydrophilic RTIL the entropy change with an exception of [BMIM][PF₆], promotes complex formation while the corresponding enthalpy change is either positive or gives rather small contribution to the complex stability. The stability constants correlate well with crown ether assisted extraction degree of cesium from water into RTIL indicating an importance of complex stability for the extraction process.

Keywords: RTIL, stability constants, complexes, cesium, 18-crown-6, ¹³³Cs NMR, extraction

1. INTRODUCTION

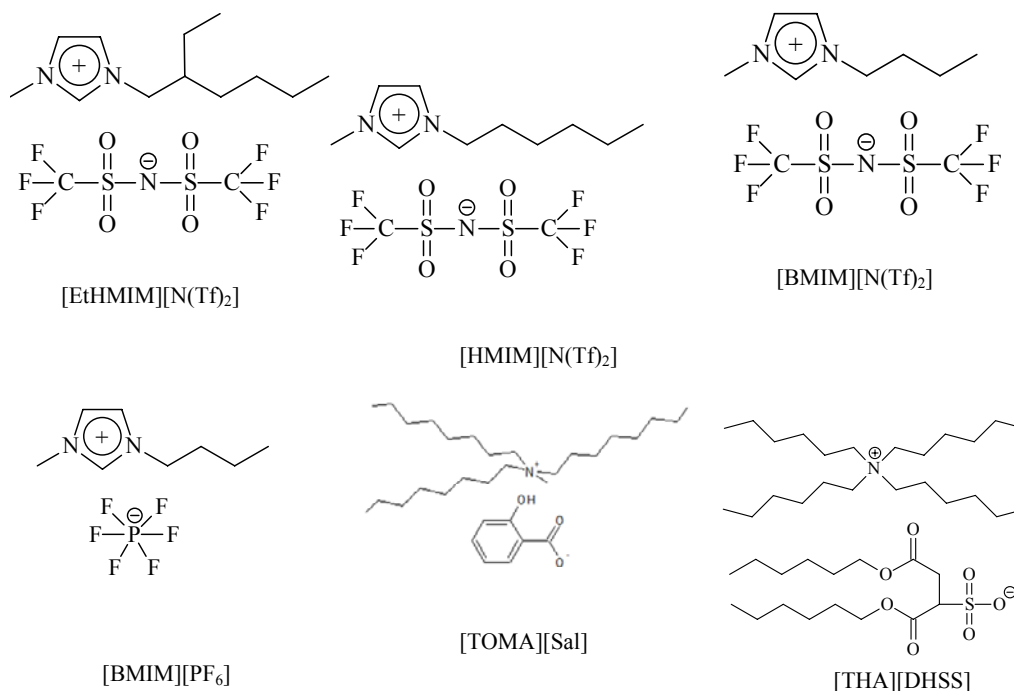
Since 1967 crown ethers are intensively studied and successfully applied for metal ion extraction in water/molecular liquid separations. It was demonstrated that cation-selective nature of crown ethers facilitates their implementation in the removal of Cs⁺ and Sr²⁺ from liquid nuclear wastes. The development of a new class of hydrophobic solvents – room-temperature ionic liquids (RTILs) gave a new impulse to the crown ether enhanced separations [1,2].

RTILs are attracting increasing attention in solvent extraction processes due to such important advantages over conventional organic diluents as negligible vapor pressure, low flammability, moisture stability, unusual extraction regularities and possibility to eliminate aqueous phase acidification [1-6]. It is demonstrated that extraction efficacy of RTIL can be modulated by chelating agent administration. Dai *et al.* [3], for example, first discovered that highly efficient extraction of strontium ions can be achieved when dicyclohexane-18-crown-6 is combined with RTILs. Rogers *et al.* [2], and Bartsch *et al.* [6], reported the extraction of various alkali metal ions with crown ethers in RTILs. Visser and Roberts demonstrated that octyl(phenyl)-*N,N*-diisobutylcarbamoylmethylphosphine oxide dissolved in RTILs enhances the extractability of lanthanides and actinides in comparison to conventional organic solvents [7]. The extraction of silver ions was found to be greatly enhanced by a combined application of RTIL and calyx[4]arene compared to that of chloroform [8]. In addition the task-specific RTILs with coordination capacity built in the RTIL cation have been reported [9,10]. Recently the efficiency of chelate extraction of 3d-cations with 8-sulfonamidoquinoline [11], Pu(IV) with carbamoylmethylphosphine oxide [12] and uranyl ion with tributylphosphate (TBP) [13] from aqueous phase into RTIL is reported. The higher selectivity of dibenzo-18-

crown-6 to K^+ over Na^+ in *N*-octadecylisoquinolinium tetrakis[3,5-bis(trifluoromethyl)phenyl]borate compared with that in molecular solvents suggests that RTIL provides a unique solvation environment for the complexation of crown ethers with the ions [14].

Besides the issues of cation, ligand and complex solubility in water and in RTIL, the relative stabilities of complex formation in both phases are of significant importance for extraction selectivity. Unfortunately, almost nothing is known about the numerical values of complex formation constants in RTILs. Some publications report a significant increase of complex stability in a series of RTILs relative to DMSO [15] and to water [14,16,17]. The data on the thermodynamic functions for cesium have been published in the recent years only for hydrophilic RTIL [17].

Present work aims to diminish this gap by studying the complex formation of cesium ions by 18-crown-6 (L, 18C6) in six hydrophobic RTILs: trioctylmethylammonium salicylate ([TOMA][Sal]), tetrahexylammonium dihexylsulfosuccinate ([THA][DHSS]), 1-butyl-3-methylimidazolium hexafluorophosphate ([BMIM][PF₆]), 1-butyl-3-methylimidazolium bis(trifluoromethyl)sulphonylimide ([BMIM][N(Tf)₂]), 1-hexyl-3-methylimidazolium bis(trifluoromethyl)sulphonylimide ([HMIM][N(Tf)₂] and 1-(2-ethylhexyl)-3-methylimidazolium bis(trifluoromethyl)sulphonylimide ([EtHMIM][N(Tf)₂] by ¹³³Cs NMR technique with an emphasis on thermodynamic data and relevance to extraction process, studied in a parallel way [18].



Scheme 1. Structures of RTILs.

EXPERIMENTAL

2.1. Reagents

Cesium nitrate (Merck, reagent purity) was dried at 110 °C for one day before use, 18-crown-6 (Fluka) was dried at 35 °C and used without further purification.

Trioctylmethylammonium salicylate. Aliquat[®] 336 (Aldrich; 2:1 mol/mol mixture of methyltriethyl- and methyltridecylammonium chloride) was mixed with 30% excess of sodium salicylate in 200 mL of chloroform. The mixture was shaken for 4 hr and then was 20 times rinsed with a large amount of distilled water. Then the solvent was evaporated and the liquid residue was heated up to 100 °C under reduced pressure for 5 hr. After cooling to room temperature a white solid matter was obtained with a density 0.943 g·cm⁻³; $T_{\text{melt}}=32.8\pm 0.4$ °C, $T_f=14\pm 2$ °C. Yield: 90%. The NMR spectra indicated: ¹H NMR (500 MHz, Bruker DRX500, solvent CDCl₃, TMS) 0.88 (9 H), 1.24 (30 H), 1.59 (6 H), 3.19 (3 H), 3.27 (6 H), 7.20 (1 H), 7.92 ppm (1 H); ¹³C NMR (126 MHz, solvent DMSO-D₆, TMS) 13.80 (C*CH₃), 21.93 (C*H₂CH₃), 21.25, 25.68, 28.27, 28.32, 31.04 (various CH₂CH₂ fragments); 47.41 (CH₃N); 60.50 (CH₂N); 115.35, 115.62, 120.73, 129.73, 130.88 (aromatic C); 163.17 (COH); 171.00 ppm (COO). Analyses, found: C, 76.06; H, 11.64; N: 2.62; calc.: C, 76.49; H, 11.89; N: 2.62.

After equilibration with water at ambient temperature the solid product transforms into a slightly yellowish viscous liquid with 0.942 g·cm⁻³ density and a freezing point below -18 °C. Water content measured by Karl Fisher titration constituted 0.18% wt (0.09 mol·dm⁻³) for a solid product and 4.83% wt (2.52 mol·dm⁻³) for RTIL samples equilibrated with water.

Tetrahexylammonium dihexylsulfosuccinate was synthesized according to [19] as a transparent viscous liquid (yield: 85%), analysed by NMR, and then used without further purification. The NMR spectra revealed: ¹H NMR (500 MHz, solvent CDCl₃, TMS) 0.88 (18 H), 1.33 (36 H), 1.55 (12 H), 3.2 (12 H), 4.1 (3 H) ppm; ¹³C NMR (126 MHz, solvent DMSO-D₆, TMS) 13.64, 13.69, 13.71 (CH₃); 20.91, 21.76 (C*H₂CH₃), 21.87, 24.82, 24.85, 25.34, 27.95, 27.99, 30.47, 30.75, 30.82 (CH₂CH₂ fragments); 34.01 (OOC*CH₂CH-); 57.63 (CH₂N); 63.89 (CH₂O); 168.31, 170.97 COOR). **Analyses**, found: C, 66.67; H, 11.31; N: 1.97, S: 4.49; calc.: C, 66.71; H, 11.34; N: 1.94, S: 4.45. An absence of halogen-ions was proved by AgNO₃ test.

1-butyl-3-methylimidazolium hexafluorophosphate. A 1000-mL, one-necked, round-bottomed flask was equipped with a magnetic stirrer and charged with 367.2 g (2.10 mol, 1 equiv.) of 1-butyl-3-methylimidazolium chloride, and 387.3 g (2.10 mol, 1 equiv.) of potassium hexafluorophosphate in 700 mL of distilled water. The reaction mixture stirring at room temperature for 2 hr led finally to the two-phase system. The organic phase was separated and washed with water (5 times by 40 mL) until the aqueous fraction observed to be free of chloride (AgNO₃). Then 400 mL of dichloromethane was added. The dichloromethane solution was mixed with activated charcoal, stirred for 2 hr, filtered and dried over anhydrous magnesium sulfate. After 1 hr, the suspension was filtered and the volatile material was removed by rotary evaporation. The resulting colourless or light-yellow viscous liquid was dried under reduced pressure (0.5 mm Hg) at 70 °C for 12 hr. Yield 462 g (77.3 %). ¹H NMR

(300 MHz, DMSO_{D6}): 0.91 (3H, t, NHCH₂CH₂CH₂CH₃), 1.27 (2H, m, NCH₂CH₂CH₂CH₃), 1.77 (2H, p, NCH₂CH₂CH₂CH₃), 3.85 (3H, s, NCH₃), 4.16 (2H, t, NCH₂CH₂CH₂CH₃), 7.72 (2H, m, C(5)H, C(4)H), 9.09 (1H, s, C(2)H). **Analyses**, found: C, 33.97; H, 5.37; N, 9.95; F, 39.91; P, 10.78; calc.: C, 33.81; H, 5.32; N, 9.86; F, 40.11; P, 10.90.

1-butyl-3-methylimidazolium bis(trifluoromethyl)sulphonylimide. A 500-mL, one-necked, round-bottomed flask was equipped with a magnetic stirrer and charged with 143.693 g (0.5 mol, 1 equiv.) of lithium bis(trifluoromethylsulfonyl)imide, and 87.25 g (0.5 mol, 1 equiv) of 1-butyl-3-methylimidazolium chloride dissolved in 80 mL of distilled water. The reaction mixture was stirred at room temperature for 2 hr forming a two-phase system. Then 200 mL of dichloromethane was added. The lower organic layer was separated and washed with water (5 times by 20 mL) until the aqueous fraction observed to be free of chloride (AgNO₃). The dichloromethane solution was mixed with activated charcoal, stirred for 2 hr, filtered and dried over anhydrous magnesium sulfate. After 1 hr, the suspension was filtered and the volatile material was removed by rotary evaporation. The resulting colourless viscous liquid was dried under reduced pressure (0.5 mm Hg) at 70 °C for 12 hr. Yield 162.6 g (77.5 %). ¹H NMR (250 MHz, DMSO_{d6}): 0.89 (3H, t, NHCH₂CH₂CH₂CH₃), 1.25 (2H, m, NCH₂CH₂CH₂CH₃), 1.76 (2H, p, NCH₂CH₂CH₂CH₃), 3.84 (3H, s, NCH₃), 4.15 (2H, t, NCH₂CH₂CH₂CH₃), 7.72 (2H, m, C(5)H, C(4)H), 9.09 (1H, s, C(2)H). **Analyses**, found: C, 28.67; H, 3.63; N, 9.94; F, 27.30; S, 15.23; O, 15.23; calc.: C, 28.64; H, 3.61; N, 10.02; F, 27.18; S, 15.29; O, 15.26.

1-hexyl-3-methylimidazolium bis(trifluoromethyl)sulphonylimide was provided by Solvent Innovation, puriss. 99%, CAS number 382150-50-7.

1-(2-ethylhexyl)-3-methylimidazolium bis(trifluoromethyl)sulphonylimide, synthesized similarly as described in [20], was kindly presented by Dr. V.E. Baulin from A.N. Frumkin Institute of Physical Chemistry and Electrochemistry of RAS: ¹H NMR (200 MHz, CDCl₃, δ) 0.85 (m, 6H, 2CH₂CH₃), 1.25 (m, 8H, 4CH₂), 1.75 (m, 1H, CH₂CHCH₂), 3.92 (s, 3H, CH₃N), 4.00 (d, J=7.0 Hz, 2H, CH₂N), 7.25(s, 1H_{arom}), 7.36 (s, 1H_{arom}), 8.65 (s, 1H_{arom}). **Analyses**, found: C, 35.40; H, 4.85; F, 24.00; N: 8.81; S: 13.52; calc.: C, 35.36; H, 4.88; F, 23.97; N: 8.84, S: 13.49.

2.2. Sample Preparation

The exact mass of solid cesium nitrate was mixed with the calculated mass of solid 18C6, and then 1 mL of RTIL was added. Within each series of 9 to 11 samples, the concentration of cesium was kept constant at a level of 0.005 mol·dm⁻³, whereas the concentration of the ligand varied as the ligand-to-metal mole ratio changed steadily from 0 to 10 or to 20. The dissolution process was performed within 3 to 5 minutes at 110 °C because a sufficient reduction of solvent viscosity was found to occur in this time. The establishment of equilibrium controlled by periodic NMR measurement of some selected samples took 1 to 2 hr. Generally, all samples measured were allowed to equilibrate in closed glass tubes at room temperature for 24 hr before NMR measurement. The pH measurements of the samples

indicated neutral solutions for all RTIL. Control was maintained with METLER Toledo 320 pH meter, calibrated by standard buffer solutions (Oy FF-Chemicals).

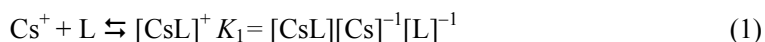
None of the RTILs used in a present study have been specially dried, as far as all of them after stability constants measurements have been used for cesium extraction from an aqueous phase. The water content in each sample was controlled with Karl Fisher method and with ^1H NMR by a comparison of water and RTIL NMR bands integral intensities.

2.3. NMR Measurements

^{133}Cs NMR was recorded with Bruker AVANCE II 300 spectrometer, operating at 39.38 MHz, in a 5 mm diameter sample tube with temperature steadily adjusted to several values between 27 and 50 $^\circ\text{C}$. After each temperature change, the sample was kept in the probehead for 10 minutes before initiating the measurement. The external standard placed in a 1 mm coaxial inner tube represented a 1:1 vol/vol mixture of aqueous solution of NaCl and CsCl with D_2O (added for lock), which provided a $0.04 \text{ mol}\cdot\text{dm}^{-3}$ concentration of each cation. Downfield shifts are denoted as positive.

2.4. NMR Data treatment, complex formation constants evaluation

Generally, the complex formation equilibrium can be described by simple reactions:



For [TOMA][Sal], [THA][DHSS], [BMIM][PF₆], only CsL have been found at any Cs/L molar ratios. An experimentally observed δ_{obs} single time-averaged ^{133}Cs chemical shift of “free” cation and a ligand-bonded cation can be given by an equation (2) [16]:

$$\delta_{\text{obs}} = (\delta_{\text{Cs}} + K_1[\text{L}]\delta_{\text{CsL}})/(1 + K_1[\text{L}]) \quad (2)$$

where

$$[\text{L}] = C_{\text{L}} - C_{\text{Cs}}X_{\text{CsL}} \quad (3)$$

$$X_{\text{CsL}} = (\delta_{\text{obs}} - \delta_{\text{Cs}})/(\delta_{\text{CsL}} - \delta_{\text{Cs}}) \quad (4)$$

C_{L} is a total concentration of the ligand, $[\text{L}]$ is a free concentration of the ligand, C_{Cs} is total concentration of Cs and X_{CsL} is a mole fraction of CsL; δ_{Cs} represents chemical shift of a free cation and δ_{CsL} corresponds to the crown ether coordinated species CsL.

The free ligand concentration $[L]$ was obtained by an iteration method using equations (2), (3) and (4). The stability constant K_1 was calculated by the non-linear curve-fitting program SigmaPlot [21] operating with 9 to 11 experimental points for a curve. All iterations have been performed without fixation of either δ_{CsL} or δ_{Cs} values, treating them equally as any of δ_{obs} experimental points. Thus, calculated and experimental δ_{Cs} values have been obtained, providing additional fitting degree estimate, Tables 1,2.

For $[BMIM][N(Tf)_2]$, $[HMIM][N(Tf)_2]$ and $[EtHMIM][N(Tf)_2]$ both CsL and CsL_2 complexes are formed. Thus, the two-step formation scheme was treated by both HypNMR software [22] and SigmaPlot [21]. The standard deviation for the measured $\log K_1$ values meets the requirements for crown ether complexes with alkali cations [23], except those measured in $[BMIM][N(Tf)_2]$, $[HMIM][N(Tf)_2]$ and $[EtHMIM][N(Tf)_2]$ where it was higher due to superposition of CsL and CsL_2 species. For $\log K_2$ an interval of $[Cs]/[L]$ ratios was much broader than for $\log K_1$ and the accuracy of measurement was therefore sufficiently higher.

The typical titration curves are presented at Figure 1. Values of calculated $\ln K_1$ and $\ln K_2$ were then plotted versus $1/T$. A linear relationship was obtained in all cases, indicating the constancy of ΔH_1 and ΔH_2 within the temperature range 27 to 50 °C, Figure 2. Then the values ΔH_n , ΔG_n , $T\Delta S_n$ ($n=1,2$) were calculated, using reaction isobar equation and an Aqua Solution Software [24]. The experimental results are presented in Tables 1,2,3,4. The values of $\log K_n$, ΔG_n and δ_{calc} for 25 °C are obtained by data extrapolation.

In Tables 3 and 4 the experimental data are given along with those obtained previously for hydrophilic RTILs: N-butyl-4-methyl-pyridinium tetrafluoroborate ($[BMPy][BF_4]$), 1-butyl-3-methylimidazolium tetrafluoroborate ($[BMIM][BF_4]$), 1-butyl-3-methylimidazolium dicyanamide ($[BMIM][N(CN)_2]$) and N-butylpyridinium methylsulphate ($[BPy][MeSO_4]$) and molecular solvents.

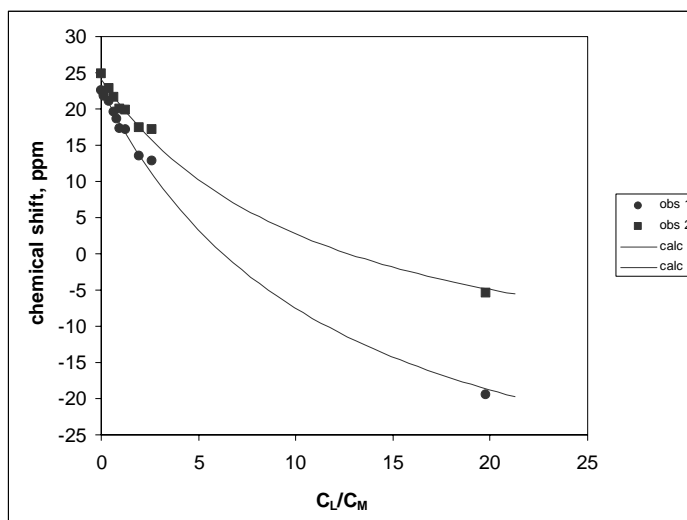


Figure 1. Variation of ^{133}Cs NMR chemical shift versus ligand-to-cesium mole ratio (C_L/C_M) in $[THA][DHSS]$ at 27 °C (1); and 50 °C (2). Solid line represents the least square fit using Eq. (2).

Table 1. Stability Constants, Chemical Shifts and Thermodynamic Quantities ΔG_1 , ΔH_1 , ΔS_1 of $[\text{Cs}(\text{18C6})]^+$ Complex Formation at 27 to 50 °C.

T, °C	$\delta_{\text{Cs calc}}$, Ppm	$\delta_{\text{Cs obs}}$, ppm	$\delta_{\text{CsL calc}}$, ppm	log K ₁	ΔG_1 , kJ/mol	ΔH_1 , kJ/mol	ΔS_1 , J/(mol·K)	T ΔS_1 , kJ/mol
[HMIM][NTf ₂]								
27	-30.6±6	-31.24	-4.4±0.9	4.40±0.53	-25.3±2.9	-9.5±0.4	53±15	15.8±2.9
35	-30.3±0.7	-31.20	-4.0±0.9	4.36±0.54	-25.1±2.9	-9.5±0.4	51±15	15.6±2.9
43	-30.3±0.7	-31.18	-3.8±0.9	4.33±0.49	-24.9±2.9	-9.5±0.4	49±15	15.4±2.9
50	-30.1±0.6	-30.89	-3.7±0.9	4.28±0.44	-24.6±2.9	-9.5±0.4	47±15	15.1±2.9
[BMIM][NTf ₂]								
27	-29.6 ±0.5	-39.31	-5±4	3.37±0.85	-19.3±1.9	-6.8±1.9	41.6±6.1	12.5±1.9
35	-29.6 ±0.5	-29.31	-4±5	3.33±0.90	-19.1±1.9	-6.8±1.9	39.9±6.1	12.3±1.9
43	-29.6±0.4	-29.27	-3±5	3.25±0.79	-18.6±2.0	-6.8±1.9	37.3±6.1	11.8±2.0
50	-29.5±0.5	-29.23	-3±5	3.31±0.86	-19.0±2.0	-6.8±1.9	37.8±6.1	12.2±2.0
[EtHMIM][NTf ₂]								
27	-30.5 ±0.1	-30.55	-3.7±0.1	3.46±0.10	-19.9±1.9	9±18	96±59	28.9±1.9
43	-30.4 ±0.1	-30.55	-3.2±0.1	3.20±0.25	-18.4±1.9	9±18	87±54	27.4±1.9
50	-30.4 ±0.1	-30.55	-3.0±0.1	4.15±0.40	-23.9±1.9	9±18	74±50	32.9±1.9
[BMIM][PF ₆]								
27	-90.5±1.5	-90.04	-6±14	2.34±0.22	-13.4±1.4	-21.0±1.4	-25.3±4.5	-7.6±1.3
32	-89.9±1.5	-89.61	1±16	2.24±0.22	-13.2±1.4	-21.0±1.4	-25.6±4.5	-7.8±1.3
37	-89.7±1.4	-89.51	3±16	2.20±0.21	-13.1±1.4	-21.0±1.4	-25.5±4.5	-7.9±1.3
42	-89.5±1.4	-89.35	5±17	2.16±0.21	-13.0±1.4	-21.0±1.4	-24.8±4.5	-8.0±1.4
[TOMA][Sal]								
35	31.8±0.7	32.97	-24.3±1.9	1.45±0.07	-8.5±0.2	3.9±0.2	40.3±0.7	12.4±0.2
43	32.5±0.8	33.79	-18.6±2.0	1.47±0.06	-8.8±0.2	3.9±0.2	40.2±0.7	12.7±0.2
50	33.2±0.8	34.48	-14.6±2.0	1.48±0.07	-9.1±0.3	3.9±0.2	40.2±0.7	13.0±0.3
[THA][DHSS]								
27	22.9 ±0.3	22.53	-43±2	0.77±0.04	-4.4±0.3	2.1±0.3	21.7±1.1	6.5±0.3
35	23.4 ±0.2	23.38	-33±2	0.77±0.04	-4.6±0.3	2.1±0.3	21.7±1.1	6.7±0.3
43	23.8±0.2	23.85	-26±2	0.79±0.04	-4.7±0.4	2.1±0.3	21.5±1.1	6.8±0.4
50	24.1±0.4	24.89	-21±3	0.79±0.08	-4.9±0.4	2.1±0.3	21.7±1.1	7.0±0.4

3. RESULTS AND DISCUSSION

Within the temperature range 27 to 50 °C all the ¹³³Cs resonances reveal a single time averaged signal for all solutions studied indicating the fast exchange of “free” and coordinated metal species even for highly viscous solutions. At the same time ¹³³Cs chemical shifts demonstrate different features depending on particular RTIL. At 25 °C the δ_{Cs} values are observed to be negative and rather close to each other within – 30 ppm for RTIL [BMIM][N(Tf)₂], [HMIM][N(Tf)₂] and [EtHMIM][N(Tf)₂], whereas those for [TOMA][Sal] and [THA][DHSS] are found to be positive (20 to 30 ppm). Chemical shift in [BMIM][PF₆] reveals the highest known negative value – 90 ppm, Table 3.

Table 2. Stability Constants, Chemical Shifts and Thermodynamic Quantities ΔG_1 , ΔH_1 , ΔS_1 of $[\text{Cs}(18\text{C}6)_2]^+$ Complex Formation in RTIL at 27 to 50 °C.

T, °C	δ_{CsLcalc} , ppm	$\delta_{\text{CsL}_2\text{calc}}$, ppm	$\log K_2$	ΔG_2 , kJ/mol	ΔH_2 , kJ/mol	ΔS_2 , J/(mol·K)	T ΔS_2 , kJ/mol
[HMIM][NTf₂]							
27	-4.5±0.2	-49±2	1.11±0.05	-6.4±0.6	-17.8±0.3	-38.0±0.9	-11.4±0.3
35	-4.1±0.2	-47±2	1.02±0.05	-6.0±0.6	-17.8±0.3	-35.7±0.9	-11.0±0.3
43	-4.0±0.2	-45±3	0.95±0.06	-5.8±0.6	-17.8±0.3	-34.2±0.9	-10.8±0.3
50	-3.9±0.2	-42±4	0.89±0.08	-5.5±0.6	-17.8±0.3	-32.5±0.9	-10.5±0.3
[EtHMIM][NTf₂]							
27	-3.6±0.5	-50±3	1.14±0.06	-6.6±0.2	-17.5±0.3	-36.3±1.0	-10.9±0.2
35	-3.5±0.5	-49±3	1.05±0.07	-6.2±0.2	-17.5±0.3	-34.1±1.0	-10.5±0.2
43	-3.2±0.5	-47±4	0.99±0.08	-6.0±0.2	-17.5±0.3	-32.6±1.0	-10.3±0.2
50	-3.0±0.4	-46±4	0.92±0.08	-5.7±0.2	-17.5±0.3	-31.0±1.0	-10.0±0.2
[BMIM][NTf₂] [26]^a							
25	-6.5±0.7	-47±1	1.29±0.07	-7.4±0.7	-41.3±0.7	-114±1	-33.9±0.2

^a The $\log K_2$, ΔG_2 , ΔH_2 , and ΔS_2 values from [26] are refined in a present work.

Thus, ¹³³Cs NMR chemical shifts of Cs⁺ cation in RTILs span a very broad range from – 90 ppm ([BMIM][PF₆]) to 90 ppm ([BMIM][N(CN)₂]) clearly indicating their dependence on the RTIL's anion nature, but not the cations one. Indeed, for all three [N(Tf)₂] based RTIL the chemical shifts of Cs⁺ are the same within the experimental error. At the same time the highly negative shift for [BMIM][PF₆] is rather close to those observed for [BMPy][BF₄] and [BMIM][BF₄] (~ – 70 ppm).

An increase of crown ether concentration in RTIL up to 1:1 cation/ligand molar ratio resulted in the corresponding monotonous increase of δ_{obs} for [BMIM][N(Tf)₂], [HMIM][N(Tf)₂], [EtHMIM][N(Tf)₂] and at a higher ligand excess for [BMIM][PF₆] up to ~ – 5 ppm, which corresponded to [Cs18C6]⁺ species.

By contrast, the chemical shifts of ¹³³Cs decreased as 18C6 was added to the [TOMA][Sal] and [THA][DHSS] solution. Thus, complex formation diminishes the differences in Cs⁺ environment and makes chemical shifts δ_{CsL} more close to each other for all RTIL, relative to δ_{Cs} . This observation is consistent with the fact that in all solvents 18C6 occupies the major part of cesium coordination sphere in more or less similar way. However, the resonances of ¹³³Cs in [CsL]⁺ still remain different in values and signs indicating different solvation and/or different ligand conformation of a complex, Table 3.

For [BMIM][N(Tf)₂], [HMIM][N(Tf)₂], [EtHMIM][N(Tf)₂] an excess of 18C6 over [Cs][L] 1:1 molar ratio leads to decrease of a chemical shift indicating the CsL₂ complex formation. The upfield shift followed by a sharp break and a downfield shift which gradually approaches an almost the same limiting value for all three N(Tf)₂-based RTIL's can be explained by the formation of a strong CsL complex followed by addition of a second molecule of a ligand to form a “sandwich” CsL₂ complex. A similar break was also found for such molecular solvents as propylene carbonate, acetonitrile, and DMFA [25].

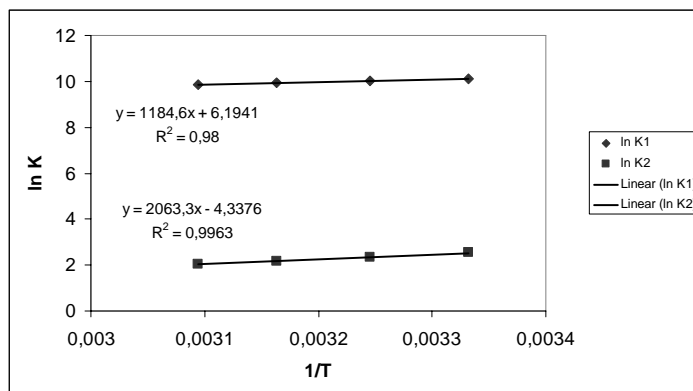


Figure 2. The dependence of $\ln K_1$ and $\ln K_2$ versus $1/T$ for cesium complexes in $[\text{HMIM}][\text{NTf}_2]$.

In $[\text{TOMA}][\text{Sal}]$, $[\text{THA}][\text{DHSS}]$, $[\text{BMIM}][\text{PF}_6]$, as well as in hydrophilic $[\text{BPy}][\text{MeSO}_4]$, $[\text{BMIM}][\text{N}(\text{CN})_2]$, $[\text{BMIM}][\text{BF}_4]$ and $[\text{BMPy}][\text{BF}_4]$ the change of chemical shift was monotonic within the whole range of $[\text{L}]/[\text{Cs}]$ ratios studied, indicating the existence of only a single CsL complex, and the absence of CsL_2 species, Figure 1. Otherwise either the change in chemical shift direction for an opposite one at 1:1 metal-to-ligand mole ratio is observed in molecular solvents [25,26] and in $[\text{BMIM}][\text{N}(\text{Tf})_2]$, $[\text{HMIM}][\text{N}(\text{Tf})_2]$, $[\text{EtHMIM}][\text{N}(\text{Tf})_2]$, or the monotonic change of a chemical shift within the ligand-to-metal mole ratio variation does not fit the CsL scheme. Although such a brakeless change itself does not guaranty the lack of CsL_2 species formation [25], in our case the calculations fit only CsL scheme. Our attempts to treat the experimental NMR data for $[\text{TOMA}][\text{Sal}]$, $[\text{THA}][\text{DHSS}]$, $[\text{BMIM}][\text{PF}_6]$ as a superposition of CsL and CsL_2 by HypNMR have failed. This is also an argument in favor of only one type of complex formation: CsL . Thus, complexes CsL_2 if any, are very weak in these systems. Our observations make $[\text{TOMA}][\text{Sal}]$, $[\text{THA}][\text{DHSS}]$, $[\text{BMIM}][\text{PF}_6]$ similar to such solvent as water, where also no any formation of CsL_2 complex was found [25].

It is interesting to note that chemical shifts of $[\text{Cs}(\text{18C6})_2]^+$ are essentially independent of solvent's nature, Table 3, providing almost the same values for RTIL and for molecular solvents. This observation indicates that in a "sandwich"-type complex the two crown ether molecules effectively shield the cesium ion from interaction with solvent. By contrast, the chemical shifts of $[\text{Cs}(\text{18C6})]^+$ are strongly solvent dependent both in RTIL and in molecular solvents.

Generally, chemical shift of ^{133}Cs seems to depend rather on an anion's nature of RTIL, than on the cation's one. This can be expected reasonably, as the co-ordination sphere of Cs^+ in RTIL is formed by anions. These anions are partly substituted by 18C6 due to complex formation, while the remaining ones provide the cause for differences in the chemical shifts of complexes. Indeed, the chemical shifts of Cs^+ and $[\text{Cs}(\text{18C6})]^+$ are almost the same in $[\text{BMIM}][\text{BF}_4]$ and $[\text{BMPy}][\text{BF}_4]$ as well as in $[\text{BMIM}][\text{N}(\text{Tf})_2]$, $[\text{HMIM}][\text{N}(\text{Tf})_2]$ and $[\text{EtHMIM}][\text{N}(\text{Tf})_2]$. This is consistent with formation of similar species $[\text{Cs}(\text{BF}_4)_n]^{1-n}$ and $[\text{Cs}(\text{18C6})(\text{BF}_4)_{n-x}]^{1-n+x}$ in both $[\text{BF}_4]$ based RTIL, as well as $\{\text{Cs} \cdot [\text{N}(\text{Tf})_2]_m\}^{1-m}$ and $\{\text{Cs}(\text{18C6}) \cdot [\text{N}(\text{Tf})_2]_{m-x}\}^{1-m+x}$ in those $[\text{N}(\text{Tf})_2]$ -based. Meanwhile, for $[\text{BMIM}][\text{N}(\text{CN})_2]$ and $[\text{THA}][\text{DHSS}]$ the chemical shifts of δ_{Cs} and δ_{CsL} are definitely different, demonstrating different environment of cesium in both species relative to those mentioned above.

Table 3. Chemical Shifts and Stability Constants of Cesium Complexes with 18C6 in RTILs and in molecular solvents at 25 °C.

Solvent	DN ^c	δ_{Cs} Calc	δ_{CsL} calc	δ_{CsL2} Calc	logK ₁	logK ₂	Reference
1,2-Dichloroethane	0	-	-	-	7.98	2.58	[29]
Acetonitrile	14.1	24.1 ^b	14.8 ^b	-53 (7) ^b	4.8 (0.2) ^a	0.6 ^c	[23 ^a ,25 ^b]
Propylene carbonate	15.1	-36.5	-8.1 (0.2)	-44.5 (0.3)	4.50 ^a	1.0 ^b	[23 ^a ,25 ^b]
Acetone	17.0	-35.8 ^b	-6.4 ^b	-47 (9) ^b	4.51(0.04) ^a	1.5 ^b	[23 ^a ,25 ^b]
[HMIM][NTf ₂]		-30.7 (0.6)	-5 (1.0)	-50 (4)	4.4 (0.1) ^a	1.13 (0.07)	Present Work
DMFA	26.6	-0.8 ^b	3.37 ^b	-48 (1) ^b	3.64(0.02) ^a	0.4 ^b	[23 ^a ,25 ^b]
[EtHMIM][NTf ₂]		-30.6 (0.2)	-3.9 (0.2)	-51 (4)	3.4 (0.4)	1.16 (0.08)	Present Work
[BMIM][NTf ₂]		-29.6 (0.5)	-6.5 (0.7) -5 (4)	-47 (1)	3.4 (0.5)	1.29 (0.07)	[26] Present Work
DMSO	29.8	68.0 ^b	23.6 ^b	-49 (2) ^b	3.04(0.02) ^a	0 ^b	[23 ^a ,25 ^b]
[BMIM][N(CN) ₂]		91 (1)	34 (1)	-	3.03 (0.08)		[17]
[BMIM][BF ₄]		-68 (4)	-22 (4)	-	2.8 (0.3)		[17]
[BMPy][BF ₄]		-70 (7)	-16 (5)	-	2.6 (0.3)		[17]
[BMIM][PF ₆]		-91 (2)	-7 (14)		2.4 (0.2)		Present Work
[TOMA][Sal]		31 (0.7)	-29 (1)	-	1.43 (0.05)		Present Work
[BPy][MeSO ₄]		23.3 (0.5)	-7 (5)	-	1.20 (0.13)		[26]
Water	33	~0	-	-	0.96(0.03) ^a	-	[23] ^a
[THA][DHSS]		22.5 (0.3)	-47 (2)	-	0.76 (0.06)		Present Work

a log K₁ values for 25 oC, I = 0 – 0.1 mol/dm³, IUPAC selection; b chemical shifts from [25] are reported with a correction related to the reference treatment in our paper; c donor number from ref. [27].

The stability constants of cesium complexes in hydrophobic RTILs demonstrate much less difference than chemical shifts, although some analogy can definitely be detected. The logK₁ values for CsL in [HMIM][N(Tf)₂], [BMIM][N(Tf)₂], [BMIM][PF₆], [TOMA][Sal] and [THA][DHSS] at 25 °C were evaluated to be 4.4; 3.4; 2.4; 1.43 and 0.76. With an exception of [THA][DHSS], all of them are higher, then the stability constant of CsL in water (0.98). As it was noted for hydrophilic RTIL, the magnitude of logK₁ for hydrophobic RTILs falls inside, but not outside the range of those for molecular solvents, with location between acetonitrile and water.

The logK₁ value for an alkali metal cation with crown ether in molecular solvents is correlated [25,27] with donor number (DN) of the solvent [28], Table 3, although some exceptions for [Cs18C6]⁺ are known (pyridine: DN 33.1; log K₁ =5.7 [25]). In this sense, the log K₁ values obtained in the present study suggest that hydrophobic RTILs [HMIM][N(Tf)₂], [BMIM][N(Tf)₂], [BMIM][PF₆], [TOMA][Sal] have DN between 33 (water) and 14 (acetonitrile), e.g. span the same range that polar molecular solvents do, but are rather far

from such nonpolar solvent as 1,2-dichloroethane (DN 0 [29]). This observation spreads out the data reported by Nishi *et al.* [14] for Li, Na, K, Rb and Cs complexes with dibenzo-18-crown-6 in a hydrophobic RTIL *N*-octadecylisoquinolinium tetrakis[3,5-bis(trifluoromethyl)phenyl]borate, which is demonstrated to have DN between 4.4 (nitrobenzene) and 0 (1,2-dichloroethane).

The $\log K_2$ values for [EtHMIM][N(Tf)₂] and [HMIM][N(Tf)₂] appeared to be 2 to 3 log units lower than $\log K_1$: 1.16; 1.13 respectively, Table 2. These values correspond well to those found for molecular solvents, Table 3 and for [BMIM][N(Tf)₂].

An increase of temperature decreases the stability constants of CsL for [HMIM][N(Tf)₂], [BMIM][N(Tf)₂] and [BMIM][PF₆], but increases them for [TOMA][Sal] and [THA][DHSS]. The linear plots of $\ln K_1$ and $\ln K_2$ versus $1/T$ gave the possibility to estimate both ΔH_1 and ΔH_2 values, Figure 2. The thermodynamic quantities for the formation of [Cs18C6]⁺ in RTIL are summarized in Tables 1 to 4 together with those for molecular solvents.

With an exception of [THA][DHSS] and [TOMA][Sal], the cesium nitrate solubility in RTIL is much less than in water, the metal-solvent interaction is likely to be stronger in water, than in RTIL, *i.e.* less energy is needed for breaking the metal-(RTIL anion) bonds. Thus the differences in metal-solvent interactions are expected to make complex formation more exothermic in RTIL than in water. Indeed, for CsL formation ΔH_1 is negative for all hydrophilic RTILs, [HMIM][N(Tf)₂], [BMIM][N(Tf)₂], [BMIM][PF₆] and almost for all polar molecular solvents.

Table 4. Thermodynamic Quantities ΔG_1 , ΔH_1 , ΔS_1 of Cesium Complexes Formation with 18C6 in RTIL and in molecular solvents at 25 °C.

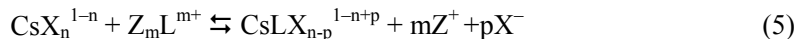
Solvent	ΔH_1 , ^a kJ/mol	ΔS_1 , J/(mol·K)	ΔH_2 , ^a kJ/mol	ΔS_2 , J/(mol·K)	Reference
Acetonitrile	-17 (1)	35			[23] ^a
Propylene carbonate	-43.3	-17.6			[23]
Acetone	-52.8 (0.4)	-27.2			[23]
DMFA	-49.2 (0.8)	-28.4			[23]
[EtHMIM][NTf ₂]	9 (18)	100 (60)	-17.5 (0.3)	-36.5 (1.0)	Present work
[HMIM][NTf ₂]	-9.5 (0.4)	53 (15)	-17.8 (0.3)	-38.3 (0.9)	Present work
[BMIM][NTf ₂]	-6.8 (1.9)	41.5 (6.1)	-41.3 (0.7) ^b	-114 (1) ^b	Present work
[BMIM][N(CN) ₂]	-47 (2)	-30 (2)			[17]
[BMIM][BF ₄]	-80 (3)	-65 (3)			[17]
[BMIM][PF ₆]	-21.0 (1.4)	-25.4 (4.5)			Present work
[BMPy][BF ₄]	-47 (1)	-32 (1)			[17]
[TOMA][Sal]	3.85 (0.25)	40.3 (0.7)			Present work
Water	-17 (1)	-39			[23]
[THA][DHSS]	2.1 (0.3)	21.6 (1.1)			Present work

^a Ref. [23], 25 °C, $I = 0 - 0.1 \text{ mol/dm}^3$, IUPAC selection; ^b Ref. [26].

Generally, it can be seen that enthalpy change promotes complex formation in hydrophilic RTIL, whereas the corresponding change of entropy is negative and provides the decomposition of $[\text{Cs}(18\text{C}6)]^+$. However, this not the case of hydrophobic RTILs $[\text{HMIM}][\text{N}(\text{Tf})_2]$, $[\text{BMIM}][\text{N}(\text{Tf})_2]$, $[\text{TOMA}][\text{Sal}]$, $[\text{THA}][\text{DHSS}]$, that reveal a positive entropy change like acetonitrile. Moreover, the entropy change gives the dominating contribution to CsL stability in $[\text{BMIM}][\text{N}(\text{Tf})_2]$, $[\text{TOMA}][\text{Sal}]$ and $[\text{THA}][\text{DHSS}]$. Only one hydrophobic RTIL ($[\text{BMIM}][\text{PF}_6]$) demonstrates the same behavior as hydrophilic RTILs and polar molecular solvents.

Thus, the thermodynamic quantities indicate clearly, that the contributions to the overall stability of CsL complex may differ rather significantly. The reaction enthalpies and entropies, reveal greater diversity, than $\log K_1$ depending on RTIL composition. The complexation of Cs^+ is the most exothermic in $[\text{BMIM}][\text{BF}_4]$. Moreover, the observed ΔH_1 value is the highest known for CsL in both molecular solvents and RTIL. At the same time the corresponding entropy change for this solvent is also the highest, diminishing the enthalpy contribution to the $\log K_1$. The data listed in Table 4 obviously indicate, that both cation and anion of RTIL affect the complex formation stability and thermodynamic functions change.

This is not simply explained in terms of the solvation of the cesium ion and 18C6. The tentative scheme of complex formation in RTIL (5) is more complicated than that one in molecular solvents [30,31]. In general, both ions forming the ionic liquid (its cation Z^+ and anion X^-) may react with cesium complex constituents. Z^+ is competing with cesium for the ligand, while X^- solvates cesium, resisting complex formation:

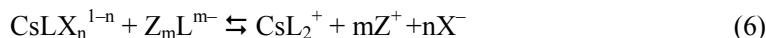


The NMR chemical shift data indicate that crown ether does not substitute all RTIL anions X^- in coordination sphere of cesium in CsL complexes. This observation agrees well with X-ray structural data for cesium complexes with 18-crown-6 in solid state [32,33] and in an aqueous solution [34], as well as with classical molecular dynamics simulations [35]. In all these structures cesium is located above the mean oxygen plane of the crown-ether ring since its size is larger than the cavity size of 18C6 (170 and 130 pm respectively [23]).

Thus the exposed part of Cs^+ may strongly interact with RTIL anions making coordination number equal to 8 or 9 as it is observed crystallographically for molecular solvents.

On the other hand, a strong influence of the ionic liquid cation, Z^+ , on $\log K_1$, ΔH_1 and ΔS_1 values of complex formation is observed when RTILs $[\text{BMIM}][\text{BF}_4]$ and $[\text{BMPy}][\text{BF}_4]$ are compared, indicating Z^+ -crown ether interactions of various intensity. Such an interaction has also analogues among molecular solvents. For example, for AN, nitromethane (NM) and even for chloroform 18-crown-6·2AN, 18-crown-6·2NM and 18-crown-6·2 CH_2Cl_2 solvates have been isolated and their structures have been determined by X-ray crystallography [36-39]. Hence, both cation and anion of RTIL have an impact on the resultant stability constant and thermodynamic quantities of chelated compound.

For ML_2 complexes in hydrophobic RTIL the situation is significantly different from that for ML complexes: ΔH_2 is more negative than ΔH_1 , at the same time ΔS_2 is negative, while ΔS_1 is positive. For the second crown ether molecule coordination in $[\text{BMIM}][\text{N}(\text{Tf})_2]$, $[\text{HMIM}][\text{N}(\text{Tf})_2]$ and $[\text{EtHMIM}][\text{N}(\text{Tf})_2]$, (6):



a possible explanation could be associated with a very weak X^- bonding in the CsLX_n^{1-n} species. An extreme case, when $n = 0$, is also possible. This is consistent with poor coordinating ability of the $\text{N}(\text{Tf})_2^-$ anion towards alkali and alkaline earth cations [40]. Alternatively, in $[\text{BMIM}][\text{PF}_6]$, $[\text{BMIM}][\text{BF}_4]$, $[\text{BMPy}][\text{BF}_4]$ and $[\text{BMIM}][\text{N}(\text{CN})_2]$, the solvent's anion X^- is bound to cesium more tightly and prevents CsL_2^+ complex formation. Such an interpretation is supported by a much better extraction of CsNO_3 from water into RTIL for $[\text{TOMA}][\text{Sal}]$, $[\text{THA}][\text{DHSS}]$ and $[\text{BMIM}][\text{PF}_6]$ relative to $[\text{BMIM}][\text{N}(\text{Tf})_2]$, $[\text{HMIM}][\text{N}(\text{Tf})_2]$ and $[\text{EtHMIM}][\text{N}(\text{Tf})_2]$ in an absence of 18C6. Notably, the 1,2-dichloroethane (1,2-DCE) with a very low donating ability also fits this scheme, Figure 3.

Formation of crown ether complexes promotes cesium extraction [18] into hydrophobic RTIL from water if the complex stability in RTIL is higher than in water, Table 5. Indeed for $[\text{BMIM}][\text{N}(\text{Tf})_2]$, $[\text{HMIM}][\text{N}(\text{Tf})_2]$, $[\text{EtHMIM}][\text{N}(\text{Tf})_2]$, $[\text{BMIM}][\text{PF}_6]$ and $[\text{TOMA}][\text{Sal}]$ $\log K_1^{\text{RTIL}} > \log K_1^{\text{water}}$ and cesium content in RTIL increases due to 18C6 administration. For $[\text{THA}][\text{DHSS}]$ $\log K_1^{\text{RTIL}} < \log K_1^{\text{water}}$ and crown ether decreases cesium content in RTIL. The $\log D_{\text{Cs}}^{18\text{C}6}$ values have the same order of magnitude for RTILs, 1,2-dichloroethane and other volatile organic diluents [41-43], while the hazardous properties of the latter are much higher.

It should be noted that the complex stability in RTIL increases as the RTIL ability to extract cesium without 18C6 (D_{Cs}) decreases, Figure 3. Meanwhile, there are no simple relationships between $\log K_1$ ($\log \beta_{1,2}$) and crown ether assisted extraction efficiency ($D_{\text{Cs}}^{18\text{C}6}$), Table 5. This happens due to a superposition of at least two phenomena: the relative stability of complexes is superimposed on a relative solubility of the crown ether and its complexes in the RTIL/water systems. However, when the ligand's extraction (D_{L}) and D_{Cs} are taken into account then a perfect linear relationship between $[\log D_{\text{Cs}}^{18\text{C}6} - \log D_{\text{Cs}} - \log D_{\text{L}}]$ and $\log \beta_{1,2}$, is observed, Figure 4.

Table 5. Stability Constants of Cesium Complexes Formation with 18C6 in RTIL and Extraction Efficacy from Water^a.

Solvent	W, % ^c	$\log \beta_{2(1)}$	$\log D_{\text{Cs}}$	$\log D_{\text{Cs}}^{18\text{C}6}$	$\log D_{18\text{C}6}$	$\log [D_{\text{Cs}}^{18\text{C}6} / (D_{\text{Cs}} D_{18\text{C}6})]$
$[\text{HMIM}][\text{NTf}_2]$	1.3	5.57	-1.24	0.82	0.25	1.81
$[\text{EtHMIM}][\text{NTf}_2]$	0.7	4.56	-0.81	0.56	-0.27	1.64
$[\text{BMIM}][\text{NTf}_2]$	0.5	4.55	-0.67	1.56	0.77	1.46
$[\text{BMIM}][\text{PF}_6]$	1.9 0.92 ^h	2.3	-0.59 -0.59 ^f -1.17 ^h	-0.20 ~ -1 ^h	0.13 0.15 ^h	0.26
$[\text{TOMA}][\text{Sal}]$	7.6	1.45	0.69	0.83	0.49	-0.38
$[\text{THA}][\text{DHSS}]$	4.4	0.77	1.21	0.25	-0.12	-0.84
1,2-dichloroethane		10.56 ^b	-7.7 ^j	0.8 ^c	0.03 ^d	6.93

^a Extraction data for RTIL are taken from [18] for 22 °C, $\text{pH}_{\text{water}}=5-7$; $[\text{Cs}]_0=0.0015$ mol/L, $[\text{18C6}]_0=0.15$ and phases volume ratio $V_{\text{water}}/V_{\text{RTIL}}=10$; $D_{\text{Cs}}=[\text{Cs}]_{\text{RTIL}}/[\text{Cs}]_{\text{water}}$; $D_{\text{Cs}}^{18\text{C}6}=[\text{Cs}]_{\text{RTIL}}/[\text{Cs}]_{\text{water}}$ in presence of 0.15 mol/L 18C6 in RTIL; $D_{18\text{C}6}=[\text{18C6}]_{\text{RTIL}}/[\text{18C6}]_{\text{water}}$ in presence of Cs^+ ; $\beta_{2(1)} = K_1$ if no CsL_2 complexes are formed, and $\beta_{2(1)} = K_1 K_2$ if CsL_2 complex exists in a particular RTIL; all $\beta_{2(1)}$ values correspond to 25 °C; ^b Ref. [29], ^c Ref. [41], picrate salt; ^d Ref. [42], ^e W -equilibrium water content in RTIL phase after extraction in presence of 18C6, mass %; ^f Ref. [6]; ^j Ref. [43], picrate salt; ^h Ref. [2].

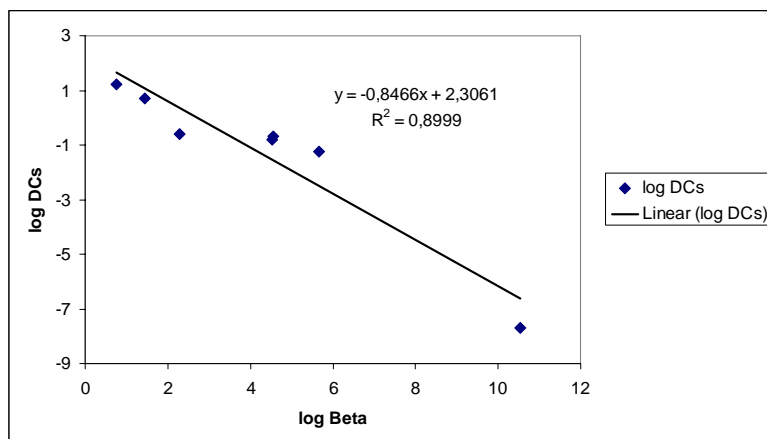


Figure 3. Plot of $\log D_{Cs}$ vs. $\log \beta_{1,2}$ for [TOMA][Sal], [THA][DHSS], [BMIM][PF₆], [BMIM][N(Tf)₂], [HMIM][N(Tf)₂], [EtHMIM][N(Tf)₂] and 1,2-dichloroethane at 22-25 °C.

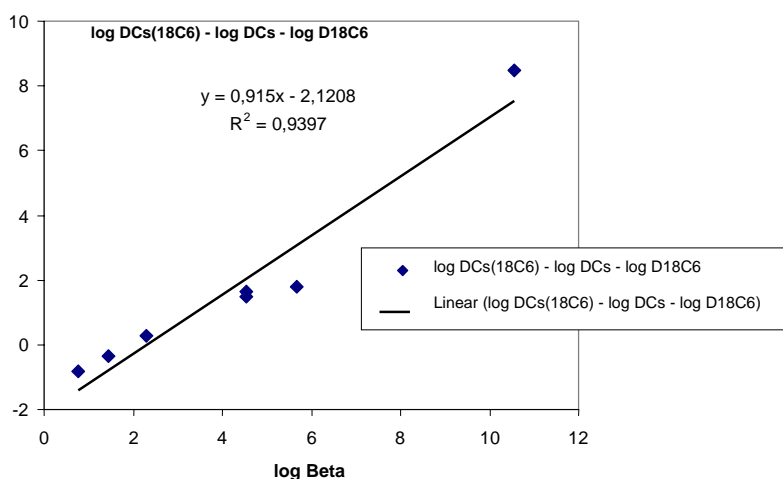


Figure 4. Plot of $[\log D_{Cs}^{18C6} - \log D_{Cs} - \log D_{18C6}]$ vs. $\log \beta_{1,2}$ for [TOMA][Sal], [THA][DHSS], [BMIM][PF₆], [BMIM][N(Tf)₂], [HMIM][N(Tf)₂], [EtHMIM][N(Tf)₂] and 1,2-dichloroethane at 22-25 °C.

This linearity has a certain background. When an aqueous phase of cesium nitrate is in equilibrium with a RTIL organic phase containing crown ether L, the distribution ratio (D_{Cs}^{18C6}) for such RTIL's as [TOMA][Sal], [THA][DHSS] and [BMIM][PF₆], where only CsL species are formed is represented by a simple equation (7):

$$D_{Cs}^{18C6} = ([Cs]^{RTIL} + [CsL]^{RTIL}) / ([Cs]^w + [CsL]^w) \quad (7)$$

where the superscripts "RTIL" and "w" denote organic and aqueous phase, respectively. When the total concentration $[L]^t \gg [Cs]^t$ and the stabilities of complexes in both phases are high enough ($\log K_1^{RTIL} \geq 1$; $\log K_1^w \geq 1$), then $[Cs]^{RTIL} \ll [CsL]^{RTIL}$ and $[Cs]^w \ll [CsL]^w$. In

this case the equilibrium concentrations of $[Cs]^{RTIL}$ and $[Cs]^w$ in (7) can be neglected. The equation (7) is therefore transformed into (8):

$$D_{Cs}^{18C6} = [CsL]^{RTIL}/[CsL]^w \quad (8)$$

or

$$D_{Cs}^{18C6} = (K_1^{RTIL}[Cs]^{RTIL}[L]^{RTIL})/(K_1^w[Cs]^w[L]^w) \quad (9)$$

as far as $[Cs]^{RTIL}/[Cs]^w = D_{Cs}$ and $[L]^{RTIL}/[L]^w = D_L$, then

$$D_{Cs}^{18C6} = K_1^{RTIL}D_{Cs}D_L/K_1^w \quad (10)$$

or

$$\log D_{Cs}^{18C6} = \log K_1^{RTIL} + \log D_{Cs} + \log D_L - \log K_1^w \quad (11)$$

Thus the plot of $(\log D_{Cs}^{18C6} - \log D_{Cs} - \log D_L)$ versus $\log K_1^{RTIL}$ should be linear with a slope 1. For [BMIM][N(Tf)₂], [HMIM][N(Tf)₂], [EtHMIM][N(Tf)₂] the equations (7), (9), (10) and (11) become more complicated due to formation of CsL₂ complexes and the lack of such complexes in water. For a molecular solvent 1,2-DCE the equation (7) and its derivatives have to involve additionally the formation equilibrium for neutral complexes CsL(NO₃) in both RTIL and aqueous phases. However, surprisingly all seven solvents fit equation (11) with a slope 0.92 and a correlation coefficient R²=0.94.

This indicates clearly an importance of complex stability contribution for hydrophobic RTILs in cesium extraction processes. At the same time this trend is strongly modulated by a relative solubility of 18-crown-6 and alkali metal nitrate in water and in a RTIL phase.

ACKNOWLEDGMENTS

The authors would like to thank the Russian Foundation for Basic Research (projects no. 07-08-00246 and no. 08-03-91319) and the Academy of Science of Finland for their financial support of this work.

REFERENCES

- [1] Earle, MJ; Seddon, KR. Ionic Liquids. Green solvents for future. *Pure Appl. Chem.*, 2000, 72, 1391-1398. In: VA; Cocalia, JD; Holbray, KE; Gutowski, NJ; Bridges, RD; Rogers, Separations of metal ions using ionic liquids: the challenges of multiple mechanisms. *Tsinghua Science Technol.*, 2006, 11, 188-193.
- [2] Visser, AE; Swatloski, RP; Reichert, WM; Griffin, ST; Rogers, RD. Traditional extractants in nontraditional solvents: Groups 1 and 2 extraction by crown ethers in room temperature ionic liquids. *Ind. Eng. Chem. Res.*, 2000, 39, 3596-3604.

- [3] Dai, S; Ju, YH; Barnes, CE. Solvent extraction of strontium nitrate by crown ether using room-temperature ionic liquids. *J. Chem. Soc; Dalton Trans.*, 1999, 1201-1202.
- [4] Luo, H; Dai, S; Bonnesen, PV; Buchana, AC. Separation of fission products based on ionic liquids containing aza-crown ether fragment. *J. Alloy Comp.*, 2006, 418, 195-199.
- [5] Po-Yu Chen: The assessment of removing strontium and cesium cations from aqueous solutions based on the combined methods of ionic liquid extraction and electrodeposition. *Electrochim. Acta*, 2007, 52, 5484-5492.
- [6] Chun, S; Dzyuba, SV; Bartsch, RA. Influence of Structural Variation in Room-Temperature Ionic Liquids on the Selectivity and Efficiency of Competitive Alkali Metal Salt Extraction. *Anal. Chem.*, 73, 3737-3741 (2001).
- [7] Visser, AE; Roberts, RD. Room-temperature ionic liquids: new solvents for f-element separations and associated solution chemistry. *J. Solid State Chemistry.*, 2003, 171, 109-113.
- [8] Shimojo, K; Goto, M. Solvent Extraction and Stripping of Silver Ions in Room-Temperature Ionic Liquids Containing Calixarenes. *Anal. Chem.*, 2004, 76, 5039-5044.
- [9] Visser, AE; Swatloski, RP; Reichert, WM; Mayton, R; Sheff, S; Wierzbicki, A; Davies, JH; Rogers RD. Task-specific ionic liquids Incorporating Novel Cations for the Coordination and Extraction of Hg^{2+} and Cd^{2+} : Synthesis, Characterization and Extraction Studies. *Environ. Sci. Technol.*, 2002, 36, 2523-2529.
- [10] Visser, AE; Swatloski, RP; Reichert, WM; Mayton, R; Sheff, S; Wierzbicki, A; Davis, JH; Jr; Rogers, RD. Task-specific ionic liquids for extraction of metal ions from aqueous solution. *Chem. Commun.*, 2001, 135-136.
- [11] Ajioka, T; Oshima, S; Hirayama, N. Use of 8-sulfonamidoquinoline derivatives as chelate extraction reagents in ionic liquid extraction system. *Talanta*, 2008, 74, 903-908.
- [12] Lohithakshan, KV; Aggarwal, SK. Solvent extraction studies of Pu(IV) with CMPO in 1-octyl-3-methyl imidazolium hexafluorophosphate (C8mimPF6) room temperature ionic liquid (RTIL). *Radiochimica Acta*, 2008, 96, 93-97.
- [13] Dietz, ML; Stepinski, DC. Anion concentration-dependent partitioning mechanism in the extraction of uranium into room-temperature ionic liquids. *Talanta*, 2008, 75, 598-603.
- [14] Nishi, N; Murakami, H; Imakura, H; Kakiuchi, T. Facilitated transfer of alkali-metal cations by dibenzo-18-crown-6 across the electrochemically polarized interface between an aqueous solution and a hydrophobic room-temperature ionic liquid. *Anal. Chem.*, 2006, 78, 5805-5812.
- [15] Lewandowski, A; Osinska, M; Stepniak, I. Stability of Ag^+ Complexes with Cryptand 222 in Ionic Liquids. *J. Incl. Phenom. Macrocycl. Chem.*, 2005, 52, 237-240.
- [16] Popov, K; Rönkkömäki, H; Hannu-Kuure, M; Kuokkanen, T; Lajunen, M; Vendilo, V; Oksman, P; Lajunen, LHJ. Stability of Crown-Ether Complexes with Alkali-Metal Ions in Ionic Liquid-Water mixed Solvents. *J. Incl. Phenom. Macrocycl.*, Chem. 2007, 59, 377-381.
- [17] Popov, KI; Rönkkömäki, H; Hannu-Kuure, M; Kuokkanen, T; Lajunen, M; Vendilo, A; Glazkova, IV. Lajunen, LHJ. Stability Constant of the Sodium Complex with Dibenzo-18-Crown-6 in Mixed Water-Ionic Liquid Solvent. *Russ. J. Coord. Chem.*, 2007, 33, 393-395.

- [18] Djigailo, DI; Smirnova, SV; Torocheshnikova, II; Vendilo, AG; Popov, KI; Pletnev, IV. 18-Crown-6 assisted extraction of cesium from water into room temperature ionic liquids. *Molecules*, in press, 2009.
- [19] Moulton, R; Davis, JH. Ionic liquids containing a sulfonate anion. US Patent 20050131118, 2005.
- [20] Khadilkar, BM; Reberio, GL. Microwave-Assisted Synthesis of Room-Temperature Ionic Liquid Precursor in Closed Vessel. *Organic Process Research & Development*, 6, 826-828 (2002); Bonhate P; Dias A.-P; Papageorgiou N; Kalyanasundaram K; Grätzel M. Hydrophobic, Highly Conductive Ambient-Temperature Molten Salts. *Inorganic Chemistry*, 1996, 35, 1168-1178.
- [21] Sigmaplot for Windows, Version 4.0, 1986-1997 SPSS Inc.
- [22] Frassinetti, C; Alderighi, L; Gans, P; Sabatini, A; Vacca, A; Ghelli, S. Determination of protonation constants of some fluorinated polyamines by means of ^{13}C NMR data processed by the new computer program HypNMR2000. Protonation sequence in polyamines. *Anal. Biochem.*, 2003, 376, 1041-1052.
- [23] Arnaud-Neu, F; Delgado, R; Chaves, S. Critical evaluation of stability constants and thermodynamic functions of metal complexes of crown ethers. *Pure Appl. Chem.*, 2003, 75, 71-102.
- [24] Pettit, LD; Sukhno, IV; Buzko, VY. The Adjustment, Estimation and Uses of Equilibrium Constants in Aqueous Solution. Aqua Solution Software, Version 1.2, IUPAC and Academic Software, UK, available at: www.iupac.org.
- [25] Mei, E; Popov, AI; Dye, JL. Complexation of the cesium cation by macrocyclic polyethers in various solvents. A cesium-133 Nuclear Magnetic Resonance study of the thermodynamics and kinetics of exchange. *J. Phys. Chem.*, 1977, 81, 1677-1681.
- [26] Vendilo, AG; Rönkkömäki, H; Hannu-Kuure, M; Lajunen, M; Asikkala, J; Petrov, AA; Krasovsky, VG; Chernikova, EA; Oksman, P; Lajunen, LHJ; Popov, KI. Stability Constants of cesium complexes with 18-crown-6 in ionic liquids. *Koord Khim.* 34, 645-650 (2008); *Russ. J. Coord. Chem.*, 2008, 34, 635-640.
- [27] Smetana, AJ; Popov, AI. Lithium-7 Nuclear Magnetic Resonance and Calorimetric Study of Lithium Crown Complexes in Various Solvents. *J. Solut. Chem.*, 1980, 9, 183-196.
- [28] Gutmann, V; Vichera, E. Coordination reactions in non aqueous solutions - the role of the donor strength. *Inorg.Nucl. Chem.Lett.*, 1966, 2, 257-260.
- [29] Kikuchi, Y; Sakamoto, Y. Complex formation of alkali metal ions with 18-crown-6 and its derivatives in 1,2-dichloroethane. *Anal. Chim. Acta*, 2000, 403, 325- 332.
- [30] Ohtsu, K; Ozutsumi, K. Thermodynamics of Solvation of 18-crown-6 and its Alkali-Metal Complexes in Various solvents. *J. Inclusion Phenom. Macrocycl. Chem.*, 2003, 45, 217-224.
- [31] Ozutsumi, K; Ohtsu, K; Kawashima, T. Thermodynamics of Complexation of 18-Crown-6 with Sodium, Potassium, Rubidium Caesium and Ammonium Ions in N,N-dimethylformamide. *J. Chem.Soc. Faraday Trans.*, 1994, 90, 127-131.
- [32] Gjikaj, M; Adam, A. Complexation of Alkali Triflates by Crown Ethers: Synthesis and Crystal Structure of $\text{Na}(12\text{-crown-4})_2[\text{SO}_3\text{CF}_3]$, $\text{Na}(15\text{-crown-5})[\text{SO}_3\text{CF}_3]$, $[\text{Rb}(18\text{-crown-6})][\text{SO}_3\text{CF}_3]$ and $[\text{Cs}(18\text{-crown-6})][\text{SO}_3\text{CF}_3]$. *Z. Anorg.Allg.Chem.*, 2006, 632, 2475-2480.

- [33] Ellerman, J; Bauer, W; Schuetz, M; Heinemann, FW. Moll, M. Chemie Polyfunktioneller Moleculer 130 Mitt.[1]: Spaltprodukte, Kristallstrukturen und Festkoerper-NMR-Spektern. Monatshefte fur Chemie, 1998, 129, 547-566.
- [34] Ozutsumi, K; Natsuhara, M; Ohtaki, H. An X-ray Diffraction Study on the structure of 18-crown-6 Ether Complexes with Alkali Metal Ions in Aqueous Solutions. *Bull. Chem. Soc. Jpn.*, 1989, 62, 2807-2818.
- [35] Dang, LX. Mechanism and Thermodynamics of Ion Selectivity in Aqueous Solutions of 18-crown-6 Ether: A molecular Dynamic Study. *J. Am.Chem.Soc.*, 1995, 117, 6954-6969.
- [36] de Boer, JAA; Reinhoudt, DN; Harkema, S; van Hummel, GJ; de Jong, F. Thermodynamic Constants of Complexes of Crown Ethers and Uncharged Molecules and X-ray Structure of the 18-Crown-6 \cdot (CH₃NO₂)₂. *J. Am. Chem. Soc.*, 1982, 104, 4073-4076.
- [37] Rogers, RD; Richards, PF; Voss, EJ. Neutral Solvent/Crown Ether Interactions, 4. Crystallization and Low Temperature (-150 °C) Structural Characterization of 18-Crown-6 \cdot 2(CH₃CN). *J. Inklus. Phenom.*, 1988, 6, 65-71.
- [38] Garrell, RL; Smyth, JC; Fronczek, FR; Gandour, RD. Crystal Structure of the 2:1 Acetonitrile Complex of 18-Crown-6. *J. Inclusion Phenom.*, 1988, 6, 73-78.
- [39] Jones, PG; Hiemisch, O; Blaschette, A. Bildung und Kristallstruktur des Komplexes [(18-Krone-6)(CH₂Cl₂)₂]. *Z. Naturforsch.*, 1994, 49b, 852-854.
- [40] Jensen, MP; Dzielawa, JA; Ricket, P; Dietz, ML. EXAFS Investigations of the Mechanism of Facilitated Ion Transfer into a Room-Temperature Ionic Liquid. *J. Am. Chem. Soc.*, 2002, 124, 10664-10665.
- [41] Abramov, AA. Extraction of cations with crown ethers. *Vestn. Mosk. Univ. (Moscow University Bull.) Ser. 2000*, 2, 41, №1, 3-15.
- [42] Takeda, Y; Kawarabayashi, A; Endo, K; Yahata, T; Kudo, Y; Katsuta, S. Solvent Extraction of Alkali Metal (Li-Cs) Picrates with 18-Crown-6 into Various Diluents. Elucidation of Fundamental Equilibria which Govern the Extraction-Ability and – Selectivity. *Anal. Sci.*, 1998, 14, 215-223.
- [43] Levitskaia, TG; Maya, L; van Berkel, GJ; Moyer, B. A. Anion Partitioning and Ion-Pairing Behavior of Anions in the Extraction of Cesium Salts by 4,5''-Bis(*tert*-octylbenzo)dibenzo-24-crown-8 in 1,2-Dichloroethane. *Inorg. Chem.*, 2007, 46, 261-272.

Chapter 10

MACROCYCLES ROLE IN COMPETITIVE TRANSPORT AND EXTRACTION OF METAL CATIONS

Azizollah Nezhadali

Associate Prof. of Anal. Chem. Dept. of Chem. Payame Noor University (PNU),
Mashhad, Iran.

ABSTRACT

A considerable number of investigation of the transport and extraction of transition and post- transition metal cations through bulk liquid and polymer inclusion membranes using a wide range of synthetic macrocyclic ionophores have now be reported by researchers. A motivation for these studies has been the potential for obtaining new metal ion separation processes for use in the range of industrial and analytical applications. A variety of membrane types have been used in metal ion transport experiments. A lot of competitive transport experiments involving metal ion transport from an aqueous source phase across an organic membrane phase into an aqueous receiving phase have been studied using open-chain mixed-donor ligands or macrocycles as the ionophore in the organic phase. For similar source and receiving phases the presence of the ionophore in the organic phase acts as a carrier for the metal ion until the concentrations in both aqueous source and receiving phases equalize and the system reaches equilibrium. It is well known that transport efficiency and selectivity can be influenced by a range of parameters with the transport limiting step differing from one system to another one. This chapter reports some of the factors that affect on the selectivity and efficiency of a macrocyclic ligand for transport and extraction of metal cations. A macrocycle has an important role to selecting a cation from a mixture of cations during the transport or extraction process. In the arrangement of transport process for carriers with protonation capability, the metal ion in the source phase comes into contact with the protonated or free ionophore at the source phase/ organic phase interface. A neutral complex is formed at this interface and the donor groups on the ligand are deprotonated upon complexation. The metal-ligand complex then diffuses through the organic phase until it comes into contact with the more acidic receiving phase where the metal ion is displaced by protons. The protonated form of the ligand then moves back through the organic phase to repeat the cycle. Typically, both aqueous phases are buffered appropriately in order to maintain

the required pH gradient. The direction of the proton transport is in the opposite direction to that of the metal ions and this enables the concentration of the transported ion to exceed the equilibrium concentration. Among the multidentate ligands, the macrocyclic ones which have many properties in common with the naturally occurring ionophores and distinguished by special arrangement of binding sites that controls their coordination environment and stereochemistry display remarkable and often unique stabilities and selectivities for complexation of various cations.

INTRODUCTION

Synthetic multidentate ligands which are capable of complexing and discriminating between simple cations very effectively and, therefore, of promoting ion extraction and transport in biological and liquid-liquid membranes are important in chemistry, biology and industry. The possibility of variations in ligand structure has paved the way for detailed studies of the dependence of complex stabilities and selectivities upon the relationship between cation and ligand structure, the nature and number of ligand donor atom and etc.

Among the multidentate ligands, the macrocyclic ones which have many properties in common with the naturally occurring ionophores and distinguished by special arrangement of binding sites that controls their coordination environment and stereochemistry display remarkable and often unique stabilities and selectivities for complexation of various cations.

The industrial importance of metal ion separation has made the study of metal ion transport behaviour an area of increasing research interest. Metal ion transport involves the transfer of metal selective cation from an aqueous source phase through an organic selective membrane into a second aqueous or receiving phase. For transport or separation of ions, ligands can use which are capable to form selectively a complex with a specific ion. The ligands which are soluble in organic phase, but nearly insoluble in aqueous phase are used as carriers through the membranes which transport the metal cations from aqueous source phase into the aqueous receiving phase.

Carrier mediated transport of metal cations through bulk membranes has been studied in a range of synthetic systems [1-3]. The selective transport of cations through liquid membranes by macrocyclic ligands also observed quantitatively in the late 1970s and early 1980s in both single and competitive cation systems as has been reviewed by Izatt and *et al.* [4].

Molecular recognition is an important characteristic of much natural chemical process. A prominent example is the selective transport of Na^+ and K^+ in nerve action [5]. The discovery of macrocyclic compounds and of their unusual cation complexation provided scientists with new incentives to design and synthesize new host molecules capable of highly selective recognition toward a variety of guests. The expected importance of this synthetic ability to future molecular recognition studies is exemplified by the awarding of the Noble Prize in 1987 to Pedersen [6], Lehn [7] and Cram [8] for their pioneering work in the area of macrocycle synthesize. Other important synthetic contributions have been made by a large number of workers [9-13].

Understanding host-guest recognition of the level requires quantifying the interaction involved. This quantification provides a basis for evaluating guest selectivity sequences and binding strengths. Correlation of the quantified properties of macrocycles with their

molecular structure as allowed scientists to obtain desired selectivities. The selectivity of a particular macrocycle for one cation over another as measured by the relative $\log K$ values is surprisingly nonvariant as a function of solvent in solvent systems [13-18].

An effective way to use the molecular recognition capability of macrocycles to make actual separation is to incorporate these ligands into solvent extraction and liquid membrane systems. If it is desired to test the selectivity of macrocycles, this should be done using competitive transport from cation mixtures. The kinetics of extraction of cations by macrocycles is usually quite rapid. This is particularly true with neutral macrocycles where a cation and its accompanying anion are extracted to maintain transport. Selectivity is usually determined entirely by the thermodynamics of solvent extraction. Unfortunately, few extraction equilibrium constants have been reported for cation-anion macrocycle combinations. These values have been useful in developing and understanding various schemes for obtaining desired selectivity and high transport rates with liquid membrane systems. In the following sections, the role of ion solvation, ion pairing in the source phase, and proton-ionizable macrocycles in determining cation selectivity in membrane systems will be presented and discussed.

ION SOLVATION EFFECTS

Traditionally, ion parameters were chosen in a somewhat unsystematic way to reproduce the solvation free energy and to give the correct ion size when compared with scattering results. Which experimental observable one chooses to reproduce should in principle depend on the context within which the ionic force field is going to be used [19]. A macrocycle with its hydrophobic exterior and electron-rich cavity is studied to bind and solvate a cation in a hydrophobic organic phase. However, the ease of extraction of the cation is also a function of the cation hydration energy. Hence, large cation diameter and minimal cation charge are favorable properties for an efficient cation extraction. These principles can be used effectively in designing separation systems. For example, the selectivity for K^+ over Na^+ with I 8C6 is enhanced with increasing hydrophobicity of the membrane or extraction - system solvent. On the other hand, the amount of K^+ extraction and, hence the rate of liquid membrane transport is decreased with increasing source phase solvent hydrophobicity. In systems with neutral macrocycles, the type of anion that accompanies the cation-macrocycle complex in the extraction step is important in determining selectivity sequences. By analog with transport results in bulk liquid membrane systems [20], the K_{ex} values for extraction of the type shown in eq.1:



are expected to vary by orders of magnitude depending on the solvation energy of the anion.

SOURCE-PHASE ION PAIRING

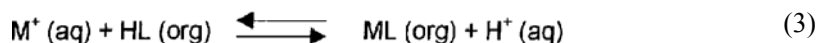
Extraction of a cation (M^+) and accompanying anion (A^-) by a neutral macrocyclic ligand (L) is often more easily modeled and quantities using equations involving the 1:1 extraction of a neutral metal-anion complex, MA_m , by L (organic) to form MA_mL as indicated in eq. (2):



Among the elements, there are many that form stable and soluble ion pairs in aqueous solution. One such set includes the halide and thiocyanate complexes of Zn^{2+} , Cd^{2+} and Hg^{2+} . These cations form a series of complexes with these anions ranging from MA^+ to MA_4^{2-} with a large variation in log K values from element to element [21].

USE OF PROTON-IONIZABLE MACROCYCLES

Use of a proton-ionizable macrocycle makes it possible to minimize anion solvation and other effects on the extraction and membrane transport. In this way, the selectivity for a particular cation can be controlled almost entirely by the choice of macrocycle. Two types of these macrocycles are pyridono and triazolo. The action of these types of macrocycles is illustrated in eq. (3):



It is apparent that extraction of the metal ion from the membrane source phase is accompanied by the loss of a proton into the source phase. A reverse process occurs at the membrane-receiving phase interface. Allowing a pH gradient will enhance the concentration factors and rapidity of transport.

The driving force for carrier-mediated membrane transport is the difference between the concentrations of any transporting complex at the membrane interfaces with the source and receiving phases. Interfacial equilibria even determine the magnitude of the concentration gradients before full system equilibrium is reached in membrane-phase, diffusion limited transport. Full system equilibrium is reached when the concentration gradient terms (ΔC) equal zero, regardless of the transport-limiting step and mechanism. The relative magnitudes of these concentrations gradients for interfacial equilibria can be calculated from the extraction equilibrium constant expressions if both the K_{ex} values and the aqueous species concentration gradients are known.

TRANSPORT THROUGH BIOLOGICAL MEMBRANES

Membrane is any delicate sheet that separates one region from another blocking or permitting (selectively or completely) the passage of substances. The skin, for example, can be considered a membrane that separates the exterior from the interior of the body; cellophane, used in chemical laboratories to separate solutions, acts as a membrane too. Membranes can be classified as impermeable, permeable, semipermeable or selectively permeable. An impermeable membrane is that through which no substance can pass. Semipermeable membranes are those that let only solvents, like water, to pass through it. Permeable membranes are those that let solvent and solutes, like ions and molecules, to pass across it. There are also selectively permeable membranes, i.e., membranes that besides allowing the passage of solvent, let only some specific solutes to pass while blocking others.

The biological activity of sodium and potassium ions depends largely on the fact that they are not uniformly distributed in most cells. In general, the concentration of potassium inside a cell is much higher than sodium, while the reverse is true outside the cell. The asymmetry of ion distribution in a resting cell is disturbed by a fast exchange of sodium and potassium ions upon extraction [22].

TRANSPORT BULK LIQUID MEMBRANE

The most common configuration encountered in artificial transport systems involves a three phase arrangement consisting of two aqueous phases (source and receiving phase) separated by an immiscible membrane phase [14-18]. In the majority of bulk liquid systems, the membrane phase consists of a water immiscible organic solvent such as chloroform, dichloromethane, toluene or hexanol [23-24]. Solvents of this type are capable of solubilising most classes of natural and synthetic ionophores reported so far. As is the case in some natural systems, the driving force for many transport experiments results from the presence of a metal ion concentration gradient between the source and receiving phase. In such a case, the metal ion concentration will initially be higher in the source phase but as transport proceeds, this concentration will drop and that in the receiving phase will rise. Ultimately equilibrium will be reached when the metal ion concentration- in both the source and receiving phases are equal and transport will cease. Under appropriate conditions, transport can also be driven by the back diffusion of a species from the receiving phase to the source phase, a process called exchange diffusion [25].

The membrane phase will normally not permit the diffusion of species contained in the source phase in the absence of an ionophore. Such synthetic membranes thus resemble lipid bilayer membrane (which is impervious to species such as alkali metal ions); however, in the presence of an ionophore, selective transport is exhibited by these membranes [26-27].

In the context of transport behaviour, efficiency is synonymous with high mass transfer of the species being transported. The physical dimensions of a transport cell affect the transport efficiency of a given system. Fig. 1, shows a typical bulk liquid membrane cell.

Efficiency can be enhanced by increasing the interfacial contact area between the aqueous and membrane phases. Another important consideration in bulk liquid membrane (BLM) systems relates to whether the respective phases are stirred (and their stirring rates)

[28]. Typically, in many reported bulk liquid membrane systems, the organic membrane phase was stirred more or less thoroughly using a magnetic spin bar [24]. However, the aqueous phases were either not stirred or stirring was less efficient than in the membrane phase.

If the metal-ion complex of an uncharged ligand such as 18-crown-6 is transported across a hydrophobic ligand membrane, then in order to maintain neutrality, a counter - ion must accompany the complexed cation forming an ion-pair. The nature of the inorganic or organic anion present has been demonstrated to affect the cation flux. The strength of complexation of the cation by the ionophore must neither be too high nor is too low if efficient transport to occur. If the stability is too low, the uptake from the source phase will be inhibited. If complexation is too strong, the cation will not be as readily released into the receiving phase. In both cases, the overall rate of transport will be inhibited [24].

METAL ION TRANSPORT ACROSS SUPPORTED LIQUID MEMBRANE

Analysis of trace metal cations in natural waters i.e., in the concentration range 10^{-2} to 10^{-8} mol/lit despite the availability of very sensitive analytical tools, is still a challenging task. Methods allowing reliable and real time analysis as well as automatic need to be developed for water quality control. Thus, the development of techniques based on preconcentration of specific elements or compounds with minimum sample perturbation and handling, and which can be readily coupled to several type sensitive detectors such as fluorescence, voltametry etc., is of most important. The supported liquid membrane (SLM) is one of the newly emerging tools which is well suited for this purpose [29-34]. It is a separation method in which an organic solvent immiscible in water containing a complexing agent, R, selective towards the target metal (carrier) is immobilized on a thin, macroporous, hydrophobic membrane and interposed between two aqueous phases (Fig. 2). One of the aqueous phases is the source (test) solution containing the metal ion to be transported and the other is the strip solution into which test metal ions are trapped by a complexing agent, L, stronger than R, present. By using strip solution volumes much smaller than the source solution volumes, the analyte can be concentrated. Thus, target elements can be separated and concentrated at the same time in this method which makes SLM a potentially attractive technique for trace element determination [35].

The metal ion transport may be proton driven or counter anion or cation driven (Fig.2). The majority of the works reported in the literature on SLM are based on the proton driven mechanism with most applications being used for industrial separation and recovery of target elements. The advantage of SLM is that metal transport can be done at their natural pH values and no modification of the test medium such as adding an electrolyte is required. SLM can use in various fields, particularly in industrial, clinical, pharmaceutical and environmental fields [36-38]. It has been used, for instance, recovery and enrichment of metals from hydrometallurgical samples [39-40], extraction of noble metals such as Am [41], removal of toxic heavy metals [42], organic pollutants and actinides from waste water [43].

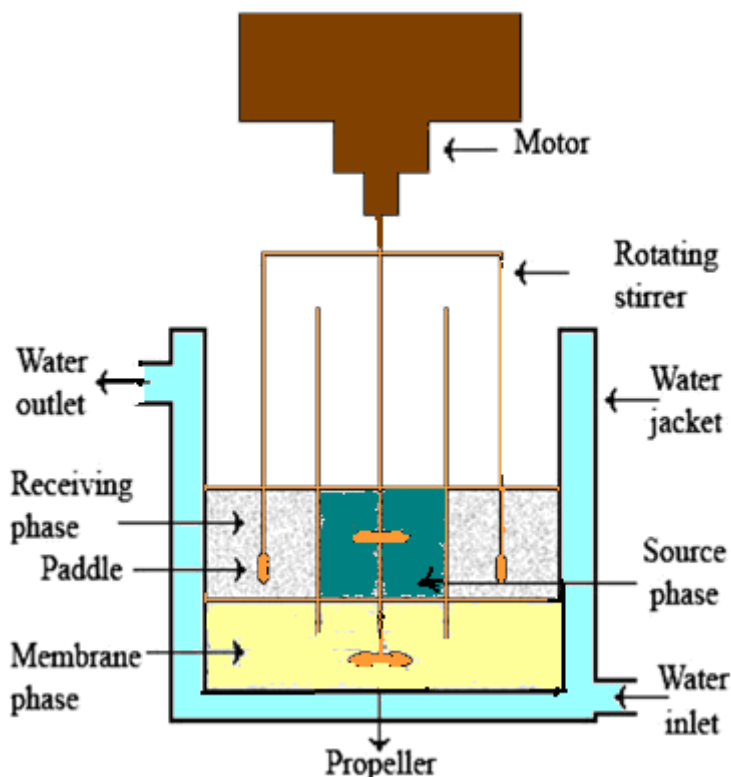


Figure 1. A typical liquid membrane cell.

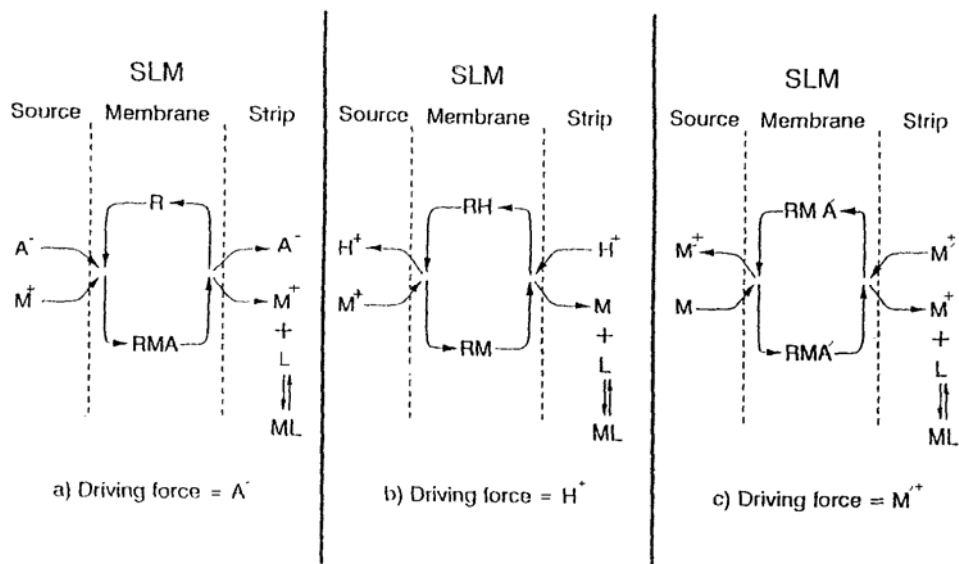


Figure 2. Mechanism of transport of metal ions across supported liquid membrane. A schematic description. Symbols used: RH organic metal ion carrier; A^- = anion in the source solution; M = metal ion in the source solution; M' = metal ions in the strip acting as the counter cation; A' = metal complexing anion in the strip solution.

COMPARISON OF SOME MEMBRANE SYSTEMS

Macrocyclic compounds such as the crown ethers have been the subjects of intensive research in recent years due to their selective interactions with particular cations [44]. One way of exploiting the selectivity of macrocycles to make separations is to use them as cation carriers in liquid membranes. Many researchers have reported the incorporation of several macrocycles into emulsion and bulk liquid membrane [6-10]. Members of the crown ether class of macrocyclic compounds interact selectively with particular alkali metal cations primarily according to the fit of the cation into the crown cavity. This type of selectivity has been observed in homogeneous solution, solvent extraction and liquid membrane systems.

The alkali metal, crown ether size related selectivities observed in bulk liquid membrane (BLM) can also be obtained in the other liquid membrane systems. However, usually the macrocycle structure must be modified before it can be used in the other membranes. Specifically, in order for the crown ether to remain in the membrane phase of these other, membrane types, hydrophobic constituent groups must be added to the macrocyclic backbone. Studies in both the BLM and emulsion liquid membrane (ELM) systems have shown that the addition of alkyl and cycloalkyl substituent groups increase the hydrophobicity of the macrocycle with minimal reduction of its complexing ability. On the other hand, benzoviny, and other electron withdrawing substituent groups reduce macrocycle complexing power. Hence, the alkyl and cycloalkyl substitution is preferred.

DIFFERENT TRANSPORT RATES

Although the use of the same macrocyclic core yields similar selectivity in different membrane systems, changes in solvent, macrocycle hydrophobicity, membrane thickness, volume ratios, membrane surface area and species concentrations can drastically alter the rate of cation transport and/or flux [35]. The transport rates are primarily a function of membrane surface area for which the order is: ELM \gg hollow fiber supported liquid membrane (HFSLM) \gg thin sheet supported liquid membrane (TSSLM) $>$ BLM [25]. The large transport rate in the ELM is particularly impressive when considering the fact that the species concentrations are much lower than in the other systems.

ADVANTAGES AND DISADVANTAGES OF SOME MEMBRANE SYSTEMS

Bulk Liquid Membrane (BLM)

The BLM is an excellent system for screening macrocycle carriers but its utility stops at that point. This statement is supported by the particular advantages and disadvantages of the system. The system requires small amounts of materials. In this system, somewhat hydrophilic membrane solvents and macrocycles can be used. Macrocycle core structures can thus be tested before the more difficult task of synthesizing highly- substituted hydrophobic analogs is undertaken. However, the bulk system is not commercially available, transport

rates are small, relatively large data standard deviations are observed, and it is difficult to sort out surface active effects in the system.

Thin Sheet Supported Liquid Membrane (TSSLM)

This system is easy to model due to the relatively small standard deviations in the data obtained and the regular geometry of the TSSLM. However, there are several disadvantages : transport rates are small; extremely hydrophobic solvents and macrocycles are required; surface effects can foul the transport, and the system is not commercially available.

Emulsion Liquid Membrane (ELM)

This system has a very thin membrane and immense surface area with rapid transport being the result. Surface activity involving any ligands is relatively unimportant since an emulsion is already present. Desired species can be concentrated from the source to the receiving phase because of the ratio of volumes of the two water phases. In order to obtain these advantages, a moderately hydrophobic membrane solvent and macrocycle along with a receiving phase complexing agent must be used. Furthermore, the effect on emulsion stability factors such as pH, ionic strength, and physical factors must be closely monitored. The most important industrial disadvantage of the ELM is the need to break the emulsion to recover the receiving phase.

Hollow Fiber Supported Liquid Membrane (HFSLM)

The surface area and membrane thickness of this system yield rapid transport, although not as rapid as the ELM system. This system has the engineering advantage of easy introduction of source and receiving phases to the system. However, fouling due to surface effects and the necessity of using quite hydrophobic solvents and difficult-to-prepare hydrophobic macrocycles are important disadvantages.

Polymer Inclusion Membrane (PIM)

A major reason for the limited use of SLMs on a large industrial scale is the membrane stability or lifetime, which, in general, is far too low for commercial applications. This is possibly a major motivation for the development of PIM.

In SLM the capillary force or interfacial tension is responsible for the binding of the membrane liquid phase to the supporting pores [45-46]. This form of adhesive force is, however, weak and membrane breakdown can easily occur via several destabilizing mechanisms including lateral shear forces, emulsion formation and leaching of the membrane liquid phase to the aqueous phase, which can be worsened by an osmotic flow [45-46]. In contrast, in PIM, as we have discussed previously, the carrier, plasticizer and base membrane

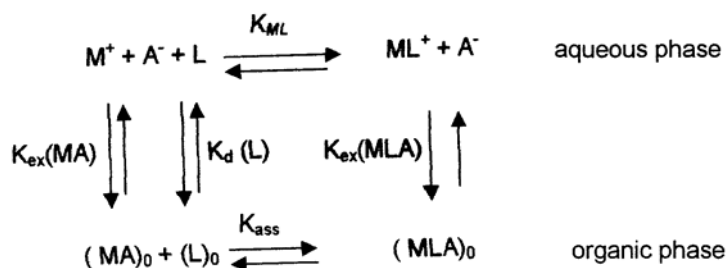
are well integrated into a relatively homogeneous thin film [35]. Although several FTIR studies [47-48] have revealed no signs of covalent bond formation between the carrier, plasticizer and the base membrane skeleton, it is most likely that they are bound to one another by a form of secondary bonding such as hydrophobic, vander Waals or hydrogen bonds. These secondary bonds are much stronger than interfacial tension or capillary forces. Consequently, PIM are considerably more stable than SLM as clearly evidenced in the PIM. Uphill transport of the target solute across the membrane can be achieved with a suitable ionic composition in the source and receiving compartments. However, because of different complexation mechanisms involved, the transport characteristics and choices of the ionic compositions for both the source and receiving phases with respect to each type of carrier are distinctively different. Fig. 3. shows a typical PIM experimental set up.

LIQUID-LIQUID EXTRACTION

Solvent extraction, process based on simple organic complexing extractants are often used commercially for the recovery and purification of metal ions [49]. Although not used commercially, the extraction of metal-ion solutions using macrocyclic ligands has been investigated extensively. Such metal ion extraction depends upon number of parameters. These include ligand structure, the stability of the individual metal/ligand complexes, solvent and the nature of the accompanying anion .

A series of equilibria for solvent extraction of a univalent metal ion (M) using an electrically neutral ligand (L) is shown in Scheme I, where the complex extracted has a composition of 1:1:1 for metal ion, ligand and counter ion [49]. There are two formation processes of a metal ion-ligand complex in aqueous and organic phases. These processes are generally competitive in solvent extraction and depend considerably on the complexing ability of the ligand in the aqueous phase and its hydrophilicity. On the evaluation of the equilibrium constants, therefore, the species formed in both phases should be considered carefully. On the assumption that the complexed salt does not dissociate in the organic phase containing a nonpolar solvent, and that the aqueous and organic solution have an equal volume, the following equilibrium constants are defined as shown in Scheme I.

$$K_{ex}(MA) = [MA]_0 / ([M^+][A^-]) \quad (4)$$



Scheme I

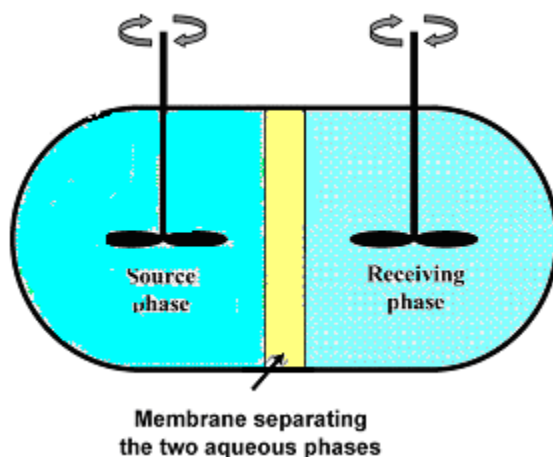


Figure 3. A typical PIM experimental set up.

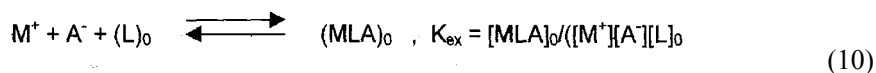
$$K_d(L) = [L]_o / ([L]) \quad (5)$$

$$K_{ass} = [MLA]_o / ([MA]_o [L]_o) \quad (6)$$

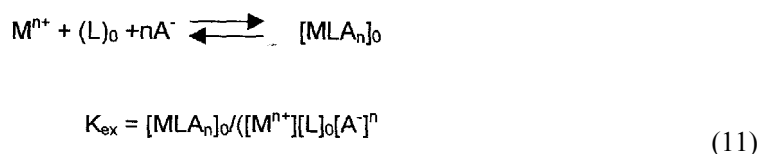
$$K_{ML} = [ML^+] / ([M^+][L]) \quad (7)$$

$$K_{ex}(MLA) = [MLA]_o / ([ML^+][A^-]) \quad (8)$$

where $K_{ex}(MA)$ is the distribution constant of the metal salt between aqueous and organic phases; $K_d(L)$ is the distribution constant of the ligand between aqueous and organic phases; K_{ass} is the association constant of the metal salt with the ligand in the organic phase; K_{ML} is the stability constant of the metal ion-ligand complex in the aqueous phase, $K_{ex}(MLA)$ is the distribution constant of the complex salt between aqueous and organic phases subscript “0” and its lack mean the organic and aqueous phases, respectively, and the brackets denote their concentrations. The above equilibria can be summarized as



or for a system involving M^{n+} ,



Here we assume that no third phase formation and no volume change occurs on mixing the two phases.

BULK LIQUID MEMBRANE TRANSPORT AND PH EFFECT

Cation transport studies are a useful and convenient way to assess ionophore activity within series of ligands. The most useful information that can be obtained from this type of experiment is probably the actual rate at which cations are transported from source to a receiving phase via a suitable membrane.

Membrane can be defined as a barrier that permits the migration of ions across a concentration gradient. This usually involves the presence of a suitable ligand (ionophore) in the membrane which acts as a carrier for the transport of the metal cation across the membrane from the aqueous source phase to the aqueous receiving phase.

A variety of membrane types have been used in metal ion transport experiments [35]. One of the liquid membranes which usually employed for transport studies is bulk liquid membrane immiscible with aqueous phases. When the source and receiving phases are similar, the presence of the ligand in the organic membrane phase will promote the transport of the metal cation until the concentrations in both phases are equal and the system reaches to equilibrium. The transport of metal ions can be driven past the fifty percent equilibrium position by a number of methods. One procedure is to use a proton pump, or pH gradient which operates the back diffusion of protons from the receiving phase into the source phase as shown in Fig. 4.

In the arrangement shown in Fig. 4 the metal ion in the source phase comes into contact with the protonated ionophore at the source phase/ organic phase interface. A neutral complex is formed at this interface and the donor groups on the ligand are deprotonated upon complexation. The metal-ligand complex then diffuses through the organic phase until it comes into contact with the more acidic receiving phase where the metal ion is displaced by protons. The protonated form of the ligand then moves back through the organic phase to repeat the cycle. Typically, both aqueous phases are buffered appropriately in order to maintain the required pH gradient. The direction of the proton transport is in the opposite direction to that of the metal ions and this enables the concentration of the transported ion to exceed the equilibrium concentration.

EXPERIMENTAL REMARKS

The common notations in use nowadays for crown ethers and cryptands like 18- crown-6 and [2.2.2] cryptand have been expended in various ways during recent years to neutral ligands, contain heteroatom other than O and N, aromatic nuclei and chains other than -CH₂-CH₂- [50-52]. Multidentate monocyclic ligands with any type of donor atoms are called coronands (crown compounds), while the term crown ether is reserved for cyclic oligoethers containing oxygen only. Moreover, a subdivision of the coronands, cryptands and podands according- to the number of arms or bridges is demonstrated, whilst the minimum number of donor atoms, chain segments and anchor groups are stated [52].

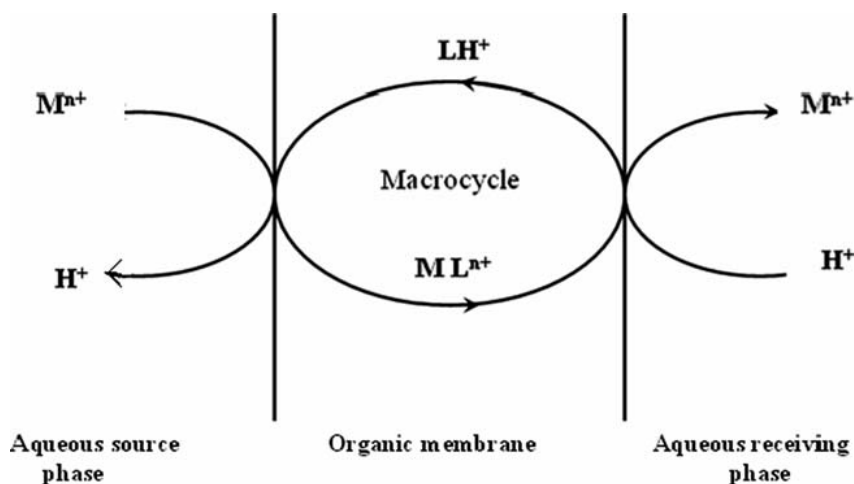


Figure 4. A Schematic representation of the transport of a metal ion-across an organic membrane phase.

Acyclic synthetic ionophores behave very similar to cyclic species and thus should be useful [53-56]. Additions to the available crown ethers and cryptands some acyclic ionospheres having oxygen and sulfur as the binding sites have been studied in connection with the extraction of precious metal ions [57]. Some podands containing larger aromatic group with hetero donor atoms wrap themselves around the cations such as Na^+ and Rb^+ ion in a helical manner to make pseudo cavity in solid and solution states. Podands possessing the sulfur-oxygen and nitrogen mixed donor atoms with the simple aromatic groups, such as phenyl group, have been much less frequently studied. Under these circumstances, L. F. Lindoy et al. [14] have been studied some ligands possessing sulfur and nitrogen atoms with simple moieties such as phenyl (ph) or alkyl groups at all ends (Scheme II), which were as the strong gonophores for Ag(I) ion rather than Co(II), Ni(II), Cu(II), Zn(II), Ag(I), Cd(II) and Pb(II) cations. Under the conditions employed, a common feature of all the studies based on 1–6 is the high transport [58] and solvent extraction [59] selectivity for silver(I) relative to the other six metals presented in the respective source phases. An increase in lipophilicity of the ionophore may also increase the efficiency of uptake of a metal salt from an aqueous source phase but also retard its transfer to the (aqueous) receiving phase. Many of these factors (for example, lipophilicity and thermodynamic stability considerations) will also influence extraction efficiency in corresponding two phase solvent extraction experiments. The selectivity for silver observed across all extraction and transport experiments strongly suggests that the origins of such behaviour in the case of the transport experiments is largely the selective transfer of silver across the source phase/membrane phase interface.

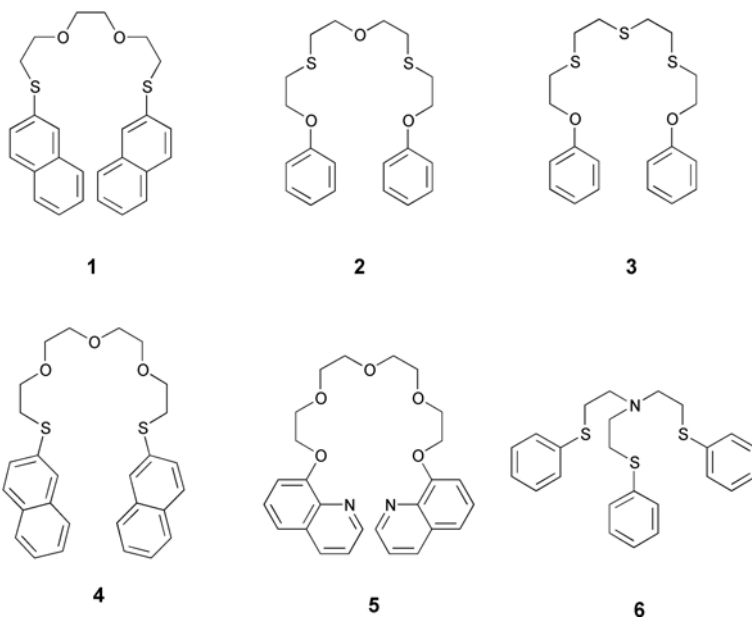
For the mentioned systems the NS3-donor tripodal ligand **6** shows the highest thermodynamic stability for silver [14, 56] and also exhibits the highest extraction efficiency for this ion (a trace of cadmium is also extracted). For this system 42% of the silver originally in the source phase was extracted (given the relative volumes and concentrations of the source and organic phases, the theoretical maximum that might be attained for 1:1 complexation is 50%). Thus, the $\log K$ value for the silver complex appears to dominate in promoting the passage of silver from the aqueous to the organic phase in this case. In contrast, the transport experiment involving **6** yielded a J (transport rate) value for silver ion transport that lies intermediate in the range observed for 1–5 [14, 56]. Such behaviour is perhaps best explained

by assuming that the substantial thermodynamic stability of the silver complex of **6** strongly aids its transfer into the chloroform phase (see above) while simultaneously (partially) inhibiting its loss from the membrane to the aqueous receiving phase. The observed J values for silver ion transport by the remaining ionophores **1–5** show the following order: **2** (S2O3) = **3** (S3O2) > **5** (N2O5) > **1** (S2O2) > **4** (S2O3). All are effective transporters of silver ion into the respective receiving phases with efficiencies that are somewhat higher than found for this ion under similar conditions using mixed nitrogen– sulfur donor macrocyclic ionophores [54]. However, in the absence of additional data concerning such factors as the relative lipophilicity (and associated solvation influences) of these systems and their complex ion species [59] it is difficult to speculate further concerning the origins of the above order.

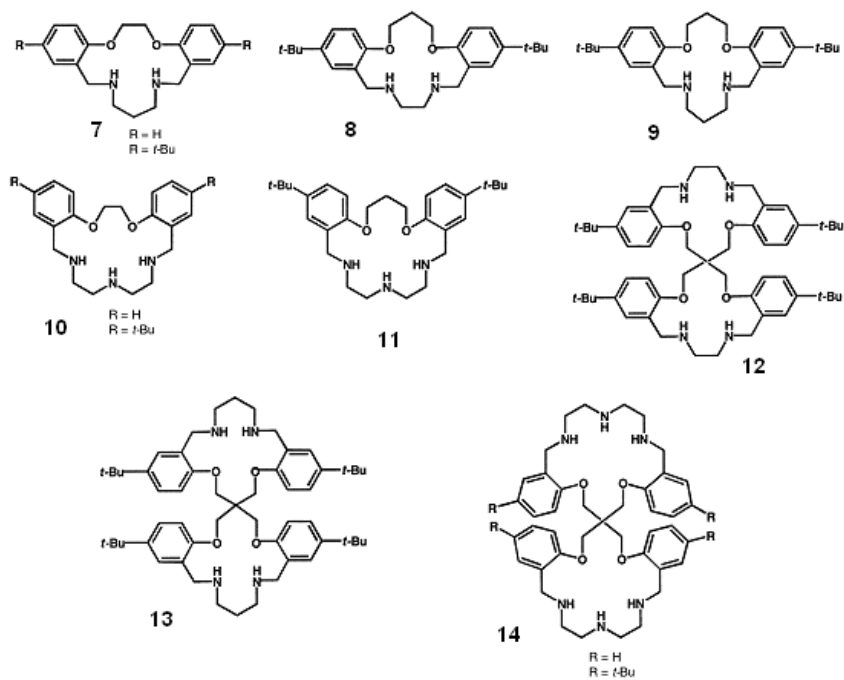
In view of the above, the steady increase in copper(II) transport in a solvent extraction process the selectivity for metal ions depends almost entirely on the difference in the lipophilicity of the corresponding metal complexes. Consequently, the selectivity is usually low and numerous extraction stages are often required to increase the selectivity. This flexibility in process design is, however, not available in membrane extraction systems. A common feature of all the transport studies based on compounds **7–14** (Scheme III) was their clear selectivity for copper (II) relative to the other six metals present in each source phase [15, 59].

Efficiency on passing from compounds **7**(R = H) to **7**(R = *t*-Bu) to **9** appears most likely to be largely a reflection of the increasing lipophilicity along this ligand series rather than any marked change in the inherent metal–donor binding abilities of the respective rings (all form similar 6-membered chelate rings incorporating the amine donors). Comparison of the transport ability of compounds **8** with that of **7** (R = *t*-Bu) indicates that the former is the more efficient ionophore for copper even though both the macrocyclic ring size and the degree of lipophilic substitution is similar for both ligands. The different behaviour apparently reflects the ability of **8** to form a more stable 5-membered chelate ring involving its two nitrogen donors. Indeed, the stability constant for this system [15] indicates that **8** binds copper(II) the most strongly of the O2N2-donor macrocycles of type **7–9**. In each case for transport experiments the values were calculated using the concentration difference between the source and receiving phases at the termination of the experiment (for the metal ions of interest). Owing to the additivity of errors inherent in this process, calculated metal-ion values for the membrane phase of less than 5 percent of the total metal originally present in the source phase were disregarded. Somewhat unexpectedly, a significant amount of nickel(II), between 16 and 20 percent of the total nickel originally present in the source phase, was found in the respective organic phases for each of the O2N2-donor systems investigated. Clearly, nickel is extracted from the source phase but does not cross the organic–receiving phase interface under the conditions employed. This result serves to demonstrate a subtlety that influences competitive metal ion transport in systems of the present type. The thermodynamic binding constants for the nickel(II) complexes of compounds **6–9** are all considerably lower than the corresponding values for copper(II). In view of this, it seems likely that the above ‘partial’ transport (that is, loss of nickel from the source phase) is a reflection of the previously documented relatively sluggish dissociation kinetics observed for nickel complexes of the present type relative to their copper(II) analogues [15]. Behaviour of the above type, in which a metal ion (or metal ions) is kinetically ‘locked’ in the organic membrane phase, appears to have received little attention previously in competitive transport studies[59]. This is somewhat surprising since clearly such partial ‘blockage’ of the

membrane phase has implications for the overall efficiency of the metal ion transport process as well as potential for influencing the observed selectivity pattern. The stability constants for the complexes of compounds **10** (R = H), **10** (R = *t*-Bu) and **11** (all of which incorporate an O₂N₃-donor set) for a given metal show only relatively minor variation, even though all values, as expected, are significantly higher than for the corresponding complexes of the related O₂N₂-donor systems discussed above. In particular, it is noted that, where values were obtainable, the stabilities of the nickel(II) complexes are very similar, as are those observed for the corresponding copper(II) complexes. Comparison of the *J* values for the copper(II) complexes of the 17-membered ring systems **10** (R = H) and **10**(R = *t*-Bu) shows that only a quite minor increase in transport occurs in the latter case [56]. While an increase might be expected because of the additional lipophilicity, the overall effect of appending the *t*-Bu substituents is much attenuated in these larger ring systems. However, closer inspection of the data for the system incorporating **10** (R = *t*-Bu) indicates that the amount of copper remaining in the organic phase (31 percent of the total) is very much higher than that for the system based on the corresponding unsubstituted ring, **10** (R = H) [15]. Thus, in the case of **10** (R = *t*-Bu), the effect of the added lipophilicity is to promote loss of copper from the source phase while inhibiting its loss from the membrane phase. Incorporation of an extra methylene group between the oxygen donors of compound **10** (R = *t*-Bu) to yield **11** leads to an overall decrease in transport efficiency towards copper(II). However, as above, this *t*-butyl derivative promotes retention of copper in the membrane phase (26 percent of the total) so that, while loss of this cation from the source phase is promoted, loss from the membrane phase to the receiving phase is again inhibited. As before, all three membrane phases incorporating the O₂N₃-donor rings of types **10** and **11** were found to incorporate nickel(II) after 24 hours; for these cases the amount of nickel retained ranged from 12 to 17 percent. Comparison of the transport efficiency towards copper(II) of compound **12** with that of **13** shows, as before, that it is the system capable of forming 5-membered chelate rings involving each pair of nitrogen donors (namely **12**) that gives rise to the higher *J* value. The values for nickel in the organic phases were 20 and 14 percent for **12** and **13**, respectively, with the former system also incorporating a small amount of silver (5 percent) in its membrane phase after 24 hours. Since compound **12** is an especially effective ionophore for copper, it was chosen for a parallel solvent extraction experiment in order to provide results that were directly comparable with those from the transport experiment. Identical source and organic phases to those used in the transport experiment were employed. On shaking the buffered (pH 4.9) seven-metal aqueous source phase with the chloroform phase at 25 °C for 24 hours the latter phase was found to have taken up: nickel(II), 17 percent; copper(II), 55 percent; and silver(I), 18 percent of the respective available metal present. Qualitatively, but not quantitatively, this metal-ion uptake is similar to that found in the membrane phase at the completion of the corresponding transport experiment. This result serves to confirm both the similarities (namely, the same metals occur in the organic phase in both experiments) and differences (the concentrations of these metals are not the same, except for nickel which is not lost from the organic phase in the transport runs) arising from the different natures of the solvent extraction and membrane transport experiments.



Scheme II.



Scheme III.

REFERENCES

- [1] Lehn, J. M. (1979). *Pure, Appl. Chem.*, 51, 979.
- [2] Painter, G. R. & Pressman, B. C. (1982). *Top Current Chem.*, 101, 83.
- [3] Cox, B. G. & Scheneider, H. (1992). "Coordination and Transport Properties of Macrocyclic Compounds in Solutions" in *Studies of Physical and Theoretical Chemistry, Vol. 76*, Elsevier.
- [4] Izatt, R. M., Clark, G. A., Bradshaw, J. S. & Christensen, J. (1986). *J. Sep. Purif.*, 15, 21.
- [5] Stein, W. D. & Lieb, W. R. (1986). "Transport and Diffusion Across Cell Membrane," Academic press, New York.
- [6] Pedersen, C. (1988). *J.Incl.Phenom.*, 6, 337.
- [7] Lehn, J. M. (1988). *J.Incl.Phenom.*, 69, 351.
- [8] Cram, D. J. (1988). *J. Incl.Phenom.*, 69, 397.
- [9] Izatt, R. M. & Christensen, J. J. (1987). Synthesis of Mcrocycles, the Design of selective complexing Agents ", *John Wiley*, New York.
- [10] Sutherl, I. O. (1986). *Chem.Soc.Rev.*, 15963.
- [11] Lehn, J. M. (1985). *Science*, 227, 849.
- [12] Rebek, J. (1984). *Acc.Chem.Res.*, 17, 258.
- [13] Lee, S. S., Il Yoon, K. M., Park, J., Jung; H., Lindoy, L. F., Nezhadali, A. & Gh. Rounaghi, (2002). *J. Chem. Soc., Dalton Trans.*, 2180.
- [14] Kim, J., Leong, A. J., Lindoy, L. F., Kim, J. Nachbaur, J., Nezhadali, A., Rounaghi, Gh. & Wei,G. (2000). *J. Chem. Soc., Dalton Trans.*, 3453.
- [15] Melnikova, M. F., Nezhadali, A., Gh. Rounaghi; McMurtrie, J. C., Kim, J., Gloe, K., Langer, M., Lee, S. S., Lindoy, L. F. Nishimura, T., Min Park, K. & Seo, J. (2004). *J. Dalton Trans.*, 122.
- [16] Nezhadali, A. (2006). *J. Incl. Phenom.*, 54, 307.
- [17] Izatt, R. M., Bradshaw, J. S., Nielsen, S. A. & Lamb, J. D. (1985). *J. Christensen and D. Sen, Chem. Rev.*, 85, 271.
- [18] Nezhadali, A., Hosseini, H.A. & Langara, P. (2009). *Polish J. Chem.* 83, 573.
- [19] Lamb, J. D., Christensen, J. J., Izatt, S. R., Bedke, K., Astin, M. S. & Izatt, R. M. (1980). *J. Am.Chem.Soc.*, 102, 3399.
- [20] Smith, R. M. & Martell, A. E. (1976). "Critical Stability Constants", *vol. 4*, Plenum press, New York.
- [21] Ctloch, P. B. & Titus, E. O. (1973). "In Progress in Inorg. Chemistry, Ed. S. J. Lippard, John Wiley and Sons, Toronto, 18, 287.
- [22] Lindoy, L. F. & Baldwin, D. S. (1989). *Pure Appl. Chem.*, 61, 909.
- [23] Ronaghi, Gh & Khoshnood, R. S. (2006). *J. Incl. Phenom.*, 55, 309.
- [24] Leong, A. J. (1994). Ph.D Thesis, James Cook University.
- [25] Nezhadali, A. (2008). *Chemistry*, 4, 286.
- [26] Nezhadali, A. & Akbarpour, M. (2008). *E- J. Chem.*, 5, 271.
- [27] Nezhadali, A. Hakimi, & M. Hydari, (2008). *E-J. Chem.* 5, 52.
- [28] Fyles, T. M. & Hansen, S. P. (1988). *Can. J. Chem.*, 66, 1445.
- [29] Izatt; R. M., Clark, C. A., Bradshaw; J. S., Lamb, J. D. & J. Christensen, (1986). *Pure Appl.Chem.*, 58, 1453.

- [30] Jonsson, J. A. & Mathiasson, L. *Trends Anal Chem.*, 11, 106.
- [31] Nijenhuis, W. F., de Jong, F. & Reinhoudt, D. N. (1993). *Red Tray. Pays-Base*, 112, 317.
- [32] Parthasarathy, N. & Buffle, J. (1991). *Anal. Chim. Acta*, 254, 9.
- [33] Cox, J. A., Bhatnagar, A. & Francis, R. W. (1990). *Talanta*, 37, 1037.
- [34] Long Nghiem, D., Patrick, M., Ian, D., Jilka, M. P., Robert, W. C. & Spas, D. K. (2006). *J. Membr. Sci.*, 281, 7.
- [35] Papantoni, M., Djane, N. K., Ndunga, K., Jonsson, J. A. & Mathiasson, L. (1995). *Analyst*, 120, 1471.
- [36] Parthasarathy, N. & Buffle, J. (1994). *Anal. Chim. Acta*, 284, 649.
- [37] Noble, R. D. & Way, J. D. (Eds.), (1987). *Liquid Membrane, Theory and Applications*, ACS Symp. Ser., vol. 347, American Chemical Society, Washington DC.
- [38] Danesi, P. R. (1984). *J. Membr. Sci.*, 20, 231.
- [39] Dnesi, P. R., Rechley-Yinger, L., Cianetti, C. & Rickert, P. G. (1984). *Solv. Extr. Ion Exch.*, 2, 781.
- [40] Alexander, P. R. & Callahan, R. W. (1987). *J. Membr. Sci.*, 35, 67.
- [41] Takeuchi, H., Takashashi, K. & Nakano, M. N. (1990). *Water Treat.*, 5, 222.
- [42] Muscatello, A. C., Nanrati, J. D. N. & Price, Y. M. (1987). *ACS Symp. Ser.*, 162,.
- [43] Izatt, R. M., Lamb, J. D. & Bruning, R. L. (1988). *Sep. Sci. Technol.*, 23, 1645.
- [44] Kemperman, A. J. B., Bargeman, D., vandenBoomgaard, T. & Strathmann, H. (1996). *Sep. Sci. Technol.*, 31, 2733.
- [45] Danesi, P. R., Reichley-Yinger, L. & Rickert, P. G. (1987). *J. Membr. Sci.*, 31, 117.
- [46] Gherrou, A., Kerdjoudj, H., Molinari, R., Seta, P. & Drioli, E. (2004). *J. Membr. Sci.*, 228, 149.
- [47] Arous, O., Kerdjoudj, H. & Seta, P. (2004). *J. Membr. Sci.*, 241, 177,.
- [48] Dalton, O. R. F. (1977). Canadian Mining and Metallurgical Bulletin, In: Buncel, E., Shin, H. S., Bannard, R. A. B., Purdon, J. G., & Cox, B. G. (1984). *Talanta*, 31, 585.
- [49] Curtis, N. F. (1968). *Coord. Chem. Rev.*, 3, 3.
- [50] Pedersen, C. J. & Frensdorff, H. K. (1972). *Angew. Chem.*, 84, 16.
- [51] Weber, E. & Vogtle, F. (1980). *Inorg. Chim. Acta*, 45, L65.
- [52] Chowdhury, A. & Kamada, S. (1994). *Chem. Lett.*, 589.
- [53] Nezhadali, A., Hakimi, M. & Naemi, A. (2008). *Asian J. Chem.* 20, 1451.
- [54] Nezhadali, A., Langara, & P. Hosseini, H. A. (2008). *J. Chin. Chem. Soc.* 55, 271.
- [55] Zamani, H. A., Nezhadali, A. & Saghravanian, M. (2008). *Anal. Letters*, 41, 2727.
- [56] Tavakoli, L., Yamini, Y., Ebrahimzadeh, H., Nezhadali, A., Shariati, S. & Nourmohammadian, F. (2008). *J. Hazardous Mater.* 152, 737.
- [57] Bushmann, H. J. & Schollmeyer, E. (2000). *Inorg. Chem. Acta*, 298, 120.
- [58] Chartres, J. D., Groth, A. M., Lindoy, L. F. & Meehan, G. V. (2002). *J. Chem. Soc., Dalton Trans.*, 371.
- [59] Nezhadali, A. (2000). Ph. D Thesis, Ferdowsi University and The University of Sydney.

Chapter 11

CHIRAL CALIXARENES

Abdulkadir Sirit^a, Mustafa Yilmaz^a and Richard A. Bartsch^b

^aDepartment of Chemistry, Selçuk University, 42099 Konya, Turkey.

^bDepartment of Chemistry and Biochemistry, Texas Tech University, Lubbock, Texas 79409-1061, USA.

ABSTRACT

The development of calixarene-based host molecules containing chiral residues at either the lower or the upper rims of the calixarene macrocyclic ring is reviewed in this chapter. These supramolecular models are of particular significance for understanding the interactions between biological molecules, design of asymmetric catalysis systems, development of new pharmaceutical agents, and analysis and separation of enantiomers.

Keywords: Chiral calixarene, molecular recognition

INTRODUCTION

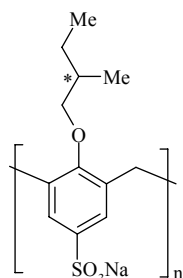
The design and synthesis of calixarene-based chiral macromolecules[1-3] is of interest in many areas of chemistry and biochemistry, including the separation, analysis and preparation of enantioselective receptors, asymmetric catalysts, biologically active molecules, additives in capillary electrophoresis, chiral stationary phases for GC and HPLC and chiral solvating agents for NMR spectroscopy.

Two principal approaches can be used to prepare chiral calixarenes: The first is the synthesis of ‘inherently’ chiral calixarenes that are built up of achiral moieties and consequently owe their chirality only to the fact that the calixarene molecule is not planar. In the literature, several strategies, including fragment condensation, and regio- and stereoselective functionalization at the lower rim, have been reported for the preparation of inherently chiral calixarenes. The second approach is the attachment of a chiral moiety to the upper or lower rim of calixarene macrocycle.

From a practical point of view, the second approach is preferable. Enantiomerically pure derivatives can be obtained relatively easily without racemization if homochiral reagents are used. The inherently chiral calixarenes generally require more complex synthetic procedures and a difficult resolution on an appropriate scale

This chapter describes the developments in the design, synthesis and applications of chiral calixarenes bearing enantiomerically pure substituents and is organized according to the type of chiral unit attached to the calixarene framework in the synthesis of chiral calixarene.

One of the earliest examples is a chiral calix[6]arene derivative **2** reported by Shinkai and coworkers in 1987 from the reaction of (*S*)-1-bromo-2-methylbutane with calix[6]arene-*p*-hexasulphonate [4,5]. Since that time, a number of research groups have incorporated various chiral residues at either the upper or lower rims of the calixarene macrocyclic ring.



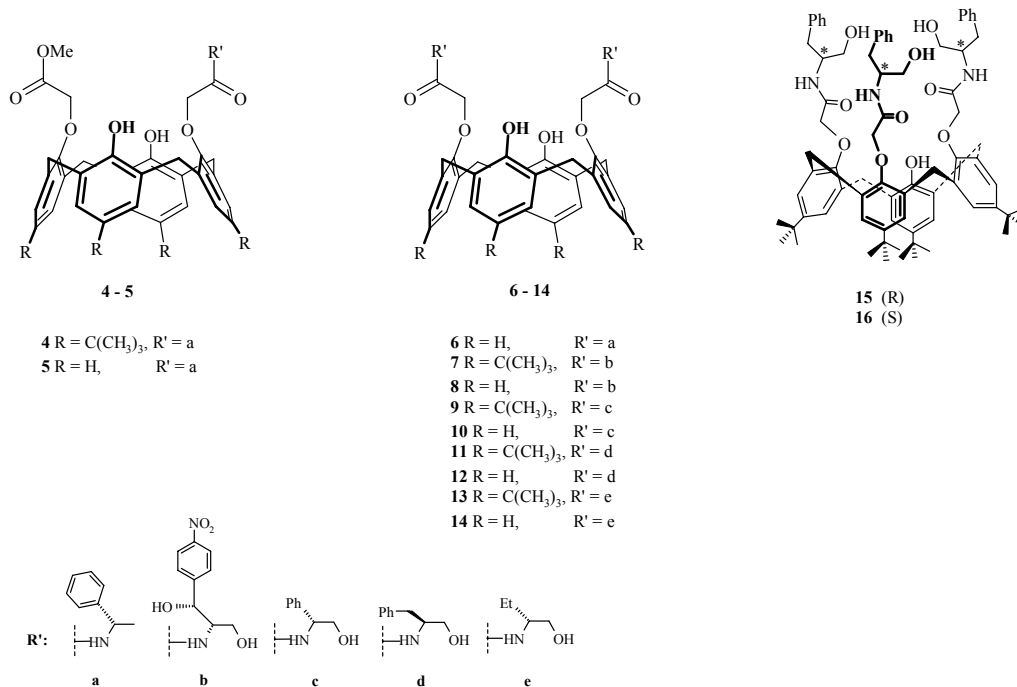
1 $n = 4$
2 $n = 6$
3 $n = 8$

To date only a few reviews and monograph chapters [6-14] have appeared in the literature describing the synthesis, properties and applications of chiral calixarenes. Among the most popular chiral building blocks employed are amino acids, peptides, amino alcohols, sugars, tartaric acid esters, binaphthyl, glycidyl, menthone, and guanidinium groups which offer a wide range of possibilities for providing calix[4]arenes with asymmetric features.

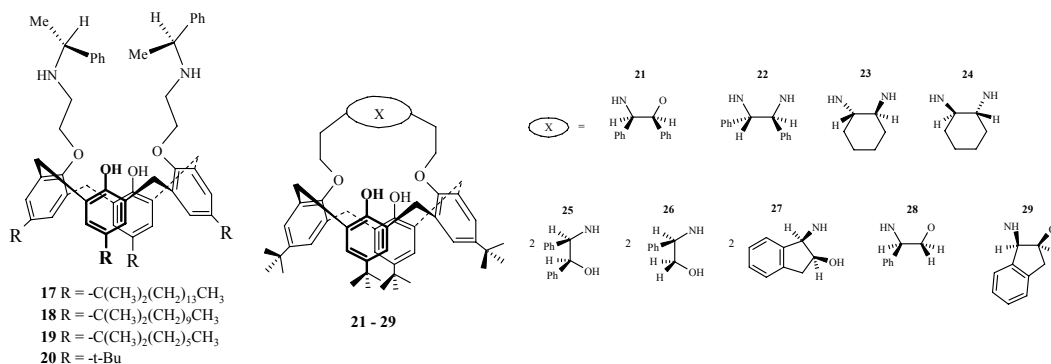
AMINES AND AMINO ALCOHOLS

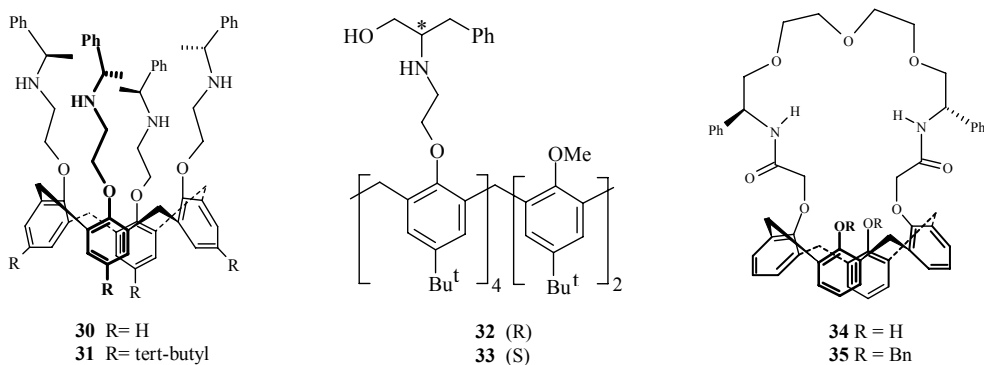
Many approaches have been developed with chiral amino alcohols and amines as chiral sources. Chiral mono-, di- and triamide derivatives **4-16** of calix[4]arene have been constructed by the aminolysis reaction of calix[4]arene esters with primary amines or amino alcohols [15-17]. Receptors **4-14** exhibited different chiral recognition abilities towards the enantiomers of racemic amines due to hydrogen bonding, as well as π - π interactions. Appreciably larger *K* values were obtained for chiral receptors **7-14**, which also bear an -OH group. Such supplemental functional groups seem to provide for better complexation and chiral recognition due to hydrogen bonding with -OH groups. It appears that chiral calix[4]arenes must interact with minimum of three possible recognition groups (carbonyl oxygen, amide nitrogen, phenoxy oxygen, phenyl group, and hydroxy groups) in order to exhibit enantioselective binding with chiral amines. The extraction properties of compounds

9-14 toward selected α -amino acid methyl esters were also studied in a liquid-liquid extraction system.

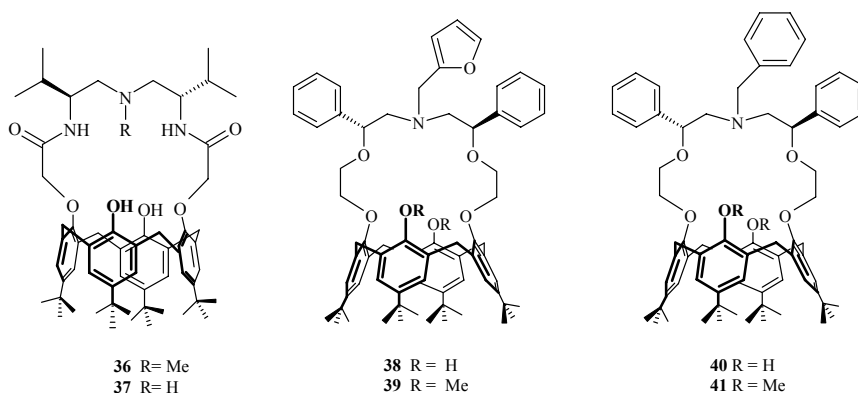


Starting with the bromo and tosyl derivatives, a series of chiral nitrogen-containing calix[n]arene and calix[4]crown derivatives were prepared bearing optically pure amine, 1,2-diphenyl-1,2-oxyamino, α,β -amino alcohol or α,β -diamine groups at the lower rim [18-23]. Chiral receptors **20**, **21** and **25** showed good to excellent chiral recognition abilities towards the enantiomers of mandelic acid, dibenzoyltartaric acid and 2-hydroxy-3-methylbutyric acid; whereas calix[4]arenes **17-19** with long tertiary alkyl groups at the upper rim and (*S*)-1-phenylethylamine groups on the lower rim can form heat-set gels and egg-like vesicles enantioselectively with *D*-2,3-dibenzoyltartaric acid. This was the first example of heat-set gels resulting from a difference in interaction between two component gelators [24].

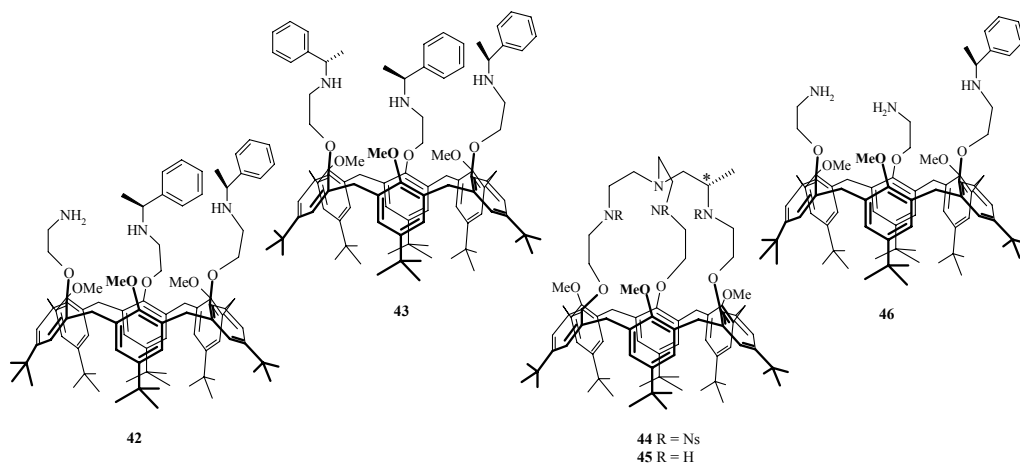




Similarly chiral calix[4](azoxa)crown ethers and calix[4](aza)crowns were synthesized by reaction of diacid chloride or dibromo derivatives of calix[4]arene with chiral diamines derived from (*R*)-phenyl glycine [25,26], L-valine [27] and (*R*)-styrene oxide [28–29] as chiral sources. In liquid–liquid extraction experiments, compound **35** exhibited selectivity for Li^+ among the alkali metal cations and a good extraction ability for transition metal cations, suggesting its potential use in different fields, such as a sensor for ions as well as for chiral molecules. The chiral recognition ability of the receptors has been studied by ^1H and ^{13}C NMR, and UV spectrophotometry. Compounds **36** and **38–41** showed strong binding and different chiral recognition abilities for the enantiomers of racemic carboxylic acids and α -amino acid esters respectively. The results indicate that the multiple hydrogen bonding, steric hindrance, structural rigidity or flexibility and π – π stacking between the aromatic groups may be responsible for the enantiomeric recognition

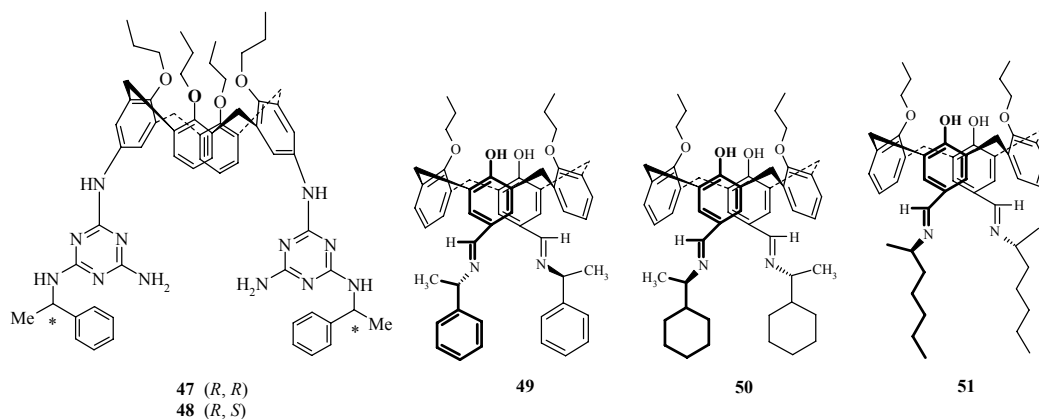


Jabin and coworkers first reported the synthesis of enantiopure calix[6]aza-cryptands from 1,3,5-tris-*O*-methylated calix[6]arene [30]. NMR studies showed that the tetra protonated derivative **44.4H⁺** displayed remarkable host–guest properties towards polar neutral molecules and enantioselective recognition with chiral guests. Similarly optically pure calix[6]arenes **42**, **43** and **46** with chiral amine arms were synthesized in high yields from the known symmetrically 1,3,5-trismethylated calix[6]arene [31]. The chiral derivative **46** undergoes a conformational change with the three ammonium arms forming a tris-cationic chiral binding site which caps the cavity. The obtained polarized host (**46.3H⁺**) thus obtained behaved as a remarkable endo-receptor for small polar neutral molecules.



In their efforts to synthesize the chiral dimelamine derivatives **47** and **48** of calix[4]arene Timmerman, Reinhoudt and coworkers started with the reaction of diamino calix[4]arene with cyanurichloride, followed by stepwise substitution of the remaining chlorine atoms by ammonia and (*R*)- or (*S*)-methylbenzylamine in several steps [32,33].

Chiral Schiff base calix[4]arene derivatives **49–51** were prepared by the condensation of a calix[4]arene dialdehyde and the chiral amines in high yields [34]. Chiral receptor **50** showed enantioselective recognition ability toward (*R*)- and (*S*)-phenylethylamine (up to $K_R/K_S = 2.67$) among all of the chiral hosts studied. More stable complexes were obtained with *n*-butylamine compared with 3-morpholinopropylamine. The results revealed that the size/shape-fit concept plays a crucial role in the formation of inclusion complexes of host compounds with guest molecules of various structures.

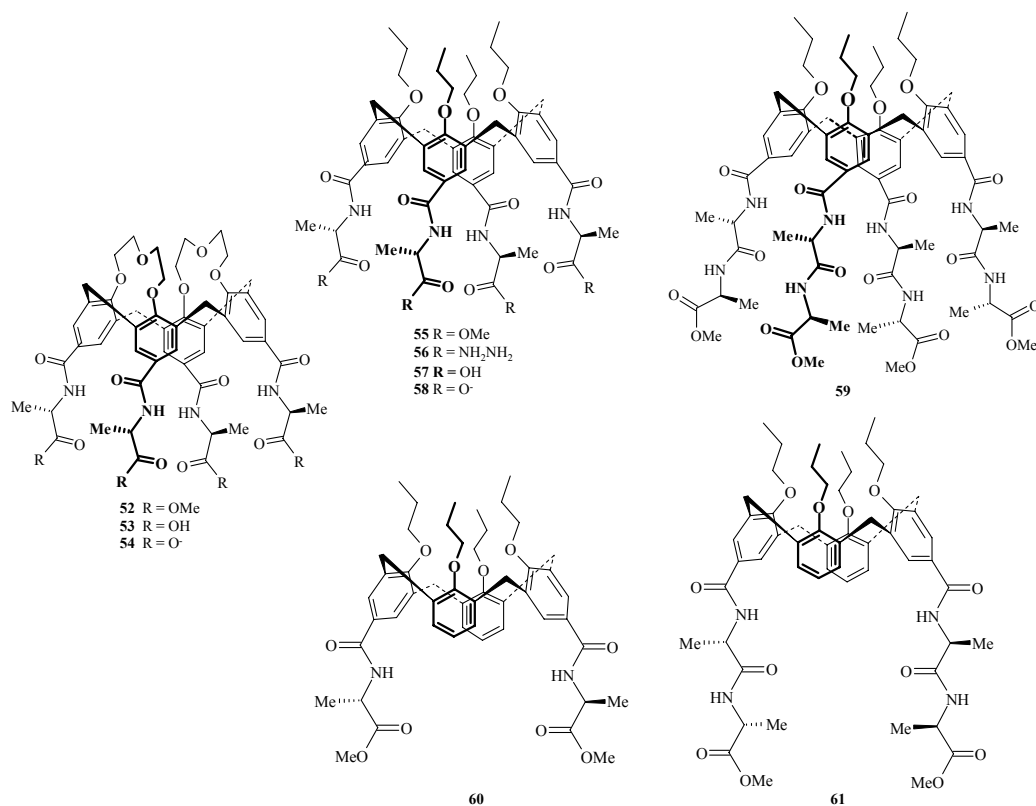


AMINO ACID DERIVATIVES AND PEPTIDES

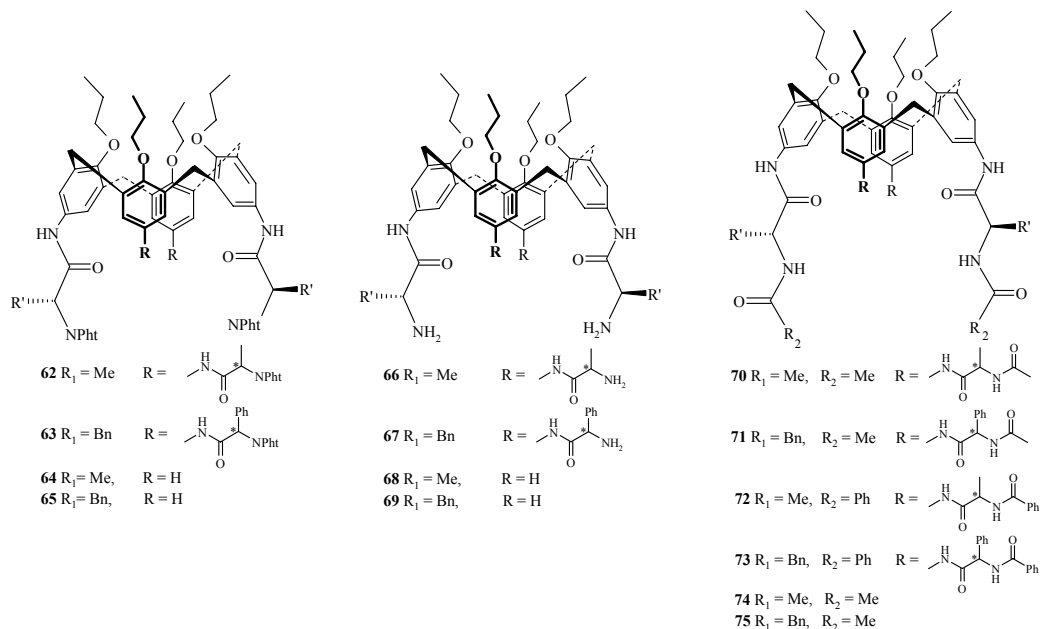
Due to the pivotal role of peptide hydrogen bonds in biological systems, considerable effort has been devoted to the design and synthesis of calixarene derivatives containing optically active amino acids and peptides. Attachment of amino acids or peptides to a

calixarene framework can be achieved through the terminal amine or carboxylic acid groups [35].

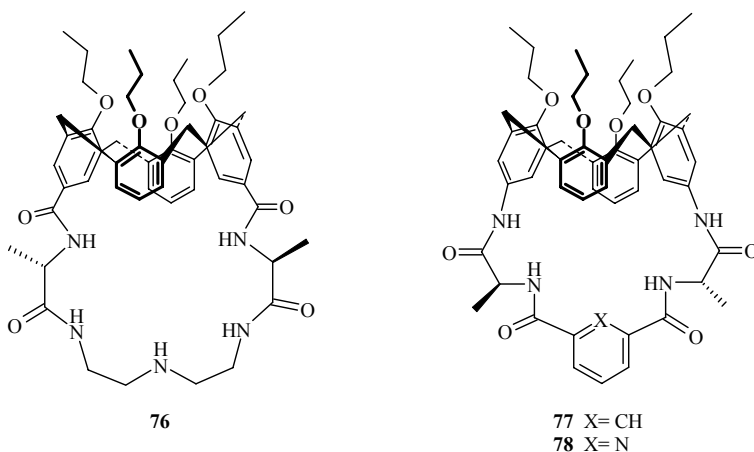
Ungaro and coworkers reported the synthesis and inclusion properties of new chiral hosts **52-61**, with two or four *L*-alanine or *L*-alanyl-*L*-alanine units on the upper rim *N*-linked calix[4]arenes [36,37]. Water soluble peptidocalix[4]arenes **54** and **58** exhibited noticeable recognition ability toward amino acids and aromatic ammonium cations. A remarkable influence of the rigidity of the calix[4]arene platform in determining the recognition properties of mobile **54** and rigid cone **58** water soluble peptidocalix[4]arene receptors was observed.



The same group has also described the synthesis and recognition properties of upper rim C-linked peptidocalix[4]arenes **62-75** with two or four *L*-alanine or *L*-phenylalanine units. These compounds represent a novel class of chiral receptors in that the amino acid units are linked to the calix[4]arene platform through their carboxy groups rather than through nitrogen as in all previously described *N*-linked peptidocalix[4]arenes [38,39].

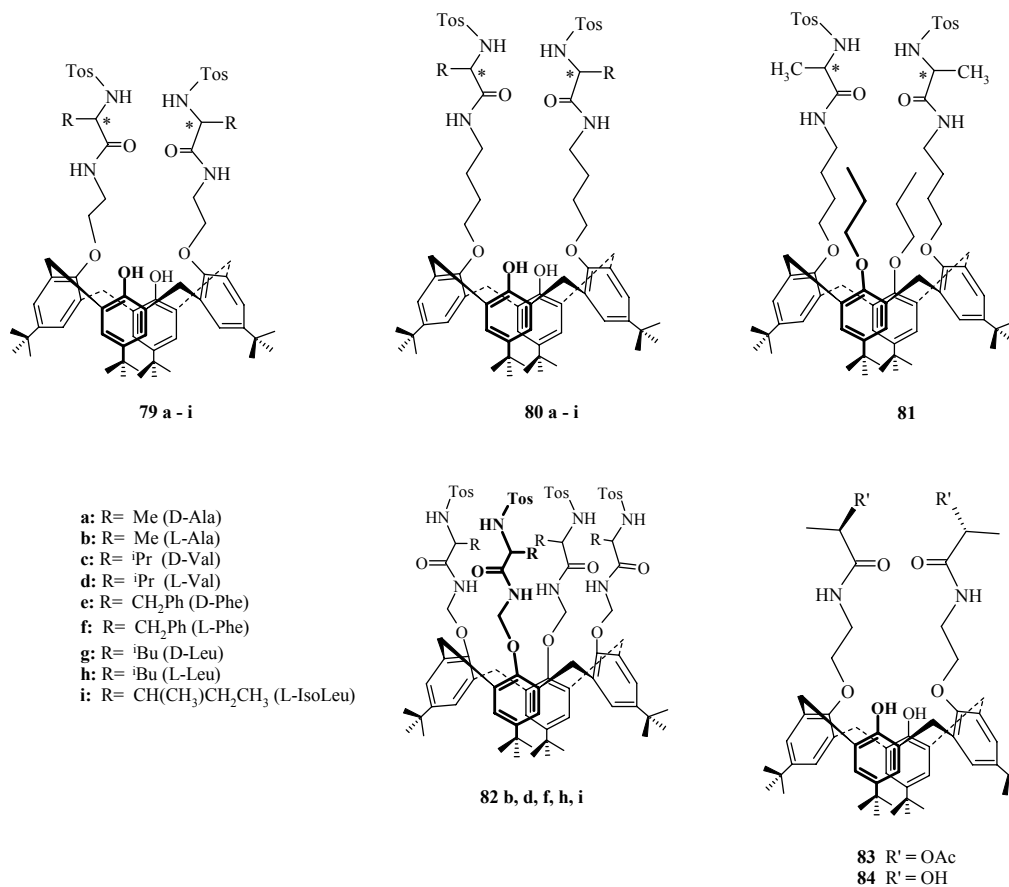


Interestingly, some of the upper rim bridged *N*-linked peptidocalix[4]arenes (e.g., **76**) behaved as vancomycin mimics and showed promising antibiotic activity toward Gram-positive bacterial strains as a consequence of their ability to bind the *D*-alanyl-*D*-alanine (*D*-ala-*D*-ala) terminal portions of peptoglycans [40,41]. The two neutral macrobicyclic anion receptors **77** and **78** displayed good complexation ability for carboxylate anions [42].

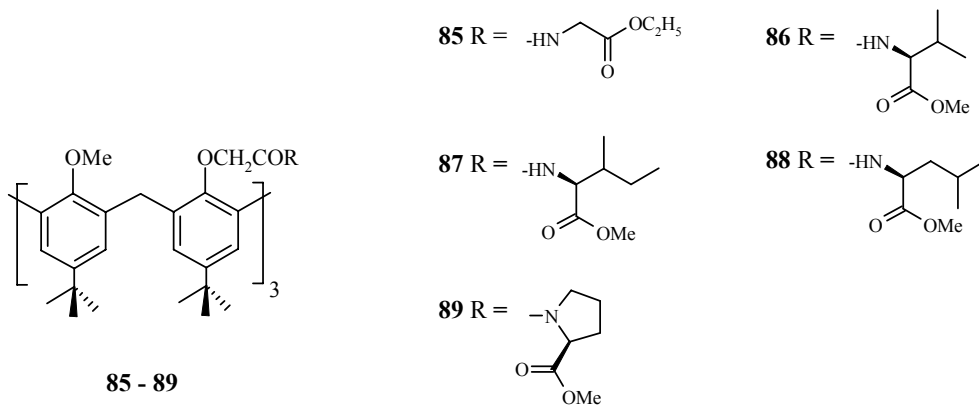


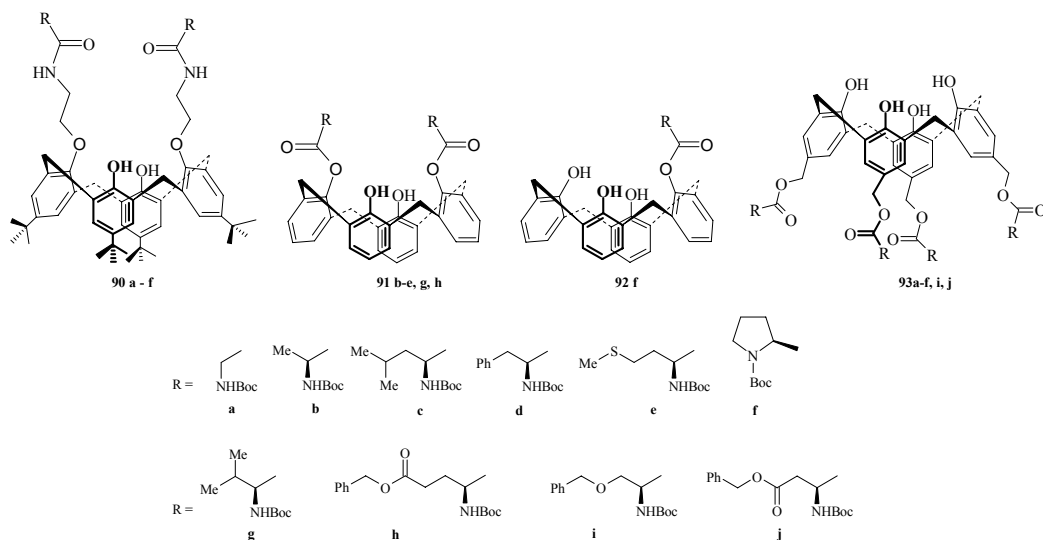
A range of chiral calix[4]arenes functionalized on the lower rim with α -hydroxyamide and amino acid groups have been prepared as a class of receptors selective for anions that are bound through hydrogen bonding with the NH group [43-45]. It was found that the calix[4]arene derivatives **79-81** and **84** might be suitable for the synthesis of hydrophobic neutral anion receptors which are able to bind anions in a 1:1 stoichiometry through hydrogen

bonding. High binding constants are observed and the better selectivity was obtained for *N*-tosyl-*L*-alaninate presumably due to additional π - π interactions between the tosyl groups.

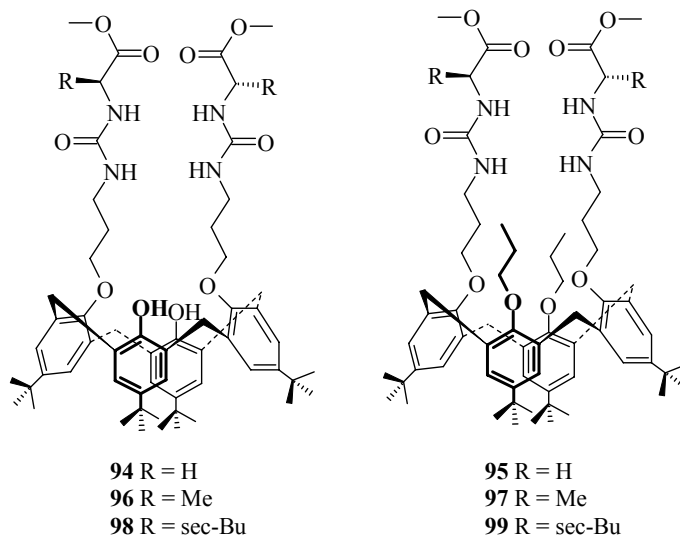


Huang and coworkers synthesized [46,47] a series of the calixarene amide (**85-90**) and ester (**91-93**) derivatives by reaction of calix[*n*]arenes or their diamino derivatives with *N*-Boc-*L*-amino acids or *N*-chloroacetyl amino acid ester.

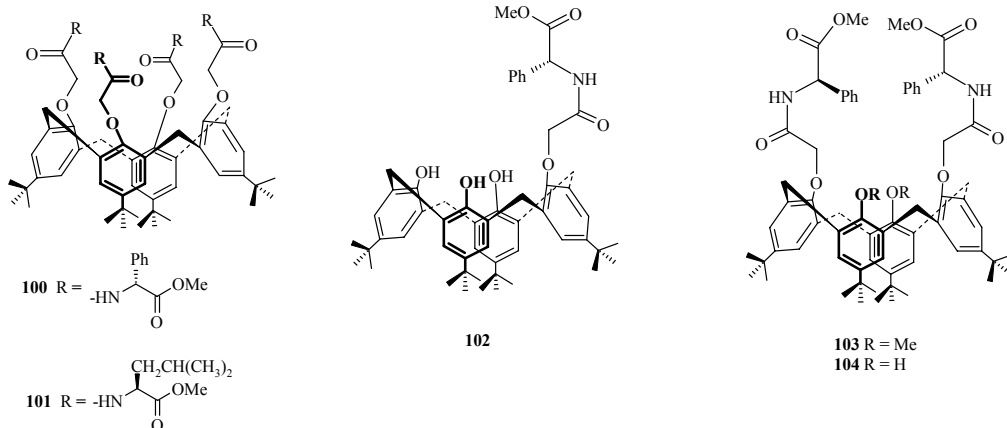




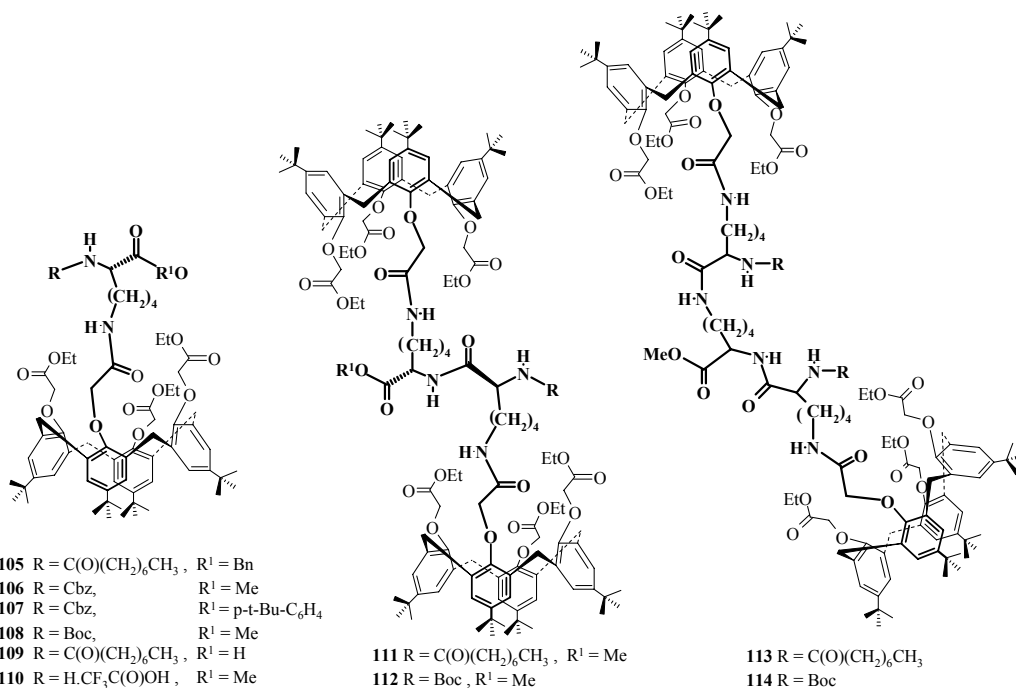
Bisurea calix[4]arene-based receptors **94-99** possessing amino acid moieties were obtained by nucleophilic addition reactions of the methyl esters of glycine, *L*-alanine, or *L*-isoleucine with isocyanatocalix[4]arenes. Ligand **97** with alanine residues close to the urea binding groups showed a remarkable ability to distinguish *D*-*N*-acetylphenylalaninate from the corresponding *L*-isomer [48].



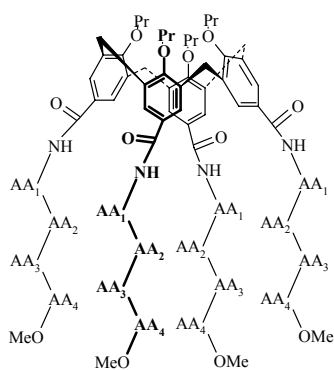
In other work, mono, di and tetrasubstituted chiral calix[4]arene derivatives **100-104** with amino acid residues on the lower rims were prepared to probe for possible hydrogen-bonding motifs with OH and amidic functions [49].



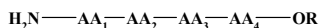
In 2003, Xu and coworkers [50] described the design and synthesis of calix[4]arene amino acids **105-110**, which were used as building blocks for assembling nanoscale, multivalent entity calix-peptides **111**, **112** and calix-peptide-dendrimers **113**, **114**.



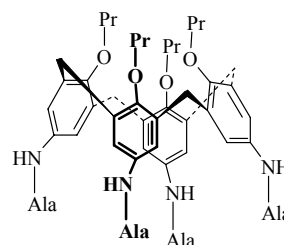
N-linked tetrapeptidocalix[4]arene derivatives **115-131** were prepared by coupling a cone calix[4]arene tetracarboxylic acid chloride with tetrapeptides [51,52]. The inhibition activity of tetrapeptidocalix[4]arenes **115-130** towards tissue and microbial transglutaminase was evaluated by in vitro assays with a labeled substrate.



115 - 130

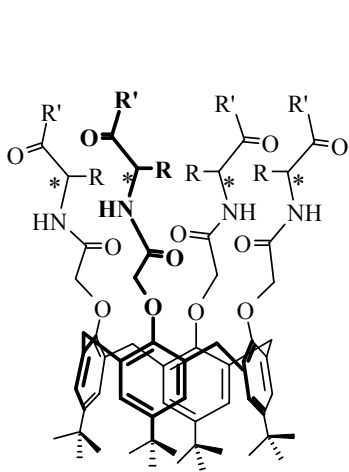


115	Gly—Phe—Gly—Tyr
116	Gly—Gly—Phe—Asp
117	Gly—Leu—Gly—Lys
118	Gly—Val—Phe—Tyr
119	Gly—Phe—Val—Tyr
120	Gly—Trp—Ala—Tyr
121	Gly—Ala—Leu—Tyr
122	Gly—Yrp—Ala—Tyr
123	Gly—Phe—Gly—Phe
124	Gly—Phe—Leu—Phe
125	Gly—Val—Leu—Phe
126	Gly—Leu—Val—Phe
127	Gly—Phe—Val—Phe
128	Gly—Leu—Phe—Phe
129	Gly—Val—Phe—Phe
130	Gly—Leu—Gly—Phe

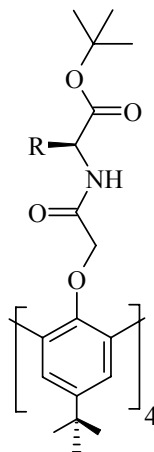
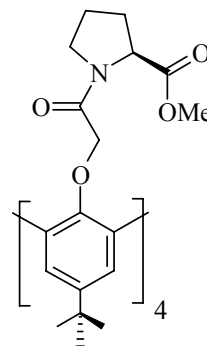


131

Warner coworkers described the first chiral separations of three binaphthyl derivatives (BNHP, BINOL, and BNA) using (*N*-*L*-alaninoacyl)calix[4]arene (**132**) and (*N*-*L*-valinoacyl)calix[4]arene (**133**) as pseudostationary phases in capillary electrophoresis [53,54]. All three binaphthyl derivatives were baseline resolved when chiral selector **133** or a mixture of sodium dodecyl sulfate and **132** was used as an additive to the buffer. The results showed an optimum buffer pH of 11, and concentration of 40 mM Na₂HPO₄ for the separation.

132 R = CH(CH₃)₂; R' = OH

133 R = Me; R' = OH

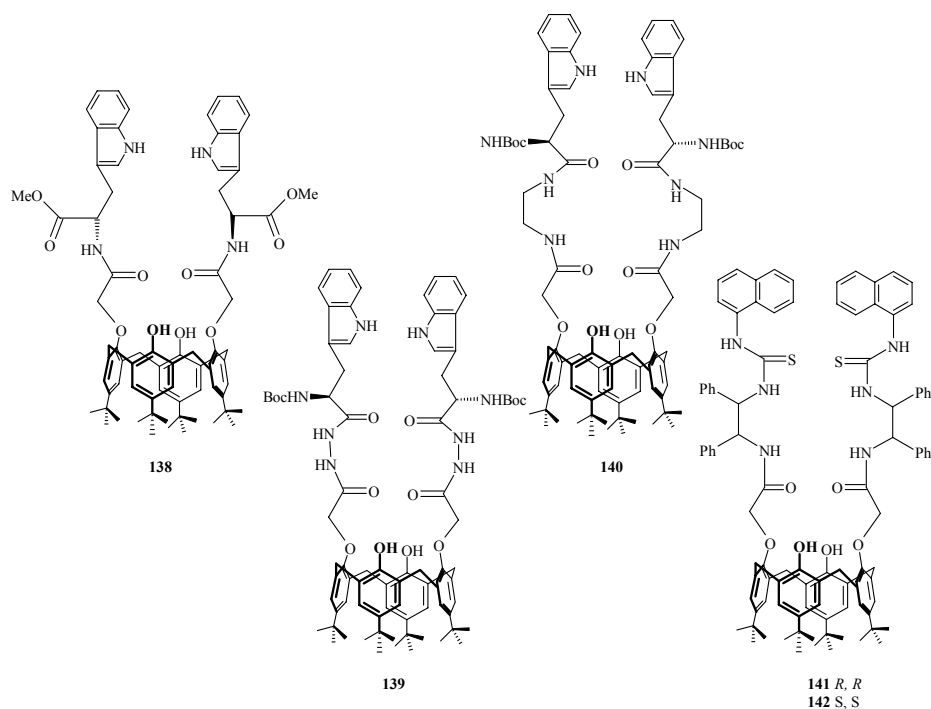
134 R = -CH₃135 R = -CH(CH₃)₂136 R = -CH₂CH(CH₃)₂

137

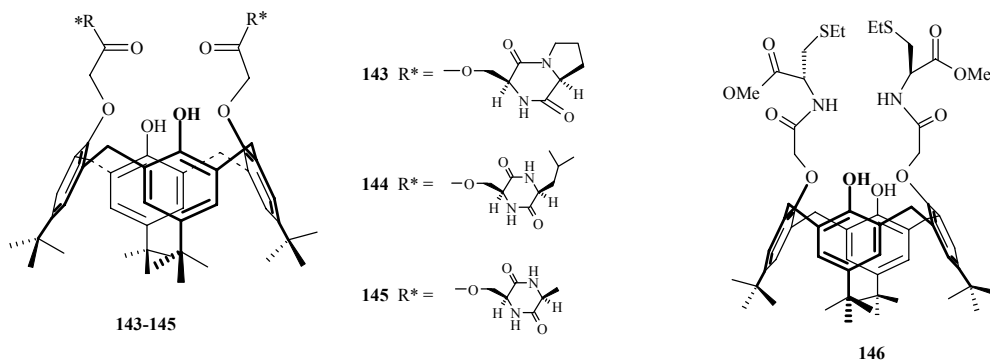
Wenzel coworkers [55] reported the synthesis of chiral calix[4]arenes **132-137** by attaching optically pure amino acid esters of alanine, valine, leucine, and proline through the hydroxyl groups of the phenol rings and examined as chiral solvating agents in NMR spectroscopy.

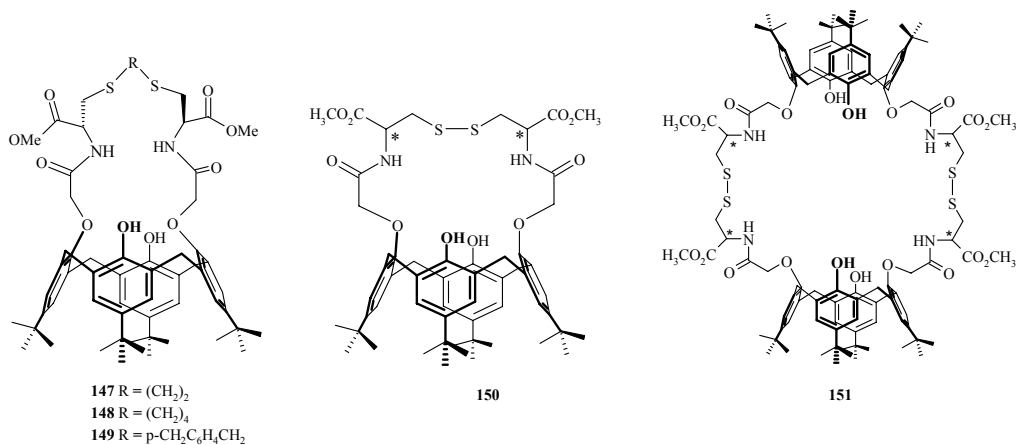
Chiral fluorescence calix[4]arenes **138-142** functionalized on the lower rim with *L*-tryptophan or diphenylethylenediamine units have been prepared by He and coworkers [56,57]. The enantioselective recognition of these receptors towards a series of chiral carboxylates was studied by fluorescence titration and ¹H NMR spectroscopy. Receptors **138**

and **139** were found to be highly selective fluorescent sensors for *N*-Boc-protected alanine and mandelate anion respectively. Receptors **141** and **142** exhibited good enantioselective fluorescent responses for phenylglycinol (up to $K_I/K_D = 4.85$, $\Delta\Delta G_0 = -3.90$ kJ mol⁻¹). According to the results, a relatively rigid structure, good structural preorganization, steric effects, π - π stacking and multiple hydrogen bonds induced the enantioselective recognition ability.

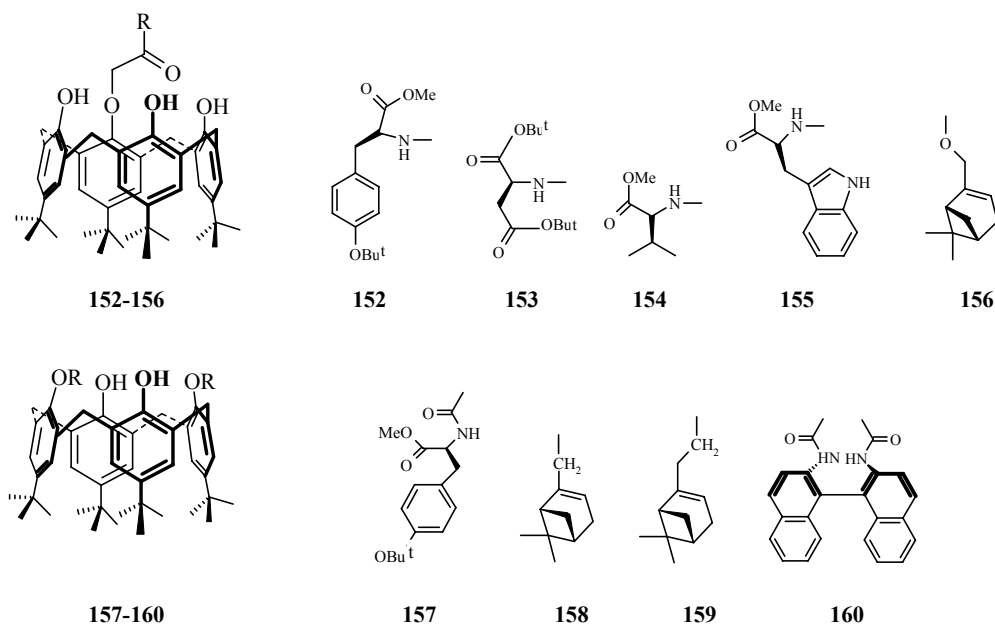


Cheng and coworkers [58-60] reported the preparation of a series of chiral calix[4]arene derivatives **143-151** by reaction of calix[4]arene diacid dichloride with various amino acid derivatives. Receptors **143-145** were found to bind much more favorably with (*R*)-methyl lactate than with its (*S*)-enantiomer and thereby rendering it as a new candidate for chiral gas sensor coatings. Receptor **150** was found to be an efficient receptor for the biologically important phosphate ion.

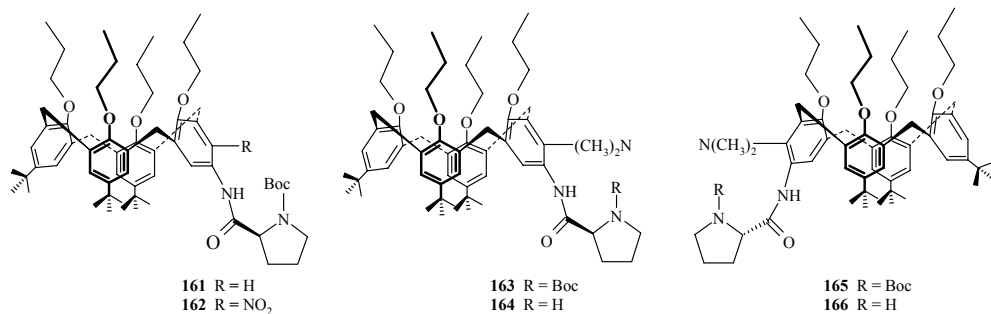




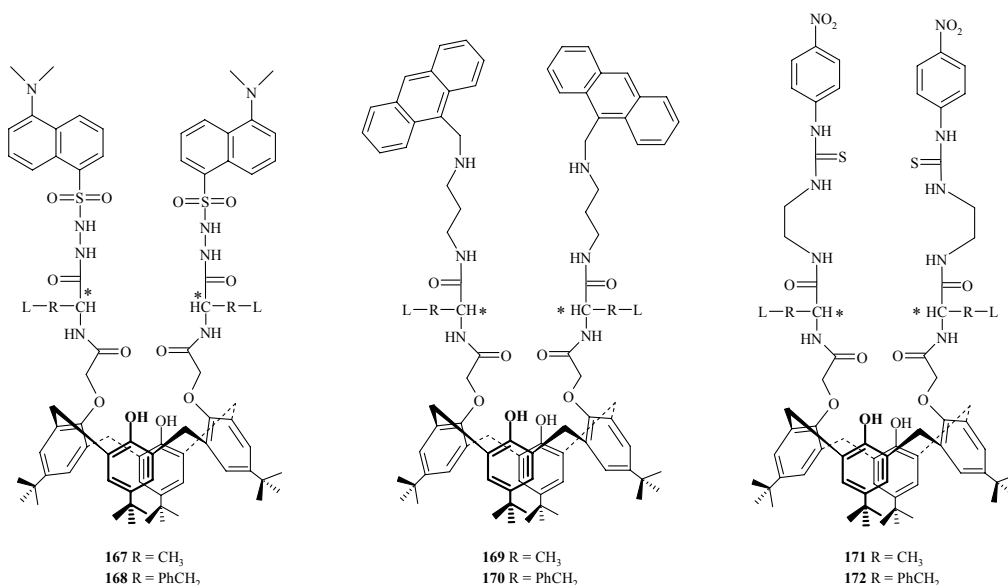
Neri and colleagues described the synthesis of optically active calix[4]arene derivatives **152-160** with different chiral pendant units such as amino acid, pinene-like, and binaphthyl groups [61]. The application of these derivatives in enantioselective catalysis was evaluated by testing the catalytic activities of the corresponding Ti(IV)/calixarene complexes, prepared in situ by an asymmetric aldol reaction.



Boc-*L*-proline-appended calix[4]arene derivatives **161-166** were synthesized by Huang and coworkers [62-64] and employed as novel bifunctional organocatalysts in an enantioselective direct aldol reaction. It was found that the inherently chiral catalysts **164** and **166** could promote the aldol reaction between 4-nitrobenzaldehyde and cyclohexanone in the presence of acetic acid in high yields and with good enantioselectivities.



Calix[4]arene based chiral receptors (**167-172**) containing hydrazide, dansyl, anthracene and *p*-nitrophenyl isothiocyanate groups were constructed by He coworkers, [65-67] who examined their enantioselective recognition abilities by fluorescence, UV/Vis absorption and ¹H NMR spectroscopy in chloroform. The results indicated that receptors **167**, **168** and **171** exhibited excellent enantioselectivities towards *N*-protected alanine, phenylalanine and α -phenylglycine anions. This was attributed to cooperative action of the hydrazide and amide units in binding the amino acid anion by multiple hydrogen bonds. Receptors **169** and **170** exhibited good chiral recognition abilities towards the enantiomers of *D*- and *L*-tetrabutylammonium malate, forming a 1:1 complexes between the host and guest. Sensitive fluorescent responses and good enantioselective recognition abilities reveal that these receptors can be employed as fluorescent or chromogenic chemosensors for chiral anions.

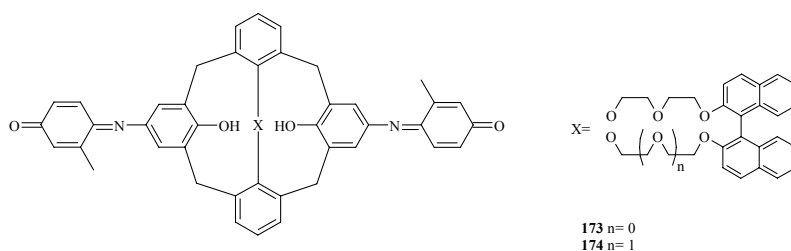


FLUORESCENT GROUPS

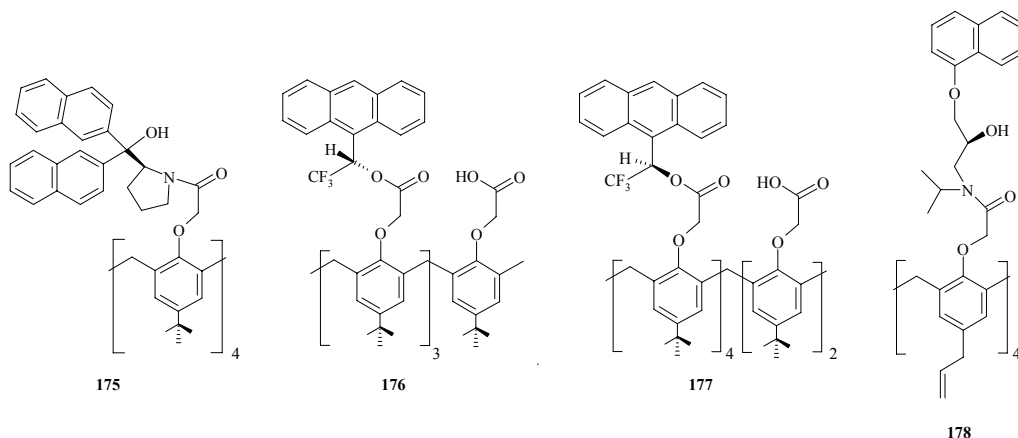
The use of fluorescently labelled chiral calixarenes for enantioselective recognition of chiral amines and amino alcohols have attracted considerable interest because such receptors

potentially provide a real-time technique for determination of the enantiomeric composition of chiral molecules [68-71]. Calixarene-based enantioselective fluorescence receptors are generally composed of a fluorophore and a chiral moiety attached to the calix[4]arene skeleton. The organic fluorophores are usually arranged in proximity to hydrogen bonding and chiral centres in the host molecule in such a way that binding of the guest species results in quenching of the fluorescence [72].

Kubo and coworkers first reported the synthesis of chromogenic receptors (**S**)-**173** and **174** containing indophenol indicator units as part of the calixarene core [73-75]. Ligand (**S**)-**173** and to some extent (**S**)-**174** were found to selectively recognize (*R*)-phenylglycinol in ethanol solution associated with a remarkable color change. This was the first chiral sensor for the colorimetric determination of amine enantiomers.

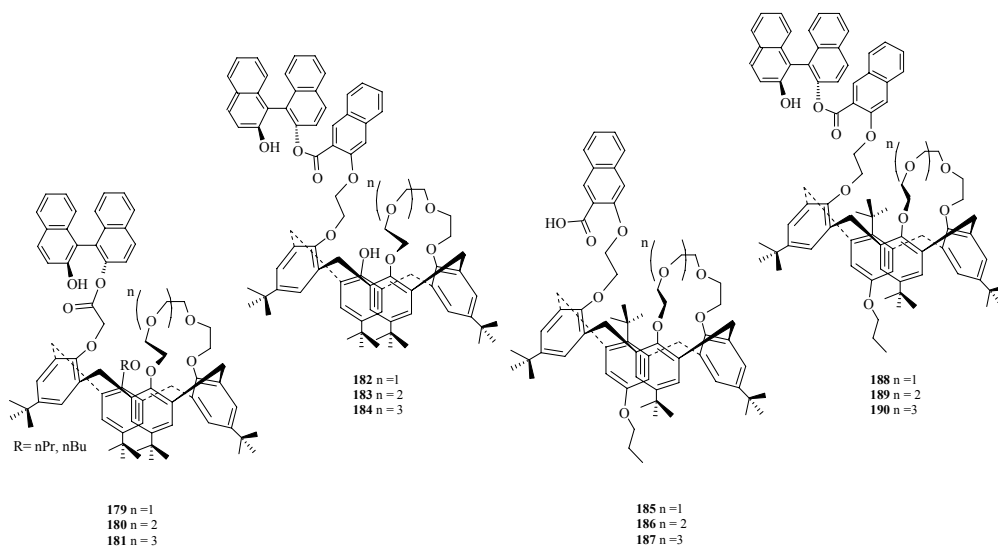


Diamond and coworkers [76-78] prepared chiral calix[*n*]arene derivatives **175-178** with (*S*)-di-2-naphthylprolinol, (*R/S*)-1-(9-anthryl)-2,2,2-trifluoroethanol and (*S*)-propranolol groups. The (*S*)-di-2-naphthylprolinol tetramer **175** was shown to exhibit significant ability to discriminate between enantiomers of 1-phenylethylamine (PEA), phenylglycinol and norephedrine; whereas **178** a propranolol amide derivative of *p*-allylcalix[4]arene, exhibited different chiral recognition abilities towards both enantiomers of phenylalaninol on the basis of the quenching of the fluorescence emission in chloroform.

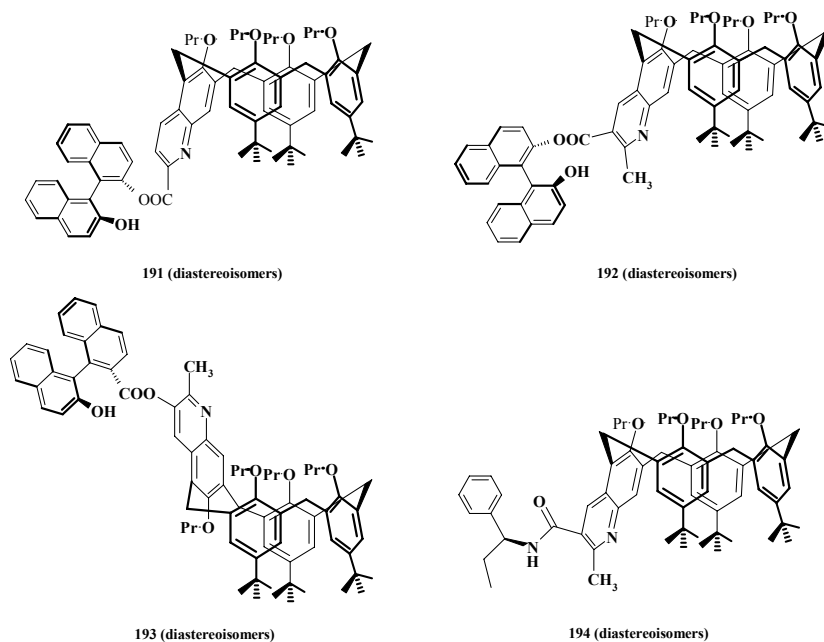


Synthesis and recognition ability of tri-*O*-alkylated and tetra-*O*-alkylated inherently chiral fluorescent calix[4]crowns in the cone and partial cone conformations were reported by Huang and coworkers [79-81] using (*S*)-BINOL-attached calix[4]arenes **179-181** and **188-190**. One of the tetra-*O*-alkylated inherently chiral fluorescent calix[4]arene-crown-6

compounds in the partial cone conformation **187** was found to exhibit considerable enantioselective recognition capability towards the enantiomers of leucinol.

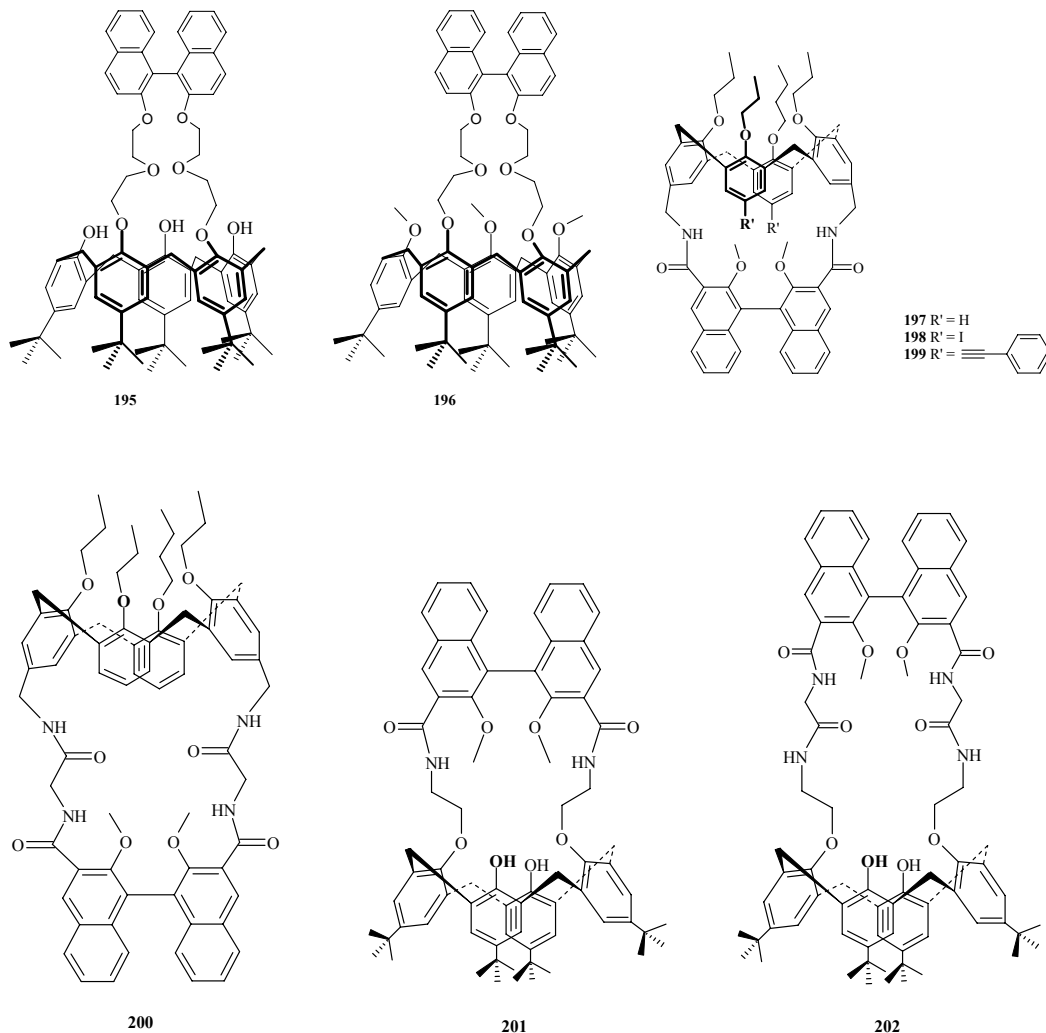


The same group also described the preparation of chiral calix[4]arenes **191-194** derived from (*S*)-BINOL or (*R*)-phenylglycinol and employed in the synthesis of inherently chiral calix[4]quinolines on the upper rim [82]. Their optical resolutions were conveniently achieved through the separation of their diastereomers.



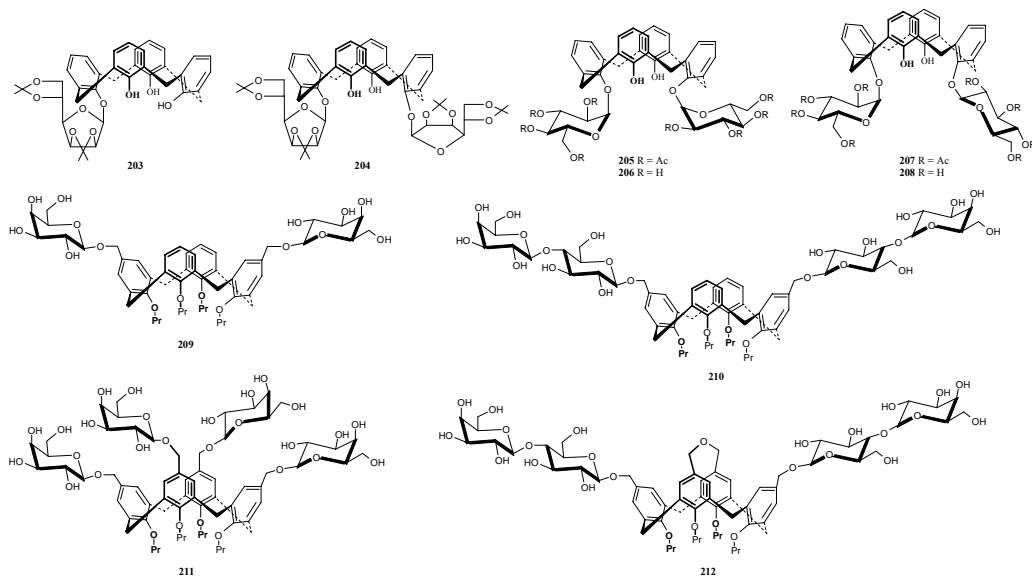
Upper and lower rim binaphthyl-bridged calix[*n*]arenes **195-202** were synthesized by exploiting selective functionalization of the calix[*n*]arene skeleton [83,84]. The calix[5]arene

complexes $[(R)\text{-195.Cu}^{2+}]$ and $[(S)\text{-195.Cu}^{2+}]$ were used as binary hosts to recognize carbohydrates; whereas the upper rim binaphthyl bridged calix[4]arene **197** strongly and selectively complexed with the silver(I) cation.

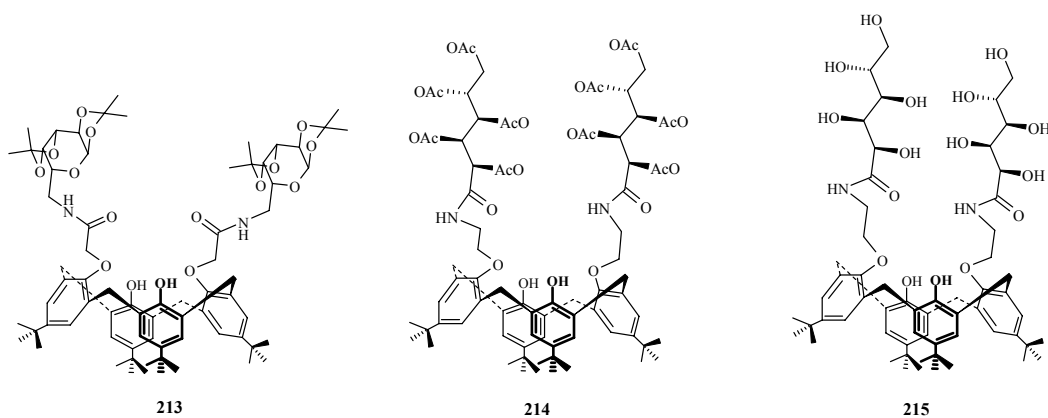


SUGARS

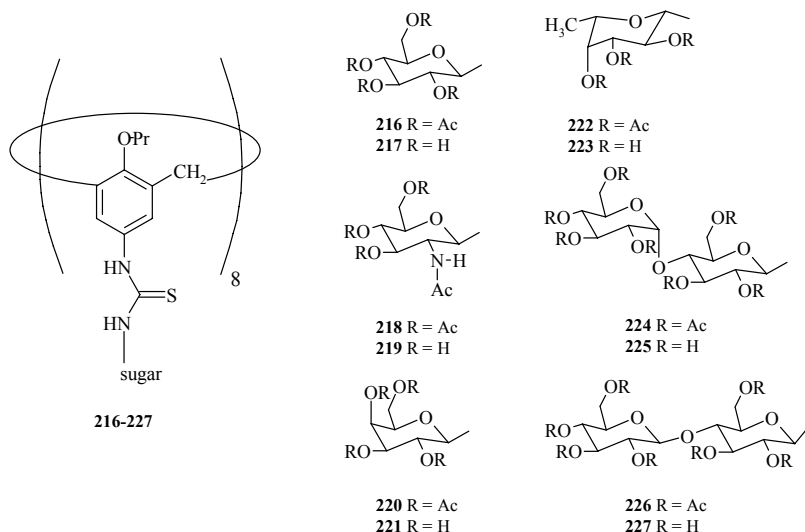
A new family of carbohydrate-containing calixarene derivatives named calixsugars was introduced by Dondoni and Ungaro [85,86] who synthesized a variety of upper- and lower-rim glycosylated calix[4]arenes. Tetrapropoxy calix[4]arenes with two or four hydroxymethyl groups on the upper rim were coupled with perbenzoylated thioethyl *D*-galactoside and *D*-lactoside and β -linked bis- and tetrakis-*O*-galactosyl calix[4]arenes **209-212** were obtained. *D*-mannofuranose and *D*-glucopyranose were attached on the lower rim of the calix[4]arenes **203-208** by glycosylation of the phenolic hydroxyl groups via a Mitsunobu reaction.



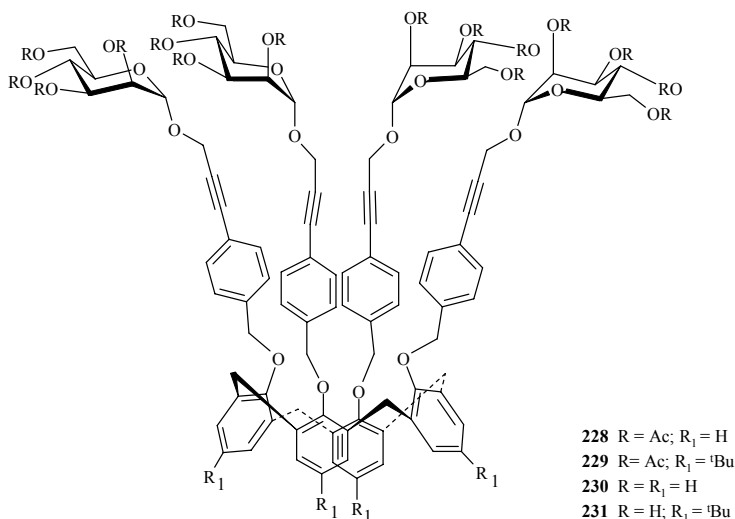
Lhotak and coworkers [87] reported the preparation of calix[4]arene derivatives **213-215** using the reaction between the appropriate acyl chloride and an amino calix[4]arene or an aminosaccharide derivative. The introduction of sugar moieties onto the lower rim of calix[4]arene leads to novel receptors, the usefulness of which has been demonstrated by their interactions with various monosaccharide derivatives.



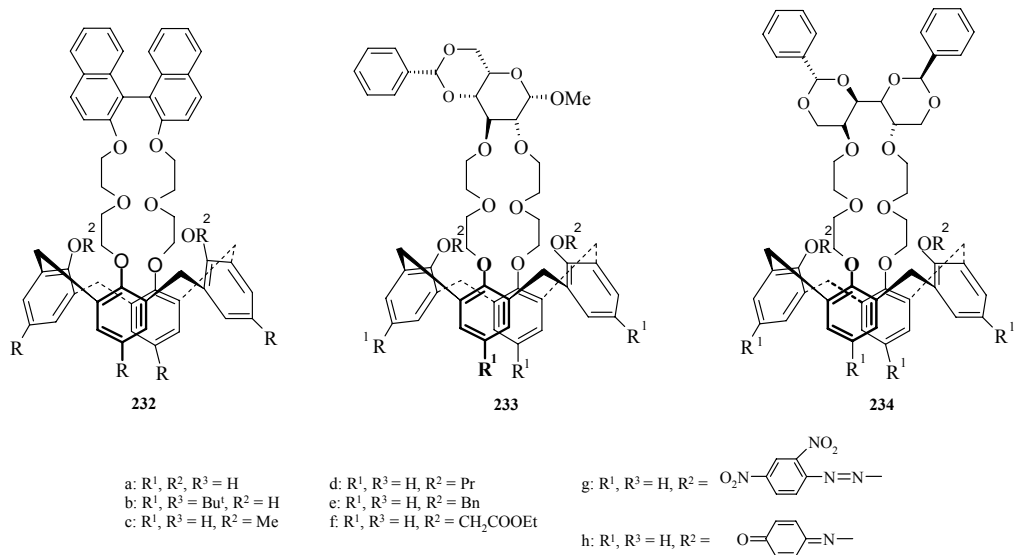
An efficient approach for the introduction of eight mono- or disaccharide sugar moieties (*D*-glucose, *N*-acetyl-*D*-glucosamine, *D*-galactose, *L*-fucose, *D*-maltose and *D*-cellobiose) on the upper rim of calix[8]arene using thioureido linkers was described by Consoli coworkers [88]. It was reported that the glycolix[8]arenes **216-227** may act as biomimetic carbohydrate systems and as hosts for highly polar organic molecules.



The synthesis and biological activity of tetrakis(mannopyranosyl) calix[4]arenes **228-231** with a deepened cavity were described using the Sonogashira reaction of propargyl α -D-mannopyranoside and 25,26,27,28-tetrakis(4'-iodobenzoyloxy) calix[4]arene for the assembly of the sugar moieties onto the calix[4]arene scaffold [89].

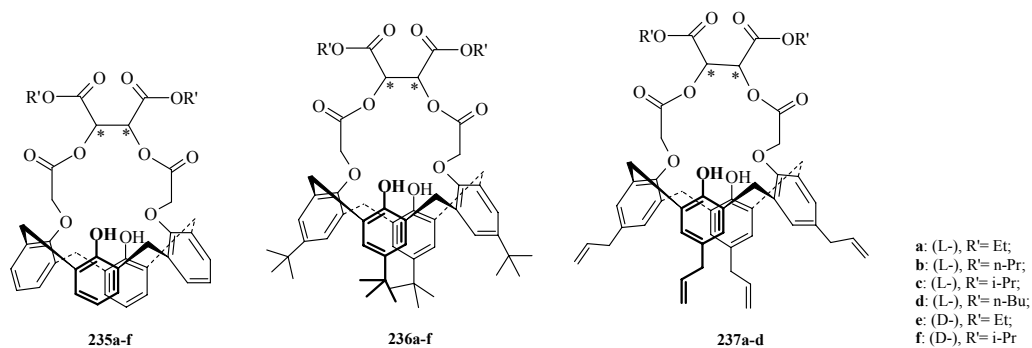


Chromogenic 1,3-calix[4]arene-crown-6 derivatives comprised of 1,1'-binaphthyl, α -D-glucoside and D-mannitol moieties in the crown ether ring and supplied with 2,4-dinitrophenylazo indicator groups were prepared by Bitter, Kubinyi and coworkers [90,91]. Receptors **232e** and **233g** exhibited noticeable chiral recognition of α -methylbenzylamine enantiomers. The UV fluorescence of (*R*)-**232e**/*S*-**232e** arising from the binaphthyl moiety is quenched by K⁺ ions.

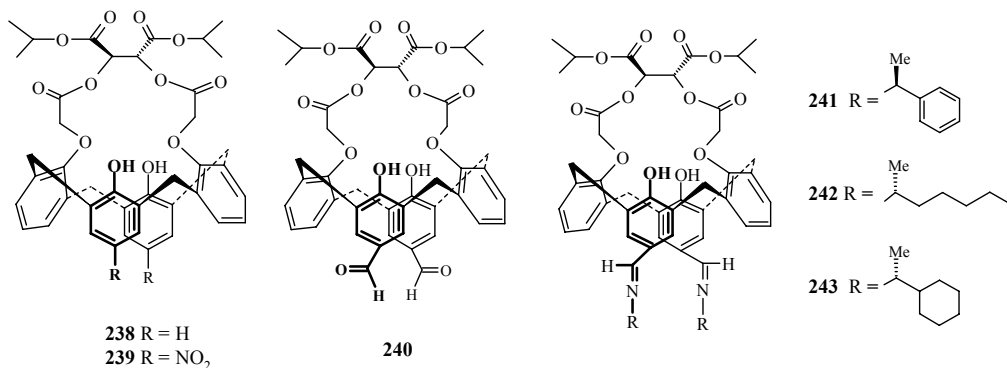


TARTARIC ACID DERIVATIVES

In the design of chiral calixarenes, tartaric acid and its derivatives can be used as building blocks. The attachment of enantiomerically pure units derived from tartaric acid to the lower rim provides a calixarene with novel properties. Huang coworkers [92] synthesized a new kind of chiral calix[4]arene derivatives **235–237** by incorporating tartaric acid ester moieties prepared from the reactions of chloroacetyl chloride with esters of tartaric acid.

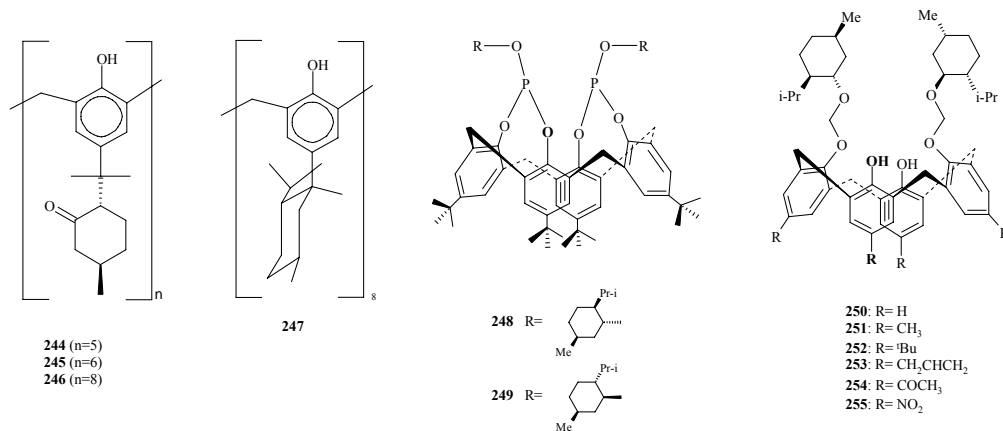


We have described the synthesis of new chiral calix[4]arene derivatives **238–243** containing tartaric acid ester moieties on the lower rim and various functionalities including aldehyde, nitro and Schiff base groups on the upper rim [93,94]. Chiral hosts **238** and **239** showed enantiomeric recognition toward *rac*-serine methyl ester hydrochloride and 1,2-propanediol, respectively due to the multiple hydrogen bonding. On the other hand, chiral selectors **241–243** showed good recognition ability for the enantiomers of phenylalanine and alanine methyl ester hydrochlorides (up to $K_D/K_L = 4.36$, $\Delta\Delta G_0 = -3.65$ kJ mol⁻¹).



MENTHONE DERIVATIVES

The synthesis of new chiral calixarenes **244-247** with different ring sizes was achieved by Schurig coworkers using (*p*-hydroxy-phenyl)-menthone and (-)-menthone and a one-pot procedure similar to that described by Gutsche and coworkers [95,96]. Chiral calix[4]arene iso-menthyl bisphosphite **248** and menthyl bisphosphite **249** were prepared [97] by reaction of *p*-tert-butyl-calix[4]arene with (1*S*,2*R*,5*R*)-(+)-iso-menthyl or (1*R*,2*S*,5*R*)-(-)-menthyl phosphorodichloridites, respectively, in the presence of triethylamine.

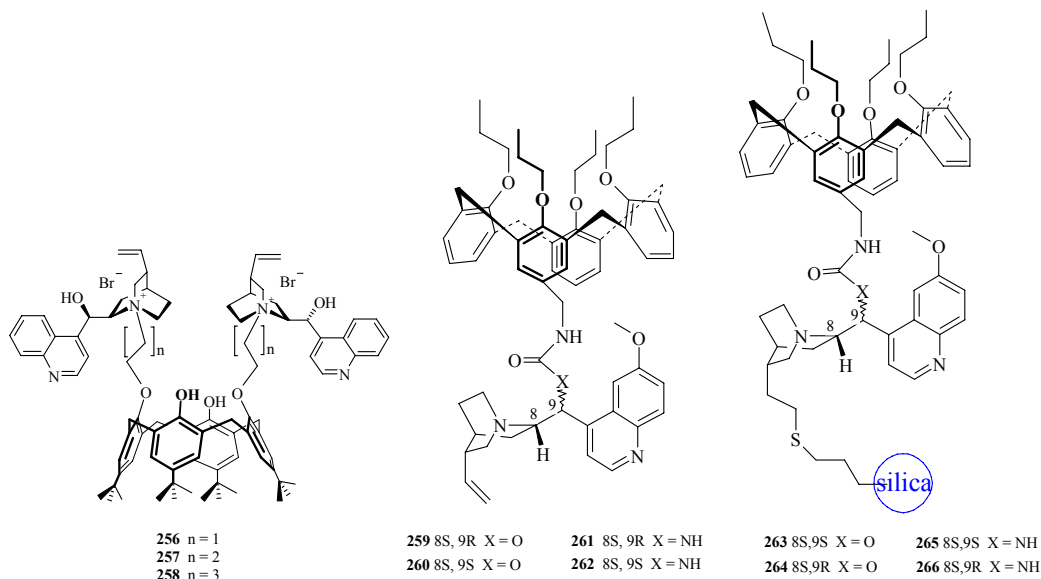


Lopez coworkers reported [98] that complex formation between the antibiotic levofloxacin and a series of chiral calix[4]arene derivatives **250-255** possessing two (+)-isomenthyl substituents on the lower rim were analyzed on the basis of quantum mechanical calculations at the density functional (for model systems) and semi-empirical levels.

CINCHONA ALKALOIDS

Cinchona alkaloids are versatile organic catalysts and resolving agents in asymmetric synthesis. They are commercially available in enantiomerically pure forms and can be used

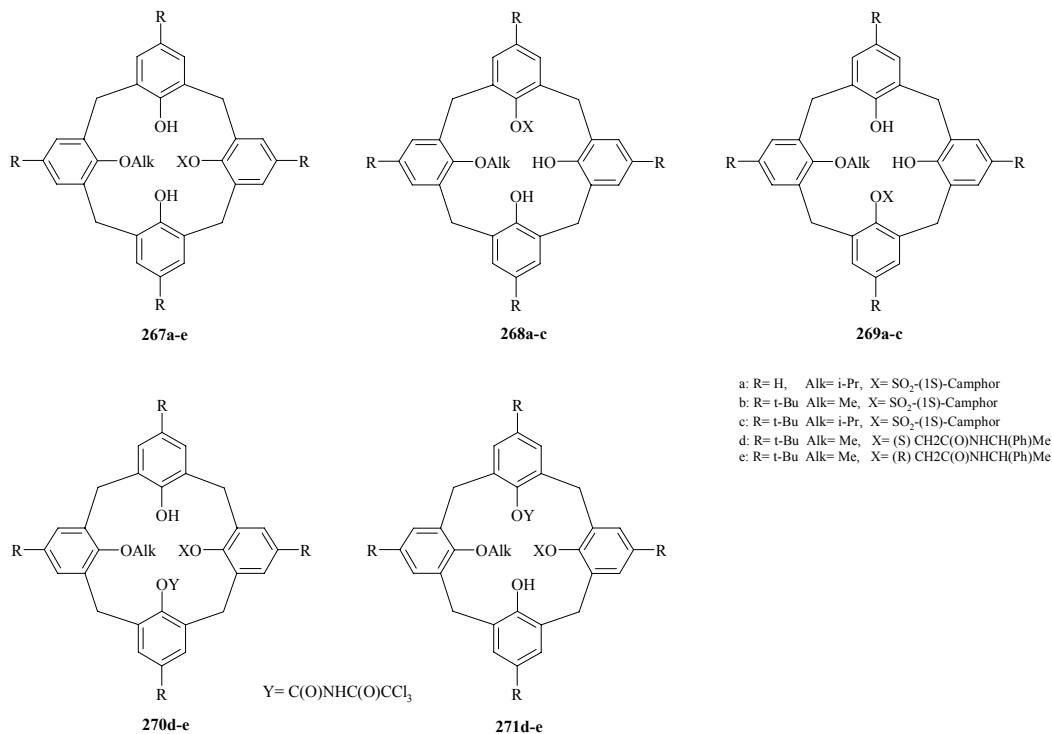
as chiral subunits for the synthesis of chiral calixarenes. Recently, the preparation of the first calixarene-based, chiral phase-transfer catalysts derived from cinchona alkaloids was achieved by our group in two steps from *p*-*tert*-butylcalix[4]arene [99]. The catalytic efficiency of the chiral calix[4]arenes **256-258** was evaluated by carrying out the phase transfer alkylation of *N*-(diphenylmethylene)glycine ethyl ester with benzyl bromide. Benzilation of glycine imine using calix[4]arene-based dimeric catalyst **256** as a chiral phase-transfer catalyst in toluene/chloroform mixture (7:3 v/v) at 0 °C gave the best enantioselectivities up to 57% ee and yields in the presence of aqueous NaOH.



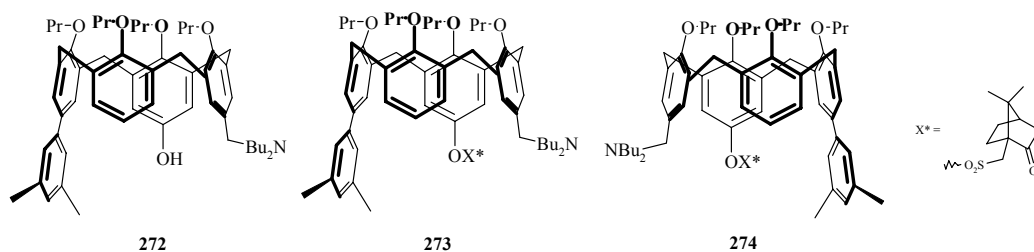
The synthesis and chromatographic evaluation of novel carbamate and urea-linked, cinchona-calixarene hybrid-type receptors **259-262** and chiral stationary phases **263-266**, derived from 9-amino(9-deoxy)-quinine (AQN), 9-amino(9-deoxy)-epiquinine (eAQN), quinine (QN) and its corresponding C9-epimer (eQN) were described [100,101]. The QN- and AQN-derived chiral stationary phases **264** and **266** showed enantioselectivities for open-chain amino acids, preferentially binding the (*S*)-enantiomers. In contrast, the eQN and eAQN congeners **263** and **265** exhibited broad chiral recognition capacity for open-chain as well as cyclic amino acids, and preferential binding of the (*R*)-enantiomers.

CAMPOR SULFONYL CHLORIDE

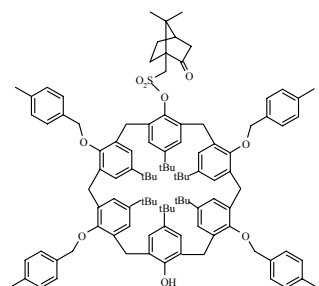
Several syntheses of chiral calixarenes from camphor sulfonyl chloride have been presented by various groups. Kalchenko and coworkers [102-104] described the synthesis of chiral calix[4]arenes **267-271** by reaction of calix[4]arene monoalkyl ethers with 1(*S*)-camphor-10-sulfonyl chloride and (*R*)- or (*S*)-*N*-(1-phenylethyl)bromoacetamides. Enantiomerically pure, inherently chiral calix[4]arene derivatives **270d,e** and **271d,e** were prepared using chiral receptors **267d,e** in preparative yields and high diastereomeric excess.



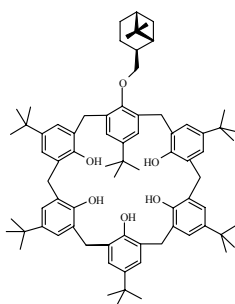
Shimizu coworkers [105] reported the preparation of chiral calix[4]arene derivatives **273** and **274** bearing a camphorsulfonyl group and used them for the optical resolution of racemic, inherently chiral, wide rim ABCD-type calix[4]arene **272** fixed in the cone conformation. The chiral calix[4]arene **272** was employed as an organocatalyst in asymmetric Michael addition reactions of thiophenols.



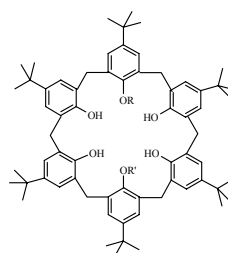
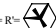
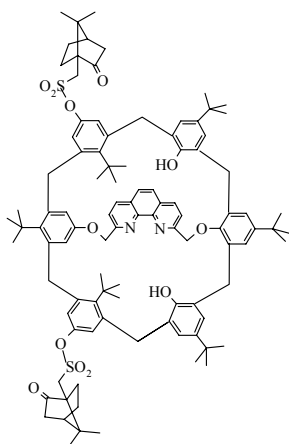
Luning and coworkers [106] prepared a series of new chiral derivatives of the 1,10-phenanthroline-bridged calix[6]arene **275-281** carrying camphorsulfonyl or myrtanyl groups. The compounds were tested as ligands for copper ions in the Cu(I)-catalyzed cyclopropanations of styrene and indene.



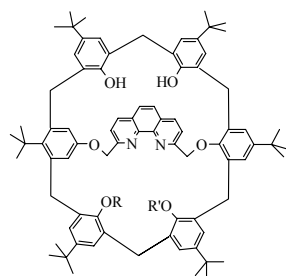
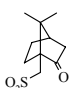
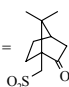
275



276

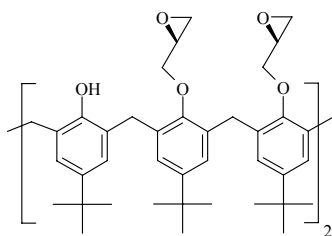
277 R = CH₃, R' = H278 R = R' = CH₃

279

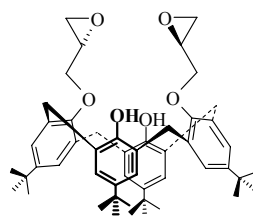
280 R = , R' = H281 R = H, R' = 

EPOXIDES AND GLYCIDYL GROUPS

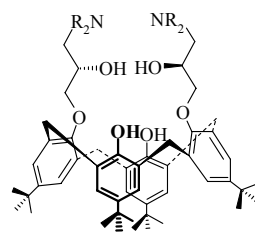
Glycidyl groups and epoxides have also been employed for the introduction of chirality into calixarenes. A series of chiral calix[*n*]arenes with β-amino alcohol groups **284–285** and **289–292** were synthesized by reaction of *p*-*tert*-butylcalix[4]arene and *p*-*tert*-butylcalix[6]arene with glycidyl tosylate followed by the regio- and stereoselective ring-opening reactions with different amines [107,108]. The monofunctionalized ligands **289** and **290** were reported to be useful catalysts in the asymmetric transfer hydrogenation of acetophenone in the presence of [Ru(*p*-cymene)Cl₂]₂ and showed good enantioselectivities (ee max = 90%) and very good conversions (conversion max = 97%)

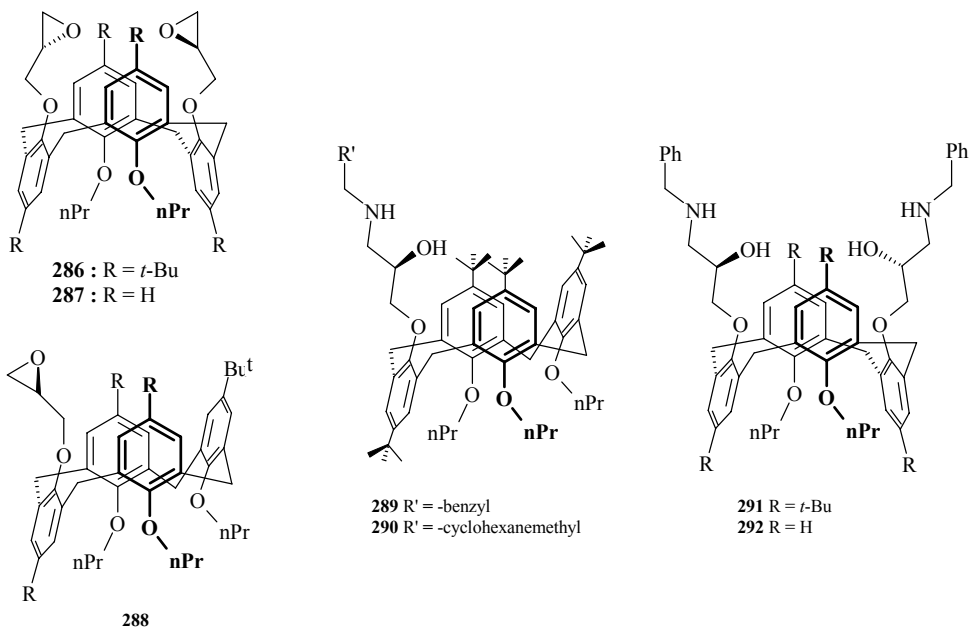


282



283

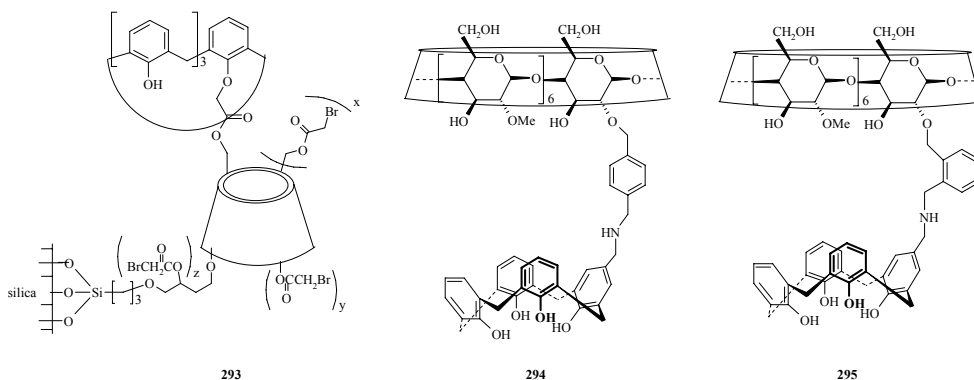
284 R = H
285 R = Me



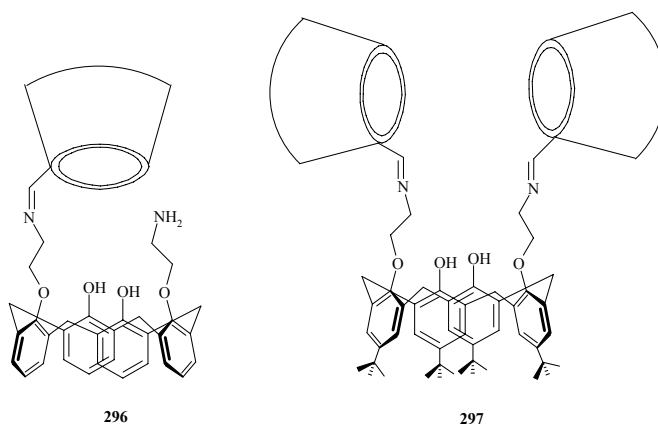
CYCLODEXTRINS

Cyclodextrins have also been used as chiral residues for the synthesis of calixarenes. For example, a calix[4]arene-capped [3-(2-*O*- β -cyclodextrin)-2-hydroxypropoxy]-propylsilyl-appended silica particle **293** was synthesized and used as a chiral stationary phase for the separation of chiral drugs by HPLC [109].

Reinhoudt and coworkers described the preparation of novel host molecules **294** and **295** starting from heptakis(6-*O*-*tert*-butyldimethylsilyl) β -cyclodextrin [110]. The cyclodextrin-calix[4]arene receptors **294** and **295** were found to be very effective hosts for fluorescent dye molecules. The strongly enhanced binding capacity is attributed to additional environmental shielding of the guest by the upper rim of the calix[4]arene which can move over the secondary hydroxy face of the cyclodextrin cavity.

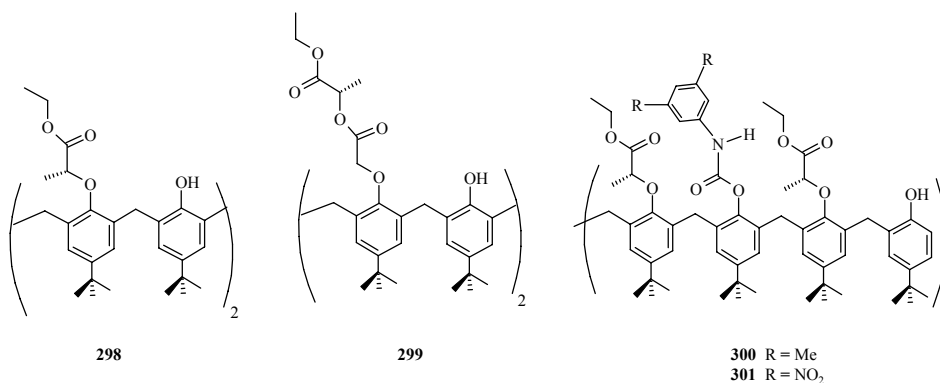


Similarly, the syntheses of novel calix[4]arene-tethered mono- (**296**) and bis(beta-cyclodextrin) (**297**) and their molecular recognition behavior with fluorescence dyes, i.e., acridine red (AR) and sodium 2-(*p*-toluidino)-6-naphthalenesulfonate (TNS), as well as some structurally related guests, i.e., methyl orange (MO), ethyl orange (EO), tropaeolin OO (TOO), brilliant green (BG), crystal violet (CV), and rhodamine B (RhB) in aqueous buffer solution were investigated by Liu, Inoue and coworkers [111].



ETHYL LACTATE

Recently, ethyl lactate derivatives **298-301** of *p*-*tert*-butylcalix[4]arene were obtained as chiral solvating agent for the differentiation of the NMR spectra of enantiomeric mixtures of amino acid derivatives [112]. The origin of enantiodiscrimination in solution was investigated by NMR spectroscopy and compared with model chiral auxiliaries.

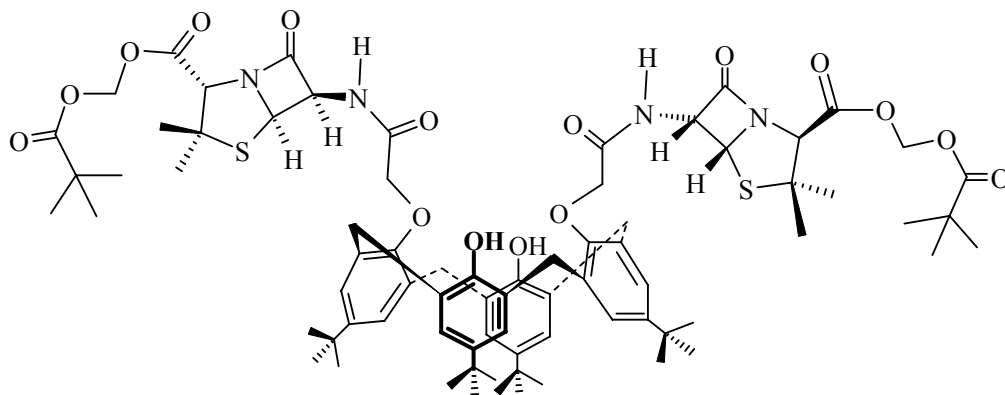


GUANIDINIUM SALTS

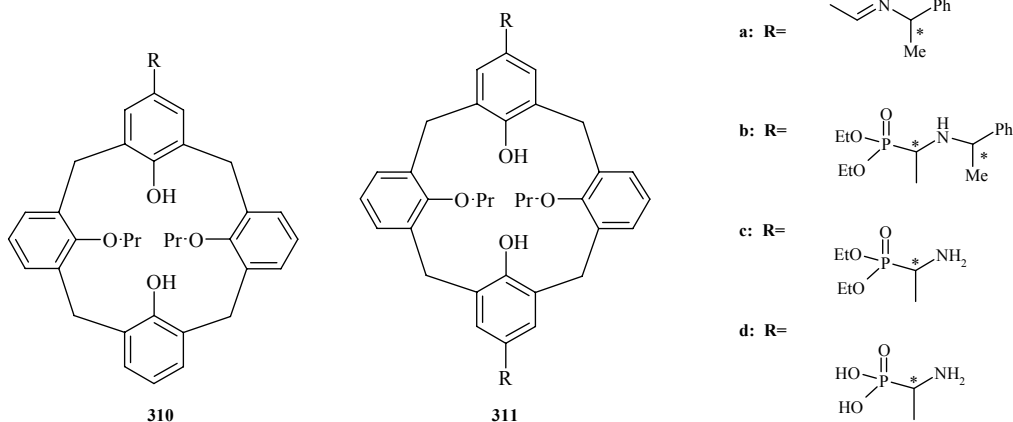
Chiral bicyclic guanidinium moieties were introduced on the lower rim of *p*-*tert*-butylcalix[4]arene and exhibited high enantioselective recognition ability for aromatic amino

Mesitylene-based chiral calix[4]arene derivatives **307** and **308** were prepared by Thondorf and coworkers [116] in the 1,3-alternate conformation by attachment of homochiral residues to the four exo-hydroxy groups.

Penicillin has also been attached on the lower rim of the *p-tert*-butylcalix[4]arene to produce calixarene-based podands shaped as potent drug dispensers [117]. It was reported that the penicillinic podand **309** represents a new kind of potentially therapeutically active calixarene derivative.

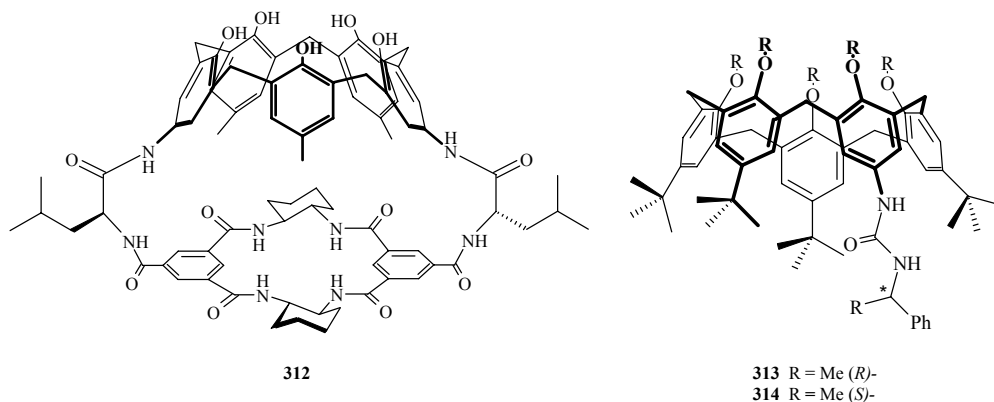
**309**

Chiral calix[4]arene alpha-aminophosphonic acids **310d** and **311d** were synthesized by Kalchenko and coworkers [118] through diastereoselective Pudovik-type addition of sodium ethyl phosphites to the chiral calixarene imines **310a** and **311a**, removal of the chiral auxiliary and dealkylation of phosphonate fragments. The calix[4]arene diacids were reported to exhibit enantioselective inhibitory activity toward porcine kidney alkaline phosphatase.

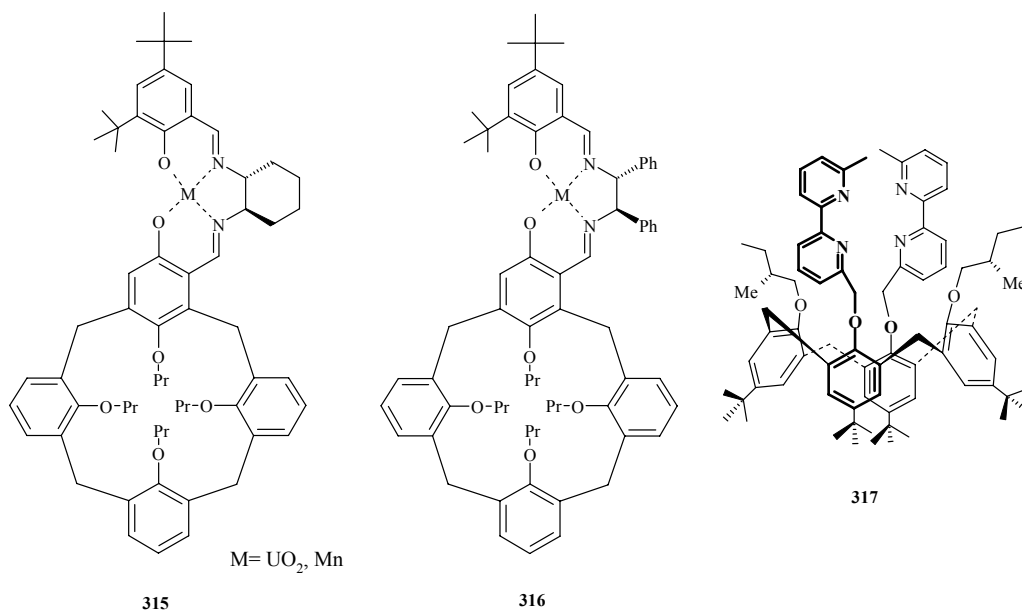


Recently Haino and coworkers [119] reported a calix[5]arene-based artificial receptor **312** capped with a chiral macrocycle. The chiral receptor exhibited strong binding and different chiral recognition ability towards chiral ethyltrimethylammonium derivatives via cation- π and/or hydrogen bonding interactions.

Another type of calix[5]arene receptor **313** and **314** with a urea unit on the upper rim and a fixed cone conformation was reported by Parisi and coworkers [120]. The chiral receptors were demonstrated to show a strong affinity for biogenic amines, α -amino acids, and lysine derivatives.

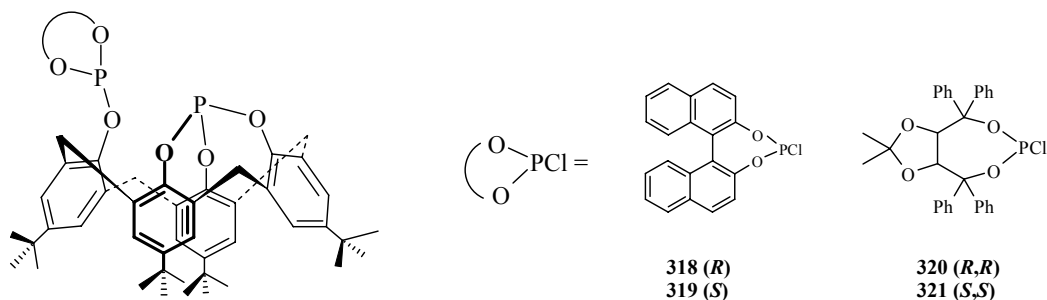


Tomaselli and coworkers [121] described the first example of chiral (salen) Mn^{III} and UO₂ complexes (**315** and **316**, respectively) containing a calix[4]arene framework. The (Salen) Mn^{III} calix[4]arene complexes were employed as catalysts in epoxidation reactions of styrene, dihydronaphthalene and of some standard *cis*- β -alkylstyrenes and high enantioselectivity up to 72% *ee* has been obtained.

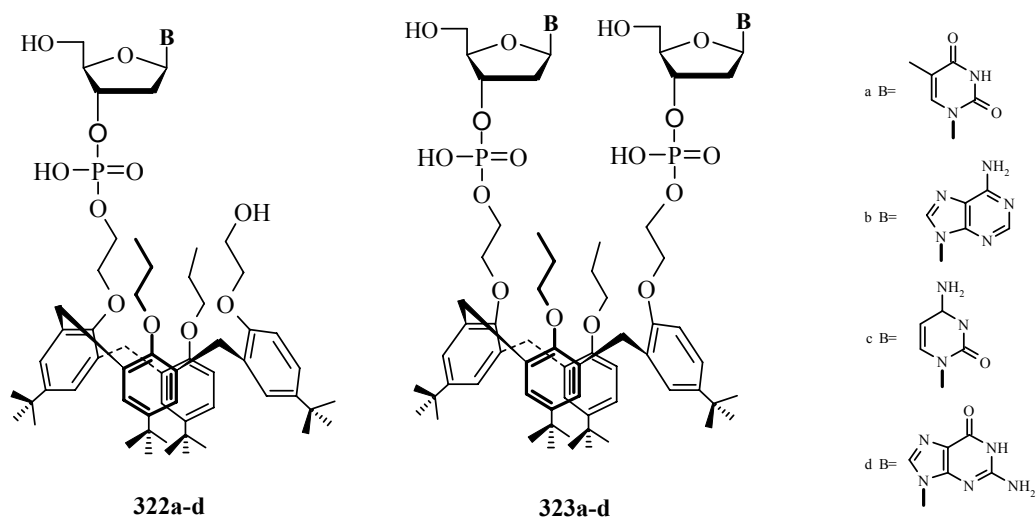


Regnouf-de-Vains and coworkers [122] introduced the chiral (*S*)-2-methylbutyl substituent close to the complexing site of a bis[(bipyridinyl)methoxy]-calixarene podand **317** resulting in the induction of an enantiomeric excess of *ca.* 30% in the corresponding Cu(I) complex.

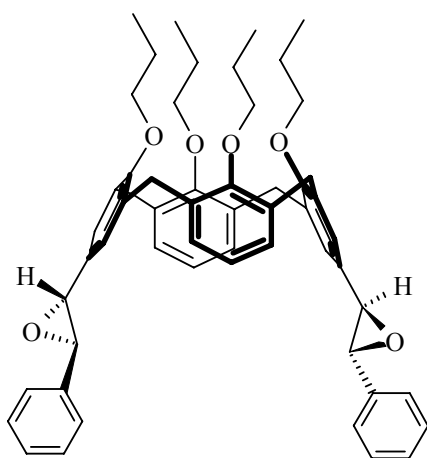
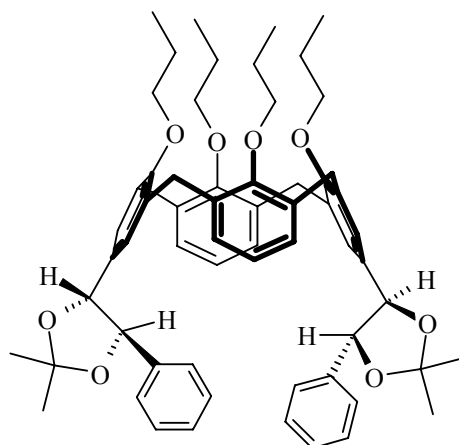
Leeuwen, Kamer and coworkers have reported [123] the preparation of chiral diphosphite ligands **318-321** constructed on a calix[4]arene backbone via lower-rim functionalization of a *p*-*tert*-butylcalix[4]arene core. High enantiomeric excess (up to 94%) were obtained in the rhodium-catalyzed asymmetric hydrogenation of prochiral olefins with TADDOL-containing diphosphites **320** and **321**.



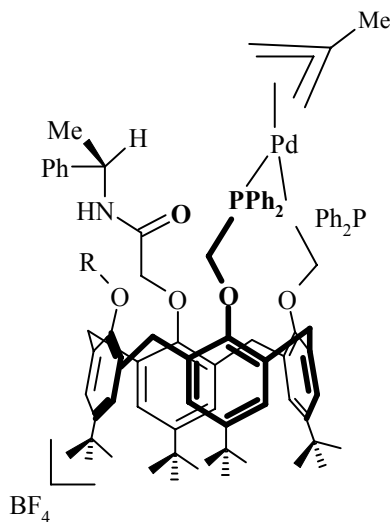
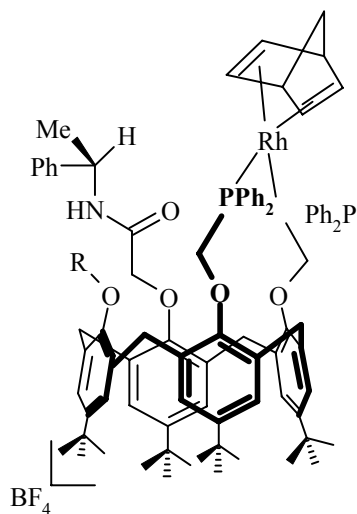
Consoli and coworkers reported a series of chiral calix[4]arenes **322a-d** and **323a-d** bearing thymine, adenine, cytosine, guanine 2'-deoxynucleotide residues via phosphoester bonds [124,125]. Preliminary results regarding their assembling in apolar solvents and host properties toward biologically interesting guests are also included.

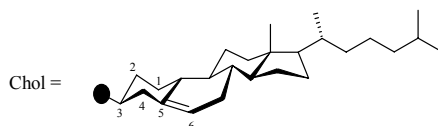
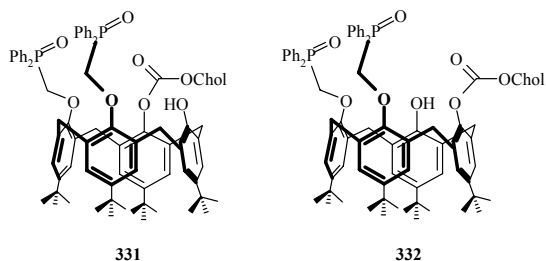


Enantioselective synthesis of a chiral calix[4]arene bis-epoxide **324** was recently reported by Bonini and coworkers [126] via a direct asymmetric reaction on the parent 1,3-diformyl calix[4]arene in excellent yield and >99% ee. Epoxide **324** was enantioselectively converted into the corresponding bis-dioxolane **325**.

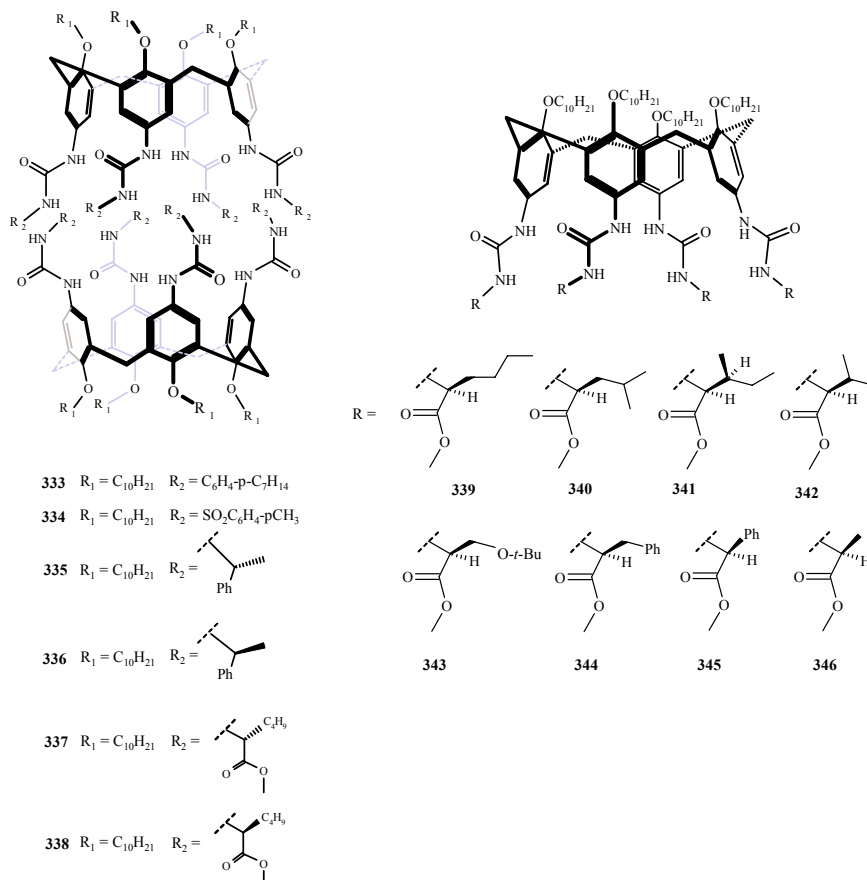
324 (*R,R*), (*R,R*)325 (*R,R*), (*R,R*)

Chiral diphosphine and phosphinite calix[4]arenes **326-332** were prepared by Matt and coworkers [127,128] and employed in allylic alkylation with 67% ee and hydrogenation with 48% ee. Despite these poor transfers of chirality, excellent results were obtained in terms of conversion (100%).

326 R = H
327 R = SiMe₃328 R = H
329 R = SiMe₃
330 R = CH₂C(O)NHC*H(Me)Ph



Molecular capsules are formed when calix[4]arenes dimerize with appropriate functional groups. The synthesis of molecular capsules using non-covalent interactions is a very attractive area of supramolecular chemistry. Rebek and coworkers [129,130] described the optically active tetraureas **333-346**, prepared through reaction of the tetraamine calix[4]arene with the appropriate isocyanates derived from amino acid methyl esters, have self-complementary recognition sites and assemble into dimeric structures.



REFERENCES

- [1] Gutsche, CD; Muthukrishnan, R. *J. Org. Chem.*, 1978, 43, 4905-4906.
- [2] Gutsche, CD. In *Calixarenes, Monographs in Supramolecular Chemistry*; Stoddart, J. F., Ed; The Royal Society of Chemistry: Cambridge, UK, 1989.
- [3] Gutsche, CD. In *Calixarenes Revisited*; JF; Stoddart, (Eds.), The Royal Society of Chemistry: Cambridge, UK, 1998.
- [4] Shinkai, S; Arimura, T; Satoh, H; Manabe, O. *J. Chem. Soc., Chem. Commun.*, 1987, 1495-1496.
- [5] Arimura, T; Kawabata, H; Matsuda, T; Muramatsu, T; Satoh, H; Fujio, K; Manabe, O; Shinkai, S. *J. Org. Chem.*, 1991, 56, 301-306.
- [6] Vysotsky, MO; Schmidt, C; Böhmer, V. In *Advances in Supramolecular Chemistry*; Gokel, G., Ed; Jai Press: Stanford, 2000, Vol. 7, 139-233.
- [7] Ludwig, R. *Microchim. Acta*, 2005, 152, 1-19.
- [8] Casnati, A; Sansone, F; Ungaro, R. *Acc. Chem. Res.*, 2003, 36, 246-254.
- [9] Fulton, DA; Stoddart, F. *Bioconjugate Chem.*, 2001, 12, 655-672.
- [10] Shinkai, S. *Tetrahedron*, 1993, 49, 8933-8968.
- [11] Mutihac, L; Buschmann, HJ; Mutihac, RC; Schollmeyer, E. *J. Incl. Phenom. Macrocyclic Chem.*, 2005, 51, 1-10.
- [12] Hembury, GA; Borovkov, VV; Inoue, Y. *Chem. Rev.*, 2008, 108, 1-73.
- [13] Baldini, L; Casnati, A; Sansone, F; Ungaro, R. *Chem. Soc. Rev.*, 2007, 36, 254-266.
- [14] Sirit, A; Yilmaz, M. *Turk J Chem*, 2009, 33, 159-200.
- [15] Kocabas, E; Durmaz, M; Alpaydin, S; Sirit, A; Yilmaz, M. *Chirality*, 2008, 20, 26-34.
- [16] Kocabas, E; Karakucuk, A; Sirit, A; Yilmaz, M. *Tetrahedron: Asymmetry*, 2006, 17, 1514-1520.
- [17] Erdemir, S; Tabakci, M; Yilmaz, M. *J. Incl. Phenom. Macrocycl. Chem.*, 2007, 59, 197-202.
- [18] Zheng, YS; Zhang, C. *Org. Lett.*, 2004, 6, 1189-1192.
- [19] Zheng, YS; Xiao, Q. *Chinese Journal of Chemistry*, 2005, 23, 1289-1291.
- [20] Zheng, YS; Zhang, C; Tian, ZF; Jiang, A. *Synth. Commun.*, 2004, 34, 679-688.
- [21] Liu, XX; Zheng, YS. *Tetrahedron Lett.*, 2006, 47, 6357-6360.
- [22] Tabakci, M; Tabakci, B; Yilmaz, M. *J. Incl. Phenom. Macrocycl. Chem.*, 2005, 53, 51-56.
- [23] Erdemir, S; Tabakci, M; Yilmaz, M. *Tetrahedron: Asymmetry*, 2005, 17, 1258-1263.
- [24] Zhou, JL; Chen, XJ; Zheng, YS. *Chem. Commun.*, 2007, 5200-5202.
- [25] Sirit, A; Karakucuk, A; Memon, S; Kocabas, E; Yilmaz, M. *Tetrahedron: Asymmetry*, 2004, 15, 3595-3600.
- [26] Sirit, A; Kocabas, E; Memon, S; Karakucuk, A; Yilmaz, M. *Supramol. Chem.*, 2005, 17, 251-256.
- [27] He, Y; Xiao, Y; Meng, L; Zeng, Z; Wu, X; Wu, CT. *Tetrahedron Lett.*, 2002, 43, 6249-6253.
- [28] Demirtas HN; Bozkurt, S; Durmaz, M; Yilmaz, M; Sirit, A. *Tetrahedron: Asymmetry*, 2008, 19, 2020-2025.
- [29] Demirtas HN; Bozkurt, S; Durmaz, M; Yilmaz, M; Sirit, A. *Tetrahedron*, 2009, 65, 3014-3018.

- [30] Garrier, E; Le Gac, S; Jabin, I. *Tetrahedron: Asymmetry*, 2005, 16, 3767-3771.
- [31] Darbost, U; Zeng, X; Giorgi, M; Jabin, I. *J. Org. Chem.*, 2005, 70, 10552-10560.
- [32] Prins, LJ; Jolliffe, KA; Hulst, R; Timmerman, P; Reinhoudt, DN. *J. Am. Chem. Soc.*, 2000, 122, 3617-3627.
- [33] Ishi-i, T; Crego-Calama, M; Timmerman, P; Reinhoudt, DN; Shinkai, S. *J. Am. Chem. Soc.*, 2002, 124, 14631-14641.
- [34] Durmaz, M; Alpaydin, S; Sirit, A; Yilmaz, M. *Tetrahedron:Asymmetry*, 2006, 17, 2322-2327.
- [35] Sansone, F; Casnati, A; Ungaro, R. *Acc. Chem. Res.*, 2003, 36, 246-254.
- [36] Sansone, F; Barbosa, S; Casnati, A; Fabbi, M; Pochini, A; Ungaro, R. *Eur. J. Org. Chem.*, 1998, 897-905.
- [37] Sansone, F; Barbosa, S; Casnati, A; Sciotto, D; Ungaro, R. *Tetrahedron Lett.*, 1999, 40, 4741-4744.
- [38] Lazzarotto, M; Sansone, F; Baldini, L; Casnati, A; Cozzini, P; Ungaro, R. *Eur. J. Org. Chem.*, 2001, 595-602.
- [39] Sansone, F; Baldini, L; Casnati, A; Chierici, E; Faimani, G; Ugozzoli, F; Ungaro, R. *J. Am. Chem. Soc.*, 2004, 126, 6204-6205.
- [40] Casnati, A; Fabbi, M; Pelizzi, N; Pochini, A; Sansone, F; Ungaro, R. *Bioorg. Med. Chem. Lett.*, 1996, 6, 2699-2704.
- [41] Frish, L; Sansone, F; Casnati, A; Ungaro, R; Cohen, Y. *J. Org. Chem.*, 2000, 65, 5026-5030.
- [42] Sansone, F; Baldini, L; Casnati, A; Lazzarotto, M; Ugozzoli, F; Ungaro, R. *Proc. Nat. Acad. Sci.*, U.S.A., 2002, 99, 4842-4847.
- [43] Ben Sdira, S; Felix, CP; Giudicelli, MB. A; Seigle-Ferrand, PF; Perrin, M; Lamartine, R. *J. Org. Chem.*, 2003, 68, 6632-6638.
- [44] Ben Sdira, S; Felix, C; Giudicelli, MB; Vocanson, F; Perrin, M; Lamartine, R. *Tetrahedron Lett.*, 2005, 46, 5659-5663.
- [45] Ben Sdira, S; Baudry, R; Felix, CP; Giudicelli, MB. A; Lamartine, R. *Tetrahedron Lett.*, 2004, 45, 7801-7804.
- [46] Zhang, WC; Zheng, YS; Wang, WG; Zheng, QY; Huang, ZT. *Chin. J. Chem.*, 2003, 21, 931-936.
- [47] Yuan, HS; Zhang, Y; Hou, YJ; Zhang, XY; Yang, XZ; Huang, ZT. *Tetrahedron*, 2000, 56, 9611-9617.
- [48] Yakovenko, AV; Boyko, VI; Kalchenko, VI; Baldini, L; Casnati, A; Sansone, F; Ungaro, R. *J. Org. Chem.*, 2007, 72, 3223-3231.
- [49] Frkanec, L; Višnjevac, A; Kojić-Prodić, B; Žinić, M. *Chem. Eur. J.*, 2000, 6, 442-453.
- [50] Xu, H; Kinsel, GR; Zhang, J; Li, M; Rudkevich, DM. *Tetrahedron*, 2003, 59, 5837-5848.
- [51] Francese, S; Cozzolino, A; Caputo, I; Esposito, C; Martino, M; Gaeta, C; Troisi, F; Neri, P. *Tetrahedron Letters*, 2005, 46, 1611-1615.
- [52] Brewster, RE; Shuker, SB. *J. Am. Chem. Soc.*, 2002, 124, 7902-7903.
- [53] Pena SM; Zhang Y; Warner IM. *Anal. Chem.*, 1997, 69, 3239-3242.
- [54] Sanchez Pena, M; Zhang, Y; Thibodeaux, S; McLaughlin, ML; Munoz de la Pena, A; Warner, IM. *Tetrahedron Lett.*, 1996, 37, 5841-5844.
- [55] Smith, KJ; Wilcox, JD; Mirick, GE; Wacker, LS; Ryan, NS; Vensel, DA; Readling, R; Domush, HL; Amonoo, EP; Shariff, SS; Wenzel, T. *J. Chirality*, 2003, 15, 150-158.

- [56] Qing, GY; He, YB; Wang, F; Qin, HJ; Hu, CG; Yang, X. *Eur. J. Org. Chem.*, 2007, 1768-1778.
- [57] Qing, GY; Qin, HJ; Yong-Bing, H; Hu, CG; Wang, F; Hu, L. *Supramol. Chem.*, 2008, 20, 265-271.
- [58] Hu, X; He, J; Chan, ASC; Han, X; Cheng, JP. *Tetrahedron: Asymmetry*, 1999, 10, 2685-2689.
- [59] Guo, W; Wang, J; Wang, C; He, JQ; He, XW; Cheng, JP. *Tetrahedron Lett.*, 2002, 43, 5665-5667.
- [60] Hu, X; Chan, ASC; Han, X; He, J; Cheng, JP. *Tetrahedron Lett.*, 1999, 40, 7115-7118.
- [61] Gaeta, C; De Rosa, M; Fruilo, M; Soriente, A; Neri, P. *Tetrahedron: Asymmetry*, 2005, 16, 2333-2340.
- [62] Xu, ZX; Li, GK; Chen, CF; Huang, ZT. *Tetrahedron*, 2008, 64, 8668-8675.
- [63] Xu, ZX; Zhang, C; Zheng, QY; Chen, CF; Huang, ZT. *Org. Lett.*, 2007, 9, 4447-4450.
- [64] Xu, ZX; Zhang, C; Yang, Y; Chen, CF; Huang, ZT. *Org. Lett.*, 2008, 10, 477-479.
- [65] Liu, SY; He, YB; Qing, GY; Xu, KX; Qin, HJ. *Tetrahedron: Asymmetry*, 2005, 16, 1527-1534.
- [66] Qing, GY; He, YB; Chen, ZH; Wu, XJ; Meng, LZ. *Tetrahedron: Asymmetry*, 2006, 17, 3144-3151.
- [67] Qing, GY; He, YB; Zhao, Y; Hu, CG; Liu, SY; Yang, X. *Eur. J. Org. Chem.*, 2006, 1574-1580.
- [68] Pu, L. *Chem. Rev.*, 2004, 104, 1687-1716.
- [69] Lin, J; Li, ZB; Zhang, HC; Pu, L. *Tetrahedron Lett.*, 2004, 45, 103-106.
- [70] Zhao, J; Fyles, TM; James, TD. *Angew. Chem. Int. Ed.*, 2004, 43, 3461-3464.
- [71] Zhao, J; Davidson, MG; Mahon, MF; Kociok-Kohn, G; James, TD. *J. Am. Chem. Soc.*, 2004, 126, 16179-16186.
- [72] Jennings, K; Diamond, D. *Analyst*, 2001, 126, 1063-1067.
- [73] Kubo, Y. *Synlett*, 1999, 161-174.
- [74] Kubo, Y; Maeda, S; Tokita, S; Kubo, M. *Nature*, 1996, 382, 522-524.
- [75] Kubo, Y; Hirota, N; Maeda, S; Tokita, S. *Anal. Sci.*, 1998, 14, 183-189.
- [76] Grady, T; Harris, SJ; Smyth, MR; Diamond, D. *Anal. Chem.*, 1996, 68, 3775-3782.
- [77] Jennings, K; Diamond, D. *Analyst*, 2001, 126, 1063-1067.
- [78] Grady, T; Joyce, T; Smyth, MR; Harris, SJ; Diamond, D. *Anal. Commun.*, 1998, 35, 123-125.
- [79] Luo, J; Zheng, QY; Chen, CF; Huang, ZT. *Tetrahedron*, 2005, 61, 8517-8528.
- [80] Cao, YD; Luo, J; Zheng, QY; Chen, CF; Wang, MX; Huang, ZT. *J. Org. Chem.*, 2004, 69, 206-208.
- [81] Luo, J; Zheng, QY; Chen, CF; Huang, ZT. *Chem. Eur. J.*, 2005, 11, 5917-5928.
- [82] Miao, R; Zheng, QY; Chen, CF; Huang, ZT. *J. Org. Chem.*, 2005, 70, 7662-7671.
- [83] Li, SY; Zheng, QY; Chen, CF; Huang, ZT. *Tetrahedron: Asymmetry*, 2005, 16, 2816-2820.
- [84] Pinkhassik, E; Stibor, I; Casnati, A; Ungaro, R. *J. Org. Chem.*, 1997, 62, 8654-8659.
- [85] Dondoni, A; Marra, A; Scherrmann, MC; Casnati, A; Sansone, F; Ungaro, R. *Chem. Eur. J.*, 1997, 3, 1774-1782.
- [86] Marra, A; Scherrmann, MC; Dondoni, A; Casnati, A; Minari, P; Ungaro, R. *Angew. Chem., Int. Ed. Engl.*, 1994, 33, 2479-2481.
- [87] Budka, J; Tkadlecová, M; Lhoták, P; Stibor, I. *Tetrahedron*, 2000, 56, 1883-1887.

- [88] Grazia, ML; Consoli, GML; Cunsolo, F; Geraci, C; Mecca, T; Neri, P. *Tetrahedron Lett.*, 2003, 44, 7467-7470.
- [89] Pérez-Balderas, F; Santoyo-González, F. *Synlett*, 2001, 1699-1702.
- [90] Bitter, I; Kőszegi, É; Grün, A; Bakó, P; Pál, K; Grofcsik, A; Kubinyi, M; Balázs, B; Tóth, G. *Tetrahedron: Asymmetry*, 2003, 14, 1025-1035.
- [91] Kubinyi, M; Pál, K; Baranyai, P; Grofcsik, A; Bitter, I; Grün, A. *Chirality*, 2004, 16, 174-179.
- [92] Yuan, HS; Huang, ZT. *Tetrahedron: Asymmetry*, 1999, 10, 429-437.
- [93] Karakucuk, A; Durmaz, M; Sirit, A; Yilmaz, M; Demir, AS. *Tetrahedron: Asymmetry*, 2006, 17, 1963-1968.
- [94] Durmaz, M; Alpaydin, S; Sirit, A; Yilmaz, M. *Tetrahedron: Asymmetry*, 2007, 18, 900-905.
- [95] Soi, A; Pfeiffer, J; Jauch, J; Schurig, V. *Tetrahedron: Asymmetry*, 1999, 10, 177-182.
- [96] Jauch, J; Schurig, V. *Tetrahedron: Asymmetry*, 1997, 8, 169-172.
- [97] Maji, P; Krishnamurthy, SS; Nethaji, N. *Polyhedron*, 2008, 27, 3519-3527.
- [98] Lambert A; Regnouf-de-Vains JB; Rinaldi, D; Ruiz-Lopez MF. *J. Phys. Org. Chem.* 2006, 19, 157-166.
- [99] Bozkurt, S; Durmaz, M; Yilmaz, M; Sirit, A. *Tetrahedron: Asymmetry*, 2008, 19, 618-623.
- [100] Krawinkler, KH; Maier, NM; Sajovic, E; Lindner, W. *J. Chromatogr. A*, 2004, 1053, 119-131.
- [101] Krawinkler, KH; Maier, NM; Ungaro, R; Sansone, F; Casnati, A; Lindner, W. *Chirality*, 2003, 15, 17-29.
- [102] Boyko, VI; Yakovenko, AV; Matvieiev, YI; Kalchenko, OI; Shishkin, OV; Shishkina, SV; Kalchenko, VI. *Tetrahedron*, 2008, 64, 7567-7573.
- [103] Yakovenko, AV; Boyko, VI; Danylyuk, O; Suwinska, K; Lipkowski, J; Kalchenko, VI. *Org. Lett.*, 2007, 7, 1183-1185.
- [104] Boyko, VI; Shivanyuk, A; Pyrozhenko, VV; Zubatyuk, RI; Shishkin, OV; Kalchenko, VI. *Tetrahedron Lett.*, 2006, 47, 7775-7778.
- [105] Shirakawa, S; Kimura, T; Murata, SI; Shimizu, S. *J. Org. Chem.*, 2009, 74, 1288-1296.
- [106] Konrad, S; Bolte, M; Näther, C; Lüning, U. *Eur. J. Org. Chem.*, 2006, 4717-4730.
- [107] Quintard, A; Darbost, U; Vocanson, F; Pellet-Rostaing, S; Lemaire M. *Tetrahedron: Asymmetry*, 2007, 18, 1926-1933.
- [108] Neri, P; Bottino, A; Geraci C; Piattelli, M. *Tetrahedron: Asymmetry*, 1996, 7, 17-20.
- [109] Thamarai Chelvi, SK; Yong, EL; Gong, Y. *J. Chromatogr., A* 2008, 1203, 54-58.
- [110] van Dienst, E; Snellink, BHM; von Piekartz, I; Engbersen, JFJ; Reinhoudt, DN. *J. Chem. Soc., Chem. Commun.*, 1995, 151-152.
- [111] Liu, Y; Chen, Y; Li, L; Huang, G; You, CC; Zhang, HY; Wada, T; Inoue, Y. *J. Org. Chem.*, 2001, 66, 7209-7215.
- [112] Uccello-Barretta, G; Berni, MG; Balzano, F. *Tetrahedron: Asymmetry*, 2007, 18, 2565-2572.
- [113] Liu, F; Lu, GY; He, WJ; Hu, J; Mei, YH; Zhu, LG. *Synthesis*, 2001, 4, 607-611.
- [114] Liu, F; Lu, GY; He, WJ; Liu, MH; Zhu, LG. *Thin Solid Films*, 2004, 468, 244-249.
- [115] Paquet, V; Zumbuehl, A; Carreira, EM. *Bioconjugate Chem.*, 2006, 17, 1460-1463.
- [116] Parzuchowski, P; Böhmer, V; Biali, SE; Thondorf, I. *Tetrahedron: Asymmetry*, 2000, 11, 2393-2402.

-
- [117] Salem, AB; Regnouf-de-Vains, JB. *Tetrahedron Lett.*, 2001, 42, 7033-7036.
- [118] Cherenok, S; Vovk, A; Muravyova, I; Shivanyuk, A; Kukhar, V; Lipkowski, J; Kalchenko, V. *Org. Lett.*, 2006, 8, 549-552.
- [119] Haino, T; Fukuoka, H; Iwamoto, H; Fukazawa, Y. *Supramol. Chem.*, 2008, 20, 51-57.
- [120] Ballistreri, FP; Notti, A; Pappalardo, S; Parisi, MF; Pisagatti, I. *Org. Lett.*, 2003, 5, 1071-1074.
- [121] Amato, ME; Ballistreri, FP; Pappalardo, A; Tomaselli, GA; Toscano, RM; Williams, DJ. *Eur. J. Org. Chem.*, 2005, 16, 3562-3570.
- [122] Regnouf-de-Vains, JB; Lamartine, R; Fenet, B. *Helv. Chim. Acta*, 1998, 81, 661-668.
- [123] Marson, A; Freixa, Z; Kamer, PCJ; van Leeuwen, PWNM. *Eur. J. Inorg. Chem.*, 2007, 4587-4591.
- [124] Consoli, GML; Granata, G; Galante, E; Cunsolo, F; Geraci, C. *Tetrahedron Lett.*, 2006, 19, 3245-3249.
- [125] Consoli, GML; Granata, G; Garozzo, D; Mecca, T; Geraci, C. *Tetrahedron Lett.*, 2007, 48, 7974-7977.
- [126] Bonini, C; Chiummiento, L; Funicello, M; Lopardo, MT; Lupattelli, P; Laurita, A; Cornia, A. *J. Org. Chem.*, 2008, 73, 4233-4236.
- [127] Dieleman, C; Steyer, S; Jeunesse, C; Matt, D. *J. Chem. Soc., Dalton Trans.*, 2001, 2508-2517.
- [128] Steyer, S; Jeunesse, C; Harrowfield, J; Matt, D. *J. Chem. Soc., Dalton Trans.*, 2005, 1301-1309.
- [129] Castellano, RK; Kim, BH; Rebek Jr., J. *J. Am. Chem. Soc.*, 1997, 119, 12671-12672.
- [130] Castellano, RK; Nuckolls, C; Rebek, J Jr. *J. Am. Chem. Soc.*, 1999, 121, 11156-11163.

Chapter 12

NEW TRENDS IN MODIFICATIONS AND APPLICATIONS OF RESORCINARENES

*Cezary A. Kozłowski**, *Wiesława Kudelska* and *Joanna Konczyk*

Institute of Chemistry and Environment Protection, Jan Długosz University, 42-201
Częstochowa, Armii Krajowej 13/15, Poland

ABSTRACT

Easily accessible, resorcinarenes are valuable three dimensional building blocks for the coordination chemistry. They can be functionalized by introducing many different ligand moieties containing atoms O, S, N, P both at upper and lower rim. The possibility of the modifications of resorcinarenes resulted in the formation of coordination preorganized structures of molecular dimensions and complexes which can selectively encapsulate a variety of molecules. All the fascinating properties of resorcinarenes make this class of compounds very prospective from the point of view of supramolecular chemistry and creation valuable receptor molecules as well as new systems mimicking nature. In this connection, chiral derivatives of resorcinarenes are particular interest due to new possibilities of activities and applications. Recent developments of the resorcinarenes application as ion carriers for alkali metal, alkaline earth metal cations as well as transition metal ions removal and separation will be presented. The effect of structural studies of ring size variation, lower and upper rim functionalization on the selectivity and efficiency of solvent extraction and liquid membrane metal ions transport will be also described.

We present the recent applications of resorcinarenes and their derivatives as new ion carrier immobilized in polymers and as analytical devices achieved *via* their attachment to solid supports.

Keywords: Resorcin[4]arenes, synthesis, application, structure study, metal complexes.

* Corresponding author: Fax: +48 34 3665322. E-mail address: c.kozlowski@ajd.czyst.pl

1. INTRODUCTION

Resorcinol-derived calixarenes, calix[4]resorcinarenes, resorcin[4]arenes **1** (Figure 1), resorcarenes have been of continuous interest to the scientific community due to their widespread applications. Resorcinarenes are very popular scaffolds widely useful as building blocks for the synthesis cation, anion and bifunctional receptors, container molecules, and self- assembling systems.

The cavity of the resorcinarenes provides a site for the binding of organic guest molecular species and the selectivity of resorcinarenes to particular analytes can be controlled by altering the size of the cavity as well as the peripheral substituted groups. Structural variations at the wide or narrow rim of hydrogen bonded resorcinarenes may result in new highly active compounds, that at present possess many applications: as the stationary phase in HPLC [1], active substances in medicine [2], catalysts in asymmetric reactions [3-5]. Furthermore, resorcinarene can exhibit liquid - crystalline behavior by appropriate choice of the R groups on the resorcinarene [6-8].

The resorcin[4]arene skeleton is well suited for the construction of cyclochiral/inherently chiral molecules due to its immanent curvature that can be preserved. The attractiveness of the this type of compounds is connected with relative easy synthetic procedure, using the Mannich reaction, and where after resolution, so the first applications of molecules possessing this type of chirality were reported early in 2004 [9] and now they are still worthy of special interest.

New trends in chemistry of calixarenes and resorcinarenes modification of their structures are of a great importance for practical applications in modern separation science as well as nano- and biotechnologies [10,11]. Recent advertences reports concerning resorcinarenes of various structures requires their detailed study and knowledge of their reactivity mechanisms. Resorcinarenes serve as starting material for the preparation of more sophisticated molecules such as cavitands, carceplexes, hemicarceplexes [12-15].

This chapter surveys recent developments concerning the trends in the synthesis and applications modified resorcinarenes.

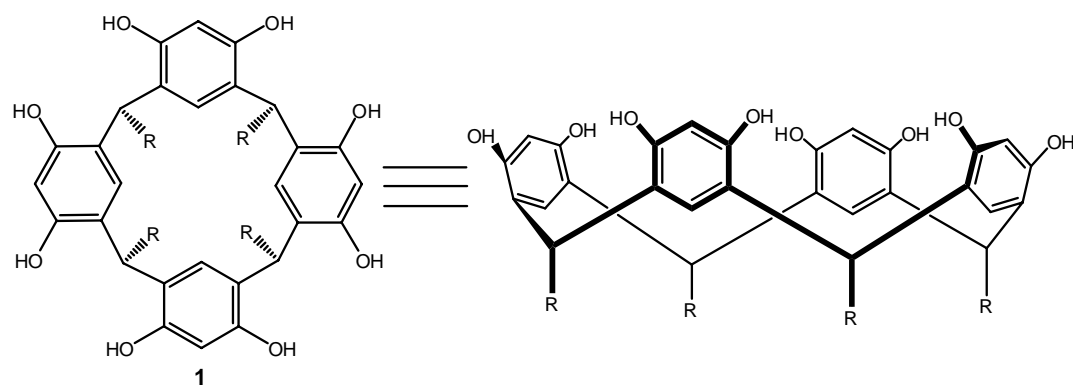


Figure 1. Resorcin[4]arenes.

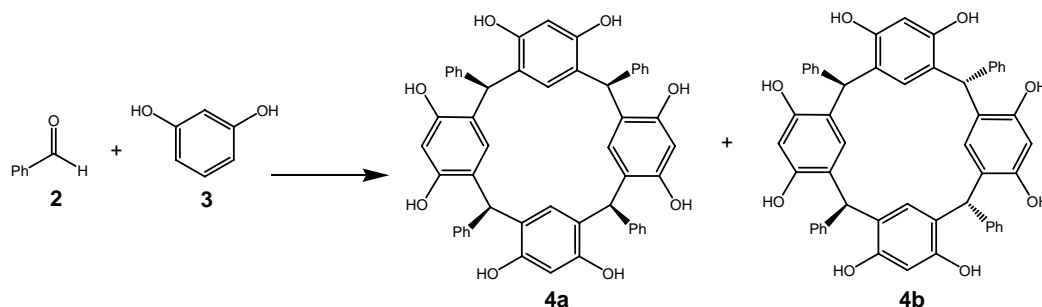


Figure 2. Formation of resorcinarene diastereoisomers.

2. SYNTHESIS OF RESORCINARENES MODIFIED AT THE WIDE (UPPER) RIM OF MOLECULE

Many methods for the complete and selective functionalization of resorcinarenes at the wide rim of macrocycle are still developed in order to preorganize multiple binding and/or catalytic subunits in close spatial proximity. Uninterruptedly developing modifications them with numerous recognition features have caused binding selectivity increased as well as stronger host - dash associations with slower dissociation rates.

The earliest report of the synthesis of resorcinarene, which could not be characterized, date back to the 1872's [16]. In 1940 the tetrameric structure of resorcinarene was established [17] and in 1980 Hogberg [18, 19] developed the most efficient synthetic procedure still in use today. The acid - catalyzed condensation of resorcinol with any aliphatic or aromatic aldehyde provides resorcinarenes. Several research group proposed the applications in the above mentioned reaction also other catalysts: *p*-toluenesulfonic acid [20], some conventional Lewis acid [21,22], more recently trifluoromethanesulfonic salts [23,24]. Lately, lanthanide(III) nitro-benzenesulfonates and *p*-toluenesulfonate complexes of lanthanide(III), iron(III), and copper(II) were successfully applied to the formation of resorcinarene. Of the four diastereoisomers formed, the all *cis* (rccc) isomer **4a** and the *cis-trans-trans* (rctt) **4b** (Figure 2) were isolated in the reaction with benzaldehyde **2**, with the relative ratio depending on the reaction conditions used [25].

The continuation of application of microwave irradiation in the synthesis of novel resorcinarenes, resorcinarene phtalonitrile and novel metal phtalocyanine (Cu, Zn, Co, Ni) polymers **5a-d** containing resorcinarene groups (Figure 3) allowed reduce reaction times and enhance the reactions yields in comparison with classical methods [26].

2.1. *O*-Functionalization Phenolic Fragments of Resorc[4]arenes

Functionalization of resorcarenens through the phenolic hydroxyl groups or the *ortho* position has led to the availability of a number of resorcarenene based resorcinarenes.

Ito et al. [27] prepared fully protected resorcinarenes **6a-j**, with acid labile groups *t*-butylcarbonyl and *t*-butylcarbonylmethyl (Figure 4) by the condensation of resorcinol with aldehydes, separation two isomers formed C_{4v} (ccc) and C_{2v} (ctt), and finally protection

hydroxyl functions. Dissolution inhibition effects of the protected resorcinarenes were investigated using a 70/30 copolymer of 4-hydroxystyrene with *t*-butyl acrylate as a matrix polymer and 0.26 N tetramethylammonium hydroxide as a developer.

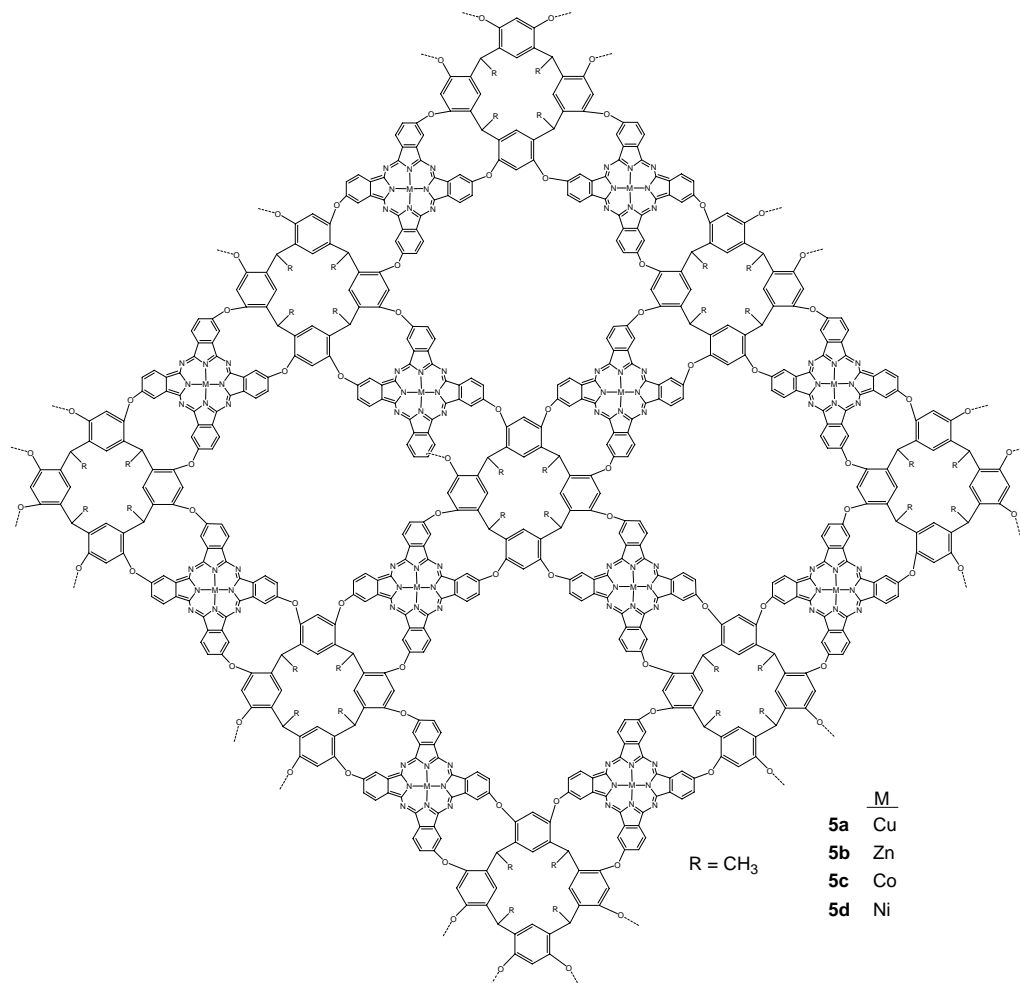


Figure 3. Metal phthalocyanine polymer with resorcinarenes.

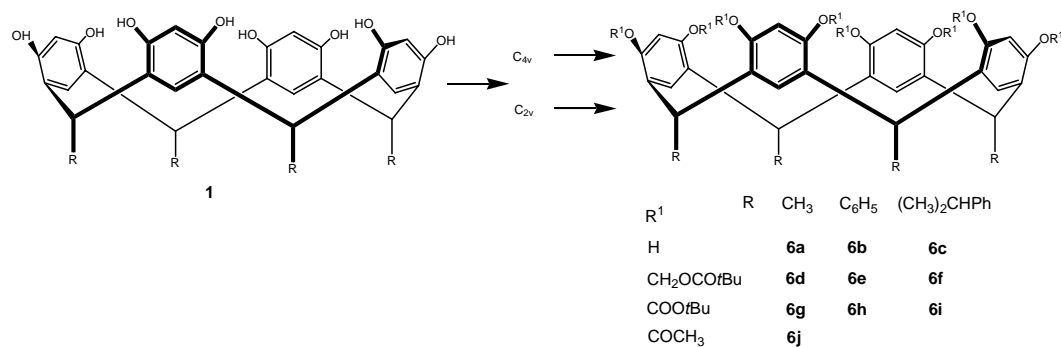


Figure 4. Protected resorcinarenes.

All the resorcinarene derivatives investigated in this study show a mutually similar and strong loading effect, much stronger than the small bifunctional inhibitors. Furthermore, resorcinarene derivatives can bring the dissolution rate of the copolymer down to < 5%, while the maximum dissolution rate reduction achieved with the bifunctional compounds is only 75-65%.

The *O*-alkylation of the racemic C_4 -symmetric heptyl and *C*-propyl resorcinarenes **7a,b** with 2- and 3-picolyyl chloride in the presence of base afforded the tetra-picolyyl ethers **8a-c** (Figure 5) in high yields, respectively. The pyridine-functionalized resorcinarenes were applied to metal complexations. It was found, that such modified resorcinarenes solubilize copper and nickel salts and form insoluble products with silver and palladium. The copper complex form a linear polymer containing two structurally distinct bridges [28].

The *O*-dansylation of *C*-propyl resorcinarene with dansyl chloride results in tetradansylated or octadansylated resorcinarenes **9, 10** (Figure 6), depending on the ratio of the used substrates [29]. Partially substituted compounds adopts a boat conformation with C_{2v} symmetry in solution and in solid state, while completely substituted resorcinarene at room temperature in solution adopts a time averaged C_{4v} symmetry, which turns into stable boat conformation at low temperatures and in the solid state. In the solid state both tetra- and octa-resorcinarenes exhibit a multitude of intra- and intermolecular interactions between the adjacent dansyl moieties and also with the aromatic parts of the macrocyclic skeleton. The relative fluorescence intensity increases with the increase in number of dansyl units in the resorcinarenes, but is clearly less than the intensity of the reference compound-dansylphenolate. Direct protonation of dansyl moieties leads to a decrease in the absorption and fluorescence spectra.

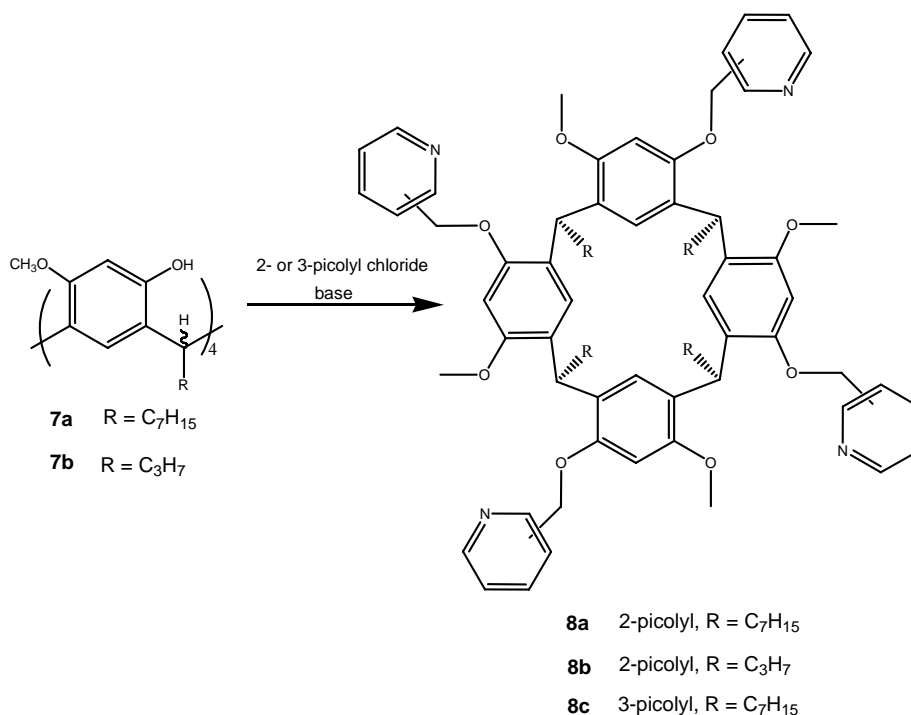


Figure 5. The pyridine - functionalized resorcinarenes.

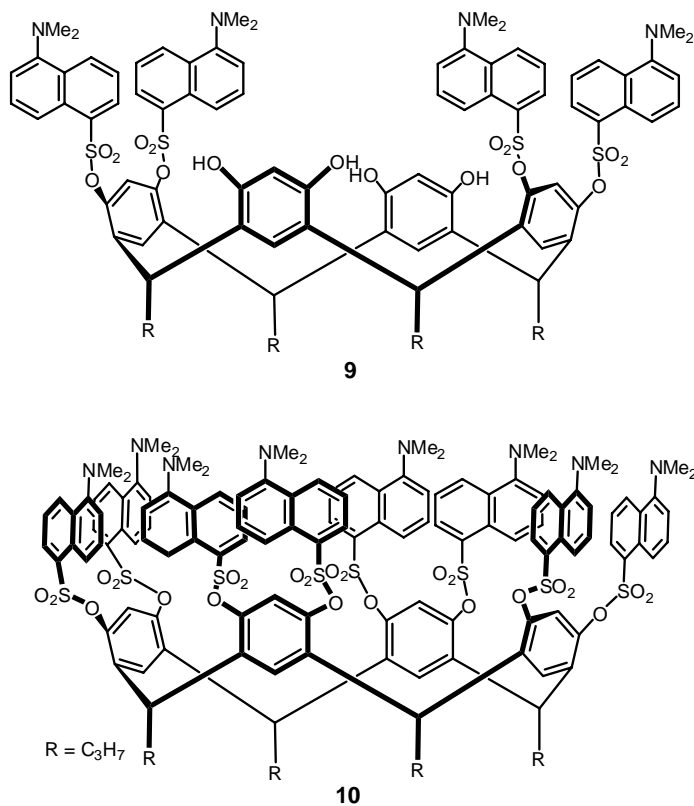


Figure 6. Partial and completed dansylated resorcinarenes.

New example of octa *O*-phosphorylated *C*-phenyl resorcinarene **11** (Figure 7) was obtained in one step by the reaction of resorcinarene with hexaethyltriimidophosphite and then by treatment with hydrogen peroxide-urea adduct [30].

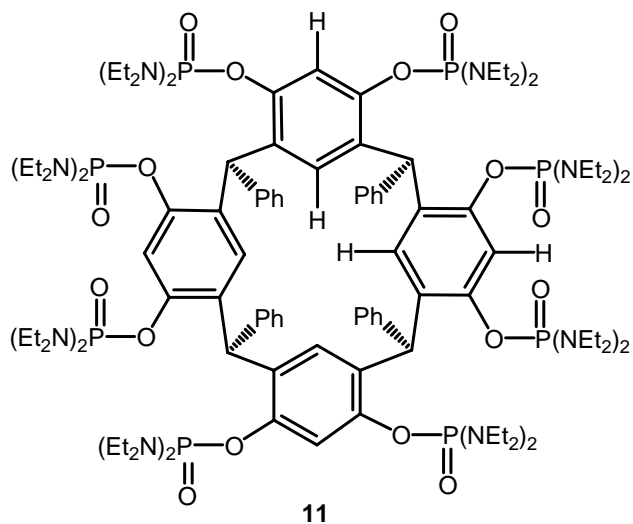


Figure 7. Structure of octa *O*-phosphorylated *C*-phenyl resorcinarene.

Hydrazides of carboxylic acids show unique complexation properties [31] so in order to combine the unusual character of resorcinarene and acylhydrazides, Podyachew et al. synthesized and characterized *C*-alkyl resorcinarenes bearing acetyl hydrazide groups on the upper rim of molecules by the hydrazinolysis of ester group containing resorcinarene [32].

Tetraaryl resorcinarene in the past years received less attention in comparison with tetraalkyl resorcinarenes, due to poor solubility in common organic solvents used as medium during chemical modifications. In order to obtain rigid stable conformations of resorcinarenes, which might result in much selective recognition, a selective and efficient procedure to introduce ferrocenes (Fc) on the upper rim, or on the lower rim, or both sides of rim molecule was reported. Known *C*-tetraaryl, *C*-*p*-hydroksyphenyl and *C*-tetraferrocenyl resorcinarenes **12a-c** [37-39] were fully alkylated with α -chloroacetate to give activated *O*-acetyl ester ethyl resorcinarene **13a-c**, then these compounds were treated with hydrazine to yield acetylhydrazine derivatives **14a-c**, from which the multi-ferrocenyl hydrazone of resorcinarenes were obtained by the reaction with ferrocenecarboaldehyde **15a-c** (Figure 8) [40].

Han and Yan introduced multi-functional carbamoyloxy groups on the wide rim of tetraaryl and tetraferrocenyl resorcinarenes **16a-c**, **17a-c** also by direct alkylation with *N,N*-dialkyl α -chloroacetamide or by aminolysis of the activated resorcinarene acetate **13** with suitable amines (Figure 9). The X-ray single crystal analysis of these resorcinarene amides show *rcctt* and *rccc* configuration [41]. One of intensively developing trends in the chemistry of resorcinarenes is the creation and investigation of new hosts with extended cavities, which open the new possibility of applications.

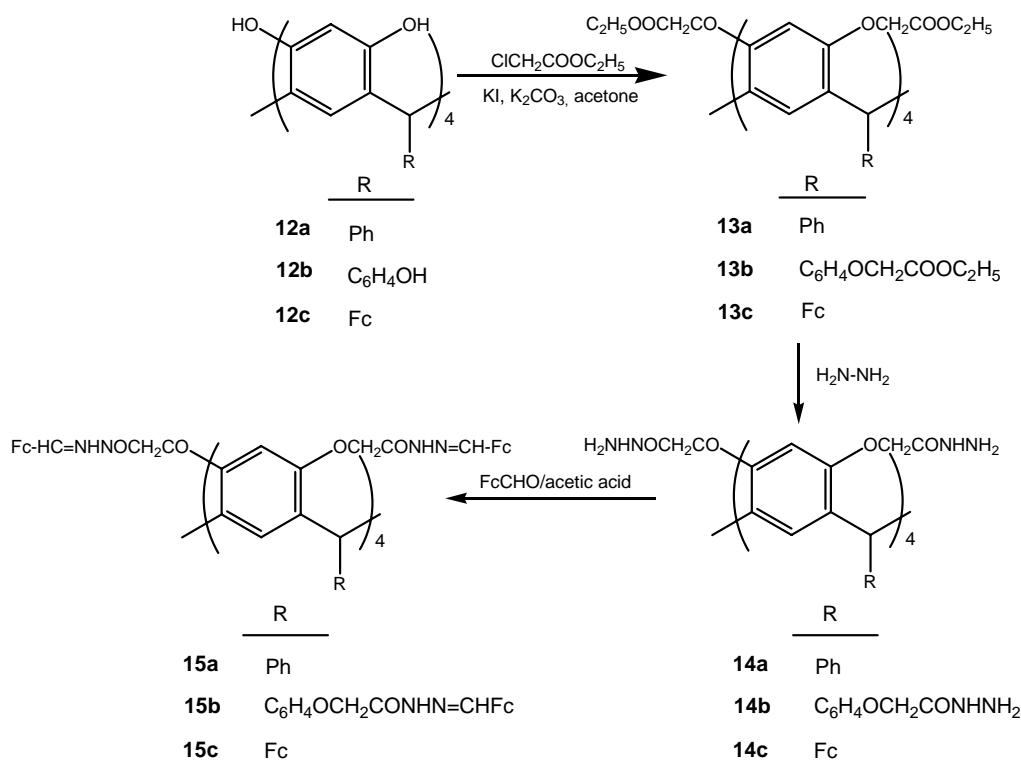


Figure 8. Synthesis of multi-ferrocenyl resorcinarenes.

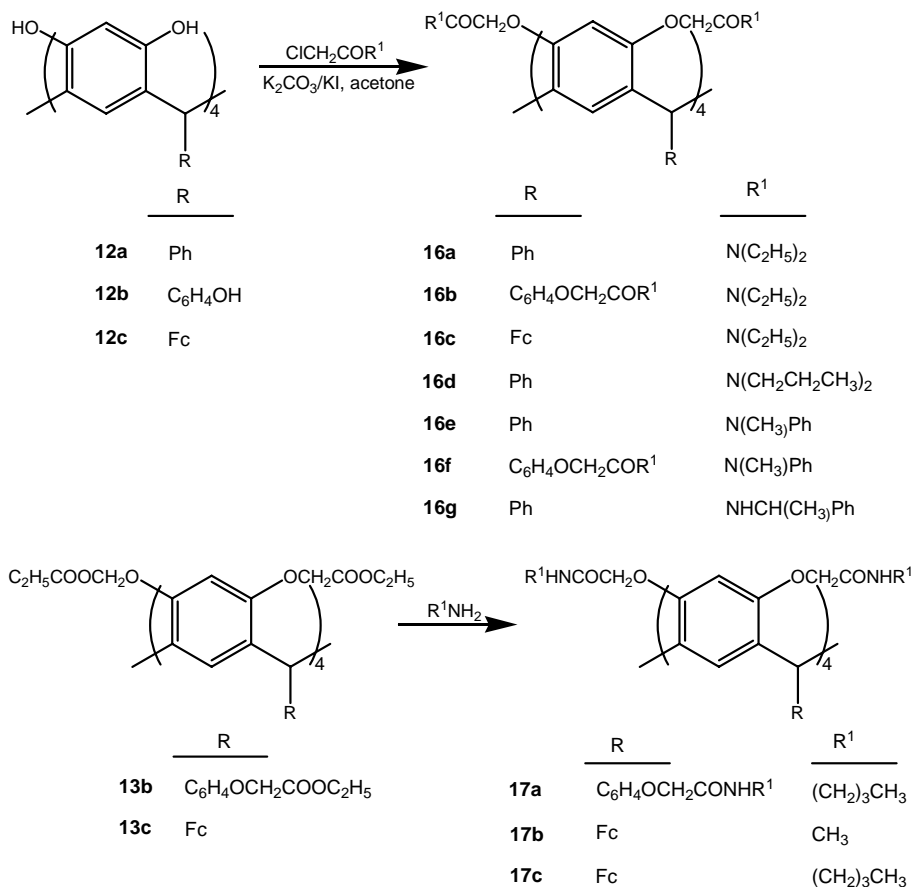


Figure 9. Synthesis of resorcinarene amides.

Condensation of acetylhydrazides **18** with aldehydes afford acetylhydrazone derivatives of resorcinarenes **19a-e** (Figure 10). The complexation properties of octahydrozones were investigated by liquid-liquid extraction method towards alkali, alkali-earth and transition metals ions. In spite of the high coordination capacity of resorc[4]arenes, octa-*O*-acetylhydrozones do not extract alkali metal cations but show excellent selectivity towards transition and soft heavy metal cations [33].

The synthesis of the two series of dendrimers with vinyl ferrocene and stilbene was carried out applying the convergent Fréchet approach [34] that consists in three steps. The first one is the synthesis of the two conjugated dendrons, which is followed by the selective formation of resorcinarenes and finally the alkylation between dendrons and resorcinarenes. Dendrons containing styryl and ferrocenylvinyl groups having *trans* conformations were obtained using Heck reactions. The $\chi^{(3)}$ values estimated from the third-harmonic generation (THG) Maker-fringe technique for the phenyl and ferrocenyl-ended resorcinarene dendrimers dispersed in thin solid films are the order of 10^{-13} and 10^{-12} esu, respectively [35]. Ferrocenyl-bearing dendrimers **22**, **23** with a resorcinarene core, high molecular weight (Figure 12) were prepared by Williamson reaction of *C*-alkyl resorcinarenes with ferrocenyl-ended dendrons containing π -conjugated systems. No electronic communication between metal centers was observed by cyclic voltammetry [36].

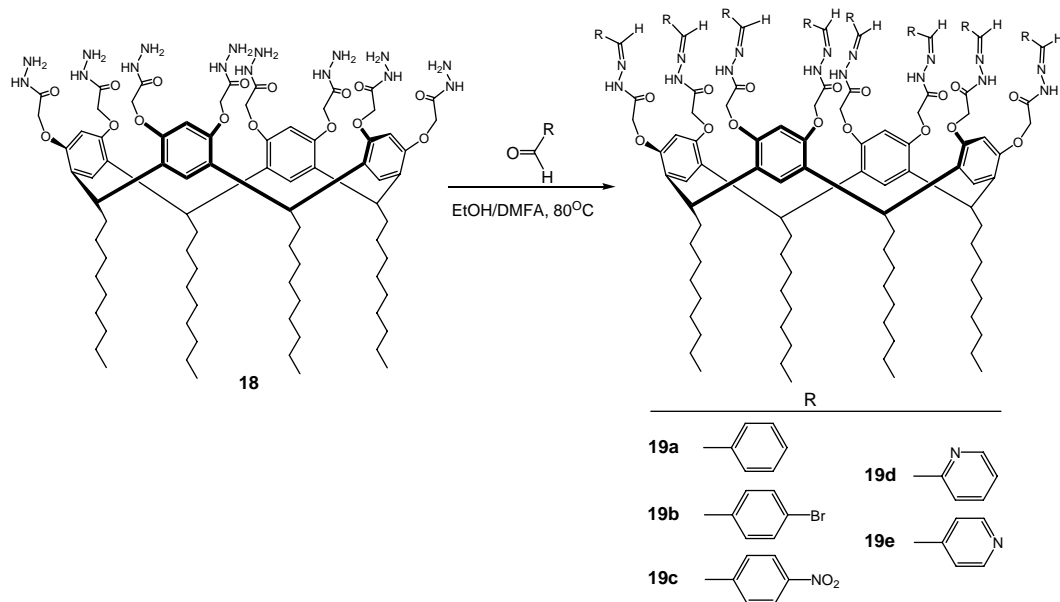


Figure 10. Synthesis of hydrazones.

Victorovna-Lijanova et al. [34] prepared phenyl and ferrocenyl ended resorcinarene-based dendrimers **20**, **21** (Figure 11).

Enantiomerically pure C_4 -symmetric alkyl resorcin[4]arenes with known absolute configuration were alkylated (with 2-bromobenzyl bromide) and then Pd-catalysed intramolecular C-C cross – coupling reactions gave inherently (*M,R*)-(-) and (*P,S*)-(+)-chiral tetrabiaryl ethers [42].

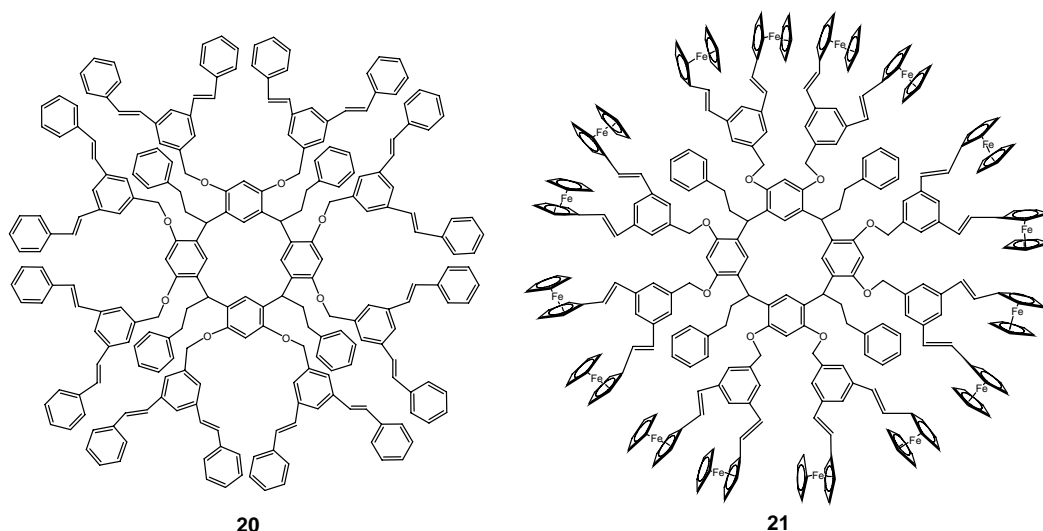


Figure 11. Resorcinarene dendrimers.

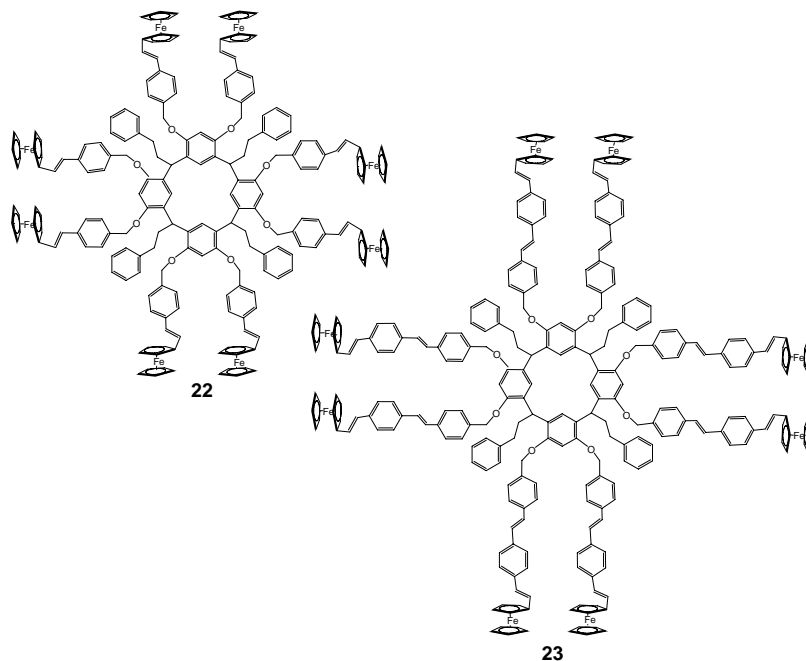


Figure 12. Ferrocenyl - bearing dendrimers with a resorcinarene core.

Salorinne and Nissinen prepared tetramethoxy resorcinarene tribenzo-bis-crown-5 ethers **24** and *m*- and *p*- tribenzo-bis-crown-6 ethers **25** (Figure 13), both of which have three benzene rings in the crown bridges on their upper rim, by the reaction of the appropriate ditosylate with tetramethoxy resorcinarene [43] in the presence of CsCO_3 as the base. Investigations of alkali metal complexation indicate that only *m*-tribenzo-bis-crown-6 as host showed affinity in binding alkali metal cations (K^+ , Rb^+ , Cs^+) with the highest affinity towards Cs^+ cation [44].

2.2. C-N(S)- Functionalization of Phenolic Fragments of Resorcin[4]arenes

Since 1993 [45], still widely used approach to the formation of nitrogen - functionalized resorcinarenes include regioselective aminomethylation of resorcinarene octaols with primary amine groups and formaldehyde under Mannich conditions. This approach led to wide spectrum of C_4 -symmetrical tetraoxazine derivatives of resorcinarenes, which can be readily transformed into wide spectrum of aminoresorcinarenes with widely variable solubility and extremely diverse structural and functional properties.

Luostarinen et al. [46] employed this strategy for construction tetra- and diaminoresorcinarenes **27a-h** from corresponding C_{4v} -tetra- or C_{2v} -bisoxazine derivatives of resorcinarenes **26a-h**. Subsequent the mild acylation of these resorcinarenes **27a-h** with butoxycarbonyl (Boc) anhydride or *p*-nitrophenyl ester (acetate or 4-methylbenzoate) proceeds selectively at the nitrogen atom to give resorcinareneamides **28a-j**. The complete acylation of **28** with acetic anhydride in pyridine afforded octaacetates **29a-d** in 40-90% yields (Figure 14). In the crystalline state the compounds obtained bind chloride anions through hydrogen bonds and electrostatic interactions and to display a chiral arrangement of

hydrogen bonded functional groups located at the wide rim of the macrocycle [46]. This procedure, namely the fourfold Mannich-type heterocyclization were also used for preparation resorcinarene oxazines bearing four 2,2,6,6-tetramethylpiperidine-*N*-oxyl radical moieties at the wide rim of macromolecule **30a-c** (Figure 15). The model studies revealed that these resorcinarene tetranitroxides are efficient scavengers of superoxide and peroxy radicals [47].

Analogous procedure was applied to synthesis of conformationally cyclochiral amido substituted on the upper rim of resorcinarenes **34a-j** (Figure 16) by using two – step sequence of reactions; Mannich reaction, removal of the *N,O*-acetal bridge and subsequent *N*-substitution with an acetyl (Ac), *t*-butoxycarbonyl (Boc) and *t*-butylaminocarbonyl (Bac) groups. Ethyl nitroacetate was found as mild and efficient agent for *N,O*- acetal removal [48]. The synthesis of chiral C_4 -symmetric resorcinarenes substituted with L-amino acid derivatives **34** were obtained by using this methodology. Compounds of that type can exist in two relatively stable inherently chiral C_4 -symmetric (*M*) and (*P*) conformations. However, because of diastereomeric preferences the amino acid substituted resorcinarene exhibit considerable diastereomeric excesses for the induced conformational inherent chirality (up to 95%). The formation of such chiral arrangements is responsible for pronounced effects in chiroptical spectra [49].

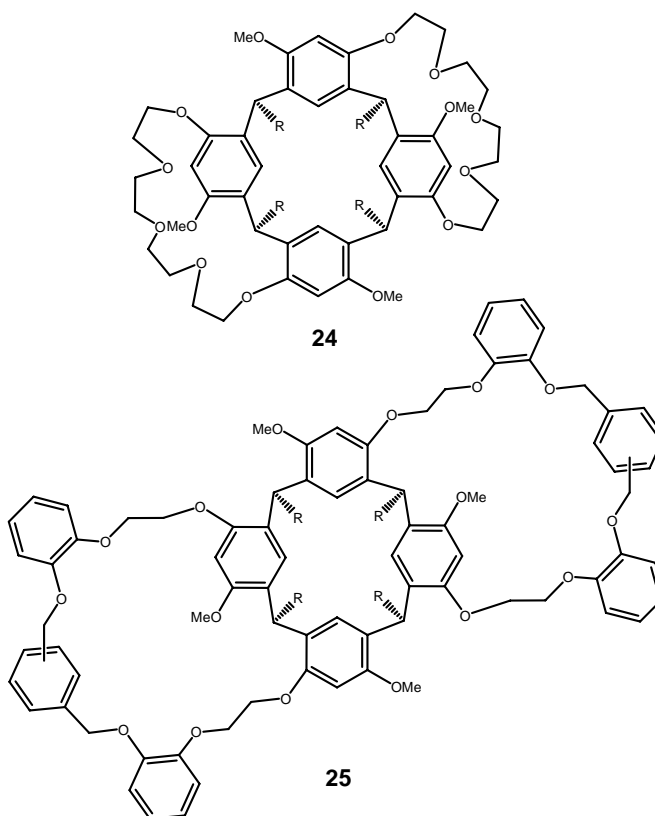


Figure 13. Structure of tetramethoxy resorcinarene tribenzo-bis-crown ethers.

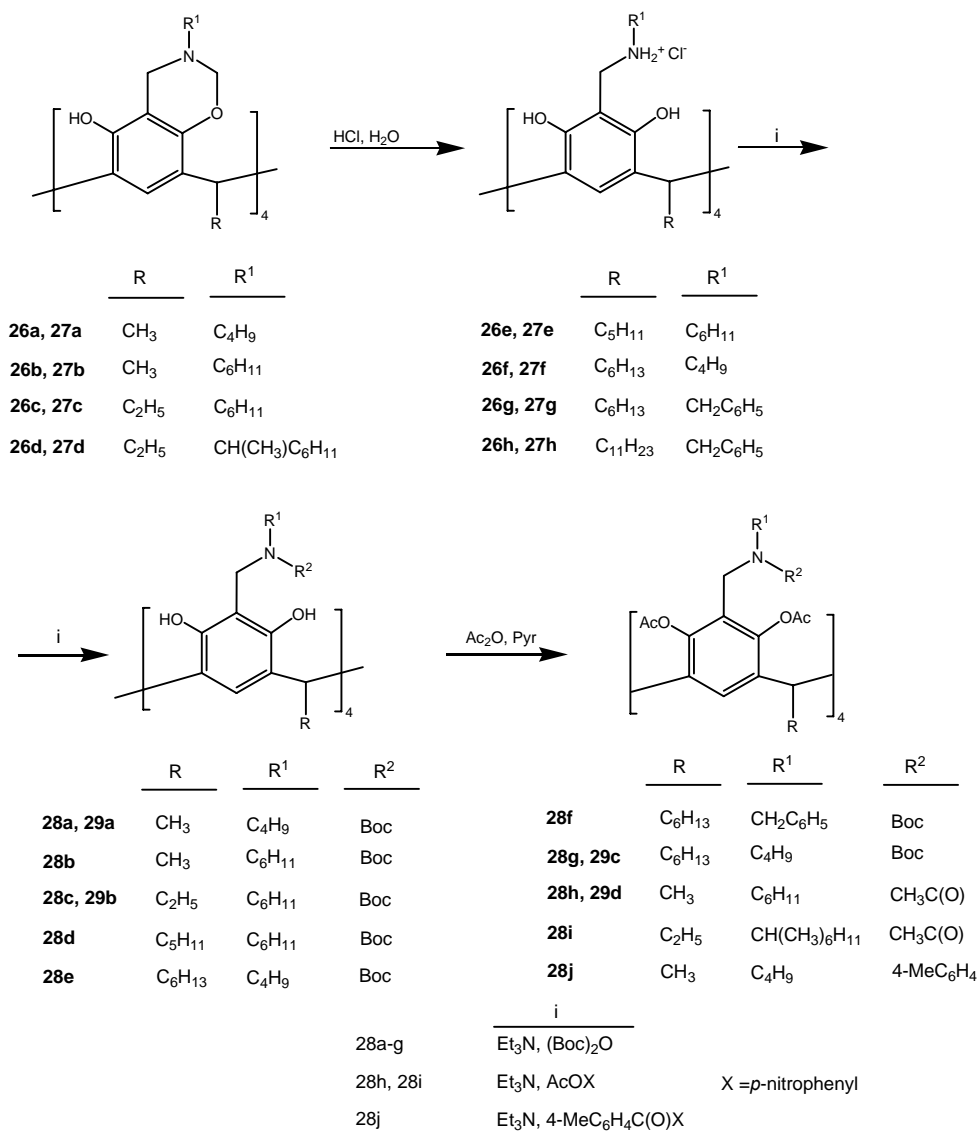


Figure 14. Synthesis of tetraaminoresorcinarenes.

Polish group reported the highly diastereoselective synthesis of chiral boron- derivatives of resorcinarene **38a-g** (Figure 17) *via* Mannich reaction from boron-chelates **37** obtained from chiral amino alcohols **36** [*S*-alaninol, (*S*)-2-amino-1-butanol, (*R*)-2-amino-1-butanol, (*S*)-valinol, (*S*)-isoleucinol, (*S*)-leucinol, (*R*)-phenylglycinol] and triethylboranes. Reactions with the (*S*)-amino alcohol led to boron derivatives *out*-(*P*, *S*, *S*, *S_N*, *S_B*). In the reactions with (*R*)-amino alcohol, *out*-(*m*, *R*, *R*, *R_N*, *R_B*) diastereoisomers were prepared, but with the same location of the ethyl group linked to the boron atom as well as the orientation to the resorcinarene cavity [50].

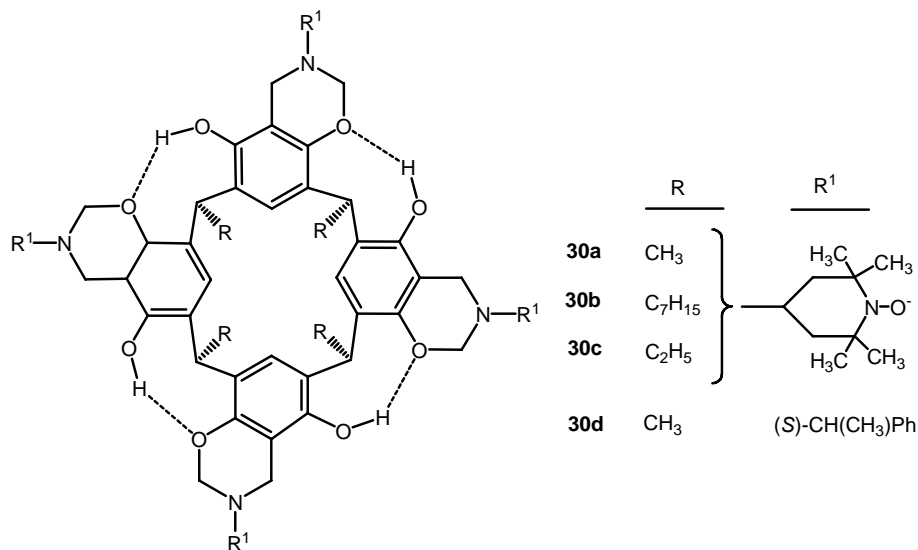


Figure 15. Chemical structures of spin labeled resorcinarenes.

A partially functionalized resorcinarene derivative **39** (Figure 18), having two sulfur donor atoms in its pendant arms was synthesized [51]. This synthesis was accomplished by the reaction of resorcinarene with ethanethiol and formaldehyde. The cation complexation properties of this receptor with various metal cations (alkali, alkaline earth, heavy and transition) show that **39** is able to interact only with the silver cation in MeOH, forming a complex of 1:1 stoichiometry. Hosting capacity of **39** for mercury was enhanced in MeOH, acetonitrile and DMF to form 1:2 complexes (ligand : metal cation) stoichiometry, but in propylene carbonate the 1:1 complex was formed.

3. SYNTHESIS OF RESORCINARENES MODIFIED AT THE NARROW RIM OF THE MOLECULE

Functionalization of resorcinarene in the lower rim has led to the availability of number of resorcinarene based derivatives to create new hosts with advantageous properties.

Botta et al. reported the synthesis of chiral basket resorcin[4]arenes **40** and **41**, each containing two 1,2-diaminocyclohexane and 1,2-diphenylethylenediamine bridges (Figure 19), respectively, starting from known resorcinarenes octamethyl ether tetra ester [52]. This synthesis involves hydrolysis ester function to tetracarboxylic acid, conversion into the corresponding tetra acid chloride and finally aminolysis with enantiomeric 1,2-diaminocyclohexane or 1,2-diphenylethylenediamine. Molecular modeling conformational investigations on the possible conformations of bis(diamido) derivatives produced a series of low-energy conformers, in which the four aromatic rings lie in a *flattened cone* arrangement, whereas both the joint chains are extended outwards in an arrangement tentatively designed as “open wings” and “folded wings”. Examination of the collision-induced decomposition (CID) spectra of the proton bonded diastereomeric $[M \cdot H \cdot A]^+$ complexes between **41** and a number of chiral amino acids guests (A = tyrosine methyl ester, tryptophan, amphetamine)

led to the conclusion that the host had a pronounced selectivity towards the enantiomers of tyrosine methyl ester and amphetamine, whereas the chirality of tryptophan was ineffective [53]. When the same macrocyclic tetracarboxylic acid chlorides in the *cone* conformation [52] was coupled with the appropriate terminal amino groups of four dipeptides, differing for composition and stereochemistry, four *cone* *N*-linked peptido-resorcin[4]arenes tetrafunctionalized at the feet were obtained. The studies interaction between peptidoresorcin[4]arenes (M) and homologue dipeptides as guests (G), both in solution and in the gas phase show the formation relatively stable host-guest complexes [M·G]. The NMR spectra revealed that hydrogen bonding interaction is at the basis of the G recognition by M, ESI mass spectroscopy allowed detection complexes [M·H·G_n]⁺ (where n = 1,2), which were shown to have different stabilities by the different collisional energies required to undergo dissociation [54]. One of observing trends in chemistry of resorcinarenes is elaboration efficient methods for preparation of interesting compounds, earlier not described in literature due to difficulties in the synthesis starting materials.

Russian group [55] reported the synthesis of the first representative resorcinarenes **42a-d** bearing four phosphinophenyl fragments at the lower rim of molecule (Figure 20) by reaction of resorcinarene with 4-dialkoxyphosphorylbenzaldehydes (alkyl = ethyl, isopropyl), under acidic conditions, in 73 and 53% yields, respectively. The starting phosphonates were obtained in the catalytic reaction of appropriate trialkyl phosphites with 4-bromobenzaldehyde [56-59].

The acid-catalyzed reaction of resorcinol with phosphono acetals or ethoxyvinylphosphonic acid esters gave **43a-g**, but in the case of hydrolytically labile compounds **43a-e** resorcinarenes **44a-e** with phosphorylmethyl groups at the lower rim of molecule were obtained, in high yields (Figure 21) [60].

The synthetic outcome of this reaction depend on nature starting phosphonates and experimental conditions. When the alkyl substituent in alkoxy groups at phosphorus atom is not very long (Et, Pr, *i*-Pr, Bu, *i*-Bu), a partial hydrolysis of the initially hydrolytically labile products formed takes place to eventually afford resorcinarenes with alkoxyhydroxylphosphoryl group. The longer alkyl substituent (heptyl, didodecyl) in starting vinylphosphonates results in formation stable resorcinarenes with diaalkoxyphosphoryl fragments on the lower rim of molecule. Reaction of resorcinol **3** with dichlorophosphonate **45** in acidic media led to water-soluble stable resorcinarene **46** bearing four fragments of phosphonic acid on the lower rim of molecule (Figure 22).

4. APPLICATIONS

During the past few decades resorcinarenes have been shown to co-crystallize and complex neutral molecules, forming often unpredictably solvates and other complexes with molecules present in the medium of crystallization. The aim of several research group studies is to further investigations of this class of compounds to gain new insights into the nature of possible interactions and to probe the properties of forming structures.

Shivanuyk reported that the highly stable hexameric resorcinarene nanocapsule **47**·8H₂O reversibly entraps inclusion complexes of calix[4]arenes **48a** and thiacalix[4]arene **48b** with

tetramethylammonium and trimethylsulfonium cations to give highly stable multicomponent assemblies (Figure 23) [61].

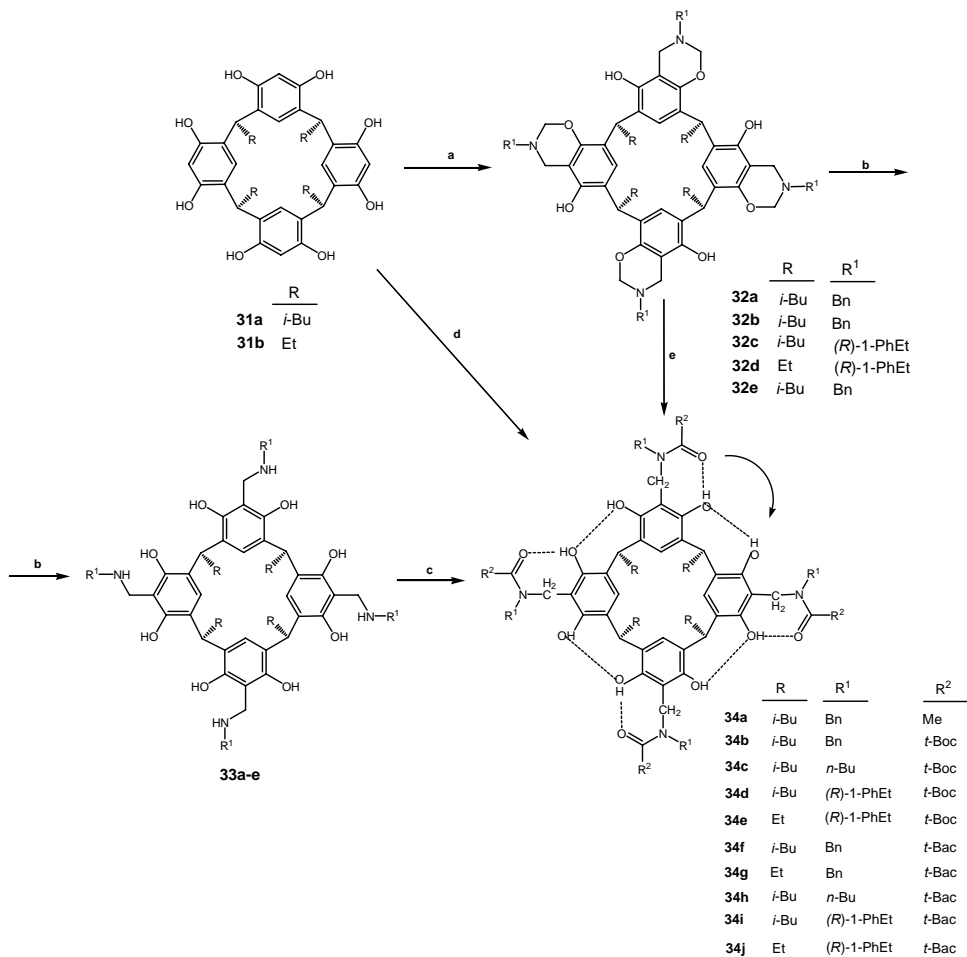


Figure 16. Synthesis of cyclochiral resorcinarenes.

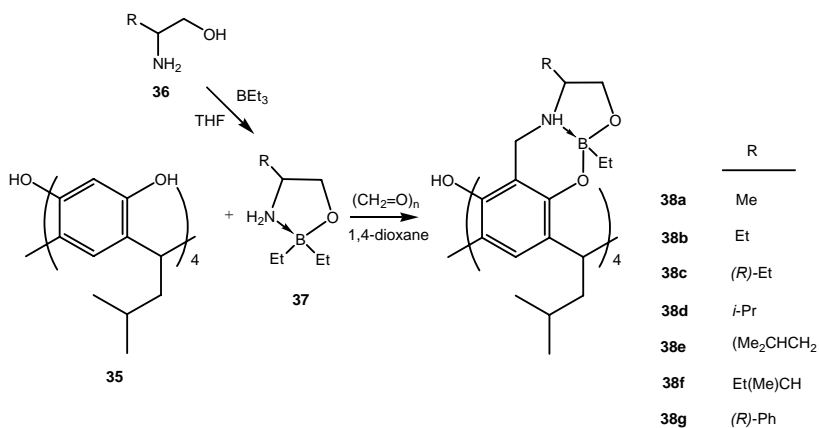


Figure 17. Synthesis of boron derivatives of resorcinarene.

The attention of Busi et al. have been focused on self-assembly and capsule formation properties of unsubstituted and substituted alkyl resorcinarenes with mono- and diquaternary alkyl ammonium cations under various conditions. In continuation of this subject resorcinarenes were crystallized with tetramethyl ammonium bromide and with other ammonium salts. Some unexpected results were observed when tetramethylated *C*-hexyl resorcinarene was co-crystallized with tetramethyl ammonium bromide. A solid state capsular structure was formed which is held together solely by the cation π -interactions and complementary geometry of the spherical guest cation and the concave resorcinarene host [62].

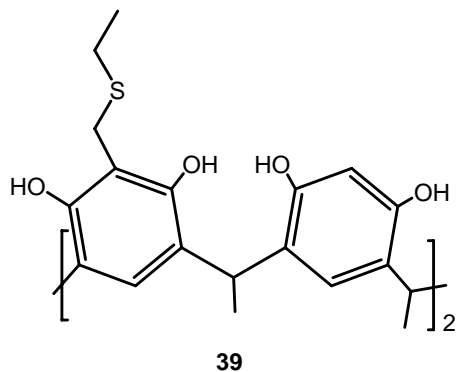


Figure 18. Resorcinarene with sulfur atoms.

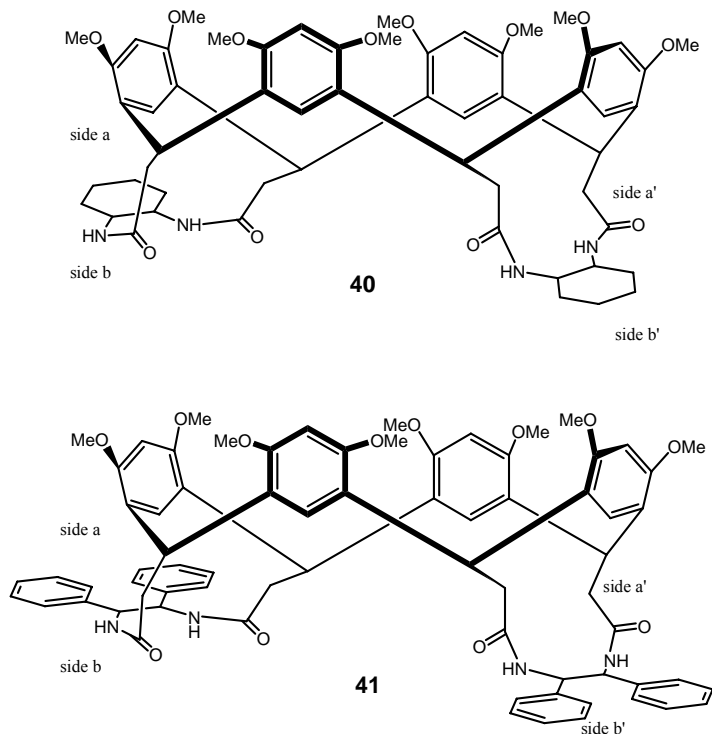


Figure 19. Chemical structure of chiral basket resorcin[4]arenes.

Co-crystallization of the C_4 -tetraisobutyl resorcin[4]arene with 1,4-bis-(pyridyl)ethane (bpe) from MeOH, regardless of the molar ratio of resorcinarene to 1,4-bis-(pyridyl)ethane, provided a molecular solid of the multicomponent host-guest complex 1:2, solvated with one half methanol molecule and one water molecule. The bpe ligands in both *cis* and *trans*-stereo configurations exist in the complex of which *trans*-bpe groups as guests are encapsulated in the capsules constructed by two pairs of opposition bowls of resorcinarene [63].

Matheny et al. investigated the self-assembly of the tetradentate ligand 1,2-bis-(5'-pyrimidyl)ethane with *C*-methyl calix[4]resorcinarene. These components formed in acetonitrile chain-link-hydrogen-bonded capsules in the ratio of 1:1:4. The reaction of the resorcinarene with ligand in a mixed solvent of methanol and dichloromethane, the linear ribbons or resorcinarenes interlocked by intricate hydrogen-bonding patterns that include methanol, water, the bipyramide ligand, and two disordered dichloromethane molecules were obtained [64].

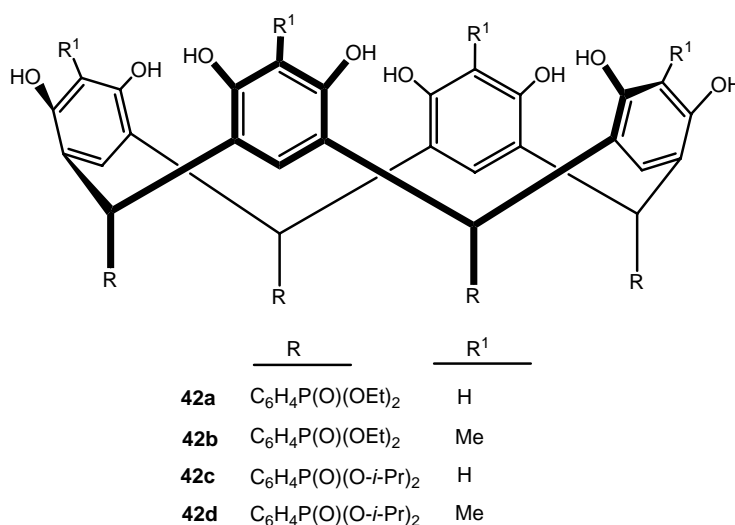


Figure 20. Synthesis of phosphorylmethyl derivatives of resorcinarene.

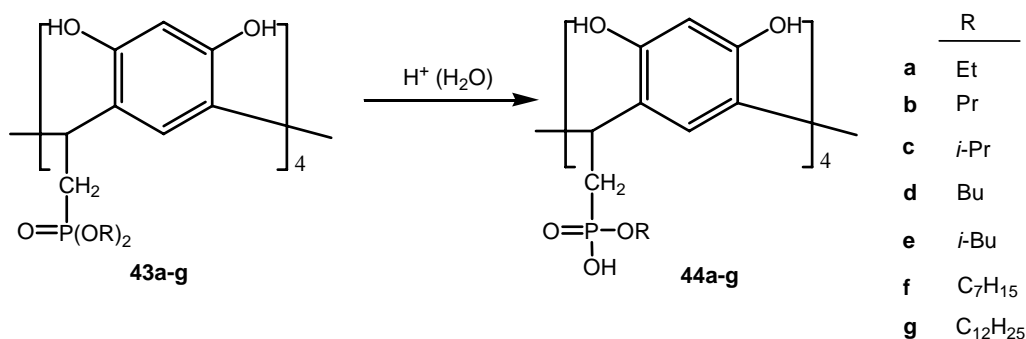


Figure 21. Synthesis of resorcinarenes with dialkoxyphosphoryl groups.

According to Aoyama et al. observations [65, 66], upper-rim unsubstituted resorcinarenes are promising hosts for sugar complexation due to hydrogen-bonding interactions between the hydroxyl groups both resorcinarene and sugars.

The goal of Kalenius et al. [67] investigation was to clarify the effects of the configuration of the sugar ring and the size of sugar. On the basis negative-polarization electrospray ionization quadrupole ion trap and electrospray ionization Fourier-transform ion cyclotron resonance mass-spectroscopy analysis, it was found that deprotonated *C*-tetraethyl and *C*-tetraphenyl resorcinarenes form noncovalent 1:1 complexes with neutral saccharides, which exhibited clear size and structure selectivity in their complexation. In the case of monosaccharides, hexoses formed much more abundant and kinetically stable complexes than pentose or deoxyhexoses molecule. A comparison of mono-, di-, and oligosaccharides revealed that both the relative abundance and stability of the complexes increase up to biose and triose, however as the sugar chain is increased, the resorcinarene affinity towards saccharides decreases, although the complexation still occurs [67].

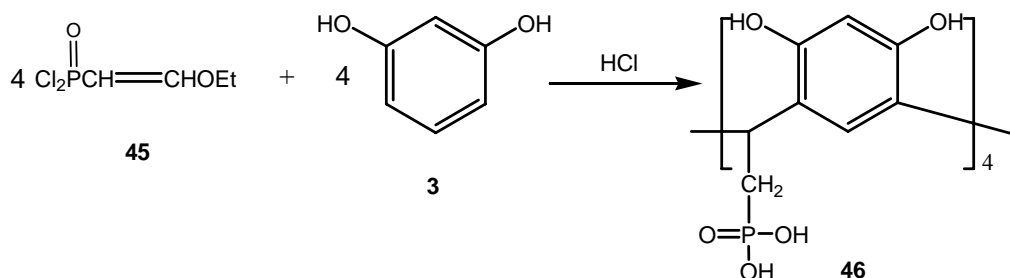


Figure 22. Synthesis of water-soluble resorcinarenes.

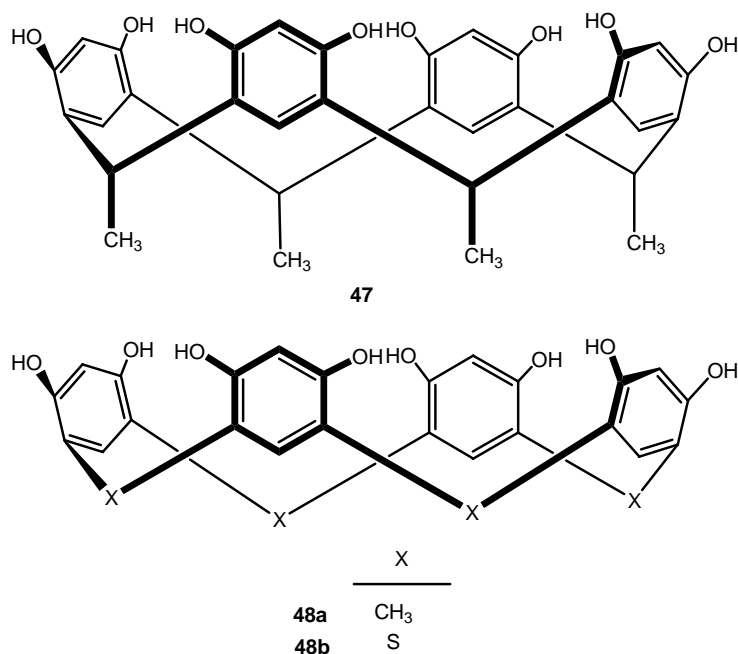


Figure 23. Resorcinarene and calixarene quest of hexameric nanocapsule.

O'Farrell et al. [68] applied Mannich conditions for preparation a series of sulfonated resorcinarenes containing pyrrolidine or piperidine groups **49a-h** (Figure 24), analogous to resorcinarene, which contains optically pure prolinylmethyl substituent attached to the resorcinol rings of a tetrasulfonated resorcinarene [69-71]. This reference compound is an exceptional chiral NMR shift reagent for water soluble substrates with phenyl or bicyclic aromatic ring. Certain new derivatives with different hydroxyproline substituent groups are specially effective at causing enantiomeric discrimination in the spectra of water-soluble cationic and anionic compounds with pyridyl, phenyl, and bicyclic aromatic rings. Mono-substituted anthryl-containing compounds form host-guest complexes with the calixarenes, as do naphthyl rings substituted at the 2,3- or 1,8-positions. While no one of these reagents is consistently the most effective the resorcinarene with *trans*-4-hydroxyproline and *trans*-3-hydroxyproline moieties generally produce the largest nonequivalence in the ^1H NMR spectra of substrates.

Hayashida et al. elaborated the synthesis a novel cyclophane-based resorcinarene tetramers **50a,b** and dodecamers **51a,b** (Figure 25) and showed their unique properties as multivalent host of histone as well as hydrophobic well-known fluorescent guest (*6-p*-toluidinonaphthalene-2-sulfonate, TNS). The oligomers prepared **51a,b** were constructed with a tetraaza[6.1.6.1]-paracyclophane or pentakis(cyclophane) skeleton [72] and 4 or 12 resorcinarenes having heptacarboxylic acid residues that connect to the macrocycle through amide linkages. The binding constants of tetramer **50a,b** and dodecamer **51a,b** with histone were $1.3 \cdot 10^7$ and $8.4 \cdot 10^7 \text{ M}^{-1}$, respectively, by means surface plasma resonance (SPR) measurements.

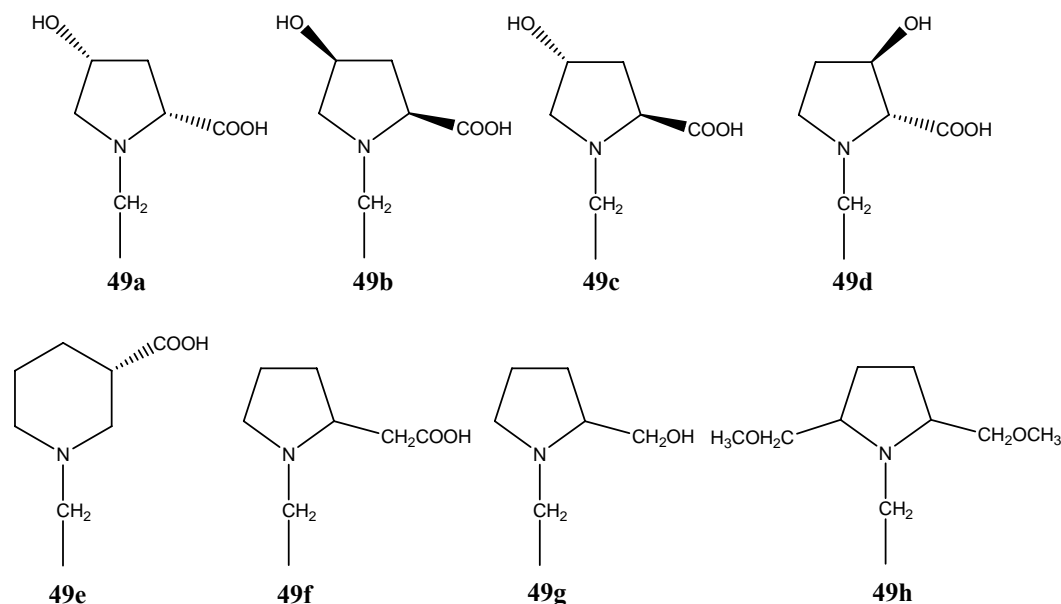


Figure 24. Substituent groups successfully attached to the sulfonated resorcinarene.

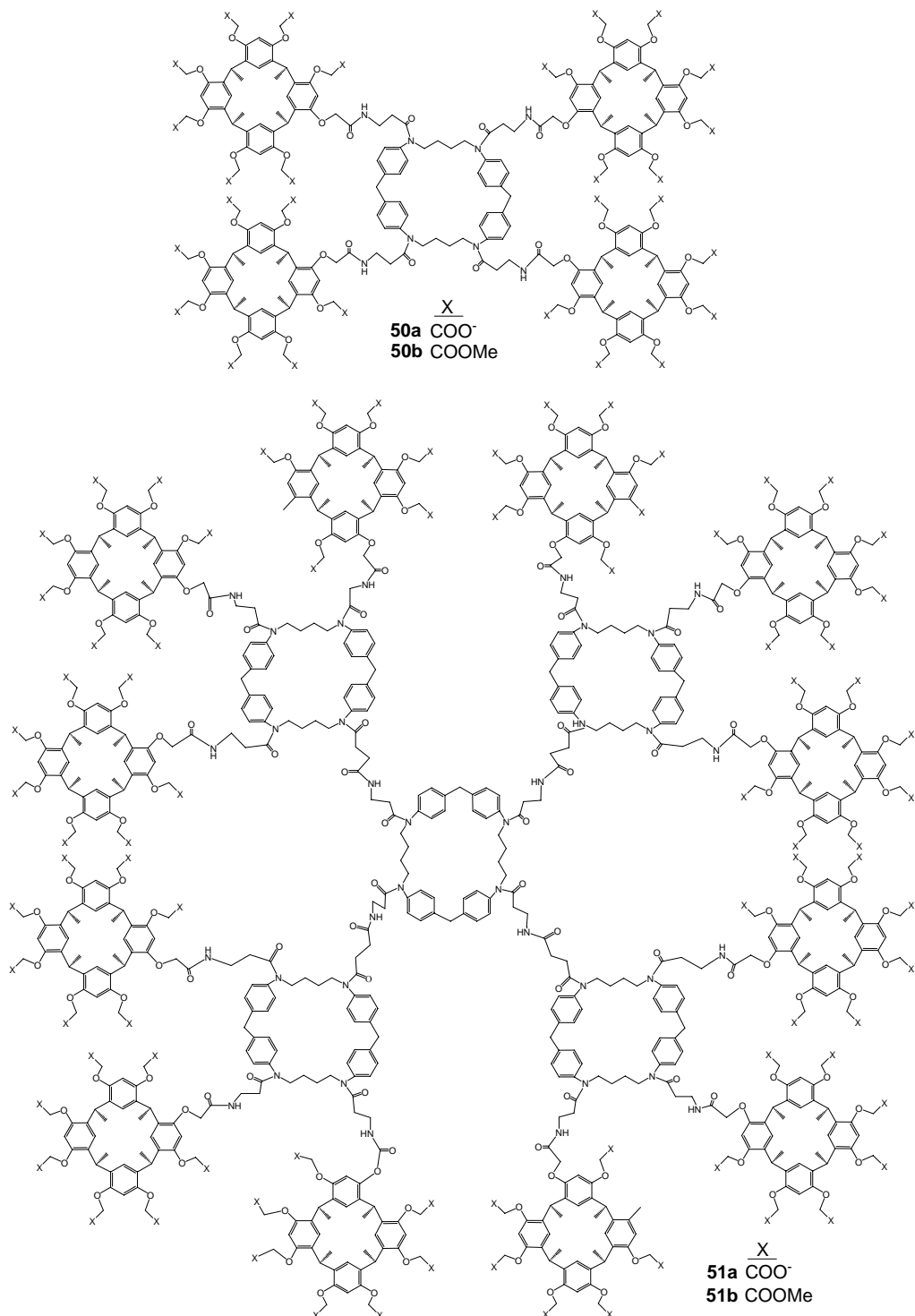


Figure 25. Anionic resorcinarene and cyclophane-based resorcinarene oligomers.

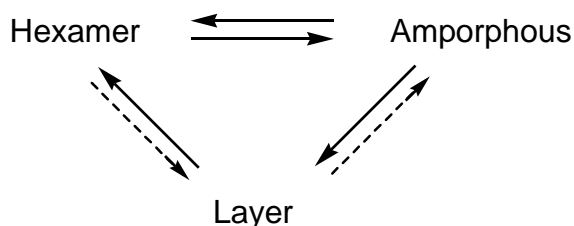
The resorcinarene oligomers act as guest carriers from the bulk aqueous phase to histone surfaces. The present cyclophane-based resorcinarene oligomers are favourable candidate as

receptor recognized histones. Moreover, the development of supramolecular formed with cyclophane-based resorcinarene oligomers and a fluorescence probe as a guest may be promising to detect trimethylated histones [73].

TiO₂ is a poor visible light absorber and therefore anatase TiO₂ has restricted applicability as an effective material in the photoelectric conversion in solar cells and photocatalysis. Such limitation can be overcome if its surface modifications is made by *C*-alkyl resorcinarene.

Misra et al. [74] developed a simple method for the synthesis of *C*-undecyl-resorcinarene-capped anatase TiO₂ nanoparticles **52** (Figure 26) that could be isolated and redispersed in different nonaqueous solvents. The adsorption of C₁₁-resorcinarene onto the surface of TiO₂ nanoparticles led the shifting of the onset wavelength of optical absorption in the visible region.

Some resorcinarene (*C*-nonylresorcinarene), in contrast to methylresorcinarene can exist in three isolable phase systems: a layer structure, a hexamer and an amorphous phase, the three are in thermal equilibrium [75].



The most stable is the layer structure to which the other two revert under appropriate thermal conditions. The hexameric structure is moderately stable for resorcinarenes when long pendant alkyl chains present a non-polar exterior to non-polar solvents. On heating in a non-polar solvent, the hexamer dissociates to give the insoluble amorphous phase. In a non-polar solvent, the amorphous phase revert to the ordered hexamer at lower temperatures, when heating is prolonged the amorphous phase is ultimately converted to the layer phase.

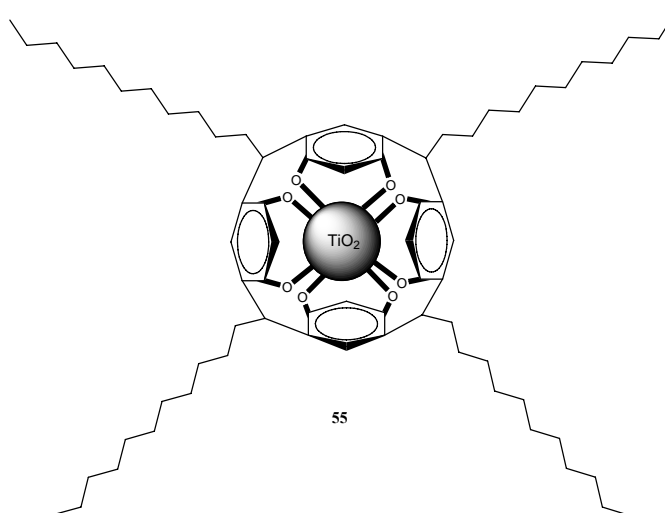


Figure 26. Schematic representation of C₁₁-resorcinarene-TiO₂ complex consisting of a TiO₂ core and a C₁₁-resorcinarene ligand.

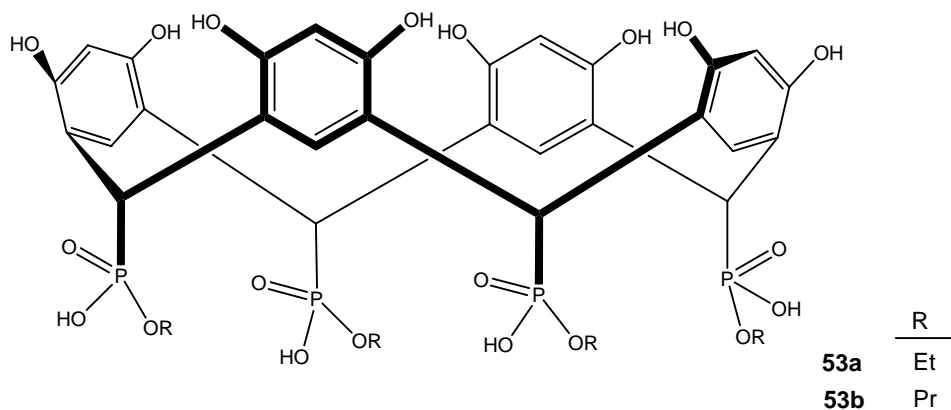


Figure 27. Structure of resorcinarene with alkyldiethylphosphonate groups.

Some investigations are still devoted to recognize the structural organization and properties of mixed solutions of polymers (polyelectrolytes) with amphiphilic resorcinarenes in order to develop new materials with predicted properties, including the catalytic one. It was found, that amphiphilic resorcinarenes **53a,b** containing the alkyldiethylphosphonate groups at the lower rim of molecule in the *cone* conformation (Figure 27) [76] form with several poly(ethyleneimines), having different molecular weights, (polyelectrolytes) in a water - DMF medium, the combined polymer – colloidal structures (aggregates) due to various noncovalent interactions. These systems prove the high catalytic activity in hydrolysis of phosphorus acid esters (acceleration by 10^3 and more times at pH 7 - 8) [77].

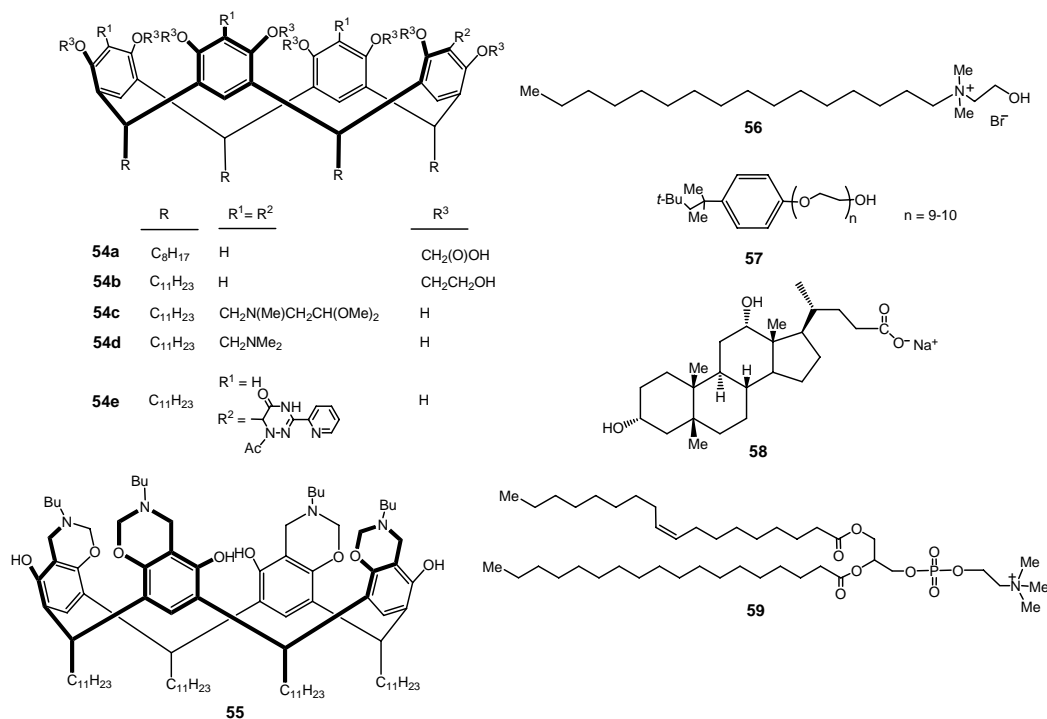


Figure 28. Structure of amphiphilic modified resorcinarenes and surfactants.

It was found that a series of amphiphilic modified resorcinarene **54a-d** (Figure 28) and synthetic (**56** and **57**) natural (**58**, **59**) surfactants in a medium of low polarity form aggregates. Analysis of the IR absorption spectra of solutions resorcinarene (**54b-e**, **55**) and their mixtures with cationic surfactant **56** in chloroform solutions showed that with an increase in the concentration of the solutions the molar intensity coefficients of the functionally active O-H bonds and relatively neutral C-H bonds decrease down to the critical micelle concentrations, which is related to micelle formation with pronounced specific features for different resorcinarene structures [78].

Shen et al. [79] reported the capability of the amphiphilic *C*-undecyl resocinarene **60** bearing hydrophilic octa aminoamido groups on the upper rim of molecule in aqueous media to form well defined multiwalled microtubes (Figure 29). This study manifests a feasible method that aims to completely change the structure resorcinarenes from a microtube to a sheet-like morphology by selectively elimination length hydrophilic groups. Molecules with hydrazinyl groups in the hydrophilic segments resulted in sheet-like structures. Furthermore, this work demonstrated a simple approach for the preparation of gold microtubes using resorcinarene-based microtubes as a skeleton. By using the obtained microtube as a template, gold colloids are directly introduced into the self-assembled microtubes.

The main aim of numerous studies which are still realized is deeper comprehension of the factors determining the different affinities of chiral biomolecules towards various chiral receptors, their selective binding transporters and their sensivity to specific anions.

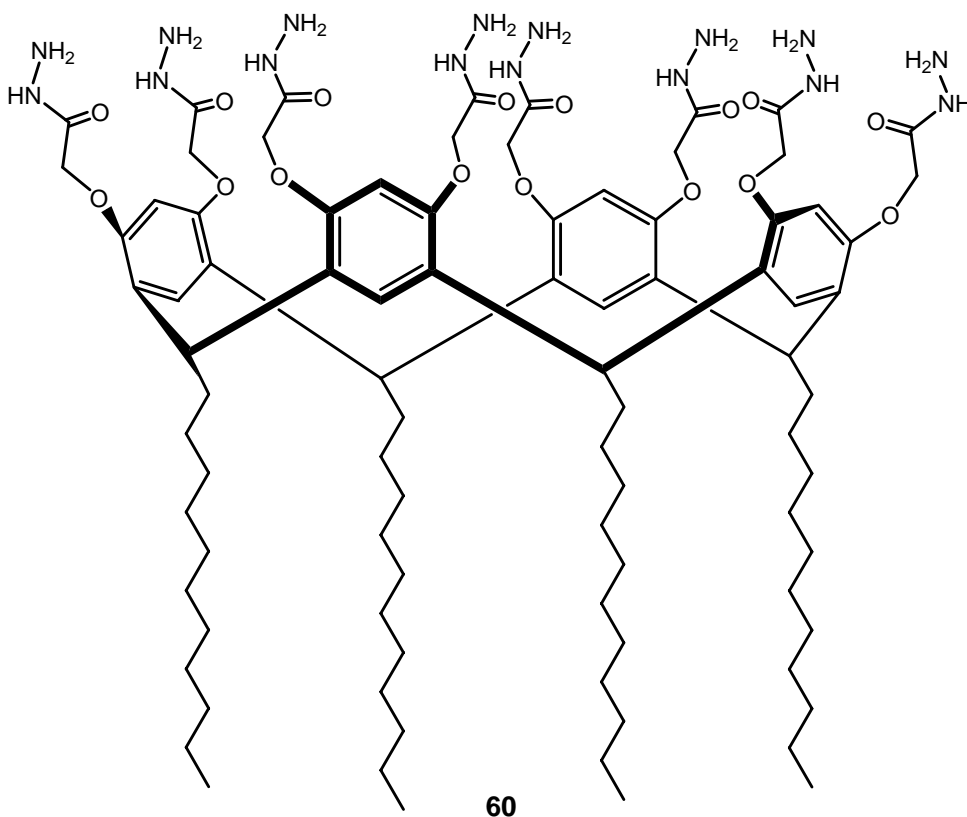


Figure 29. Structure of amphiphilic *C*-undecyl resocinarene.

Botta et al. [80] reported results on the specific noncovalent interactions between the enantiomers amphetamine and several chiral amido[4]resorcinarene receptors, containing either flexible **61a-c** or rigid pendants **62a,b** (Figure 30) indicate that the gas-phase kinetics and enantioselectivities of the base-induced displacement reactions between the 2-aminobutane enantiomers and the diastereomeric $[M \cdot H \cdot A]^+$ complexes are mainly determined by structural and dynamic factors.

Investigations of interactions of resorcinarenes and their modified derivatives are still important with point of view design, synthesis and applicability such compounds as unique hosts. Fluorescence from a common probe pyrene was used to study interactions involving C- ethyl resorcinarene and its tetra-morpholine derivative in basic media [81]. It was found that these compounds efficiently quench the pyrene fluorescence due to presence of long - range interactions with pyrene. Effectiveness of cesium ion as the quencher of pyrene fluorescence was reduced in the presence morpholine-appended resorcinarene [82].

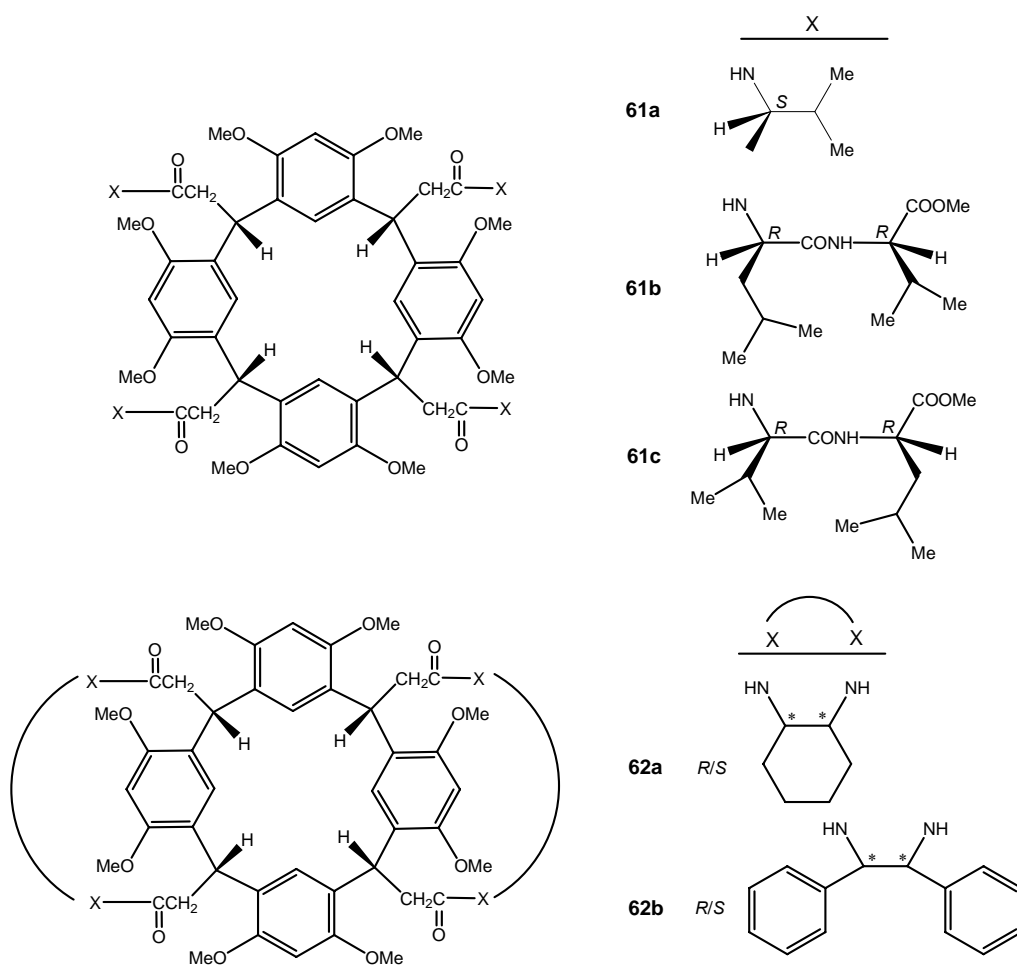


Figure 30. Selected amino[4]resorcinarenes.

Richardson et al. [83] characterized the sensing behaviour of two amphiphilic calix[4]resorcinarenes **63a,b** (Figure 31) in terms of modifications to their surface pressure-area isotherms, their UV-Vis solution and LB film spectra, for a wide number of analytes such as acids, amine, thiols. Lysine and calix-type molecule in LB film form create strong interactions. Barret et al. reported the syntheses resorcinarenes labeled with donor (D) and acceptor (A) fluorophores attached to the lower rim of resorcinarene monomers [84, 85]. Pyrene and perylene were chosen as the respective donor and acceptor fluorophores. Starting from *tert*-butyldimethylsilyl (TBS) protected monohydroxy resorcinarene [86] esterification with 1-pyrene carboxylic acid via the acid chloride, provided the protected pyrene ester. For the acceptor, perylene alkyne [87] was reacted with resorcinarene azide, generated from alcohol via the mesylate, in a copper mediated reaction to afford the protected compounds. Deprotection both and gave resorcinarenes **64** and **65** (Figure 32).

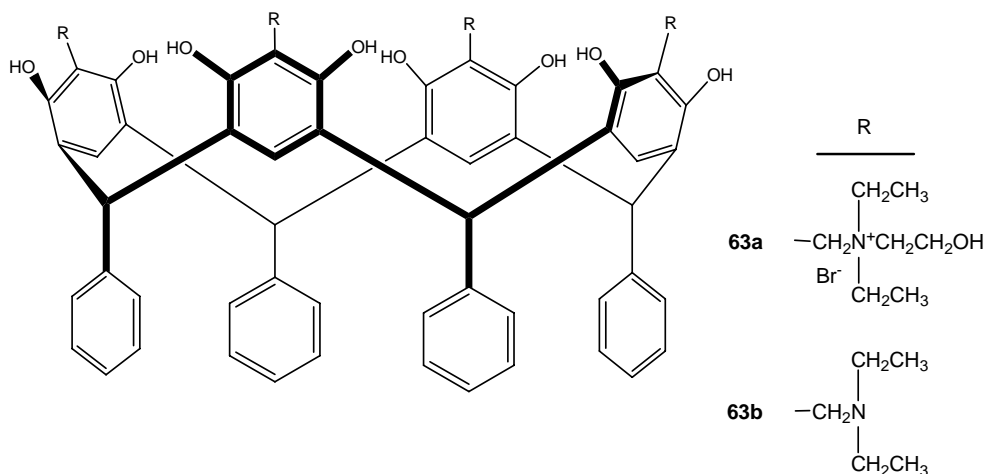


Figure 31. Chemical structure of the calix[4]resorcinarenes.

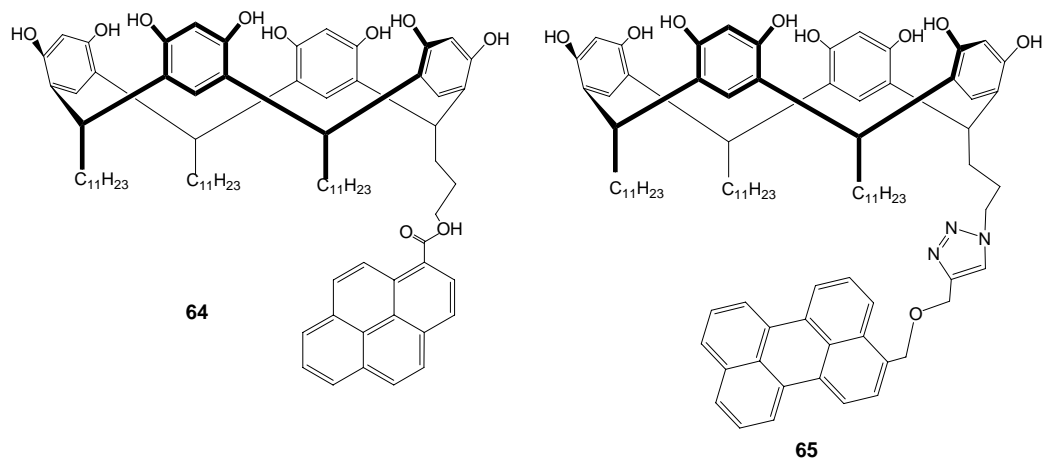


Figure 32. Resorcinarenes labeled with donor and acceptor fluorophores.

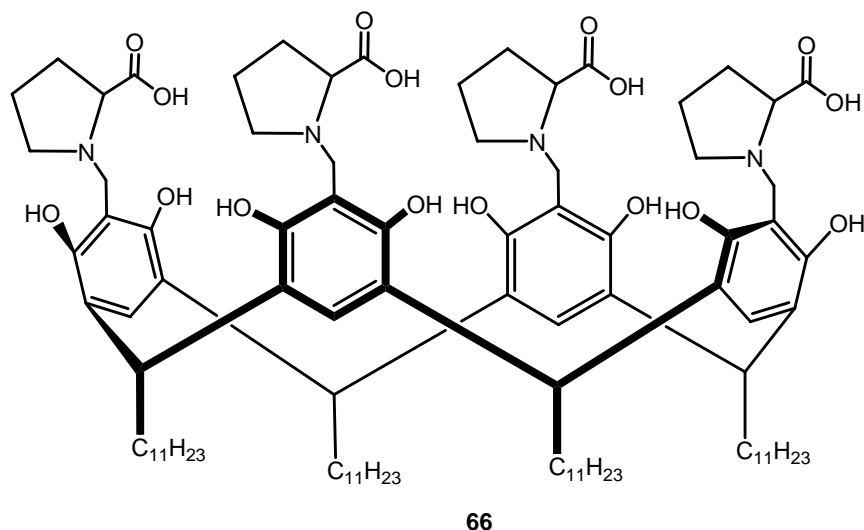


Figure 33. Molecular formula of prolyl-bearing resorcinarene.

Separately, the labeled resorcinarenes **64** and **65** in wet chloroform with tetrahexyl ammonium bromide showed clean formation of the respective encapsulation complexes by ^1H NMR. When dilute solutions of **64** and **65** resorcinarene hexamers in wet chloroform were mixed, the change in the fluorescence emission spectra was followed with time. Applications of fluorescence resonance energy transfer allowed to monitor the dynamics of hydrogen-bonded hexameric assemblies formed from labeled resorcinarenes. The results reveal the factors that influence the dynamic assembly of macrocycles into hexameric capsules. They include the concentration of mixing, the importance of temperature, stability of the capsules to polar additives, and the necessity to water to facilitate the capsule formation [88]. Mixing of substoichiometric ratios of tetramethylsulfonated *C*-methyl or *C*-pentyl- resorcinarenes and tertiary ammonium derivative of phenothiazine (promazine) resulted in formation of crystallohydrates that were transformed into ionic complexes when host : guest ratio approached stoichiometric one. The driving forces of promazine coordination rely on Coulomb interaction with sulfonato-groups on the upper rim of the macrocycle and cation π -interactions with aromatic cavities of resorcinarenes [89].

Prolyl-bearing amphiphilic resorcinarene **66** (Figure 33), which self-assemble as stable solid lipid nanoparticles can be further functionalized at their surface with proteins, and interact with specific antibodies. In order to achieve surface modification, solid lipid nanoparticles were submitted to chemical activation using 1-(3-dimethylaminopropyl)-3-ethylcarbodiimide and *N*-hydroxysuccinimide and subsequently reacted with bovine serum albumin to produce proteo-solid lipid nanoparticles. The evidence of the successful grafting of bovine serum albumin at the surface of resorcinarene **66** solid lipid nanoparticle arises from their capability of interacting with surface bound polyclonal specific antibodies. Interactions with proteo - solid lipid nanoparticle were investigated by means of SPR. The results demonstrate that there is an interaction between the bovine serum albumin modified resorcinarene **66** solid lipid nanoparticles and surface-bound anti- bovine serum albumin antibodies. Proteo - solid lipid nanoparticle were immobilized on a gold surface on the basis of their recognition properties vs. antibodies [90]. Researchers are still actively designing and

testing ion-selective carriers for membrane separation systems which avoid some of the difficulties encountered in solvent extraction.

REFERENCES

- [1] Pietraszkiewicz, O; Pietraszkiewicz, M. *Pol. J. Chem.*, 1998, 72, 2418.
- [2] Menger, FM; Bian, J; Sizova, E; Martinson, DE; Seredyuk, VA. *Org. Lett.*, 2004, 2, 261.
- [3] Arnott, G; Hunter, R. *Tetrahedron*, 2006, 62, 992.
- [4] Buckley, BR; Boxhall, JY; Page, PCB; Chan, Y; Elsegood, MRJ; Heaney, H; Holmes, KE; McIldowie, MJ; McKee, V; McGrath, MJ; Mocerino, M; Poulton, AM; Sampler, EP; Skelton, BW; White, AH. *Eur. J. Org. Chem.*, 2006, 5117.
- [5] Buckley, BR; Page, PCB; Chan, Y; Heaney, H; Klaes, M; McIldowie, MJ; McKee, V; Mattay, J; Mocerino, M; Moreno, E; Skelton, BW; White, AH. *Eur. J. Org. Chem.*, 2006, 5135.
- [6] Bonsignore, S; Cometti, G; Dalcanale, E; Du Vosel, A. *Liq. Cryst.*, 1990, 8, 639.
- [7] Cometti, G; Dalcanale, E; Du Vosel, A; Levelut, AM. *J. Chem. Soc., Chem. Commun.*, 1990, 163.
- [8] Purse, BW; Shivanyuk, A; Rebek, J. *Chem. Commun.*, 2002, 2612.
- [9] Cort, AD; Murua, JIM; Pasquini, C; Pons, M; Schiaffino, L. *Chem.- Eur. J.*, 2004, 10, 3301.
- [10] Sliwa, W; Kozlowski, C. *Calixarenes and Resorcinarenes. Synthesis, Properties and Applications*, 1. Edition - February 2009, Wiley-VCH, Weinheim.
- [11] Vicens, J; Harrowfield, J. (Eds.), *Calixarenes in the Nanoworld*, Springer Verlag 2007
- [12] S. M. Biro, J. Rebek, Jr, *Chem. Soc. Rev.*, 2007, 36, 93.
- [13] Alexander, W. *Chem. Commun.*, 2006, 1581.
- [14] Krock, L; Shivanyuk, A; Goodin, DB; J. Rebek, Jr, *Chem. Commun.*, 2004, 272.
- [15] Beyeh, NK; Kogej, M; Ahman, A; Rissanen, K; Schalley, CA. *Angew. Chem. Int. Ed.*, 2006, 45, 5214.
- [16] Baeyer, A. *Ber. Dtsch. Chem. Ges.*, 1872, 5, 25.
- [17] Niederl, JB; Vogel, HJ. *J. Am. Chem. Soc.*, 1940, 62, 2512.
- [18] Hogberg, AGS. *J. Org. Chem.*, 1980, 45, 4498.
- [19] Hogberg, AGS. *J. Am. Chem. Soc.*, 1980, 102, 6046.
- [20] Roberts, BA; Cave, GWV; Raston, CL; Scott, JL. *Green Chem.*, 2001, 3, 280.
- [21] Curtis, ADM. *Tetrahedron Lett.*, 1997, 38, 4295.
- [22] Pieroni, OL; Rodriguez, NM; Vuano, BM; Cabaleiro, MC. *J. Chem. Res., Synop.*, 1994, 188.
- [23] Barrett, AGM; Braddock, DC; Henschke, JP; Walker, ER. *J. Chem. Soc., Perkin Trans.*, 1999, 1, 873.
- [24] Peterson, KE; Smith, RC; Mohan, RS. *Tetrahedron Lett.*, 2003, 44, 7723.
- [25] Deleersnyder, K; Mehdi, H; Horvath, IT; Binnemans, K; Parac-Vogt, TN. *Tetrahedron*, 2007, 63, 9063.
- [26] Kantar, C; Agar, E; Sasmaz, S. *Dyes and Pigments*, 2008, 77, 487.
- [27] Ito, H; Nakayama, T; Sherwood, M; Miller, D; Ueda, M. *Chem. Mater.*, 2008, 20, 341.
- [28] McIldowie, MJ; Mocerino, M; Ogden, MI; Skelton, BW; *Tetrahedron*, 2007, 63, 10817.

- [29] Beyeh, NK; Aumanen, J; Åhman, A. M. Luostarinen, H. Mansikkamaki, M. Nissinen, J. Korppi-Tommola, K. Rissanen, *New J. Chem.*, 2007, 31, 370.
- [30] Mustafina, AR; Zagidullina, IYa; Maslennikova, VI; Serkova, OS., Guzeeva, TV. Kononov, AI. *Russ. Chem. Bull. Int. Edit.*, 2007, 56, 313.
- [31] Machkhoshvili, RI; Schechelokov, RN. *Russ. J. Coord. Chem.*, 2000, 26, 677.
- [32] Podyachew, SN; Syakev, VV; Sudakova, SN; Shagidullin, RR; Osyanina, DV; Avvakumova, LV; Buzykin, BI; Latypov, SK; Bauer, I; Habicher, WD; Kononov, AI. *J. Inclusion. Phenom.*, 2007, 58, 55.
- [33] Podyachew, SN; Burmakina, NE; Syakev, VV; Sudakova, SN; Shagidullin, RR; Kononov, AN. *Tetrahedron*, 2009, 65, 408.
- [34] Victorovna-Lijanovna, I; Reyes-Valderrama, MI; Maldondo, JL; Ramos-Ortiz, G; Klimova, T; Martínez-García, M. *Tetrahedron*, 2008, 64, 4460.
- [35] Hawker, CJ; Frechet, JMJ. *J. Am. Chem. Soc.*, 1990, 112, 7638.
- [36] Reyes-Valderrama, MI; Vázquez-García, RA; Klimova, T; Klimova, E; Ortiz-Frade, L; Martínez-García, M. *Inorg. Chim. Acta*, 2008, 361, 1597.
- [37] Atwood, JL; Szumna, A. *Chem. Commun.*, 2003, 940.
- [38] Botta, B; Caporuscio, F; Subissati, D; Taffi, A; Botta, M; Fillipi, A; Speranza, M. *Angew. Chem., Int. Ed.*, 2006, 45, 2717.
- [39] Eisler, DJ; Puddephatt, RJ. *Cryst. Growth Des.*, 2005, 5, 57.
- [40] Han, J; Cai, YH; Liu, L; Yan, CG; Li, Q. *Tetrahedron*, 2007, 63, 2275.
- [41] Han, J; Yan, ChG. *J. Incl. Phenom. Macrocycl. Chem.*, 2008, 61, 119.
- [42] Paletta, M; KLaes, M; Neuman, B; Stammler, H.G; Grimme, S; Mattay, J. *Eur. J. Org. Chem.*, 2008, 555.
- [43] McIldowie, MJ; Mocerino, M; Skelton, BW; White, AH. *Org. Lett.*, 2000, 2, 3869.
- [44] Salorinne, K; Nissinen, M. *Tetrahedron*, 2008, 64, 1798.
- [45] Matsushita, Y; Matsui, T. *Tetrahedron Lett.*, 1993, 34, 7433.
- [46] Luostarinen, M; Nissinen, M; Nieger, M; Shivanyuk, A; Rissanen, K. *Tetrahedron*, 2007, 63, 1254.
- [47] Vovk, AI; Shivanyuk, AM; Bugas, RV; Muzychka, OV; Melnyk, AK. *Bioorg. Med. Chem. Lett.*, 2009, 19, 1314.
- [48] Szumna, A. *Org. Biomol. Chem.*, 2007, 5, 1358.
- [49] Kuberski, B; Pecul, M; Szumna, A. *Eur. J. Org. Chem.*, 2008, 3069.
- [50] Wzorek, A; Mattay, J; Iwanek, W. *Tetrahedron: Asymmetry*, 2007, 18, 815.
- [51] de Namor, AFD; Chaaban, JK. *J. Phys. Chem.*, 2008, 112, 2070.
- [52] Botta, B; D'Acquarica, I; Nevola, L; Sacco, F; Lopez, ZV; Zappa, G; Frascchetti, C; Speranza, M; Taffi, A; Caporuscio, F; Letzel, MC; Mattay, J. *Eur. J. Org. Chem.*, 2007, 5995.
- [53] Botta, B; Di Giovanni, MC; Delle Monache, G; De Rosa, MC; Gacs, E; Botta, M; Corelli, F; Taffi, A; Santini, A; Benedetti, E; Pedone, C; Misti, D. *J. Org. Chem.*, 1994, 59, 1532.
- [54] Botta, B; D'Acquarica, I; Monache, GD; Subissati, D; Uccello-Barretta, G; Mastrini, M; Nazzi, S; Speranza, M. *Eur. J. Org. Chem.*, 2007, 72, 9283.
- [55] Gavrilova, EL; Naumova, AA; Burišov, AR; Pudovik, MA; Krasil'nikova, EA; Kononov, AI. *Russ. Chem. Bull., Int. Ed.*, 2007, 56, 2348.
- [56] Tavs, P. *Chem. Ber.*, 1970, 103, 2428.

- [57]Sentemov, VV; Krasil'nikova, EA; Berdnik, IV. *Zh. Obshch. Khim.*, 1989, 59, 2692, (*J. Gen. Chem. USSR*, 1989, 59, Engl. Transl.).
- [58]Sentemov, VV; Gavrilova, EL; Krasil'nikova, EA. *Zh. Obshch. Khim.*, 1993, 63, 48 (*Russ. J. Gen. Chem. USSR*, 1993, 63, Engl. Transl.).
- [59]Krasil'nikova, EA; Sentemov, VV; Gavrilova, EL. *Zh. Obshch. Khim.*, 1993, 63, 848 (*Russ. J. Gen. Chem.*, 1993, 63, Engl. Transl.).
- [60]Burilov, AR; Knyazeva, IR; Sadykova, YUM; Pudovik, MA; Habicher, WD; Baier, I; Kononov, AI. *Russ. Chem. Bull. Int. Ed.*, 2007, 56, 1144.
- [61]Shivanyuk, A. *J. Am. Chem. Soc.*, 2007, 129, 14196.
- [62]Busi, S; Saxell, H; Frohlich, R; Rissanen, K. *Cryst. Eng. Comm.*, 2008, 10, 1803.
- [63]Wang, XL; Liu, SQ; Zhang, QF. *J. Chem. Crystallogr.*, 2008, 38, 851.
- [64]Matheny, JM; Bosch, E; Barnes, CL. *Crystal Growth & Design*, 2007, 7, 984.
- [65]Aoyama, Y; Tanaka, Y; Sugahara, S. *J. Am. Chem. Soc.*, 1989, 111, 5397.
- [66]Kikuchi, Y; Tanaka, Y; Sutarto, S; Kobayashi, K; Toi, H; Aoyama, Y. *J. Am. Chem. Soc.*, 1992, 114, 10302.
- [67]Kalenius, E; Kekalainen, T; Neitola, R; Beyeh, K; Rissanen, K; Vainiotalo, P. *Chem. Eur. J.*, 2008, 14, 5220.
- [68]O'Farrell, CM; Chudomel, JM; Collins, JM; Dignam, CF; Wenzel, T. *J. Org. Chem.*, 2008, 73, 2843.
- [69]Yunagihara, R; Tominaga, M; Aoyama, Y. *J. Org. Chem.*, 1994, 59, 6865.
- [70]Dignam, CF; Richards, CJ; Zopf, JJ; Wacker, LS; Wenzel, TJ. *Org. Lett.*, 2005, 7, 1773.
- [71]Dignam, CF; Zopf, JJ; Richards, CJ; Wenzel, TJ. *J. Org. Chem.*, 2005, 70, 8071.
- [72]Hayashida, O; Uchiyama, M. *J. Org. Chem.*, 2007, 72, 610.
- [73]Hayashida, O; Takaoka, Y; Hamachi, I. *Tetrahedron Lett.*, 2005, 46, 6589.
- [74]Misra, TK; Chen, J; Liu, CY. *J. Colloid. Interface Sci.*, 2007, 310, 178.
- [75]Stirling, CJM; Johan Fundin, L; Williams, NH. *Chem. Commun.*, 2007, 1748.
- [76]Burilov, AR; Volodina, Yu; Popova, EV; Gazivov, AS; Knyazeva, IR; Pudovik, MA; Habicher, WD; Kononov, AI. *Zh. Obshch. Khim.*, 2006, 76, 433 (*Russ. J. Gen. Chem.*, 2006, 76, 412 Engl. Transl.).
- [77]Pashirova, TN; Lukashenko, SS; Kosacheva, EM; Rizvanova, LZ; Gainanova, GA; Kudryavtseva, LA. *Russ. Chem. Bull. Int. Ed.*, 2007, 56, 959.
- [78]Ryzhkina, IS; Timosheva, AP; Chernova, AV; Shagidullin, RR; Gazizova, AA; Habicher, WD; Krause, T; Vagapova, LI; Kononov, AI. *Russ. Chem. Bull. Int. Ed.*, 2007, 56, 475.
- [79]Sun, Y; Yan, CG; Yao, Y; Han, Y; Shen, M. *Adv. Funct. Mater.*, 2008, 18, 3981.
- [80]Botta, B; Taffi, A; Caporuscio, F; Botta, M; Nevola, L; D'Acquarica, I.; Frascetti, C; Speranza, M. *Chem. Eur. J.*, 2008, 14, 3585.
- [81]Matsushita, YI; Takanao, M. *Tetrahedron Lett.*, 1993, 34, 7433.
- [82]Pandey, S; Ali, M; Bishnoi, A; Azam, A; Pandey, S; Chawla, HM. *J. Fluores.*, 2008, 18, 533.
- [83]Sugden, MW; Richardson, TH; Davies, F; Higson, SPJ; Faul, CFJ. *Colloids and Surfaces A: Physicochem. Eng. Aspects*, 2008, 321, 43.
- [84]Barret, ES; Dale, TJ; Rebek, J. Jr., *J. Am. Chem. Soc.*, 2007, 129, 3818.
- [85]Barret, ES; Dale, TJ; Rebek, J. Jr, *Chem. Commun.*, 2007, 4224.
- [86]Hauke, F; Myles, AJ; Rebek, J. Jr, *Chem. Commun.*, 2005, 4164.
- [87]Skorobogatyi, MV; Pchelintseva, AA; Petrunina, AL; Stepanova, AI; Andronova, VL; Galegov, GA; Malakhov, AD; Korshun, VA. *Tetrahedron*, 2006, 62, 1279.

[88]Barret, ES; Dale, TJ; Rebek, J. Jr., *J. Am. Chem. Soc.*, 2008, 130, 2344.

[89]Kazakova, EK; Syakev, VV; Morozova, JE; Makarova, NA; Muslinkina, LA; Evtugyn, GA; Konovalov, AI. *J. Incl. Phenom. Macrocycl. Chem.*, 2007, 59, 143.

[90]Ehrler, S; Pieleś, U; Wirth-Heller, A; Shahgaldian, P. *Chem. Commun.*, 2007, 2605.

Chapter 13

IMINE MACROCYCLICS: BUILDING BLOCKS IN POLYMER SYNTHESIS

Mircea Grigoras and Loredana Vacareanu*

“P. Poni” Institute of Macromolecular Chemistry, Electroactive Polymers Department,
41A Gr. Ghica Voda Alley, 700487-Iasi, Romania.

ABSTRACT

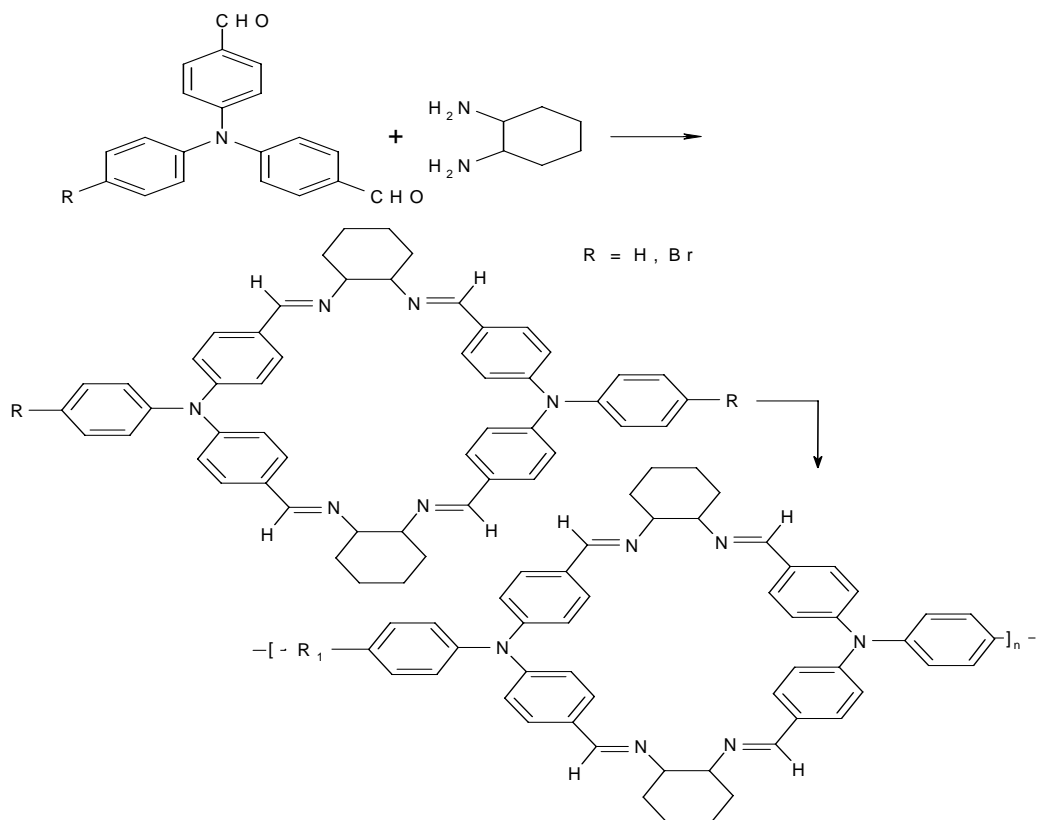
Two imine macrocycles with rhomboidal shape have been synthesized in excellent yields through [2+2] cyclocondensation reaction between (R,R)-1,2-diaminocyclohexane with 4,4'-bisformyl triphenylamine and 4,4'-bisformyl 4''-bromo triphenylamine. The macrocycles structure was assigned by electrospray ionization mass spectrometry (EIS-MS), ¹H-NMR, and elemental analysis. UV and FTIR spectroscopy and TG measurements were also used to characterize these compounds. These macrocycles have used as bricks in building of polymers containing macrocycles in the main chain (polyrhombimines). Chemical and electrochemical oxidative polymerization of rhombimine (R=H) and Suzuki polycondensation (R=Br) were applied in order to obtaining polymers containing imine macrocycles in the main polymer chain.

1. INTRODUCTION

Now, it is recognized that macrocyclic compounds have played an essential role in the birth of supramolecular chemistry [1-3]. Crown ethers, cyclodextrins, cucurbiturils, cryptands, calixarenes and many other cyclic compounds are well known hosts, able to selectively recognize specific guests by noncovalent interactions. They have been much used for the investigation of the supramolecular interactions and building of new supramolecular architectures. Macrocycles can self-organize to form various supramolecular assemblies: tubular channels [4-8], tubular liquid crystals [9-11], porous organic solids or to form with

* Corresponding author: E-mail:grim@icmpp.ro

guests interlocked structures, such as rotaxanes and catenanes, polyrotaxanes and polycatenanes [12-15], nanocapsules and nanoreactors, etc [16-18]. On the other hand, arylamine-based oligomers and polymers have attracted much attention due to their unique properties that allow them to have potential application in organic electronics, photonics and spintronics [19-21]. Particularly, triphenylamine-based polymers have good hole-transporting properties, high light-emitting efficiencies, photoconductivity and photorefractivity, large two-photon absorption cross sections and stabilization effect of high-spin polyradicals in organic magnets. Due to the good electron-donating nature of triphenylamine (TPA), its polymers have been widely used as hole-transporting materials for a number of applications, such as xerography, organic field-effect transistors, photorefractive systems, light emitting diodes etc [22-24]. The interesting properties are associated with the presence of TPA unit that contains the nitrogen center (the electroactive site) linked to three electron-rich phenyl groups in a propeller-like geometry [25].



The purpose of this chapter is to present our recent results about synthesis and characterization of imine macrocycles (**3a**, **3b**) obtained by [2+2] cyclocondensation of 4,4'-diformyl triphenylamine (**1a**) and 4,4'-diformyl 4'-bromo triphenylamine (**1b**) with (R,R)-1,2-diaminocyclohexane (**2**). Their use as monomers in chemical and electrochemical polymerization and palladium (0)-catalyzed polycondensation is also discussed. To our knowledge, there are only few reports describing synthesis of polymers containing covalently linked macrocycles: crown ethers in the main chain of polyesters and polyamides [26,27] or

phenylene ethynylene macrocycles in the side chain of polyacetylene [28] or polymethacrylate [29]. Recent developments in the shape-persistent phenylene-ethynylene macrocycles synthesis and their self-assembling behavior have reviewed by Moore and Zhao [11]. These macrocycles were synthesized by multisteps method and the overall yield was very low. Also, an interesting review on the design and characterization of cyclic compounds as building blocks for tubular aggregates and their behavior as multifunctional nanoobjects was recently published [30].

2. SYNTHESIS OF IMINE MACROCYCLES

The shape-persistent imine macrocycles [31] derived from (R,R)-1,2-diaminocyclohexane and aromatic dialdehydes [32-51] have been attracted much attention in the last years due to their exotic shapes and potential applications in supramolecular chemistry and materials science as guest-host complexes, tubular channels, porous organic solids, nanocapsules and nanoreactors, etc [11,31b]. They are build of a rigid diamine and π -conjugated dialdehyde and have specific two-dimensional shapes: rhombus, triangle, rectangle, etc. (Figure 1).

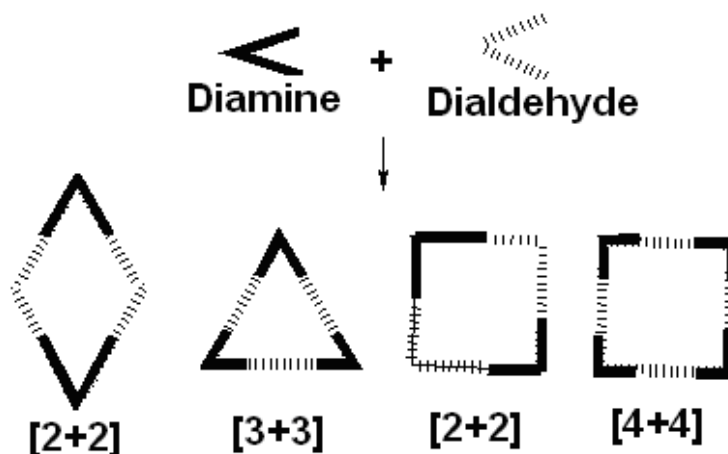


Figure 1. Schematic representation of imine macrocyclic shapes.

The most frequently shape of imine macrocycles is rhomb obtained by [2+2] cyclocondensation and triangle obtained by [3+3] cyclocondensation. Unlike arylene-ethynylene macrocycles, imine homologues can be obtained in a single step reaction, with quantitative yield. Chiral cyclic compounds are also accessible starting from optically active diamine, i.e., (R,R)-1,2-diaminocyclohexane and they can selectively encapsulate chiral guests.

The common strategy used for obtaining of imine macrocycles is based on one-pot synthesis using Schiff base condensation reaction between aldehyde and amine compounds. The reaction is reversible, highly selective and the intermediate reaction products are dynamically interconvertible. The composition of the library is determined by the thermodynamic stability of the library members [52]. Therefore, under thermodynamically

controlled conditions and dynamic combinatorial chemistry, the imine condensation proceeded to completion generating with almost quantitative yield the most stable macrocycle. The reversibility of the imine condensation allows to self-correct the eventually errors in the bond-forming step and finally to obtain with high efficiency the thermodynamically stable product. Formation of macrocyclics is favoured over linear oligomerization if diamine, dialdehyde or both reactants have a predisposed structure for the formation of cyclic products: a bent structure with restricted conformations [39].

Previously, we have studied synthesis of some imine polymers by solution polycondensation of 3,6-*bis*formyl N-alkyl carbazole and 4,4'-*bis*formyl triphenylamine with aromatic diamines [53-55]. Both dialdehyde comonomers have a bent structure with in plane-projected angle between the two Ar-CHO linkages close by 120°. When diamine partner has also a bent structure, i.e. 3,6-diamino N-alkyl carbazole, formation of conjugated macrocycles of different shapes and dimensions has been evidenced [55].

The size and shape of macrocycle can be designed by choice of the diamine and dialdehyde geometry [34,38]. (1R,2R)-*trans*-1,2-Diaminocyclohexane is a rigid molecule with *ortho* NH₂ functions occupying equatorial positions and having in plane-projected angle between the two C-NH₂ close to 60°. With linear dialdehyde, i.e., terephthaldehyde or its derivatives, chiral trianglimines are obtained as main product by [3+3] cyclocondensation [32,33,36,40,41,42-44,46,47,48,50,51]. When dialdehyde has a bent structure with an angle between aldehyde groups close to 120°, then rhombimines by [2+2] cyclocondensation are obtained [34,39,44,47,49,51]. Therefore, the shape of macrocycle can be anticipated from dialdehyde and diamine geometry.

Imine macrocycles with more complex shapes and three-dimensional (3D) shapes have also obtained using aromatic aldehydes containing three or four aldehyde groups and aliphatic diamine (1,2-diaminoethane, 1,3-diaminopropane or 1,4-diaminobutane) or aromatic triamine; 1,3,5-(*p*-aminophenyl)benzene) under dynamic combinatorial synthesis. Thus, an octahedral nanocontainer (**6**) was synthesized by condensation reaction between the tetraformylcavitand **4** with 1,2-diaminoethane (**5**) [56]. The macrocycle **6** is composed of six cavitands connected together with 12 diamino units (Figure 2). With 1,3-diaminopropane and 1,4-diaminobutane [56] or 1,3-diaminobenzene [57,58] hemicarcerands (**7**) have been synthesized by connecting two cavitands (**4**) with four diamine molecules as linkers.

When amine compound was 1,3,5-tris(*p*-aminophenyl)benzene a rhombicuboctahedron nanocapsule (**5**) with a cavity volume of almost 5000 Å³ was obtained (Figure 3). The hollow nanosphere has an inner diameter of 30 Å and by open portals can encapsulate organic guest molecules with high affinity and insulate them from the bulk phase [59].

A very nice and aesthetically shape, polyimine nanocube, was synthesized by Xu and Warmuth [60] starting from an aromatic trialdehyde, *tris*formyl-trihexadecyloxycyclotriphenylene and linear diamines; 1,4-phenylenediamine or benzidine. Trialdehyde, has the three aldehyde groups oriented in the *x*, *y* and *z* directions in space having angles between them close to 90°, the molecule being a suitable corner piece in strain-free nanocube synthesis. It was observed that by acid-catalyzed [8+12] cyclocondensation between 8 equiv of trialdehyde with 12 equiv of 1,4-phenylenediamine or benzidine, chiral nanocubes are synthesized in high yield (95 and 84 %, respectively). The cube vertices are occupied by the eight cyclophenylene units while the twelve edges are formed from linear diamines (Figure 4).

When trialdehyde is 1,3,5-trisformylbenzene, containing aldehyde groups in the same plane, with (R,R)-1,2-diaminocyclohexane yielded selectively a [4+6] cycloimine spherand [39] (Figure 5).

All these macrocyclic structures have cavities suitable for the encapsulation of guests ranging in size from gases to liquids and solids. The potential applications of these iminospherands proposed by Warmouth et al. [56] are in drug- and pesticide-delivery systems, wastewater detoxification, separation technology and molecular reactors. Chiral iminospherands could find applications in chiral separations [39,60].

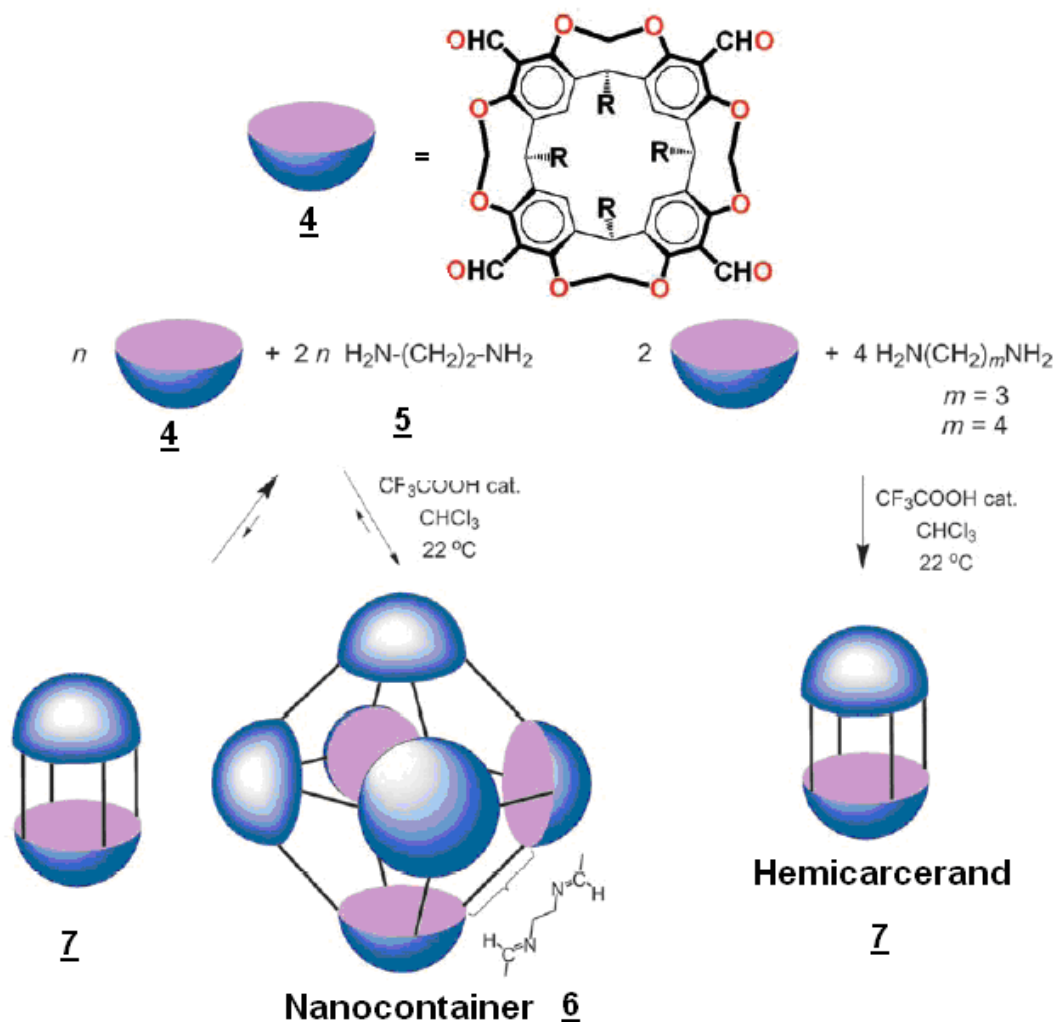


Figure 2. The thermodynamically controlled condensation of cavitant **4** with aliphatic diamines [Reproduced with permission from reference 56].

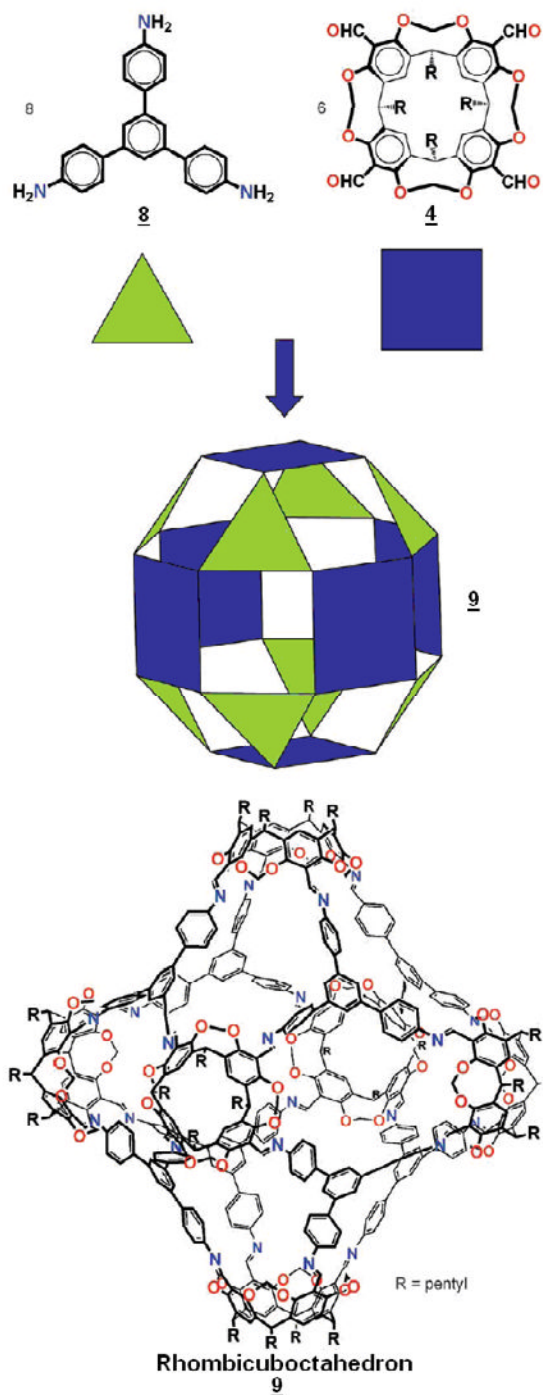


Figure 3. Synthesis of rhombicuboctahedron nanocapsule (9) by [6+8] cycloaddition between 1,3,5-(p-aminophenyl)benzene (8) and tetraformyl derivative (4) [Reproduced with permission from reference 59].

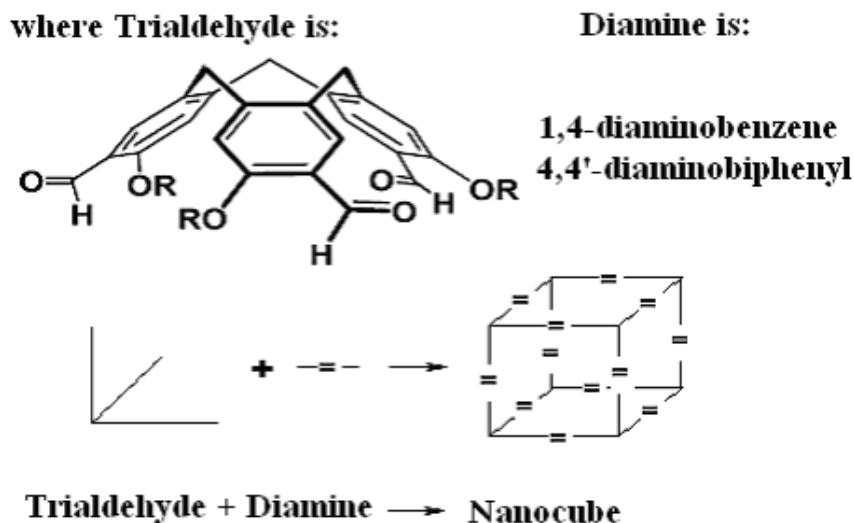


Figure 4. Schematic representation of nanocube synthesis.

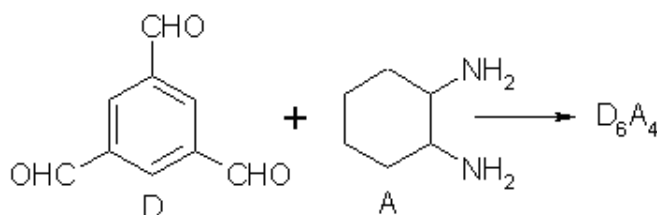


Figure 5. [4+6] Cyclocondensation of 1,3,5-triformylbenzene with (R,R)-1,2-diaminocyclohexane [39].

3. SYNTHESIS OF TRIPHENYLAMINE-BASED IMINE MACROCYCLES

In order to obtain polymers containing imine macrocycles covalently linked in the backbone, functionalized macrocycles has to be firstly synthesized. Triphenylamine is a good starting compound in synthesis of macrocycles because it contains three positions (*para*) more reactive, able to be functionalized with three identical or different groups.

We have synthesized two triphenylamine-based imine macrocycles in one-pot method by cyclocondensation of 4,4'-diformyl triphenylamine (**1a**) or 4,4'-diformyl 4''-bromo-triphenylamine (**1b**) with (R,R)-1,2-diaminocyclohexane (**2**) (Figure 6). **1a** was synthesized by formylation of triphenylamine using a high excess of POCl₃/DMF mixture [55,61]. However, even using a very high ratio between formylating reactant (POCl₃/DMF) to triphenylamine, always a mixture of 4-formyl- and 4,4'-diformyl triphenylamine is present in the final reaction product. The pure dialdehyde was separated by flash chromatography on a

silica gel column using ethyl acetate/hexane (1:10) as eluent. **1b** was synthesized similarly with **1a** but starting from 4-bromo triphenylamine [62].

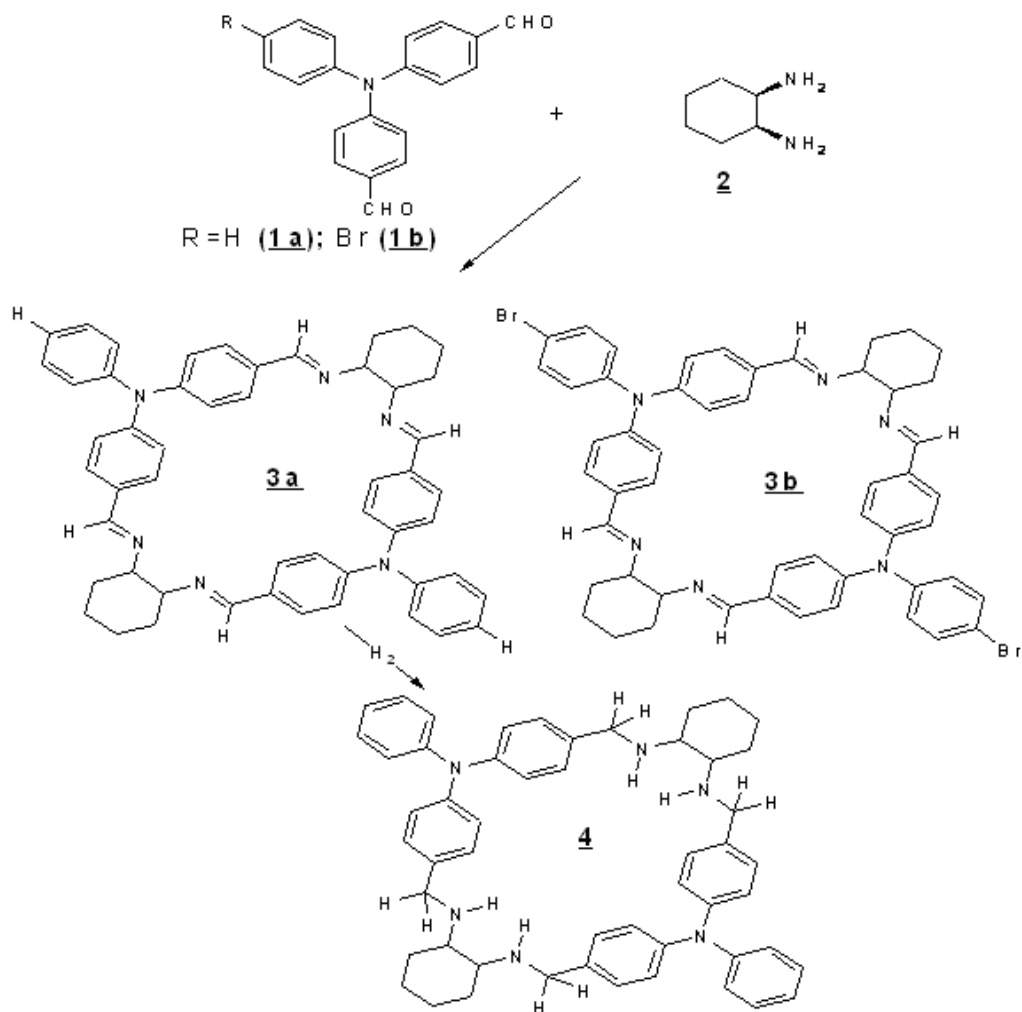


Figure 6. Synthesis of triphenylamine-based rhombimine macrocycles.

Condensation of **1** with **2**, in dichloromethane at room temperature or under reflux using equimolar ratio between partners yielded the target rhombimines **3a** and **3b** in nearly quantitative yield without the use of dehydrating conditions and without any external template [63].

It is noteworthy that the [2+2] macrocycle is the main cyclic compound observed by ESI-MS spectroscopy in the crude product of all condensation reactions between **1** and **2**, at equimolar feed ratio. The rhombimine shape of macrocycles **3** was anticipated because (1*R*,2*R*)-*trans*-1,2-diaminocyclohexane (**2**) is a rigid molecule with equatorial positioned *ortho* NH₂ functions and the angle between the two cyclohexyl-N bond is close of 60°

Dialdehydes **1a**, **1b** have the angle between OHC-C₆H₄-N-C₆H₄-CHO bonds close to 120 °. Therefore, free-strain macrocycles (**3a**, **3b**) of rhomboidal shape should be obtained as the dominant product by [2+2] cyclocondensation and all analysis methods confirmed this assumption.

3.1. Characterization of Imine Macrocylics

The pure product **3a** was obtained by purification from N,N-dimethylformamide as colorless powder. The macrocycle is soluble in chlorinated solvents, CH₂Cl₂, CHCl₃ or CCl₄ and poor soluble in DMF, THF or DMAc. However **3a** was completely soluble in DMF at reflux temperature and by cooling, the solution immediately became as a gel-like and macrocycle was separated by filtration and drying. The thermal stability of macrocycle was studied by TG measurements in nitrogen atmosphere and typical curves for **3a** and **3b** are reproduced in Figures 7 and 8. They showed a very good thermal stability up to 340 °C with onset degradation temperature 348 °C and 322 °C, respectively and high melting temperature (325 °C for **3a**).

Compound **3b** has also a good thermal stability but between 50-150 °C it showed a 7% weight loss due to hosted molecules of solvent that leaved their host.

The structure of the compounds was assigned on the basis of elemental analysis as well as ESI-MS, FTIR, ¹H-NMR and UV spectroscopy. Elemental analysis data are in good agreement with the theoretical one. X-ray data showed the both compounds are crystalline but good crystals suitable for structure determination could not be obtained.

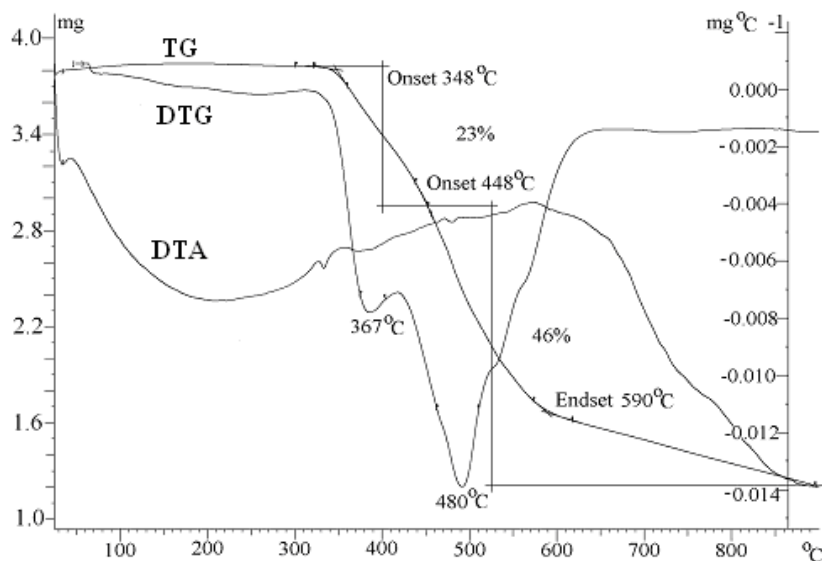


Figure 7. TG, DTG and DTA curves for **3a**.

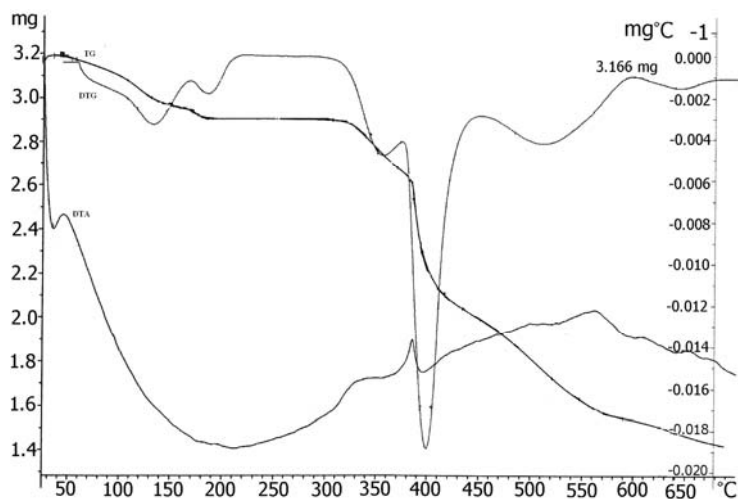


Figure 8. TG, DTG and DTA curves for **3b**.

The FTIR spectra of macrocycles **3a** and **3b** (Figure 9) does not show any absorption for aldehyde C=O (1680 cm^{-1}) and amine N-H (3390 and 3315 cm^{-1}) stretches, while absorption bands characteristic to C=N (1634 cm^{-1}) and C=C (1607 and 1507 cm^{-1}) are observed. The absorption bands localized between 697 and 837 cm^{-1} (ν C-H aromatic from benzene rings), 1268 - 1286 cm^{-1} (the stretching vibration of tertiary amine) and 2856 - 2930 cm^{-1} (C-H aliphatic from cyclohexane) are also evidenced in **3a** and **3b**.

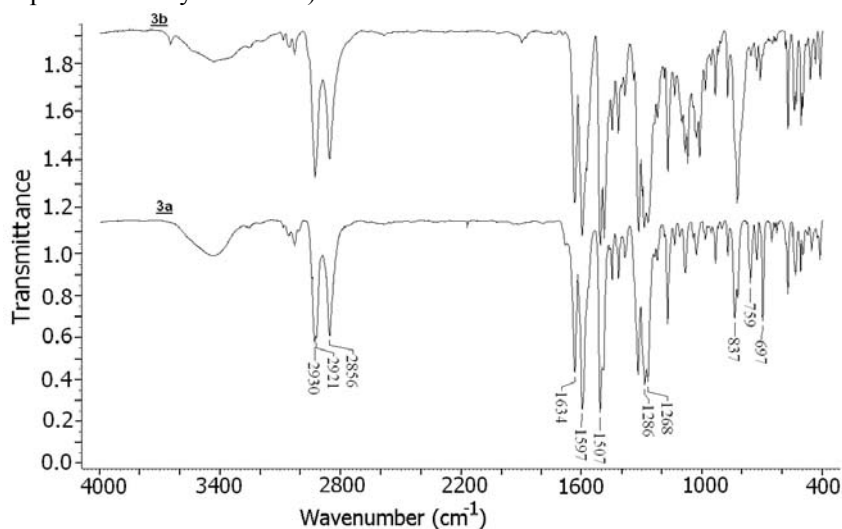


Figure 9. FTIR spectra (KBr) of **3a** and **3b**.

The ESI-MS spectra (macrocycle solution in chloroform/methanol = 3/1) presented in Figure 10 showed signals with the molecular ion peak at 759.3 Da (**3a**⁺+1) and fragmentation ions peak at 380.15 Da , for **3a** and 917.09 Da (**3b**⁺+1), 839.2 Da (**3a**⁺+1-Br) and fragmentation peak at 458.06 Da for **3b**, that are consistent with the chemical structures proposed in Figure 6.

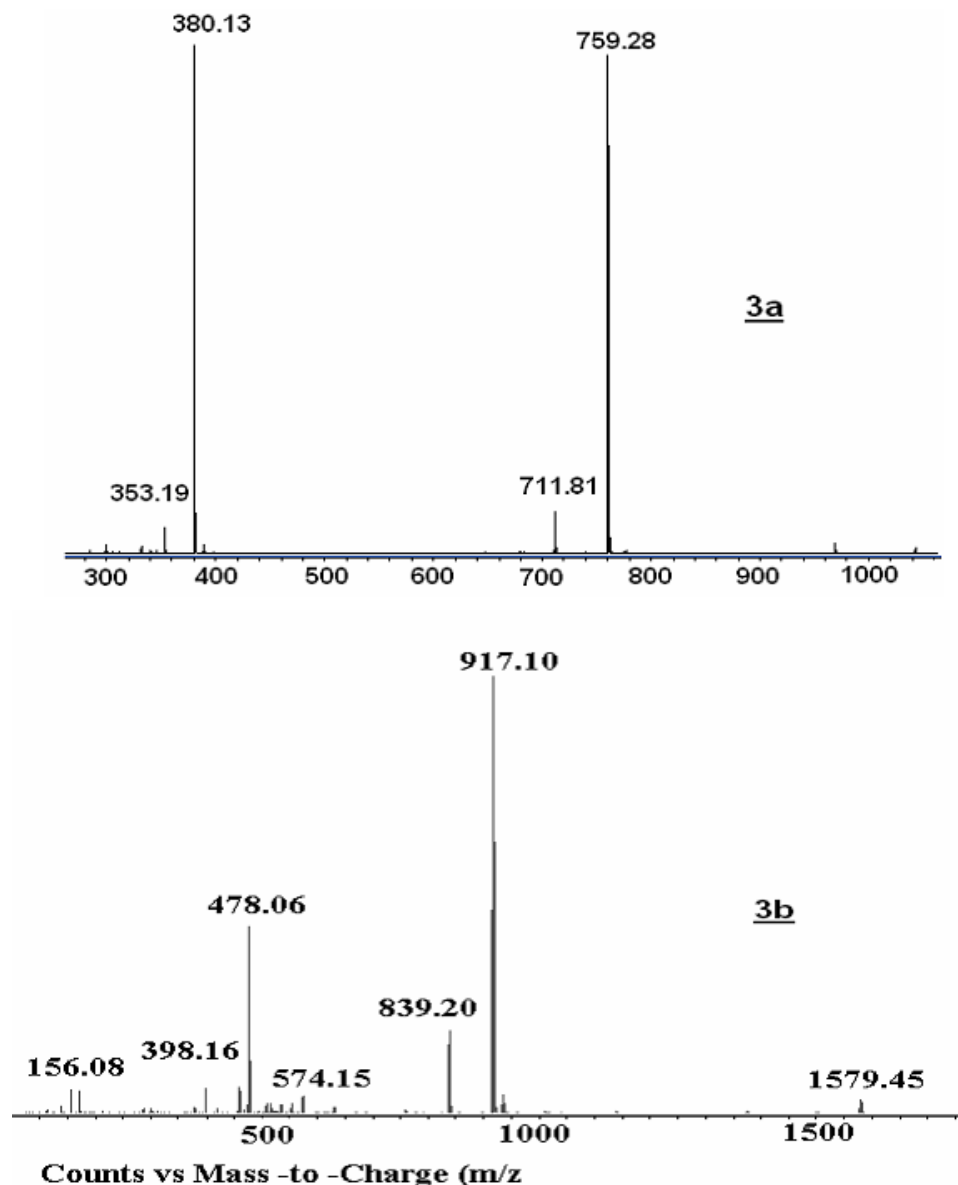


Figure 10. ESI-MS of 3a and 3b.

The $^1\text{H-NMR}$ spectrum of **3a** (Figure 11 and 12) is consistent with the proposed structure, showing only a singlet signal at 7.91 ppm for the four imine protons suggesting a highly symmetric macrocycle. The assignment of signals is: $\delta=7.91$ (s, 4H, $\text{CH}=\text{N}$), 7.34 (d, $J=8.8$ Hz, 8H, nitrogen *meta* aromatic protons in $=\text{CH}-\text{C}_6\text{H}_4-\text{N}-$), 7.24 (t, $J=8.0$ Hz, 4H, *meta* protons in $-\text{N}-\text{C}_6\text{H}_5$), 7.03-7.06 (m, 6H, *ortho* and *para* protons in $-\text{N}-\text{C}_6\text{H}_5$), 6.97 (d, $J=8.8$ Hz, nitrogen *ortho* aromatic protons in $=\text{CH}-\text{C}_6\text{H}_4-\text{N}$), 3.22-3.24 (m, 4H, $-\text{CH}-\text{N}=\text{}$), 2.05 (d, $J=11.6$ Hz, 4H of C_6H_{10} ring), 1.88 (d, $J=7.6$ Hz, 8H of C_6H_{10} ring) and 1.48 (q, $J=10.4$ Hz, 4H of C_6H_{10} ring). Some signals positioned at 7.26, 2.96 and 2.88 ppm came from CHCl_3 and DMF included in the macrocycle.

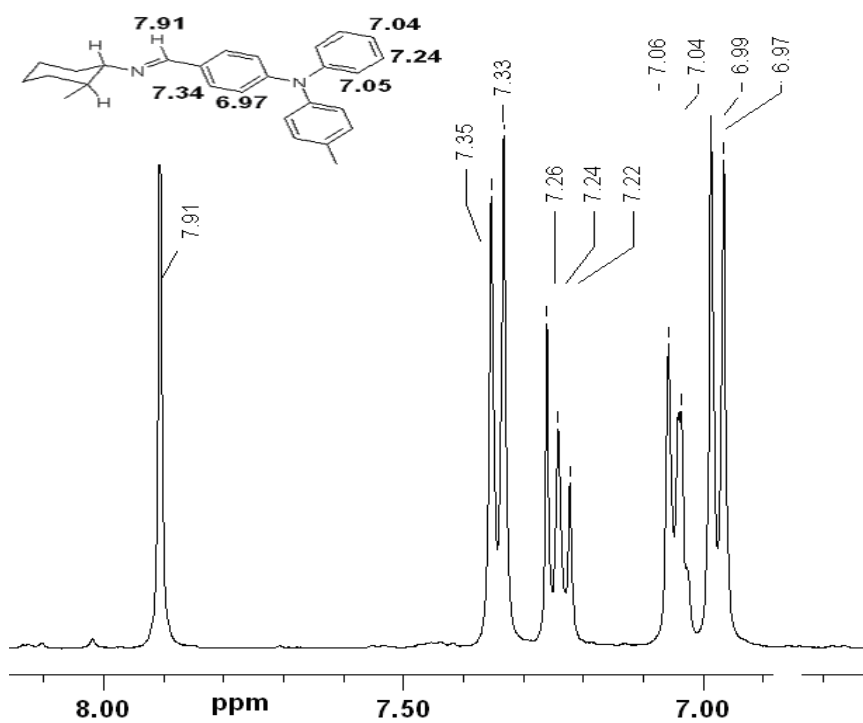


Figure 11. $^1\text{H-NMR}$ spectrum (CDCl_3 , 25 $^\circ\text{C}$) (aromatic region) of 3a, after recrystallization from DMF.

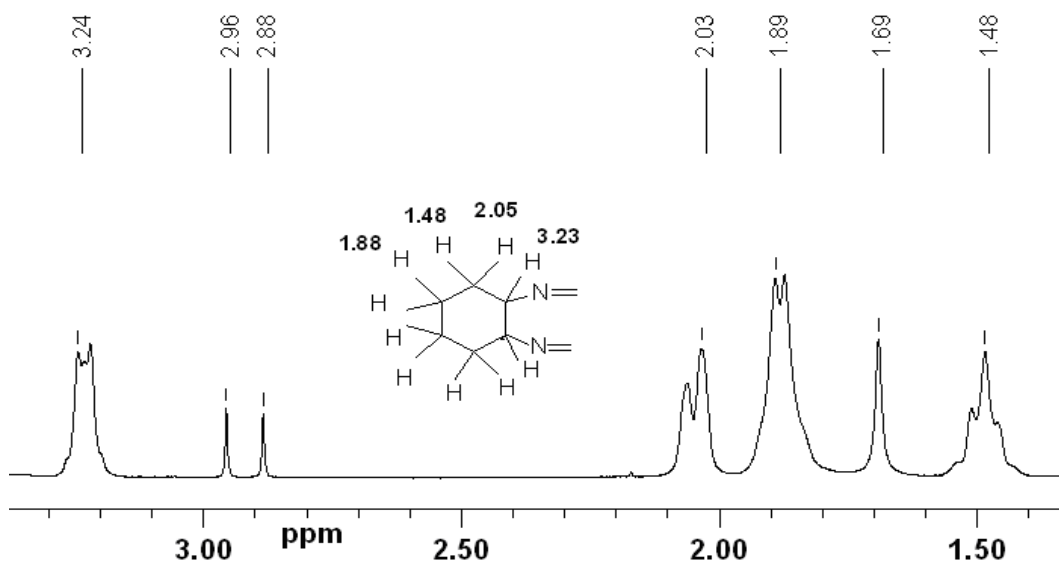


Figure 12. $^1\text{H-NMR}$ spectrum, CDCl_3 , room temperature, (aliphatic region) of 3a (recrystallized from DMF).

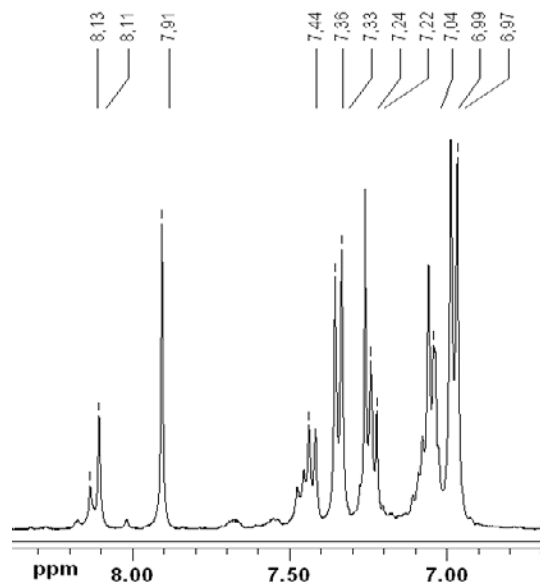


Figure 13. ¹H-NMR spectrum (CDCl₃, 25 °C) (aromatic region) of 3a, (presented in Figure 11) registered again but after several days.

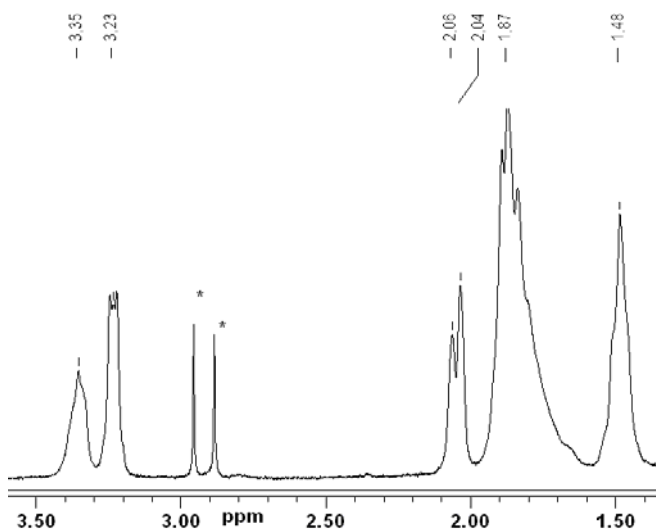


Figure 14. ¹H-NMR spectrum, CDCl₃, room temperature, (aliphatic region) of 3a (presented in Figure 12) registered after several days.

When the CDCl₃ solution of **3a** was left in the NMR tube for several days at room temperature and N₂ atmosphere and then registered again its proton NMR spectrum showed significant modifications, mostly observed in the aromatic region (Figure 13). Thus, new signals appeared for imine (8.11-8.13 ppm), aromatic (7.42-7.44 ppm) and -CH-N= diamine

(3.35 ppm) protons (Figure 14), suggesting presence of two non-equivalent triphenylamine groups. The intensities of the new signals integrals are correlated between them.

The imine linkage in Schiff base compounds could adopt *E* or *Z* configuration, therefore **3** should exist as all-*E*, all-*Z* or *E-Z* isomers. However, it is recognized that *E* isomer is the only product obtained due to its higher thermodynamical stability. In addition, *E* isomer can exist in many conformations, as *syn* or *anti* rotamers (Figure 15), with a preference for *syn* conformer [32]. In the first rotamer, imine and =N-CH- (from cyclohexane) hydrogens are in *syn* position. Therefore, the changes observed in the NMR spectrum of **3a** can be assigned to an isomerization (interconversion) process that takes place in solution by a ring inversion (Figure 16).

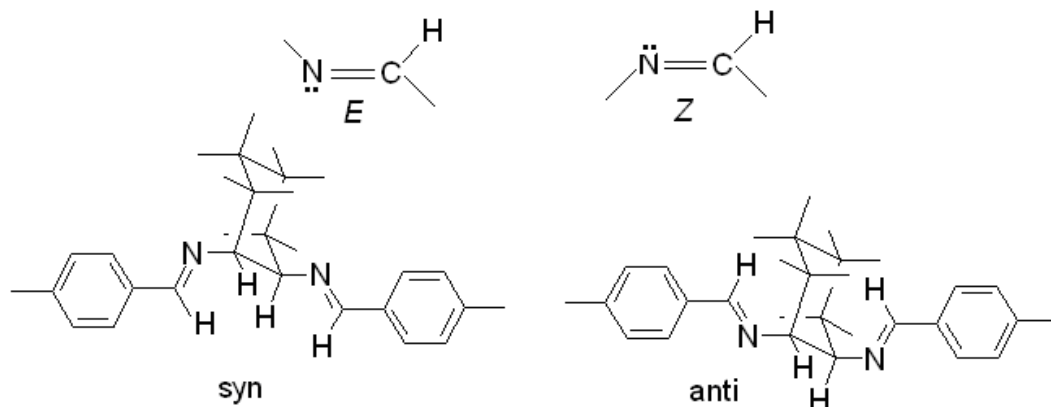


Figure 15. *E/Z* and *syn/anti* isomers.

Interconversion between *anti* and *syn* conformers (Figure 16) take place *via* the concerted rotation of triphenylamine group around flexible cyclohexane-N bonds.

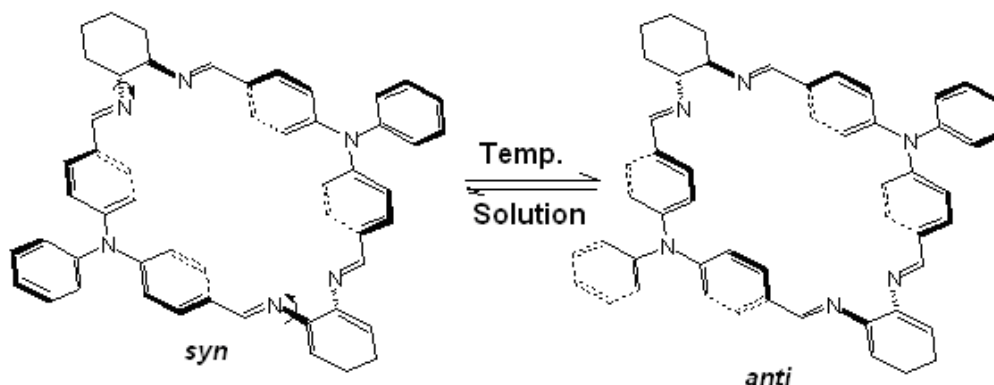


Figure 16. Interconversion of *syn-anti* rotamers.

Kuhnert et al. [44] has observed a similar dependent $^1\text{H-NMR}$ spectrum of the macrocycle obtained from **2** and N-ethyl 3,6-carbazole dialdehyde and assigned this change to a ring inversion of carbazole groups.

UV absorption spectra of **3a** showed also important changes in the shape and positions of the absorption maxima of the CHCl_3 solution. Thus, **3a** in *anti* conformation presented three absorption maxima (in CHCl_3 solution), the first two being characteristic of the $\pi\text{-}\pi^*$ transitions in triphenylamine group (240-250 and 336 nm). The third absorption can be attributed to imine linkages conjugated with triphenylamine moiety (356 nm). After few minutes the solution showed a new broad absorption band at 422 nm and its intensity gradually increased in time (correlated with the disappearance of the 356 nm band) and after 24 h attained the saturate level. In the same time the intensity of 336 nm band decreased. We assume that **3a** obtained by crystallization from DMF has an *anti* conformation but in CHCl_3 solution it spontaneously isomerized to *syn* rotamer, more thermodynamically stable, having lower sterical hindrances and more extended conjugation. Because in the NMR spectrum at least three signals for imine protons can be observed, a mixture of the rotamers was present with different torsion angles (ω).

ESI-MS spectrum of **3a** (recovered after keeping in CHCl_3 solution for some days) is unchanged (Figure 10), therefore the modifications observed from $^1\text{H-NMR}$ and UV spectra couldn't be associated with hydrolysis of imine linkage or formation of larger macrocycles ([3+3] or [4+4] type). The raw product obtained from synthesis showed a similar NMR spectrum with that presented in Figure 13 and 14.

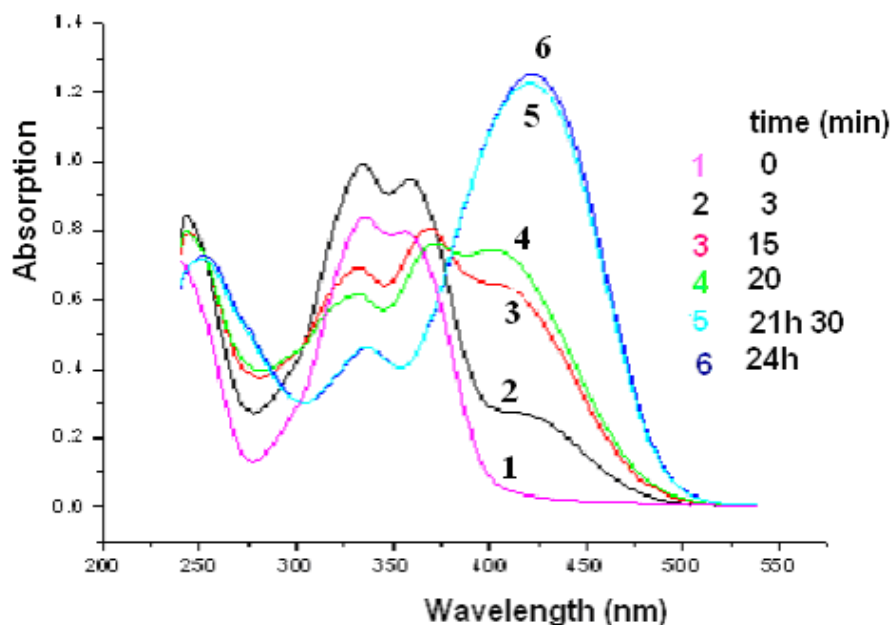


Figure 17. In time-evolution of UV spectra (CHCl_3) of **3a**.

Reduction of **3a** with NaBH_4 in methanol/THF mixture gave rhombamine **4a** in almost quantitative yield. In the H-NMR spectrum, signal assigned to imine protons (7.9-8.2 ppm) has disappeared and new signals at 3.5-3.9 ppm ($-\text{CH}_2-$) and 2.3 ppm ($-\text{NH}-$) have appeared.

A dibromine-functionalized rhombimine, **3b**, was synthesized by a similar protocol as **3a**, from **1b** and **2** and recrystallized from CCl_4 /ethyl acetate (9/1 v/v). The ^1H -NMR spectrum (Figure 18) is very similar with that of **3a** obtained from synthesis. The presence of solvent (ethyl acetate) in macrocycle **3b** was observed by ^1H -NMR where signals for ethyl acetate (4.13, 2.04 and 1.26 ppm), about one solvent molecule for two macrocycles, can be observed, even if the compound was dried at $40\text{ }^\circ\text{C}$ *in vacuo* for 24 h. TG curves showed also a 3-7 % weight loss between $100\text{-}180\text{ }^\circ\text{C}$ due to removing of the solvent included in the macrocycle (Figure 8). Therefore, **3b** had a *syn* conformation.

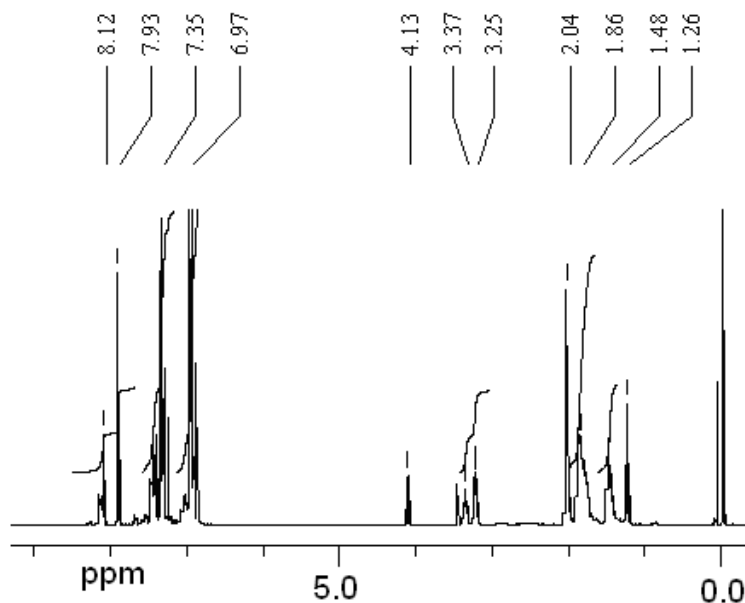


Figure 18. ^1H -NMR spectrum (CDCl_3) of **3b** after recrystallization from CCl_4 /ethyl acetate. Signals at 1.26, 2.04 and 4.13 ppm are from ethyl acetate.

4. SYNTHESIS OF TRIPHENYLAMINE-BASED POLYRHOMBIMINES

Imine macrocycles **3a** and **3b** can be introduced into polymers as part of the backbone. The coupling can take place directly or through a spacer. Macrocycle **3a** can be considered as a monomer. Having two unsubstituted positions (*para*), active for encatennation, **3a** can be considered as monomer in chemical and electrochemical oxidative polymerization. For instance, the chemical oxidative polymerization (FeCl_3 as oxidant) of triarylamine derivatives, 4-alkyl triphenylamine [64,65], 4-methoxy, 4-cyano and 4-nitro triphenylamine [66], di(1-naphthyl)-4-anisilamine [67] and di(1-naphthyl) p-tolylamine [68] has been reported. The polymers have relatively high molecular weights, are soluble in organic solvents and can be processed as free-standing films with good thermal stability.

The electrochemical behavior of macrocycle **3a** was studied using repeated potential scan polymerization with a standard three-electrode cell. Figure 19 presents the repeated potential scan electropolymerization of **3a** in 0.2 M tetrabutylammonium tetrafluoroborate (electrolyte)

and methylene chloride as solvent. The potential is scanned anodically at a scan rate of 50 mV/sec. At 1.4 V there is a peak for the one-electron TPA group oxidation.

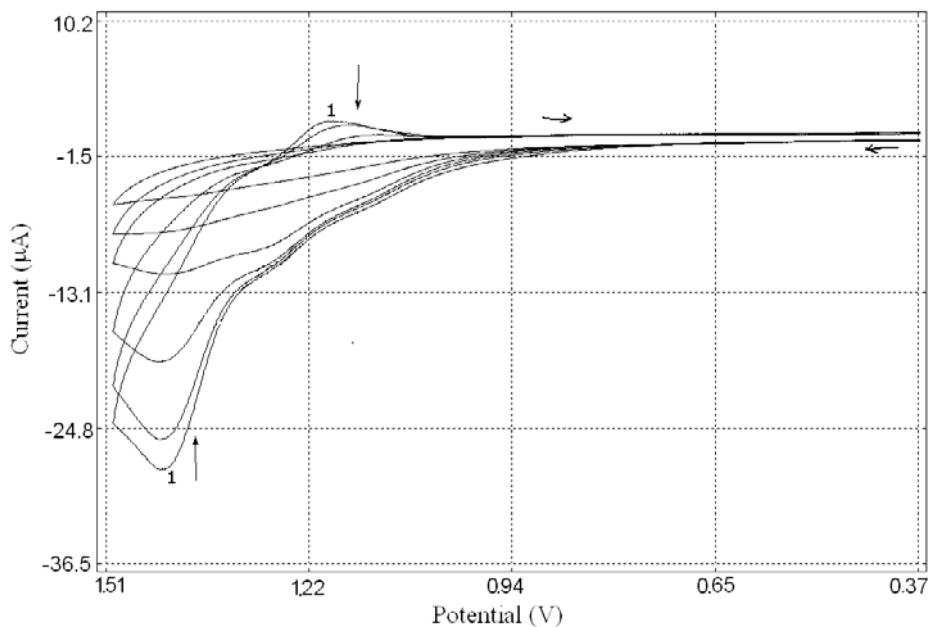


Figure 19. Cyclic voltammograms of **3a** (2mM) at 20 °C in CH₂Cl₂ containing 0.2M Bu₄NBF₄ at a Pt working electrode. Scan rate = 50 mV/s.

Upon reductive scanning a cathodic process with a peak at 1.2V is observed corresponding to the reduction of the oxidized monomer. Repeated scanning over this potential range has resulted in the deposition of a thin film on the working electrode. In the same time, the current response of both the anodic and cathodic polymer redox processes decreases, as the result of the deposition of a non-conductive polymer film on electrode.

The chemical oxidative polymerization of **3a** was carried out using FeCl₃ as oxidant in CHCl₃ solution, at room temperature (Figure 20). At low molar ratio FeCl₃/**3a** =1-2, no polymer was obtained, even the initially yellow color of monomer solution turned on to red-brick by adding the oxidant. Probably the oxidant is inactive due to its complexing by imine groups. At high molar ratio (>5) a precipitate was deposited on the flask' walls during the polymerization. Finally, a brick-colored and insoluble product was obtained.

Based on literature data [64-68], the oxidative chemical and electrochemical polymerization is believed to proceed through 4',4'' positions of TPA.

FTIR spectrum, very similar with that of **3a**, showed an additional weak signal at 1692 cm⁻¹ assigned to carbonyl groups resulted from hydrolysis of some imine linkages (Figure 21). The side reactions are favored by HCl traces resulted from oxidative process. Unfortunately, the polymer insolubility didn't allow obtaining more information about its structure and molecular weight and introduction of the bulky substituents in the macrocycle could improve polymer processability and characterization.

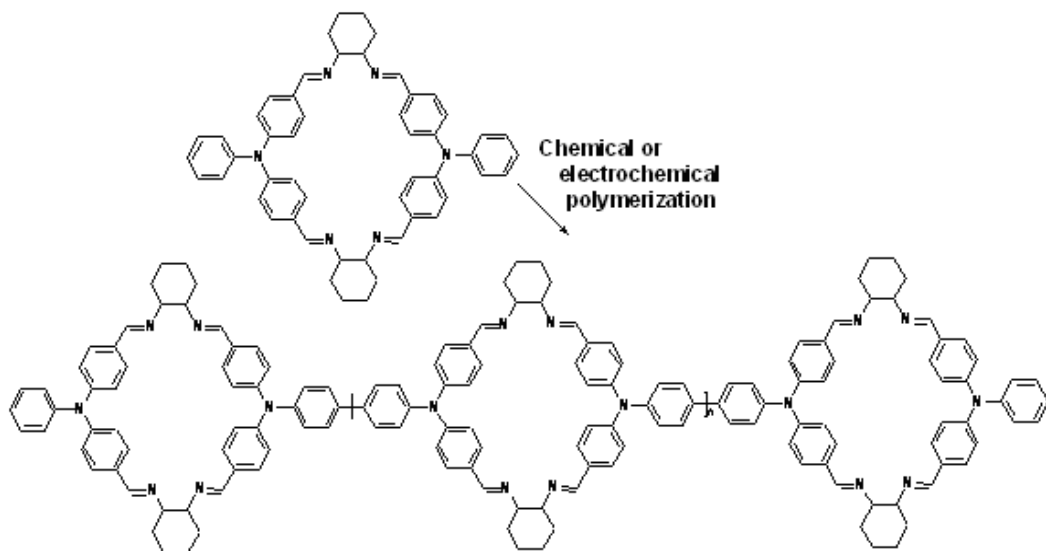


Figure 20. Synthesis of polyrhombimine by chemical or electrochemical oxidative polymerization of 3a.

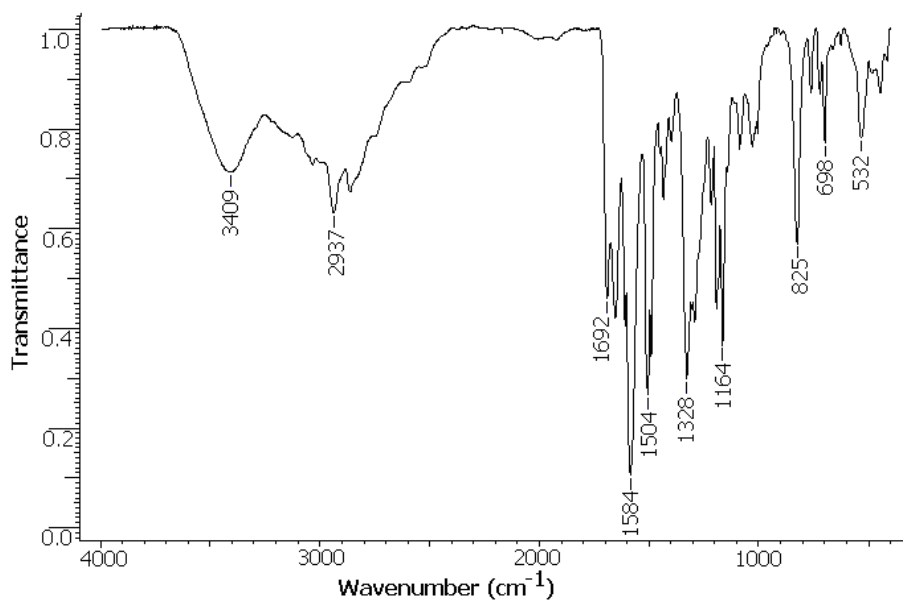


Figure 21. FTIR spectrum of poly-3a synthesized by chemical oxidative polymerization.

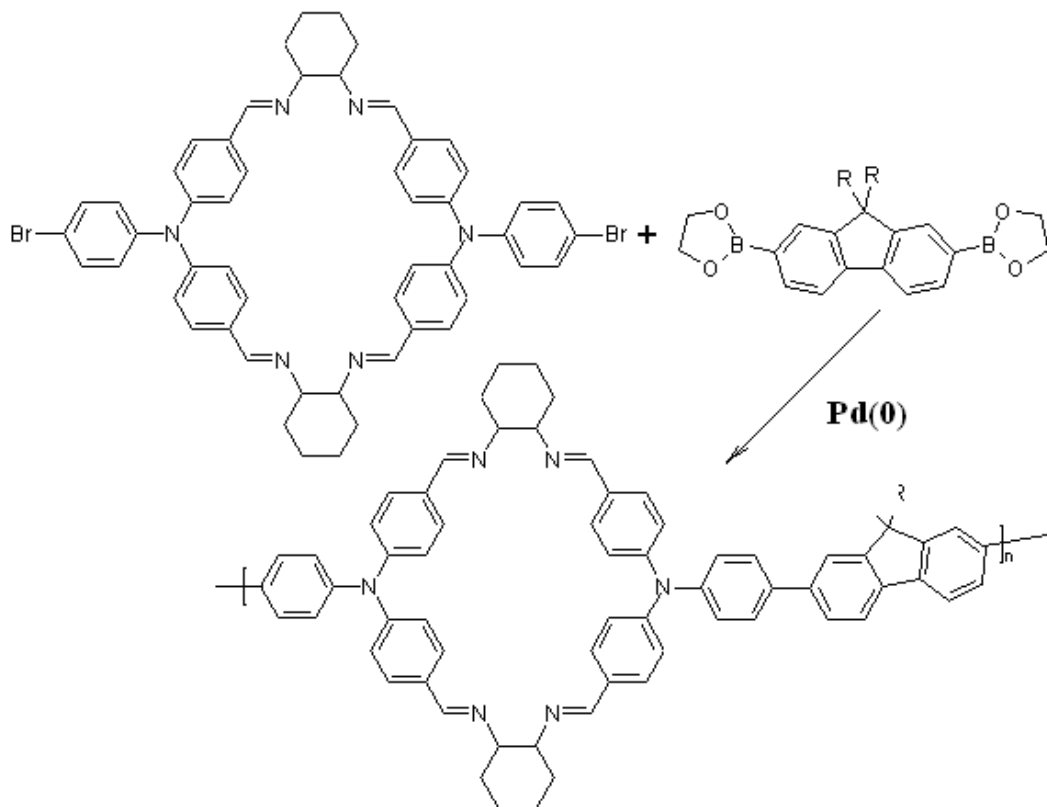


Figure 22. Synthesis of polyrhombimine by Suzuki polycondensation of 3b using fluorene bisboronic acid derivative.

Macrocycle 3b, containing two functional bromine atoms is an adequate comonomer for use in metal-catalyzed polycondensation reactions. The palladium-catalyzed cross-coupling *via* Suzuki reaction of *bis*bromine-substituted macrocycle with 9,9-dihexylfluorene diboronic acid *bis*(1,3-propanediol)ester was carried out in a two-phase system of toluene and aqueous potassium carbonate at reflux temperature using a feed ratio of 1/1 between the components (Figure 22). The copolymer was obtained in low yield as an orange-brick solid, mostly soluble in chloroform and having low molecular weight ($M_n = 1840$, $DPI = 2.43$). The molecular weight measured by GPC based on polystyrene standards should be taken as the minimum estimation because of the different structure of the polymer. The very poor solubility of macrocycle in usual solvents used in Suzuki polycondensation is a disadvantage because the reaction had to be carried out at high dilution and very long time (when side reactions are important) to obtain acceptable yields.

$^1\text{H-NMR}$ spectrum of the polymer is presented in Figure 23. New signals in the aliphatic region (0.71, 1.01, 2.08 ppm) can be observed and are assigned to hexyl substituents from fluorene monomer. Aromatic protons of fluorene and triphenylamine have appeared in the same region and all signals are broadened.

Polymer showed also two signals for imine protons (7.92 and 8.12 ppm) suggesting the existence of macrocycles in the main chain as *syn* conformer.

Both polymers contain rhombimine macrocycles in the main chain and space filling models of the polymers are presented in Figure 24.

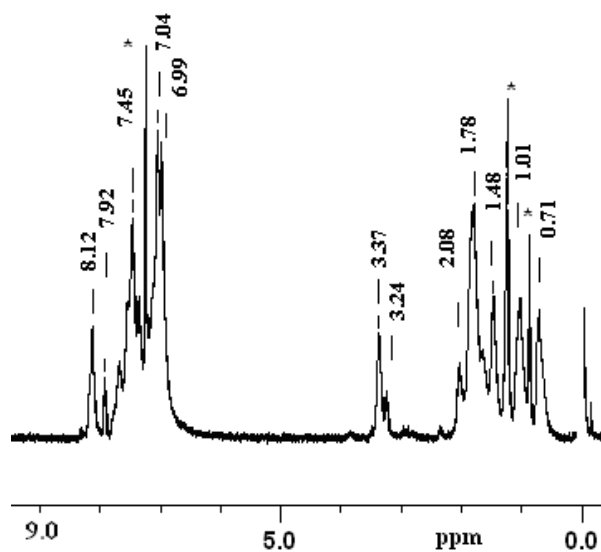


Figure 23. ^1H -NMR spectrum of polymer synthesized by Suzuki polycondensation.

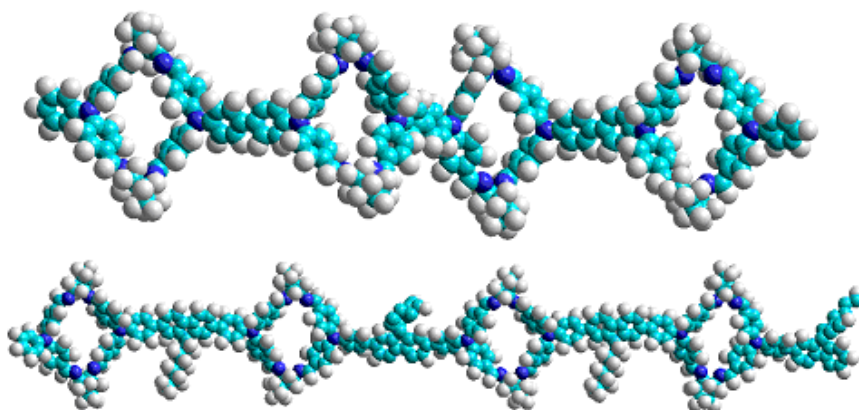


Figure 24. Space filling models for polyrhombimines obtained by chemical oxidation of 3a (up) or Suzuki polycondensation of 3b (down).

Macrocycles and corresponding polymers contain cavities where small solvent molecules can be hosted. The inclusion of solvent molecules (DMF or ethyl acetate) by 3a and 3b was observed by NMR and TG spectroscopy in the samples, even after high-vacuum drying at 40–60 °C. The presence of imine sites opens new opportunities for modification of imine macrocycles by Lewis acid complexation and inorganic or organic acid quaternization observed by optical spectroscopy. For instance, UV spectrum (CH_2Cl_2) of poly-3b showed absorptions at 238, 330 (shoulder) and 366 nm and emission at 450 nm. In the presence of metallic ions, Sn^{2+} and Fe^{3+} the absorption maximum (366 nm) is shifted at 378 and 464 nm,

respectively. Therefore, the polymer films could be used as sensors for detection of different metallic ions.

5. CONCLUSIONS

The first polymer containing large imine macrocycles in the main chain was synthesized by palladium (0)-catalyzed polycondensation of *bis*bromine imine macrocycle with 9,9-dihexylfluorene diboronic acid bis(1,3-propanediol)ester. The polymer structure was confirmed by NMR spectroscopy and has a low molecular weight due to low solubility of the monomer and polymer during the polymerization reaction. Chemical oxidative polymerization of 3a, carried out with FeCl₃ in CHCl₃, led to a brick colored and insoluble polymer with FTIR spectrum similar with 3a. The use of imine macrocycles as monomers in synthesis of polymers opens new research directions and possible applications. These polymer structures represent new materials with interesting properties and applications.

ACKNOWLEDGMENTS

The authors thank the Romanian National Authority for Scientific Research (UEFISCSU) for financial support (Grant PN II-IDEI-993).

REFERENCES

- [1] Cram, D. J. *Angew. Chem. Int. Ed.*, 1988, 27, 1009-1020;
- [2] Pedersen, C. J. *Angew. Chem. Int. Ed.*, 1988, 27, 1021-1027.
- [3] Lehn, JM. *Angew. Chem. Int. Ed.*, 1988, 27, 89-112.
- [4] Hoger, S; Morisson, DL; Enkelmann, V. *J. Am. Chem. Soc.*, 2002, 124, 6734-6736.
- [5] Henze, O; Lentz, D; Schafer, A; Franke, P; Schluter, AD. *Chem.-Eur. J.*, 2002, 8, 357-365.
- [6] Grave, C; Lentz, D; Schafer, A; Samori, P; Rabe, J. P; Franke, P; Schluter, AD. *J. Am. Chem. Soc.*, 2003, 125, 6907-6918.
- [7] Zhao, D; Moore, JS. *J. Org. Chem.*, 2002, 67, 3548-3554.
- [8] Gallant, AJ; MacLachlan, M. J. *Angew. Chem. Int. Ed.*, 2003, 42, 5307-5310.
- [9] Hoger, S; Cheng, XH; Ramminger, AD; Enkelmann, V; Rapp, A; Mondeshki, M; Schnell, I. *Angew. Chem. Int. Ed.*, 2005, 44, 2801-2805.
- [10] Sessler, JL; Callaway, W; Dudek, SP; Date, RH; Lynch, V; Bruce, DW. *Chem. Commun.*, 2003, 2422-2423.
- [11] Zhao, D; Moore, JS. *Chem. Commun.*, 2003, 807-818 and references therein.
- [12] Gibson, HW; Bheda, MC; Engen, PT. *Progr. Polym. Sci.*, 1994, 19, 843-945.
- [13] Nepogodiev, SA; Stoddart, JF. *Chem. Rev.*, 1998, 98, 1959-1976.

- [14] Raymo, FM; Stoddart, JF. *Chem. Rev.*, 1999, 99, 1643-1663. d) Sauvage, J. P; Dietrich-Buchecker, C. Eds. *Molecular Catenanes, Rotaxanes and Knots*; Wiley-VCH, Weinheim, 1999.
- [15] Takata, T; Kihara, N; Furusho, Y. *Adv. Polym., Sci.*, 2004, 171, 1-76.
- [16] Cram, DJ; Cram, JM. *Container Molecules and their Guests*, Royal Society of Chemistry, Cambridge. UK 1994.
- [17] Jasat, A; Sherman, JC. *Chem. Rev.*, 1999, 99, 931- 968.
- [18] Warmuth, R; Yoon, J. *Acc. Chem. Res.*, 2001, 34, 95-105.
- [19] Kraft, A; Grimsdale, AC; Holmes, AB. *Angew. Chem. Int. Ed.*, 1998, 37, 402-428.
- [20] Mitchke, U; Bäuerle, P. *J. Mater. Chem.*, 2000, 10, 1471-1507.
- [21] Friend, RH; Gymer, RW; Holmes, AB; Burroughes, JH; Marks, RN; Taliani, C; Bradley, DDC; Santos, DAD; Brédas, JL; Lögdlund, M; Salaneok, WP. *Nature*, 1999, 397, 121-128.
- [22] Law, KY. *Chem. Rev.*, 1993, 93, 449-486
- [23] Forrest, SR. *Chem. Rev.*, 1997, 97, 1793-1896.
- [24] Walzer, K; Maening, B; Pfeifer, M; Leo, K. *Chem. Rev.*, 2007, 107, 1233-1271.
- [25] Lambert, C; Gaschler, W; Schmalzlin, E; Meerholz, K; Brauchle, C. *J. Chem. Soc., Perkin Trans., II* 1999, 577-588.
- [26] Delaviz, Y; Gibson, HW. *Macromolecules*, 1992, 25, 18-20.
- [27] Delaviz, Y; Gibson, HW. *Macromolecules*, 1992, 25, 4859-4862.
- [28] Kaneko, T; Horie, T; Matsumoto, S; Teraguchi, M; Aoki, T. *Macromol. Chem. Phys.*, 2009, 210, 23-36.
- [29] Opris, DM; Franke, P; Schluter, AD. *Eur. J. Org. Chem.*, 2005, 822-837.
- [30] Pasini, D; Ricci, M. *Curr. Org. Synth.*, 2007, 4, 59-80.
- [31] for relevant reviews on imine macrocycles, see: (a) Borisova, NE; Reshetova, MD; Ustynyuk, YA. *Chem. Rev.*, 2007, 107, 46-79. (b) MacLachlan, MJ. *Pure Appl. Chem.*, 2006, 78, 873-878.
- [32] Gawronski, J; Kolbon, H; Kwit, M; Katrusiak, A. *J. Org. Chem.*, 2000, 65, 5768-5773.
- [33] Kwit, M; Gawronski, J. *Tetrahedron: Asymmetry*, 2003, 14, 1303-1308.
- [34] Gawronski, J; Brzostowska, M; Kwit, M; Plutecka, A; Rychlewska, U. *J. Org. Chem.*, 2005, 70, 10147-10150.
- [35] Kwit, M; Skowronek, P; Kolbon, H; Gawronski, J. *Chirality*, 2005, 17, 93-100.
- [36] Gawronski, J; Gawronska, K; Grajewski, J; Kwit, M; Plutecka, A; Rychlewska, U. *Chem. Eur. J.*, 2006, 12, 1807-1817.
- [37] Kaik, M; Gawronski, M. *Org. Lett.*, 2006, 8, 2921-2924.
- [38] Gawronski, J; Kwit, M; Grajewski J; Gajewy J; Długokinska A. *Tetrahedron: Asymmetry*, 2007, 18, 2632-2637.
- [39] Skowronek, P; Gawronski, J. *Org. Lett.*, 2008, 10, 4755-4758.
- [40] Chadim, M; Budesinsky, M; Hodacova, J; Zavada, J; Junk, PC. *Tetrahedron: Asymmetry*, 2001, 12, 127-133.
- [41] Hodackova, J; Budesinsky, M. *Org. Lett.*, 2007, 9, 5641-5643.
- [42] Kuhnert, N; Lopez-Periago, AM. *Tetrahedron Lett.*, 2002, 43, 3329-3332.
- [43] Kuhnert, N; Strassnig, C; Lopez-Periago, AM. *Tetrahedron: Asymmetry*, 2002, 13, 123-128.
- [44] Kuhnert, N; Rossignolo, GM; Lopez-Periago, A. *Org. Biomol. Chem.*, 2003, 1, 1157-1170.

- [45] Kuhnert, N; Burzclaff, N; Patel, C; Lopez-Periago, A. *Org. Biomol. Chem.*, 2005, 3, 1911-1921
- [46] Kuhnert, N; Lopez-Periago, A; Rossignolo, GM. *Org. Biomol. Chem.*, 2005, 3, 524-537.
- [47] Kuhnert, N; Patel, C; Jami, F. *Tetrahedron Lett.*, 2005, 46, 7575-7579.
- [48] Gao, J; Martell, AE. *Org. Biomol. Chem.*, 2003,1, 2795-2800.
- [49] Gao, J; Martell, AE. *Org. Biomol. Chem.*, 2003,1 2801-2806.
- [50] Gao, J; Reibenspies, JH; Zingaro, RA; Wooley, FR; Martell, AE; Clearfield, A. *Inorg. Chem.*, 2005, 44, 232-241.
- [51] Srimurugan, S; Viswanathan, B; Varadarajan, TK; Varghese, B. *Org. Biomol. Chem.*, 2006, 4, 3044-3047.
- [52] Corbett, PT; Leclaire, J; Vial, L; West, KR; Wietor, JL; Sanders, JKM; Otto, S. *Chem. Rev.*, 2006,106, 3652-3711.
- [53] Grigoras, M; Antonoaia, NC. *Eur. Polym. J.*, 2005, 41, 1079-1089.
- [54] Grigoras, M; Stafie, L; Totolin, M. *Rev. Roum. Chim.*, 2008, 53, 787-794.
- [55] Grigoras, M; Stafie, L. *Des. Mon. Polym.*, 2009, 12, 177-196.
- [56] Liu, X; Liu, Y; Li, G; Warmuth, R. *Angew. Chem. Int. Ed.*, 2006, 45, 901-906.
- [57] Ro, S; Rowan, SJ; Pease, AR; Cram, DJ; Stoddart, JF. *Org. Lett.*, 2000, 2, 2411-2414.
- [58] Quan, MLC; Cram, DJ. *J. Am. Chem. Soc.*, 1991, 113, 2754-2755.
- [59] Liu, Y; Liu, X; Warmuth, R. *Chem.-Eur. J.*, 2007, 13, 8953-8959.
- [60] Xu, D; Warmuth, R. *J. Am. Chem. Soc.*, 2008, 130, 7520-7521.
- [61] Mallejol, T; Gmoh, S; Meziane, MAA; Blanchard-Desce, M; Mougin, O. *Synthesis*, 2005, 11, 1771-1774.
- [62] Paul, GK; Mwaura, J; Argun, AA; Taranekar, P; Reynolds, JR. *Macromolecules*, 2006, 39, 7789-7792.
- [63] Vacareanu (Stafie), L; Barboiu, V; Timpu, D; Grigoras, M. *Chem. J. Mold.*, 2009, 4, 97-102.
- [64] Sim, JH; Yamada, K; Lee, SH; Yokokura, S; Sato, H. *Synth. Met.*, 2007, 157, 940-944.
- [65] Ogino, K; Kanegae, A; Yamaguchi, R; Sato, H; Kurjata, J. *Macromol. Rapid Commun.*, 1999, 20, 103-106.
- [66] Lin, HY; Liou, GS. *J. Polym. Sci. Part A: Polym. Chem.*, 2009, 47, 285-294.
- [67] Lin, HY; Liou, GS; Lee, WY; Chen, WC. *J. Polym. Sci. Part A: Polym. Chem.*, 2007, 45, 1727-1736.
- [68] Nomura, M; Shibasaki, Y; Ueda, M; Tugita, K; Ichikawa, M; Taniguchi, Y. *Macromolecules*, 2004, 37, 1204-1210.

Chapter 14

**THE RECOGNITION AND ACTIVATION OF
MOLECULES AND ANIONS BY POLYAZA
MACROCYCLIC LIGANDS AND THEIR COMPLEXES**

Tong-Bu Lu

MOE Key Laboratory of Bioinorganic and Synthetic Chemistry / State Key Laboratory of Optoelectronic Materials and Technologies / School of Chemistry and Chemical Engineering, Sun Yat-Sen University, Guangzhou 510275, China.

ABSTRACT

Molecular recognition and activation occur frequently in biological systems to achieve the physiological actions, and it is important to understand the process of recognition between receptors and substrates. In this chapter, we present the recent progress in the recognition of molecules and anions by cryptands, protonated cryptands and cryptates, the chiral recognition of amino acids by chiral polyaza macrocyclic ligands, the asymmetrical catalysis by chiral macrocyclic complexes, and the activations of bicarbonate and nitriles by dinuclear cryptates.

INTRODUCTION

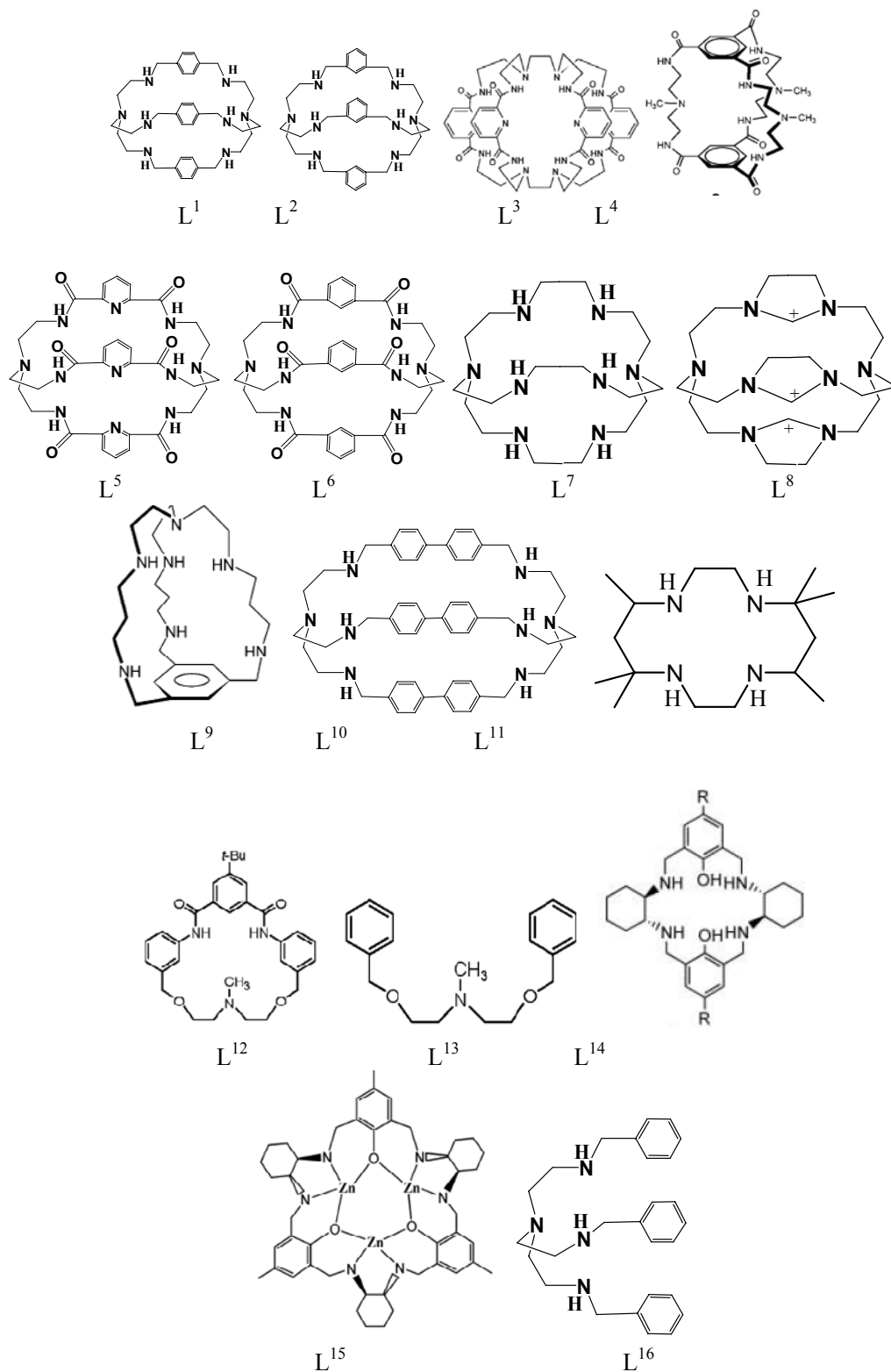
The recognition was defined as a process involving both binding and selecting of substrate(s) by a given receptor molecule,[1] and the recognized substrate within the receptor can be activated by multi-supramolecular interactions between the substrate and a receptor. Since the first report of the crown ethers and their complexes by Pedersen,[2] there has been continuous interest in the design and synthesis of macrocyclic receptors for the recognition and activation of molecules and anions. Among them, polyaza macrocyclic ligands (including cryptands) draw particular attention due to their high stability and selectivity to metal ions, the good capability to recognize anions upon protonation, and facility to synthesis. Many reviews have been published in the past decade to deal with the synthesis and coordination

behaviors of these polyaza macrocyclic ligands and their complexes.[3-10] The recognition of polyaza macrocyclic ligands and their complexes to molecules and anions depends on the size match between the substrates and receptors, the dimensionality, flexibility and rigidity of the polyaza macrocyclic ligands, the M...M separations in the dinuclear cryptates, the counter anions, pH values and temperature etc. Thus, the selectivity of polyaza macrocyclic ligands and their complexes to molecules and anions can be improved by changing the above mentioned factors. In this chapter, we will present the recent progress in the recognition of molecules and anions by cryptand, protonated cryptands, and cryptates, and the chiral recognition of amino acids by chiral polyaza macrocyclic ligands, as well as the activation of bicarbonate and nitriles by dinuclear cryptates through both coordination interactions and intermolecular supramolecular interactions, and transfer them to carbonate monoesters and alcohol, respectively.

THE RECOGNITION BY CRYPTANDS AND PROTONATED CRYPTANDS

The polyaza macrocyclic ligands, upon protonated, can encapsulate the different anions within their cavity through both electrostatic and hydrogen bonding interactions between the protonated amines and the guest anions. The recognition depends on the size match between the receptors (macrocyclic ligands) and the substrates (molecules and anions), the degree of protonation of the polyaza macrocyclic ligands (pH value), the counteranion etc.

The hexaprotonated azacryptand $[\text{H}_6\text{L}^1]^{6+}$ shows cascade-like coordination,[11] with two fluoride ions inside two tren-based cavity, bridged by a water molecule (Figure 1a). For larger chloride and bromide, $[\text{H}_6\text{L}^1]^{6+}$ can only encapsulate a single Cl^-/Br^- within its tren-based cavity, and the other pole is occupied by a water molecule (Figure 1b). The association constants of $\log K$, determined by NMR titration in aqueous solution at pH 5, are 3.15(5), 3.37(3) and 3.34(4) for F^- , Cl^- and Br^- anions, respectively. Under different preparation condition, single Cl^-/Br^- encapsulated cascade complexes of $[\text{H}_6\text{L}^1(\text{Cl})]^{5+}$ and $[\text{H}_6\text{L}^1(\text{Br})]^{5+}$ were obtained,[12] in which the Cl^-/Br^- is located almost on the centre of the cryptand cavity (Figure 1c). The shape of protonated cryptand $[\text{H}_6\text{L}^1]^{6+}$ changes from olivary in $[\text{H}_6\text{L}^1(\text{Cl}/\text{Br})(\text{H}_2\text{O})]^{5+}$ to pumpkin-shaped in $[\text{H}_6\text{L}^1(\text{Cl}/\text{Br})]^{5+}$, and the distances between the bridgehead nitrogen atoms in $[\text{H}_6\text{L}^1(\text{Cl}/\text{Br})]^{5+}$ (6.240 Å for Cl^- and 6.486 Å for Br^-) are much shorter than those observed in $[\text{H}_6\text{L}^1(\text{Cl}/\text{Br})(\text{H}_2\text{O})]^{5+}$ (10.039 Å for Cl^- and 10.377 Å for Br^-). The iodide anion is too large to encapsulate into the cavity of $[\text{H}_6\text{L}^1]^{6+}$ at room temperature, thus it locates outside the cryptand cavity as counteranion, and the cavity of the receptor is occupied by a water trimer (Figure 1d).[12] However, under the heating condition, the iodide anion can enter the cryptand cavity of $[\text{H}_8\text{L}^1]^{8+}$ to form a iodide encapsulated complex of $[\text{H}_8\text{L}^1(\text{I})]^{7+}$ via N-H...I and C-H...I interactions (Figure 1e).[13] When L^2 with larger windows is used as a receptor, the iodide anion can be encapsulated into the cavity of $[\text{H}_6\text{L}^2]^{6+}$ at room temperature to form a complex of $[\text{H}_6\text{L}^2(\text{I})]_5 \cdot 4\text{H}_2\text{O}$ (Figure 1f).[14] In addition, this receptor can also encapsulate two Cl^- inside the cryptand cavity to form a proton bridged complex of $[\text{H}_4\text{L}^2(\text{ClHCl})](\text{Cl})_3 \cdot n\text{H}_2\text{O}$ (Figure 1g).[14] Proton bridged two fluoride $[\text{FHF}]^-$ can also be encapsulated into the cryptands cavity of L^3 and L^4 to form complexes of $n\text{BuN}^+[\text{L}^3(\text{FHF})] \cdot 3\text{H}_2\text{O}$ (Figure 1h)[15] and $\text{Me}_4\text{N}^+[\text{L}^4(\text{FHF})]$ (Figure 1i),[16] respectively.



Scheme 1

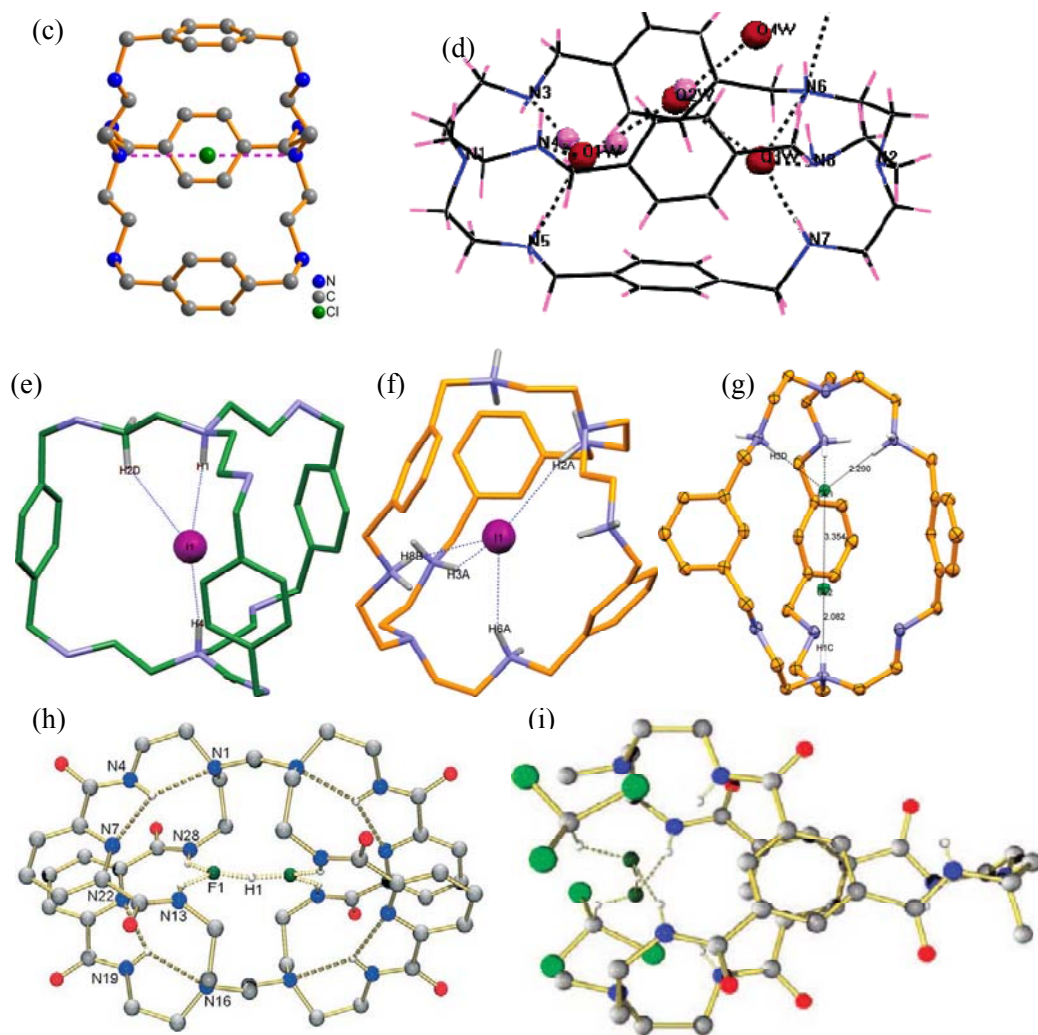


Figure 1. The structures of cascade complexes of (a) $[\text{H}_6\text{L}^1(\text{F}_2)(\text{H}_2\text{O})]^{4+}$, (b) $[\text{H}_6\text{L}^1(\text{Cl})(\text{H}_2\text{O})]^{5+}$, (c) $[\text{H}_6\text{L}^1(\text{Cl})]^{5+}$, (d) $[\text{H}_6\text{L}^1(\text{H}_2\text{O})_3]^{6+}$, (e) $[\text{H}_8\text{L}^1(\text{I})]^{5+}$, (f) $[\text{H}_6\text{L}^2(\text{I})]^{5+}$, (g) $[\text{H}_4\text{L}^2(\text{ClHCl})]^{3+}$, (h) $[\text{L}^3(\text{FHF})]^-$, and (i) $[\text{L}^4(\text{FHF})]^-$.

It's interesting to note that the protonated cryptand L^1 shows both size and temperature dependent encapsulation for tetrahedral anions.[17] At room temperature, the smaller ClO_4^- can be encapsulated inside the cavity of $[\text{H}_6\text{L}^1]^{6+}$ to form a cascade complex of $[\text{H}_6\text{L}^1(\text{ClO}_4)]^{5+}$ (Figure 2a), while the larger H_2PO_4^- cannot be encapsulated inside the cavity of $[\text{H}_6\text{L}^1]^{6+}$ and $[\text{H}_8\text{L}^1]^{8+}$, as the window of $[\text{H}_6\text{L}^1]^{6+}/[\text{H}_8\text{L}^1]^{8+}$ is too small to let H_2PO_4^- enter, thus the reactions of L^1 with H_3PO_4 at pH = 2 and 1 gave $[\text{H}_6\text{L}^1(\text{H}_2\text{O})_2](\text{H}_2\text{PO}_4)_6$ and $[\text{H}_8\text{L}^1(\text{H}_2\text{O})_3](\text{H}_2\text{PO}_4)_8$ (Figures 2b and 2c), respectively. At higher temperature, the window of $[\text{H}_6\text{L}^1]^{6+}/[\text{H}_8\text{L}^1]^{8+}$ can be enlarged, thus H_2PO_4^- can be encapsulated into the cavity of H_8L^1 under heating condition to generate a cascade complex of $[\text{H}_8\text{L}^1(\text{H}_2\text{PO}_4)](\text{H}_2\text{PO}_4)_7$ (Figure 2d). Other tetrahedral anions, such as SO_4^{2-} , can also be encapsulated inside the cavity of protonated cryptands $[\text{H}_8\text{L}^2]^{8+}$ and $[\text{H}_2\text{L}^5]^{2+}$ to generate two cascade complexes of $[\text{H}_8\text{L}^2(\text{SO}_4)](\text{SO}_4)_2(\text{HSO}_4)_2$ (Figure 2e) and $[\text{H}_2\text{L}^5(\text{SO}_4)]$ (Figure 2f), respectively.[18] In

addition, the cryptands L^5 and L^6 also show the F^- anion encapsulation,[19,20] and the analogous cryptand to L^5 show the SO_4^{2-} anion encapsulation.[21]

In comparison with the protonated cryptands L^1 and L^2 , the protonated cryptand L^7 with smaller cavity can recognize the smaller halides of F^- and Cl^- anions rather than Br^- anion, and the reactions of $[H_6L^7]^{6+}$ with the mixed anions of F^-/Br^- and Cl^-/Br^- generate two complexes of $[H_6L^7(F)](Br)_5$ (Figure 2g) and $[H_6L^7(Cl)](Br)_5$ (Figure 2h), respectively,[22] in which only F^- and Cl^- can be encapsulated inside the cavity of L^7 , and the Br^- anions are located outside the cavity as counteranion. Moreover, the protonated cryptand L^8 can only recognize F^- to form a complex of $[H_2L^8(F)](BF_4)_2(ClO_4)_2$ (Figure 2i),[23] as the cavity of L^8 is even smaller than that of L^7 , with the bridgehead $N\cdots N$ distances in $[H_2L^8(F)]^{4+}$, $[H_6L^7(F)]^{5+}$, and $[H_6L^7(Cl)]^{5+}$ are 5.16, 6.58 and 6.65 Å, respectively.

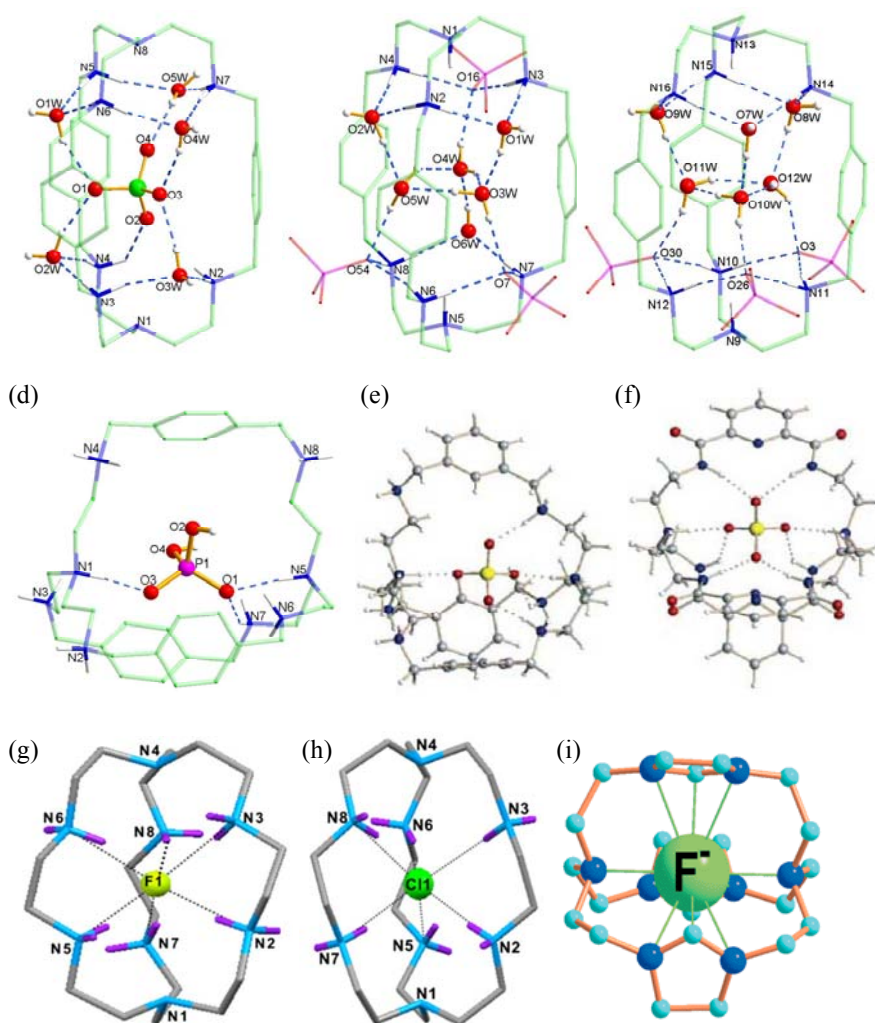


Figure 2. The structures of (a) $[H_6L^1(ClO_4)]^{5+}$, (b) and (c) two $\{[(H_8L^1)(H_2O)_3](H_2PO_4)_3(H_2O)_3\}^{5+}$ cations, (d) $[(H_8L)(H_2PO_4)]^{7+}$, (e) $[H_8L^2(SO_4)]^{6+}$, (f) $[H_2L^5(SO_4)]$, (g) $[H_6L^7(F)]^{5+}$, (h) $[H_6L^7(Cl)]^{5+}$, and (i) $[H_2L^8(F)]^{4+}$.

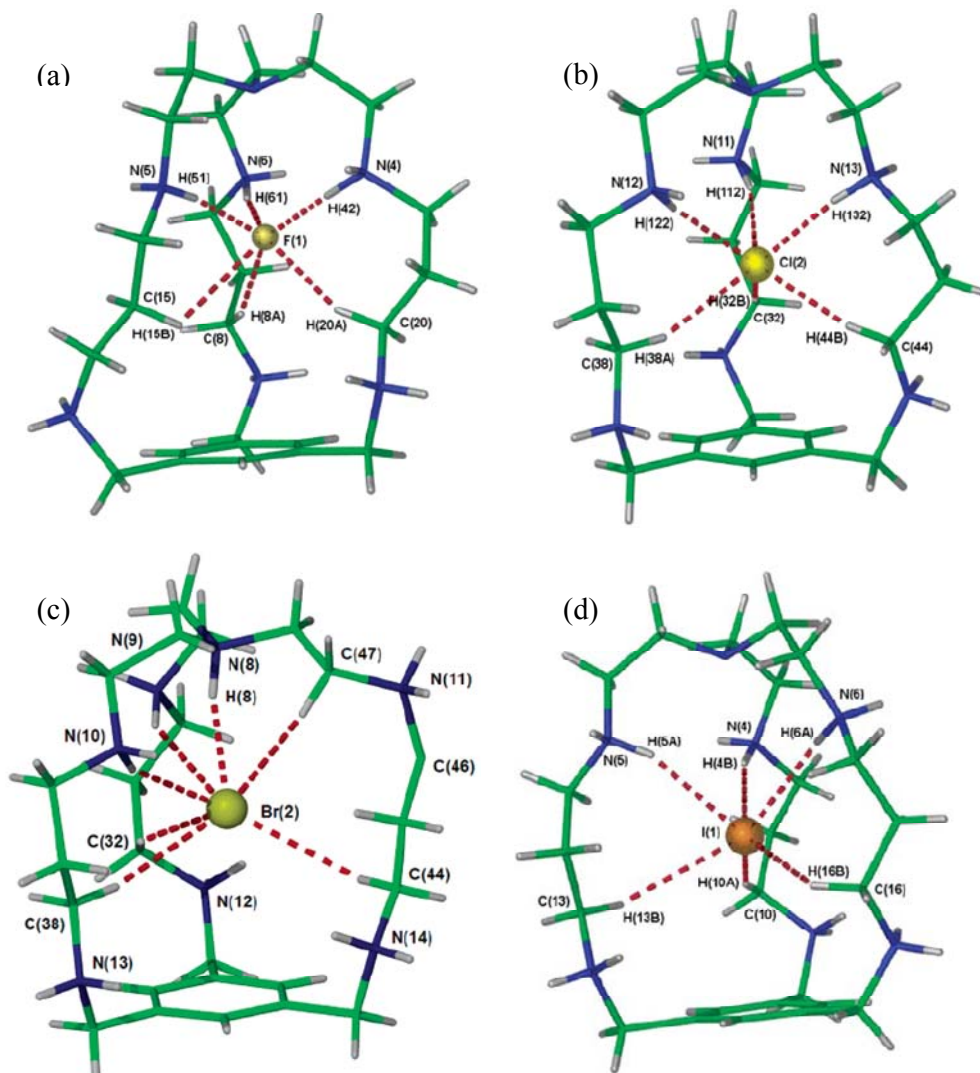


Figure 3. The structures of (a) $[\text{H}_6\text{L}^9(\text{F})]^{5+}$, (b) $[\text{H}_6\text{L}^9(\text{Cl})]^{5+}$, (c) $[\text{H}_6\text{L}^9(\text{Br})]^{5+}$, and (d) $[\text{H}_6\text{L}^9(\text{I})]^{5+}$.

Steed and co-workers synthesized a polyaza cryptand L^9 . [24] They found that the protonated L^9 exhibits remarkable strong and selective fluoride binding comparable to the most effective bis(tren) cryptands, only through three $\text{NH}\cdots\text{F}^-$ and three $\text{CH}\cdots\text{F}^-$ interactions, with the first F^- binding constant of $\log K_1$ observed for $[\text{H}_6\text{L}^9]^{6+}$ as high as 9.54(12). While the first association constants of $\log K_1$ is dramatically decreased to 4.19(13) for Cl^- , and there is no obvious binding of $[\text{H}_6\text{L}^9]^{6+}$ to Br^- and NO_3^- . The strong affinity of $[\text{H}_6\text{L}^9]^{6+}$ towards F^- can be attributed to the size match between the cavity of $[\text{H}_6\text{L}^9]^{6+}$ and F^- anion. The results of crystal structure analyses indicate that the average $\text{N}\cdots\text{F}^-$ distance for $[\text{H}_6\text{L}^9(\text{F})]^{5+}$ is only 2.648 Å (Figure 3a), this distance is much shorter than the corresponding $\text{N}\cdots\text{F}^-$ distances of 2.835 and 2.859 Å for $[\text{H}_6\text{L}^7(\text{F})](\text{F})_5$ [25] and $[\text{H}_6\text{L}^7(\text{F})](\text{Br})_5$ [21] respectively, suggesting a very good match between the cavity of $[\text{H}_6\text{L}^9]^{6+}$ and F^- anion. While the average $\text{N}\cdots\text{Cl}^-$ distance of 3.164(8) Å for $[\text{H}_6\text{L}^9(\text{Cl})]^{5+}$ (Figure 3b) is even longer than the corresponding $\text{N}\cdots\text{Cl}^-$ distances of 3.085 Å for $[\text{H}_6\text{L}^7(\text{Cl})](\text{Cl})_5$ [26] indicating the cavity of $[\text{H}_6\text{L}^9]^{6+}$ is not a

good match the size of Cl^- . Interestingly, the fluoride complex exhibits a rather long anion...centroid separation of 4.506 Å, while the anion...centroid separations remain remarkably constant at ca. 3.6 Å for all the other Cl^- , Br^- and I^- anions (Figures 3b-3d). The fact that this rather short distance of 3.6 Å does not increase with increasing halide size suggests that the halide anions are in repulsive contact with the aromatic ring, thus the binding of all halides except F^- should be destabilized. Besides the above mentioned instances, the anions recognitions by other cryptands have also been investigated.[27-33]

Beside anions, the small solvent molecules can also be encapsulated into the cavity of protonated L^1 . The reaction of $\text{L}^1 \cdot 8\text{HClO}_4$ and NaOH in $\text{H}_2\text{O}/\text{MeOH}$ at a pH 7 generated a complex of $[\text{H}_4\text{L}^1(\text{H}_2\text{O} \cdot \text{MeOH})]^{4+}$ (Figure 4a), in which one methanol and one water molecules, instead of two water or two methanol molecules, were simultaneously encapsulated inside the cavity of $[\text{H}_4\text{L}^1]^{4+}$, indicating three non-hydrogen atoms are preferably accommodated in the cavity of $[\text{H}_4\text{L}^1]^{4+}$. [34] More interesting, upon increasing the pH value to 9, two protons in $[\text{H}_4\text{L}^1]^{4+}$ was removed to get $[\text{H}_2\text{L}^1]^{2+}$, in which the configuration of L^1 was changed, and the encapsulated water-methanol binary molecules were released (Figure 4a). The encapsulation and release of $\text{H}_2\text{O}/\text{MeOH}$ can be interconverted in $\text{H}_2\text{O}/\text{MeOH}$ by adjusting pH values to 7 and 9, respectively (Figure 4a). In addition, the $[\text{H}_4\text{L}^1]^{4+}$ can also encapsulate $\text{H}_2\text{O}/\text{MeCN}/\text{H}_2\text{O}$ molecules within its cavity (Figure 4b). [35]

The outside counteranions can also affect the hydrogen bonding environments of the cavity of protonated L^1 , leading to the formation of different water clusters within the cavity. It has been found that a water dimer (Figure 5a) and a circular water trimer (Figure 5b), a linear water trimer (Figure 5c), and a quasi-prismatic hexamer water cluster (Figure 5d) were encapsulated inside the cavity of $[\text{H}_6\text{L}^1]^{6+}$, when H_2PO_4^- , $[\text{CH}_3(\text{C}_6\text{H}_4\text{-}p)\text{SO}_3^-]$ and SO_4^{2-} were used as counteranions, respectively. [36]

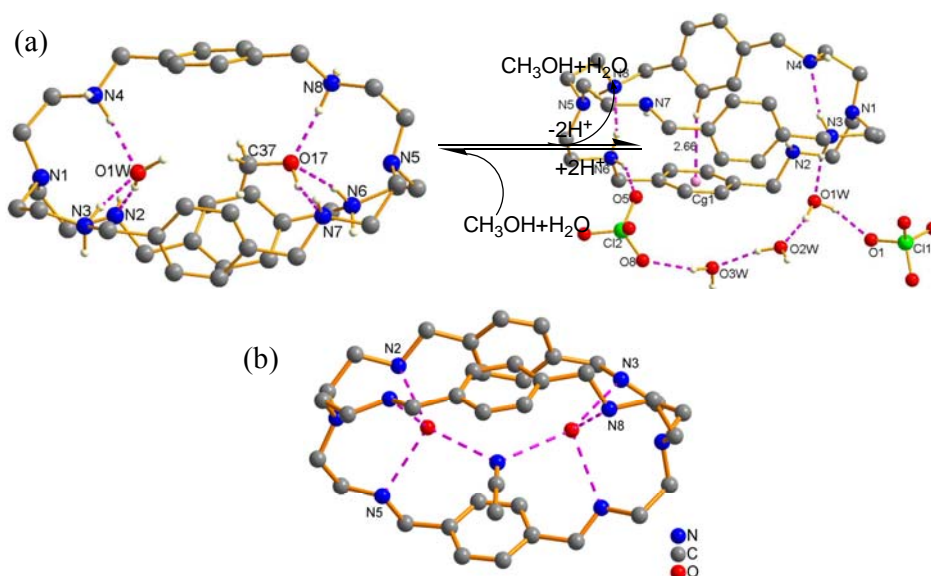


Figure 4. (a) The structures of $[\text{H}_4\text{L}^1(\text{H}_2\text{O} \cdot \text{MeOH})]^{4+}$ (left) and $[\text{H}_2\text{L}^1]^{2+}$ (right), and the reversible encapsulation and release of $\text{H}_2\text{O}/\text{MeOH}$ at pH 7 and 9, respectively. (c) The encapsulation of $\text{H}_2\text{O}/\text{MeCN}/\text{H}_2\text{O}$ molecules in the cavity of $[\text{H}_4\text{L}^1]^{4+}$.

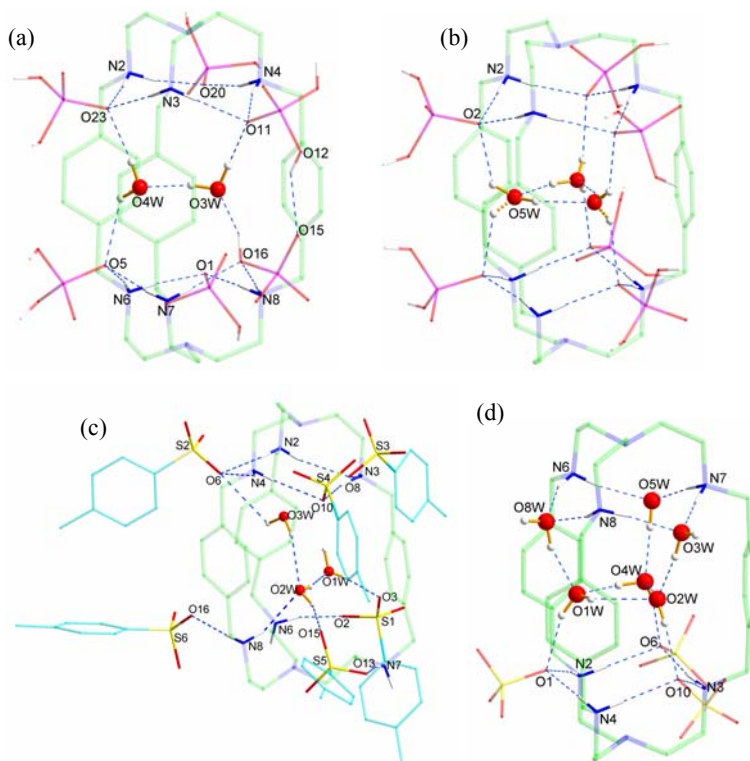


Figure 5. The structures of (a) a water dimer, (b) a circular water trimer, (c) a linear water trimer, and (d) a quasi-prismatic hexamer water cluster encapsulated inside the cavity of $[H_6L^1]^{6+}$.

THE RECOGNITION BY CRYPTATES

The polyaza cryptands can incorporate two metal ions at the two poles, leaving two axial sites vacant and favorable for the coordination of an anion. The recognition of these dinuclear cryptates to anions depends on the flexibility and rigidity of the cryptands, as well as the $M \cdots M$ separations in the cryptates. Increasing the rigidity of a cryptate may improve its selectivity, as the $M \cdots M$ distance can be fixed within a narrow range for a rigid cryptate, thus it can recognize an anion with particular size and shape. We found that the rigid cryptate $[Co_2L^1]^{4+}$ can recognize the Cl^- and Br^- rather than F^- and I^- ,^[37] in which Cl^- and Br^- can be encapsulated inside the cavity of $[Co_2L^1]^{4+}$ to form Cl^-/Br^- bridged cryptates of $[Co_2L^1(Cl)]^{3+}$ (Figure 6a) and $[Co_2L^1(Br)]^{3+}$, with the association constants ($\log K$) of 5.7(1) and 5.2(1) for Cl^- and Br^- , respectively. While the association constant ($\log K$) of $[Co_2L^2]^{4+}$ with Cl^- is only 4.2(1), indicating the stability of $[Co_2L^1(Cl)]^{3+}$ is higher than that of $[Co_2L^2(Cl)]^{3+}$ due to the rigid conformation of L^1 . The F^- anion is too small to form fluoride bridged cryptate of $[Co_2L^1(F)]^{3+}$. While the I^- is too large to encapsulate inside the cryptate cavity, it locates outside the cavity as counteranion, and the two axial positions are occupied by a water molecule and an OH^- group, respectively (Figure 6b). The $Co \cdots Co$ separations in $[Co_2L^1(Cl)]^{3+}$, $[Co_2L^1(Br)]^{3+}$, and $[Co_2L^1(OH)(H_2O)]^{3+}$ are 4.866, 5.034, and 6.482(2), respectively.

Beside the encapsulation of halides, the dinuclear cryptate $[\text{Cu}_2\text{L}^1]^{4+}$ can also recognize linear anions. Ghosh and co-workers found that the cryptate $[\text{Cu}_2\text{L}^1]^{4+}$ can encapsulate linear anion of N_3^- to generate a Cu-NNN-Cu unit inside the cryptand cavity (Figure 6c), with the Cu...Cu separation of 6.188 Å.[38] The cryptate $[\text{Cu}_2\text{L}^1]^{4+}$ can also encapsulate linear CN⁻ anion inside its cavity to form a complex of $[\text{Cu}_2\text{L}^1(\text{CN})]^{3+}$ (Figure 6d), with the Cu...Cu separation of 5.177(1) Å.[39] The Cu...Cu separation is expanded to 11.305(6) Å in a dinuclear cryptate $[\text{Cu}_2\text{L}^{10}]^{4+}$ with long ellipsoidal cavity,[40] and this cryptate can recognize longer linear anion such as 1,4-benzenedicarboxylate, but not 1,3- and 1,2-benzenedicarboxylate.

It's interesting to note that $[\text{Cu}_2\text{L}^1]^{4+}$ can also bind imidazolate (im^-) anion within its cavity to form a sandwich-like dinuclear cryptate $[\text{Cu}_2\text{L}^1(\text{im})]^{3+}$ (Figure 6e).[41] The cryptate $[\text{Cu}_2\text{L}^1(\text{im})]^{3+}$ is stabilized by the strong $\pi\cdots\pi$ interactions between the imidazolate ring and two phenyl rings, with the distances of 3.21 and 3.24 Å, respectively (Figure 6f), as well as the strong $\text{CH}\cdots\pi$ interaction between the imidazolate ring with the third perpendicular phenyl ring, with the edge to face distance of only 3.38 Å.

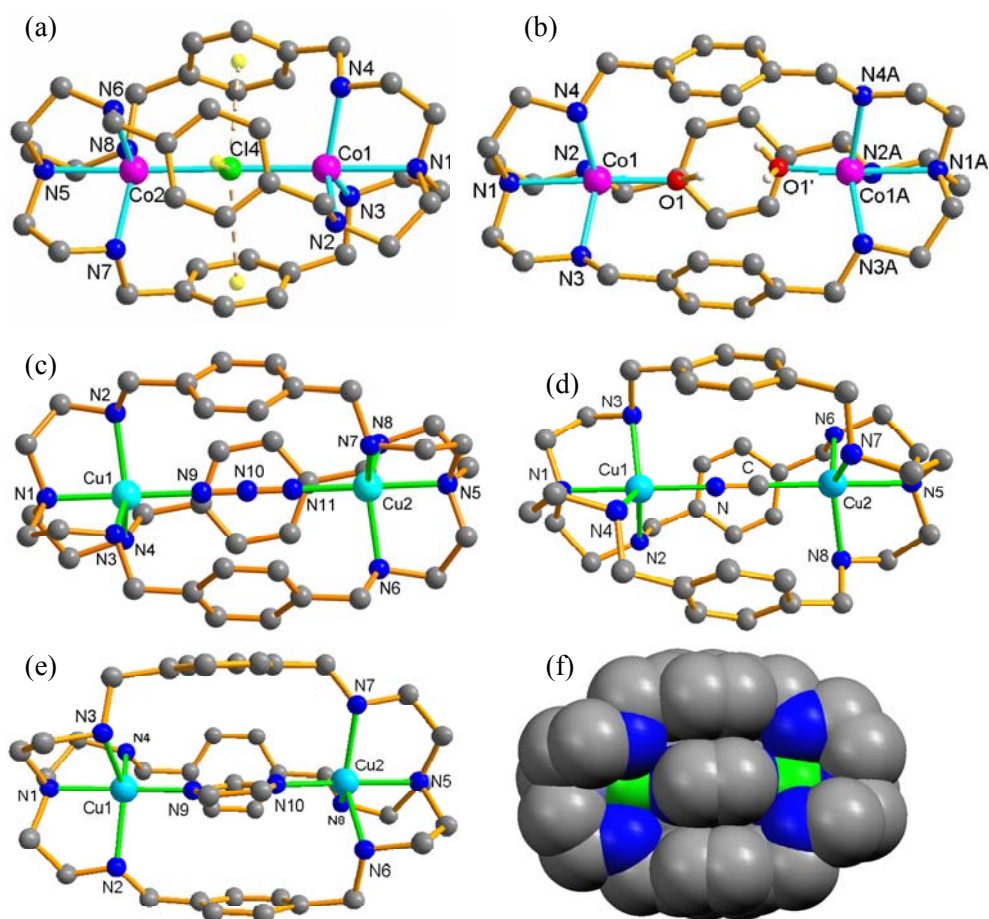


Figure 6. The structures of (a) $[\text{Co}_2\text{L}^1(\text{Cl})]^{3+}$, (b) $[\text{Co}_2\text{L}^1(\text{OH})(\text{H}_2\text{O})]^{3+}$ (c) $[\text{Cu}_2\text{L}^1(\text{N}_3)]^{3+}$, (d) $[\text{Cu}_2\text{L}^1(\text{CN})]^{3+}$, and (e) $[\text{Cu}_2\text{L}^1(\text{im})]^{3+}$. (f) The space filling mode of $[\text{Cu}_2\text{L}^1(\text{im})]^{3+}$.

It's also interesting to note that the chiral macrocyclic complex receptor can recognize the chiral substrate. For instance, the reaction of racemic $[\text{Ni}(\alpha\text{-rac-L}^{11})](\text{ClO}_4)_2$ with racemic $d\text{-Phe}^-$ generate a racemic mixture ($\text{Phe}^- = \text{phenylalanine anion}$), in which the SS and RR enantiomers in $[\text{Ni}(\alpha\text{-rac-L}^{11})]^{2+}$ recognize l - and $d\text{-Phe}^-$ respectively to give two monomers of $[\text{Ni}(SS\text{-L})(l\text{-Phe})]^+$ (Figure 7a) and $[\text{Ni}(RR\text{-L})(d\text{-Phe})]^+$ (Figure 7b).[42] All the $[\text{Ni}(SS\text{-L})(l\text{-Phe})]^+$ monomers are connected through the intermolecular hydrogen bonds to form a novel 1D right-handed homochiral helical chain of $\{[\text{Ni}(SS\text{-L})(l\text{-Phe})]\}_n^{n+}$ (Figure 7c), and all the $[\text{Ni}(RR\text{-L})(d\text{-Phe})]^+$ monomers are connected through the same intermolecular hydrogen bonds to form a 1D left-handed homochiral helical chain of $\{[\text{Ni}(RR\text{-L})(d\text{-Phe})]\}_n^{n+}$ (Figure 7d). The spontaneous resolution occurs during the reaction, in which each crystal crystallizes into enantiopure. More interestingly, The reaction of $[\text{Ni}(SS\text{-L})(d\text{-Phe})](\text{ClO}_4)$ with $[\text{Ni}(RR\text{-L})(l\text{-Phe})](\text{ClO}_4)$ also gives complexes of $[\text{Ni}(SS\text{-L})(l\text{-Phe})](\text{ClO}_4)$ with $[\text{Ni}(RR\text{-L})(d\text{-Phe})](\text{ClO}_4)$, in which the SS and RR enantiomers preferentially coordinate to l - and $d\text{-Phe}^-$ respectively, thus l - and $d\text{-Phe}^-$ anions in $[\text{Ni}(SS\text{-L})(d\text{-Phe})](\text{ClO}_4)$ and $[\text{Ni}(RR\text{-L})(l\text{-Phe})](\text{ClO}_4)$ are interchanged to form two stable enantiomers of $[\text{Ni}(SS\text{-L})(l\text{-Phe})](\text{ClO}_4)$ and $[\text{Ni}(RR\text{-L})(d\text{-Phe})](\text{ClO}_4)$.

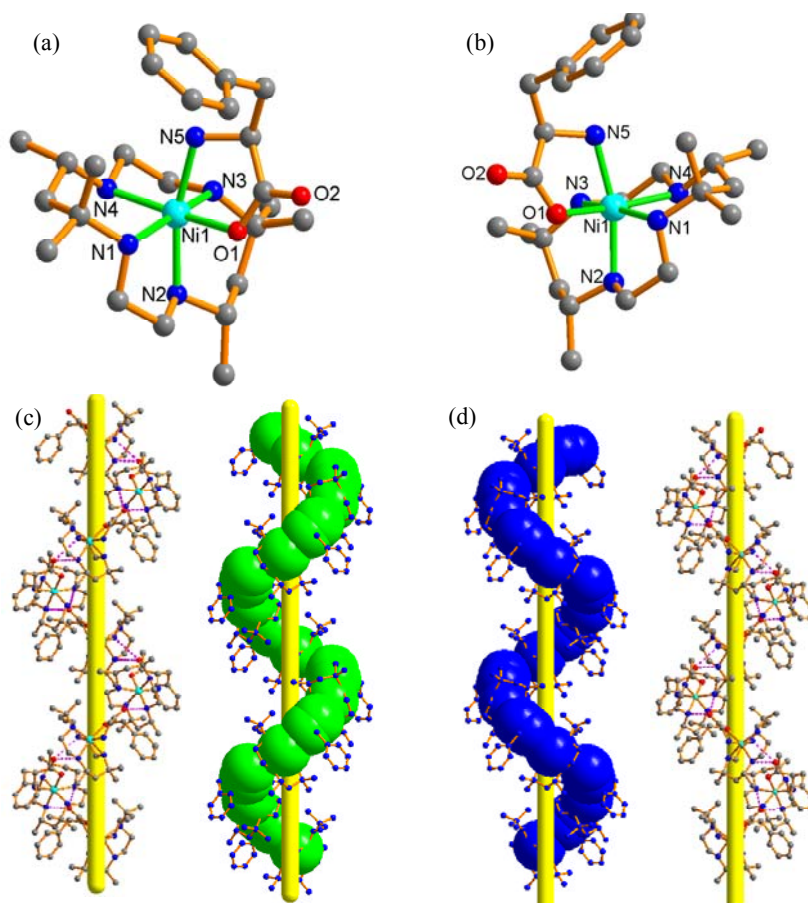
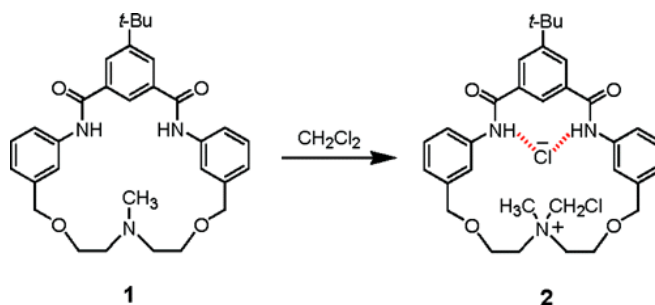


Figure 7. The structures of (a) $[\text{Ni}(SS\text{-L})(l\text{-Phe})]^+$ and (b) $[\text{Ni}(RR\text{-L})(d\text{-Phe})]^+$. (c) Side view of 1D hydrogen bonded right-handed helical chain of $\{[\text{Ni}(SS\text{-L})(l\text{-Phe})]\}_n^{n+}$, and (d) the 1D hydrogen bonded left-handed helical chain of $\{[\text{Ni}(RR\text{-L})(d\text{-Phe})]\}_n^{n+}$.



Scheme 2

THE ACTIVATION BY POLYAZA MACROCYCLIC LIGANDS AND THEIR COMPLEXES

Smith and co-workers found[43] that the polyaza macrocyclic ligand L^{12} (**1**) can cleavage the C-Cl bond of methylene chloride efficiently to generate the quaternary ammonium salt **2** (see Scheme 2). When methylene chloride is the solvent and the concentration of **1** is below 0.5 mM, the reaction exhibits ideal pseudo-first-order kinetics, with the second-order rate constant of $1.8 \times 10^{-4} \text{ M}^{-1} \text{ s}^{-1}$ at 298 K (determined by HPLC). The reaction half-life at 298 K is only 2.0 min, while the reaction half-life for acyclic amine L^{13} under identical conditions was determined to be 80 000 min, indicating that **1** reacts with methylene chloride about 50 000 times faster than structurally related L^{13} . The reaction is greatly inhibited by polar solvents such as methanol and DMSO. The results of detailed calculations using DFT and second-order Møller-Plesset demonstrate that the methylene chloride firstly encapsulate inside the cavity of **1** through the weak hydrogen bonding interactions between a chlorine atom of CH_2Cl_2 and the macrocyclic NH's, as well as two hydrogen atoms of CH_2Cl_2 and two macrocyclic ether oxygen atoms (Figure 8a), then the macrocyclic nitrogen attacks the electrophilic carbon of encapsulated CH_2Cl_2 through a transition state (Figure 8b) to generate the product of **2** (Figure 8c).

It's interesting to note that multinuclear metal complexes with chiral polyaza macrocyclic ligands exhibit the asymmetric catalytic properties. The dinuclear copper(II) complex with a chiral macrocyclic ligand L^{14} can enantioselectively catalyze the coupling reaction of 2-naphthol at 273 K in the presence of 10 mol% of catalyst in CCl_4 solution, with the yield of 79%, and the enantiomeric excess of 80%.[44] The trinuclear Zn(II) complex with a chiral macrocyclic ligand L^{15} also shows the high catalytic activity and enantioselectivity of asymmetric Aldol reaction in DMSO at room temperature, with the yield of 95% and the enantiomeric excess of 94% (see Scheme 3).[45]

Nelson and co-workers found[46] that the reactions of $\text{Cu}(\text{ClO}_4)_2$ with L^2 in water and $\text{CH}_3\text{OH}/\text{CH}_3\text{CN}$ gave the products of $[\text{Cu}_2\text{L}^2(\mu\text{-CO}_3)(\text{H}_3\text{O})]\text{Br}_3$ and $[\text{Cu}_2\text{L}^2(\mu\text{-O}_2\text{COCH}_3)](\text{ClO}_4)_3$, respectively. They presumed that the generation of $\text{O}_2\text{COCH}_3^-$ by $[\text{Cu}_2\text{L}^2]^{4+}$ in methanol may follow a mechanism of CO_2 insertion into the M-OCH₃ bond. If this mechanism is correct, the mononuclear complex $[\text{CuL}^{16}]^{2+}$ in methanol should easily generate the complex $[\text{CuL}^{16}(\text{O}_2\text{COCH}_3)]^+$. However, we found[47] that the corresponding mononuclear complexes $[\text{Cu}(\text{tren})(\text{H}_2\text{O})](\text{ClO}_4)_2$ and $[\text{CuL}^{16}(\text{H}_2\text{O})](\text{ClO}_4)_2$ in

CH₃OH/CH₃CN (1:1) do not generate the methylcarbonate species, even if NaOCH₃ is added and the solution is left under open atmospheric conditions for several days. This suggests that alkylcarbonate formation does not result from CO₂ insertion into the M-OCH₃ bond. Further investigation[47] on this reaction indicates that the cryptate [Cu₂L²]⁴⁺ can facilely absorb the atmospheric CO₂ even under acidic conditions to form μ-O₂COH⁻ bridged cryptate [Cu₂L²(μ-O₂COH)]³⁺, and it can be efficiently transformed to alkylcarbonate in alcohol solutions. The alkylcarbonate formation involves two step reactions (see Scheme 4): Firstly, the initial coordinated water molecule deprotonates, gives a species of [Cu₂(OH)L²]³⁺, and the OH⁻ attacks the carbon atom of CO₂ to form a μ-O₂COH⁻ bridged cryptate [Cu₂L²(μ-O₂COH)]³⁺. Secondly, the synchronous activation by two Cu(II) atoms onto a μ-O₂COH⁻ leads to increased positive charge on the carbon atom in the μ-O₂COH⁻ bridge, thus the electrophilic carbon atom of μ-O₂COH⁻ in [Cu₂L²(μ-O₂COH)]³⁺ is facilely attacked by the primary alcohols to form a tetrahedral intermediate, then it converts into μ-O₂COR⁻ bridged cryptate of [Cu₂L²(μ-O₂COR)]³⁺ by elimination of water. The μ-O₂COH⁻ formation is necessary for esterification.

Though L¹ and L² have similar structures, their dinuclear Cu(II) cryptates show different reactivity. As we mentioned before, the dinuclear complex [Cu₂L²]⁴⁺ dissolved in acetonitrile can easily take up atmospheric CO₂ in an open vessel to form a μ-O₂COH⁻ bridged cryptate of [Cu₂L¹(μ-O₂COH)]³⁺ within a few minutes. On the contrary, [Cu₂L¹]⁴⁺ does not take up atmospheric CO₂, but cleaves the C-C bond of acetonitrile at room temperature to produce a cyano-bridged dinuclear cryptate [Cu₂L¹(CN)]³⁺ and methanol, due to the strong recognition between the receptor and the substrate (cyanide anion).[48] The cleavage rate was determined spectrophotometrically in acetonitrile at 890 nm and 293 K, with the observed rate constant and half time of 1.52 × 10⁻⁴ s⁻¹ and 76 min, respectively. Further investigations[49] indicate the dinuclear zinc(II) cryptate [Zn₂L¹]⁴⁺ can also cleave the C-C bond of nitriles such as acetonitrile, propionitrile and benzonitrile at room temperature under open atmospheric conditions, resulting in the cyano-bridged cryptate [Zn₂L¹(CN)]³⁺ (Figure 9a) and methanol, ethanol and phenol, respectively. The cleavage rate was determined by measuring the concentration of formed methanol in acetonitrile solution at 293 K using GC measurements, with the observed rate constant and half time of 3.0 × 10⁻⁴ s⁻¹ and 39 min, respectively. This indicates the cleavage rate for [Zn₂L¹]⁴⁺ is faster than that of [Cu₂L¹]⁴⁺. The HPLC measurements indicate that the C-C bond cleavage of (*S*)-(+)-2-methylbutyronitrile by [Zn₂L¹]⁴⁺ produced (*R*)-(-)-2-butanol only, demonstrating that the cleavage reaction proceeds through an S_N2 pathway (Walden inversion). In this process (Scheme 5), the nitrogen atom of (*S*)-(+)-2-methylbutyronitrile binds to one Zn(II) atom in the [Zn₂L¹]⁴⁺ receptor through its electron pair, and the other Zn(II) atom possibly interacts with the filled π orbital of the *sp*-hybridized (*S*)-(+)-2-methylbutyronitrile carbon atom. This should result in electron flow from the π bond to the Zn(II) atom and increases the “leaving ability” of cyanide, thus the electrophilic alkyl carbon atom is attached by a water molecule through an S_N2 type process, resulting in an inversion of the configuration and producing (*R*)-(-)-2-butanol and a receptor-substrate complex of [Zn₂L¹(CN)]³⁺. It is interesting to note that [Cu₂L¹(OH)(OH₂)]³⁺, in which the two axial positions are occupied by H₂O and OH⁻, respectively (Figure 9b), do not cleave the C-C bond of acetonitrile at room temperature. This suggests that the empty axial positions for both Cu(II) and Zn(II) cryptates are necessary for the C-C bond cleavage of nitriles.

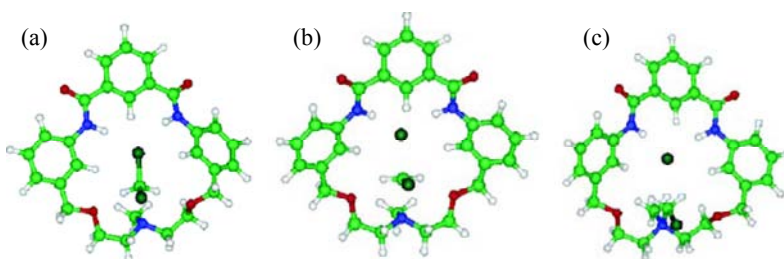
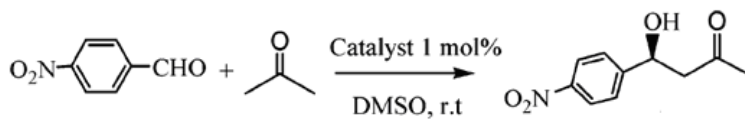
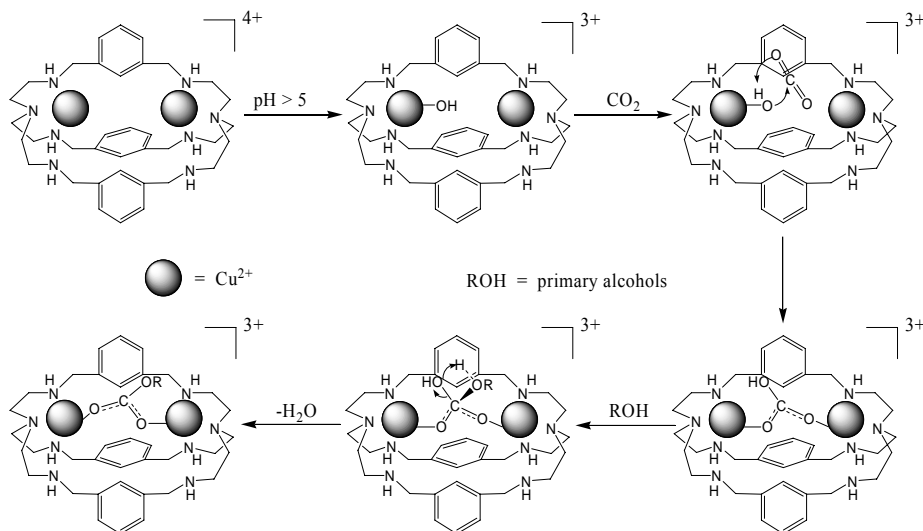


Figure 8. The calculated solution-state structures of (a) the pre-reaction complex, (b) the transition state, and (c) the product for the reaction of 1 (L^{12}) with methylene chloride.



Scheme 3.



Scheme 4

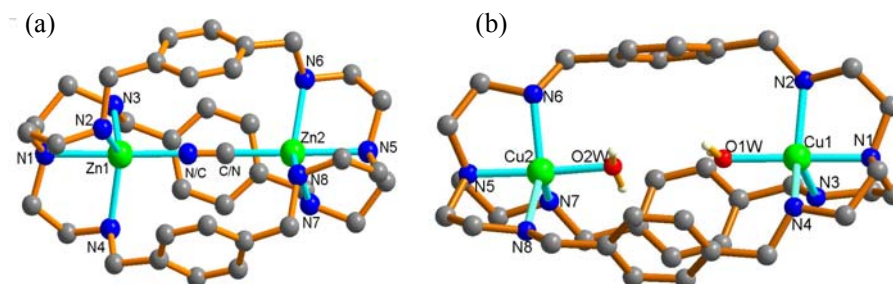
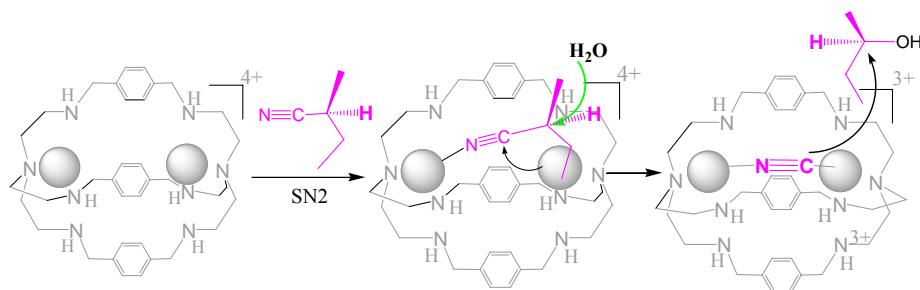


Figure 9. The structures of (a) $[Zn_2L^1(CN)]^{3+}$ and (b) $[Cu_2L^1(OH)(OH_2)]^{3+}$.



Scheme 5

ACKNOWLEDGMENTS

This work was supported by NSFC (20625103, 20831005, 20821001) and 973 Program of China (2007CB815305).

REFERENCES

- [1] Lehn, JM. Supramolecular chemistry-scope and perspectives molecules, supermolecules and molecular devices (Nobel lecture). *Angew. Chem. Int. Ed. Engl.*, 1988, 27, 89-112.
- [2] Pedersen, CJ. Cyclic polyethers and their complexes with metal salts. *J. Am. Chem. Soc.*, 1967, 89, 7017-7036.
- [3] McKee, V; Nelson, J; Town, RM. Caged oxoanions. *Chem. Soc. Rev.*, 2003, 32, 309-325.
- [4] Borman-James, K. Alfred Werner revisited: the coordination chemistry of anions. *Acc. Chem. Res.*, 2005, 38, 671-678.
- [5] Amendola, V; Bonizzoni, M; Esteban-Gómez, D; Fabbrizzi, L; Licchelli, M; Sancenón, F; Taglietti, A. Some guidelines for the design of anion receptors. *Coord. Chem. Rev.*, 2006, 250, 1451-1470.
- [6] Kang, SO; Hossain, MA; Bowman-James, K. Influence of dimensionality and charge on anion binding in amide-based macrocyclic receptors. *Coord. Chem. Rev.*, 2006, 250, 3038-3052.
- [7] Kang, SO; Begum, RA; Bowman-James, K. Amide-based ligands for anion coordination. *Angew. Chem. Int. Ed.*, 2006, 45, 7882-7894.
- [8] O'Neil, EJ; Smith, BD. Anion recognition using dimetallic coordination complexes. *Coord. Chem. Rev.*, 2006, 250, 3068-3080.
- [9] Wichmann, K; Antonioli, B; Söhnle, T; Wenzel, M; Gloe, K; Gole, K; Price, JR; Lindoy, LF; Blake, A; Schröder, M. Polyamine-based anion receptors: Extraction and structural studies. *Coord. Chem. Rev.*, 2006, 250, 2987-3003.
- [10] Vigato, PA; Tamburini, S; Bertolo, L. The development of compartmental macrocyclic Schiff bases and related polyamine derivatives. *Coord. Chem. Rev.*, 2007, 251, 1311-1492.
- [11] Hossain, MA; Morehouse, P; Powell, D; Bowman-James, K. Tritopic (cascade) and ditopic complexes of halides with an azacryptand. *Inorg. Chem.*, 2005, 44, 2143-2149.

- [12]Lakshminarayanan, PS; Kumar, DK; Ghosh, P. Counteranion-controlled water cluster recognition in a protonated octaamino cryptand. *Inorg. Chem.*, 2005, 44, 7540-7546.
- [13]Lakshminarayanan, PS; Ravikumar, I; Suresh, E; Ghosh, P. Molecular recognition studies of an octaaminocryptand upon different degree of protonation. *Cryst. Growth Des.*, 2008, 8, 2842-2852.
- [14]Ravikumar, I; Lakshminarayanan, PS; Suresh, E; Ghosh, P. Spherical versus linear anion encapsulation in the cavity of a protonated azacryptand. *Inorg. Chem.*, 2008, 47, 7992-7999.
- [15]Kang, SO; Powell, D; Day, VW; Bowman-James, K. Trapped bifluoride. *Angew. Chem. Int. Ed. Engl.*, 2006, 45, 1921-1925.
- [16]Kang, SO; Day, VW; Bowman-James, K. Cyclophane capsule motifs with side pockets. *Org. Lett.*, 2008, 10, 2677-2680.
- [17]Yang, LZ; Li, Y; Jiang, L; Feng, XL; Lu, TB. Size and temperature dependent encapsulation of tetrahedral anions by a protonated cryptand host. *CrystEngComm*, 2009, DOI, 10.1039/b904838c.
- [18]Kang, OS; Hossain, AM; Powell, D; Bowman-James, K. Encapsulated sulfates: insight to binding propensities. *Chem. Commun.*, 2005, 328-330.
- [19]Kang, OS; Llinares, JM; Powell, D; VanderVelde, D; Bowman-James, K. New polyamide cryptand for anion binding. *J. Am. Chem. Soc.*, 2003, 125, 10152-10153.
- [20]Kang, OS; VanderVelde, D; Powell, D; Bowman-James, K. Fluoride-facilitated Deuterium exchange from DMSO-*d*₆ to polyamide-based cryptands. *J. Am. Chem. Soc.*, 2004, 126, 12272-12273.
- [21]Kang, OS; Powell, D; Bowman-James, K. Anion binding motifs: topicity and charge in amidocryptands. *J. Am. Chem. Soc.*, 2005, 127, 13478-13479.
- [22]Arunachalam, M; Suresh, E; Ghosh, P. Hexabromide salt of a tiny octaazacryptand as a receptor for encapsulation of lower homolog halides: structural evidence on halide selectivity inside the tiny cage. *Tetrahedron*, 2007, 63, 11371-11376.
- [23]Zhang, BG; Cai, P; Duan, CY; Miao, R; Zhu, LG; Niitsu, T; Inoue, H. Imidazolidinium-based robust crypt with unique selectivity for fluoride anion. *Chem. Commun.*, 2004, 2206-2207.
- [24]Ilioudis, CA; Tocher, DA; Steed, JW. A highly efficient, preorganized macrobicyclic receptor for halides based on CH and NH...anion interactions. *J. Am. Chem. Soc.*, 2004, 126, 12395-12402.
- [25]Dietrich, B; Dilworth, B; Lehn, JM; Souchez, JP; Cesario, M; Guilhem, J; Pascard, C. Anion cryptates: synthesis, crystal structures, and complexation constants of fluoride and chloride inclusion complexes of polyammonium macrocyclic ligands. *Helv. Chim. Acta*, 1996, 79, 569-587.
- [26]Hossain, MA; Linares, JM; Miller, CA; Seib, L; Brown-James, K. Further insight to selectivity issues in halide binding in a tiny octaazacryptand. *Chem. Commun.*, 2000, 2269-2270.
- [27]Bernier, N; Carvalho, S; Li, F; Delgado, R; Félix, V. Anion recognition by a macrobicycle based on a tetraxadiaz macrocycle and an isophthalamide head unit. *J. Org. Chem.*, 2009, 74, 4819-4827.
- [28]Fowler, CJ; Haverlock, TJ; Moyer, BA; Shriver, JA; Gross, DE; Marquez, M; Sessler, JL; Hossain, MA; Brown-James, K. Enhanced anion exchange for selective sulfate extraction: overcoming the Hofmeister bias. *J. Am. Chem. Soc.*, 2008, 130, 14386-14387.

- [29] Gac, SL; Jabin, I. Synthesis and study of calix[6]cryptamides: a new class of heteroditopic receptors that display versatile host-guest properties toward neutral species and organic associated ion-pair salts. *Chem. Eur. J.*, 2008, 14, 548-557.
- [30] Hisaki, I; Sasaki, S; Hirose, K; Tobe, Y. Synthesis and anion-selective complexation of homobenzylic tripodal thiourea derivatives. *Eur. J. Org. Chem.*, 2008, 14, 548-557.
- [31] Ambrosi, G; Formica, M; Fusi, V; Giorgi, L; Guerri, A; Micheloni, M; Paoli, P; Pontellini, R; Rossi, P. A new macrocyclic cryptand with squaramide moieties: an overstructured Cu^{II} complex that selectively binds halides: synthesis, acid/base- and ligational behavior, and crystal structures. *Chem. Eur. J.*, 2007, 13, 702-712.
- [32] Kaewtong, C; Fuangswasdi, S; Muangsin, N; Chaichit, N; Vicens, J; Pulpoka, B. Novel C_{3v}-symmetrical N₇-hexahomotriazacalix[3]cryptand: a highly efficient receptor for halide anions. *Org. Lett.*, 2006, 8, 1561-1564.
- [33] Katayev, EA; Ustynyuk, YA; Sessler, JL. Receptors for tetrahedral oxyanions. *Coord. Chem. Rev.*, 2006, 250, 3004-3007.
- [34] Yang, LZ; Jiang, L; Feng, XL; Lu, TB. Unusual pH value dependent encapsulation and release of water-methanol binary guests by a cryptand host. *CrystEngComm*, 2008, 10, 649-651.
- [35] Ravikumar, I; Lakshminarayanan, PS; Suresh, E; Ghosh, P. Recognition of water-acetonitrile-water cluster in a tetraprotonated picrate salt of octaaminocryptand. *Cryst. Growth Des.*, 2006, 6, 2630-2633.
- [36] Li, Y; Jiang, L; Feng, XL; Lu, TB. Anion dependent water clusters encapsulated inside a cryptand cavity. *Cryst. Growth Des.*, 2008, 8, 3689-3694.
- [37] Chen, JM; Zhuang, XM; Yang, LZ; Jiang, L; Feng, XL; Lu, TB. Anion recognition of chloride and bromide by a rigid dicobalt(II) cryptate. *Inorg. Chem.*, 2008, 47, 3158-3165.
- [38] Ravikumar, I; Suresh, E; Ghosh, P. A perfect linear Cu-NNN-Cu unit inside the cryptand cavity and perchlorate entrapment within the channel formed by the cascade complex. *Inorg. Chem.*, 2006, 45, 10046-10048.
- [39] Bond, AD; Derossi, S; Harding, CJ; McInnes, EJJ; Mckee, V; McKenzie, CJ; Nelson, J; Wolowska, J. Cascade complexation: a single cyano bridge links a pair of Cu(II) cations. *Dalton Trans.*, 2005, 2403-2409.
- [40] Boiocchi, M; Bonizzoni, M; Fabbrizzi, L; Piovani, G; Taglietti, A. A dimetallic cage with a long ellipsoidal cavity for the fluorescent detection of dicarboxylate anions in water. *Angew. Chem. Int. Ed.*, 2004, 43, 3847-3852.
- [41] Zhuang, XM; Lu, TB; Chen, S. Cyanide and imidazolate bridged macrocyclic dinuclear Cu^{II} complexes: Synthesis, structure and magnetic properties. *Inorg. Chim. Acta*, 2005, 358, 2129-2134.
- [42] Ou, GC. Jiang, L; Feng, XL; Lu, TB. Spontaneous resolution of a racemic nickel(II) complex and helicity induction via hydrogen bonding: The effect of chiral building blocks on the helicity of one-dimensional chains. *Inorg. Chem.*, 2008, 47, 2710-2718.
- [43] Lee, JJ; Stanger, KJ; Noll, BC; Gonzalez, C; Marquez, M; Smith, BD. Rapid fixation of methylene chloride by a macrocyclic amine. *J. Am. Chem. Soc.*, 2005, 127, 4184-4185.
- [44] Gao, J; Reibenspies, JH; Martell, AE. Structurally defined catalysts for enantioselective oxidative coupling reactions. *Angew. Chem. Int. Ed.*, 2003, 42, 6008-6012.
- [45] Gao, J; Zingaro, RA; Reibenspies, JH; Martell, AE. Direct observation of enantioselective synergism at trimetallic centers. *Org. Lett.*, 2004, 6, 2453-2455.

-
- [46]Dussart, Y; Harding, C; Dalgaard, P; Mckenzie, C; Kadirvelraj, R; McKee, V; Nelson, J. Cascade chemistry in azacryptand cages: bridging carbonates and methylcarbonates. *J. Chem. Soc., Dalton Trans.*, 2002, 1704-1713.
- [47]Chen, JM; Wei, W; Feng, XL; Lu, TB. CO₂ fixation and transformation by a dinuclear copper cryptate under acidic conditions. *Chem. Asian J.*, 2007, 2, 710-719.
- [48]Lu, TB; Zhuang, XM; Li, YW; Chen, S. C-C bond cleavage of acetonitrile by a dinuclear copper(II) cryptate. *J. Am. Chem. Soc.*, 2004, 126, 4760-4761.
- [49]Yang, LZ; Li, Y; Zhuang, XM; Jiang, L; Chen, JM; Luck, RL; Lu, TB. Mechanistic studies of C-C bond cleavage of nitriles by dinuclear metal cryptates. *Chem. Eur. J.*, 2009, in press.

*Chapter 15***NEW THERAPEUTICALLY AGENT WITH INCREASED
ANTIFUNGAL ACTIVITY**

***Mariana Spulber¹, Mariana Pinteala¹, Adrian Fifere¹,
Valeria Harabagiu¹ and Bogdan C Simionescu^{1,2}***

¹Petru Poni Institute of Macromolecular Chemistry, Iasi.

²The Gh Asachi Technical University, Iasi.

ABSTRACT

The effect of various native cyclodextrins and hydroxy propyl- β -cyclodextrin onto flucytosine water solubility has been investigated in phosphate buffer aqueous solution of the same pH value (7.0-7.2) and 37° C, corresponding to human body normal conditions, using Higuchi and Connors phase solubility method. The cyclodextrins increase the drug solubility, making drug molecules more available for cell metabolism; the complexation stoichiometry is obtained by using two different methods (the phase solubility and Rose-Drago method). The enhancement of the solubility and the characteristics of the obtained phase diagram recommend the analyzed cyclodextrins as useful therapeutic agents promoters for sulconazole nitrate in conditions mimic to those characteristic for human bodies. The best results were obtained for hydroxypropyl β -cyclodextrin and β -cyclodextrin, that is why the flucytosine- β -cyclodextrin and hydroxypropyl β -cyclodextrin water soluble inclusion complex were used for further studies. The formation of inclusion complex between β -cyclodextrins and flucytosine has been studied and fully described in our previous work [1]. In this paper we are describing also, the results obtained concerning the antifungal activity of this new compounds. As expected the new inclusion complexes presents an important increase of the antifungal activity, illustrated by the reduction of the minimal inhibitory concentrations for 50 % and 90 % of the tested strains decreased. Also, the acute toxicity of the flucytosine - β cyclodextrin and hydroxypropyl β cyclodextrin complex is smaller comparing with the pure drug, analyzed alone. These results recommend the described conjugates as future promising therapeutic agents.

INTRODUCTION

In the last decades, because the range of clinically important fungi has broadened, and the number of immunosuppressed patients increased the prevalence of resistance to antifungal agents is increasing [2]. In this context the interest in developing new antifungal agents or reducing the dosage, with the resistance reducing has continuously increased.

Cyclodextrins (CDs), with lipophilic inner cavities and hydrophilic outer surfaces, are molecules known for being capable of interacting with a large variety of guest molecules to form noncovalent inclusion complexes (Figure 1). Cyclodextrins comprise a family of three wellknown industrially produced major, and several rare, minor cyclic oligosaccharides. The three major cyclodextrins are crystalline, homogeneous, nonhygroscopic substances, which are torus-like macro-rings built up from glucopyranose units. The α -cyclodextrin (cyclomaltohexaose, cyclohexaglucan, cyclohexaamylose, α -CD, ACD, C₆A) comprises six glucopyranose units, β -CD (cyclomaltoheptaose, cycloheptaglucan, cycloheptaamylose, β -CD, BCD, C₇A) comprises seven such units, and γ -CD (cyclooctaglucan, cyclooctaamylose, δ -CD, GCD, C₈A) comprises eight such units (Figure 1).

Cyclodextrins (CDs) are capable of interacting with a large variety of guest molecules to form noncovalent inclusion complexes. In an aqueous solution, the slightly apolar cyclodextrin cavity is occupied by water molecules which are energetically unfavored (polar-apolar interaction), and therefore can be readily substituted by appropriate “guest molecules” which are less polar than water. The dissolved cyclodextrin is the “host” molecule, and the “driving force” of the complex formation is the substitution of the water molecules by an appropriate “guest” molecule. One, two, or three cyclodextrin molecules contain one or more entrapped “guest” molecules [5-9].

Complexation process with native or modified CDs increases guest solubility and stability against the effects of light, heat, and oxidation. The most common application of CDs in the pharmaceutical industry is to enhance the solubility, the dissolution rate, and the bioavailability of poorly water-soluble drugs [4]. That is why a large variety of drugs encapsulated through noncovalent interactions into unmodified or modified cavity are described in the literature [6, 7, 10]. The protective role played by CD molecules has been intensively described in the literature protects the host molecules from reactive oxygen species. On the other hand, complexation with CD results in considerable decrease in antioxidant ability of the included host molecules [11-17].

Flucytosine (5-FC), a fluorinated analogue of cytosine, the oldest synthetic antifungal agents, received a special attention in the last years, because of increasingly usage in combination with a number of antifungal agents for lethal invasive mycosis treatment and alone as a possible new therapeutic for colorectal carcinoma [18]. 5-FC usage is limited by its major side effects including hepatotoxicity, causing severe liver necrosis [19] and bone-marrow depression inducing life-threatening leucycytopenia, thrombocytopenia, and pancytopenia [20].

Complexation of 5-FC with cyclodextrin offers the possibility to improve the aqueous solubility of 5-FC, without modifying the drug original structure, increasing 5-FC bioavailability, and reducing its toxicity [5-8].

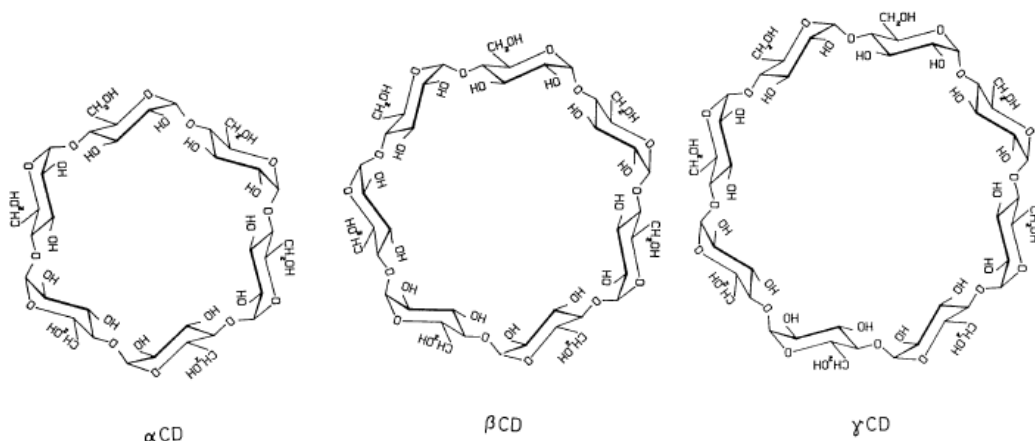


Figure 1. Chemical structure of α , β and γ cyclodextrin [3].

Cyclodextrins (CDs) act as host molecules to form inclusion complexes rather nonspecifically with a wide variety of guest molecules. The hydrophobic cavity of native cyclodextrins and their derivatives is capable of binding guest molecules of the appropriate size and shape. Complexation of guest compounds with cyclodextrins can alter guest solubility, increase stability against the effects of light, heat, and oxidation, mask unwanted physiological effects, and reduce volatility [21].

Due to its molecular structure 5-FC is a suitable guest for the cyclodextrins' macrocycle. The effectiveness of solubilization of a sparingly soluble hydrophobic compound in aqueous medium by means of its guest-host inclusion complexation with cyclodextrins depends mainly on the respective cyclodextrin and of the formed inclusion complex and on the stoichiometry and the equilibrium binding constant of the complex formed in aqueous solution [22, 23].

We have therefore collected the data for a comparative study of the water solubility enhancement of the inclusion complexes between 4 different hosts as α -, β -, γ - and hydroxypropyl- β -cyclodextrin (α -, β -, γ -, and HP β -CD) and 5-FC [5-8]. Binding constants were measured spectrophotometrically at the maximum wavelength absorption of the pure and complexed guest, in phosphate buffer aqueous solutions at pH value 7.0-7.2. Such value was chosen in order to avoid acid catalyzed hydrolysis of the host, and is similar to living bodies' conditions [24-26].

We also synthesized cyclodextrin-5-FC inclusion complexes, in order to increase the bioavailability of 5-FC, with the consequent reduction of the dosage, the treatment period and the gravity of all possible side effects [5-8]. These new complexes were tested from antifungal activity efficiency point of view, in order to evaluate their potential applications as therapeutic agents.

MATERIALS AND METHODS

1. Materials

α -, β -, γ -CD (Aldrich), HP β -CD (Cyclolab) and 5-FC (Fluka) were used as received. Stock phosphate buffer solutions were prepared according to the literature reports [24] and used within few days, after checking the real pH value with a Titroline Titrimeter. Freshly double distilled decarbonated water was used for the preparation of the buffers, which were used as solvents for the preparation of the measurement of the binding constants.

2. Methods

2.1. UV visible spectroscopy studies were performed on a Specord 200 Analytik Jena 200 spectrophotometer. To reach the thermal equilibrium the samples were maintained at 37°C for 1 hour under stirring before the experiment.

2.2. Solubility studies

Solubility studies were carried out according to the Higuchi and Connors method [25]. α -, β -, γ -CD and HP β -CD solutions of different concentrations ranging between 0.5 and 40 10^{-1} M were added to a supersaturated solution of 5-FC in equal volumes and shaken at $37 \pm 1^\circ\text{C}$ for 24 hours or more, until the solution becomes clear. After reaching equilibrium, the solutions were filtered. The concentration of 5-FC in the filtrate was determined spectrophotometrically, considering the absorbance at the maximum absorption wavelength nm with reference to a suitably constructed standard curve, after 1/100 dilution (Figure 1).

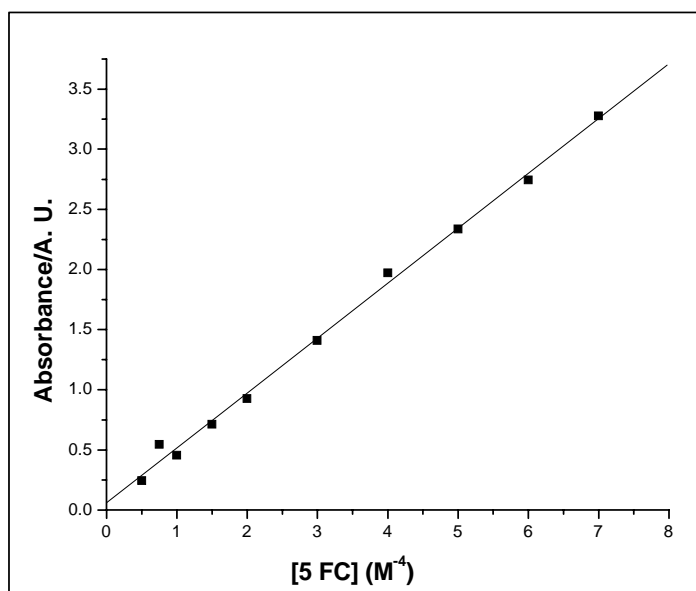


Figure 1. 5-FC calibration curve.

2.3. Determination of the stoichiometry by Rose-Drago method

The binding constants were determined by using two solution of the same molarity of guest (5-FC) and host (α -, β -, γ -CD, HP β -CD) (0.5×10^{-4} M) which were mixed in different proportions in order to obtain various solutions with the same total concentration and different ratio between host and guest. In the mixed solutions, the host concentration varied from 4×10^{-6} to $2,88 \times 10^{-5}$ M. ϵ C was determined using inclusions complexes obtained by coprecipitation. The binding constants values were determined using these solutions according with the method described in the literature [25].

2.4. Preparation of the solid complex

The inclusion complexes (C) were prepared by freeze drying method. An aqueous solution containing 5-FC and β -CD, or HP β -CD in a 1:1 molar ratio was frozen by immersion in liquid nitrogen and freeze-dried in a Martin Christ, ALPHA 1-2LD Freeze-Dryer. The aqueous solution was obtained by dissolving 7.74×10^{-4} mol 5-FC and 7.74×10^{-4} mol cyclodextrin in 25 ml distilled water and stirring it at room temperature for 48 h.

2.5. Pharmacological studies

2.5.1. Anti-fungal activity studies

Antifungal activity studies were performed on 32 yeast strains belonging to *Candida* genus, isolated from fungemia episodes from patients hospitalized in Iasi, using the testing method M27-A2 recommended by CLSI (NCCLS) to evaluate the antifungal susceptibility of the yeasts [27].

The yeast strain subcultures were obtained by incubating the initial strains at 35°C for 48 hours. Yeast strain inocula were obtained using stock cultures, by the suspension of five colonies of approximately 1 mm in diameter in saline solution. Pure 5-FC, β -CD-5-FC and HP β -CD-5-FC inclusion complexes solutions (3.2 (pure 5-FC) and (3.2 (complexed SULC) micromoles/ml, containing 3.2 micromoles active substance) in DMSO were diluted to the final concentrations (32; 16; 8; 4; 2; 1; 0.5; 0.125; and 0.0625 microg/ml) in DMSO and each solution was inoculated on the yeast strain inoculum. Suspension density adjustment was performed spectrophotometrically, so that the absorbance of each suspension to correspond to that produced by McFarland standard 0.5 at 530 nm. The final density of the suspensions varied from 1×10^6 to 2.5×10^6 . These suspensions were diluted 1:100 with sterile saline solution and 1:20 in RPMI 1640-MOPS, so that the final cell density to vary from 0.5×10^3 to 2.5×10^3 . The witness suspension was obtain by adding 900 microl yeast inoculum to 100 microl RPMI 1640-MOPS DMSO 1:10 dilution. The growth was evaluated by comparing the turbidity from each vial containing the antifungal agent to the turbidity of a 1:4 dilution in RPMI of the witness. Minimal inhibitory concentrations (MIC) were calculated as the minimal antifungal agent concentration that caused 50 % and 90% (MIC90 and MIC50) growth inhibition.

The best results were obtained on *C. Krusei* and *C. norvegensis*, isolated from fungemia episodes obtained from Cantacuzino Institute, Bucharest.

2.5.2. Acute toxicity studies

Acute toxicity studies were performed on laboratory mice, on nulliparous and nonpregnant healthy young females with age between 8 and 12 weeks old, and weight around

20±0.2 g. The animals were housed individually, respecting the same microclimate (temperature around 22°±3°C, the relative humidity 55% and an alternation 12 hours artificial light, 12 hours darkness) and feeding conditions. The animals were randomly selected, marked to permit individual identification, and kept in their cages for at least 5 days prior to dosing, in order to allow the acclimatization to the laboratory conditions. The administration of the pure and complexed 5-FC was made in a constant volume of 2 ml/100 g body weight in aqueous solutions [28]. The dose volume was administered by gavage using a stomach tube. The experiments were performed on Wistar SD1 NRM1 White/C57Bi6 mice, offered by the Cantacuzino Institute, Bucharest.

The acute toxicity (LD50) was established using the Dixon and Mood method [29, 30].

RESULTS AND DISCUSSIONS

1. Phase Solubility Behavior

As described in the literature the solubility of 5-FC in water is low, being equal to 10.5 g.L⁻¹ at 25°C, as already reported [31]. In Figure 2 it is shown the solubility curve obtained for 5-FC in presence of α -, β -, γ - and HP β -CD (Figure 2) in distilled water.

5-FC water solubility in phosphate buffer aqueous solutions presents a linear rapid increase with increasing CD concentration for all studied systems, corresponding to 1/1, 1/1.5 5-FC/CD molar ratio. This particular behavior indicates that the 5-FC water solubility enhancement depends dramatically of CD concentration until and after the complexation stoichiometry is reached. The obtained curves can be classified, in general, as type AL (linear isotherms), as described in literature [25]. An increase of 5-FC solubility between 47 for HP β -CD and 37 times for β -CD and just 1.5 fold for γ -CD was obtained. These results were extremely encouraging, especially toward the usage of the β -CD and HP β -CD for formulations with 5-FC.

Supposing a 1:1 stoichiometric ratio between components the apparent solubility constant, K1:1, was calculated from the slope of the linear portion of the curve, according to Equation 1 [25]:

$$K1:1 = \frac{Slope}{S_0 \cdot (1 - Slope)} \quad (\text{Eq 1})$$

where: S_0 is the solubility of 5-FC in the absence of CDs and

Slope is the experimental slope of the obtained curves.

The obtained results are summarized in Table 1

Table 1. The slopes and K1:1 values obtained for the inclusion complexes.

Complex	α -CD-5-FC	β -CD-5-FC	γ -CD-5-FC	HP β -CD-5-FC
Slope	0.34	0.85	0.04	0.92
K1:1	0.6 M ⁻¹	7 M ⁻¹	0.05 M ⁻¹	38 M ⁻¹

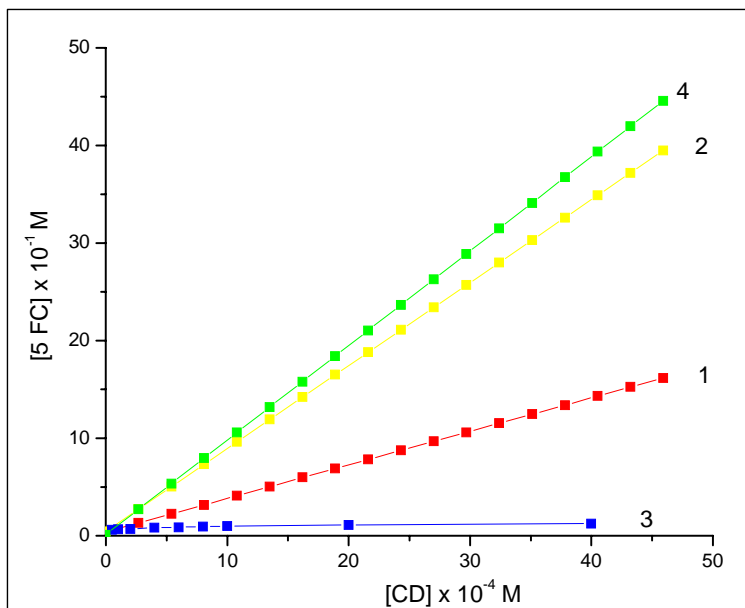


Figure 2. Phase solubility diagrams for 5-FC in presence of α -CD (1), β -CD (2), γ -CD (3), HP β -CD (4).

The values of solubility were found between 0.05 M^{-1} and 38 M^{-1} in the following series: γ CD < α -CD < β -CD < HP β -CD. All the obtained values are not so high indicated that the dissociation rate is high enough to ensure a fast release and entrance of the 5-FC at the level a cell membrane. The solubility of the 5-FC increases in all above-mentioned systems, in normal physiological conditions, the apparent solubility constants are higher enough to ensure the usage of all analyzed cyclodextrins for complexation with 5-FC.

As seen from the presented data solubility of the tested drug increases more for the β -CD and HP β -CD, the obtained values recommend these 2 systems for future analysis.

2. Rose-Drago Method

Plotting the values of $A_{\text{obs}} - A_{\text{guest}}$ as a function of $\frac{[H]_t}{[H]_t + [G]_t}$ complex concentrations (modified Job's plot) [26] could be estimated the stoichiometry of the complexation process for all the cyclodextrins used in these experiments (Figure 3).

From Figure 3 it can be seen that the maximum X of the four curves obtained for the four described cyclodextrins is around 0.5- 0.55, these values indicate that the stoichiometry for the inclusion phenomena is 1:1, as described in the literature [24]. This obtained values are in accord with those provided by the analysis of phase solubility diagrams of the analyzed cyclodextrins and 5-FC.

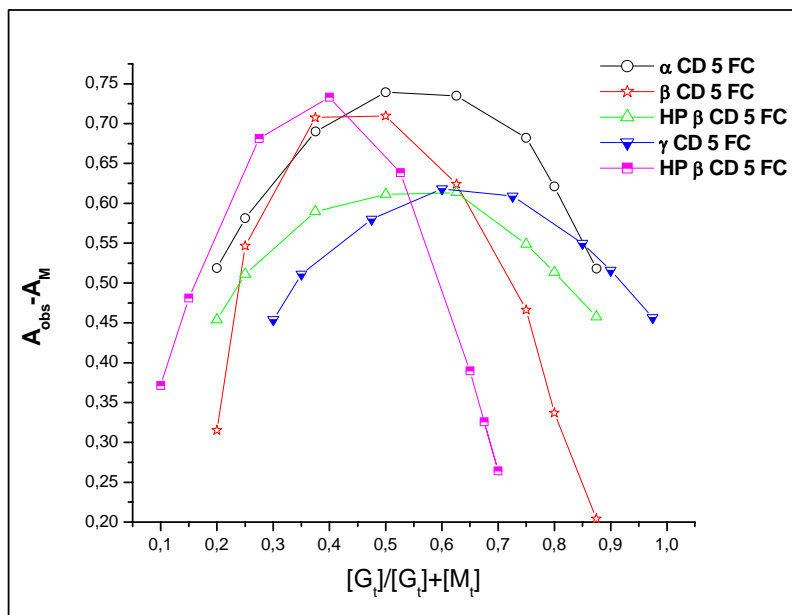


Figure 3. Modified Job's plot for the systems CD 5-FC

3. In Vitro Antifungal Activity Studies

As already described in a previous paper, the inclusion complex obtained by freeze drying between 5-FC and β -CD or HP β -CD were characterized and it was proved their formation [6, 7]. The authors observed an improving of the dissolution rate of the pure drug after complexation, making the new obtained compound a proper candidate for therapy. All the results can be summarized in Table 2 and 3 and Figure 4.

The data presented in Table 2 indicate that 5-FC is efficient in antifungal treatments, the growth inhibition is 100% for different *Candida* strains tested in our experiment. The determined sensibility rate was 93.73 % for all analyzed stains, the best results are obtained for two strains (*C. krusei* and *C. norvegensis*) known to behave as resistant fungi. As an example we present the microscopic images of the culture of *Candida albicans* on the culture media in the absence and presence of the 5-FC in concentration of 0.032 micromoles/ml.

The percentage variability of the inactivated strains depends in 89.57 % proportion on 5-FC concentration, the multiple correlation coefficient having the value $R^2 = 0.8957$. The regression of the inactivated strains depending on the antifungal substance concentration has the following equation: $y = 0.4068 \ln(x) + 0.1749$.

From Table 3 one can see that the inclusion complexes β -CD-5-FC and HP β -CD-5-FC present an higher antifungal activity comparing with the free drug, due to the increase of the hydro solubility of the complex comparing with the pure 5-FC. It can be observed that MIC 50 is reduced 2 times and 6 times for the inclusion complexes of 5-FC with β -CD and HP- β -CD. Also, MIC90 is reduced four and respectively, eight times for the complexed 5-FC with β -CD and HP β -CD, comparing with the free drug alone, indicating also the possible reduction of the treatment dosage and of the gravity of all side effects in case of using these

compounds for mycosis treatment. These results are also sustained by the microscopic images of the culture of *Candida albicans* on the culture media in the absence and presence of 5-FC, β -CD-5-FC and HP β -CD-5-FC in concentration of 0.032, 0.008 and 0.0076 micromoles 5-FC /ml. The growth inhibition is clear in the four images, sustained by the reduction of the fungal cells density on the culture media (Figure 4).

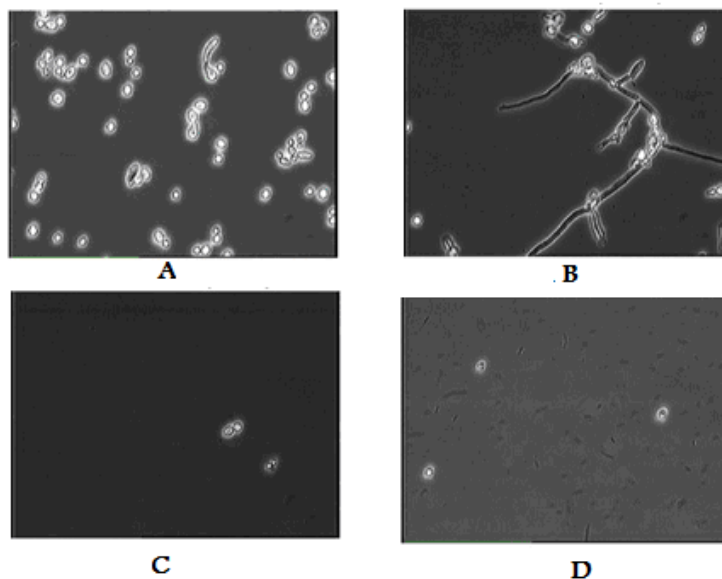


Figure 4. *Candida albicans* cultures- witness at 35⁰C (A), in the presence of 5-FC (0.0032 mmol/ml) (B), in the presence of β -CD-5-FC (0.008 mmol/ml) (C), and HP β -CD-5-FC (0.0076 mmol/ml).

Table 2. The frequency of MIC of 5-FC for the 32 tested strains.

Concentration of 5-FC (microg/ml)	0,5	1	2	4	8	16	32	64
Absolute frequency (<i>n</i>)	19	5	2	0	3	1	1	1
Cumulative frequency (%)	59.37	75.00	81.25	81.25	90.62	93.75	96.87	100

Table 3. In vitro susceptibility of the analyzed 32 strains at pure and complexed 5-FC (the synthesis of the data).

Antifungal agent	Concentration (micromol/ml)	Geometric average (micromol/ml)	CMI50 (micromol/ml)	CMI90 (micromol/ml)
5-FC	0.0005-0.032	0.0001163	0.0005	0.0008
5-FC β CD	0.00025-0.008	0.0000262	0.00025	0.0002
5-FC HP β CD	0.0002-0.0076	0.0000245	0.000083	0.0001

5-FC is efficient in the treatment of the *Candida* species in concentrations higher than 32 microg/ml (0.032 micromoles/ml)

The minimal inhibitory concentration of the antifungal agent required for growth inhibition is reduced in the presence of the cyclodextrin.

The performed tests proved that there are significant differences between the antifungal effect of the native substance and of the complexed substance. The improvement of *in vitro* antifungal effect of complexed 5-FC, characterized by the decrease of the active concentrations necessary to inactivate the yeasts and also by the decrease of the minimal inhibitory concentrations for 50 % and 90 % of the strains, can be observed.

4. Acute Toxicity Studies

The acute toxicity studies data show, that the acute toxicity of the β -CD-5-FC and HP β -CD-5-FC inclusion complex is smaller, comparing with the free 5-FC, analyzed separately. The oral LD50 for the β -CD-5-FC lyophilized complex is 1.4, and respectively 1.55 micromole 5-FC/kg body weight, higher than the value of LD50 obtained for free 5-FC 1.25 micromole/kg body weight.

The inclusion complex showed an improved bioavailability, and a reduction of the toxicity comparing with the pure SULC, aspect sustained by the absence of any hepatic, hematological and/or renal anomalies at 1.4 and 1.55 micromole 5-FC complexed/kg body weight.

CONCLUSION

From the solubility studies is easy to analyze the effect induced by the presence of cyclodextrins on the solubility of the 5-FC in water, the solubility rises up to 47 times, the effect being maxim for β -CD and HP β -CD, which forms the most stable complexes with 5-FC. The phase diagrams obtained for all native cyclodextrin and derivative indicate a 1:1 complexation, sustained by Rose Drago method. Considering all the serious side effects induced by 5-FC administration, the complexation with the cyclodextrins seems a useful method to increase the safety of drug administration.

Inclusion complex of flucytosine and β -CD, or HP β -CD was prepared by freeze-drying method in a molar ratio 1:1. The inclusion efficacy was confirmed by all the data already described in the literature [5-8]. Complexation by inclusion increases flucytosine solubility and dissolution in water for the two analyzed cyclodextrins, due to the low crystallinity of the complex. Due to this aspect, cyclodextrin based supramolecular systems represent an interesting formulation platform for delivery of drugs with poor physicochemical and biopharmaceutical properties.

The inclusion complex shows an acute toxicity smaller than the pure drug, oral 1.4 and 1.5 micromole 5 FC complexed/kg body weight, due to higher solubility and bioavailability of the complexed drug. Also, the *in vitro* antifungal activity of the complexed drug is higher (MIC50 is half and MIC90 is four time smaller), than of the pure biological active compound.

The increase of the bioavailability of the drug in β -CD and HP β -CD-5-FC inclusion complexes, combined with the decrease of the active dose and of the toxic effects proves the efficacy of the therapeutic usage of these inclusion complexes.

REFERENCES

- [1] Spulber, M; Pinteala, M; Fifere, A; Harabagiu, V; Simionescu, BC. *J Incl Phenom Macrocycl Chem.*, 2008, 62, 117-125.
- [2] Vermes, A; Guchelaar, AJ; Dankert, J. *Journal of Antimicrobial Chemotherapy*, 2000, 46, 171-179.
- [3] Rajeswari, C; Alka, A; Javed, A; Khar, RK. *AAPS PharmSciTech*, 2005, 6, 329-357.
- [4] Szejtli, J. *Chem. Rev.*, 1998, 98, 1743-1753.
- [5] Spulber, M; Pinteala, M; Harabagiu, V; Simionescu, BC. *J Incl Phenom Macrocycl Chem.*, 2008, 61, 41-51.
- [6] Spulber, M; Pinteala, M; Fifere, A; Moldoveanu, C; Mangalagiu, I; Harabagiu, V; Simionescu, BC. *J Incl Phenom Macrocycl Chem.*, 2008, 62, 135-142.
- [7] Spulber, M; Pinteala, M; Fifere, A; Harabagiu, V; Simionescu, BC. *J Incl Phenom Macrocycl Chem.*, 2008, 62, 117-125.
- [8] Miron, L; Mares, M; Nastasa, V; Spulber, M; Pinteala, M; Fifere, A; Harabagiu, V; Simionescu, B.C. *J Incl Phenom Macrocycl Chem.*, 2009, 63, 159-162.
- [9] Fifere, A; Budtova, T; Tarabukina, E; Pinteala, M; Spulber, M; Peptu, C; Harabagiu, V; Simionescu, B.C. *J Incl Phenom Macrocycl Chem.*, DOI: 10.1007/s10847-009-9539-4.
- [10] Loftsson, T; Brewster, ME. *J Pharm Sci*, 1996, 85, 1017-1025.
- [11] Polyakov, N; Leshina, TV; Konovalova, TA; Hand, EO; Kispert, LD. *Free Radical Biol. Med.*, 2004, 36, 872-880.
- [12] Lyng, SMO; Passos, M; Fontana, JD. *Process Biochemistry.*, 2005, 40, 865-872.
- [13] Ionita, G; Ionita, P; Sahini, VE; Luca, C. *Journal of Inclusion Phenomena and Macrocyclic Chemistry*, 2001, 39, 269-271.
- [14] Damiani, E; Tursilli, R; Casolari, A; Astolfi, P; Greci, L; Scalia, S. *Free Radical Research.*, 2005, 39, 41-49.
- [15] Tursilli, R; Casolari, A; Iannuccelli, V; Scalia, S. *Journal of Pharmaceutical and Biomedical Analysis*, 2006, 40, 910-914.
- [16] Simeoni, S; Scalia, S; Benson, HAE *International Journal of Pharmaceutics*, 2004, 280, 163-171.
- [17] Godwin, DA; Wiley, CJ; Felton, LA. *European Journal of Pharmaceutics and Biopharmaceutics*, 2006, 62, 85-93.
- [18] Francis, P; Walsh, TJ. *Clinical Infectious Diseases*, 1992, 15, 1003-1018.
- [19] Scholer, HJ. Flucytosine. In: Speller ED, Wiley Chichester Eds, *Antifungal Chemotherapy*, 1997, 35-106.
- [20] Viviani, MA. *Journal of Antimicrobial Chemotherapy*, 1995, 35, 241-244.
- [21] Hedges, AR. *Chem. Rev.*, 1998, 98, 2035-2044.
- [22] Stoescu, V. Bazele farmacologice ale practicii medicale. Editura Medicala- Bucuresti, Ed. a 7-a, rev. si compl, 2001.
- [23] Kopecky, F; Kopecka, B; Kaclik, P. *Journal of Inclusion Phenomena and Macrocyclic Chemistry*, 2001, 39, 215-217.
- [24] D'Anna, F; Lo Meo, P; Riela, S; Gruttadauria, M; Noto, R. *Tetrahedron.*, 2001, 57, 6823-27.
- [25] Higuchi, T; Connors, KA. *Adva. Anal. Chem. Instr.*, 1965, 4, 212-7.

- [26] Hirose, K. *Journal of Inclusion Phenomena and Macrocyclic Chemistry*, 2001, 39, 193-209.
- [27] National Committee for Clinical Laboratory Standards. Reference method for broth dilution antifungal susceptibility testing of yeasts. Approved standard, 2nd ed. M27-A2. National Committee for Clinical Laboratory Standards, Wayne, Pa, 2002.
- [28] Dixon, WJ; Mood, AM. . *J Amer. Statist Assoc*, 1948, 43, 109-126.
- [29] OECD Guidance Document on Acute Oral Toxicity. Environmental Health and Safety Monograph Series on Testing and Assessment No. 24, 2000.
- [30] OECD Guidance document on the Recognition, Assessment and use Clinical Signs as Humane Endpoints for Experimental Animals Used in Safety Evaluation. Environmental Health and Safety Monograph Series on Testing and Assessment No 19, 2000.
- [31] Polak, A; Grensén, M. *European Journal of Biochemistry*, 1973, 32, 276-282.

Chapter 16

FOOD ANTIOXIDANTS CYCLODEXTRIN INCLUSION COMPOUNDS: MOLECULAR SPECTROSCOPIC STUDIES AND MOLECULAR MODELLING

Aida Moreira da Silva^{1,2*}

¹College of Agriculture of Coimbra, Department of Food Science and Technology,
Bencanta, P-3040-316 Coimbra, Portugal.

²Research Unit Molecular Physical-Chemistry, University of Coimbra,
3000-535 Coimbra, Portugal.

ABSTRACT

Certain plant-derived foods are rich in chlorogenic, caffeic and gallic acids, potent antioxidants. Its interaction with β -cyclodextrin leads to formation of inclusion compounds which affect the physicochemical properties of the guest molecule. Raman and ¹H-NMR spectroscopic studies of the interactions between β -cyclodextrin (β -CD) and included *PPO* (polyphenol oxidase) substrate molecules, chlorogenic acid, (CGA) and caffeic acid (CA) in aqueous and solid medium are reported.

Data analysis by Job's method shows that all the complexes have 1:1 stoichiometry in the studied range of temperatures. Values for the apparent association constant of the inclusion compound are estimated at different temperatures. The obtained thermodynamic parameters are compared with previously reported values for other inclusion systems. These molecules also provide characteristic vibrations with group frequencies for probing the guest on complex formation. The results confirm that inclusion occurs.

This work was complemented by evaluating the energy differences involved in the inclusion reactions for the considered guests and the energies involved in the conformational changes occurring both in the included guests and in the CD macrocycles. Molecular modelling was carried out for the inclusion complexes using the Gaussian 98 system of programs (Gaussian 98, 1998). Inclusion modes for the 1:1 inclusion complexes of gallic, caffeic and chlorogenic acids in β -cyclodextrin (β -CD) and the

* Corresponding author: E-mail: aidams@esac.pt

structures of the included and free host (β -CD) and guest molecules were determined at the HF/6-31G//HF/PM3 level. In addition, the total energy for the 1:1 inclusion as well as the interaction energies between CD and the guest molecules in their non-relaxed inclusion complex geometries were evaluated.

Keywords: β -cyclodextrin, Polyphenol Oxidase (PPO), Polyphenolic Compounds, Enzymatic Browning, Raman Spectroscopy, $^1\text{H-NMR}$ Spectroscopy, Molecular Modelling

1. INTRODUCTION

In certain plant-derived foods, such as juices, enzymatic browning - initiated by the enzyme polyphenol oxidase; *o*-diphenol: oxygen oxidoreductase EC 1.10.3.1 or *PPO* - occurs due to the oxidation and subsequent condensation of naturally occurring phenolic compounds, such as caffeic acid (CA), chlorogenic acid (CGA), and gallic acid (GA) (Figure 1), and results in an undesirable pigmentation of the product. These phenolic compounds are also important antioxidants *in vitro* (Olthof et al., 2002). The control of enzymatic browning in fresh plant products is a problem for the food processing industry since the utilization of sulfites, the most effective inhibitor of browning, became restricted. Much effort has gone into discovering alternative to sulfites such as various antioxidants and their derivatives. Thus, the minimally processed plant products offer a significant economic use for sulphite alternatives such as cyclodextrins.

β -Cyclodextrin (cyclomalto-heptaose, β -CD) – a short, hollow, truncated cone shaped molecule – is a cyclic oligosaccharide composed by seven $\alpha(1-4)$ linked gluco-pyranose units in normal chair conformation (Scheme I). β -CD interacts with other molecules, which may get into the cavity thus originating inclusion compounds. β -CD is a chiral cyclic oligosaccharide whose natural enantiomer is R-(+). Both in the crystalline hydrate and in aqueous media, the β -CD molecule interacts with water molecules, some of which are removed when a guest of suitable size goes into the cavity.

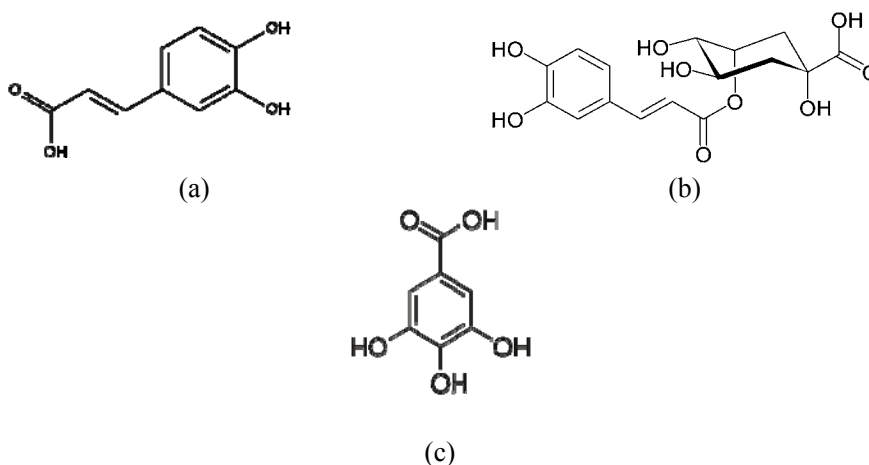
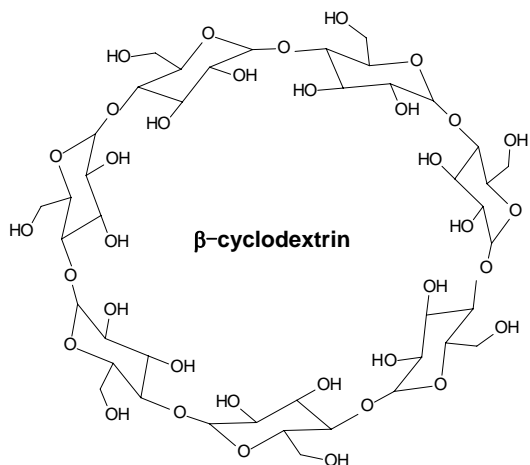


Figure 1. Some phenolic compounds (a) caffeic acid (CA); (b) chlorogenic acid (CGA); (c) gallic acid (GA).



Scheme I.

In this chapter, $^1\text{H-NMR}$ and Raman spectroscopic studies of the interactions between β -CD and *PPO* substrate molecules in aqueous medium (at defined temperatures) and solid state, are reported. Inclusion modes for the 1:1 inclusion complexes of gallic, caffeic and chlorogenic acids in β -cyclodextrin (β -CD) and the structures of the included and free host (β -CD) and guest molecules were determined at the HF/6-31G//HF/PM3 level. In addition, the total energy for the 1:1 inclusion reactions, the changes in the conformational energies of both β -CD and the guest molecules, as well as the interaction energies between β -CD and the guest molecules in their non-relaxed inclusion complex geometries were evaluated.

2. CHARACTERIZATION OF PHENOLIC- β -CD INCLUSION COMPOUNDS

β -CD, the host molecule, was kindly offered by *Wacker Chemie*, Munchen, Germany, and the guest molecules, Chlorogenic acid (1,3,4,5-tetrahydroxycyclohexanecarboxylic acid; (CGA)), caffeic acid, (3,4-dihydroxycinnamic acid; (CA)), and gallic acid (3,4,5-trihydroxybenzoic acid; (GA)), D_2O and CDCl_3 (99.5% isotopic purity) were obtained from *Aldrich*, Madrid.

2.1. The $^1\text{H-NMR}$ Experiment

$^1\text{H-NMR}$ spectra were recorded at temperature range of 20–40°C with a *Varian UNITY-500* NMR spectrometer at 499.824 MHz. D_2O was used as solvent and trichloromethane (CDCl_3 , $\delta=7.20$ relative to TMS) was used as external reference. The residual water signal was reduced by using Presat sequence.

The stoichiometries of the inclusion compounds were determined using a method due to Job (Job, 1928) and generally known as the continuous variation method or Job's method. This method involves running a series of experiments varying the host to guest initial concentrations while maintaining constant the sum of the initial molar concentrations of the

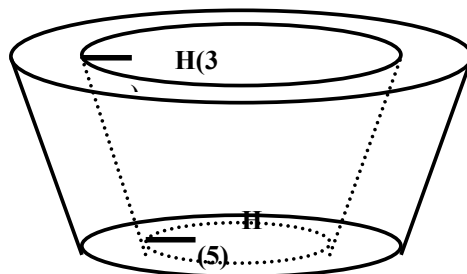
host and guest ($[\beta\text{-CD}]_0 + [\text{G}]_0$), at well defined r values ($r = [\beta\text{-CD}]_0 / ([\beta\text{-CD}]_0 + [\text{G}]_0)$ or $r = [\text{G}]_0 / ([\beta\text{-CD}]_0 + [\text{G}]_0)$). In particular, 10 mM D₂O solutions of the guest (G) and of β -CD were mixed to constant volume (*i.e.*, the sum of the initial concentrations of β -CD and G remains equal to 10 mM, $[\beta\text{-CD}]_0 + [\text{G}]_0 = 10$ mM), and to defined values of r (r took values from 1/10 to 9/10, in steps of 1/10).

The stoichiometries were finally determined by plotting $\Delta\delta.[\beta\text{-CD}]_0$ or $\Delta\delta.[\text{G}]_0$ against r and finding the r values corresponding to the maxima of these distributions.

2.1.1. Stoichiometry of inclusion compounds

The H(3) and H(5) protons of β -CD form two inner 'crowns' of hydrogen atoms, in the wider and narrower rims of β -CD, respectively (see Scheme II). These 'crowns' of protons have strategic positions for reporting host-guest interactions in the cavity. Since both H(3) and H(5) are appreciably shifted to lower frequencies and point to the inside of the cavity, it can be inferred that the formed species are inclusion complexes (Figure 1(a)). On the other hand, the $\Delta\delta$ s of H(6') resonances of the guest molecule shows significant chemical shifts perturbations. So, the H(5), H(3) and H(6') NMR signals were used for probing the *guest*. β -CD interaction (Figure 2 (a) and (b)).

For a 500 MHz spectrometer, and a typical value of the largest observed chemical shift difference ($\Delta\delta_{\text{max}} = 0.2$), the fast exchange condition (*i.e.*, the exchange rate larger than the reciprocal of the largest observed frequency shift in Hz) implies that inclusion and release of the guest (G) should occur at least 100 times/s. (Moreira da Silva *et al.*, 1999). Under these conditions, the frequency of a proton signal is obtained by averaging the frequencies of the free and complexed species, weighted by their mole fractions. From this relationship, one easily arrives at $[C]/[\beta\text{-CD}]_0 = \Delta\delta/\Delta\delta_{\text{max}}$, that is, $\Delta\delta$ provides a means for measuring the concentration of the inclusion compound [C]. Plotting $\Delta\delta.[\beta\text{-CD}]_0$ or $\Delta\delta.[\text{G}]_0$ for both guest molecules, CA or CGA, against r leads to maxima at $r = 0.5$ (see Figure 2 b), pointing to 1:1 stoichiometries (Job, 1928). These distributions are roughly symmetrical, suggesting the presence of associations with a single stoichiometry, in this case, of the 1:1 type. In fact, competitive formation of associations with distinct stoichiometries would give rise to asymmetric "Job's plot".



Scheme II.

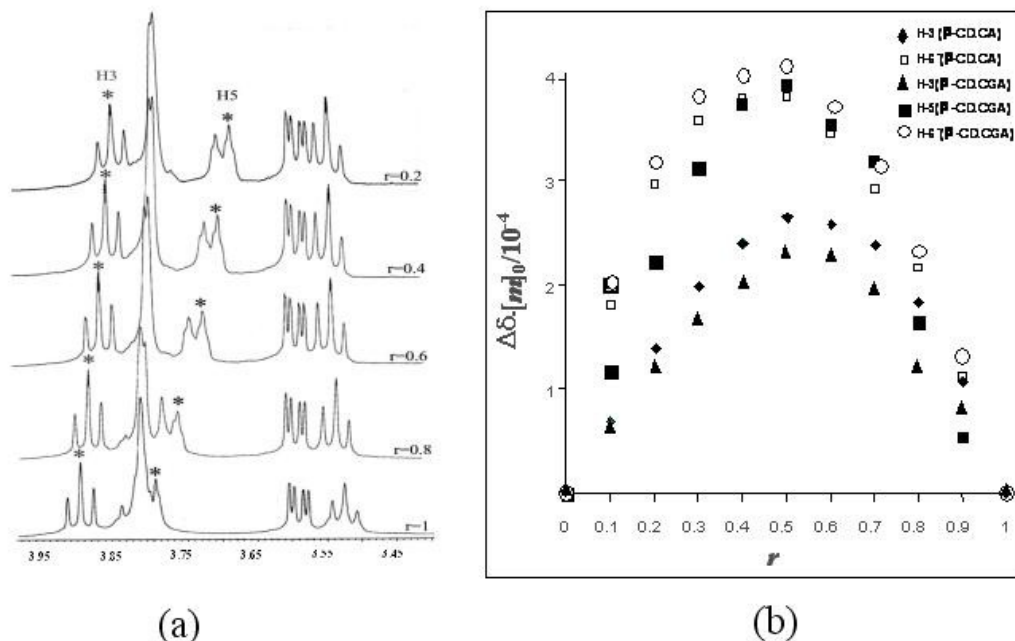


Figure 2. (a) Typical 500 MHz ¹H NMR spectra for mixtures of β-CD and caffeic acid CA, D₂O solutions with different values of *r*, in the region of the H(3) and H(5) signals. (b) Continuous variation plots of 500 MHz ¹H-NMR spectra, for mixtures of β-CD and Guest, (Chlorogenic acid, CGA and Caffeic acid, CA) in D₂O solutions with different values of *r* in the region of the H(5) and H(3) signals and H(6') from Guest molecules.

2.1.2. Apparent inclusion constants of inclusion compounds

The equilibrium for the inclusion process in aqueous solution involves hydrated forms of β-CD and G, and represents a substitution of water molecules in the β-CD cavity by the incoming guest molecule. The apparent association constant, K_{app} , at measuring the extent of complex formation at defined temperatures, from 20 °C up to 40 °C, was estimated by the Benesi-Hildebrand method (Benesi & Hildebrand, 1949). The guest concentration was set at 0.2 mM and that of the β-CD varied from 2 to 12 mM, one of the species observed in the presence of a large excess of the other component (Table 1). The K_{app} was determined following the shift of the chosen H(6') peaks from the guest molecule, CGA or CA, that occurs at 3525.23 Hz (6.901 ppm) and 3533.04 Hz (7.071 ppm), respectively (Irwin et al., 1994, Rodrigues et al., 2002). The results are summarized in Table 2.

Different K_{app} values point to distinct host-guest interactions. At the lower temperature, 20°C, leads to more stable inclusion compounds than higher temperatures up to 40°C. So, as the temperature increases, both inclusion systems tend to dissociate and at 40°C they became appreciably weaker than at room temperature.

Table 1. Chemical shift differences (Hz) for the H(6') protons of the Guest ([chlorogenic acid] = [caffeic acid] = 0.2 mM in mixtures of a D₂O solution of β-CD, T = 25 °C.

[β-CD] ₀ /mM	Δδ H(6')/Hz	
	CGA	CA
0	0	0
2	15.68	0.83
3	18.31	1.06
4	21.06	2.10
5	20.64	2.10
6	24.96	2.70
7	25.98	3.78
8	25.88	4.60
9	27.51	5.84
1	28.40	6.00
11.	29.19	6.57
1	30.22	6.81

Table 2. The apparent association constant, K_{app}, measuring the extent of complex formation, versus temperature (K_{app} was estimated by the Benesi-Hildebrand regression method).

Temperature/°C	K _{app} /M ⁻¹	
	Chlorogenic Acid	Caffeic Acid
20	537	879
25	248	766
30	199	563
35	140	393
40	63	390

2.1.3. Complexation thermodynamics of β-CD.CGA

Since the range of temperatures values is too short (20, 25, 30, 35 and 40 °C) and the number of points scarce, only estimates of ΔH° and ΔS° based on the linear regression of ln K_{app} versus 1/T from the van't Hoff equation (Eq. 1), that allow us to calculate these thermodynamic parameters of the inclusion process,

$$\ln K_{\text{app}} = \Delta S^\circ/R - \Delta H^\circ/RT \quad (\text{Eq. 1})$$

yielding,

$$CA.\beta\text{-CD}: \Delta H^\circ \approx -0.8 \text{ kJ mol}^{-1}, \Delta S^\circ \approx 20.0 \text{ J mol}^{-1},$$

$$CGA.\beta\text{-CD}: \Delta H^\circ \approx -0.2 \text{ kJ mol}^{-1}, \Delta S^\circ \approx 73.0 \text{ J mol}^{-1},$$

For an appreciable number of β -CD inclusion compounds, it has been previously shown that the corresponding ΔS° and ΔH° values fall in one ΔS° versus ΔH° straight line whose slope, the compensation or isoequilibrium temperature, $T_{\text{iso}_{\text{eq}}} = \Delta(\Delta H^\circ)/\Delta(\Delta S^\circ)$, takes the value 27 °C (290 K) (Rekharsky & Inoue, 1998). This important general result has been taken as indicating that the inclusion formation is largely independent of the chemical properties of the guest molecule, thus suggesting that one the driving forces for inclusion is the removal of high-enthalpy water molecules from the cyclodextrin cavity, where these reside in an unfavourable, predominantly hydrophobic environment (Sanger, 1980).

Since the ΔS° and ΔH° values for the CA. β -CD and CGA. β -CD are positive and negative respectively, the inclusion processes became spontaneous for all temperature studied, below and up to $T_{\text{iso}_{\text{eq}}} = \Delta_{\text{CA,CGA}}(\Delta H^\circ)/\Delta_{\text{CA,CGA}}(\Delta S^\circ)$ assuming that ΔS° and ΔH° are constant in the considered temperature range. In addition, these points (ΔS° , ΔH°) fall within the uncertainty range in the general straight line for β -CD inclusion compounds (Figure 3).

This correlation means a compensation mechanism, enthalpy-entropy compensation, that suggests an interaction among cyclodextrins and several substrates. The substrates in this correlation are different but since they are under the same conditionalisms that have similar characteristics. In fact, substrates are restricted in shape and specially restricted in dimension, because they form inclusion compounds with β -CD. Moreover, substrates are restricted in molecular properties due the hydrophobic character of the included fragment in β -CD.

2.2. The Raman Experiment

β -CD was recrystallized by cooling a concentrated aqueous solution from *ca.* 80 °C to room temperature, in a Dewar flask. The guest molecule, CGA or CA (3.5 mmol) was well dispersed in 10 mL distilled water before adding it dropwise to β -CD solution (5 g dissolved in 100 mL of hot water, 70 °C). The mixture was then vigorously stirred over night on a magnetic stirrer at room temperature. White precipitates were filtered and dried for 1-2 days over ambient atmosphere. Filtration allowed separation of the β -CD excess. Non-included guest compound was lost by evaporation.

A sample of each one of the inclusion compounds was inserted in a Kimax capillary tube which, in turn, was put into laser beam. All the Raman spectra were recorded on a *T64000 Jobin Yvon* spectrometer, working in the subtractive configuration (*i.e.*, double premonochromator stage in subtractive configuration, plus third stage spectrograph), with relevant slit widths set to 320 nm and the intermediate slit between premonochromator and spectrograph wide open (14 mm). The detecting device was a CCD detector, and an integration time of 15 s was used. Spectral data for the 2800-3800 cm^{-1} overall region were collected in 10 subregions, hence corresponding to a total acquisition time of 150 s. An He-Ne laser, 632.8 nm (from Spectra-Physics) provided *ca.* 20 mW at the sample position. Integrated intensities were determined using the Microcal TM Origin 6.0® data analysis software.

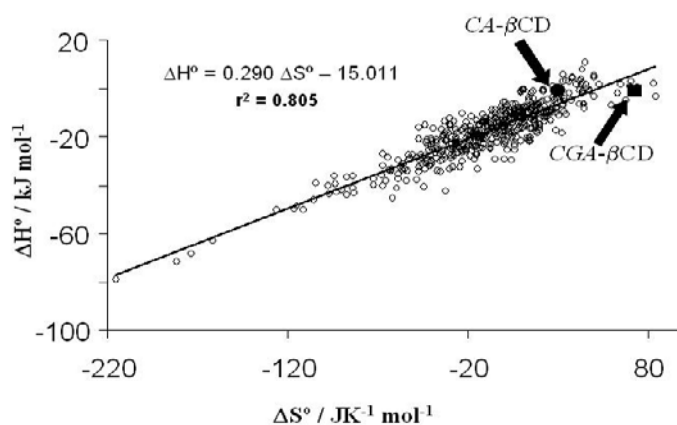


Figure 3. Enthalpy-Entropy Compensation plots for 1:1 inclusion compounds of various guests with β -CD (from reference Rekharsky & Inoue, 1998) and the inclusion compounds CA- β -CD and CGA- β -CD.

2.2.1. The Raman experiment shows that inclusion also occurs in solid state

The *PPO* (polyphenol oxidase) substrate molecules CA and CGA show characteristic vibrational bands in the 1550-1800 cm^{-1} region as inclusion process probes. These molecules have the C=O group and the vibrational sensitivity of this oscillator to π electrons is very useful as a vibrational probe of the interactions of CA or CGA and β -CD. Moreover CA and CGA have a phenyl group that presents one of ring stretching vibrations *ca.* 1600 cm^{-1} . Finally, the bond C=C is also present in the two compounds (Sánchez-Cortés & Garcia-Ramos, 2000).

The Raman spectrum of β -CD in the region 200-1800 cm^{-1} and the Raman spectra of X- β -CD compounds (X = CA or CGA) in the region 1550-1800 cm^{-1} are presented in Figure 4 a) and b), respectively.

According to the previous results, the more relevant spectral features presented in these spectra are ν_{CC} (*ca.* 1600 cm^{-1}), $\nu_{\text{C=O}}$ (1658-1706 cm^{-1}) and $\nu_{\text{C=C}}$ (1624-1627 cm^{-1}).

Two types of spectral comparisons emerge from these spectra:

- i) Between the pure guests molecules, X (X = CA or CGA)
- ii) Between X and X- β -CD, for a particular guest X (X = CA or CGA).

The inclusion process can be assessed through comparison *ii*) which, in turn, leads to conclusions concerning *solvent effects* and/or *specific interactions* affecting $\nu_{\text{C=O}}$. In general terms, comparison *ii*) reveals

- a) Frequency shifts of band maxima and
- b) Significant changes in asymmetric band envelopes.

While *a*) may be due to *bulk solvent effects* and/or *specific interactions* namely, of the hydrogen bonding type, *b*) implies overlapping of bands and strongly suggests the occurrence of *non specific interactions*.

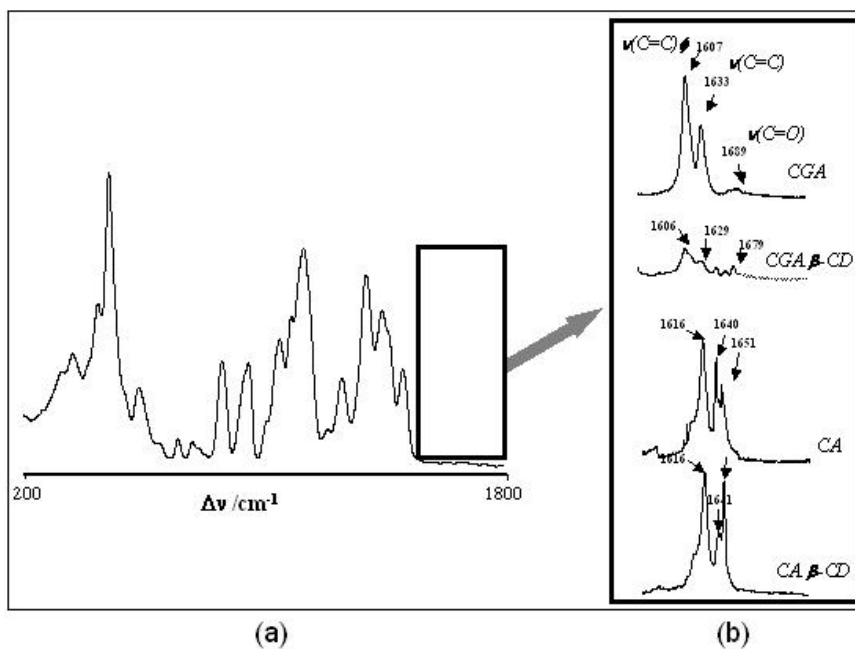


Figure 4. (a) β -CD Raman spectrum presents a window in the region of 1550-1800 cm^{-1} . (b) Raman spectra of the inclusion compounds β -CD.CGA and β -CD.CA compared with the Raman spectra of the guest molecule alone, in the region 1550-1800 cm^{-1} .

2.3. Model Calculations Study

Following the Raman and $^1\text{H-NMR}$ spectroscopic studies of the interactions between cyclodextrin and included phenolase substrate molecules, chlorogenic (CGA), caffeic (CA) and gallic (GA) acids, in aqueous and solid media, the study was complemented. The structures of the included and the free host and guest molecules were elucidated, by evaluating the energy differences involved in the inclusion reactions for the considered guests and the energies involved in the conformational changes occurring both in the included guests and in the β -CD macrocycle.

Molecular modelling was carried out for the inclusion complexes using the Gaussian 98 system of programs (Gaussian 98, 1998). Due to the large number of atoms in the β -CD moiety, the geometry full optimization stage of the calculation was kept at the semi-empirical PM3 level and the single point energy calculations for the optimized geometries were performed at the Hartree-Fock level with the 6-31G basis set. The geometry optimized structures were visualized with GaussView®.

At the level of calculations herein performed, consideration of solvent effects by a Self-Consistent Reaction Field method would yield solvation energies below or surrounding the predicted errors of the calculations. Even with a higher level of calculation, a dielectric continuum could not adequately model a hydrogen-bond solvent with a relative permittivity as high as water. For these reasons, no solvent effects were considered in the present calculations. Considering the level and basis set used in these calculations and the fact that

they were applied to isolated molecular systems, the results can only be used to draw qualitative inferences for the inclusion reactions.

The total energies for the 1:1 inclusion reactions, ΔE_{total} , the changes in the conformational energies of both β -CD, $\Delta E_{\beta\text{-CD}}$ ($=E_{\beta\text{-CDincomplex}} - E_{\text{isolated}\beta\text{-CD}}$), and the guest molecules, ΔE_{guest} ($=E_{\text{guestincomplex}} - E_{\text{isolatedguest}}$), and the interaction energies between β -CD and the guests in their non-relaxed inclusion complex geometries, ΔE_{int} ($=\Delta E_{\text{total}} - \Delta E_{\beta\text{-CD}} - \Delta E_{\text{guest}}$), are presented in Table 3. It can be seen that the conformational energy changes for β -CD amount approximately to 90% of ΔE_{total} for GA, to 22% for CA and 20% for CGA. While ΔE_{guest} is negligible for both GA and CA, for CGA, ΔE_{guest} approximately doubles $\Delta E_{\beta\text{-CD}}$, thus suggesting that, in this case, the major conformational changes occur in CGA and not in β -CD.

The optimized structures for the inclusion complexes of GA, CA and CGA in β -CD are shown in Figures 5, 6 and 7.

Table 3. Energy values (kJ mol⁻¹) for the inclusions of GA, CA and CGA in β -CD.

Inclusion reaction	$\Delta E_{\beta\text{-CD}}$	ΔE_{guest}	ΔE_{int}	ΔE_{total}
$\beta\text{CD} + \text{GA} \rightarrow \beta\text{-CD.GA}$	18	0	2	20
$\beta\text{-CD} + \text{CA} \rightarrow \beta\text{-CD.CA}$	14	2	48	64
$\beta\text{-CD} + \text{CGA} \rightarrow \beta\text{-CD.CGA}$	11	21	23	55

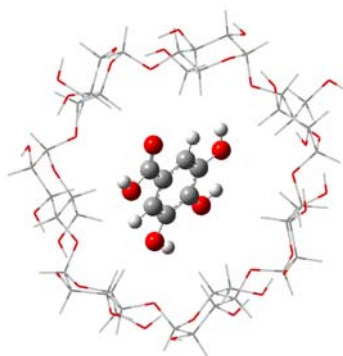


Figure 5. PM3 structure for the inclusion complex GA. β -CD.

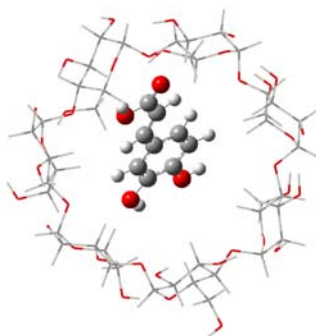


Figure 6. PM3 structure for the inclusion complex CA. β -CD.

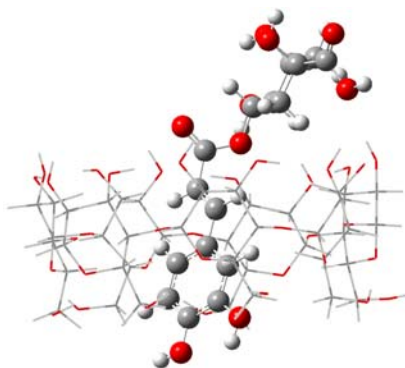


Figure 7. PM3 structure for the inclusion complex CGA.β-CD.

Table 4 lists close contacts between guest atoms and β-CD atoms whose distances are below 2Å.

Table 4. Guest-host close contacts for the inclusion complexes of GA, CA and CGA in β-CD (the first atom belongs to the guest).

inclusion complex	H...HC5	H...HC3	H...HC6	(H)O...HC5	OH...HC5
GA. β-CD	—	—	—	1	1
CA. β-CD	2	1	1	—	—
CGA. β-CD	2	1	1	—	—

CONCLUSION

The results herein reported indicate that these systems are inclusion compounds and satisfy the basic requirements (K_{app} in the range 10^2 - 10^4 M^{-1}) for use in the pharmaceutical and functional food industries. In addition, the K_{app} obtained at $T = 25^\circ C$ value herein obtained for CGA.β-CD is of the same order of magnitude of a previously determined value obtained by ultra violet-visible spectrophotometry (Irwin et al., 1994).

A linear $\Delta H^\circ - \Delta S^\circ$ relationship has been reported. This correlation means a compensatory enthalpy-entropy mechanism, suggesting the same type of interaction between cyclodextrins and different guest molecules: the same size of cavity and the same hydrophobic environment. In addition, the Raman experiment shows that inclusion also occurs in solid state.

The molecular modelling approach confirms experimental observations of the polyphenolics abilities to form inclusion complexes with β-CD in aqueous environment. The conformational analysis based on theoretical methods may be of significance in future studies aiming at the elucidation of the structure – activity relationships associated with the biological role of certain types of compounds displaying potential therapeutic activity (namely anticancer therapeutic properties) and may also be used to design better and more efficient inclusion carriers of food systems.

REFERENCES

- [1] Benesi, A; Hildebrand, J. *J. Am. Chem. Soc.*, 1949, 71, 2703-2707.
- [2] Gaussian, 98, Revision A.6, (1998) MJ; Frisch, GW; Trucks, HB; Schlegel, GE; Scuseria, MA; Robb, JR; Cheeseman, VG; Zakrzewski, JA; Montgomery Jr., RE; Stratmann, JC; Burant, S; Dapprich, JM; Millam, AD; Daniels, KN; Kudin, MC; Strain, O; Farkas, J; Tomasi, V; Barone, M; Cossi, R; Cammi, B; Mennucci, C; Pomelli, C; Adamo, S; Clifford, J; Ochterski, GA; Petersson, PY; Ayala, Q; Cui, K; Morokuma, DK; Malick, AD; Rabuck, K; Raghavachari, JB; Foresman, J; Cioslowski, JV; Ortiz, BB; Stefanov, G; Liu, A; Liashenko, P; Piskorz, I; Komaromi, R; Gomperts, RL; Martin, DJ; Fox, T; Keith, MA; Al-Laham, CY; Peng, A; Nanayakkara, C; Gonzalez, M; Challacombe, PMW; Gill, B; Johnson, W; Chen, MW; Wong, JL; Andres, C; Gonzalez, M; Head-Gordon, ES; Replogle, JA; Pople, Gaussian, Inc., Pittsburgh PA
- [3] GaussView 2.1, Gaussian Inc., Carnegie Office Park, Building 6, Pittsburgh, PA 15106.
- [4] Irwin, P; Pfeffer, P; Doner, L; Sapers, G; Brewster, J; Nagahashi, G; Hicks, K. *Carbohydr. Res.*, 1994, 256, 13-27.
- [5] Job, P. *Ann. Chim.*, 1928, 9, 113-135.
- [6] Moreira da Silva, A; Empis, J; Teixeira-Dias, JJC. *J. Inclusion Phenomena Macrocyclic Chem.*, 1999, 33, 81-97.
- [7] Otholf, MR.; Hollman, PCH; Katan, MB. *J. Nutrition*, 2002, 131, 66-71.
- [8] Rekharsky, M; Inoue, Y. *Chem. Reviews.*, 1998, 98, 1875-1917.
- [9] Rodrigues, E; Vaz, S; Gil, VMSS; Caldeira, M; Moreira da Silva, A. *J. Incl Phenom Macro Chem.*, 2002, 44, 395-399.
- [10] Sánchez-Cortés, S; Garcia-Ramos, JV. *Applied Spectroscopy*, 2000, 54(2), 230-238.
- [11] Sanger, W. *Angew Chem*, 1980, 19, 344-362.

Chapter 17

**A NEW SPROUTING INHIBITOR:
n@NO-SPROUT®, B-CYCLODEXTRIN/
S-CARVONE INCLUSION COMPOUND**

*Marta Costa e Silva*¹, *Cristina Galhano*^{2,3}
and Aida Moreira da Silva^{1,4*}

¹Escola Superior Agrária de Coimbra, Departamento de Ciência e Tecnologia Alimentar.

²Departamento de Ciências Exactas e do Ambiente, Bencanta, 3040-316 Coimbra.

³Unidade de Investigação CERNAS, Bencanta, 3040-316 Coimbra; Unidade de Investigação Química Física Molecular⁴, Universidade de Coimbra, 3000-535 Coimbra.

ABSTRACT

The main goal of this work was to develop a new potato sprouting inhibitor. Why? Because there is an unquestionable increasing research interest on finding alternatives to traditional chemical control methods. In fact, it is well recognized the high importance of obtaining a human health innocuous and environmentally-friendly potato anti-sprouting compound to take Chlorpropham's (CIPC) place. In many countries, this carbamate is not currently being used due to both legislative and marketing reasons. However, potato sprouting is a common significant problem during winter storage of potato tubers, which we need to prevent. Potato is the fourth most important food crop in the world, mainly due to its starch content, high quality protein, substantial amount of essential vitamins, minerals, and very low fat content.

In this work, the potential potato sprouting inhibition effect on two systems, S-carvone and the inclusion compound *n@NO-sprout*® was studied and, simultaneously, compared with the traditionally used CIPC. S-(+)-carvone, a monoterpene compound, which is the main compound if the essential oil of caraway (*Carum carvi* L.) is extracted using hydrodistillation and the supercritical method. The inclusion compound, *n@NO-sprout*®, based on β -cyclodextrin and S-carvone (yield ca. 95% (w/v)) was synthesised through the precipitation method. Firstly, small-scale bioassays were carried out using 70

* Corresponding author: Tel.: +351-239-802275; Fax +351-239-802273, E-mail: aidams@esac.pt

potato tubers/treatment. Secondly, bioassays were carried out on a large scale in semi-practical conditions at a chips industry. The obtained results showed the significant sprout inhibition effect of *n@NO-sprout*® on potato tubers. Finally, to access possible detectable flavour differences between industrial chips obtained from potato tubers which were previously submitted to the different treatments and industrial chips obtained from potato tubers which were not submitted to any treatment, sensory discriminative analysis, triangular tests, were performed. Through statistical analysis, significant differences ($p < 0.05$) were only found for the CIPC treatment.

To sum up the findings a new promising sprout inhibitor agent for potato tuber storage, the β -cyclodextrin/S-carvone inclusion compound registered as *n@NO-sprout*® was found as an alternative to CIPC.

Keywords: *n@No-sprout*®; sprout inhibitor; potato; S-carvone; β -cyclodextrin; inclusion compound; sensory discriminative analysis

1. INTRODUCTION

There is a growing concern and awareness of the scientific and general communities regarding the use of pesticides and their potential residues left in food. Therefore, several groups of researchers are attempting to develop phytochemical-based strategies for plant protection. Most pesticides tend to be rather toxic or volatile, with poor target specificity and less-than-perfect human or environmental safety, such as groundwater contamination or atmospheric ozone depletion (Chitwood, 2002; Daniels-Lake & Prange, 2007; Magro *et al.*, 2003). Moreover, because members of the plant kingdom are capable of producing an incredible variety of secondary metabolites, many investigators have ventured beyond allelopathic interactions and have looked for plant enemies antagonistic substances. Several benefits may come out from the identification of specific phytochemicals involved in these interactions whether they occur in a field or a laboratory. These compounds can be developed to be used as biocides themselves or they can serve as model compounds for the development of chemically synthesized derivatives with enhanced activity or environmental friendliness. Many phytochemicals, but certainly not all, are safer for the environment and humans rather than traditional chemicals (Chitwood, 2002).

Potato is one of the most important food crops in the world with a total production of 309344247 ton/year (FAOSTAT, s.d.). It is an important source of starch as well as essential vitamins, minerals, and dietary fiber with a very low fat content (USDA, s.d.). Potato tubers are used in industry either as seed or as raw material, both of which usually need storage for days, weeks or months. During this period of time, sprouting must be managed to maintain tuber quality and hence market value. Sprouting represents a loss of tuber material and causes an accelerated loss of water through the permeable surface of the sprout. Tubers with sprouts are considered undesirable by the marketplace particularly those with the associated wilting and sweetening effects. For fresh consumption, sprouts and flaccid tubers are unsightly and therefore less saleable. In industry, sprouted tubers do not pass through processing equipment properly. In addition, French fries, crisps and potato flakes producers prefer low reducing sugar concentrations to obtain the preferred light-coloured finished products. Also, higher levels of sugars can contribute to production of acrylamide during high-temperature processing. Given this undesirable feature, sprouting control using non-chemical and

chemical methods has been supported the potato industry. Nowadays, the most important of these methods is low-temperature storage, initially at 2-4°C, followed by storage at constant temperature (*ca.* 10°C), and treatment with chlorpropham (CIPC; isopropyl N-(3-chlorophenyl)carbamate), and to a lesser extent maleic hydrazide (MH). However, the former method originates the so-called low-temperature sweetening, leading to a high reduction of sugar content in tubers which causes browning and bitterness of processed products, features that are undesirable, as it was referred above. Sweetening can be prevented by tuber storage at higher temperatures (7-8°C) with sprout suppressants application (Costa e Silva et al., 2007a,b; Daniels-Lake & Prange, 2007). Furthermore, its common use by storage entities in Scandinavian countries, the CIPC, a widespread, synthetic, conventional sprout suppressant, has already been restricted due to its human health and environmental negative impacts. In fact, there is a growing tendency to disallow the use of chemicals in other European countries whose safety conditions was discussed by the European Community standing committee on Plant Health (OJEU, 2002a). The general worry about pesticide usage and their residues in all foodstuffs has lead the potato industry—as well as potato researchers, to find appropriate alternatives for replacing traditional sprout inhibitor methods (Costa e Silva et al., 2007a,b; Daniels-Lake & Prange, 2007).

Since long, volatile plant compounds have been used in post-harvest potato storage for many decades (Carvalho & Fonseca, 2006; Hartmans et al., 1995; Oosterhaven et al., 1995; Vaughn & Spencer 1991). Among these, (4S)-(+)-Carvone, a monoterpene, which is the main compound of the essential oil of caraway (*Carum carvi* L.) fruits, is being used as a sprouting inhibitor agent for potatoes and seed potatoes during the process storage. This compound was already registered by the European Commission to be used as flavourings in foodstuffs, which means that it brings no risk for the consumer's health (OJEU, 2002b). Carvone also appears on the Everything Added to Food in the US' (EAFUS) list which means that it was classified as Generally Recognised As Safe (GRAS) or as approved food Additives by the United States Food and Drug Administration (FDA, s.d.). Moreover, carvone was also considered as an antimicrobial agent, as an insecticide and as a biochemical environmental indicator (Carvalho & Fonseca, 2006). Talent® is currently the only commercial sprout suppressant formulation that uses carvone as its primary active ingredient. Nevertheless, it is extremely volatile and therefore unstable. This problem can be avoided with the inclusion of carvone into β -cyclodextrin (β -CD) (Del Valle, 2004; Moreira da Silva et al., 1999). β -CD, composed by seven units of D-(+)-glucopyranoside, can be topologically represented as a toroid with the larger and the smaller openings exposed, respectively, to the solvent secondary and primary hydroxyl groups.

Based on the arguments discussed, the main purpose of this work was to study the potential anti-sprouting effect of *n@NO-sprout*® comparatively to those of carvone and CIPC. For this, firstly, small scale bioassays were inducted; secondly, bioassays were carried out on a large scale in semi-practical conditions at a chips industry. Finally, a sensory discriminative analysis, triangular tests, were performed to know if there were any detectable flavour differences between industrial chips obtained from potato tubers which were previously submitted to the different treatments (carvone, *n@NO-sprout*®, CIPC) and industrial chips obtained from potato tubers which were not submitted to any treatment.

2. METHODOLOGY

β -CD (KLEPTOSE) was kindly offered by Roquette, France, and the S-carvone was purchased from Aldrich or extracted from caraway seeds by supercritical method (Baysal & Starmans, 1999) and/or hydrodistillation (Bailer *et al.*, 2001). Talent® was kindly offered by Luxan and CIPC, Batalex Novo®, was purchased from Sapec Agro.

2.1. n@NO-Sprout Preparation (Pilot Scale)

β -CD (273 g) was dissolved in 15 L of distilled water to form a clear solution, at 353 K in a B. Braun Biotech Biostat ED DCU2 Fermentor. The S-carvone (37.7 mL) was added dropwise to β -CD solution. The mixture was vigorously stirred over night with a magnetic stirrer at room temperature. The white precipitate formed was filtered and dried for 1–2 days over ambient atmosphere, ca. 90% (m/m) yield (Costa e Silva *et al.*, 2007a).

The β -CD/carvone inclusion compound was characterized by ¹H-NMR and Raman spectroscopic studies (Moreira da Silva *et al.*, 1999; 2002).

2.2. Potato Storage Experiments

The used potato tubers were produced at Escola Superior Agrária de Coimbra (ESAC) and Cooperativa Agrícola dos Lavradores do Concelho de Oliveira do Bairro (CALCOB), partners of AGRO 691 Project.

2.2.1. Small scale bioassay

This experiment was conducted for two months, at ESAC. Eight wood containers of 70 x 50 cm² were placed in a cool storage room at 283 K, and 80–90% relative humidity (RH). Seventy potato tubers, cv. Désirée (ca. 140 g/potato) making 10 kg of total weight, were layered in each container. The potato tubers of each container were submitted to different treatments (Table 1).

Table 1. Treatments and quantities used in the small scale bioassay.

Treatment	Applied quantity	Total applied quantity
S-carvone (<i>Talent</i> ®)	1.0 mL	6.0 mL
	2.0 mL	12.0 mL
	4.0 mL	24.0mL
	6.0 mL	36.0 mL
<i>n@NO-sprout</i> ®	30.0 g	180.0 g
CIPC (<i>Batalex Novo</i> ®)	3.(3) g	10.0 g
Caraway fruits	—	400.0 g

Talent[®] and *n@NO-sprout*[®] were homogenously distributed, weekly. *Batalex Novo*[®] was homogenously distributed, each two weeks. The caraway fruits were distributed only at the beginning of the experiment. One of the containers was left without any treatment, as control. The containers were placed separately, to avoid cross interactions among treatments. Number and length of the sprouts were registered in each treatment and in control, on 10 randomly chosen potato tubers, weekly. The results were submitted to a one-way ANOVA and differences among treatments were detected by the Tukey test, at the $p=0.05$ level (Zar, 1996).

2.2.2. Large scale bioassay

This experiment was also conducted for two months, at Sociedade Industrial de Aperitivos – S&A, a Chip Industry, another partner of AGRO 691 Project. The potato tubers, cv. Hermes, were placed in wood containers (600 kg capacity) passing through a continuous rolling machine. During this process, potato tubers were submitted to different three treatments: 1 - *Talent*[®] using pressurized equipment; 2 - 9.36 kg of *n@NO-sprout*[®]; 3 – 0.6 kg of *Batalex Novo*[®]. Tubers in a fourth container were left without any treatment as control. The containers were then placed in a cool storage room at 285 K and 90% RH (Relative Humidity). Results were registered and analysed as described above.

Chemical analyses and sensory evaluation of chips

Chemical analyses were carried out on chips produced in a continuous process line, according to AOAC (Association of Official Agricultural Chemists) Official Methods. The parameters evaluated were: (i) moisture content, by desiccation in a stove at 120°C of ca. 5 g of test sample; (ii) salt content, by reaction of chloride anion with potassium thiocyanide and titration with silver nitrate; (iii) fat content, by infrared method (MCT-*medium chain triacylglycerols*); (vi) colour, by comparison with the IBVL scale (IBVL, Institute for Storage and Processing of Agricultural Products, Wageningen, the Netherlands).

To know if the different treatments affected the flavour of potato after being processed, chips were analyzed by a non-trained panel (94 assessors) through triangular tests, conducted in individual booths-and the results were analysed by binomial tests.

3. RESULTS AND DISCUSSION

3.1. Potato Storage Experiments

Small scale bioassay

The results obtained in this experiment are shown in Figures 1 and 2. All treatments had a sprout inhibiting effect when compared with control, including caraway fruits. All over the experiment, carvone showed an effect statistically equivalent to CIPC in terms of both evaluated criteria. It is important to highlight results that were obtained with the new compound, *n@NO-sprout*[®]. In fact, this novel system turns out to be as effective as the two other compounds already known as anti-sprouting agents: the traditionally used CIPC and the aforementioned carvone, which in turn was already pointed out as an ecofriendly alternative

to CIPC (Carvalho & Fonseca, 2006; Daniels-Lake & Prange, 2007; Hartmans et al., 1995; Oosterhaven et al., 1995).

Among carvone treatments, despite the two higher quantities had the most evident anti-sprouting effect, in a general way, there were no significant differences. Although the two higher quantities of carvone treatments revealed better anti-sprouting effects, there were no remarkable differences regarding the sprout length. In order to know what would be the lowest carvone and/or *n@NO-sprout*® quantities to obtain the desirable anti-sprouting effect, further studies should be carried out.

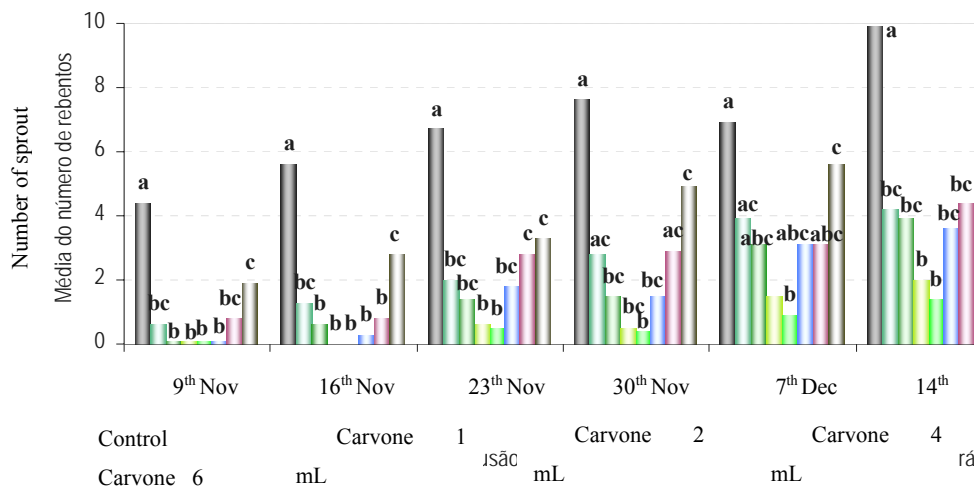


Figure 1. Number of sprouts registered in each treatment and control in the small scale bioassay. Data are means of 10 replicates. Columns with the same letter, for each observation time, are not significantly different ($p>0.05$).

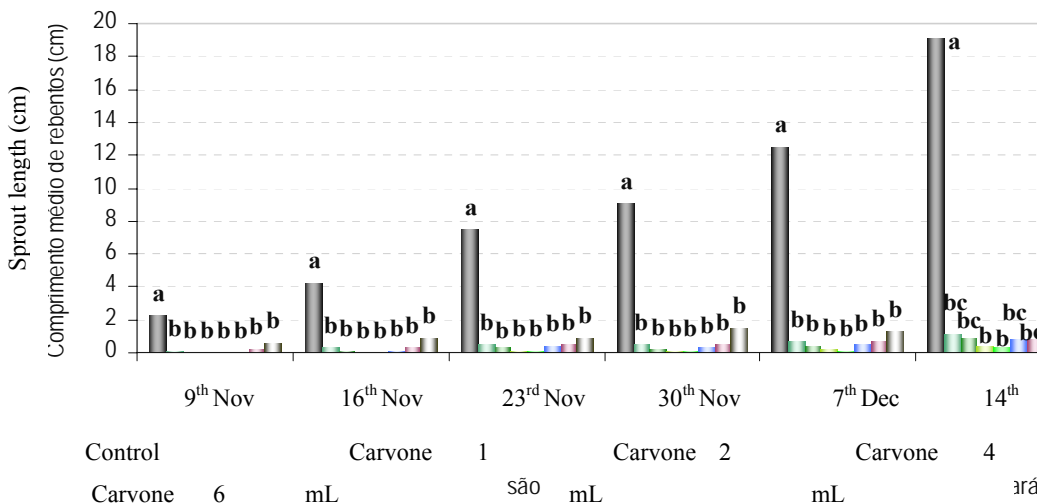


Figure 2. Sprout length registered in each treatment and in control in the small scale bioassay. Data are means of 10 replicates. Columns with the same letter, for each observation time, are not significantly different ($p>0.05$).

Large scale bioassay

The results obtained in this experiment are presented in Figure 3.

The results about the number of sprouts are not shown since no significant differences between treatments were observed. Nevertheless, the results about sprout length showed that either carvone or *n@NO-sprout*® had comparable anti-sprouting effect to CIPC. Among those three compounds, the best behaviour as a sprout inhibitor was observed with *n@NO-sprout*®. In fact, in the last observation, the sprout length in the CIPC and in the *n@NO-sprout*® treated tubers was very alike. Based on these findings, more research on the *n@NO-sprout*® capability to avoid potato sprouting is needed in order to confirm the results of this experiment. Studies with the *n@NO-sprout*® during a longer storage period under practical scale would probably confirm its potential as a promising alternative to CIPC.

The *n@NO-sprout*® potential was observed either on the small scale bioassay or on the large scale bioassay, despite the use of different potato cultivars, Desirée and Hermes, respectively. Even though it would be recommended to use the same cultivar in both bioassays this was not possible due to limited potato stock availability from the in charged partners of tuber production. Hereafter, the anti-sprouting effect of carvone as well as *n@NO-sprout*® should be tested in other potato storage cultivars to be used not only for chips but also for other processing industry or fresh consumption. Furthermore, in future similar studies it would be important to consider a higher number of replicates/observation to obtain a more significant sample.

3.2. Chemical Analyses and Sensory Evaluation of Chips

The general chemical composition of chips samples obtained from tubers, which were submitted to different treatments, is presented in Table 2. These results show that there was homogeneity in all evaluated parameters among the different treatment samples.

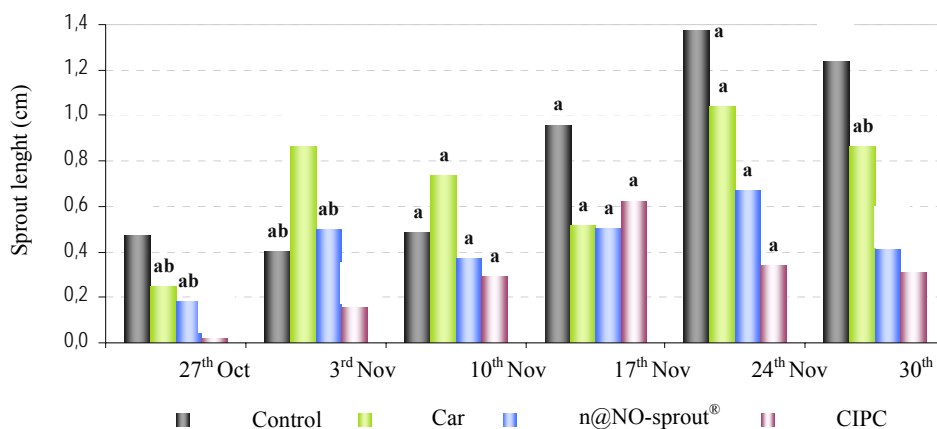



Figure 3. Sprout length registered in each treatment and in control in the large scale bioassay. Data are means of 10 replicates. Columns with the same letter, for each observation time, are not significantly different ($p > 0.05$).

Table 2. Chemical Composition and Colour of chips.

	Dry Matter % (w/w)	Fat % (w/w)	Moisture % (w/w)	Salt % (w/w)	Colour <i>IBVL Card Colour</i>
Control	21.6	35.01	0.7	1.1	9
<i>n@NO-sprout</i> ®	21.6	37.01	0.8	1.1	9
CIPC	21.6	34.48	0.8	1.3	9
<i>Talent</i> ®	21.6	33.67	0.8	1.3	9



The organoleptic characteristics of carvone exhibit a sweet, warm, herbaceous, and spicy odour. These organoleptic characteristics of carvone justify its use as a flavouring constituent in bakery goods, candies, condiment mixtures, and alcoholic liquors of the kmmel type (Burt, 2004; Carvalho & Fonseca, 2006). Although only very limited amounts of carvone could be detected within peeled tubers (Hartmans *et al.*, 1995) it was very important to know whether this had any influence on the sensory quality (“off-flavour”) of industrial potato chips. “Off-flavour” means any type of “unpotato-like” characteristics. No significant affect, due to carvone or *n@NO-sprout*, was found on the “off-flavour” during the experiment storage period.

Sensory analysis could only detect significant differences ($p < 0.05$, binomial test) between industrial chips from potatoes with no treatment and the CIPC treated potatoes. Accordingly, the results of the chemical analysis are consistent with the non-trained panel answer.

The potential of the new compound, *n@NO-sprout*®, as a sprout inhibitor was discovered in this study, under semi-practical conditions. This could be an important innovation for agro-industrial purposes and, at the same time, a human health safety and ecofriendly solution for potato sprouting. The anti-sprouting effect of carvone was already known, as was referred above. However, the application of this compound still has some limitations due to its liquid formulation and instability. The inclusion of carvone in the β -cyclodextrin molecule prevents such restrictions.

4. CONCLUSION

The results herein reported indicate that *n@No-sprout*®, a β -cyclodextrin/S-carvone inclusion compound, is a promising new alternative to CIPC. In fact, this system satisfies the basic requirements to be used as a sprout inhibitor agent for potato tuber storage, for mid-term storage period under semi-practical conditions (2 tons).

Nowadays, the only weakness for *n@NO-sprout*® use could be the higher application technology cost when compared to the corresponding traditional synthesis compound CIPC cost, since it is already commercialized as a common sprout inhibitor, for a long time. Nevertheless, the *n@NO-sprout*® application is *ca.*1.7 times less expensive than carvone. Moreover, the β -cyclodextrin price has been decreasing gradually during the last few years which could lead to a price reduction of the *n@NO-sprout*®.

REFERENCES

- [1] Bailer, J., Aichinger, T., Hackl, G., de Hueber, K. & Dachler, M. (2001). Essential oil content and composition in commercially available dill cultivars in comparison to caraway. *Industrial Crops and Products*, 14, 229-239
- [2] Baysal, T. & Starmans, D. A. J. (1999). Supercritical carbon dioxide extraction of carvone and limonene from caraway seed. *Journal of Supercritical Fluids*, 14, 225-234
- [3] Burt, S. (2004). Essential oils: their antibacterial properties and potential applications in foods - a review. *International Journal of Food Microbiology*, 94, 223- 253
- [4] Carvalho, C. C. C. R. & Fonseca, M. M. R. (2006). Carvone: Why and how should one bother to produce this terpene. *Food Chemistry*, 95, 413-422
- [5] Chitwood, D. J. (2002). Phytochemical based strategies for nematode control. *Annual Review of Phytopathology*, 40, 221-249
- [6] Costa e Silva, M., Galhano, C. I. C. & Moreira da Silva, A. M. G. (2007a). A new sprout inhibitor of potato tuber based on carvone/ β -cyclodextrin inclusion compound. *Journal of Inclusion Phenomena and Macrocyclic Chemistry*, 57, 121-124
- [7] Costa e Silva, M., Galhano, C. I. C. & Moreira da Silva, A. (2007b). S-carvone/ β -cyclodextrin inclusion compound: a new potato sprout inhibitor? *EURO FOOD CHEM XIV Proceedings*. Paris
- [8] Daniels-Lake, B. J. & Prange R. K. (2007). The canon of potato science: 41. Sprouting. *Potato Research*, 50, 379-382
- [9] Del Valle, E. M. (2004). Cyclodextrins and their uses: a review. *Process Biochemistry*, 39, 1033-1046
- [10] FAOSTAT (s.d). FAO Food and Agriculture Organization. *FAO Statistical Databases-FAOSTAT Agriculture*. Available from <http://faostat.fao.org/default.aspx>.
- [11] FDA (s.d) - U. S. Food and Drug Administration *Everything Added to Food in the United States* (EAFUS). Available from <http://www.accessdata.fda.gov/scripts/fcn/fcn-DetailNavigation.cfm?rpt=eafusListing&id=530>.
- [12] Hartmans, K. J., Diepenhorst, P., Bakker, W. & Gorris, L. G. M. (1995). The use of carvone in agriculture: sprout suppression of potatoes and antifungal activity against potato tuber and other plant diseases. *Industrial Crops and Products* 4, 3-13.
- [13] Magro, A., Rodrigues Júnior, C. & Mexia, A. (2003). A utilização de extractos de origem vegetal na inibição do crescimento fúngico. *6º Encontro Nacional de Protecção Integrada Proceedings*. Castelo Branco.
- [14] Moreira da Silva, A., Empis, J. & Teixeira-Dias, J. (1999). Inclusion of enantiomeric carvones in β -cyclodextrin: a variable temperature ¹H NMR study in aqueous solution. *Journal of Inclusion Phenomena and Macrocyclic Chemistry* 33, 81-97.
- [15] Moreira da Silva, A., Empis, J. & Teixeira-Dias, J. (2002). Inclusion of carvone enantiomers in cyclomaltoheptaose (β -cyclodextrin): thermal behaviour and H \rightarrow D and D \rightarrow H exchange. *Carbohydrate Research* 337, 2501-2504.
- [16] OJEU (2002a). Official Journal of the European Communities. Commission decision of 14 August 2002. Available from <http://eur-lex.europa.eu/LexUriServ/LexUriServ.do?uri=OJ:L:2002:221:0037:0038:EN:PDF>.
- [17] OJEU (2002b). Official Journal of the European Communities. Commission decision of 23 January 2002. Available from http://ec.europa.eu/food/fs/sfp/addit_flavor/flav17_en.pdf.

- [18] Oosterhaven, K., Poolman, B. & Smid, E. J. (1995). S-carvone as a natural potato sprout inhibiting, fungistatic, and bacteristatic compound. *Industrial Crops and Products* 4, 23-31.
- [19] USDA National Nutrient Database. (s.d.). Available from <http://www.nal.usda.gov/fnic/foodcomp/search/>.
- [20] Vaughn, S. & Spencer, G. F. (1991). Volatile monoterpenes inhibit potato tuber sprout. *American Potato Journal* 68, 821-831.
- [21] Zar, J. H. (1996). *Biostatistical Analysis*. New Jersey, USA, Prentice Hall International. V+662 pp.

Chapter 18

UREA AS AN ADDUCTOR FOR THE BRANCHED DRUG MOLECULES

A.K. Madan^{1} and Seema Thakral²*

1. Faculty of Pharmaceutical Sciences,
M.D. University, Rohtak 124-001, INDIA

2. GVM College of Pharmacy,
Sonipat 131 001, INDIA

1. INTRODUCTION

Urea has the interesting property of forming solid inclusion compounds (more commonly referred to as adducts in the earlier literature) with straight chain organic compounds [Zimmerschied *et al*, 1950]. An inclusion compound is a unique form of chemical complex formed by the inclusion of one kind of molecules, termed as *guest molecules /adductee /endocyte* into cavities of a crystalline framework composed of molecules of another kind (or into the cavity of one large molecule), called *host molecules /adductor*; the essential criterion being that “*guest*” be of a suitable size and shape so as to fit into a cavity within a solid structure formed by “*host*” molecules [Powell, 1948a; Findlay, 1962; Bhatnagar, 1968; Frank, 1975; Sinko, 2005]. Unlike the case of traditional chemical compounds, *favorable spatial complementarity* of guest and host subsystem and not the chemical reactivity determines whether inclusion can occur [Dyadin & Terekhova, 2004].

The general title for this class of compounds ‘*inclusion compounds*’ was first used by Schlenk [Schlenk, 1949] and new descriptions and modifications of available terms have been used to accommodate increase in new host molecular structures. Some of the examples are “*adducts*”, “*occlusion compounds*”, “*host-guest complexes*”, “*addition compounds*” “*clathrate complexes*”, “*molecular compounds*”, “*super molecular complexes*”, and “*supramolecular assemblies*’ [Frank, 1975; Weber, 1989; Sinko, 2005]. Various approaches

* For Correspondence: E-mail: madan_ak@yahoo.com, Phone: +91-98963-46211

and schemes for classification of inclusion compounds have been proposed by different researchers. Although the type of space in an inclusion compound cannot be precisely described without consideration of the included component, it is common place to speak of hosts as having closed cavities, channels or interlayer spaces [Powell, 1984]. Thus, while, Barrer divided inclusion compounds based on varying concept of host structure [Barrer 1949], Frank proposed a more “*convenient and workable*” classification based on organization of inclusion compounds by their structure and properties and classified them as polymolecular, monomolecular or macromolecular inclusion compounds [Frank, 1975]. Weber and Josel put forward a system of classification and nomenclature of inclusion compounds based upon host-guest interaction and topology of the host-guest aggregate, proposed to be applicable to the then known and future possible types of inclusion compounds [Weber & Josel, 1983]. Inclusion compounds/clathrates were also classified according to shape of cavity into cryptoclathrates (compounds having cage structure), tubuloclathrates (unidimensional non-intersecting or intersecting channel type inclusion compounds) and intercaloclathrates (layered inclusion compounds) [Dyadin & Terekhova, 2004]. These have also been divided into two general subtypes on the basis of the relative topological relationship between host and guest [Steed & Atwood, 2000] as per the following:

1. *Cavitands*: These are hosts possessing intramolecular cavities. Thus the cavity available for guest binding is an intrinsic molecular property of the host and exists both in solution as well as in the solid state. This is a typical feature of monomolecular clathrates and these hosts are exemplified by crown ethers, cyclodextrins, cryptands, rotaxanes and catenanes.

2. *Clathrands*: These are the hosts with extramolecular cavities and the guest molecules are located within the architecture of a solid host material. Association of host and guest components in these cases is strictly a solid phenomena exhibiting disassociation on dissolution in a solvent. The inclusion spaces within these solid hosts include a wide variety of topologies, such as linear or intersecting tunnels, isolated cages, and two-dimensional inter-lamellar regions within layered hosts. Zeolites, graphite, urea, thiourea, deoxycholic acid, tri-ortho-thymodite fall into this category. Within this broad range of these solid inclusion compounds, host molecules can be further subdivided into hard and soft hosts depending upon stability of host structure [Harris, 1997] as per the following:

Hard host are the host compounds which remain stable even after removal of the guest component.

Soft hosts are those in which the host structure undergoes substantial reorganization following removal of the guest component[s]. For inclusion compounds of soft hosts, the guest component generally acts as an essential template for not only the formation of the host structure but also for maintaining the stability of the host structure. Urea and thiourea inclusion compounds are the representative examples of this class [Harris, 1997].

Inclusion phenomena are quite widespread in chemistry and inclusion compounds have become one of the significant components of chemical structure and behavior [Powell, 1984]. There is a broad actual field of practical and research applications based upon inclusion compounds [Atwood & Steed, 2004; Vaidya, 2004]. Some of the more important and extensively studied host molecules along with the organization and topology of the cavities formed by these are summarized in **Table 1**.

Table 1 Characteristics of various adductors

S. No.	Name of the adductor	Organization of host molecules	Shape of the cavity	Size of the cavity (Å)	References
1	Urea	Polymolecular	Hexagonal channels	5.25	George and Harris, 1995
2	Thiourea	Polymolecular	Hexagonal channels	7	Harris, 1997
3	Deoxy-choleic acids	Polymolecular	Channel like	4	Bishop and Dance, 1989
4	4-4'-dinitrobiphenyl	Polymolecular	Face-centered channels	4	Rapson <i>et al</i> , 1946.
5	Hydroquinone	Hexa-molecular	Cage-like(open ended two interpenetrating cup)	4 (diameter of cage)	Hagan, 1962
6	Water (liquid or gas hydrates)	Two types			Frank, 1975
		a) 46 water molecules with 8 guest moieties.	Eight cage-like cavities 2 dedecahedrons 6 tetradecahedrons	5 6	Klotz, 1970
		b) 136 water molecules with 32 guest moieties.	24 dodecahedrons 8 dodecahedrons	16.5 7	Panka, 1968
7	Phenol	12 phenol molecules	Rhombohedral cage	-	Lahr and Williams, 1959
8	Dianin's compound	Hexamolecular	Hourglass shaped cage	11 Å long 6.2 Å long	Flippen and Karle, 1971
9	Tri-othymodite	Polymolecular	Elongated cage for of guest molecules (length < 9.5) Channel for guest molecules longer than 9.5.		Wlliams and Lawton, 1975
10	Cyclodextrins	Monomolecular	Ring-shaped enclosure α Cyclodextrins β Cyclodextrins γ Cyclodextrins	6 8 10	D'Souza and Lipkowitz, 1998
11	Zeolites	Macromolecular	Interconnected cavities	Variable	Nicoloni <i>et al</i> , 1987
12	Amylose	Polymolecular	Helical coils	8	Rundle and Balwin, 1943

Since there are numerous applications of inclusion compounds, therefore, it has always been desirable to constitute certain general guidelines to simplify easy construction of new clathrate compound [Davies *et al*, 1983; Weber, 1989]. However, most of the classical clathrate hosts have been discovered by accident and not via directed synthesis [Davies, 1981]. Efforts have also been made to create new host compounds simply by altering an individual section of a known host constitution [MacNicol *et al*, 1978; Weber, 1989]. However, easy construction of new clathrate compounds i.e. *Directed Host Design* with regard to numerous applications of clathrate compounds, is also being actively investigated [MacNicol & Wilson, 1976; Weber *et al*, 1984; Hart *et al*, 1985; Jacobs *et al* 2005].

A considerable amount of research effort in the study of inclusion compounds is dedicated to the applications in the pharmaceutical industry towards improvement of pharmaceutical characteristics. The problems faced by formulation development scientists during design and development of an optimum formulation are quite typical [Allen *et al*, 2005]. The recent trends in drug discovery has led to identification of probable drug moieties possessing higher molecular weight, greater $\log k_{(\text{octanol/water})}$ and reduced water solubility. Thus, approximately 40 % of the drugs being discovered are known to possess poor solubility and therefore their bioavailability upon oral administration is incomplete or irregular owing to low dissolution rate [Szejtli, 1997; Huh *et al*, 2007]. In case of the complete absorption, sometimes the time for orally administered drug to attain the minimum effective blood concentration is too long, tending to delay the onset of pharmacological action. Some of the drugs are chemically unstable and because of their autodecomposition, polymerization or degradation by atmospheric oxygen, moisture and light, a dosage form with satisfactory shelf life can not be formulated. Some drugs possess physical instability, which may be demonstrated by volatilization or sublimation of contents or by hygroscopicity [Yoshioka & Stella, 2000]. On the other hand, some of the good drug candidates have unpleasant odor or have bitter or irritating taste. Dose of some of the drug candidates is extremely low; therefore, content uniformity is naturally problematic. As a consequence of extremely high biological activity of these potent drugs, working with powders of such drugs is rather hazardous. Moreover, it is comparatively problematic to handle drugs in liquid state. [Szejtli, 1997; Allen *et al*, 2005].

Macrocyclic chemistry incorporating inclusion of a drug molecule with an appropriate host moiety can be considered as a viable solution for the above listed problems of drug formulation. Till date, an important tool with respect to exploitation of inclusion phenomena in improvement in pharmaceutical characteristics has been the use of cyclodextrins (CDs) as the host molecule [Szejtli, 1996; Loftsson *et al*, 2004a]. These starch derivatives interact via dynamic complex formation [Loftsson *et al*, 2004b] and other mechanisms in a way that camouflages undesirable physicochemical properties including poor dissolution profile and limited drug stability. CDs based formulations are being marketed for improving pharmaceutical characteristics as diverse as enhanced solubility and dissolution profile [Chowdary & Nalluri, 2000; Cavallari & Abertini, 2002], increased photostability [Loftsson & Peterson, 1998; Nagase *et al*, 2001], increased thermal stability in solid state [Cwiertnia *et al*, 1999], stability against intramolecular cyclization in solid state [Li *et al*, 2002], stability against hydrolysis, and hence increased shelf life [Uekama *et al*, 1983; Singhla *et al*, 2002], for colon-specific delivery and controlled drug release [Yano *et al*, 2002; Chowdary & Kamalakara, 2003], reduced irritation [Blanchard *et al*, 2000], taste masking of bitter drugs [Andersen *et al*, 1984], and as flavor stabilizing agents [Chittiteeranon *et al*, 2007]. The

database on CDs-drug complexes is increasing tremendously as evidenced by enormous number of research papers/ patents being reported during past 25 years.

However, in addition to the above listed advantages, there are quite a number of limiting factors which restrict the applicability of CDs to certain types of drugs, because not all the drugs are suitable for complexation in CDs. There are several general preconditions for the formation of medicinally useful CDs complex of a drug molecule, the important ones include; more than five atoms (C, P, S, N) forming skeleton of the drug molecule; drug solubility of less than 10 mg cm^{-3} ; drug melting point below 250°C (otherwise cohesive forces between the molecules are too strong), molecular mass between 100 and 400 and a low dose of the drug. Furthermore, a high K_a stability constant for drug-CD complex ($> ca. 10^4 \text{ dm}^3 \text{ mol}^{-1}$) may result in reduced bioavailability (as the complex is practically not absorbed; only the released molecularly dispersed drug molecules are absorbed) while a low stability constant ($> ca. 10^4 \text{ dm}^3 \text{ mol}^{-1}$) may upon removal of water lead to the formation of intimate mixture of drug and CDs rather than inclusion compound [Cramer *et al*, 1967; Stella *et al*, 1999]. With some drugs, complexation with CDs results in no essential advantages while with some, increased degradation rate and reduced shelf life have been reported possibly due to unfavorable steric arrangement of the drug in the complex [Chin *et al*, 1968; Bekers *et al*, 1991]. Although a study published in 1957 suggested that orally administered CDs were highly toxic [French, 1957], but subsequent animal toxicity studies in rats and dogs have shown this not to be the case. CDs are now approved for use in orally administered formulations [Thompson, 1997]. β -cyclodextrins, upon parental administration, is not metabolized but accumulated in the kidneys as insoluble cholesterol complex, resulting in nephrotoxicity [Irie & Uekama, 1997].

In comparison to CDs, no alternate adductor has been extensively investigated for pharmaceutical use. Among the established adductors, there is some limitation on to the choice of adductors available mainly owing to their specific toxicity e.g. thiourea, selenourea, hydroquinone or instability in intestinal fluids e.g. deoxycholeic acid. The new synthetic hosts which are being introduced recently are highly specific i.e. their molecular (or ionic) recognition capacity prefers a given ion or molecule. These types of hosts deliver highly specific and sensitive sensors, or entrapping agents, sequestrators, for specific ions. Thus these hosts have very restricted fields and amounts. Produced for a limited market, generally by complex synthetic procedures, majority of these hosts continue to be expensive specialty chemicals [Szejtli, 1997].

However, urea, an age old chemical and a component of normal physiological processes of body, is also known to form inclusion compounds with a variety of organic substances. Urea, as the major nitrogen-containing end product of protein metabolism by mammals, is synthesized in the liver through urea cycle and secreted into the blood stream (normal blood urea level: 2.5 -7.5 mmol/l blood). The adult human body discharges almost 50 g (1.8 oz) of urea daily. In addition small amount of urea is excreted in sweat along with sodium chloride [Nelson & Cox, 2005]. It can be naturally expected that the human organism is well adapted to urea within the physiological range of concentrations and even beyond. This may partly explain why urea has not been rigorously studied with toxicological tests. Nevertheless, urea appears to cause little or no toxicity to most mammalian species (ruminants are more sensitive because of microbial ammonia production) and humans at reasonable dose levels. Hence, urea is of low concern to human health [INCHEM, 1997]. An estimated human exposure (EHE) level for urea can only be given very crudely, and it can probably vary widely depending on the food consumed and as a tentative value, 3 g/day (about 40 mg/kg body weight/day) is

proposed. [INCHEM, 1997] Urea has been categorized as generally regarded as safe (GRAS) as per FAO/WHO [FAO, 1989]. Traditionally, US FDA has generally accepted as safe for oral dosage forms excipient ingredients that have been reviewed and approved or acknowledged as safe for use in food. Food ingredients that have been categorized as GRAS by Joint Expert Committee on Food Additives (JECFA) have generally been accepted as safe for use as excipient in oral dosage form of drug. [Pino & Sullivan, 2006]

Though extensive use of CDs has positioned them as an important enabling and functional excipients, there lies unlimited potential to explore urea inclusion compounds as a solution to problems associated with the formulation development of drug substances. Urea offers following distinct advantages over CDs:

- Urea is an ideal host for formulation of sparingly soluble drug into an immediate release dosage form. Owing to its excellent solubility in water (1000 mg/ml [Budavari, 1996] compared to ~ 500mg/ml for the most soluble CDs [Loftsson *et al*, 2004a], urea is expected to release the included endocytes instantaneously on coming in contact with water, irrespective of the value of the stability constant for drug–urea complex.
- Urea can act as an adductor for both linear aliphatic compounds and substituted cyclic compounds (through the modified technique), while CDs, owing to their large cage-like cavity, can include only substituted cyclic compounds [Ueda *et al*, 1999].
- Owing to larger cavity of CDs cages, there are chances of isomerization of guest molecules even when included within the cage. Hence, CDs are known to fasten photo-degradation of some of the drugs [Sortino *et al*, 2001]. In contrast, the guest molecules constrained within the narrow hexagonal tunnels formed by urea molecules are unlikely to isomerize owing to spatial limitations.
- Urea being a part of normal physiological processes, has been categorized as generally regarded as safe (GRAS) as per FAO/WHO [FAO, 1989]. With some of the derivatized CDs, issues need to be resolved regarding their toxicological potential [Rowe *et al*, 2003].
- Though pharmaceutical industry is a cost insensitive industry, but the very fact that urea is very cheap compared to CDs, can not be overlooked.

Thus, despite its unique characteristics like high solubility, stability, inexpensiveness, biodegradability and easy availability, urea has been overlooked by drug formulators. As a consequence, immense potential of urea as an adductor for drug molecules need to be explored for the improvement of various pharmaceutical characteristics of diverse nature.

2. UREA AS AN ADDUCTOR

Urea is quite versatile and has continued to demand attention ever since its discovery. Its laboratory synthesis from ammonia and cyanic acid dealt a deathblow to the vital force theory. This small molecule is biologically important, and has commercial as well as industrial utility [Mavrovic and Shirley, 1982]. Urea is used in many commercial protein

supplements in veterinary practice and is sometimes used in mixing feed on the farm. The first solid dispersions created for pharmaceutical applications were prepared utilizing urea as a matrix and sulfathiazole [Sekiguchi and Noboru, 1961] though urea has been investigated as a carrier for solid dispersions of drugs [Okonogi *et al*, 1997; Modi & Tayade, 2006; Habib & Attia, 1985]. However, for over the past 70 years a major amount of chemical research involving urea has been undertaken due to the capacity of urea to form inclusion compounds with a large variety of organic materials.

Urea, usually, reveals a tetragonal structure in X-ray diffraction patterns, depicting extensive hydrogen bonding, wherein each carbonyl oxygen is involved in a hydrogen bond with both anti hydrogen of each adjacent molecule. Urea lattice consists of ribbons of molecules linked in a head-to-tail fashion along the tetragonal *c*-axis [Zavodnik *et al*, 1999]. However, it was in 1940 that Bengen stumbled upon the fact that *n*-octyl alcohol and many unbranched organic molecules form an inclusion compound with urea. [Bengen, 1951; Bengen & Schlenk, 1949]. It is now well established that when subjected to crystallization in the presence of straight-chain hydrocarbons, urea generally forms a *hexagonal helical structure surrounding a canal like void space*. Different terms **canal**, **channel**, **tube**, **tunnel** have been used by various authors to describe the urea host cavities extended in one dimension [Bishop & Dance, 1988]. Weber and Josel proposed the terms **helical tubuland** for the host structure and **helical tubulate** for the host-guest complex [Weber & Josel, 1983]. Ever since this accidental discovery of urea adducts, the chemistry of urea inclusion compounds have received much attention and the novelty of urea-complex formation has prompted many research groups to investigate fundamental study of its characteristics.

The urea inclusion compounds generally crystallize in long, hexagonal prisms or occasionally as hexagonal plates (for example with cetyl alcohol). [Schlenk, 1949; Smith, 1952]. The unit cell is hexagonal and the structure has six urea molecules per unit cell (space group $p6_122$) [Bishop & Dance, 1988] (**Fig. 1**). The overall structure of the crystal is that of parallel tubes in which the hydrocarbon molecules are held together in a loose network of hydrogen bond between the nitrogen and oxygen atoms (**Fig. 2**). The urea molecule is coplanar with the walls of the hexagonal prism, and the prisms are packed into a distinctive honeycomb lattice. The lattice is stabilized by the maximum possible number of hydrogen bonds: the two donors by each NH_2 , and four acceptors by each oxygen atom [Takemoto & Sonoda, 1984]. Thus, the typical urea inclusion compound exists in a hexagonal crystal lattice, similar to the tetragonal lattice of pure urea in that there is extensive hydrogen bonding but dissimilar in that each anti-hydrogen is hydrogen bonded to different carbonyl oxygen. The hydrogen bonds between neighboring molecules in tetragonal urea form lead to a rather loose structure [Bishop & Dance, 1988].

Urea host channels have minimum van der Waals diameters of 5.5-5.8 Å [George & Harris, 1995]. A comparison of the diameter of urea channel with the cross section of *n*-octane, benzene, 3-methylpentane and 2, 2, 4-trimethylpentane revealed that whilst 3-methylpentane can be accommodated in the channel but 2, 2, 4-trimethylpentane cannot be accommodated. This determining factor as to whether or not a molecule can act as a guest molecule is thus its ability to fit into the space available in the urea channel [Schlenk, 1949].

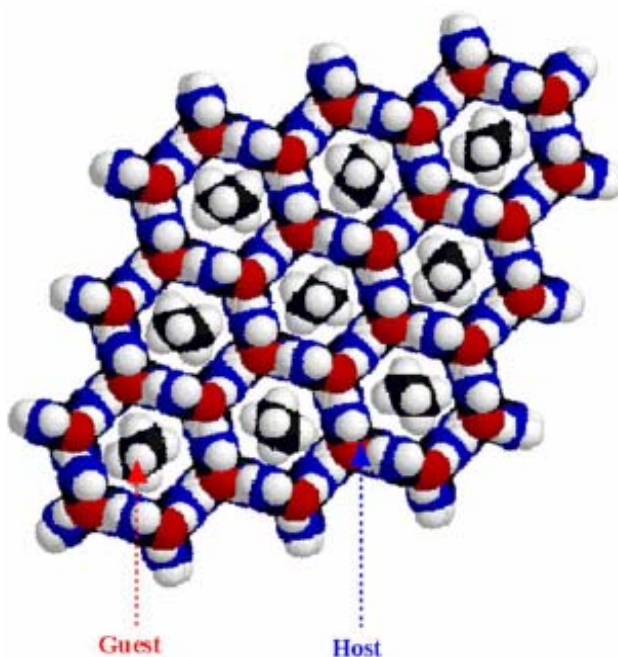


Fig. 1 The hexadecane-urea inclusion compounds at ambient temperature, showing nine complete tunnels with van der Waals radii, viewed along the tunnel axis. The guest molecules have been inserted into the tunnels illustrating orientational disorder (Reproduced from Harris, 1994 by permission of Royal Society of Chemistry).

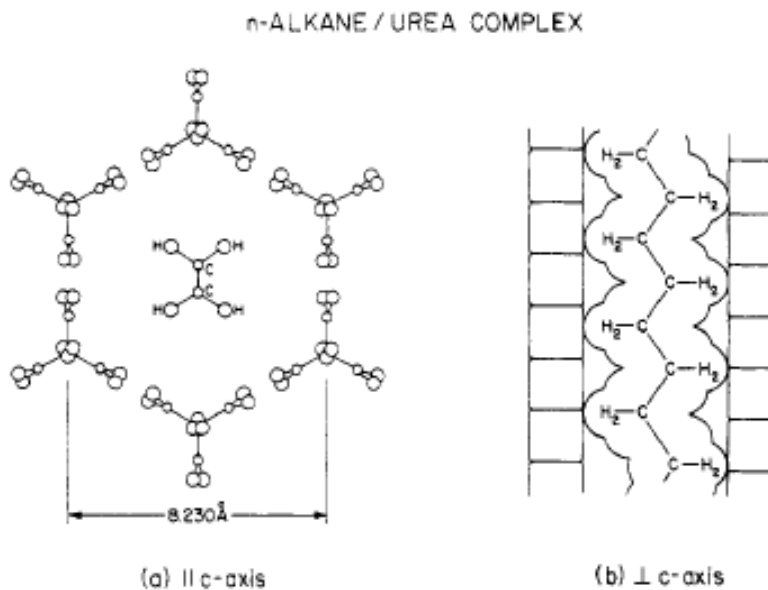


Fig. 2 Schematic model of complexes of n-alkanes in the hexagonal structure of urea (a) viewed along the long c axis of the n-alkane and (b) viewed perpendicular to the c axis. (Reproduced with permission from Suryanarayan et al, 1982. Copyright 2010, American Chemical Society)

Other than hydrocarbons, urea forms inclusion compounds with other linear organic compounds like alcohols, esters and ether derivatives, aldehydes, ketones, carboxylic acids, dicarboxylic acids, amines nitriles, thioalcohols and thioethers [Schlenk & Holman, 1950; Truter, 1951; Linstead & Whallwy, 1950; Schiessler & Flitter, 1950; Tied and Trutter, 1952; Aylward and Wood, 1956; Schiessler and Neiswender, 1957; Radell *et al*, 1961]. The degree of unsaturation or the isomerism of the double bonds does not seem to affect the ability of the guest molecules to form inclusion compounds [Schlenk and Holman, 1950]. Some degree of substitution of the carbon chain is allowed: e.g. 1-bromohexane forms an inclusion compound whilst 2-bromooctane does not. On the other hand 2, 2-difluorooctane does form an inclusion compound, probably because of the smaller size of the fluorine atoms. In the case of oxygen derivatives of *n*-alkanes, neither the hydroxyl group in 2-octanol, nor the carbonyl group in 2-heptanone prevents inclusion compound formation [Zimmerschild *et al*, 1950; Redlich *et al*, 1950]. Urea also forms inclusion compounds with a number of butane & butadiene derivatives, which on γ -irradiation can form **stereo-regular polymers** [White, 1960].

Competitive inclusion has also been studied between tetradecane and its isomers in binary mixtures. The more highly branched compounds form an insignificant amount (0.5-2%) of inclusion compound even when present at > 75% content in the binary mixture. The less highly branched hydrocarbons give about 1% inclusion compound at < 25% content and 8.5 - 10% inclusion compound at < 90% content in the binary mixture [Ovezov *et al*, 1977].

Thus, there are two main criteria which determine whether or not a particular urea inclusion compound will be formed, namely the *length of the carbon backbone of the guest*, and the *degree of branching* or substitution in the guest carbon skeleton [Fetterly, 1964]. In terms of the length of the carbon backbone, also called *anchor length*, the guests must have a carbon skeleton consisting of six or more atoms in order to successfully form an inclusion compound with urea. [Swern, 1955]. In terms of the degree of branching or substitution in a guest molecule, little or no branching or substitution is usually a requirement for urea inclusion compound formation with smaller guest molecules of a given family. With respect to larger molecules of a given family increasing the length of the carbon backbone increases the enthalpy of complexation, so a degree of branching or substitution is tolerable [Findlay, 1964; Hollingswoth & Harris, 1996].

It has been demonstrated that with some guest moieties, urea can also give inclusion compounds other than linear hexagonal tunnels like, rhombohedral space groups $R3c$ with α,ω -disubstituted alkanes 15 to 39 Å in length as guests [Lenne *et al*, 1968] or pseudo-hexagonal in orthorhombic space group $Pbcn$ with 1,4-dichlorobutane as guest [Otto, 1972].

The conventional urea inclusion compounds have been extensively investigated with respect to the structural aspects, dynamic and conformational properties of guest molecules, chemical reactions, and other applied aspects [Harris, *et al* 1991; Hollingswoth *et al* 1999; Weber *et al* 2000; Welberry, 2001; Harris, 2003]. Urea inclusion compounds have been extensively reviewed [Frank, 1975; Takemoto & Sonoda, 1984; Bishop & Dance, 1988; Hollingswoth & Harris, 1996; Harris, 1997; Harris, 2004; Harris, 2007].

3. GENERAL APPLICATIONS OF UREA INCLUSION COMPOUNDS

Since the urea inclusion compounds display a selectivity which is essentially governed by the size of available channels, much work has been carried out to exploit this selectivity in separating the components of mixtures on an industrial scale. Some of the significant applications are as listed below:

3.1 Petroleum industry

The formation of urea complexes with long chain organic compounds was found to be a powerful technique for isolation of alpha olefins and normal olefins from petroleum streams [Oswald, 1991; Gupta *et al*, 1998]. Both batch and fluidized-bed methods have been developed for these processes, although zeolites are now routinely used in such applications [Hollingsworth & Harris, 1996].

3.2 Chromatography

Urea inclusion compounds have been studied at laboratory scale as stationary phases, to obtain information on the behavior and properties of these compounds under gas chromatographic conditions, to draw conclusions concerning their stability and selectivity and finally to use them as stationary phases for analytical purposes. Similarly, interactions occurring in gas-solid chromatographic systems involving a common adsorbent or support coated with host molecules have also been studied using a wide-pore silica as a strongly absorbing substance and an inert chromatographic support. [Karr, 1955; Karr & Comberinati, 1965].

3.3 Purification of fatty acids

Owing to its low cost, low toxicity, and simplicity, fractionation based upon adduction with urea has been most frequently used for the purification of fatty acids from fish oil [Abu-Nasr, *et al*, 1954; Ratnayake *et al* 1988] and from several vegetal oils e.g. blackcurrant oil, borage oil, linseed oil, rapeseed oil [Hayes, 2002].

3.4 Non-linear optics

The potential to exploit inclusion phenomena in the field of non-linear optics has received considerable attention in recent years. The material studied was the urea inclusion compounds containing 1, 10-dibromodecane guest molecules, and its successful application as dichroic filter has been demonstrated. However, the commercial applications of these compounds in X-ray polarimetry is still to be exploited [Collins *et al*, 2002].

3.5 Improvement of handling characteristics

A novel solution to the handling of viscous, adhesive materials and potent or dangerous compounds is the formation of a urea inclusion compound with appropriate substances in these categories. Liquid non-ionic polyoxyethylene surfactants have been complexed with urea to form a solid powder which is easily handled [Varadaraj & Brons, 1998].

As evident from above, presently material applications based upon urea inclusion compounds are comparatively scarce in comparison to, for example to the wide range applications that exploit the properties of microporous inorganic materials. [Hollingsworth & Harris, 1996] However, the development of fundamental understanding of structural, dynamic and chemical properties of urea is expected to lead the way towards the future design and development of applications of these materials. Amongst the dynamic properties being exploited recently for development of applications in pharmaceutical industry, has been the phenomena of co-inclusion in presence of a suitable rapidly adductible molecule/ endocyte.

UREA CO-INCLUSION COMPOUNDS

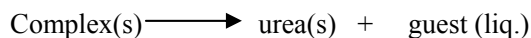
As evident from above discussion, urea is a well known adductor for linear long chain organic compounds and is used commercially as an adductor for linear molecules. In general, molecules containing cyclic groups such as benzene and cyclohexane do not form inclusion compounds with urea, presumably because these structural components are too wide to fit inside the narrow urea tunnel. However, 1-phenyl-octadecane in which the ring is located at the end of a long chain, forms inclusion compound with urea. The long chain of this compound is readily adducted and apparently the unit cell can easily withstand the distortions caused by occasional benzene group [Findlay, 1962]. Also, 3-methyl heptane (normally a non-adductible endocyte, NNAE) forms an adduct with urea only when a more slender hydrocarbon (e.g. $n\text{-C}_6\text{H}_{14}$) –a rapidly adductible endocyte (RAE) serves as a "**pathfinder**" [Findlay, 1962; Schlenk, 1949]. The endocytes possessing a sufficiently long n -alkane chain and hence easily adductible within urea channels are herein named as rapidly adductible endocytes (RAE) while sufficiently substituted and /or cyclic endocytes which are known to be non-adductible in urea are termed as normally non-adductible endocytes (NNAE) [Thakral & Madan 2008a].

The phenomena of co-inclusion of a NNAE in the presence of RAE in urea lattice were reported in literature [Swern, 1949] but not much investigated further. However, the aforementioned reports were exploited for co-inclusion of vitamin A palmitate in urea in the presence of a suitable RAE resulting in improved pharmaceutical characteristics of vitamin A palmitate [Madan and Grover, 1993; Madan, 1994]. Thus the possibility of co-inclusion of liquid or solid NNAE drugs in the presence of a RAE leading to formation of stable free flowing solid of urea based channel lattice complex was explored. Due to the presence of cyclic and/or substituted moieties in their molecular structure, the NNAE drugs are not known to get adducted in urea under any known conditions. However, in presence of a suitable RAE, small amount of NNAE drug co-adducts and formation of mixed crystals results. However, presence of either cyclic and/or highly branched groups in NNAE drug results in distortion of unit cells of hexagonal urea following co-inclusion with RAE. Any distortion of unit cells of

hexagonal urea leads to decrease in heat of decomposition of hexagonal urea and facilitate rapid dissolution. Since the drug is already at molecular level, therefore, the release of drug from the distorted lattice results in an almost rapid and instantaneous release of medicament. Moreover, when enclosed in a network of host molecules, the guest moiety is naturally shielded from the atmospheric oxygen. Further as the guest molecule is entrapped within the host framework, there is restricted movement along bond axis leading to reduced possibility of photoisomerisation. Hence, urea based inclusion complexes of drugs in the presence of a suitable RAE are characterized by improved solubility and stability profile. Urea co-inclusion compounds of NNAE drug(s) can be easily prepared through a modified technique which has been diagrammatically illustrated in **Fig. 3**.

Urea co-inclusion compounds of a NNAE drug can be prepared by initially dissolving NNAE drug in methanolic solution of urea. Subsequently, a known amount of RAE is incorporated in the above solution leading to an immediate precipitation of the crystals of urea co-inclusion compound. After keeping the solution at room temperature for 2-3 hrs, crystals can be separated from the mother liquor by vacuum filtration, dried and packed in suitable containers [Madan & Grover, 1993; Bajaj & Madan, 1994; Madan, 1994].

Considerable heat evolution is observed during formation of urea inclusion compounds, the magnitude of which provides information about the physicochemical nature of formation. Also, urea inclusion compounds are known to decompose endothermally below the melting point of urea, with a concurrent change in the crystal lattice of urea and loss in weight. Energetically, the decomposition involves the process [McAdie, 1963]:



The increase of heat content on decomposition or the heat of formation of urea inclusion compounds has been determined by various methods and found to be closely proportional to the length of carbon main chain of the compound to be included for a homologous series [Zimmerschied *et al*, 1950]. Heat of decomposition has been interpreted as mainly due to heat of fusion and difference in energy of hydrogen bonds between urea in the adduct and pure urea [Redlich *et al*, 1950]. Higher value of heat of decomposition can be expected for urea inclusion compounds having a guest molecule possessing longer carbon chain [McAdie, 1963]. Thus an estimate of heat of decomposition gives an insight into relative stability of the urea inclusion compound.

A calorimetric method was developed by Zimmerschied *et al* [Zimmerschied *et al*, 1950] to determine the stoichiometric ratio between urea and endocycle. The method involves addition of successive small increments of RAE to a mixture of urea and methanol in a calorimeter until temperature ceases to rise. Plotting rise in temperature vs. moles of RAE added gives a smooth sigmoid shape curve as depicted in **Fig 4**. From the point of intersection of the lines of extrapolation of the initial rate of temperature rise and final temperature level, the moles of RAE reacting with the present amount of urea can be easily calculated. [Zimmerschied *et al*, 1950]

However, the same procedure with slight modification can also be exploited for the determination of minimum ratio of RAE and drug for formation of co-inclusion compounds with urea. Thus, measurement of temperature rise following addition of small increments of RAE to a methanolic solution of urea containing excess of the NNAE drug is performed.

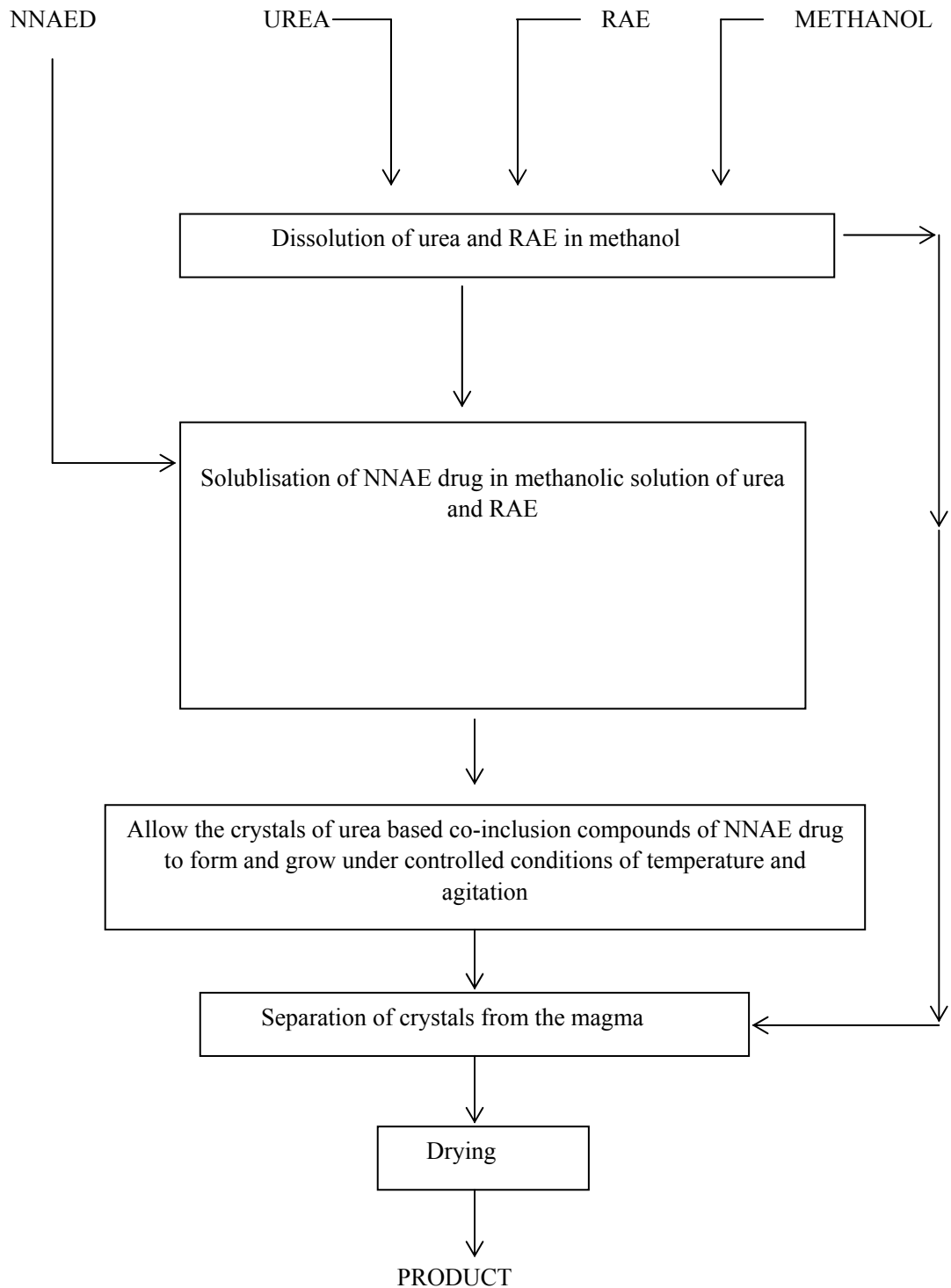


Fig. 3 Preparation of urea based co-inclusion compounds of NNAE drugs [Madan and Grover, 1993; Madan, 1994].

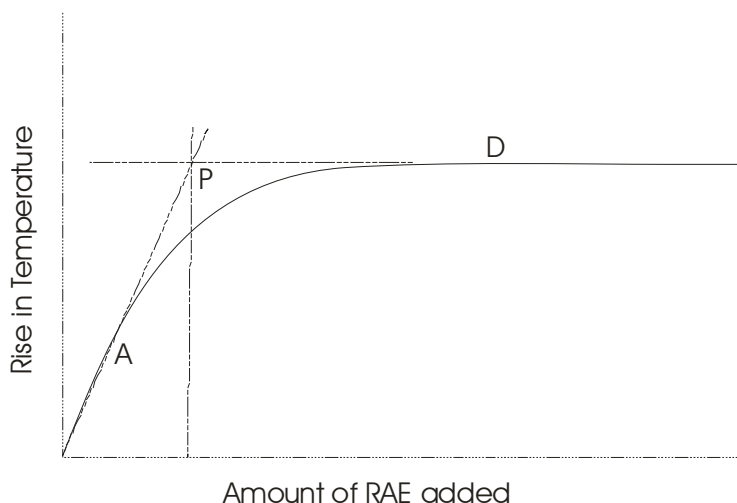


Fig. 4 Representative plot showing increase in temperature following incremental addition of RAE to methanolic solution of urea.

Plotting rise in temperature vs. moles of RAE added yields a characteristic curve depicted in **Fig. 5**. While the curve for addition of RAE to methanolic solution of urea had a smooth sigmoid shape, in presence of drug, the same curve demonstrated the following sequence of events i.e., an initial temperature rise (A), followed by intermediate final temperature (B), subsequent temperature rise (C) and then achievement of a final temperature (D). The second stage of temperature rise is due to displacement of NNAE with RAE as evidenced by the fact that the overall temperature rise is found to be similar to that of RAE alone. The point of intersection (P) of the lines of extrapolation of the initial rate of temperature rise and intermediate final temperature allows calculation of minimum amount of RAE required for adduction of NNAE in urea [Thakral & Madan 2008a; Thakral & Madan, 2008d].

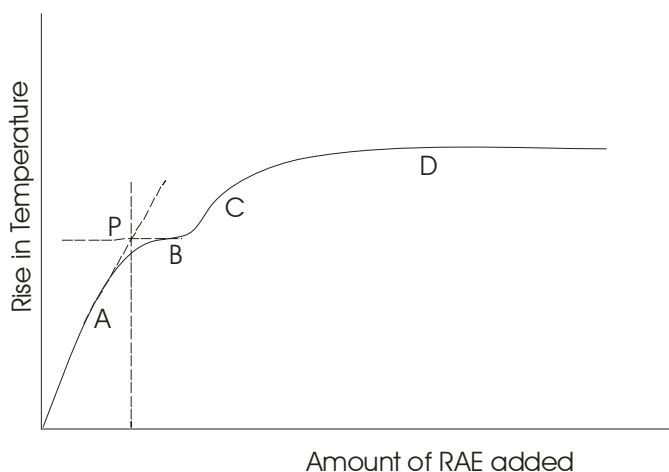


Fig. 5 Representative plot showing increase in temperature following addition of successive increments of RAE to methanolic solution of urea and NNAE drug

Once, the minimum amount of RAE required for adduction of a NNAE drug is known, urea inclusion compounds containing varying proportions of drug and RAE can be prepared. The extent of NNAE drug incorporated into urea co-inclusion compound determines degree of distortion of the unit cell of normal hexagonal urea. These distortions in turn destabilize the host-guest complex, as evident by decrease in heat of decomposition of hexagonal urea and hence facilitate rapid dissolution. Moreover, increasing the relative proportion of RAE will tend to impart better protection to the incorporated drug from the atmospheric oxygen and moisture. Hence, in brief, it is possible to vary proportion of NNAE drug and RAE in order to formulate each capsule containing unit dose of the drug with optimized dissolution and stability profile.

5. CHARACTERIZATION OF INCLUSION COMPOUNDS

The characteristic of inclusion compounds is the containment of guest molecules in empty spaces in a host lattice with weak host-guest interaction forces and stronger host-host interaction forces. One consequence of this is that the host molecules constitute a regular crystallographic lattice while the array of guest molecules can be disordered in some fashion. These characteristics have implications for structure determination by infrared spectroscopy, differential scanning calorimetry and X-ray diffraction analysis [Bishop & Dance, 1988].

5.1 Infrared Spectroscopy

IR spectra of pure urea indicate that molecule has planar and tetragonal structure, as evident by bands at 1682 cm^{-1} due to C=O stretching, at 1628 and 1599 cm^{-1} due to N-H bending vibrations, and at 1467 cm^{-1} due to the N-C-N antisymmetric stretching vibration. [Keller, 1948.; Waldron & Badger, 1950; Stewart, 1957]. These vibrational modes are sensitive to the structural transformation occurring when urea forms inclusion compounds with guest molecules. Thus IR spectra of all urea inclusion compounds have been shown to exhibit similar changes from the spectrum of tetragonal urea, although in varying degree [Fischer & McDowell, 1960].

The most striking change in adduct spectra occurs in the N-H stretching frequency region. The out-of-phase vibration occurring at 3436 cm^{-1} in the tetragonal urea is lowered to 3420 cm^{-1} , whereas the in-phase vibration is shifted from 3333 cm^{-1} to 3220 cm^{-1} in going from tetragonal to hexagonal unit cell. An increase in the strength of the hydrogen bond is apparent. Thus shorter hydrogen bonds of the tetragonal structure are situated in a much more favorable position for hydrogen bonding to occur during complex formation and the stability of the adduct is mainly due to these bonds. In addition to the van der waals forces, strong hydrogen bonds further stabilize the complexes. Although crystallography data shows no shortening of the bond length of longer hydrogen bonds, spectral analysis indicates a slight shortening [Yamaguchi *et al*, 1957; Barlow & Corish, 1959; Mecke & Kutzelnigg, 1960; Durie & Harrison, 1962].

5.2 Differential Scanning Calorimetry

Differential scanning calorimetry (DSC) is a technique for measuring the energy necessary to establish a nearly zero temperature difference between a substance and an inert reference material, as the two specimens are subjected to the identical temperature regimes in an environment heated or cooled at a controlled rate. While the DSC thermogram of pure urea exhibits a single melting endotherm characteristic of tetragonal form of urea (134.59 °C), the thermogram of urea inclusion compound is known to exhibit a low temperature endotherm corresponding to the complex decomposition. [McAdie, 1962 & 1963; White, 1988] Thus, urea inclusion compounds are reported to melt incongruently in two steps. The first step involves the collapse of urea inclusion compound to yield guest moiety and tetragonal solid urea while the second step involves melting of tetragonal urea [Farina *et al*, 1979}. Furthermore, the disappearance of sharp melting endotherm of otherwise crystalline NNAE drug may indicate the presence of the drug in an amorphous state.

5.3 Polycrystalline X-Ray Diffraction

It has been confirmed that X-ray powder diffraction analysis was the most positive method of confirming the formation of a complex. The honeycomb network made of urea has been shown to be the only crystalline part of the complex. The guest molecules are trapped and isolated from one another in the honeycomb and do not contribute to the crystal structure except slight distortions caused by bulky guests. Uncomplexed or dissociated tetragonal urea gave characteristic but different set of interplanar spacings from that of a complex. In analyzing the X-ray data, the following interplanar spacings are indicative of the urea inclusion compounds: 3.25 to 3.29, 3.39 to 3.41, 3.53 to 3.59, 3.83 to 3.88, 4.09 to 4.15 and 7.08 to 7.19 Å. [Radell & Brodman, 1965; Brodman & Radell, 1967].

The following interplanar spacings characterize tetragonal urea: 2.51 to 2.53, 2.80 to 2.84, 3.03 to 3.06, 3.6 to 3.63 and 3.97 to 4.04 Å. The 3.97 to 4.04 Å is the only exclusively characteristic line for uncomplexed urea. [Radell *et al*, 1964]

Furthermore, absence of major peaks of otherwise crystalline NNAE drug substantiates the fact that the drug may be in an amorphous state. These observations indicate transformation of NNAE drug from crystalline to amorphous state following the formation of an inclusion compound with urea in presence of RAE.

In addition to above, NMR [Zwanziger *et al*, 1999; Schmider *et al*, 2001], ESR [Griffith, 1964] and Raman [Casal, 1984; Guillaume *et al*, 1993; Smart *et al*, 1994] methods have also been used for studying structural and dynamic features of urea inclusion compounds.

6. IMPROVEMENT OF PHARMACEUTICAL CHARACTERISTICS USING UREA CO-INCLUSION COMPOUNDS

Global research efforts in pharmaceutical industry and academia are directed towards improvement of pharmaceutical characteristics of existing as well as new drugs in order to enhance quality and clinical performance of a pharmaceutical product. Among the numerous approaches investigated for the purpose, exploitation of co-inclusion phenomena for urea inclusion compounds has received attention lately and promising results have been achieved using the said approach. The improvements in physical and chemical properties of drugs is summarized below:

6.1 Improvement in dissolution profile of drugs

Drug dissolution (release of drug from the dosage form) is of primary importance for all conventional solid oral dosage forms in particular and can be rate limiting step for the absorption of drugs administered orally. Physicochemically, dissolution is the process by which a solid substance enters the solvent phase to yield a solution [Sinko, 2005]. Dissolution of the drug substance is a multistep process involving heterogeneous reactions/interactions between the phases of solute-solute and solute-solvent phases and at the solute-solvent interface. From the dosage form perspective, dissolution of the active pharmaceutical ingredient is often the rate determining step in presenting the drug in solution to the absorbing membrane [Kramer *et al*, 2005].

Dissolution test has turned out to be a critical test for measuring product performance and may be considered as an indicator of potential drug release and absorption characteristics of a product in humans as well as in animals. A dissolution test is often considered a surrogate for the assessment of bioavailability of drugs in the body. Tests to characterize the dissolution behavior of the dosage form are usually conducted using methods and apparatus that have been standardized virtually worldwide over past years, as part of the ongoing efforts to harmonize pharmaceutical manufacturing and quality control on global basis. Hence, over the last quarter century, the dissolution test has emerged as a most powerful and valuable tool to guide formulation development, monitor the manufacturing process, assesses product quality, and in some cases to predict *in vivo* performance of solid dosage forms [Hendriksen *et al*, 2003; Jamzad & Fassihi, 2006].

Co-inclusion of a NNAE drug having adequate anchor length inside the urea hexagonal channels in the presence of a suitable RAE has shown instantaneous and complete release of the included drug contents in the dissolution medium for various drugs. The technique demonstrated release of ~ 100% of drug content in the dissolution medium for urea co-inclusion compounds of drugs possessing adequate solubility like enalapril maleate [Thakral & Madan, 2007] and amiloride hydrochloride [Thakral & Madan, 2008a]. A marked improvement in dissolved percentage and dissolution efficiency with the urea co-inclusion compounds of these drugs was noticeable as compared to the same for pure drugs (**Fig. 6**).

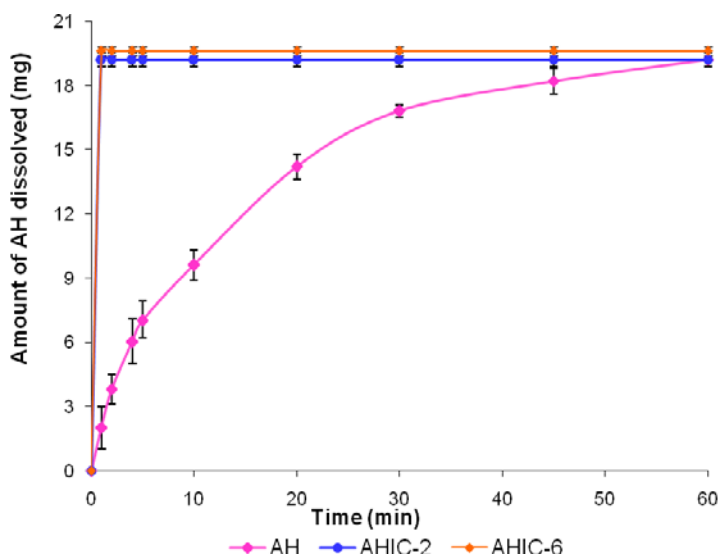


Fig. 6 Dissolution profiles of water soluble NNAE drug and drug-RAE-urea co-inclusion compounds containing varying proportions of drug and RAE. Each point is the average of three measurements; error bars indicate \pm standard deviation. (Drug: Amiloride hydrochloride [Thakral and Madan, 2008a])

With sparingly soluble drugs like, famotidine [Bajaj & Madan, 1994], *cis*-RA [Thakral & Madan, 2008b], gliclazide [Thakral & Madan, 2008c] and glipizide [Thakral & Madan, 2008e] however, a different dissolution profile was demonstrated (Fig. 7). When urea co-inclusion compound system of these drugs are exposed to an aqueous medium, the urea hexagonal host lattice dissolves rapidly and leads to an immediate release of the included guest (i.e. drug and RAE) at the molecular level. Thus, a high supersaturation ratio is developed upon addition of the contents to the dissolution medium. However, such a high supersaturation can not be sustained [Miller 1984] and it leads to the spontaneous/primary nucleation for obvious reasons. As these drugs possess limited aqueous solubility under the present dissolution conditions, the initially released drug molecules subsequently tend to crystallize in excess of solubility. This may be caused by non-sink conditions of the dissolution media. In case the drug possesses a high membrane permeability, the released drug molecules may rapidly permeate through biological barriers *in vivo* and a built-up of concentration at the site of dissolution may not actually occur. Thus complete dissolution and subsequent permeation of the drug can be expected *in vivo*. Urea inclusion compound formation can be exploited as a valuable tool for development of immediate release formulations for potent poorly soluble drugs possessing sufficient anchor length in their molecular structure [Thakral & Madan, 2008b].

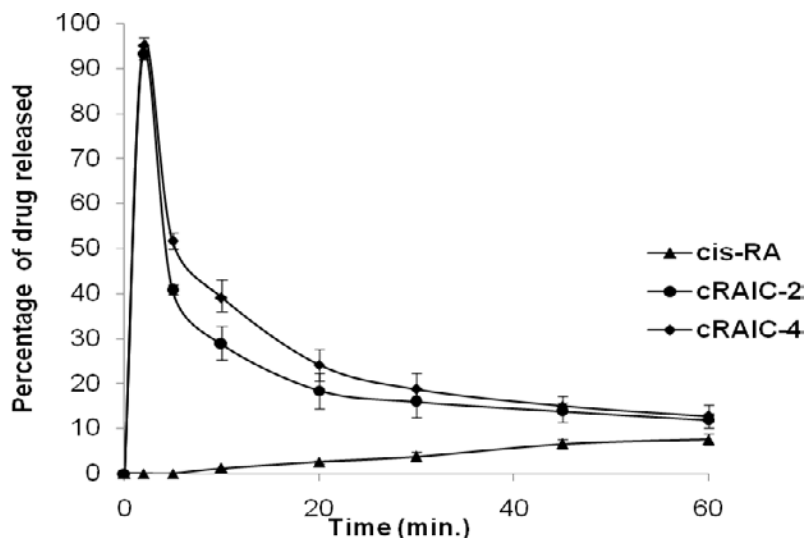


Fig. 7 Dissolution profile of sparingly water soluble drug and its co-inclusion compounds with urea containing varying proportions of drug and RAE. Each point is the average of three measurements; error bars indicate \pm standard deviation (drug: *Cis-retinoic acid*) [reproduced from Thakral and Madan, 2008b]

6.2 Good content uniformity

Progress in pharmaceutical research has produced very potent drugs, which require careful formulation and production in order to produce solid oral dosage forms with acceptable homogeneity and physical stability. Any failure to comply with content uniformity leads to either over dosage or under dosage, both of which are highly undesirable for obvious reasons. In drug manufacturing, it is a challenge to achieve content uniformity when mixing a small amount of one material with a much larger amount of another material [Sallam & Orr, 1983]. Even if the powder is properly formulated, there are greater chances of demixing or segregation of component due to difference in particle size and density difference attributed to continuous vibrations of the machines. In urea co-inclusion compounds, all the components - urea, NNAE drug and RAE, are bound together at the molecular level, thus alleviating any chances of demixing or segregation. The phenomena of urea inclusion compound formation have shown to impart good content uniformity to the resulting product which can be of great significance specifically with low dose drugs, possessing sufficient anchor length [Thakral & Madan, 2007, 2008 a,b,c and d]

6.3 Improved chemical stability

Stability of drugs towards exposure to light and oxidation in air is a topic of great practical interest but of considerable complexity. The primary focus of any controls instituted for product administration include precautionary product- labeling statement that product

efficacy and safety is maintained. International convention for harmonization (ICH) has issued guidelines and protocols for the conduct of stability studies of air/photo sensitive drugs [ICH].

Drug degradation is a complex phenomenon which may involve single or many degradation mechanisms. However, the chemistry of drug within an inclusion complex involve features, which may be quite distinct from those of uncomplexed substances since the interior of the cavity constitutes as isolated environment where the included species are usually present as single molecules restricting the photochemistry to intermolecular events [Glass *et al*, 2004]. Thus, when presented in the form of urea inclusion compound, an included moiety is contained within the narrow, hexagonal, parallel and non-intersecting channels stabilized by hydrogen bonds between urea molecules. The containment of guest moiety within these channels may tend to restrict its molecular motion and also prevent direct availability of incident photons to conjugated double bonds, which provide necessary energy for isomerization. Thus, urea inclusion compound formation tends to reduce photo/ air sensitivity of included guest species, which may be a degradation-labile drug having sufficient anchor length. The same has been demonstrated using vitamin A palmitate and *cis*-RA as the candidate drugs [Madan, 1994. Thakral & Madan, 2008b]

However, inclusion of a bulky guest is known to cause distortions in the vicinity of aromatic ring in the surrounding hexagonal channels formed of urea molecules. These distortions in turn, weaken the intermolecular hydrogen bonds and destabilize the structure. Increasing the proportion of RAE in the co-inclusion compound will reduce frequency of these distortions and may lead to improved stability of the urea lattice as a whole. Thus the extent of photoprotection can be further improved by modifying the relative proportion of RAE in the co-inclusion compound of drug in urea [Thakral & Madan, 2008b].

6.4 Improved moisture stability

Knowledge of the water content of pharmaceutical solids (proteins, drugs, and excipients) is essential to obtain a solid dosage form with optimal chemical, physical, microbial and shelf-life properties. Water content influences the chemical stability, microbial stability, flow properties, compaction, hardness, and dissolution rate of dosage forms of pharmaceuticals, proteins, biopharmaceuticals, nutraceuticals and phytochemicals. [Kontny & Zografí, 1995]. The inclusion compounds of urea, in which urea exists in its hexagonal form have been shown to exhibit quite reduced moisture sorption and improved moisture stability as compared to that of the pure tetragonal form of urea (**Fig. 8**). The fact, that urea inclusion compounds are more stable than the tetragonal form of urea, is also be supplemented by differential thermal analysis study. Also the co-inclusion of nicorandil, a moisture sensitive drug, in urea complex along with RAE has been demonstrated to lead to reduction in moisture sensitivity of the drug itself [Thakral & Madan, 2008d]. The drug being included in the hexagonal channels formed by urea molecules is not exposed to atmosphere and hence manifests reduced degradation.

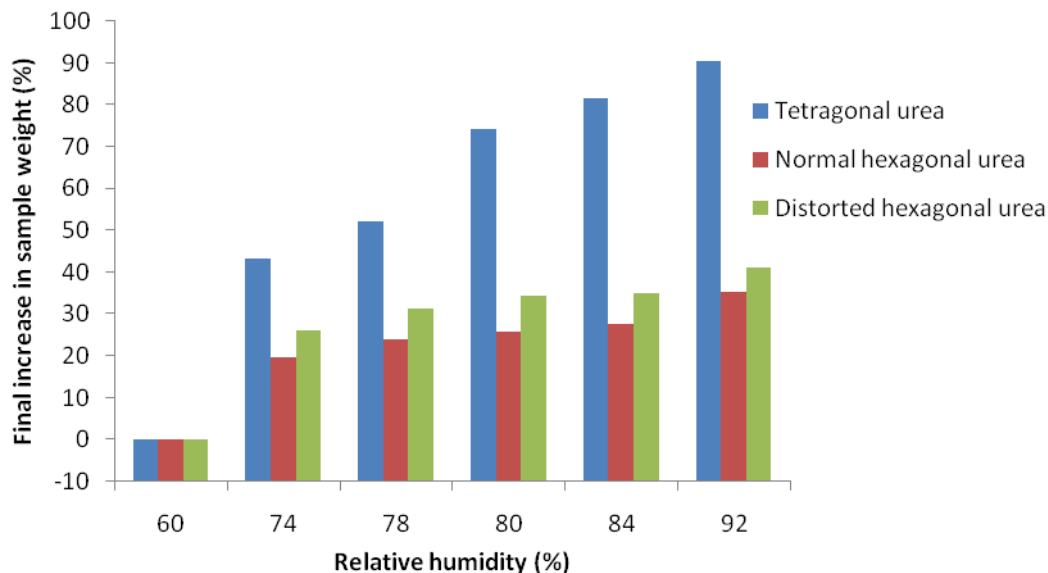


Fig. 8 Figure showing moisture uptake by samples of tetragonal urea, normal hexagonal urea (UOA) and distorted hexagonal urea (NRDIC) under various relative humidity conditions. (With kind permission from Springer Science + Business Media: Thakral and Madan, 2008d)

6.5 Safe handling characteristics

A novel solution to the handling of viscous, adhesive materials and potent or dangerous compounds having the minimum required anchor length is the formation of a urea inclusion compound. The approach has already been successfully utilized at commercial scale for easy handling of waxy surfactants and other compounds. Inclusion of drugs into hexagonal urea cavities as inclusion compounds can improve safe handling characteristic of drugs (specifically important with respect to anti-cancer drugs) not only by reducing transdermal absorption of drug but also by improved content uniformity for potent drugs [Thakral & Madan, 2008b].

6.6 Conversion of liquid drug into solid

Incorporation of liquid drug into urea lattice results in the transformation of a liquid drug into free flowing powder which can be easily formulated and handled. The same has been exemplified through use of vitamin A palmitate and vitamin E. [Madan, 1994; Bajaj & Madan, 2004]

Various applications of urea inclusion compounds for the improvement of pharmaceutical characteristics have been summarized in Table 2.

Table 2: Applications of urea as an adductor for improvement of pharmaceutical characteristics

S.No.	Name of the drug	Characters improved	Reference
1	Vitamin A palmitate	Improved photo and air-stability Liquid drug converted to free flowing solid	Madan, 1994
2	Famotidine	Improved dissolution profile	Bajaj and Madan, 1995
3	Vitamin E	Improved air-stability Liquid drug converted to free flowing solid	Bajaj and Madan, 1999
4	Amiloride hydrochloride	Improved dissolution profile, good content uniformity	Thakral and Madan, 2008a
5	Glipizide	Improved dissolution profile, good content uniformity	Thakral and Madan, 2008c
6	Enalapril maleate	Improved dissolution profile, good content uniformity	Thakral and Madan, 2007
7	<i>Cis</i> -retinoic acid	Improved dissolution profile Improved photostability Safe handling characteristics good content uniformity	Thakral and Madan, 2008b
8	Nicorandil	Improved moisture stability, good content uniformity	Thakral and Madan, 2008d
9	Gliclazide	Improved dissolution profile, good content uniformity	Thakral and Madan, 2008e

CONCLUSION

Urea – a widely used as an adductor for diverse range of linear organic compounds- can also be utilized for adduction of cyclic/ branched drug molecules having sufficient anchor length in the presence of suitable RAE, through a modified technique. Resulting co-inclusion compounds of drug in urea offer wide range of applications of diverse nature, which are exemplified, but not limited by, steep improvement in dissolution profile of poorly soluble drugs; improved content uniformity especially important for potent drugs; protection from moisture, light, atmospheric oxygen leading to improved stability and shelf life; conversion of liquid medicaments into solids and improvement in safe handling characteristics. Thus, urea inclusion compounds are gradually emerging as simple and viable substitute for solid dispersions for the improvement in dissolution profile of poorly soluble drugs and as substitute for microcapsules for stabilization of air/moisture/photo sensitive drugs. However, further studies are needed to exploit the full potential of urea as an adductor, which can be a promising alternative also to cyclodextrins for improvement of pharmaceutical characteristics. There are exciting prospects for the continued studies on urea co-inclusion compounds to unravel their potential applications.

REFERENCES

- Abu-Nasr, A.M.; Potts, W.M. & Holman, R.T. (1954). Highly unsaturated fatty acids. II. Fractionation by urea inclusion compounds. *J. Am. Oil Chemists Soc.* 31, 16-20.
- Allen, L.V.; Popovich, N.G. & Ansel, H.C., (2005). *Ansel's Pharmaceutical dosage forms and Drug Delivery Systems*. 8th Edn, Philadelphia: Lippincott Williams and Wilkins, 93-140.
- Andersen, F.M.; Bungard, H. & Mengel, H.B. (1984). Formation, bioavailability and organoleptic properties of an inclusion complex of femoxetine with β -cyclodextrin. *Int. J. Pharm.* 21, 51-60.
- Atwood, J. L. & Steed, J.W. (2004). *Encyclopedia of Supramolecular Chemistry*. Vol. 2, New York: Marcel Dekker, 1538-1549.
- Aylward, F. & Wood, P.D.S. (1956). Urea adducts of glyceryl esters. *Nature* 17, 146.
- Bajaj, V. & Madan, A.K. (1994). A process for preparation of urea complexes of vitamin E and its esters. *Indian Patent* 182620 dated 24th Oct.
- Bajaj, V. and Madan, A.K. (1995). Highly Distorted Urea based Channel Complexes as an Alternative to Solid Dispersions for Improving Content Uniformity and Dissolution Rate, *Proceedings of the First Regional Conference of IEEE Engineering in Medicine & Biology Society and 14th Conference of the Biomedical Engineering Society of India – An International Meet*, New Delhi, 4.67-4.68.
- Barlow, G.B. & Corish, P.J. (1959). Infrared absorption spectra of some urea complexes. *J. Chem. Soc.* 1706-1710.
- Barrer, R.M. (1949). *Quart. Rev.* 3, 293.
- Bengen, M. F. & Schlenk, Jr., W. (1949). *Experimentia* 5, 200.
- Bengen, M.F. (1951). *Angew. Chem.* 63, 207.
- Bekker, O.; Beijnen, J.H.; Kempers, Y.A.G.; Bult, A. & Underberg, W.J.M. (1991). Effect of cyclodextrins complexation on the chemical stability of doxorubicin and daunorubicin in aqueous solution. *Int. J. Pharm.* 72, 123-130.
- Bhatnagar, V.M. (1968). Clathrate compounds of urea and thiourea. *J. Struc. Chem.* 8(3),
- Bishop, R. & Dance, I.G. (1988). New type of helical inclusion networks. *Topics Current Chem.* 149, 139-188.
- Blanchard, J.; Ugwu, S.O.; Bhardwaj, R. & Dorr, R.T. (2000). Development and testing of an improved of phenytoin using 2-hydroxypropyl-beta-cyclodextrin. *Pharm. Dev. Technol.* 5, 333-338.
- Budavari, S., (1996). The Merck index. 12th edn. Merck &Co., NJ.
- Cammer, F.; Saenger, W. & Satz H.C. (1967) Inclusion compounds. XIX. The formation of inclusion compounds of alpha cyclodextrin in aqueous solution, thermodynamics and kinetics. *J. Am. Chem. Soc.* 89, 14-20.
- Casal, H. L. (1984). Raman spectroscopic determination of the integrity of urea inclusion compounds. *Appl. Spectro.* 38, 306-309.
- Cavallari, C.; Abertini, B.; Rodriguez, M.L.G. & Rodriguez, L. (2002). Improved dissolution behavior of steam granulated piroxicam. *Eur. J. Pharm. Biopharm.* 54, 65-73.
- Chenite, A. & Brisse, F. (1991). Structure and conformation of PEO in the trigonal form of the PAE urea complex at 173 K. *Macromol.* 24, 2221-2225.

- Chittiteeranon, P.; Soontaros, S. & Pongsawasdi, P. (2007). Preparation and characterization of inclusion complexes containing fixolide, a synthetic musk fragrance and cyclodextrins. *J. Inclusion Phenom. Macrocyclic Chem* 57, 69-73.
- Chin, T.; Chung, P. & Lach, J.L. (1968). Influence of cyclodextrins on ester hydrolysis. *J. Pharm. Sci.* 57, 44-48.
- Chowdary, K.P.R. & Kamalakara, R.G. (2003). Controlled release of nifedipine from mucoadhesive tablets of its inclusion complexes with β -cyclodextrin. *Pharmazie* 58, 721-724.
- Chowdary, K.P.R. & Nalluri, B.N. (2000). Nimesulide and beta-cyclodextrin inclusion complexes: physicochemical characterization and dissolution rate studies. *Drug Dev Ind Pharm.* 26, 1217-1220.
- Collins, S.P.; Laundry, D.; Harris, K.D.M.; Kariuki, B.M.; Bauer, C.L.; Brown, S.D. & Thompson, P.J. (2002). X-ray linear dichroism in an α,ω -dibromoalkane/urea inclusion compound and its application to polarization analysis of magnetic diffraction *J. Phys. Condensed Mater.* 14, 123- 129.
- Cammer, F.; Saenger, W. & Satz H.C. (1967) Inclusion compounds. XIX. The formation of inclusion compounds of alpha cyclodextrin in aqueous solution, thermodynamics and kinetics. *J. Am. Chem. Soc.* 89, 14-20.
- Cwiertnia, B.; Hladon, T. & Stobiecki, M. (1999). Stability of diclofenac sodium in the inclusion complex in the beta cyclodextrin in the solid state. *J. Pharm. Pharmacol.* 51, 1213-1218.
- D'Souza, V.T. & Lipkowitz, K.B. (1998). Editors. Cyclodextrins: Introduction. *Chem. Rev.* 98, 1741-1742
- Davies, J. E. D.; Lipkowski, J. & Orville-Thomas, W. J. (198). Preface. *J. Mol. Struct.* 75, 1.
- Davies, J. E. D.; Kemula, W.; Powell, H. M. & Smith, N. O. (1983). Inclusion compounds. Past, present and future. *J. Incl. Phenom. Macrocyclic Chem.* 1, 3-44.
- Durie, R.A. & Harrison, R.J. (1962). Effects of urea-adduct formation and physical state on the infra-red spectra of n-paraffin hydrocarbons. *Spectrochimica Acta* 18, 1505-1514.
- Dyadin, Y.A. & Terekhova, I.S. (2004). Classical description of inclusion compounds. In Atwood, J. L.; Steed, J.W. (eds.), *Encyclopedia of Supramolecular Chemistry*. Vol. 2, Marcel Dekker, New York, pp 253-260.
- FAO/WHO, (1989). Evaluation of certain food additives and contaminants. Thirty-third report of the joint FAO/WHO expert committee on food additives (JECFA). *World Health Organ Tech Rep Ser*, No. 776.
- Farina, Mario; Silvestro, G. Di & Grassi, M. (1979). Solid-liquid diagram of polyethylene-perhydrotriphenylene mixtures. Congruent melting of an inclusion compound containing a macromolecular constituent. *Macromol. Chem. Phys.* 180, 1041-1047.
- Fetterly, L.C. (1964). in *Non-stoichiometric compounds*. Mandelcorn, Academic Press, New York, 491.
- Findlay, R.A. (1962). Adductive Crystallization. In Schoen, H.M, Mcketta, J.J. (eds.), *Interscience Library of Chemical Engineering and Processing. New Chemical Engineering Separation Techniques. Vol. 1*, New York: Interscience Publishers, 257-318.
- Fischer, P.H.H. & McDowell, C.A. (1960). The infrared absorption spectra of urea-hydrocarbon adducts. *Can. J. Chem.* 38, 187-193.
- Flippen, J. L. & Karle, J. (1971). Heptanol as a Guest Molecule in Dianin's Compound. *J. Phys. Chem.* 75, 3566-3567.

- Frank, S.G. (1975). Inclusion Compounds. *J. Pharm. Sci.* 64, 1585-1604.
- French, D. (1957). The Schardinger dextrans. *Adv. Carbohydr. Chem.* 12, 189-260.
- George, A.R. & Harris, K.D. (1995). *J. Mol. Graphics* 13, 138-141.
- Glass, B.D.; Novak, C. & Brown, M.E. (2004). The thermal and photostability of solid pharmaceuticals- a review. *J. Thermal Anal. Calorimetry* 77, 1-22.
- Griffith, O. H. (1964). Electronic spin resonance and molecular motion of RCH_2CHOOR' radicals in X-irradiated ester- urea inclusion compounds. *J. Chem. Phys.* 41, 1093-1105.
- Guillaume, F.; Baghdadi, A. E. & Dianoux, A.J. (1993). Dynamics of alkyl-type chains in crystals. *Physica Scripta* 49, 691-694.
- Gupta, A. A.; Swamy, K. K.; Prakash, S.; Rai, M. M. & Bhatnagar, A. K. (1998). Process for recovery of solid and reusable urea from the urea adduction process. *United States Patent* 5847209.
- Habib, F. S. & Attia, M. A. (1985). Effect of Particle Size on the Dissolution Rate of Monophenylbutazone Solid Dispersion in Presence of Certain Additives. *Drug Dev. Ind. Pharm.*, 11(11) 2009 – 2019
- Hagan, M. (1962). *Clathrate Inclusion compounds*. Rienhold, New York, N.Y.
- Hart, H.; Lin, L.T.W & Ward, D.L. (1985). N,N' -ditritylurea, a versatile host for crystalline host-guest complexes. *J. Chem. Soc. Chem. Commun.* 5, 293-294.
- Harris, K.D.M.; Smart, S.S. & Hollingsworth, M.D. (1991). Structural properties of α,ω -dibromoalkane/urea inclusion compounds, a new type of interchannel guest molecule ordering. *J. Chem. Soc. Faraday Trans.* 87, 3423-3429.
- Harris, K.D.M. (1997). Meldola lecture: Understanding properties of urea and thiourea inclusion compounds. *Chem. Soc. Rev.* 76, 279-289.
- Harris, K.D.M. (2003). Local structural aspects of one-dimensional solid inclusion compounds. *Phase Transitions* 76, 205-218.
- Harris, K.D.M. (2004). Urea inclusion compounds. In Atwood, J. L.; Steed, J.W.(eds.), *Encyclopedia of Supramolecular Chemistry*. Vol. 2, Marcel Dekker, New York, pp 1538-1549.
- Harris, K.D.M. (2007). Fundamental and applied aspects of urea and thiourea inclusion compounds. *Supramol. Chem.* 9, 47-53.
- Hayes, D. (2002). Urea Inclusion Compound formation. *Inform* 13, 781-801.
- Hendriksen, B. A.; Felix, M.V. S.; Bolger, M.B. 2003. The composite solubility versus pH profile and its role in intestinal absorption prediction. *AAPS PharmSci*, 5 (1) Article 4 (<http://www.pharmsci.org>).
- Hollingsworth, M.D. & Harris, K.D.M. (1996). Urea inclusion compounds. In Atwood, J.L., *Comprehensive Supramolecular Chemistry, Chapter 4*, New York: Interscience Pub, 192-234.
- Hollingsworth, M.D.; Werner-Zwanziger, U.; Brown, M.E.; Chaney, J.D.; Huffamn, J.C.; Harris, K.D.M. & Sharon, P.S. (1999). Spring-loading at the molecular level: relaxation of guest-induced strain in channel inclusion compounds *J. Am. Chem. Soc.* 121, 9732-9734.
- Hoor, M.J. (1996). The formation of urea. Controverseries and confusion. *J. Chem. Edu.* 73, 42-45.
- Huh, K.M.; Lee, S.C.; Ooya, J. & Park, K. (2007). Polymeric delivery system for poorly soluble drugs. *Encyclopedia Pharm. Tech. Swarbrick, J.* 3rd edn, Vol 5, 2912.

- INCHEM, (1997). International Chemical Safety Cards. ICSC: 0595. Urea. OECD Screening Information dataset. By International Program on Chemical safety.
- International Conference on harmonization. 1997. "Guidelines for the photostability testing of new drug substances and products. *Federal Register* **62**, 27115-27122.
- Irie, T. & Uekama, K. (1997). Pharmaceutical applications of cyclodextrins: III. Toxicological issues and safety evaluation. *J. Pharm. Sci.* **85(11)**, 1142-68.
- Jacobs, A.; Nassimbeni, L.R.; Su, H. & Taljaard, B. (2005). Xanthenol clathrates: structure, thermal stability, guest exchange and kinetics of desolvation. *Org. Biomol. Chem.* **3**, 1319-1322.
- Jamzad, S.; Fassih, R. 2006. Role of surfactant and pH on dissolution properties of fenofibrate and glipizide- a technical note. *AAPS PharmSciTech.* **7**, E1-E6.
- Karr, C. Jr. (1955). Separation process utilizing urea paraffin chromatography. *United States Patent* 2,912,426, 18 April.
- Karr, C. & Comberati, J.R. (1965). The analysis of straight-chain aliphatics by urea partition chromatography and gas-solid chromatography. *J. Chromatog.* **18**, 394-397.
- Keller, W.E. (1948). Evidence of planer structure of urea. *J. Chem. Phys.* **16**, 1003-1004.
- Kontny, M.J. & Zograf, G. (1995). Sorption of water by solids. In *Physical characterization of pharmaceutical solids*. Brittain HG (ed.), Marcel Dekker Inc., New York, p. 387-418.
- Krammer, J.; Grady, L.T. & Gajendran, J. (2005). Historical development of dissolution testing. In Dressman, J.; Kramer, J. *Pharmaceutical dissolution testing*. Taylor & Francis, Boca Raton, pp 1-38.
- Lahr, P.H. & Williams, H.L. (1959). Properties of some rare gas clathrate compounds. *J. Phys. Chem.* **63**, 1432-1434.
- Lenne, H.U.; Mez, H.C. & Schlenk, W. (1968). The lengths of molecules in inclusion channels of urea and thiourea. *Justus Liebigs Ann.Chem.* **73**, 70-96.
- Li, J.; Guo, Y. & Zograf, G. (2002). The solid-state stability of amorphous quinapril in the presence of beta-cyclodextrins. *J Pharm Sci.* **91**, 229-243.
- Linstead, R.P. & Whallwy, M. (1950). The formation of crystalline complexes between urea and esters, and their application to separation of mixtures of esters. *J. Chem. Soc.* **80** 2987-2989.
- Loftsson, T. & Peterson, D.S. (1998). Cyclodextrin solubilization of ETH-615, a zwitterionic drug. *Drug Dev. Ind. Pharm.* **24**, 365-370.
- Loftsson, T.; Brewster, M.E. & Masson, M. (2004a). Role of cyclodextrins in improving oral drug delivery. *Am. J. Drug Deliv.* **2** (4), 1-15.
- Loftsson, T.; Masson, M. & Brewster, M.E. (2004b). Self association of cyclodextrins and cyclodextrin complexes. *J. Pharm. Sci.* **93**, 1091-9.
- MacNicol, D.D. & Wilson, D.R. (1976). New strategy for the design of inclusion compounds: discovery of the 'hexa-hosts' *J. Chem. Soc. Chem. Commun.* **13**, 494.
- MacNicol, D.D.; McKendrick, J.J. & Wilson, D.R. (1978). Clathrates and molecular inclusion phenomena. *Chem. Soc. Rev.* **7**, 65.
- Madan, A.K. (1994). Microencapsulation of low dose drugs. Ph.D. Thesis, IIT Delhi.
- Madan, A.K. & Grover, P.D. (1993). A process for preparation of urea based inclusion compounds of vitamin A esters. *Indian Patent* 180627 dated 20th Jan.
- Mavrovic, I. & Shirley, A.R. (1982). Urea In Kirk-Othner, *Encyclopedia of Chemical Technology*, Vol. 23, 3rd Edition, Wiley-Interscience Publication, New York, 548-574.

- McAdie, H.D. (1962). Thermal decomposition of molecular complexes. I Urea *n*-paraffin Inclusion Compounds. *Can. J. Chem.* 40, 2195- 2203.
- McAdie, H.D. (1963). Thermal decomposition of molecular complexes. III Urea inclusion compounds of monosubstituted aliphatic series. *Can. J. Chem.* 41, 2144- 2153.
- Miller, S. A. (1984) Liquid solid operations and equipments. In: Perry, R. H., Green, D. W. & Maloney, J. O. (eds) *Perry's chemical engineers' handbook*, 7th edn, McGraw-Hill Book Company, New York, pp 18–37
- Modi A. & Tayade, P. (2006). Enhancement of dissolution profile by solid dispersion (Kneading) technique. *AAPS PharmSciTech.*; 7(3): Article 68. DOI: 10.1208/pt070368
- Nagase, Y.; Hirata, M. & Wada, K. (2001). Improvement of some pharmaceutical properties of DY-9760e by sulfobutyl ether beta-cyclodextrin. *Int. J. Pharm.* 229, 163-172.
- Nelson, D.L. & Cox, M.M. (2005). Amino acid oxidation and the production of urea. *Lehinger Principles of Biochemistry*. 4th edition. W.H. Freeman and Company, New York. Chapter 18, 656-688.
- Nicolini, C.; Ramôa F.; Ribeiro, E.J. & Duckstein, L. (1987). Zeolites: Science and Technology. Springer, Netherland.
- Okonogi, S.; Yonemochi, E.; Oguchi, T.; Puttipipatkachorn, S. & Samamoto K. (1997). Enhanced dissolution of ursodeoxycholic acid from the solid dispersion. *Drug Dev Ind Pharm.* 23, 1115-1121.
- Oswald, A.A.; Chen, F.J.; Espino, R.L. & Peng, K.L. (1991). Multistep process for the manufacture of novel polyolefin lubricants. *United States Patent* 5017279.
- Otto, J. (1972). Bestimmung der Wirtsstruktur von 1,4-Dichlorbutan-Harnstoff, ein Beitrag zur Bestätigung eines allgemeinen Bauprinzips für die Einschlussverbindungen des Harnstoffs und des Thioharnstoffs. *Acta Crystallogr.* B28, 543-551.
- Ovezov, A.A.; Aidogdyev, A. & Sergeinko, S.R. (1977). *Izv. Akad. Nauk. Turkm. SSR, Ser. Fiz.-Tekh., Khim. Geol. Nauk*, 6, 72-75 (*Chem. Abs.*, 1978, 88, 79912).
- Pino, R.G. & Sullivan, T.N. (2006). Regulation in Pharmaceutical Excipients. In Katdare, A. and Chaubal, M.V., *Excipient development for pharmaceutical, biotechnology and drug delivery systems. Informa Healthcare*, New York, 46.
- Powell, H.M. (1948a). The structure of molecular compounds. Part IV. Clathrate compounds. *J. Chem. Soc.* 61-72.
- Powell, H.M. (1948b). Compound formation by molecular imprisonment. *Research (London)* 1, 353-357.
- Powell, H.M. (1984). Introduction. In Atwood, J.W.; Davis, J.E.D.; MacNicol, D.D. (eds.), *Inclusion Compounds*. Vol. 1, London : Academic Press , pp. 1-28.
- Radell, J.; Connolly, J.W. & Yuhas, L.D. (1961b). Urea inclusion compounds of alkynes. *J. Org. Chem.* 26, 2022-2024.
- Rapson, W.S. & Saunder, D.H. & Stewart, E.T. (1946). *J. Chem. Soc.* 1110.
- Ratnayake, W.M.N.; Olsson, B. & Matthews, D. (1946). *J. Chem. Soc.* Ackman, R.G. 1988. Preparation of omega-3-PUFA concentrates from fish oils via urea complexation. *Fat Sci. Technol.* 90, 381-386.
- Redlich, O.; Gable, C.M.; Dunlop, A.K. & Millar, R.W. (1950). Addition compounds of urea and organic substances. *J. Am. Chem. Soc.* 72, 4153-4160.
- Rowe, R.C.; Sheskey, P.J.; Weller, P.W. 2003. *Handbook of Pharmaceutical Excipients*. The Pharmaceutical Press, London, 412-413.

- Rundle R.E.; Baldwin, R.R. (1943). The configuration of starch and the starch-iodine complex. I. the dichroism of flow of starch-iodine solutions. *J. Am. Chem. Soc.* 65, 554-558.
- Sallam, E.A. & Orr, N.A. (1983). Studies relating to the content uniformity of ethinyloestradiol tablets 10 mg: effect of particle size of excipients. *Expo. Congr. Int. Technol. Pharm.*, 3rd, 28-37.
- Schiessler, R.W. & Flitter, D. (1950). Urea and thiourea adduction of C₅-C₄₂-hydrocarbons. *J. Am. Chem. Soc.* 74, 1720-1723.
- Schiessler, R.W. & Neiswender, D.D. (1957). Urea complexes of higher methylalkanes. *J. Org. Chem.* 22, 697-698.
- Schlenk, H. & Holman, R.H. (1950a). The urea complexes of unsaturated fatty acids. *Science*, 112, 19-20.
- Schlenk, H. & Holman, R.H. (1950b). Separation and stabilization of fatty acids by urea complexes. *J. Am. Chem. Soc.* 72, 5001-5004.
- Schlenk, W. (1949). Urea addition of aliphatic compounds. *Ann. Chem.* 565, 204-240.
- Schmider, J.; Fritsch, G.; Haisch, T. & Miller, K. (2001). Solid state ²H NMR studies of *n*-alkanes confined in solid matrices. *Mol. Cryst. Liq. Cryst.* 356, 99-109.
- Sekiguchi, K. & Noboru, O. (1961). Studies on Absorption of Eutectic Mixture. I. A Comparison of the Behavior of Eutectic Mixture of Sulfathiazole and that of Ordinary Sulfathiazole in Man. *Chem. Pharm. Bull.* 9(11), 866-872
- Sergienko, S.R.; Oveznov, A.A. & Aidogdyev, A. (1975). *Dokl. Akad. Nauk. SSSR.* 223, 1150; *Chem. Abst.* 83, 192506.
- Singhla, A.K.; Garg, A. & Aggarwal, D. (2002). Paclitaxel and its formulations. *Int. J. Pharm.* 235, 179-192.
- Sinko, P.J. (2005). *Martin's Physical Pharmacy and Pharmaceutical Sciences*. Lippincot Williams and Wilkins, Philadelphia.
- Smart, S.S.; Baghdagi, A.E.; Guillaume, F. & Harris, K.D.M. (1994). Conformational and vibrational properties of α,ω - dihalogenoalkane/urea inclusion compounds, a Raman scattering investigation. *J. Chem. Soc. Faraday Trans.* 90, 1313-1322
- Smith, A.E. (1952). The crystal structure of urea -hydrocarbon complexes. *Acta Crystallogr.* 5, 224- 235.
- Smith, A.E. (1955). Crystal structure and bond character of urea complexes. *Am. Chem. Soc. Div. Petrol. Chem. Symposium*, 33, 5-9.
- Sortino, S; Guiffrida, S.; De Guldi, G. et al, (2001). The photochemistry of flutamide and its inclusion complex with beta-cyclodextrin: Dramatic effect of microenvironment on the nature and on the efficiency of the photodegradation pathways. *Photochem Photobiol.* 73, 6-13.
- Steed, J.W. & Atwood, J.L. (2000). Definition and development of supramolecular chemistry. In *Supramolecular Chemistry*. John Wiley & Sons, Chichester, Chapter 1. pp 1-6.
- Stella, V.J.; Rao, V.M.; Zannou, E.A. & Zia, V. (1999) Mechanism of drug release from cyclodextrin complex. *Adv. Drug Del. Rev.* 36(1), 3-16.
- Stewart, J.E. (1957). Infrared absorption spectra of urea, thiourea, and some thiourea-alkali halide complexes. *J. Chem. Phys.* 26, 248 -254.
- Stuart, A.A.V. (1956). On the infrared spectrum of urea in urea-cetane complex. *Reucil*, 75, 907-911.

- Suryanarayana, D.; Chamulltrat, W.; Kavan, L. (1982). ESR characterization of the dynamic properties of urea-n-alkane adducts using peroxy spin probes. *J. Phys. Chem.* 86, 4822-4825.
- Swern, D. (1955) Urea and thiourea complexes in separating organic compounds. *Ind. Eng. Chem.* 47, 216-221.
- Szejtli, J. & Osa, T. (1996). *Comprehensive Supramolecular Chemistry, vol. 3, : Cyclodextrins, Pergamon, Oxford*, 1996.
- Szejtli, J. (1997). Utilization of cyclodextrins in industrial products and processes. *J. Mater. Chem.* 7, 575-587.
- Takemoto, K. & Sonoda, N. (1984). Inclusion compounds of urea, thiourea and selenourea. In Atwood, J.W., Davis, J.E.D., MacNicol, D.D. (eds.), *Inclusion Compounds*. Vol. 2, Academic Press, London, pp. 47-67.
- Thakral, S. & Madan, A.K. (2007). Urea inclusion compounds of enalapril maleate for improvement of pharmaceutical characteristics. *J. Pharm. Pharmacol.* 59 (11) 1501-1507.
- Thakral, S. & Madan, A.K. (2008a). Adduction of amiloride hydrochloride in urea through a modified technique for the dissolution enhancement. *J. Pharm. Sci.* 97, 3, 1191-1202.
- Thakral, S. & Madan, A.K., (2008b). Urea co-inclusion compounds of 13-*cis* retinoic acid for simultaneous improvement of dissolution profile, photostability and safe handling characteristics. *J. Pharm. Pharmacol* 60, 7, 823-900.
- Thakral, S. & Madan, A.K. (2008c). Urea inclusion compounds of glipizide for improvement in dissolution rate. *J. Inclusion Phenom. Macrocyclic Chem.* 60, 203-209.
- Thakral, S. & Madan, A.K., (2008d). Reduction in moisture sensitivity/ uptake of moisture sensitive drugs through adduction in urea. *J. Pharm. Innovation*, 3, 4, 249-257.
- Thakral, S. & Madan, A.K. (2008e). Improvement of dissolution profile of gliclazide through co-inclusion in urea. British Pharmaceutical Conference 2008, Manchester, UK, 7-9th Sept, 2008.
- Thompson, D.O. (1997) Cyclodextrins-enabling excipients: their present and future use in pharmaceuticals. *Crit. Rev. Ther. Drug. Carrier Syst.* 14, 1-104.
- Tied, J. & Trutter, E.V. (1952). The component of wool wax. Part I. The Aliphatic alcohols. *J. Chem. Soc.* 4628-4630.
- Truter, E.V. (1951). Urea complexes of some branched-chain and cyclic esters. *J. Chem. Soc.* 2416-2419.
- Ueda, H.; Wakamiya, T.; Endo, H.; Nagase, H.; Tomono, K. & Nagai, T. (1999). Interaction of cyclomaltonaose (delta-CD) with several drugs. *Drug Dev Ind Pharm* 25, 951-955.
- Uekama, K.; Fujinaga, T. & Hirayama, F. (1983). Improvement of the oral bioavailability of digitalis glycosides by cyclodextrin complexation. *J. Pharm. Sci.* 72, 1338-1341.
- Uekama, K.; Ikegami, K. & Wang, Z. (1992). Inhibitory effect of 2-hydroxypropyl- β -cyclodextrin on crystal-growth of nifedipine during storage: superior dissolution and oral bioavailability compared with polyvinylpyrrolidone K-30. *J. Pharm. Pharmacol.* 44, 73-78
- Vaidya, S. (2004). Clathrates – An exploration of the chemistry of caged compounds. *Resonance* 9, 18-31.
- Varadaraj, R. & Brons, C.H. (1998). Urea-surfactant clathrates and their use in bioremediation of hydrocarbon contaminated soils and water. *United States Patent* 5705690, 6. Jan.

- Vasanthan, N.; Shin, I. D. & Tonelli, A. E. (1996). *Macromol.* 29, 263.
- Waldron, R.D. & Badger, R.M. (1950). The planarity of urea molecule. *J. Chem. Phys.* 18, 566.
- Weber, Th.; Boysen, H. & Frey, F. (2000). Longitudinal positional ordering of *n*-alkane molecules in urea inclusion compounds. *Acta Crystallogr.* B56, 132-141.
- Weber, E. (1989). Clathrate chemistry today-Some problems and reflections. *Topics Current Chem.* 140, 3-20.
- Weber, E.; Csoregh, I.; Stensland, B. & Czugler, M. (1984). A novel clathrate design: selective inclusion of uncharged molecules via the binaphthyl hinge and appended coordinating groups. X-ray crystal structures and binding modes of 1,1'-binaphthyl-2,2'-dicarboxylic acid host/hydroxylic guest inclusions. *J. Am. Chem. Soc.* 106, 3297-3299.
- Weber, E. & Josel, H.P., (1983). *J. Incl. Phenom.* 1, 79.
- Welberry, T.R. (2001). Diffuse X-ray scattering and strain effects in disordered crystals. *Acta Crystallogr.* A57, 244-255.
- White, D.M. (1960). Stereospecific polymerization in urea canal complexes. *J. Am. Chem. Soc.* 82, 5678-5685.
- Williams, D.J. & Lawton, D. (1975). Deviations from C₃ symmetry of the tri-O-thymotide molecule in different crystalline environments.: X-ray determinations of the unsolvated form and of typical cavity and channel inclusion compounds. *Tetrahedron Lett.* 16, 111-114.
- Wu, N.; Fu, L.; Su, M.; Aslam, M.; Wong, K.C. & Dravid, V.P. (2004). Interaction of fatty acid monolayers with Cobalt nanoparticles. *Nano Lett.* 4, 383-386.
- Yano, H.; Hirayama, F.; Kamada, M.; Arima, H. & Uekama, K. (2002). Colon specific delivery of prednisolone-appended alpha-cyclodextrin conjugate: alleviation of systemic side effect after oral administration. *J Control Release* 79, 103-112.
- Yoshioka, S. & Stella, V.J. (2006). *Stability of drugs and dosage forms*. Springer, Netherlands, p106-107.
- Zavodnik V.; Stash, A.; Tsirelson, V.; Vries, R. & Feil, D. (1999). Electron density study of urea using TDS-corrected X-ray diffraction data: quantitative comparison of experimental and theoretical results. *Acta Cryst.* B55, 45 -54.
- Zimmerschied, W.J.; Dinerstein, R.A.; Wietkamp, A.W. & Marschner, R.F. (1949). Complexes of urea with linear aliphatic compounds. *J. Am. Chem. Soc.* 71, 2947.
- Zwanziger, U.W.; Brown, M.E.; Chaney, J.D.; Still, E.J. & Hollingsworth, M.D. (1999). Deuterium NMR studies of guest motions in urea inclusion compound of 1,6-dibromohexane with analytical evaluation of spectra in fast motion limit. *Appl. Magn. Reson.* 17, 265-281.

INDEX

A

- absorption, 71, 86, 95, 160, 179, 182, 185, 190, 195, 201, 203, 205, 218, 258, 260, 297, 356, 385, 401, 403, 412, 420, 425, 430, 455, 456
absorption coefficient, 195, 258
absorption spectra, 182, 205, 260, 403
acceleration, 138, 402
acceptor, 22, 76, 87, 106, 166, 218, 405
accessibility, 276
accidental, 20
acclimatization, 458
accommodation, 35, 110
accounting, 92, 93
accuracy, 29, 79, 88, 258, 261, 311
acetate, 27, 29, 36, 72, 126, 232, 234, 235, 236, 271, 387, 390, 418, 426, 430
acetic acid, 155, 170, 355
acetone, 72, 73, 96
acetonitrile, xv, 72, 73, 74, 108, 155, 170, 202, 203, 205, 306, 313, 315, 317, 393, 397, 446, 450, 451
acetophenone, 366
achievement, 233
acidic, xi, xv, 20, 25, 26, 28, 32, 38, 39, 41, 61, 72, 149, 158, 161, 166, 181, 182, 189, 190, 206, 208, 215, 232, 233, 325, 336, 394, 446, 451
acidification, 33, 306
acidity, 26, 31, 32, 72, 166, 275
acoustic, 85
acrylate, 384
acrylonitrile, 243
activated carbon, 71
activation, xvi, 86, 183, 244, 406, 435, 446
activation energy, 183
acute, xvii, 453, 458, 462
acylation, 390
adamantane, 110, 132
additives, 152, 168, 246, 343
adducts, xii, 69, 71, 93, 108, 194
adenine, 372
adenosine, 297
adhesive force, 333
adipate, 110
adjustment, 132, 457
administration, 306, 318, 458, 462
ADP, 197
adsorption, 71, 85, 86, 89, 95, 164, 167, 168, 243, 246, 249, 401
adsorption isotherms, 167, 168
aerobic, 150
Ag, 74, 186, 212, 216, 218, 321, 337
age, 457
agent, xviii, 23, 148, 161, 165, 170, 306, 330, 333, 368, 391, 457, 461, 478, 479, 484
agents, xvi, xvii, 20, 23, 156, 283, 301, 343, 353, 363, 453, 454, 455, 481
aggregates, 53, 75, 76, 80, 179, 244, 246, 249, 402, 403, 413
aggregation, 243, 246, 256, 276, 277
agricultural, 233, 246
agriculture, 243, 244, 246, 249, 485
aid, 26, 39, 132, 137
air, 85, 88, 92, 369
alanine, 275, 348, 349, 351, 353, 354, 356, 362
albumin, 406
alcohol, 30, 31, 72, 111, 150, 158, 243, 345, 366, 392, 405, 436, 446
alcohols, 73, 77, 111, 112, 122, 159, 256, 344, 356, 392, 446
aldehydes, 239, 383, 388, 414
alicyclic, 156, 162
aliphatic amines, 181, 186
alkali, xvi, 21, 57, 73, 75, 91, 109, 306, 311, 315, 318, 320, 321, 322, 329, 332, 346, 381, 388, 390, 393
alkaline, xi, xvi, 20, 23, 25, 26, 27, 38, 111, 181, 197, 201, 202, 203, 206, 222, 245, 318, 370, 381, 393

- alkaline earth metals, 222
 alkaline phosphatase, 370
 alkaloids, 160, 363
 alkane, 166, 303
 alkanes, 91, 110
 alkenes, 239
 alkylation, 364, 373, 385, 388
 alpha, 370
 alternative, xviii, 60, 92, 180, 466, 478, 481, 483, 484
 alternatives, xvii, 466, 477, 479
 alters, 73, 156
 Amadori, 245
 ambivalent, 24
 amide, 22, 34, 57, 149, 151, 152, 155, 215, 273, 344, 350, 356, 357, 399, 448
 amine, xi, 20, 34, 37, 39, 149, 150, 151, 152, 155, 156, 158, 159, 160, 162, 170, 187, 197, 200, 215, 338, 345, 346, 348, 357, 390, 405, 413, 414, 420, 445, 450
 amines, xi, 20, 35, 73, 149, 153, 182, 187, 188, 344, 347, 356, 366, 371, 387, 436
 amino groups, 24, 32, 37, 152, 160, 163, 286, 394
 aminoglycosides, 149
 ammonia, 152, 347
 ammonium, 22, 24, 26, 35, 39, 40, 43, 49, 59, 155, 249, 346, 348, 396, 406, 445
 ammonium salts, 24, 396
 amorphous, 401
 amphetamine, 393, 404
 amphiphilic compounds, 253
 amphoteric, 152
 amplitude, 84
 amyloid, 276
 amylopectin, xiv, 231, 232, 234, 241, 243
 anaerobic, 150
 analgesics, 283
 analog, 159, 161, 162, 327
 analytical tools, 330
 anatase, 401
 anger, 471
 aniline, xiv, 86, 281, 284, 285, 292, 293
 animals, 458, 464
 anion, 40, 321, 323, 448, 449, 450
 anions, 227, 234, 323, 435
 anisotropy, 57, 259
 ANOVA, 481
 antagonistic, 478
 antagonists, 157
 antenna, 195
 anthracene, xiii, 109, 177, 181, 186, 201, 210, 356
 antibacterial, 485
 antibacterial properties, 485
 antibiotic, 149, 150, 151, 152, 154, 155, 168, 169, 349, 363
 antibiotics, 147, 148, 149, 152, 153, 155
 anticancer, 475
 antioxidant, 454
 argument, 314
 arithmetic, 272
 aromatic compounds, 302
 aromatic diamines, 414
 aromatic hydrocarbons, 181
 aromatic rings, 76, 81, 86, 90, 124, 149, 150, 152, 153, 393, 399
 ASI, 225
 Asia, 272
 Asian, 228, 342, 451
 aspirin, 304
 assessment, 91, 321
 assignment, 32, 34, 37, 58, 296, 421
 assumptions, 36, 260
 asymmetric molecules, 33
 asymmetric synthesis, 138
 asymmetry, 329
 atmosphere, 419, 423, 471, 480
 ATP, 195, 196, 197
 attachment, xvi, 24, 275, 343, 362, 370, 381
 attacks, 445, 446
 attractiveness, 382
 availability, 21, 179, 283, 284, 297, 330, 383, 393, 483
 averaging, 42, 468
 avoidance, 32
 awareness, 478
 azacrown ethers, 20, 21
 A β , 276

B

- back, xv, 57, 194, 325, 329, 336, 383
 bacteria, 150, 151, 152, 169
 bacterial, 169, 246, 349
 bacterial strains, 349
 bacterium, 155
 barbiturates, 161
 barley, xiii, 231, 237, 238, 239, 240, 241
 barrier, 95, 336
 barriers, 56
 basicity, 23, 24, 25, 27, 50, 58, 59, 166, 232, 233
 basis set, 473
 battery, 79
 behavior, 27, 36, 39, 53, 56, 57, 59, 60, 61, 106, 107, 115, 119, 120, 123, 132, 133, 139, 160, 164, 168, 169, 190, 201, 236, 237, 243, 244, 248, 317, 368, 382, 413, 426, 450, 458

bell, 186
 benefits, 478
 benzene, 56, 72, 73, 77, 85, 86, 109, 112, 120, 125, 137, 163, 182, 285, 286, 292, 293, 294, 299, 303, 390, 414, 416, 420
 beverages, 148
 bias, 449
 bicarbonate, xvi, 435, 436
 binding energies, 86
 binding energy, 87, 183
 binuclear, 186, 221
 bioaccumulation, 243
 bioassay, 480, 481, 482, 483
 bioassays, xviii, 477, 479, 483
 bioavailability, 454, 455, 462
 biochemistry, 106, 282, 343
 bioenergetics, 195
 biofuels, xiii, 231, 233, 241
 biogenic amines, 371
 biological activity, 147, 283, 329, 361
 biological systems, xiii, xvi, 70, 71, 231, 347, 435
 biologically active compounds, xiv, 251, 252
 biomacromolecules, 106
 biomass, 233
 biomedical applications, 23
 biomimetic, 360
 biomolecular, 31
 biomolecules, xiii, 231, 304, 403
 biosynthesis, 283
 biotechnologies, 382
 birth, 411
 bismuth, 234
 blends, 156
 BLM, 329, 332
 blocks, xvi, 344, 352, 362, 381, 382, 413, 450
 body weight, 458, 462
 boiling, 87, 91
 bonding, 76, 84, 108, 155, 158, 159, 160, 162, 164, 188, 196, 254, 255, 257, 275, 276, 282, 285, 292, 296, 302, 318, 334, 344, 346, 349, 357, 362, 370, 394, 397, 436, 441, 445, 450, 472
 bonds, 21, 22, 24, 33, 35, 42, 43, 44, 49, 50, 51, 53, 54, 55, 57, 59, 84, 90, 156, 161, 196, 197, 234, 235, 242, 253, 282, 316, 334, 347, 372, 403, 419, 424, 444
 borate, 307, 316
 borderline, 206
 bottleneck, 253
 boundary conditions, 118
 bovine, 406
 breakdown, 333
 bromine, 429
 Bruker DRX, 308

buffer, xvi, 166, 262, 271, 310, 353, 368, 453, 455, 456, 458
 building blocks, xvi, 344, 352, 362, 381, 382, 413, 450
 bypass, 178

C

Ca²⁺, 23, 74, 195, 197, 201, 222, 245
 cadmium, 337
 caffeic acid, xvii, 465, 466, 467, 469, 470
 calcitonin, 276
 calcium, 242, 245, 249
 calibration, 216, 456
 calixarenes, xii, 69, 70, 71, 72, 73, 75, 77, 80, 81, 83, 86, 88, 89, 90, 92, 93, 94, 343, 344, 356, 362, 363, 364, 366, 367, 382, 399, 411
 calorimetric measurements, 284
 calorimetry, 112, 283, 285, 292, 293, 297, 299
 calyx, 306
 CAM, 279
 Candida, 457, 460, 461
 candidates, 42, 91
 capacitance, 85
 capillary, 31, 52, 86, 129, 138, 148, 159, 160, 170, 262, 271, 282, 333, 343, 353, 471
 caprolactone, 110
 caps, 346
 capsule, 92, 396, 406, 449
 caraway, xviii, 477, 479, 480, 481, 485
 carbamic acid, 73
 carbazole, 414, 425
 carbohydrate, 149, 150, 151, 152, 232, 359, 360
 carbohydrates, 233, 245, 246, 359
 carbon, 23, 33, 34, 35, 38, 39, 40, 71, 77, 91, 95, 96, 110, 111, 112, 122, 124, 138, 150, 151, 161, 163, 167, 169, 234, 239, 273, 302, 445, 446, 485
 carbon atoms, 33, 110, 111, 112, 138, 163
 carbon dioxide, 91, 95, 485
 carbon monoxide, 234, 239
 carbonates, 451
 carbonization, 241
 carbonyl groups, 427
 carboxyl, 169, 273, 274, 292, 296
 carboxyl groups, 273
 carboxylates, 353
 carboxylic, xiv, 149, 150, 153, 155, 156, 158, 164, 169, 202, 281, 284, 286, 287, 288, 292, 294, 300, 346, 348, 387, 405
 carboxylic acids, 346, 387
 carboxylic groups, 153
 carcinoma, 454

- carrier, xv, xvi, 216, 301, 325, 328, 330, 331, 333, 336, 381
- CAS, 105, 309
- catalysis, xvi, 20, 22, 138, 343, 355, 435
- catalyst, 138, 238, 239, 240, 241, 364, 445
- catalytic activity, 234, 238, 402, 445
- catalytic effect, 233, 237
- catalytic properties, 138, 241, 445
- catechol, 130
- cathodic process, 427
- cavitation, 256
- cavities, xii, 21, 24, 28, 69, 71, 80, 86, 90, 91, 92, 93, 94, 106, 108, 109, 110, 137, 190, 234, 256, 387, 406, 415, 430, 454
- C-C, 389, 445, 446, 451
- CDA, 148, 170
- cell, xvii, 25, 79, 169, 297, 329, 331, 426, 453, 457, 459
- cell metabolism, xvii, 453
- ceramics, 232, 246
- cereals, 239, 244
- cesium, xiv, xv, 305, 306, 307, 309, 310, 313, 314, 315, 316, 317, 318, 319, 320, 321, 322, 404
- CH₄, 91, 96
- channels, 71, 90, 369, 411, 413
- charcoal, 308, 309
- charge density, 20, 222
- chelates, 22, 23, 24, 58, 392
- chelating agents, 21, 23, 24
- chelators, xi, 19, 23, 29, 55, 61
- chemical energy, 59, 195
- chemical oxidation, 430
- chemical properties, 168, 178, 179, 471
- chemical reactions, 76, 113
- chemical structures, 24, 33, 420
- chemicals, 478, 479
- chemotherapy, 463
- chiral catalyst, 355
- chiral center, 158, 167, 274
- chiral molecules, 132, 346, 357, 382
- chiral recognition, xvi, 150, 151, 152, 156, 157, 158, 159, 160, 161, 162, 163, 164, 165, 166, 167, 168, 169, 274, 344, 345, 346, 356, 357, 361, 364, 370, 435, 436
- chirality, xiii, xiv, 147, 251, 274, 343, 366, 373, 382, 391, 394
- chloride, 72, 111, 154, 195, 232, 234, 235, 236, 308, 309, 346, 352, 360, 362, 364, 385, 390, 393, 405, 427, 436, 445, 447, 449, 450, 481
- chloride anion, 390, 481
- chlorine, 149, 150, 152, 347, 445
- chlorobenzene, 93
- chloroform, 72, 73, 86, 306, 308, 317, 329, 338, 339, 356, 357, 364, 403, 406, 420, 429
- chlorogenic acid, xvii, 465, 466, 467
- CHP, 297
- chromatography, 138, 148, 160, 162, 167, 169, 170, 282, 417
- chromium, 234
- circular dichroism, 112, 140, 284, 285, 292, 293, 302
- classes, 148, 149, 155, 180, 218, 329
- classical, 25, 27, 32, 34, 52, 178, 217, 317, 383
- classification, 301
- clean air, 85
- cleavage, 197, 445, 446, 451
- closure, 76
- clusters, 55, 71, 441, 450
- C-N, 197, 200, 390, 414
- Co, xiii, 170, 231, 232, 234, 235, 238, 239, 240, 241, 245, 337, 383, 397, 442
- CO₂, 25, 28, 29, 36, 91, 95, 128, 129, 134, 239, 240, 247, 445, 446, 451
- coal, 233, 241
- coatings, 85, 354
- collaboration, 186, 197
- colloids, 403
- combined effect, 168
- communication, 95, 388
- communities, 478
- community, 224, 382
- compensation, 156, 163, 164, 165, 255, 257, 471
- competition, 35, 73, 212, 276
- competitive process, 194
- complement, 76, 80
- complementarity, 87, 282
- complex systems, 243
- complexity, 34, 168
- components, 45, 49, 70, 73, 87, 108, 119, 194, 232, 237, 240, 243, 244, 258, 397, 429, 458
- composition, 46, 71, 77, 80, 81, 87, 158, 159, 161, 167, 168, 178, 241, 246, 249, 286, 317, 334, 357, 394, 413, 483, 485
- comprehension, 403
- compressibility, 303
- computer simulation, 168
- computing, 32
- concentrates, 236
- concentration ratios, 115, 116
- conception, 169
- condensation, 79, 86, 343, 347, 383, 413, 414, 415, 418, 466
- conditioning, 233, 243, 246, 249
- conductive, 427
- conductivity, xiii, 85, 231, 233, 236, 249

configuration, 44, 87, 108, 148, 167, 169, 275, 329, 387, 389, 398, 424, 441, 446, 471
conformational analysis, 56, 84, 475
conformational states, 165
confusion, 30
conjugation, 425
constituent groups, 332
constraints, 70, 75, 80, 85
construction, 91, 190, 216, 382, 390
consumption, 478, 483
contamination, 478
contrast agent, 23
control, xvii, 29, 178, 234, 235, 237, 243, 254, 466, 477, 478, 481, 482, 483, 485
convergence, 53
conversion, 95, 259, 366, 373, 401
cooling, 308, 419, 471
copolymer, 110, 384, 385, 429
copolymers, 243
copper, 57, 59, 160, 183, 190, 236, 245, 338, 339, 365, 383, 385, 405, 445, 451
corn, xiv, 231, 234, 236, 239, 241, 243, 247
correlation, 34, 48, 52, 61, 83, 119, 132, 257, 274, 320, 460, 471, 475
correlation coefficient, 48, 52, 320, 460
correlations, 45, 115, 116
Coulomb, 24, 45, 406
Coulomb interaction, 406
coupling, 41, 217, 352, 389, 426, 429, 445, 450
covalent, 35, 75, 160, 275, 285, 334, 374
covalent bond, 35, 160, 334
covalent bonding, 160
CRC, 246, 247, 249
critical micelle concentration, 403
critical temperature, 167
crops, 233, 478
crosslinking, xiii, 231
crown, xiv, xv, 20, 21, 22, 56, 57, 70, 72, 75, 78, 80, 84, 138, 148, 180, 181, 203, 217, 218, 305, 306, 307, 308, 310, 311, 313, 314, 315, 317, 318, 319, 320, 321, 322, 323, 330, 332, 336, 337, 345, 346, 357, 361, 390, 391, 412, 435
crystal lattice, 71, 80, 90
crystal structure, 57, 70, 71, 72, 93, 186, 188, 201, 212, 245, 248, 440, 449, 450
crystal structures, 70, 72, 449, 450
crystalline, xii, 54, 69, 71, 72, 88, 91, 161, 252, 254, 255, 296, 382, 390, 419, 454, 466
crystallinity, 462
crystallization, 78, 148, 394, 397, 425
crystals, 86, 90, 91, 93, 95, 96, 411, 419
C-terminal, 169, 275
culture, 460, 461

culture media, 460, 461
curve-fitting, 26, 311
cyanide, 194, 446
cyclic voltammetry, 220, 388
cyclohexane, 25, 128, 131, 132, 135, 393, 420, 424
cyclohexanol, 111, 112, 126, 128, 131, 132, 134
cyclohexanone, 355
cyclohexyl, 418
cyclotron, 77, 398
cytosine, 372, 454

D

DAD, 432
D-amino acids, 169
data analysis, 40, 52, 259, 471
DCI, 77
decay, 197, 260
decomposition, xiii, 79, 87, 93, 231, 233, 234, 236, 237, 238, 239, 240, 242, 248, 317, 393
decomposition temperature, 87, 242
decoupling, 39
definition, 137, 159
deformation, 71, 90, 235
degradation, 148, 152, 161, 238, 239, 240, 241, 242, 246, 277, 282, 419
degrading, 246
degrees of freedom, 255
dehydration, xiv, 165, 281, 285, 286, 292, 293, 296, 299
delivery, 277, 283, 301, 462
delocalization, 235
dendrimers, 352, 388, 389, 390
density, 95, 235, 254, 288, 308, 363, 457, 461
deoxynucleotide, 372
deposition, 70, 71, 85, 427
depressants, 232, 236, 246
depression, 454
desiccation, 481
desorption, 77, 86, 88
destruction, 291
detachment, 183, 215
detection, 24, 70, 75, 85, 179, 216, 394, 431, 450
detoxification, 415
deuterium oxide, 164
deviation, 169, 258, 292
DFT, xi, 20, 41, 42, 43, 44, 45, 46, 48, 50, 51, 52, 53, 61, 234, 445
diamines, 346, 414, 415
dichloroethane, 220, 316, 318, 319, 322
dielectric constant, 256
dielectric permittivity, 42
diesel, 247

dietary, 478
 dietary fiber, 478
 differentiation, 368
 diffraction, 93, 96
 diffusion, 86, 90, 207, 261, 328, 329, 336
 diffusion process, 86
 dihedral angles, 235
 dimensionality, 436, 448
 dimer, 94, 137, 152, 161, 441, 442
 dimeric, 71, 92, 94, 190, 221, 364, 374
 dimerization, 161, 164
 dimethylformamide, 73, 322, 419
 diodes, 412
 dipeptides, 169, 275, 394
 dipole, 148, 159, 160, 161, 163, 166, 169, 254, 255
 dipole moment, 254, 255
 dipole moments, 255
 direct observation, 140
 discipline, 178
 discrimination, xii, 105, 106, 107, 113, 114, 115,
 116, 118, 119, 120, 121, 122, 123, 124, 125, 132,
 133, 136, 137, 138, 139, 158, 161, 162, 164, 166,
 167, 399
 disorder, 72, 255
 dispersion, 255, 273
 displacement, 164, 273, 404
 disposition, 57, 180, 188
 dissociation, 25, 26, 234, 235, 261, 303, 338, 383,
 394, 459
 distilled water, 308, 309, 457, 458, 471, 480
 distribution, 26, 36, 49, 50, 111, 167, 178, 183, 197,
 210, 234, 262, 272, 319, 329, 335
 diversification, 273
 diversity, 113, 122, 178, 317
 DMF, 223, 393, 402, 417, 419, 421, 422, 425, 430
 DMFA, 313, 315, 316
 DNA, 75
 donor, xv, 22, 23, 24, 25, 29, 36, 56, 57, 76, 87, 106,
 166, 178, 180, 187, 196, 201, 202, 206, 208, 210,
 212, 215, 217, 218, 232, 233, 234, 247, 315, 322,
 325, 326, 336, 337, 338, 393, 405
 donors, 23, 187, 188, 206, 215, 222, 338
 dosage, 454, 455, 460
 dosing, 458
 drug carriers, xiv, 106, 251
 drug delivery, 277, 283, 301
 drug delivery systems, 277, 283
 drugs, 157, 161, 283, 301, 367, 454, 462
 drying, 419, 430, 457, 460, 462
 DSC, 98, 225, 237, 242
 DSC diagrams, 242
 DTA curve, 419, 420
 dyes, 259, 283, 368

dynamic factors, 404

E

earth, xvi, 195, 201, 202, 244, 318, 381, 388, 393
 economic problem, 241
 effusion, 71, 77, 79
 egg, 345
 elaboration, 394
 electrical conductivity, 249
 electrodeposition, 321
 electrodes, 24, 26, 27, 86
 electrolyte, 26, 32, 246, 330, 426
 electrolytes, 303
 electromagnets, 31
 electromigration, 301
 electromotive force, 25
 electron, xiii, 22, 24, 77, 91, 166, 178, 181, 182, 186,
 191, 197, 210, 217, 218, 235, 254, 327, 332, 412,
 427, 446
 electron density, 235, 254
 electron pairs, 24, 166, 254
 electronegativity, 163
 electrons, 76, 81, 166, 235, 472
 electrophoresis, 129, 148, 160, 170, 262, 271, 282,
 343, 353
 electrostatic force, 108
 electrostatic interactions, 22, 24, 45, 83, 156, 164,
 169, 254, 257, 390
 EMF, 25, 26
 emission, xiii, 177, 178, 180, 181, 182, 183, 185,
 186, 187, 189, 190, 191, 194, 195, 197, 200, 201,
 202, 203, 205, 207, 210, 212, 216, 217, 218, 260,
 357, 406, 430
 emitters, 181
 enantiomer, 162, 164, 166, 167, 168, 354, 466
 enantiomers, xiii, xvi, 132, 138, 147, 148, 156, 158,
 159, 160, 161, 162, 163, 164, 166, 167, 168, 343,
 344, 345, 346, 356, 357, 358, 361, 362, 364, 394,
 404, 444, 485
 encapsulated, 57, 92, 189, 397, 436, 438, 439, 441,
 442, 445, 450, 454
 encapsulation, 20, 21, 22, 24, 92, 106, 108, 406, 415,
 438, 441, 443, 449, 450
 endothermic, 286
 energy transfer, 190, 191, 195, 201, 406
 entanglement, 277
 enthalpy, 163, 257
 entrapment, 92, 450
 entropy, xiv, xv, 56, 73, 80, 83, 84, 156, 160, 161,
 163, 164, 165, 254, 255, 256, 257, 261, 281, 284,
 285, 286, 292, 293, 296, 297, 299, 306, 317, 471,
 475

- environment, xvi, 33, 43, 70, 85, 107, 108, 111, 148, 163, 183, 207, 212, 241, 243, 253, 256, 307, 313, 314, 326, 471, 475, 478
- environmental control, 86
- environmental effects, 53
- enzymatic, 148, 282, 466
- enzymes, 22, 130, 136, 277, 282
- epoxides, 366
- EPR, 232, 247, 248
- equality, 41
- equilibrium, xv, 26, 28, 32, 35, 38, 43, 46, 47, 49, 50, 53, 57, 73, 86, 88, 96, 114, 116, 118, 167, 259, 261, 273, 309, 310, 318, 319, 320, 325, 327, 328, 329, 334, 336, 401, 455, 456, 469
- Erk, 228
- erosion, 244
- ESI, 75, 76, 394, 418, 419, 420, 421, 425
- ester, 123, 152, 187, 350, 362, 364, 387, 390, 393, 405, 429, 431
- esterification, 164, 405, 446
- esters, 73, 77, 153, 303, 344, 346, 351, 353, 362, 374, 394, 402
- ethane, 41, 397
- ethanol, 74, 108, 170, 202, 203, 247, 357, 446
- ether, 321, 323
- ethers, 20, 21, 22, 56, 57, 70, 73, 75, 148, 180, 306, 320, 322, 323, 332, 336, 337, 346, 364, 385, 389, 390, 391, 411, 412
- ethyl acetate, 72, 126, 418, 426, 430
- ethylene, 110, 127, 256
- ethylene glycol, 256
- ethylene oxide, 110
- ethylenediamine, 127
- evaporation, 78, 83, 86, 308, 309, 471
- evolution, 425
- EXAFS, 323
- exchange diffusion, 329
- exchange rate, 259, 261, 468
- excitation, 195, 202, 205, 260
- exclusion, 32, 158, 233, 255
- excretion, 232
- experimental condition, 290, 394
- exposure, 86, 91
- extraction, xv, xvi, 22, 306, 307, 310, 318, 320, 321, 322, 325, 326, 327, 328, 329, 330, 332, 334, 337, 338, 339, 344, 346, 369, 381, 388, 407, 449, 485
- extraction process, xv, 306, 307, 320, 325, 338
- extrapolation, 83, 311
- FAO, 485
- fat, xviii, 477, 478, 481
- fats, 238, 241
- feeding, 458
- feet, 394
- females, 457
- fermentation, 149, 152
- ferrocenyl, 387, 388, 389
- fertility, 243
- fiber, 179, 332, 478
- fiber optics, 179
- film, 85, 86, 89, 90, 405
- films, 71, 85, 86, 89, 388, 426
- filtration, 419
- financial support, 224, 320, 431
- first generation, 252
- Fischer-Tropsch synthesis, 247
- fission, 321
- fixation, 311, 450, 451
- flammability, 306
- flavor, 485
- flexibility, 22, 36, 39, 45, 56, 57, 60, 70, 72, 75, 78, 80, 83, 84, 87, 110, 180, 252, 273, 338, 346, 436, 442
- flotation, 232, 236, 246
- flow, 333, 446
- fluctuations, 40
- fluid, 160, 162
- fluoride, 436, 440, 442, 449
- fluoride ions, 436
- fluorinated, 322, 454
- fluorine, 138
- fluorogenic, xiii, 177, 179, 180, 206, 207, 209, 218
- fluorometric, 271
- fluorophores, xiii, 177, 206, 357, 405
- flushing, 85
- focusing, xiii, 147, 148
- folded conformations, 215
- folding, 277
- folic acid, 283
- food, xiii, xviii, 148, 177, 178, 232, 233, 244, 245, 247, 282, 466, 475, 477, 478, 479, 485
- Food and Drug Administration, 479, 485
- food processing industry, 466
- foodstuffs, 479
- formaldehyde, 390, 393
- Formica, 450
- fouling, 333
- Fourier, 77, 398
- free energy, 44, 70, 73, 84, 87, 91, 156, 255, 257, 272, 284, 285, 297, 327
- free radicals, 248
- free volume, 93

F

- failure, 73, 96
- family, 138, 151, 186, 197, 202, 215, 252, 359, 454

freedom, 255
 freeze-dried, 457
 freezing, 308
 frequency distribution, 262
 fructose, 244, 245
 fruits, 479, 480, 481
 FTICR, 77, 85
 FTIR, xvi, 334, 411, 419, 420, 427, 428, 431
 FT-IR, 245
 FTIR spectroscopy, xvi, 411
 fullerene, 109
 functionalization, xvi, 206, 343, 358, 372, 381, 383
 fungal, 457, 461
 fungi, 246, 454, 460

G

G4, 120, 126
 G8, 123
 gas, 33, 42, 44, 50, 53, 70, 75, 76, 77, 78, 79, 80, 82, 83, 84, 85, 87, 89, 91, 95, 96, 148, 202, 232, 233, 239, 275, 354, 394, 404
 gas chromatograph, 87, 148
 gas phase, 44, 70, 77, 78, 80, 82, 83, 84, 202, 232, 233, 275, 394
 gas sorption, 95, 96
 gases, xii, 69, 92, 95, 96, 240, 241, 415
 gasification, 237, 238, 239, 240
 Gaussian, xvii, 53, 55, 262, 272, 465, 473, 476
 gel, 152, 179, 237, 418, 419
 gelation, 243
 gels, 232, 233, 236, 243, 248, 249, 345
 generation, 239, 388, 445
 geometrical parameters, 55
 Gibbs, 78, 82, 83, 84
 Gibbs energy, 78, 84
 glass, 20, 25, 26, 27, 30, 31, 32, 79, 179, 309
 glucose, 106, 152, 232, 233, 235, 237, 242, 244, 245, 252, 253, 282, 291, 297, 360
 glucoside, 361
 glutamic acid, 275
 glycerol, 245
 glycine, 271, 346, 351, 364
 glycol, 110, 256
 glycopeptides, 147, 148, 149, 150, 162, 169
 glycosylated, 359
 glycosylation, 359
 gold, 86, 179, 403, 406
 GPC, 429
 grafting, 406
 grain, 237, 238, 239, 240, 241
 grains, xiii, 231, 237, 238, 239, 240, 241, 244, 249
 gram-positive, 150, 152, 169, 349

granules, 232, 241
 graph, 46
 gravimetric analysis, 91
 gravity, 455, 460
 greenhouse, 249
 groundwater, 478
 growth, xiii, 147, 233, 457, 460, 461
 growth inhibition, 457, 460, 461
 guanine, 372
 guidelines, 32, 35, 448
 gums, 234

H

H1, 51, 128, 130, 131, 135, 269, 270, 271, 272, 311, 312, 313, 316, 317
 H₂, 50, 51, 91, 96, 128, 130, 131, 135, 311, 313, 316, 317
 half-life, 445
 halogen, 163, 308
 halogenated, 91
 handling, 330
 harmonization, 110
 harvest, 479
 hate, xiv, 305
 H-bonding, 35, 39, 40, 53, 57, 60, 87, 148, 155, 156, 158, 159, 160, 161, 162, 163, 164
 health, xvii, 477, 479, 484
 heat, 235, 237, 261, 262, 345, 454, 455
 heat capacity, 261
 heating, xii, 57, 69, 93, 234, 238, 239, 242, 401, 436, 438
 heavy metal, xiii, 231, 232, 236, 244, 330, 388
 heavy metals, 232, 236, 330
 heavy water, 27, 31
 height, 38
 helicity, 450
 helix, 275
 hematological, 462
 hepatotoxicity, 454
 herbicide, 167
 herbicides, 157, 167
 heterocycles, 181
 heterogeneous, 168, 234
 hexafluorophosphate, 307, 308, 321
 hexane, 72, 85, 86, 418
 high pressure, 96
 high-level, 107, 113, 136
 high-performance liquid chromatography, 147, 148, 170
 histidine, 111
 histone, 399, 400
 HOMO, 234, 235

homogeneity, 157, 483
 homogenous, 22, 252
 homolog, 449
 homolytic, 248
 hospitalized, 457
 hot water, 471
 HPLC, 148, 149, 150, 152, 161, 162, 163, 170, 343,
 367, 382, 445, 446
 human, xvi, xvii, 179, 453, 477, 478, 479, 484
 humans, 478
 humidity, 88, 458, 480
 hybrid, 364
 hybrids, 275
 hydrate, 107, 466
 hydration, 45, 247, 256, 273, 285, 291, 327
 hydrazine, 387
 hydro, xv, 43, 53, 85, 106, 132, 157, 158, 234, 253,
 276, 282, 291, 306, 307, 311, 314, 315, 316, 317,
 332, 403, 454, 460
 hydrocarbon, 24, 138, 150, 272, 303
 hydrocarbons, 85, 181, 234
 hydrodynamics, 71
 hydrogen atoms, 44, 441, 445, 468
 hydrogen bonds, 35, 43, 84, 195, 234, 253, 256, 273,
 276, 334, 347, 354, 356, 390, 444
 hydrogen peroxide, 386
 hydrogenation, 234, 241, 366, 372, 373
 hydrolysis, 196, 234, 393, 394, 402, 425, 427, 455
 hydrolyzed, 243
 hydrophilic, xv, 43, 53, 106, 132, 253, 276, 282, 291,
 306, 307, 311, 314, 315, 316, 317, 332, 403, 454
 hydrophilic groups, 403
 hydrophilicity, 122, 334
 hydrophobic interactions, 156, 159, 160, 161, 164,
 187, 256, 257, 273, 276, 285, 291, 292, 296
 hydrophobicity, 158, 256, 274, 299, 300, 327, 332
 hydroxide, 29, 384
 hydroxides, 236
 hydroxyl, 74, 75, 76, 108, 113, 120, 130, 137, 138,
 210, 232, 233, 234, 235, 236, 241, 242, 252, 253,
 254, 256, 273, 282, 292, 296, 353, 359, 383, 384,
 398, 479
 hydroxyl groups, 108, 113, 120, 138, 232, 233, 234,
 235, 236, 241, 242, 252, 253, 254, 282, 292, 296,
 353, 359, 383, 398, 479
 hydroxyproline, 399
 hydroxypropyl, xiv, xvii, 275, 281, 284, 297, 299,
 300, 302, 453, 455
 hypothesis, 72
 hysteresis, 88, 237
 hysteresis loop, 237

I

id, 485
 identification, 37, 38, 113, 132, 165, 458, 478
 identity, 156, 163
 images, 460, 461
 imaging, 23
 immersion, 457
 immobilization, 243
 implementation, 179, 306
 impurities, 79, 152
 in situ, 86, 178, 355
 in vitro, 150, 352, 462, 466
 in vivo, 138, 150
 inactive, 427
 incentives, 326
 inclusion parameters, 87
 indication, 51, 52, 285, 293, 299
 indicators, 179
 indole, 181
 induction, 255, 371, 450
 industrial, xv, xviii, 179, 251, 300, 325, 326, 330,
 333, 478, 479, 484
 industry, xviii, 236, 326, 454, 466, 478, 479, 483
 inert, 275
 inertness, 22
 infancy, 24
 inferences, 474
 inflammatory, 157, 162
 infrared, 91, 481
 infrared spectroscopy, 91
 inhibition, xviii, 352, 384, 457, 460, 461, 477
 inhibitor, xvii, xviii, 276, 283, 466, 477, 478, 479,
 483, 484, 485
 inhibitors, 385
 inhibitory, xvii, 369, 370, 453, 457, 461, 462
 innovation, 309, 484
 inoculum, 457
 inorganic, 20, 106, 108, 109, 110, 121, 248, 282,
 330, 430
 inorganic salts, 108
 insecticide, 479
 insertion, 294, 300, 445
 insight, 39, 93, 166, 449
 inspection, 32, 43, 84, 339
 instability, 484
 instruments, 31, 77, 85
 integration, 179, 247, 471
 intercalation, xii, 69, 71, 90
 interdisciplinary, 61
 interface, xv, 92, 165, 321, 325, 328, 336, 337, 338,
 369
 interfacial tension, 333

interference, 85, 222
intermolecular, 39, 53, 54, 79, 106, 107, 108, 110, 111, 113, 114, 120, 132, 136, 385, 436, 444
intermolecular interactions, 79, 106, 107, 108, 110, 113, 114, 385
interval, 28, 311
intrinsic, 34, 35, 70, 75, 85, 92, 111, 180, 218
invasive, 454
inversion, 39, 73, 222, 424, 425, 446
inversions, 45
investigative, 178
iodine, 191, 193
ion channels, 369
ion transport, xv, 325, 326, 330, 336, 337, 338
ionic, xi, xiii, xiv, 20, 23, 25, 26, 27, 29, 32, 36, 39, 42, 44, 46, 47, 50, 73, 106, 115, 118, 155, 156, 158, 161, 164, 169, 170, 178, 243, 305, 306, 317, 320, 321, 322, 327, 333, 334, 406
ionic liquids, xiv, 305, 306, 320, 321, 322
ionizable groups, 168
ionization, xvi, 24, 25, 70, 75, 76, 77, 155, 157, 169, 235, 286, 290, 303, 398, 411
ionization energy, 235
iron, 110, 245, 248, 383
irradiation, 383
irritation, 283
isoelectric point, 161
isolation, 215
isoleucine, 351
isomerization, 138, 424
isomers, 35, 50, 113, 120, 122, 123, 283, 383, 424
isothermal, 89, 261
isotherms, 87, 88, 89, 167, 168, 405, 458
isotope, xi, 20, 30, 41
isotropic, 51, 52
ITC, 261
iteration, 311

K

K⁺, 26, 27, 29, 36, 201, 307, 326, 361, 390
KBr, 126, 420
ketones, 239
KH, 97, 247, 378
kidney, 370
kinetic parameters, 86
kinetics, 77, 304, 322, 327, 338, 404, 445
KOH, 25, 27, 30, 32, 57
Krebs cycle, 194

L

L1, 271, 272, 437, 438, 439, 441, 442, 446
L2, 315, 436, 437, 439, 445, 446
labeling, 34, 37, 47
lactones, 160
Langmuir-Blodgett, 85
lanthanide, 197, 248, 383
lanthanum, 234, 248
laser, 179, 471
lattice, 39, 40, 71, 90, 91
lattices, 90
leaching, 333
left-handed, 444
legality, 37
lending, 254
leucine, 152, 353
life-threatening, 454
lifetime, 190, 259, 260, 333
light emitting diode, 412
limitation, 107, 401
limitations, xi, 19, 50, 258, 484
Lincoln, 141, 279
linear, 23, 26, 27, 32, 33, 35, 37, 43, 47, 51, 52, 57, 87, 165, 167, 205, 241, 257, 258, 259, 273, 286, 302, 311, 316, 318, 320, 385, 397, 414, 441, 442, 443, 449, 450, 458, 470, 475
linear dependence, 26
linear regression, 43, 51, 52, 286, 470
linkage, 424, 425
links, 450
lipid, 329, 406
lipids, 236
lipophilic, 338, 454
liposomes, 180
liquid chromatographic methods, xiii, 147
liquid chromatography, 147, 148, 170, 301
liquid crystals, 411
liquid nitrogen, 457
liquid phase, 73, 333
liquids, xii, xiv, 31, 41, 69, 87, 305, 306, 320, 321, 322, 415
lithium, 27, 73, 309, 322
liver, 454
loading, 156, 385
local anesthetic, 160
localization, 235
location, 77, 95, 122, 273, 274, 275, 288, 294, 300, 315, 392
lover, 31
low molecular weight, 429, 431
low temperatures, 86, 95, 385
low-level, 107, 113

low-temperature, 479
luminescence, 190, 195, 207, 222
LUMO, 235
lying, 51, 52, 201, 253, 254, 255
lysine, 275, 371

M

machines, 59
macrocyclics, 414
macromolecules, 343, 369
magnesium, 242, 308, 309
magnetic, 23, 30, 31, 42, 51, 129, 140, 271, 308, 309, 330, 450, 471, 480
magnetic field, 30
magnetic properties, 450
magnetic resonance spectroscopy, 271
magnets, 30, 31, 412
maize, 247
maltodextrin, 246
maltose, 244, 245, 360
management, 246
manganese, 245
manners, 234
mannitol, 361
market, 478
market value, 478
marketing, xvii, 477
marketplace, 478
marrow, 454
masking, 277
mass spectrometry, xvi, 70, 75, 77, 91, 411
mass transfer, 329
materials science, 413
matrix, xiii, 71, 76, 86, 177, 202, 253, 384
maximum water sorption, 88
measurement, 32, 33, 38, 40, 50, 56, 80, 118, 261, 309, 310, 311, 456
measures, 165, 243
mechanical properties, 243
media, xi, 20, 26, 28, 30, 33, 45, 61, 72, 73, 138, 232, 233, 394, 403, 404, 460, 461, 466, 473
melamine, 76
melting, 242, 419
melting temperature, 419
membranes, xv, 180, 325, 326, 329, 332, 336
Mendeleev, 101
Merck, 172, 247, 308
mercury, 393
metabolic, 283
metabolism, xvii, 453
metabolites, 478
metal oxide, 232

metal salts, xiii, 231, 232, 233, 236, 237, 240, 241, 245, 448
metallurgy, 236
metals, xiii, 178, 187, 190, 195, 197, 201, 202, 208, 222, 232, 234, 236, 243, 245, 246, 330, 337, 338, 339, 388
methane, 239, 240, 241
methanol, 72, 155, 170, 201, 202, 256, 397, 420, 425, 441, 445, 446
methionine, 167, 168
methyl group, 136, 152, 273
methylation, 158, 273
methylene, 36, 39, 59, 72, 91, 273, 339, 427, 445, 447, 450
methylene chloride, 72, 427, 445, 447, 450
methylene group, 39, 59, 273, 339
Mg²⁺, 195, 201, 222, 245
mice, 244, 457
micelle formation, 403
micelles, 180, 236
microbial, 352
microcalorimetry, xiv, 251, 258, 262
microclimate, 458
microelectrode, 30
microenvironment, 106, 108, 259, 260, 262
microflora, 247
micronutrients, 243
microscopy, 179
microtubes, 403
microwave, 234, 383
microwave heating, 234
migration, 336
mimicking, xvi, 22, 381
mineralogy, 246
minerals, xviii, 243, 246, 477, 478
mining, 237
mixing, 336, 406
MLC, 433
mobility, 24, 39, 40, 41, 42, 45, 53, 56, 90, 180, 286
model system, 93, 304, 363
modeling, xi, 20, 42, 43, 55, 61, 71, 166, 285, 303, 393
models, xvi, 22, 42, 43, 44, 45, 50, 51, 52, 53, 54, 59, 106, 138, 220, 282, 302, 343, 430
modulation, xiii, 177
modules, 217
MOE, 435
moieties, xvi, 76, 84, 91, 93, 149, 150, 151, 152, 153, 156, 158, 162, 164, 179, 187, 190, 191, 210, 215, 234, 242, 275, 337, 343, 351, 360, 361, 362, 368, 381, 385, 391, 399, 450
moisture, 306, 481
moisture content, 481

molar ratio, 95, 96, 189, 190, 191, 207, 211, 212, 215, 219, 220, 261, 310, 313, 397, 427, 457, 458, 462
 molar ratios, 95, 207, 212, 220, 310
 molar volume, 288, 289, 290, 291, 296, 303
 mole, 28, 35, 309, 310, 311, 314, 468
 molecular dynamics, 53, 83, 292, 303, 317
 molecular mass, 149, 150, 152
 molecular orbitals, 254
 molecular sensors, xiii, 177, 178, 179, 206, 210, 218
 molecular structure, xii, 33, 35, 55, 60, 69, 74, 87, 106, 167, 303, 327, 369, 455
 molecular weight, 79, 239, 252, 388, 402, 426, 427, 429, 431
 Møller, 445
 molybdenum, 234
 monolayers, 369
 monomer, 181, 183, 187, 426, 427, 429, 431
 monomeric, 76, 190
 monomers, 76, 405, 412, 431, 444
 monosaccharide, 360
 monosaccharides, 398
 monoterpenes, 486
 montmorillonite, 246
 morphology, 403
 Mössbauer, 247, 248
 motion, 40, 59, 90
 motivation, xv, 325, 333
 movement, 59, 84
 MRI, 23
 multiplicity, 33
 mutant, 276

N

Na⁺, 27, 29, 30, 74, 165, 205, 218, 307, 326
 N-acety, 120, 150, 151, 152, 273, 351, 360
 NaCl, 28, 29, 126, 310
 nanocapsules, 412, 413
 nanocubes, 414
 nanoparticles, 179, 401, 406
 nanoreactors, 412, 413
 nanotechnology, 91
 naphthalene, 59, 79, 121, 123, 131, 181, 186, 187
 NATO, 225
 natural, 106, 108, 138, 242, 243, 244, 247, 326, 329, 330, 403, 466, 486
 NdCl₃, 245
 NEC, 160
 necrosis, 454
 nematode, 485
 nerve, 326
 nesting, 221

network, xii, 53, 54, 69, 70, 87, 90, 237
 Ni, xiv, 143, 144, 231, 232, 234, 235, 238, 239, 240, 241, 244, 316, 321, 337, 383, 444
 nickel, 245, 338, 339, 385, 450
 Nielsen, 341
 nimodipine, 134
 nitrate, xvii, 22, 39, 41, 57, 208, 232, 234, 235, 236, 308, 309, 316, 319, 320, 321, 453, 481
 nitrates, 26
 nitric acid, 34
 nitrobenzene, 73, 120, 126, 316
 nitrogen, 23, 24, 34, 36, 45, 50, 56, 152, 156, 181, 183, 186, 188, 197, 201, 202, 210, 212, 215, 273, 292, 337, 338, 344, 345, 348, 390, 412, 419, 421, 436, 445, 446, 457
 noble metals, 330
 non-steroidal anti-inflammatory drugs, 157
 normal, xvii, 46, 53, 55, 122, 155, 168, 170, 453, 459, 466
 normal conditions, xvii, 453
 normalization, 119
 NS, 129, 376
 N-terminal, 163
 nuclear, 33, 129, 140, 306
 nuclear magnetic resonance, 129, 140
 nuclei, 25, 26, 27, 28, 33, 35, 37, 38, 39, 40, 45, 49, 336
 nucleotides, 60
 nucleus, 32, 33, 35, 36
 nulliparous, 457

O

oat, xiii, 231, 237, 238, 239, 240, 241, 247
 observations, 33, 39, 96, 118, 123, 140, 314, 398, 475
 OECD, 464
 OH-groups, 106, 299
 oil, xviii, 89, 246, 477, 479, 485
 oils, 485
 olefins, 372
 oligoethers, 336
 oligomeric, 77
 oligomerization, 414
 oligomers, 399, 400, 412
 oligosaccharide, 248, 466
 oligosaccharides, 106, 252, 282, 398, 454
 opposition, 397
 optical, xiii, 113, 120, 122, 124, 147, 177, 180, 207, 212, 215, 218, 220, 246, 358, 365, 401, 430
 optical properties, 212
 optics, 179
 optimization, 54, 169, 473

oral, 462
ores, 232, 236, 246
organ, 75, 110, 183
organic compounds, 70, 85, 87, 111, 113, 132, 138
organic matter, 246, 249
organic solvent, 20, 71, 86, 91, 155, 159, 168, 197, 256, 306, 329, 330, 387, 426
organic solvents, 20, 71, 159, 168, 197, 306, 387, 426
organoleptic, 484
organometallic, 75, 110
orientation, 247, 254, 292, 392
oscillator, 472
osmotic, 333
oxidation, 191, 193, 241, 245, 427, 430, 454, 455, 466
oxidative, xvi, 411, 426, 427, 428, 431, 450
oxide, 110, 306, 346
oxides, 243
oxygen, 20, 21, 36, 70, 76, 81, 83, 84, 88, 197, 222, 234, 235, 242, 253, 254, 256, 317, 336, 337, 339, 344, 445, 454, 466
ozone, 478

P

pairing, 40, 75, 187, 196, 327
palladium, 205, 385, 412, 429, 431
paramagnetic, 23
parameter, 87, 166, 253, 261
Paris, 300, 301, 485
particles, 71, 138, 151
partition, 165
patients, 454, 457
Pb, 220, 221, 222, 337
PCM, xii, 20, 43, 44, 53
penalty, 95
peptide, xiv, 149, 156, 157, 159, 251, 275, 276, 347, 352
peptide bonds, 156
peptide chain, xiv, 251, 276
peptides, xiv, 147, 149, 169, 251, 252, 275, 276, 303, 344, 347, 352
perchlorate, 221, 222, 450
periodic, 309
permeable membrane, 329
permit, 20, 25, 253, 329, 458
permittivity, 473
perturbation, 164, 167, 168, 330
perturbations, 468
perylene, 405
pesticide, 415, 479
pesticides, 478

PET, 181, 182, 187, 197, 201, 210, 211
petrochemical, 148
pH values, 28, 29, 33, 181, 182, 187, 189, 190, 191, 206, 208, 210, 211, 215, 330, 436, 441
pharmaceutical, xvi, 148, 155, 277, 283, 301, 330, 343, 454, 475
pharmaceutical industry, 454
pharmaceuticals, 283
pharmacological, 148
phase diagram, xvii, 89, 453, 462
phase transformation, 92, 95
phase transitions, xii, 69, 71, 93
phase-transfer catalysis, 20
phenol, 84, 112, 138, 167, 273, 353, 446
phenolic, 75, 84, 149, 150, 152, 158, 256, 273, 359, 383, 466
phenolic compounds, 466
phenylalanine, 111, 120, 127, 256, 260, 273, 348, 356, 362, 444
phosphate, xvi, 187, 232, 271, 354, 453, 455, 456, 458
phosphonates, 394
phosphorus, 394, 402
photocatalysis, 401
photocatalytic, 193
photoconductivity, 412
photoinduced electron transfer, 197, 210
photolysis, 194
photon, 182, 412
photonics, 412
physical chemistry, 303
physical factors, 333
physicochemical, xvii, 148, 149, 153, 243, 249, 282, 462, 465
physicochemical properties, xvii, 148, 149, 153, 249, 282, 465
physiological, xvi, 283, 435, 455, 459
phytochemicals, 478
pigments, 283
planar, 43, 44, 109, 210, 222, 232, 235, 343
plants, 243
plasma, 77, 399
plasticity, 237, 243, 246, 249
plasticizer, 333
play, 70, 107, 120, 123, 156, 157, 159, 161, 162, 163, 166, 178, 181, 244, 254, 273, 292
PM3, xvii, 466, 467, 473, 474, 475
polar groups, 73, 120, 161, 273, 286, 291
polar media, 45
polarity, 74, 107, 108, 109, 110, 111, 124, 132, 160, 168, 256, 403
polarizability, 166, 255
polarization, 91, 398

- pollutants, 330
 polyacrylamide, 249
 polyamide, 449
 polyamides, 412
 polyamine, 24, 25, 26, 27, 30, 31, 33, 61, 181, 182, 186, 187, 189, 190, 194, 195, 196, 197, 201, 202, 206, 448
 polycondensation, xvi, 411, 412, 414, 429, 430, 431
 polycrystalline, xii, 69
 polyelectrolytes, 402
 polyene, 149
 polyesters, 412
 polyether, 20, 70, 80, 84
 polyethylene, 110
 polymer, xv, xvi, 85, 110, 325, 384, 385, 402, 411, 427, 429, 430, 431
 polymer chains, 110
 polymer film, 427, 431
 polymer films, 431
 polymer structure, 431
 polymerization, xvi, 411, 412, 426, 427, 428, 431
 polymers, xvi, 91, 106, 110, 179, 249, 381, 383, 402, 411, 412, 414, 417, 426, 430, 431
 polymorphism, 71, 169
 polypeptide, 149, 154, 276
 polypeptides, 277
 polypropylene, 110
 polysaccharide, xiii, 231, 232, 233, 242
 polysaccharides, xiii, 148, 231, 232, 233, 234, 240, 241, 243, 244, 245, 246, 247, 248, 249
 Polysaccharides, 231, 233, 236, 237, 243
 polystyrene, 429
 poor, 109, 318, 373, 387, 401, 419, 429, 462, 478
 population, 36, 42, 46, 244
 pores, 71, 91, 333
 porosity, 88, 91
 porous, 71, 91, 95, 411, 413
 porous materials, 95
 potassium, 91, 242, 249, 308, 329, 429, 481
 potato, xiv, xvii, xviii, 231, 234, 236, 237, 239, 241, 242, 245, 247, 249, 477, 478, 479, 480, 481, 483, 484, 485, 486
 potatoes, 479, 484, 485
 potentiometric study, 196
 powder, xii, 69, 93, 95, 96, 419
 powders, 88, 96
 power, 20, 122, 332
 PPA, 266, 273
 PPO, xvii, 465, 466, 467, 472
 precipitation, xviii, 208, 477
 preconditioning, 158
 prediction, 27, 87
 preference, 207, 424
 press, 174, 249, 322, 341, 451
 pressure, xii, 69, 71, 79, 80, 86, 88, 89, 93, 96, 306, 308, 309, 405
 prevention, 243
 probability, 130
 probe, 205, 217, 218, 256, 351, 394, 401, 404, 472
 process control, xiii, 177, 178
 producers, 478
 production, xiii, 231, 233, 234, 236, 237, 238, 239, 240, 241, 242, 244, 247, 283, 478, 483
 profit, 197
 profitability, 244
 program, 26, 35, 39, 42, 48, 53, 54, 224, 261, 311, 322
 propane, 95
 propionic acid, 266
 propranolol, 357
 propylene, 110, 313, 393
 protection, 241, 383, 478
 protective role, 454
 protein, xviii, 75, 152, 158, 276, 277, 477
 protein folding, 277
 proteins, xiv, 148, 240, 241, 251, 252, 276, 277, 280, 406
 protic, 25
 protocol, 36, 53, 426
 protons, xv, 27, 33, 34, 35, 36, 40, 41, 50, 56, 60, 182, 187, 195, 205, 218, 286, 287, 288, 294, 300, 325, 336, 421, 424, 425, 429, 441, 468, 470
 pseudo, 337, 445
 pulse, 39
 purification, 92, 132, 308, 334, 419
 PVC, 180
 pyrene, 181, 404, 405
 pyridine ring, 59, 186
 pyrolysis, 241
- Q**
- quadrupole, 77, 398
 quality control, 330
 quantum, xi, 20, 33, 61, 179, 181, 186, 259, 284, 363
 quantum dots, 179
 quantum yields, 181
 quartz, 85, 86
 quaternary ammonium, 445
 quinine, 364
- R**
- race, 158, 161, 162, 167, 169, 344, 346, 365, 385, 444, 450

- racemization, 147, 344
radiopharmaceuticals, 23
radiotherapy, 23
radius, 24
rain, 244
Raman, xvii, 248, 301, 465, 466, 467, 471, 472, 473, 475, 480
Raman spectra, 248, 471, 472, 473
random, 232
RAS, 305, 309
raw material, 478
reactant, 130, 261, 417
reactants, 113, 414
reaction medium, 111
reaction time, 383
reactive oxygen, 454
reactive oxygen species, 454
reactivity, 77, 382, 446
reading, 27
reagent, xiv, 77, 156, 233, 281, 308, 399
reagents, 76, 285, 286, 292, 293, 321, 344, 399
real time, 178, 330
reality, 21, 31, 41
recovery, 39, 85, 330, 334
recrystallization, xii, 69, 426
recrystallized, 71, 422, 426, 471
red shift, 182, 205, 297
redox, 427
reflection, 119, 122, 338
refractive index, 86
regression, 43, 51, 52, 166, 257, 286, 460, 470
regression analysis, 43, 286
regression equation, 52
regression line, 257
regression method, 470
regular, 253, 333
regulation, 24
relationship, xii, 37, 70, 87, 105, 110, 115, 116, 117, 122, 125, 133, 139, 165, 257, 274, 311, 318, 326, 468, 475
relationships, 32, 51, 52, 87, 114, 116, 249, 318, 475
relatives, 190
relaxation, 39, 40, 42, 262, 271, 304
relaxation time, 39, 40
relaxation times, 39
relevance, 86, 307
reliability, 32
renal, 462
renewable energy, 244
reparation, 249
repeatability, 25
residuals, 28
residues, xvi, 252, 275, 276, 277, 343, 344, 351, 367, 370, 372, 399, 478, 479
resistance, 454
resistivity, 247
resolution, 148, 155, 156, 158, 161, 162, 168, 179, 344, 365, 382, 444, 450
resorcinol, 383, 394, 399
resources, 244
response time, 179, 216
retention, 95, 155, 156, 158, 159, 160, 161, 163, 164, 165, 166, 167, 168, 169, 339
Reynolds, 103, 433
rheological properties, xiii, 231
rheology, 233, 248
rhodium, 372
ribose, 244, 245
rice, 249, 484
rigidity, 41, 57, 72, 87, 108, 110, 178, 182, 346, 348, 436, 442
rings, 22, 24, 59, 124, 149, 150, 152, 154, 155, 186, 235, 252, 338, 353, 390, 399, 420, 443, 454
risk, 479
rolling, 481
room temperature, xiv, 95, 96, 305, 308, 309, 320, 321, 322, 385, 418, 422, 423, 427, 436, 438, 445, 446, 457, 469, 471, 480
room-temperature, 306, 321
rotations, 90
runoff, 246
rural, 244
rural population, 244
Russian Academy of Sciences, 69
ruthenium, 181, 190, 194
rye, xiii, 231, 237, 238, 239, 240, 241
- S**
- safety, 462, 478, 479, 484
Salen, 371
saline, 457
salmon, 276
salt, 25, 55, 57, 91, 121, 232, 233, 236, 239, 242, 275, 318, 334, 335, 337, 445, 449, 450, 481
salt formation, 25
salts, xi, 19, 30, 57, 76, 108, 109, 222, 232, 233, 234, 236, 237, 238, 241, 245, 246, 247, 248, 383, 385, 450
sample, 31, 79, 178, 238, 239, 310, 330, 471, 481, 483
saturation, 158, 233, 236
scaffold, 222, 361
scaffolds, 382
scaling, 47, 51, 52

- scarcity, 75
scattering, 255, 327
Schiff, 203, 347, 362, 413, 424, 448
Schiff base, 347, 362, 413, 424, 448
Schmid, 169, 175
scientific community, 224, 382
SCN, 109
scripts, 485
search, 42, 91, 244, 486
searches, 50
searching, xiv, 251
second generation, xiii, 231, 242
secret, 107
seed, 478, 479, 485
seeds, 480
selecting, xv, 325, 435
self-assembling, 413
self-assembly, 71, 85, 396, 397
self-organization, 131
semi-natural, 106
sensing, xiii, 178, 181, 186, 190, 194, 195, 206, 207, 218, 405
sensitivity, 87, 179, 180, 212, 258, 259, 275
sensors, xiii, 24, 70, 85, 86, 177, 178, 179, 180, 195, 206, 210, 215, 217, 218, 354, 431
series, 28, 37, 38, 39, 76, 87, 93, 111, 113, 114, 124, 126, 158, 160, 215, 253, 307, 309, 328, 334, 336, 338, 345, 350, 353, 354, 363, 365, 366, 372, 388, 393, 399, 403, 459, 467
serine, 274, 362
serum, 406
serum albumin, 406
shape, xvi, 30, 32, 38, 46, 55, 71, 87, 108, 110, 111, 166, 168, 178, 218, 274, 347, 411, 413, 414, 418, 425, 436, 442, 455, 471
shaping, 246
shear, 237, 333
short-range, 40, 53, 164
short-term, 244
shoulder, 430
side effects, 454, 455, 460, 462
sign, 57, 288
signal transduction, 179, 215
signaling, 179, 180, 201, 215, 217, 218
signalling, xiii, 177, 181, 212, 215
signals, 27, 28, 29, 32, 33, 37, 38, 39, 40, 46, 47, 57, 261, 288, 294, 420, 421, 423, 425, 426, 429, 468, 469
signs, 82, 313, 334
silane, 138
silica, 138, 151, 152, 160, 179, 367, 418
silver, 186, 306, 337, 339, 359, 385, 393, 481
similarity, 34, 37, 38, 123
simulation, 33, 42, 91, 248, 256
simulations, xii, 20, 43, 45, 53, 57, 83, 317
sine, 35
single crystals, 71, 90, 93, 207
single-crystalline, xii, 69
skeleton, 22, 110, 132, 254, 334, 357, 358, 382, 385, 399, 403
skin, 329
SMS, 228
sodium, 27, 29, 30, 111, 121, 130, 137, 205, 234, 242, 249, 308, 329, 353, 368, 370
sodium hydroxide, 29
software, xi, 20, 25, 39, 44, 50, 53, 61, 311, 471
soil, 231, 232, 233, 242, 243, 244, 246, 249
soil erosion, 243
soils, 243, 246, 249
solar, 401
solar cell, 401
solar cells, 401
sol-gel, 179
solid phase, 20, 93
solid state, 57, 72, 73, 83, 84, 90, 91, 92, 93, 183, 185, 197, 209, 212, 215, 220, 234, 252, 254, 255, 283, 296, 317, 385, 396, 467, 472, 475
solid-state, xii, 22, 69, 91, 106, 185
solubility, xvi, 73, 75, 156, 158, 207, 210, 218, 253, 261, 277, 282, 297, 307, 316, 318, 320, 387, 390, 429, 431, 453, 454, 455, 458, 459, 460, 462
solvation, 53, 70, 74, 75, 87, 165, 166, 286, 292, 307, 313, 317, 327, 328, 338, 473
solvent molecules, 33, 71, 73, 77, 78, 79, 80, 81, 86, 91, 95, 96, 215, 222, 255, 430, 441
solvents, 20, 71, 73, 83, 86, 95, 96, 159, 168, 197, 288, 306, 311, 313, 314, 315, 316, 317, 320, 321, 322, 329, 332, 333, 372, 387, 401, 419, 426, 429, 445, 456
sorbents, 91
sorption, 71, 87, 88, 89, 90, 91, 95, 96, 242
sorption isotherms, 87, 88
soybean, 247
spacers, 56, 57
spatial, 110, 178, 255, 383
speciation, 26
specificity, xiii, 106, 107, 177, 179, 180, 478
spectrophotometric, 140, 190, 258
spectrophotometric method, 258
spectrophotometry, 112, 346, 475
spectroscopy, xi, xiv, 19, 27, 32, 33, 57, 61, 70, 77, 86, 91, 179, 181, 251, 258, 259, 260, 262, 283, 297, 302, 343, 353, 356, 368, 394, 398, 418, 419, 430, 431, 456

- spectrum, 29, 31, 37, 39, 46, 47, 48, 57, 76, 185, 195, 261, 287, 288, 298, 390, 421, 422, 423, 424, 425, 426, 427, 428, 429, 430, 431, 472, 473
- speed, 242
- spheres, 40, 232, 233
- spin, 33, 39, 40, 85, 330, 393, 412
- spine, 208
- SPR, 86, 399, 406
- sprouting, xvii, xviii, 477, 478, 479, 481, 482, 483, 484
- SPSS, 322
- stabilization, 56, 249, 254, 275, 276, 301, 412
- stabilize, 71, 80, 238, 284
- stabilizers, 244
- stages, 36, 148, 240, 242, 338
- stainless steel, 79
- standard deviation, 311, 333
- standards, 20, 247, 429, 464
- starch, xiv, xviii, 231, 232, 233, 234, 236, 237, 239, 240, 241, 242, 243, 245, 246, 247, 248, 249, 282, 477, 478
- starch granules, 245
- starch polysaccharides, 245
- starches, 232, 233, 234, 236, 241, 242, 244, 247
- statistical analysis, xviii, 48, 61, 478
- statistics, 42
- steel, 79
- steric, 75, 85, 130, 131, 148, 155, 156, 158, 159, 160, 161, 162, 163, 164, 167, 169, 233, 234, 235, 273, 275, 346, 354
- sterile, 457
- STO, 44, 53
- stochastic, 167
- stock, 457, 483
- stoichiometry, xii, xvii, 69, 70, 76, 82, 87, 108, 114, 115, 116, 118, 137, 208, 220, 257, 258, 259, 261, 262, 283, 286, 293, 300, 349, 393, 453, 465, 468
- stomach, 458
- storage, xvii, xviii, 88, 91, 95, 195, 242, 246, 477, 478, 479, 480, 481, 483, 484
- strain, 149, 150, 254, 255, 414, 419, 457
- strains, xvii, 349, 453, 457, 460, 461, 462
- strategies, 148, 179, 343, 478, 485
- strategy use, 413
- strength, xi, 20, 22, 25, 26, 27, 32, 36, 52, 70, 85, 109, 111, 115, 118, 178, 249, 253, 254, 256, 303, 322, 330, 333
- Streptomyces, 149, 152, 153, 154, 155
- stress, 109, 178, 237
- stretching, 420, 472
- strong interaction, 76, 80, 110, 119, 132, 273, 405
- strontium, 306, 321
- structural changes, 296
- structural characteristics, 162
- styrene, 346, 365, 371
- substances, xiii, 31, 231, 237, 240, 241, 252, 256, 273, 303, 329, 382, 454, 478
- substitution, 21, 59, 123, 212, 273, 296, 297, 332, 338, 347, 391, 454, 469
- substrates, xiii, xvi, 24, 86, 178, 191, 243, 255, 385, 399, 435, 436, 471
- sucrose, 165, 246
- sugar, 150, 151, 152, 153, 156, 158, 164, 245, 360, 361, 398, 478
- sugars, 152, 158, 245, 246, 344, 398, 478
- sulfate, 155, 308, 309, 353, 449
- sulfites, 466
- sulfur, 91, 156, 206, 222, 223, 337, 338, 393, 396
- sulfuric acid, 88
- summaries, 133
- sunflower, 247
- superconducting, 30
- superconducting magnets, 30
- supercritical, xviii, 160, 477, 480
- superoxide, 391
- superposition, 46, 181, 311, 314, 318
- supplemental, 344
- supply, 156
- supported liquid membrane, 330, 331, 332
- suppression, 485
- supramolecular chemistry, xiii, xvi, 22, 75, 106, 107, 108, 109, 113, 139, 140, 177, 178, 179, 195, 251, 374, 381, 411, 413
- supramolecular complex, 108
- surface area, 79, 89, 90, 237, 256, 332, 333
- surface layer, 89
- surface modification, 401, 406
- surface tension, 129
- surfactant, 179, 303, 304, 403
- surfactants, 138, 402, 403
- susceptibility, 31, 47, 457, 461, 464
- suspensions, 246, 457
- swelling, 86, 232, 245
- switching, 183
- symmetry, 44, 50, 54, 72, 87, 221, 253, 385
- synchronous, 446
- synergistic, 137, 161
- synergistic effect, 137, 161

T

- taste, 282
- TBP, 306
- TCC, 150, 297
- teicoplanin, 148, 149, 150, 151, 152, 155, 156, 157, 158, 159, 162, 163, 164, 165, 166, 167, 168, 169

- temperature dependence, 71, 78, 81, 82, 83, 156,
 159, 163, 183, 257, 292
 temperature gradient, 79
 tensile, 249
 tensile strength, 249
 tension, 129, 165, 333
 ternary complex, 196
 textile, 282
 therapeutic agents, xvii, 453, 455
 therapy, 460
 thermal decomposition, xiii, 231, 233, 237, 242
 thermal degradation, 242
 thermal equilibrium, 401, 456
 thermal evaporation, 86
 thermal properties, 240, 245
 thermal stability, xiii, 70, 231, 233, 237, 239, 419,
 426
 thermodynamic cycle, 82
 thermodynamic function, 74, 82, 83, 84, 307, 317,
 322
 thermodynamic parameters, xiv, xvii, 74, 77, 78, 85,
 87, 161, 164, 165, 245, 251, 257, 261, 262, 284,
 285, 286, 300, 465, 470
 thermodynamic properties, 70, 75
 thermodynamic stability, 22, 92, 337, 413
 thermodynamics, 73, 257, 275, 322, 327, 470
 thermogravimetric, xiii, 91, 231
 thermogravimetric analysis, 91
 thermogravimetry, 87
 thermolysis, 234, 237, 238, 239, 240, 241, 242, 244,
 245
 thin film, 70, 71, 185, 334, 427
 thin films, 71
 three-dimensional, 76, 80, 90, 132, 414
 threonine, 161, 168
 threshold, xii, 69, 87
 thrombocytopenia, 454
 thymine, 372
 TILs, 306
 time-frame, 76
 tissue, 352
 title, xi, 19, 24, 42
 titration, xi, 20, 25, 26, 27, 28, 29, 30, 31, 32, 33, 34,
 35, 36, 37, 38, 41, 46, 50, 58, 183, 187, 194, 200,
 201, 203, 205, 220, 233, 236, 258, 259, 261, 271,
 308, 311, 353, 436, 481
 toluene, 72, 73, 85, 86, 92, 93, 329, 364, 429
 topological, 276
 topology, xiii, 177, 178
 torus, 252, 292, 294, 454
 total energy, xvii, 466, 467
 total product, 478
 toxic, 23, 236, 330, 369, 462, 478
 toxic effect, 462
 toxicity, xvii, 254, 453, 454, 457, 458, 462
 toxins, 161
 TPA, 412, 427
 trajectory, 84
 transduction, 85, 179, 180, 217
 transfer, xiii, 20, 77, 78, 82, 83, 84, 160, 165, 178,
 181, 182, 190, 191, 195, 197, 201, 210, 220, 254,
 282, 291, 302, 304, 321, 326, 337, 338, 364, 366,
 406, 436
 transformation, 92, 95, 96, 106, 451
 transformations, 95
 transglutaminase, 352
 transistors, 85, 412
 transition, xiii, xv, xvi, 22, 87, 91, 92, 93, 186, 187,
 190, 197, 201, 202, 205, 206, 212, 220, 231, 232,
 234, 241, 242, 243, 245, 246, 247, 325, 346, 381,
 388, 393, 445, 447
 transition metal, xiii, xv, xvi, 186, 187, 197, 201,
 202, 205, 206, 212, 220, 231, 234, 241, 242, 243,
 245, 247, 325, 346, 381, 388
 transition metal ions, xiii, xvi, 197, 201, 205, 206,
 212, 220, 231, 234, 241, 242, 243, 381
 transitions, 84, 93, 222, 425
 translation, 35
 translational, 255
 translocation, 189
 transparent, 52, 308
 transport, xv, xvi, 20, 71, 90, 91, 180, 325, 326, 327,
 328, 329, 330, 331, 332, 333, 334, 336, 337, 338,
 339, 381
 transport processes, 180
 transportation, 95
 triacylglycerols, 481
 trial, 50
 trimer, 436, 441, 442
 Trp, 127, 129, 152, 159, 164, 169, 263, 264, 266,
 267, 269, 270, 271, 274
 tryptophan, 111, 129, 275, 353, 393
 tubers, xvii, xviii, 477, 478, 479, 480, 481, 483, 484
 tubular, 411, 413
 tungsten, 234
 two-dimensional (2D), 33, 89, 413
 tyramine, 273
 tyrosine, 111, 256, 260, 273, 276, 393

U

- ubiquitin, 276
 uncertainty, 292, 471
 unfolded, 277
 universe, 147
 uranium, 321

urea, 76, 351, 364, 371, 386
USDA, 478, 486
UV, xvi, 149, 190, 258, 262, 263, 264, 265, 268,
269, 270, 271, 283, 293, 297, 298, 299, 346, 356,
361, 405, 411, 419, 425, 430, 456
UV absorption, 425
UV absorption spectra, 425
UV spectrum, 430

V

vacuum, 44, 52, 54, 79, 86, 88, 430
valence, 51, 234
validity, 37, 70, 77, 163
valine, 346, 353
van der Waals, xiv, 71, 92, 93, 108, 164, 254, 255,
257, 273, 281, 282, 285, 286, 292, 300
van der Waals forces, 273, 292
vanadium, 234
vancomycin, 148, 149, 151, 152, 153, 160, 161, 162,
163, 164, 165, 166, 349
vapor, 71, 75, 77, 78, 79, 80, 81, 85, 86, 87, 88, 89,
93, 207, 306
variability, 24, 460
variation, xvi, 87, 150, 159, 220, 286, 314, 328, 339,
381, 467, 469
verapamil, 155, 159
vesicles, 345
vibration, 420
vibrational circular dichroism, 284, 302
viscosity, 236, 237, 309
visible, 195, 202, 218, 401, 456, 475
visualization, 52
vitamins, xviii, 477, 478
voids, 91
volatile substances, 244
volatility, 455
volatilization, 77, 238

W

warfarin, 158, 159
waste water, 330
wastewater, 232, 236, 415

water absorption, 90
water clusters, 71, 441, 450
water diffusion, 90
water quality, 330
water sorption, 71, 88, 89
water-soluble, 22, 24, 30, 181, 394, 398, 399, 454
weak interaction, 75, 277
weakness, xiv, 281, 484
weight loss, 79, 237, 238, 240, 242, 419, 426
wheat, xiii, 231, 237, 239, 240, 241, 245
windows, 436
winter, xvii, 477
wood, 233, 247, 480, 481
workers, 22, 23, 31, 33, 37, 57, 58, 91, 110, 224,
326, 440, 443, 445
worry, 479

X

X-ray analysis, 96
X-ray crystallography, 57, 91, 222, 317
X-ray diffraction, 55, 59, 61, 74, 90, 91, 95, 207,
220, 284
X-ray diffraction data, 59, 90
xylene, 72, 73, 86

Y

yeast, 457
yield, xviii, 93, 110, 138, 186, 238, 239, 241, 242,
243, 259, 308, 333, 339, 372, 387, 413, 414, 418,
425, 429, 445, 473, 477, 480

Z

zeolites, 70, 71
zinc, 58, 183, 244, 245, 446
Zinc, 196, 241
Zn, 189, 190, 192, 196, 197, 202, 207, 208, 238, 239,
240, 241, 328, 337, 383, 445, 446
zolmitriptan, 161
zwitterions, 369